Volume 31, Number 1 January 2023
ISSN:1521-1398 PRINT,1572-9206 ONLINE

Journal of Computational Analysis and Applications

EUDOXUS PRESS,LLC

Journal of Computational Analysis and Applications
ISSNno.'s:1521-1398 PRINT,1572-9206 ONLINE

SCOPE OF THE JOURNAL

An international publication of Eudoxus Press, LLC
(published quarterly) www.eudoxuspress.com.

Editor in Chief: George Anastassiou
Department of Mathematical Sciences,
University of Memphis, Memphis, TN 38152-3240, U.S.A
ganastss@memphis.edu, ganastss2@gmail.com
http://web0.msci.memphis.edu/~ganastss/jocaaa/

The main purpose of "J.Computational Analysis and Applications" is to publish high quality research articles from all subareas of Computational Mathematical Analysis and its many potential applications and connections to other areas of Mathematical Sciences. Any paper whose approach and proofs are computational,using methods from Mathematical Analysis in the broadest sense is suitable and welcome for consideration in our journal, except from Applied Numerical Analysis articles. Also plain word articles without formulas and proofs are excluded. The list of possibly connected mathematical areas with this publication includes, but is not restricted to: Applied Analysis, Applied Functional Analysis, Approximation Theory, Asymptotic Analysis, Difference Equations, Differential Equations, Partial Differential Equations, Fourier Analysis, Fractals, Fuzzy Sets, Harmonic Analysis, Inequalities, Integral Equations, Measure Theory, Moment Theory, Neural Networks, Numerical Functional Analysis, Potential Theory, Probability Theory, Real and Complex Analysis, Signal Analysis, Special Functions, Splines, Stochastic Analysis, Stochastic Processes, Summability, Tomography, Wavelets, any combination of the above, e.t.c.

"J.Computational Analysis and Applications" is a peer-reviewed Journal. See the instructions for preparation and submission **of articles to JOCAAA.**

Journal of Computational Analysis and Applications(JoCAAA) is published by **EUDOXUS PRESS,LLC**,1424 Beaver Trail Drive,Cordova,TN38016,USA,anastassioug@yahoo.com http://www.eudoxuspress.com. **Annual Subscription Prices**:For USA and Canada,Institutional:Print $500, Electronic OPEN ACCESS. Individual:Print $250. For any other part of the world add $150 more(handling and postages) to the above prices for Print. No credit card payments.

Copyright©2023 by Eudoxus Press,LLC,all rights reserved.JoCAAA is printed in USA.

JoCAAA is reviewed and abstracted by Elsevier-Scopus, available also via EBSCO publishing and EBSCO.

It is strictly prohibited the reproduction and transmission of any part of JoCAAA and in any form and by any means without the written permission of the publisher.It is only allowed to educators to Xerox articles for educational purposes.The publisher assumes no responsibility for the content of published papers.

Editorial Board

Associate Editors of Journal of Computational Analysis and Applications

Francesco Altomare
Dipartimento di Matematica
Universita' di Bari
Via E.Orabona, 4
70125 Bari, ITALY
Tel+39-080-5442690 office
+39-080-3944046 home
+39-080-5963612 Fax
altomare@dm.uniba.it
Approximation Theory, Functional Analysis, Semigroups and Partial Differential Equations, Positive Operators.

Ravi P. Agarwal
Department of Mathematics
Texas A&M University - Kingsville
700 University Blvd.
Kingsville, TX 78363-8202
tel: 361-593-2600
Agarwal@tamuk.edu
Differential Equations, Difference Equations, Inequalities

George A. Anastassiou
Department of Mathematical Sciences
The University of Memphis
Memphis, TN 38152,U.S.A
Tel.901-678-3144
e-mail: ganastss@memphis.edu
Approximation Theory, Real Analysis,
Wavelets, Neural Networks, Probability, Inequalities.

J. Marshall Ash
Department of Mathematics
De Paul University
2219 North Kenmore Ave.
Chicago, IL 60614-3504
773-325-4216
e-mail: mash@math.depaul.edu
Real and Harmonic Analysis

Dumitru Baleanu
Department of Mathematics and Computer Sciences,
Cankaya University, Faculty of Art and Sciences,
06530 Balgat, Ankara,
Turkey, dumitru@cankaya.edu.tr
Fractional Differential Equations
Nonlinear Analysis, Fractional Dynamics

Carlo Bardaro
Dipartimento di Matematica e Informatica
Universita di Perugia
Via Vanvitelli 1
06123 Perugia, ITALY
TEL+390755853822
+390755855034
FAX+390755855024
E-mail carlo.bardaro@unipg.it
Web site:
http://www.unipg.it/~bardaro/
Functional Analysis and Approximation Theory, Signal Analysis, Measure Theory, Real Analysis.

Martin Bohner
Department of Mathematics and Statistics, Missouri S&T
Rolla, MO 65409-0020, USA
bohner@mst.edu
web.mst.edu/~bohner
Difference equations, differential equations, dynamic equations on time scale, applications in economics, finance, biology.

Jerry L. Bona
Department of Mathematics
The University of Illinois at Chicago
851 S. Morgan St. CS 249
Chicago, IL 60601
e-mail:bona@math.uic.edu
Partial Differential Equations, Fluid Dynamics

Luis A. Caffarelli
Department of Mathematics
The University of Texas at Austin
Austin, Texas 78712-1082
512-471-3160
e-mail: caffarel@math.utexas.edu
Partial Differential Equations

George Cybenko
Thayer School of Engineering
Dartmouth College
8000 Cummings Hall,
Hanover, NH 03755-8000
603-646-3843 (X 3546 Secr.)
e-mail:george.cybenko@dartmouth.edu
Approximation Theory and Neural Networks

Sever S. Dragomir
School of Computer Science and Mathematics, Victoria University,
PO Box 14428,
Melbourne City,
MC 8001, AUSTRALIA
Tel. +61 3 9688 4437
Fax +61 3 9688 4050
e-mail: sever.dragomir@vu.edu.au
Inequalities, Functional Analysis, Numerical Analysis, Approximations, Information Theory, Stochastics.

Oktay Duman
TOBB University of Economics and Technology,
Department of Mathematics, TR-06530, Ankara, Turkey,
e-mail: oduman@etu.edu.tr
Classical Approximation Theory, Summability Theory, Statistical Convergence and its Applications

J .A. Goldstein
Department of Mathematical Sciences
The University of Memphis
Memphis, TN 38152
901-678-3130
e-mail: jgoldste@memphis.edu
Partial Differential Equations, Semigroups of Operators

H. H. Gonska
Department of Mathematics
University of Duisburg
Duisburg, D-47048
Germany
011-49-203-379-3542
e-mail: heiner.gonska@uni-due.de
Approximation Theory, Computer Aided Geometric Design

John R. Graef
Department of Mathematics
University of Tennessee at Chattanooga
Chattanooga, TN 37304 USA
e-mail: John-Graef@utc.edu
Ordinary and functional differential equations, difference equations, impulsive systems, differential inclusions, dynamic equations on time scales, control theory and their applications

Weimin Han
Department of Mathematics
University of Iowa
Iowa City, IA 52242-1419
319-335-0770
e-mail: whan@math.uiowa.edu
Numerical analysis, Finite element method, Numerical PDE, Variational inequalities, Computational mechanics

Tian-Xiao He
Department of Mathematics and Computer Science
P.O. Box 2900, Illinois Wesleyan University
Bloomington, IL 61702-2900, USA
Tel (309)556-3089
Fax (309)556-3864
e-mail: the@iwu.edu
Approximations, Wavelet, Integration Theory, Numerical Analysis, Analytic Combinatorics

Margareta Heilmann
Faculty of Mathematics and Natural Sciences, University of Wuppertal
Gaußstraße 20
D-42119 Wuppertal, Germany,
heilmann@math.uni-wuppertal.de
Approximation Theory (Positive Linear Operators)

Xing-Biao Hu
Institute of Computational Mathematics
AMSS, Chinese Academy of Sciences
Beijing, 100190, CHINA
e-mail: hxb@lsec.cc.ac.cn
Computational Mathematics

Seda Karateke
Department of Computer Engineering,
Faculty of Engineering,
Istanbul Topkapi University,
Istanbul, Zeytinburnu 34087, Turkey
e-mail: sedakarateke@topkapi.edu.tr
Approximation Theory, Neural Networks

Jong Kyu Kim
Department of Mathematics
Kyungnam University
Masan Kyungnam,631-701,Korea
Tel 82-(55)-249-2211
Fax 82-(55)-243-8609
e-mail: jongkyuk@kyungnam.ac.kr
Nonlinear Functional Analysis,
Variational Inequalities, Nonlinear
Ergodic Theory, ODE, PDE,
Functional Equations.

Robert Kozma
Department of Mathematical Sciences
The University of Memphis
Memphis, TN 38152, USA
e-mail: rkozma@memphis.edu
Neural Networks, Reproducing Kernel
Hilbert Spaces,
Neural Percolation Theory

Mustafa Kulenovic
Department of Mathematics
University of Rhode Island
Kingston, RI 02881, USA
e-mail: kulenm@math.uri.edu
Differential and Difference
Equations

Burkhard Lenze
Fachbereich Informatik
Fachhochschule Dortmund
University of Applied Sciences
Postfach 105018
D-44047 Dortmund, Germany
e-mail: lenze@fh-dortmund.de
Real Networks, Fourier Analysis,
Approximation Theory

Alina Alb Lupas
Department of Mathematics and
Computer Science
Faculty of Informatics
University of Oradea
2 Universitatii Street,
410087 Oradea, Romania
e-mail: alblupas@gmail.com
e-mail: dalb@uoradea.ro
Complex Analysis, Topological
Algebra, Mathematical Analysis

Razvan A. Mezei
Computer Science Department
Hal and Inge Marcus School of
Engineering
Saint Martin’s University
Lacey, WA 98503, USA
e-mail: RMezei@stmartin.edu
Numerical Approximation, Fractional
Inequalities.

Hrushikesh N. Mhaskar
Department Of Mathematics
California State University
Los Angeles, CA 90032
626-914-7002
e-mail: hmhaska@gmail.com
Orthogonal Polynomials,
Approximation Theory, Splines,
Wavelets, Neural Networks

Ram N. Mohapatra
Department of Mathematics
University of Central Florida
Orlando, FL 32816-1364
tel.407-823-5080
e-mail: ram.mohapatra@ucf.edu
Real and Complex Analysis,
Approximation Th., Fourier
Analysis, Fuzzy Sets and Systems

Gaston M. N'Guerekata
Department of Mathematics
Morgan State University
Baltimore, MD 21251, USA
tel: 1-443-885-4373
Fax 1-443-885-8216
Gaston.N'Guerekata@morgan.edu
nguerekata@aol.com
Nonlinear Evolution Equations,
Abstract Harmonic Analysis,
Fractional Differential Equations,
Almost Periodicity & Almost
Automorphy

M.Zuhair Nashed
Department Of Mathematics
University of Central Florida
PO Box 161364
Orlando, FL 32816-1364
e-mail: znashed@mail.ucf.edu
Inverse and Ill-Posed problems,
Numerical Functional Analysis,
Integral Equations, Optimization,
Signal Analysis

Mubenga N. Nkashama
Department OF Mathematics
University of Alabama at Birmingham
Birmingham, AL 35294-1170
205-934-2154
e-mail: nkashama@math.uab.edu
Ordinary Differential Equations,
Partial Differential Equations

Vassilis Papanicolaou
Department of Mathematics
National Technical University of
Athens
Zografou campus, 157 80
Athens, Greece
tel: +30(210) 772 1722
Fax +30(210) 772 1775
e-mail: papanico@math.ntua.gr
Partial Differential Equations,
Probability

Choonkil Park
Department of Mathematics
Hanyang University
Seoul 133-791
S. Korea,
e-mail: baak@hanyang.ac.kr
Functional Equations

Svetlozar (Zari) Rachev,
Professor of Finance, College of
Business, and Director of
Quantitative Finance Program,
Department of Applied Mathematics &
Statistics
Stonybrook University
312 Harriman Hall, Stony Brook, NY
11794-3775
tel: +1-631-632-1998,
svetlozar.rachev@stonybrook.edu

Alexander G. Ramm
Mathematics Department
Kansas State University
Manhattan, KS 66506-2602
e-mail: ramm@math.ksu.edu
Inverse and Ill-posed Problems,
Scattering Theory, Operator Theory,
Theoretical Numerical Analysis,
Wave Propagation, Signal Processing
and Tomography

Tomasz Rychlik
Polish Academy of Sciences
Instytut Matematyczny PAN
00-956 Warszawa, skr. poczt. 21
ul. Śniadeckich 8
Poland
e-mail: trychlik@impan.pl
Mathematical Statistics,
Probabilistic Inequalities

Boris Shekhtman
Department of Mathematics
University of South Florida
Tampa, FL 33620, USA
Tel 813-974-9710
e-mail: shekhtma@usf.edu
Approximation Theory, Banach
spaces, Classical Analysis

T. E. Simos
Department of Computer
Science and Technology
Faculty of Sciences and Technology
University of Peloponnese
GR-221 00 Tripolis, Greece
Postal Address:
26 Menelaou St.
Anfithea - Paleon Faliron
GR-175 64 Athens, Greece
e-mail: tsimos@mail.ariadne-t.gr
Numerical Analysis

Jagdev Singh
JECRC University, Jaipur, India
jagdevsinghrathore@gmail.com
Fractional Calculus, Mathematical
Modelling, Special Functions,
Numerical Methods

H. M. Srivastava
Department of Mathematics and
Statistics
University of Victoria
Victoria, British Columbia V8W 3R4
Canada
tel.250-472-5313; office,250-477-
6960 home, fax 250-721-8962
e-mail: harimsri@math.uvic.ca
Real and Complex Analysis,
Fractional Calculus and Appl.,
Integral Equations and Transforms,
Higher Transcendental Functions and
Appl.,q-Series and q-Polynomials,
Analytic Number Th.

I. P. Stavroulakis
Department of Mathematics
University of Ioannina
451-10 Ioannina, Greece
e-mail: ipstav@cc.uoi.gr
Differential Equations
Phone +3-065-109-8283

Jessada Tariboon
Department of Mathematics
King Mongut's University of
Technology N. Bangkok
1518 Pracharat 1 Rd., Wongsawang,
Bangsue, Bangkok, Thailand 10800
e-mail: jessada.t@sci.kmutnb.ac.th
Time scales

Differential/Difference Equations,
Fractional Differential Equations

Manfred Tasche
Department of Mathematics
University of Rostock
D-18051 Rostock, Germany
manfred.tasche@mathematik.uni-rostock.de
Numerical Fourier Analysis, Fourier Analysis, Harmonic Analysis, Signal Analysis, Spectral Methods, Wavelets, Splines, Approximation Theory

Juan J. Trujillo
University of La Laguna
Departamento de Analisis Matematico
C/Astr.Fco.Sanchez s/n
38271. LaLaguna. Tenerife.
SPAIN
Tel/Fax 34-922-318209
e-mail: Juan.Trujillo@ull.es
Fractional: Differential Equations-Operators-Fourier Transforms, Special functions, Approximations, and Applications

Xiao-Jun Yang
State Key Laboratory for Geomechanics and Deep Underground Engineering, China
University of Mining and Technology, Xuzhou 221116, China
Local Fractional Calculus and Applications, Fractional Calculus and Applications, General Fractional Calculus and Applications, Variable-order Calculus and Applications, Viscoelasticity and Computational methods for Mathematical Physics.dyangxiaojun@163.com

Xiang Ming Yu
Department of Mathematical Sciences
Southwest Missouri State University
Springfield, MO 65804-0094
417-836-5931
e-mail: xmy944f@missouristate.edu
Classical Approximation Theory, Wavelets

Richard A. Zalik
Department of Mathematics
Auburn University
Auburn University, AL 36849-5310
USA.
Tel 334-844-6557 office
Fax 334-844-6555
e-mail: zalik@auburn.edu
Approximation Theory, Chebychev Systems, Wavelet Theory

Ahmed I. Zayed
Department of Mathematical Sciences
DePaul University
2320 N. Kenmore Ave.
Chicago, IL 60614-3250
773-325-7808
e-mail: azayed@condor.depaul.edu
Shannon sampling theory, Harmonic analysis and wavelets, Special functions and orthogonal polynomials, Integral transforms

Ding-Xuan Zhou
Department Of Mathematics
City University of Hong Kong
83 Tat Chee Avenue
Kowloon, Hong Kong
852-2788 9708,Fax:852-2788 8561
e-mail: mazhou@cityu.edu.hk
Approximation Theory, Spline functions, Wavelets

Xin-long Zhou
Fachbereich Mathematik, Fachgebiet Informatik
Gerhard-Mercator-Universitat Duisburg
Lotharstr.65, D-47048 Duisburg, Germany
e-mail:Xzhou@informatik.uni-duisburg.de
Fourier Analysis, Computer-Aided Geometric Design, Computational Complexity, Multivariate Approximation Theory, Approximation and Interpolation Theory

Instructions to Contributors
Journal of Computational Analysis and Applications

An international publication of Eudoxus Press, LLC, of TN.

Editor in Chief: George Anastassiou
Department of Mathematical Sciences
University of Memphis
Memphis, TN 38152-3240, U.S.A.

1. Manuscripts files in Latex and PDF and in English, should be submitted via email to the Editor-in-Chief:

Prof.George A. Anastassiou
Department of Mathematical Sciences
The University of Memphis
Memphis,TN 38152, USA.
Tel. 901.678.3144
e-mail: ganastss@memphis.edu

Authors may want to recommend an associate editor the most related to the submission to possibly handle it.

Also authors may want to submit a list of six possible referees, to be used in case we cannot find related referees by ourselves.

2. Manuscripts should be typed using any of TEX,LaTEX,AMS-TEX,or AMS-LaTEX and according to EUDOXUS PRESS, LLC. LATEX STYLE FILE. (Click HERE to save a copy of the style file.)They should be carefully prepared in all respects. Submitted articles should be brightly typed (not dot-matrix), double spaced, in ten point type size and in 8(1/2)x11 inch area per page. Manuscripts should have generous margins on all sides and should not exceed 24 pages.

3. Submission is a representation that the manuscript has not been published previously in this or any other similar form and is not currently under consideration for publication elsewhere. A statement transferring from the authors(or their employers,if they hold the copyright) to Eudoxus Press, LLC, will be required before the manuscript can be accepted for publication.The Editor-in-Chief will supply the necessary forms for this transfer.Such a written transfer of copyright,which previously was assumed to be implicit in the act of submitting a manuscript,is necessary under the U.S.Copyright Law in order for the publisher to carry through the dissemination of research results and reviews as widely and effective as possible.

4. The paper starts with the title of the article, author's name(s) (no titles or degrees), author's affiliation(s) and e-mail addresses. The affiliation should comprise the department, institution (usually university or company), city, state (and/or nation) and mail code.

The following items, 5 and 6, should be on page no. 1 of the paper.

5. An abstract is to be provided, preferably no longer than 150 words.

6. A list of 5 key words is to be provided directly below the abstract. Key words should express the precise content of the manuscript, as they are used for indexing purposes.

The main body of the paper should begin on page no. 1, if possible.

7. All sections should be numbered with Arabic numerals (such as: 1. INTRODUCTION) .
Subsections should be identified with section and subsection numbers (such as 6.1. Second-Value Subheading).
If applicable, an independent single-number system (one for each category) should be used to label all theorems, lemmas, propositions, corollaries, definitions, remarks, examples, etc. The label (such as Lemma 7) should be typed with paragraph indentation, followed by a period and the lemma itself.

8. Mathematical notation must be typeset. Equations should be numbered consecutively with Arabic numerals in parentheses placed flush right, and should be thusly referred to in the text [such as Eqs.(2) and (5)]. The running title must be placed at the top of even numbered pages and the first author's name, et al., must be placed at the top of the odd numbed pages.

9. Illustrations (photographs, drawings, diagrams, and charts) are to be numbered in one consecutive series of Arabic numerals. The captions for illustrations should be typed double space. All illustrations, charts, tables, etc., must be embedded in the body of the manuscript in proper, final, print position. In particular, manuscript, source, and PDF file version must be at camera ready stage for publication or they cannot be considered.

Tables are to be numbered (with Roman numerals) and referred to by number in the text. Center the title above the table, and type explanatory footnotes (indicated by superscript lowercase letters) below the table.

10. List references alphabetically at the end of the paper and number them consecutively. Each must be cited in the text by the appropriate Arabic numeral in square brackets on the baseline.
References should include (in the following order):
initials of first and middle name, last name of author(s)
title of article,

name of publication, volume number, inclusive pages, and year of publication.

Authors should follow these examples:

Journal Article

1. H.H.Gonska,Degree of simultaneous approximation of bivariate functions by Gordon operators, (journal name in italics) *J. Approx. Theory*, 62,170-191(1990).

Book

2. G.G.Lorentz, (title of book in italics) *Bernstein Polynomials* (2nd ed.), Chelsea,New York,1986.

Contribution to a Book

3. M.K.Khan, Approximation properties of beta operators,in(title of book in italics) *Progress in Approximation Theory* (P.Nevai and A.Pinkus,eds.), Academic Press, New York,1991,pp.483-495.

11. All acknowledgements (including those for a grant and financial support) should occur in one paragraph that directly precedes the References section.

12. Footnotes should be avoided. When their use is absolutely necessary, footnotes should be numbered consecutively using Arabic numerals and should be typed at the bottom of the page to which they refer. Place a line above the footnote, so that it is set off from the text. Use the appropriate superscript numeral for citation in the text.

13. After each revision is made please again submit via email Latex and PDF files of the revised manuscript, including the final one.

14. Effective 1 Nov. 2009 for current journal page charges, contact the Editor in Chief. Upon acceptance of the paper an invoice will be sent to the contact author. The fee payment will be due one month from the invoice date. The article will proceed to publication only after the fee is paid. The charges are to be sent, by money order or certified check, in US dollars, payable to Eudoxus Press, LLC, to the address shown on the Eudoxus homepage.

No galleys will be sent and the contact author will receive one (1) electronic copy of the journal issue in which the article appears.

15. This journal will consider for publication only papers that contain proofs for their listed results.

Characteristics of Mexican hat wavelet transform in a class of generalized quotient space

Abhishek Singh*,[1], Aparna Rawat[1] and Shubha Singh[2]

December 24, 2022

Abstract

In this paper, Mexican hat wavelet transformation is defined on the space of tempered generalized quotients by employing the structure of exchange property. We study the exchange property for the Mexican hat wavelet transform by applying the theory of the Mexican hat wavelet transform of distributions. Further, different properties of Mexican hat wavelet transform are investigated on the space of tempered generalized quotients.

Key words: Wavelet transform; Exchange property; Distribution space; Tempered generalized quotient
Mathematics Subject Classification(2010): 44A15; 44A35; 46F99; 54B15

1

1 Introduction

The wavelet transform $(Wf)(b,a)$ of a square integrable function f, is given by

$$(Wf)(b,a) = \int_{-\infty}^{\infty} f(t)\overline{\psi_{b,a}}(t)dt, \tag{1.1}$$

where

$$\psi_{b,a}(t) = (\sqrt{a})^{-1}\psi\left(\frac{t-b}{a}\right), \quad b,t \in \mathbb{R}^n, \text{ and } a > 0. \tag{1.2}$$

The inversion formula for (1.1) is given by

$$\frac{2}{C_\psi}\int_0^{\infty}\left[\int_{-\infty}^{\infty}(\sqrt{a})^{-1}(Wf)(b,a)\psi\left(\frac{x-b}{a}\right)db\right]\frac{da}{a^2} = f(x), \quad x \in \mathbb{R}^n, \tag{1.3}$$

---

[1]* Corresponding author (mathdras@gmail.com) [1]Department of Mathematics and Statistics, Banasthali Vidhyapith, Banasthali, India
[2]Department of Physics, Banaras Hindu University, Varanasi

where the admissibility condition C_ψ is given by

$$\frac{C_\psi}{2} = \int_0^\infty \frac{|\hat{\psi}(u)|^2}{|u|} dv = \int_0^\infty \frac{|\hat{\psi}(-u)|^2}{|u|} du < \infty \qquad [3, \text{p. } 64].$$

The Mexican hat wavelet is constructed by taking the negative second derivative of a Gaussian function and is given by [24]

$$\psi(t) = e^{-(\frac{t^2}{2})}(1-t^2) = -\frac{d^2}{dt^2} e^{-(\frac{t^2}{2})} \tag{1.4}$$

such that

$$\psi_{b,a}(t) = -a^{\frac{3}{2}} D_t^2 e^{-\frac{(b-t)^2}{2a^2}}, \qquad \left(D_t = \frac{d}{dt}\right). \tag{1.5}$$

Thus, (1.1) can be reduced to

$$(Wf)(b,a) = -a^{\frac{3}{2}} \int_{\mathbb{R}} f(t)\ D_t^2 e^{-\frac{(b-t)^2}{2a^2}} dt, \qquad a \in \mathbb{R}_+ \tag{1.6}$$

which then, under certain conditions on f is

$$(Wf)(b,a) = -a^{\frac{3}{2}} \int_{\mathbb{R}} f^{(2)}(t)\ \ e^{-\frac{(b-t)^2}{2a^2}} dt, \qquad a \in \mathbb{R}_+. \tag{1.7}$$

Let a function $k_a(b-t)$ be defined by

$$k_a(b-t) = \frac{1}{\sqrt{2\pi a}} e^{\left(\frac{-(b-t)^2}{2a}\right)}, \tag{1.8}$$

where $t \in \mathbb{R},\ b = \sigma + i\omega$ and $a \in \mathbb{R}_+$. Then

$$D_t^2 k_{a^2}(b-t) = \frac{1}{\sqrt{2\pi a}} D_t^2 \left(e^{\frac{-(b-t)^2}{2a^2}}\right). \tag{1.9}$$

Therefore, by (1.5)

$$\psi_{b,a}(t) = -(2\pi)^{\frac{1}{2}} a^{\frac{5}{2}} D_t^2 k_{a^2}(b-t)$$

and hence the Mexican hat wavelet transform is given by

$$\begin{aligned} (Wf)(b,a) &= (2\pi)^{\frac{1}{2}} a^{\frac{5}{2}} \int_{\mathbb{R}} f(t) D_t^2 k_{a^2}(b-t) dt \\ &= (2\pi)^{\frac{1}{2}} a^{\frac{5}{2}} \int_{\mathbb{R}} f^{(2)}(t) k_{a^2}(b-t) dt \\ &= (2\pi)^{\frac{1}{2}} a^{\frac{5}{2}} (f^{(2)} * k_{a^2})(b), \quad b \in \mathbb{C},\ a \in \mathbb{R}_+, \end{aligned} \tag{1.10}$$

where $k_{a^2}(b-t) = \frac{1}{\sqrt{2\pi a}} e^{\frac{-(b-t)^2}{2a^2}}$.

The most general theory of the MHWT is investigated on the generalized function space $(\mathscr{W}^{\gamma}_{\alpha,\beta})'$ developed by Pathak *et al.* [8]. It is proved that the MHWT $(Wf)(b,a)$ of $f \in (\mathscr{W}^{\gamma}_{\alpha,\beta})'$, is given by $\langle f^{(2)}(t), k_{a^2}(b-t)\rangle$ is an analytic function in the strip $\frac{\alpha}{\gamma} < \operatorname{Re} b < \frac{\beta}{\gamma}$ for some $\alpha, \beta, \gamma \in \mathbb{R}$.

Recently, the wavelet transform has been comprehensively studied in many functions, distributions, and tempered distribution spaces. Several interesting properties and applications in generalized function spaces have been developed (See, for example, [6, 9, 10, 11, 12, 13, 17, 18, 19, 20, 21]. On the other hand, Mikusiński's algebraic approach gave a new transformation to the theory of functional analysis. The space of generalized quotients (Boehmians) is the recent generalization of the Schwartz distribution and the motivation for the expansion is in the core of Mikusiński operators. Its application to function spaces with the involvement of convolution provides different generalized function spaces. Hence, many integral transforms have been investigated in such spaces [1, 5, 7, 14, 15, 16, 22, 23].

Let $\mathscr{S}(\mathbb{R}^n)$ and $\mathscr{S}(\mathbb{R}^n \times \mathbb{R}_+)$ be the spaces of functions with continuous derivatives which are rapidly decreasing on $\mathbb{R}^n$ and $\mathbb{R}^n \times \mathbb{R}_+$. The dual of $\mathscr{S}$ is represented by $\mathscr{S}'$ that is known as the space of tempered distributions. The spaces $\mathscr{S}$ and $\mathscr{S}'$ have been introduced and developed in [2]. The class $\mathscr{S}'$ of tempered distributions is contained in $(\mathscr{W}^{\gamma}_{\alpha,\beta})'$. Therefore the Mexican hat wavelet transform theory can be made applicable to $\mathscr{S}'$. Further, the Mexican hat wavelet transform can be expanded to the space of tempered generalized quotient, as the space is a natural expansion of tempered distributions. Here, we extend the Mexican hat wavelet transformation to a class of generalized quotient space that have quotients of sequences in the form of f_n/φ_n, where the numerator contains terms of the sequence from some set $\mathscr{S}'$ and the denominator is a delta sequence such that it satisfies the following condition

$$f_n * \varphi_m = f_m * \varphi_m, \quad \forall m, n \in \mathbb{N}. \tag{1.11}$$

Further, the delta sequences are defined as sequences of functions $\{\varphi_n\} \in \mathscr{S}$ that satisfies

1. $\int_{\mathbb{R}^n} \varphi_n(x)dx = 1$ for all $n = 1, 2, 3, \cdots$.

2. There exists a constant $C > 0$ such that
$$\int_{\mathbb{R}^n} |\varphi_n(x)|\, dx \leq C \text{ for all } n = 1, 2, 3, \cdots.$$

3. $\lim_{n\to\infty} \int_{\|x\|\geq\epsilon} \|x\|^k \, |(\varphi_j(x))|\, dx = 0$ for every $k \in \mathbb{N}$ and $\epsilon > 0$.

In particular, we extend the transformation to generalized quotient space by defining an exchange property for the Mexican hat wavelet transform. In the next section, we introduce some of the basic results required for the investigation of MHWT on the generalized quotient space. Section 3 describes some algebraic properties of MHWT in the context of tempered generalized quotients.

2 The exchange property

In this section, the space of tempered generalized quotients is constructed by applying the exchange property. This construction for generalized quotients indicates that the role of convergence is not necessary.

Theorem 2.1. *For a function $f \in \mathscr{S}'$ and $t \in \mathbb{R}$,*

$$(Wf)(b,a) = (2\pi)^{\frac{1}{2}} a^{\frac{5}{2}} (f^{(2)} * k_{a^2})(b) = (2\pi)^{\frac{1}{2}} a^{\frac{5}{2}} \lim_{n\to\infty} ((f^{(2)} * k_{a^2}) e^{-\frac{t^2}{2n}})(b).$$

Proof. Consider,

$$\begin{aligned} (2\pi)^{\frac{1}{2}} a^{\frac{5}{2}} \lim_{n\to\infty} ((f^{(2)} * k_{a^2}) e^{-\frac{t^2}{2n}})(b) &= (2\pi)^{\frac{1}{2}} a^{\frac{5}{2}} \lim_{n\to\infty} \int_{\mathbb{R}} f^{(2)}(t) k_{a^2}(b) e^{-\frac{t^2}{2n}} dt \\ &= a^{\frac{3}{2}} \lim_{n\to\infty} \int_{\mathbb{R}} f^{(2)}(t) e^{-\frac{(b-t)^2}{2a^2}} e^{-\frac{t^2}{2n}} dt \\ &= a^{\frac{3}{2}} \int_{\mathbb{R}} f^{(2)}(t) e^{-\frac{(b-t)^2}{2a^2}} dt. \end{aligned}$$

Therefore,

$$(Wf)(b,a) = (2\pi)^{\frac{1}{2}} a^{\frac{5}{2}} \lim_{n\to\infty} ((f^{(2)} * k_{a^2}) e^{-\frac{t^2}{2n}})(b).$$

□

Theorem 2.2. *For $f \in \mathscr{S}'$ and $\varphi \in \mathscr{S}$, we have*

$$(W(f * \varphi))(b,a) = (Wf)(b,a) * \varphi.$$

Proof. By using [4, Lemma 4.3.8], $(f * \varphi) \in \mathscr{S}'$ and hence $(W(f * \varphi))(b,a)$ is defined. Also, by Theorem 2.1

$$(W(f * \varphi))(b,a) = (2\pi)^{\frac{1}{2}} a^{\frac{5}{2}} \lim_{n\to\infty} (((f^{(2)} * \varphi) * k_{a^2}) e^{-\frac{t^2}{2n}})(b).$$

Consider,

$$\begin{aligned} (2\pi)^{\frac{1}{2}} a^{\frac{5}{2}} (((f^{(2)} * \varphi) * k_{a^2}) e^{-\frac{t^2}{2n}})(b) &= (2\pi)^{\frac{1}{2}} a^{\frac{5}{2}} \int_{\mathbb{R}} (f^{(2)} * \varphi)(t) k(b-t, a^2) e^{-\frac{t^2}{2n}} \, dt \\ &= a^{\frac{3}{2}} \int_{\mathbb{R}} (f^{(2)} * \varphi)(t) e^{-\frac{(b-t)^2}{2a^2}} e^{-\frac{t^2}{2n}} \, dt \\ &= a^{\frac{3}{2}} \int_{\mathbb{R}} \langle f^{(2)}(s), \varphi(t-s) \rangle e^{-\frac{(b-t)^2}{2a^2}} e^{-\frac{t^2}{2n}} \, dt \\ &= a^{\frac{3}{2}} \int_{\mathbb{R}} \langle f^{(2)}(s), \varphi(t-s) \rangle \psi_n(t) dt, \qquad (2.1) \end{aligned}$$

where $\psi_n(t) = e^{-\frac{(b-t)^2}{2a^2}} e^{-\frac{t^2}{2n}}$.

By [8, Lemma 4.3], we have

$$a^{\frac{3}{2}} \int_{-m}^{m} \langle f^{(2)}(s), \varphi(t-s) \rangle \psi_n(t) dt = a^{\frac{3}{2}} \left\langle f^{(2)}(s), \int_{-m}^{m} \varphi(t-s)\psi_n(t) dt \right\rangle, \ \forall m > 0,$$

which converges to

$$a^{\frac{3}{2}} \left\langle f^{(2)}(s), \int_{-m}^{m} \varphi(t-s)\psi_n(t) dt \right\rangle \text{ as } m \to \infty,$$

Therefore,

$$\begin{aligned} \int_{-\infty}^{\infty} \langle f^{(2)}(s), \varphi(t-s) \rangle e^{-\frac{(b-t)^2}{2a^2}} e^{-\frac{t^2}{2n}} \ dt &= \left\langle f^{(2)}(s), \int_{-\infty}^{\infty} \varphi(t-s)\psi_n(t) \ dt \right\rangle \\ &= \langle f^{(2)}(s), (\varphi * \psi_n)(s) \rangle. \qquad (2.2) \end{aligned}$$

Let us now consider,

$$\begin{aligned} (2\pi)^{\frac{1}{2}} a^{\frac{5}{2}} ((f^{(2)} * k_{a^2}) * \varphi)(b) &= (2\pi)^{\frac{1}{2}} a^{\frac{5}{2}} \int_{\mathbb{R}} (f^{(2)} * k_{a^2})(b-t)\varphi(t) \ dt \\ &= (2\pi)^{\frac{1}{2}} a^{\frac{5}{2}} \int_{-M}^{M} \langle f^{(2)}(s), k_{a^2}(b-t-s) \rangle \varphi(t) \ dt, \end{aligned}$$

where supp $\varphi \subseteq [-P, P]$. Now by [8, Lemma 4.3],

$$\begin{aligned} (2\pi)^{\frac{1}{2}} a^{\frac{5}{2}} ((f^{(2)} * k_{a^2}) * \varphi)(b) &= (2\pi)^{\frac{1}{2}} a^{\frac{5}{2}} \int_{-M}^{M} \langle f^{(2)}(s), k_{a^2}(b-t-s) \rangle \varphi(t) \ dt \\ &= (2\pi)^{\frac{1}{2}} a^{\frac{5}{2}} \left\langle f^{(2)}(s), \int_{-\infty}^{\infty} k_{a^2}(b-t-s)\varphi(t) \ dt \right\rangle \\ &= (2\pi)^{\frac{1}{2}} a^{\frac{5}{2}} \left\langle f^{(2)}(s), \int_{-\infty}^{\infty} \frac{1}{\sqrt{2\pi} a} \psi(t-s)\varphi(t) \ dt \right\rangle \\ &= a^{\frac{3}{2}} \left\langle f^{(2)}(s), \int_{-\infty}^{\infty} \psi(t-s)\varphi(t) \ dt \right\rangle \\ &= a^{\frac{3}{2}} \langle f^{(2)}(s), (\varphi * \psi)(s) \rangle. \qquad (2.3) \end{aligned}$$

From (2.2) and (2.3), we obtain

$$(W(f * \varphi))(b, a) = (Wf)(b, a) * \varphi.$$

□

Definition 2.3. For a family $\{\varphi_j\}_{j \in J}$, where $\varphi_j \in \mathcal{S}$, we define

$$M\Big(\{\varphi_j\}_J \Big) = \{x \in \mathbb{R}^n : \varphi_j(x) = 0, \ \ \forall j \in J\}. \qquad (2.4)$$

A family of pairs $\{(f_j,\varphi_j)\}_J$, where $f_j \in \mathcal{S}'$ and $\varphi_j \in \mathcal{S}$, have the exchange property if

$$f_j * \varphi_k = f_k * \varphi_j, \forall j,k \in J. \tag{2.5}$$

Let set $\mathcal{A}$ denotes the collection of $\{(f_j,\varphi_j)\}_J$, where $f_j \in \mathcal{S}'(\mathbb{R}^n)$ and $\varphi_j \in \mathcal{S}(\mathbb{R}^n)$, $\forall j \in J$, with exchange property such that $M\bigg(\ \{\varphi_j\}_J\ \bigg) = \emptyset$.

If $M\left(\{\varphi_j\}_J\right) = \emptyset$ and $M\left(\{\lambda_k\}_K\right) = \emptyset$, then $M\Big(\{\varphi_j * \lambda_k\}_{J\times K}\Big) = \emptyset$.

Theorem 2.4. *If $\{(f_j,\varphi_j)\}_J \in \mathcal{A}$, then there exists a unique $F \in \mathcal{S}'(\mathbb{R}^n \times \mathbb{R}_+)$ such that F is the Mexican hat wavelet transform of the family of functions $\{(f_j,\varphi_j)\}_J$, i.e., $F = (W\{(f_j,\varphi_j)\}_J)$.*

Proof. Let us consider family of sequences $\{(f_j,\varphi_j)\}_J \in \mathcal{A}$, where $f_j \in \mathscr{S}'(\mathbb{R}^n)$ and $\varphi \in \mathscr{S}$, $\forall j \in J$, with exchange property such that $|\varphi(x)| > \epsilon$, for some $\epsilon > 0$, and $x \in M\left(\{\varphi_j\}_J\right)^c$. Then, in some open neighborhood of x, we define

$$F = \frac{(Wf_j)}{\varphi_j}. \tag{2.6}$$

Case 1: We show that for some open neighborhood of x we have a quotient F that is unique in that neighborhood, i.e., F does not depend on $j \in J$. Let U and V be some open neighborhood of x such that $|\varphi_j(x)| > \epsilon$, $\forall x \in U$ and $|\varphi_k(x)| > \epsilon$, $\forall x \in V$. Then since $\{(f_j,\varphi_j)\} \in \mathcal{A}$, hence it satisfy the exchange property and therefore,

$$f_j * \varphi_k = f_k * \varphi_j,\ \forall j,k \in J. \tag{2.7}$$

Applying Mexican hat wavelet transform to (2.7), we get

$$\begin{aligned} (W(f_j * \varphi_k)) &= (W(f_k * \varphi_j)) \\ (Wf_j) * \varphi_k &= (Wf_k) * \varphi_j \quad \text{(by Theorem 2.2)} \\ \frac{(Wf_j)}{\varphi_j} &= \frac{(Wf_k)}{\varphi_k}. \end{aligned} \tag{2.8}$$

Hence, we get a quotient $F = \dfrac{(Wf_j)}{\varphi_j}$ on $U \cap V$.

Case 2: We need to show that $F \in \mathscr{S}'(\mathbb{R}^n \times \mathbb{R}_+)$ is unique. From (2.6) and (2.8), for any $j,k \in J$, we have

$$(Wf_k) = F\varphi_k,\ \forall k \in J \tag{2.9}$$

such that there exists a unique $F \in \mathscr{S}'(\mathbb{R}^n \times \mathbb{R}_+)$ which implies exchange property.

Clearly, for a total sequence, say $\{\varphi_j\}_{\mathbb{N}}$, where $\varphi_j \in \mathcal{S}(\mathbb{R}^n)$ for all $j \in \mathbb{N}$, there is an $f_j \in \mathcal{S}'(\mathbb{R}^n)$ such that $(Wf_j) = \varphi_j F$. Hence, $\{(f_j,\varphi_j)\}_{\mathbb{N}} \in \mathcal{A}$ and $F = (W(\{(f_j,\varphi_j)\}_{\mathbb{N}}))$. $\square$

For the family of pairs of sequences $\{(f_j,\varphi_j)\}_J,\ \{(g_k,\lambda_k)\}_K \in \mathcal{A}$ has an Equivalence Relation, i.e., $\{(f_j,\varphi_j)\}_J\ \ \{(g_k,\phi_k)\}_K$ if

$$f_j * \lambda_k = g_k * \varphi_j, \quad \forall j \in J,\ k \in K. \tag{2.10}$$

Theorem 2.5. *Let* $\{(f_j,\varphi_j)\}_J, \{(g_k,\lambda_k)\}_K \in \mathcal{A}$*. Then* $\{(f_j,\varphi_j)\}_J \sim \{(g_k,\lambda_k)\}_K$ *iff* $(W(\{(f_j,\varphi_j)\}_J)) = (W(\{(g_k,\lambda_k)\}_K))$*.*

Proof. Let $\{(f_j,\varphi_j)\}_J \sim \{(g_k,\lambda_k)\}_K$, hence, they satisfy the exchange property, defined as

$$f_j * \lambda_k = g_k * \varphi_k,\ \forall j \in J, k \in K.$$

Let F and G denotes the Mexican hat wavelet transform of some family of sequences such that $F = (W(\{(f_j,\varphi_j)\}_J))$ and $G = (W(\{(g_k,\lambda_k)\}_K))$. Now, consider,

$$\begin{aligned} \varphi_j F * \lambda_k &= (Wf_j) * \lambda_k \\ &= (W(f_j * \lambda_k)) \\ &= (W(g_k * \varphi_j)) \\ &= (Wg_k) * \varphi_j \\ &= \lambda_k G * \varphi_j. \end{aligned}$$

Now, by applying Lemma 2, we get $F = G$.
Conversely, we need to show that the family of sequences $\{(f_j,\varphi_j)\}_J$ and $\{(g_k,\lambda_k)\}_K$ are equivalent. Let us consider

$$\begin{aligned} & F = G \\ \Longrightarrow\quad & (Wf_j) * \lambda_k = (Wg_k) * \varphi_j \\ \Longrightarrow\quad & (W(f_j * \lambda_k)) = (W(g_k * \varphi_j)) \\ \Longrightarrow\quad & f_j * \lambda_k = g_k * \varphi_j. \end{aligned} \tag{2.11}$$

Hence, $\{(f_j,\varphi_j)\}_J \sim \{(g_k,\lambda_k)\}_K$. ☐

From the above theorem it is shown that there is an equivalence relation on $\mathcal{A}$ and hence splits $\mathcal{A}$ into equivalence classes. The equivalence class contains the generalized quotient $\dfrac{f_n}{\varphi_n}$ and is denoted by $\left[\dfrac{f_n}{\varphi_n}\right]$. These equivalence classes are called generalized quotients or Boehmians and the space of all such generalized quotients is denoted by $\mathcal{B}$.

Definition 2.6. Let $X = \left[\dfrac{f_n}{\varphi_n}\right] \in \mathscr{B}$, then the MHWT of X as a generalized quotient is defined by,

$$Y = (WX)(b,a) = \left[\frac{(Wf_n)(b,a)}{\varphi_n}\right].$$

It is well defined since, if $X = \left[\frac{f_n}{\varphi_n}\right] = Y = \left[\frac{g_n}{\psi_n}\right]$ in $\mathscr{B}$, then

$$\begin{aligned} f_m * \psi_n &= g_n * \varphi_m \ \ \forall m, n \in \mathbb{N} \\ (W(f_m * \psi_n))(b,a) &= (W(g_n * \varphi_m))(b,a) \\ (Wf_m)(b,a) * \psi_n &= (Wg_n)(b,a) * \varphi_m \quad \text{(by Theorem 2.2)} \\ \left[\frac{(Wf_n)(b,a)}{\varphi_n}\right] &= \left[\frac{(Wg_n)(b,a)}{\psi_n}\right]. \end{aligned}$$

Further, by considering the map $f \ \rightarrow \left[\frac{f*\delta_n}{\delta_n}\right]$, any $f \in \mathcal{W}'(-\infty,\infty)$ can be considered as an element of $\mathscr{B}$ by [4, Theorem 4.3.9], i.e., if $X = \left[\frac{f*\delta_n}{\delta_n}\right]$, then

$$(WX)(b,a) = \left[\frac{W(f*\delta_n)(b,a)}{\delta_n}\right] = \left[\frac{(Wf)(b,a)*\delta_n}{\delta_n}\right] = (Wf)(b,a).$$

This definition extends the theory of MHWT to more general spaces than $(\mathscr{W}^{\gamma}_{\alpha,\beta})'$.

From Theorem 2.4 and Theorem 2.5, it is clear that the Mexican hat wavelet transform is a bijection from the space of generalized quotients to the space of distributions.

Theorem 2.7. *For every* $\mathcal{X} \in \mathcal{B}_{\mathscr{S}'(\mathbb{R}^n)}$ *there exists a delta sequence* (φ_n) *such that* $\mathcal{X} = [\{(f_n, \varphi_n)\}_{\mathbb{N}}]$ *for some* $f_n \in \mathscr{S}'(\mathbb{R}^n)$.

Proof. Let $(\phi_n) \in \mathscr{S}(\mathbb{R}^n)$, be a delta sequence and $X \in \mathcal{B}_{\mathscr{S}'(\mathbb{R}^n)}$. Then, $(WX)*\phi_n \in \mathscr{S}'$, since $(WX) \in \mathscr{S}'$. Consequently, $(WX)*\phi_n = (Wg_n)$ for some $g_n \in \mathscr{S}'$. Therefore, we have

$$X = \left[\frac{g_n * \phi_n}{\phi_n * \phi_n}\right]. \tag{2.12}$$

Hence, $f_n = (g_n * \phi_n) \in \mathscr{S}'$ and by using the property of delta sequences $\phi_n * \phi_n \in \mathscr{S}$ is a delta sequence. This completes the proof. ☐

Conclusions

The space of generalized quotients includes regular operators, distributions, ultra-distributions and also objects which are neither regular operators nor distributions. It may be concluded here that the space of tempered generalized quotient is constructed in a simple way by using the exchange property. This new construction is further used to represent the Mexican hat wavelet transform of tempered generalized quotients with its algebraic properties. This space of generalized quotient can be applied to examine Mexican hat wavelet transformation on various manifolds.

Acknowledgement

The first author (AS) is supported by National Board for Higher Mathematics(DAE), Government of India, through sanction No. 02011/7/2022 NBHM(R.P.)/ R&D-II/10010 and the third author is supported by DST under WOS-A, Government of India.

References

[1] Arteaga, C. and Marrero, I. (2012). The Hankel Transform of Tempered Boehmians via the Exchange Property. *Applied Mathematics and Computation*, **219**(3), 810-818.

[2] Atanasiu, D. and Mikusiński, P. (2005). On the Fourier transform and the Exchange Property. *International Journal of Mathematics and Mathematical Sciences*, **16**,2579-2584.

[3] Chui, C. K. (1992). *An Introduction to Wavelets*. New York: Academic Press.

[4] Kalpakam NV (1998) Topics in the theory of Boehmians and their integral transforms. (Doctoral dissertation)

[5] Loonker, D., Banerji, P.K., Debnath, L. (2010). On the Hankel transform for Boehmians. *Integral Transforms and Special Functions*, **21**(7), 479-486.

[6] Mala, A., Singh, A., Banerji, P. K. (2018). Wavelet transform of L c, d-space. Integral Transforms and Special Functions, 29(6), 431-441.

[7] Mikusiński, P. (1983). Convergence of Boehmains. *Japanese Journal of Mathematics*, **9**(1), 159-179.

[8] Pathak RS, Singh Abhishek (2016) Mexican hat Wavelet Transform of Distributions. Integral Transforms Special Functions, 27(6):468-483

[9] Pathak, R. S., and Singh, A. (2016). Distributional Wavelet Transform. *Proceedings of the National Academy of Sciences, India Section A: Physical Sciences*, **86**(2), 273-277.

[10] Pathak, R. S., Singh, A. (2016). Wavelet transform of Generalized functions in $K'\{M_p\}$ spaces. *Proceedings Mathematical Sciences*, **126**(2), 213-226.

[11] Pathak, R. S., Singh, A. (2017) Wavelet transform of Beurling-Bjrck type ultradistributions. *Rendiconti del Seminario Matematico della Universita di Padova*, **137**(1), 211-222.

[12] Pathak, R. S., Singh, A. (2019) PaleyWienerSchwartz type theorem for the wavelet transform. *Applicable Analysis*, **98**(7), 1324-1332.

[13] Rawat, A., Singh, A. (2021). Mexican hat wavelet transform of generalized functions in $\mathcal{G}'$ spaces. Proceedings-Mathematical Sciences, 131(2), 1-13.

[14] Roopkumar, R. (2003). Wavelet Analysis on a Boehmian Space. *International Journal of Mathematics and Mathematical Sciences*, **15**, 917-926.

[15] Roopkumar, R. (2009). Convolution Theorems for Wavelet Transform on Tempered Distributions and their extension to Tempered Boehmians. *Asian-European Journal of Mathematics*, **2**(1), 117-127.

[16] Singh, A. (2015). On the Exchange Property for the Hartley Transform. *Italian J. Pure Appl. Math*, **35**, 373-380.

[17] Singh, A., Mala, A. (2019). The continuous wavelet transform on ultradistribution spaces. In Colloquium Mathematicum (Vol. 157, pp. 189-201). Instytut Matematyczny Polskiej Akademii Nauk.

[18] Singh, A., Raghuthaman, N., Rawat, A., Singh, J. (2020). Representation theorems for the Mexican hat wavelet transform. Mathematical Methods in the Applied Sciences, 43(7), 3914-3924.

[19] Singh, A. (2020). Distributional Mexican hat wavelet transform. The Journal of Analysis, 28(2), 533-544.

[20] Singh, A., Raghuthaman, N., Rawat, A. (2021). PaleyWienerSchwartz Type Theorem for Ultradistributional Wavelet Transform. Complex Analysis and Operator Theory, 15(4), 1-11.

[21] Singh, A. (2021). Some Characterizations of Wavelet Transform. National Academy Science Letters, 44(2), 143-145.

[22] Singh, A., Rawat, A., Dhawan, S. (2022). On the exchange property for the wavelet transform. The Journal of Analysis, 1-9.

[23] Singh, A., Rawat, A., Singh, S., Banerji, P. K. (2022). On the wavelet transform for boehmians. Proceedings of the National Academy of Sciences, India Section A: Physical Sciences, 92(3), 331-336.

[24] Srivastava, H. M., Singh, A., Rawat, A., Singh, S. (2021). A family of Mexican hat wavelet transforms associated with an isometry in the heat equation. Mathematical Methods in the Applied Sciences, 44(14), 11340-11349.

Maxwell Cattaneo double diffusive convection (DDC) in a viscoelastic fluid layer

Monal Bharty[1], Atul. K. Srivastava[2], Hrisikesh Mahato[3]
Department of Mathematics, School of Natural Sciences,
Central University of Jharkhand,
Ranchi−825305, India
Emails: priyabharty58@gmail.com[1], atulshaswat@gmail.com[2]
hrishikesh.mahato@cuj.ac.in[3]

December 28, 2022

Abstract

The onset of Maxwell-Cattaneo DDC in a viscoelastic fluid layer is studied using linear stability analysis with the help of normal mode technique. The parabolic advection diffusion equation, which presupposes classical fickian diffusion for both heat and salt, controls the evaluation of temperature and salinity. Analytically, the onset criteria for stationary and oscillatory convection is derived. Since the onset of stationary (steady case) convection is unaffected by Maxwell-Cattaneo effects as well as visco-elastic parameters, oscillatory convection rather than stationary convection is the key to visualize the effects of different parameters in this paper. Two different scenarios for oscillatory convection have been discussed (i) when Maxwell-Cattaneo coefficient for salinity $C_S = 0$ and (ii) when Maxwell-Cattaneo coefficient for temperature $C_T = 0$. Also a comparative study for these two cases i.e. $C_S = 0$ and $C_T = 0$ is performed for different controlling parameters like relaxation parameter (λ_1), retardation parameter (λ_2), diffusion ratio (τ), solutal Rayleigh number (Ra_S) and Prandtl number (Pr) with the help of graphs.

Keywords

DDC, Maxwell-Cattaneo Effect (M-C Effect), Viscoelastic binary fluid, Rayleigh number, Thermal Convection.

1 Introduction

The viscoelastic fluid flow is of significant importance in many fields of science, engineering, and technology, including geophysics, bioengineering, and the processing of materials in the nuclear, chemical, and petroleum sectors [15][4]. Unique patterns of instabilities, such as overstability, which cannot be predicted or seen in Newtonian fluid, are present in viscoelastic fluids. For almost 40 years [5], the literature has explored the nature of convective motions in a thin horizontal layer of viscoelastic fluid heated from below in the context of the classical Rayleigh-Benard convection geometry. The key papers by Vest and Arpaci [5] provided the first thorough study of the linear stability of a layer of an upper-convected Maxwell fluid, in which stress exhibits an elastic response to strain typified by a single viscous relaxation period. Due to the high viscosity of the polymeric fluids, flow instability and turbulence are much less common than in Newtonian fluids. For a very long time, it has been widely accepted that in realistic experimental conditions, oscillatory convection cannot occur in viscoelastic fluids .However, recent studies on the elastic behaviour of single long DNA strands in buffer solutions have revealed how to make a fluid in which oscillatory viscoelastic convection might be observed. Recently, this notion was confirmed by Kolodner [21], who found oscillatory convection in DNA suspensions in annular geometry. Theoretically, these studies reignite interest in heat convection in viscoelastic fluids.

Sushila et. al. [25] studied a hybrid analytical algorithm for the thin film flow problem that arises in non-Newtonian fluid. They looked at the thin film flow of a third-grade fluid down an inclined plane in their paper. For the local fractional transport equation that occurs in fractal porous media, in [14], a an effective computational technique is presented. Mehta et. al. [22] investigated heat generation/absorption and the effect of joule heating on radiating MHD mixed convection stagnation point flow along vertical stretched sheet embedded in a permeable medium. The use of an unique fractional derivative in the analysis of heat and mass transfer for the slipping flow of viscous fluid with SWCNT's subject to Newtonian heating is explored by [17]. Whereas heat and mass transfer fractional second grade fluid with slippage and ramped wall temperature using Caputo-Fabrizio fractional derivative approach is investigated by [24].

Due to a variety of real-world situations where the Fourier law of heat flux is insufficient, the dynamics of Maxwell-Cattaneo (or non-fourier) fluids have drawn interest. In his investigation of the theory of gases, Maxwell argued that the relationship between heat flow and temperature gradient not only contain a finite relaxation time but also not be instantaneous. In the case of solid, Cattaneo [3] established a comparable relation, which Oldroyd [11] developed further. Later additions were important, such as those by Fox [20] and Carrassi, Morro[18]. The classical Fourier law of heat conduction expresses the heat flux within a medium is proportional to the local temperature gradient in the system. i.e.

$$V_T = -K\nabla T \tag{1}$$

In which V_T is heat flux, T is temperature and K the thermal conductivity. A well consequence of this law is that the heat purturbation propagate with a infinite velocity. To eliminate this unphysical feature, Maxwell-Cattaneo law is one of the various modifications fourier law and takes the form:

$$\tau_T \frac{DV_T}{Dt} = -V_T - K\nabla T \tag{2}$$

Where the relaxation time is τ_T and the thermal conductivity is K. The derivative $\frac{D}{Dt}$ here represents the time derivative following the motion so that:

$$\frac{DV_T}{Dt} = \left(\frac{\partial}{\partial t} + V.\nabla\right) V_T \tag{3}$$

Where t is time and V is velocity. When a finite speed heatwave [6],[1],[2] is solved by the inclusion of finite relaxation periods, the parabolic heat equation of Fourier fluids, in which heat diffuses at infinite speed, is transformed into a hyperbolic heat equation. The significance of the thermal relaxation term is typically expressed by the dimensionless Maxwell-Cattaneo coefficient C_T, which is the ratio of the thermal relaxation time to twice the thermal diffusion time.

$$C_T = \frac{\tau_T K}{2\rho C_P d^2} = \frac{\tau_T \kappa}{2d^2} = \frac{\left(\frac{\tau_T}{2}\right)}{\tau_\kappa} \tag{4}$$

where thermal diffusion time is $\tau_\kappa (= \frac{d^2}{\kappa})$, density is ρ, specific heat at constant pressure is C_P, length is d and thermal diffusivity is κ. Thus the classical Fourier law has $C_T = 0$.

Numerous physical scenarios have been investigated when it comes to the Maxwell-Cattaneo heat transport effect, including nano-fluid and nano-material [7], biological tissue [26] and stellar interiors [16] in the context of DDC. Many factors, including the coefficient definition, affect the Maxwell-Cattaneo effect's potential importance. Eltayeb [9] discussed convection instabilities of Maxwell-Cattaneo fluids. In his study, he used three distinct forms of the time derivative of the heat flux to explore the linear and weakly nonlinear stabilities of a horizontal layer of fluid obeying the Maxwell-Cattaneo relationship of heat flux and temperature. While Eltayeb, Hughes, and Proctor [10] have examined the convection instability of a Maxwell-Cattaneo fluid in the presence of a vertical magnetic field and have discussed about the instability of a Benard layer under a vertical uniform magnetic field. The DDC of Maxwell-Cattaneo fluid has been studied by Hughes, Proctor and Eltayeb [8]. The consequences of include the Maxwell-Cattaneo (M-C) effects on the commencement of DDC, in which two factors alter the density of a fluid but diffuse at separate rates, were investigated in that study. For both temperature and salinity they considered Maxwell-Cattaneo effect. The modified salinity evolution equation is expressed as:

$$\tau_{\mathscr{C}} \frac{DV_{\mathscr{C}}}{Dt} = -V_{\mathscr{C}} - \kappa_{\mathscr{C}} \nabla \mathscr{C} \tag{5}$$

by analogy with temperature equation when M-C effect is included. where $\mathscr{C}$

is salt concentration, κ is salinity diffusivity, $\tau_{\mathscr{C}}$ the relaxation time for salinity and $V_{\mathscr{C}}$ is salt flux. Most of the above discussed work is related with the Newtonian fluid.

The onset of DDC in viscoelastic fluid (non-Newtonian fluid)layer is investigated by Malashetty and Swamy [19]. They analysed the stability of a binary viscoelastic fluid layer using linear and weakly nonlinear methods in that study. In view of importance viscoelastic fluid as discussed above, in this paper we carry out a linear stability analysis for a Maxwell-Cattaneo DDC in a viscoelastic fluid layer. Here, we focus on the scenario in which the M-C coefficients are extremely small, driven by geophysical and astrophysical concerns. Therefore, even when $C_T, C_S << 1$, new mechanisms for oscillatory instability might develop, given that the initial gradients of temperature and salinity are relatively significant. This is because the modified equations now describe singular perturbations in the time domain.

The work is presented in the following way. The physical problem is discussed in sect. 2 with a brief mathematical formulation. In sect. 3, the linear stability analysis in oscillatory convection for two cases i.e ($C_T = 0$ and $C_S = 0$) for the free-free boundaries is covered. The results and discussion are included in sect. 4, where we described results shown with the help of graph drawn for different parameters by fixing the values of all other parameters and discussed whether these parameters stabilise or destabilise the system. Last but not least, sect. 5 brings to a close a few key aspects of the analysis.

2 Mathematical model

2.1 The physical domain

We consider DDC in a horizontal layer of an incompressible binary viscoelastic Maxwell-Cattaneo fluid confined between two parallel horizontal planes at $z = 0$ and $z =$ d, a distance d apart with the vertically downward gravity g acting on it. Origin is set in the lower boundary of a Cartesian frame of reference, horizontal component x and vertical component z increases upwards. The surfaces are stretched indefinitely in both x and y directions while maintaining a consistent temperature gradient ΔT across the porous layer. To account for the impact of density fluctuations, we presum that the Oberbeck-Boussinesq approximation is used.

2.2 Governing equations

The momentum equation is modelled using the viscoelastic fluid of the Oldroyd type. The basic governing equations are

$$\left(1+\lambda_1\frac{\partial}{\partial t}\right)\left[\rho_0\left(\frac{\partial V}{\partial t}+V.\nabla V\right)+\nabla p-\rho g\right]=\mu\left(1+\lambda_2\frac{\partial}{\partial t}\right)\nabla^2 V \tag{6}$$

$$\left(\frac{\partial T}{\partial t}+(V.\nabla)T\right)=-\nabla.V_T \tag{7}$$

$$\tau_T\left(\frac{\partial U_T}{\partial t}+\nabla.(VU_T)\right)=-U_T-K\nabla^2T \tag{8}$$

$$\left(\frac{\partial \mathscr{C}}{\partial t}+(V.\nabla)\mathscr{C}\right)=-\nabla.V_{\mathscr{C}} \tag{9}$$

$$\tau_{\mathscr{C}}\left(\frac{\partial U_{\mathscr{C}}}{\partial t}+\nabla.(VU_{\mathscr{C}})\right)=-U_{\mathscr{C}}-K_{\mathscr{C}}\nabla^2\mathscr{C} \tag{10}$$

$$\nabla.V=0 \tag{11}$$

where $U_T=\nabla.V_T$, $U_{\mathscr{C}}=\nabla.V_{\mathscr{C}}$, $V=(u,v,w)$ is velocity, μ is viscosity, λ_1 is relaxation parameter, λ_2 is retardation parameter, ρ is density, K is thermal conductivity, $K_{\mathscr{C}}$ is salt conductivity, V_T is heat flux and $V_{\mathscr{C}}$ is salt flux. The formula for the relationship between reference density, temperature, and salinity is:-

$$\rho=\rho_0\left[1-\beta_T(T-T_0)+\beta_{\mathscr{C}}(\mathscr{C}-\mathscr{C}_0)\right] \tag{12}$$

Temperature and salinity's appropriate boundary conditions are:-

$$T=T_0+\Delta T \text{ at } z=0 \text{ and } T=T_0 \text{ at } z=d \tag{13}$$

$$\mathscr{C}=\mathscr{C}_0+\Delta\mathscr{C} \text{ at } z=0 \text{ and } \mathscr{C}=\mathscr{C}_0 \text{ at } z=d \tag{14}$$

2.3 Initial state

It is considered that the fluid is in a quiescent initial state, which is represented by

$$\begin{aligned} V_b=(0,0,0)\,,P=P_b(z),T=T_b(z),\mathscr{C}=\mathscr{C}_b(z),\rho=\rho_b(z),\\ V_{T_b}=(0,0,V_T(z))\,,V_{\mathscr{C}_b}=(0,0,V_{\mathscr{C}}(z)) \end{aligned} \tag{15}$$

Using (2.3) in Eqs. (6) – (12) yield

$$\frac{dp_b}{dz}=-\rho_b g,\frac{d^2T_b}{dz^2}=0,\frac{d^2\mathscr{C}_b}{dz^2}=0 \tag{16}$$

The initial state solution for temperature and salinity fields are given by:-

$$T_b(z)=T_l-\Delta T\frac{z}{d},\mathscr{C}_b(z)=\mathscr{C}_l-\Delta\mathscr{C}\frac{z}{d} \tag{17}$$

2.4 Perturbed state

On the initial state, we superimpose a disturbance of the type:-

$$\begin{aligned} V = V_b(z) + V'(x,y.z,t), T = T_b(z) + T'(x,y,z.t), \mathscr{C} = \mathscr{C}_b(z) + \mathscr{C}'(x,y,z,t),\\ P = P_b(z) + P'(x,y,z,t), \rho = \rho_b(z) + \rho'(x,y,z,t), V_T = V_{T_b} + V_T'(x,y,z,t),\\ V_{\mathscr{C}} = V_{\mathscr{C}_b} + V_{\mathscr{C}}'(x,y,z,t) \end{aligned} \tag{18}$$

where perturbations are indicated by primes. Introducing (18) in Eqs. (6) − (11), and using basic state from Eq. (16), The resulting equations are then non-dimensionalized using the following transformations

$$(x,y,z) = d(x^*,y^*,z^*), t = \frac{d^2}{\kappa_{Tz}}t^*, \lambda_1 = \frac{\kappa_{Tz}}{d^2}\lambda_1*, (V') = \frac{\kappa_{Tz}}{d}(V^*), P' = \frac{\mu\kappa_{Tz}}{K_z}P^*,$$

$$\lambda_2 = \frac{\kappa_{Tz}}{d^2}\lambda_2*, V_T = \Delta T\frac{K}{d}V_T^*, V_{\mathscr{C}} = \Delta T\frac{\kappa}{d}V_{\mathscr{C}}^*, T^{'} = (\Delta T)\,T^*, \mathscr{C}^{'} = (\Delta\mathscr{C})\,\mathscr{C}^* \tag{19}$$

After eliminating the asterisks for simplicity, we arrived at the non-dimensional, linear governing equations, which are

$$\left(1+\lambda_1\frac{\partial}{\partial t}\right)\left[\frac{1}{Pr}\frac{\partial}{\partial t}\nabla^2 V - Ra_T\nabla_1^2 T + Ra_S\nabla_1^2\mathscr{C}\right] - \left(1+\lambda_2\frac{\partial}{\partial t}\right)\nabla^4 V = 0 \tag{20}$$

$$\frac{\partial T}{\partial t} = w - U_T \tag{21}$$

$$2C_T\frac{\partial U_T}{\partial t} = -U_T - \nabla^2 T \tag{22}$$

$$\frac{\partial \mathscr{C}}{\partial t} = w - U_{\mathscr{C}} \tag{23}$$

$$2C_S\frac{\partial U_{\mathscr{C}}}{\partial t} = -U_{\mathscr{C}} - \tau\nabla^2\mathscr{C} \tag{24}$$

where the Prandtl number Pr, thermal Rayleigh number Ra_T, solutal Rayleigh number Ra_S, Diffusivity ratio τ, Maxwell-Cattaneo coefficient for temperature C_T and Maxwell-Cattaneo coefficient for salinity $C_{\mathscr{C}}$ are defined as: $Pr = \frac{\nu}{\kappa_{T_Z}}$, $Ra_T = \frac{\beta_T g\Delta T dK_Z\nu}{\kappa_{T_Z}}$, $Ra_S = \frac{\beta_S g\Delta\mathscr{C} dK_Z\nu}{\kappa_{T_Z}}$, $\tau = \frac{\kappa_{\mathscr{C}}}{\kappa}$, $C_T = \frac{\tau_T\kappa}{2d^2}$, $C_S = \frac{\tau_{\mathscr{C}}\kappa_{\mathscr{C}}}{2d^2}$, and u, v and w are x, y and z component of velocity respectively.
The boundaries are assumed to be impermeable, isothermal and stress free, therefore we have the following conditions

$$w = \frac{\partial^2 w}{\partial z^2} = T = \mathscr{C} = 0 \text{ at } z = 0, 1. \tag{25}$$

3 Linear Stability Analysis

In this part, we employ linear theory to forecast the thresholds of both marginal and oscillatory convections. Assuming that the amplitudes are small enough, the time-dependent periodic disturbances in a horizontal plane are used to solve the eigenvalue problem specified by Eqs. (20)–(24) subject to the boundary conditions (20) is solved as follows:

$$\begin{pmatrix} w \\ T \\ \mathscr{C} \\ U_T \\ U_{\mathscr{C}} \end{pmatrix} = \begin{pmatrix} W(z) \\ \Theta(z) \\ \Phi(z) \\ \zeta(Z) \\ \gamma(Z) \end{pmatrix} e^{i(lx+my)+\sigma t} \tag{26}$$

where the growth rate is represented by the complex quantity σ and the horizontal wave numbers l and m. W, Θ, Φ, ζ and γ are the amplitudes of stream function, temperature field, solute field, heat flux and solute flux respectively.

$$\begin{aligned}\left[(1+\lambda_1\sigma)\left(\frac{\sigma}{Pr}(D^2-a^2)\right)+(1+\lambda_2\sigma)(D^2-a^2)^2\right]W+(1+\lambda_1\sigma)Ra_Ta^2\Theta \\ -(1+\lambda_1\sigma)Ra_Sa^2\Phi=0\end{aligned} \tag{27}$$

$$-W+\sigma\Theta+\zeta=0 \tag{28}$$

$$(D^2-a^2)\Theta+(2C_T\sigma+1)\zeta=0 \tag{29}$$

$$-W+\sigma\Phi+\gamma=0 \tag{30}$$

$$\tau(D^2-a^2)\Phi+(2C_S\sigma+1)\gamma=0 \tag{31}$$

where $D=\frac{d}{dz}$ and $a^2=l^2+m^2$. on the free boundary. we take the solution of Eqn. (27)-(31) satisfying the boundary condition for free-free case:

$$[W(z),\Theta(z),\Phi(z),\zeta(z),\gamma(z)]=[W_0,\Theta_0,\Phi_0,\zeta_0,\gamma_0]\sin(n\pi z),(n=1,2,3,...) \tag{32}$$

Substituting Eq. (32) into (27)-(31), and considering $n=1$, we get a matrix equation

$$\begin{bmatrix} M_1 & -a^2Ra_T & a^2Ra_S & 0 & 0 \\ -1 & \sigma & 0 & 1 & 0 \\ 0 & -\alpha & 0 & 2C_T\sigma+1 & 0 \\ -1 & 0 & \sigma & 0 & 1 \\ 0 & 0 & -\tau\alpha & 0 & 2C_S\sigma+1 \end{bmatrix}\begin{bmatrix} W_0 \\ \Theta_0 \\ \Phi_0 \\ \zeta_0 \\ \gamma_0 \end{bmatrix}=\begin{bmatrix} 0 \\ 0 \\ 0 \\ 0 \\ 0 \end{bmatrix} \tag{33}$$

where $\alpha=a^2+\pi^2$, $M_1=\left[\frac{-\sigma}{Pr}+\frac{(1+\lambda_2\sigma)\alpha}{(1+\lambda_1\sigma)}\right]\alpha$.

For non-trivial solution of W, Θ, Φ, ζ and γ, we need to make the determinant of the above matrix as zero, we get

$$Ra_T=\left(\sigma+\frac{\alpha}{(2C_T\sigma+1)}\right)\left[\frac{M_1}{a^2}-\frac{Ra_S(2C_S\sigma+1)}{\sigma(2C_S\sigma+1)+\tau\alpha}\right] \tag{34}$$

3.1 Stationary state

We have $\sigma = 0$ at the stability margin for the direct bifurcation, or stable onset. The Rayleigh number at which a marginally stable steady mode occurs therefore becomes

$$Ra_T^{st} = \frac{\alpha^3}{a^2} - \frac{Ra_S}{\tau} \tag{35}$$

We obtained the result which is comparable to that of Turner [13]. This result also indicate that stationary Rayleigh number is independent of the viscoelastic parameters and Maxwell-Cattaneo coefficients. The stationary Rayleigh number Ra_T^{st} given by Eq. (35) attains the critical value

$$Ra_{T,C}^{st} = \frac{27}{4}\pi^4 - \frac{Ra_S}{\tau} \tag{36}$$

for the wave number $a_c = \frac{\pi}{\sqrt{2}}$.
When $Ra_S = 0$, Eq. (36) gives

$$Ra_{T,C}^{st} = \frac{27}{4}\pi^4 \tag{37}$$

which is classical outcome of Newtonian fluid layer mentioned in the book of Chandrashekhar [23].

3.2 Oscillatory motion

In general, σ, the growth rate, is a complex quantity with the formula $\sigma = \sigma_r + i\omega$. While the system will become unstable for $\sigma_r > 0$, it is always stable for $\sigma_r < 0$. $\sigma_r = 0$ for the neutral stability state.

1. The case of C_S=0

we put C_S=0 in Eq. (34), and get

$$Ra_T = \left(\sigma + \frac{\alpha}{2C_T\sigma + 1}\right)\left[\left(\frac{-\sigma\alpha}{Pra^2} + \frac{(1+\lambda_2\sigma)\alpha^2}{(1+\lambda_1\sigma)a^2}\right) - \frac{Ra_S}{\sigma + \tau\alpha}\right] \tag{38}$$

then put $\sigma = i\omega(\omega$ is real) in Eq. (38) and get

$$Ra_T = \Pi_1 + (i\omega)\,\Pi_2 \tag{39}$$

The expression for Π_1 is given by

$$\Pi_1 = D_1 - D_2 - D_3 + D_4 - D_5$$

The fact that Ra_T is a physical quantity proves that it is real. Hence, from Eq. (39) it follows that either $\omega = 0$ (steady onset) or $\Pi_2 = 0$ ($\omega \neq 0$, oscillatory onset). For oscillatory onset $\Pi_2 = 0(\omega \neq 0)$ and this provides a dispersion relation of the form

$$B_1\left(\omega^2\right)^3 + B_2\left(\omega^2\right)^2 + B_3\left(\omega^2\right) + B_4 = 0 \tag{40}$$

where the constants $B_1 = Q_1, B_2 = Q_1Q_7 + Q_2 - Q_3Q_5 - Q_3Q_8, B_3 = Q_2Q_7 - Q_4Q_5 - Q_3Q_6 - Q_3Q_7Q_8 - Q_4Q_8 + Q_9 + Q_3Q_{10}, B_4 = -Q_4Q_6 - Q_4Q_7Q_8 + Q_7Q_9 + Q_4Q_{10}$

Now Eq. (39) with $\Pi_2 = 0$, gives oscillatory Rayleigh number Ra_T^{osc} at the margin of stability as

$$Ra_T^{osc} = \Pi_1. \tag{41}$$

Also, to cause the oscillatory convection, ω^2 must be positive. The symbols $D_1, D_2, D_3, D_4, D_5, Q_1, Q_2, Q_3, Q_4, Q_5, Q_6, Q_7, Q_8, Q_9, Q_{10}, Q_{11}, Q_{12}, Q_{13}, Q_{14}, Q_{15}, Q_{16}$ and Π_2 are defined in Appendix-I

2. **The case of C_T=0**

we put C_T=0 in Eq. (34), and get

$$Ra_T = (\sigma + \alpha)\left[\left(\frac{-\sigma\alpha}{Pra^2} + \frac{(1+\lambda_2\sigma)\alpha^2}{1+\lambda_1\sigma)a^2}\right) - \frac{Ra_S(2C_S\sigma + 1)}{(\sigma(2C_S\sigma + 1) + \tau\alpha)}\right] \tag{42}$$

then put $\sigma = i\omega(\omega$ is real) in Eq. (42) and get

$$Ra_T = \Pi_1' + (i\omega)\,\Pi_2' \tag{43}$$

The expression for Π_1' is given by

$$\Pi_1' = F_1 - F_2 + F_3 + F_4 - F_5$$

For oscillatory onset $\Pi_2' = 0$ $(\omega \neq 0)$ and this provides a dispersion relation of the form

$$C_1\left(\omega^2\right)^3 + C_2\left(\omega^2\right)^2 + C_3\left(\omega^2\right) + C_4 = 0 \tag{44}$$

where the constants $C_1 = P_1P_6^2 - P_2P_6^2P_7$, $C_2 = P_1 + 2P_2P_5P_6P_7 - P_2P_7 - P_3P_6^2P_7 + P_6^2P_8 + P_2P_6P_9$, $C_3 = P_1P_5^5 - 2P_1P_5P_6 - P_2P_4 - P_2P_5^2P_7 + 2P_3P_5P_6P_7 - P_3P_7 - 2P_5P_6P_8 + P_8 - P_2P_5P_9 + P_3P_6P_9 + P_2P_9$, $C_4 = -P_3P_4 - P_3P_5^2P_7 + P_5^2P_8 - P_3P_5P_9 + P_3P_9$

Now Eq. (43) with $\Pi_2' = 0$, gives oscillatory Rayleigh number Ra_T^{osc} at the margin of stability as

$$Ra_T^{osc} = \Pi_1'. \tag{45}$$

Also, to cause the oscillatory convection, ω^2 must be positive. The symbols $F_1, F_2, F_3, F_4, F_5, P_1, P_2, P_3, P_4, P_5, P_6, P_7, P_8, P_9, P_{10}, P_{11}, P_{12}, P_{13}, P_{14}$ and Π_2' are defined in Appendix-I

4 Result and discussion

In this paper, Linear stability has been investigated in the presence of Maxwell-Cattaneo DDC for viscoelastic fluid. The onset of instability is examined for various controlling parameters such as Prandtl number (Pr), diffusivity ratio (τ), relaxation parameter(λ_1), retardation parameter (λ_2), solutal Rayleigh number (Ra_S), Maxwell-Cattaneo coefficient for temperature (C_T) and Maxwell-Cattaneo coefficient for salinity (C_S). In most physical contexts, the Maxwell-Cattaneo effect is so negligible that we have concentrated on the case where C is smaller than 1, where C is used in the discussion to signify either C_T or C_S. Because C is so small, the Maxwell-Cattaneo effect only manifests itself for concomitantly strong heat and salinity gradients.

In the (a, Ra_T) plane, Fig. 1(a)-(f) illustrate the neutral curves of oscillatory convection for C_S, λ_1, λ_2, τ, Pr and Ra_S when $C_T = 0$ while Fig 1(a')-(f') illustrate the neutral curves when $C_S = 0$ for C_T, λ_1, λ_2, τ, Pr and Ra_S. Fig. 1(a) illustrates how C_S affects the system's stability whereas the impact of C_T is depicted in Fig. 1(a'). With a rise in C_S, the minimum Rayleigh number increases, but with a rise in C_T, the minimum Rayleigh number decreases. So, clearly it is shown that C_S has stabilizing while C_T has destabilizing effect on the stability of the system.

Fig. 1(b) and Fig. 1(b') show the influence of relaxation parameter λ_1 on the stability of the system for $C_T = 0$ and $C_S = 0$ respectively. We can see that raising λ_1 causes the lowest value of the Rayleigh number, Ra_T, is decreases, indicating that λ_1 has a destabilising influence on the Maxwell-Cattaneo DDC in viscoelastic fluid for both situations, where ($C_T = 0$ and $C_S = 0$). Also, it is shown graphically that for different values of λ_1 the case $C_S = 0$ is more stable as compare to $C_T = 0$. Fig. 1(c) and Fig. 1(c') demonstrate that when the value of λ_2 grows, the lowest Rayleigh number similarly rises, stabilising the system. For different values of λ_2, $C_S = 0$ case is more stable. Viscoelastic parameter behaviour is clear and consistent with what [12] said.

The influence of diffusion ratio τ on the system's stability is depicted in Fig 1(d) for $C_T = 0$ and in Fig 1(d') for $C_S = 0$. It is shown the minimum of critical Rayleigh number rises with rise in the value of (τ). It occurs because $\tau = \frac{\kappa_{\mathscr{C}}}{\kappa}$ has an inverse relationship to thermal diffusivity κ. Therefore, when the diffusivity ratio τ increases, the value of thermal diffusivity falls, implying an increase in the Rayleigh number. Also, for different values of τ, $C_S = 0$ is more stable.

Fig 1(e) and Fig 1 (e') show graphs for various values of Prandtl number Pr when $C_T = 0$ and $C_S = 0$ respectively. For the case $C_T = 0$, the system becomes stabilised as a result of the minimum of Ra_T value increasing together with the value of Prandtl number Pr. The fact that Pr is inversely proportional to thermal diffusivity explains it. It has been demonstrated that as the value of Pr increases, the minimum Rayleigh number drops and the system becomes unstable as a result for $C_S = 0$.

The graphs for various Ra_S values on the (a, Ra_T) plane for $C_T = 0$ and $C_S = 0$ are shown in Fig 1(f) and Fig 1(f') respectively. So, for $C_T = 0$, as Ra_S values rise, the minimum of Rayleigh number rises as well, which causes the system to stabilise. It has been seen that the system becomes unstable when the value of Ra_S rises because the minimum Rayleigh number decreases for $C_S = 0$.

5 Conclusion

We have attempted to understand the onset of Maxwell-Cattaneo DDC in a binary viscoelastic fluid layer. With the use of the normal mode technique, linear stability analysis for stationary and oscillatory convection is carried out in this study. Because the Maxwell-Cattaneo coefficients have no effect on stationary states, we have generated graphs for oscillatory convection rather than stationary convection.
The conclusions are as follows.

1. The onset of oscillatory convection is found to be delayed by C_S, λ_2, τ, Pr, and Ra_S, whereas the onset of oscillatory convection is found to be advanced by increasing the value of λ_1, which decreases the value of Rayleigh number corresponding to oscillaory convection in the case of $C_T = 0$.

2. λ_2, τ are found to delay the onset of oscillatory convection whereas on increasing the value of C_T, λ_1, Pr and Ra_S the value of Rayleigh number corresponding to oscillaory convection decreases, thus it advances the onset of convection for the case $C_S = 0$.

According to Maxwell-Cattaneo law, there is currently relatively limited study being done on thermal instability. The Maxwell-Cattaneo law for heat flux and temperature relation with various external effects, such as Electrohydrodynamics, radiation, rotation, etc., can therefore be applied to diverse types of fluids in the future.

Appendix-I

$D_1 = \omega^2 Q_8 \left(1 - \frac{Q_{11}}{Q_{16}\omega^2+1}\right)$, $D_2 = \frac{\omega^2 Q_{12}}{Q_3\omega^2+Q_4}\left(1 - \frac{Q_{11}}{Q_{16}\omega^2+1}\right)$, $D_3 = \frac{\omega^2 Q_{13}}{Q_7+\omega^2}\left(1 - \frac{Q_{11}}{Q_{16}\omega^2+1}\right)$, $D_4 = \frac{\omega^2 Q_{14}}{(Q_3\omega^2+Q_4)(Q_{16}\omega^2+1)}$, $D_5 = \frac{Q_5}{(Q_7+\omega^2)(Q_{16}\omega^2+1)}$, $Q_1 = 4C_T^2\alpha^2\lambda_1\lambda_2$, $Q_2 = \lambda_1\lambda_2\alpha^2 - 2C_T\lambda_1\lambda_2\alpha^2$, $Q_3 = \lambda_1^2 a^2$, $Q_4 = a^2$, $Q_5 = 4Ra_S C_T^2\tau\alpha$, $Q_6 = Ra_S\tau\alpha - 2C_T Ra_S\tau\alpha$, $Q_7 = \tau^2\alpha^2$, $Q_8 = \frac{\alpha}{Pra^2}$, $Q_9 = \alpha^3(\lambda_2-\lambda_1)$ $Q_{10} = \alpha Ra_S$, $Q_{11} = 2C_T$, $Q_{12} = (\lambda_2 - \lambda_1)\alpha^2$, $Q_{13} = Ra_S$, $Q_{14} = \alpha^3\lambda_1\lambda_2$, $Q_{15} = Ra_S\tau\alpha^2$, $Q_{16} = 4C_T^2$, $\Pi_2 = \frac{(Q_1\omega^4+Q_2\omega^2)}{(Q_3\omega^2+Q_4)} - \frac{(Q_5\omega^2+Q_6)}{Q_7+\omega^2} - Q_8 + \frac{Q_9}{(Q_3\omega^2+Q_4)} + \frac{Q_{10}}{(Q_7+\Omega^2)}$, $F_1 = \omega^2 P_{10}$, $F_2 = \frac{P_{11}\omega^2}{P_2\omega^2+P_3}$, $F_3 = \frac{\omega^2 Q_{13}((Q_5-Q_6\omega^2)-1)}{(Q_5-Q_6\omega^2)^2+\omega^2}$, $F_4 = \frac{\omega^2 Q_{12}}{Q_2\omega^2+Q_3}$, $F_5 = \frac{Q_9+Q_4(Q_5-Q_6\omega^2)}{(Q_5-Q_6\omega^2)^2+\omega^2}$, $P_1 = \alpha^2\lambda_1\lambda_2$, $P_2 = a^2\lambda_1^2$, $P_3 = a^2$, $P_4 = Ra_S\tau\alpha$, $P_5 = \tau\alpha$, $P_6 = 2C_S$, $P_7 = \frac{\alpha^2}{Pra^2}$, $P_8 = (\lambda_2 - \lambda_1)\alpha^3$, $P_9 = 2Ra_S\alpha C_S$, $P_{10} = \frac{\alpha}{a^2 Pr}$, $P_{11} = (\lambda_2 - \lambda_1)\alpha^2$, $P_{12} = \alpha^3\lambda_1\lambda_2$, $P_{13} = 2C_S Ra_S$, $P_{14} = Ra_S\alpha$, $\Pi_2' = \frac{P_1\omega^2}{P_2\omega^2+P_3} - \frac{P_4}{(P_5-P_6\omega^2)^2+\omega^2} - P_7 + \frac{P_8}{P_2\omega^2+P_3} - \frac{P_9((P_5-P_6\omega^2)-1)}{(P_5-P_6\omega^2)^2+\omega^2}$

Acknowledgment

Author, Monal Bharty, sincerely thanks Central University of Jharkhand for providing financial support in the form of a research fellowship. This work is only presented in the 5th International Conference on Mathematical Modelling, Applied Analysis and Computation-2022 (ICMMAAC-22) held in JECRC University, Jaipur (India).

References

[1] B. Straughan, *Heat waves*, New York, NY: Springer, 2011.

[2] B. Straughan, Tipping points in Cattaneo-Christov thermohaline convection, *Proc. R. Soc. A*, 467, 7–18 (2011).

[3] C. Cattaneo, Sulla conduzione del calore, *Atti Mat. Fis. Univ. Modena*, 3, 83–101 (1948).

[4] C.W. Horton, F.T. Rogers, Convection currents in a porous medium. *J. Appl. Phys.*, 16, 367-370 (1945).

[5] C.M. Vest, V.S. Arpaci, Overstability of a viscoelastic fluid layer heated from below, *J.Fluid Mech*, 36, 613-623 (1969).

[6] D.D. Joseph, L.Preziosi, Heat waves, *Rev.Mod. Phys.*, 61, 41–73 (1989).

[7] D. Jou, A. Sellitto, FX. Alvarez, Heat waves and phonon-wall collisions, *nanowires. Proc. R. Soc. A*, 467, 2520–2533 (2011).

[8] D.W. Hughes, M.R.E. Proctor, I.A. Eltayeb, Maxwell–Cattaneo double-diffusive convection:limiting cases, *J. Fluid Mech.*, vol. 927 (2021).

[9] I. A. Eltayeb, Convective instabilities of Maxwell–Cattaneo fluids, *Proc. R. Soc. A*, 473 (2017) https://doi.org/10.1098/rspa.2016.0712

[10] I. A. Eltayeb, D. W. Hughes, M. R. E. Proctor, The convective instability of a Maxwell–Cattaneo fluid in the presence of a vertical magnetic field, *Proc. R. Soc. A*, 476 (2020) https://doi.org/10.1098/rspa.2020.0494

[11] J.G. Oldroyd, On the formulation of rheological equations of state, *Proc. R. Soc. Lond. A*, 200, 523–541 (1950).

[12] J. Kang, Fu, Ceji. Fu, W. Tan, Thermal convective instability of viscoelastic fluids in a rotating porous layer heated from below, *J. Non-Newtonian Fluid Mechanics*, 166, 93-101 (2011).

[13] J.S. Turner, *Buoyancy Effects in Fluids*, Cambridge University Press, London, 1973.

[14] J. Singh, An efficient computational method for local fractional transport equation occurring in fractal porous media, *Comput. Appl. Math*, 39, 137(2020).

[15] J.Zhou, I. Papautsky, Viscoelastic microfluidics: progress and challenges, *Microsyst and Nanoeng*, 6, 1-24 (2020).

[16] L. Herrera, N. Falcón, Heat waves and thermohaline instability in a fluid, *Phys. Lett. A*, 201, 33–37 (1995).

[17] M. Ahmad, M. I. Asjad, J. Singh, Application of novel fractional derivative to heat and mass transfer analysis for the slippage flow of viscous fluid with SWCNT's subject to Newtonian heating, *Math. Methods Appl. Sci*, (2021) https://doi.org/10.1002/mma.7332

[18] M. Carrassi, A. Morro, A modified Navier-Stokes equation, and its consequences on sound dispersion, *Nuovo Cimento B*, 9, 321–343 (1972).

[19] M.S. Malashetty, M. Swamy, The onset of double diffusive convection in a viscoelastic fluid layer, *Int. J. Non Newtonian Fluid Mech.*, vol. 165, 1129-1138 (2010).

[20] N. Fox, Low temperature effects and generalized thermoelasticity, *IMA J. Appl. Maths*, 5, 373–386 (1969).

[21] P. Kolodner, Oscillatory convection in viscoelastic DNA suspensions, *J.Non- Newtonian Fluid Mech*, 75, 167–192 (1998).

[22] R. Mehta, R. Kumar, H. Rathore, J. Singh, Joule heating effect on radiating MHD mixed convection stagnation point flow along vertical stretching sheet embedded in a permeable medium and heat generation/absorption, *Heat Transfer (Wiley)*, 51(8), 7369-7386 (2022).

[23] S. Chandrasekhar, *Hydrodynamic and Hydromagnetic Stability*, Dover, New York, 1981.

[24] S. U. Haq, S. U. Jan, S. I. A. Shah, I. Khan, J. Singh, Heat and mass transfer of fractional second grade fluid with slippage and ramped wall temperature using Caputo-Fabrizio fractional derivative approach, *AIMS Mathematics*, 5(4), 3056-3088 (2020).

[25] Sushila, J. Singh, D. Kumar, D. Baleanu, A hybrid analytical algorithm for thin film flow problem occurring in non-Newtonian fluid mechanics, *Ain Shams Eng. J*, 12(2), 2297-2302 (2021).

[26] W. Dai, H. Wang, PM. Jordan, RE. Mickens, A. Bejan, A mathematical model for skin burn injury induced by radiation heating, *Int. J. Heat Mass Transfer*, 51, 5497–5510 (2008).

Figure 1: Oscillatory neutral stablity curves for different values of: 1(a) Maxwell-Cattaneo coefficient for solute C_S when $C_T = 0$; 1(a') Maxwell-Cattaneo coefficient for temperature C_T when $C_S = 0$.

Figure 2: Oscillatory neutral stability curves for different values of: 1(b) relaxation parameter λ_1 when $C_T = 0$; 1(b') relaxation parameter λ_1 when $C_S = 0$.

Figure 3: Oscillatory neutral stability curves for different values of: 1(c) retardation parameter λ_2 when $C_T = 0$; 1(c') retardation parameter λ_2 when $C_S = 0$.

Figure 4: Oscillatory neutral stability curves for different values of: 1(d) diffusivity ratio τ when $C_T = 0$; 1(d') diffusivity ratio τ when $C_S = 0$.

Figure 5: Oscillatory neutral stability curves for different values of: 1(e) Prandtl number Pr when $C_T = 0$; 1(e') Prandtl number Pr when $C_S = 0$.

Figure 6: Oscillatory neutral stability curves for different values of: 1(f) solutal Rayleigh number Ra_S when $C_T = 0$; 1(f') solutal Rayleigh number Ra_S when $C_S = 0$.

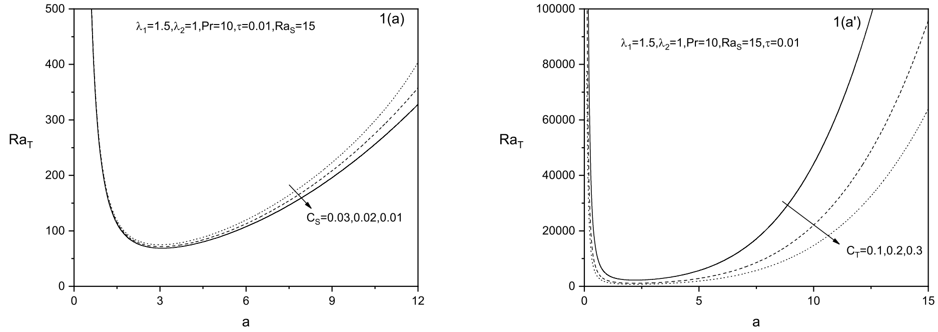

Figure 1

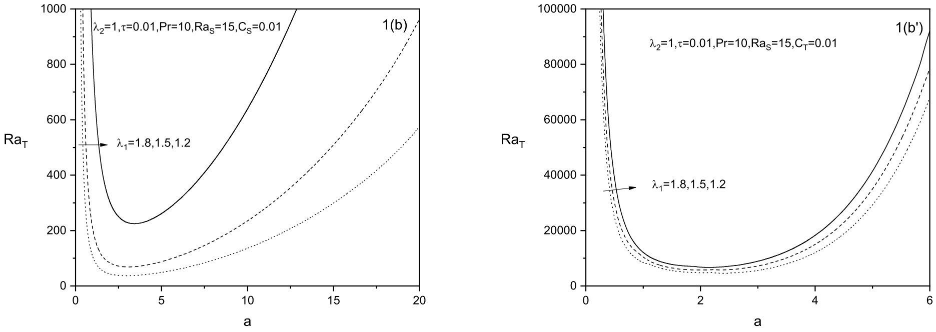

Figure 2

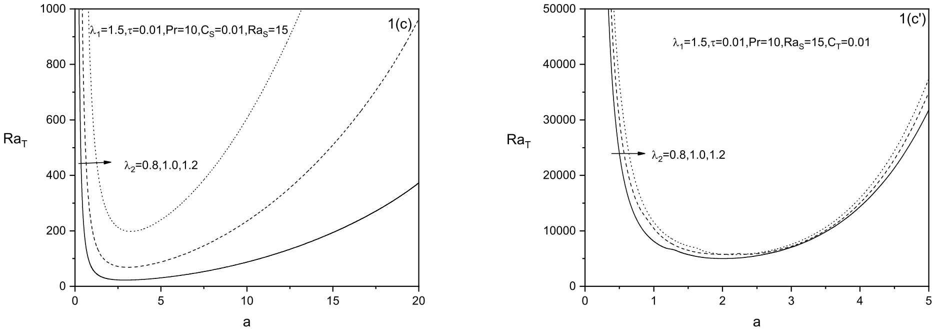

Figure 3

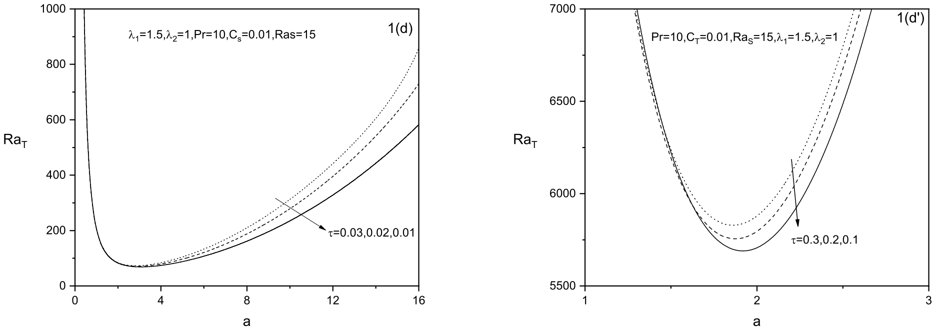

Figure 4

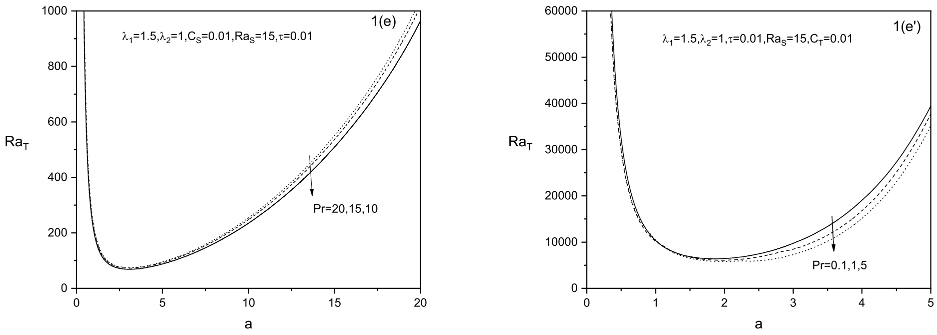

Figure 5

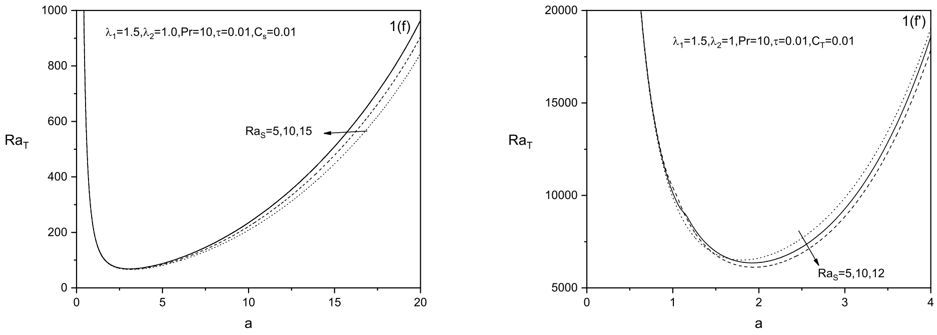

Figure 6

J. COMPUTATIONAL ANALYSIS AND APPLICATIONS, VOL. 31, NO.1, 2023, COPYRIGHT 2023 EUDOXUS PRESS, LLC

Some New Results for the $\mathcal{M}$-Transform Involving the Incomplete H- and $\overline{H}$-Functions

Sanjay Bhatter[1], Sapna Meena[1], Jagdev Singh[2] and
Sunil Dutt Purohit[3,*]
[1]Department of Mathematics, Malaviya National Institute of Technology, Jaipur, India.
sbhatter.maths@mnit.ac.in, sapnabesar1996@gmail.com
[2]Department of Mathematics, JECRC University, Jaipur, India.
jagdevsinghrathore@gmail.com
[3]Department of HEAS (Mathematics), Rajasthan Technical University, Kota, India.
sunil_a_purohit@yahoo.com

Abstract

In this paper, we construct some new image formulas for the incomplete H-and $\overline{H}$-functions under the Akel's $\mathcal{M}$-transform. We also provide image formulas for the incomplete Meijer's G-functions, incomplete Fox-Wright functions and Fox's H-function, as special cases of our main findings in corollaries.

Key Words and Phrases. Incomplete gamma function; $\mathcal{M}$-transform; Incomplete H-functions; Incomplete $\overline{H}$-functions; Mellin-Barnes type contour; Incomplete Fox-Wright generalized hypergeometric functions.
MSC2010. 26A33, 33B20,33C60, 33E20, 44A40 .

1 Introduction and Preliminaries

Integral transforms have been useful in solving numerous differential and integral problems for many years. It is possible to convert differential and integral operators from one domain under consideration into multiplication operators in another domain by using the right integral transform.

The Laplace transform, the Fourier integral transform, the Mellin transform are the classical integral transforms used to solve differential equations, integral equations, and in analysis and the theory of functions. For further information, see the research papers [5, 10, 12, 13].

---

[*] Corresponding author

Akel's $\mathcal{M}$-transform

Akel in [1] recently, introduced the following $\mathcal{M}$-transform in this sequence:

$$\mathcal{M}_{\rho,m}[f(x)](u,v,w) = \int_0^\infty \frac{e^{-ux-\frac{v}{x}}}{(x^m + w^m)^\rho} f(wx)\, dx, \tag{1}$$

with $\rho \in \mathbb{C}, \mathfrak{Re}(\rho) > 0, m \in \mathbb{N}$ and $u, v \in \mathbb{C}$, $w \in \mathbb{R}^+$ are called the transform variables.

The $\mathcal{M}$-transform given by (1), depends on a number of parameters, so that it covers many known integral transforms as its special cases. This transform has the duality relations with well-known transforms such as the Laplace transform, the natural transform and the Srivastava-Luo-Raina $\mathbb{M}$-transform.
This transform is a precious tool for solving certain initial and boundary value problems with certain variable coefficients. Additional ionformation on this transform, may be found in [1].

The incomplete H-and $\overline{H}$-functions

The incomplete H-functions $\gamma_{p,\,q}^{m,\,n}$ and $\Gamma_{p,\,q}^{m,\,n}$ have studied and defined by Srivastava et al. [13] in the form of Mellin-Barness contour integral as follow:

$$\gamma_{p,\,q}^{m,\,n}(z) = \gamma_{p,\,q}^{m,\,n}\left[z \,\middle|\, \begin{array}{c} (\mathfrak{g}_1, \nu_1, y), (\mathfrak{g}_j, \nu_j)_{2,p} \\ (\mathfrak{h}_j, \omega_j)_{1,q} \end{array} \right] = (2\pi\iota)^{-1} \int_{\pounds} g(\vartheta, y)\; z^{-\vartheta}\; d\vartheta, \tag{2}$$

and

$$\Gamma_{p,\,q}^{m,\,n}(z) = \Gamma_{p,\,q}^{m,\,n}\left[z \,\middle|\, \begin{array}{c} (\mathfrak{g}_1, \nu_1, y), (\mathfrak{g}_j, \nu_j)_{2,p} \\ (\mathfrak{h}_j, \omega_j)_{1,q} \end{array} \right] = (2\pi\iota)^{-1} \int_{\pounds} G(\vartheta, y)\; z^{-\vartheta}\; d\vartheta, \tag{3}$$

where,

$$g(\vartheta, y) = \frac{\gamma(1-\mathfrak{g}_1-\nu_1\vartheta, y) \prod\limits_{j=1}^{m} \Gamma(\mathfrak{h}_j+\omega_j\vartheta) \prod\limits_{j=2}^{n} \Gamma(1-\mathfrak{g}_j-\nu_j\vartheta)}{\prod\limits_{j=m+1}^{q} \Gamma(1-\mathfrak{h}_j-\omega_j\vartheta) \prod\limits_{j=n+1}^{p} \Gamma(\mathfrak{g}_j+\nu_j\vartheta)}, \tag{4}$$

and

$$G(\vartheta, y) = \frac{\Gamma(1-\mathfrak{g}_1-\nu_1\vartheta, y) \prod\limits_{j=1}^{m} \Gamma(\mathfrak{h}_j+\omega_j\vartheta) \prod\limits_{j=2}^{n} \Gamma(1-\mathfrak{g}_j-\nu_j\vartheta)}{\prod\limits_{j=m+1}^{q} \Gamma(1-\mathfrak{h}_j-\omega_j\vartheta) \prod\limits_{j=n+1}^{p} \Gamma(\mathfrak{g}_j+\nu_j\vartheta)}. \tag{5}$$

This family of incomplete H-functions characterized as (2) and (3) exist for $x \geq 0$, according to the conditions specified by Srivastava [13].

Srivastava in [13] developed a generalisation for the family of incomplete H-functions, referred as the incomplete $\overline{H}$-functions, which is described by:

$$\begin{aligned}\overline{\gamma}^{\mathsf{m},\,\mathsf{n}}_{\mathsf{p},\,\mathsf{q}}(z) &= \overline{\gamma}^{\mathsf{m},\,\mathsf{n}}_{\mathsf{p},\,\mathsf{q}}\left[z \,\middle|\, \begin{matrix} (\mathfrak{g}_1, \nu_1; \mathfrak{G}_1; y),\ (\mathfrak{g}_\mathsf{j}, \nu_\mathsf{j}; \mathfrak{G}_\mathsf{j})_{2,\,\mathsf{n}},\ (\mathfrak{g}_\mathsf{j}, \nu_\mathsf{j})_{\mathsf{n}+1,\,\mathsf{p}} \\ (\mathfrak{h}_\mathsf{j}, \omega_\mathsf{j})_{1,\mathsf{m}},\ (\mathfrak{h}_\mathsf{j}, \omega_\mathsf{j}; \mathfrak{H}_\mathsf{j})_{\mathsf{m}+1,\,\mathsf{q}} \end{matrix}\right] \\ &= (2\pi\iota)^{-1} \int_{\pounds} \overline{g}(\vartheta, y)\ z^{-\vartheta}\ d\vartheta, \end{aligned} \tag{6}$$

and

$$\begin{aligned}\overline{\Gamma}^{\mathsf{m},\,\mathsf{n}}_{\mathsf{p},\,\mathsf{q}}(z) &= \overline{\Gamma}^{\mathsf{m},\,\mathsf{n}}_{\mathsf{p},\,\mathsf{q}}\left[z \,\middle|\, \begin{matrix} (\mathfrak{g}_1, \nu_1; \mathfrak{G}_1; y),\ (\mathfrak{g}_\mathsf{j}, \nu_\mathsf{j}; \mathfrak{G}_\mathsf{j})_{2,\,\mathsf{n}},\ (\mathfrak{g}_\mathsf{j}, \nu_\mathsf{j})_{\mathsf{n}+1,\,\mathsf{p}} \\ (\mathfrak{h}_\mathsf{j}, \omega_\mathsf{j})_{1,\mathsf{m}},\ (\mathfrak{h}_\mathsf{j}, \omega_\mathsf{j}; \mathfrak{H}_\mathsf{j})_{\mathsf{m}+1,\,\mathsf{q}} \end{matrix}\right] \\ &= (2\pi\iota)^{-1} \int_{\pounds} \overline{G}(\vartheta, y)\ z^{-\vartheta}\ d\vartheta, \end{aligned} \tag{7}$$

where

$$\overline{g}(\vartheta, y) = \frac{[\gamma(1-\mathfrak{g}_1-\nu_1\vartheta, y)]^{\mathfrak{G}_1} \prod\limits_{\mathsf{j}=1}^{\mathsf{m}} \Gamma(\mathfrak{h}_\mathsf{j}+\omega_\mathsf{j}\vartheta) \prod\limits_{\mathsf{j}=2}^{\mathsf{n}} [\Gamma(1-\mathfrak{g}_\mathsf{j}-\nu_\mathsf{j}\vartheta)]^{\mathfrak{G}_\mathsf{j}}}{\prod\limits_{\mathsf{j}=\mathsf{m}+1}^{\mathsf{q}} [\Gamma(1-\mathfrak{h}_\mathsf{j}-\omega_\mathsf{j}\vartheta)]^{\mathfrak{H}_\mathsf{j}} \prod\limits_{\mathsf{j}=\mathsf{n}+1}^{\mathsf{p}} \Gamma(\mathfrak{g}_\mathsf{j}+\nu_\mathsf{j}\vartheta)}, \tag{8}$$

and

$$\overline{G}(\vartheta, y) = \frac{[\Gamma(1-\mathfrak{g}_1-\nu_1\vartheta, y)]^{\mathfrak{G}_1} \prod\limits_{\mathsf{j}=1}^{\mathsf{m}} \Gamma(\mathfrak{h}_\mathsf{j}+\omega_\mathsf{j}\vartheta) \prod\limits_{\mathsf{j}=2}^{\mathsf{n}} [\Gamma(1-\mathfrak{g}_\mathsf{j}-\nu_\mathsf{j}\vartheta)]^{\mathfrak{G}_\mathsf{j}}}{\prod\limits_{\mathsf{j}=\mathsf{m}+1}^{\mathsf{q}} [\Gamma(1-\mathfrak{h}_\mathsf{j}-\omega_\mathsf{j}\vartheta)]^{\mathfrak{H}_\mathsf{j}} \prod\limits_{\mathsf{j}=\mathsf{n}+1}^{\mathsf{p}} \Gamma(\mathfrak{g}_\mathsf{j}+\nu_\mathsf{j}\vartheta)}. \tag{9}$$

Numerous authors are actively working on the development and wide variety of implications for these incomplete functions, such as in [3, 15], authors established modified saigo fractional integral operators involving the product of a general class of multivariable polynomials and the multivariable H-function and an integral operator involving the family of incomplete H-function in its kernel, respectively. The authors of [11] investigated applications of the incomplete H-function on the influence of environmental pollution on the occurrence of biological populations, whereas the authors of [6, 7] developed an equation of internal blood pressure involving incomplete $\overline{H}$-functions and specific expansion formulae for the incomplete H-functions.

The main purpose of this paper is to give new image formulas for incomplete H- and $\overline{H}$-functions under Akel's $\mathcal{M}$-transform. And by giving suitable values to the involved parameters, we also present some special cases of our main findings.

The paper is organized in the following way. In Section 2, we establish the Akel's $\mathcal{M}$-transform image formulae for the incomplete H- and $\overline{H}$-functions. In Section 3 , we derive some interesting and important special cases of our main findings. Finally, a brief conclusion in Section 4.

2 The $\mathcal{M}$-Transform of Incomplete H- and $\overline{H}$-Functions

In this segment, we establish new image formulas for the incomplete H- and $\overline{H}$-functions under the Akel's $\mathcal{M}$-transform.

Theorem 1. *If $\rho \in \mathbb{C}, \mathfrak{Re}(\rho) > 0, m \in \mathbb{N}$ and $u, v \in \mathbb{C}$, $w \in \mathbb{R}^+$, then the following image formula exists for $\gamma^{\mathsf{m,\,n}}_{\mathsf{p,\,q}}[z]$:*

$$\mathcal{M}_{\rho,m}\left\{\gamma^{\mathsf{m,\,n}}_{\mathsf{p,\,q}}\left[zx \,\middle|\, \begin{matrix}(\mathfrak{g}_1,\nu_1,y),(\mathfrak{g}_{\mathsf{j}},\nu_{\mathsf{j}})_{2,\mathsf{p}}\\ (\mathfrak{h}_{\mathsf{j}},\omega_{\mathsf{j}})_{1,\mathsf{q}}\end{matrix}\right]\right\}(u,v,w) = \frac{w^{-m\rho}}{u\,m}\,\frac{1}{2\pi\iota}\int_{\pounds}\mathbb{B}\left(\rho-\frac{\xi}{m},\frac{\xi}{m}\right)(uw)^{\xi}$$
$$\gamma^{\mathsf{m,\,n+1}}_{\mathsf{p+1,\,q}}\left[z\frac{w}{u} \,\middle|\, \begin{matrix}(\mathfrak{g}_1,\nu_1,y),(\xi,1)_{uv},(\mathfrak{g}_{\mathsf{j}},\nu_{\mathsf{j}})_{2,\mathsf{p}}\\ (\mathfrak{h}_{\mathsf{j}},\omega_{\mathsf{j}})_{1,\mathsf{q}}\end{matrix}\right]d\xi. \tag{10}$$

Here, $\mathbb{B}(x, y)$ represents the classical Euler-Beta function.

Proof. To get the result (1), first we take the L.H.S of (10) and use the definition (1), we have

$$\mathcal{M}_{\rho,m}\left\{\gamma^{\mathsf{m,\,n}}_{\mathsf{p,\,q}}\left[zx \,\middle|\, \begin{matrix}(\mathfrak{g}_1,\nu_1,y),(\mathfrak{g}_{\mathsf{j}},\nu_{\mathsf{j}})_{2,\mathsf{p}}\\ (\mathfrak{h}_{\mathsf{j}},\omega_{\mathsf{j}})_{1,\mathsf{q}}\end{matrix}\right]\right\}(u,v,w) = \int_0^{\infty}\frac{e^{-ux-\frac{v}{x}}}{(x^m+w^m)^{\rho}}\,\gamma^{\mathsf{m,\,n}}_{\mathsf{p,\,q}}(zw\,x)\,dx$$
$$= \int_0^{\infty}\frac{e^{-ux-\frac{v}{x}}}{(x^m+w^m)^{\rho}}\,\frac{1}{2\pi\iota}\int_{\pounds} g(\vartheta,y)z^{-\vartheta}(wx)^{-\vartheta}\,d\vartheta\,dx$$

On interchanging the orders of the integration

$$= \frac{1}{2\pi\iota}\int_{\pounds} g(\vartheta,y)z^{-\vartheta}\int_0^{\infty}\frac{e^{-ux-\frac{v}{x}}}{(x^m+w^m)^{\rho}}(wx)^{-\vartheta}\,dx\,d\vartheta$$

Now, on utilizing [1, pg. 6, Eqn. (2.11)], we get

$$= \frac{1}{2\pi\iota}\int_{\pounds} g(\vartheta,y)z^{-\vartheta}\,\frac{w^{-\vartheta-m\rho}\,u^{\vartheta-1}}{m\,\Gamma(\rho)}\,H^{2,\,1}_{1,\,2}\left[u\,w \,\middle|\, \begin{matrix}(1,\frac{1}{m})\\ (1-\vartheta,1)_{uv},(\rho,\frac{1}{m})\end{matrix}\right]d\vartheta$$
$$= \frac{w^{-m\rho}}{um\,\Gamma(\rho)}\frac{1}{2\pi\iota}\int_{\pounds} g(\vartheta,y)\left(z\frac{w}{u}\right)^{-\vartheta}\frac{1}{2\pi\iota}\int_{-\iota\infty}^{+\iota\infty}(u\,w)^{\xi}\Gamma(\frac{\xi}{m})\Gamma_{uv}(1-\xi-\vartheta)\Gamma(\rho-\frac{\xi}{m})d\xi\,d\vartheta$$

On changing the order of the integrations and after some adjustment of terms

$$= \frac{w^{-m\rho}}{u\,m}\,\frac{1}{2\pi\iota}\int_{\pounds}\frac{\Gamma(\frac{\xi}{m})\,\Gamma(\rho-\frac{\xi}{m})}{\Gamma(\rho)}\,(uw)^{\xi}\,\frac{1}{2\pi\iota}\int_{\pounds} g(\vartheta,y)\,\Gamma_{uv}(1-\xi-\vartheta)\left(z\frac{w}{u}\right)^{-\vartheta}d\vartheta\,d\xi, \tag{11}$$

using (2), we obtain the required R.H.S of (10). □

Theorem 2. *If $\rho \in \mathbb{C}, \mathfrak{Re}(\rho) > 0, m \in \mathbb{N}$ and $u, v \in \mathbb{C}$, $w \in \mathbb{R}^+$, then the following image formula exists for $\Gamma^{\mathsf{m,\,n}}_{\mathsf{p,\,q}}[z]$:*

$$\mathcal{M}_{\rho,m}\left\{\Gamma^{\mathsf{m,\,n}}_{\mathsf{p,\,q}}\left[zx \,\middle|\, \begin{matrix}(\mathfrak{g}_1, \nu_1, y), (\mathfrak{g}_{\mathsf{j}}, \nu_{\mathsf{j}})_{\mathsf{2,p}} \\ (\mathfrak{h}_{\mathsf{j}}, \omega_{\mathsf{j}})_{\mathsf{1,q}}\end{matrix}\right]\right\}(u,v,w) = \frac{w^{-m\rho}}{u\,m}\,\frac{1}{2\pi\iota}\int_{\pounds}\mathbb{B}\left(\rho - \frac{\xi}{m}, \frac{\xi}{m}\right)(uw)^{\xi}$$
$$\Gamma^{\mathsf{m,\,n+1}}_{\mathsf{p+1,\,q}}\left[z\frac{w}{u} \,\middle|\, \begin{matrix}(\mathfrak{g}_1, \nu_1, y), (\xi, 1)_{uv}, (\mathfrak{g}_{\mathsf{j}}, \nu_{\mathsf{j}})_{\mathsf{2,p}} \\ (\mathfrak{h}_{\mathsf{j}}, \omega_{\mathsf{j}})_{\mathsf{1,q}}\end{matrix}\right] d\xi. \tag{12}$$

Here, $\mathbb{B}(x, y)$ represents the classical Euler-Beta function.

Proof. To get the result (12), we take the Akel's $\mathcal{M}$-transform presented in (1) of (3), then on interchanging the order of the integrations and making use of the known result given in [1, p. 6, Eq. (2.11)], and after some small arrangements of the terms, we easily get the right hand side assertion of (12). ☐

Theorem 3. *If $\rho \in \mathbb{C}, \mathfrak{Re}(\rho) > 0, m \in \mathbb{N}$ and $u, v \in \mathbb{C}$, $w \in \mathbb{R}^+$, then the following image formula exists for $\overline{\gamma}^{\mathsf{m,\,n}}_{\mathsf{p,\,q}}[z]$:*

$$\mathcal{M}_{\rho,m}\left\{\overline{\gamma}^{\mathsf{m,\,n}}_{\mathsf{p,\,q}}\left[zx \,\middle|\, \begin{matrix}(\mathfrak{g}_1, \nu_1; \mathfrak{G}, y), (\mathfrak{g}_{\mathsf{j}}, \nu_{\mathsf{j}}; \mathfrak{G}_{\mathsf{j}})_{\mathsf{2,n}}, (\mathfrak{g}_{\mathsf{j}}, \nu_{\mathsf{j}})_{\mathsf{n+1,p}} \\ (\mathfrak{h}_{\mathsf{j}}, \omega_{\mathsf{j}})_{\mathsf{1,m}}, (\mathfrak{h}_{\mathsf{j}}, \omega_{\mathsf{j}}; \mathfrak{H}_{\mathsf{j}})_{\mathsf{m+1,q}}\end{matrix}\right]\right\}(u,v,w)$$
$$= \frac{w^{-m\rho}}{u\,m}\,\frac{1}{2\pi\iota}\int_{\pounds}\mathbb{B}\left(\rho - \frac{\xi}{m}, \frac{\xi}{m}\right)(uw)^{\xi}$$
$$\overline{\gamma}^{\mathsf{m,\,n+1}}_{\mathsf{p+1,\,q}}\left[z\frac{w}{u} \,\middle|\, \begin{matrix}(\mathfrak{g}_1, \nu_1; \mathfrak{G}, y), (\xi, 1; 1)_{uv}, (\mathfrak{g}_{\mathsf{j}}, \nu_{\mathsf{j}}; \mathfrak{G}_{\mathsf{j}})_{\mathsf{2,n}}, (\mathfrak{g}_{\mathsf{j}}, \nu_{\mathsf{j}})_{\mathsf{n+1,p}} \\ (\mathfrak{h}_{\mathsf{j}}, \omega_{\mathsf{j}})_{\mathsf{1,m}}, (\mathfrak{h}_{\mathsf{j}}, \omega_{\mathsf{j}}; \mathfrak{H}_{\mathsf{j}})_{\mathsf{m+1,q}}\end{matrix}\right] d\xi. \tag{13}$$

Here, $\mathbb{B}(x, y)$ represents the classical Euler-Beta function.

Proof. To get the result (3), first we take the L.H.S of (13) and use the definition (1), we have

$$\mathcal{M}_{\rho,m}\left\{\overline{\gamma}^{\mathsf{m,\,n}}_{\mathsf{p,\,q}}\left[zx \,\middle|\, \begin{matrix}(\mathfrak{g}_1, \nu_1; \mathfrak{G}_1; y),\ (\mathfrak{g}_{\mathsf{j}}, \nu_{\mathsf{j}}; \mathfrak{G}_{\mathsf{j}})_{\mathsf{2,\,n}},\ (\mathfrak{g}_{\mathsf{j}}, \nu_{\mathsf{j}})_{\mathsf{n+1,\,p}} \\ (\mathfrak{h}_{\mathsf{j}}, \omega_{\mathsf{j}})_{\mathsf{1,m}},\ (\mathfrak{h}_{\mathsf{j}}, \omega_{\mathsf{j}}; \mathfrak{H}_{\mathsf{j}})_{\mathsf{m+1,\,q}}\end{matrix}\right]\right\}(u,v,w)$$
$$= \int_0^{\infty}\frac{e^{-ux-\frac{v}{x}}}{(x^m + w^m)^{\rho}}\,\overline{\gamma}^{\mathsf{m,\,n}}_{\mathsf{p,\,q}}(zw\,x)\,dx$$
$$= \int_0^{\infty}\frac{e^{-ux-\frac{v}{x}}}{(x^m + w^m)^{\rho}}\,\frac{1}{2\pi\iota}\int_{\pounds}\overline{g}(\vartheta, y)z^{-\vartheta}(wx)^{-\vartheta}\,d\vartheta\,dx$$

On interchanging the orders of the integration

$$= \frac{1}{2\pi\iota}\int_{\pounds}\overline{g}(\vartheta, y)z^{-\vartheta}\int_0^{\infty}\frac{e^{-ux-\frac{v}{x}}}{(x^m + w^m)^{\rho}}(wx)^{-\vartheta}\,dx\,d\vartheta$$

5

Now, on utilizing [1, pg. 6, Eqn. (2.11)], we get

$$= \frac{1}{2\pi\iota}\int_{\pounds} \overline{g}(\vartheta, y) z^{-\vartheta}\, \frac{w^{-\vartheta-m\rho}\, u^{\vartheta-1}}{m\,\Gamma(\rho)}\, H^{2,\,1}_{1,\,2}\left[u\,w \,\middle|\, \begin{matrix} (1, \frac{1}{m}) \\ (1-\vartheta, 1)_{uv}, (\rho, \frac{1}{m}) \end{matrix}\right] d\vartheta$$

$$= \frac{w^{-m\rho}}{um\,\Gamma(\rho)}\frac{1}{2\pi\iota}\int_{\pounds} \overline{g}(\vartheta, y) \left(z\frac{w}{u}\right)^{-\vartheta} \frac{1}{2\pi\iota}\int_{-\iota\infty}^{+\iota\infty} (u\,w)^{\xi}\Gamma(\frac{\xi}{m})\Gamma_{uv}(1-\xi-\vartheta)\Gamma(\rho-\frac{\xi}{m})d\xi\, d\vartheta$$

On changing the order of the integrations and after some adjustment of terms

$$= \frac{w^{-m\rho}}{u\,m}\,\frac{1}{2\pi\iota}\int_{\pounds} \frac{\Gamma(\frac{\xi}{m})\,\Gamma(\rho-\frac{\xi}{m})}{\Gamma(\rho)}\,(uw)^{\xi}\,\frac{1}{2\pi\iota}\int_{\pounds} \overline{g}(\vartheta, y)\,\Gamma_{uv}(1-\xi-\vartheta)\left(z\frac{w}{u}\right)^{-\vartheta} d\vartheta\, d\xi, \tag{14}$$

using (6), we obtain the required R.H.S of (13). ☐

Theorem 4. *If $\rho \in \mathbb{C}, \mathfrak{Re}(\rho) > 0, m \in \mathbb{N}$ and $u, v \in \mathbb{C}$, $w \in \mathbb{R}^{+}$, then the following image formula exists for $\overline{\Gamma}^{\mathsf{m},\,\mathsf{n}}_{\mathsf{p},\,\mathsf{q}}[z]$:*

$$\mathcal{M}_{\rho,m}\left\{\overline{\Gamma}^{\mathsf{m},\,\mathsf{n}}_{\mathsf{p},\,\mathsf{q}}\left[zx \,\middle|\, \begin{matrix} (\mathfrak{g}_1, \nu_1; \mathfrak{G}, y), (\mathfrak{g}_{\mathsf{j}}, \nu_{\mathsf{j}}; \mathfrak{G}_{\mathsf{j}})_{2,\mathsf{n}}, (\mathfrak{g}_{\mathsf{j}}, \nu_{\mathsf{j}})_{\mathsf{n}+1,\mathsf{p}} \\ (\mathfrak{h}_{\mathsf{j}}, \omega_{\mathsf{j}})_{1,\mathsf{m}}, (\mathfrak{h}_{\mathsf{j}}, \omega_{\mathsf{j}}; \mathfrak{H}_{\mathsf{j}})_{\mathsf{m}+1,\mathsf{q}} \end{matrix}\right]\right\}(u, v, w)$$
$$= \frac{w^{-m\rho}}{u\,m}\,\frac{1}{2\pi\iota}\int_{\pounds} \mathbb{B}\left(\rho-\frac{\xi}{m}, \frac{\xi}{m}\right)(uw)^{\xi}$$
$$\overline{\Gamma}^{\mathsf{m},\,\mathsf{n}+1}_{\mathsf{p}+1,\,\mathsf{q}}\left[z\frac{w}{u} \,\middle|\, \begin{matrix} (\mathfrak{g}_1, \nu_1; \mathfrak{G}, y), (\xi, 1; 1)_{uv}, (\mathfrak{g}_{\mathsf{j}}, \nu_{\mathsf{j}}; \mathfrak{G}_{\mathsf{j}})_{2,\mathsf{n}}, (\mathfrak{g}_{\mathsf{j}}, \nu_{\mathsf{j}})_{\mathsf{n}+1,\mathsf{p}} \\ (\mathfrak{h}_{\mathsf{j}}, \omega_{\mathsf{j}})_{1,\mathsf{m}}, (\mathfrak{h}_{\mathsf{j}}, \omega_{\mathsf{j}}; \mathfrak{H}_{\mathsf{j}})_{\mathsf{m}+1,\mathsf{q}} \end{matrix}\right] d\xi. \tag{15}$$

Here, $\mathbb{B}(x, y)$ represents the classical Euler-Beta function.

Proof. To get the result (15), we take the Akel's $\mathcal{M}$-transform presented in (1) of (7), then on interchanging the order of the integrations and making use of the known result given in [1, p. 6, Eq. (2.11)], and after some small arrangements of the terms, we easily get the right hand side assertion of (15). ☐

3 Special Cases

In this section, we derive some interesting and important special cases of our main findings by giving some particular values to the parameters involved in the definitions of $\mathcal{M}$-transform (1) and incomplete H-functions (2) and (3).
(1) Taking $\mathsf{n} = \mathsf{p}$, $\mathsf{m} = 1$, substitute q with $\mathsf{q}+1$ and choosing appropriate parameters such as $z = -z$, $\mathfrak{g}_{\mathsf{j}} \to (1-\mathfrak{g}_{\mathsf{j}})$ $(\mathsf{j} = 1, \cdots, \mathsf{p})$, and $\mathfrak{h}_{\mathsf{j}} \to (1-\mathfrak{h}_{\mathsf{j}})$ $(\mathsf{j} = 1, \cdots, \mathsf{q})$, the incomplete H-functions (2) and (3) convert, respectively, to the incomplete Fox-Wright ${}_{\mathsf{p}}\Psi^{(\gamma)}_{\mathsf{q}}$- and ${}_{\mathsf{p}}\Psi^{(\Gamma)}_{\mathsf{q}}$-functions (see [13, Eqs. (6.3)

and (6.4)]):

$$\gamma^{1,\,\mathsf{p}}_{\mathsf{p},\,\mathsf{q}+1}\left[-z\left|\begin{array}{c}(1-\mathfrak{g}_1,\nu_1,y),(1-\mathfrak{g}_\mathsf{j},\nu_\mathsf{j})_{2,\mathsf{p}}\\(0,1),(1-\mathfrak{h}_\mathsf{j},\omega_\mathsf{j})_{1,\mathsf{q}}\end{array}\right.\right]={}_{\mathsf{p}}\Psi^{(\gamma)}_{\mathsf{q}}\left[\begin{array}{r}(\mathfrak{g}_1,\nu_1,y),(\mathfrak{g}_\mathsf{j},\nu_\mathsf{j})_{2,\mathsf{p}}\,;\\(\mathfrak{g}_\mathsf{j},\omega_\mathsf{j})_{1,\mathsf{q}}\,;\end{array}\;z\right]\tag{16}$$

and

$$\Gamma^{1,\,\mathsf{p}}_{\mathsf{p},\,\mathsf{q}+1}\left[-z\left|\begin{array}{c}(1-\mathfrak{g}_1,\nu_1,y),(1-\mathfrak{g}_\mathsf{j},\nu_\mathsf{j})_{2,\mathsf{p}}\\(0,1),(1-\mathfrak{h}_\mathsf{j},\omega_\mathsf{j})_{1,\mathsf{q}}\end{array}\right.\right]={}_{\mathsf{p}}\Psi^{(\Gamma)}_{\mathsf{q}}\left[\begin{array}{r}(\mathfrak{g}_1,\nu_1,y),(\mathfrak{g}_\mathsf{j},\nu_\mathsf{j})_{2,\mathsf{p}}\,;\\(\mathfrak{g}_\mathsf{j},\omega_\mathsf{j})_{1,\mathsf{q}}\,;\end{array}\;z\right].\tag{17}$$

Using above relations (16) and (17), in (10) and (12), respectively, we will get the following corollaries.

Corollary 1. *If $\rho\in\mathbb{C},\mathfrak{Re}(\rho)>0,m\in\mathbb{N}$ and $u,v\in\mathbb{C}$, $w\in\mathbb{R}^+$, then the following image formulae exist for ${}_{\mathsf{p}}\Psi^{(\gamma)}_{\mathsf{q}}[z]$ and ${}_{\mathsf{p}}\Psi^{(\Gamma)}_{\mathsf{q}}[z]$:*

$$\begin{aligned}\mathcal{M}_{\rho,m}\left\{{}_{\mathsf{p}}\Psi^{(\gamma)}_{\mathsf{q}}\left[zx\left|\begin{array}{c}(\mathfrak{g}_1,\nu_1,y),(\mathfrak{g}_\mathsf{j},\nu_\mathsf{j})_{2,\mathsf{p}}\\(\mathfrak{h}_\mathsf{j},\omega_\mathsf{j})_{1,\mathsf{q}}\end{array}\right.\right]\right\}(u,v,w)&=\frac{w^{-m\rho}}{u\,m}\frac{1}{2\pi\iota}\int_{\pounds}\mathbb{B}\left(\rho-\frac{\xi}{m},\frac{\xi}{m}\right)(uw)^{\xi}\\&\quad{}_{\mathsf{p}+1}\Psi^{(\gamma)}_{\mathsf{q}}\left[z\frac{w}{u}\left|\begin{array}{c}(\mathfrak{g}_1,\nu_1,y),(\xi,1)_{uv},(\mathfrak{g}_\mathsf{j},\nu_\mathsf{j})_{2,\mathsf{p}}\\(\mathfrak{h}_\mathsf{j},\omega_\mathsf{j})_{1,\mathsf{q}}\end{array}\right.\right]d\xi\end{aligned}\tag{18}$$

and

$$\begin{aligned}\mathcal{M}_{\rho,m}\left\{{}_{\mathsf{p}}\Psi^{(\Gamma)}_{\mathsf{q}}\left[zx\left|\begin{array}{c}(\mathfrak{g}_1,\nu_1,y),(\mathfrak{g}_\mathsf{j},\nu_\mathsf{j})_{2,\mathsf{p}}\\(\mathfrak{h}_\mathsf{j},\omega_\mathsf{j})_{1,\mathsf{q}}\end{array}\right.\right]\right\}(u,v,w)&=\frac{w^{-m\rho}}{u\,m}\frac{1}{2\pi\iota}\int_{\pounds}\mathbb{B}\left(\rho-\frac{\xi}{m},\frac{\xi}{m}\right)(uw)^{\xi}\\&\quad{}_{\mathsf{p}+1}\Psi^{(\Gamma)}_{\mathsf{q}}\left[z\frac{w}{u}\left|\begin{array}{c}(\mathfrak{g}_1,\nu_1,y),(\xi,1)_{uv},(\mathfrak{g}_\mathsf{j},\nu_\mathsf{j})_{2,\mathsf{p}}\\(\mathfrak{h}_\mathsf{j},\omega_\mathsf{j})_{1,\mathsf{q}}\end{array}\right.\right]d\xi.\end{aligned}\tag{19}$$

Here, $\mathbb{B}(x,y)$ indicates the classical Euler-Beta function.

(2) Letting $(\nu_\mathsf{j})_{1,\mathsf{p}}=1=(\omega_\mathsf{j})_{1,\mathsf{q}}$, the functions (2) and (3) convert into Meijer's incomplete ${}^{(\gamma)}G^{\mathsf{m},\,\mathsf{n}}_{\mathsf{p},\,\mathsf{q}}$- and ${}^{(\Gamma)}G^{\mathsf{m},\,\mathsf{n}}_{\mathsf{p},\,\mathsf{q}}$- functions:

$$\gamma^{\mathsf{m},\,\mathsf{n}}_{\mathsf{p},\,\mathsf{q}}(z)\left[z\left|\begin{array}{c}(\mathfrak{g}_1,1,y),(\mathfrak{g}_\mathsf{j},1)_{2,\mathsf{p}}\\(\mathfrak{h}_\mathsf{j},1)_{1,\mathsf{q}}\end{array}\right.\right]={}^{(\gamma)}G^{\mathsf{m},\,\mathsf{n}}_{\mathsf{p},\,\mathsf{q}}\left[z\left|\begin{array}{c}(\mathfrak{g}_1,y),(\mathfrak{g}_\mathsf{j})_{2,\mathsf{p}}\\(\mathfrak{h}_\mathsf{j})_{1,\mathsf{q}}\end{array}\right.\right]\tag{20}$$

and

$$\Gamma^{\mathsf{m},\,\mathsf{n}}_{\mathsf{p},\,\mathsf{q}}(z)\left[z\left|\begin{array}{c}(\mathfrak{g}_1,1,y),(\mathfrak{g}_\mathsf{j},1)_{2,\mathsf{p}}\\(\mathfrak{h}_\mathsf{j},1)_{1,\mathsf{q}}\end{array}\right.\right]={}^{(\Gamma)}G^{\mathsf{m},\,\mathsf{n}}_{\mathsf{p},\,\mathsf{q}}\left[z\left|\begin{array}{c}(\mathfrak{g}_1,y),(\mathfrak{g}_\mathsf{j})_{2,\mathsf{p}}\\(\mathfrak{h}_\mathsf{j})_{1,\mathsf{q}}\end{array}\right.\right].\tag{21}$$

Using above relations (20) and (21) in (10) and (12), respectively, we get the following corollaries.

Corollary 2. *If $\rho \in \mathbb{C}, \mathfrak{Re}(\rho) > 0, m \in \mathbb{N}$ and $u, v \in \mathbb{C}$, $w \in \mathbb{R}^+$, then the following image formulae exist for ${}^{(\gamma)}G^{\mathsf{m,\,n}}_{\mathsf{p,\,q}}[z]$ and ${}^{(\Gamma)}G^{\mathsf{m,\,n}}_{\mathsf{p,\,q}}[z]$, respectively:*

$$\mathcal{M}_{\rho,m}\left\{ {}^{(\gamma)}G^{\mathsf{m,\,n}}_{\mathsf{p,\,q}}\left[zx \,\middle|\, \begin{array}{c} (\mathfrak{g}_1, 1, y), (\mathfrak{g}_\mathsf{j}, 1)_{\mathsf{2,p}} \\ (\mathfrak{h}_\mathsf{j}, 1)_{\mathsf{1,q}} \end{array} \right]\right\}(u,v,w) = \frac{w^{-m\rho}}{u\,m}\,\frac{1}{2\pi\iota}\int_{\pounds} \mathbb{B}\left(\rho - \frac{\xi}{m}, \frac{\xi}{m}\right)(uw)^{\xi}$$
$$ {}^{(\gamma)}G^{\mathsf{m,\,n+1}}_{\mathsf{p+1,\,q}}\left[z\frac{w}{u} \,\middle|\, \begin{array}{c} (\mathfrak{g}_1, 1, y), (\xi, 1)_{uv}, (\mathfrak{g}_\mathsf{j}, 1)_{\mathsf{2,p}} \\ (\mathfrak{h}_\mathsf{j}, 1)_{\mathsf{1,q}} \end{array} \right] d\xi \tag{22}$$

and

$$\mathcal{M}_{\rho,m}\left\{ {}^{(\Gamma)}G^{\mathsf{m,\,n}}_{\mathsf{p,\,q}}\left[zx \,\middle|\, \begin{array}{c} (\mathfrak{g}_1, 1, y), (\mathfrak{g}_\mathsf{j}, 1)_{\mathsf{2,p}} \\ (\mathfrak{h}_\mathsf{j}, 1)_{\mathsf{1,q}} \end{array} \right]\right\}(u,v,w) = \frac{w^{-m\rho}}{u\,m}\,\frac{1}{2\pi\iota}\int_{\pounds} \mathbb{B}\left(\rho - \frac{\xi}{m}, \frac{\xi}{m}\right)(uw)^{\xi}$$
$$ {}^{(\Gamma)}G^{\mathsf{m,\,n+1}}_{\mathsf{p+1,\,q}}\left[z\frac{w}{u} \,\middle|\, \begin{array}{c} (\mathfrak{g}_1, 1, y), (\xi, 1)_{uv}, (\mathfrak{g}_\mathsf{j}, 1)_{\mathsf{2,p}} \\ (\mathfrak{h}_\mathsf{j}, 1)_{\mathsf{1,q}} \end{array} \right] d\xi. \tag{23}$$

Here, $\mathbb{B}(x, y)$ indicates the classical Euler-Beta function.

(3) If we put $y = 0$ in (3), we get the Fox's H-function

$$\Gamma^{\mathsf{m,\,n}}_{\mathsf{p,\,q}}\left[z \,\middle|\, \begin{array}{c} (\mathfrak{g}_1, \nu_1, 0), (\mathfrak{g}_\mathsf{j}, \nu_\mathsf{j})_{\mathsf{2,p}} \\ (\mathfrak{h}_\mathsf{j}, \omega_\mathsf{j})_{\mathsf{1,q}} \end{array} \right] = H^{\mathsf{m,\,n}}_{\mathsf{p,\,q}}\left[z \,\middle|\, \begin{array}{c} (\mathfrak{g}_\mathsf{j}, \nu_\mathsf{j})_{\mathsf{1,p}} \\ (\mathfrak{h}_\mathsf{j}, \omega_\mathsf{j})_{\mathsf{1,q}} \end{array} \right]. \tag{24}$$

Using relation (24), we obtain the subsequent corollaries.

Corollary 3. *If $\rho \in \mathbb{C}, \mathfrak{Re}(\rho) > 0, m \in \mathbb{N}$ and $u, v \in \mathbb{C}$, $w \in \mathbb{R}^+$, then the following image formula exists for $H^{\mathsf{m,\,n}}_{\mathsf{p,\,q}}[z]$:*

$$\mathcal{M}_{\rho,m}\left\{ H^{\mathsf{m,\,n}}_{\mathsf{p,\,q}}\left[zx \,\middle|\, \begin{array}{c} (\mathfrak{g}_\mathsf{j}, \nu_\mathsf{j})_{\mathsf{1,p}} \\ (\mathfrak{h}_\mathsf{j}, \omega_\mathsf{j})_{\mathsf{1,q}} \end{array} \right]\right\}(u,v,w) = \frac{w^{-m\rho}}{u\,m}\,\frac{1}{2\pi\iota}\int_{\pounds} \mathbb{B}\left(\rho - \frac{\xi}{m}, \frac{\xi}{m}\right)(uw)^{\xi}$$
$$ H^{\mathsf{m,\,n+1}}_{\mathsf{p+1,\,q}}\left[z\frac{w}{u} \,\middle|\, \begin{array}{c} (\xi, 1)_{uv}, (\mathfrak{g}_\mathsf{j}, \nu_\mathsf{j})_{\mathsf{1,p}} \\ (\mathfrak{h}_\mathsf{j}, \omega_\mathsf{j})_{\mathsf{1,q}} \end{array} \right] d\xi. \tag{25}$$

Here, $\mathbb{B}(x, y)$ indicates the classical Euler-Beta function.

(4) If we put $v = 0$ in (1), then the Akel's $\mathcal{M}$-transform converts into the Srivastava-Luo-Raina $\mathbb{M}$-transform (see [1]):

$$\mathcal{M}_{\rho,m}[f(x)](u, 0, w) = \mathbb{M}_{\rho,m}[f(x)](u, w), \tag{26}$$

here, $\mathbb{M}_{\rho,m}[f(x)](u, w)$ is the Srivastava-Luo-Raina $\mathbb{M}$-transform, defined in [14]. Using relation (26) in (10) and (12), we obtain the results derived by Bansal et al. [2, p. 720, Eqs. (2.1) and (2.2)],

$$\mathbb{M}_{\rho,m}\left\{\gamma^{\mathsf{m},\,\mathsf{n}}_{\mathsf{p},\,\mathsf{q}}\left[zx\,\middle|\,\begin{matrix}(\mathfrak{g}_1,\nu_1,y),(\mathfrak{g}_{\mathsf{j}},\nu_{\mathsf{j}})_{2,\mathsf{p}}\\(\mathfrak{h}_{\mathsf{j}},\omega_{\mathsf{j}})_{1,\mathsf{q}}\end{matrix}\right]\right\}(u,w)=\frac{w^{-m\rho}}{u\,m}\frac{1}{2\pi\iota}\int_{\pounds}\mathbb{B}\left(\rho-\frac{\xi}{m},\frac{\xi}{m}\right)(uw)^{\xi}\,\gamma^{\mathsf{m},\,\mathsf{n}+1}_{\mathsf{p}+1,\,\mathsf{q}}\left[z\frac{w}{u}\,\middle|\,\begin{matrix}(\mathfrak{g}_1,\nu_1,y),(\xi,1),(\mathfrak{g}_{\mathsf{j}},\nu_{\mathsf{j}})_{2,\mathsf{p}}\\(\mathfrak{h}_{\mathsf{j}},\omega_{\mathsf{j}})_{1,\mathsf{q}}\end{matrix}\right]d\xi \tag{27}$$

and

$$\mathbb{M}_{\rho,m}\left\{\Gamma^{\mathsf{m},\,\mathsf{n}}_{\mathsf{p},\,\mathsf{q}}\left[zx\,\middle|\,\begin{matrix}(\mathfrak{g}_1,\nu_1,y),(\mathfrak{g}_{\mathsf{j}},\nu_{\mathsf{j}})_{2,\mathsf{p}}\\(\mathfrak{h}_{\mathsf{j}},\omega_{\mathsf{j}})_{1,\mathsf{q}}\end{matrix}\right]\right\}(u,w)=\frac{w^{-m\rho}}{u\,m}\frac{1}{2\pi\iota}\int_{\pounds}\mathbb{B}\left(\rho-\frac{\xi}{m},\frac{\xi}{m}\right)(uw)^{\xi}\,\Gamma^{\mathsf{m},\,\mathsf{n}+1}_{\mathsf{p}+1,\,\mathsf{q}}\left[z\frac{w}{u}\,\middle|\,\begin{matrix}(\mathfrak{g}_1,\nu_1,y),(\xi,1),(\mathfrak{g}_{\mathsf{j}},\nu_{\mathsf{j}})_{2,\mathsf{p}}\\(\mathfrak{h}_{\mathsf{j}},\omega_{\mathsf{j}})_{1,\mathsf{q}}\end{matrix}\right]d\xi. \tag{28}$$

Remark. *If we take* $v = 0$ *in* (18) *and* (19)*, then we get the known results obtained by Bansal et al. [2, p. 720-721, Eqs. (2.3) and (2.4)].*

4 Conclusion

In this paper, we have derived image formulas for the incomplete H- and $\overline{H}$-functions under the Akel's $\mathcal{M}$-transform. Furthermore, from our key findings various special cases can be evaluated by giving suitable values to the involved parameters and variables with applications in engineering and science, some of which are clearly indicated in section 3.

References

[1] M. Akel, A new gneneralized integral transform and applications, *arXiv preprint* arXiv:2207.13093, 2022.

[2] M. K. Bansal, D. Kumar, J. Singh, A. Tassaddiq, and K. S. Nisar, Some new results for the Srivastava−Luo−Raina $\mathbb{M}$-transform pertaining to the incomplete H-functions, *AIMS Math*, **5**(1), 717-722, 2020.

[3] M.K. Bansal, S. Lal, D. Kumar, S. Kumar, and J. Singh, Fractional differential equation pertaining to an integral operator involving incomplete Hfunction in the kernel, *Mathematical Methods in the Applied Sciences*, 1-8, 2020.

[4] B. Davis, *Integral Transforms and Their Applications*, 3rd ed.; Springer: New York, NY, USA, 2002.

[5] L. Debnath and D. Bhatta, *Integral Transforms and Their Applications*, Third Edi- tion, Chapman and Hall (CRC Press), Taylor and Francis Group, London and New York, 2016.

[6] N. Jangid, S. Joshi, S.D. Purohit, and D.L. Suthar, Fractional derivatives and expansion formulae of incomplete H and $\overline{H}$-functions, *Advances in the Theory of Nonlinear Analysis and its Application*, **5**(2), 193-202, 2021.

[7] D. Kumar, M.K. Bansal, K.S. Nisar, and J. Singh, Mathematical modelling of internal blood pressure involving incomplete $\overline{H}$-functions, *Journal of Interdisciplinary Mathematics*, **22**(7), 1213-1221, 2019.

[8] A.M. Mathai, R.K. Saxena, and H.J. Haubold, *The H-function theory and applications*, Springer-Verlag, New York, 2010.

[9] A.M. Mathai, R.K. Saxena, *The H-function with applications in statistics and other disciplines*, Wiley Eastern Limited, New Delhi; John Wiley ans Sons, New York, 1978.

[10] S. Meena, S. Bhatter, K. Jangid, and S.D. Purohit, Certain integral transforms concerning the product of family of polynomials and generalized incomplete functions, *Moroccan Journal of Pure and Applied Analysis*, **6**(2), 243-254, 2020.

[11] S.D. Purohit, A.M. Khan, D.L. Suthar, and S. Dave, The impact on raise of environmental pollution and occurrence in biological populations pertaining to incomplete H-function, *National Academy Science Letters*, **44**(3), 263-266, 2021.

[12] I.N. Sneddon, *The use of integral transforms*, Tata McGraw-Hill, New York, 1974.

[13] H.M. Srivastava, R.K. Saxena, and R.K. Parmar, Some families of the incomplete H-functions and the incomplete $\overline{H}$-functions and associated integral transforms and operators of fractional calculus with applications, *Rus. J. Math. Phys.*, **25**, 116-138, 2018.

[14] H.M. Srivastava, M.J. Luo, R.K. Raina, A new integral transform and its applications, *Acta Math. Sci.*, **35**, 1386-1400, 2015.

[15] D. L. Suthar, B. Debalkie, and M. Andualem, Modified Saigo fractional integral operators involving multivariable H-function and general class of multivariable polynomials, *Advances in Difference Equations*, **1**(2019), 1-11, 2019.

J. COMPUTATIONAL ANALYSIS AND APPLICATIONS, VOL. 31, NO.1, 2023, COPYRIGHT 2023 EUDOXUS PRESS, LLC

Approximate solutions of space and time fractional telegraph equations using Taylor series expansion method

*Shweta Dubey, †S. Chakraverty, and ‡M. Kundu

December 29, 2022

The study investigates the telegraph equations by considering space and time fractional derivatives. Caputo's concept of fractional derivatives is used here. We are focusing to generalize the solutions of integer order telegraph equations to fractional order telegraph equations. In this case, approximate solutions for fractional order telegraph equations have been obtained using Taylor series expansion. Additionally, it has been shown quantitatively how the solutions converge by using the number of terms in the series solutions.

Keywords

Telegraph equation, Caputo fractional derivative, Taylor series.

Mathematics Subject Classification

65M99

1 Introduction

Recent research suggests that fractional order derivatives are essential for a wide range of physical phenomena viz. rheology, damping law, heat-diffusion, wave dynamics, signal processing, etc. Researchers have used different types of analytical and numerical methods to handle such problems. Techniques including modified extended tanh method [1], novel analytical technique [2], coupled transformation method [3], Galerkin and collocation methods [4], etc. are some

---

*shwetadubey9452@gmail.com (Department of Mathematics, National Institute of Technology Rourkela, India)

†sne_ chak@yahoo.com (Department of Mathematics, National Institute of Technology Rourkela, India)

‡mkundu@nitrkl.ac.in (Department of Chemical Engineering, National Institute of Technology Rourkela, India)

recent endeavors in this paradigm. Moreover, the semi-analytical homotopy perturbation method (HPM) has been used to tackle fractional models such as the heat-conduction equation [5], convection-diffusion problem [6], and wave equation [7] etc. Additionally, Dubey et al. have used local fractional natural homotopy analysis method [8, 9] and some coupling techniques such as the local fractional variational iteration technique with the local fractional natural transform [10] and local fractional homotopy perturbation method with local fractional natural transform operator [11] to solve various types of physical problems.

The studied of fractional telegraph equations (FTEs) have gained popularity due to various applications they can be applied to, such as modeling reaction diffusion, transmission and propagation of electrical signals, etc.

The general FTE [12] is given as,

$$D_x^p\phi(x,t) = aD_t^q\phi(x,t) + bD_t^r\phi(x,t) + c\phi(x,t) + h(x,t)$$

,

where $1 < p,\ q \leq 2,\ 0 < r \leq 1,\ x,t \geq 0,\ \phi(0,t) = f_1(t),\ \phi_x(0,t) = f_2(t)$ and a, b, c are constants.

Various authors have solved telegraph equations using different numerical and analytical techniques. The analytical solution for FTE with respect to time has been obtained by chen et al. [13] by using method of separating variables. The space-fractional telegraph equation (SFTE) and time-fractional telegraph equation (TFTE) and related telegraph process have been disscussed by Orsingher and Zaho [14] and Orsingher and Beghin [15]. Moreover, some other methods such as variational iteration method [16], HPM [17], differential transform method [18] have also been used to handle FTEs.

The Taylor series expansion method (TSEM) is applied by Demir et al. [19] for different fractional partial differential equation (PDE). In this study, we use Taylor series of an analytical solution of the integer order differential equation. This Taylor series solution can be reach out to the approximate or exact solution of fractional differential equation (FDE). Our approach changes the terms of Taylor series expansion for derivatives in the sense of fractionals and integers so that their relationship remains unaltered. Applications of this method demonstrate that it may be used to solve any differential equation derived from FDEs with ease and effectiveness, provided that the differential equation has an analytical or approximative solution. Here, the Caputo concept of the fractional derivative is utilised.

Here, Taylor series is applied on SFTEs and TFTEs. Firstly, the Taylor series expansion for analytical solution obtained from integer order telegraph equation is determined and then the expansion has been extended for FDE.

The rest of the paper follows this format: Methodology of the Taylor series expansion method is described in Section 2. Section 3 includes solutions of SFTEs and TFTEs. This section also covers convergency tables and graphical solutions. Finally, Section 4 concludes this article with a brief summary.

2 Taylor series expansion method

In this section, TSEM has been discussed to handle space and time fractional PDEs.

2.1 Fundamental approach to solve space-fractional PDEs

Let us consider a genaral form space-fractional PDE as

$$D_x^{\alpha}\phi(x,t) = \eta\left(\phi, \frac{\partial\phi}{\partial t}, \cdots \frac{\partial^n\phi}{\partial t^n}, x, t\right), \quad k-1<\alpha\leq k,\ x>0,\ t>0. \tag{1}$$

To find the solution of Eq. (1), we must first calculate the solution to its integer order version by using the expression $\alpha = k$, which is represented as

$$D_x^{k}\phi(x,t) = \eta\left(\phi, \frac{\partial\phi}{\partial t}, \cdots \frac{\partial^n\phi}{\partial t^n}, x, t\right), \quad t>0,\ x>0. \tag{2}$$

From the exact answer of Eq. (1), one can get the approximation or exact solution (2). To do this, we must modify the terms in the Taylor series expansion of integer order differential equation (2). In the infinite Taylor series expansion of the solution of Eq. (2), the first k terms remain the same. Moreover, the fractional derivative with respect to x is used in place of the integer order derivative with respect to x in order to maintain the relationship between the terms of the Taylor series and to satisfy the boundary conditions of the fractional differential equation.

To solve Eq. (2) with respect to x, a primitive Taylor series form is shown below.

$$\phi(x,t) = \sum_{n=0}^{\infty} \frac{\partial^n\phi(0,t)}{\partial x^n}\frac{x^n}{n!}. \tag{3}$$

The solution of Eq. (1) is thus expressed in the following way:

$$\phi(x,t) = \sum_{n=0}^{k-1} \frac{\partial^n\phi(0,t)}{\partial x^n}\frac{x^n}{n!} + \sum_{n=1}^{\infty}\sum_{j=0}^{k-1} \frac{\partial^{kn+j}\phi(0,t)}{\partial x^{kn+j}}\frac{x^{n\alpha+j}}{\Gamma(n\alpha+j+1)}. \tag{4}$$

2.2 Fundamental approach to solve time-fractional PDEs

Let us consider a genaral form time-fractional PDE as

$$D_t^{\alpha}\phi(x,t) = \eta\left(\phi, \frac{\partial\phi}{\partial x}, \cdots \frac{\partial^n\phi}{\partial x^n}, x, t\right), \quad k-1 < \alpha \leq k,\, t > 0. \tag{5}$$

For obtaing the solution of Eq. (5), we have to determine the solution for integer order form of Eq. (5) by taking $\alpha = k$, which is written as

$$D_t^{k}\phi(x,t) = \eta\left(\phi, \frac{\partial\phi}{\partial x}, \cdots \frac{\partial^n\phi}{\partial x^n}, x, t\right), \quad t > 0. \tag{6}$$

If we alter the terms of the Taylor series expansion in the solution of the integer order differential equation, we can obtain the approximate or precise solution of Equation (5) from the exact solution of Eq. (6). The initial k terms of the infinite Taylor series expansion of solution of Eq. (6) are unaltered. Additionally, in order to maintain the relationship between the terms of the Taylor series and to satisfy the boundary conditions of the fractional differential equation, the integer order derivative with respect to t is substituted by the fractional derivative with respect to t.

For the solution of Eq. (6) with regard to t, the sketched Taylor series form is shown below.

$$\phi(x,t) = \sum_{n=0}^{\infty} \frac{\partial^n\phi(x,0)}{\partial t^n}\frac{t^n}{n!}. \tag{7}$$

Then the solution of Eq. (5) is given in the following format.

$$\phi(x,t) = \sum_{n=0}^{k-1} \frac{\partial^n\phi(x,0)}{\partial t^n}\frac{t^n}{n!} + \sum_{n=1}^{\infty}\sum_{j=0}^{k-1} \frac{\partial^{kn+j}\phi(x,0)}{\partial t^{kn+j}}\frac{t^{n\alpha+j}}{\Gamma(n\alpha+j+1)}. \tag{8}$$

3 Numerical examples

3.1 Solution of SFTE

Take a look at a general SFTE example [20].

$$\frac{\partial^{2\alpha}\phi}{\partial x^{2\alpha}} = \frac{\partial^2\phi}{\partial t^2} + 4\frac{\partial\phi}{\partial t} + 4\phi \quad t \geq 0,\, 0 < \alpha \leq 1, \tag{9}$$

with initial conditions

$$\phi(0,t) = 1 + e^{-2t},\ \phi_x(0,t) = 2. \tag{10}$$

The exact solution of Eq. (9) with initial conditions (10) is given as

$$\phi(x,t) = e^{2x} + e^{-2t}. \tag{11}$$

The Taylor series expansion of the exact solution (11) is below.

$$\phi(x,t)=\left(e^{-2t}+1+2x+\frac{4x^2}{2!}+\frac{8x^3}{3!}+\cdots\right). \tag{12}$$

As discussed in the procedure, the solution to Eq. (9) is given by

$$\phi(x,t)=\left(1+e^{-2t}+\frac{2x^{\alpha}}{\Gamma(\alpha+1)}+\frac{4x^{2\alpha}}{\Gamma(2\alpha+1)}+\frac{8x^{3\alpha}}{\Gamma(3\alpha+1)}+\cdots\right). \tag{13}$$

To demonstrate how well the approach works, we will check its convergence by increasing the number of terms in the series solution. In perspective of this, Convergency Table 1 contains values for the fractional value α, with $\alpha = 0.8$ and a fixed value of $t = 0.1$, while x ranges from 0 to 1.

Table 1: Convergency chart for the solution of the SFTE.

x	$\phi(x, t = 0.1)$						
	3 terms	5 terms	7 terms	9 terms	13 terms	16 terms	17 terms
0	1.818730	1.818730	1.818730	1.818730	1.818730	1.818730	1.818730
0.1	2.159061	2.240025	2.241460	2.241473	2.241473	2.241473	2.241473
0.2	2.411281	2.680719	2.694812	2.695188	2.695194	2.695194	2.695194
0.3	2.638323	3.195128	3.249704	3.252453	3.252541	3.252541	3.252541
0.4	2.850420	3.793880	3.937923	3.949311	3.949894	3.949895	3.949895
0.5	3.052055	4.483454	4.791251	4.825739	4.828286	4.828291	4.828291
0.6	3.245725	5.268850	5.843929	5.929557	5.938111	5.938144	5.938144
0.7	3.433014	6.154317	7.133256	7.318560	7.342541	7.342702	7.342703
0.8	3.615007	7.143644	8.699801	9.062343	9.121244	9.121873	9.121876
0.9	3.792495	8.240293	10.587472	11.244084	11.374845	11.376950	11.376964
1.0	3.966073	9.447488	12.843557	13.962366	14.230392	14.236641	14.236689

The surface of the graph in Fig. 1 depicts the exact solution of the telegraph equation given in Eq. (11) for $\alpha = 1$. Further, the surface of graphs in Figs. 2 and 3 show the approximate solutions of the SFTE for $\alpha = 0.5$ and 0.3 respectively.

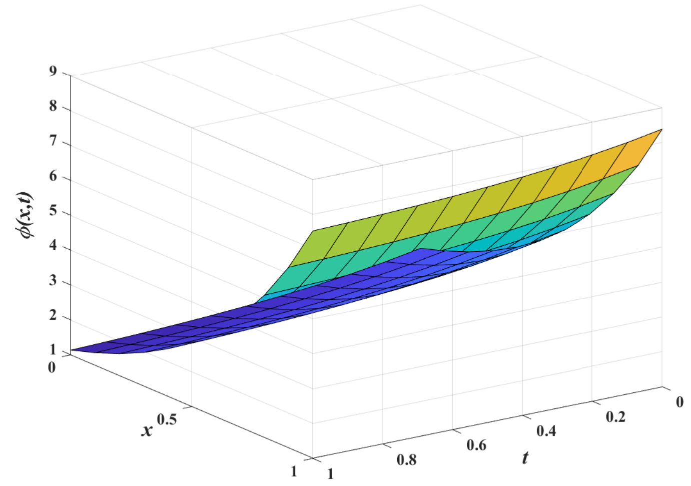

Figure 1: Exact solution of SFTE (11) for $\alpha = 1$

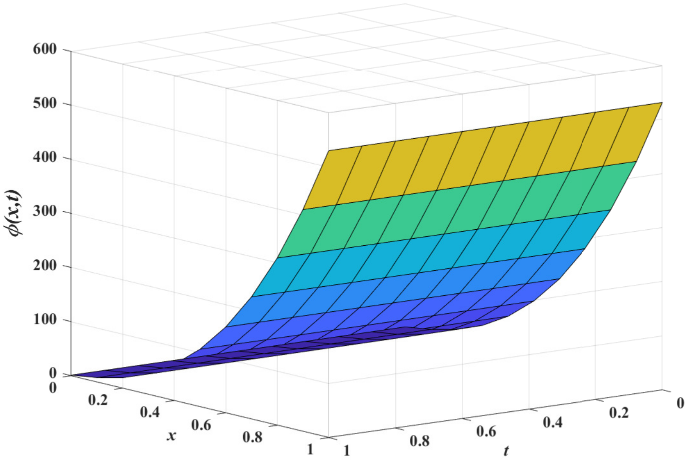

Figure 2: Approximate solution of SFTE (13) for $\alpha = 0.3$

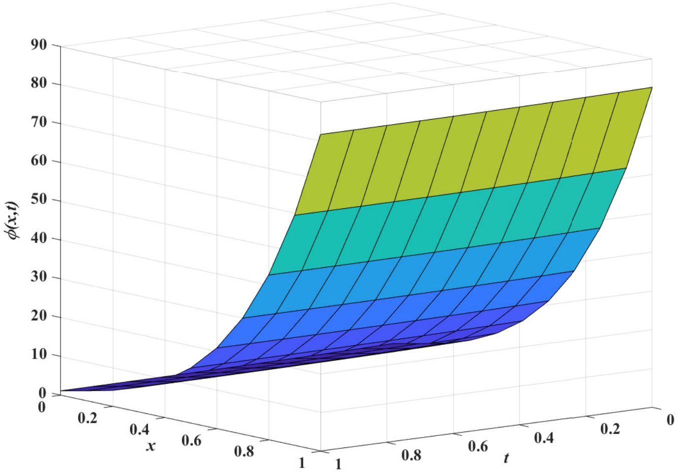

Figure 3: Approximate solution of SFTE (13) for $\alpha = 0.5$

3.2 Solution of TFTE

Take a look at the following TFTE [20],

$$\frac{\partial^{\alpha}\phi(x,t)}{\partial t^{\alpha}}=\frac{\partial^{2}\phi(x,t)}{\partial x^{2}}-\frac{\partial\phi(x,t)}{\partial t}-\phi(x,t),\quad x,t\geq 0,\ 0<\alpha\leq 2 \tag{14}$$

with initial conditions

$$\phi(x,0)=e^{-x},\quad \phi_t(x,0)=-e^{-x}. \tag{15}$$

This equation has the following exact solution for $\alpha=2$,

$$\phi(x,t)=e^{-(x+t)}. \tag{16}$$

The Taylor series expansion for exact solution (16) as below

$$\phi(x,t)=e^{-2t}\left(1-t+\frac{4x^{2}}{2!}+\frac{8x^{3}}{3!}+\cdots\right). \tag{17}$$

The method allows us to arrive at the following solution to Eq. (14),

$$\phi(x,t)=e^{-x}\left(1-t+\frac{t^{\alpha}}{\Gamma(\alpha+1)}-\frac{t^{\alpha+1}}{\Gamma(\alpha+2)}+\frac{t^{2\alpha}}{\Gamma(2\alpha+1)}-\frac{t^{2\alpha+1}}{\Gamma(2\alpha+2)}+\cdots\right). \tag{18}$$

Here, we examine whether the approximation solution for the fractional value of α is convergent. The calculated values of $\phi(x,t)$ for $\alpha=1.7, x=0.1$, and t ranging from 0 to 1 are shown in Table 2. This table indicates that the computed result $\phi(x,t)$ converges up to four places of decimal in the approximation of the tenth term.

The graphical illustration for exact and approximate solutions has been shown. The graph in Fig. 4 has been plotted for the exact solution (16). In Figs. 5 and 6, the surfaces of the graphs show the approximate solutions (18) for $\alpha=1.2$ and 1.7.

Table 2: Convergency chart for the solution of the TFTE.

t	$\phi(x = 0.1, t)$						
	2 terms	3 terms	4 terms	5 terms	6 terms	7 terms	8 terms
0	0.9048374	0.9048374	0.9048374	0.9048374	0.9048374	0.9048374	0.9048374
0.1	0.8426171	0.8499774	0.8482249	0.8485619	0.8485076	0.8485151	0.8485142
0.2	0.7888023	0.8057117	0.8016857	0.8024599	0.8023350	0.8023524	0.8023503
0.3	0.7390122	0.7665189	0.7599697	0.7612292	0.7610260	0.7610542	0.7610508
0.4	0.6920779	0.7309256	0.7216762	0.7234549	0.7231680	0.7232079	0.7232030
0.5	0.6473983	0.6981743	0.6860848	0.6884097	0.6880347	0.6880868	0.6880804
0.6	0.6045998	0.6677937	0.6527476	0.6556410	0.6551744	0.6552392	0.6552313
0.7	0.5634244	0.6394591	0.6213556	0.6248370	0.6242755	0.6243535	0.6243440
0.8	0.5236826	0.6129314	0.5916817	0.5957681	0.5951090	0.5952006	0.5951894
0.9	0.4852285	0.5880266	0.5635508	0.5682577	0.5674985	0.5676040	0.5675911
1.0	0.4479456	0.5645982	0.5368238	0.5421650	0.5413035	0.5414232	0.5414086

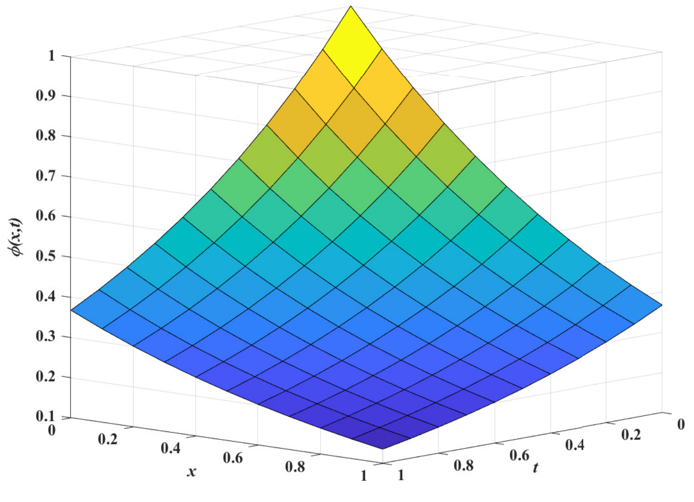

Figure 4: Exact solution of TFTE (16) for $\alpha = 2$

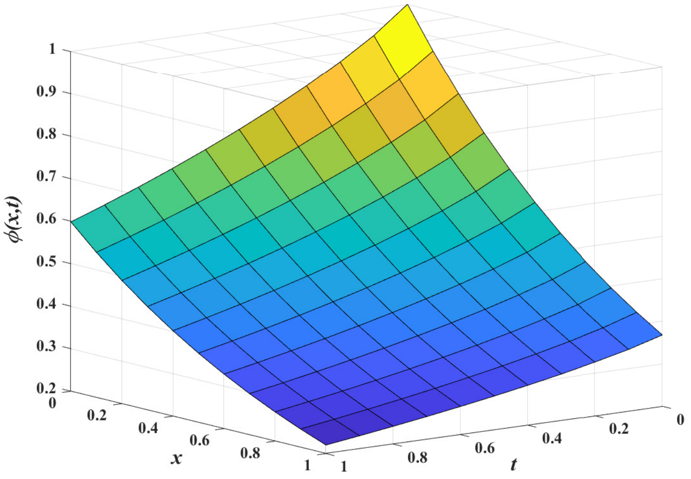

Figure 5: Approximate solution of TFTE (18) for $\alpha = 1.2$

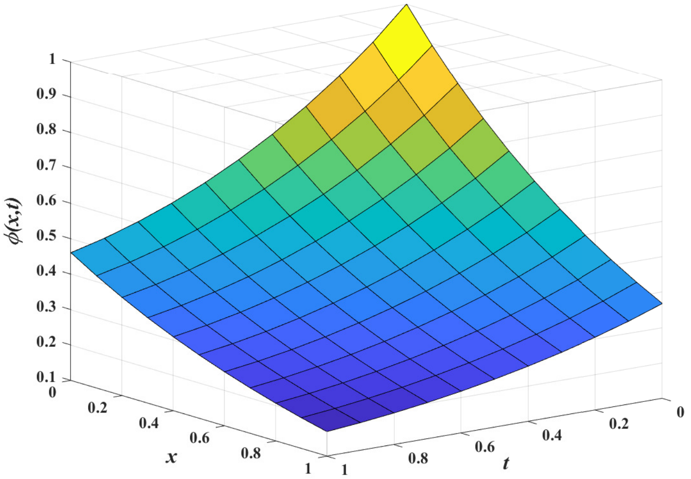

Figure 6: Approximate solution of TFTE (18) for $\alpha = 1.7$

4 Conclusion

If the integer order PDEs have analytical solutions, the Taylor series expansion method works well enough for fractional order PDEs. Numerical examples of this method demonstrate that it may be used to solve any differential equation derived from FDEs with ease and effectiveness, provided that the differential equation has an analytical or approximative solution. By extending the Taylor series expansion of the analytical solution, this study has determined the approximate solutions of the SFTE and TFTE. Furthermore, the infinitive series solution obtained in numerical examples 3.1 and 3.2 is identical to that given in [20], confirming the validity of the considered method. Additionally, the convergency Tables 1 and 2 demonstrate the efficacy of the method. As we can observe that the recorded values in Tables 1 and 2 are being closure enough if the number of terms increases. Furthermore, a graphic illustration is used to show both the exact and approximative solutions for integer and fractional values of α. Using the MATLAB programme, the 3D graphs for the solution of SFTE and TFTE are shown. The discussed method can also be used to analyse ODEs and PDEs with fractional derivatives with exponential and Mittag-Leffler kernels in future iterations of the research.

References

[1] S. Dubey and S. Chakraverty, "Application of modified extended tanh method in solving fractional order coupled wave equations," *Mathematics and Computers in Simulation*, vol. 198, pp. 509–520, 2022.

[2] R. M. Jena, S. Chakraverty, and D. Baleanu, "A novel analytical technique for the solution of time-fractional ivancevic option pricing model," *Physica A: Statistical Mechanics and its Applications*, vol. 550, p. 124380, 2020.

[3] S. Edeki, R. Jena, S. Chakraverty, and D. Baleanu, "Coupled transform method for time-space fractional black-scholes option pricing model," *Alexandria Engineering Journal*, vol. 59, no. 5, pp. 3239–3246, 2020.

[4] E. Zayed, Y. Amer, and R. Shohib, "The fractional complex transformation for nonlinear fractional partial differential equations in the mathematical physics," *Journal of the Association of Arab Universities for Basic and Applied Sciences*, vol. 19, pp. 59–69, 2016.

[5] S. Dubey and S. Chakraverty, "Homotopy perturbation method for solving fuzzy fractional heat-conduction equation," in *Advances in Fuzzy Integral and Differential Equations.* Springer, 2022, pp. 159–169.

[6] S. Momani and A. Yıldırım, "Analytical approximate solutions of the fractional convection–diffusion equation with nonlinear source term by he's homotopy perturbation method," *International Journal of Computer Mathematics*, vol. 87, no. 5, pp. 1057–1065, 2010.

[7] S. Dubey and S. Chakraverty, “Solution of fractional wave equation by homotopy perturbation method,” *Wave Dynamics*, p. 263, 2022.

[8] V. P. Dubey, J. Singh, A. M. Alshehri, S. Dubey, and D. Kumar, “Analysis of local fractional coupled helmholtz and coupled burgers’ equations in fractal media,” *AIMS Mathematics*, vol. 7, no. 5, pp. 8080–8111, 2022.

[9] V. P. Dubey, D. Kumar, H. M. Alshehri, S. Dubey, and J. Singh, “Computational analysis of local fractional lwr model occurring in a fractal vehicular traffic flow,” *Fractal and Fractional*, vol. 6, no. 8, p. 426, 2022.

[10] V. P. Dubey, J. Singh, A. M. Alshehri, S. Dubey, and D. Kumar, “Forecasting the behavior of fractional order bloch equations appearing in nmr flow via a hybrid computational technique,” *Chaos, Solitons & Fractals*, vol. 164, p. 112691, 2022.

[11] V. P. Dubey, D. Kumar, J. Singh, A. M. Alshehri, and S. Dubey, “Analysis of local fractional klein-gordon equations arising in relativistic fractal quantum mechanics,” *Waves in Random and Complex Media*, pp. 1–21, 2022.

[12] D. KUMAR, J. SINGH, and S. KUMAR, “Analytic and approximate solutions of space-time fractional telegraph equations via laplace transform,” *Walailak Journal of Science and Technology (WJST)*, vol. 11, no. 8, pp. 711–728, 2014.

[13] J. Chen, F. Liu, and V. Anh, “Analytical solution for the time-fractional telegraph equation by the method of separating variables,” *Journal of Mathematical Analysis and Applications*, vol. 338, no. 2, pp. 1364–1377, 2008.

[14] E. Orsingher and X. Zhao, “The space-fractional telegraph equation and the related fractional telegraph process,” *Chinese Annals of Mathematics*, vol. 24, no. 01, pp. 45–56, 2003.

[15] E. Orsingher and L. Beghin, “Time-fractional telegraph equations and telegraph processes with brownian time,” *Probability Theory and Related Fields*, vol. 128, no. 1, pp. 141–160, 2004.

[16] A. Sevimlican, “An approximation to solution of space and time fractional telegraph equations by he’s variational iteration method,” *Mathematical Problems in Engineering*, vol. 2010, 2010.

[17] A. Yıldırım, “He’s homotopy perturbation method for solving the space-and time-fractional telegraph equations,” *International Journal of Computer Mathematics*, vol. 87, no. 13, pp. 2998–3006, 2010.

[18] J. Biazar and M. Eslami, “Analytic solution for telegraph equation by differential transform method,” *Physics Letters A*, vol. 374, no. 29, pp. 2904–2906, 2010.

[19] A. Demir, S. Erman, B. Özgür, and E. Korkmaz, “Analysis of fractional partial differential equations by taylor series expansion,” *Boundary Value Problems*, vol. 2013, no. 1, pp. 1–12, 2013.

[20] S. Dubey and S. Chakraverty, “Hybrid techniques for approximate analytical solution of space-and time-fractional telegraph equations,” *Pramana*, vol. 97, no. 1, pp. 1–13, 2023.

J. COMPUTATIONAL ANALYSIS AND APPLICATIONS, VOL. 31, NO.1, 2023, COPYRIGHT 2023 EUDOXUS PRESS, LLC

An $M/G/1$ Feedback retrial queue with working vacation and a waiting server

S.Pazhani Bala Murugan[1] and R.Keerthana[2]
[1,2]Department of Mathematics, Annamalai University,
Annamalainagar-608002, Tamilnadu, India.
*Corresponding Author E-Mail: spbm1966@gmail.com

December 27, 2022

Abstract

An $M/G/1$ feedback retrial queue with working vacation and a waiting server is taken into consideration in this study. Both retrial times and service times are assumed to follow general distribution and the waiting server follows an exponential distribution. During the working vacation period customers are served at a lesser rate of service. Before going for a vacation the server waits for some arbitrary amount of time and so is called a waiting server. We obtain the probability generating function (PGF) for the number of customers and the mean number of customers in the invisible waiting area by utilizing the supplementary variable technique. We compute the mean waiting time. Out of interest a few special cases are conferred. Numerical outcomes are exhibited.

Keywords: Retrial queue, Working vacation, Supplementary variable technique, Waiting server, Feedback.

Mathematics Subject Classification 2010: 60K25, 90B22

1 Introduction

Retrial queues are expressed by the fact that if a customer observed that the server is occupied then they are entered into the invisible waiting area called an orbit. In recent years numerous researchers have examined the retrial queue. For a more in-depth analysis of the retrial queues, we can refer[1,2,3].

In Queueing theory queueing models with server vacation has a most impactful application. In addition to the vacation strategy Servi and Finn [4] developed a newest vacation strategy, called as Working Vacation (WV). In the WV period the server provides a lesser rate of service to the customers than during the regular service period. Wu and Takagi [5] examined M/G/1/Multiple Working

Vacation (MWV). Pazhani Bala Murugan and Santhi[7] studied the $M/G/1$ retrial queue with MWV. For a comprehensive study on WV we can refer [8]. Whenever the system becomes empty the server leaves from the regular service period (RS) and goes on a WV, but in a waiting server model the server wait for a arbitrary amount of time before going to WV.

The server wait option is representative of many queueing mechanisms used in real life, especially when interacting with people. For a detailed study on waiting server model we can refer [9,10,11]. In queueing models, some customers rejoin the orbit after receiving the service to receive it again out of dissatisfaction. This is referred to as feedback. For a broad analysis of feedback retrial queues we can refer[12,13,14,15].

In this article, we consider an $M/G/1$ feedback retrial queue with multiple WV and a waiting server. This article has the following structure. We explain the model in segment 2. In segment 3 performance measures are established. Segment 4 discusses some special cases. In segment 5 numerical outcomes are exhibited . The conclusion is given in segment 6.

2 Model Description

We examined an $M/G/1$ retrial queue with switch over time to working vacation where the primary customer's arrival follows a Poisson process with a rate of λ and service discipline is first-in-first-out(FIFO). If an approaching customer discovers that the server is occupied, then they exit the service area because we assume that there is no waiting area and they join the orbit. At a service completion instant, only the customer at the head of the orbit is permitted to approach the server. The retrial time follows a general distribution with a distribution function G(x) for the regular service period, let $g(x)$ and $G^*(\theta)$ signifies the pdf and LST respectively, and for WV period, let $L(x), l(x), L^*(\theta)$ signifies the distribution function, pdf and LST respectively. On the service completion epoch of each customer, if there is a contest between the primary customer and an orbit customer. The service time in the RS period follows a general distribution with the distribution function $R_s(x), r_s(x)$ and $R_s^*(\theta)$ as its pdf and LST respectively. The service delivered in the WV period follows a general distribution with $W_v(x), w_v(x), W_v^*(\theta)$ as its distribution function, pdf, LST. The server waits for an arbitrary period of time once the orbit turns empty, which follows an exponential distribution with a rate of α. After completion of the waiting time, the server goes for WV, which follows an exponential distribution with a rate of β. After getting the service, customers either rejoin the orbit with probability m or depart the system with probability $n(= 1 - m)$. Inter-arrival times, retrial times, service time in RS periods and WV periods are all presumed to be independent of one another.

Let's use the subsequent random variables.

$O(t)$- Size of the orbit at time "t".

$G^0(t), R_s^0(t)$- the remaing retrial time and remaining service time in RS period.

$L^0(t), W_v^0(t)$- the remaing retrial time and remaining service time in WV period.

At time "t" the four distinct states of the server are

$$E(t) = \begin{cases} 0 \text{ - if the server is not being occupied in WV} \\ 1 \text{ - if the server is not being occupied in RS period} \\ 2 \text{ - if the server is being occupied in WV} \\ 3 \text{ - if the server is being occupied in RS period} \end{cases}$$

so that the supplementary variables $L^0(t), G^0(t), W_v^0(t)$ and $R_s^0(t)$ are introduced in order to obtain the bivariate Markov Processes $\{(O(t), B(t)); t \geq 0\}$, where

$$B(t) = \begin{cases} L^0(t), & \text{if } E(t) = 0; \\ G^0(t), & \text{if } E(t) = 1; \\ W_v^0(t), & \text{if E(t)=2;} \\ R_s^0(t), & \text{if E(t)=3.} \end{cases}$$

$$\begin{aligned}
W_{0,0} &= \lim_{t\to\infty} P[O(t) = 0,\ E(t) \ = 0] \\
R_{0,0} &= \lim_{t\to\infty} P[O(t) = 0,\ E(t) \ = 1] \\
W_{0,h} &= \lim_{t\to\infty} P[O(t) = h,\ E(t) \ = 0,\ x < L^0(t) \ \leq x + dx];\ h \geq 1 \\
R_{0,h} &= \lim_{t\to\infty} P[O(t) = h,\ E(t) \ = 1,\ x < G^0(t) \ \leq x + dx];\ h \geq 1 \\
W_{1,h} &= \lim_{t\to\infty} P[O(t) = h,\ E(t) \ = 2,\ x < W_v^0(t) \ \leq x + dx];\ h \geq 0 \\
R_{1,h} &= \lim_{t\to\infty} P[O(t) = h,\ E(t) \ = 3,\ x < R_s^0(t) \ \leq x + dx];\ h \geq 0
\end{aligned}$$

The above mentioned are the limiting probabilities which we have defined.

$$R_s^*(\theta) = \int_0^\infty e^{-\theta x} r_s(x)dx \qquad W_v^*(\theta) = \int_0^\infty e^{-\theta x} w_v(x)dx$$

$$L^*(\theta) = \int_0^\infty e^{-\theta x} l(x)dx \qquad G^*(\theta) = \int_0^\infty e^{-\theta x} g(x)dx$$

$$W_{0,h}^*(\theta) = \int_0^\infty e^{-\theta x} W_{0,h}(x)dx \qquad W_{0,h}^*(0) = \int_0^\infty W_{0,h}(x)dx$$

$$W_{1,h}^*(\theta) = \int_0^\infty e^{-\theta x} W_{1,h}(x)dx \qquad W_{1,h}^*(0) = \int_0^\infty W_{1,h}(x)dx$$

$$R_{0,h}^*(\theta) = \int_0^\infty e^{-\theta x} R_{0,h}(x)dx \qquad R_{0,h}^*(0) = \int_0^\infty R_{0,h}(x)dx$$

$$R_{1,h}^*(\theta) = \int_0^\infty e^{-\theta x} R_{1,h}(x)dx \qquad R_{1,h}^*(0) = \int_0^\infty R_{1,h}(x)dx$$

$$
\begin{aligned}
W_0^*(z,\theta) &= \sum_{h=1}^{\infty} W_{0,h}^*(\theta) z^h & W_0^*(z,0) &= \sum_{h=1}^{\infty} W_{0,h}^*(0) z^h \\
W_0(z,0) &= \sum_{h=1}^{\infty} W_{0,h}(0) z^h & W_1^*(z,\theta) &= \sum_{h=0}^{\infty} W_{1,h}^*(\theta) z^h \\
W_1^*(z,0) &= \sum_{h=0}^{\infty} W_{1,h}^*(0) z^h & W_1(z,0) &= \sum_{h=0}^{\infty} W_{1,h}(0) z^h \\
R_0^*(z,\theta) &= \sum_{h=1}^{\infty} R_{0,h}^*(\theta) z^h & R_0^*(z,0) &= \sum_{h=1}^{\infty} R_{0,h}^*(0) z^h \\
R_0(z,0) &= \sum_{h=1}^{\infty} R_{0,h}(0) z^h & R_1^*(z,\theta) &= \sum_{h=0}^{\infty} R_{1,h}^*(\theta) z^h \\
R_1^*(z,0) &= \sum_{h=0}^{\infty} R_{1,h}^*(0) z^h & R_1(z,0) &= \sum_{h=0}^{\infty} R_{1,h}(0) z^h
\end{aligned}
$$

The above mentioned are the Laplace Steiltjes Transform and PGF which we have defined.
In steady state the system was illustrated by the subsequent differential difference equations:

$$
\begin{aligned}
\lambda W_{0,0} &= nW_{1,0}(0) + \alpha R_{0,0} & (1) \\
-\frac{d}{dx} W_{0,h}(x) &= -(\beta+\lambda) W_{0,h}(x) + nW_{1,h}(0) l(x) \\
&\quad + mW_{1,h-1}(0) l(x); \quad h \geq 1 & (2) \\
-\frac{d}{dx} W_{1,0}(x) &= -(\lambda+\beta) W_{1,0}(x) + W_{0,1}(0) w_v(x) + \lambda W_{0,0} w_v(x) & (3) \\
-\frac{d}{dx} W_{1,h}(x) &= -(\lambda+\beta) W_{1,h}(x) + \lambda W_{1,h-1}(x) + W_{0,h+1}(0) w_v(x) \\
&\quad + \lambda \int_0^{\infty} W_{0,h}(x) dx \; w_v(x); h \geq 1 & (4) \\
(\lambda+\alpha) R_{0,0} &= nR_{1,0}(0) & (5) \\
-\frac{d}{dx} R_{0,h}(x) &= -\lambda R_{0,h}(x) + nR_{1,h}(0) g(x) + mR_{1,h-1}(0) g(x) \\
&\quad + \beta \int_0^{\infty} W_{0,h}(x) dx \; g(x); \quad h \geq 1 & (6) \\
-\frac{d}{dx} R_{1,0}(x) &= -\lambda R_{1,0}(x) + R_{0,1}(0) r_s(x) + \beta r_s(x) \int_0^{\infty} W_{1,0}(x) dx & (7)
\end{aligned}
$$

$$\begin{aligned}-\frac{d}{dx}R_{1,h}(x) &= -\lambda R_{1,h}(x)+\lambda R_{1,h-1}(x)+\beta r_s(x)\int\limits_0^\infty W_{1,h}(x)dx\\ &\quad +R_{0,h+1}(0)r_s(x)+\lambda r_s(x)\int\limits_0^\infty R_{0,h}(x)dx;\quad h\geq 1 \qquad (8)\end{aligned}$$

Taking the LST from (2) to (8) on both sides results

$$\begin{aligned}\theta W^*_{0,h}(\theta)-W_{0,h}(0) &= (\lambda+\beta)W^*_{0,h}(\theta)-nW_{1,h}(0)L^*(\theta)\\ &\quad -mW_{1,h-1}(0)L^*(\theta);\quad h\geq 1 \qquad (9)\end{aligned}$$

$$\begin{aligned}\theta W^*_{1,0}(\theta)-W_{1,0}(0) &= (\lambda+\beta)W^*_{1,0}(\theta)-W_{0,1}(0)W^*_v(\theta)\\ &\quad -\lambda W_{0,0}W^*_v(\theta) \qquad (10)\end{aligned}$$

$$\begin{aligned}\theta W^*_{1,h}(\theta)-W_{1,h}(0) &= (\lambda+\beta)W^*_{1,h}(\theta)-W_{0,h+1}(0)W^*_v(\theta)\\ &\quad -\lambda W^*_{1,h-1}(\theta)-\lambda W^*_{0,h}(0)W^*_v(\theta);\quad h\geq 1 \qquad (11)\end{aligned}$$

$$\begin{aligned}\theta R^*_{0,h}(\theta)-R_{0,h}(0) &= \lambda R^*_{0,h}(\theta)-nR_{1,h}(0)G^*(\theta)-\beta G^*(\theta)W^*_{0,h}(0)\\ &\quad -mR_{1,h-1}(0)G^*(\theta);\quad h\geq 1 \qquad (12)\end{aligned}$$

$$\begin{aligned}\theta R^*_{1,0}(\theta)-R_{1,0}(0) &= \lambda R^*_{1,0}(\theta)-R_{0,1}(0)R^*_s(\theta)-\beta R^*_s(\theta)W^*_{1,0}(0)\\ &\quad -\lambda R_{0,0}R^*_s(\theta) \qquad (13)\end{aligned}$$

$$\begin{aligned}\theta R^*_{1,h}(\theta)-R_{1,h}(0) &= \lambda R^*_{1,h}(\theta)-\lambda R^*_{1,h-1}(\theta)-R^*_s(\theta)R_{0,h+1}(0)\\ &\quad -\beta R^*_s(\theta)W^*_{1,h}(0)-\lambda R^*_s(\theta)R^*_{0,h}(0);\quad h\geq 1 \qquad (14)\end{aligned}$$

Summing over h from 1 to infinity $\times$ (9) with z^h and results,

$$\begin{aligned}W^*_0(z,\theta)[\theta-(\lambda+\beta)] &= W_0(z,0)-L^*(\theta)[(n+mz)W_1(z,0)\\ &\quad -nW_{1,0}(0)] \qquad (15)\end{aligned}$$

Summing over h from 1 to infinity $\times$ (11) with z^h and comprise with (10) results,

$$\begin{aligned}W^*_1(z,\theta)[\theta-(\lambda+\beta-\lambda z)] &= W_1(z,0)-\frac{W^*_v(\theta)}{z}W_0(z,0)\\ &\quad -\lambda W_{0,0}W^*_v(\theta)-\lambda W^*_v(\theta)W^*_0(z,0) \qquad (16)\end{aligned}$$

Placing $\theta=\lambda+\beta$ in (15), results

$$W_0(z,0) = L^*(\lambda+\beta)[(n+mz)W_1(z,0)-nW_{1,0}(0)] \qquad (17)$$

Placing $\theta=0$ and (Sub.) (17) in (15), results

$$W^*_0(z,0) = \frac{(1-L^*(\lambda+\beta))((n+mz)W_1(z,0)-nW_{1,0}(0))}{\lambda+\beta} \qquad (18)$$

Placing $\theta = \lambda + \beta - \lambda z$ and (Sub.) (17) and (18) in (16), results

$$W_1(z,0) = \frac{\begin{bmatrix} [\lambda z(\lambda+\beta)W_{0,0} - n[L^*(\lambda+\beta)(\lambda+\beta-\lambda z) \\ \hfill +\lambda z]W_{1,0}(0)]W_v^*(\lambda+\beta-\lambda z) \end{bmatrix}}{Dr_1(z)} \tag{19}$$

(Sub.)(19) in (17), results

$$W_0(z,0) = \frac{\begin{bmatrix} (\lambda+\beta)z[(n+mz)\lambda W_v^*(\lambda+\beta-\lambda z)W_{0,0} \\ \hfill -nW_{1,0}(0)]L^*(\lambda+\beta) \end{bmatrix}}{Dr_1(z)} \tag{20}$$

Let $f(z) = (\lambda+\beta)z - W_v^*(\lambda+\beta-\lambda z)(L^*(\lambda+\beta)(\lambda+\beta-\lambda z)+\lambda z)$, for $f(z) = 0$ we obtain $f(0) < 0$ and $f(1) > 0$ which $\Rightarrow$ that $\exists$ a real root $z_1 \in (0,1)$.
At $z = z_1$(20) is converted in to

$$W_{1,0}(0) = \lambda W_v^*(\lambda - \lambda z_1 + \beta)(n+mz)W_{0,0} \tag{21}$$

(Sub.) (21) in (19), results

$$W_1(z,0) = \frac{\lambda W_v^*(\lambda+\beta-\lambda z)UP(z)}{Dr_1(z)}W_{0,0} \tag{22}$$

where,

$$UP(z) = z(\lambda+\beta) - (n+mz)W_v^*(\lambda+\beta-\lambda z_1)[\lambda z + L^*(\lambda+\beta)(\lambda+\beta-\lambda z)]$$

(Sub.) (21) in (20), results

$$W_0(z,0) = \frac{\begin{bmatrix} \begin{bmatrix} (n+mz)\lambda z(\lambda+\beta)[W_v^*(\lambda+\beta-\lambda z) \\ \hfill -W_v^*(\lambda-\lambda z_1+\beta)] \end{bmatrix} L^*(\lambda+\beta) \end{bmatrix}}{Dr_1(z)} \tag{23}$$

(Sub.) (21) and (22) in (18), results

$$W_0^*(z,0) = \frac{\begin{bmatrix} \begin{bmatrix} (1-L^*(\lambda+\beta))\lambda z(n+mz)[W_v^*(\lambda+\beta-\lambda z) \\ \hfill -W_v^*(\lambda+\beta-\lambda z_1)] \end{bmatrix} \end{bmatrix}}{Dr_1(z)} \tag{24}$$

Placing $\theta = 0$ and (Sub.) (22), (23) and (24) in (16), results

$$W_1^*(z,0) \ = \ \frac{W_{0,0}\lambda(1-W_v^*(\lambda+\beta-\lambda z))UP(z)}{(\lambda+\beta-\lambda z)Dr_1(z)} \tag{25}$$

Summing over h from 1 to infinity × (12) with z^h and results

$$\begin{aligned} R_0^*(z,\theta)(\theta-\lambda) &= R_0(z,0)-G^*(\theta)[(n+mz)R_1(z,0)-nR_{1,0}(0)] \\ &\quad -W_0^*(z,0)\beta G^*(\theta) \end{aligned} \tag{26}$$

(Sub.) $W_{1,0}(0)=(n+mz)\lambda W_v^*(\lambda+\beta-\lambda z_1)W_{0,0}$ in (1), we get

$$\alpha R_{0,0} = \lambda(1-(n+mz)W_v^*(\lambda+\beta-\lambda z_1))W_{0,0}$$

Placing $\theta=\lambda$ and (Sub.) $R_{1,0}(0)=\lambda(1-(n+mz)W_v^*(\lambda+\beta-\lambda z_1))W_{0,0}-\lambda R_{0,0}$ in (26), results

$$\begin{aligned} R_0(z,0) &= [(n+mz)R_1(z,0)-\lambda(1-(n+mz)W_v^*(\lambda+\beta-\lambda z_1))W_{0,0} \\ &\quad -\lambda R_{0,0}+\beta W_0^*(z,0)]G^*(\lambda) \end{aligned} \tag{27}$$

Summing over h from 1 to infinity × (14) with z^h and comprise with (13) results

$$R_1^*(z,\theta)[\theta-\lambda+\lambda z]=R_1(z,0)-\left[\frac{R_0(z,0)}{z}+\beta W_1^*(z,0)+\lambda R_0^*(z,0)+\lambda R_{0,0}\right]R_s^*(\theta) \tag{28}$$

Placing $\theta\ =0$ and (Sub.) (27) and $nR_{1,0}(0)=(1-(n+mz)W_v^*(\lambda+\beta-\lambda z_1))\lambda W_{0,0}-\lambda R_{0,0}$ in (26), results

$$\begin{aligned} R_0^*(z,0) &= \Big[(n+mz)R_1(z,0)-(1-(n+mz)W_v^*(\lambda+\beta-\lambda z_1))\lambda W_{0,0} \\ &\quad -\lambda R_{0,0}+\beta W_0^*(z,0)\Big]\Big[\frac{(1-G^*(\lambda))}{\lambda}\Big] \end{aligned} \tag{29}$$

Placing $\theta\ =\lambda-\lambda z$ and (Sub.) (27) and (29) in (28), results

$$R_1(z,0)=\frac{\left[\begin{array}{r} R_s^*(\lambda-\lambda z)\Big[\beta zW_1^*(z,0)+\beta[(1-z)G^*(\lambda)+z]W_0^*(z,0) \\ -[(1-(n+mz)W_v^*(\lambda+\beta-\lambda z_1))\lambda W_{0,0}+\lambda R_{0,0}] \\ [(1-z)G^*(\lambda)+z]+\lambda zR_{0,0}\Big] \end{array}\right]}{z-(n+mz)R_s^*(\lambda-\lambda z)[z+G^*(\lambda)(1-z)]} \tag{30}$$

(Sub.) (30) in (27), results

$$R_0(z,0)=\frac{\left[\begin{array}{r} zG^*(\lambda)\ \Big[\beta(n+mz)R_s^*(\lambda-\lambda z)W_1^*(z,0)+\beta W_0^*(z,0) \\ -\lambda(1-(n+mz)W_v^*(\lambda+\beta-\lambda z_1))W_{0,0} \\ -\lambda(1-(n+mz)R_s^*(\lambda-\lambda z))R_{0,0}\Big] \end{array}\right]}{z-(n+mz)R_s^*(\lambda-\lambda z)\big[(1-z)G^*(\lambda)+z\big]} \tag{31}$$

(Sub.) (30) in (29), results

$$R_0^*(z,0) = \frac{\begin{bmatrix}(1-G^*(\lambda))z\ [\beta W_1^*(z,0)(n+mz)R_s^*(\lambda-\lambda z)+\beta W_0^*(z,0) \\ \qquad -\lambda(1-(n+mz)W_v^*(\lambda+\beta-\lambda z_1))W_{0,0} \\ \qquad -\lambda(1-(n+mz)R_s^*(\lambda-\lambda z))R_{0,0}]\end{bmatrix}}{\lambda\big\{z-(n+mz)R_S^*(\lambda-\lambda z)\big[(1-z)G^*(\lambda)+z\big]\big\}} \tag{32}$$

Placing $\theta = 0$ and (Sub.) (30), (31) and (32) in (28), results

$$R_1^*(z,0) = \frac{\begin{bmatrix}\Big\{W_0^*(z,0)[G^*(\lambda)(1-z)+z]\beta+\lambda z R_{0,0}-[G^*(\lambda)(1-z)+z] \\ \qquad \times[\lambda(1-(n+mz)W_v^*(\lambda+\beta-\lambda z_1))W_{0,0}+\lambda R_{0,0}] \\ \qquad +\beta W_1^*(z,0)z\Big\}(1-R_s^*(\lambda-\lambda z))\end{bmatrix}}{(\lambda-\lambda z)\ \Big[\ z-(n+mz)R_s^*(\lambda-\lambda z)[z+G^*(\lambda)(1-z)]\Big]} \tag{33}$$

We define $W_v(z) = W_0^*(z,0) + W_1^*(z,0) + W_{0,0}$

$$\begin{aligned}W_v(z) =& \frac{W_{0,0}}{(\lambda+\beta-\lambda z)D_1(z)}\Big\{\lambda z(W_v^*(\lambda+\beta-\lambda z)-W_v^*(\lambda+\beta-\lambda z_1)) \\ &\times(\lambda+\beta-\lambda z)(1-L^*(\lambda+\beta))+\lambda(1-W_v^*(\lambda+\beta-\lambda z)) \\ &\times[z(\lambda+\beta)-[\lambda z+L^*(\lambda+\beta)(\lambda+\beta-\lambda z)]W_v^*(\lambda+\beta-\lambda z_1) \\ &\times(n+mz)]+(\lambda+\beta-\lambda z)[z(\lambda+\beta)-(n+mz)W_v^*(\lambda+\beta-\lambda z) \\ &\times(\lambda z+L^*(\lambda+\beta)(\lambda+\beta-\lambda z))]\Big\}\end{aligned} \tag{34}$$

when the server is on WV period, as the PGF for the number of customers in orbit.
(Sub.) (24) and (25) in (32), results

$$\begin{aligned}R_0^*(z,0) =& \frac{z(1-G^*(\lambda))W_{0,0}}{(\lambda+\beta-\lambda z)Dr_1(z)Dr_2(z)}\Big\{\beta(n+mz)(1-W_v^*(\lambda+\beta-\lambda z)) \\ &\times R_s^*(\lambda-\lambda z)\big\{(\lambda+\beta)z-(n+mz)W_v^*(\lambda+\beta-\lambda z_1)[\lambda z \\ &+(\lambda+\beta-\lambda z)L^*(\lambda+\beta)]\big\}+\beta z(\lambda+\beta-\lambda z)(1-L^*(\lambda+\beta)) \\ &\times(n+mz)(W_v^*(\lambda+\beta-\lambda z)-W_v^*(\lambda+\beta-\lambda z_1))-(\lambda+\beta-\lambda z) \\ &\times(1-(n+mz)W_v^*(\lambda+\beta-\lambda z_1))\big\{(\lambda+\beta)z-W_v^*(\lambda+\beta-\lambda z) \\ &\times(n+mz)[\lambda z+(\lambda+\beta-\lambda z)L^*(\lambda+\beta)]\big\}-\frac{\lambda}{\alpha}(\lambda+\beta-\lambda z) \\ &\times(1-(n+mz)W_v^*(\lambda+\beta-\lambda z_1))(1-(n+mz)R_s^*(\lambda-\lambda z)) \\ &\times\big\{(\lambda+\beta)z-W_v^*(\lambda+\beta-\lambda z)[\lambda z+(\lambda+\beta-\lambda z)L^*(\lambda+\beta)]\big\}\Big\}\end{aligned} \tag{35}$$

(Sub.) (24), (25) in (33), results

$$
\begin{aligned}
R_1^*(z,0) \quad = \quad & \frac{(1-R_s^*(\lambda-\lambda z))W_{0,0}}{Dr_2(z)(\lambda+\beta-\lambda z)Dr_1(z)}\Big\{[\lambda z+G^*(\lambda)(\lambda+\beta-\lambda z)](n+mz) \\
& \times[1-L^*(\lambda+\beta)][W_v^*(\lambda+\beta-\lambda z)-W_v^*(\beta+\lambda-\lambda z_1)]\beta z \\
& -(1-(n+mz)W_v^*(\lambda+\beta-\lambda z_1))[\lambda z+G^*(\lambda)(\lambda+\beta-\lambda z)] \\
& \times\big\{(\lambda+\beta)z-(n+mz)W_v^*(\lambda+\beta-\lambda z)[\lambda z+(\lambda+\beta-\lambda z) \\
& \times L^*(\lambda+\beta)]\big\}+(W_v^*(\lambda+\beta-\lambda z)-W_v^*(\lambda+\beta-\lambda z_1))\beta z \\
& \times(\lambda+\beta)L^*(\lambda+\beta)-\frac{\lambda}{\alpha}(1-(n+mz)W_v^*(\lambda+\beta-\lambda z_1))G^*(\lambda) \\
& \times(\lambda+\beta-\lambda z)\big\{(\lambda+\beta)z-[\lambda z+(\lambda+\beta-\lambda z)L^*(\lambda+\beta)] \\
& \times W_v^*(\lambda+\beta-\lambda z)(n+mz)\big\}+m\Big[[\lambda\beta z^2W_v^*(\lambda+\beta-\lambda z_1) \\
& +\beta^2zW_v^*(\lambda+\beta-\lambda z_1)W_v^*(\lambda+\beta-\lambda z)L^*(\lambda+\beta) \\
& \times+W_v^*(\lambda+\beta-\lambda z_1)\lambda\beta zL^*(\lambda+\beta)W_v^*(\lambda+\beta-\lambda z)(1-z)] \\
& \times(n+mz)-[\beta^2z^2+\lambda\beta z^2]W_v^*(\lambda+\beta-\lambda z)\Big]\Big\}
\end{aligned}
\tag{36}
$$

We define $R_S(z)=R_0^*(z,0)+R_1^*(z,0)+R_{0,0}$

$$
\begin{aligned}
R_S(z) \quad = \quad & \frac{W_{0,0}}{(\lambda+\beta-\lambda z)(Dr_1(z)Dr_2(z))}\Bigg\{z(1-G^*(\lambda))\Big\{(1-W_v^*(\lambda+\beta-\lambda z)) \\
& \times R_s^*(\lambda-\lambda z)\beta(n+mz)\Big[(\lambda+\beta)z-(n+mz)W_v^*(\lambda+\beta-\lambda z_1) \\
& \times[\lambda z+(\lambda+\beta-\lambda z)L^*(\lambda+\beta)]\Big]+\beta z(1-L^*(\lambda+\beta))(\lambda+\beta-\lambda z) \\
& \times(n+mz)(W_v^*(\lambda+\beta-\lambda z)-W_v^*(\lambda+\beta-\lambda z_1))-(\lambda+\beta-\lambda z) \\
& \times(1-(n+mz)W_v^*(\lambda+\beta-\lambda z_1))\Big[(\lambda+\beta)z-W_v^*(\lambda+\beta-\lambda z) \\
& \times[\lambda z+(\lambda+\beta-\lambda z)L^*(\lambda+\beta)](n+mz)\Big]\Big\}+(1-R_s^*(\lambda-\lambda z)) \\
& \times\Big\{[\lambda z+(\lambda+\beta-\lambda z)G^*(\lambda)][W_v^*(\lambda+\beta-\lambda z)-W_v^*(\lambda+\beta-\lambda z_1)] \\
& \times\beta z(n+mz)[1-L^*(\lambda+\beta)]-(1-(n+mz)W_v^*(\lambda+\beta-\lambda z_1)) \\
& \times[\lambda z+G^*(\lambda)(\lambda+\beta-\lambda z)][(\lambda+\beta)z-(n+mz)W_v^*(\lambda+\beta-\lambda z) \\
& \times[\lambda z+L^*(\lambda+\beta)(\lambda+\beta-\lambda z)]]+\beta z(\lambda+\beta)(W_v^*(\lambda+\beta-\lambda z) \\
& -W_v^*(\lambda+\beta-\lambda z_1))L^*(\lambda+\beta)\Big\}+m\Big[[\beta^2zW_v^*(\lambda+\beta-\lambda z_1) \\
& \times W_v^*(\lambda+\beta-\lambda z)L^*(\lambda+\beta)+\lambda\beta z^2W_v^*(\lambda+\beta-\lambda z_1)+(1-z) \\
& \times\lambda\beta zW_v^*(\lambda+\beta-\lambda z_1)L^*(\lambda+\beta)](n+mz)-[\beta^2z^2+\lambda\beta z^2] \\
& \times W_v^*(\lambda+\beta-\lambda z)\Big]+\frac{\lambda}{\alpha}(\lambda+\beta-\lambda z)(1-W_v^*(\lambda+\beta-\lambda z_1)) \\
& \times(n+mz)[(\lambda+\beta)z-(n+mz)W_v^*(\lambda+\beta-\lambda z)[\lambda z+L^*(\lambda+\beta) \\
& \times(\lambda+\beta-\lambda z)][mG^*(\lambda)R_s^*(\lambda-\lambda z)-G^*(\lambda)](1-z)\Bigg\}
\end{aligned}
\tag{37}
$$

where,

$$\begin{aligned} Dr_1(z) &= z(\lambda+\beta)-(n+mz)W_v^*(\lambda+\beta-\lambda z)[\lambda z \\ &\quad +L^*(\lambda+\beta)(\lambda+\beta-\lambda z)] \qquad (38) \\ Dr_2(z) &= z-(n+mz)R_s^*(\lambda-\lambda z)[G^*(\lambda)(1-z)+z] \qquad (39) \end{aligned}$$

when the server is on RS period, as the PGF for the number of customers in the orbit.
Again, we define $R(z) = R_S(z) + W_v(z)$

$$\begin{aligned} R(z) &= \frac{W_{0,0}}{(\lambda+\beta-\lambda z)D_1(z)D_2(z)}\Bigg\{z(1-G^*(\lambda))\Big[(1-W_v^*(\lambda+\beta-\lambda z))\beta \\ &\quad \times(n+mz)R_s^*(\lambda-\lambda z)\big[(\lambda+\beta)z-(n+mz)W_v^*(\lambda+\beta-\lambda z_1)[\lambda z \\ &\quad +(\lambda+\beta-\lambda z)L^*(\lambda+\beta)]\big]+\beta z(\lambda-\lambda z)(n+mz)(1-L^*(\lambda+\beta)) \\ &\quad \times(W_v^*(\lambda+\beta-\lambda z)-W_v^*(\lambda+\beta-\lambda z_1))-(\lambda+\beta-\lambda z)(1-(n+mz) \\ &\quad \times W_v^*(\lambda+\beta-\lambda z_1))\big[(\lambda+\beta)z-(n+mz)W_v^*(\lambda+\beta-\lambda z)[L^*(\lambda+\beta) \\ &\quad \times(\lambda+\beta-\lambda z)+\lambda z]\big]\Big]+(1-R_s^*(\lambda-\lambda z))\Big[[\lambda z+(\lambda+\beta-\lambda z)G^*(\lambda)] \\ &\quad \times\beta z(n+mz)[1-L^*(\lambda+\beta)][W_v^*(\lambda+\beta-\lambda z)-W_v^*(\lambda+\beta-\lambda z_1)] \\ &\quad -(1-(n+mz)W_v^*(\lambda+\beta-\lambda z_1))[\lambda z+G^*(\lambda)(\lambda+\beta-\lambda z)]\big[(\lambda+\beta)z \\ &\quad -(n+mz)W_v^*(\lambda+\beta-\lambda z)[\lambda z+(\lambda+\beta-\lambda z)L^*(\lambda+\beta)]\big]+(\lambda+\beta) \\ &\quad \times\beta z(W_v^*(\lambda+\beta-\lambda z))-W_v^*(\lambda+\beta-\lambda z_1))L^*(\lambda+\beta)+m\Big\{[\lambda\beta z^2 \\ &\quad \times W_v^*(\lambda+\beta-\lambda z_1)+\beta^2 zW_v^*(\lambda+\beta-\lambda z_1)W_v^*(\lambda+\beta-\lambda z)L^*(\lambda+\beta) \\ &\quad +W_v^*(\lambda+\beta-\lambda z_1)\lambda\beta zW_v^*(\lambda+\beta-\lambda z)L^*(\lambda+\beta)(1-z)](n+mz) \\ &\quad -[\beta^2z^2+\lambda\beta z^2]W_v^*(\lambda+\beta-\lambda z)\Big]+\frac{\lambda}{\alpha}(\lambda+\beta-\lambda z)(1-(n+mz) \\ &\quad \times W_v^*(\lambda+\beta-\lambda z_1))[(\lambda+\beta)z-(n+mz)W_v^*(\lambda+\beta-\lambda z)[\lambda z \\ &\quad +(\lambda+\beta-\lambda z)L^*(\lambda+\beta)][mG^*(\lambda)R_s^*(\lambda-\lambda z)-G^*(\lambda)](1-z)\big] \\ &\quad +\Big[(\lambda+\beta-\lambda z)(W_v^*(\lambda+\beta-\lambda z)-W_v^*(\lambda+\beta-\lambda z_1))(1-L^*(\lambda+\beta)) \\ &\quad \times\lambda z+\lambda(1-W_v^*(\lambda+\beta-\lambda z))[z(\lambda+\beta)-(n+mz)W_v^*(\lambda+\beta-\lambda z_1) \\ &\quad \times(\lambda z+L^*(\lambda+\beta)(\lambda+\beta-\lambda z))]+(\lambda+\beta-\lambda z)[z(\lambda+\beta)-(n+mz) \\ &\quad \times W_v^*(\lambda+\beta-\lambda z)(\lambda z+L^*(\lambda+\beta)(\lambda+\beta-\lambda z))]\Big]\Big[z-R_s^*(\lambda-\lambda z) \\ &\quad \times[z+(1-z)G^*(\lambda)]\Big]\Bigg\} \qquad (40) \end{aligned}$$

where $Dr_1(z)$ and $Dr_2(z)$ are given in (38) and (39) as the PGF for the number of customers in the orbit. Make use of the normalizing condition $R(1) = 1$ to findout that $W_{0,0}$ araise in (41). Using L'Hospitals rule and (Sub.) $z = 1$ in

(40) results,

$$W_{0,0} = \frac{1-\rho_s}{\left[\begin{array}{l} \left\{\dfrac{O}{\beta G^*(\lambda)[\lambda+\beta-W_v^*(\beta)(\lambda+\beta L^*(\lambda+\beta))]}\right\} \\ -\left\{\dfrac{P+mT}{G^*(\lambda)[\lambda+\beta-W_v^*(\beta)(\lambda+\beta L^*(\lambda+\beta))]}\right\} \\ +\left\{\dfrac{\beta W_v^*(\lambda+\beta-\lambda z_1)L^*(\lambda+\beta)(1-G^*(\lambda))}{G^*(\lambda)[\lambda+\beta-W_v^*(\beta)(\lambda+\beta L^*(\lambda+\beta))]}+Q\right\} \end{array}\right]} \quad (41)$$

$$R_{0,0} = \frac{\lambda}{\alpha}(1-W_v^*(\lambda+\beta-\lambda z_1))W_{0,0} \quad (42)$$

where,

$$\begin{aligned} O &= (\lambda-\lambda W_v^*(\lambda+\beta-\lambda z_1)+\beta)[\lambda+\beta G^*(\lambda) \\ &\quad -W_v^*(\beta)(\lambda+\beta L^*(\lambda+\beta))] \\ P &= \lambda E(R_s)W_v^*(\beta)[\lambda+\beta-W_v^*(\lambda+\beta-\lambda z_1)(\lambda+\beta L^*(\lambda+\beta))] \\ T &= \beta[L^*(\lambda+\beta)[W_v^*(\lambda+\beta-\lambda z)-W_v^*(\lambda+\beta-\lambda z_1)] \\ &\quad -W_v^*(\lambda+\beta-\lambda z)[1-L^*(\lambda+\beta)W_v^*(\lambda+\beta-\lambda z_1)]] \\ &\quad -\frac{\lambda}{\beta^2}(1-W_v^*(\lambda+\beta-\lambda z_1))\left[1+\frac{\beta}{\alpha}\right] \\ Q &= \frac{\lambda}{\alpha}(1-W_v^*(\lambda+\beta-\lambda z_1))G^*(\lambda) \\ \rho_s &= \frac{\lambda E(R_s)}{G^*(\lambda)} - \frac{m}{G^*(\lambda)} \end{aligned}$$

$E(R_s)$ is the mean service time and the system's stability condition $\rho_s < 1$ is obtained from (41).

3 The Model's Performance Measures

Mean Orbit Length in WV period:
We assume that W_v - mean orbit size and L_v - mean waiting time of the customer in the orbit during WV period.
Then

$$\begin{aligned} W_v &= \frac{d}{dz}W_v(z)\Big|_{z=1} \\ &= \frac{d}{dz}[W_1^*(z,0)+W_0^*(z,0)]\Big|_{z=1} \\ &= \frac{d}{dz}\left[\frac{S(z)}{(\lambda+\beta-\lambda z)Dr_1(z)}+\frac{K(z)}{Dr_1(z)}\right]W_{0,0}\Big|_{z=1} \end{aligned}$$

$$= \left[\begin{array}{c} \dfrac{\left[\begin{array}{c} Dr_1(z)(\lambda+\beta-\lambda z)S'(z) \\ -S(z)[(\lambda+\beta-\lambda z)Dr_1'(z)-Dr_1(z)\lambda] \end{array}\right]}{Dr_1(z))^2(\lambda+\beta-\lambda z)} \\ +\left[\dfrac{K'(z)Dr_1(z)-Dr_1'(z)K(z)}{(Dr_1(z))^2}\right] \end{array}\right] W_{0,0}\Bigg|_{z=1}$$

where,

$$\begin{aligned} K(z) &= \lambda z(1-L^*(\lambda+\beta))(n+mz)[W_v^*(\lambda+\beta-\lambda z)-W_v^*(\lambda+\beta-\lambda z_1)] \\ Dr_1(z) &= z(\lambda+\beta)-(n+mz)W_v^*(\lambda+\beta-\lambda z)(L^*(\lambda+\beta) \\ &\quad (\lambda+\beta-\lambda z)+\lambda z) \\ S(z) &= \lambda(1-W_v^*(\lambda+\beta-\lambda z))\big[z(\lambda+\beta)-(n+mz)W_v^*(\lambda+\beta-\lambda z_1) \\ &\quad \times(L^*(\lambda+\beta)(\lambda+\beta-\lambda z)+\lambda z)\big] \end{aligned}$$

Differentiating $S(z), K(z)$ and $Dr_1(z)$ with respect to z, we get

$$\begin{aligned} S'(z) &= \lambda^2 W_v^{*'}(\lambda+\beta-\lambda z)[z(\lambda+\beta)-(n+mz)W_v^*(\lambda+\beta-\lambda z_1) \\ &\quad \times(\lambda+\beta-\lambda z)L^*(\lambda+\beta)+\lambda z]+(1-W_v^*(\lambda+\beta-\lambda z))\lambda \\ &\quad \times[\lambda+\beta-(n+mz)(\lambda-\lambda L^*(\lambda+\beta))W_v^*(\lambda+\beta-\lambda z_1)] \\ &\quad -m[(\lambda+\beta-\lambda z)L^*(\lambda+\beta)+\lambda z]W_v^*(\lambda+\beta-\lambda z_1) \\ K'(z) &= (1-L^*(\lambda+\beta))(n+mz)\lambda[W_v^*(\lambda+\beta-\lambda z)-W_v^*(\lambda+\beta-\lambda z_1)] \\ &\quad +(n+mz)\lambda z(1-L^*(\lambda+\beta))(-\lambda W_v^{*'}(\lambda+\beta-\lambda z)) \\ &\quad +m\lambda z(1-L^*(\lambda+\beta))[W_v^*(\lambda+\beta-\lambda z)-W_v^*(\lambda+\beta-\lambda z_1)] \\ Dr_1'(z) &= (\lambda+\beta)+(n+mz)\lambda W_v^{*'}(\lambda+\beta-\lambda z)(\lambda z+(n+mz)L^*(\lambda+\beta) \\ &\quad (\lambda+\beta-\lambda z))-W_v^*(\lambda+\beta-\lambda z)(\lambda-\lambda L^*(\lambda+\beta)) \\ &\quad -m(\lambda z+(n+mz)L^*(\lambda+\beta)(\lambda+\beta-\lambda z))W_v^*(\lambda+\beta-\lambda z) \end{aligned}$$

At $z=1$ L_v turns

$$= \left[\begin{array}{c} \left[\dfrac{\beta Dr_1(1)S'(1)-S(1)[\beta Dr_1'(1)-\lambda Dr_1(1)]}{(\beta Dr_1(1))^2}\right] \\ +\left[\dfrac{Dr_1(1)K'(1)-K(1)Dr_1'(1)}{(Dr_1(1))^2}\right] \end{array}\right] W_{0,0}$$

we know that $L_v = \dfrac{W_v}{\lambda}$
where,

$$\begin{aligned} S(1) &= \lambda(1-W_v^*(\beta))[\beta+\lambda-W_v^*(\lambda+\beta-\lambda z_1)(\lambda+\beta L^*(\lambda+\beta))] \\ S'(1) &= \lambda^2 W_v^{*'}(\beta)[\lambda+\beta-W_v^*(\lambda+\beta-\lambda z_1)(\lambda+\beta L^*(\lambda+\beta))] \\ &\quad +\lambda(1-W_v^*(\beta))[\lambda+\beta-W_v^*(\lambda+\beta-\lambda z_1)(\lambda-\lambda L^*(\lambda+\beta))] \\ &\quad -m(\lambda+\beta L^*(\lambda+\beta))W_v^*(\lambda+\beta-\lambda z_1) \end{aligned}$$

$$\begin{aligned}
K(1) &= \lambda(1-L^*(\lambda+\beta))(W_v^*(\beta)-W_v^*(\beta-\lambda z_1+\lambda)) \\
K'(1) &= \lambda(1-L^*(\lambda+\beta))\big[W_v^*(\beta)-W_v^*(\beta+\lambda-\lambda z_1)-W_v^{*'}(\beta)\lambda \\
&\quad +m[W_v^*(\beta)-W_v^*(\beta+\lambda-\lambda z_1)]\big] \\
Dr_1(1) &= \beta-(\lambda+\beta L^*(\lambda+\beta))W_v^*(\beta)+\lambda \\
Dr_1'(1) &= \beta+[\lambda W_v^{*'}(\beta)+mW_v^*(\beta)][\lambda+L^*(\lambda+\beta)\beta] \\
&\quad +\lambda-[\lambda-\lambda L^*(\lambda+\beta)]W_v^*(\beta)
\end{aligned}$$

Mean Orbit Length in RS period:
We assume that L_s - mean orbit size and W_s - mean waiting time of the customer in the orbit during WV period.

$$\begin{aligned}
L_s &= \frac{d}{dz}R_S(z)\Big|_{z=1} \\
&= \frac{d}{dz}[R_1^*(z,0)+R_0^*(z,0)]\Big|_{z=1} \\
&= \frac{d}{dz}\left[\frac{Nr_1(z)(1-G^*(\lambda))+Nr_2(z)Nr_3(z)}{Dr_1(z)(\lambda+\beta-\lambda z)Dr_2(z)}\right]W_{0,0}\Big|_{z=1}
\end{aligned}$$

$$L_s = \frac{\left[\begin{array}{r}
\big[Dr_2'(z)2Nr_1'(z)(\lambda Dr_1(z)-(\lambda+\beta-\lambda z)Dr_1'(z)) \\
+(\lambda+\beta-\lambda z)Dr_1(z)Nr_1''(z)(Dr_2'(z)-Dr_2''(z)Nr_1'(z))\big] \\
\times(1-G^*(\lambda))+2(\lambda+\beta-\lambda z)Nr_2'(z)Dr_2'(z)(Nr_3'(z)Dr_1(z) \\
-Nr_3(z)Dr_1'(z))+Nr_3(z)[2\lambda Nr_2'(z)Dr_2'(z)+(\lambda+\beta-\lambda z) \\
Dr_2'(z)Nr_2''(z)-(\lambda+\beta-\lambda z)Dr_2''(z)Nr_2'(z)]Dr_1(z)
\end{array}\right]}{2(Dr_1(z)(\lambda+\beta-\lambda z)Dr_2'(z))^2}W_{0,0}\Big|_{z=1}$$

where,

$$\begin{aligned}
Nr_1(z) &= \beta z(n+mz)R_s^*(\lambda-\lambda z)(1-W_v^*(\lambda+\beta-\lambda z))\big\{(\lambda+\beta)z \\
&\quad -(n+mz)W_v^*(\lambda+\beta-\lambda z_1)[(\lambda+\beta-\lambda z)L^*(\lambda+\beta)+\lambda z]\big\} \\
&\quad +(\lambda+\beta-\lambda z)\beta z^2(n+mz)(1-L^*(\lambda+\beta))[W_v^*(\lambda+\beta-\lambda z) \\
&\quad -W_v^*(\lambda+\beta-\lambda z_1)]-(1-(n+mz)W_v^*(\lambda+\beta-\lambda z_1))\big\{(\lambda+\beta) \\
&\quad \times z-(n+mz)W_v^*(\lambda+\beta-\lambda z)[(\lambda+\beta-\lambda z)L^*(\lambda+\beta)+\lambda z]\big\} \\
&\quad \times z(\lambda+\beta-\lambda z)-\frac{z\lambda}{\alpha}(1-(n+mz)R_s^*(\lambda-\lambda z))(\lambda+\beta-\lambda z) \\
&\quad \times(1-(n+mz)W_v^*(\lambda+\beta-\lambda z_1))\big\{(\lambda+\beta)z-(n+mz) \\
&\quad \times W_v^*(\lambda+\beta-\lambda z)[(\lambda+\beta-\lambda z)L^*(\lambda+\beta)+\lambda z]\big\} \\
Nr_2(z) &= (1-R_s^*(\lambda-\lambda z)) \\
Dr_1(z) &= (\lambda+\beta)z-(n+mz)W_v^*(\lambda+\beta-\lambda z)[L^*(\lambda+\beta) \\
&\quad \times(\lambda+\beta-\lambda z)+\lambda z] \\
Dr_2(z) &= z-(n+mz)R_s^*(\lambda-\lambda z)[(1-z)G^*(\lambda)+z]
\end{aligned}$$

$$\begin{aligned}
Nr_3(z) &= \beta z[(\lambda+\beta-\lambda z)G^*(\lambda)+\lambda z](1-L^*(\lambda+\beta))(W_v^*(\lambda+\beta-\lambda z) \\
&\quad -W_v^*(\lambda+\beta-\lambda z_1))-(1-W_v^*(\lambda+\beta-\lambda z_1))[(\lambda+\beta-\lambda z) \\
&\quad \times G^*(\lambda)+\lambda z]\{(\lambda+\beta)z-W_v^*(\lambda+\beta-\lambda z)(\lambda+\beta-\lambda z)L^*(\lambda+\beta) \\
&\quad +\lambda z)\}+\beta z(\lambda+\beta)(W_v^*(\lambda+\beta-\lambda z)-W_v^*(\lambda+\beta-\lambda z_1)) \\
&\quad \times L^*(\lambda+\beta)-\frac{\lambda}{\alpha}(1-W_v^*(\lambda+\beta-\lambda z_1))G^*(\lambda)(\lambda+\beta-\lambda z) \\
&\quad \times\big\{(\lambda+\beta)z-W_v^*(\lambda+\beta-\lambda z)[\lambda z+(\lambda+\beta-\lambda z)L^*(\lambda+\beta)\big\} \\
&\quad +m\Big[\big[\lambda\beta z^2W_v^*(\lambda+\beta-\lambda z_1)+\beta^2zW_v^*(\lambda+\beta-\lambda z_1)L^*(\lambda+\beta) \\
&\quad \times W_v^*(\lambda+\beta-\lambda z)+\lambda\beta zW_v^*(\lambda+\beta-\lambda z_1)W_v^*(\lambda+\beta-\lambda z) \\
&\quad \times L^*(\lambda+\beta)(1-z)\big](n+mz)-[\beta^2z^2+\lambda\beta z^2]W_v^*(\lambda+\beta-\lambda z)\Big]
\end{aligned}$$

At $z=1$ L_s turns

$$L_s=\frac{\left[\begin{array}{r}(1-G^*(\lambda))\big[2Nr_1'(1)Dr_2'(1)(\lambda Dr_1(1)-\beta Dr_1'(1))+\beta Dr_1(1) \\ (Dr_2'(1)Nr_1''(1)-Nr_1'(1)Dr_2''(1))\big]+2\beta Nr_2'(1)Dr_2'(1) \\ (Dr_1(1)Nr_3'(1)-Nr_3(1)Dr_1'(1))+Nr_3(1)Dr_1(1)[2\lambda \\ Nr_2'(1)Dr_2'(1)+\beta Dr_2'(1)Nr_2''(1)-\beta Nr_2'(1)Dr_2''(1)]\end{array}\right]}{2(\beta Dr_1(1)Dr_2'(1))^2}W_{0,0}$$

as it is known that $W_s=\dfrac{L_s}{\lambda}$,
where,

$$\begin{aligned}
Nr_1'(1) &= -\beta\lambda W_v^*(\beta)+\beta\lambda E(R_s)(1-W_v^*(\beta))[\lambda+\beta-\beta W_v^*(\lambda+\beta-\lambda z_1) \\
&\quad \times L^*(\lambda+\beta)-\lambda W_v^*(\lambda+\beta-\lambda z_1)]-\beta^2L^*(\lambda+\beta)W_v^*(\beta)+\beta^2 \\
&\quad \times L^*(\lambda+\beta)W_v^*(\lambda+\beta-\lambda z_1)+\lambda[\beta+\lambda-\beta W_v^*(\beta)L^*(\lambda+\beta) \\
&\quad -\lambda W_v^*(\beta)]-\lambda^2W_v^*(\lambda+\beta-\lambda z_1)+\lambda^2W_v^*(\lambda+\beta-\lambda z_1)W_v^*(\beta) \\
&\quad +\lambda\beta W_v^*(\lambda+\beta-\lambda z_1)W_v^*(\beta)L^*(\lambda+\beta)+\frac{\lambda}{\alpha}[-m+\lambda E(R_s)] \\
&\quad \times\beta(1-W_v^*(\lambda+\beta-\lambda z_1))\{(\lambda+\beta)-W_v^*(\beta)[\lambda+\beta L^*(\lambda+\beta)]\} \\
&\quad +\beta m\{(\lambda+\beta)-W_v^*(\beta)[\lambda+\beta L^*(\lambda+\beta)]\}W_v^*(\lambda+\beta-\lambda z_1) \\
Nr_3(1) &= (1-W_v^*(\beta))\{\beta G^*(\lambda)W_v^*(\lambda+\beta-\lambda z_1)(\lambda+\beta L^*(\lambda+\beta))-\beta\lambda \\
&\quad -\beta\lambda G^*(\lambda)-\beta^2G^*(\lambda)\}+(1-W_v^*(\lambda+\beta-\lambda z_1))\{\beta\lambda W_v^*(\beta) \\
&\quad \times L^*(\lambda+\beta)-\lambda^2(1-W_v^*(\beta))\}+\beta^2L^*(\lambda+\beta)(W_v^*(\beta) \\
&\quad -W_v^*(\lambda+\beta-\lambda z_1))-\frac{\lambda}{\alpha}\beta G^*(\lambda)(1-W_v^*(\lambda+\beta-\lambda z_1)) \\
&\quad \times\{\lambda+\beta-W_v^*(\beta)(L^*(\lambda+\beta)\beta+\lambda)\}+\big\{\lambda\beta W_v^*(\lambda+\beta-\lambda z_1) \\
&\quad -\beta W_v^*(\beta)[\lambda+\beta-\beta W_v^*(\lambda+\beta-\lambda z_1)L^*(\lambda+\beta)]\big\}m \\
Nr_2'(1) &= -\lambda E(R_s)
\end{aligned}$$

$$
\begin{aligned}
Nr_1''(1) &= (W_v^*(\beta)-W_v^*(\lambda+\beta-\lambda z_1))[(1-L^*(\lambda+\beta))(\beta\lambda(1-G^*(\lambda))\\
&\quad +\beta^2G^*(\lambda))+\beta^2L^*(\lambda+\beta)]+G^*(\lambda)(\lambda+\beta+\lambda W_v^*(\beta))\\
&\quad \times(\beta W_v^*(\lambda+\beta-\lambda z_1)-\lambda)-\beta\lambda L^*(\lambda+\beta)(1-W_v^*(\lambda+\beta-\lambda z_1))\\
&\quad \times(W_v^*(\beta)+\beta W_v^{*'}(\beta))+G^*(\lambda)W_v^*(\lambda+\beta-\lambda z_1)[\lambda+\beta-\beta W_v^*(\beta)\\
&\quad \times L^*(\lambda+\beta)+\lambda W_v^*(\beta)]\lambda-\beta G^*(\lambda)[\lambda+\beta-\lambda^2W_v^{*'}(\beta)+\lambda W_v^*(\beta)]\\
&\quad +[\lambda W_v^{*'}(\beta)(\beta L^*(\lambda+\beta)-\lambda)+\lambda W_v^*(\beta)W^*(\lambda+\beta)][\beta G^*(\lambda)\\
&\quad \times W_v^*(\lambda+\beta-\lambda z_1)-\lambda(1-W_v^*(\lambda+\beta-\lambda z_1))]+\frac{\lambda}{\alpha}G^*(\lambda)\\
&\quad \times(1-W_v^*(\lambda+\beta-\lambda z_1))\big\{\lambda(\lambda+\beta)-\lambda^2W_v^*(\beta)-2\lambda\beta W_v^*(\beta)\\
&\quad \times L^*(\lambda+\beta)-\lambda^2\beta W_v^{*'}(\beta)-\lambda\beta^2W_v^{*'}(\beta)L^*(\lambda+\beta)+\lambda\beta W_v^*(\beta)\\
&\quad -\beta(\lambda+\beta)\big\}+m\Big[\beta W_v^*(\lambda+\beta-\lambda z_1)\Big[[L^*(\lambda+\beta)\beta+\lambda]\\
&\quad \times[3(W_v^*(\beta)-W_v^{*'}(\beta)-\lambda E(R_s))+m(1-W_v^*(\beta))-4]\\
&\quad -3(1-W_v^*(\beta))[\lambda-\lambda L^*(\lambda+\beta)]\Big]+\beta(\lambda+\beta)\Big[2(1-W_v^*(\beta)\\
&\quad +\lambda W_v^{*'}(\beta))+\lambda E(R_s)[2+W_v^*(\beta)]\Big]+\beta[1-L^*(\lambda+\beta)][2(2\beta-\lambda)\\
&\quad \times[W_v^*(\beta)-W_v^*(\lambda+\beta-\lambda z_1)]-\lambda\beta W_v^{*'}(\beta)]-\lambda\beta^2[1-L^*(\lambda+\beta)]\\
&\quad \times W_v^*(\beta)+(\lambda+\beta)W_v^*(\lambda+\beta-\lambda z_1)(3\beta-2\lambda)+[L^*(\lambda+\beta)\beta+\lambda]\\
&\quad \times\Big[\beta\lambda W_v^{*'}(\beta)[3W_v^*(\lambda+\beta-\lambda z_1)-2]+W_v^*(\beta)[W_v^*(\lambda+\beta-\lambda z_1)\\
&\quad \times(2\lambda-m\beta-\beta)+\beta]\Big]\frac{\lambda}{\alpha}\Big[\{(\lambda+\beta)(1-W_v^*(\lambda+\beta-\lambda z_1))[\beta+2\beta\\
&\quad -\lambda+\lambda\beta E(R_s)]-2\beta mW_v^*(\lambda+\beta-\lambda z_1)\}+\Big\{[\lambda\beta(W_v^{*'}(\beta)\\
&\quad -E(R_s))-m\beta W_v^*(\beta)-2\beta+\lambda](1-W_v^*(\lambda+\beta-\lambda z_1))+2\beta m\\
&\quad \times W_v^*(\lambda+\beta-\lambda z_1)\Big\}[L^*(\lambda+\beta)\beta+\lambda]-\beta(1-W_v^*(\lambda+\beta-\lambda z_1))\\
&\quad \times[\lambda-\lambda L^*(\lambda+\beta)]W_v^*(\beta)\Big]\Big]\\
Dr_1(1) &= \beta+\lambda-(\lambda+\beta L^*(\lambda+\beta))W_v^*(\beta)\\
Dr_1'(1) &= \beta+[\lambda W_v^{*'}(\beta)+mW_v^*(\beta)][\lambda+L^*(\lambda+\beta)\beta]\\
&\quad +\lambda-[\lambda-\lambda L^*(\lambda+\beta)]W_v^*(\beta)\\
Dr_2'(1) &= G^*(\lambda)-E(R_s)\lambda-m\\
Dr_2''(1) &= -2(1-G^*(\lambda))[\lambda E(R_s)+m]-E(R_s^2)\lambda^2-2\lambda mE(R_s)\\
Nr_2''(1) &= -\lambda^2E(R_s^2)
\end{aligned}
$$

$$
\begin{aligned}
Nr_3'(1) \quad = \quad & \{(1-W_v^*(\beta))(2\beta\lambda E(R_s)+\beta\lambda^2E(R_s^2))+2\beta\lambda^2E(R_s)W_v^{*'}(\beta)\} \\
& \times[\lambda+\beta-W_v^*(\lambda+\beta-\lambda z_1)(\lambda+\beta L^*(\lambda+\beta))]+2\beta\lambda E(R_s) \\
& \times(1-W_v^*(\beta))[\lambda+\beta+\lambda W_v^*(\lambda+\beta-\lambda z_1)(L^*(\lambda+\beta)-1)] \\
& +2\beta\lambda[W_v^{*'}(\beta)(\lambda+\beta L^*(\lambda+\beta))+(1-W_v^*(\beta))(2-L^*(\lambda+\beta) \\
& \times W_v^*(\lambda+\beta-\lambda z_1))]+2\beta^2L^*(\lambda+\beta)(W_v^*(\lambda+\beta-\lambda z_1) \\
& -W_v^*(\beta))+2\lambda^2(1-W_v^*(\beta))(1-W_v^*(\lambda+\beta-\lambda z_1))+2\lambda[\lambda \\
& +\lambda W_v^{*'}(\beta)(\lambda+\beta L^*(\lambda+\beta))+\lambda W_v^*(\beta)(L^*(\lambda+\beta)-1)] \\
& \times(1-W_v^*(\lambda+\beta-\lambda z_1))+\frac{\lambda^2}{\alpha}(1-W_v^*(\lambda+\beta-\lambda z_1))\big\{[\lambda+\beta \\
& -W_v^*(\beta)[\lambda+\beta L^*(\lambda+\beta)]][4\beta+\lambda\beta-1]E(R_s)+2\beta\lambda W_v^{*'}(\beta) \\
& \times[\lambda+\beta L^*(\lambda+\beta)]E(R_s)+\lambda\beta E(R_s^2)[\lambda+\beta-W_v^*(\beta) \\
& (\lambda+\beta L^*(\lambda+\beta))]\big\}
\end{aligned}
$$

4 Special cases

(a) If the service time distribution follows an exponential distribution, no retrial, no service among the vacation period and there is no feedback then, the present model will be remodeled as analysis of M/M/1 queue with server vacations and a waiting server.
(b) If the server does not wait after the completion of the RS period and there is no feedback then, the present model will be remodeled as an M/G/1 retrial queue with multiple working vacation.

5 Numerical results

The curved graph constructed in Figure 1 and the values tabulated in the Table 1 are obtained by setting the fixed values $\mu_v = 3.6$, $\mu_s = 9.8$, $\mu_{vr} = 3.5$, $\mu_{sr} = 5.3$, $\alpha = 1$, $m = 0.4$ and altering the values of λ from 1 to 2 incremented with 0.2 and increasing the values of β from 0.3 to 1.1 in steps of 0.4, we observed that as λ rises L_v falls and hence the stability of the model is verified.

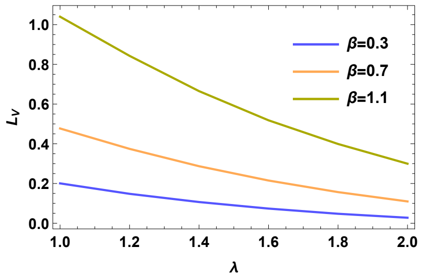

Figure 1: λ versus L_v

λ	$\beta = 0.3$	$\beta = 0.7$	$\beta = 1.1$
1.0	0.2006	0.4771	1.0399
1.2	0.1479	0.3744	0.8428
1.4	0.1066	0.2870	0.6651
1.6	0.0737	0.2149	0.5181
1.8	0.0475	0.1566	0.3990
2.0	0.0275	0.1097	0.2997

Table 1: λ versus L_v

The curved graph constructed in Figure 2 and the values tabulated in the Table 2 are obtained by setting the fixed values $\mu_v = 6.6$, $\mu_s = 10.8$, $\mu_{vr} = 3.5$, $\mu_{sr} = 5.3$, $\alpha = 1.7$, $m = 0.3$ and altering the values of λ from 1 to 2 incremented with 0.2 and increasing the values of β from 0.2 to 0.6 in steps of 0.2. We observed that as λ rises W_v falls which is expected.

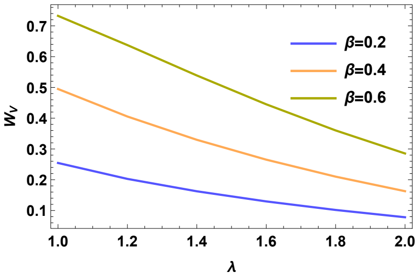

Figure 2: λ versus W_v

λ	$\beta = 0.2$	$\beta = 0.4$	$\beta = 0.6$
1.0	0.2545	0.4949	0.7325
1.2	0.2027	0.4054	0.6375
1.4	0.1624	0.3297	0.5388
1.6	0.1295	0.2652	0.4451
1.8	0.1018	0.2100	0.3602
2.0	0.0781	0.1628	0.2853

Table 2: λ versus W_v

The curved graph constructed in Figure 3 and the values tabulated in the Table 3 are obtained by setting the fixed values $\mu_v = 0.1$, $\mu_s = 10$, $\mu_{vr} = 1.5$, $\mu_{sr} = 4.5$, $\alpha = 0.6$, $m = 0.3$ and altering the values of λ from 1 to 2 incremented with 0.2 and increasing the values of β from 1.3 to 1.7 in steps of 0.2. We observed that as λ rises L_s also rises which shows the stability of the model.

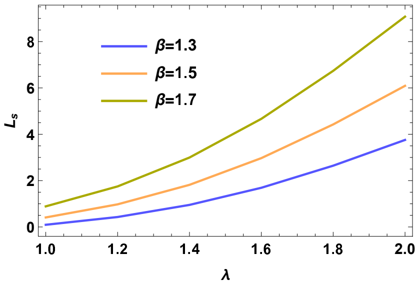

Figure 3: λ versus L_s

λ	$\beta = 1.3$	$\beta = 1.5$	$\beta = 1.7$
1.0	0.0939	0.4101	0.8883
1.2	0.4295	0.9762	1.7499
1.4	0.9517	1.8173	2.9956
1.6	1.6909	2.9705	4.6665
1.8	2.6447	4.4248	6.7373
2.0	3.7557	6.0909	9.0768

Table 3: λ versus L_s

The curved graph constructed in Figure 4 and the values tabulated in the Table 4 are obtained by setting the fixed values $\mu_v = 9.3$, $\mu_s = 11$, $\mu_{vr} = 4.5$, $\mu_{sr} = 5.5$, $\alpha = 1.5$, $m = 0.5$ and altering the values of λ from 1 to 2 incremented with 0.2 and increasing the values of β from 0.3 to 0.5 in steps of 0.1. From the graph, we studied that as λ rises W_s falls which shows the stability of the model.

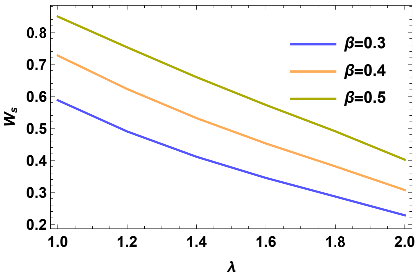

Figure 4: λ versus W_s

λ	$\beta = 0.3$	$\beta = 0.4$	$\beta = 0.5$
1.0	0.5875	0.7271	0.8489
1.2	0.4899	0.6225	0.7527
1.4	0.4107	0.5315	0.6595
1.6	0.3447	0.4523	0.5726
1.8	0.2865	0.3808	0.4904
2.0	0.2280	0.3069	0.4018

Table 4: λ versus W_s

6 Conclusion

In this paper, an $M/G/1$ feedback retrial queue with working vacation and a waiting server is evaluated. We obtained the PGF for the number of customers and the mean number of customers in the orbit. We worked out the mean waiting time. We also derived the performance measures. We performed some particular cases. We illustrated some numerical results.

References

[1] Yang T. and Templeton J.G.C., *A Survey on Retrial Queue*, Queue. Syst., 2 (1987), 201-233.

[2] Falin G.I., *A Survey on Retrial Queues*, Queueing Systems Theory and Applications, 7 (1990), 127-168.

[3] Falin G.I. and Templeton J.G.C., *Retrial queues*, Chapman and Hall, London, (1997).

[4] Servi L. and Finn S., "M/M/1 queue with working vacations (M/M/1/WV)", *Perform. Eval*, 50 (2002), 41-52 .

[5] Wu D. and Takagi H., "M/G/1 queue with multiple working vacations", *Perform. Eval*, 63 (2006), 654-681.

[6] Kalyanaraman R. and Pazhani Bala Murugan S., "A single server retrial queue with vacation", *J.Appl.Math.and Informatics*, 26(3-4) (2008), 721-732.

[7] Pazhani Bala Murugan S. and Santhi K., "An M//G/1 retrial queue with multiple working vacation", *International Journal of Mathematics and its Applications*, 4(2-D) (2016), 35-48.

[8] Chandrasekaran V.M., Indhira K., Saravanarajan M.C. and Rajadurai P., "A survey on working vacation queueing models", *International Journal of Pure and Applied Mathematics*, 106(6) (2016), 33-41.

[9] Gupta P. and Kumar N., Performance Analysis of Retrial Queueing Model with Working Vacation, Interruption, Waiting Server, Breakdown and Repair, *J. Sci. Res.,* 13(3) (2021), 833-844.

[10] Boxma O.J., Schlegel S. and Yechiali U., "M/G/1 queue with waiting server timer and vacations", *American Mathematical Society Translations*, 2(207) (2002), 25-35.

[11] Kalidass K. and Kasturi Ramanath, "Time dependent analysis of M/M/1 queue with server vacations and a waiting server", *QTNA*, August, (2011), 23-26.

[12] Krishna Kumar B., Pavai madheswari and Vijayakumar A., "The M/G/1 retrial queue with feedback and starting failures", *Applied Mathematical modelling*, 26 (2002), 1057-1075.

[13] Jau-chuan ke, Fu-min chang, "Modified vacation Policy for M/G/1 retrial queue with balking and feedback", *Computers and Industrial Engineering*, 57 (2009), 433-443.

[14] Rajadurai P., Saravanarajan M. C. and Chandrasekaran V.M., "A study on M/G/1 feedback retrial queue with subject to server breakdown and repain under multiple working vacation policy", Alexandria University, *Alexandria Engineering Journal*, 57 (2018), 947-962.

[15] Gnanasekar M.M.N. and Indhira K., Analysis of an M/G/1 Retrial Queue with Delayed Repair and Feedback under Working Vacation policy with Impatient Customers, *Mathematical Models: Methods and Applications*, 14(10) 2022, 1-18.

[16] Artalejo J.R.,*Accessible bibliography on retrial queue*, Math. Comput. Modell., 30 (1999), 1-6.

[17] Artalejo J.R. and Falin G., *Standard and retrial queueing systems: A Comparitive Analysis*, Rev. Math. Comput., 15 (2002), 101-129.

[18] Gomez-Corral A., "Stochastic analysis of a single server retrial queue with general retrial time", *Naval Res. Log.*, 46 (1999), 561-581.

[19] Medhi J., *Stochastic Models in Queueing Theory*, Second Edition (2003).

J. COMPUTATIONAL ANALYSIS AND APPLICATIONS, VOL. 31, NO.1, 2023, COPYRIGHT 2023 EUDOXUS PRESS, LLC

An Application of Incomplete I-Functions with Two Variables to Solve the Nonlinear Differential Equations Using S-Function

Rahul Sharma[1], Jagdev Singh[2], Devendra Kumar[3], Yudhveer Singh[4*]

December 28, 2022

Department of Mathematics, Amity School of Applied Sciences, Amity University Rajasthan, Jaipur-303002, Rajasthan, India[1]
Department of Mathematics, JECRC University, Jaipur-303905, Rajasthan, India[2]
Department of Mathematics, University of Rajasthan, Jaipur-302004, Rajasthan, India[3]
Amity Institute of Information Technology, Amity University Rajasthan, Jaipur-303002, Rajasthan, India[4]

Abstract

In this article, we evaluate the approximate solutions of Nonlinear Differential Equations (NoLDEs) with the association of S-function, incomplete H-functions (IHFs) and incomplete I-functions (IIFs) with two variables by using the Hermite, Legendre and Jacobi polynomials. Here, we introduce incomplete I-functions with two variables. The NoLDEs are significantly applicable in fluid dynamics, vibration problems, population dynamics, electromagnetism, chemical kinetics, combustion theory, economics and finance. Recently, it was implemented to solve the resistance less circuit with a nonlinear capacitor under influence of external periodic force.

This method is established as an application of improper integrals, polynomials and special functions. The obtained results are helpful to get the solution of various problems of mathematical physics and engineering in approximate aspects.

Keywords: Incomplete H-functions, Incomplete I-functions, q-Gamma functions, S-function, Laplace transform, Improper Integral.
MSC2020: 33B20, 33D05, 33E12, 44A10.

1 Introduction and Preliminaries:

Earlier, Nonlinear differential equations play remarkable roles in the field of Engineering and Physics. Numerous authors have given their outputs to solving these equations by several methods. In the nineteen century, many Mathematicians like Gadre [9], Saxena et al. [16], Srivastava [24] and Srivastava et al. [25] worked on NoLDEs system. In last two decades many more authors such as Chaurasia et al. [5], Sharma [17], Singh [20], Singh et al. [21, 22, 23], Bansal et al. [1, 2, 3, 4] and Kumar et al. [11, 12] have also paid their attention in this branch of Applied Mathematics.

In the section 1, we defined the incomplete H-functions, incomplete I-functions with two variables and S-function. Section 2, shows some important theorems that will be used to solve the NoLDEs given in the section 3.

Special functions are well known tool which are uses in various fields of Engineering and Physics. The incomplete Gamma functions (IGFs) $\gamma(s,y)$ and $\Gamma(s,y)$ are investigated by Prym [14]. The incomplete Gamma functions are base of the recently developed incomplete forms of special functions like incomplete H-functions, incomplete $\overline{H}$-functions, incomplete I-functions and incomplete $\aleph$-functions.
The incomplete Gamma functions $\gamma(s,y)$ and $\Gamma(s,y)$ are defined, by

$$\gamma(s,y) = \int_0^y t^{s-1}e^{-t}dt, \quad (\mathbb{R}(s) > 0;\ y \geq 0). \tag{1}$$

$$\Gamma(s,y) = \int_y^\infty t^{s-1}e^{-t}dt, \quad (y \geq 0;\ \mathbb{R}(s) > 0 \ when\ y = 0). \tag{2}$$

The IGFs holds the decomposition formula $\gamma(s,y) + \Gamma(s,y) = \Gamma(s)$, here $\Gamma(.)$ is well known gamma function.
Pochhammer symbol $(\mu)_\lambda$ defined as:

$$(\mu)_\lambda = \frac{\Gamma(\mu+\lambda)}{\Gamma(\mu)} = \begin{cases} 1, & \text{if} \quad \lambda = 0; \mu \in \mathbb{C}\backslash\{0\} \\ (\mu)(\mu+1)\dots(\mu+n-1), & \text{if} \quad \lambda = n \in \mathbb{N}; \mu \in \mathbb{C}, \end{cases} \tag{3}$$

provided $\Gamma(\mu)$ exists. Here $\mathbb{C}$ and $\mathbb{N}$ are as usual denote the set of complex and natural numbers respectively.

Definition 1: In terms of the incomplete gamma functions (IGFs) $\Gamma(s,x)$ and $\gamma(s,x)$, the IHFs [26] is defined $\gamma_{P,Q}^{M,N}(z)$ and $\Gamma_{P,Q}^{M,N}(z)$ as follows:

$$\begin{aligned} \gamma_{P,Q}^{M,N}(z) &= \gamma_{P.Q}^{M,N}\left[z \,\middle|\, \begin{matrix} (f_1,F_1,t),(f_j,F_j)_{2,P} \\ (w_j,W_j)_{1,Q} \end{matrix} \right] \\ &:= \frac{1}{2\pi i}\int_L \varphi(s,t)z^s ds, \end{aligned} \tag{4}$$

where

$$\varphi(s,t) = \frac{\gamma(1-f_1+F_1s,t)\prod_{j=1}^{M}\Gamma(w_j-W_js)\prod_{j=2}^{N}\Gamma(1-f_j+F_js)}{\prod_{j=M+1}^{Q}\Gamma(1-w_j+W_js)\prod_{j=N+1}^{P}\Gamma(f_j-F_js)}, \tag{5}$$

2

and

$$\begin{aligned}\Gamma_{P,Q}^{M,N}(z) &= \Gamma_{P,Q}^{M,N}\left[z \,\middle|\, \begin{matrix}(f_1,F_1,t),(f_j,F_j)_{2,P}\\ (w_j,W_j)_{1,Q}\end{matrix}\right]\\ &:= \frac{1}{2\pi i}\int_L \phi(s,t) z^s ds, \end{aligned} \tag{6}$$

where

$$\phi(s,t) = \frac{\Gamma(1-f_1+F_1 s,t)\prod_{j=1}^{M}\Gamma(w_j-W_j s)\prod_{j=2}^{N}\Gamma(1-f_j+F_j s)}{\prod_{j=M+1}^{Q}\Gamma(1-w_j+W_j s)\prod_{j=N+1}^{P}\Gamma(f_j-F_j s)}, \tag{7}$$

The IHFs $\gamma_{P,Q}^{M,N}(z)$ and $\Gamma_{P,Q}^{M,N}(z)$ are exist for all $t \geq 0$ and for more existing conditions (see, [26]).

Definition 2: We introduce the incomplete I-functions with two variables ${}^{(\Gamma)}I^{0,n:m_1,n_1;m_2,n_2}_{p_l,q_l,r;p_{l^{(1)}},q_{l^{(1)}},r_{(1)};p_{l^{(2)}},q_{l^{(2)}},r_{(2)}}$ as follows:

$${}^{(\Gamma)}I^{0,n:m_1,n_1;m_2,n_2}_{p_l,q_l,r;p_{l^{(1)}},q_{l^{(1)}},r_{(1)};p_{l^{(2)}},q_{l^{(2)}},r_{(2)}}\left[\begin{matrix} z_1\\ z_2\end{matrix} \,\middle|\, \begin{matrix}\left(e_1,E_1^{(1)},E_1^{(2)},x\right),\left(e_j,E_j^{(1)},E_j^{(2)}\right)_{2,n}\\ \ldots,\left(f_{jl},F_{jl}^{(1)},F_{jl}^{(2)}\right)_{m+1,q_l},\end{matrix}\right.$$

$$,\left(e_{jl},E_{jl}^{(1)},E_{jl}^{(2)}\right)_{n+1,p_l},(e_j^{(1)},E_j^{(1)})_{1,n_1},\left(e_{jl^{(1)}}^{(1)},E_{jl^{(1)}}^{(1)}\right)_{n_1+1,p_l^{(1)}},$$
$$\left(f_j^{(1)},F_j^{(1)}\right)_{1,m_1},\left(f_{jl^{(1)}}^{(1)},F_{jl^{(1)}}^{(1)}\right)_{m_1+1,q_l^{(1)}},$$

$$\left.\begin{matrix}(e_j^{(2)},E_j^{(2)})_{1,n_2},\left(e_{jl^{(2)}}^{(2)},E_{jl^{(2)}}^{(2)}\right)_{n_2+1,p_l^{(2)}}\\ \left(f_j^{(2)},F_j^{(2)}\right)_{1,m_2},\left(f_{jl^{(2)}}^{(2)},F_{jl^{(2)}}^{(2)}\right)_{m_2+1,q_l^{(2)}}\end{matrix}\right]$$

$$= \frac{1}{(2\pi\omega)^2}\int_{L_1}\int_{L_2}\theta\left(\xi_1,\xi_2,x\right) z_1^{\xi_1} z_2^{\xi_2}\theta_1(\xi_1)\theta_2(\xi_2)d\xi_1 d\xi_2 \quad (\omega=\sqrt{-1}), \tag{8}$$

where
$\theta\left(\xi_1,\xi_2,x\right) = \frac{\Gamma(1-e_1+\sum_{i=1}^{2}E_j^{(i)}\xi_i,x)\prod_{j=2}^{n}\Gamma(1-e_j+\sum_{i=1}^{2}E_j^{(i)}\xi_i)}{\sum_{i=1}^{r}\left[\prod_{j=n+1}^{p_l}\Gamma\left(e_{jl}-\sum_{i=1}^{2}E_{jl}^{(i)}\xi_i\right)\prod_{j=1}^{q_l}\Gamma\left(1-f_{jl}+\sum_{i=1}^{2}F_{jl}^{(i)}\xi_i\right)\right]}$,

and,
$\theta_i(\xi_i) = \frac{\prod_{j=1}^{m_i}\Gamma(f_j^{(i)}-F_j^{(i)}\xi_i)\prod_{j=1}^{n_i}\Gamma(1-e_j^{(i)}+E_j^{(i)}\xi_i)}{\sum_{i^{(i)}=1}^{r^{(i)}}\left[\prod_{j=m_i+1}^{q_{l^{(i)}}}\Gamma\left(1-f_{jl^{(i)}}^{(i)}+F_{jl^{(i)}}^{(i)}\xi_i\right)\prod_{j=n_i+1}^{p_{i^{(i)}}}\Gamma\left(e_{jl^{(i)}}^{(i)}-E_{jl^{(i)}}^{(i)}\xi_i\right)\right]}$, $(i=1,2)$.

Now, We can define lower form of the incomplete I-function with two variables

${}^{(\gamma)}I^{0,n:m_1,n_1;m_2,n_2}_{p_l,q_l,r;p_{l^{(1)}},q_{l^{(1)}},r^{(1)};p_{l^{(2)}},q_{l^{(2)}},r^{(2)}}$ as follows:

$$
{}^{(\gamma)}I^{0,n:m_1,n_1;m_2,n_2}_{p_l,q_l,r;p_{l^{(1)}},q_{l^{(1)}},r^{(1)};p_{l^{(2)}},q_{l^{(2)}},r^{(2)}}\left[\begin{array}{c|l} z_1 & \left(e_1,E_1^{(1)},E_1^{(2)},x\right),\left(e_j,E_j^{(1)},E_j^{(2)}\right)_{2,n} \\ z_2 & \ldots,\left(f_{jl},F_{jl}^{(1)},F_{jl}^{(2)}\right)_{m+1,q_l}, \end{array}\right.
$$

$$
,\left(e_{jl},E_{jl}^{(1)},E_{jl}^{(2)}\right)_{n+1,p_l},(e_j^{(1)},E_j^{(1)})_{1,n_1},\left(e_{jl^{(1)}}^{(1)},E_{jl^{(1)}}^{(1)}\right)_{n_1+1,p_l^{(1)}}, \\
\left(f_j^{(1)},F_j^{(1)}\right)_{1,m_1},\left(f_{jl^{(1)}}^{(1)},F_{jl^{(1)}}^{(1)}\right)_{m_1+1,q_l^{(1)}},
$$

$$
\left.\begin{array}{l} (e_j^{(2)},E_j^{(2)})_{1,n_2},\left(e_{jl^{(2)}}^{(2)},E_{jl^{(2)}}^{(2)}\right)_{n_2+1,p_l^{(2)}} \\ \left(f_j^{(2)},F_j^{(2)}\right)_{1,m_2},\left(f_{jl^{(2)}}^{(2)},F_{jl^{(2)}}^{(2)}\right)_{m_2+1,q_l^{(2)}} \end{array}\right]
$$

$$
=\frac{1}{(2\pi\omega)^2}\int_{L_1}\int_{L_2}\theta\left(\xi_1,\xi_2,x\right)z_1^{\xi_1}z_2^{\xi_2}\theta_1(\xi_1)\theta_2(\xi_2)d\xi_1 d\xi_2 \quad (\omega=\sqrt{-1}),
$$

where
$\theta\left(\xi_1,\xi_2,x\right)=\frac{\gamma(1-e_1+\sum_{i=1}^{2}E_j^{(i)}\xi_i,x)\prod_{j=2}^{n}\Gamma(1-e_j+\sum_{i=1}^{2}E_j^{(i)}\xi_i)}{\sum_{i=1}^{r}\left[\prod_{j=n+1}^{p_l}\Gamma\left(e_{jl}-\sum_{i=1}^{2}E_{jl}^{(i)}\xi_i\right)\prod_{j=1}^{q_l}\Gamma\left(1-f_{jl}+\sum_{i=1}^{2}F_{jl}^{(i)}\xi_i\right)\right]}$,

and,
$\theta_i(\xi_i)=\frac{\prod_{j=1}^{m_i}\Gamma(f_j^{(i)}-F_j^{(i)}\xi_i)\prod_{j=1}^{n_i}\Gamma(1-e_j^{(i)}+E_j^{(i)}\xi_i)}{\sum_{i^{(i)}=1}^{r^{(i)}}\left[\prod_{j=m_i+1}^{q_{l^{(i)}}}\Gamma\left(1-f_{jl^{(i)}}^{(i)}+F_{jl^{(i)}}^{(i)}\xi_i\right)\prod_{j=n_i+1}^{p_{i^{(i)}}}\Gamma\left(e_{jl^{(i)}}^{(i)}-E_{jl^{(i)}}^{(i)}\xi_i\right)\right]}$, $(i=1,2)$.

Decomposition formula satisfying in case of incomplete I-functions with two variables defined in (1) and (2) as ${}^{(\gamma)}I_Q^P[z_i]+{}^{(\Gamma)}I_Q^P[z_i]=I_Q^P[z_i]$.

Here, $z_i\neq 0;\ f_j\ (j=1,\ldots,p);\ e_j\ (j=1,\ldots,q);\ e_j^{(i)}\ (j=1,\ldots,n_i);\ e_{jl^{(i)}}^{(i)}\ (j=n_i+1,\ldots,p_{l^{(i)}});\ f_j^{(i)}\ (j=1,\ldots,m_i);\ f_{jl^{(i)}}^{(i)}\ (j=m_i+1,\ldots,q_{l^{(i)}});\ i=1,\ 2$ are complex numbers and $E_j,\ F_j,\ E_{jl^{(i)}}^{(i)},\ F_{jl^{(i)}}^{(i)}$ are positive real numbers for standardization purpose such that

$$
A_l^{(i)}=\sum_{j=1}^{n}E_j^{(i)}+\sum_{j=n+1}^{p_i}E_{jl}^{(i)}+\sum_{j=1}^{n_i}E_j^{(2)}+\sum_{j=n_i+1}^{p_{i^{(i)}}}E_{jl^{(i)}}^{(i)} \\
-\sum_{j=1}^{q_i}F_{jl^{(i)}}^{(i)}-\sum_{j=1}^{m_i}F_j^{(i)}-\sum_{j=m_i+1}^{q_{i^{(i)}}}F_{jl^{(i)}}^{(i)}\leq 0 \quad (i=1,2),
$$

The integral path is a contour starting from $L-l\infty$ to $L+l\infty$ and the poles of $\Gamma(f_j^{(i)}-F_j^{(i)}\xi_i),\ j=1,\ldots,m_i,\ i=1,2$ are separated from those of $\Gamma(1-a_j+\sum_{i=1}^{2}E_j^{(i)}\xi_i),\ j=1,\ldots,n$ and $\Gamma(1-e_j^{(i)}+E_j^{(i)}\xi_i),\ j=1,\ldots,n_i,\ i=1,2$

4

to the left of the contour L_k. The existence conditions for multiple Mellin-Barnes contours can be obtained with the help of two variables I-function [18] as $|arg z_i| < \frac{\pi}{2}\bar{A}_i^{(i)}$, where

$$\bar{A}_l^{(k)} = \sum_{j=1}^{n} E_j^{(i)} - \sum_{j=n+1}^{p_l} E_{jl}^{(i)} - \sum_{j=1}^{q_l} F_{jl}^{(i)} + \sum_{j=1}^{n_i} E_j^{(i)} - \sum_{j=n_i+1}^{p_{l^{(i)}}} E_{jl^{(i)}}^{(i)} + \sum_{j=1}^{m_i} F_j^{(i)} - \sum_{j=m_i+1}^{q_{l^{(i)}}} F_{jl^{(i)}}^{(i)} > 0 \quad (i = 1, 2).$$

for more detail conditions (see [13, 18, 10, 19]).

Definition 3: The S-function introduced and investigated by Saxena et al. [7] and defined as:

$$\underset{(p,q)}{\overset{(a,b,c,d,e)}{\mathrm{S}}}(y) = \underset{(p,q)}{\overset{(a,b,c,d,e)}{\mathrm{S}}}(\alpha_1, \alpha_2, \ldots, \alpha_p; \beta_1, \beta_2, \ldots, \beta_q; y) = \sum_{n=0}^{\infty} \frac{(\alpha_1)_n \ldots (\alpha_p)_n}{(\beta_1)_n \ldots (\beta_q)_n} \frac{(c)_{nd,e}}{\Gamma_e(na+b)} \frac{y^n}{n!}, \tag{9}$$

where $e \in \mathbb{R};\ a, b, c, d \in \mathbb{C};\ Re(a) > 0, \alpha_i\ (i = 1, 2, \ldots, p),\ \beta_j\ (j = 1, 2, \ldots, q)$, $Re(a) > eRe(d)$ and $p < q + 1$. Pochhammer symbol $(\mu)_\lambda$ defined in (3).
Here, the k-Pochhammer symbol $(y)_{n,k}$ and k-Gamma function $\Gamma_q(y)$ defined by Diaz et al. [6].
If we put $c = d = e = 1$ in S-function, it reduces to the generalized M-series. Similarly, we can convert S-function to other functions named Generalized k-Mittag-Leffler function, k-function, generalized Mittag-Leffler function and Mittag-Leffler function.

2 Theorems

In this section, we use the linear approximation of the Hermite, Legendre and Jacobi polynomials to obtain the approximate solution of general NoLDEs which given below:

$$\ddot{\mathrm{x}} + \omega \underset{(p,q)}{\overset{(a,b,c,d,e)}{\mathrm{S}}} \left[y \left(\frac{x}{L} \right)^{2\Lambda'} \right] \Gamma^{M,N}_{P,Q} \left[z \left(\frac{x}{L} \right)^{2\Lambda} \,\middle|\, \begin{matrix} (f_1, F_1, t), (f_j, F_j)_{2,P} \\ (w_j, W_j)_{1,Q} \end{matrix} \right] = NF(t), \tag{10}$$

$$\ddot{\mathrm{x}} + \omega \underset{(p,q)}{\overset{(a,b,c,d,e)}{\mathrm{S}}} \left[y \left(1 + \frac{x}{L} \right)^{\nu'} \right] \Gamma^{M,N}_{P,Q} \left[z \left(1 + \frac{x}{L} \right)^{\nu} \,\middle|\, \begin{matrix} (f_1, F_1, t), (f_j, F_j)_{2,P} \\ (w_j, W_j)_{1,Q} \end{matrix} \right] = NF(t), \tag{11}$$

$$\ddot{\mathrm{x}}+\omega \underset{(p,q)}{\overset{(a,b,c,d,e)}{\mathrm{S}}}\left[y\left(\frac{x}{L}\right)^{\Lambda}\right]{}^{(\Gamma)}I^{0,n:m_1,n_1;m_2,n_2}_{p_l,q_l,r;p_{l^{(1)}},q_{l^{(1)}},r^{(1)};p_{l^{(2)}},q_{l^{(2)}},r^{(2)}}\left[\begin{array}{c|c} z_1\left(\frac{x}{L}\right)^{\nu} & A^* \\ z_2\left(\frac{x}{L}\right)^{\lambda} & B^* \end{array}\right] = NF(t), \quad (12)$$

where

$A^*=\left(e_1,E_1^{(1)},E_1^{(2)},s\right),\left(e_j,E_j^{(1)},E_j^{(2)}\right)_{2,n},\left(e_{jl},E_{jl}^{(1)},E_{jl}^{(2)}\right)_{n+1,p_l},$
$(e_j^{(1)},E_j^{(1)})_{1,n_1},\left(e^{(1)}_{jl^{(1)}},E^{(1)}_{jl^{(1)}}\right)_{n_1+1,p_l^{(1)}},(e_j^{(2)},E_j^{(2)})_{1,n_2},\left(e^{(2)}_{jl^{(2)}},E^{(2)}_{jl^{(2)}}\right)_{n_2+1,p_l^{(2)}}$
and
$B^*=\ldots,\left(f_{jl},F_{jl}^{(1)},F_{jl}^{(2)}\right)_{m+1,q_l},\left(f_j^{(1)},F_j^{(1)}\right)_{1,m_1},\left(f^{(1)}_{jl^{(1)}},F^{(1)}_{jl^{(1)}}\right)_{m_1+1,q_l^{(1)}},$
$\left(f_j^{(2)},F_j^{(2)}\right)_{1,m_2},\left(f^{(2)}_{jl^{(2)}},F^{(2)}_{jl^{(2)}}\right)_{m_2+1,q_l^{(2)}}.$

Under the effect of external periodic force, these NoLDEs defined in (10), (11) and (12) used in the theory of resistance less circuits. To solve these Nonlinear differential equations, we use Hermite, Legendre and Jacobi polynomials.
Now, we derive some new integrals as theorems that will use to solve the above given NoLDEs.

Theorem 1:

$$\int_{-\infty}^{\infty} x^{2\sigma}e^{-x^2}H_n(x)\underset{(p,q)}{\overset{(a,b,c,d,e)}{\mathrm{S}}}\left(yx^{2\rho'}\right) \Gamma^{M,N}_{P,Q}\left[zx^{2\rho}\left|\begin{array}{l}(f_1,F_1,t),(f_j,F_j)_{2,P}\\(w_j,W_j)_{1,Q}\end{array}\right.\right]dx=\sqrt{\pi}2^{n-2\sigma}L_1(k) \Gamma^{M,N+1}_{P+1,Q+1}\left[z2^{-2\rho}\left|\begin{array}{l}(-2\sigma-2\rho'k,2\rho),(f_1,F_1,t),(f_j,F_j)_{2,P}\\(w_j,W_j)_{1,Q},(n/2-\sigma-\rho'k,\rho)\end{array}\right.\right], \quad (13)$$

where,

$$L_1(k)=\sum_{k=0}^{\infty}\frac{(\alpha_1)_k\ldots(\alpha_p)_k}{(\beta_1)_k\ldots(\beta_q)_k}\frac{(c)_{kd,e}}{\Gamma_e(ka+b)}\frac{y^k}{k!}2^{-2\rho' k}.$$

Proof: By using the results of (6) and (9) in (13), we arrive at

$$\int_{-\infty}^{\infty} x^{2\sigma}e^{-x^2}H_n(x) \left[\sum_{k=0}^{\infty}\frac{(\alpha_1)_k\ldots(\alpha_p)_k}{(\beta_1)_k\ldots(\beta_q)_k}\frac{(c)_{kd,e}}{\Gamma_e(ka+b)}\frac{\left(yx^{2\rho'}\right)^k}{k!}\frac{1}{2\pi i}\int_L\phi(s,t)\left(zx^{2\rho}\right)^s ds\right]dx,$$

here $\phi(s,t)$ defined in (7).
Provided under the given condition, interchange the order of contour integral

and integral. We get,

$$\sum_{k=0}^{\infty}\frac{(\alpha_1)_k\ldots(\alpha_p)_k}{(\beta_1)_k\ldots(\beta_q)_k}\frac{(c)_{kd,e}}{\Gamma_e(ka+b)}\frac{y^k}{k!}$$
$$\frac{1}{2\pi i}\int_L\phi(s,t)z^s\left[\int_{-\infty}^{\infty}x^{2(\sigma+\rho' k+\rho s)}e^{-x^2}H_n(x)dx\right]ds.$$

By using improper integral given below

$$\int_{-\infty}^{\infty}x^{2\sigma}e^{-x^2}H_n(x)dx=2^{n-2\sigma}\sqrt{\pi}\frac{\Gamma(2\sigma+1)}{(\sigma-n/2+1)}. \tag{14}$$

After little simplification we get the desire result.

Theorem 2:

$$\int_{-1}^{1}(1+x)^{\Lambda-1}P_n(x)\overset{(a,b,c,d,e)}{\underset{(p,q)}{\mathrm{S}}}\left[y\,(1+x)^{\nu'}\right]$$
$$\Gamma_{P,Q}^{M,N}\left[z\,(1+x)^{\nu}\left|\begin{array}{l}(f_1,F_1,t),(f_j,F_j)_{2,P}\\(w_j,W_j)_{1,Q}\end{array}\right.\right]dx=2^{\Lambda}L_2(k)\Gamma_{P+2,Q+2}^{M,N+2}$$
$$\left[z2^{\nu}\left|\begin{array}{l}(1-\Lambda-\nu' k,\nu),(1-\Lambda-\nu' k,\nu),(f_1,F_1,t),(f_j,F_j)_{2,P}\\(w_j,W_j)_{1,Q},(\Lambda-\nu' k-n,\nu),(1-\Lambda-\nu' k+n,\nu)\end{array}\right.\right], \tag{15}$$

where,

$$L_2(k)=\sum_{k=0}^{\infty}\frac{(\alpha_1)_k\ldots(\alpha_p)_k}{(\beta_1)_k\ldots(\beta_q)_k}\frac{(c)_{kd,e}}{\Gamma_e(ka+b)}\frac{y^k}{k!}2^{\nu' k}.$$

Proof: By using the known result given in (p.316, eq.15, [8]), we can get the proof of the Theorem 2 in similar manner as we did in the Theorem 1 .

Theorem 3:

$$\int_{-1}^{1}(1-x)^{\lambda}(1+x)^{\delta}x^nP_n^{(\lambda,\delta)}(x)\overset{(a,b,c,d,e)}{\underset{(p,q)}{\mathrm{S}}}(yx^{\rho})$$
$${}^{(\Gamma)}I_{p_l,q_l,r;p_{l^{(1)}},q_{l^{(1)}},r^{(1)};p_{l^{(2)}},q_{l^{(2)}},r^{(2)}}^{0,n:m_1,n_1;m_2,n_2}\left[\begin{array}{c}z_1x^{\nu}\\z_2x^{\mu}\end{array}\left|\begin{array}{c}A^*\\B^*\end{array}\right.\right]=2^{\lambda+\delta+n+1}L_3(k)$$
$${}^{(\Gamma)}I_{p_l+2,q_l+1,r;p_{l^{(1)}},q_{l^{(1)}},r^{(1)};p_{l^{(2)}},q_{l^{(2)}},r^{(2)}}^{0,n+2:m_1,n_1;m_2,n_2}\left[\begin{array}{c}z_12^{\nu}\\z_22^{\mu}\end{array}\left|\begin{array}{c}C^*\\D^*\end{array}\right.\right], \tag{16}$$

where,

$A^*=\left(e_1,E_1^{(1)},E_1^{(2)},s\right),\left(e_j,E_j^{(1)},E_j^{(2)}\right)_{2,n},\left(e_{jl},E_{jl}^{(1)},E_{jl}^{(2)}\right)_{n+1,p_l},$
$(e_j^{(1)},E_j^{(1)})_{1,n_1},\left(e_{jl^{(1)}}^{(1)},E_{jl^{(1)}}^{(1)}\right)_{n_1+1,p_l^{(1)}},(e_j^{(2)},E_j^{(2)})_{1,n_2},\left(e_{jl^{(2)}}^{(2)},E_{jl^{(2)}}^{(2)}\right)_{n_2+1,p_l^{(2)}}$
$B^*=\ldots,\left(f_{jl},F_{jl}^{(1)},F_{jl}^{(2)}\right)_{m+1,q_l},\left(f_j^{(1)},F_j^{(1)}\right)_{1,m_1},\left(f_{jl^{(1)}}^{(1)},F_{jl^{(1)}}^{(1)}\right)_{m_1+1,q_l^{(1)}},$

$\left(f_j^{(2)}, F_j^{(2)}\right)_{1,m_2}, \left(f_{jl^{(2)}}^{(2)}, F_{jl^{(2)}}^{(2)}\right)_{m_2+1,q_l^{(2)}}$

$C^* = (-\lambda - n - \rho k, \nu, \mu), (-\delta - n - \rho k, \nu, \mu), \left(e_1, E_1^{(1)}, E_1^{(2)}, s\right),$
$\left(e_j, E_j^{(1)}, E_j^{(2)}\right)_{2,n}, \left(e_{jl}, E_{jl}^{(1)}, E_{jl}^{(2)}\right)_{n+1,p_l}, (e_j^{(1)}, E_j^{(1)})_{1,n_1},$
$\left(e_{jl^{(1)}}^{(1)}, E_{jl^{(1)}}^{(1)}\right)_{n_1+1,p_l^{(1)}}, (e_j^{(2)}, E_j^{(2)})_{1,n_2}, \left(e_{jl^{(2)}}^{(2)}, E_{jl^{(2)}}^{(2)}\right)_{n_2+1,p_l^{(2)}}$

$D^* = \ldots, \left(f_{jl}, F_{jl}^{(1)}, F_{jl}^{(2)}\right)_{m+1,q_l}, (-1 - \lambda - \delta - 2(n - \rho k), 2\nu, 2\mu),$
$\left(f_j^{(1)}, F_j^{(1)}\right)_{1,m_1}, \left(f_{jl^{(1)}}^{(1)}, F_{jl^{(1)}}^{(1)}\right)_{m_1+1,q_l^{(1)}}, \left(f_j^{(2)}, F_j^{(2)}\right)_{1,m_2},$
$\left(f_{jl^{(2)}}^{(2)}, F_{jl^{(2)}}^{(2)}\right)_{m_2+1,q_l^{(2)}}$

and

$L_3(k) = \sum_{k=0}^{\infty} \frac{(\alpha_1)_k \ldots (\alpha_p)_k}{(\beta_1)_k \ldots (\beta_q)_k} \frac{(c)_{kd,e}}{\Gamma_e(ka+b)} \frac{y^k}{k!} 2^{\rho k}.$

Proof: By using the result given in (p.261, eq.15, [15]), we can get the proof of the Theorem 3 in similar manner as we did in the Theorem 1 .

3 Polynomials and Linear Approximation

Here, we solve the NoLDEs given in (10), (11) and (12) by using Hermite, Legendre and Jacobi polynomials respectively.

3.1 Hermite Polynomials and Linear Approximation

Here, we solve the NoLDE given in equation (10) as follows:

$$\ddot{x} + f(x) = NF(t), \tag{17}$$

where

$$f(x) = \omega \underset{(p,q)}{\overset{(a,b,c,d,e)}{\mathrm{S}}} \left[y \left(\frac{x}{L}\right)^{2\Lambda'} \right] \Gamma_{P,Q}^{M,N} \left[z \left(\frac{x}{L}\right)^{2\Lambda} \middle| \begin{matrix} (f_1, F_1, t), (f_j, F_j)_{2,P} \\ (w_j, W_j)_{1,Q} \end{matrix} \right], \tag{18}$$

which can be written in terms of Hermite polynomials in the interval (–L, L), We get

$$f(x) = \sum_{n=0}^{\infty} \eta_n H_n \left(\frac{x}{L}\right), \tag{19}$$

where coefficient η_n is defined by

$$\eta_n = \frac{\int_{-\infty}^{\infty} f(Lx) H_n(x) x^{2\rho} e^{-x^2} dx}{\int_{-\infty}^{\infty} [H_n(x)]^2 e^{-x^2} dx}. \tag{20}$$

The series given in equation (20) truncated after two terms then, we get a linear approximation $f^*(x)$ as follows:

$$f^*(x) = \eta_0 H_0\left(\frac{x}{L}\right) + \eta_1 H_1\left(\frac{x}{L}\right). \tag{21}$$

Now, we can write linear approximation $f^*(x)$ by using equation (18) as

$$\begin{aligned} f^*(x) = \omega \overset{(a,b,c,d,e)}{\underset{(p,q)}{\mathrm{S}}} & \left[y\left(\frac{x}{L}\right)^{2\Lambda'}\right] \\ & \Gamma^{M,N}_{P,Q}\left[z\left(\frac{x}{L}\right)^{2\Lambda} \middle| \begin{matrix} (f_1,F_1,t),(f_j,F_j)_{2,P} \\ (w_j,W_j)_{1,Q} \end{matrix}\right], \end{aligned} \tag{22}$$

putting $H_0(x) = 1$ and $H_1(x) = 2x$ in (21), we have

$$f^*(x) = \eta_0 + 2\eta_1\left(\frac{x}{L}\right). \tag{23}$$

To obtain the values of η_0 and η_1, we consider $n = 0, n = 1$ and using equation (18) in (22), then we have

$$\eta_0 = \frac{\int_{-\infty}^{\infty} \omega \overset{(a,b,c,d,e)}{\underset{(p,q)}{\mathrm{S}}} \left(yx^{2\Lambda'}\right) A_H H_0(x) x^{2\rho} e^{-x^2} dx}{\int_{-\infty}^{\infty} \left[H_0(x)\right]^2 e^{-x^2} dx}, \tag{24}$$

and

$$\eta_1 = \frac{\int_{-\infty}^{\infty} \omega \overset{(a,b,c,d,e)}{\underset{(p,q)}{\mathrm{S}}} \left(yx^{2\Lambda'}\right) A_H H_1(x) x^{2\rho} e^{-x^2} dx}{\int_{-\infty}^{\infty} \left[H_1(x)\right]^2 e^{-x^2} dx}, \tag{25}$$

where
$A_H = \Gamma^{M,N}_{P,Q}\left[zx^{2\Lambda} \middle| \begin{matrix} (f_1,F_1,t),(f_j,F_j)_{2,P} \\ (w_j,W_j)_{1,Q} \end{matrix}\right]$
Further, using Theorem 1 and result (p.193, eq.(6), [15]) with $n = 0$ in equation (24), we get

$$\begin{aligned} \eta_0 &= 2^{-2\sigma}\omega L_1(k) \\ & \Gamma^{M,N+1}_{P+1,Q+1}\left[z2^{-2\rho} \middle| \begin{matrix} (-2\sigma-2\rho' k, 2\rho),(f_1,F_1,t),(f_j,F_j)_{2,P} \\ (w_j,W_j)_{1,Q},(-\sigma-\rho' k,\rho) \end{matrix}\right], \end{aligned} \tag{26}$$

similarly, we can obtained

$$\begin{aligned} \eta_1 &= 2^{-2\sigma}\omega L_1(k) \\ & \Gamma^{M,N+1}_{P+1,Q+1}\left[z2^{-2\rho} \middle| \begin{matrix} (-2\sigma-2\rho' k, 2\rho),(f_1,F_1,t),(f_j,F_j)_{2,P} \\ (w_j,W_j)_{1,Q},(1/2-\sigma-\rho' k,\rho) \end{matrix}\right]. \end{aligned} \tag{27}$$

Now, on replacing $f(x)$ by $f^*(x)$ and using (23), we can express (17) as

$$\ddot{\mathrm{x}} + \eta_0 + 2\eta_1\left(\frac{x}{L}\right) = NF(t), \tag{28}$$

If $\delta^2 = 2\eta_1/L$ and $\delta_1^2 = \eta_0$, then (28) can be written as

$$\ddot{\mathrm{x}} + \delta^2 x + \delta_1^2 = NF(t). \tag{29}$$

Apply Laplace transform in equation (29) to find the approximate solution under the given constraints

$$y = L(L-1) \text{ and } \dot{\mathrm{x}} = 0 \text{ if } t = 0,$$

$$x^* = \left[L(L-1) + \frac{\delta_1^2}{\delta}\right]\cos\delta t - \frac{\delta_1^2}{\delta} + \frac{N}{\delta}\int_0^t F(u)\sin\delta(t-u)du. \tag{30}$$

The obtained approximate solution is general in nature.

3.2 Legendre Polynomials and Linear Approximation

The main objective of this section is to solve the NoLDE defined in (11) as follows:

$$\ddot{\mathrm{x}} + f(x) = NF(t), \tag{31}$$

where

$$f(x) = \omega \overset{(a,b,c,d,e)}{\underset{(p,q)}{\mathrm{S}}}\left[y\left(1+\frac{x}{L}\right)^{\nu'}\right] \Gamma_{P,Q}^{M,N}\left[z\left(1+\frac{x}{L}\right)^{\nu} \middle| \begin{matrix} (f_1,F_1,t),(f_j,F_j)_{2,P} \\ (w_j,W_j)_{1,Q} \end{matrix}\right], \tag{32}$$

which can be written in terms of Legendre polynomials in the interval (–L, L). We get

$$f(x) = \sum_{n=0}^{\infty} \tau_n P_n\left(\frac{x}{L}\right), \tag{33}$$

where coefficient τ_n is defined by

$$\tau_n = \frac{\int_{-1}^{1} f(Lx)P_n(x)(1+x)^{\Lambda-1}dx}{\int_{-1}^{1}\left[P_n(x)\right]^2 dx}. \tag{34}$$

Truncated the series (34) after two terms. We get a linear approximation $f^*(x)$ as follows:

$$f^*(x) = \tau_0 P_0\left(\frac{x}{L}\right) + \tau_1 P_1\left(\frac{x}{L}\right). \tag{35}$$

Now, we can write linear approximation $f^*(x)$ by using equation (32) by

$$f^*(x) = \omega \overset{(a,b,c,d,e)}{\underset{(p,q)}{\mathrm{S}}}\left[y\left(1+\frac{x}{L}\right)^{\nu'}\right] \Gamma_{P,Q}^{M,N}\left[z\left(1+\frac{x}{L}\right)^{\nu} \middle| \begin{matrix} (f_1,F_1,t),(f_j,F_j)_{2,P} \\ (w_j,W_j)_{1,Q} \end{matrix}\right], \tag{36}$$

Putting $P_0(x) = 1$ and $P_1(x) = x$ in (35), we have

$$f^*(x) = \tau_0 + \tau_1 \left(\frac{x}{L}\right). \tag{37}$$

Use equation (36) in (34) with $n = 0$ and $n = 1$, to obtain the values of τ_0 and τ_1 respectively as

$$\tau_0 = \frac{\int_{-1}^{1} \omega \overset{(a,b,c,d,e)}{\underset{(p,q)}{\mathrm{S}}} \left[y\,(1+x)^{\nu'}\right] A_L P_0(x)(1+x)^{\Lambda-1} dx}{\int_{-1}^{1} \left[P_0(x)\right]^2 dx}, \tag{38}$$

and

$$\tau_1 = \frac{\int_{-1}^{1} \omega \overset{(a,b,c,d,e)}{\underset{(p,q)}{\mathrm{S}}} \left[y\,(1+x)^{\nu'}\right] A_L P_1(x)(1+x)^{\Lambda-1} dx}{\int_{-1}^{1} \left[P_1(x)\right]^2 dx}, \tag{39}$$

where

$$A_L = \Gamma^{M,N}_{P,Q}\left[z\,(1+x)^{\nu} \,\middle|\, \begin{matrix} (f_1, F_1, t), (f_j, F_j)_{2,P} \\ (w_j, W_j)_{1,Q} \end{matrix}\right]$$

Further, using Theorem 2 and result (p.175, eq.(12), [15]) with $n = 0$ in (38), we get

$$\tau_0 = \omega 2^{\Lambda-1} L_2(k) \Gamma^{M,N+2}_{P+2,Q+2} \left[z2^{\nu} \,\middle|\, \begin{matrix} (1-\Lambda-\nu' k, \nu), (1-\Lambda-\nu' k, \nu), (f_1, F_1, t), (f_j, F_j)_{2,P} \\ (w_j, W_j)_{1,Q}, (\Lambda-\nu' k, \nu), (1-\Lambda-\nu' k, \nu) \end{matrix}\right], \tag{40}$$

Similarly, we can evaluate for $n = 1$

$$\tau_1 = 3\omega 2^{\Lambda-1} L_2(k) \Gamma^{M,N+2}_{P+2,Q+2} \left[z2^{\nu} \,\middle|\, \begin{matrix} (1-\Lambda-\nu' k, \nu), (1-\Lambda-\nu' k, \nu), (f_1, F_1, t), (f_j, F_j)_{2,P} \\ (w_j, W_j)_{1,Q}, (\Lambda-\nu' k-1, \nu), (2-\Lambda-\nu' k, \nu) \end{matrix}\right]. \tag{41}$$

Now, on replacing $f(x)$ by $f^*(x)$ and use (37), we can express in (31) as

$$\ddot{\mathrm{x}} + \delta_1^2 + \delta^2 x = NF(t), \tag{42}$$

where $\delta^2 = \tau_1/L$ and $\delta_1^2 = \tau_0$. Apply the Laplace transform in (42) to find the approximate solution under the constraints

$$x = L(L-1) \text{ and } \dot{\mathrm{x}} = 0 \text{ if } t = 0,$$

$$x^* = \left[L(L-1) + \frac{\delta_1^2}{\delta}\right] \cos \delta t - \frac{\delta_1^2}{\delta} + \frac{N}{\delta} \int_0^t F(u) \sin \delta (t-u) du. \tag{43}$$

The obtained approximate solution is general in nature.

3.3 Jacobi Polynomials and Linear Approximation

Here, our aim is to solve the NoLDE given in (12) is as follows:

$$\ddot{\mathrm{x}} + f(x) = NF(t), \tag{44}$$

where

$$f(x) = \omega \overset{(a,b,c,d,e)}{\underset{(p,q)}{\mathrm{S}}} \left[y \left(\frac{x}{L}\right)^{\Lambda} \right] {}^{(\Gamma)}I^{0,n:m_1,n_1;m_2,n_2}_{p_l,q_l,r;p_{l(1)},q_{l(1)},r_{(1)};p_{l(2)},q_{l(2)},r_{(2)}} \left[\begin{array}{c|c} z_1 \left(\frac{x}{L}\right)^{\nu} & A^* \\ z_2 \left(\frac{x}{L}\right)^{\mu} & B^* \end{array} \right], \tag{45}$$

where A^* and B^* are defined in (12), which can be written in terms of Jacobi polynomials in the interval (–L, L). We have

$$f(x) = \sum_{n=0}^{\infty} C_n^{(\iota,\kappa)} P_n^{(\iota,\kappa)} \left(\frac{x}{L}\right), \tag{46}$$

where coefficient $C_n^{(\iota,\kappa)}$ is defined by

$$C_n^{(\iota,\kappa)} = \frac{\int_{-1}^{1} f(Lx) P_n^{(\iota,\kappa)}(x)(1-x)^{\iota}(1+x)^{\kappa} dx}{\int_{-1}^{1} \left[P_n^{(\iota,\kappa)}(x)\right]^2 (1-x)^{\iota}(1+x)^{\kappa} dx}. \tag{47}$$

Truncated the above given series after two terms. We get a linear approximation $f^*(x)$ as follows:

$$f^*(x) = C_0^{(\iota,\kappa)} P_0^{(\iota,\kappa)} \left(\frac{x}{L}\right) + C_1^{(\iota,\kappa)} P_1^{(\iota,\kappa)} \left(\frac{x}{L}\right). \tag{48}$$

Now, we can write linear approximation $f^*(x)$ by using equation (45) by

$$f^* = \omega \overset{(a,b,c,d,e)}{\underset{(p,q)}{\mathrm{S}}} \left[y \left(\frac{x}{L}\right)^{\Lambda} \right] {}^{(\Gamma)}I^{0,n:m_1,n_1;m_2,n_2}_{p_l,q_l,r;p_{l(1)},q_{l(1)},r_{(1)};p_{l(2)},q_{l(2)},r_{(2)}} \left[\begin{array}{c|c} z_1 \left(\frac{x}{L}\right)^{\nu} & A^* \\ z_2 \left(\frac{x}{L}\right)^{\mu} & B^* \end{array} \right], \tag{49}$$

Putting $P_0^{(\iota,\kappa)} = 1$ and $P_1^{(\iota,\kappa)} = \frac{\iota-\kappa}{2} + \frac{(2+\iota+\kappa)x}{2}$ in (48), we have

$$f^*(x) = C_0^{(\iota,\kappa)} + C_1^{(\iota,\kappa)} \left[\frac{\iota-\kappa}{2} + \frac{(2+\iota+\kappa)x}{2} \right]. \tag{50}$$

Use equation (47) in (45) with $n = 0$ and $n = 1$, to obtain the values of $C_0^{(\iota,\kappa)}$ and $C_1^{(\iota,\kappa)}$ with the help of Theorem 3 and aid a result (p.260, eq.(11), [15]) with $n = 0$ in equation (47), we get $C_0^{(\iota,\kappa)}$ as follows:

$$C_0^{(\iota,\kappa)} = \frac{\omega L_3(k)\Gamma(2+\iota+\kappa)}{\Gamma(1+\iota)\Gamma(1+\kappa)} \\ {}^{(\Gamma)}I^{0,n+2:m_1,n_1;m_2,n_2}_{p_l+2,q_l+1,r;p_{l^{(1)}},q_{l^{(1)}},r^{(1)};p_{l^{(2)}},q_{l^{(2)}},r^{(2)}}\left[\begin{array}{c|c} z_1 2^{\nu} & C^{**} \\ z_2 2^{\mu} & D^{**}\end{array}\right], \quad (51)$$

where
$C^{**} = (-\iota-\rho k,\nu,\mu),(-\kappa-\rho k,\nu,\mu),\left(e_1,E_1^{(1)},E_1^{(2)},s\right),\left(e_j,E_j^{(1)},E_j^{(2)}\right)_{2,n},$
$\left(e_{jl},E_{jl}^{(1)},E_{jl}^{(2)}\right)_{n+1,p_l},(e_j^{(1)},E_j^{(1)})_{1,n_1},\left(e_{jl^{(1)}}^{(1)},E_{jl^{(1)}}^{(1)}\right)_{n_1+1,p_l^{(1)}},(e_j^{(2)},E_j^{(2)})_{1,n_2},$
$\left(e_{jl^{(2)}}^{(2)},E_{jl^{(2)}}^{(2)}\right)_{n_2+1,p_l^{(2)}}$
$D^{**} = \ldots,\left(f_{jl},F_{jl}^{(1)},F_{jl}^{(2)}\right)_{m+1,q_l},(-1-\iota-\kappa-2\rho k,2\nu,2\mu),\left(f_j^{(1)},F_j^{(1)}\right)_{1,m_1}$
$,\left(f_{jl^{(1)}}^{(1)},F_{jl^{(1)}}^{(1)}\right)_{m_1+1,q_l^{(1)}},\left(f_j^{(2)},F_j^{(2)}\right)_{1,m_2},\left(f_{jl^{(2)}}^{(2)},F_{jl^{(2)}}^{(2)}\right)_{m_2+1,q_l^{(2)}}.$

Similarly, we can obtain $C_1^{(\iota,\kappa)}$ as

$$C_1^{(\iota,\kappa)} = \frac{2\omega L_3(k)\Gamma(3+\iota+\kappa)}{\Gamma(2+\iota)\Gamma(2+\kappa)} \\ {}^{(\Gamma)}I^{0,n+2:m_1,n_1;m_2,n_2}_{p_l+2,q_l+1,r;p_{l^{(1)}},q_{l^{(1)}},r^{(1)};p_{l^{(2)}},q_{l^{(2)}},r^{(2)}}\left[\begin{array}{c|c} z_1 2^{\nu} & C^{***} \\ z_2 2^{\lambda} & D^{***}\end{array}\right], \quad (52)$$

where
$C^{***} = (-\iota-1-\rho k,\nu,\mu),(-\kappa-1-\rho k,\nu,\mu),\left(e_1,E_1^{(1)},E_1^{(2)},s\right),$
$\left(e_j,E_j^{(1)},E_j^{(2)}\right)_{2,n},\left(e_{jl},E_{jl}^{(1)},E_{jl}^{(2)}\right)_{n+1,p_l},(e_j^{(1)},E_j^{(1)})_{1,n_1},$
$\left(e_{jl^{(1)}}^{(1)},E_{jl^{(1)}}^{(1)}\right)_{n_1+1,p_l^{(1)}},(e_j^{(2)},E_j^{(2)})_{1,n_2},\left(e_{jl^{(2)}}^{(2)},E_{jl^{(2)}}^{(2)}\right)_{n_2+1,p_l^{(2)}}$
$D^{***} = \ldots,\left(f_{jl},F_{jl}^{(1)},F_{jl}^{(2)}\right)_{m+1,q_l},(-3-\iota-\kappa-2\rho k,2\nu,2\mu),\left(f_j^{(1)},F_j^{(1)}\right)_{1,m_1}$
$,\left(f_{jl^{(1)}}^{(1)},F_{jl^{(1)}}^{(1)}\right)_{m_1+1,q_l^{(1)}},\left(f_j^{(2)},F_j^{(2)}\right)_{1,m_2},\left(f_{jl^{(2)}}^{(2)},F_{jl^{(2)}}^{(2)}\right)_{m_2+1,q_l^{(2)}}.$

Now, on replacing $f(x)$ by $f^*(x)$ and use equation (50), we can write equation (44) as

$$\ddot{\mathrm{x}} + \delta^2 x + \frac{\iota-\kappa}{2+\iota+\kappa}\left(\delta^2-\delta_1^2\right) = NF(t), \quad (53)$$

where $\delta^2 = \frac{2+\iota+\kappa}{2L}$ and $\delta_1^2 = \frac{2+\iota+\kappa}{(\kappa-\iota)L}C_0^{(\iota,\kappa)}$.
Apply the Laplace transform in equation (53) to find the approximate solution under the constraints

$$x = L(L-1) \text{ and } \dot{\mathrm{x}} = 0 \text{ if } t = 0,$$

$$x^* = \left[L(L-1) + \frac{(\iota-\kappa)\delta}{2+\iota+\kappa}\left(1-\frac{\delta_1^2}{\delta}\right)\right] \cos\delta t - \frac{(\iota-\kappa)\delta}{2+\iota+\kappa}\left(1-\frac{\delta_1^2}{\delta}\right) + \frac{N}{\delta}\int_0^t F(u)\sin\delta(t-u)du. \tag{54}$$

The obtained approximate solution is general in nature.

Similarly, we can prove all of the above results and theorems for lower forms of the incomplete H-function $\gamma_{P,Q}^{M,N}[z]$ and incomplete I-function with two variables ${}^{(\gamma)}I^{0,n:m_1,n_1;m_2,n_2}_{p_l,q_l,r;p_{l^{(1)}},q_{l^{(1)}},r^{(1)};p_{l^{(2)}},q_{l^{(2)}},r^{(2)}}[z_i]$.

4 Conclusion

In this article, we introduced the approximate solution of NoLDE associated with incomplete H-functions, incomplete I-functions with two variables and S-function with the help of Hermite, Legendre and Jacobi polynomials. These obtained results are general and effectively used in the field of Science, Mathematics, Statistics, Economics and finance. These findings can be used to solve the problem of a resistance less circuit involving a nonlinear capacitor under the influence of external periodic force.

References

[1] Bansal, M. K., Jolly, N., Jain, R., and Kumar, D. (2019). An integral operator involving generalized Mittag-Leffler function and associated fractional calculus results. *The Journal of Analysis*, 27(3), 727-740.

[2] Bansal, M. K., Kumar, D., and Jain, R. (2019). Interrelationships Between Marichev–Saigo–Maeda Fractional Integral Operators, the Laplace Transform and the $\overline{H}$-Function. *International Journal of Applied and Computational Mathematics*, 5(4), 1-13.

[3] Bansal, M. K., Kumar, D., Khan, I., Singh, J., and Nisar, K. S. (2019). Certain unified integrals associated with product of M-series and incomplete H-functions. *Mathematics*, 7(12), 1191.

[4] Bansal, M. K., Kumar, D., Singh, J., Tassaddiq, A., and Nisar, K. S. (2020). Some new results for the Srivastava–Luo–Raina M-transform pertaining to the incomplete H-functions. *AIMS Math*, 5(1), 717-722.

[5] Chaurasia V. B. L., and Saxena, V. (2007). Applications of certain special functions to non-linear differential equation involving $\bar{H}$-function. *Acta Ciencia Indica.*, XXXIVM(1), 307-318.

[6] Diaz, R., and Pariguan, E. (2004). On hypergeometric functions and Pochhammer k-symbol. *arXiv preprint math/0405596.*

[7] Daiya, J., and Saxena, R. K. (2015). Integral transforms of the S-functions. *Le Matematiche*, 70(2), 147-159.

[8] Erdélyi, A., Magnus, W., Oberhettinger, F., and Tricomi, F. G. (1953). *Higher Transcendental Functions Vol. II.* New York, Toronto and London: McGraw-Hill Book Company.

[9] Garde R. M. (1967). Applications of Jacobi polynomials to non-linear oscillations–1, Free oscillations. *Proc Nat Acad Sci India*. 37, 119-120.

[10] Jayarama, P., Madam, V. N. T., and Kurumujji, S. K. (2014). A study of I-function of several complex variables. *International Journal of Engineering Mathematics*, 2014.

[11] Kumar, D., Singh, J., Purohit, S. D., and Swroop, R. (2019). A hybrid analytical algorithm for nonlinear fractional wave-like equations. *Mathematical Modelling of Natural Phenomena*, 14(3), 304.

[12] Kumar, D., Singh, J., Prakash, A., and Swroop, R. (2019). Numerical simulation for system of time-fractional linear and nonlinear differential equations. *Progr. Fract. Differ. Appl*, 5(1), 65-77.

[13] Prasad, Y. N. (1986). Multivariable I-function. *Vijnana Parishad Anusandhan Patrika*. 29(4), 231-235.

[14] Prym, F. E. (1877). Zur theorie der gamma function. *The Journal fur die Reine und Angewandte Mathematik*. 82, 165–172.

[15] Rainville, E. D. (1960). *Special functions (Vol. 5)*. New York.

[16] Saxena, R. K., and Kushwaha, R. S. (1970). Applications of Jacobi polynomials to non-linear oscillations. *In Proceedings of the National Academy of Sciences, India*. 40, 65-72.

[17] Sharma, M. (2008). Fractional integration and fractional differentiation of the M-series. *Fractional calculus and applied analysis*, 11(2), 187-191.

[18] Sharma, C. K., and Mishra, P. L. (1991). On the I-function of two variables and its properties. *Acta Ciencia Indica Math*. 17, 667-672.

[19] Sharma, R., Singh, J., Kumar, D., and Singh, Y. (2022). Certain unified integrals associated with product of the general class of polynomials and incomplete I-functions. *International Journal of Applied and Computational Mathematics*, 8(1), 1-11.

[20] Singh, P. (2007). Applications of Hermite, Legendre and Jacobi polynomials and linear approximation to some non-linear differential equations associated with H-function. *Vijnana Parishad Anusandhan Patrika*. 50(1), 41-61.

[21] Singh, J., Kumar, D., and Bansal, M. K. (2019). Solution of nonlinear differential equation and special functions. *Mathematical Methods in the Applied Sciences*, 43(5), 2106-2116.

[22] Singh, J., Kumar, D., Baleanu, D., and Rathore, S. (2018). An efficient numerical algorithm for the fractional Drinfeld–Sokolov–Wilson equation. *Applied Mathematics and Computation*. 335, 12-24.

[23] Singh, J., Secer, A., Swroop, R., and Kumar, D. (2019). A reliable analytical approach for a fractional model of advection-dispersion equation. *Nonlinear Engineering*, 8(1), 107-116.

[24] Srivastava, B. M. (1975). Solvable potentials for the Chebyshev and associated Laguerre equations. *Jnanabha Sect A*. 5, 181-187.

[25] Srivastava, B. M., and Singh, F. (1976). Application of Jacobi polynomials to non-linear differential equation associated with H-function. *Vijnana Parishad Anusandhan Patrika*. 19(1), 25-34.

[26] Srivastava, H. M., Saxena, R. K., and Parmar, R. K. (2018). Some Families of the Incomplete H-Functions and the Incomplete $\overline{H}$-Functions and Associated Integral Transforms and Operators of Fractional Calculus with Applications. *Russian Journal of Mathematical Physics*, 25(1), 116-138.

J. COMPUTATIONAL ANALYSIS AND APPLICATIONS, VOL. 31, NO.1, 2023, COPYRIGHT 2023 EUDOXUS PRESS, LLC

SEAIQHRDP mathematical model Analysis for the transmission dynamics of COVID-19 in India

M. Ankamma Rao[1] and A.Venkatesh[2]*

[1,2]Department of Mathematics,
AVVM Sri Pushpam College (Affiliated to Bharathidasan University),
Poondi, Thanjavur(Dt), Tamilnadu, India-613 503.

December 28, 2022

Abstract

Mathematical modeling is one of the most used techniques for analyzing and preventing the transmission of COVID-19. To control this pandemic, it is essential to classify the infected population. So in this article, a new SEAIQHRDP model was formulated to investigate the transmittal dynamics of COVID-19. This model contains nine compartments Susceptible(S) class, Exposed(E) class, Asymptomatic(A) class, Infected(I) class, Quarantined(Q) class, Hospitalized(H) class, Recovered(R) class, Death(D) class, and Insusceptible (P) class. This model was fitted to the daily and cumulative confirmed COVID-19 cases in the period between 30th January 2020 and 13th January 2021 in India. Sensitivity analysis concerning R_0 was performed to classify the significance of parameters. Contour plots for R_0 were executed and the effect of various parameters on the infected classes had shown graphically. The necessity of stringent face mask usage and social seclusion is highlighted by optimal control analysis as a key factor in the dramatic reduction of infection rates. So the optimal control technique was adopted to lessen the disease mortality by taking both nonpharmaceutical and pharmaceutical intervention strategies as control functions and comparing infectives and recoveries with and without controls.

Keywords: : mathematical model, Stability analysis, Basic reproduction number, Sensitivity analysis, optimal strategy
Subject Classification: 00A71

1 Introduction

The world has been trembling with a new infectious disease COVID-19. The World Health Organization (WHO) has declared it was a universal pandemic on 11th March 2020 [14]. originally The COVID-19 disease was revealed in December 2019 in Wuhan, Hubei, China. Later it increased rapidly and spread in all countries in the world. As of August 28th, 2022, the total confirmed cases of 596,873,121 and death cases of 6,459,684 of COVID-19 had been reported to WHO [15]. On January 30th, 2020 the first COVID-19 case [28] was placed in Kerala, India. A total of 44,389,176 confirmed cases and 527,556 death cases were placed in India as of August 28th, 2022. Initially, some countries implemented strictly non-pharmacological interventions namely as use of face masks social distancing, and hygiene to resist the extent of the COVID-19 pandemic. Due to these safety measures, the virus spread slowed down gradually but not ceased completely. Since the vaccination process had started, the COVID-19 cases decreased day by day and it became under control. But still now in some countries COVID- cases raises unexpectedly.

---

*Corresponding author: avenkateshmaths@gmail.com

Mathematical modeling is a prominent technique for forecasting and controlling the transmission dynamics of epidemic diseases. Alexander Krämeret al.[1] H.W. Hethcote [16], R.M.May & R.M Anderson, [38] Brauer F & Chavez CC) [6]. Some standard mathematical models such as SIR, SEIR, SEIAR, SEIRD, etc. were broadly used to estimate the future trend of a pandemic. The standard SIR model Kermack WO & McKendrick [20] described the spread of the virus using the compartments of susceptible, infected, and recovered. By incorporating the new compartments, we get new models to detect the communication dynamics of contagious diseases. An SEIR model by Mwalili S et al. cite 26 was developed by adding an Exposed compartment to the SIR model which contained distinctive reaction and administration activity factors. This model is used widely to forecast the direction of the COVID-19 graph in China among other countries. Through the SEIR model, the influence of control strategies was studied by Lin Q et al.[22] and formulated the SEIR extension model. A generalized SEIR model Read JM et al.[34] was advanced in the latent period to cover the communication dynamics of COVID-19. During the incubation period, it consists of one more compartment as asymptomatic individuals in the SEIR model. The isolated class in SEIJR was interchanged with the asymptomatic class in SEIAR. By using this model, Bailey et al [2] displayed related properties to the SEIJR model Peng L et al. [30]. General models such as SIR, SEIR, SEIRD, SEIJR, etc. were not suitable for forecast the effect of the widespread disease since they comprise a finite number of parameters and disregarded essential classes such as asymptomatic infected, quarantine, Hospitalization, etc. SIDARTHE model of Giordano et al.[11] is an extension of the SEIR model which consists of undetected as well as detected infected populations.

The field of FDEs has developed greatly over the past few decades as a result of its applicability in numerous branches of research and technology. To study malaria transmission, Rehman, Attiq ul, and colleagues devised a 9 compartment FDE model [35]. By considering both the government's activity and the individual's response, Danane, Jaouad et al.[8] established a seven-compartment FDE model. Supriya, Yadav, and colleagues [42] created the FDE model to investigate the COVID-19 trend using an effective and potent analytical q-HASTM approach. By Jagdev Singh, a fractional guava fruit model with memory effect was developed [41]

In general, before showing any symptoms an individual exposed to the virus will become infectious i.e. pre-symptomatic through an incubation period of 5 days Liu C et al. [23]. Many reports have shown that a huge number of individuals who were exposed to the virus did not show any symptoms i.e., they all remain asymptomatic. The pre-symptomatic or asymptomatic individuals were capable to diffuse the virus to others. Since the reported asymptomatic cases in India are high, it was necessary to include the asymptomatic class in the epidemiological model. As for the total of parameters and accurateness model, the above-discussed models were not perfect for long-term predictions. Therefore one more compartment dead population had been incorporated in the SEIAR model presented through Huang et al.[15] to improve the accurateness model for long-term prediction.

Raj Kishore et.al [33] developed the SEIQRDP model by including the quarantine class (Q) and insusceptible class (P) and predicted the number of active cases. By

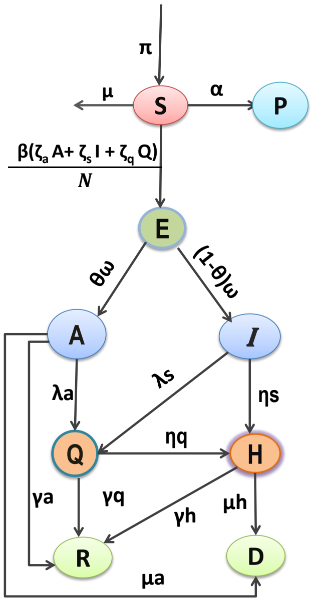

Figure 1: Flow Chart of SEAIQHRDP model

incorporating an asymptomatic class Singh HP et al [39] introduced the SEAIQRDT model and forecast the confirmed cases. When the best optimal control technique is used early in a pandemic, the intensity of epidemic peaks tends to decline, spreading the maximum impact of an epidemic across a longer time. Massad, Eduardo et al [25] developed an optimal control model to analyze the effect of vaccination on the zika virus. To analyze the COVID-19 trend in the future, Bandekar SR and Minighosh [3] devised an 11 compartments mathematical model. They then employed an optimal control strategy to reduce the disease fatality.

By taking into account all of the aforementioned discussions, We developed a new SEAIQHRDP model by including a new class—hospitalization—to the SEAIQRDP model in order to examine the transmission of COVID-19. Later an optimal control strategy with three control variables was applied to the proposed model to moderate the outspread of COVID-19 optimally.

The following sections in this manuscript were systematized as follows: SEAIQHRDP model formulation was presented in section 2. In section 3 The elementary properties of the recommended model such as positivity and boundedness, disease-free equilibrium's local stability, and R_0 expression in various parameters were executed. Section 3 finished Parameter estimation, model fitting, and model justification. Sect.5 performed the sensitive analysis concerning R_0 and the impact of parameters on infected populations. Section 6 implemented and solved an optimal control problem analytically. The work ends with the conclusion in Section 7

2 Model formation

By considering all the above discussions, in this study, a new mathematical model SEAIQHRDP was formulated. In this model, the class S(t) contained the susceptible individuals at time t, the class E(t) contained exposed individuals (these were contaminated but does not contaminate others within the reaction time), the class A(t) contained asymptomatic infected individuals (despite no symptoms appeared in them but capable to infect others), the class I(t) contains the symptomatic individuals (these persons having symptoms and were capable to infect others), the class Q(t) contained the quarantined individuals (these were infected but isolated), the class H(t) contained the hospitalization individuals (these were infected and undergo medical treatment), the class R(t) contained the recovered individuals, the class D(t) contained the death individuals, and the class P(t) contained the insusceptible individuals those are incapable of getting infected due to either pre-isolated or following the WHO rules strictly.

Let Λ and μ be the constant recruitment rate and normal death rate in the susceptible population. Let β be the virus contact rate. Let ζ_a, ζ_q, and ζ_s be the adjustment factors for asymptomatic infected, symptomatic infected, and quarantine populations. $\beta\zeta_a$, $\beta\zeta_q$ and $\beta\zeta_h$ were the virus transmission factors of asymptomatic, symptomatic, and quarantine populations to susceptible populations. These were time-dependent factors in computations. This model has the potency of disease is $\triangle = \frac{\zeta_a A+\zeta_s I+\zeta_q Q}{N}$.

Let α be the protection rate at which the susceptible individuals move to insusceptible individuals. This included the influence of control measures. Let θ be the fraction at which the exposed individuals move to asymptomatic individuals. Then $(1-\theta)$ is the fraction at which exposed individuals move to symptomatic infected individuals at a velocity ω. Let λ_a and λ_s be the quarantine rates at which the asymptomatically infected individuals and symptomatically infected individuals were quarantined. Let η_s and η_q hospitalization rates at which the symptomatic and quarantine populations had certain complications due to severe symptoms shall be hospitalized. Let γ_a, γ_q, and γ_h be the recovery rates at which the asymptomatic infected, quarantined, and hospitalized individuals were recovered from the disease. There will be a possibility to die, in asymptomatic individuals before getting symptoms and after admitting to the hospital. Let μ_a and μ_h be the mortality rates of asymptomatic and hospitalized individuals. By using all the above conditions, The relation between these nine compartments and corresponding parameters were shown in Figure.1 and table 1

The arrangement of nonlinear differential equations for the proposed model in India was

$$\frac{ds}{dt} = \Lambda - \beta \triangle S - (\alpha+\mu)S \tag{1.1}$$

$$\frac{dE}{dt} = \beta \triangle S - (\omega+\mu)E \tag{1.2}$$

$$\frac{dA}{dt} = \theta\omega E - (\lambda_a+\gamma_a+\mu_a+\mu)A \tag{1.3}$$

$$\frac{dI}{dt} = (1-\theta)\omega E - (\lambda_s+\eta_s+\mu)I \tag{1.4}$$

$$\frac{dQ}{dt} = \lambda_a A + (\lambda_s I - (\eta_q+\gamma_q+\mu)Q \tag{1.5}$$

$$\frac{dH}{dt} = \eta_s I + \eta_q Q - (\gamma h+\mu_h+\mu)H \tag{1.6}$$

$$\frac{dR}{dt} = \gamma_a A + \gamma_q Q + \gamma_h H - \mu R \tag{1.7}$$

$$\frac{dD}{dt} = \mu_a A + \mu_h H \tag{1.8}$$

$$\frac{dP}{dt} = \alpha S. \tag{1.9}$$

with non negative primary conditions are $S(0)=S_0$, $E(0)=E_0$, $A(0)=A_0$, $I(0)==I_0$, $Q(0)=Q_0$, $H(0)=H_0$,$R(0)=R_0$, $D(0)=D_0$and $P(0)=P_0$.

Table 1: SEAIQHRDP model parameter's complete depiction.

parameter	description
Λ	Recruitment rate of human
θ	Proportion of exposed individuals
ω	Conversion rate of exposed to asymptomatically infected populace
α	Protection rate of susceptible individuals to insusceptible populace
ζ_a,ζ_s,ζ_q	Adjustment factor for asymptomatic, symptomatic and quarantine populace
β	Transmission rate of virus
λ_a	Quarantine rate of asymptomatic infected populace
λ_s	Quarantine rate of symptomatic infected populace
η_s	Hospitalization rate of symptomatic infected populace
η_q	Hospitalization rate of quarantine infected populace
γ_a	The rate of recovery from asymptomatic infected populace
γ_q	The rate of recovery from quarantine populace
γ_h	The rate of recovery from hospitalization populace
μ_a	The rate of mortality from asymptomatic populace
μ_h	The rate of mortality from hospitalization populace
μ	Normal mortality rate of human populace

3 SEAIQHRDP model analysis

3.1 Positivity and boundedness

Theorem 1. *All the solutions* $(S(t), E(t), A(t), I(t), Q(t), H(t), R(t), D(t), P(t)) \in \mathbb{R}^9_+$ *of the system (1) with primary conditions remain non negative and were uniformly bounded in the region* Ω *for all time* $t \geq 0$.

Proof 1. *Assumed that* $(S(t), E(t), A(t), I(t), Q(t), H(t), R(t), D(t), P(t)) \in \mathbb{R}^9_+$ *be a solution of (1) for* $t \in [0, t_0]$, *where* $t_0 \geq 0$.

From the equation (1.1),

$\frac{ds}{dt} = \Lambda - (\zeta_a A + \zeta_s I + \zeta_q Q)\frac{S}{N} - (\alpha + \mu)S \geq \Lambda - \phi(t)S$

where $\phi(t) = \beta(\zeta_a A + \zeta_s I + \zeta_q Q)\frac{S}{N} + (\alpha + \mu)$

$\Rightarrow \frac{ds}{dt} \geq \Lambda - \phi(t)S$

After integration, $S(t) = S^0 \exp(-\int_0^t \phi(s)\,ds)\int_0^t e^{\int_0^s \phi(u)\,du)} > 0.$

Hence, for all $t \in$ *[0,* t_0*), we get* $S(t) > 0$

From the equation (1.2),

$\frac{dE}{dt} = (\zeta_a A + \zeta_s I + \zeta_q Q)\frac{S}{N} - (\omega + \mu)E \geq -(\omega + \mu)E$

$\Rightarrow \frac{dE}{dt} \geq -(\omega + \mu)E$

$\Rightarrow E(t) \geq E^0 \exp(-\int_0^t (\omega + \mu)\,ds) \geq 0$

i.e, $E(t) \geq 0$

From the equation (1.3),

$\frac{dA}{dt} = \theta\omega E - (\lambda_a + \gamma_a + \mu_a + \mu)A \geq -(\lambda_a + \gamma_a + \mu_a + \mu)A$

$\Rightarrow \frac{dA}{dt} \geq -(\lambda_a + \gamma_a + \mu_a + \mu)A$

$\Rightarrow A(t) \geq A^0 \exp(-\int_0^t (\lambda_a + \gamma_a + \mu_a + \mu)\,ds \geq 0$

i.e,$A(t) \geq 0$

From the equation (1.4),

$\frac{dI}{dt} = (1 - \theta)\omega E - (\lambda_s + \eta_s + \mu)I \geq -(\lambda_s + \eta_s + \mu)I$

$\Rightarrow \frac{dI}{dt} \geq -(\lambda_s + \eta_s + \mu)I$

$\Rightarrow I(t) \geq I^0 \exp(-\int_0^t(\lambda_s + \eta_s + \mu)\, ds \geq 0$
i.e,$I(t) \geq 0$

From the equation of (1.5),
$\frac{dQ}{dt} = \lambda_a A + (\lambda_s I - (\eta_q + \gamma_q + \mu)Q \geq -(\eta_q + \gamma_q + \mu)Q$
$\Rightarrow \frac{dQ}{dt} \geq -(\eta_q + \gamma_q + \mu)Q$
$\Rightarrow Q(t) \geq Q^0 \exp(-\int_0^t(\eta_q + \gamma_q + \mu)\, ds \geq 0$
i.e,$Q(t) \geq 0$

From the equation (1.6),
$\frac{dH}{dt} = \eta_s I + \eta_q Q - (\gamma_h + \mu_h + \mu)H \geq -(\gamma_h + \mu_h + \mu)H$
$\Rightarrow \frac{dH}{dt} \geq -(\gamma_h + \mu_h + \mu)H$
$\Rightarrow H(t) = H^0 \exp(-\int_0^t(\gamma_h + \mu_h + \mu)\, ds \geq 0$
i.e, $H(t) \geq 0$

From the equation (1.7),
$\frac{dR}{dt} = \gamma_a A + \gamma_q Q + \gamma_h H - \mu R \geq \mu R$
$\Rightarrow \frac{dR}{dt} \geq \mu R$
$\Rightarrow R(t) \geq R^0 \exp(-\int_0^t \mu)\, ds \geq 0$
i.e,$R(t) \geq 0.$

Similarly we can prove that $D(t) \geq 0$ *and* $P(t) \geq 0.$

Hence $(S(t), E(t), A(t), I(t), Q(t), H(t), R(t), D(t), P(t))$ *of (1) with primary conditions for all* $t \in [0, t_0]$ *are non negative solutions in* Ω.

We prove that the boundedness of the solutions (S, E, A, I, Q, H, R,D,P) of system (1).

The positivity of the solutions implies that $\frac{dS}{dt} \leq \Lambda - (\alpha + \mu)S$.

From the above equation, we can write that
$\lim_{t\to\infty} supS \leq \frac{\Lambda}{(\alpha+\mu)}$ *and* $S \leq \frac{\Lambda}{(\alpha+\mu)}$.

consider the entire population$N = S + E + A + I + Q + H + R + D + P$.

By derivation of above equation gives $\frac{dN}{dt} \leq \Lambda - (\alpha + \mu)N$ *which leads to* $\lim_{t\to\infty} supN \leq \frac{\Lambda}{(\alpha+\mu)}$.

This implies that $N \leq \frac{\Lambda}{(\alpha+\mu)}$.
$S + E + A + I + Q + H + R + D + P \leq \frac{\Lambda}{(\alpha+\mu)}$.

Hence all the solution trajectories $(S(t), E(t), A(t), I(t), Q(t), H(t), R(t), D(t), P(t)$ *with primary conditions were uniformly bounded in the region*
$\Omega = (S(t), E(t), A(t), I(t), Q(t), H(t), R(t), D(t), P(t)) \in \mathbb{R}^9_+ : 0 \leq (S, E, A, I, Q, H, R, D, P) \leq \frac{\Lambda}{(\alpha+\mu)}$.

3.2 Basic reproduction number

The basic reproduction number, symbolized as R_0, was a prominent parameter in the analysis of contagious disease and it was defined as the total number of secondary cases arising through a primary case in susceptible individuals. If $R_0 > 1$ then the secondary cases were more than one, so that disease will continue in the population and become an epidemic. If $R_0 < 1$ then the secondary cases were less than one, so that disease cannot spread and die out as soon as possible. If $R_0 = 1$ then there is only one secondary case so that the disease is stable. Since at protection rate α population was protected, the susceptible individuals became $S = N(1 - \alpha)$. The disease-free equilibrium point $E^0 = (N(1 - \alpha), 0, 0, 0, 0, 0, 0, 0)$ of system (1) exists. Through Next Generation Matrix O.Diekmann et al [29] P.van den Driessche & Watmough [32] and Khajanchi, S et al [21], R_0 value will be calculated mathematically.

$$\mathcal{F} = \begin{pmatrix} \beta\zeta_a(1-\alpha) + \beta\zeta_s(1-\alpha) + \beta\zeta_q(1-\alpha) \\ 0 \\ 0 \\ 0 \\ 0 \end{pmatrix} \& \mathcal{V} = \begin{pmatrix} (\omega+\mu)E \\ -\theta\omega E + (\lambda_a + \gamma_a + \mu_a + \mu)I_a \\ -(1-\theta)\omega E + (\lambda_s + \eta_s + \mu)I_s \\ -\lambda_a I_a - (\lambda_s I_s + (\eta_q + \gamma_q + \mu)Q \end{pmatrix}$$

At disinfection state $E = A = I = Q = H = 0$,The Jacobian of two matrices $\mathcal{F}$ and $\mathcal{V}$ are

$$F = \begin{pmatrix} 0 & \beta\zeta_a(1-\alpha) & \beta\zeta_s(1-\alpha) & \beta\zeta_q(1-\alpha) \\ 0 & 0 & 0 & 0 \\ 0 & 0 & 0 & 0 \\ 0 & 0 & 0 & 0 \end{pmatrix}$$

$$V = \begin{pmatrix} \omega+\mu & 0 & 0 & 0 \\ -\theta\omega & \lambda_a + \gamma_a + \mu_a + \mu & 0 & 0 \\ -(1-\theta)\omega & 0 & \lambda_s + \eta_s + \mu & 0 \\ 0 & -\lambda_a & -\lambda_s & \eta_q + \gamma_q + \mu \end{pmatrix}$$

Therefore R_0 was obtained from equation $R_0 = \rho(FV^{-1})$,where ρ represented the matrix FV^{-1} spectral radius. Hence, the reproduction number was

$$R_0 = \frac{(1-\theta)\beta\omega\zeta_s(1-\alpha)}{(\lambda_s+\eta_s+\mu)(\omega+\mu)} + \frac{\beta\theta\omega\zeta_a(1-\alpha)}{(\lambda_a+\gamma_a+\mu_a+\mu)(\omega+\mu)} + \frac{\beta\zeta_q((1-\theta)(\lambda_a+\gamma_a+\mu_a+\mu)\omega\lambda_s+(\lambda_s+\eta_s+\mu)\theta\omega\lambda_a)(1-\alpha)}{(\lambda_a+\gamma_a+\mu_a+\mu)(\lambda_s+\eta_s+\mu)(\eta_q+\gamma_q+\mu)(\omega+\mu)} \tag{1}$$

3.3 Disease-free equilibrium Stability analysis

The Jacobian matrix J_{E^0} of the classification of equations (1) at the equilibrium point $E^0(\frac{\Delta}{\mu}, 0, 0, 0, 0, 0, 0, 0, 0)$ was
$J_{E^0} =$

$$\begin{pmatrix} -(\alpha+\mu) & 0 & -\beta\zeta_a(1-\alpha) & -\beta\zeta_s(1-\alpha) & -\beta\zeta_q(1-\alpha) & 0 & 0 & 0 & 0 \\ 0 & \omega+\mu & \beta\zeta_a(1-\alpha) & \beta\zeta_s(1-\alpha) & \beta\zeta_q(1-\alpha) & 0 & 0 & 0 & 0 \\ 0 & \theta\omega & -(\lambda_a+\gamma_a+\mu_a+\mu) & 0 & 0 & 0 & 0 & 0 & 0 \\ 0 & (1-\theta)\omega & 0 & -(\lambda_s+\eta_s+\mu) & 0 & 0 & 0 & 0 & 0 \\ 0 & 0 & \lambda_a & \lambda_s & -(\eta_q+\gamma_q+\mu) & 0 & 0 & 0 & 0 \\ 0 & 0 & 0 & \eta_s & \eta_q & -(\gamma_h+\mu_h+\mu) & 0 & 0 & 0 \\ 0 & 0 & \gamma_a & 0 & \gamma_q & \gamma_h & -\mu & 0 & 0 \\ \alpha & 0 & 0 & 0 & 0 & 0 & 0 & 0 & 0 \\ 0 & 0 & 0 & \mu_a & 0 & \mu_h & 0 & 0 & 0 \end{pmatrix}$$

The characteristic equation of the matrix J_{E^0} was $\mid J_{E^0} - \lambda I \mid = 0$
$(\lambda+\mu)(\lambda+(\alpha+\mu))(\lambda^9 + a_1\lambda^8 + a_2\lambda^7 + a_3\lambda^6 + a_4\lambda^5 + a_5\lambda^4 + a_6\lambda^3 + a_7\lambda^2 a_8\lambda + a_9) = 0$
where $a_1 = (A + G + J + K + t + E + I)$
$a_2 = (G + J + K)t + A(G + J + K + t + E + I) + (G + J + K + I + t)E + (G + J + K + E + t)I + BF + CH + G(J + K) + JK),$
$a_3 = A(G + J + K + E + I)\mu + GE + JE + GI + KE + JI + KI + EI + BF + CH + GJ + GK + JK) + ... + I(J + K)\mu,$
$a_4 = A(GEI + JEI + KEI + BFJ + CGH + BFK + CHJ + CHK + GJK + (EI + BF + CH)\mu + ... + BFKI + GJKE + GJKI,$
$a_5 = A(FK\lambda_a D + GH\lambda_s D + HK\lambda_s D + (BFI + GJE + GKE + GJI + JKE + JKI + F\lambda_a D)\mu + ... + CHJKt + h\mu DII,$
$a_6 = A(BFJKI + GHK\lambda_s D + (BFJI + BFKI + GJKE + GJKI + FK\lambda_a D + GH\lambda_s D)\mu +$

$... + (FK\lambda_a DI + BFJKI)\mu,$
$a_7 = A(GJKEI + CGHJK + FK\lambda_a DI + BFJKI + GHK\lambda_s D)\mu,$
$a_8 = 0$ and $a_9 = 0$
Here $A = (\alpha + \mu)$,B=$\beta\zeta_a(1 - \alpha)$ and $C = \beta\zeta_s(1 - \alpha)$, $D = \beta\zeta_q(1 - \alpha)$, $E = (\mu + \omega)$, $F = \theta\omega$,
$G = (\lambda_a+\gamma_a+\mu_a+\mu)$, $H = (1-\theta)$, $I = (\lambda_s+\eta_s+\mu)$, $J = (\eta_q+\gamma_q+\mu)$, $K = ((\gamma_h+\mu_h+\mu)$.
Hence J_{E^0} is singular because one of the eigenvalues is zero. Therefore at the disease-free equilibrium, the stability of the system (1) does not exists by using eigenvalues.

Theorem 2. *The Disease-Free Equilibrium* $E^0 = (\frac{\Lambda}{\mu}, 0, 0, 0, 0, 0, 0)$ *was locally asymptotically stable for* $R_0 < 1$ *and unstable for* $R_0 > 1$

Since the J_{E^0} has zero eigen value, according to Kermack WO [20] and singh HP[39], the theorem was satisfied that is the Disease-Free Equilibrium $E^0 = (\frac{\Lambda}{\mu}, 0, 0, 0, 0, 0, 0)$ was locally asymptotically stable for $R_0 < 1$ and unstable for $R_0 > 1$.

Table 2: Fitted parameters and their sensitivity indices list of SEAIQHRDP model

parameter	value	References	sensitivity indices
π	varies	-	-
ζ_a	0.4	Gumel AB et al.[12]	0.4547
ζ_s	0.4	Nadim SS et al.[27]	0.2416
ζ_q	0.3	Biswas, Sudhanshu Kumar et al [4]	0.3037
θ	0.7	Fergusonm.N et al. [10]	-0.0015
ω	0.1	R. Li et al. [36]	-0.1048
β	0.9714	evaluated	1.0000
α	0.0016	evaluated	-0.07158
λ_a	0.4614	evaluated	-0.1764
λ_s	0.1143	evaluated	-0.0997
η_s	0.1840	evaluated	-0.1418
η_q	0.0742	evaluated	-0.0948
γ_a	0.1302	evaluated	-0.2757
γ_q	0.1661	evaluated	-0.2088
γ_h	0.1777	evaluated	-0.2278
μ_a	0.0035	evaluated	-0.0207
μ_h	0.1544	evaluated	-0.0233
μ	0.0000391	Worldmeter.info/coronavirus [16]	-0.1070

4 Numerical simulation

In this sector, the numerical simulation of confirmed cases of COVID-19 for India was performed and the simulation results were compared with actual data [21] from 30th, January 2020 to 13th, January 2021. The SEAIQHRDP model fitted to daily and cumulative confirmed coronavirus cases in India which illustrates a satisfactory estimation. The model parameters β, α, λ_a, λ_s, η_s, η_q, γ_a, γ_q, γ_h, μ_a, μ_h and μ were estimated by using a nonlinear least squares regression method (LSQNONLIN function) in MATLAB.

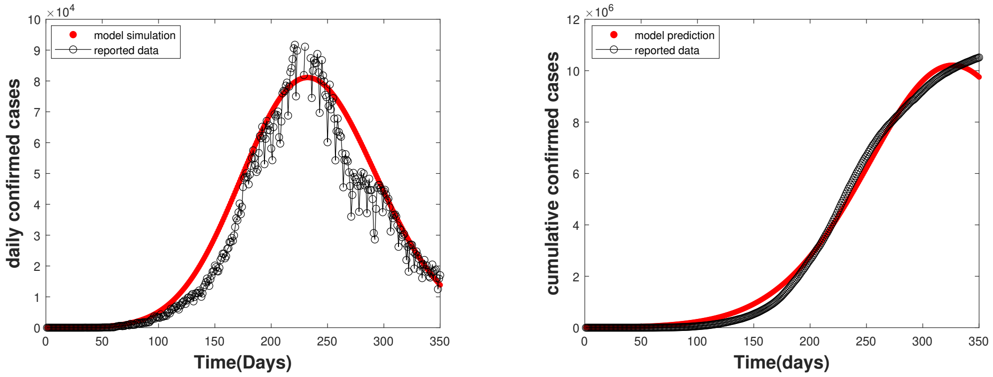

(a) (b)

Figure 2: The model fitting of reported (a) daily confirmed cases and (b) cumulative confirmed cases of COVID-19 in India.

The minimizing error was

$$R(\Phi) = \sum_{t=1}^{n} (Q_t(\Phi) - Q_t\bar{(}\Phi))^2 \tag{2}$$

where $Q_t(\Phi)$ and $Q_t\bar{(}\Phi)$ were a cumulative number of confirmed cases through actual data and model prediction. In Table 2, the values for the estimated and fixed parameters were shown. The fundamental reproduction numberR_0 was determined as 2.089 using the fixed and model parameters in Table 2.

In Figure.2 the curve fitting was taken from 30th, January 2020 to 13th, January 2021 in apicovid19india.org [13] in India. The black curve represented the reported COVID-19 cases and the red curve denoted the model simulation COVID-19 cases.

5 Sensitivity analysis

Sensitivity analysis was used in defining the impact of different factors in the spread of COVID-19. This analysis was used to identify the growth and reduction in basic reproduction numbers concerning numerous parameters. A complete chapter on the sensitivity analysis of the dengue virus was obtained in Rodrigues H et al. [37] and Burattini, M.N et al [6]. Whenever the significant parameters were recognized, different strategies will be executed to get optimum results. To identify such parameters, the sensitivity index of R_0 concerning various parameters was estimated. The normalized sensitivity index of R_0 is defined as

$$\Gamma_q^{R_0} = \frac{\partial R_0}{\partial q} \times \frac{q}{R_0}.$$

where q was the significant parameter, whose sensitivity on R_0 obtained by using normalized forward sensitivity index method Biswas, S et al [5].

The highest sensitive parameter on reproduction number was the parameter whose index was high in magnitude. If the sensitivity of parameter q was positive, R_0 was increased whenever the parameter q increased. Similarly, the sensitivity of parameter q was negative, R_0 was decreased whenever the parameter q increased. From Figure.3

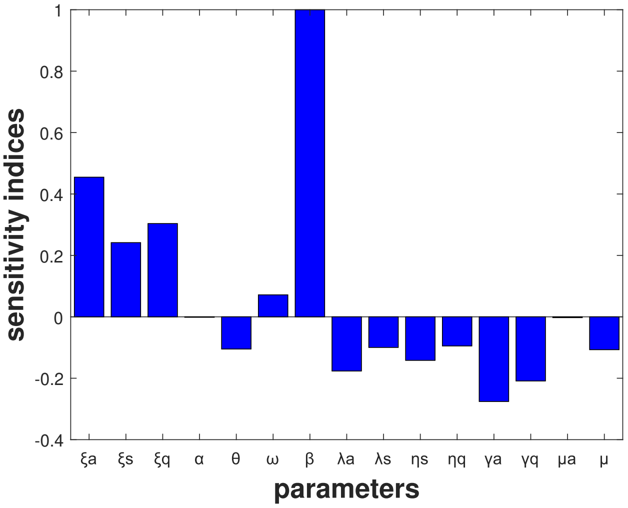

Figure 3: Normalized local sensitivity indices of R_0 with respect to each model parameter.

it was observed the parameters θ, λ_a, λ_s, η_s, η_q, γ_a, γ_q, μ_a have negative indices with R_0 and the parameters ζ_a, ζ_s , ζ_q, β, ω, μ share positive indices with R_0. So that R_0 value increased as the parameters ζ_a, ζ_s and ζ_q increased and R_0 value decreased as the parameters θ, η_s, η_q and γ_q increased. Hence the sensitive analysis determined that the parameters ζ_a, ζ_s, ζ_q, β, θ, η_s,γ_a and γ_q were more effective parameters. The sensitivity indices of various parameters had been displayed in Table 2.

Figure.4(a) represented that R_0 Contour Plot with respect to virus transmission rate (β) and quarantine rate (λ_s) from symptomatic population. This figure described a reduction in R_0 with a decrease in virus transmission rate (β) and an increase in quarantine rate (λ_s) from the symptomatic population. Figure.4(b) explained R_0 Contour Plot with respect to virus transmission rate (β) and hospitalization rate (η_s) from symptomatic population. This figure described a reduction in R_0 with a decrease in virus transmission rate β and an increase in hospitalization rate (η_s) from the symptomatic population. Figure.4(c) displayed R_0 Contour Plot with respect to quarantine rate (λ_a) from asymptomatic population and recovery rate (γ_q) from quarantine population. This figure demonstrated reduction in R_0 with an increase in quarantine rate (λ_a) from an asymptomatic population and an increase in recovery rate (γ_q) from quarantine population. Figure.4(d) expressed the Contour Plot of the Basic Reproduction Number concerning hospitalization rate (η_s) from symptomatic population and hospitalization rate (η_q) from quarantine population. This figure illustrated R_0 rises with a decrease in hospitalization rate (η_s) from the symptomatic population and hospitalization rate (η_q) from the quarantine population.

5.1 COVID-19 Prevalence changes with various parameters

From Figure.5 to Figure.9, It was perceived that the asymptomatic infected and symptomatic infected individuals were reduced if the protection rate (α) from susceptible individuals, quarantine rate (λ_a) from asymptomatic individuals, quarantine rate (λ_s) from symptomatic individuals, hospitalization rate (η_q) from quarantine individuals and hospitalization rate (η_s) from symptomatic individuals increased.

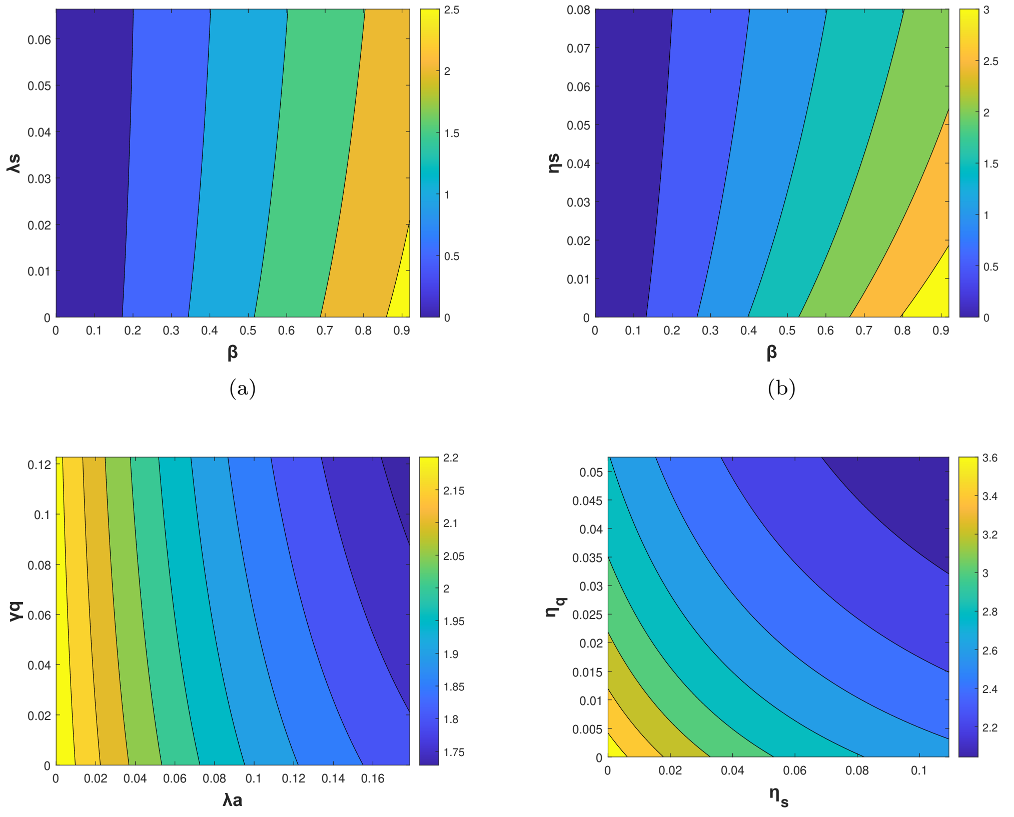

(a) (b)

(c) (d)

Figure 4: Contour plots of basic reproduction number R_0 with respect to (a) $(\beta,\ \lambda_s)$, (b) $(\beta\ \eta_s)$, (c) $(\lambda_a,\ \gamma_q)$ and (d) $(\eta_s,\ \eta_q)$.

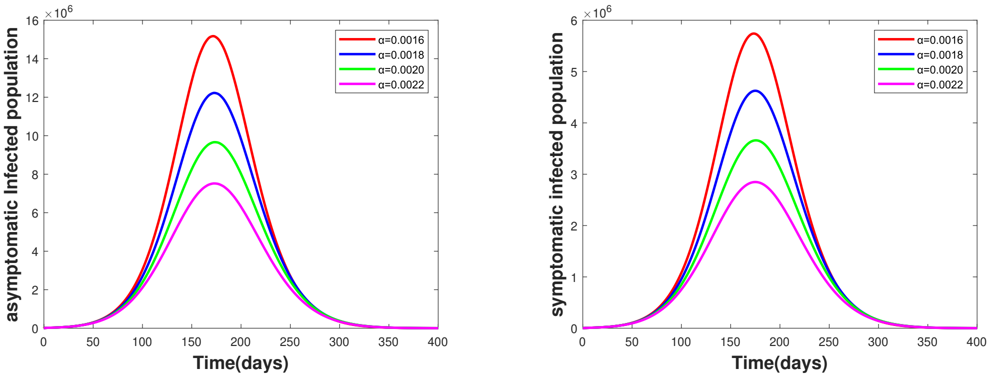

(a) (b)

Figure 5: Effect of parameter α on (a) asymptomatic infected populace and (b) symptomatic infected populace

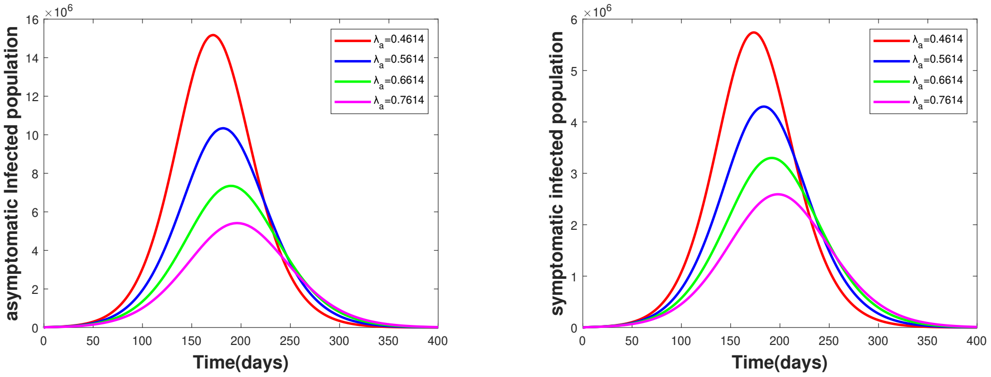

(a) (b)

Figure 6: Effect of parameter λ_a on (a) asymptomatic infected populace and (b) symptomatic infected populace

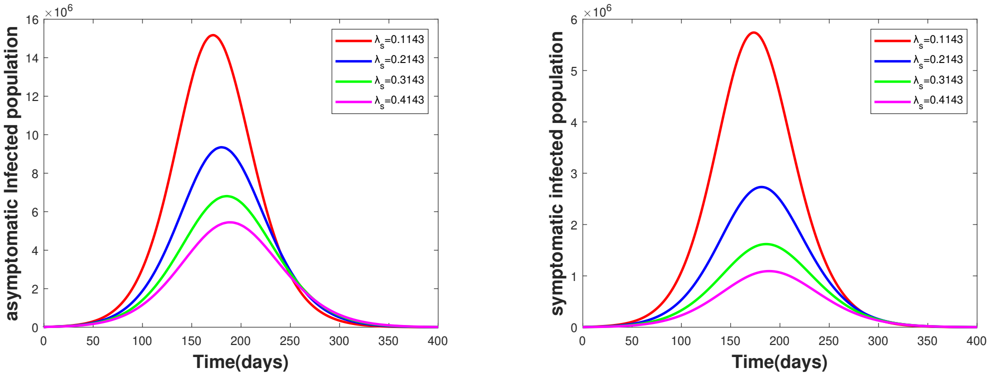

(a) (b)

Figure 7: Effect of parameter λ_s on (a) asymptomatic infected populace and (b) symptomatic infected populace

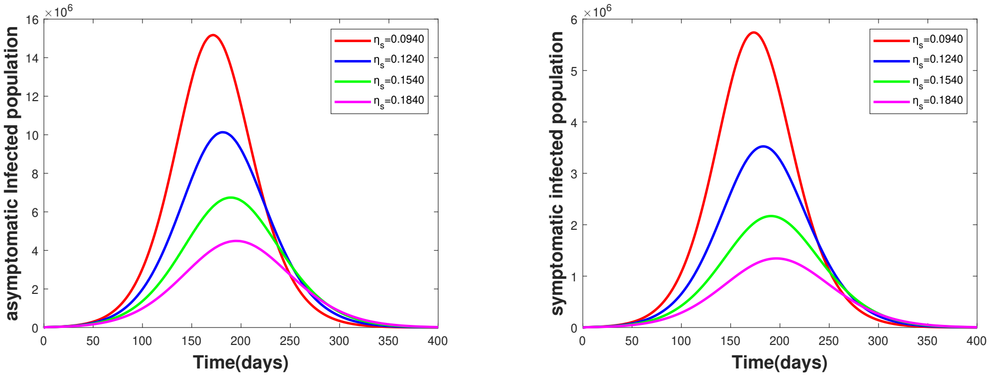

(a) (b)

Figure 8: Effect of parameter η_q on (a) asymptomatic infected populace and (b) symptomatic infected populace

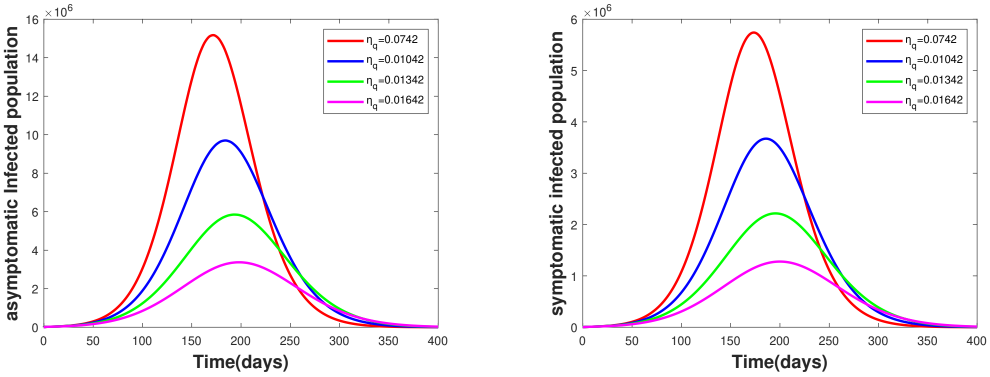

(a) (b)

Figure 9: Effect of parameter η_s on (a) asymptomatic infected populace and (b) symptomatic infected populace

6 Optimal control

6.1 Optimal control problem

The effectiveness of control techniques was crucial in decreasing the spread of the COVID-19 virus. It was essential to improve a policy that minimizes both the number of infected populations and related costs. In this phase, the optimal control technique was a tremendously useful tool for defining such a strategy. Now we study the impact of pharmacological interventions to diminish the spread of the virus. To achieve this, the system(1) can be extended by including three control variables $u_1(t)$, $u_2(t)$ and $u_3(t)$ where

(a) Control $u_1(t)$ represented the degree of protection provided by government interventions. The function of this control variable was to enhance the protection rate α.

(b) Control $u_2(t)$ described the treatment of asymptomatic infected individuals. The function of this control variable was to develop the quarantine rate (λ_a) from asymptomatic infected individuals.

(c) Control $u_3(t)$ characterized the treatment of symptomatic infected (both quarantine and hospitalization) individuals. The function of this control variable was to improve the quarantine rate (λ_s) and hospitalization rate (η_s) from symptomatic infected individuals. The three control variable values were assumed between 0 and 1.

There was no efforts made in these controls if $u_1 = u_2 = u_3 = 0$ and maximum efforts had been placed if $u_1 = u_2 = u_3 = 1$

By considering all the above suppositions, the optimal control model was formulated as

$$\frac{ds}{dt} = \pi - \beta\frac{(\zeta_a A+\zeta_s I_s+\zeta_q Q)S}{N} - (\alpha + u_1 + \mu)S$$
$$\frac{dE}{dt} = \beta\frac{(\zeta_a A+\zeta_s I_s+\zeta_q Q)S}{N} - (\omega + \mu)E$$
$$\frac{dA}{dt} = \theta\omega E - (\lambda_a + u_2)A + \gamma_a + \mu_a + \mu)A$$
$$\frac{dI}{dt} = (1-\theta)\omega E - (\lambda_s + u_3 + \eta_s + u_3 + \mu)I$$
$$\frac{dQ}{dt} = (\lambda_a + u_2)A + (\lambda_s + u_3)I - (\eta_q + \gamma_q + \mu)Q$$
$$\frac{dH}{dt} = (\eta_s + u_3)I + \eta_q Q - (\gamma_h + \mu_h + \mu)H$$
$$\frac{dR}{dt} = \gamma_a A + \gamma_q Q + \gamma_h H - \mu R$$
$$\frac{dD}{dt} = \mu_a A + \mu_h H$$
$$\frac{dP}{dt} = \alpha S$$

Now we detect $u_1(t)$, $u_2(t)$ and $u_3(t)$'s optimal values that minimize the objective functional

$\mathcal{J}(u_1(t), u_2(t), u_3(t))=\int_0^{t_f} \ (C_1A + C_2I + C_3Q + C_4H + \frac{1}{2}(C_5u_1^2 + C_6u_2^2 + C_7u_3^2) \ dt$

subject to the system (2), which contained the sum of asymptomatic infected, symptomatic infected, quarantined, and hospitalized population, besides the optimal controls $u_1(t)$, $u_2(t)$ and $u_3(t)$. These were bounded and Lebesgue integral functions Kirschner D et al [9] and S. Lenhart and J.T.Workman [40]). Here The positive coefficients C_1, C_2, C_3, C_4, C_5, C_6 and C_7 were corresponding balancing weight constants parameters of stated infected variables and optimal controls.

The main purpose was to determine the optimal controls variables $u_1^*(t)$,$u_2^*(t)$,$u_3^*(t)$ such that

$$\mathcal{J}(u^*(t)) = \min_{u_1,u_2,u_3 \in U} \mathcal{J}((u_1(t), u_2(t), u_3(t))$$

where Φ= $\{u_1, u_2, u_3$: $u_1, u_2, u_3/ \ u_1, u_2, u_3 : [0, t_f] \to [0, 1]$ are lebsegue integrable$\}$.

Through Pontryagin's maximum principle Pontryagin, L et al [31], we derived the essential conditions for this optimal control problem. The Lagrangian function was given

by
$\mathcal{L}(S,E,A,I,Q,H,R,u_1(t),u_2(t),u_3(t)) = C_1A+C_2I+C_3Q+C_4H+\frac{1}{2}(C_4u_1^2+C_5u_2^2+C_5u_3^2$
The Hamiltonian function $\mathcal{H}$ obtained as
$\mathcal{H} = C_1A+C_2I+C_3Q+C_4H+\frac{1}{2}(C_4u_1^2+C_5u_2^2+C_5u_3^2+\lambda_1\frac{dS}{dt}+\lambda_2\frac{dE}{dt}+\lambda_3\frac{dA}{dt}+\lambda_4\frac{dI}{dt}+\lambda_5\frac{dQ}{dt}+\lambda_6\frac{dH}{dt}+\lambda_7\frac{dR}{dt}+\lambda_8\frac{dD}{dt}+\lambda_9\frac{dP}{dt}$
where λ_1 λ_2, λ_3 , λ_4, λ_5, λ_6 and λ_7 are the adjoint variables.
The of differential equation form of adjoint variables were as follows.

$$\frac{d\lambda_1}{dt} = -\frac{\partial\mathcal{H}}{\partial S} = (\lambda_1-\lambda_2\beta(\frac{(\zeta_aA+\zeta_sI_s+\zeta_qQ)}{N}+(\lambda_1-\lambda_8(\alpha+u_1)+\lambda_1u_1$$
$$\frac{d\lambda_2}{dt} = -\frac{\partial\mathcal{H}}{\partial E} = (\omega+\mu)\lambda_2-\lambda_4-\lambda_3\theta\omega-\lambda\omega$$
$$\frac{d\lambda_3}{dt} = -\frac{\partial\mathcal{H}}{\partial A} = -C_1+(\lambda_1-\lambda_2)\beta\frac{\zeta_aS}{N}+(\lambda_3-\lambda_5)(\lambda_a+u_2)+((\lambda_3-\lambda_8)\mu_a+\mu\lambda_3$$
$$\frac{d\lambda_4}{dt} = -\frac{\partial\mathcal{H}}{\partial I} = -C_2+(\lambda_1-\lambda_2)\beta\frac{\zeta_sS}{N}+(\lambda_4-\lambda_5)(\lambda_s+u_3)+(\lambda_4-\lambda_6)(\eta_s+u_3)+\mu\lambda_4$$
$$\frac{d\lambda_5}{dt} = -\frac{\partial\mathcal{H}}{\partial Q} = -C_3+(\lambda_1-\lambda_2)\beta\frac{\zeta_qS}{N}+(\lambda_5-\lambda_6)\eta_q+(\lambda_5-\lambda_7)\gamma_q+\mu\lambda_5$$
$$\frac{d\lambda_6}{dt} = -\frac{\partial\mathcal{H}}{\partial H} = -C_4+(\lambda_6-\lambda_7)\gamma_h+(\lambda_6-\lambda_8)\mu_h+\mu)$$
$$\frac{d\lambda_7}{dt} = -\frac{\partial\mathcal{H}}{\partial R} = \mu\lambda_7$$
$$\frac{d\lambda_8}{dt} = -\frac{\partial\mathcal{H}}{\partial D} = 0$$
$$\frac{d\lambda_9}{dt} = -\frac{\partial\mathcal{H}}{\partial P} = 0$$

we minimize Hamilton function relating to control variables $u_1^*(t)$,$u_2^*(t)$ and $u_3^*(t)$.
Using the optimal conditions $\frac{\partial\mathcal{H}}{\partial u_1}=0$, $\frac{\partial\mathcal{H}}{\partial u_2}=0$ and $\frac{\partial\mathcal{H}}{\partial u_3}=0$, we get

$$\frac{\partial\mathcal{H}}{\partial u_1} = C_5u_1-\alpha\lambda_1+\alpha\lambda_9S=0 \Rightarrow u_1^* = \frac{(\lambda_1-\lambda_9)\alpha S}{NC_5}$$
$$\frac{\partial\mathcal{H}}{\partial u_2} = C_6u_2-\lambda_3A+\lambda_5A=0 \Rightarrow u_2^* = \frac{(\lambda_3-\lambda_5)A}{C_6}$$
$$\frac{\partial\mathcal{H}}{\partial u_3} = C_7u_3-((\lambda_4-\lambda_5+(\lambda_4-\lambda_6)I=0 \Rightarrow u_3^* = \frac{((\lambda_4-\lambda_5)+(\lambda_4-\lambda_6))I}{C_7}$$

6.2 Optimal control model simulation

With the values of the parameters mentioned in Table 2, numerical simulation was conducted for the optimal control problem (2) in MATLAB by using an iterative fourth-order Runge-Kutta method (Kamien, M et al [19] and Lukes, D.L.[24]) for the period [0,400]. The baseline weight parameters were taken as $C_1 = 1$, $C_2 = 1$, $C_3 = 1$, $C_4 = 1$,$C_5 = 40$, $C_6 = 40$ and $C_7 = 45$.

In Figure.10, variations of exposed, asymptomatic infected, symptomatic infected, quarantine, hospitalization, and dead populace with and without control had performed. This figure shows that, in comparison to the infected population without control, the infected population decreased quickly under control.

In Figure.11, variations of recovered and insusceptible Populace with and without control were executed. This graph demonstrates that the disinfected population under control swiftly rose in comparison to the disinfected population without control.

According to Figure.12, the best controls, u_1,u_2 and u_3 combined their efforts extremely well to increase the protection rate (α) from susceptible individuals, the quarantine rates (λ_a, λ_s)from asymptomatic infected and symptomatic infected individuals, and the hospitalization rates (η_q, η_s) from symptomatic and quarantine individuals.

From these figures we perceived that in the presence of optimal control strategy the number of susceptible, exposed, asymptomatic infected, symptomatic infected, quarantined, hospitalized, and dead individuals were reduced rapidly while the number of recovered and insusceptible individuals were increased swiftly comparing with the populations without control strategy.

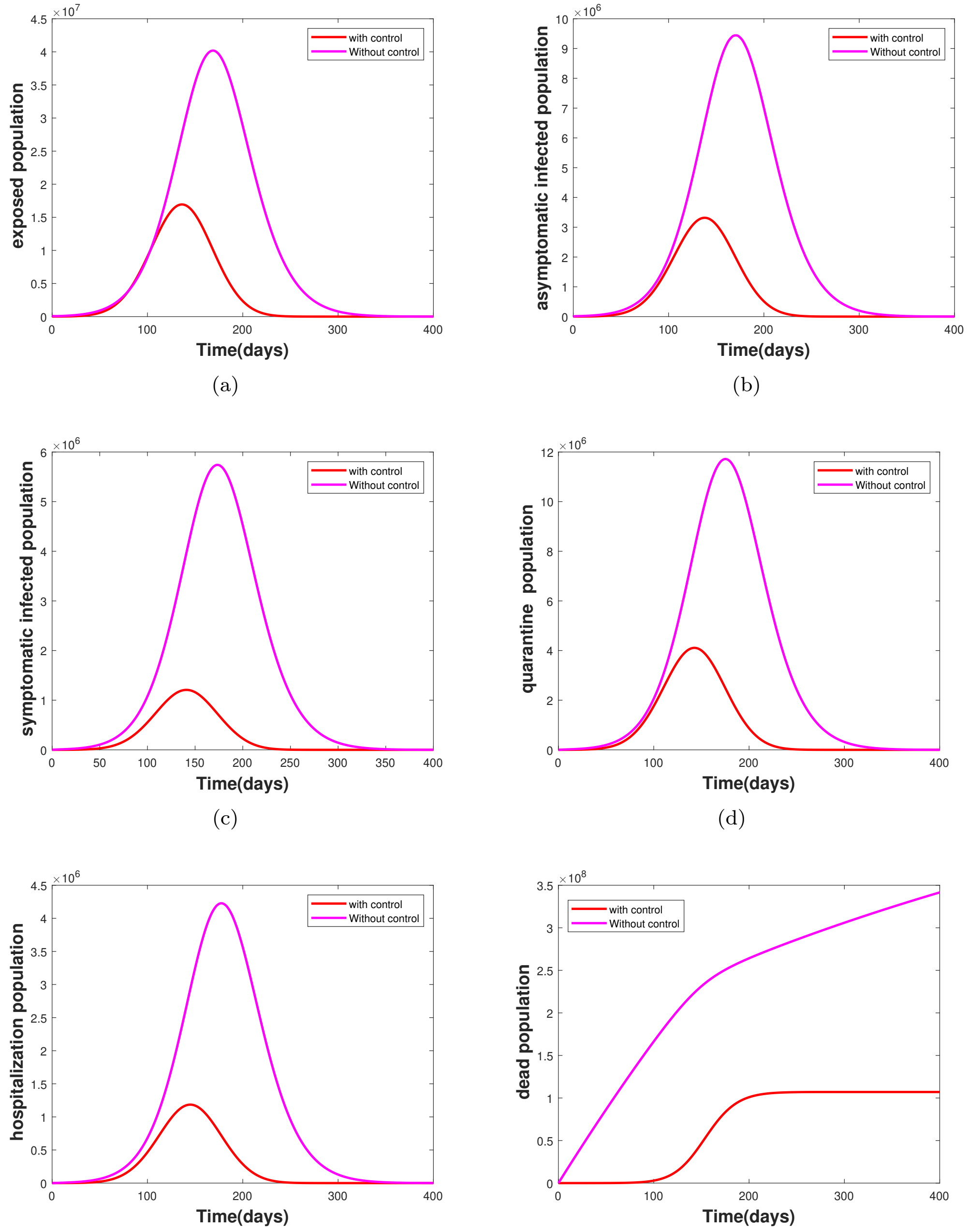

(a) (b) (c) (d) (e) (f)

Figure 10: Variations of (a) exposed (b) asymptomatic (c) symptomatic infected (d) quarantine (e) hospitalization and (f) dead populations with and without control

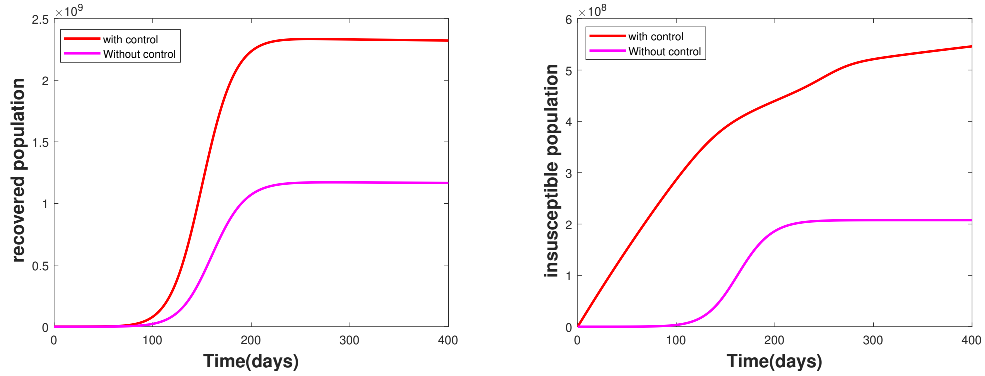

(a) (b)

Figure 11: Variations of (a) recovered (b) insusceptible population with and without control

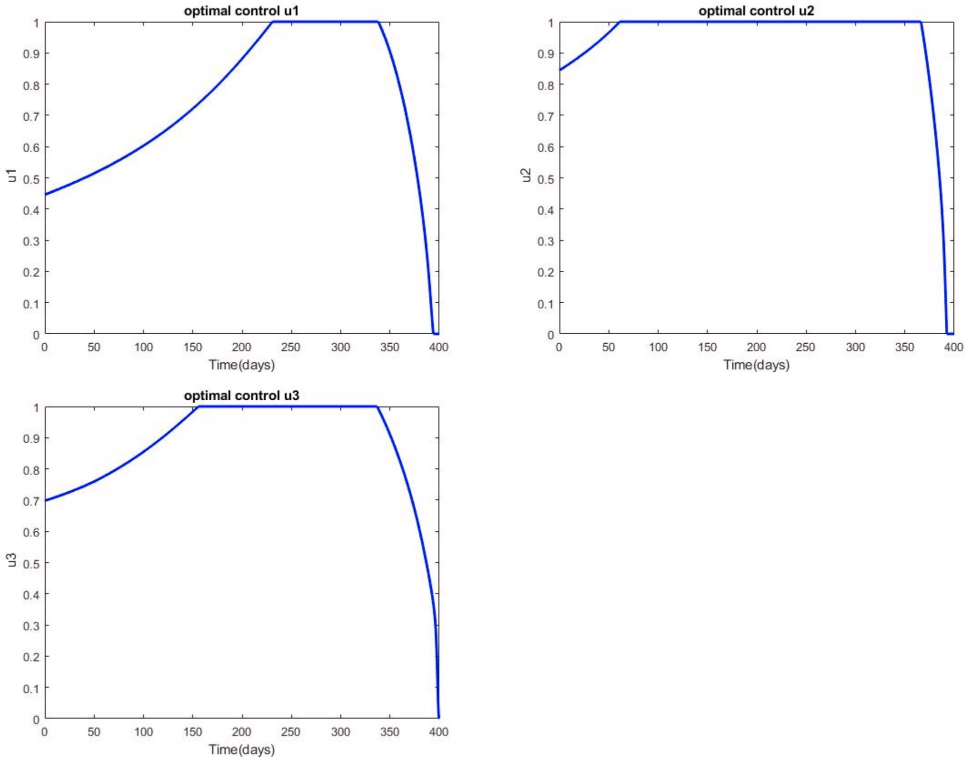

Figure 12: Dynamics of Optimal Controls u_1, u_2 and u_3

7 Conclusion

Epidemiological models aid in understanding the dynamics of infectious illness transmission. The deterministic mathematical model with 9 compartments was thoroughly studied in this paper. First, the elementary properties of the model such as the positivity and boundedness of the SEAIQHRDP model, the expression of R_0, and the local stability of the disease-free equilibrium were performed. Our suggested model has 18 parameters, but we only calculated 11 of them based on the sensitivity analysis. Through sensitivity analysis, it was observed that just eight parameters are very sensitive concerning clinically unwell or infected patients. The time series behavior of the infected populations for 400 days was examined concerning variations in parameters. From this, the spread of infections can be slowed down by increasing the protection rate, hospitalization rate, and quarantine rate. The best optimal control analysis was then carried out by including three control factors, one of which was increased protection, and the other two were improved quarantine and medical facilities for both identified and unidentified affected people. Through the Optimal control strategy, it was found that the infected populations were reduced rapidly, and disinfected populations were increased compared with the infected and disinfected populations without optimal control technique. When the best control approach is used early in a pandemic, the intensity of epidemic peaks tends to decline, spreading the maximum impact of an epidemic across a longer period. Finally, this study leads to the conclusion the rising of infections can be controlled only if the implementation of rapid testing, quarantine centers, and medical facilities. Additionally, we intend to increase the scope of our modeling work by including vaccination and the impact of environmental contaminants in the future.

References

[1] Alexander Krämer, Mirjam Kretzschmar, Klaus Krickeberg. "Krickeberg Modern Infectious Disease Epidemiology." 2010 : 209–221.(2010)

[2] Bai Y, Liu K, Chen Z. " Early transmission dynamics of novel coronavirus pneumonia epidemic in Shaanxi Province [J]." Chin J Nosocomiol 30(6):834–838(2020)

[3] Bandekar SR, Ghosh M." Mathematical modeling of COVID-19 in India and its states with optimal control." Model Earth Syst Environ. 2022;8(2):2019-2034. doi:10.1007/s40808-021-01202-8(2020)

[4] Biswas SK, Ghosh JK, Sarkar S, Ghosh U."COVID-19 pandemic in India: a mathematical model study." Nonlinear Dyn. 2020;102(1):537-553. doi:10.1007/s11071-020-05958-z(2020)

[5] Biswas SK, Ghosh U, Sarkar S. "Mathematical model of zika virus dynamics with vector control and sensitivity analysis.", Infect. Dis. Model. 5, 23–41 (2020)

[6] Brauer F, Chavez CC. "Mathematical models in population biology and epidemiology." Springer, New York, NY. https://doi. org/10.1007/978-1-4614-1686-9 (2012)

[7] Burattini MN, Massad E, Coutinho, FAB. "Estimation of R_0 from the initial phase of an outbreak of a vector-borne infection." Trop. Med. Int. Health 15(1), 120–26 (2010)

[8] Danane J, Hammouch Z, Allali K, Rashid S, Singh J. "A fractional-order model of coronavirus disease 2019 (COVID-19) with governmental action and individual reaction." Math Methods Appl Sci. 2021 Aug 25:10.1002/mma.7759. doi: 10.1002/mma.7759.(2021)

[9] D. Kirschner, S. Lenhart, S. Serbin. "Optimal control of the chemotherapy of HIV." Journal of Mathematical Biology, vol. 35, no. 7, pp. 775–792,(1997).

[10] Fergusonm.N et al Report 9: Impact of non-pharmaceutical interventions (NPIs) to reduce COVID19 mortality and healthcare demand, in https://doi.org/10.25561/77482 (2020).

[11] Giordano G, Blanchini F, Bruno R, Colanary P, Filippo AD, Matteo AD, Colaneri M. "Modelling the COVID-19 epidemic and implementation of population-wide interventions in Italy." Nat Med 26:855–860.(2020)

[12] Gumel AB, Ruan S, Day T, Watmough J, Brauer F, van den Driessche P, Gabrielson D, Bowman C, Alexander ME, Ardal S, Wu J, Sahai BM. "Modelling strategies for controlling SARS outbreaks." Proc Biol Sci. 2004 Nov 7;271(1554):2223-32. (2020)

[13] https://api.covid19india.org/documentation/csv/ Coronavirus outbreak in India. Google sheets

[14] https://www.who.int/director-general/speeches/detail/who-director-general-s-opening-remarks-at-the-media-briefing-on-COVID-19-11-march-2020

[15] https://covid19.who.int

[16] https://www.Worldmeter.info/coronavirus

[17] Huang G, Pan Q, Zhao S, Gao Y, Gao X. "Prediction of COVID-19 outbreak in China and optimal return date for university students based on propagation dynamics". J Shanghai Jiaotong Univ 25:140–146. (2020)

[18] H.W. Hethcote. "The mathematics of infectious diseases". SIAM Review 42.4 ,pp. 599-653. ISSN: 00361445(2000)

[19] Kamien, MI, Schwartz NL. "Dynamic Optimization: The Calculus of Variations and Optimal Control in Economics and Management". Modern Economy, Vol.11 No.7, July 15, 2020 (2020)

[20] Kermack WO, McKendrick AG "A contribution to the mathematical theory of epidemics". Proceedings of the London. Series A Contain Papers Mathematical Phys Charact 115(772):700–721 (1927)

[21] Khajanchi S, Bera S, Roy TK. "Mathematical analysis of the global dynamics of a HTLV-I infection model, considering the role of cytotoxic T-lymphocytes". Math. Comput.Simul. 180, 354–378 (2021)

[22] Lin Q, Zhao S, Gao D, Lou Y, Yang S, Musa S, Wang M, Cai Y, Wang W, Yang L. "A conceptual model for the outbreak of Coronavirus disease (COVID-19) in Wuhan, China with individual reaction and governmental action". Int J Infect Dis 93:211–216.(2020)

[23] Liu C, Ding G, Gong J, Wang L, Cheng K, Zhang D. "Studies on mathematical models for SARS outbreak prediction and warning". Chin Sci Bull 49(21):2245–2251(2004)

[24] Lukes DL. ”Differential equations, classical to controlled”. Mathematical Science Engineering 162. AcademicPress, New York (1982)

[25] Massad E, Coutinho FAB, Wilder-Smith A. Modelling an optimum vaccination strategy against ZIKA virus for outbreak use. Epidemiol Infect. 2019;147:e196. doi:10.1017/S0950268819000712(2019)

[26] Mwalili S, Kimathi M, Ojiambo V, Gathungu D, Mbogo R. ”SEIR model for COVID-19 dynamics incorporating the environment and social distancing.” BMC Res Notes. 2020 Jul 23;13(1):352(2020)

[27] Nadim SS, Ghosh I, Chattopadhyay J. ”Short-term predictions and prevention strategies for COVID-19.” A model-based study. Appl Math Comput. 2021 Sep 1;404:126251.(2021)

[28] NCBI: ”First confirmed case of COVID-19 infection in India: a case report.” https://www.ncbi.nlm.nih.gov/pmc/articles/ PMC7530459(2020)

[29] O. Diekmann, J. Heesterbeek, J. Metz. ”On the definition and the computation of the basic reproduction ratio R_0 in models for infectious diseases in heterogeneous populations.” J. Math. Biol. 28, 365–382 (1990)

[30] Peng L, Yang W, Zhang D, Zhuge C, Hong L. ”Epidemic analysis of COVID-19 in China by dynamical modeling.” medRxiv 2020.02.16.20023465; doi: https://doi.org/10.1101/2020.02.16.20023465(2020).

[31] Pontryagin, L.S., Boltyanskii, V.G., Gamkrelidze, R.V., Mishchenko, E.F. ”The Mathematical Theory of Optimal Processes.” Wiley-Interscience, New York (1962)

[32] P. van den Driessche, J. Watmough. ”Reproduction numbers and sub-threshold endemic equilibria for compartmental models of disease transmission.” Math. Biosci. 180(1–2), 29–48(2002)

[33] Raj Kishore, B.Sahoo, D.Swain, Kisor K. Sahu. ”Analysis of COVID19 Outbreak in India using SEIR model.” arXiv preprint arXiv:2010.13610 (2010)

[34] Read JM, Bridgen JR, Cummings DA, Ho A, Jewell CP. ”Novel coronavirus 2019-nCoV: early estimation of epidemiological parameters and epidemic predictions.” MedRxiv 2020.01.23.20018549; doi: https://doi.org/10.1101/2020.01.23.20018549 (2020)

[35] Rehman, Attiq ul, Ram Singh, Jagdev Singh. ”Mathematical analysis of multi-compartmental malaria transmission model with reinfection.” Chaos, Solitons and Fractals, volume 163, 112527, ISSN 0960-0779, https://doi.org/10.1016/j.chaos.2022.112527.(2022)

[36] R Li, Pei S, Chen B, Song Y, Zhang T, Yang W, Shaman J. ”Substantial undocumented infection facilitates the rapid dissemination of novel coronavirus (SARS-CoV-2).” Science. 2020 May 1;368(6490):489-493. doi: 10.1126/science.abb3221(2020)

[37] Rodrigues H, Teresa M, Delfim F, Torres M. ”Sensitivity Analysis in a Dengue Epidemiological Model.” Conference Paper, Open Access Volume 2013, Article ID 721406, https://doi.org/10.1155/2013/721406(2013)

[38] RM May, Anderson RM. ”Population biology of infectious diseases.” Part II. Nature. 1979 Aug 9; 280(5722): 455-61. doi: 10.1038/280455a0. PMID: 460424(1979)

[39] Singh HP, Kumari p, Singh S. ”SEIAQRDT model for the spread of novel coronavirus (COVID-19): A case study in India.” Appl Intell (Dordr). 2021;51(5):2818-2837. doi: 10.1007/s10489-020-01929-4. Epub 2020 Nov 13. PMID: 34764566; PMCID: PMC7662031(2020)

[40] S. Lenhart, Workman JT. ”Optimal Control Applied to Biological Models, Mathematical and Computational Biology Series.” Chapman Hall CRC,(2007)

[41] Singh J, Ganbari B, Kumar D, Baleanu D. ”Analysis of fractional model of guava for biological pest control with memory effect.” J Adv Res. 2020 Dec 10;32:99-108. doi: 10.1016/j.jare.2020.12.004. PMID: 34484829; PMCID: PMC8408328(2020)

[42] Supriya Yadav, Devendra Kumar, Jagdev Singh, Dumitru Baleanu. ”Analysis and dynamics of fractional order Covid-19 model with memory effect.” Results in Physics, volume 24,2021, 104017, ISSN 2211-3797, https://doi.org/10.1016/j.rinp.2021.104017 (2021)

J. COMPUTATIONAL ANALYSIS AND APPLICATIONS, VOL. 31, NO.1, 2023, COPYRIGHT 2023 EUDOXUS PRESS, LLC

On nonempty intersection properties in metric spaces

A. Gupta[1]* and S. Mukherjee[1]

[1]Department of Mathematics,
NIT Meghalaya, Shillong-793003, Meghalaya, India

Abstract

The classical Cantor's intersection theorem states that in a complete metric space X, intersection of every decreasing sequence of nonempty closed bounded subsets, with diameter approaches zero, has exactly one point. In this article, we deal with decreasing sequences $\{K_n\}$ of nonempty closed bounded subsets of a metric space X, for which the Hausdorff distance $H(K_n, K_{n+1})$ tends to 0, as well as for which the excess of K_n over $X \setminus K_n$ tends to 0. We achieve nonempty intersection properties in metric spaces. The obtained results also provide partial generalizations of Cantor's theorem.

Keywords Metric space · Atsuji space · Hausdorff metric · Nested sequence · Cantor's intersection theorem

Mathematics Subject Classification (2020) 54E50 · 54A20

1 Introduction

In metric spaces, there are some marvellous nonempty intersection theorems. Cantor's theorem (see [14]) asserts that in a complete metric space X, the intersection of every decreasing sequence $\{K_n\}$ of nonempty closed subsets of X with diameter $\delta(K_n) \to 0$ has exactly one point. This intersection theorem is widely used in the fields related to mathematical analysis. Kuratowski provided a generalization of Cantor's theorem using Kuratowski measure of non-compactness, α:

$$\alpha(A) = \inf\left\{\varepsilon > 0 : \exists\ X_i, i = 1, \cdots, n, X_i \subset X, \delta(X_i) < \varepsilon, A = \cup_i X_i\right\},$$

where A is a subset of a complete metric space X. Kuratowski's theorem (see [6, 15]) states that for each decreasing sequence $\{K_n\}$ of nonempty closed subsets of a complete metric space X with $\lim\limits_{n\to\infty} \alpha(K_n) \to 0$, $\bigcap\limits_{n=1}^{\infty} K_n$ is nonempty

---

*Corresponding author. *E-mail address:* ajitkumar.gupta@nitm.ac.in and compact. Later, this theorem is further generalized by Horvath [3] using the same measure of compactness α. In [9], Mitrovic et al. have studied the generalization of Horvath's results; and they applied this generalization for best approximation in [10]. Recently, Souza and Alves [15] extended both Cantor's theorem and Kuratowski's theorem from metric spaces to admissible spaces.

An Atsuji space, which is more general than compact spaces, has the property that each continuous function on it is uniformly continuous. A metric space X is said to be an Atsuji space if the set of limit points X' is compact in X and for each $\epsilon > 0$ the complement of the set $N_\epsilon(X') := \bigcup\limits_{x \in X'} B(x, \epsilon)$, in X, is uniformly discrete, where $B(x, \epsilon)$ denotes the open ball centered at x and with radius ϵ. For a metric space, the property of being an Atsuji space lies in between the compactness and the completeness. A detailed study on Atsuji spaces can be found in [4].

This article presents various results on nonempty intersection of decreasing sequence of nonempty closed bounded subsets in metric spaces and in Atsuji spaces using Hausdorff distance $H(A, B)$ and the functional $\hat{d}$, defined as $\hat{d}(A) = \sup\limits_{x \in A} d(x, X \setminus A)$, where A, B are subsets of a metric space X. These obtained results are also compared with the Cantor's intersection theorem.

The article is organized as follows. Some preliminary results, needed for the rest part of the article, are discussed in Section 2. In Section 3 and Section 4, we consider decreasing sequence $\{K_n\}$ of nonempty closed bounded subsets of a metric space X and discuss their nonempty intersection results in the cases for which the Hausdorff distance $H_n := H(K_n, K_{n+1}) \to 0$, and $\hat{d}(K_n) := \sup\limits_{x \in K_n} d(x, X \setminus K_n) \to 0$, respectively.

2 Preliminaries

Given a metric space (X, d), we denote the set of all nonempty bounded subsets of X and the set of all nonempty bounded closed subsets of X by $B(X)$ and $C_b(X)$, respectively. Further given $A \subset X$, A', A^o, $N_\epsilon(A)$ and ∂A denote the set of all limit points, interior points, ϵ-neighborhood and boundary of A, respectively. The diameter of A is given by $\delta(A) = \sup\limits_{x,y \in A} d(x, y)$.

Definition 2.1. [2] The *Hausdorff distance*, H, of two nonempty subsets A, B of a metric space (X, d) is defined as

$$H(A, B) = \max\left\{\sup_{x \in A} d(x, B),\ \ \sup_{x \in B} d(x, A)\right\},$$

where $d(x, A) = \inf\limits_{y \in A} d(x, y)$.

It is well-known that the distance function H is a metric, provided A, B are closed and bounded.

Definition 2.2. [7] A sequence $\{x_n\}$ in a metric space (X, d) is said to be *absolutely convergent sequence* if $\sum_{i=1}^{\infty} d(x_i, x_{i+1})$ is finite.

Lemma 2.3. [7] In a metric space X, every Cauchy sequence $\{x_n\}$ contains an absolutely convergent subsequence.

Theorem 2.4. [5] A metric space X is an Atsuji space if and only if each sequence $\{x_n\}$ with $\lim\limits_{n\to\infty} I(x_n) = 0$, has a limit point in X, where $I(x) = d(x, X \setminus \{x\}), x \in X$.

Definition 2.5. [8] A subset S of a metric space X is said to be metrically convex if for any distinct points $x, y \in S$, there is a point $z \in S \setminus \{x, y\}$ that satisfies $d(x, y) = d(x, z) + d(z, y)$.

Theorem 2.6. [8] Consider a complete and metrically convex metric space X. Then, for any distinct points $x, y \in X$, there is a metric segment with the end points x, y.

3 Nonempty intersection results using Hausdorff distance

By a decreasing sequence $\{K_n\}$ of subsets of a metric space X, we mean $K_{n+1} \subset K_n, \ \forall \ n \in \mathbb{N}$, and we denote $H(K_n, K_{n+1})$ by H_n. Clearly $H_n \le \delta(K_n)$. The following theorem furnishes a partial generalization of Cantor's intersection theorem, which we will discuss in Subsection 3.1. It is well known that, in a metric space X, if for each decreasing sequence $\{F_n\} \subset C_b(X)$ with $\delta(F_n) \to 0$, $\bigcap\limits_{n=1}^{\infty} F_n \neq \emptyset$, then X is complete.

Theorem 3.1. A metric space X is complete if and only if for every decreasing sequence $\{K_n\} \subset C_b(X)$ with $\sum_{n=1}^{\infty} H_n$ converges, $\bigcap\limits_{n=1}^{\infty} K_n \neq \emptyset$.

Proof. Let X be a complete metric space. For $a_1 \in K_1$, $\epsilon > 0$, there exists $a_2 \in K_2$ such that $d(a_1, a_2) \le H(K_1, K_2) + \epsilon$. Again, for $a_2 \in K_2$ and $\epsilon > 0$ as above, there exists $a_3 \in K_3$ such that $d(a_2, a_3) \le H(K_2, K_3) + \epsilon^2$. Proceeding this way, we get $d(a_r, a_{r+1}) \le H(K_r, K_{r+1}) + \epsilon^r, \ r \ge 1$. This implies, $\{a_i\}$ is a Cauchy sequence. Let $a_i \to a \in X$. Then, $a \in \bigcap\limits_{i=1}^{\infty} K_n$.

For the converse, consider a decreasing sequence $\{F_n\} \subset C_b(X)$ with $\delta(F_n) \to 0$. Then, the sequence $\{x_n\} \subset X$ with $x_n \in F_n$ is a Cauchy sequence. So, by Lemma 2.3, it has an absolutely convergent subsequence, say, $\{x_{p_i}\}_{i=1}^{\infty}$. Let K_i be the closure of the set $\{x_{p_i}, x_{p_{i+1}}, x_{p_{i+2}}, ...\}, \ i = 1, 2, 3, ...$. Observing $H_i \le d(x_{p_i}, x_{p_{i+1}})$, we have $\sum_{i=1}^{\infty} H_i < \infty$. Then, by the hypothesis, $\bigcap\limits_{i\in\mathbb{N}} K_i \neq \emptyset$. And hence, $\bigcap\limits_{n\in\mathbb{N}} F_n \neq \emptyset$. This completes the proof. $\square$

Following examples validate the statement of the above theorem.

Example 3.2. Let $K_n = \left[-\frac{1}{n}, \frac{1}{n}\right] \subset \mathbb{R}$. Then $\sum_{n=1}^{\infty} H_n$ converges, and $\bigcap\limits_{n\in\mathbb{N}} K_n = \{0\}$.

Example 3.3. Consider the sequence space $X = (l^p, \|\cdot\|_p)$, for some p with $1 \leq p \leq \infty$ and choose $K_n = \{e_i\}_{i\geq n}$, where $e_i = (\delta_{ij})_{j=1}^{\infty}$. Then $\{K_n\}$ is a decreasing sequence in $C_b(X)$. It can be easily checked that $\sum_{n=1}^{\infty} H_n$ doesn't converge and $\bigcap\limits_{n=1}^{\infty} K_n = \emptyset$.

Example 3.4. Let $X = \mathbb{Q}$ with standard metric. Then X is not complete. Let r be a fixed irrational. Define $K_n = \{x \in X : r - 1/n \leq x \leq r + 1/n\}$. Then $K_n \in C_b(X)$ and decreasing. Although $\sum_{n=1}^{\infty} H_n$ converges, $\bigcap\limits_{n=1}^{\infty} K_n = \emptyset$.

3.1 Comparison with Cantor's theorem

It is worth noting that Examples 3.2-3.4 also validate the result of Cantor's intersection theorem. Therefore it is fairly natural to ask: *What advantage Theorem 3.1 provides over the Cantor's theorem?* The answer lies in the fact that $H_n \leq \delta(K_n)$.

In Cantor's intersection theorem, $\delta(K_n) \to 0$ is the sufficient condition to have nonempty intersection. But in the case when $\delta(K_n) \not\to 0$, Cantor's theorem does not provide a conclusion whether $\bigcap\limits_{n=1}^{\infty} K_n$ is empty or nonempty. In such case, if $\sum_{n=1}^{\infty} H_n$ converges, then Theorem 3.1 ensures $\bigcap\limits_{n=1}^{\infty} K_n$ is nonempty. For instance,

Example 3.5. Let $K_n \subset \mathbb{R}^2$ be the region (including boundaries) bounded by the curves $4n(y - 1/n) = -x^2$, and $4n(y + 1/n) = x^2$, $n \in \mathbb{N}$. Then $\delta(K_n) \not\to 0$, and so Cantor's theorem becomes inconclusive here. However, $\sum_{n=1}^{\infty} H_n$ is convergent, and $\bigcap\limits_{n\in\mathbb{N}} K_n$ is the set $\{(x, 0) : -2 \leq x \leq 2\}$.

3.2 Nonempty intersection in Atsuji space

In Theorem 3.1, we see that the condition "$\sum_{n=1}^{\infty} H_n < \infty$", is sufficient to have $\bigcap\limits_{n\in\mathbb{N}} K_n \neq \emptyset$, in complete metric spaces. A more general condition, namely "$H_n \to 0$", is not sufficient to have the nonempty intersection. For instance,

Example 3.6. The functions e_i, defined as $e_i(t) = t^i, t \in [0, 1], i \in \mathbb{N}$, are in the normed space $X = (C[0, 1], \|\cdot\|_\infty)$, and the sets $K_n := \{e_i\}_{i=n}^{\infty}$, $n \in \mathbb{N}$, are closed bounded subsets of X. Here, $H_n = \|e_n - e_{n+1}\|_\infty \to 0$, but $\bigcap\limits_{n=1}^{\infty} K_n = \emptyset$.

However, in Atsuji spaces, which are also complete, "$H_n \to 0$" is sufficient to have the nonempty intersection.

Theorem 3.7. If X is an Atsuji space, then for each decreasing sequence $\{K_n\} \subset C_b(X)$ with $H_n \to 0$, $\bigcap\limits_{n=1}^{\infty} K_n \neq \emptyset$.

Proof. Given a decreasing sequence $\{K_n\} \subset C_b(X)$ such that $H_n \to 0$. For the sequence $\{K_n\}$, there exists $a_n \in K_n$ (as in the proof of Theorem 3.1) such that for any fixed $\epsilon \in (0,1)$ and for all $n \geq 1$ we have, $d(a_n, a_{n+1}) \leq H_n + \epsilon^n \to 0$, as $n \to \infty$. If $a_n = c$, for infinitely many values of n, then $c \in \bigcap\limits_{n=1}^{\infty} K_n$. Otherwise, if the terms of the sequence $\{a_n\}$ are distinct, except for at most finitely many n, then this implies $I(a_n) \to 0$. Therefore, by Theorem 2.4, $\{a_n\}$ has a limit point lying in $\bigcap\limits_{n=1}^{\infty} K_n$. □

The converse of Theorem 3.7, in general, is not true. That means if "$H_n \to 0$" suffices to have the nonempty intersection property, the space is not necessarily an Atsuji space. This is evident from the following example.

Example 3.8. Consider $X = \mathbb{N} \cup M$ with the standard Euclidean metric on $\mathbb{R}$, where $M = \{n + 1/2m : m, n \in \mathbb{N}\}$. Let $\{K_i\} \subset C_b(X)$ be a decreasing sequence with $H_i \to 0$. Then, as in the proof of Theorem 3.7, there exists $a_i \in K_i$ such that $|a_i - a_{i+1}| \to 0$. It can be shown that either $\{a_i\}$ is eventually constant, say $p \in X$, or $\{a_i\}$ converges to some positive integer k. In either case $\bigcap\limits_{i=1}^{\infty} K_i \neq \emptyset$, as it contains either p or k. Thus we get, for each decreasing sequence $\{K_i\} \subset C_b(X)$ with $H_i \to 0$, $\bigcap\limits_{i=1}^{\infty} K_i \neq \emptyset$, but the space X is not an Atsuji space because $X' = \mathbb{N}$.

We notice that Theorem 3.7 provides a generalization of Cantor's intersection theorem in Atsuji spaces.

4 Nonempty intersection results using $\hat{d}$

Jain and Kundu, in [4], considered a functional $I : X \to \mathbb{R}$ defined as, $I(x) = d(x, X \setminus \{x\})$. Here we consider a more general functional, $\hat{d}$, acting on the subsets of a metric space X, defined by $\hat{d}(A) = \sup\limits_{x \in A} d(x, X \setminus A)$, $A \subset X$. This is also known as the excess of A over $X \setminus A$. This functional gives the radius of the inscribed ball inside a regular body in the Euclidean space $\mathbb{R}^2$. For subsets A, B of a metric space X, we conclude the following as well:

1. $\hat{d}(A) \leq \hat{d}(B)$, if $A \subset B$, and $A \in B(X)$,
2. $\hat{d}(A) = 0$ if and only if $A = \emptyset$ or $A \subset [X \setminus A]'$,
3. For an unbounded set A, $\hat{d}(A)$ can be finite or infinite. For example, in the euclidean space $\mathbb{R}^2$, consider $A_1 = \{(x, 0) : x \in \mathbb{R}\}$, and $A_2 = \{(x, y) : x, y \geq 0\}$, then $\hat{d}(A_1) = 0$, and $\hat{d}(A_2) = \infty$,

4. If $A = X$, then $\hat{d}(A)$ is finite or infinite, depending on X is bounded or unbounded, respectively. (We take $d(x, \emptyset) = \sup\{d(x, A) : A \subset X\}$, $x \in X$.)

Proposition 4.1. Let $A, B \in B(X)$. Then

(a) $H(X \setminus A, X \setminus B) \leq \max\{\hat{d}(A), \hat{d}(B)\}$.

(b) $\max\{\hat{d}(A), \hat{d}(B)\} \leq H(A, B)$, provided $A \cap B = \emptyset$.

Proof. (a) For $A, B \in B(X)$, we have

$$\begin{aligned}
&H(X \setminus A, X \setminus B)\\
&= \max\{\sup_{p \in X\setminus A} d(p, X \setminus B), \sup_{q \in X \setminus B} d(X \setminus A, q)\}\\
&= \max\{\sup_{p \in B\setminus A} d(p, X \setminus B), \sup_{q \in A \setminus B} d(q, X \setminus A)\} \qquad (4.1)\\
&\leq \max\{\sup_{p \in B} d(p, X \setminus B), \sup_{q \in A} d(q, X \setminus A)\}\\
&= \max\{\hat{d}(B), \hat{d}(A)\}. \qquad (4.2)
\end{aligned}$$

(b) Suppose $A \cap B = \emptyset$, then

$$\begin{aligned}
H(A, B) &= \max\{\sup_{x \in A} d(x, B), \sup_{y \in B} d(A, y)\}\\
&\geq \max\{\sup_{x \in A} d(x, X \setminus A), \sup_{y \in B} d(X \setminus B, y)\}\\
&= \max\{\hat{d}(A), \hat{d}(B)\}.
\end{aligned}$$

□

Remark 4.2. For two subsets A, B with $A \subset B$ in a metric space X, in general, $\hat{d}(B)$ and $H(A, B)$ are not comparable, even in Atsuji spaces.

Theorem 4.3. Let X be an Atsuji space. Then, for each decreasing sequence $\{K_n\} \subset C_b(X)$ with $\hat{d}(K_n) \to 0$, $\bigcap_{n=1}^{\infty} K_n \neq \emptyset$.

Proof. Consider $x_n \in K_n$. Then, $I(x_n) = d(x_n, X \setminus \{x_n\}) \leq d(x_n, X \setminus K_n) \leq \sup_{x \in K_n} d(x, X \setminus K_n) = \hat{d}(K_n)$, which by the hypothesis tends to 0. Hence, using Theorem 2.4, the sequence $\{x_n\}$ has a limit point lying in $\bigcap_{i=1}^{\infty} K_n$. □

The converse of Theorem 4.3, in general, does not hold.

Example 4.4. Consider the set X as in Example 3.8, with the standard Euclidean metric d on $\mathbb{R}$. Let $\{K_i\} \subset C_b(X)$ be a decreasing sequence with $\hat{d}(K_i) \to 0$. Then, as in the proof of Theorem 4.3, there exists $x_i \in K_i \setminus K_{i+1}$ such that $I(x_i) \to 0$. If the range set, $R = \{x_i\}_{i \geq 1}$, is infinite and $R \subset M$, consider $x_i = n_i + 1/2m_i$. If $\{m_i\}_{i\geq 1} = \{p_1, p_2, ..., p_q\}$, a finite set, then $d(n_i+1/2p_j, X\backslash\{n_i+1/2p_j\}) = d(n_i+1/2p_j, n_i+1/2(p_j+1)) = \frac{1}{2}d(1/p_j, 1/(p_j+1)) \geq \inf\limits_{1\leq j\leq q} \frac{1}{2}d(1/p_j, 1/(p_j+1)) > 0$, which is a contradiction to $I(x_i) \to 0$. Hence, there is a subsequence $\{m_{t_i}\}$ of $\{m_i\}$ with $m_{t_i} \to \infty$ as $i \to \infty$. And so, it can be proved that in the case either $R \subset M$ or $R \not\subset M$; the sequence $\{x_i\}$ has a subsequence converging to some $p \in \mathbb{N}$. Therefore $p \in \bigcap\limits_{i=1}^{\infty} K_i$. Thus we get, for each decreasing sequence $\{K_i\} \subset C_b(X)$ with $\hat{d}(K_i) \to 0$, $\bigcap\limits_{i=1}^{\infty} K_i \neq \emptyset$. Although, the space X is not an Atsuji space.

Theorem 4.5. If X is a metric space, and for each decreasing sequence $\{K_n\} \subset C_b(X)$ with $\hat{d}(K_n) \to 0$, $\bigcap\limits_{n=1}^{\infty} K_n \neq \emptyset$, then X is complete.

Proof. Consider a decreasing sequence $\{F_n\} \subset C_b(X)$ with $\delta(F_n) \to 0$. Then, the sequence $\{x_n\}$ with $x_n \in F_n$ is a Cauchy sequence in X. Let K_n be the closure of the set $\{x_i\}_{i\geq n}$. Since $\{x_n\}$ is Cauchy, for each $\epsilon > 0$, there is an $N \in \mathbb{N}$ such that $\sup\limits_{n\geq N+1} d(x_N, x_n) < \epsilon$, that is, $\sup\limits_{x\in K_{N+1}} d(x_N, x) < \epsilon$, which further implies $\hat{d}(K_{N+1}) = \sup\limits_{x\in K_{N+1}} d(x, X \setminus K_{N+1}) < \epsilon$. Thus $\hat{d}(K_n) \to 0$. So, by the hypothesis $\bigcap\limits_{n=1}^{\infty} K_n \neq \emptyset$. Hence, $\bigcap\limits_{n=1}^{\infty} F_n \neq \emptyset$ and this completes the proof. $\square$

4.1 Comparison with Cantor's theorem

We observe that, in general, $\hat{d}$ and δ are not comparable. For instance,

Example 4.6. Consider a set $X = \{x, y\}$, $x \neq y$, equipped with a metric d. Let $A = \{x\}$. Then, $\hat{d}(A) = d(x, y) > 0$, and $\delta(A) = 0$.

But if $X = \mathbb{R}^2$, with standard Euclidean metric, and $A = B[0, r]$, then $\hat{d}(A) = r < 2r = \delta(A)$.

We shall show that in metrically convex metric spaces, $\hat{d}$ is always dominated by δ.

Lemma 4.7. Let (X, d) be a metric space. Then, for all $x, y \in X$ and $r \in [0, d(x, y)]$, $B[x, r] \cap B[y, d(x, y) - r] = S[x, r] \cap S[y, d(x, y) - r]$, where $S[x, r] := \{z \in X : d(x, z) = r\}$.

Proof. Let us denote $B[x, r] \cap B[y, d(x, y) - r]$ and $S[x, r] \cap S[y, d(x, y) - r]$ by $B^{\cap}$ and $S^{\cap}$, respectively. If $B^{\cap}$ is empty, there is nothing to prove. Let $B^{\cap} \neq \emptyset$ and $z \in B^{\cap}$. We claim $z \notin B_1 \cup B_2$, where $B_1 = B[x, r] \setminus S[x, r]$, $B_2 = B[y, d(x, y) - r] \setminus S[y, d(x, y) - r]$. If possible, let $z \in B_1$. Then $d(x, y) \leq d(x, z) + d(z, y) < r + d(x, y) - r = d(x, y)$, which is a contradiction. Similarly, we prove $z \notin B_2$. Thus, $z \in B^{\cap} \cap [B_1 \cup B_2]^c = B^{\cap} \cap [{B_1}^c \cap {B_2}^c]$, where B^c

denotes the complement of a set B in X. This implies $z \in S^{\cap}$, and so $B^{\cap} \subset S^{\cap}$. Hence, $B^{\cap} = S^{\cap}$. $\square$

Theorem 4.8. Let A be a nonempty bounded proper subset in a complete metrically convex space X. Then $\hat{d}(A) \leq \delta(A)$.

Proof. Let (X, d) be an metrically convex space. By Theorem 2.6, X is a connected metric space too. We shall achieve the conclusion in the following steps.

Step 1 : First we show that for each $\epsilon > 0$ the set $N_\epsilon(A) \setminus A$ is not empty.
Step 2 : We show that for each $\epsilon > 0$ we have $B(a, r + \epsilon) = N_\epsilon(B)$, where $B = B(a, r)$.
Step 3 : Finally we prove that $\hat{d}(A) \leq \delta(A)$.

Step 1. On the contrary, let us assume $N_\epsilon(A) \setminus A = \emptyset$. This implies, A is open and for all $x \in A$, $B(x, \epsilon) \subset A$. Since A is open, $\partial A \not\subset A$. This implies, "$\exists\ b \in \partial A$ such that $b \notin B(x, \epsilon)$ for all $x \in A$", which is a contradictory statement in itself.

Step 2. Observe that, $N_\epsilon(B) \subset B(a, r+\epsilon)$ follows from the triangle inequality. Conversely, suppose $y \in B(a, r + \epsilon)$. If $y \in B$ then $y \in B(y, \epsilon) \subset N_\epsilon(B)$. Suppose $y \in B(a, r + \epsilon) \setminus B$. Then, consider the ball $B(y, \epsilon)$. If $B(y, \epsilon) \cap B = \emptyset$, then $B(y, \epsilon) \cap \partial B = \emptyset$. Therefore, $d(q, y) \geq \epsilon$, for all $q \in \partial B$. By Theorem 2.6 and Lemma 4.7, since $r \in [0, d(a, y)]$, there is a $u \in X$ such that $\psi(r) = u \in B[a, r] \cap B[y, d(a, y) - r] = S[a, r] \cap S[y, d(a, y) - r] = \partial B \cap S[y, d(a, y) - r]$, where ψ is an isometry from $[0, d(a, y)]$ to X. This implies $d(a, y) = d(a, u) + d(u, y) \geq r + \epsilon$, a contradiction. Hence, $B(y, \epsilon) \cap B \neq \emptyset$, and therefore $y \in B(z, \epsilon)$ for some $z \in B$. Thus, $B(a, r + \epsilon) \subset N_\epsilon(B)$.

Step 3. Since $\partial B \neq \emptyset$, $\inf\limits_{p \in X \setminus B} d(a, p) = d(a, q) = r$, for some $q \in \partial B$. Now, let x be an element in A. If $x \in A^{\circ}$, then consider a ball $B(x, r')$, where $r' = \sup\{r > 0 : B(x, r) \subset A\}$. There must be a point in $N_\epsilon(B(x, r'))$ which lies in $N_\epsilon(A) \setminus A$. Hence, $[N_\epsilon(B(x, r')) \setminus B(x, r')] \cap [N_\epsilon(A) \setminus A] \neq \emptyset$. Therefore, $d(x, X \setminus A) = r' \leq \delta(A)$. On the other hand, if $x \in \partial A$, then $d(x, X \setminus A) = 0 \leq \delta(A)$. Hence, $\hat{d}(A) \leq \delta(A)$. $\square$

Since the metric spaces with Takahashi's convex strustures ([12]) and the normed spaces are metrically convex metric spaces, so Theorem 4.8 is applicable to these spaces too. Due to Theorem 4.8, Theorem 4.3 induces a generalization of Cantor's intersection theorem in metrically convex Atsuji spaces.

Example 4.9. Consider the metric space $X = \{(x, y) \in \mathbb{R}^2 : -3 \leq x, y \leq 3\}$, with standard Euclidean metric on $\mathbb{R}^2$. The space X is a metrically convex Atsuji space. Let $K_n \subset X$ be the region (including boundaries) bounded by the curves $n(1 + \frac{1}{n})^2(y - 1/n) = -x^2$, and $n(1 + \frac{1}{n})^2(y + 1/n) = x^2$, $n \in \mathbb{N}$. Here $\delta(K_n) \not\to 0$, and so Cantor's theorem becomes indecisive. However, $\hat{d}(K_n) \to 0$, and $\bigcap\limits_{n \in \mathbb{N}} K_n$ is the set $\{(x, 0) : -1 \leq x \leq 1\}$.

5 Conclusion

For a pair of consecutive elements K_n, K_{n+1} from a decreasing sequence $\{K_n\}$ of nonempty closed bounded subsets of a metric space, it is observed that H_n is less than or equal to the diameter of K_n, where H_n is the Hausdorff distance between K_n and K_{n+1}. Therefore, $H_n \to 0$ is the necessary condition for Cantor's intersection theorem. However, the condition $H_n \to 0$ in not sufficient to have nonempty $\bigcap\limits_{n\in\mathbb{N}} K_n$ in complete metric spaces; extra conditions on H_n is required for that. We have shown that the condition $\sum_{n=1}^{\infty} H_n < \infty$, is sufficient to have nonempty intersection in complete metric spaces; while, $H_n \to 0$ is sufficient to have nonempty intersection in Atsuji spaces. Further, in Atsuji spaces, we have provided sufficient condition for nonempty $\bigcap\limits_{n\in\mathbb{N}} K_n$ using the concept of excess of a set.

Nonempty intersection theorems, and the generalizations of such theorems like Cantor's theorem, Kuratowski's theorem, Horvath's theorem, etc. play an important role to study the best approximations, fixed point results, etc. (for example, see [3, 9, 10, 13]). In case of set-valued mappings, researchers have been studying the fixed point results for mappings from a metric space to the subspaces of the hyperspace of nonempty closed subsets endowed with the Hausdorff distance (for example, see [1, 11]). Findings of this manuscript, can further be applied in these directions.

References

[1] N. A. Assad and W. A. Kirk, Fixed point theorems for set-valued mappings of contractive type, *Pacific J. Math.*, 43, 553–562 (1972).

[2] J. Henrikson, Completeness and total boundedness of the Hausdorff metric, *MIT Undergrad. J. Math.*, 1, 69-80 (1999).

[3] C. Horvath, Measure of non-compactness and multivalued mappings in complete metric topological vector spaces, *J. Math. Anal. Appl.*, 108, 403–408 (1985).

[4] T. Jain, S. Kundu, Atsuji completions: Equivalent characterisations, *Topology Appl.*, 154, 28–38 (2007).

[5] S. Kundu and T. Jain, Atsuji spaces: Equivalent conditions, *Topology Proc.*, 30, 301–325 (2006).

[6] K. Kuratowski, Sur les espaces complets, *Fund. Math.*, 15, pp. 301–309 (1930).

[7] H. M. MacNeille, Extensions of measure, *Proc. Natl. Acad. Sci.*, 24, pp. 188–193 (1938).

[8] A. Martinon, Distance to the intersection of two sets, *Bull. Austral. Math. Soc.*, 70, pp. 329–341 (2004).

[9] Z. D. Mitrovic and I. D. Arandjelovic, Existence of generalised best approximations, *Nonlinear Convex Anal.*, 15, pp. 787–792 (2014).

[10] Z. D. Mitrovic and I. D. Arandjelovic, Generalized scalar equilibrium problem with applications to best and coupled best approximations, *J. Fixed Point Theory Appl.*, 19, pp. 1613–1624 (2017).

[11] S. B. Nadler Jr., Multi-valued contraction mappings, *Pacific J. Math.*, 30, pp. 475–488 (1969).

[12] W. Phuengrattana and S. Suantai, Existence and convergence theorems for generalized hybrid mappings in uniformly convex metric spaces, *Indian J. Pure Appl. Math.*, 45, pp. 121–136 (2014).

[13] T. Shimizu and W.Takahashi, Fixed points of multivalued mappings in certain convex metric spaces, *Topol. Methods Nonlinear Anal.*, 8, pp. 197–203 (1996).

[14] G. F. Simmons, *Introduction to Topology and Modern Analysis*, McGraw-Hill, New York, 1963.

[15] J. A. Souza and R. W. M. Alves, CantorKuratowski theorem in admissible spaces, *Topology Appl.*, 252, pp. 158–168 (2019).

J. COMPUTATIONAL ANALYSIS AND APPLICATIONS, VOL. 31, NO.1, 2023, COPYRIGHT 2023 EUDOXUS PRESS, LLC

Goal programming approach to solve linear transportation problems with multiple objectives

Vishwas Deep Joshi[1], Keshav Agarwal[2], Jagdev Singh[3]
[1,2,3] Department of Mathematics, JECRC University Jaipur, Rajasthan, INDIA
Email: [1]vdjoshi.or@gmail.com*, [2]keshavaggarwal58@gmail.com, [3]jagdevsinghrathor@gmail.com
*Corresponding author

December 28, 2022

Abstract

In multi-objective transportation, due to the conflicting nature of objectives, no method is available to find the best compromise optimal solution. In this paper, we present a method to obtain a compromised solution for multi-objective transportation problems under a weighted environment. In which, a modified weighted model is presented that provides us with an efficient solution according to the priorities of the decision maker. To measure the efficiency of the method, a numerical example is included and the results are compared with previously reported work for the same numerical problems to illustrate the feasibility and the applicability of the proposed method.

Keywords- Multi-objective optimization; transportation problem; compromise solution; goal programming

1 Introduction

With the growing population of this competitive world the demand for the goods is growing day by day and to fulfil the demands, the businesses have to outperform themselves every time. Due to this, the management of the business faces a lot of challenges and single objective transportation is not enough to meet the needs of this competitive market. Just Minimizing the transportation cost cannot be the only objective, they must take other factors into consideration and solving such type of problem with multiple objectives which need to be fulfilled simultaneously gives birth to a new branch of transportation problem that we call multi-objective transportation problem (MOTP).

In a classic transportation problem, a product is to be transported from m sources to n destinations and there is a penalty p_{ij} associated with transporting a unit of product. This penalty may be cost or delivery time or safety of delivery, or something else depending upon the decision maker (DM). Over a period of time, many algorithms have been developed to obtain initial basic feasible solutions like the North-west corner rule, least cost method, and Vogel's approximation method. Veena Adlakha and Kowalski [2](1997) proposed a very effective algorithm (Absolute point method) that can be used to directly obtain optimal cost without using the MODI method. These methods are applicable when all the decision parameters are given in a precise way, but as already discussed in real life situations, not all transportation problems are single-objective.

Past many years a lot of work has been done in developing an algorithm to solve multi-objective transportation problems. Every algorithm gives varying results and it is very difficult to say which is the best method to obtain a compromised solution (For multi-objective transportation, a compromised solution is a feasible solution that is favoured more by the DM over all other feasible solutions, taking into consideration all criteria contained in the multi-objective function).The quality of the solution totally depends on the DM.

Lee and Moore [7](1973) inspected the optimization of transportation problems with multiple objectives. Isermann and Diaz [6] (1979) formulated different algorithms for all the non-dominated solutions for linear multi-objective transportation problems. The fuzzy programming technique was applied by Bit, Biswal, and Alam [3] (1992) to solve the multi-objective transportation problem. For the first time in the early 1960s, Charnes and Cooper suggested the concept of goal programming (GP) and a very good literature review was given. It has been found extensive in various fields. Since 1960, numerous works have been done and a lot of applications have been proposed. A review of GP formulations and their applications was given by Lee and Olson [8](1999). Edward L. Hannan [4] (1981) illustrated GP with fuzzy goals having a linear membership function. Zangiabadi and Maleki [13](2013) presented the application of fuzzy goal programming to linear MOTP using a non-linear membership function. Despite its recognition and a huge variety of applications, there's no assurance that GP will offer Pareto an optimal solution.

In multi-objective problems, we can assign different weights to the objective according to the importance of the objective and obtain varying results for different weights assigned by the DM. Due to the overlapping existence of priorities, it is rare to find an optimal solution that optimizes all of them at the same. Here in this paper, we have discussed the weighted sum method and the algorithm proposed by Nomani [10](2016) and a comparison has been made with the proposed model with the help of numerical examples. The proposed model is a new weighted method that helps obtain compromised solutions according to the priorities given by the DM for different goals.

2 Multi-objective linear transportation problem (MOLTP)

In today's aggressive environment, a single-objective transportation assignment is insufficient to deal with all real-life decision-making issues. So, to address all real-life conditions on transportation problems, the DM regularly wishes to consider more than one non-commensurable or conflicting objective in transportation problems. The problem wherein more than one target is optimized concurrently is referred to as a multi-objective transportation problem (MOTP). The reason for defining the multi-objective transportation problem in the mathematical programming framework is to optimize numerous objectives concurrently subject to a set of constraints Other than transportation expense the objectives can include shipping time, degradation of goods, secure shipping of items, energy consumption, etc

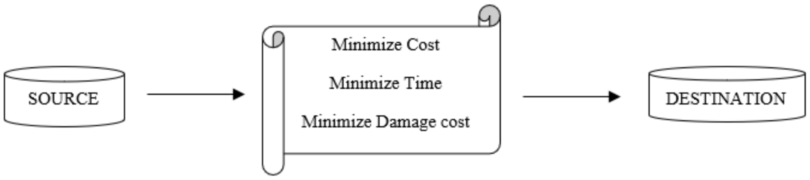

The mathematical model of MOTP is written as follows:

$$Min\ F_k(x_ij) = \sum_{i=1}^{m}\sum_{j=1}^{n} p_{ij}^{k} x_{ij}, \qquad k = 1, 2, \ldots, K$$

Subject to:

$$\sum_{j=1}^{n} x_{ij} = s_i, \qquad i = 1, 2, 3, \ldots, m$$

$$\sum_{i=1}^{m} x_{ij} = dj, \qquad j = 1, 2, 3, \ldots, n$$

$$x_{ij} \geq 0, \quad i = 1, 2, 3, \ldots m, and\ \ j = 1, 2, \ldots, n$$

Where m is no. of source, n is no. of destination, d_n is capacity of destination, s_m is capacity of sources, p_{ij}^{k} is penalty of k^{th} objective, F_k is k^{th} objective and x_{ij} is unknown qty to be shipped.

3 Methods for solving MOLTP

3.1 Weighted sum method

For solving a MOLTP the method of the weighted sum is highly used to obtain varying results for different weights. The basic idea of this method is to assign weight $n_k \geq 0$ to each objective function F_k and minimize the new objective function $\sum_{k=1}^{K} n_k F_k$ with respect to problem constraints. This method is very easy to use but the solution majorly depends on the weights given by the DM and it should be decided beforehand. Using the weighted sum method, the following normalized single-objective optimization problem is obtained:

$$Minimize \;\; F = n_1F_1 + n_2F_2 + \ldots + n_KF_K$$

Subject to:

$$\sum_{j=1}^{n} x_{ij} = s_i, \qquad i = 1, 2, 3, \ldots, m$$

$$\sum_{i=1}^{m} x_{ij} = dj, \qquad j = 1, 2, 3, \ldots, n$$

$$x_{ij} \geq 0, \quad i = 1, 2, 3, \ldots m, and \;\; j = 1, 2, \ldots, n$$

Where the weights $n_k, k = 1, 2, \ldots K$, corresponding to the objective function satisfy the following conditions $n_1 + n_2 + \ldots + n_k = 1 \; k = 1, 2, \ldots K$
Using the above method, single solution points are obtained for different weights that reflect the preferences of the decision-maker. This method fails when DM have no idea about preference.

3.2 Method proposed by Nomani(2016)

In 2016, Mohammad Asim Nomani, Irfan and Ahmed proposed a model to obtain a compromised solution for a MOLTP. This model focuses on converting multiobjective optimization into a new single objective optimization where the objective is to $minimize \; \mu^{'} = \sum \mu(1 - n_k)$, where μ is the general deviation variable for all objectives and n_k is the weight assigned to the k^{th} objective.

Consider the following multi-objective optimization problem:

$$Minimize \; F(x) = [F_1(x), F_2(x), \ldots, F_K(x)]$$

$$Subject \; to \;\; x \in S$$

Where x is an n-dimensional decision maker variable and S is the set of feasible solutions. Each objective is transformed into constraints with an upper bound of $F_k^* + \mu(1 - n_k)$, where F_k^* is an ideal solution obtained when each objective $F_k, k = 1, 2, \ldots, K$ is solved independently of other objectives.
The problem reduces as:

$$Minimize \; \mu^{'} = \sum_{k=1}^{K} \mu(1 - n_k)$$

Subject to:

$$F_k \leq F_k^* + \mu(1 - n_k); \qquad x_{ij} \geq 0$$

In this model, instead of using a deviation variable alone, a factor $(1-n_k)$ has been introduced. This method is capable of providing a solution even if DM has no priority for objectives.

4 Proposed Method

In this section, we will discuss the proposed method and later we will see a comparison between the results obtained by these three methods. Let us consider a multi-objective optimization problem:

$$Minimize \;\; F(x) = [F_1(x), F_2(x), \dots, F_K(x)]$$

Like Nomani's model, this model also focuses on converting the multi-objective problem into a single objective problem. The main idea is to minimize the deviation of each objective from its ideal solution. To do so a deviation variable μ was introduced.

The model is formulated as:

$$Minimize \; \mu^{'} = \sum_{k=1}^{K} \mu(1-n_k)$$

Subject to

$$\sum_{i=1}^{m}\sum_{j=1}^{n} p_{ij}^{k} x_{ij} \leq F_k^{*} + \frac{\mu(1-n_k}{(F_u^k - F_l^k)} \quad k = 1,2,\dots,K$$

$$\sum_{j=1}^{n} x_{ij} = s_i, \qquad i = 1,2,3,\dots,m$$

$$\sum_{i=1}^{m} x_{ij} = dj, \qquad j = 1,2,3,\dots,n$$

$$0 \leq n_k \leq 1, k = 1,2,\dots,K$$

$$x_{ij} \geq 0, i = 1,2,\dots,m \;\; and \; j = 1,2,3,\dots,n$$

Here in this model a factor $\frac{1}{(F_u^k - F_l^k)}$ is introduced alongside with existing $\mu(1-n_k)$. F_u^k and F_l^k represent upper and lower bounds in which the compromised solution will lie. The solution cannot exceed this range. For a k^{th} objective, this range can be obtained by using the ideal allocation. For upper bound max (Solution obtained by substituting others allocation in kth objective) and for lower bound the optimal solution of k^{th} objective is it's lower bound and this lower bound is the ideal solution F_k^{*}.

Step by Step method:

Step 1: Solve all the K objectives as a single objective problem without considering other objectives.
Step 2: Obtain the range for every objective as stated above.
Step 3: Now develop a model for the problem as described above and define weights for the objectives if DM has any.
Now simply evaluate and a compromised solution will be obtained.

5 Numerical illustration

The first example that we will be considering is used by many authors and they have obtained different solutions. Ringuest and Rinks [11](1987) used this problem to illustrate the MOLTP. In this paper, we have formulated the problem like a real-life problem to make a better understanding of the problem.

Example 1: Let us consider a problem in which Jethalal wants to transport TVs from its 3 Factories situated in Delhi, Mumbai and Bangalore, to the 4 warehouses at Bhopal, Dehradun, Kolkata and Chennai. The Factory capacity of Delhi is 8 thousand TVs, Mumbai is 19 thousand TVs and Bangalore is 17 thousand TVs. The warehouse requirement at Bhopal is 11 thousand TVs, Dehradun is 3 thousand TVs, Kolkata is 14 thousand TVs and Chennai is 16 thousand TVs. Jethalal wants to minimize the transportation cost as well as the safety cost for the TVs. The cost of transportation and safety per unit is given in the table below (in thousands)

Safety,Transportation	**Bhopal**	**Dehradun**	**Kolkata**	**Chennai**
Delhi	1,4	2,4	7,3	7,4
Mumbai	1,5	9,8	3,9	4,10
Banglore	8,6	9,2	4,5	6,1

Solution The first step is to obtain a solution for both the objectives separately ignoring the other objective. The solution obtained is as follows:
$X^1 = (x_{11} = 5, x_{12} = 3, x_{21} = 6, x_{24} = 13, x_{33} = 14, x_{34} = 3)$
$F_1(X^1) = 143(ideal solution), F_1(X^2) = 208,$
Upper and lower bounds of the objective function F_1 is $143 \leq F_1 \leq 208$
$X^2 = (x_{13} = 8, x_{21} = 11, x_{22} = 2, x_{23} = 6, x_{32} = 1, x_{34} = 16)$
$F_2(X^2) = 167(ideal solution), F_2(X^1) = 265,$
Upper and lower bounds of the objective function F_2 is $167 \leq F_2 \leq 265$
Now since we have the bounds, we can formulate the mathematical model of the problem using the proposed model.

$$Minimize\ \mu^{'} = \mu(1 - n_1) + \mu(1 - n_2)$$

Subject to:

$$\sum_{i=1}^{3}\sum_{j=1}^{4} p_{ij}^{1} x_{ij} \leq 143 + \frac{\mu(1 - n_1)}{(208 - 143)}$$

$$\sum_{i=1}^{3}\sum_{j=1}^{4} p_{ij}^{2} x_{ij} \leq 167 + \frac{\mu(1-n_2)}{(265-167)}$$

$$\sum_{j=1}^{4} x_{ij} = s_i, \quad i = 1,2,3$$

$$\sum_{i=1}^{3} x_{ij} = d_j, j = 1,2,3,4$$

$$n_1 + n_2 = 1$$

$$0 \leq n_k \leq 1$$

$$k = 1,2; \quad x_{ij} \geq 0$$

Now simply allot the weight to the objective function and solve the LPP. Make sure the weights are non-negative and their sum is exactly equal to 1. We have used Lingo 19.0 to solve the LLP.

	Weights (n_1, n_2)	**Proposed method**	**Nomani**	**Weighted sum**
1	$n_1 = 0.1, n_2 = 0.9$	197;169	186;171	208;167
2	$n_1 = 0.2, n_2 = 0.8$	186;171	176;175	186;171
3	$n_1 = 0.3, n_2 = 0.7$	176;175	172;180	176;175
4	$n_1 = 0.4, n_2 = 0.6$	172;180	168;185	176;175
5	$n_1 = 0.5, n_2 = 0.5$	168;185	164;190	176;175
6	$n_1 = 0.6, n_2 = 0.4$	148;180	160;195	156;200
7	$n_1 = 0.7, n_2 = 0.3$	160;195	156;200	156;200
8	$n_1 = 0.8, n_2 = 0.2$	156;200	154;210	156;200
9	$n_1 = 0.9, n_2 = 0.1$	152;220	150;230	143;265

Comparison of solution of Example 1 by the proposed method, Nomani method, weighted sum

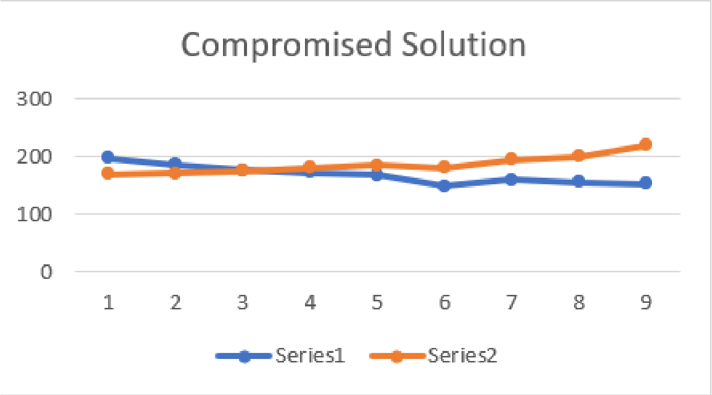

7

Figure 1 Graphical representation of solution with different priorities

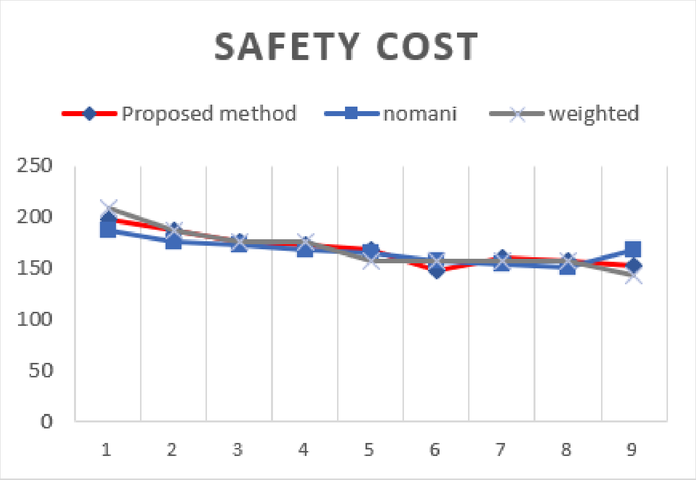

Figure 2 Comparison of safety costs obtained by different methods

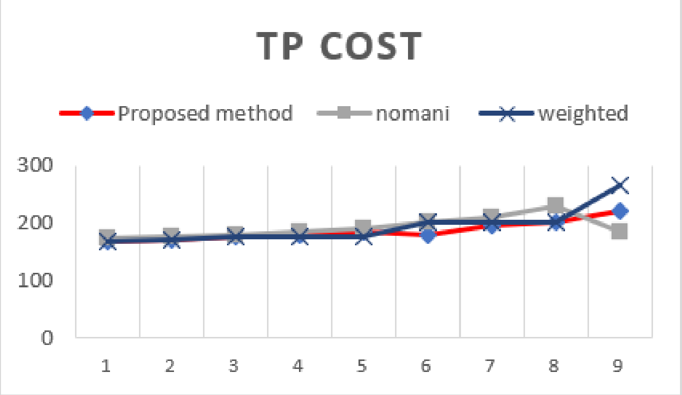

Figure 3 Comparison of TP cost obtained by different methods

Let us now consider a 3-objective problem. This example is already used by authors to compare varying results. Diaz [6](1979) used this example to illustrate the approach. Like the previous problem, we have formulated it like real life problem for better understanding.

Example 2: Madhavi Bhide have a business selling Pickel and she wants to deliver the pickle to various locations across India. She has manufacturing units in Mumbai, Ahmedabad, Chandigarh, and Mirzapur and needs to supply at Ratlam, Nagpur, Patna, Panji, and Kota. The supply capacity of Mumbai is 500 boxes, Ahmedabad is 400 boxes, Chandigarh is 200 boxes, and Mirzapur is 900 boxes. Demand at Ratlam is 400 boxes, Nagpur is 400 boxes, Patna is 600 boxes, Panji is 200 boxes, and Kota is 400 boxes. She wants to minimize the delivery time, transportation cost and packaging cost. The cost time and packing cost per unit are given below (in hundreds).

Cost,Time,Packing cost	**Ratlam**	**Nagpur**	**Patna**	**Panji**	**Kota**
Mumbai	9,2,2	12,9,4	9,8,6	6,1,3	9,4,6
Ahmedabad	7,1,4	3,9,8	7,9,4	7,5,9	5,2,2
Chandigarh	6,8,5	5,1,3	9,8,5	11,4,3	3,5,6
Mirzapur	6,2,6	8,8,9	11,6,6	2,9,3	2,8,1

Solution: The first step is to obtain a solution for all three objectives separately ignoring the other objectives. The solution obtained is as follows:
$X^1 = (x_{13} = 5, x_{22} = 3, x_{23} = 1, x_{31} = 1, x_{32} = 1, x_{41} = 3, x_{44} = 2, x_{45} = 4)$
$F_1(X^1) = 102, F_1(X^2) = 164, F_1(X^3) = 134,$
Upper bound = Max 164,134 = 164
Upper and lower bounds of the objective function F_1 is $102 \leq F_1 \leq 164$
$X^2 = (x_{11} = 3, x_{14} = 2, x_{21} = 1, x_{25} = 4, x_{32} = 2, x_{41} = 1, x_{42} = 2, x_{43} = 6)$
$F_2(X^2) = 72(ideal solution), F_2(X^1) = 141, F_2(X^3) = 122,$
Upper bound = Max 141,122 = 141
Upper and lower bounds of the objective function F_2 is $72 \leq F_2 \leq 141$
$X^3 = (x_{11} = 3, x_{12} = 2, x_{21} = 1, x_{23} = 3, x_{32} = 2, x_{43} = 3, x_{44} = 2, x_{45} = 4)$
$F_3(X^3) = 64(ideal solution), F_3(X^2) = 90, F_3(X^1) = 94,$
Upper bound = Max 90,94 = 94
Upper and lower bounds of the objective function F_3 is $64 \leq F_2 \leq 94$
Now since we have the bounds, we can formulate the mathematical model of the problem using the proposed model.

$$Minimize\ \mu^{'} = \mu(1-n_1) + \mu(1-n_2) + \mu(1-n_3)$$

Subject to:

$$\sum_{i=1}^{4}\sum_{j=1}^{5} p_{ij}^{1} x_{ij} \leq 102 + \frac{\mu(1-n_1)}{(164-102)}$$

$$\sum_{i=1}^{4}\sum_{j=1}^{5} p_{ij}^{2} x_{ij} \leq 72 + \frac{\mu(1-n_2)}{(141-72)}$$

$$\sum_{i=1}^{4}\sum_{j=1}^{5} p_{ij}^{3} x_{ij} \leq 64 + \frac{\mu(1-n_2)}{(94-64)}$$

$$\sum_{j=1}^{5} x_{ij} = s_i, \quad i = 1,2,3,4$$

$$\sum_{i=1}^{4} x_{ij} = d_j, \quad j = 1,2,3,4,5$$

$$n_1 + n_2 + n_3 = 1 \ \ 0 \leq n_k \leq 1 \quad k = 1,2,3$$

Now simply allot the weight to the objective function and solve the LPP. Make sure the weights are non-negative and their sum is exactly equal to 1. We have used Lingo 19.0 to solve the LLP.

	Weights (n_1, n_2, n_3)	**Proposed method**	**Nomani**	**Weighted sum**
1	$n_1 = 0.1, n_2 = 0.9, n_3 = 0.0$	147;76;94	147;76;94	157;72;86
2	$n_1 = 0.2, n_2 = 0.8, n_3 = 0.0$	142;78;98	142;78;98	157;72;86
3	$n_1 = 0.3, n_2 = 0.7, n_3 = 0.0$	134;85;96	134;85;96	142;78;98
4	$n_1 = 0.4, n_2 = 0.0, n_3 = 0.6$	114;99;89	124;109;78	129;126;64
5	$n_1 = 0.5, n_2 = 0.0, n_3 = 0.5$	119;101;91	118;110;83	105;128;84
6	$n_1 = 0.6, n_2 = 0.0, n_3 = 0.4$	117;106;88	117;108;84	105;128;84
7	$n_1 = 0.0, n_2 = 0.3, n_3 = 0.7$	134;93;83	139;99;74	153;89;75
8	$n_1 = 0.0, n_2 = 0.2, n_3 = 0.8$	135;97;78	141;102;72	134;122;64
9	$n_1 = 0.0, n_2 = 0.1, n_3 = 0.9$	141;102;72	140;110;68	134;122;64
10	$n_1 = 0.3, n_2 = 0.3, n_3 = 0.4$	126;92;94	124;99;87	127;104;76
11	$n_1 = 0.3, n_2 = 0.4, n_3 = 0.3$	126;92;94	129;95;87	141;86;82
12	$n_1 = 0.4, n_2 = 0.3, n_3 = 0.3$	124;97;91	124;99;87	112;110;88

Comparison of solution of Example 2 by the proposed method, Nomani method, weighted sum

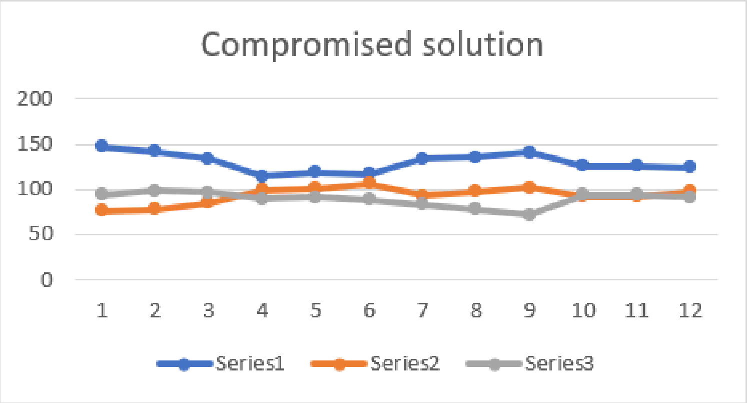

Figure 4 Graphical representation of solution with different priorities

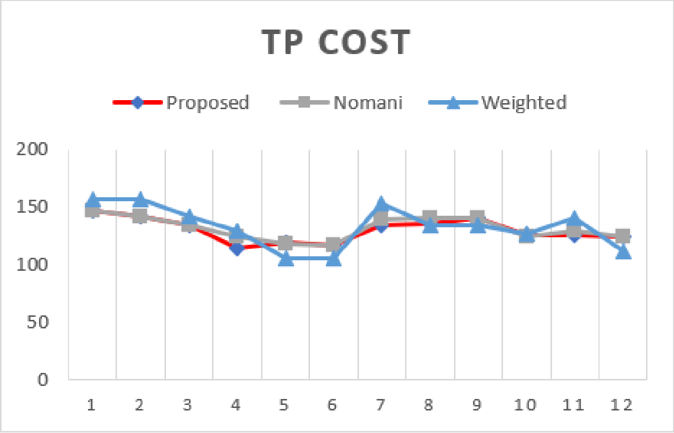

Figure 5 Comparison of transportation costs obtained by different methods

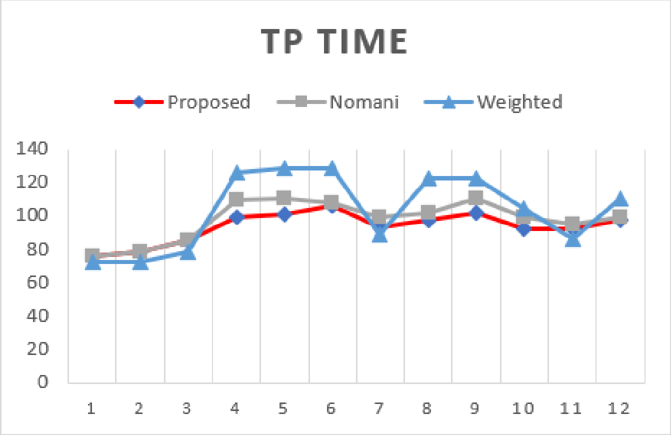

Figure 6 Comparison of transportation time obtained by different methods

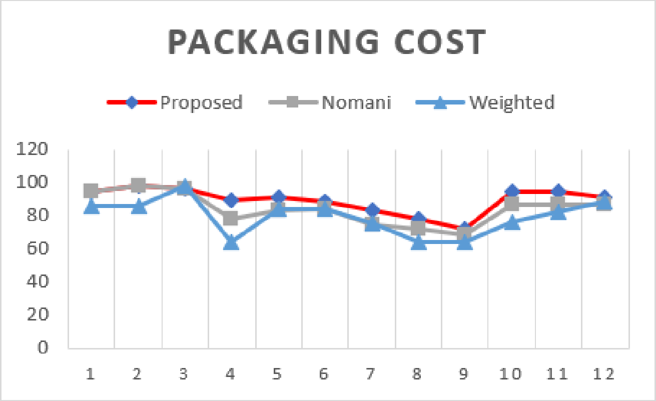

Figure 7 Comparison of packaging cost obtained by different methods

6 Conclusion

In this paper, we discussed a new modified goal programming model and a comparison was made with existing weighted models. The proposed model is capable of providing varying results for a MOTP. LINGO 19.0 was used to solve all the mathematical models. As further development, we plan to extend this method for Fractional MOTP, Rough MOTP and Fixed charge MOTP.

References

[1] Waiel F Abd El-Wahed. A multi-objective transportation problem under fuzziness. *Fuzzy sets and systems*, 117(1):27–33, 2001.

[2] Veena Adlakha and Krzysztof Kowalski. A quick sufficient solution to the more-for-less paradox in the transportation problem. *Omega*, 26(4):541–547, 1998.

[3] AK Bit, MP Biswal, and SS1185389 Alam. Fuzzy programming approach to multicriteria decision making transportation problem. *Fuzzy sets and systems*, 50(2):135–141, 1992.

[4] Edward L Hannan. On fuzzy goal programming. *Decision sciences*, 12(3):522–531, 1981.

[5] Frank L Hitchcock. The distribution of a product from several sources to numerous localities. *Journal of mathematics and physics*, 20(1-4):224–230, 1941.

[6] Heinz Isermann. The enumeration of all efficient solutions for a linear multiple-objective transportation problem. *Naval Research Logistics Quarterly*, 26(1):123–139, 1979.

[7] Sang M Lee and Laurence J Moore. Optimizing transportation problems with multiple objectives. *AIIE transactions*, 5(4):333–338, 1973.

[8] Sang M Lee and David L Olson. Goal programming. In *Multicriteria decision making*, pages 203–235. Springer, 1999.

[9] Gurupada Maity and Sankar Kumar Roy. Solving multi-choice multi-objective transportation problem: a utility function approach. *Journal of uncertainty Analysis and Applications*, 2(1):1–20, 2014.

[10] Mohammad Asim Nomani, Irfan Ali, and A Ahmed. A new approach for solving multi-objective transportation problems. *International journal of management science and engineering management*, 12(3):165–173, 2017.

[11] Jeffrey L Ringuest and Dan B Rinks. Interactive solutions for the linear multiobjective transportation problem. *European Journal of operational research*, 32(1):96–106, 1987.

[12] Rachana Saini, Vishwas Deep Joshi, and Jagdev Singh. On solving a mfl paradox in linear plus linear fractional multi-objective transportation problem using fuzzy approach. *International Journal of Applied and Computational Mathematics*, 8(2):1–13, 2022.

[13] Maryam Zangiabadi and Hamid Reza Maleki. Fuzzy goal programming technique to solve multiobjective transportation problems with some non-linear membership functions. 2013.

J. COMPUTATIONAL ANALYSIS AND APPLICATIONS, VOL. 31, NO.1, 2023, COPYRIGHT 2023 EUDOXUS PRESS, LLC

Dynamical analysis of fractional yellow fever virus model with efficient numerical approach

Chandrali Baishya[1,*], Sindhu J. Achar[1], P. Veeresha[2], Devendra Kumar[3]

December 28, 2022

[1]Department of Studies and Research in Mathematics, Tumkur University,
Tumkur-572103, Karnataka, India
Email: baishyachandrali@gmail.com, sindhuachar6@gmail.com
[2] Department of Mathematics, CHRIST (Deemed to be University),
Bengaluru-560029, India
Email: pveeresha.maths@gmail.com & pundikala.veeresha@christuniversity.in
[3] Department of Mathematics, University of Rajasthan, Jaipur-302004, Rajasthan,
India
Email: devendra.maths@gmail.com

Abstract

In this paper, we have projected the theoretical and numerical investigation of the mathematical model representing the yellow fever virus transmission from infected mosquitoes to humans or vise-versa through mosquito bites in the framework of the Caputo derivative. Theoretical aspects of the dynamics of susceptible individuals, exposed individuals, infected individuals, toxic infected individuals, recovered and immune individuals, and susceptible mosquitoes and infected mosquitoes have been analyzed by using the theory of fractional calculus such as boundedness, uniqueness and existence of the solutions. Sufficient conditions for the global stability of the virus-free point of equilibrium are inspected. T validate the theoretical results numerical analysis is performed using the generalized Adams-Bashforth-Moultan method.

Keywords: Predator-Prey, Yellow Fever Virus, Predictor-Corrector Method.
2000 Mathematics Subject Classification: 34A34, 92D30.

---

[*] Corresponding Author

1 Introduction

Infectious illness outbreaks have become the greatest threat to mankind over time, resulting in the loss of many lives. They may also bring economic and political upheaval if they are not handled properly. Yellow fever (YF) virus which belongs to a family of about 70 viruses was the first human virus discovered. YF is an intense viral disease spread by infected female 'Aedes aegypti' mosquitoes. These mosquitoes are also the vector of Zika virus, dengue and chikungunya [1, 2]. In Africa, sylvatic and peridomestic Aedes species transmit rural and intermediate YF. The incubation period of the virus on the infected individuals is generally 3 to 6 days [3]. Vomiting, nausea, lack of appetite, muscle pain with backache, slight fever, headache, jaundice, and weariness are some of the symptoms that patients experience [4]. Nonetheless, these symptoms fade after four or five days, while other individuals may continue to the infection's toxicity phase, in which 50 percent of instances lead to death within eight to ten days [5]. Although YF is compartmentalized as viral hemorrhagic fever, it causes 1000 times more risk to death than the virus like Ebola [1].

Among the scientific community, the study of disease dynamics has remained a popular issue [6, 7]. To help humankind in fighting against YF by understanding its dynamics mathematically, a few mathematicians have contributed their expertise in modeling this infection [8,9]. In the recent times, fractional derivatives namely the Caputo, Riemann-Liouville, Gr*ü*nwald Letnikov, Jumarie, and Caputo-Fabrizio are investigated by the researchers in search of new behavioral findings while representing real world problems using such derivatives. Notably, many results associated with memory, hereditary, longrange memory, random walk, anomalous diffusion, non-Markovian processes, and others made the concept of fractional derivatives a highly significant to take into account [10–14]. Over the years, theories of these derivatives have also been developed to a great extent [15–18]. Many phenomena related to mathematical biology and their interdisciplinary fields [18, 19] have been studied using these fractional derivatives [20, 21]. They have been used to model many complex phenomena of disease dynamics [22–24].

This work aims to examine the qualitative nature of the yellow fever virus mathematical model with interaction of seven categories of the population namely susceptible , YF exposed, YF infected, toxic-infected individuals, recovered and immune individuals, susceptible mosquitoes, and infected mosquitoes incorporating the Caputo fractional derivative. Adams-Bashforth-Moulton method has been used to perform the numerical simulation [25–29]. The rest of the paper is structured as follows: in Section 2, we provide some elementary definitions, theorems and lemmas of fractional calculus which is followed by the formulation of the model in Section 3. Sections 4, 5, 6 dispense the existence and uniqueness, boundedness, the existence of various points of equilibrium and their local stability respectively. Sections 7 depicts the numerical method and simulation in detail. Finally, we discuss the concluding remarks in Section 8.

2 Some Essential Theorems

In the present work, we have used the Caputo fractional derivatives because it supports the integer order initial condition. In this section, we have presented certain theorems those have been applied to determine the theoretical results corresponding to the solution of the projected model. The Caputo fractional derivative is denoted by ${}^{C}D$.

Definition 2.1. [15] (Caputo Fractional Derivative) Suppose $g(\mathrm{t})$ is k times continuously differentiable function and $g^{(k)}(\mathrm{t})$ is integrable in $[\mathrm{t}_0, T]$. The fractional derivative of the order α established by Caputo sense for $g(\mathrm{t})$,is

$$ {}^{C}_{\mathrm{t}_0}D^{\alpha}_{\mathrm{t}} g(\mathrm{t}) = \frac{1}{\Gamma(k-\alpha)} \int_{\mathrm{t}_0}^{\mathrm{t}} \frac{g^{(k)}(\tau)}{(\mathrm{t}-\tau)^{\alpha+1-k}} d\tau $$

where $\Gamma(\cdot)$ refers to Gamma function, $\mathrm{t} > a$ and k is a positive integer with the property that $k-1 < \alpha < k$.

Lemma 1. [17] Consider the system

$$ {}^{C}_{\mathrm{t}_0}D^{\alpha}_{\mathrm{t}} v(\mathrm{t}) = g(\mathrm{t}, v),\ \mathrm{t} > \mathrm{t}_0, \tag{1} $$

choosing the initial condition as $v(\mathrm{t}_0)$, where $0 < \alpha \leq 1$ and $g : [\mathrm{t}_0, \infty) \times \Omega \to \mathbb{R}^n, \Omega \in \mathbb{R}^n$. When $g(\mathrm{t}, v)$ holds the locally Lipchitz conditions concerning to v, Eq.1 has a unique solution on $[\mathrm{t}_0, \infty) \times \Omega$.

Lemma 2. [18] We assume that $g(\mathrm{t})$ is a continuous function on $[\mathrm{t}_0, +\infty)$ satisfying

$$ {}^{C}_{\mathrm{t}_0}D^{\alpha}_{\mathrm{t}} g(\mathrm{t}) \leq -\lambda g(\mathrm{t}) + \xi,\ g(\mathrm{t}_0) = g_0, $$

where $\mathrm{t}_0 \geq 0$ is the initial time, $0 < \alpha \leq 1,\ \lambda \neq 0,\ (\lambda, \xi) \in \mathbb{R}^2$. Then,

$$ g(\mathrm{t}) \leq (g(\mathrm{t}_0) - \frac{\xi}{\lambda}) E_{\alpha}[-\lambda(\mathrm{t}-\mathrm{t}_0)^{\alpha}] + \frac{\xi}{\lambda} $$

Lemma 3. [18] Let $v(\mathrm{t}) \in \mathbb{R}_+$ be a derivable and continuous function. Then, at any time $\mathrm{t} > \mathrm{t}_0$,

$$ {}^{C}_{\mathrm{t}_0}D^{\alpha}_{\mathrm{t}} (v(\mathrm{t}) - v^* - v^* ln \frac{v(\mathrm{t})}{v^*}) \leq (1 - \frac{v^*}{v}) {}^{C}_{\mathrm{t}_0}D^{\alpha}_{\mathrm{t}} v(t), \quad v^* \in \mathbb{R}_+, \quad \forall \alpha \in (0,1). $$

3 Model Formulation

Yusuf and Daniel's [9] work has inspired the mathematical model described in this study. We observe that fractional derivatives influence coexistence. When a new virus emerges, it is never completely eradicated from the world. A fraction of humans will always be infected by that virus in some part of the universe. This nature of the virus's existence prompts us to model YF infection by incorporating fractional derivatives. In this paper, the YF virus mathematical model has been proposed within the population of humans and mosquitoes. It has been assumed that both populations mix freely without any barriers. Since there is a high risk of YF transmission from travelers, their vaccination is essential. It is assumed that some portion of the travelers is vaccinated. Again, a part of the infected population may become toxic. It is also assumed that once an individual becomes toxic, he or she does not recover. In the present model, the human population has been subdivided into five different compartments namely: $S_H(t), E_H(t), I_H(t), T_H(t), R_H(t)$ which represents the density of susceptible, YF exposed, YF infected, toxic-infected individuals, and recovered and immune individuals respectively. In the same way, the mosquito population is divided into two categories: $S_V(t), I_V(t)$ represent the density of susceptible mosquitoes and infected mosquitoes respectively. We have considered the Caputo sense fractional derivative to represent the projected model. The present model is as follows:

$$\begin{aligned}
{}_{t_0}^{C}D_t^{\alpha} S_H &= r + (1-\sigma)\lambda - \theta\beta_1 S_H I_V - \rho S_H - d S_H, \qquad (2)\\
{}_{t_0}^{C}D_t^{\alpha} E_H &= \theta\beta_1 S_H I_V - \mu E_H - d E_H,\\
{}_{t_0}^{C}D_t^{\alpha} I_H &= (1-\xi)\mu E_H - \psi I_H - (d+\Lambda) I_H,\\
{}_{t_0}^{C}D_t^{\alpha} T_H &= \xi \mu E_H - (d+\Lambda) T_H\\
{}_{t_0}^{C}D_t^{\alpha} R_H &= \psi I_H + \sigma\lambda + \rho S_H - d R_H,\\
{}_{t_0}^{C}D_t^{\alpha} S_V &= \nu - \theta\beta_2 S_V I_H - \phi S_V,\\
{}_{t_0}^{C}D_t^{\alpha} I_V &= \theta\beta_2 S_V I_H - \phi I_V.
\end{aligned}$$

with initial condition $S_H(t_0) = S_H(0)$, $E_H(t_0) = E_H(0)$, $I_H(t_0) = I_H(0)$, $T_H(t_0) = T_H(0)$, $R_H(t_0) = R_H(0)$, where t_0 is the initial time. All the parameters $r, \sigma, \lambda, \theta, \beta_1, \rho, d, \mu, \xi, \psi, \Lambda, \nu, \beta_2, \phi$ are non-negative. Where, r is the birth rate of human, σ is the vaccinated proportion of immigrants, λ is the arrival rate of immigrants per individual per time, and θ is the daily biting rate. β_1 and β_2 represent the transmission probability of YF from mosquitoes to human and from human to mosquitoes respectively. ρ is the effective vaccination rate of susceptible humans, d is the natural death rate of human, μ is the rate at which E_H progresses to I_H, ξ is the proportion of E_H which converts to the toxic case, ψ is the recovery rate of human, Λ is the death rate of human-induced due to YF, ν is the birth rate of mosquitoes, and ϕ is the natural death rate of the vectors.

4 Existence of the solutions

The existence of the solution of the model 2 is demonstrated using the Fixed-Point Theorem. Due to the complex and non-local nature of the system 2, there are no precise algorithms or approaches for evaluating the exact solutions. However, the existence of the solution is assured if certain conditions are met. To initiate the process of establishing the existence of the solution, the system 2 is rewritten as:

$$\begin{aligned}
&{}^{C}_{t_0}D^{\alpha}_{t}[S_H(t)] = \mathfrak{P}_1(t,S_H),\ {}^{C}_{t_0}D^{\alpha}_{t}[E_H(t)] = \mathfrak{P}_2(t,E_H),\ {}^{C}_{t_0}D^{\alpha}_{t}[I_H(t)] = \mathfrak{P}_3(t,I_H),\\
&{}^{C}_{t_0}D^{\alpha}_{t}[T_H(t)] = \mathfrak{P}_4(t,T_H),\ {}^{C}_{t_0}D^{\alpha}_{t}[R_H(t)] = \mathfrak{P}_5(t,R_H),\ {}^{C}_{t_0}D^{\alpha}_{t}[S_V(t)] = \mathfrak{P}_6(t,S_V),\\
&{}^{C}_{t_0}D^{\alpha}_{t}[I_V(t)] = \mathfrak{P}_7(t,I_V).
\end{aligned} \tag{3}$$

The above system can be transformed into Volterra type integral equation as:

$$\begin{aligned}
S_H(t)-S_H(0) &= \frac{1}{\Gamma(\alpha)}\int_0^t \mathfrak{P}_1(\tau,S_H(\tau))(t-\tau)^{\alpha-1}d\tau,\\
E_H(t)-E_H(0) &= \frac{1}{\Gamma(\alpha)}\int_0^t \mathfrak{P}_2(\tau,E_H(\tau))(t-\tau)^{\alpha-1}d\tau,\\
I_H(t)-I_H(0) &= \frac{1}{\Gamma(\alpha)}\int_0^t \mathfrak{P}_3(\tau,I_H(\tau))(t-\tau)^{\alpha-1}d\tau,\\
T_H(t)-T_H(0) &= \frac{1}{\Gamma(\alpha)}\int_0^t \mathfrak{P}_4(\tau,T_H(\tau))(t-\tau)^{\alpha-1}d\tau,\\
R_H(t)-R_H(0) &= \frac{1}{\Gamma(\alpha)}\int_0^t \mathfrak{P}_5(\tau,R_H(\tau))(t-\tau)^{\alpha-1}d\tau,\\
S_V(t)-S_V(0) &= \frac{1}{\Gamma(\alpha)}\int_0^t \mathfrak{P}_6(\tau,S_V(\tau))(t-\tau)^{\alpha-1}d\tau,\\
I_V(t)-I_V(0) &= \frac{1}{\Gamma(\alpha)}\int_0^t \mathfrak{P}_7(\tau,I_V(\tau))(t-\tau)^{\alpha-1}d\tau.
\end{aligned} \tag{4}$$

Theorem 4.1. In the region $\Omega \times [t_0,T]$, where

$$\Omega = \{(S_H, E_H, I_H, T_H, R_H, S_V, I_V) \in \mathbb{R}^7 : max\{|S_H|, |E_H|, |I_H|, |T_H|, |R_H|, |S_V|, |I_V|\} \le \mathfrak{M}\},$$

and $T < +\infty$, the Lipschitz condition is satisfied and contraction occurs by the kernel $\mathfrak{P}_1$ if $0 \le \theta\beta_1\mathfrak{M} + \rho + d < 1$.

Proof: We consider the two functions S_H and $\bar{S}_H$ such as:

$$||\mathfrak{P}_1(t,S_H) - \mathfrak{P}_1(t,\bar{S}_H)|| = ||(r + (1-\sigma)\lambda - \theta\beta_1 S_H I_V - \rho S_H - dS_H)$$

$$\begin{aligned}
&-(r+(1-\sigma)\lambda-\theta\beta_1\bar{S}_H I_V-\rho\bar{S}_H-d\bar{S}_H)||.\\
&\leq(\theta\beta_1\mathfrak{M}+\rho+d)||S_H(t)-\bar{S}_H(t)||\\
&=\zeta_1||S_H(t)-\bar{S}_H(t)||, \qquad (5)
\end{aligned}$$

where $\zeta_1=\theta\beta_1\mathfrak{M}+\rho+d$. As a result, the Lipschitz condition is met for $\mathfrak{P}_1$ and if $0\leq\zeta_1<1$, then $\mathfrak{P}_1$ follows contraction. Similarly, it can be shown and illustrated in case of the other equations as follows:

$$\begin{aligned}
&||\mathfrak{P}_2(t,E_H)-\mathfrak{P}_2(t,\bar{E}_H)||\leq\zeta_2||E_H(t)-\bar{E}_H(t)||,\ ||\mathfrak{P}_3(t,I_H)-\mathfrak{P}_3(t,\bar{I}_H)||\leq\zeta_3||I_H(t)-\bar{I}_H(t)||,\\
&||\mathfrak{P}_4(t,T_H)-\mathfrak{P}_4(t,\bar{T}_H)||\leq\zeta_4||T_H(t)-\bar{T}_H(t)||,\ ||\mathfrak{P}_5(t,R_H)-\mathfrak{P}_5(t,\bar{R}_H)||\leq\zeta_5||R_H(t)-\bar{R}_H(t)||,\\
&||\mathfrak{P}_6(t,S_V)-\mathfrak{P}_6(t,\bar{S}_V)||\leq\zeta_6||S_V(t)-\bar{S}_V(t)||,\ ||\mathfrak{P}_7(t,I_V)-\mathfrak{P}_7(t,\bar{I}_V)||\leq\zeta_7||I_V(t)-\bar{I}_V(t)||, \qquad (6)
\end{aligned}$$

where $\zeta_2=(\mu+d)$, $\zeta_3=(\psi+d+\Lambda)$, $\zeta_4=(d+\Lambda)$, $\zeta_5=(\psi+d+\Lambda)$, $\zeta_6=(\theta\beta_2\mathfrak{M}+\phi)$ and $\zeta_7=\phi$. $\mathfrak{P}_i$, $i=2,3,4,5,6,7$ are the contraction if $0<\zeta_i<1$, $i=2,3,4,5,6,7$. Using system 4, the recursive form can now be written as follows:

$$\begin{aligned}
\kappa_{1,n}(t)&=S_{H_n}(t)-S_{H_{n-1}}(t)=\frac{1}{\Gamma(\alpha)}\int_0^t(\mathfrak{P}_1(\tau,S_{H_{n-1}})-\mathfrak{P}_1(\tau,S_{H_{n-2}}))(t-\tau)^{\alpha-1}d\tau,\\
\kappa_{2,n}(t)&=E_{H_n}(t)-E_{H_{n-1}}(t)=\frac{1}{\Gamma(\alpha)}\int_0^t(\mathfrak{P}_2(\tau,E_{H_{n-1}})-\mathfrak{P}_2(\tau,E_{H_{n-2}}))(t-\tau)^{\alpha-1}d\tau,\\
\kappa_{3,n}(t)&=I_{H_n}(t)-I_{H_{n-1}}(t)=\frac{1}{\Gamma(\alpha)}\int_0^t(\mathfrak{P}_3(\tau,I_{H_{n-1}})-\mathfrak{P}_3(\tau,I_{H_{n-2}}))(t-\tau)^{\alpha-1}d\tau,\\
\kappa_{4,n}(t)&=T_{H_n}(t)-T_{H_{n-1}}(t)=\frac{1}{\Gamma(\alpha)}\int_0^t(\mathfrak{P}_4(\tau,T_{H_{n-1}})-\mathfrak{P}_4(\tau,T_{H_{n-2}}))(t-\tau)^{\alpha-1}d\tau,\\
\kappa_{5,n}(t)&=R_{H_n}(t)-R_{H_{n-1}}(t)=\frac{1}{\Gamma(\alpha)}\int_0^t(\mathfrak{P}_5(\tau,R_{H_{n-1}})-\mathfrak{P}_5(\tau,R_{H_{n-2}}))(t-\tau)^{\alpha-1}d\tau,\\
\kappa_{6,n}(t)&=S_{V_n}(t)-S_{V_{n-1}}(t)=\frac{1}{\Gamma(\alpha)}\int_0^t(\mathfrak{P}_6(\tau,S_{V_{n-1}})-\mathfrak{P}_6(\tau,S_{V_{n-2}}))(t-\tau)^{\alpha-1}d\tau,\\
\kappa_{7,n}(t)&=I_{V_n}(t)-I_{V_{n-1}}(t)=\frac{1}{\Gamma(\alpha)}\int_0^t(\mathfrak{P}_7(\tau,I_{V_{n-1}})-\mathfrak{P}_7(\tau,I_{V_{n-2}}))(t-\tau)^{\alpha-1}d\tau. \qquad (7)
\end{aligned}$$

The prerequisites are: $S_{H_0}(t)=S_H(0)$, $E_{H_0}(t)=E_H(0)$, $I_{H_0}(t)=I_H(0)$, $T_{H_0}(t)=T_H(0)$, $R_{H_0}(t)=R_H(0)$, $S_{V_0}(t)=S_V(0)$, $I_{V_0}(t)=I_V(0)$.
By applying the norm to the first equation of the system 7, we obtained

$$\begin{aligned}
||\kappa_{1,n}(t)||&=||S_{H_n}(t)-S_{H_{n-1}}(t)||\\
&=||\frac{1}{\Gamma(\alpha)}\int_0^t(\mathfrak{P}_1(\tau,S_{H_{n-1}})-\mathfrak{P}_1(\tau,S_{H_{n-2}}))(t-\tau)^{\alpha-1}d\tau||\\
&\leq\frac{1}{\Gamma(\alpha)}\int_0^t||(\mathfrak{P}_1(\tau,S_{H_{n-1}})-\mathfrak{P}_1(\tau,S_{H_{n-2}}))(t-\tau)^{\alpha-1}d\tau||. \qquad (8)
\end{aligned}$$

Using Lipchitz condition 5, we get

$$||\kappa_{1,n}(t)|| \leq \frac{1}{\Gamma(\alpha)}\zeta_1 \int_0^t ||\kappa_{1,n-1}(\tau)d\tau||. \tag{9}$$

Similarly,

$$\begin{gathered} ||\kappa_{2,n}(t)|| \leq \frac{1}{\Gamma(\alpha)}\zeta_2 \int_0^t ||\kappa_{2,n-1}(\tau)d\tau||,\ ||\kappa_{3,n}(t)|| \leq \frac{1}{\Gamma(\alpha)}\zeta_3 \int_0^t ||\kappa_{3,n-1}(\tau)d\tau||, \\ ||\kappa_{4,n}(t)|| \leq \frac{1}{\Gamma(\alpha)}\zeta_4 \int_0^t ||\kappa_{4,n-1}(\tau)d\tau||,\ ||\kappa_{5,n}(t)|| \leq \frac{1}{\Gamma(\alpha)}\zeta_5 \int_0^t ||\kappa_{5,n-1}(\tau)d\tau||, \\ ||\kappa_{6,n}(t)|| \leq \frac{1}{\Gamma(\alpha)}\zeta_6 \int_0^t ||\kappa_{6,n-1}(\tau)d\tau||,\ ||\kappa_{7,n}(t)|| \leq \frac{1}{\Gamma(\alpha)}\zeta_7 \int_0^t ||\kappa_{7,n-1}(\tau)d\tau||. \end{gathered} \tag{10}$$

As a result, it yields
$S_{H_n}(t) = \sum_{i=1}^n \kappa_{1,i}$, $E_{H_n}(t) = \sum_{i=1}^n \kappa_{2,i}$, $I_{H_n}(t) = \sum_{i=1}^n \kappa_{3,i}$, $T_{H_n}(t) = \sum_{i=1}^n \kappa_{4,i}$,
$R_{H_n}(t) = \sum_{i=1}^n \kappa_{5,i}$, $S_{V_n}(t) = \sum_{i=1}^n \kappa_{6,i}$, $I_{V_n}(t) = \sum_{i=1}^n \kappa_{7,i}$.
This theorem will be used to illustrate the next theorem.

Theorem 4.2. The solution of the fractional model 2 exists and will be unique, if we acquire some t_α such that

$$\frac{1}{\Gamma(\alpha)}\zeta_i t_\alpha < 1,\ \ i = 1,2,3,...,7.$$

Proof: Applying equations 9 and 10 recursively, we have

$$\begin{gathered} ||\kappa_{1,n}(t)|| \leq ||S_{H_n}(0)|| \left[\frac{1}{\Gamma(\alpha)}\zeta_1 t\right]^n,\ ||\kappa_{2,n}(t)|| \leq ||E_{H_n}(0)|| \left[\frac{1}{\Gamma(\alpha)}\zeta_2 t\right]^n, \\ ||\kappa_{3,n}(t)|| \leq ||I_{H_n}(0)|| \left[\frac{1}{\Gamma(\alpha)}\zeta_3 t\right]^n,\ ||\kappa_{4,n}(t)|| \leq ||T_{H_n}(0)|| \left[\frac{1}{\Gamma(\alpha)}\zeta_4 t\right]^n, \\ ||\kappa_{5,n}(t)|| \leq ||R_{H_n}(0)|| \left[\frac{1}{\Gamma(\alpha)}\zeta_5 t\right]^n,\ ||\kappa_{6,n}(t)|| \leq ||S_{V_n}(0)|| \left[\frac{1}{\Gamma(\alpha)}\zeta_6 t\right]^n, \\ ||\kappa_{7,n}(t)|| \leq ||I_{V_n}(0)|| \left[\frac{1}{\Gamma(\alpha)}\zeta_7 t\right]^n. \end{gathered} \tag{11}$$

As a result, the existence and continuity are established. To illustrate that the above relations formulate the solution of the model 2, we assume the following:

$$S_H(t) - S_{H_0}(t) = S_{H_n}(t) - \Delta_{1n}(t),\ E_H(t) - E_{H_0}(t) = E_{H_n}(t) - \Delta_{2n}(t), \tag{12}$$

$$I_H(t) - I_{H_0}(t) = I_{H_n}(t) - \Delta_{3n}(t),\ T_H(t) - T_{H_0}(t) = T_{H_n}(t) - \Delta_{4n}(t), \tag{13}$$

$$R_H(t) - R_{H_0}(t) = R_{H_n}(t) - \Delta_{5n}(t),\ S_V(t) - S_{V_0}(t) = S_{V_n}(t) - \Delta_{6n}(t), \tag{14}$$

$$I_V(t) - I_{V_0}(t) = I_{V_n}(t) - \Delta_{7n}(t). \tag{15}$$

In order to achieve the desired outcomes, set that

$$||\Delta_{1n}(t)|| = ||\frac{1}{\Gamma(\alpha)}\int_0^t (\mathfrak{P}_1(\tau, S_H) - \mathfrak{P}_1(\tau, S_{H_{n-1}}))d\tau|| \tag{16}$$

This implies,

$$||\Delta_{1n}(t)|| \leq \frac{1}{\Gamma(\alpha)}\zeta_1 ||S_H - S_{H_{n-1}}||t. \tag{17}$$

Continuing the same procedure recursively, we get

$$||\Delta_{1n}(t)|| \leq \left(\frac{1}{\Gamma(\alpha)}\zeta_1 t\right)^{n+1}\mathfrak{M}. \tag{18}$$

At certain t_α, we have

$$||\Delta_{1n}(t)|| \leq \left(\frac{1}{\Gamma(\alpha)}\zeta_1 t_\alpha\right)^{n+1}\mathfrak{M}. \tag{19}$$

From equation [**?**], we observe that $||\Delta_{1n}(t)||$ approaches to 0 as n tends to ∞, provided $\left(\frac{1}{\Gamma(\alpha)}\zeta_1 t_\alpha\right) < 1$. Similarly, it may be demonstrated that
$||\Delta_{2n}(t)||$, $||\Delta_{3n}(t)||$, $||\Delta_{4n}(t)||$, $||\Delta_{5n}(t)||$, $||\Delta_{6n}(t)||$, $||\Delta_{7n}(t)||$ tends to 0. Hence the proof.
We shall now demonstrate the uniqueness for the solution of the system 2. Let us assume that there is a different set of solutions, namely $\hat{S}_H$, $\hat{E}H$, $\hat{I}_H$, $\hat{T}_H$, $\hat{R}_H$, $\hat{S}_V$, $\hat{I}_V$ for the system 2. Then, as a result of the first equation, we have

$$S_H(t) - \hat{S}_H(t) = \frac{1}{\Gamma(\alpha)}\int_0^t (\mathfrak{P}_1(t, S_H) - \mathfrak{P}_1(t, \hat{S}_H))d\tau. \tag{20}$$

Using the norm, the equation above becomes:

$$||S_H(t) - \hat{S}_H(t)|| = \frac{1}{\Gamma(\alpha)}\int_0^t ||(\mathfrak{P}_1(t, S_H) - \mathfrak{P}_1(t, \hat{S}_H))d\tau||. \tag{21}$$

By applying the Lipschitz condition,

$$||S_H(t) - \hat{S}_H(t)|| \leq \frac{1}{\Gamma(\alpha)}\zeta t||S_H - \hat{S}_H||.$$

This results in,

$$||S_H(t) - \hat{S}_H(t)||\left(1 - \frac{(1-\alpha)}{\Gamma(\alpha)}\zeta t\right) \leq 0.$$

Since $\left(1 - \frac{1}{\Gamma(\alpha)}\zeta_1 t\right) > 0$, we much have $||S_H(t) - \hat{S}_H(t)|| = 0$. This implies $S_H(t) = \hat{S}_H(t)$.

5 Boundedness

In this Section, we have established the boundedness of the solution of the system 2.

Theorem 5.1. The solution of the system 2 is uniformly bounded.

Proof. Considering the function, $\mathfrak{L}(t) = S_H(t) + E_H(t) + I_H(t) + T_H(t) + R_H(t) + S_V(t) + I_V(t)$.
and applying fractional derivative on it, we get

$$\begin{aligned}
{}_{t_0}^{C}D_t^{\alpha}\mathfrak{L}(t) + d\mathfrak{L}(t) &= {}_{t_0}^{C}D_t^{\alpha}[S_H(t) + E_H(t) + I_H(t) + T_H(t) + R_H(t) + S_V(t) + I_V(t)] \\
&\quad + d[S_H(t) + E_H(t) + I_H(t) + T_H(t) + R_H(t) + S_V(t) + I_V(t)] \\
&= r + \lambda - \Lambda(I_H + T_H) + \nu - \phi(S_V + I_V) + d(S_V + I_V) \\
&\leq r + \lambda + \nu + dS_V + dI_V. \qquad (22)
\end{aligned}$$

The solution exists and is unique in
$\mho = \{(S_H, E_H, I_H, T_H, R_H, S_V, I_V)/max\{|S_H|, |E_H|, |I_H|, |T_H|, |R_H|, |S_V|, |I_V|\} \leq \mathfrak{M}\}$.
The above inequality yields,

$${}_{t_0}^{C}D_t^{\alpha}\mathfrak{L}(t) + d\mathfrak{L}(t) \leq r + \lambda + \nu + 2d\mathfrak{M}.$$

By the Lemma 2, we get

$${}_{t_0}^{C}D_t^{\alpha}\mathfrak{L}(t) \leq (\mathfrak{L}(t_0) - \frac{1}{d}(r+\lambda+\nu+2d\mathfrak{M})E_{\alpha}[-\eta(t-t_0)^{\alpha}] + \frac{1}{d}(r+\lambda+\nu+2d\mathfrak{M}) \to r+\lambda+\nu+2d\mathfrak{M}$$

as $t \to \infty$. Therefore, all the solution of the system 2 that initiates in $\mho$ remained bounded in
$\Theta = \{(S_H, E_H, I_H, T_H, R_H, S_V, I_V) \in \mho_+ | \mathfrak{L}(t) \leq r + \lambda + \nu + 2d\mathfrak{M} + \varepsilon, \quad \varepsilon > 0\}$. ☐

6 Existence of points of equilibrium

In this section, we find the points of equilibrium of the system 2. We have the following points of equilibrium for the fractional order system 2:

1. The disease-free equilibrium point is $\bar{\mathfrak{I}} = (\frac{r+\lambda(1-\sigma)}{d+\rho}, 0, 0, 0, \frac{\rho(r+\lambda)+d\lambda\sigma}{d^2+d\rho}, \frac{\nu}{\phi}, 0)$ and it always exists.
2. The endemic equilibrium point $\tilde{\mathfrak{I}} = (\tilde{S_H}, \tilde{E_H}, \tilde{I_H}, \tilde{T_H}, \tilde{R_H}, \tilde{S_V}, \tilde{I_V})$ exists if $\nu\theta^2\mu\beta_1\beta_2(1-\xi)(r+\lambda(1-\sigma)) > \phi^2(d+\mu)(d+\rho)(d+\Lambda+\psi)$. Coexistence equilibrium point can be obtained by solving the algebraic equations given below:

$$r + (1-\sigma)\lambda - \theta\beta_1\tilde{S_H}\tilde{I_V} - \rho\tilde{S_H} - d\tilde{S_H} = 0, \; \theta\beta_1\tilde{S_H}\tilde{I_V} - \mu\tilde{E_H} - d\tilde{E_H} = 0,$$

$$
\begin{aligned}
&(1-\xi)\mu\tilde{E_H}-\psi\tilde{I_H}-(d+\Lambda)\tilde{I_H}=0,\ \xi\mu\tilde{E_H}-(d+\Lambda)\tilde{T_H}=0,\\
&\psi\tilde{I_H}+\sigma\lambda+\rho\tilde{S_H}-d\tilde{R_H}=0,\ \nu-\theta\beta_2\tilde{S_V}\tilde{I_H}-\phi\tilde{S_V}=0,\\
&\theta\beta_2\tilde{S_V}\tilde{I_H}-\phi\tilde{I_V}=0.
\end{aligned}
$$

Solving these equations we obtain,

$$
\begin{aligned}
\tilde{S_H}&=\frac{r+\lambda(1-\sigma)}{d+\rho+\tilde{I_V}\theta\beta_1},\\
\tilde{E_H}&=\frac{\tilde{I_V}\theta\beta_1(r+\lambda(1-\sigma))}{(d+\mu)(d+\rho+\tilde{I_V}\theta\beta_1)},\\
\tilde{T_H}&=\frac{\tilde{I_V}\theta\mu\xi\beta_1(r+\lambda(1-\sigma))}{(d+\mu)(d+\Lambda+\psi)(d+\rho+\tilde{I_V}\theta\beta_1)},\\
\tilde{R_H}&=\frac{1}{d}\left(\lambda\sigma+\frac{\rho(r+\lambda(1-\sigma))}{d+\rho+\tilde{I_V}\theta\beta_1}+\frac{\tilde{I_V}\phi^2\psi}{\theta\beta_2(\nu-\tilde{I_V}\phi)}\right),\\
\tilde{I_H}&=\frac{\tilde{I_V}\phi^2}{\theta\beta_2(\nu-\tilde{I_V}\phi)},\\
\tilde{S_V}&=\frac{\nu(\nu-\tilde{I_V}\phi)}{\phi(\nu-\tilde{I_V}\phi)+\tilde{I_V}\phi^2},\\
\tilde{I_V}&=\frac{-\phi^2(d+\mu)(d+\rho)(d+\Lambda+\psi)+\nu\theta^2\mu\beta_1\beta_2(1-\xi)(r+\lambda(1-\sigma))}{\theta\phi^2\beta_1(d+\mu)(d+\Lambda+\psi)+\theta\mu\beta_2(1-\xi)(r+\lambda(1-\sigma))}.
\end{aligned}
$$

Clearly, $\tilde{I_V}>0$ if $\nu\theta^2\mu\beta_1\beta_2(1-\xi)(r+\lambda(1-\sigma))>\phi^2(d+\mu)(d+\rho)(d+\Lambda+\psi)$ and hence the endemic equilibrium point exists if this condition is satisfied.

7 Numerical Simulation

Here, we have evaluated the model 2 numerically taking into consideration the influences of various parameters on the dynamics of YF transmission. We have considered the initial values as: $S_{H_0}(t)=0.62$, $E_{H_0}(t)=0.23$, $I_{H_0}(t)=0.1$, $T_{H_0}(t)=0.05$, $R_{H_0}(t)=0$, $S_{V_0}(t)=0.9$, $I_{V_0}(t)=0.1$. Values of the parameters are considered as:$r=\frac{4.94}{10^5}$, $\theta=3$, $\beta_1=0.6$, $\beta_2=0.5$, $\sigma=\frac{0.5}{10^6}$, $\lambda=\frac{1}{10^6}$, $\rho=0.01$, $d=\frac{4.94}{10^5}$, $\mu=0.31$, $\xi=0.15$, $\psi=0.143$, $\Lambda=\frac{3.5}{10}$, $\nu=0.051$, $\phi=0.051$. It is assumed that 50 of the immigrants are vaccinated. From the Figures 1 it is visible that, the daily biting rate θ influences the infected human and infected mosquito population. For $\alpha=1$, these populations tends to grow and reaches the peak, and thereafter they start to decrease and tend to extinction. As the fractional values are incorporated, it is notable that, there is a delay in extinction of the I_H and I_V population. As the value of α further decreases, we notice that infections in human and mosquitoes are never eradicated. In fact a small portion of population are always with infection.

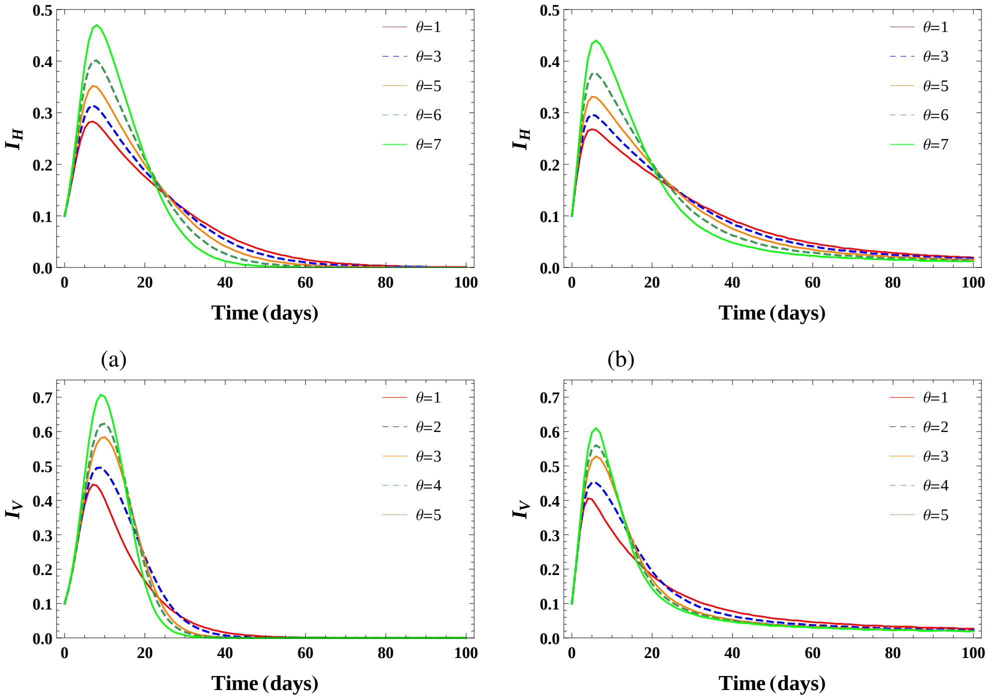

(a) (b)

(c) (d)

Figure 1: Profile of I_H and I_V for distinct values of θ for (A) $\alpha = 1$, (B) $\alpha = 0.65$, (C) $\alpha = 1$, (D) $\alpha = 0.65$

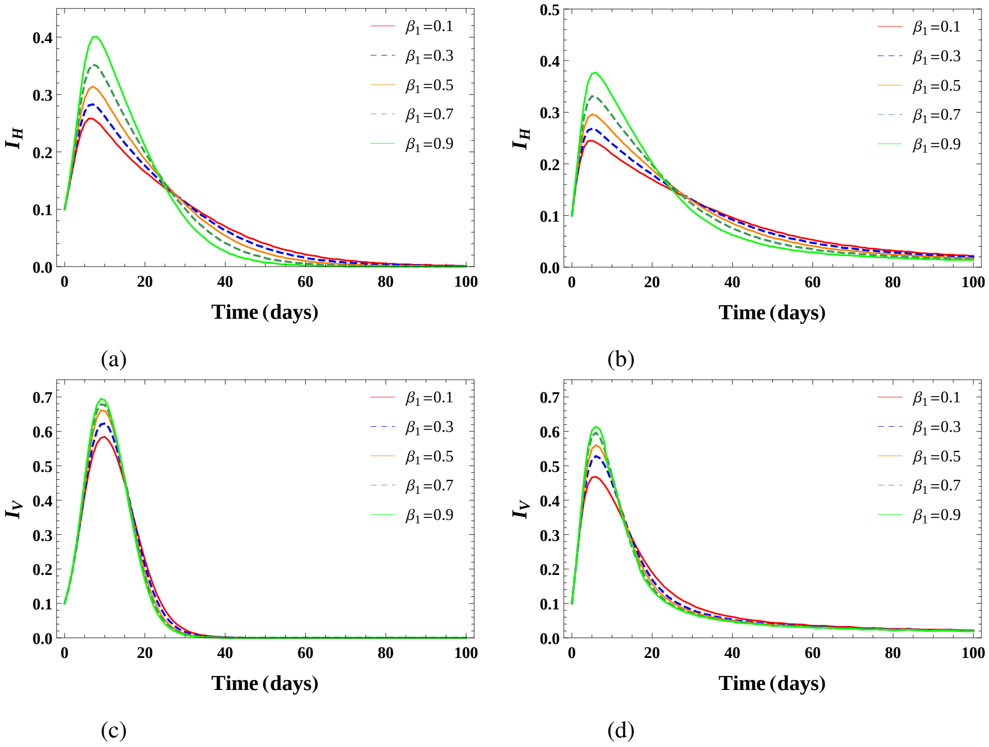

(a) (b) (c) (d)

Figure 2: Profile of I_H and I_V for distinct values of β_1 for (A) $\alpha = 1$, (B) $\alpha = 0.65$, (C) $\alpha = 1$, (D) $\alpha = 0.65$

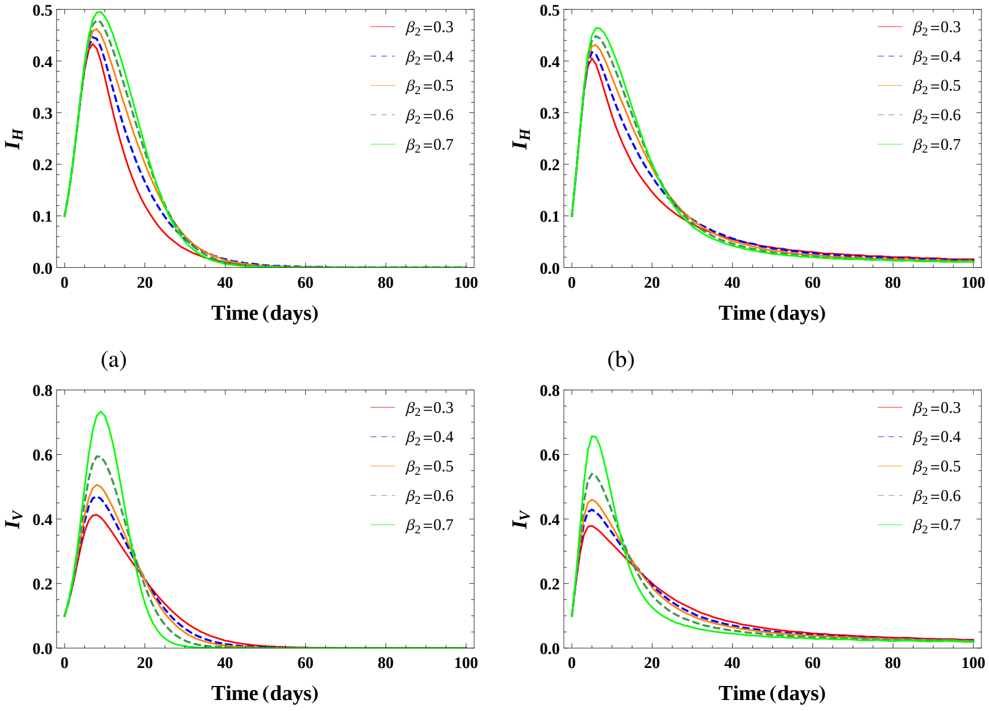

(a) (b)

(c) (d)

Figure 3: Profile of I_H and I_V for distinct values of β_2 for (A) $\alpha = 1$, (B) $\alpha = 0.65$, (C) $\alpha = 1$, (D) $\alpha = 0.65$

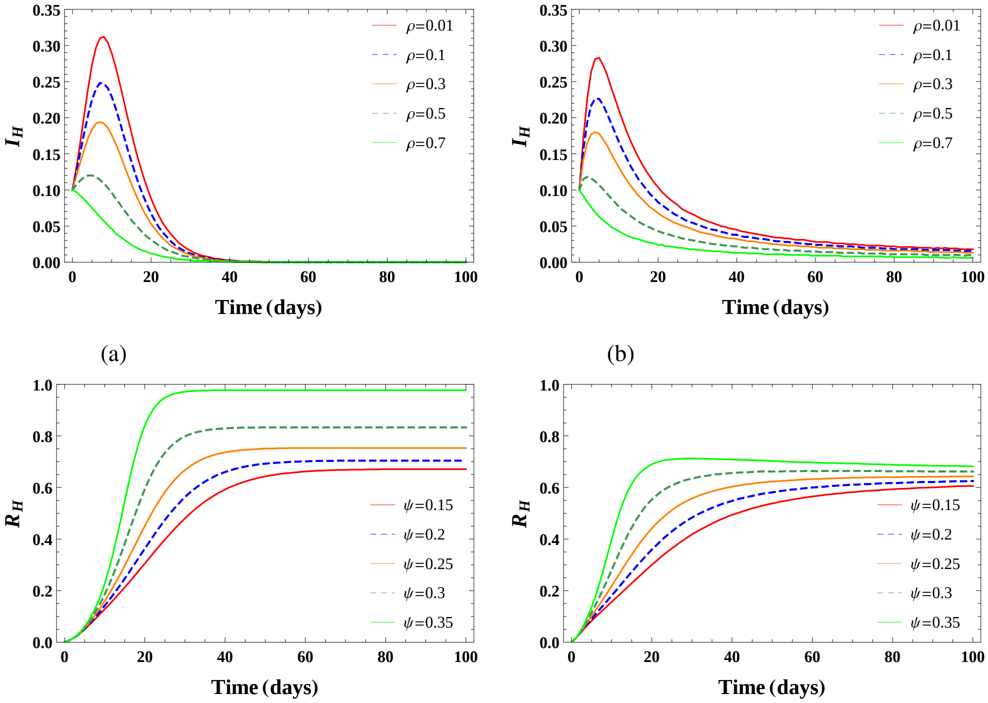

(a) (b)

(c) (d)

Figure 4: Profile of I_H and R_H for distinct values of (A) ρ and $\alpha = 1$, (B) ρ and $\alpha = 0.65$, (C) ψ and $\alpha = 1$, (D)ψ and $\alpha = 0.65$

The variations in the profiles of I_H and I_V for different values of β_1 are depicted in Figures 2. Figures 3 shows the variation in the profile of I_H and I_V for distinct values of β_2. From the above graphs it is visible that, as the value of β_1 and β_2 increases, the I_H and I_V population tends to grow and attains maximum value. Subsequently, they start decreasing and reach nullity which results in extinction of the I_H and I_V population. But decrease in the value of fractional derivative results in existence of the infection among the populations for longer duration. Figure 4 represents the varied profile of I_H for discrete values of effective vaccination rate of susceptible population. From the figure it is notable that, as the vaccination rate increases, the infected host population keeps on decreasing. Further, as the time progress, the infection extincts due to the influence of vaccination. As the fractional values are introduced, a fall in the infected population peak is notable. Figure 4 also depicts the profile of R_H for different recovery rate ψ and various fractional values. It may be observed that, as the value of recovery rate ψ is increased, the total recovery population also increases and leads to reduction of the

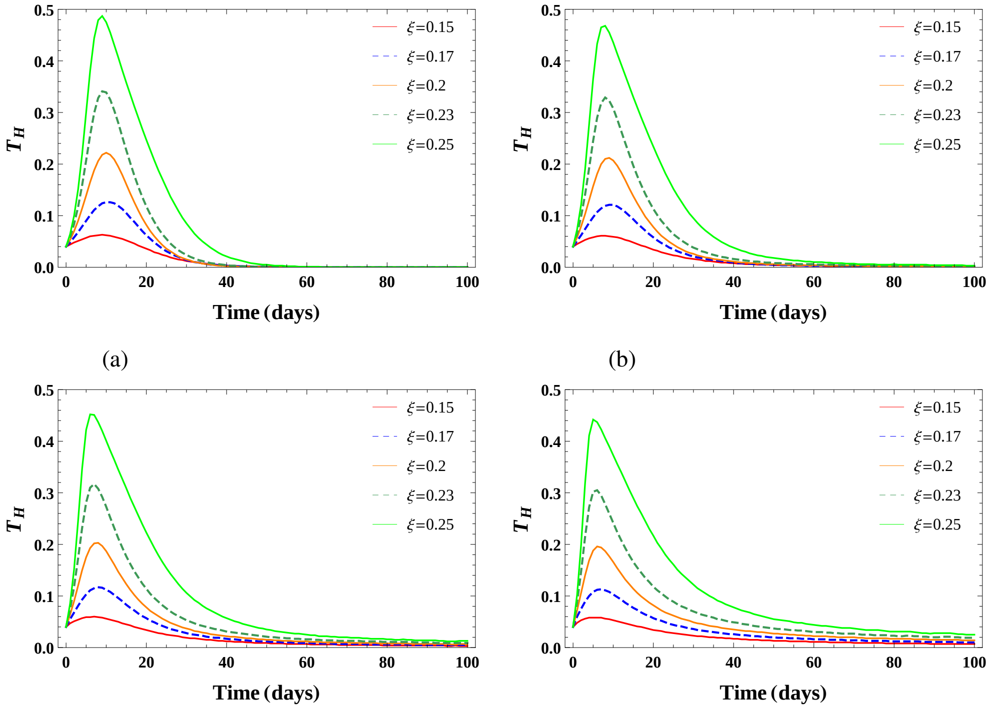

(a) (b)

(c) (d)

Figure 5: Profile of T_H for distinct values of ξ for (A) $\alpha = 1$, (B) $\alpha = 0.95$, (C) $\alpha = 0.85$, (D) $\alpha = 0.65$

epidemic in the host population.Figure 5 presents the dynamics of the toxic population as the proportion of exposed population deteriorates into toxic case at the rate ξ. As the value of ξ increases, the population of toxic ones grows. Further, since there is no recovery in toxic population, they die and hence population tends to extinction.

8 Conclusion

The fractional dynamics of the YF model is investigated in the present work in Caputo sense. Boundedness, existence, continuity, and uniqueness of the solution have been established. In the figures we have demonstrated the profile of the infected human and infected vectors under the influence of the biting rate, transmission rate from mosquitoes to human and human to mosquitoes, vaccination rate of susceptible population, recovery rate, and toxicity rate in presence of the Caputo fractional derivatives. We have observed that the Caputo derivative provides more realistic information than that of the classical derivative. The reseason behind this claim is that it does not show the extinction of the infection from the environment. Graphical representations establish that the Adams-Bashfort-Moulton predictor-corrector method gives expected depiction of the results for analyzing the dynamics of the projected model. Numerical analysis of disease dynamics in the framework of various fractional derivatives can enrich the applications of mathematics for betterment of humankind as a future direction of studies of fractional calculus.

References

[1] T. P. Monath, "Dengue and yellow fever-challenges for the development and use of vaccines," *New England Journal of Medicine*, vol. 357, no. 22, pp. 2222–2225, 2007.

[2] T. P. Monath and P. F. Vasconcelos, "Yellow fever," *Journal of clinical virology*, vol. 64, pp. 160–173, 2015.

[3] M. Kung'aro, L. S. Luboobi, and F. Shahada, "Reproduction number for yellow fever dynamics between primates and human beings," *Commun. Math. Biol. Neurosci.*, 2014.

[4] T. P. Monath, "Treatment of yellow fever," *Antiviral research*, vol. 78, no. 1, pp. 116–124, 2008.

[5] T. P. Monath and A. D. Barrett, "Pathogenesis and pathophysiology of yellow fever," *Advances in virus research*, vol. 60, pp. 343–397, 2003.

[6] W. O. Kermack and A. G. McKendrick, "Contributions to the mathematical theory of epidemics-I," *Bulletin of mathematical biology*, vol. 53, no. 1-2, pp. 33–55, 1991.

[7] A. S. Quintero and R. E. Gutierrez-Carvajal, "Modeling the Evolution of SARS-CoV-2 Using a Fractional-Order SIR Approach," *TecnoLogicas*, vol. 24, no. 51, 2021.

[8] L. Esteva, C. Vargas, and H. M. Yang, "A model for yellow fever with migration," vol. 1, no. 6, 2019.

[9] T. T. Yusuf and D. O. Daniel, "Mathematical modeling of yellow fever transmission dynamics with multiple control measures," *Asian Research Journal of Mathematics*, pp. 1–15, 2019.

[10] C. Baishya, “An operational matrix based on the Independence polynomial of a complete bipartite graph for the Caputo fractional derivative,” *SeMA Journal*, pp. 1–19, 2021.

[11] M. R. Ali and R. Sadat, “Construction of Lump and optical solitons solutions for (3+ 1) model for the propagation of nonlinear dispersive waves in inhomogeneous media,” *Optical and Quantum Electronics*, vol. 53, no. 5, pp. 1–13, 2021.

[12] C. Baishya and P. Veeresha, “Laguerre polynomial-based operational matrix of integration for solving fractional differential equations with non-singular kernel,” *Proceedings of the Royal Society A*, vol. 477, 2021.

[13] P. Veeresha, “A numerical approach to the coupled atmospheric ocean model using a fractional operator,” *Mathematical Modelling and Numerical Simulation with Applications (MMNSA)*, vol. 1, no. 1, pp. 1–10, 2021.

[14] M. R. Ali, W.-X. Ma, and R. Sadat, “Lie symmetry analysis and invariant solutions for (2+ 1) dimensional Bogoyavlensky-Konopelchenko equation with variable-coefficient in wave propagation,” *Journal of Ocean Engineering and Science*, 2021.

[15] I. Podlubny, *Fractional differential equations: an introduction to fractional derivatives, fractional differential equations, to methods of their solution and some of their applications*. Elsevier, 1998.

[16] J. Losada and J. J. Nieto, “Properties of a new fractional derivative without singular kernel,” *Progr. Fract. Differ. Appl*, vol. 1, no. 2, pp. 87–92, 2015.

[17] B. Wang and L.-Q. Chen, “Asymptotic stability analysis with numerical confirmation of an axially accelerating beam constituted by the standard linear solid model,” *Journal of Sound and Vibration*, vol. 328, no. 4-5, pp. 456–466, 2009.

[18] H. L. Li, L. Zhang, C. Hu, Y.-L. Jiang, and Z. Teng, “Dynamical analysis of a fractional-order predator-prey model incorporating a prey refuge,” *Journal of Applied Mathematics and Computing*, vol. 54, no. 1-2, pp. 435–449, 2017.

[19] C. Baishya, S. J. Achar, P. Veeresha, and D. G. Prakasha, “Dynamics of a fractional epidemiological model with disease infection in both the populations,” *Chaos: An Interdisciplinary Journal of Nonlinear Science*, vol. 31, no. 4, 2021.

[20] M. A. Dokuyucu, E. Celik, H. Bulut, and H. M. Baskonus, “Cancer treatment model with the Caputo-Fabrizio fractional derivative,” *The European Physical Journal Plus*, vol. 133, no. 3, pp. 1–6, 2018.

[21] M. A. Khan, Z. Hammouch, and D. Baleanu, “Modeling the dynamics of hepatitis E via the Caputo–Fabrizio derivative,” *Mathematical Modelling of Natural Phenomena*, vol. 14, no. 3, 2019.

[22] E. Ahmed and H. A. El-Saka, “On fractional order models for Hepatitis C,” *Nonlinear biomedical physics*, vol. 4, no. 1, pp. 1–3, 2010.

[23] P. Veeresha, D. Kumar, “Analysis and dynamics of the Ivancevic option pricing model with a novel fractional calculus approach,” *Waves in Random and Complex Media*, pp. 1-18, 2022.

[24] S. J. Achar, C. Baishya, P. Veeresha, and L. Akinyemi, “Dynamics of fractional model of biological pest control in tea plants with Beddington-DeAngelis functional response,” *Fractal and Fractional*, vol. 6, no. 1, 2022.

[25] K. Diethelm, N. J. Ford, and A. D. Freed, “A predictor-corrector approach for the numerical solution of fractional differential equations,” *Nonlinear Dynamics*, vol. 29, no. 1, pp. 3–22, 2001.

[26] K. Diethelm and N. J. Ford, “Analysis of fractional differential equations,” *Journal of Mathematical Analysis and Applications*, vol. 265, no. 2, pp. 229–248, 2002.

[27] C. Baishya, “Dynamics of fractional stage structured predator prey model with prey refuge,” *Indian Journal of Ecology*, vol. 47, no. 4, pp. 1118–1124, 2020.

[28] S. J. Achar, C. Baishya, and M. K. Kaabar, “Dynamics of the worm transmission in wireless sensor network in the framework of fractional derivatives,” *Mathematical Methods in the Applied Sciences*, 2021.

[29] C. Baishya, “Dynamics of fractional holling type-ii predator-prey model with prey refuge and additional food to predator,” *Journal of Applied Nonlinear Dynamics*, vol. 10, no. 2, pp. 315–328, 2020.

TABLE OF CONTENTS, JOURNAL OF COMPUTATIONAL ANALYSIS AND APPLICATIONS, VOL. 31, NO. 1, 2023

Characteristics of Mexican hat wavelet transform in a class of generalized quotient space, Abhishek Singh, Aparna Rawat, and Shubha Singh,……...10

Maxwell Cattaneo double diffusive convection (DDC) in a viscoelastic fluid layer, Monal Bharty, Atul. K. Srivastava, Hrisikesh Mahato,…………………………………………………21

Some New Results for the $\mathcal{M}$-Transform Involving the Incomplete H- and $\overline{H}$-Functions, Sanjay Bhatter, Sapna Meena, Jagdev Singh, and Sunil Dutt Purohit,…………………………………38

Approximate solutions of space and time fractional telegraph equations using Taylor series expansion method, Shweta Dubey, S. Chakraverty, and M. Kundu,……………………………48

An M/G/1 Feedback retrial queue with working vacation and a waiting server, S.Pazhani Bala Murugan and R.Keerthana,………………………………………………………………………61

An Application of Incomplete I-Functions with Two Variables to Solve the Nonlinear Differential Equations Using S-Function, Rahul Sharma, Jagdev Singh, Devendra Kumar, and Yudhveer Singh,…………………………………………………………………………………80

SEAIQHRDP mathematical model Analysis for the transmission dynamics of COVID-19 in India, M. Ankamma Rao and A.Venkatesh,…………………………………………………….96

On nonempty intersection properties in metric spaces, A. Gupta and S. Mukherjee,………….117

Goal programming approach to solve linear transportation problems with multiple objectives, Vishwas Deep Joshi, Keshav Agarwal, and Jagdev Singh,…………………………………….127

Dynamical analysis of fractional yellow fever virus model with efficient numerical approach, Chandrali Baishya, Sindhu J. Achar, P. Veeresha, and Devendra Kumar,……………………..140

Volume 31, Number 2 April 2023
ISSN:1521-1398 PRINT,1572-9206 ONLINE

Journal of Computational Analysis and Applications

EUDOXUS PRESS,LLC

Journal of Computational Analysis and Applications
ISSNno.'s:1521-1398 PRINT,1572-9206 ONLINE

SCOPE OF THE JOURNAL

An international publication of Eudoxus Press, LLC
(published quarterly) www.eudoxuspress.com.

Editor in Chief: George Anastassiou
Department of Mathematical Sciences,
University of Memphis, Memphis, TN 38152-3240, U.S.A
ganastss@memphis.edu, ganastss2@gmail.com
http://web0.msci.memphis.edu/~ganastss/jocaaa/

The main purpose of "J.Computational Analysis and Applications" is to publish high quality research articles from all subareas of Computational Mathematical Analysis and its many potential applications and connections to other areas of Mathematical Sciences. Any paper whose approach and proofs are computational,using methods from Mathematical Analysis in the broadest sense is suitable and welcome for consideration in our journal, except from Applied Numerical Analysis articles. Also plain word articles without formulas and proofs are excluded. The list of possibly connected mathematical areas with this publication includes, but is not restricted to: Applied Analysis, Applied Functional Analysis, Approximation Theory, Asymptotic Analysis, Difference Equations, Differential Equations, Partial Differential Equations, Fourier Analysis, Fractals, Fuzzy Sets, Harmonic Analysis, Inequalities, Integral Equations, Measure Theory, Moment Theory, Neural Networks, Numerical Functional Analysis, Potential Theory, Probability Theory, Real and Complex Analysis, Signal Analysis, Special Functions, Splines, Stochastic Analysis, Stochastic Processes, Summability, Tomography, Wavelets, any combination of the above, e.t.c.

"J.Computational Analysis and Applications" is a peer-reviewed Journal. See the instructions for preparation and submission **of articles to JOCAAA.**

Journal of Computational Analysis and Applications(JoCAAA) is published by **EUDOXUS PRESS,LLC**,1424 Beaver Trail Drive,Cordova,TN38016,USA,anastassioug@yahoo.com http://www.eudoxuspress.com. **Annual Subscription Prices**:For USA and Canada,Institutional:Print $500, Electronic OPEN ACCESS. Individual:Print $250. For any other part of the world add $150 more(handling and postages) to the above prices for Print. No credit card payments.

Copyright©2023 by Eudoxus Press,LLC,all rights reserved.JoCAAA is printed in USA.

JoCAAA is reviewed and abstracted by Elsevier-Scopus, available also via EBSCO publishing and EBSCO.

It is strictly prohibited the reproduction and transmission of any part of JoCAAA and in any form and by any means without the written permission of the publisher.It is only allowed to educators to Xerox articles for educational purposes.The publisher assumes no responsibility for the content of published papers.

Editorial Board
Associate Editors of Journal of Computational Analysis and Applications

Francesco Altomare
Dipartimento di Matematica
Universita' di Bari
Via E.Orabona, 4
70125 Bari, ITALY
Tel+39-080-5442690 office
+39-080-3944046 home
+39-080-5963612 Fax
altomare@dm.uniba.it
Approximation Theory, Functional Analysis, Semigroups and Partial Differential Equations, Positive Operators.

Ravi P. Agarwal
Department of Mathematics
Texas A&M University - Kingsville
700 University Blvd.
Kingsville, TX 78363-8202
tel: 361-593-2600
Agarwal@tamuk.edu
Differential Equations, Difference Equations, Inequalities

George A. Anastassiou
Department of Mathematical Sciences
The University of Memphis
Memphis, TN 38152,U.S.A
Tel.901-678-3144
e-mail: ganastss@memphis.edu
Approximation Theory, Real Analysis,
Wavelets, Neural Networks, Probability, Inequalities.

J. Marshall Ash
Department of Mathematics
De Paul University
2219 North Kenmore Ave.
Chicago, IL 60614-3504
773-325-4216
e-mail: mash@math.depaul.edu
Real and Harmonic Analysis

Dumitru Baleanu
Department of Mathematics and Computer Sciences,
Cankaya University, Faculty of Art and Sciences,
06530 Balgat, Ankara, Turkey, dumitru@cankaya.edu.tr
Fractional Differential Equations
Nonlinear Analysis, Fractional Dynamics

Carlo Bardaro
Dipartimento di Matematica e Informatica
Universita di Perugia
Via Vanvitelli 1
06123 Perugia, ITALY
TEL+390755853822
+390755855034
FAX+390755855024
E-mail carlo.bardaro@unipg.it
Web site:
http://www.unipg.it/~bardaro/
Functional Analysis and Approximation Theory, Signal Analysis, Measure Theory, Real Analysis.

Martin Bohner
Department of Mathematics and Statistics, Missouri S&T
Rolla, MO 65409-0020, USA
bohner@mst.edu
web.mst.edu/~bohner
Difference equations, differential equations, dynamic equations on time scale, applications in economics, finance, biology.

Jerry L. Bona
Department of Mathematics
The University of Illinois at Chicago
851 S. Morgan St. CS 249
Chicago, IL 60601
e-mail:bona@math.uic.edu
Partial Differential Equations, Fluid Dynamics

Luis A. Caffarelli
Department of Mathematics
The University of Texas at Austin
Austin, Texas 78712-1082
512-471-3160
e-mail: caffarel@math.utexas.edu
Partial Differential Equations

George Cybenko
Thayer School of Engineering
Dartmouth College
8000 Cummings Hall,
Hanover, NH 03755-8000
603-646-3843 (X 3546 Secr.)
e-mail:george.cybenko@dartmouth.edu
Approximation Theory and Neural
Networks

Sever S. Dragomir
School of Computer Science and
Mathematics, Victoria University,
PO Box 14428,
Melbourne City,
MC 8001, AUSTRALIA
Tel. +61 3 9688 4437
Fax +61 3 9688 4050
e-mail: sever.dragomir@vu.edu.au
Inequalities, Functional Analysis,
Numerical Analysis, Approximations,
Information Theory, Stochastics.

Oktay Duman
TOBB University of Economics and
Technology,
Department of Mathematics, TR-
06530, Ankara, Turkey,
e-mail: oduman@etu.edu.tr
Classical Approximation Theory,
Summability Theory, Statistical
Convergence and its Applications

J .A. Goldstein
Department of Mathematical Sciences
The University of Memphis
Memphis, TN 38152
901-678-3130
e-mail: jgoldste@memphis.edu
Partial Differential Equations,
Semigroups of Operators

H. H. Gonska
Department of Mathematics
University of Duisburg
Duisburg, D-47048
Germany
011-49-203-379-3542
e-mail: heiner.gonska@uni-due.de
Approximation Theory, Computer
Aided Geometric Design

John R. Graef
Department of Mathematics
University of Tennessee at
Chattanooga
Chattanooga, TN 37304 USA
e-mail: John-Graef@utc.edu
Ordinary and functional
differential equations, difference
equations, impulsive systems,
differential inclusions, dynamic
equations on time scales, control
theory and their applications

Weimin Han
Department of Mathematics
University of Iowa
Iowa City, IA 52242-1419
319-335-0770
e-mail: whan@math.uiowa.edu
Numerical analysis, Finite element
method, Numerical PDE, Variational
inequalities, Computational
mechanics

Tian-Xiao He
Department of Mathematics and
Computer Science
P.O. Box 2900, Illinois Wesleyan
University
Bloomington, IL 61702-2900, USA
Tel (309)556-3089
Fax (309)556-3864
e-mail: the@iwu.edu
Approximations, Wavelet,
Integration Theory, Numerical
Analysis, Analytic Combinatorics

Margareta Heilmann
Faculty of Mathematics and Natural
Sciences, University of Wuppertal
Gaußstraße 20
D-42119 Wuppertal, Germany,
heilmann@math.uni-wuppertal.de
Approximation Theory (Positive
Linear Operators)

Xing-Biao Hu
Institute of Computational
Mathematics
AMSS, Chinese Academy of Sciences
Beijing, 100190, CHINA
e-mail: hxb@lsec.cc.ac.cn
Computational Mathematics

Seda Karateke
Department of Computer Engineering,
Faculty of Engineering,
Istanbul Topkapi University,
Istanbul, Zeytinburnu 34087, Turkey
e-mail: sedakarateke@topkapi.edu.tr
Approximation Theory, Neural
Networks

Jong Kyu Kim
Department of Mathematics
Kyungnam University
Masan Kyungnam,631-701,Korea
Tel 82-(55)-249-2211
Fax 82-(55)-243-8609
e-mail: jongkyuk@kyungnam.ac.kr
Nonlinear Functional Analysis,
Variational Inequalities, Nonlinear
Ergodic Theory, ODE, PDE,
Functional Equations.

Robert Kozma
Department of Mathematical Sciences
The University of Memphis
Memphis, TN 38152, USA
e-mail: rkozma@memphis.edu
Neural Networks, Reproducing Kernel
Hilbert Spaces,
Neural Percolation Theory

Mustafa Kulenovic
Department of Mathematics
University of Rhode Island
Kingston, RI 02881, USA
e-mail: kulenm@math.uri.edu
Differential and Difference
Equations

Burkhard Lenze
Fachbereich Informatik
Fachhochschule Dortmund
University of Applied Sciences
Postfach 105018
D-44047 Dortmund, Germany
e-mail: lenze@fh-dortmund.de
Real Networks, Fourier Analysis,
Approximation Theory

Alina Alb Lupas
Department of Mathematics and
Computer Science
Faculty of Informatics
University of Oradea
2 Universitatii Street,
410087 Oradea, Romania
e-mail: alblupas@gmail.com
e-mail: dalb@uoradea.ro
Complex Analysis, Topological
Algebra, Mathematical Analysis

Razvan A. Mezei
Computer Science Department
Hal and Inge Marcus School of
Engineering
Saint Martin’s University
Lacey, WA 98503, USA
e-mail: RMezei@stmartin.edu
Numerical Approximation, Fractional
Inequalities.

Hrushikesh N. Mhaskar
Department Of Mathematics
California State University
Los Angeles, CA 90032
626-914-7002
e-mail: hmhaska@gmail.com
Orthogonal Polynomials,
Approximation Theory, Splines,
Wavelets, Neural Networks

Ram N. Mohapatra
Department of Mathematics
University of Central Florida
Orlando, FL 32816-1364
tel.407-823-5080
e-mail: ram.mohapatra@ucf.edu
Real and Complex Analysis,
Approximation Th., Fourier
Analysis, Fuzzy Sets and Systems

Gaston M. N'Guerekata
Department of Mathematics
Morgan State University
Baltimore, MD 21251, USA
tel: 1-443-885-4373
Fax 1-443-885-8216
Gaston.N'Guerekata@morgan.edu
nguerekata@aol.com
Nonlinear Evolution Equations,
Abstract Harmonic Analysis,
Fractional Differential Equations,
Almost Periodicity & Almost
Automorphy

M.Zuhair Nashed
Department Of Mathematics
University of Central Florida
PO Box 161364
Orlando, FL 32816-1364
e-mail: znashed@mail.ucf.edu
Inverse and Ill-Posed problems,
Numerical Functional Analysis,
Integral Equations, Optimization,
Signal Analysis

Mubenga N. Nkashama
Department OF Mathematics
University of Alabama at Birmingham
Birmingham, AL 35294-1170
205-934-2154
e-mail: nkashama@math.uab.edu
Ordinary Differential Equations,
Partial Differential Equations

Vassilis Papanicolaou
Department of Mathematics
National Technical University of Athens
Zografou campus, 157 80
Athens, Greece
tel: +30(210) 772 1722
Fax +30(210) 772 1775
e-mail: papanico@math.ntua.gr
Partial Differential Equations,
Probability

Choonkil Park
Department of Mathematics
Hanyang University
Seoul 133-791
S. Korea,
e-mail: baak@hanyang.ac.kr
Functional Equations

Svetlozar (Zari) Rachev,
Professor of Finance, College of
Business, and Director of
Quantitative Finance Program,
Department of Applied Mathematics &
Statistics
Stonybrook University
312 Harriman Hall, Stony Brook, NY
11794-3775
tel: +1-631-632-1998,
svetlozar.rachev@stonybrook.edu

Alexander G. Ramm
Mathematics Department
Kansas State University
Manhattan, KS 66506-2602
e-mail: ramm@math.ksu.edu
Inverse and Ill-posed Problems,
Scattering Theory, Operator Theory,
Theoretical Numerical Analysis,
Wave Propagation, Signal Processing
and Tomography

Tomasz Rychlik
Polish Academy of Sciences
Instytut Matematyczny PAN
00-956 Warszawa, skr. poczt. 21
ul. Śniadeckich 8
Poland
e-mail: trychlik@impan.pl
Mathematical Statistics,
Probabilistic Inequalities

Boris Shekhtman
Department of Mathematics
University of South Florida
Tampa, FL 33620, USA
Tel 813-974-9710
e-mail: shekhtma@usf.edu
Approximation Theory, Banach
spaces, Classical Analysis

T. E. Simos
Department of Computer
Science and Technology
Faculty of Sciences and Technology
University of Peloponnese
GR-221 00 Tripolis, Greece
Postal Address:
26 Menelaou St.
Anfithea - Paleon Faliron
GR-175 64 Athens, Greece
e-mail: tsimos@mail.ariadne-t.gr
Numerical Analysis

Jagdev Singh
JECRC University, Jaipur, India
jagdevsinghrathore@gmail.com
Fractional Calculus, Mathematical
Modelling, Special Functions,
Numerical Methods

H. M. Srivastava
Department of Mathematics and
Statistics
University of Victoria
Victoria, British Columbia V8W 3R4
Canada
tel.250-472-5313; office,250-477-
6960 home, fax 250-721-8962
e-mail: harimsri@math.uvic.ca
Real and Complex Analysis,
Fractional Calculus and Appl.,
Integral Equations and Transforms,
Higher Transcendental Functions and
Appl.,q-Series and q-Polynomials,
Analytic Number Th.

I. P. Stavroulakis
Department of Mathematics
University of Ioannina
451-10 Ioannina, Greece
e-mail: ipstav@cc.uoi.gr
Differential Equations
Phone +3-065-109-8283

Jessada Tariboon
Department of Mathematics
King Mongut's University of
Technology N. Bangkok
1518 Pracharat 1 Rd., Wongsawang,
Bangsue, Bangkok, Thailand 10800
e-mail: jessada.t@sci.kmutnb.ac.th
Time scales

Differential/Difference Equations,
Fractional Differential Equations

Manfred Tasche
Department of Mathematics
University of Rostock
D-18051 Rostock, Germany
manfred.tasche@mathematik.uni-rostock.de
Numerical Fourier Analysis, Fourier Analysis, Harmonic Analysis, Signal Analysis, Spectral Methods, Wavelets, Splines, Approximation Theory

Juan J. Trujillo
University of La Laguna
Departamento de Analisis Matematico
C/Astr.Fco.Sanchez s/n
38271. LaLaguna. Tenerife.
SPAIN
Tel/Fax 34-922-318209
e-mail: Juan.Trujillo@ull.es
Fractional: Differential Equations-Operators-Fourier Transforms, Special functions, Approximations, and Applications

Xiao-Jun Yang
State Key Laboratory for Geomechanics and Deep Underground Engineering, China
University of Mining and Technology, Xuzhou 221116, China
Local Fractional Calculus and Applications, Fractional Calculus and Applications, General Fractional Calculus and Applications, Variable-order Calculus and Applications, Viscoelasticity and Computational methods for Mathematical Physics.dyangxiaojun@163.com

Xiang Ming Yu
Department of Mathematical Sciences
Southwest Missouri State University
Springfield, MO 65804-0094
417-836-5931
e-mail: xmy944f@missouristate.edu
Classical Approximation Theory, Wavelets

Richard A. Zalik
Department of Mathematics
Auburn University
Auburn University, AL 36849-5310
USA.
Tel 334-844-6557 office
Fax 334-844-6555
e-mail: zalik@auburn.edu
Approximation Theory, Chebychev Systems, Wavelet Theory

Ahmed I. Zayed
Department of Mathematical Sciences
DePaul University
2320 N. Kenmore Ave.
Chicago, IL 60614-3250
773-325-7808
e-mail: azayed@condor.depaul.edu
Shannon sampling theory, Harmonic analysis and wavelets, Special functions and orthogonal polynomials, Integral transforms

Ding-Xuan Zhou
Department Of Mathematics
City University of Hong Kong
83 Tat Chee Avenue
Kowloon, Hong Kong
852-2788 9708,Fax:852-2788 8561
e-mail: mazhou@cityu.edu.hk
Approximation Theory, Spline functions, Wavelets

Xin-long Zhou
Fachbereich Mathematik, Fachgebiet Informatik
Gerhard-Mercator-Universitat Duisburg
Lotharstr.65, D-47048 Duisburg, Germany
e-mail:Xzhou@informatik.uni-duisburg.de
Fourier Analysis, Computer-Aided Geometric Design, Computational Complexity, Multivariate Approximation Theory, Approximation and Interpolation Theory

Instructions to Contributors
Journal of Computational Analysis and Applications

An international publication of Eudoxus Press, LLC, of TN.

Editor in Chief: George Anastassiou

Department of Mathematical Sciences
University of Memphis
Memphis, TN 38152-3240, U.S.A.

1. Manuscripts files in Latex and PDF and in English, should be submitted via email to the Editor-in-Chief:

Prof.George A. Anastassiou
Department of Mathematical Sciences
The University of Memphis
Memphis,TN 38152, USA.
Tel. 901.678.3144
e-mail: ganastss@memphis.edu

Authors may want to recommend an associate editor the most related to the submission to possibly handle it.

Also authors may want to submit a list of six possible referees, to be used in case we cannot find related referees by ourselves.

2. Manuscripts should be typed using any of TEX,LaTEX,AMS-TEX,or AMS-LaTEX and according to EUDOXUS PRESS, LLC. LATEX STYLE FILE. (Click HERE to save a copy of the style file.)They should be carefully prepared in all respects. Submitted articles should be brightly typed (not dot-matrix), double spaced, in ten point type size and in 8(1/2)x11 inch area per page. Manuscripts should have generous margins on all sides and should not exceed 24 pages.

3. Submission is a representation that the manuscript has not been published previously in this or any other similar form and is not currently under consideration for publication elsewhere. A statement transferring from the authors(or their employers,if they hold the copyright) to Eudoxus Press, LLC, will be required before the manuscript can be accepted for publication.The Editor-in-Chief will supply the necessary forms for this transfer.Such a written transfer of copyright,which previously was assumed to be implicit in the act of submitting a manuscript,is necessary under the U.S.Copyright Law in order for the publisher to carry through the dissemination of research results and reviews as widely and effective as possible.

4. The paper starts with the title of the article, author's name(s) (no titles or degrees), author's affiliation(s) and e-mail addresses. The affiliation should comprise the department, institution (usually university or company), city, state (and/or nation) and mail code.

The following items, 5 and 6, should be on page no. 1 of the paper.

5. An abstract is to be provided, preferably no longer than 150 words.

6. A list of 5 key words is to be provided directly below the abstract. Key words should express the precise content of the manuscript, as they are used for indexing purposes.

The main body of the paper should begin on page no. 1, if possible.

7. All sections should be numbered with Arabic numerals (such as: 1. INTRODUCTION) .
Subsections should be identified with section and subsection numbers (such as 6.1. Second-Value Subheading).
If applicable, an independent single-number system (one for each category) should be used to label all theorems, lemmas, propositions, corollaries, definitions, remarks, examples, etc. The label (such as Lemma 7) should be typed with paragraph indentation, followed by a period and the lemma itself.

8. Mathematical notation must be typeset. Equations should be numbered consecutively with Arabic numerals in parentheses placed flush right, and should be thusly referred to in the text [such as Eqs.(2) and (5)]. The running title must be placed at the top of even numbered pages and the first author's name, et al., must be placed at the top of the odd numbed pages.

9. Illustrations (photographs, drawings, diagrams, and charts) are to be numbered in one consecutive series of Arabic numerals. The captions for illustrations should be typed double space. All illustrations, charts, tables, etc., must be embedded in the body of the manuscript in proper, final, print position. In particular, manuscript, source, and PDF file version must be at camera ready stage for publication or they cannot be considered.

Tables are to be numbered (with Roman numerals) and referred to by number in the text. Center the title above the table, and type explanatory footnotes (indicated by superscript lowercase letters) below the table.

10. List references alphabetically at the end of the paper and number them consecutively. Each must be cited in the text by the appropriate Arabic numeral in square brackets on the baseline.
References should include (in the following order):
initials of first and middle name, last name of author(s)
title of article,

name of publication, volume number, inclusive pages, and year of publication.

Authors should follow these examples:

Journal Article

1. H.H.Gonska,Degree of simultaneous approximation of bivariate functions by Gordon operators, (journal name in italics) *J. Approx. Theory*, 62,170-191(1990).

Book

2. G.G.Lorentz, (title of book in italics) *Bernstein Polynomials* (2nd ed.), Chelsea,New York,1986.

Contribution to a Book

3. M.K.Khan, Approximation properties of beta operators,in(title of book in italics) *Progress in Approximation Theory* (P.Nevai and A.Pinkus,eds.), Academic Press, New York,1991,pp.483-495.

11. All acknowledgements (including those for a grant and financial support) should occur in one paragraph that directly precedes the References section.

12. Footnotes should be avoided. When their use is absolutely necessary, footnotes should be numbered consecutively using Arabic numerals and should be typed at the bottom of the page to which they refer. Place a line above the footnote, so that it is set off from the text. Use the appropriate superscript numeral for citation in the text.

13. After each revision is made please again submit via email Latex and PDF files of the revised manuscript, including the final one.

14. Effective 1 Nov. 2009 for current journal page charges, contact the Editor in Chief. Upon acceptance of the paper an invoice will be sent to the contact author. The fee payment will be due one month from the invoice date. The article will proceed to publication only after the fee is paid. The charges are to be sent, by money order or certified check, in US dollars, payable to Eudoxus Press, LLC, to the address shown on the Eudoxus homepage.

No galleys will be sent and the contact author will receive one (1) electronic copy of the journal issue in which the article appears.

15. This journal will consider for publication only papers that contain proofs for their listed results.

Two step Newton's method with multiplicative calculus to solve the non-linear equations

Gurjeet Singh[1,a], **Sonia Bhalla**[1,b]

[1] Department of Mathematics, Chandigarh University, Gharuan, Punjab, India, 140413
[a] Corresponding author: gs42477@gmail.com
[b] sonia.e8843@cumail.in

Abstract

For solving non-linear equations, iterative root-finding methods are important because of the broad range of applications in science and engineering. We have constructed an iterative method based on multiplicative calculus in this paper. Some numerical results are performed to exposed the efficiency of proposed and earlier method.

Keywords: Multiplicative calculus, Non linear equations, Iterative methods, Newton's-Raphson method, Order of convergence

1 Introduction

In the field of engineering and sciences, solving nonlinear equations effectively is one of the interesting task. Sometimes it is difficult to solve these problems. Then, we rely on iterative schemes to execute the root of non-linear function $g(t) = 0$. One of the popular methods for approximating the root of a non-linear function is the Newton's method [14] defined as

$$t_{q+1} = t_q - \frac{g(t_q)}{g'(t_q)}, \quad q = 0, 1, 2, 3... \tag{1}$$

The convergence order of Newton's method is two for the simple root. Several variants of Newton's method are developed to improve the convergence order in the literature such as Halley method [23], super-Halley method [16], Euler's method [21], Weerakoon and Fernando [22] etc. All of the above mentioned methods consist second-order derivatives except Weerakoon and Fernando. From 1964 to 2012, researchers [1],[9],[15],[24] has developed fourth-order methods to find the non-linear equations roots like Traub and Ostrowski [15], Chun and Ham [9], Cordero and Torregrosa [1], Kanwar et al. [24] etc. Out of them, Kanwar et. al. introduced a method which consists second-order derivatives while other listed methods have first-order derivative. Sometime it is difficult to achieve the second-order derivative at each step of the method. So some authors [10-11] developed second-order derivative free methods to solve the non-linear equations.

But still handling of first-order or second-order derivative in iterative techniques is difficult task. Nowdays, non-linear equations $g(t) + 1 = 1$ are solved using multiplicative calculus instead of function $g(t) = 0$. Initially, in 2008 Bashirov et al. [3] discussed the theoretical foundations and various applications of multiplicative calculus. In 2009 and 2011 Misirli and Gurefe [12], Riza et al. [18], and Ozyapici & Misirli [13] used multiplicative calculus to develop multiplicative numerical methods and in 2010 Filip and Piatecki [11] used it to examine economic growth and Uzer [8] extended the multiplicative calculus to include complex valued functions of complex variables, which was previously applicable only to positive real valued functions of real variables. In 2011 Bashirov et al. [4] used it to develop multiplicative differential equations. Bashirov & Riza [5] and in 2012 Florack and van Assen [17] used in biomedical image analysis. Currently, in 2016 Ozyapici, Sensoy and Karanfiller constructed a Multiplicative Newton's method. Keeping the same fact in mind, we consider the joint four-order multiplicative Newton's method.

This paper is structured as follows. Some basic terms of Multiplicative Calculus forms Section 2. As described in Section 3, a convergence analysis is conducted to determine the fourth-order of convergence of the proposed method. In Section 4, we presents comparisons of results obtained by proposed method with some other fourth-order methods. Finally, the conclusions form Section 5.

2 Some basic terms of Multiplicative Calculus

Definition: Let $g(t)$ be a real positive valued function in the open interval (a, b). Assume function be changes in $t \in (a, b)$ s.t. $g(t)$ changes in $g(t + h)$. Then [13] multiplicative forward operator denoted as Δ^* defined as follows

$$\Delta^* g(t) = \frac{g(t+h)}{g(t)} \tag{2}$$

By considring the operator Δ^* in (2), multiplicative derivative can be defined as below

$$g^*(t) = \lim_{h \to 0} (\Delta^* g)^{1/h} \tag{3}$$

The function $g^*(t)$ is said to be multiplicative differentiable at t if the limit on R.H.S exists.

If g is positive function and the derivative of g at t exist, then q^{th} multiplicative derivatives of g exist and

$$g^{*(q)}(t) = exp\left\{(ln \circ g)^{(q)}(t)\right\} \tag{4}$$

Theorem 1: (Multiplicative Taylor Theorem in one variable) [5] Let $g(t)$ be a function in open interval (a, b) s.t the functions is $q+1$ times $*$ differentiable on (a, b). Then for any $t, t+h \in A(a, b)$, there is a number $\theta \in (a, b)$ such that

$$g(t+h) = \prod_{p=0}^{n} \Big(g^{*(p)}(t)\Big)^{\overline{p!}^{\,h^p}} . \Big(g^{*(q+1)}(t+\theta h)\Big)^{\frac{h^{q+1}}{(q+1)!}} \tag{5}$$

Theorem 2: (Multiplicative Newton's-Raphson method) [7] Assume that $g \in \mathcal{C}^2[a, b]$ and there exist a number $p \in [a, b]$ such that $g(p) = 1$. If $g^*(p) \neq 1$ and $h(t) = t - \dfrac{ln\ g(t)}{ln\ g^*(t)}$ then there exist a $\delta > 0$ such that the sequence $pk_{k=1}^{\infty}$ defined by iteration will converge to m for any initial value $p_0 \in [p-\delta, p+\delta]$

$$p_k = p_{k-1} - \frac{ln\ g(p_{k-1})}{ln\ g^*(p_{k-1})} \tag{6}$$

with error $e_{q+1} = b_2 e_q^2 + 2(b_3 - b_2^2)e_q^3 + \mathcal{O}(e_q^4)$

3 The Proposed Method and Analysis of Convergence

Here we constructed two step iterative method by considering first step as multiplicative Newton's-Raphson method and second step as considering ordinary Newton's-Raphson Scheme.

$$y_q = t_q - \frac{ln\ g(t_q)}{ln\ g^*(t_q)},$$

$$t_{q+1} = y_q - \frac{g(y_q)}{g'(y_q)}. \tag{7}$$

Where $q = 1, 2, 3, ...$ is the iteration level .
For convergence analysis, we have proved the following theorem.

Theorem 3: Suppose that for an open interval I, the function $g : I \subseteq \mathbb{R} \to \mathbb{R}$ has only one root, $s \in I$. Let $g(t)$ be a sufficiently ordinary differentiable and then multiplicative differentiable in the neighborhood of s. Then the proposed method (7) has fourth-order of convergence.
Proof: Let s be the simple root of $g(t)$ and $e_q = t_q - s$. Consider the function $H(t) = t_{q+1}$ defined by

$$H(t) = y_q - \frac{g(y_q)}{g'(y_q)},$$

where

$$y_q = t_q - \frac{ln\ g(t_q)}{ln\ g^*(t_q)} \tag{8}$$

By using Mathematica version 11.1.1 with the fact that $y'(s) = 0$ from Theorem 2, the function $H(t)$ satisfies

$$H(s) = r \quad and \quad H^{(q)}(s) = 0, q = 1, 2, 3. \tag{9}$$

Thus, $H^{(4)}(s)$ can be given as

$$H^{(4)}(s) = \frac{3(g'(t)^2 - g''(t))^2 g''(t)}{g'(t)^3}$$

By Taylor expansion of $H(t_n)$ around s with condition (9), one obtain

$$t_{q+1} = H(t_q) = H(s) + \frac{H^{(4)}}{4!} e_q^4 + \mathcal{O}(e_q^5).$$

Hence,

$$e_{q+1} = \frac{H^{(4)}(s)}{4!} e_q^4 + \mathcal{O}(e_q^5)$$

Hence, the method (8) has fourth-order of convergence.

4 Numerical Examples

Several examples are given in this section to illustrate the applicability of the proposed method. The results of proposed method denoted as (PM) is also compared with earlier methods such as two-step Newton's Method [19] denoted as (NM), Chun method [10] denoted as (CM) and Maheshwari method [6] denoted as (MM) reprsented in Table 1 - Table 4. All computations can be done in Mathematica version 11.1.1 software and the stopping criteria $|t_{q+1} - t_q| < \epsilon$ and $\epsilon = 10^{-14}$ is used. The obtained results are compared for first three iterations. Moreover, the Approximated computational order of convergence(ACOC) is computed by using the following.

$$\rho \cong \frac{ln\left|\dfrac{t_{q+1} - s}{t_q - s}\right|}{ln\left|\dfrac{t_q - s}{t_{q-1} - s}\right|}.$$

Example 1: A fraction conversion problem is considered firstly, in which nitrogen-hydrogen feed is converted to ammonia fractionally. A temperature of 500°C and a pressure of 250 atm have been used in this problem. The nonlinear form of this problem is as follows::

$$g_1(t) = -0.186 - \frac{8t^2(t-4)^2}{9(t-2)^3}, \tag{10}$$

The simplified form of equation (10) is reduces to non-linear function as

$$g_1(t) = t^4 - 7.79075t^3 + 14.7445t^2 + 2.511t - 1.674 \tag{11}$$

Since the polynomial above has a degree of four, there must be exactly four roots. Due to its definition, fraction conversion lies in the interval (0,1), so there can be only one root in this interval, and that is 0.2777595428. Using the initial guess $t_0 = 0.4$ in Table 1, it is clear that our suggested method takes fewer iterations than others.

Example 2: Consider a Kepler's Equation

$$g_2(t) = t - \alpha_1 Sin(t) - K, \tag{12}$$

where $0 \leq \alpha_1 < 1$ and $0 \leq K \leq \pi$. We solve the equation by taking $K = 0.1$ and $\alpha_1 = 0.25$. For this set of values the root is 0.13320215082857313... which is approximated by proposed and earlier methods at the initial root $t_0 = 2$ and results are shown in Table 2.

Example 3: Problems of transcendental and algebraic nature. The following equations are used to numerically analyze the proposed technique:

$$(a) \qquad g_3(t) = e^{-t} + Cost, with\ exact\ root\ s = 1.7461. \tag{13}$$

$$(b)\ g_4(t) = te^{t^2} - Sin^2 t + 3Cost - 4, with\ exact\ root\ s = 1.0651. \tag{14}$$

Table 3 and Table 4 shows the numerical outcomes starting with the initial guess 2.0 and 1.0 respectively. According to the numerical results, the proposed method requires fewer steps and reduces computation time.

Method	q	$\|t_q - t_{q-1}\|$	$\|g(t_q)\|$	ρ
NM	1	2.7402×10^{-1}	22.441	4.000
	2	2.7338×10^{-2}	9.6722×10^{-1}	
	3	3.4387×10^{-4}	4.3475×10^{-15}	
CM	1	2.5637×10^{-1}	22.4486	3.9987
	2	4.4424×10^{-2}	1.7056	
	3	5.9249×10^{-4}	1.8635×10^{-2}	
MM	1	2.5941×10^{-1}	22.4486	4.000
	2	4.1567×10^{-2}	1.5720	
	3	4.0948×10^{-4}	1.2868×10^{-2}	
PM	1	5.46149×10^{-1}	23.4486	3.999
	2	3.07797×10^{-2}	2.13315	
	3	3.44644×10^{-4}	1.0109	

Table 1: Fraction Conversion of Nitrogen-Hydrogen to Ammonia

Method	q	$\|t_q - t_{q-1}\|$	$\|g(t_q)\|$	ρ
NM	1	1.6621	1.5227	4.000
	2	6.5678×10^{-3}	5.0169×10^{-3}	
	3	2.8775×10^{-13}	2.1973×10^{-13}	
CM	1	1.6495	1.5226	4.000
	2	1.9131×10^{-2}	1.4623×10^{-2}	
	3	3.3555×10^{-10}	-2.5622×10^{-10}	
MM	1	1.6490	1.5226	4.000
	2	1.9652×10^{-2}	1.5022×10^{-2}	
	3	3.2303×10^{-10}	-2.4667×10^{-10}	
PM	1	1.66756	2.5226	4.000
	2	1.12051×10^{-3}	1.0008	
	3	9.0489×10^{-15}	1.0000	

Table 2: Kepler's Equation

Method	q	$\|t_q - t_{q-1}\|$	$\|g(t_q)\|$	ρ
NM	1	2.5389×10^{-1}	-2.8081×10^{-1}	4.000
	2	3.2728×10^{-5}	3.7935×10^{-5}	
	3	3.9104×10^{-21}	4.5325×10^{-21}	
CM	1	2.5424×10^{-1}	-2.8081×10^{-1}	4.000
	2	3.7917×10^{-4}	4.3955×10^{-4}	
	3	7.1375×10^{-16}	8.2731×10^{-16}	
MM	1	2.5418×10^{-1}	-2.8081×10^{-1}	4.000
	2	3.2177×10^{-4}	3.7299×10^{-4}	
	3	3.3377×10^{-16}	3.8688×10^{-16}	
PM	1	2.5398×10^{-1}	7.1919×10^{-1}	4.000
	2	1.1458×10^{-4}	1.0001	
	3	4.7761×10^{-18}	1.0000	

Table 3: $e^{-t} + Cost$

Method	q	$\|t_q - t_{q-1}\|$	$\|g(t_q)\|$	ρ
NM	1	4.2454×10^{-1}	103.12	3.8484
	2	3.6870×10^{-1}	13.838	
	3	1.3811×10^{-1}	1.3718	
CM	1	3.4554×10^{-1}	103.121	3.9221
	2	3.3105×10^{-1}	20.3079	
	3	2.1605×10^{-1}	3.4207	
MM	1	3.6468×10^{-1}	103.121	3.9615
	2	3.4233×10^{-1}	18.5257	
	3	2.0077×10^{-1}	2.7788	
PM	1	9.2639×10^{-1}	104.12	4.000
	2	8.4709×10^{-3}	1.0580	
	3	7.6367×10^{-9}	1.0000	

Table 4: $te^{t^2} - Sin^2t + 3Cost - 4$

5 Conclusion

Here, we developed the Joint Multiplicative Newton's method which is mixture of multiplicative Newton's method and Ordinary Newton's method. We tested the proposed method for approximating the roots of nonlinear equations and compared it with ordinary methods. The obtained results are efiicient as compared with earlier ones in terms of residual error, consecutive error and order of convergence.

References

[1] A. Cordero, J. L. Hueso, E. M. Juan, R. Torregrosa, Steffensen type methods for solving nonlinear equations, J. Comput. Appl. Math. 236(12) 3058-3064 (2012).

[2] A. Cordero, N. Garrido, J. R. Torregrosa, P. T. Nvarro, Iterative schemes for finding all roots simultaneously of nonlinear equations, Appl. Math. Lett., Volume 134,(2022)

[3] A.E. Bashirov, E.M.Kurpınar, A.Ozyapıcı, Multiplicative calculus and its applications, J. Math. Anal. Appl. 337(1), 36–48 (2008)

[4] A.E. Bashirov, E. Mısırlı, Y. Tandogdu, A. Ozyapıcı, On modeling with multiplicative differential equations. Appl. Math. J Chin. Univ. 26(4), 425–438 (2011)

[5] A.E. Bashirov, M. Riza, On complex multiplicative differentiation. TWMS J. Appl. Eng. Math. 1(1), 51–61 (2011)

[6] A. K. Maheshwari, A fourth order iterative method for solving nonlinear equations, Appl. Math. Comput. 211(2) 383 –391 (2009)

[7] A Ozyapıcı, Effective Root-Finding Methods for Nonlinear Equations Based on Multiplicative Calculi, J. Math. (2016)

[8] A. Uzer, Multiplicative type complex calculus as an alternative to the classical calculus. Comput. Math. Appl. 60(10), 2725–2737 (2010)

[9] C. Chun and Y. Ham, Some fourth-order modifications of Newton's method, Appl. Math. Comput. 197(2) 654-658 (2008).

[10] C. Chun, M. Y. Lee, B. Neta, and J. Dzunic, On optimal fourth-order iterative methods free from second derivative and their dynamics, Appl. Math. Comput. 218(11) 6427–6438 (2012).

[11] D.A. Filip, C. Piatecki, A non-Newtonian examination of the theory of exogenous economic growth, CNCSIS-UEFISCSU (project number PNII IDEI 2366/2008) and Laboratoire d'Economie d'Orleans (LEO) (2010)

[12] E. Mısırlı, Y. Gurefe, Multiplicative Adams–Bashforth–Moulton methods. Numer. Algo. 57(4), 425–439 (2011)

[13] E. Mısırlı, A. Ozyapıcı, Exponential approximations on multiplicative calculus. Proc. Jangjeon Math. Soc. 12(2), 227–236 (2009)

[14] E. Suli and D. Mayers, An Introduction to Numerical Analysis. Cambridge University Press. ISBN 0-521-00794-1. (2003).

[15] J. F. Traub, Prentice-Hall, Iterative methods for the solution of equations, Englewood Cliffs, New Jersey, 1964.

[16] J. Gutierrez and M. Hernandez, An accerlation of Newton's method, Appl. Math. Comput. 117(2-3) 223-239 (2001).

[17] L. Florack, H. van Assen, Multiplicative calculus in biomedical image analysis, J. Math. Imaging Vis. 42(1), 64–75 (2012)

[18] M. Riza, A. Ozyapıcı, E. Mısırlı, Multiplicative finite difference methods. Q. Appl. Math. 67(4),745 (2009)

[19] M. Ruiz, A. Alberto, I. K. Argyros, Two-step Newton methods. J. Complex, 30(4), 533–553 (2014)

[20] M. Shams, N. Rafiq, N. Kausar, On iterative techniques for estimating all roots of nonlinear equation and its system with application in differential equation. Adv Differ Equ 2021, 480 (2021)

[21] S. Amat, S. Busquier, and J. M. Gutierrez,Geometric Construction of Iterative Functions to Solve Nonlinear Equations, J. Comput. Appl. Math. 157(1), 197-205 (2003).

[22] S. Weekaroon and TGI. Fernando, A variant of Newton's method with accelerated third-order convergence, Appl. Math. Lett. 13 87-93 (2002).

[23] V. Kanwar and S.K. Tomar, Modified families of Newton, Halley and Chebyshev methods, Appl. Math. Comput. 192 20-26 (2007).

[24] V. Kanwar, R. Behl and K. K. Sharma, Simply constructed family of a Ostrowski's method with optimal order of convergence, J. Comput. Appl. Math. 62(11) 4021-4027 (2011).

J. COMPUTATIONAL ANALYSIS AND APPLICATIONS, VOL. 31, NO. 2, 2023, COPYRIGHT 2023 EUDOXUS PRESS, LLC

Analysis of Tripled System of Fractional Differential Equation using Certain Fixed Points Theorems with Fractional Boundary Condition

Ashok Kumar Badsara[1], Jagdev Singh[2], Richa Sharma[3]
and Virendra Singh Chouhan[4]

December 26, 2022

Abstract

This paper presents the tripled system of differential equations of fractional type with fractional integral boundary conditions as well as integer and fractional derivative. Here the Banach fixed points theorem and Scheafer's fixed points theorem are used as a main tool. To justify the results we illustrate some examples.

Key Words and Phrases: Fixed points theorem, Banach fixed point, Fractional differential equations, Fractional integral boundary conditions.

2010 AMS Subject Classification: 47H10, 26A33.

1

1 Introduction

Fractional differential equation are applicable in many streams of science and engineering like as fitting of experimental data, e electromagnetics, physics, viscoelasticity, lectro chemistry, biophysics, blood flow phenomena,porous media,biology, electrical circuits, etc. Therefore compare to models of integer order, fractional order model become more practical and realistic. Thus there has been

---

[1] Corresponding author: [4]Virendra Singh Chouhan,
[1,4]Department of Mathematics and Statistics, Manipal University Jaipur, Rajasthan
[1]Email-ashokkumarbadsra1995@gmail.com
[2]Department of Mathematics, JECRC University, Jaipur (Rajasthan)
Email- jagdevsingh05@gmail.com
[3]Department of Mathematics, Chandigarh University, Mohali (Punjab)
Email-richa.tuknait@gmail.com
[4]Email-darbarvsingh@yahoo.com(Corresponding Author)

a significant developments in problems of boundary value for the existence and uniqueness of fractional differential equations; see [1, 4, 5, 6, 8, 9, 10, 12]. and the references therein. Many authors have worked on existence and uniqueness of solution of tripled system of fractional differential equations [2, 3, 7, 11, 13, 14]. The tripled systems of fractional differential equation often exits in numerous models such as Chemostats and Microorganism Culturing, Brine Tanks, Irregular Heartbeats, Chemical Kinetics, Lidocaine and Pesticides, Predator Prey etc. [8] study fractional differential equations for Boundary value problems of nonlinear type and include nonlocal and integral boundary condition of fractional type. Inspired by the problem [9],

$$\begin{cases} {}^{C}D^{a_1}x_1(\alpha) = e_1(\alpha, x_2(\alpha), x_3(\alpha)), \alpha \in [0,1] \\ {}^{C}D^{a_2}x_2(\alpha) = e_2(\alpha, x_1(\alpha), x_3(\alpha)), \alpha \in [0,1] \\ {}^{C}D^{a_1}x_3(\alpha) = e_3(\alpha, x_1(\alpha), x_2(\alpha)), \alpha \in [0,1] \\ x_1(0) = x_1'(0) = x_1"(0) = 0, \\ {}^{C}D^{p_1}x_1(1) = \gamma_1(J^{q_1}x_1)(1), \\ x_2(0) = x_2'(0) = x_2"(0) = 0, \\ {}^{C}D^{p_2}x_2(1) = \gamma_2(J^{q_2}x_2)(1) \\ x_3(0) = x_3'(0) = x_3"(0) = 0, \\ {}^{C}D^{p_3}x_3(1) = \gamma_3(J^{q_3}x_3)(1) \end{cases}$$

Where ${}^{C}D^{a_i}$ Caputo fractional derivative with order a_i, J^q represent the Riemann-Liouville fractional integral whose order $a_1, a_2 \in (4,5]$, $p_1, p_2, p_3 \in (0,4]$ $q_1, q_2, q_3 > 0, e_1, e_2, : [0,1] \times R \to R$ are smooth functions and $\gamma_i \neq \frac{\Gamma(q_i+5)}{\Gamma(5-p_i)}, i = 1, 2, 3$. Existence and uniqueness of solution for the mentioned above tripled system of nonlinear fractional order differential equations is main focus of the paper.

2 Preliminaries

Firstly we introduce some notation, lemmas and definitions.
Definition 2.1 [6] Caputo derivative whose fractional order is a for smooth function $e : [0, \infty) \to R$ is define as

$${}^{C}D^{a}e(\alpha) = \frac{1}{\Gamma(n-a)} \int_0^{\alpha} (\alpha - t)^{n-a-1} e^{(n)}(t)dt$$

gives $e(n)(\alpha)$ exist, where [a] represents the integer part of the real number a and Γ is the Euler's Gamma function.
Definition 2.2 [12] Riemann-Liouville fractional integral of the order $a > 0$ for a smooth function

$$J^{a}e(\alpha) = \frac{1}{\Gamma(a)} \int_0^{\alpha} (\alpha - t)^{a-1} e(t)dt.$$

Lemma 2.1 [2] Let $f, g > 0$ and $e \in L_1[a,b]$ then $J^f J^g e = J^{f+g} e$

Lemma 2.2 [**2**] If e is continuous and $n \geq 0$, then

$$^{C}D^{n}J^{n}e = e$$

It follows from Lemmas 2.1 and 2.2 that if e is continuous and $\gamma > a$, then $^{C}D^{a}e = J^{\gamma-a}e$.

Lemma 2.3 [**2**] Let $\gamma > -1$ and $n > 0$. Then

$$J^{n}z^{\gamma} = \frac{\Gamma(\gamma+1)}{\Gamma(n+\gamma+1)}z^{n+\gamma}$$

Lemma 2.4 [**2**] Let $\gamma \geq 0$ and $m = [n]+1$, then

$$^{C}D^{n}x^{\gamma} = \begin{cases} 0, & \text{if} \gamma \in 0,1,2,\dots m-1 \\ \frac{\Gamma(\gamma+1)}{\Gamma(\gamma+1-n)}(z-a)^{\gamma-n}, & \text{if} \gamma \epsilon N \text{and} \gamma \geq m \\ & \text{or} \gamma \notin N, \gamma > m-1 \end{cases}$$

Lemma 2.5 [**7**] Let $a > 0$ then,

$$J^{a C}D^{a}V(\alpha) = V(\alpha) + h_0 + h_1\alpha + h_2\alpha^2 + \cdots + h_{n-1}\alpha^{n-1}$$

for some $h_i \in \mathbb{R}, i = 0,1,2,\dots n-1$, n is smallest integer grater than or equal to a.

3 Supporting Result

In this part, we establish the result required in our main proofs.

Lemma 3.1 Let $y \in H([0,1],\mathbb{R})$ and $\gamma \neq \frac{\Gamma(q+5)}{\Gamma(5-p)}$. Then the problem

$$\begin{cases} ^{C}D^{a}x(\alpha) = y(\alpha)\alpha \in [0,1] \\ x(0) = x'(0) = x''(0) = x'''(0) = 0,^{C} D^{p}x(1) = \gamma(J^{q}x)(1) \end{cases} \tag{3.1}$$

has unique solution

$$\begin{aligned} x(\alpha) &= \frac{1}{\Gamma a}\int_0^{\alpha}(\alpha-t)^{\alpha-1}y(t)dt \\ -\frac{\gamma\Gamma(5-p)\Gamma(5+q)\alpha^3}{24\Gamma(a-p)[\gamma\Gamma(5-p)-\Gamma(q+4)}&\int_0^1(1-t)^{q+a-1}y(t)dt \\ +\frac{\Gamma(5-p)\Gamma(q+5)\alpha^3}{24\Gamma(a-p)[\gamma\Gamma(5-p)-\Gamma(q+5)]}&\int_0^1(1-t)^{a-p-1}y(t)dt \end{aligned} \tag{3.2}$$

Proof: From Lemma 2.2, (3.2) is similar to

$$x(\alpha) = J^{a}y(\alpha) - h_0 - h_1\alpha - h_2\alpha^2 - h_3\alpha^3 - h_4\alpha^4 \tag{3.3}$$

3

for some $h_i \in \mathbb{R}, i$ from $0to4$.
from $x(0) = 0$ it follows $h_0 = 0$ also $x'(0) = 0 \implies h_1 = 0, x''(0) = 0 \implies h_2 = 0$ and $x'''(0) = 0 \implies h_3 = 0$. Thus (3.3) becomes

$$x(\alpha) = J^a y(\alpha) - h_4 \alpha^4 \tag{3.4}$$

Now

$$({}^C D^p x) = J^{a-p} y(\alpha) - c_4 \frac{\Gamma 5}{\Gamma(5-p)} \alpha^{4-p}$$
$$J^q x(\alpha) = J^{p+q} y(\alpha) - c_4 \frac{\Gamma 5}{\Gamma(5+q)} \alpha^{4+q}$$

From the boundary condition,

$$\begin{aligned} &({}^C D^p x)(1) = (J^q x)(1) \\ \implies & J^{a-p} y(1) - c_4 \frac{\Gamma 5}{\Gamma(5-p)} = \gamma J^{p+q} y(1) - c_4 \frac{\Gamma 5}{\Gamma(5+q)} \\ \implies & c_4 \left[\frac{\Gamma 5(\gamma \Gamma(5-p) - \Gamma(5+q))}{\Gamma(5+q)\Gamma(5-q)} \right] = \gamma J^{p+q} y(1) - J^{a-p} y(1) \\ \implies & c_4 = \frac{\Gamma(5-q)\Gamma(5+q)}{24(\gamma \Gamma(5-p) - \Gamma(5+q)} \left[\gamma J^{p+q} y(1) - J^{a-p} y(1) \right]. \end{aligned}$$

On substituting the value of c_4 in (3.4) we find solution (3.2). It clear from lemma (3) that solution of the tripled system (1.1) is given by the integral equation,

$$\begin{aligned} x_1(\alpha) &= \frac{1}{\Gamma a_1} \int_0^\alpha (\alpha - t)^{a_1 - 1} e_1(t, x_2(t), x_3(t)) dt \\ &- \frac{\gamma_1 R_1 \alpha^3}{24 \Gamma(q_1 + a_1)} \int_0^1 (1-t)^{q_1 + a_1 - 1} e_1(t, x_2(t), x_3(t)) dt \\ &+ \frac{R_1 \alpha^3}{\Gamma(a_1 - p_1)} \int_0^1 (1-t)^{a_1 - p_1 - 1} e_1(t, x_2(t), x_3(t)) dt \end{aligned}$$

$$\begin{aligned} x_2(\alpha) &= \frac{1}{\Gamma a_2} \int_0^\alpha (\alpha - t)^{a_2 - 1} e_2(t, x_2(t), x_3(t)) dt \\ &- \frac{\gamma_2 R_2 \alpha^3}{24 \Gamma(q_2 + a_2)} \int_0^1 (1-t)^{q_2 + a_2 - 1} e_2(t, x_2(t), x_3(t)) dt \\ &+ \frac{R_2 \alpha^3}{\Gamma(a_2 - p_2)} \int_0^1 (1-t)^{a_2 - p_2 - 1} e_2(t, x_2(t), x_3(t)) dt \end{aligned}$$

$$\begin{aligned} x_3(\alpha) &= \frac{1}{\Gamma a_3} \int_0^\alpha (\alpha - t)^{a_3 - 1} e_3(t, x_2(t), x_3(t)) dt \\ &- \frac{\gamma_3 R_3 \alpha^3}{24 \Gamma(q_3 + a_3)} \int_0^1 (1-t)^{q_3 + a_3 - 1} e_3(t, x_2(t), x_3(t)) dt \\ &+ \frac{R_3 \alpha^3}{\Gamma(a_3 - p_3)} \int_0^1 (1-t)^{a_3 - p_3 - 1} e_3(t, x_2(t), x_3(t)) dt \end{aligned}$$

Where

$$R_i = \frac{\Gamma(5-p_i)\Gamma(q_i+5)}{\gamma_i\Gamma(5-p_i)-\Gamma(q_i+4)},$$

for i =1, 2, 3.
Let $X = H[0,1]$ then $(X, \|.\|_X)$ is Banach space fit out with the norm.

$$\|X\|_X = (sup|x(\alpha)|\colon \alpha \in [0,1])$$

Let $B = X \times X \times X$ then $(B, \|.\|_B)$ is also a Banach space equipped with the norm.

$$\|(x_1, x_2, x_3)\|_B = \|x_1\|_X + \|x_2\|_X + \|x_3\|_X$$

Let us define an operation $F : B \to B$

$$\begin{aligned} f(x_1,x_2,x_3)(\alpha) = (f_1x_2(\alpha)x_3(\alpha), f_2x_1(\alpha)x_3(\alpha),\\ f_3x_1(\alpha)x_2(\alpha)\end{aligned}$$

Where

$$\begin{aligned}
f_1x_2(\alpha)x_3(\alpha) &= \frac{1}{\Gamma a_1}\int_0^\alpha (\alpha-t)^{a_1-1}e_1(t,x_2(t),x_3(t))dt\\
&-\frac{\gamma_1R_1\alpha^3}{24\Gamma(q_1+a_1)}\int_0^1(1-t)^{q_1+a_1-1}e_1(t,x_2(t),x_3(t))dt\\
&+\frac{R_1\alpha^3}{\Gamma(a_1-p_1)}\int_0^1(1-t)^{a_1-p_1-1}e_1(t,x_2(t),x_3(t))dt\\
f_2x_1(\alpha)x_3(\alpha) &= \frac{1}{\Gamma a_2}\int_0^\alpha (\alpha-t)^{a_2-1}e_2(t,x_2(t),x_3(t))dt\\
&-\frac{\gamma_2R_2\alpha^3}{24\Gamma(q_2+a_2)}\int_0^1(1-t)^{q_2+a_2-1}e_2(t,x_2(t),x_3(t))dt\\
&+\frac{R_2\alpha^3}{\Gamma(a_2-p_2)}\int_0^1(1-t)^{a_2-p_2-1}e_2(t,x_2(t),x_3(t))dt\\
f_3x_1(\alpha)x_2(\alpha) &= \frac{1}{\Gamma a_3}\int_0^\alpha (\alpha-t)^{a_3-1}e_3(t,x_2(t),x_3(t))dt\\
&-\frac{\gamma_3R_3\alpha^3}{24\Gamma(q_3+a_3)}\int_0^1(1-t)^{q_3+a_3-1}e_3(t,x_2(t),x_3(t))dt\\
&+\frac{R_3\alpha^3}{\Gamma(a_3-p_3)}\int_0^1(1-t)^{a_3-p_3-1}e_3(t,x_2(t),x_3(t))dt
\end{aligned}$$

We see fixed point of F are solution of tripled system(1.1). To simplify and our convenience we put.

$$\Lambda_i = \frac{1}{\Gamma(a_i+1)} + \frac{\gamma|R_i|}{24\Gamma(q_i+a_i+1)} + \frac{|R_i|}{24\Gamma(a_i-p_i+1)}$$

for i = 1, 2, 3

4 Main Theorem

We will use well know Banach fixed points theorem to prove our first result.
Theorem 4.1 Suppose that $\gamma_i \neq \frac{\Gamma(q_i+5)}{\Gamma(5-p_i)}, i = 1, 2, 3$ and the following hypothesis holds. (H 1) Assume that a non-negative continuous functions $k_i \in C[0,1], i = 1, 2$ exist such that

$$\begin{aligned}|e_i(\alpha, y_1) - e_i(\alpha, y_2)| &\leq k_i(\alpha)|y_1 - y_2|\\ |e_i(\alpha, y_2) - e_i(\alpha, y_3)| &\leq k_i(\alpha)|y_2 - y_3|\\ |e_i(\alpha, y_3) - e_i(\alpha, y_1)| &\leq k_i(\alpha)|y_3 - y_1|\\ &\forall y_1, y_2, y_3 \in \mathbb{R}\text{and}\forall\alpha \in [0,1]\end{aligned}$$

with $I_i = \sup k_i(\alpha) i = 1, 2, 3\ \alpha \in [0,1]$ and $I = \underset{i}{max} I_i$ and if $I(\eta_1 + \eta_2 + \eta_3) < 1$ where $\eta_i, i = 1, 2, 3$ and defined by (7) then on $[0,1]$ the tripled system (1) has a unique. We shall show F is contraction.
Proof. Let $(x_1, x_2, x_3), (x_1', x_2', x_3') \in B$ then $\forall\alpha \in [0,1]$

$$\begin{aligned}|f_1(x_2)(x_3)(\alpha) - f_1(x_2')(x_3')(\alpha)| &\leq \frac{1}{\Gamma a_1}\int_0^\alpha (\alpha - t)^{a_1 - 1}\\ |e_1(t, x_2(t), x_3(t) - e_1(t, x_2'(t), x_3'(t)|dt &+ \frac{|R_1|\gamma_1}{24\Gamma(q_1 + a_1)}\\ \int_0^1 (1-t)^{q_1 + a_1 - 1}|e_1(t, x_2(t), x_3(t) &- e_1(t, x_2'(t), x_3'(t)|dt\\ +\frac{|R_1|}{\Gamma(a_1 - p_1)}\int_0^1 (1-t)^{a_1 - p_1 - 1}&|e_1(t, x_2(t), x_3(t)\\ &-e_1(t, x_2'(t), x_3'(t)|dt\\ \leq I\|x_2x_3 - x_2'x_3'\|\Bigg[\frac{1}{\Gamma a_1}\int_0^\alpha (\alpha-t)^{a_1-1}dt &+ \frac{|R_1|\gamma_1}{24\Gamma(q_1 + a_1)}\\ \int_0^1 (1-t)^{q_1+a_1-1}dt + \frac{|R_1|}{\Gamma(a_1-p_1)}&\int_0^1 (1-t)^{a_1-p_1-1}dt\Bigg]\\ \leq \|x_2x_3 - x_2'x_3'\|\times\left[\frac{1}{\Gamma a_1} + \frac{|R_1|}{24\Gamma(q_1+a_1)} \right.&\left.+ \frac{|R_1|\gamma_1}{\Gamma(a_1-p_1)}\right]\end{aligned}$$

Thus

$$\|f_1(x_2)(x_3) - f_1(x_2')(x_3')\| \leq I\eta_1\|x_2x_3 - x_2'x_3'\|_x$$

Similarly

$$\|f_2(x_1)(x_3) - f_2(x_1')(x_3') \leq I\eta_2\|x_1x_3 - x_1'x_3'\|$$

and

$$\|f_2(x_1)(x_2) - f_2(x_1')(x_2') \leq I\eta_2\|x_1x_2 - x_1'x_2'\|$$

$$\|f(x_1,x_2,x_3)-f(x_1',x_2',x_3')\|_B\leq$$
$$I(\eta_1+\eta_2+\eta_3)\|(x_1,x_2,x_3)-(x_1',x_2',x_3')\|_B$$

As $I(\eta_1+\eta_2+\eta_3)<1$ therefore f is a contradiction and by Banach fixed point result, f must have unique fixed point i.e. the tripled system (1.1) has unique solution.

Theorem 4.2 Assume $\gamma_i \neq \frac{\Gamma(q_i+5)}{\Gamma(5-p_i)}, i=1,2,3$ and the following hypothesis holds.

(H 2) there exist non negative continuous function $l_1,l_2,l_3 \in C[0,1]$ such that $|e_i(\alpha,y)|\leq l_i(\alpha)$ $\forall y\in\mathbb{R}$ and $\forall\alpha\in[0,1]$ with $L_i=\underset{\alpha\in[0,1]}{sup}\, l_i(\alpha), i=1,2,3.$

Then the tripled system (1.1) defined on [0, 1] has at least one solution

Proof: To prove this result we take help of Schaefer fixed point theorems.

Step-1 F is smooth.

Since e_1,e_2 and e_3 are smooth therefore f is also smooth.

Step-2 Under the mapping f bounded set of B are mapped into bounded sets of B.

Let $\omega_\xi=(x_1,x_2,x_3)\in B; \|(x_1,x_2,x_3)\|_B\leq\xi$

where $\xi>0$ Now for $(x_1,x_2,x_3)\in\omega_\xi$ and $\forall\alpha\in[0,1]$

$$\begin{aligned}
|f_1(x_1)(x_2)(x_3)|\leq & \frac{1}{\Gamma a_1}\int_0^\alpha(\alpha-t)^{a_1-1}|e_1(t,x_2(t),x_3(t)|dt \\
&+\frac{|R_1|\gamma_1}{24\Gamma(q_1+a_1)}\int_0^1(1-t)^{q_1+a_1-1}|e_1(t,x_2(t),x_3(t)|dt \\
&+\frac{|R_1|}{\Gamma(a_1-p_1)}\int_0^1(1-t)^{a_1-p_1-1}|e_1(t,x_2(t),x_3(t)|dt \\
&\leq \omega_1\left[\frac{1}{\Gamma a_1}\int_0^\alpha(\alpha-t)^{a_1-1}dt+\frac{|R_1|\gamma_1}{24\Gamma(q_1+a_1)}\right. \\
&\left.\int_0^1(1-t)^{q_1+a_1-1}dt+\frac{|R_1|}{\Gamma(a_1-p_1)}\int_0^1(1-t)^{a_1-p_1-1}dt\right] \\
&\leq \omega_1\left[\frac{1}{\Gamma a_1}+\frac{|R_1|\gamma_1}{24\Gamma(q_1+a_1)}+\frac{|R_1|}{\Gamma(a_1-p_1)}\right]
\end{aligned}$$

Thus

$$\|f_1(x_2)(x_3)\|_X\leq\omega_1\eta_1$$

similar

$$\|f_1(x_1)(x_3)\|_X\leq\omega_2\eta_2$$

and

$$\|f_1(x_1)(x_2)\|_X\leq\omega_3\eta_3$$

$$\implies \|f_1(x_1,x_2,x_3)\|_X\leq\omega_1\eta_1+\omega_2\eta_2+\omega_3\eta_3$$

i.e. $\|f_1(x_1,x_2,x_3)\|_X \leq \infty$ Step-3. $F : B \to B$ is completely continuous operator. Let $(x_1,x_2,x_3) \in \omega_\xi$ and $\alpha_1,\alpha_2,\alpha_3 \in [0,1]$ with $\alpha_1 < \alpha_2 < \alpha_3$, then

$$|f_1(x_2)(\alpha_2) - f_1(x_2)(\alpha_1)| \leq \frac{\omega_1}{\Gamma a_1}\int_0^{\alpha_1}\left[(\alpha_2-t)^{a_1-1} - (\alpha_1-t)^{a_1-1}\right]dt$$
$$+\frac{\omega_1}{\Gamma a_1}\int_0^{\alpha_1}(\alpha_2-t)^{a_1-1} + \frac{\omega_1\gamma_1|R_1|\|\alpha_2^3-\alpha_1^3\|}{24\Gamma(q_1+a_1)}\int_0^1(1-t)^{q_1+a_1-1}dt$$
$$+\frac{\omega_1\gamma_1|R_1|\|\alpha_2^3-\alpha_1^3\|}{24\Gamma(q_2-p_1)}\int_0^1(1-t)^{a_1-p_1-1}dt \leq \frac{\omega_1}{\Gamma(a_1+1)}\left[(\alpha_2-\alpha_1)^{a_1}\right. \tag{4.1}$$
$$\left.+(\alpha_2^{a_1}-\alpha_1^{a_1})\right] + \frac{(\alpha_2-\alpha_1)^{a_1}}{\Gamma(a_1+1)} + \frac{\omega_1\gamma|R_1|\|\alpha_2^3-\alpha_1^3\|}{24\Gamma(q_1+a_1+1)} + \frac{\omega|R_1|\|\alpha_2^3-\alpha_1^3\|}{24\Gamma(a_1-p_1+1)} \tag{4.2}$$

right- hand side tends to zero when $\alpha_1 \to \alpha_2$.
Thus $\|f_1x_2(\alpha_2) - f_1x_2(\alpha_1)\|_X \to 0$ as $\alpha_1 \to \alpha_2$.
Similarly $\|f_2x_1(\alpha_2) - f_2x_1(\alpha_1)\|_X \to 0$ as $\alpha_1 \to \alpha_2$
$\|f_3x_1(\alpha_2) - f_3x_1(\alpha_1)\|_X \to 0$ as $\alpha_1 \to \alpha_2$.
Thus $\|f(x_1,x_2,x_3)(\alpha_2) - f(x_1,x_2,x_3)(\alpha_1)\|_B \to 0$ as $\alpha_1 \to \alpha_2$
Similarly $\|f(x_1,x_2,x_3)(\alpha_3) - f(x_1,x_2,x_3)(\alpha_1)\|_B \to 0$ as $\alpha_1 \to \alpha_3$
Combining step 1 to 3 and by reaction of Arzela - Ascoli theorem, $F : B \to B$ is completely continuous operation.
Step-4
Let

$$\psi = \{(x_1,x_2,x_3) \in B : (x_1,x_2,x_3) = \phi F(x_1,x_2,x_3)$$

for some $\phi \in (0,1)$ we shall show that set ψ is bounded. Let $(x_1,x_2,x_3) \in \psi \implies (x_1,x_2,x_3)(\alpha) = \phi f(x_1,x_2,x_3)(\alpha)$ for some $\phi \in (0,1)$. Then we have

$$\begin{aligned} x_1(\alpha) &= \phi f_1x_2x_3(\alpha) \\ x_2(\alpha) &= \phi f_2x_2x_3(\alpha) \\ x_3(\alpha) &= \phi f_3x_2x_3(\alpha), \forall\alpha \in [0,1] \end{aligned}$$

$$\|x_1(\alpha)\| = |\phi f_1x_2x_3(\alpha)| \leq \phi\omega_1\left[\frac{1}{\Gamma a_1}\int_0^\alpha(\alpha-t)^{a_1-1}dt\right.$$
$$+\frac{\gamma_1|R_1|}{24\Gamma(q_1+a_1)}\int_0^1(1-t)^{q_1+a_1-1}dt + \frac{|R_1|}{24\Gamma(a_1-p_1)}$$
$$\left.\int_0^1(1-t)^{a_1-p_1-1}dt\right]$$
$$\leq \omega_1\left[\frac{1}{\Gamma(a_1+1)} + \frac{\gamma_1|R_1|}{24\Gamma(q_1+a_1+1)} + \frac{|R_1|}{24\Gamma(a_1-p_1+1)}\right] \tag{4.3}$$

Thus

$$\|x_1\|_X \leq \omega_1\eta_1$$

Similarly

$$\|x_2\|_X \leq \omega_2\eta_2$$

and

$$\|x_3\|_X \leq \omega_3\eta_3$$

Hence, we get

$$\begin{aligned} \|(x_1,x_2,x_3)\|_X &\leq \omega_1\eta_1+\omega_2+\omega_3\eta_3\eta_2 \\ \|(x_1,x_2,x_3)\|_B &\leq \infty \end{aligned}$$

Thus Scheafer's fixed point result present ϕ is bounded set. f must have minimum one fixed point which is solution of tripled system (1.1).

Example 4.1. Take the following tripled system

$$\begin{cases} {}^C D^{\frac{17}{4}} x_1(\alpha) = \frac{1}{\alpha^2+16}\frac{|x_2(\alpha)x_3(\alpha|)}{1+|x_2(\alpha)x_3(\alpha)|} \\ {}^C D^{\frac{9}{2}} x_2(\alpha) = \frac{1}{\alpha^2+25}\tan^{-1}(x_1(\alpha)x_3(\alpha)), \alpha\in[0,1] \\ {}^C D^{\frac{13}{2}} x_3(\alpha) = \frac{1}{\alpha^2+49}\cot^{-1}(x_1(\alpha)x_3(\alpha)), \alpha\in[0,1] \\ x_1(0)=x_1'(0)=x_1''(0)=0, {}^C D^{\frac{1}{2}}x_1(1)=\frac{15}{16}(J^{\frac{5}{2}}x_1)(1) \\ x_2(0)=x_2'(0)=x_2''(0)=0, {}^C D^{\frac{3}{2}}x_2(1)=\frac{16}{17}(J^{\frac{7}{2}}x_2)(1) \\ x_3(0)=x_3'(0)=x_3''(0), {}^C D^{\frac{4}{3}}x_3(1)=\frac{17}{18}(J^{\frac{9}{2}}x_3)(1) \\ a_1=\frac{17}{4}, p_1=\frac{1}{2}, q_1=\frac{5}{2}, \gamma_1=\frac{15}{16}\neq\frac{\Gamma(q_1+5)}{\Gamma(5-p_1)}=160.875 \\ a_2=\frac{9}{2}, p_2=\frac{3}{2}, q_2=\frac{7}{2}, \gamma_2=\frac{16}{7}\neq\frac{\Gamma(q_2+5)}{\Gamma(5-p_2)}=422.96 \\ a_3=\frac{13}{2}, p_3=\frac{4}{3}, q_3=\frac{9}{2}, \gamma_3=\frac{17}{8}\neq\frac{\Gamma(q_3+5)}{\Gamma(5-p_3)}=4558.125 \end{cases} \tag{4.4}$$

for $\alpha\in[0,1]$ and $y_1,y_2,y_3\in\mathbb{R}$.

$$|e_i(\alpha,y_1)-e_i(\alpha,y_2)| \leq \frac{1}{\alpha^2+16}|y_1-y_2|$$

$$|e_i(\alpha,y_2)-e_i(\alpha,y_3)| \leq \frac{1}{\alpha^2+25}|y_2-y_3|$$

$$|e_i(\alpha,y_3)-e_i(\alpha,y_1)| \leq \frac{1}{\alpha^2+49}|y_3-y_1|$$

So, we can take $K_1=\frac{1}{\alpha^2+16}, K_2=\frac{1}{\alpha^2+25}, K_3=\frac{1}{\alpha^2+49}$

$$I_1 = \underset{\alpha\in[0,1]}{sup}\ K_1(\alpha) = \frac{1}{16}$$

$$I_2 = \underset{\alpha\in[0,1]}{sup}\ K_2(\alpha) = \frac{1}{25}$$

$$I_3 = \underset{\alpha\in[0,1]}{sup}\ K_3(\alpha) = \frac{1}{49}$$

and then, we have

$$I = \max\{I_1, I_2, I_3\} = \frac{1}{16}$$

Further,

$$\begin{aligned}
|R_1| &= \frac{\Gamma(5-p_1)\Gamma(q_1+5)}{|\Gamma(5-p_1)-\Gamma(q_1+5)|} = \frac{2786582\sqrt{\pi}}{1467322} = 3.37 \\
|R_2| &= \frac{\Gamma(5-p_2)\Gamma(q_2+5)}{|\Gamma(5-p_2)-\Gamma(q_2+5)|} = \frac{8968428\sqrt{\pi}}{9624241} = 1.65 \\
|R_3| &= \frac{\Gamma(5-p_3)\Gamma(q_3+5)}{|\Gamma(5-p_3)-\Gamma(q_3+5)|} = \frac{7525863\sqrt{\pi}}{9569341} = 1.39 \\
I\eta_1 &= I\left[\frac{1}{\Gamma(a_1+1)} + \frac{\alpha_1|R_1|}{24\Gamma(q_1+a_1+1)} + \frac{R_1}{24\Gamma(a_1-p_1+1)}\right] \\
&= \frac{1}{16}[0.078+0.0034+0.0007] \\
&= \frac{1}{16}[0.08211] \\
&= 0.00513 \\
I\eta_2 &= I\left[\frac{1}{\Gamma(a_2+1)} + \frac{\alpha_2|R_2|}{24\Gamma(q_2+a_2+1)} + \frac{R_2}{24\Gamma(a_2-p_2+1)}\right] \\
&= \frac{1}{16}[0.4357+0.0046+0.0036] \\
&= \frac{1}{16}[0.44066] \\
&= 0.027 \\
I\eta_3 &= I\left[\frac{1}{\Gamma(a_3+1)} + \frac{\alpha_3|R_3|}{24\Gamma(q_3+a_3+1)} + \frac{R_3}{24\Gamma(a_3-p_3+1)}\right] \\
&= \frac{1}{16}[0.00742+0.0000127+0.00332] \\
&= \frac{1}{16}[0.010752] \\
&= 0.005376
\end{aligned}$$

and then

$$I(\eta_1+\eta_2+\eta_3) = 0.005131 + 0.027 + 0.005376 = 0.0375087 < 1$$

Hence all assumptions of Theorem 4.1 are justify and consequently the tripled system (4.4) must have unique solution defined on $[0, 1]$.

Example 4.2. Now consider the following tripled system

$$\begin{cases} {}^{C}D^{\frac{5}{2}}x_1(\alpha) = \frac{\cos x_2 x_3(\alpha)}{7+\alpha} \\ {}^{C}D^{\frac{11}{4}}x_2(\alpha) = \frac{\sin x_1 x_3(\alpha)}{4+\alpha^2} \\ {}^{C}D^{\frac{17}{4}}x_3(\alpha) = \frac{\cos 2\pi x_2 x_3(\alpha)}{7+\alpha^3} \\ x_1(0) = x_1'(0) = x_1'''(0) = 0, {}^{C}D^{\frac{1}{2}}x_1(1) = \frac{13}{4}(J^{\frac{13}{2}}x_1)(1) \\ x_2(0) = x_2'(0) = x_2'''(0) = 0, {}^{C}D^{\frac{3}{2}}x_2(1) = \frac{9}{8}(J^{\frac{9}{2}}x_2)(1) \\ x_3(0) = x_3'(0) = x_3'''(0), {}^{C}D^{\frac{5}{2}}x_3(1) = \frac{6}{7}(J^{\frac{7}{2}}x_3)(1) \\ a_1 = \frac{5}{2}, p_1 = \frac{1}{2}, q_1 = \frac{13}{2}, \alpha_1 = \frac{13}{4} \neq \frac{\Gamma(q_1+5)}{\Gamma(5-p_1)} = 1023014.17 \\ a_2 = \frac{11}{4}, p_2 = \frac{3}{2}, q_2 = \frac{9}{2}, \alpha_2 = \frac{9}{8} \neq \frac{\Gamma(q_2+5)}{\Gamma(5-p_2)} = 35.895.23 \\ a_3 = \frac{17}{4}, p_3 = \frac{5}{2}, q_3 = \frac{7}{2}, \alpha_3 = \frac{6}{7} \neq \frac{\Gamma(q_3+5)}{\Gamma(5-p_3)} = 10557.42 \end{cases} \tag{4.5}$$

for $\alpha \in [0,1]$ and $B \in R$, we get

$$|e_1(\alpha, B)| = |\frac{\cos B}{7+\alpha}| \leq \frac{1}{7+\alpha}$$
$$|e_2(\alpha, B)| = |\frac{\sin B}{4+\alpha^2}| \leq \frac{1}{4+\alpha^2}$$
$$|e_3(\alpha, B)| = |\frac{\cos 2\pi B}{7+\alpha}| \leq \frac{1}{9+\alpha^3}$$

so we can take $l_1(\alpha) = \frac{1}{7+\alpha}, l_2(\alpha) = \frac{1}{4+\alpha^2}, l_3(\alpha) = \frac{1}{9+\alpha^3}$ and then, we have

$$w_1 = \underset{\alpha\in[0,1]}{sup}\ l_1(\alpha) = \frac{1}{7}$$
$$w_2 = \underset{\alpha\in[0,1]}{sup}\ l_2(\alpha) = \frac{1}{4}$$
$$w_3 = \underset{\alpha\in[0,1]}{sup}\ l_3(\alpha) = \frac{1}{9}$$

Hence all assumption of Theorem 4.2 are satisfied therefor the tripled solution (4.5).

Acknowledgement

For the helpful comments and suggestions the authors of the manuscript express sincere thanks to the editors and reviewers.

References

[1] S. Sunder, S. Bhatter, K. Jangid, S.D. Purohit, *Fractionalized mathematical models for drug diffusion*, Chaos, Solitons and Fractals, Volume 165, https://doi.org/10.1016/j.chaos.2022.112810.

[2] K. Diethelm, N. J. Ford, *Analysis of fractional differential equations*, Journal of Mathematical Analysis and Applications 265 (2) (2002) 229–248.

[3] V. Gafiychuk, B. Datsko, V. Meleshko, D. Blackmore, *Analysis of the solutions of coupled nonlinear fractional reaction diffusion equations*, Chaos Solitons and Fractals 41 (3) (2009) 1095–1104.

[4] A. Guezane-Lakoud, R. Khaldi, *Solvability of a three-point fractional nonlinear boundary value problem*, Differential Equations and Dynamical Systems 4 (20) (2012) 395–403.

[5] M. Houas, M. Benbachir, *Existence solutions for three point boundary value problem for differential equations*, J. Fract. Calc. Appl 6 (1) (2015) 160–174.

[6] R. W. Ibrahim, A. Killcman, F. H. Damag, *Existence and uniqueness for a class of iterative fractional differential equations*, Advances in Difference Equations 2015 (1) (2015) 1–13.

[7] A. Kilbas, A. Anatoli, H. Srivastava, and J. Juan, *Theory and applications of fractional differential equation*, Elsvier Publication 204, 2006.

[8] A. K. Nain, R. K. Vats, S. K. Verma, V. Sihag, *Existence of solutions of a non linear fractional differential equations with fractional derivative and fractional integral boundary conditions*,Advances and Applications in Mathematical Sciences 18 (1) (2018) 75–84.

[9] S. K. Ntouyas, *Boundary value problems for nonlinear fractional differential equations and inclusions with nonlocal and fractional integral boundary conditions*, Mathematica 33 (1) (2013) 117–138.

[10] J. Singh, A.M. Alshehri , S. Momani , S. Hadid,D. Kumar, *Computational Analysis of Fractional Diffusion Equations Occurring in Oil Pollution*, Mathematics. 2022; 10(20):3827. https://doi.org/10.3390/math10203827

[11] X.Su, *Boundary value problem for a coupled system of nonlinear fractional differential equations*,Applied Mathematics Letters 22 (1) (2009) 64–69.

[12] M. P. Yadav, R. Agarwal, S. D. Purohit, D. Kumar, D. L. Suthar, (2022) *Groundwater flow in karstic aquifer: analytic solution of dual-porosity fractional model to simulate groundwater flow*, Applied Mathematics in Science and Engineering, 30:1, 598-608, DOI: 10.1080/27690911.2022.2117913

[13] W. Yang *Positive solutions for a coupled system of nonlinear fractional differential equations with integral boundary conditions*, Computers and Mathematics with Applications 63 (1) (2012) 288–297.

[14] Y. Zhang, Z. Bai, T. Feng, *Existence results for a coupled system of nonlinear fractional three-point boundary value problems at resonance*, Computers and Mathematics with Applications 61 (4) (2011) 1032–1047.

J. COMPUTATIONAL ANALYSIS AND APPLICATIONS, VOL. 31, NO. 2, 2023, COPYRIGHT 2023 EUDOXUS PRESS, LLC

L^1-Convergence of Newly Defined Trigonometric Sums Under Some New Class of Fourier Coefficients

Priyanka, Karannvir Singh
Maharaja Ranjit Singh Punjab Technical University, Bathinda, India
priyanka.baghla@gmail.com

Tough difficulties in the trigonometric series convergence in L^1 norm is appearance of trigonometric series as Fourier series, and its L^1- convergence. Many academics investigated trigonometric series separately by examining the cosine & sine series , so as a result, modified cosine sums and sine sums were developed to assess the sharp consequences on trigonometric series's integrability & L^1-convergence, as improved sums approach respective limits closer than traditional trigonometric sums. This work presents 'KP', a new class of Fourier Coefficients, as well as advanced cosine and sine sums of trigonometric series with real coefficients. As a result, necessary & sufficient criterion for Integrability and L^1-normed convergence for trigonometric functions is achieved. Here, authors also discuss about L^1-convergence of r^{th} differential of newly defined improved trigonometric sums with Fourier coefficients are from an enlarged class KP_r.

Keywords: L^1- convergence; Integrability; Modified Sums; Dirichlet Kernel
Mathematics Subject Classifications: 42A20; 42A32

1 Introduction

Take a look at sine & cosine series

$$\sum_{\kappa=1}^{\infty} c_\kappa^* \sin \kappa y \tag{1.1}$$

$$\frac{c_0^*}{2} + \sum_{\kappa=1}^{\infty} c_\kappa^* \cos \kappa y \tag{1.2}$$

and these equations collectively written as

$$\sum_{\kappa=1}^{\infty} c_\kappa^* \psi y \tag{1.3}$$

where ψy is $\sin \kappa y$ or $\cos \kappa y$ respectively.
η^{th} sum of $\sum_{\kappa=1}^{\infty} c^*_\kappa \psi y$ is represented as $S_\eta(y)$. So $\lim_{\eta\to\infty} S_\eta(y) = Z(y)$.
Kano's[1] outcome is popularly known as sequence $\{c^*_\kappa\}$ fulfilling $\{c^*_\kappa\} \to 0$ as $\kappa \to \infty$ & $\sum_{\kappa=1}^{\infty} \kappa^2 |\Delta^2 \left(\frac{c^*_\kappa}{\kappa}\right)| < \infty$ then $\sum_{\kappa=1}^{\infty} c^*_\kappa \sin \kappa y$ and $\frac{c^*_0}{2} + \sum_{\kappa=1}^{\infty} c^*_\kappa \cos \kappa y$ are known to us as Fourier Series.

Definitions:

Convex Sequence: $\{c^*_\tau\}$ is called a convex sequence(seq.) satisfying

$$\Delta^2 c^*_\tau \geq 0, \quad \text{where} \quad \Delta c^*_\tau = c^*_\tau - c^*_{\tau+1} \quad \text{and} \quad \Delta^2 c^*_\tau = \Delta c^*_\tau - \Delta c^*_{\tau+1}.$$

Quasi-Convex Sequence([2],Vol.2, page 204): A seq. $\{c^*_\tau\}$ is called quasi-convex satisfying

$$\sum_{\tau=1}^{\infty} (\tau+1)|\Delta^2 c^*_\tau| < \infty.$$

Sequence $\{c^*_\tau\}$ is known as generalised quasi-convex satisfying

$$\sum_{\tau=1}^{\infty} \tau^{\varkappa} |\Delta^2 c^*_\tau| < \infty : \varkappa = 0, 1, 2, ...$$

'S' Class([4]: sequence $\{c^*_\tau\}$ follow class S by satisfying $c^*_\tau = 0(1)$, τ monotonically decreasing seq. converging to $0 \to \infty$ and $\exists$ a sequence $\{A^*_\tau\}$ s.t.
(a) A^*_τ is monotonically decreasing seq. converging to 0, as$\tau \to \infty$, (b) $\sum_{\tau=0}^{\infty} A^*_\tau < \infty$,
(c) $|\Delta c^*_\tau| \leq A^*_\tau \quad \forall \quad \tau$.
Convergence in L^1-norm: The series L^1-converges in (0,π) if $||f^* - S^*_\tau|| = o(1), \tau \to \infty$.
Young[5] began to work on this issue in 1913 by examining a class of convex seq., which was followed by Kolmogorov[6] in 1923 by addressing a general class of quasi-convex seq.Then Telyakovskii[4] analysed Sidon's significantly weaker class S rather than the previously defined classes for L^1- normed convergence(cgs.) of trigonometric series. Following theorems are famous about the L^1- normed cgs. of Fourier series:

Theorem 1.1:[2], Vol.2, page 204

If $\{c^*_\kappa\}$ is monotonically decreasing and $\{c^*_\kappa\}$ is convex/quasi-convex seq. , then necessary & sufficient condition for L^1-normed convergence of $\frac{c^*_0}{2} + \sum_{\kappa=1}^{\infty} c^*_\kappa \cos \kappa y$ is $c^*_\kappa \log \kappa = o(1) \quad \kappa \to \infty$.
Telyakovskˇii generalised Theorem 1.1 for expression (1.2) where the coefficients of series (1.2) satisfy the requirements of class S[7] as follows:

Theorem 1.2:[4]

When coefficients of $\frac{c_0^*}{2}+\sum_{\kappa=1}^{\infty}c_\kappa^*\cos\kappa y$ satisfying criterion of class S[7] then criterion of its L^1 convergence is that $c_\kappa^*\log\kappa=o(1)\quad\text{as}\quad\kappa\to\infty$

Many writers examined and generalised these findings by examining various generalisations of seq. classes.Recently,the coefficient seq. SJ[8] was introduced to study the integrability and L^1-cgs. of modified cosine and sine sums, which was further generalied by Krasniqi[9]. A contemporary class of Fourier coefficients is formulated in this study as:

Definition 1.3: A monotonically decreasing seq. $\{c_\eta^*\}$ with $c_\eta^*\to 0\quad\text{as}\quad\eta\to\infty$ is follow a new class KP if $\exists$ a seq. $\{A_\eta^*\}$ satisfying

$$(i)A_\eta^*\downarrow 0 \tag{1.4}$$

$$(ii)\sum\eta A_\eta^*<\infty \tag{1.5}$$

$$(iii)\left|\Delta\left(\frac{c_\eta^*}{\eta^2}\right)\right|\leq\frac{A_\eta^*}{\eta^2} \tag{1.6}$$

Here, coefficient sequence KP_r will be formulated that is enlargement of coefficient sequence KP.

Definition 1.4:: A monotonically decreasing seq. $\{c_\eta^*\}$ with $c_\eta^*\to 0\quad\text{as}\quad\eta\to\infty$ is from a new class KP_r if $\exists$ seq. $\{A_\eta^*\}$ satisfying

$$(i)A_\eta^*\downarrow 0 \tag{1.7}$$

$$(ii)\sum\eta^{r+1}A_\eta^*<\infty \tag{1.8}$$

$$(iii)\left|\Delta\left(\frac{c_\eta^*}{\eta^2}\right)\right|\leq\frac{A_\eta^*}{\eta^2} \tag{1.9}$$

Obviously, KP = KP_r when r = 0. It is obvious that $KP_{r+1}\subseteq KP_r$, but its reverse does not hold.

Example. Define $b_\eta=\frac{1}{\eta^{r+3}},$ r = 0,1,2,... Firstly we are going to demonstrate that$\{b_\eta\}\notin KP_{r+1}$

As, $b_\eta=\frac{1}{\eta^{r+3}}\to 0\quad\text{as}\quad\eta\to\infty$.

Let $\exists\ A_\eta=\frac{1}{\eta^{r+3}},r=0,1,2,3,...s.t.\sum\limits_{\eta=1}^{\infty}\eta^{r+2}A_\eta=\sum\limits_{\eta=1}^{\infty}\frac{1}{\eta}$ is divergent, means $\{b_\eta\}$ does not belong to KP_{r+1}.

But, A_η is monotonically decreasing and converging to 0 $\eta\to\infty$, &

$\sum\limits_{\eta=1}^{\infty}\eta^{r+1}A_\eta^*=\sum\limits_{\eta=1}^{\infty}\frac{1}{\eta^2}<\infty$,

Also $|\Delta(\frac{b_\eta}{\eta^2})|\leq\frac{A_\eta^*}{\eta^2},\forall\eta$.

Therefore, $\{b_\eta\}\in KP_r$.

2 Main Results:

Now we will give proof of the succeeding statement:

Theorem 2.1: If the coefficients of series (1.3) meet the class KP criteria, then it will be a Fourier series.

Explanation

$$\sum_{\kappa=1}^{\infty}\kappa^2\left|\Delta^2\left(\frac{c_\kappa^*}{\kappa}\right)\right| = \sum_{\kappa=1}^{\infty}\kappa^2\left|\Delta\left(\frac{c_\kappa^*}{\kappa}\right)-\Delta\left(\frac{c_{\kappa+1}^*}{\kappa+1}\right)\right|$$

$$= \sum_{\kappa=1}^{\infty}\kappa^2\left|\frac{c_\kappa^*}{\kappa}-\frac{c_{\kappa+1}^*}{\kappa+1}-\frac{c_{\kappa+1}^*}{\kappa+1}+\frac{c_{\kappa+2}^*}{\kappa+2}\right|$$

$$\left\{\begin{array}{ll} c_{\kappa+2}^*<c_{\kappa+1}^* \quad and \quad \kappa+2>\kappa+1 \quad \text{therefore} & \dfrac{1}{\kappa+2}<\dfrac{1}{\kappa+1} \\ & \Rightarrow \dfrac{c_{\kappa+2}^*}{\kappa+2}<\dfrac{c_{\kappa+1}^*}{\kappa+1} \end{array}\right\}$$

$$\le \sum_{\kappa=1}^{\infty}\kappa^2\left|\frac{c_\kappa^*}{\kappa}-\frac{c_{\kappa+1}^*}{\kappa+1}\right|$$

$$= \sum_{\kappa=1}^{\infty}\kappa^2\left|\kappa\frac{c_\kappa^*}{\kappa^2}-(\kappa+1)\frac{c_{\kappa+1}^*}{(\kappa+1)^2}\right|$$

$$< \sum_{\kappa=1}^{\infty}\kappa^3\left|\frac{c_\kappa^*}{\kappa^2}-\frac{c_{\kappa+1}^*}{\kappa+1^2}\right|$$

$$= \sum_{\kappa=1}^{\infty}\kappa^3\left|\Delta\left(\frac{c_\kappa^*}{\kappa^2}\right)\right|$$

$$\le \sum_{\kappa=1}^{\infty}\kappa^3\frac{A_\kappa^*}{\kappa^2} \quad \text{by} \quad \text{defined} \quad \text{class KP of Fourier Coefficients.}$$

$$= \sum_{\kappa=1}^{\infty}\kappa A_\kappa^*<\infty$$

As c_κ^* is null sequence, So by the result given by Kano[1], Theorem 1 holds. In this study, we provide latest improved trigonometric sums.

$$Z_\eta(y) = \tfrac{c_0^*}{2} + \sum_{\kappa=1}^{\eta}\left[\sum_{j=\kappa}^{\eta}\Delta\left(\tfrac{c_j^*\cos jy}{j^2}\right)\right]\kappa^2,$$

$$r_\eta(y) = \sum_{\kappa=1}^{\eta}\left[\sum_{j=\kappa}^{\eta}\Delta\left(\tfrac{c_j^*\sin jy}{j^2}\right)\right]\kappa^2.$$

Also investigated their L^1-convergence following the newly established class KP of coefficient sequences

Theorem 2.2: Suppose that coefficients of series (1.3) follow class KP, then

$$\lim_{\eta\to\infty} Z_\eta(y) = Z(y), exists \quad for \quad y \in (o,\pi] \tag{2.2.1}$$

$$Z(y) \in L^1(0,\pi] \tag{2.2.2}$$

$$||Z(y) - S_\eta(y)|| = o(1), \eta \to \infty \tag{2.2.3}$$

Theorem 2.3: If coefficients of a sequence (1.3) are from a class KPr, then

$$\lim_{\eta\to\infty} Z^r{}_\eta(y) = Z^r(y), exists \quad for \quad y \in (o,\pi] \tag{2.3.1}$$

$$Z^r(y) \in L^1(0,\pi], \qquad (r = 0,1,2,...) \tag{2.3.2}$$

$$||Z^r(y) - S^r{}_\eta(y)|| = o(1), \eta \to \infty. \tag{2.3.3}$$

3 Lemmas:

The subsequent lemmas are required to prove our main results.

Lemma 3.1[3]

Let $\eta \geq 1$ & $r \in \mathbb{Z}^+ \cup 0$, y $\in$ [s,π] So $|\tilde{D}^r_\eta(y)| \leq C_s \frac{\eta^r}{y}$ Where C_s is +ve constant rely upon s, 0<s<π & $\tilde{D}^r_\eta(y)$ is conjugate Dirichlet kernel.

Lemma 3.2[4]

Suppose $\{c^*_\eta\}$ is a sequence of $\Re$ s.t. $|c^*_\eta| \leq 1$ forall η. So the relation

$$\int_{\frac{\pi}{\eta+1}}^{\pi} |\sum_{\kappa=0}^{\eta} c^*_\kappa \tilde{D}_\kappa(y)|dy \leq N(\eta+1)$$

exists, where N is perfectly constant.
By Bernstein's inequality,

$$\int_{\frac{\pi}{\eta+1}}^{\pi} |\sum_{\kappa=0}^{\eta} c^*_\kappa \tilde{D}^r_\kappa(y)|dx \leq N(\eta+1)^{s+1} \quad \text{for s = 0,1,2,...}$$

lemma 3.3[3]

$||D^s_\eta(y)||_{L^1} = o(\eta^s \log\eta) + o(\eta^s)$, $\quad s = 0,1,2,....$, and $D^r_\eta(y)$ shows the r^{th} differentials of Dirichlet Kernel.

4 Proof of Main results:

4.1 Solution of theorem 2.1:

We will just show the evidence for cosine sums here, while the argument for sine sums will be shown on parallel paths.
To prove (2.2.1), we notice that

$$\begin{aligned} Z_\eta(y) &= \frac{c_0^*}{2} + \sum_{\kappa=1}^{\eta}\left[\sum_{j=\kappa}^{\eta}\Delta\left(\frac{c_j^*\cos jy}{j^2}\right)\right]\kappa^2 \\ &= \frac{c_0^*}{2} + \sum_{\kappa=1}^{\eta}\left[\sum_{j=\kappa}^{\eta}\left(\frac{c_j^*\cos jy}{j^2} - \frac{c_{j+1}^*\cos(j+1)y}{(j+1)^2}\right)\right]\kappa^2 \\ &= \frac{c_0^*}{2} + \sum_{\kappa=1}^{\eta} c_\kappa^*\cos\kappa y - \sum_{\kappa=1}^{\eta}\kappa^2\frac{c_{\eta+1}^*\cos(\eta+1)y}{(\eta+1)^2} \\ &= S_\eta(y) - \frac{c_{\eta+1}^*\cos(\{\eta+1\}y)\eta(\eta+1)(2\eta+1)}{6(\eta+1)^2} \end{aligned}$$

$$\lim_{\eta\to\infty} Z_\eta(y) = \lim_{\eta\to\infty} S_\eta(y) - \lim_{\eta\to\infty}\frac{c_{\eta+1}^*\eta(2\eta+1)\cos((\eta+1)y)}{6(\eta+1)}$$

Since $\cos(\eta+1)y$ is bounded in $(0,\pi]$ and $\lim_{\eta\to\infty}\frac{2\eta+1}{\eta+1} = 2$ and

$$\begin{aligned} \eta\left|c_\eta^*\right| = \frac{\eta^3 c_\eta^*}{\eta^2} &= \eta^3\sum_{\kappa=\eta}^{\infty}\left|\Delta\left(\frac{c_\kappa^*}{\kappa^2}\right)\right| \\ &\le \sum_{\kappa=\eta}^{\infty}\kappa^3\left|\Delta\left(\frac{c_\kappa^*}{\kappa^2}\right)\right| \\ &\le \sum_{\kappa=\eta}^{\infty}\kappa^3\frac{A_\kappa^*}{\kappa^2} = \sum_{\kappa=\eta}^{\infty}\kappa A_\kappa^* = 0(1) \\ & as \quad \eta\to\infty \end{aligned}$$

$\{if\sum c_\eta^*$ is convergent then $\lim_{\eta\to\infty} c_\eta^* = 0\}$

$$\text{So,}\quad \lim_{\eta\to\infty} Z_\eta(y) = \lim_{\eta\to\infty} S_\eta(y) = Z(y) \quad where$$

$$\begin{aligned} Z(y) &= \frac{c_0^*}{2} + \lim_{\eta\to\infty}\sum_{\kappa=1}^{\eta} c_\kappa^*\cos\kappa y \\ &= \lim_{\eta\to\infty} Z_\eta(y) = \lim_{\eta\to\infty} S_\eta(y) \\ &= \lim_{\eta\to\infty}(\frac{c_0^*}{2} + \sum_{\kappa=1}^{\eta} c_\kappa^*\cos\kappa y) \end{aligned}$$

$$\text{Now} \lim_{\eta\to\infty}(\sum_{\kappa=1}^{\eta} c_\kappa^* \cos\kappa y)$$

$$\begin{aligned}
&= \lim_{\eta\to\infty}(\sum_{\kappa=1}^{\eta} \frac{c_\kappa^*}{\kappa^2}\kappa^2 \cos\kappa y)\\
&= \lim_{\eta\to\infty}(\sum_{\kappa=1}^{\eta-1} \Delta(\frac{c_\kappa^*}{\kappa^2}(-D_\kappa^{''}(y)) + \frac{c_\eta^*}{\eta^2}(-D_\eta^{''}(y)))\\
&= \sum_{\kappa=1}^{\infty} \Delta(\frac{c_\kappa^*}{\kappa^2})(-D_\kappa^{''}(y))\\
&\leq \sum_{\kappa=1}^{\infty} \Delta(\frac{A_\kappa^*}{\kappa^2})(-D_\kappa^{''}(y))
\end{aligned}$$

According to the provided hypothesis & lemma 1, $\sum_{\kappa=1}^{\infty} \Delta(\frac{A_\kappa^*}{\kappa^2})(-D_\kappa^{''}(y))$ converges. Therefore Z(y)exists for y $\in$ (0,π]
This brings the proof of (2.2.1).

$$\begin{aligned}
\text{Now}||Z(y) - Z_\eta(y)|| &= \int_0^\pi |Z(y) - Z_\eta(y)|dy\\
&= \int_0^\pi |\sum_{\kappa=\eta+1}^{\infty} c_\kappa^* \cos\kappa y + \frac{\eta(2\eta+1)c_{\eta+1}^* \cos{(\eta+1)y}}{6(\eta+1)}|dy\\
&= \lim_{m\to\infty}\int_0^\pi |\sum_{\kappa=\eta+1}^{m} \frac{c_\kappa^*\kappa^2 \cos\kappa y}{\kappa^2} + \frac{\eta(2\eta+1)c_{\eta+1}^* \cos{(\eta+1)y}}{6(\eta+1)}|dy
\end{aligned}$$

We obtain by employing Abel's Transformation

$$\begin{aligned}
&= \int_0^\pi |\sum_{\kappa=\eta+1}^{\infty} \Delta\left(\frac{c_\kappa^*}{\kappa^2}\right)\left(-D_\kappa^{''}(y)\right) + \frac{c_{\eta+1}^* D_\eta^{''}(y)}{(\eta+1)^2}\\
&+ \frac{\eta(2\eta+1)c_{\eta+1}^* \cos{(\eta+1)y}}{6(\eta+1)}|dy\\
&\leq \int_0^\pi |\sum_{\kappa=\eta+1}^{\infty} \Delta\left(\frac{c_\kappa^*}{\kappa^2}\right)\left(-D_\kappa^{''}(y)\right)|dy + \int_0^\pi |\frac{c_{\eta+1}^* D_\eta^{''}(y)}{(\eta+1)^2}|dy\\
&+ \int_0^\pi |\frac{\eta(2\eta+1)c_{\eta+1}^* \cos{(\eta+1)y}}{6(\eta+1)}|dy\\
&= (i) + (ii) + (iii)
\end{aligned}$$

Evidence of part (i)

$$\int_0^\pi |\sum_{\kappa=\eta+1}^{\infty} \Delta\left(\frac{c_\kappa^*}{\kappa^2}\right)\left(-D_\kappa^{''}(y)\right)|dy = \int_0^\pi |\sum_{\kappa=\eta+1}^{\infty} \frac{\frac{A_\kappa^*}{\kappa^2}\Delta\left(\frac{c_\kappa^*}{\kappa^2}\right)\left(-D_\kappa^{''}(y)\right)}{\frac{A_\kappa^*}{\kappa^2}}|dy$$

Implementing Abel's Transformation Once More

$$
\begin{aligned}
&= \int_0^\pi | \sum_{\kappa=\eta+1}^{\infty} \Delta \frac{A_\kappa^*}{\kappa^2}) \sum_{j=1}^{\kappa} \frac{\Delta \frac{c_j^*}{j^2}}{(\frac{A_j}{j^2})} (-D_j^{''}(x))|dy \\
&\leq \sum_{\kappa=\eta+1}^{\infty} \Delta \left(\frac{A_\kappa^*}{\kappa^2} \right) \int_0^\pi | \sum_{j=1}^{\kappa} \left(\frac{\Delta \left(\frac{c_j^*}{j^2} \right)}{\frac{A_j^*}{j^2}} \right) \left(D_j^{''}(y) \right) |dy
\end{aligned}
$$

Now by given assumption

$$
\begin{aligned}
&\leq \sum_{\kappa=\eta+1}^{\infty} \Delta \left(\frac{A_\kappa^*}{\kappa^2} \right) M(\kappa+1)^3 \\
&= o \left(\sum_{\kappa=\eta+1}^{\infty} (\kappa+1)^3 \Delta \left(\frac{A_\kappa^*}{\kappa^2} \right) \right) \\
&= o(1) \quad \text{as} \quad \{c_\kappa^*\} \in \quad \text{new defined class.}
\end{aligned}
$$

Validation of (ii) component

$$
\begin{aligned}
\frac{c_{\eta+1}^*}{(\eta+1)^2} \int_0^\pi |D_\eta^{''}(y)|dy &= \frac{c_{\eta+1}^*}{(\eta+1)^2} \left(\frac{4}{\pi}(\eta^2 \log \eta) + O(\eta^2) \right) \\
&\leq c_{\eta+1}^* \left(\frac{4}{\pi} \frac{\eta^2 \log \eta}{(\eta+1)^2} + \frac{1}{(\eta+1)^2} o(\eta^2) \right) \\
&\leq c_{\eta+1}^* \left(\frac{4}{\pi} \frac{\eta^2 \log \eta}{(\eta+1)^2} + o(1) \right) \\
&= o \left(c_{\eta+1}^* \log \eta \right)
\end{aligned}
$$

Now $\log \eta \leq \eta \quad \forall \quad \eta \geq 1$
And $\eta c_\eta^* = o(1) \quad as \quad \eta \to \infty$ as already proved above.
Proof of (iii)part
(iii) part is equal to $o(\eta c_{\eta+1}^*)$ which is equal to $o(1) \quad$ as $\quad \eta \to \infty$.
Therefore $||Z(y) - Z_\eta(y)|| = o(1)$ as $\eta \to \infty$
Therefore $Z(y) \in L^1(0, \pi]$
This concludes (2.2.2).
Now we shall provide evidence of (2.2.3)

$$
\begin{aligned}
||Z - S_\eta|| &= ||Z - Z_\eta + Z_\eta - S_\eta|| \\
&\leq ||Z - Z_\eta|| + ||Z_\eta - S_\eta|| \\
&= ||Z - Z_\eta|| + ||\frac{\eta(2\eta+1)}{6(\eta+1)} c_{\eta+1}^* \cos{(\eta+1)y}|| \\
&\leq ||Z - Z_\eta|| + \frac{\eta(2\eta+1)}{6(\eta+1)} c_{\eta+1}^* \int_0^\pi |\cos{(\eta+1)y}|dy \\
&\to \quad o(1) \quad as \quad \eta \to \infty
\end{aligned}
$$

by employing the assertion (2.2.1) and (2.2.2). This brings the proof of (2.2.3) to a close. Apparently theorem 2 is developed for feeble class than class S, yet conclusions are produced for L^1 -convergence by not employing condition like $c^*_\eta \log \eta = o(1), \quad as \quad \eta \to \infty$.

4.2 Explanation of theorem 2.3:

We will just show the evidence for cosine sums here, while the argument for sine sums will be shown on parallel paths.

$$Z_\eta\,(y) = S_\eta(y) - \frac{c^*_{\eta+1}\cos\left((\eta+1)y\right)(\eta)(2\eta+1)}{6(\eta+1)}$$

$$Z^r_\eta\,(y) = S^r{}_\eta(y) - \frac{c^*_{\eta+1}\cos\left(((\eta+1)y)+r\frac{\pi}{2}\right)(\eta)(2\eta+1)(\eta+1)^r}{6(\eta+1)}$$

Since A_κ is monotonically decreasing and converging to 0 as $\kappa \to \infty$ & $\sum\limits_{\kappa=1}^{\infty} \kappa^{r+1} A_\kappa < \infty$,

So, we got $\kappa^{r+2} A_\kappa \to 0$, as $\kappa \to \infty$ and

$$\eta^{r+1} c^*_\eta = \eta^{r+3} \sum_{\kappa=\eta}^{\infty} |\Delta(\frac{a_\kappa}{\kappa^2})| \leq \sum_{\kappa=\eta}^{\infty} \kappa^{r+3} |\Delta(\frac{c^*_\kappa}{\kappa^2})| \leq \sum_{\kappa=\eta}^{\infty} \kappa^{r+3} (\frac{A^*_\kappa}{\kappa^2}) = o(1), \eta \to \infty. \tag{4.2.1}$$

As $\cos\left((\eta+1)y + r\frac{\pi}{2}\right)$ is finite in (0,π]. So,

$$\begin{aligned} z^r(y) &= \lim_{\eta\to\infty} z_\eta{}^r(y) \\ &= \lim_{\eta\to\infty} S_\eta{}^r(y) \\ &= \lim_{\eta\to\infty} (\sum_{\kappa=1}^{\eta} \kappa^r c^*_\kappa \cos(\kappa y + r\frac{\pi}{2})) \end{aligned}$$

After using Abel's Transformation, obtained as

$$\begin{aligned} \lim_{\eta\to\infty} (\sum_{\kappa=1}^{\eta} \kappa^r c^*_\kappa \cos(\kappa y + r\frac{\pi}{2})) &= \lim_{\eta\to\infty} [\sum_{\kappa=1}^{\eta-1} \Delta(\frac{c^*_\kappa}{\kappa^2})(-D^{r+2}{}_\kappa(y)) + \frac{c^*_\eta}{\eta^2} D^{r+2}{}_\eta(y)] \\ &= \sum_{\kappa=1}^{\infty} \Delta(\frac{c^*_\kappa}{\kappa^2})(-D^{r+2}{}_\kappa(y)) + \lim_{\eta\to\infty} \frac{c^*_\eta}{\eta^2} D^{r+2}{}_\eta(y) \\ &\leq \sum_{\kappa=1}^{\infty} \frac{A^*_\kappa}{\kappa^2}(-D^{r+2}{}_\kappa(y)) + \lim_{\eta\to\infty} \frac{c^*_\eta}{\eta^2} D^{r+2}{}_\eta(y) \end{aligned}$$

Using the provided assumptions, lemma 1 & (4.2.1), the series $\sum\limits_{\kappa=1}^{\infty} \frac{A^*_\kappa}{\kappa^2}(-D^{r+2}{}_\kappa(y))$ converges.

So, the limit $z^r(y)$ exists for $y \in (0, \pi]$ and (2.3.1) follows.
Take the following consideration to establish (2.3.2).

$$\begin{aligned}
z^r(y) - {z_\eta}^r(y) &= \sum_{\kappa=\eta+1}^{\infty} \kappa^r c^*_\kappa \cos(\kappa y + r\frac{\pi}{2}) + \frac{c^*_{\eta+1}\cos{(\eta+1)y + r\frac{\pi}{2}}\eta(2\eta+1)(\eta+1)^r}{6(\eta+1)} \\
&= \sum_{\kappa=\eta+1}^{\infty} \Delta(\frac{c^*_\kappa}{\kappa^2})(-{D_\kappa}^{r+2}(y)) + \frac{c^*_{\eta+1}}{(\eta+1)^2} D^{r+2}_\eta(y) \\
&+ \frac{\eta(\eta+1)^r(2\eta+1)}{6(\eta+1)} c^*_{\eta+1}\cos((\eta+1)y + r\frac{\pi}{2}) \\
&= \sum_{\kappa=\eta+1}^{\infty} \frac{A^*_\kappa}{\kappa^2}\frac{\Delta(\frac{c^*_\kappa}{\kappa^2})}{\frac{A^*_\kappa}{\kappa^2}}(-{D_\kappa}^{r+2}(y)) + \frac{c^*_{\eta+1}}{(\eta+1)^2} D^{r+2}_\eta(y) \\
&+ \frac{\eta(\eta+1)^r(2\eta+1)}{6(\eta+1)} c^*_{\eta+1}\cos((\eta+1)y + r\frac{\pi}{2}) \\
&= \sum_{\kappa=\eta+1}^{\infty} \Delta(\frac{A^*_\kappa}{\kappa^2}) \sum_{j=1}^{\kappa} \frac{\Delta(\frac{c^*_j}{j^2})}{\frac{A^*_j}{j^2}}(-{D_j}^{r+2}(y)) + (\frac{A^*_{\eta+1}}{\eta+1}) \sum_{j=1}^{\eta} \frac{\Delta(\frac{c^*_j}{j^2})}{\frac{A^*_j}{j^2}}(-{D_j}^{r+2}(y)) \\
&+ \frac{c^*_{\eta+1}}{(\eta+1)^2} D^{r+2}_\eta(y) + \frac{\eta(\eta+1)^r(2\eta+1)}{6(\eta+1)} c^*_{\eta+1}\cos((\eta+1)y + r\frac{\pi}{2})
\end{aligned}$$

After applying the lemma 2 & lemma 3

$$\begin{aligned}
||z^r(y) - {z_\eta}^r(y)|| \le & \sum_{\kappa=\eta+1}^{\infty} \Delta(\frac{A^*_\kappa}{\kappa^2}) \int_0^\pi |\sum_{j=1}^{\kappa} \frac{\Delta(\frac{c^*_j}{j^2})}{\frac{A^*_j}{j^2}}(-{D_j}^{r+2}(y))|dy \\
& + (\frac{A^*_{\eta+1}}{\eta+1}) \int_0^\pi |\sum_{j=1}^{\eta} \frac{\Delta(\frac{c^*_j}{j^2})}{\frac{A^*_j}{j^2}}(-{D_j}^{r+2}(y))|dy + \int_0^\pi |\frac{c^*_{\eta+1}}{(\eta+1)^2} D^{r+2}_\eta(y)|dy \\
& + \frac{\eta(\eta+1)^r(2\eta+1)}{6(\eta+1)} |c^*_{\eta+1}| \int_0^\pi |\cos((\eta+1)y + r\frac{\pi}{2})|dy \\
& = O(\sum_{\kappa=\eta+1}^{\infty} \kappa^{r+3}\Delta(\frac{A^*_\kappa}{\kappa^2})) + O(\eta^{r+3}(\frac{A^*_{\eta+1}}{\eta+1^2})) + O(\eta^r c^*_{\eta+1}\log\eta) \\
& + \frac{\eta(\eta+1)^r(2\eta+1)}{6(\eta+1)} \Big| c^*_{\eta+1}| \int_0^\pi |\cos\Big((\eta+1)y + r\frac{\pi}{2}\Big)\Big| dy
\end{aligned}$$

Using the reasoning provided in the explanation of theorem 2, researchers may conclude that $\sum\limits_{\kappa=\eta+1}^{\infty} \kappa^{r+3}\Delta(\frac{A_\kappa}{\kappa^2})$ converges.
$\int_0^\pi |\cos((\eta+1)y + r\frac{\pi}{2})|dy \le \frac{2}{\eta+1}$ and for $\eta \ge 1, \eta^{r+1}c^*_\eta \log\eta \le \eta^{r+2}c^*_\eta = o(1)$ as $\eta \to \infty$. This implies that

$$||z^r(y) - {z_\eta}^r(y)|| = 0(1) \qquad as \qquad \eta \to \infty. \tag{4.2.2}$$

Because,${z_\eta}^r(y)$ is a monomial, so $z^r(y) \in L^1(0,\pi]$ which completes (2.3.2). We are now proceeding on to the evidence of (2.3.3)

$$\begin{aligned}
||z^r - {S_\eta}^r|| &= ||z^r - {z_\eta}^r + {z_\eta}^r - {S_\eta}^r|| \\
&\leq ||z^r - {z_\eta}^r|| + ||{z_\eta}^r - {S_\eta}^r|| \\
&= ||z^r - {z_\eta}^r|| + ||\frac{\eta(\eta+1)^r(2\eta+1)}{6(\eta+1)}|c^*_{\eta+1}\cos((\eta+1)y + r\frac{\pi}{2})|| \\
&\leq ||z^r - {z_\eta}^r|| + \frac{\eta(\eta+1)^r(2\eta+1)}{6(\eta+1)}|c^*_{\eta+1}| \int_0^\pi |\cos((\eta+1)y + r\frac{\pi}{2})|dy
\end{aligned}$$

Further $||z^r(y) - {z_\eta}^r(y)|| = 0(1) \quad as \quad \eta \to \infty$ by using (1.11),$\int_0^\pi |\cos((\eta+1)y + r\frac{\pi}{2})|dy \leq \frac{2}{\eta+1}$ and c^*_η is a seq. converging to 0,so the (2.3.3)part of theorem 2.3 holds.

Note The scenario r = 0 in main result 2.3 gives output of main result 2.2.

Acknowledgment

Authors are thankful to MRSPTU Bathinda for enabling opportunities in paper preparation process.

References

[1] T.Kano,Coefficients of some trigonometric series,*Jour. Frac. Sci. Shihshu University*,**3**,153-621(968).

[2] N.K.Bary,*A Treatise on Trigonometric Veries* (vol 1 and vol 2),London,1964.

[3] S.Sheng,The extension of the theorems of C.V.Stanojevic and V.B.Stanojevic,*Proc. Amer. Math. Soc.*,**14**,158-60,(1939).

[4] S.A.Telyakovskii,A sufficient condition of Sidon for the integrability of trigonometric series,*Mat.Zametki*,**14**,317-28,(1973).

[5] W.H.Young, On the Fourier series of bounded functions,*Proc. London Math. Soc.*,**12**,41-70,(1993).

[6] A.N. Kolmogorov,Sur l'ordere de grandeur des coefficients de la sėrie de Fourier-Lebsque,*Bull. Acad. Polon. Sci. Ser. Sci. Math. Astronom. Phys.*,83-86,(1923).

[7] S.Sidon, Hinreichende Bedingungen f ur den Fourier-Charakter einer trigonometrischen Reihe,*J. London Math. Soc.*,**14**,579-86,(1939).

[8] J.Kaur and S.S. Bhatia,Convergence of new modified trigonometric sums in metric space L, *The journal of Non Linear Sciences and applications*,**1(3)**,179-188,(2008).

[9] Xh.Z. Krasniqi, Further results on L^1-convergence of some modified complex trigonometric sums, *J. Numer. Anal. Approx. Theory*,**44(2)**,180-189,(2015).

J. COMPUTATIONAL ANALYSIS AND APPLICATIONS, VOL. 31, NO. 2, 2023, COPYRIGHT 2023 EUDOXUS PRESS, LLC

Numerical Study of Heat and Mass Transfer of MHD Casson Fluid Flow with Cross-Diffusion and Heat Source Impacts in presence of Radiation

Shilpa[1], *Ruchika Mehta*[1*], *Sushila*[2]*and Renu Sharma*[3]
[1]*Department of Mathematics and Statistics*,
Manipal University Jaipur, Jaipur(Raj.), India
[2]*Department of Physics*,
Vivekananda Global University, Jaipur(Raj.), India
[3]*Department of Physics*,
JECRC University, Jaipur(Raj.), India
[1*]*ruchika.mehta*1981@*gmail.com*

Abstract

The current research analyzes Soret and Dufour effects on magneto hydrodynamic natural convection viscous-elastic radiative Casson fluid flow across a non-linear stretchy sheet. First, the PDEs (partial differential equations) are changed using similarity analysis into non-linear paired ODEs (ordinary differential equations). Then, using the BVP4C technique, ordinary differential equations are numerically solved. Engineering interest of substantial quantities like skin-friction coefficient, Nusselt parameter, and Sherwood parameter debated in the table with multiple significant characteristics. The current study describes that the temperature profile increases with rising thermal radiation and the Dufour effect. A declining Sherwood impression of Soret number is depicts in current study. An increasing radiation impact declines the Nusselt number.In addition, the concentration field enhances due to an increasing Soret effect.

Key words: Non-linear stretchy sheet, Soret and Dufour effects, Casson fluid, Radiation Parameter, BVP4C technique.

1 Introduction

When most organic and commercial fluids, including hemoglobin, printer inks, greasing heavy oils, watercolors, gypsum pastes, fluid cleansers, multigrade oils, ceramic materials, fruit drinks, polymeric materials and others are pressured, they modify their initial fluid properties or viscosity nature. The traditional Newton's law of viscosity is significantly deviated by these non-Newtonian fluids. Many Researchers have explore a variety of non-Newtonian viscous-elastic flow samples through evaluate their unique flow movement in order to estimate these conventional fluids' features of flow, temperature and concentration dispensation in a suitable way.

Thermal radiation is the process through which energy or heat is conveyed by electromagnetic waves. Thermal radiation is important when there is a large temperature difference between the boundary surface and the surrounding fluid. In physics and engineering, radiative impacts are essential. The effects of radiation heat transfer on various flows are critical when performing activities requiring high temperatures and space technologies. For instance, the effects of radiation are essential for observing heat transfer in the polymer sectors, where heat regulating elements have a mild influence on the quality of the finished product. Relevant are also the effects of radiation on nuclear power plants, aircraft, gas turbines, spacecraft, liquid metal fluids, and solar radiation.A comprehensive examination of mixture convective flow of Casson and Oldroyd-B fluids through a linearly stratified stretchy sheet was reported by Kumam, P.et al. [1]. Additionally Thermal radiation, chemical reactivity, and magnetization are all properties of Casson and Oldroyd-B fluids. The property of slide boundary circumstances and chemical reactive on heat and mass transport via mix convective boundary stratum flow of a non-Newtonian fluid over a non-linear stretchy sheet are studied by Ahemed et al. [2]. Ahmad. et al. [3] studied the free convection slippage flow of fractional viscous fluid by considering the thermal radiation, heat generation, chemical reaction of order first, and Newtonian heating through a porous medium by considering single-wall carbon nanotube (SWCNT).The Casson fluid form is used to explain the performance of non-Newtonian fluids. Basha et al. [4] investigated the MHD convective heat transport viscous-elastic boundary layer of the Casson fluid with Joule and viscous dissipation characteristics under the impact of chemical process and in the presence of Lorentz forces, a non-linear stretched sheet was utilized. Basha et al. [5] developed a 2D numerical form to explore the result of buoyancy forces on magnetized free convective Walters-B fluid flow across a stretched sheet with Soret impact, heat radiative, heat source/sink, and viscous dissipation. The stretchy sheet geometry is used to generate the present physical model. The electromagnetic force on a charged particle, effect on a non-linear structure is analyzed. The work focuses exclusively on contributions to the utilization of non-Newtonian Casson fluid entropy generation across an exponentially stretched sheet. Entropy generation and homogeneous–heterogeneous reactions are explored by Das et al. [6]. Instead of no-slip situation at the boundary, motion and thermal slips are measured. The buoyancy influence on 2D Casson fluid flow and mix convection over a non-linear stretched sheet is detected from Gangadhar et al. [7].

The Soret effect is related to mass flow phenomena caused by heat diffusion, while the Dufour effect is tied to the energy flux generated by the solute difference. The Soret impact is used to cope with gas concentrations with lighter and medium molecular weights. The Soret and Dufour phenomena are used to transfer heat and mass in a variety of industrial and engineering applications, such as multicomponent melts in geosciences, groundwater pollutant migration, solidification of binary alloys, chemical reactors, space cooling, isotope separation, oil reservoirs, and mixtures of gases.An unsteady free convection slip flow of second grade fluid over an infinite heated inclined plate solved with Caputo-Fabrizio fractional derivativeis studied by Haq et al. [8].Hussanan et al. [9] explored the heat transfer from a Casson fluid to a non-linearly expanding sheet using Newtonian heating and the magneto hydrodynamic flow of that fluid. Ibrahim et al. [10] constructed a mathematical model for the investigation of mixed convection on MHD Casson fluid flow through a non-linearly permeable extended sheet with radiative, viscous dispersion, heat source/sink, chemical reaction, and suction. They also used the Buogiorno's type Nano-fluid form, which includes Brownian motion and thermophoresis. The impacts of radiation parameter and chemical reactions on time dependent MHD free convection flow in a porous plate were analyzed by Matta et al. [11].Mehta. et al. [12] discussed magnetohydrodynamics varied convective stagnation point stream with a vertically extended sheet embedded in a permeable material with generation/absorption, radiation impacts, and viscous dissipation. The MHD flow stalling at the point of Casson fluid across a non-linearly extending sheet with viscous dispersion was studied from Medicare et al. [13].The MHD flow and heat transmission of Casson nano particles across a non-linear (temperature variation throughout) stretchable sheet is studied by Mustafa et al. [14]. Mukhopadhyay, s. [15] explored a boundary layer investigation for non-Newtonian fluid flow and heat transport across a non-linearly stretchy sheet. The motion field is suppressed when the Casson constraint is rised. However, as the Casson parameter is enhanced, the temperature rises. In the existence of a chemical reaction, Naduvinamani et al.[16] explored the heat and mass transport characteristics of a time dependent MHD squeeze flow of Casson fluid between two parallel plates with viscous and Joule dissipation influences. Compress flow is affected by Soret and Dufour impacts, as well as radiation parameter and heat source/sink impacts are explored. Panigrahi et al. [17] assessed the effects of Soret and Dufour on the properties of heat and mass transport in a mixture Powell-Erying fluid boundary layer flow on a non-linear stretch sheet. In the existence of thermal radiation and chemical reaction, Reddy et al.[18] studied the time independent 2D MHD convective boundary layer flow of a Casson fluid over an increasingly slope porous stretchy sheet.

Aside from the flow caused by an unstable or steady extending/shrinking sheet, the influence of the buoyant force caused by the stretching sheets could not be ignored. The importance of thermal radiation with mixed convective boundary layer (BL) flow in geothermal engineering, space technology, and nuclear reactor cooling has increased interest in the topic.Singh et al. [19] investigate thin film flow of a third-grade fluid down a inclined planeusing an effective well organized computational scheme namely homotopy perturbation Elzaki transform method.Singh et al. [20] studied the local fractional linear transport equations (LFLTE) in fractal porous media.Sumalatha and Bandari [21] investigated the impact of radiation impact and heat source/sink on the flow across a non-linearly expanding sheet of Casson fluid. Sreedevi et al. [22] studied the convective heat and mass transport flow of an electrical conducting fluid over a porous vertically stretched sheet under the assorted property of the magnetic parameter, Joule heating, thermal radiation absorption, viscous dissipation, buoyancy forces, Soret, and Dufour. Tak et al. [23] examined the impressions of radiation parameter and magnetic impact on the heat and mass transport features of natural convection around an upright surface embedded in a dripping wet Darcian porous media, taking into account the Soret and Dufour impacts. Ullah et al. [24] explored the impact of slip effects on MHD free convection flow of non-Newtonian fluid across a non-linear stretched sheet wringing wet in porous media with Newtonian heating. Ullah et al. [25] investigated a time dependent mix convection flow of Casson fluid for a non-linear extending sheet with slip and convective boundary circumstances. Furthermore explored are the impacts of thermo-diffusion, diffusion-thermo, viscous dissipation, and heat Source/Sink. The flow and heat transport characteristics of a viscous fluid over a non-linear extending sheet are investigated through studied by Vajravelu, K. [26].

Basha, H. et al. [4] are investigated the Casson fluid flow natural convection viscous-elastic boundary layer in MHD over a non-linear stretched sheet with Joule and viscous dissipation impacts under chemical reaction influence in the presence of Lorentz forces. The current work fills the gap of Basha, H. et al. [4] by involving the Soret and Dufour impacts in existence of radiation parameter, and the numerical result discussed through graphs along with table using MATLAB software.

2 Problem Structure:

The current study examines the movement of 2D; time-independent, laminar, viscous, incompressible boundary layer carrying a MHD Non-Newtonian Casson fluid across a non-linear stretched sheet. Based on the geometry that is taken into consideration, the current physical condition is modeled. On the other hand, Figure 1 gives clear clarification of the measured problems flow configuration completed with all required criteria. The contemplated flow design is consistent with the $y = 0$ plane and stream are restricted to just $y > 0$. Still, exterior forces are used in combination with axial flow side in which the surface is enhanced and the origin is fixed. In order to clearly give details the problem, the authors also established a rectangular system where the y-direction is taken perpendicular to the stretchy surface and the x-coordinate is measured along the flow direction. Also, B_0 strength is applied to the Y-coordinate, as is seen in Fig. 1. Furthermore; the free flow velocity, thermal, and volume fraction are represented by U_∞, T_∞, and C_∞.

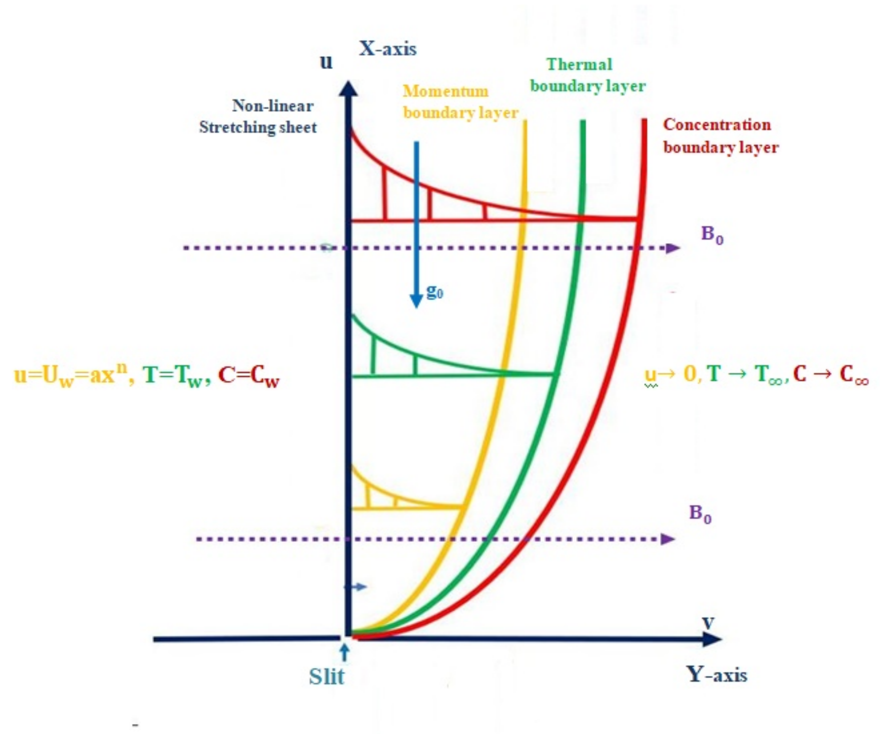
X-axis
u
Thermal boundary layer
Momentum boundary layer
Non-linear Stretching sheet
Concentration boundary layer
B_0
g_0
$u=U_w=ax^n$, $T=T_w$, $C=C_w$
$u \to 0, T \to T_\infty, C \to C_\infty$
B_0
v
Slit
Y-axis

Figure 1: Physical structure and coordinate system of the topic under investigation.

The established equation of a Casson fluid is inscribed by used Ref [4], [7], [9], and [15]

$$\tau_{mn} = \begin{cases} 2(\mu_B + \frac{\tau_y}{\sqrt{2\pi}})e_{mn} & \text{if } \pi > \pi_c \\ 2(\mu_B + \frac{\tau_y}{\sqrt{2\pi}})e_{mn} & \text{if } \pi < \pi_c \ . \end{cases} \tag{1}$$

Where $\pi = e_{mn}e_{mn}$ and e_{mn} is the $(m, n)^{th}$ section of the rate of deformation, π is the multiple of the sections of defacement rate, π_c is critical worth of the multiply founded by the non-Newtonian fluid form, μ_B is the plastic movable viscosity of the non-Newtonian fluid and τ_y is the yield stress of the fluid.

The following criteria define the controlling relations for the proposed study Ref. [4], [17], [18]

$$\frac{\partial u}{\partial x} + \frac{\partial v}{\partial y} = 0, \tag{2}$$

$$u\frac{\partial u}{\partial x}+v\frac{\partial v}{\partial y}=\nu(1+\frac{1}{\beta})\frac{\partial^2 u}{\partial y^2}-\frac{\sigma {B_0}^2 u}{\rho}+g\beta_T(T-T_\infty)+g\beta_C(C-C_\infty), \tag{3}$$

$$u\frac{\partial T}{\partial x}+v\frac{\partial T}{\partial y}=\frac{k}{\rho c_p}\frac{\partial^2 T}{\partial y^2}+\frac{Q_0}{\rho c_p}(T-T_\infty)+\frac{\mu}{\rho c_p}(1+\frac{1}{\beta})(\frac{\partial u}{\partial y})^2+\frac{\sigma {B_0}^2 u^2}{\rho c_p}$$
$$-\frac{1}{\rho c_p}\frac{\partial q_r}{\partial y}+\frac{D_m K_T}{c_s c_p}\frac{\partial^2 C}{\partial y^2}, \tag{4}$$

$$u\frac{\partial C}{\partial x}+v\frac{\partial C}{\partial y}=D_m\frac{\partial^2 C}{\partial y^2}+\frac{D_m K_T}{T_m}\frac{\partial^2 T}{\partial y^2}-k_1(C-C_\infty). \tag{5}$$

Earlier, equations (2) to (5) are in paired form, $\beta=\mu_B\frac{\sqrt{2\pi_C}}{\tau_y}$ is a parameter for the Casson fluid. And motion factors are u and v. and ν denotes kinematic viscosity, β is a number of the shear thinning Casson fluid, σ shows the electro conductivity, B_0 signifies the magneto field strength, ρ symbol for the density, k denotes thermal conductivity, T pointed for temperature, Q_0 characterizes inside heat source (>0)/sink (<0) amount, C is the occurrence of concentration, D_m defines diffusivity, and k_1 shows the chemical reactive parameter, μ symbol for the dynamic viscosity, C_p represents for the specific heat capacity, C_s is the volume fraction susceptibility, g is the gravitational force, β_T and β_C are the coefficients of thermal and mass expansion. Where the non-linear stretchy surface speed is represented by the parameters a $(a>0)$ and n. further the terms $\rho-\rho_\infty=-(\beta_T(T-T_\infty)+\beta_C(C-C_\infty))$ is buoyancy effects. Furthermore, the boundary-layer supposition suggests that corporally the conditions on a particular location are directly dependent upon those upstream. From a mathematical standpoint, the behavior of the system was converted from an elliptical to a parabola form, additionally; this change would significantly simplify the mathematical studies of the problem.

The limitations are composed by used Ref. [4]

$$u=u_w=ax^n,\ v=0,\ T=T_w,\ C=C_w,\ \ at\ y=0.$$
$$u\to 0,\qquad T\to T_\infty,\qquad C\to C_\infty,\qquad at\ \ y\to\infty. \tag{6}$$

the Roseland approximation of the radiation heat flow is defined by Ref. [18], [21]

$$q_r=\frac{-4\sigma}{3k^*}\frac{\partial T^4}{\partial y}, \tag{7}$$

Inscribe the T^4 as a linear connection of thermal with Taylor's series extension regarding expansion about T_∞ and deleting greater terms, we get

$$T^4\approx 4{T_\infty}^3 T-{T_\infty}^4. \tag{8}$$

In view of the similarity transformation, we change the dimensional governing equation into non-dimensional equations and similarity transformation are written as

$$u=ax^n f'(\eta),\qquad v=-x^{(n-1)/2}\sqrt{\frac{\nu a(n+1)}{2}}[f(\eta)+\frac{(n-1)}{(n+1)}\eta f'(\eta)], \tag{9a}$$

$$where \quad \eta = y\sqrt{\frac{a(n+1)}{2\nu}}x^{(n-1)/2}, \quad \theta(\eta) = \frac{T-T_\infty}{T_w-T_\infty}, \quad \phi(\eta) = \frac{C-C_\infty}{C_w-C_\infty}. \tag{9b}$$

With the help of equations (7) to (9b), equations (2) to (6) are diminished to the following regime with rejecting pressure gradient.

$$(1+\frac{1}{\beta})f''' = \frac{2n}{(n+1)}(f')^2 - ff'' + 2Mf' - G_T\theta - G_C\phi = 0, \tag{10}$$

$$((1+Nr))\theta'' + 2QPr\theta + Prf\theta' + (1+\frac{1}{\beta})PrEc(f'') + 2PrMEc(f')^2 + Dupr\phi'' = 0, \tag{11}$$

$$(1+ScSr)\phi'' + Scf\phi' - 2ScKr\phi = 0. \tag{12}$$

With suitable boundary circumstances

$$f(0) = 0, \quad f'(0) = 1, \quad \theta(0) = 1, \quad \phi(0) = 0, \quad at \ \eta = 0. \tag{13a}$$

$$f'(\infty) \to 0, \quad \theta(\infty) \to 0, \quad \phi(\infty) \to 0, \quad at \ \eta \to \infty. \tag{13b}$$

Where,M shows the magnetic parameter or Hartman number $M = \frac{\sigma B^2(0)}{\rho a(n+1)x^{n-1}}$, G_T and G_C represent the local Temperature Grashof number $G_T = \frac{g\beta_T(T_w-T_\infty)}{a^2x^{2n-1}\frac{(n+1)}{2}}$ and local Concentration Grashof number $G_C = \frac{g\beta_C(C_w-C_\infty)}{a^2x^{2n-1}\frac{(n+1)}{2}}$ respectively, Pr shows the Prandtl number $Pr = \frac{\nu\rho C_p k}{}$, Nr denotes the Radiation parameter $Nr = \frac{16\sigma {T_\infty}^3}{3kk^*}$, Ec denotes the Eckert number $Ec = \frac{a^2x^{2n}}{c_p(T_w-T_\infty)}$, Du specifies the Dufour number $Du = \frac{D_mK_T(C_w-C_\infty)}{c_sc_p\nu(T_w-T_\infty)}$, Sc denotes the Schmidt number $Sc = \frac{\nu}{D_m}$, Sr represents the Soret number $Sr = \frac{D_mK_T(C_w-C_\infty)}{T_m\nu(T_w-T_\infty)}$, β denotes the non-Newtonian Casson parameter$\beta = \mu_B\frac{\sqrt{2\pi_C}}{\tau_y}$, Kr shows that the chemical reaction $Kr = \frac{K_1}{a(n+1)x^{n-1}}$, where K_1 stands for porosity parameter$K_1 = \frac{\nu}{kc}$, and Q denotes the heat sorce sink $Q = \frac{Q_0}{\rho ac_px^{n-1}}$.

Physical Quantities:

Skin Friction Coefficient Cf_x: The physical amount Skin friction Cf_x that getsup due to the viscous stretch in the surroundings of the plate is well-defined as

$$Cf_x = \frac{\tau_w}{\rho u_w^2}, \quad where \ \ \tau_w = (\mu_B + \frac{\tau_y}{\sqrt{2\pi}})(\frac{\partial u}{\partial y})_{y=0}. \tag{14}$$

Heat Transfer Coefficient: The dimensionless Nusselt number(Nu_x) is specified by

$$Nu_x = \frac{xq_w}{k(T_w-T_\infty)}, \quad where \ \ q_w = -k(\frac{\partial T}{\partial y})_{y=0}. \tag{15}$$

Mass Transmission factor: The amount of mass transport is resulting through a Sherwood parameter (Sh_x) which is assumed by

$$Sh_x = \frac{xq_m}{D_m(C_w-C_\infty)}, \quad where \ \ q_m = -D_m(\frac{\partial C}{\partial y})_{y=0}. \tag{16}$$

Here τ_w denotes the shear stress along with the shrinkage wall, q_w signifies heat flux, and q_m is mass transmission quantity at wall.

Therefore, in terms of Equations (9a) to (9b), the following non-dimensional quantities are obtained:

$$ {Re_x}^{1/2}Cf_x = (\frac{n+1}{2})^{1/2}(1+\frac{1}{\beta})f''(0), $$

local Nusselt

$$Re_x{}^{-1/2} Nu_x = -(\frac{n+1}{2})^{1/2} \theta'(0),$$

local Sherwood

$$Re_x{}^{-1/2} Sh_x = -(\frac{n+1}{2})^{1/2} \phi'(0). \tag{18}$$

Where, $Re_x = \frac{u_w x}{\nu}$ is the local Reynolds number, Cf_x is Skin Friction coefficient, Nu_x is Nusselt number, Sh_x is Sherwood parameter,τ_w indicates the wall shear stress, k signifies the thermo nano-fluid conductivity, q_w shows the surface heat flux, and q_m directs the surface mass flux.

We resolve the reduced equations (10) to (12) with limit conditions (13a) and (13b) via BVP4C method.

3 Results and Discussion:

The current research attempts to provide a fundamental physical understanding and industrial level practical significance of the subject under consideration. The rheological equations (10 to 13b)are solved numerically with the BVP4C with rheological quantities heat source/sink parameter, generative/destructive, chemical reactive parameter, transverse magnetic impact, thermal diffusivity, viscous dissipation, chemical reaction, radiation parameter, Dufour and Soret effect.Such as n,G_c,G_T, β, M, Ec, Pr, Kr,Nr,Sr,Q,Du, and Sc.For existing study, The Fig. of different parameters is designed with the service of MATLAB software and shown in Fig. 2 to Fig.25. Fig. (2-4) presents how the effects of β on flow sensibility, temperature, and mass transport characteristics. Additionally, the impacts of β on the dominant motion profile are also seen in Figure 2. The flow velocity in the domain of the solution under consideration is significantly reduced by the increasing under the impression of the magnetic and non-linear stretchy parameters, like shown in Figure 2.Flow velocities are decreased for increasingβ because an enhance in β rises the dynamic viscosity when stresses are present, that significantly increases the resistance to the movement of fluid near the wall. Therefore, flow velocity was decreased.Figure 3 also displays the effect ofβ thermal dispersion. This figure shows that the thermal graph decomposes as β rises. The thermal layer is also seen to be thinning.The temperature profile drops to zero until it is close to the surface.Like this, Figure 4 depicts the effect of the Casson fluid parameter on the mass distribution field.The concentration distribution increases near the stretching surface as β increases. Greater β values result in stronger molecular scale contacts, which increase molecular mobility and, ultimately, enhance the fluid's mass distribution. A thicker concentration boundary layer is subsequently observed.Figure 5 shows that the thermal distribution enlarges at greater values of the Dufour impact Du. this can be decoded that rise in the Dufour effect Du, which reason an enhancement in the concentration gradient and a faster rate of mass diffusion. The rate of heat transport associated to the particles rises as an outcome. The thermal profiles improve as a result. Velocity and Temperature decreases with increasing Eckert parameter Ec which is shown in Fig.-6 and 7, respectively. The purpose of Figs. 8 and 9 is to see how local concentration (local concentration Grashof number G_c) affects velocity and concentration. As G_c rises, an enhancement in fluid velocity is seen. As G_c increases, the buoyant force increasingly outweighs the viscous force. As a result, the Grashof number improves fluid flow, raising both the velocity and thickness of the motion barrier layer.Additionally, since the buoyancy force tends to make the concentration gradient higher, the concentration is reduced.

Fig.10-12 shows that the influence of local temperature Grashof number G_T on motion, thermal and volume fraction. For the decrease in the thickness of the boundary layer the motion reduces with rising values of the local temperature Grashof effect. For increasing the local temperature Grashof parameter, the thermal and volume fraction profiles decrease. This decrease in temperature and concentration profiles is primarily caused by the fact that raising the local temperature uses more energy and causes more heat to flow to the surrounding fluid, which lowers the thermal and volume fraction profiles. Figure 13 shows that the mass distribution degraded at increasing Kr parameters. This decline in Solutal graph is mostly caused by the increased mass distribution that also reduces the concentration distribution. The decreased velocity profile for the increasing Magnetic field M values is depicted in Fig. 14. The resistance grows as the Lorentz forces increase, which causes the velocity distribution close to the surface to flatten. Additionally, for an increasing magnetic impact in the flow field, the factor of the velocity distribution along the axial side decrease to nil at a greater distance from a given point. Consequently, when the magnetic field increased, the velocity field degraded. Figures 15 and 16 explain the impact magnetic parameter M has on thermal and volume fraction flow formulation. The temperature distribution increased for the growing magnetic field M, as seen in Figure 15. Based to the fluid's Joule heating, the temperature field grows as the magnetic field rises since more thermal energy will be liberated into the fluid as an outcome. Even as flexibility stress parameter lowers due to an enhance in the magnetic parameter, the thermal field is augmented in the fluid flow under consideration. Figure 16 also shows how the magnetic field affects the concentration profile. The concentration distribution is seen to react as a decreasing function of magnetic number in this graph.

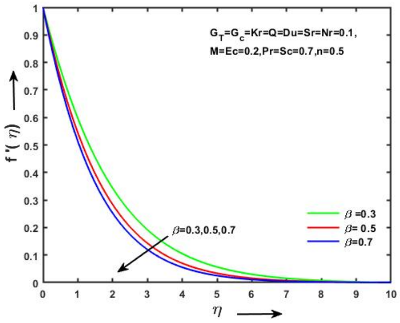

Figure 2: Motion formulation of Casson fluid parameter β.

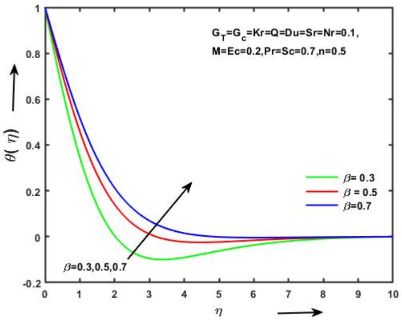

Figure 3: Thermal formulation of Casson fluid parameter β.

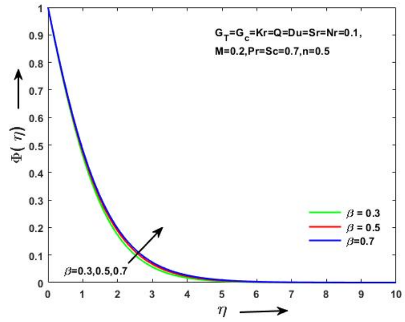

Figure 4: Concentration formulation of Casson parameter β.

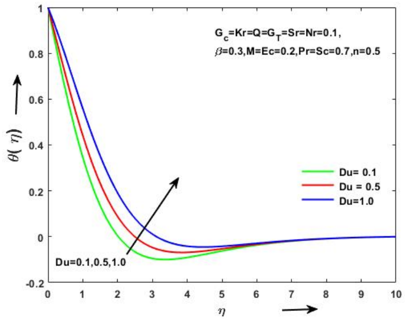

Figure 5: Temperature formulation of Dufour effect Du.

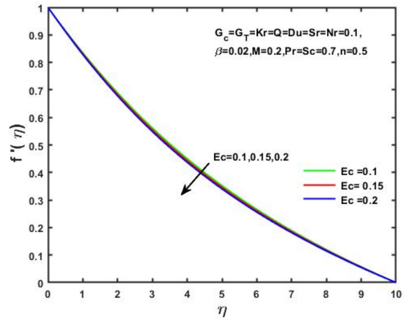

Figure 6: Velocity formulation of Eckert number Ec.

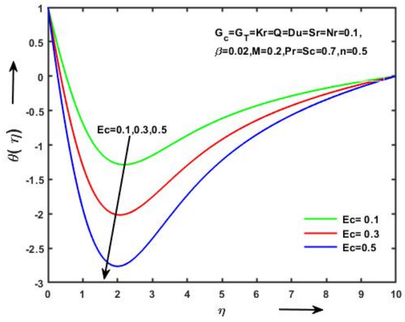

Figure 7: Temperature formulation of Eckert number Ec.

Figures (17–19) show how non-linear stretched parameters affect velocity, temperature, and concentration distribution behavior. Figures 17 illustrate how the expanding stretching variable reduces flow velocity. Additionally, at higher n numbers, this decrease in $f^{'}(\eta)$ is quite small. Since $\frac{2n}{n+1}$ is the coefficient in Equation (10) approaches 2 when $n > 1$, and an outcome the velocity profile is reduced. Additionally, the non-linear parameter n causes the velocity profile to be more disconnected. Furthermore, at a greater distance from the fixed value, the velocity profile monotonically decreased to zero. Figures 18 and 19 show, correspondingly, how the non - linear stretched parameter affects thermal and volume fraction profiles. The thermal and Solutal curves are magnified for the enhancing non - linear parameter n, as shown in Figures 18 and 19. Additionally, at a greater distance from the object, temperature and concentration exponentially decrease to zero. Also, as the non - linear stretched number n increases, the temperature and concentration boundary regions get thicker. As seen in figure.20, temperature is rising as the radiation parameter Nr and the boundary layer thickness it depends on both grow. This is because a rise in the radiation parameter heats the fluid more, which raises the temperature and thickens the layer of thermal boundaries

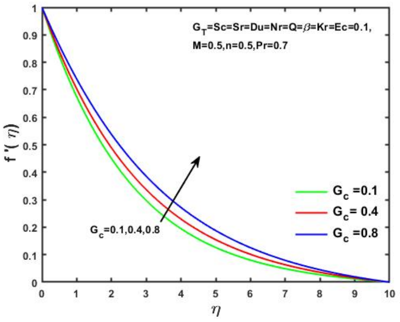

Figure 8: Velocity formulation of concentration Grashof number G_c.

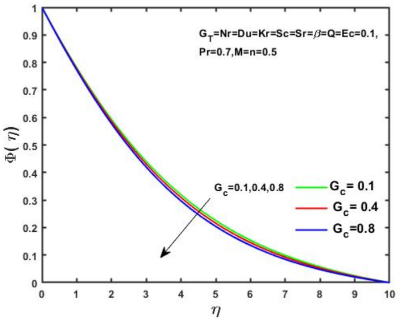

Figure 9: Concentration formulation of concentration Grashof number G_c.

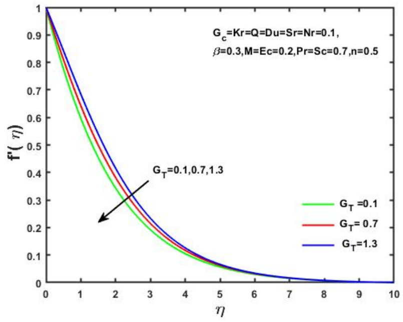

Figure 10: Velocity formulation of local thermal Grashof number G_T.

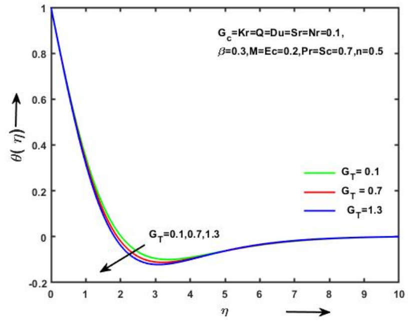

Figure 11: Temperature formulation of local thermal Grashof number G$_T$.

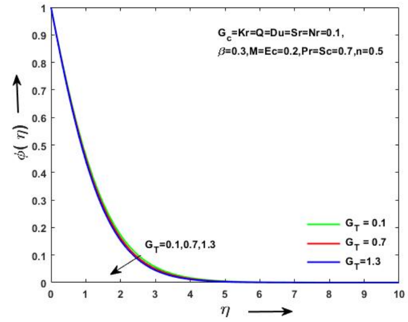

Figure 12: Concentration formulation of local thermal Grashof number G$_T$.

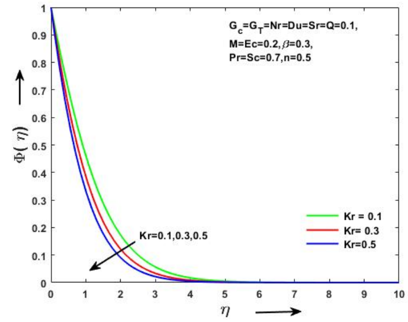

Figure 13: Concentration formulation of chemical reaction parameter Kr.

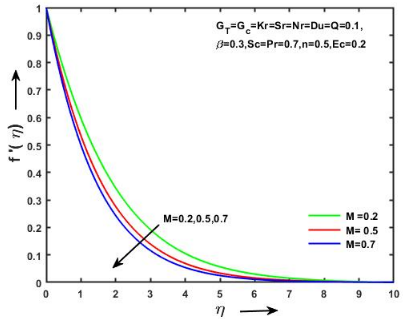

Figure 14: Velocity formulation of magnetic impact M.

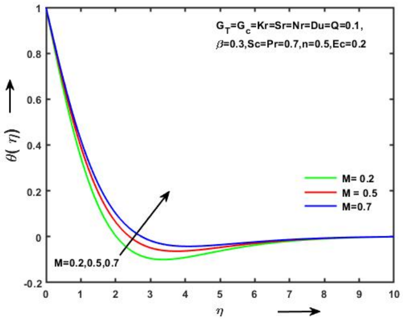

Figure 15: Temperature formulation of magnetic impact M.

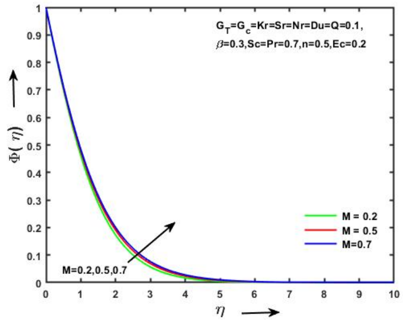

Figure 16: Volume fraction of magnetic impact M.

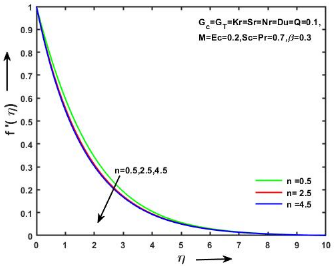

Figure 17: Motion formulation of the nonlinear parameter n.

12

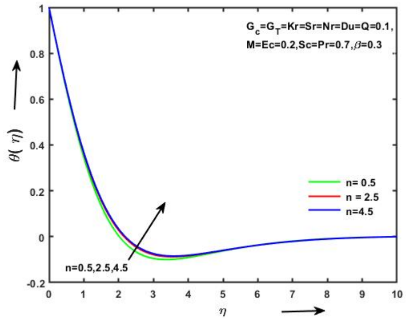

Figure 18: Temperature formulation of the nonlinear parameter n.

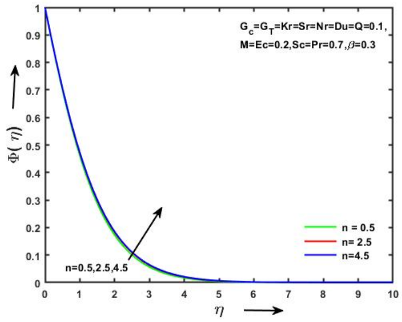

Figure 19: Concentration formulation of the nonlinear parameter n.

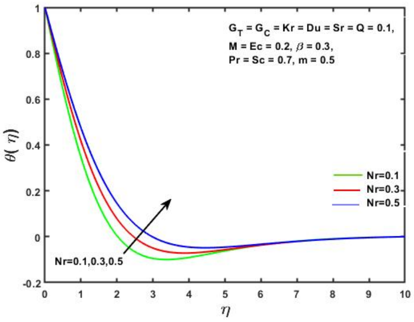

Figure 20: Temperature formulation of the Radiation parameter Nr.

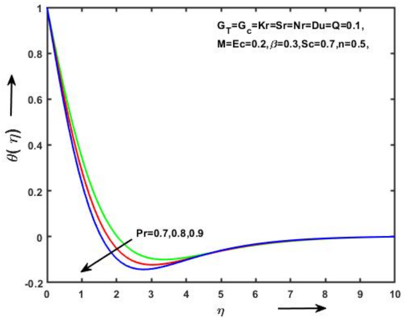

Figure 21: Temperature formulation of the Prandtl parameter Pr.

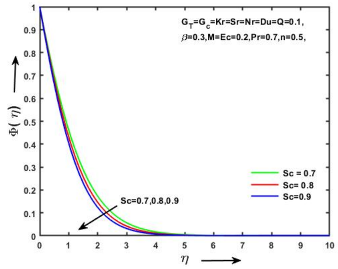

Figure 22: Concentration formulation of the Schmidt parameter Sc.

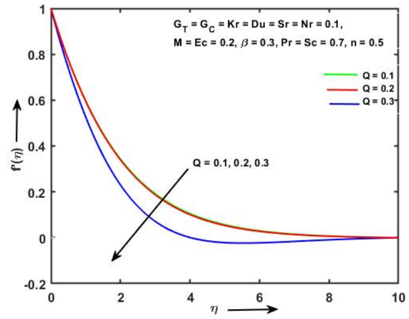

Figure 23: Motion formulations of Heat source sink Q.

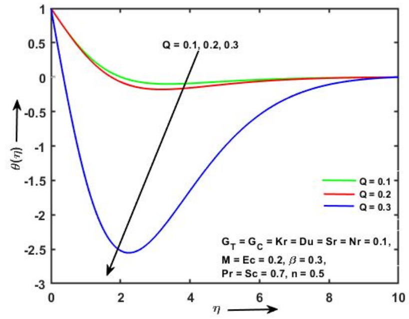

Figure 24: Temperature formulations of Heat source sink Q.

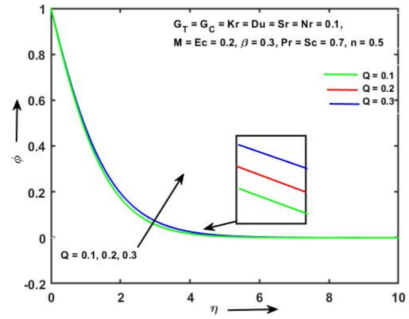

Figure 25: Concentration formulations of Heat source sink Q.

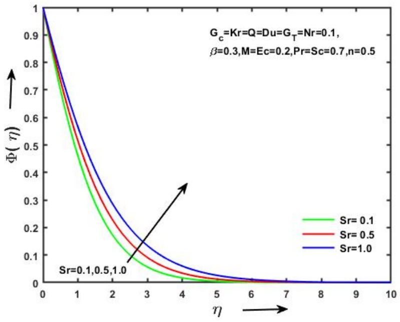

Figure 26: Concentration formulation of Soret effect Sr.

The impact of the thermal graph is displayed in Fig. 21 for various Prandtl number Pr quantities. Temperature distribution is shown to reduce for increasing in this analysis. Physically, Prandtl parameter Pr affects the thickness of the thermal boundary layer and momentum boundary layers. A larger Prandtl number denotes a thickness of the thermal boundary layer that is thinner, maintaining the boundary layer's uniform thermal distribution. The heating-boundary layer is subordinated to the magneto hydrodynamic boundary layer. Heat can dissipate more quickly in reduced Prandtl parameter fluids than in highest Prandtl parameter fluids according to their higher thermal conductivities. The impact of Schmidt parameter Sc on the dispensation of concentrations is shown in Fig.22. The volume fraction field reduces with rising Schmidt number Sc. Schmidt number, though it is constantly connected to velocity and mass diffusivities. Therefore, the fluid concentration diffusion is suppressed by rising values of Schmidt parameter Sc. In Figure 23, the motion profile reduces with the enhancing value of heat source or sink Q. Figure 24 shows how heating source or sink parameter Q affects temperature. The figure shows that as the heat sink's power rises, the non - dimensional temperature lowers, even as the heat source's power rises, the temperature rises. Therefore, as the heat sink parameter is raised, the thermal boundary layer reduces thickness, whereas the heat source effect causes it to rise. Also Fig.25 denotes the increasing concentration profile with the increasing value of heat source or sink Q. Figure 26 provided a visual representation of the consequences of thermal migration or Soret number (Sr). Sr represents the mass transfer rate between lowest to the highest solute concentrations and is essentially a ratio of temperature gradient to concentration. Figure 26 show that the concentration profile is exhibiting a rising behavior along with the rising value of Sr.

Table I: Impression of parameters of notice on skin friction, Nusselt parameter, and Sherwood parameter:

n	G_T	G_C	β	M	Pr	Ec	Sc	Q	Du	Sr	Nr	Kr	$Cf_xRe_x{}^{1/2}$	$-Nu_xRe_x{}^{-1/2}$	$-Sh_xRe_x{}^{-1/2}$
0.5	**0.1**	**0.1**	**0.3**	**0.2**	**0.7**	**0.2**	**0.7**	**0.1**	**0.1**	**0.1**	**0.1**	**0.1**	**-1.85657**	**0.65240**	**0.55783**
2.5													**-2.23135**	**0.65017**	**0.54858**
4.5													**-2.3244**	**0.64932**	**0.54636**
0.5	**0.1**												**-1.85657**	**0.6524**	**0.55783**
	0.7												**-1.59447**	**0.65546**	**0.56157**
	1.3												**-1.33728**	**0.65742**	**0.56520**
	0.1		**0.3**										**-1.85657**	**0.652401**	**0.557836**
			0.7										**-1.43724**	**0.535531**	**0.5621336**
			0.7										**-1.44060**	**0.482280**	**0.5611931**
			0.3	**0.2**									**-1.85657**	**0.652401**	**0.557836**
				0.5									**-2.33732**	**0.928422**	**0.508645**
				0.7									**-2.05587**	**0.571925**	**0.545825**

				0.2	**0.7**								**-1.85657**	**0.652401**	**0.55783**
					0.8								**-1.48080**	**0.727980**	**.561245**
					0.9								**-1.53126**	**0.79666**	**0.5589154**
			0.02		**0.7**	**0.1**							**-10.18979**	**2.044867**	**0.594878**
						0.3							**-26.32619**	**10.6900**	**0.507348**
						0.5							**-33.7957**	**18.38017**	**0.4583266**
			0.3			**0.2**	**0.7**						**-1.85657**	**0.652401**	**0.557836**
							0.8						**-2.01032**	**0.925019**	**0.558312**
							0.9						**-1.42483**	**0.648136**	**0.558312**
							0.7	**0.1**					**-1.85657**	**0.652401**	**0.557836**
								0.2					**-1.463515**	**0.626327**	**0.56106**
								0.3					**-1.63419**	**0.691826**	**0.551289**
								0.1	**0.1**				**-1.856577**	**0.652401**	**0.557836**
									0.5				**-1.9724632**	**0.809687**	**0.515012**
									1				**-1.222268**	**0.336784**	**0.573077**
									0.1	**0.1**			**-1.85657**	**0.652401**	**0.557836**
										0.5			**-1.419446**	**0.663674**	**0.494086**
										1			**-2.0097**	**0.948055**	**0.3811412**
										0.1	**0.1**		**-1.856577**	**0.652401**	**0.557836**
											0.3		**-1.34829**	**0.577117**	**0.56761**
											0.5		**-1.283884**	**0.51627**	**0.570809**
											0.1	**0.1**	**-1.856577**	**0.652401**	**0.557836**
												0.2	**-1.42427**	**0.6509020**	**0.64566**
												0.3	**-1.425672**	**0.645687**	**0.7180935**
		0.1	**0.1**	**0.5**		**0.1**	**0.1**					**0.1**	**-3.678953**	**0.75017**	**0.200603**
		0.4											**-3.2968876**	**0.7372915**	**0.20394816**
		0.8											**-2.803422**	**0.720553**	**0.208056**

Table II: validate the current values of various physical parameters to previouslyresults of Basha et al. Ref. [3] andVajraveluk. Ref. [21] respectively.

		Vajraveluk.Ref[21]		**Basha et al. Ref. [3]**		**current values**	
n	Pr	$f^{''}(0)$	$\theta'(0)$	$f^{''}(0)$	$\theta'(0)$	$f^{''}(0)$	$\theta'(0)$
1	**0.71**	**-1.0000**	**-0.4590**	**-1.00005468353233**	**-0.45908783553**	**-1.00001**	**-0.459033**
5	**0.71**	**-1.1945**	**-0.4394**	**-1.19449559110388**	**-0.4395495710690**	**-1.1945**	**-0.4394**
10	**0.71**	**-1.2348**	**-0.4357**	**-1.23488263663213**	**-0.4356401511209**	**-1.23488**	**-0.435641**
1	**7**	**-1.0000**	**-1.8953**	**-1.00005468353233**	**-1.8953100096284**	**-1.00001**	**-1.89541**
5	**7**	**-1.1945**	**-1.8610**	**-1.19449559110388**	**-1.8609911518168**	**-1.1945**	**-1.86159**
7	**7**	**-1.2348**	**-1.8541**	**-1.23488263663213**	**-1.8540100137230**	**-1.23488**	**-1.85464**

4 Conclusion:

From the current study we conclude that the mathematical outcomes for diverse physical quantities have been dissolved. The effects of the transfer of mass and heat including Soret and Dufour effects, heat absorption/ generation, Radiation parameter, chemical reaction, have been expressed for a non-linear stretchy surface in the rheology.This problem can be solved for future purpose if sheet is inclined at some angle. The boundary conditions and fluids can also be changed. The ending conclusion is

- An increasing value of Soret effect, grow the concentration of the fluid. And an increasing value of Heat source/ sink, also enhancing the concentration of the fluid

- Temperature profile is increased for an increasing value of Dufour effect
- Motion and thermal profiles of the fluid are decreased due to increased Heat source/sink
- Temperature profile of the fluid is increased when raised thermal radiation
- Motion and thermal profiles of the fluid are decreased due to enhanced Eckert number
- The decreasing skin-friction rate impression is seen for radiation parameters
- For the Soret effect, the diminishing Sherwood parameter impression is observed

References

[1] Ebrahem A Algehyne, Musaad S Aldhabani, Anwar Saeed, Abdullah Dawar, and Poom Kumam. Mixed convective flow of casson and oldroyd-b fluids through a stratified stretching sheet with nonlinear thermal radiation and chemical reaction. *Journal of Taibah University for Science*, 16(1):193–203, 2022.

[2] Sameh E Ahmed, MA Mansour, A Mahdy, and Shadia S Mohamed. Entropy generation due to double diffusive convective flow of casson fluids over nonlinearity stretching sheets with slip conditions. *Engineering Science and Technology, an International Journal*, 20(6):1553–1562, 2017.

[3] Mushtaq Ahmad, Muhammad Imran Asjad, and Jagdev Singh. Application of novel fractional derivative to heat and mass transfer analysis for the slippage flow of viscous fluid with single-wall carbon nanotube subject to newtonian heating. *Mathematical Methods in the Applied Sciences*, 2021.

[4] Hussain Basha, Naresh Kumar Nedunuri, Gudala Janardhana Reddy, and Sreenivasulu Ballem. Thermal analysis of buoyancy-motivated casson fluid flow with time-independent chemical reaction under lorentz forces. *Heat Transfer*, 50(7):7291–7320, 2021.

[5] Hussain Basha, Sreenivasulu Ballem, G Janardhana Reddy, Harish Holla, and Mikhail A Sheremet. Buoyancy-motivated dissipative free convection flow of walters-b fluid along a stretching sheet under the soret effect and lorentz force influence. *Heat Transfer*, 51(4):3512–3539, 2022.

[6] Subrata Das, Hiranmoy Mondal, Prabir Kumar Kundu, and Precious Sibanda. Spectral quasi-linearization method for casson fluid with homogeneous heterogeneous reaction in presence of nonlinear thermal radiation over an exponential stretching sheet. *Multidiscipline Modeling in Materials and Structures*, 2018.

[7] K Gangadhar, R Edukondala Nayak, and M Venkata Subba Rao. Buoyancy effect on mixed convection boundary layer flow of casson fluid over a non linear stretched sheet using the spectral relaxation method. *International Journal of Ambient Energy*, 43(1):1994–2002, 2022.

[8] Sami Ul Haq, Saeed Ullah Jan, Syed Inayat Ali Shah, Ilyas Khan, and Jagdev Singh. Heat and mass transfer of fractional second grade fluid with slippage and ramped wall temperature using caputo-fabrizio fractional derivative approach. *AIMS Mathematics*, 5(4):3056–3088, 2020.

[9] Abid Hussanan, Mohd Zuki Salleh, Hamzeh Taha Alkasasbeh, and Ilyas Khan. Mhd flow and heat transfer in a casson fluid over a nonlinearly stretching sheet with newtonian heating. *Heat transfer research*, 49(12), 2018.

[10] SM Ibrahim, G Lorenzini, P Vijaya Kumar, and CSK Raju. Influence of chemical reaction and heat source on dissipative mhd mixed convection flow of a casson nanofluid over a nonlinear permeable stretching sheet. *International Journal of Heat and Mass Transfer*, 111:346–355, 2017.

[11] Sweta Matta, Appidi L BalaSidduluMalga, and P Pramod Kumar. Radiation and chemical reaction effects on unsteady mhd free convention mass transfer fluid flow in a porous plate. *Indian Journal of Science and Technology*, 14(8):707–717, 2021.

[12] Ruchika Mehta, Ravindra Kumar, Himanshu Rathore, and Jagdev Singh. Joule heating effect on radiating mhd mixed convection stagnation point flow along vertical stretching sheet embedded in a permeable medium and heat generation/absorption. *Heat Transfer*, 51(8):7369–7386, 2022.

[13] Monica Medikare, Sucharitha Joga, Kishore Kumar Chidem, et al. Mhd stagnation point flow of a casson fluid over a nonlinearly stretching sheet with viscous dissipation. *American Journal of Computational Mathematics*, 6(01):37, 2016.

[14] M Mustafa and Junaid Ahmad Khan. Model for flow of casson nanofluid past a non-linearly stretching sheet considering magnetic field effects. *AIP advances*, 5(7):077148, 2015.

[15] Swati Mukhopadhyay. Casson fluid flow and heat transfer over a nonlinearly stretching surface. *Chinese Physics B*, 22(7):074701, 2013.

[16] NB Naduvinamani and Usha Shankar. Thermal-diffusion and diffusion-thermo effects on squeezing flow of unsteady magneto-hydrodynamic casson fluid between two parallel plates with thermal radiation. *Sādhanā*, 44(8):1–16, 2019.

[17] Satyaban Panigrahi, Motahar Reza, and Akshya Kumar Mishra. Mixed convective flow of a powell-eyring fluid over a non-linear stretching surface with thermal diffusion and diffusion thermo. *Procedia Engineering*, 127:645–651, 2015.

[18] P Bala Anki Reddy. Magnetohydrodynamic flow of a casson fluid over an exponentially inclined permeable stretching surface with thermal radiation and chemical reaction. *Ain Shams Engineering Journal*, 7(2):593–602, 2016.

[19] Jagdev Singh, Devendra Kumar, Dumitru Baleanu, et al. A hybrid analytical algorithm for thin film flow problem occurring in non-newtonian fluid mechanics. *Ain Shams Engineering Journal*, 12(2):2297–2302, 2021.

[20] Jagdev Singh, Devendra Kumar, and Sunil Kumar. An efficient computational method for local fractional transport equation occurring in fractal porous media. *Computational and Applied Mathematics*, 39(3):1–10, 2020.

[21] Chenna Sumalatha, Shankar Bandari, et al. Effects of radiations and heat source/sink on a casson fluid flow over nonlinear stretching sheet. *World Journal of Mechanics*, 5(12):257, 2015.

[22] Gandluru Sreedevi, DRV Rao, Oluwole Daniel Makinde, and G Reddy. Soret and dufour effects on mhd flow with heat and mass transfer past a permeable stretching sheet in presence of thermal radiation. 2017.

[23] Shyam Sunder Tak, Rajeev Mathur, Rohit Kumar Gehlot, and Aiyub Khan. Mhd free convection-radiation interaction along a vertical surface embedded in darcian porous medium in presence of soret and dufour's effects. *Thermal Science*, 14(1):137–145, 2010.

[24] Imran Ullah, Sharidan Shafie, and Ilyas Khan. Effects of slip condition and newtonian heating on mhd flow of casson fluid over a nonlinearly stretching sheet saturated in a porous medium. *Journal of King Saud University-Science*, 29(2):250–259, 2017.

[25] Imran Ullah, Ilyas Khan, and Sharidan Shafie. Soret and dufour effects on unsteady mixed convection slip flow of casson fluid over a nonlinearly stretching sheet with convective boundary condition. *Scientific Reports*, 7(1):1–19, 2017.

[26] K Vajravelu. Viscous flow over a nonlinearly stretching sheet. *Applied mathematics and computation*, 124(3):281–288, 2001.

J. COMPUTATIONAL ANALYSIS AND APPLICATIONS, VOL. 31, NO. 2, 2023, COPYRIGHT 2023 EUDOXUS PRESS, LLC

M/M/1 Retrial Queueing Model with Server Breakdown and Feedback

M.SEENIVASAN,
Mathematics Wings - DDE, Annamalai University,
Annamalainagar-608002, India.
Email: emseeni@yahoo.com
J.SHINY EPCIYA,
Department of Mathematics, Annamalai University,
Annamalainagar-608002, India.
Email: epciyashinydoss@gmail.com

December 28, 2022

In this article, we present M/M/1 retrial queueing system with feedback and Server breakdown. Arrival follows Poisson process. An arrival finds the system is full, the arrival enters into an orbit of size infinity. From the orbit the customers try their luck. The time between two successive retrials is called retrial time, it follows negative exponential distribution. Service time is exponentially distributed. Once the server experiences an unanticipated failure, it should be repaired and returned to normal functioning. Feedback is when unsatisfied customers join the orbit again for a service. Matrix geometric method is engaged to determined performance measures. Some graphical representations are also acquired.

AMS subject classification number— 90B22, 60K30 and 60K25
Key Words —- Retrial Queue, Arrival Rate, Server Breakdown, Feedback, Matrix Geometric Method (MGM).

1 Introduction

Queueing model can be found in variety of real-life scenarios. Queueing system with feedback have several uses in the manufacturing, computing and telecommunications systems. In queueing theory in which customer arrives who finds the sever and waiting places are engaged, may retry after an irregular measurement of time is known as retrial queue. During the period of getting service the server may get sudden breakdown and send to repair, at that time the customer wait to get complete service. After getting a service the customer has to decide to leave the system or to continue the service. The unsatisfied customer goes to the orbit for another service is called feedback. Artalejo (2012) determined M/M/1 retrial queue with finite population. A survey of retrial queues was explored by Falin (1990). M/M/1 retrial queueing system with variable service rates in priority service was analyzed by Ayyappan Govindan et al (2011). Neuts (1981) discussed several matrix geometric stochastic model solutions. Praveen Deora et al (2021) analyzed the cost analysis and optimization of machine repair model with working vacation and feedback policy.

This model has been investigated by Choi, et al (1998) analyzed multi-server retrial queue with feedback and loss. Choi and Kulkarni (1992) explored feedback retrial queueing model. Chuen-Horng Lin and Jau-Chuan Ke (2011) determined multi server retrial queue with loss and feedback. Retrial queue with server breakdown has been investigated by Kalyanaraman and Seenivasan (2011) analyzed multi-server retrial queue with breakdown and geometric loss. Seenivasan et al investigated different type of queueing models and their characteristics behavior. With the help of that research criteria we developed the concept using in retrial queueing model.

Following is an overview of the remaining sections of this article. Construction of our model is presented in section 2. Section 3 includes some numerical examples. Section 4 describes the system performance measures, as well as the summary follows in the end part of this article. [1]

2 Construction of the model

In this article, we concentrated on retrial queue with server breakdown and Feedback. Arriving customer follows Poisson process with rate λ. Assuming that the server is free, the incoming customer will be served instantly, and if the server is occupied, he will joining the orbit. After certain uneven estimations of time, customers from orbit attempt their luck. In retrial, each customer is viewed as equivalent to a primary customer. The retrial time is exponentially distributed with rate ν. The service time is exponential distributed with service rate μ. Eventually when the server could open to unforeseen breakdown with rate α and after it ought to be fixed and goes to normal service with rate ϕ. Server will wait unless there is no queue at the ending of the vacation. Assuming that the served customer decide to leaves the framework forever with rate $\beta^{'} = (1-\beta)$ (or) he rejoins the orbit again for another service at a rate β (it is called feedback). Our model's transition diagram is depicted in (Figure. 1).

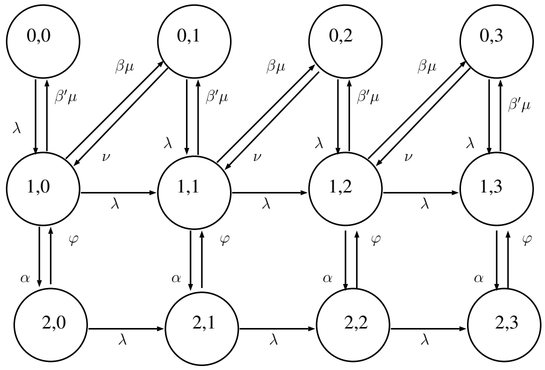

---

[1] Corresponding Author: M.Seenivasan, Mathematics Wings - DDE, Annamalai University, Annamalainagar - 608002, Tamilnadu, India.
Email: emseeni@yahoo.com

Figure 1. Transition Diagram

Let $A(t), B(t) : t \geq 0$ be a stochastic process with state space at time t,
A(t) = 0, server is idle,
A(t) = 1, server is working,
A(t) = 2, server gets breakdown.
B(t) indicates no. of customers in the orbit.
Lexicographical series is given by:
$\Omega = (0,0)U(1,0)U(i,j); i = 0,1, j = 1,2, ..., n \geq 1$
Infinitesimal generated matrix Q:

$$Q = \begin{pmatrix} K_{00} & L_{00} & \cdots & \cdots & \cdots & \cdots & \cdots & \cdots \\ N_{00} & M_{00} & L_{00} & \cdots & \cdots & \cdots & \cdots & \cdots \\ 0 & N_{00} & M_{00} & L_{00} & \cdots & \cdots & \cdots & \cdots \\ 0 & \cdots & N_{00} & M_{00} & \cdots & \cdots & \cdots & \cdots \\ 0 & \cdots & \cdots & N_{00} & \cdots & \cdots & \cdots & \cdots \\ \cdots & \cdots & \cdots & \cdots & \cdots & \cdots & \cdots & \cdots \end{pmatrix}$$

Where

$$K_{00} = \begin{pmatrix} -(\lambda) & \lambda & 0 \\ \beta^{'}\mu & -(\lambda+\alpha+\mu) & \alpha \\ 0 & \varphi & -(\lambda+\varphi) \end{pmatrix}; \; L_{00} = \begin{pmatrix} 0 & 0 & 0 \\ \beta\mu & \lambda & 0 \\ 0 & 0 & \lambda \end{pmatrix};$$

$$N_{00} = \begin{pmatrix} 0 & \nu & 0 \\ 0 & 0 & 0 \\ 0 & 0 & 0 \end{pmatrix}; \; M_{00} = \begin{pmatrix} -(\lambda+\nu) & \lambda & 0 \\ \beta^{'}\mu & -(\lambda+\alpha+\mu) & \alpha \\ 0 & \varphi & -(\lambda+\varphi) \end{pmatrix};$$

We define $\pi_{ij} = \{A = i, B = j\}$=$\lim_{t\to\infty} Pr\{A(t) = i, B(t) = j\}$, where j indicates no. of customers in the orbit & i indicates the server state.
From the balance equation $\Pi Q = 0$. (1)
$\pi_0 K_{00} + \pi_1 N_{00} = 0$ (2)
$\pi_0 L_{00} + \pi_1 M_{00} + \pi_2 N_{00} = 0$ (3)
$\pi_1 L_{00} + \pi_2 M_{00} + \pi_3 N_{00} = 0$ (4)
.
.
.
$\pi_i L_{00} + \pi_{i+1} M_{00} + \pi_{i+2} N_{00} = 0$ (5)
And $\pi_j = \pi_0 R^j$ for$j \geq 1$. (6)
We can assuming that R is a rate matrix.
$\pi_0[K_{00} + RN_{00}] = 0$ (7)
$\pi_0[R^2 N_{00} + RM_{00} + L_{00}] = 0$ (8)
The normalizing condition is
$\Pi_0 \left[I - R\right]^{-1} e = 1$ (9)
'e' is a column vector with all elements equal to 1.
Π partitioned as $\Pi = (\Pi_0, \Pi_1, \Pi_2)$ is a static prob. vector of the (reducible) generator matrix is $D = L_{00} + M_{00} + N_{00}$.

$$D = \begin{pmatrix} -(\lambda+\nu) & (\lambda+\nu) & 0 \\ \mu & -(\mu+\alpha) & \alpha \\ 0 & \varphi & -\varphi \end{pmatrix} \tag{10}$$

And Π could be displayed to be stationary in order that $\Pi D = 0$ & $\Pi e = 1$.

$$\Pi_0 = [1 + \frac{\lambda + \nu}{\mu} + \frac{\alpha(\lambda + \nu)}{\varphi\mu}]^{-1}; \Pi_1 = \frac{\lambda + \nu}{\mu}\Pi_0; \Pi_2 = \frac{\alpha(\lambda + \nu)}{\varphi\mu}\Pi_0.$$

The static condition adopts the format actually determined by the drift condition. $\Pi L_{00} e < \Pi N_{00} e$. Equation (10) determines D's static probability. After obtaining rate matrix R, our probability vectors Πj's ($j \geq 1$) are calculated using Eqs. (6) and (9).

3 Numerical Study

By changing the values of the parameter λ & fixing all other parameters

Case i

If $\lambda = 0.10$, $\mu = 2.0$, $\beta = 0.4$,$\beta^{'} = 0.6$,$\alpha = 0.30$, $\varphi = 0.50$, $\nu = 0.05$ & $R = \begin{pmatrix} 0.3950 & 0.2226 & 0.0247 \\ 0.5926 & 0.1838 & 0.0370 \\ 0.4938 & 0.1868 & 0.1975 \end{pmatrix}$

Table 1. Probability vectors

Π_j	π_{0j}	π_{1j}	π_{2j}	Total
π_0	0.2436	0.0203	0.0361	0.3000
π_1	0.1261	0.0647	0.0139	0.2047
π_2	0.0950	0.0426	0.0083	0.1459
π_3	0.0668	0.0305	0.0056	0.1029
π_4	0.0472	0.0215	0.0039	0.0726
π_5	0.0333	0.0152	0.0027	0.0512
π_6	0.0235	0.0107	0.0019	0.0316
π_7	0.0166	0.0076	0.0014	0.0256
π_8	0.0117	0.0053	0.0010	0.0180
π_9	0.0083	0.0038	0.0007	0.0128
π_{10}	0.0058	0.0027	0.0005	0.0090
π_{11}	0.0041	0.0012	0.0003	0.0063
π_{12}	0.0029	0.0008	0.0002	0.0044
π_{13}	0.0020	0.0006	0.0002	0.0031
π_{14}	0.0014	0.0004	0.0001	0.0022
π_{15}	0.0010	0.0003	0.0001	0.0016
π_{16}	0.0007	0.0002	0.0001	0.0011

π_{17}	0.0005	0.0001	0.0000	0.0007
π_{18}	0.0004	0.0001	0.0000	0.0006
π_{19}	0.0003	0.0001	0.0000	0.0004
π_{20}	0.0002	0.0001	0.0000	0.0003
Total				0.9999

The prob. vectors in table 1 were calculated by using the matrix R in Equation (7) and Equation (9), we get the vector $\Pi_0 = (0.2436\ 0.0203\ 0.0361)$. Utilizing Π_0 in Equation (6), the rest of the vectors are obtained. Hence the sum of the probability is affirmed to be $0.9999 \approx 1$.

Case ii

If $\lambda = 0.15$, $\mu = 2.0$, $\beta = 0.4$,$\beta' = 0.6$, $\alpha = 0.30$, $\varphi = 0.50$, $\nu = 0.05$ & $R = \begin{pmatrix} 0.4548 & 0.2665 & 0.0394 \\ 0.6064 & 0.2264 & 0.0525 \\ 0.4665 & 0.2100 & 0.2711 \end{pmatrix}$

Table 2. Probability vectors

Π_j	π_{0j}	π_{1j}	π_{2j}	Total
π_0	0.1364	0.0171	0.0338	0.1873
π_1	0.0882	0.0473	0.0154	0.1509
π_2	0.0760	0.0375	0.0101	0.1236
π_3	0.0621	0.0309	0.0077	0.1006
π_4	0.0505	0.0251	0.0062	0.0818
π_5	0.0411	0.0204	0.0050	0.0665
π_6	0.0334	0.0166	0.0040	0.0540
π_7	0.0272	0.0135	0.0033	0.0440
π_8	0.0221	0.0110	0.0027	0.0358
π_9	0.0179	0.0089	0.0022	0.0290
π_{10}	0.0146	0.0073	0.0018	0.0237
π_{11}	0.0119	0.0059	0.0014	0.0192
π_{12}	0.0096	0.0048	0.0012	0.0156
π_{13}	0.0078	0.0039	0.0009	0.0126
π_{14}	0.0064	0.0032	0.0008	0.0104
π_{15}	0.0052	0.0026	0.0006	0.0084
π_{16}	0.0042	0.0021	0.0005	0.0068
π_{17}	0.0034	0.0017	0.0004	0.0055
π_{18}	0.0028	0.0014	0.0003	0.0045

π_{19}	0.0023	0.0011	0.0003	0.0037
π_{20}	0.0018	0.0009	0.0002	0.0029
π_{21}	0.0015	0.0007	0.0002	0.0024
π_{22}	0.0012	0.0006	0.0001	0.0019
π_{23}	0.0010	0.0005	0.0001	0.0021
π_{24}	0.0008	0.0004	0.0001	0.0013
π_{25}	0.0007	0.0003	0.0001	0.0011
π_{26}	0.0005	0.0003	0.0001	0.0009
π_{27}	0.0004	0.0002	0.0001	0.0007
π_{28}	0.0004	0.0002	0.0000	0.0006
π_{29}	0.0003	0.0001	0.0000	0.0004
π_{30}	0.0002	0.0001	0.0000	0.0003
Total				0.9998

The prob. vectors in table 2 were calculated by using the matrix R in Equation (7) and Equation (9), we get the vector $\Pi_0 = (0.1364\ 0.0171\ 0.0338)$. Utilizing Π_0 in Equation (6), the rest of the vectors are obtained. Hence the sum of the probability is affirmed to be $0.9998 \approx 1$.

Case iii

If $\lambda = 0.20$, $\mu = 2.0$, $\beta = 0.4$,$\beta^{'} = 0.6$, $\alpha = 0.30$, $\varphi = 0.50$, $\nu = 0.05$ & $R = \begin{pmatrix} 0.4827 & 0.2894 & 0.0517 \\ 0.6034 & 0.2543 & 0.0647 \\ 0.4310 & 0.2160 & 0.3319 \end{pmatrix}$

Table 3. Probability vectors

Π_j	π_{0j}	π_{1j}	π_{2j}	Total
π_0	0.0849	0.0142	0.0305	0.1296
π_1	0.0627	0.0348	0.0154	0.1129
π_2	0.0579	0.0303	0.0106	0.0988
π_3	0.0508	0.0268	0.0085	0.0861
π_4	0.0443	0.0233	0.0072	0.0748
π_5	0.0386	0.0203	0.0062	0.0651
π_6	0.0335	0.0177	0.0054	0.0566
π_7	0.0292	0.0154	0.0047	0.0493
π_8	0.0253	0.0133	0.0040	0.0416
π_9	0.0220	0.0116	0.0035	0.0371
π_{10}	0.0192	0.0101	0.0031	0.0324
π_{11}	0.0166	0.0088	0.0027	0.0281
π_{12}	0.0145	0.0076	0.0023	0.0244

π_{13}	0.0126	0.0066	0.0020	0.0212
π_{14}	0.0109	0.0058	0.0017	0.0184
π_{15}	0.0095	0.0050	0.0015	0.0160
π_{16}	0.0083	0.0044	0.0013	0.0140
π_{17}	0.0072	0.0038	0.0011	0.0121
π_{18}	0.0062	0.0033	0.0010	0.0105
π_{19}	0.0054	0.0029	0.0009	0.0092
π_{20}	0.0047	0.0025	0.0008	0.0080
π_{21}	0.0041	0.0022	0.0007	0.0070
π_{22}	0.0036	0.0019	0.0006	0.0061
π_{23}	0.0031	0.0016	0.0005	0.0052
π_{24}	0.0027	0.0014	0.0004	0.0045
π_{25}	0.0023	0.0012	0.0004	0.0039
π_{26}	0.0020	0.0011	0.0003	0.0034
π_{27}	0.0018	0.0009	0.0003	0.0030
π_{28}	0.0015	0.0008	0.0002	0.0025
π_{29}	0.0013	0.0007	0.0002	0.0022
π_{30}	0.0012	0.0006	0.0002	0.0020
π_{31}	0.0010	0.0005	0.0002	0.0017
π_{32}	0.0009	0.0005	0.0001	0.0015
π_{33}	0.0008	0.0004	0.0001	0.0013
π_{34}	0.0007	0.0003	0.0001	0.0011
π_{35}	0.0006	0.0003	0.0001	0.0010
π_{36}	0.0005	0.0003	0.0001	0.0009
π_{37}	0.0004	0.0002	0.0001	0.0007
π_{38}	0.0003	0.0002	0.0001	0.0006
π_{39}	0.0003	0.0002	0.0000	0.0005
π_{40}	0.0002	0.0001	0.0000	0.0003
Total				0.9980

The prob. vectors in table 3 were calculated by using the matrix R in Equation (7) and Equation (9), we get the vector $\Pi_0 = (0.0849\ 0.0142\ 0.0305)$. Utilizing Π_0 in Equation (6), the rest of the vectors are obtained. Hence the sum of the probability is affirmed to be $0.9980 \approx 1$.

Case iv

If $\lambda = 0.25$, $\mu = 2.0$,$\beta = 0.4$,$\beta^{'} = 0.6$, $\alpha = 0.30$, $\varphi = 0.50$, $\nu = 0.05$ & $R = \begin{pmatrix} 0.4938 & 0.3055 & 0.0617 \\ 0.5926 & 0.2768 & 0.0741 \\ 0.3950 & 0.2161 & 0.3827 \end{pmatrix}$

Table 4. Probability vectors

Π_j	π_{0j}	π_{1j}	π_{2j}	Total
π_0	0.0570	0.0119	0.0275	0.0964
π_1	0.0416	0.0267	0.0149	0.0877
π_2	0.0444	0.0247	0.0105	0.0796
π_3	0.0407	0.0227	0.0086	0.0720
π_4	0.0369	0.0206	0.0075	0.0650
π_5	0.0334	0.0186	0.0067	0.0587
π_6	0.0301	0.0168	0.0060	0.0529
π_7	0.0272	0.0152	0.0054	0.0478
π_8	0.0245	0.0137	0.0049	0.0431
π_9	0.0221	0.0123	0.0044	0.0388
π_{10}	0.0200	0.0111	0.0040	0.0351
π_{11}	0.0180	0.0100	0.0036	0.0316
π_{12}	0.0163	0.0091	0.0032	0.0286
π_{13}	0.0147	0.0082	0.0029	0.0258
π_{14}	0.0132	0.0074	0.0026	0.0232
π_{15}	0.0119	0.0067	0.0024	0.0210
π_{16}	0.0108	0.0060	0.0021	0.0189
π_{17}	0.0097	0.0054	0.0019	0.0170
π_{18}	0.0088	0.0049	0.0017	0.0154
π_{19}	0.0079	0.0044	0.0016	0.0139
π_{20}	0.0071	0.0040	0.0014	0.0125
π_{21}	0.0064	0.0036	0.0013	0.0113
π_{22}	0.0058	0.0032	0.0012	0.0102
π_{23}	0.0052	0.0029	0.0010	0.0091
π_{24}	0.0047	0.0026	0.0009	0.0082
π_{25}	0.0043	0.0024	0.0008	0.0075
π_{26}	0.0038	0.0021	0.0008	0.0067
π_{27}	0.0035	0.0019	0.0007	0.0061
π_{28}	0.0033	0.0017	0.0006	0.0054
π_{29}	0.0028	0.0016	0.0006	0.0050
π_{30}	0.0025	0.0014	0.0005	0.0044
π_{31}	0.0023	0.0013	0.0005	0.0041
π_{32}	0.0021	0.0012	0.0004	0.0037

π_{33}	0.0019	0.0010	0.0004	0.0033
π_{34}	0.0017	0.0009	0.0003	0.0029
π_{35}	0.0015	0.0008	0.0003	0.0026
π_{36}	0.0014	0.0008	0.0003	0.0025
π_{37}	0.0012	0.0007	0.0002	0.0021
π_{38}	0.0011	0.0006	0.0002	0.0018
π_{39}	0.0010	0.0006	0.0002	0.0018
π_{40}	0.0009	0.0005	0.0002	0.0016
π_{41}	0.0008	0.0005	0.0002	0.0015
π_{42}	0.0007	0.0004	0.0001	0.0012
π_{43}	0.0007	0.0004	0.0001	0.0012
π_{44}	0.0006	0.0003	0.0001	0.0010
π_{45}	0.0005	0.0003	0.0001	0.0009
π_{46}	0.0005	0.0003	0.0001	0.0009
π_{47}	0.0004	0.0002	0.0001	0.0007
Total				0.9990

The prob. vectors in table 4 were calculated by using the matrix R in Equation (7) and Equation (9), we get the vector $\Pi_0 = (0.0570\ 0.0119\ 0.0275)$. Utilizing Π_0 in Equation (6), the rest of the vectors are obtained. Hence the sum of the probability is affirmed to be $0.9990 \approx 1$.

4 Performance Measures

The following performance measures were discovered using steady-state probabilities.

- Pr{server is in idle} $E(I) = \Pi_0$ (11)
- Pr{server is on busy period} $E(B) = \sum_{j=1}^{\infty} j\pi_{1j}$ (12)
- Pr{server gets breakdown} $E(BD) = \sum_{j=1}^{\infty} j\pi_{2j}$ (13)
- Pr{Total no. of customers in the system} $E(N) = E(I) + E(B) + E(BD)$ (14)
- Pr{No customer in the orbit} $PNCO = \sum_{i=0}^{2} \pi_{i0}$ (15)

Table 5. Performance Measures

λ	0.1	0.15	0.2	0.25
E(I)	0.6917	0.6327	0.5954	0.5660
E(B)	0.7077	1.3304	2.0656	3.6330
E(BD)	0.1297	0.3255	0.6596	1.0317
E(N)	2.3764	4.3319	6.6537	9.8917
PNCO	0.3000	0.1873	0.1296	0.0964

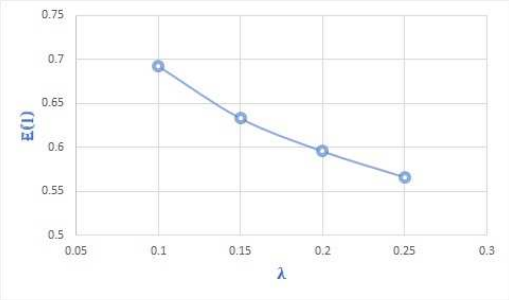

Figure 2. Arrival rate versus E(I)

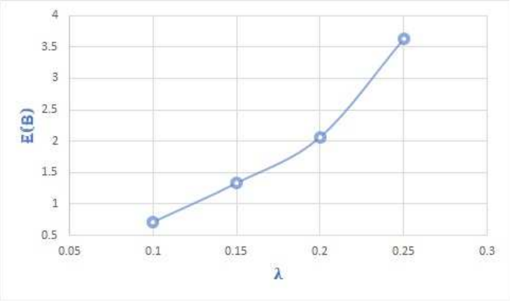

Figure 3. Arrival rate versus E(B)

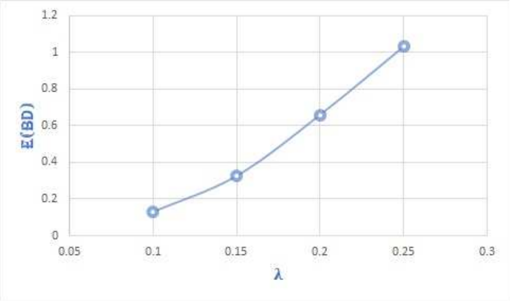

Figure 4. Arrival rate versus E(BD)

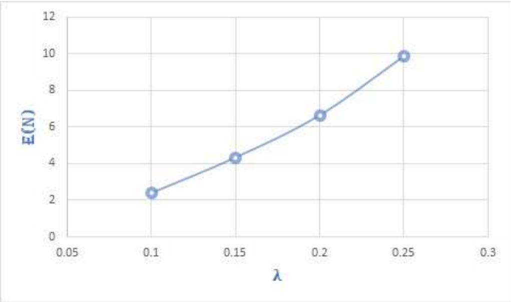

Figure 5. Arrival rate versus E(N)

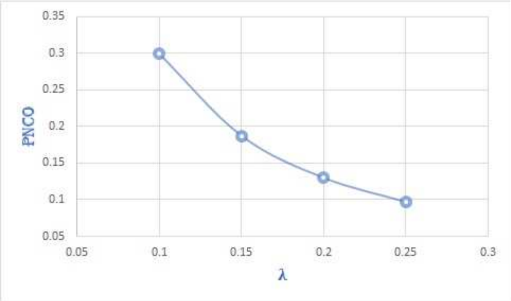

Figure 6. Arrival rate versus PNCO

The values of arrival rate have been varied from 0.1 to 2.5 As the arrival increases, Prob. that server is on idle and Prob. that orbit has no customer are decreases(refer Fig. 2 & Fig. 6). Similarly, if arrival rate increases, then Prob. that server is on busy period, Prob. that server gets breakdown and Prob. that total customers in the system are gradually increases (refer Fig. 3, Fig. 4 & Fig. 5).

5 Summary

This article focused on M/M/1 retrial queue with breakdown & feedback by utilizing Matrix geometric method. Using this type of model we can able to manage the time during the server breakdown and customer who is not satisfied are also able to get a servers again without any issues. By this producing this method the steady state probability vectors are obtained. From that some system performance measures are also determined with graphical representations.

References

[1] Artalejo. J. R. Lopez-Herrero M. J., The single server retrial queue with finite population, A BSDE approach, (2012).

[2] Ayyappan Govindan Muthu Ganapathy Subramanian and Gopal Sekar, Single Server Retrial Queueing System with Variable Service Rates in Priority Service

by Matrix Geometric Method, International Journal of Applied Mathematics & Computation, vol.3, pp. 216-231, (2011).

[3] Choi. B. D. Kim. Y. C. and Lee. Y. W., The M/M/c retrial queue with Geometric loss and Feedback, Computers Math. Applic. vol.36, pp. 41-52, (1998).

[4] Choi. B. D. Kulkarni. V. G., Feedback retrial queueing system, Stochastic Model Relat. Fields, pp. 93-105, (1992).

[5] Chuen-Horng Lin Jau-Chuan Ke., On the multiserver retrial queue with geometric loss and feedback, computational algorithm and parameter optimization, International Journal of Computer Mathematics, vol.88, pp. 1083-1101,(2011).

[6] Falin. G.I., A survey of retrial queues, Queueing Syst.,7, pp. 127-168, (1990).

[7] Kalyanaraman. R. Seenivasan. M., A multi Server Retrial Queue with Breakdown and Geometric loss, International Journal of Computational Cognition, vol. 9, pp. 44 - 48, (2011).

[8] Neuts, M.F., Markov chains with applications queueing theory, which have a matrix geometric invariant probability vector, Adv Appl Prob, Vol. 10, pp. 185-212, (1978).

[9] Neuts. M.F., Matrix-Geometric solutions in stochastic models, vol. 2 of johnsHopkins's series in the mathematical series, Johns HopkinsUniversity Press, Baltimore, USA, (1981).

[10] Praveen Deora, Umesh Kumari, and DC Sharma, Cost analysis and optimization of machine repair model with working vacation and feedback policy, International Journal of Applied Computational Mathematics, Vol. 6, pp. 1-14, (2021).

[11] Praveen Kumar Agrawal, Anamika Jain, and Madhu Jain, M/M/1 queueing model with working vacation and two type of server breakdown, Phys Conf Ser, Vol. 1849, (2021).

[12] Seenivasan, M., Senthilkumar, R., Subasri K S., "M/M/2 Heterogeneous Queueing System Having Unreliable Server with Catastrophes and Restoration", Materials Today: Proceedings Vol. 51(8) Pp. 2332 – 2338, 2021.

[13] Seenivasan, M., Chakravarthy, V J., Abinaya, R., "Markovian Queueing Model with Server Breakdown, Single Working Vacation and Catastrophe", Springer Book Series, vol-881, Pp. 409-421, 2022.

[14] Seenivasan, M., and Shiny Epciya, J. "M/M/1 queue Server Breakdown, Single Working Vacation, Feedback and State Dependent Customer", IEEE Xplore, Pp. 1-5, 2022.

[15] Seenivasan, M., and Chandiraleka. S. "Single Server Queueing Model with Multiple Working Vacation and with Server Breakdown", IEEE Xplore, Pp. 1-5, 2022.

J. COMPUTATIONAL ANALYSIS AND APPLICATIONS, VOL. 31, NO. 2, 2023, COPYRIGHT 2023 EUDOXUS PRESS, LLC

Norm retrieval by vectors and projections

Suman Dowerah[†][*] and Saikat Mukherjee[†]

[†]Department of Mathematics, NIT Meghalaya, Shillong 793003, India

December 28, 2022

Abstract

Norm retrieval was introduced for Hilbert space frames for the first time by Bahmanpour et. al. in the year 2015. In order for a subspace as well as its orthogonal complement to do norm retrieval, it was proved by Bahmanpour et. al. that norm retrieval is a necessary requirement. Basically, norm retrieval refers to the process of reconstructing the signal's norm from the intensity measurements. We give a few characterizations for norm retrieval by vectors and subspaces under the action of bounded linear operators.

2020 Mathematics Subject Classification 42C15, 46C15
Keywords: Norm retrieval; Phase retrieval; Frames; Hilbert spaces; Signal reconstruction

1 Introduction

For any orthonormal basis $\{u_1, u_2, u_3, \dots\}$, a vector $v \in \mathcal{H}$ can be explicitly represented as $v = \sum\limits_i \langle v, u_i \rangle u_i$. Thus orthonormal bases help to reconstruct a vector. In a similar manner, frames, having more flexible structure, also help to reconstruct a vector in a stable way. Duffin and Schaeffer [9] for the first time introduced frames for Hilbert spaces in the year 1952. Frames provides us with a reconstruction formula for lost signals. Daubechies et. al. popularized frames through their work in [7]. Over the last few decades, frame theory has become a prestigious area of research. Researchers worked various generalizations of frames, for instance, K-frame [13], fusion frame [5], wavelet frame [6] and many more. Basically, frames help us to recover and reconstruct the signal, that was lost or distorted, in a stable manner.

Reconstruction of signal is one of the important and significant problems in engineering especially in signal processing. Here a signal can be thought as a vector. This process of regaining the original signal becomes challenging when there is a partial loss of information. Sometimes it happens that we only have the intensity measurements or the phaseless measurements of the lost signal. In such case, phase retrieval sequences help to reconstruct or regain the signal from its intensity measurements or phaseless measurements. Phase retrieval was introduced by Balan et al. [2] for Hilbert space frames in the year 2006. Since then mathematicians have started to work in this area. Phase retrieval is one of the challenging engineering problems. It includes a broad range of applications in many fields, such as speech recognition technology, X-ray crystallography, etc.

---

[*] Corresponding author. *E-mail address:* sumandowerah@nitm.ac.in

Norm retrieval means regaining or reconstructing the lost signal's norm from its intensity measurements or phaseless measurements. Norm retrieval for Hilbert spaces was discussed for the first time by Bahmanpour et. al. [1] in the year 2015. It was proved in [1] that norm retrieval is the necessary requirement for a subspace so that the subspace along with its orthogonal complement do phase retrieval. We note that if a sequence does phase retrieval then it will always do norm retrieval. In the last few years, it is observed that researchers have worked on norm retrieval frames [10], norm retrieval subspaces in finite dimensional Hilbert spaces [4]; and in infinite dimensional Hilbert spaces [15]. Apart from these, pertubation of norm retrieval frames is discussed in [11]. Being highly influenced as well as encouraged by the above mentioned work we explore norm retrieval sequences for vectors under the action of bounded linear operators, T. We also provide a method for construction of norm retrieval subspaces.

We stick to the following notations throughout paper. $\mathcal{H}, \mathcal{K}$ represents separable Hilbert spaces, $\mathcal{B}(\mathcal{H})$ represents the space of linear and bounded operators from $\mathcal{H}$ to $\mathcal{H}$. I, Λ, Λ_i represents a countable index set.

The paper is organised as follows. In Section 2, we give some preliminary background on norm retrieval sequences for finite and infinite dimensional spaces and we highlight some of the important results in these fields. We provide characterizations of norm retrieval sequences and and norm retrieval subspaces in Section 3.

2 Preliminaries

We recall the fundamental definitions and basic results that will be helpful for the paper. Frames are mathematical tools that are used to reconstruct signals.

Definition 2.1. [6] Consider a sequence, say $\varphi = \{\varphi_i\}_{i\in I}$, in $\mathcal{H}$. If for all $x \in \mathcal{H}$, there exist constants $0 < A_1 \leq A_2 < \infty$ such that φ satisfies

$$A_1\|x\|^2 \leq \sum_{i\in I} |\langle x, \varphi_i\rangle|^2 \leq A_2\|x\|^2.$$

Then φ is called a frame for $\mathcal{H}$. Here the constants A_1 is known as the lower frame bound, A_2 is known as the upper frame bound. The frame φ is called Parseval frame if $A_1 = A_2 = 1$.

For example, consider an orthonormal basis, say, $\{e_n\}$ for $\mathcal{H}$, then the sequence $\{e_1, e_1, e_2, e_3, e_4, \dots\}$ is a frame for $\mathcal{H}$. The associated frame bounds are $A_1 = 1$, $A_2 = 2$.

The frame operator, S, is a mapping $S : \mathcal{H} \to \mathcal{H}$ defined as

$$Sx = \sum_{i\in I} \langle x, \varphi_i\rangle \varphi_i, \quad \forall x \in \mathcal{H}.$$

The reconstruction formula given by frame operator and frame elements is as follows:

$$x = \sum_{i\in I} \langle x, S^{-1}\varphi_i\rangle \varphi_i = \sum_{i\in I} \langle x, \varphi_i\rangle S^{-1}\varphi_i, \quad \forall x \in \mathcal{H}.$$

We note that this representation is not unique, owing to the fact that frame elements are not necessarily linearly independent. Frames are one of the essential tools for restoring a signal. There are many different types of frames. One special type of frame is the scalable frame [14]. A scalable frame is a frame, φ, for $\mathcal{H}$ such that there exists scalars, say $c_1, c_2, c_3, \dots$ with $c_i \geq 0$ for which $\{c_i\varphi_i\}_{i\in I}$ is a Parseval frame for $\mathcal{H}$. We refer the readers [6] for more information in frame theory.

Definition 2.2. [2] Consider a sequence $\varphi = \{\varphi_i\}_{i\in I} \in \mathcal{H}$. We say φ performs phase retrieval for $\mathcal{H}$, if for $x, y \in \mathcal{H}$, φ satisfies

$$|\langle x, \varphi_i\rangle| = |\langle y, \varphi_i\rangle|, \quad \forall\, i \in I,$$

then $x = cy$ and c satisfies $|c| = 1$.

The sequence of vectors $\{e_i + e_j\}_{i<j}$, where e_i's are standard orthonormal basis, performs phase retrieval for ℓ_2. If a sequence does phase retrieval in a finite dimension space then it is also a frame, but it may not necessarily be a frame in an infinite dimension space.

In [3], Cahill et. al. thoroughly discussed phase retrieval by subspaces or projections.

Definition 2.3. [3] Suppose $W = \{W_i\}_{i\in I} \subset \mathcal{H}$ is a collection of closed subspaces with corresponding projections $P = \{P_i\}_{i\in I}$. Then W or P does phase retrieval whenever $x, y \in \mathcal{H}$, P satisfies

$$\|P_i x\| = \|P_i y\| \qquad \forall\, i \in I,$$

we have $x = cy$ and c satisfies $|c| = 1$.

Bahmanpour et. al. [1] introduced norm retrieval for frames in Hilbert spaces in the year 2015. In his attempt to pass the phase retrieval condition by subspaces to its orthogonal complements, Bahmanpour proved in [1] that the property of norm retrieval is a necessary requirement. A norm retrieval sequence helps to reconstruct partially lost signal's norm.

Definition 2.4. [1] A sequence of vectors $\varphi = \{\varphi_i\}_{i\in I}$ in $\mathcal{H}$ does norm retrieval if for $x, y \in \mathcal{H}$, φ satisfies

$$|\langle x, \varphi_i\rangle| = |\langle y, \varphi_i\rangle| \quad \forall\ i \in I,$$

then $\|x\| = \|y\|$.

It is obvious for scalable frames, parseval frames, tight frames to do norm retrieval. An orthonormal basis will always do norm retrieval for the corresponding space. It is to be noted that if a sequence performs phase retrieval for $\mathcal{H}$ then the sequence also performs norm retrieval for $\mathcal{H}$, however the converse is not true. For example, orthonormal bases do norm retrieval but not phase retrieval.

Norm retrieval by projections is defined as follows.

Definition 2.5. [1] Consider a family of subspaces, say $\{W_i\}_{i\in I}$, in an infinite dimensional Hilbert space $\mathcal{H}$ and define the orthogonal projections, say $\{P_i\}_{i\in I}$, onto $\{W_i\}_{i\in I}$. Then $\{W_i\}_{i\in I}$ (or $\{P_i\}_{i\in I}$) performs norm retrieval for $\mathcal{H}$ if for $x, y \in \mathcal{H}$, $\{P_i\}_{i\in I}$ satisfies $\|P_i x\| = \|P_i y\|$, $\forall\ i \in I$, we have $\|x\| = \|y\|$.

Norm retrieval can be thought as having an advantage of one free measurement when one tries to do phase retrieval.

The next proposition gives us a method to construct norm retrieval subspaces with the help of dimension of the subspaces.

Proposition 2.6. *[4] If $\{W_i\}_{i=1}^m$ are subspaces in $\mathbb{R}^n$ such that they do norm retrieval then $\sum\limits_{i=1}^m \dim W_i \geq n$. Moreover, if $\exists\ k_1, k_2, \ldots, k_m \in \mathbb{N}$ with $k_i \leq n$ such that for some $L \in \mathbb{N}$ $\sum\limits_{i=1}^m k_i = Ln$ then there exist subspaces $\{W_i\}_{i=1}^m$ that perform norm retrieval in $\mathbb{R}^n$ where $\dim W_i = k_i$ for $1 \leq i \leq m$.*

The above result can easily be generalized as follows.

Theorem 2.7. *Suppose $\{k_i\}_{i=1}^m$ are natural numbers such that $k_i \leq n$ and $\sum\limits_{i=1}^m k_i \geq n$. If for some $l \in \mathbb{N}$ with $1 \leq l \leq m$, $\sum\limits_{i=1}^l k_i$ is a multiple of n, then there exist subspaces $\{W_i\}_{i=1}^m$ in $\mathbb{R}^n$ satisfying $\dim W_i = k_i$ such that $\{W_i\}_{i=1}^m$ performs norm retrieval.*

We recall the following properties of projection operators.

Lemma 2.8. *[12] Consider any two Hilbert spaces, say, $\mathcal{H}_1$, $\mathcal{H}_2$ and $T \in \mathcal{B}(\mathcal{H}_1, \mathcal{H}_2)$. Consider a closed subspace, say, W_1, of $\mathcal{H}_1$ and another closed subspace, say, W_2, of $\mathcal{H}_2$. Then the following statements are true.*

(i) $P_{W_1} T^* P_{W_2} = P_{W_1} T^*$ *if and only if* $TW_1 \subset W_2$.

(ii) $P_{W_1} T^* P_{\overline{TW_1}} = P_{W_1} T^*$

3 Main Results

We begin this section by studying norm retrieval sequences under the action of bounded linear operators.

In [1], it was shown that orthogonal projections preserve the norm retrieval property. However in [4], it is shown that the norm retrieval property is not preserved by invertible operators. For instance, $\varphi = \{(1,0),(0,1)\}$ does norm retrieval for $\mathbb{R}^2$; consider an invertible on $\mathbb{R}^2$ defined by $T(x_1,x_2) = (x_1+x_2, x_2)$; but $T\varphi = \{(1,0),(1,1)\}$ does not do norm retrieval for $\mathbb{R}^2$.

Remark 3.1. $\varphi = \{\varphi_i\}_{i\in I}$ perform norm retrieval for $\mathcal{H} \iff$ for $c_i \neq 0$, $c\varphi = \{c_i\varphi_i\}_{i\in I}$ perform norm retrieval for $\mathcal{H}$. Indeed, this can be easily verified from the fact that $|\langle x, c_i\varphi_i\rangle| = |\langle y, c_i\varphi_i\rangle| \iff |\langle x, \varphi_i\rangle| = |\langle y, \varphi_i\rangle|, \quad \forall i \in I$.

Theorem 3.2. *Suppose $\{\varphi_i\}_{i\in I}$ performs norm retrieval for $\mathcal{H}$. Consider $T \in \mathcal{B}(\mathcal{H})$, such that T is an isometry. Then $\{T^*\varphi_i\}_{i\in I}$ performs norm retrieval for $\mathcal{H}$.*

Proof. Suppose $x, y \in \mathcal{H}$ such that $|\langle x, T^*\varphi_i\rangle| = |\langle y, T^*\varphi_i\rangle| \implies |\langle Tx, \varphi_i\rangle| = |\langle Ty, \varphi_i\rangle|, \quad \forall \; i \in I$. Using the fact that $\{\varphi_i\}_{i\in I}$ performs norm retrieval for $\mathcal{H}$ and T is an isometry, we get $\|x\| = \|y\|$. □

Corollary 3.3. *Suppose $T \in \mathcal{B}(\mathcal{H})$ is an unitary operator and let $\varphi = \{\varphi_i\}_{i\in I}$ be a sequence of vectors in $\mathcal{H}$. Then, φ doing norm retrieval for $\mathcal{H}$ is equivalent to $T\varphi$ doing norm retrieval for $\mathcal{H}$.*

In [8] it was shown that phase retrieval is preserved by non-zero idempotent operators for the range space. Theorem 3.4 shows that idempotent operators also preserves norm retrieval for the range space.

Theorem 3.4. *Consider $T \in \mathcal{B}(\mathcal{H})$, a non-zero idempotent operator and let $\varphi = \{\varphi_i\}_{i\in I}$ be a sequence of vectors in $\mathcal{H}$. Then φ doing norm retrieval for $R(T^*)$ is equivalent to $\{T\varphi_i\}_{i\in I}$ doing norm retrieval for $R(T^*)$.*

Proof. We note that for every $x_1, x_2 \in R(T^*)$, there exists $y_1, y_2 \in \mathcal{H}$ such that $T^*y_1 = x_1$, $T^*y_2 = x_2$. Then we have,

$$\begin{aligned} |\langle x_1, T\varphi_i\rangle| = |\langle x_2, T\varphi_i\rangle| &\iff |\langle T^*y_1, T\varphi_i\rangle| = |\langle T^*y_2, T\varphi_i\rangle| \\ &\iff |\langle T^*y_1, \varphi_i\rangle| = |\langle T^*y_2, \varphi_i\rangle| \\ &\iff |\langle x_1, \varphi_i\rangle| = |\langle x_2, \varphi_i\rangle|, \end{aligned}$$

for all $i \in I$. Hence the theorem holds. □

Theorem 3.5. *Given a closed subspace W of a Hilbert space $\mathcal{H}$, every norm sequence for $\mathcal{H}$ can be uniquely decomposed into norm retrieval sequences for W and $W^{\perp}$.*

Proof. Suppose $\varphi = \{\varphi_i\}_{i\in I}$ does norm retrieval for $\mathcal{H}$ and P_w is the orthogonal projection onto W. Then φ can be uniquely decomposed as $P_w\varphi$ and $(I-P_w)\varphi$, where $P_w\varphi = \{P_w\varphi_i\}_{i\in I}$. The conclusion follows from the facts that for $x, y \in W$,

$$|\langle x, \varphi_i\rangle| = |\langle x, P_w\varphi_i\rangle| = |\langle y, P_w\varphi_i\rangle| = |\langle y, \varphi_i\rangle|, \ \forall\ i \in I;$$

and for $x, y \in W^\perp$,

$$|\langle x, \varphi_i\rangle| = |\langle x, (I-P_w)\varphi_i\rangle| = |\langle y, (I-P_w)\varphi_i\rangle| = |\langle y, \varphi_i\rangle|, \ \forall\ i \in I.$$

□

Corollary 3.3 shows that the norm retrieval property for vectors is preserved by unitary operators. We now show that the norm retrieval property for subspaces is also preserved by unitary operators.

Theorem 3.6. *Consider $W = \{W_i\}_{i\in I}$ is a collection of closed subspaces in $\mathcal{H}$. Further, let $T : \mathcal{H} \to \mathcal{K}$ be unitary. If W does norm retrieval for $\mathcal{H}$, then TW does norm retrieval for $\mathcal{K}$.*

Proof. For $y_1, y_2 \in \mathcal{K}$, let $\|P_{TW_i}y_1\| = \|P_{TW_i}y_2\|$ for all $i \in I$. Since T is surjective, $\exists\ x_1, x_2 \in \mathcal{H}$ such that $Tx_1 = y_1$ and $Tx_2 = y_2$. We note that for $k = 1, 2$, we have $P_{TW_i}y_k = P_{TW_i}Tx_k = P_{TW_i}TP_{W_i}x_k + P_{TW_i}TP_{W_i^\perp}x_k = P_{TW_i}TP_{W_i}x_k = TP_{W_i}x_k$. Thus, we get $\|TP_{W_i}x_1\| = \|TP_{W_i}x_2\|$. Using the fact that T is isometry and $\{W_i\}_{i\in I}$ do norm retrieval, we obtain $\|y_1\| = \|y_2\|$. □

The following two examples show that if we drop the condition that T is isometry or the condition that T is surjective then we may lose the property of norm retrievality of $\{TW_i\}_{i\in I}$.

Example 3.7. Consider the subspaces $W_1 = x$-axis and $W_2 = y$-axis in $\mathbb{R}^2$. Clearly, $\{W_1, W_2\}$ does norm retrieval for $\mathbb{R}^2$. Define $T_1 : \mathbb{R}^2 \to \mathbb{R}^2$ as $T_1(x_1, x_2) = (x_1 + x_2, x_2)$. Thus T_1 is not an isometry. Now $T_1W_1 = x$-axis and $T_1W_2 = \text{span}\{(x, x) : x \in \mathbb{R}\}$. However $\{T_1W_1, T_1W_2\}$ does not do norm retrieval in $\mathbb{R}^2$. This can be easily verified at $(1, 1)$ and $(1, -3)$.

Example 3.8. Consider the subspaces $W_1 = x$-axis and $W_2 = y$-axis in $\mathbb{R}^2$. We note that $\{W_1, W_2\}$ does norm retrieval for $\mathbb{R}^2$. Define $T_2 : \mathbb{R}^2 \to \mathbb{R}^3$ as $T_2(x_1, x_2) = (x_1, x_2, 0)$. Clearly T_2 is not surjective. Now $T_2W_1 = x$-axis and $T_2W_2 = y$-axis in $\mathbb{R}^3$. But $\{T_2W_1, T_2W_2\}$ does not do norm retrieval in $\mathbb{R}^3$. This can be easily verified for $(0, 0, 1)$ and $(0, 0, 2)$.

Let $\{P_i\}_{i=1}^m$ be projections onto subspaces $\{W_i\}_{i=1}^m$ of $\mathbb{C}^n$. Consider any orthonormal bases $\{\varphi_{ij}\}_{j=1}^{I_i}$ of $\{W_i\}_{i=1}^m$ and a sub collection $S \subseteq \{(i, j) : 1 \leq i \leq m, 1 \leq j \leq I_i\}$. It was shown in [4] that if $\{P_i\}_{i=1}^m$ does norm retrieval and $x \perp \text{span}\{\varphi_{ij}\}_{(i,j)\in S}$, $y \perp \text{span}\{\varphi_{ij}\}_{(i,j)\in S^c}$ then $\text{Re}\langle x, y\rangle = 0$. In fact $\langle x, y\rangle = 0$ for an arbitrary Hilbert space, this is eveident from the following result. A similar result for weaving norm retrival subspaces was proved in [8].

Theorem 3.9. *Let $\{P_i\}_{i\in\Lambda}$ be projections onto subspaces $\{W_i\}_{i\in\Lambda}$ of $\mathcal{H}$. Given any orthonormal bases $\{\varphi_{ij}\}_{j\in\Lambda_i}$ of $\{W_i\}_{i\in\Lambda}$ and a sub collection $S\subset\{(i,j): i\in\Lambda, j\in\Lambda_i\}$. If $\{P_i\}_{i\in\Lambda}$ does norm retrieval then $\{\varphi_{ij}\}^{\perp}_{(i,j)\in S}\perp\{\varphi_{ij}\}^{\perp}_{(i,j)\in S^c}$.*

Proof. Given $S\subset\{(i,j): i\in\Lambda, j\in\Lambda_i\}$. Let $x\in\{\varphi_{ij}\}^{\perp}_{(i,j)\in S}$ and $y\in\{\varphi_{ij}\}^{\perp}_{(i,j)\in S^c}$. We note that for each $i\in\Lambda$,

$$\begin{aligned}\|P_i(x+y)\|^2=\sum_{j\in\Lambda_i}|\langle x+y,\varphi_{ij}\rangle|^2&=\sum_{\substack{j\in\Lambda_i\\(i,j)\in S^c}}|\langle x,\varphi_{ij}\rangle|^2+\sum_{\substack{j\in\Lambda_i\\(i,j)\in S}}|\langle y,\varphi_{ij}\rangle|^2.\\&=\sum_{j\in\Lambda_i}|\langle x-y,\varphi_{ij}\rangle|^2\\&=\|P_i(x-y)\|^2.\end{aligned}$$

Therefore, we get $\|x+y\|^2=\|x-y\|^2$ for all $i\in\Lambda$. Thus $\mathrm{Re}\langle x,y\rangle=0$.

Similarly, we obtain $\|P_i(x+iy)\|^2=\|P_i(x-iy)\|^2 \implies \|x+iy\|^2=\|x-iy\|^2\implies \mathrm{Im}\langle x,y\rangle=0$ for all $i\in\Lambda$. Hence, $x\perp y$. ☐

Corollary 3.10. *Consider a sequence of vectors $\varphi=\{\varphi_i\}_{i\in I}$ in $\mathcal{H}$. For non-trivial $J\subset I$, let $W_1=span\{\varphi_i\}_{i\in J}$ and $W_2=span\{\varphi_i\}_{i\in J^c}$. If φ does norm retrieval then $W_1^{\perp}\subset W_2$.*

Proof. Since φ does norm retrieval, so by Theorem 3.9 we have $W_1^{\perp}\perp W_2^{\perp}$. Hence the conclusion follows. ☐

In [4], it has been proved that corollary 3.11 is true for $\mathbb{R}^n$. We extend it to $\mathcal{H}^n$ where $\mathcal{H}^n$ is an n-dimensional Hilbert space.

Corollary 3.11. *Every norm retrieval set with n elements is orthogonal in $\mathcal{H}^n$, where $\mathcal{H}^n$ is an n-dimensional Hilbert space.*

Proof. Consider a norm retrieval collection $\{\varphi_i\}_{i=1}^n$ in $\mathcal{H}^n$. If possible, suppose for some k with $1\le k\le n$, φ_k is not orthogonal to another element of this collection. Let $W_1=\mathrm{span}\{\varphi_i\}_{i\neq k}$ and $W_2=\mathrm{span}\{\varphi_k\}$. Then $W_1^{\perp}$ can not be a subset W_2, a contradiction to Corollary 3.10. ☐

References

[1] S. Bahmanpour, J. Cahill, P. G. Casazza, J. Jasper and L. Woodland, Phase retrieval and norm retrieval, Trends in Harmonic Analysis and its Applications, *Contemp. Math*, Amer. Math. Soc., Providence, RI, 650, 2015, pp.3–14.

[2] R. Balan, P. Casazza and D. Edidin, On signal reconstruction without phase, *Applied and Computational Harmonic Analysis*, 20(3), 345–356 (2006).

[3] J. Cahill, P. G. Casazza, J. Peterson and L. Woodland, Phase retrieval by projections, *Houstan J. Math.*, 42(2), 537–558 (2016).

[4] P. G. Casazza, D. Ghoreishi, S. Jose and J. C. Tremain, Norm retrieval and Phase retrieval by projections, *Axioms*, 6(1), 6 (2017).

[5] P. Casazza and G. Kutyniok, Frames of subspaces, *Contemp. Math.*, AMS, 345, 2004, pp.87–114.

[6] O. Christensen, *An introduction to frames and Riesz bases*, Boston: Birkh*ä*user, 2003.

[7] I. Daubechies, A. Grossmann and Y. Meyer, Painless nonorthogonal expansions, *J. Math. Phys.*, 27, 1271–1283 (1986).

[8] S. Dowerah and S. Mukherjee, Weaving phase retrieval and weaving norm retrieval, *Int. J. Appl. and Comput. Math.*, 8(4), 198 (2022).

[9] R. J. Duffin and A. C. Schaeffer, A class of nonharmonic Fourier series, *Trans. Amer. Math. Soc.*, 72(2), 341–366 (1952).

[10] M. A. H. Fard and S. Moazeni, Signal reconstruction without phase by norm retrievable frames, *Linear and Multilinear Algebra*, 69(8), 1484–1499 (2021).

[11] M. A. H. Fard and L. M. Rad, Norm Retrievable Frames and Their Perturbation in Finite Dimensional Complex Hilbert Spaces, *Numerical Functional Analysis and Optimization*, 38(1), 51–57 (2016).

[12] L. Găvruţa, On the duality of fusion frame, *J. Math. Anal. Appl.*, 333(2), 871–879 (2007).

[13] L. Găvruţa, Frames for operators, *Appl. Comput. Harmon. Anal.*, 32, 139–144 (2012).

[14] G. Kutyniok, K. A. Okoudjou, F. Philipp and E. K. Tuley, Scalable frames, *Linear Algebra and its Applications*, 438, 2225–2238 (2013).

[15] Y. Zhou, Norm Retrieval by Projections on Infinite-Dimensional Hilbert Spaces, *Ann. Appl. Math.*, 33, 324–330 (2017).

J. COMPUTATIONAL ANALYSIS AND APPLICATIONS, VOL. 31, NO. 2, 2023, COPYRIGHT 2023 EUDOXUS PRESS, LLC

Non Markovian retrial queue, balking, disaster under working breakdown and working vacation

P. Manoharan[1] and S. Subathra[2]
[1,2]Department of Mathematics, Annamalai University,
Annamalainagar-608002, Tamilnadu, India.
*Corresponding Author E-Mail: manomaths.hari@gmail.com

December 29, 2022

Abstract

Any arriving customer who arrives and finds that the server is free, enters the service station and the remaining customers connect into the orbit. When the normal busy server is running, the system may at any time become defective due to a disaster. All users are forced to quit the system due to a disaster, which also brings about the failure of the main server. When a primary server breaks, it is shipped out for repair, and the repair process starts instantly. The server stops running as soon as the orbit is empty at a typical service finish instant. During the working breakdown or working vacation, the replacement server offers arriving customers a lower level of service. The arriving customer receives service instantly if the server is idle. If not, he will choose whether to leave the system without service or returning to receive service. Using the supplementary variable technique, we calculate the steady state PGF for system and orbit sizes. We generate performance measures and particular cases. With the use of specific numerical examples, we analyse the model.
Keywords: Retrial queue, balking, disaster, working breakdown, working vacation.

Mathematics Subject Classification 2010: 60K25, 90B22

1 Introduction

Previously, various authors investigated queueing models with varying service rates. These models drive almost made the assistance rate subject to the framework's circumstance, like lines in irregular conditions, lines with breakdown, and working breakdown. Retrial lines with repeated tasks are distinguished in a retrial queueing system by the fact that an arriving customer sees the server busy upon arrival and is encouraged to leave the support area and join a retry line known as orbit. After a specific measure of time has elapsed, the client in orbit might make another assistance demand. It makes no difference to the other customers in the orbit if any random customer in the orbit repeats the service request. Such queues assume a novel part in PC and broadcast communications frameworks. Rajadurai [8,9], estimated a Non-Markovian retrial queue including calamity and working breakdown. Kalidass and Ramanath (2012) pioneered "The concept of working breakdowns". If a regular busy server fails due to a disaster at any time, the system ought to be ready with a reinforcement (reserve) server in the event that the primary server falls flat. It makes no difference to the other customers in the orbit if any random customer in the orbit repeats the service request. The main server rejoins the system and becomes operational as soon as the repair is fulfilled. Furthermore, the operational breakdown service can reduce customer complaints as the principal server is being repaired, as well as the cost of customers who are waiting. As a result, a more sensible repair strategy for problematic queueing framework is the working breakdown service. Rajadurai et al [10], considered inconsistent queueing frameworks with different highlights, one of which is that when a server falls flat, it is sent for fix, during which time it stops offering support to essential clients until the assistance channel is fixed, and the client who was simply being served before the server disappointment trusts that the leftover help will finish.

2 Model Description

In this model the arrival follows Poisson process with rate λ and the service discipline is FIFO. Since there is no waiting area, this is assumed. When a customer arrives and determines that the server is busy, they are joined to the orbit. If an orbital customer is permitted access to the server. Laplace-Stieltjes Transforms (LST) represent inter retrial times as $\Upsilon^*(\theta)$ and have an arbitrary distribution function $\Upsilon(t)$. In normal service period (NS period), service time have general distribution function S(t), with LST as $S^*(\theta)$. We assume that the disaster occur only when the main service is in progress and disaster follows a negative exponential distribution with rate δ. When the disaster occurs all customers are clear out and the primary server is dispatched for maintenance. The repair time follows an exponential distribution with parameter η. The server gives a lower rate of service follows an arbitrary distribution function $S_w(t)$ to arriving customers during the working breakdown period, with LST as $S_w^*(\theta)$. The server resumes normal operation after the repair is finished. As soon as the service is finished and the orbit is empty, the server goes on vacation. The duration of the vacation period is determined by an exponential distribution with the parameter θ. If there are still users in the system at the time the vacation ends, the server will begin a new busy period. Otherwise, he awaits the arrival of a customer. The server gives a lesser rate of service follows an arbitrary distribution function $S_w(t)$ to arriving customers during the working vacation period, with LST as $S_w^*(\theta)$. A vacation interruption occurred if the server quits

his vacation to return to the normal busy period after discovering that there is a customer in the orbit. Working breakdown and working vacation are both regarded as low service in this situation (LS period). If the server is idle, the customer arrives and gets served instantly. If not, he will choose whether to leave the system with probability $(1-r)$ or joining the orbit with probability r.
Let $\Upsilon^0(t)$ denotes the elapsed retrial time, $S^0(t)$ denotes the elapsed service time in NS period , $S_w^0(t)$ denotes the elapsed service time in LS period .
Let $F(t)$ denotes the size of the orbit at time "t". and we use the subsequent random variable as follows.
Let's use the subsequent random variables.
$F(t)$- Size of the orbit at time "t".
At time "t" the four distinct states of the server are

$$\Theta(t) = \begin{cases} 0, & \text{if the server is idle in LS period} \\ 1, & \text{if the server is idle in NS period} \\ 2, & \text{if the server is busy in LS period} \\ 3, & \text{if the server is busy in NS period} \end{cases}$$

o generate bivariate Markov Process, $\{(F(t), \Theta(t)); t \geq 0\}$ further supplementary variables $\Upsilon^0(t)$, $S^0(t)$, and $S_w^0(t)$ are introduced. The sequence of periods at which a NS or LS periods completion occurs is $\{t_m, m = 1, 2, 3, ...\}$. The Markov chain that is formed by the random vector sequences $Z_m = \{F(t_m+), \Theta(t_m+)\}$ is incorporated into the retrial queueing system. The concerned embedded Markov chain is ergodic if and only if $\rho < \Upsilon^*(\lambda)\big[$ See Sennott et al.,[12]$\big]$ where $\rho = \frac{\lambda r}{\delta}(1 - S^*(\delta))$ pretaining to our model.
Following are the limiting probabilities

$$\begin{aligned}
\Omega_{0,1} &= \lim_{t\to\infty} P\{\Theta(t) = 1,\ F(t) \ = 0\}, \\
\Omega_{0,2} &= \lim_{t\to\infty} P\{\Theta(t) = 0,\ F(t) \ = 0\}, \\
\Upsilon_m(x) &= \lim_{t\to\infty} P\{\Theta(t) = 1,\ F(t) \ = m,\ x \leq \Upsilon^0(t) < x + dx\}, \\
&\qquad\qquad\qquad\qquad x \geq 0,\ m \geq 1 \\
\Omega_{m,1}(x) &= \lim_{t\to\infty} P\{\Theta(t) = 3,\ F(t) \ = m,\ x \leq S^0(t) < x + dx\}; \\
&\qquad\qquad\qquad\qquad x \geq 0,\ m \geq 0,
\end{aligned}$$

$$\begin{aligned}
\Omega_{m,2}(x) &= \lim_{t\to\infty} P\{\Theta(t) = 2,\ F(t) \ = m,\ x \leq S_w^0(t) < x + dx\}; \\
&\qquad\qquad\qquad\qquad x \geq 0,\ m \geq 0.
\end{aligned}$$

Following are the probability generating function

$$\begin{aligned}
\Upsilon(z,x) &= \sum_{m=1}^{\infty} \Upsilon_m(x) z^m; & \Upsilon(z,0) &= \sum_{m=1}^{\infty} \Upsilon_m(0) z^m; \\
\Upsilon^*(\theta) &= \int_0^{\infty} e^{-\theta x} r(x) dx; & \Omega_1(z,x) &= \sum_{m=0}^{\infty} \Omega_{m,1}(x) z^m; \\
\Omega_1(z,0) &= \sum_{m=0}^{\infty} \Omega_{m,1}(0) z^m; & S^*(\theta) &= \int_0^{\infty} e^{-\theta x} \mu(x) dx; \\
\Omega_2(z,x) &= \sum_{m=0}^{\infty} \Omega_{m,2}(x) z^m; & \Omega_2(z,0) &= \sum_{m=0}^{\infty} \Omega_{m,2}(0) z^m; \\
S_w^*(\theta) &= \int_0^{\infty} e^{-\theta x} \mu_w(x) dx;
\end{aligned}$$

We are using the following hazard rate functions. Let $r(x)$ denotes the conditional retrial completion rate of $\Upsilon(x)$

and $r(x)dx = \dfrac{d\Upsilon(x)}{1-\Upsilon(x)}$.

Let $\mu(x)$ denotes the conditional normal service completion rate of $S(x)$

and $\mu(x)dx = \dfrac{dS(x)}{1-S(x)}$.

Let $\mu_w(x)$ denotes the conditional lower service completion rate of $S_w(x)$

and $\mu_w(x)dx = \dfrac{dS_w(x)}{1-S_w(x)}$.

The system was demonstrated in steady state by the following differential difference equations:

$$\begin{aligned}
\lambda\Omega_{0,1} &= (\theta+\eta)\Omega_{0,2}, & (1) \\
(\lambda+\theta+\eta)\Omega_{0,2} &= \int_0^{\infty} \Omega_{0,1}(x)\mu(x)dx + \int_0^{\infty} \Omega_{0,2}(x)\mu_w(x)dx \\
&\quad +\delta\int_0^{\infty} \Omega_{m,1}(x)dx, m \geq 0, & (2) \\
\frac{d\Upsilon_m(x)}{dx} &= -(\lambda+r(x))\Upsilon_m(x), m \geq 1, & (3) \\
\frac{d\Omega_{0,1}(x)}{dx} &= -(\lambda+\delta+\mu(x))\Omega_{0,1}(x) + \lambda(1-r)\Omega_{0,1}(x), m = 0 & (4) \\
\frac{d\Omega_{m,1}(x)}{dx} &= -(\lambda+\delta+\mu(x))\Omega_{m,1}(x) + \lambda(1-r)\Omega_{m,1}(x) \\
&\quad +\lambda r\Omega_{m-1,1}(x), m \geq 1, & (5)
\end{aligned}$$

$$\frac{d\Omega_{0,2}(x)}{dx} = -(\lambda+\eta+\theta+\mu_w(x))\Omega_{0,2}(x)+\lambda(1-r)\Omega_{0,2}(x), m=0, \quad (6)$$

$$\frac{d\Omega_{m,2}(x)}{dx} = -(\lambda+\eta+\theta+\mu_w(x))\Omega_{m,2}(x)+\lambda(1-r)\Omega_{m,2}(x) +\lambda r\Omega_{m-1,2}(x), m\geq 1. \quad (7)$$

At $x=0$,

$$\Upsilon_m(0) = \int_0^\infty \Omega_{m,1}(x)\mu(x)dx+\int_0^\infty \Omega_{m,2}(x)\mu_w(x)dx,\ m\geq 1, \quad (8)$$

$$\Omega_{0,1}(0) = \int_0^\infty \Upsilon_1(x)r(x)dx+(\theta+\eta)\int_0^\infty \Omega_{0,2}(x)dx+\lambda\Omega_{0,1},\ m=0, \quad (9)$$

$$\Omega_{m,1}(0) = \int_0^\infty \Upsilon_{m+1}(x)r(x)dx+(\theta+\eta)\int_0^\infty \Omega_{m,2}(x)dx +\lambda\int_0^\infty \Upsilon_m(x)dx,\ m\geq 1, \quad (10)$$

$$\Omega_{m,2}(0) = \begin{cases}\lambda\Omega_{0,2}, & m=0,\\ 0, & m\geq 1,\end{cases} \quad (11)$$

The normalizing condition is

$$1 = \Omega_{0,1}+\Omega_{0,2}+\sum_{m=0}^{\infty}\Big[\int_0^\infty \Omega_{m,1}(x)dx+\int_0^\infty \Omega_{m,2}(x)dx\Big] +\sum_{m=1}^{\infty}\int_0^\infty \Upsilon_m(x)dx$$

Multiply the equations (2) - (8) by the proper powers of z

$$\frac{d\Upsilon(z,x)}{dx}+(\lambda+r(x))\Upsilon(z,x) = 0 \quad (12)$$

$$\frac{d\Omega_1(z,x)}{dx}+(\lambda(1-rz)-\lambda(1-r)+\delta+\mu(x))\Omega_1(z,x) = 0 \quad (13)$$

$$\frac{d\Omega_2(z,x)}{dx}+(\lambda(1-rz)-\lambda(1-r)+\theta+\eta+\mu_w(x))\Omega_2(z,x) = 0 \quad (14)$$

$$\Upsilon(z,0) = \int_0^\infty \Omega_1(z,x)\mu(x)dx+\int_0^\infty \Omega_2(z,x)\mu_w(x)dx -\int_0^\infty \Omega_{0,1}(x)\mu(x)dx-\int_0^\infty \Omega_{0,2}(x)\mu_w(x)dx \quad (15)$$

Using the equation (2) in equation (15), we get

$$\Upsilon(z,0) = \int_0^\infty \Omega_1(z,x)\mu(x)dx+\int_0^\infty \Omega_2(z,x)\mu_w(x)dx+\delta\int_0^\infty \Omega_1(z,x)dx -(\lambda+\theta+\eta)\Omega_{0,2} \quad (16)$$

Multiply the equations $(10)-(11)$ by the proper powers of z

$$\begin{aligned}\Omega_1(z,0) &= \frac{1}{z}\int_0^\infty \Upsilon(z,x)r(x)dx+\lambda\int_0^\infty \Upsilon(z,x)dx+\lambda\Omega_{0,1} \\ &\quad +(\eta+\theta)\int_0^\infty \Omega_2(z,x)dx \qquad (17)\\ \Omega_2(z,0) &= \lambda\Omega_{0,2} \qquad (18)\end{aligned}$$

Solving the first order linear differential equations $(13),(14),(15)$ which yields,

$$\begin{aligned}\Upsilon(z,x) &= \Upsilon(z,0)[1-\Upsilon(x)]e^{-\lambda x} \qquad (19)\\ \Omega_1(z,x) &= \Omega_1(z,0)[1-S(x)]e^{-B(z)x} \qquad (20)\\ \Omega_2(z,x) &= \Omega_2(z,0)[1-S_w(x)]e^{-B_w(z)x} \qquad (21)\end{aligned}$$

where $B(z)=(\lambda r(1-z)+\delta)$, $B_w(z)=(\lambda r(1-z)+\theta+\eta)$.
Substituting the equations (19) and (21)in equation (17), we get

$$\Omega_1(z,0) = \frac{\Upsilon(z,0)}{z}\Big[\Upsilon^*(\lambda)+z(1-\Upsilon^*(\lambda))\Big]+\lambda\Omega_{0,1}+\lambda\Omega_{0,2}U(z) \qquad (22)$$

where, $U(z) = \dfrac{(\eta+\theta)(1-S_w^*(B_w(z))}{B_w(z)}$.
Substituting the equations (20) and (21) in equation (16), we get

$$\Upsilon(z,0) = \Omega_1(z,0)[S^*(B(z))+S(z)]+\Omega_2(z,0)S_w^*(B(z))-(\lambda+\theta+\eta)\Omega_{0,2}. \qquad (23)$$

where $S(z)=\dfrac{\delta(1-S^*(B(z)))}{\delta+\lambda r(1-z)}$
Using equations (18) and (22) in equation (23) and get

$$\begin{aligned}\Upsilon(z,0) &= \frac{z\Omega_{0,2}}{Dr_1(z)}\Big\{[\theta+\eta+\lambda U(z)][S^*(B(z))+S(z)]+\lambda(S_w^*(B_w(z))-1)\\ &\quad -(\theta+\eta)\Big\}, \qquad (24)\end{aligned}$$

Substituting the equation (24) in equation (22), we get

$$\begin{aligned}\Omega_1(z,0) &= \frac{\Omega_{0,2}}{Dr_1(z)}\Big\{[\lambda(S_w^*(B_w(z))-1)-(\theta+\eta)][\Upsilon^*(\lambda)+z(1-\Upsilon^*(\lambda))]\\ &\quad +z[\theta+\eta+\lambda U(z)])\Big\} \qquad (25)\end{aligned}$$

where $Dr_1(z)=z-[S^*(B(z))+S(z)][\Upsilon^*(\lambda)+z(1-\Upsilon^*(\lambda))]$. Using the equations (24), (25) and (18) in equations (19), (20) and (21), then the limiting PGF's are $\Upsilon(z,x)$, $\Omega_1(z,x)$, and $\Omega_2(z,x)$.

3 Steady state results

If $\rho < \Upsilon^*(\lambda)$, The PGF's are listed below.
(i) The amount of orbiting customers as the server is not being utilized

$$\begin{aligned}\Upsilon(z) &= \frac{(1-\Upsilon^*(\lambda))}{\lambda Dr_1(z)}\Big\{z\Omega_{0,2}\big[(\lambda U(z)+\theta+\eta)[S^*(B(z))+S(z)] \\ &\quad +\lambda(S_w^*(B_w(z))-1)-(\theta+\eta)\big]\Big\} \qquad (26)\end{aligned}$$

(ii) The amount of orbiting customers as the server is regularly busy

$$\begin{aligned}\Omega_1(z) &= \frac{(1-S^*(B(z)))}{B(z)Dr_1(z)}\Big\{\Omega_{0,2}\big[(\lambda U(z)+\theta+\eta)z+[\lambda(S_w^*(B_w(z))-1) \\ &\quad -(\theta+\eta)][\Upsilon^*(\lambda)+z(1-\Upsilon^*(\lambda))]\big]\Big\} \qquad (27)\end{aligned}$$

(iii) PGF is used to determine the total number of users in orbit $(C_s(z))$.

$$\begin{aligned}C_s(z) &= \Omega_{0,1}+\Omega_{0,2}+\Upsilon(z)+z(\Omega_1(z)+\Omega_2(z)), \\ C_s(z) &= \frac{\Omega_{0,2}}{Dr_1(z)}\Big\{B(z)\Big(z-(S^*(B(z))+S(z))(\Upsilon^*(\lambda)+z(1-\Upsilon^*(\lambda)))\Big) \\ &\quad \times\Big(\frac{\eta+\theta}{\lambda}+1\Big)+\Big((U(z)+\frac{1}{\lambda}(\theta+\eta))(S^*(B(z))+S(z)) \\ &\quad +(S_w^*(B_w(z))-1)-\frac{1}{\lambda}(\theta+\eta)\Big)z(1-\Upsilon^*(\lambda))B(z)+(1-S^*(B(z)) \\ &\quad \times\Big((\lambda U(z)+\theta+\eta)z+(\lambda(S_w^*(B_w(z))-1)-(\theta+\eta))(\Upsilon^*(\lambda) \\ &\quad +z(1-\Upsilon^*(\lambda)))\Big)z+B(z)\Big(z-(S^*(B(z))+S(z))(\Upsilon^*(\lambda) \\ &\quad +z(1-\Upsilon^*(\lambda)))\Big)\frac{\lambda zU(z)}{(\theta+\eta)}\Big\}.\end{aligned}$$

(iv) PGF is used to determine the total number of users in orbit $(C_o(z))$.

$$\begin{aligned}C_o(z) &= \Omega_{0,1}+\Omega_{0,2}+\Upsilon(z)+\Omega_1(z)+\Omega_2(z), \\ C_o(z) &= \frac{\Omega_{0,2}}{Dr_1(z)}\Big\{B(z)\Big(z-(S^*(B(z))+S(z))(\Upsilon^*(\lambda)+z(1-\Upsilon^*(\lambda)))\Big) \\ &\quad \times\Big(\frac{\eta+\theta}{\lambda}+1\Big)+\Big((U(z)+\frac{1}{\lambda}(\theta+\eta))(S^*(B(z))+S(z)) \\ &\quad +(S_w^*(B_w(z))-1)-\frac{1}{\lambda}(\theta+\eta)\Big)z(1-\Upsilon^*(\lambda))B(z)+(1-S^*(B(z)) \\ &\quad \times\Big((\lambda U(z)+\theta+\eta)z+(\lambda(S_w^*(B_w(z))-1)-(\theta+\eta))(\Upsilon^*(\lambda) \\ &\quad +z(1-\Upsilon^*(\lambda)))\Big)+B(z)\Big(z-(S^*(B(z))+S(z))(\Upsilon^*(\lambda) \\ &\quad +z(1-\Upsilon^*(\lambda)))\Big)\frac{\lambda U(z)}{(\theta+\eta)}\Big\}. \qquad (28)\end{aligned}$$

(v) The amount of orbiting customers as the server is lower speed service

$$\Omega_2(z) \quad = \quad \frac{\lambda\Omega_{0,2}U(z)}{\theta+\eta} \tag{29}$$

Using normalizing condition , we find $\Omega_{0,1}$, $\Omega_{0,2}$ by putting $z = 1$ and we apply L's hospital rule,
$\Omega_{0,1} + \Omega_{0,2} + \Upsilon(1) + \Omega_1(1) + \Omega_2(1) = 1,$

$$\Omega_{0,2} = \frac{\Upsilon^*(\lambda) - \frac{\lambda r}{\delta}(1 - S^*(\delta))}{\left[\begin{array}{r} \Upsilon^*(\lambda)(\frac{\eta+\theta}{\lambda} + 1) + \frac{\lambda r}{\theta+\eta}(1 - S_w^*(\theta+\eta)) \\ +\frac{\lambda}{\delta}\Upsilon^*(\lambda)(1-r)(1 - S^*(\delta)) + \frac{\eta+\theta}{\delta}\Upsilon^*(\lambda)(1-r) \\ \times(1 - S^*(\delta)) - \frac{\lambda r}{\delta}S_w^*(\theta+\eta)(1 - S^*(\delta)) - \frac{\lambda}{\delta}S_w^*(\theta+\eta) \\ \times\Upsilon^*(\lambda)(1-r) + \frac{\lambda}{\theta+\eta}\Upsilon^*(\lambda)(1-r)(1 - S_w^*(\theta+\eta) \end{array}\right]} \tag{30}$$

$$\Omega_{0,1} = \frac{\Upsilon^*(\lambda) - \frac{\lambda r}{\delta}(1 - S^*(\delta))}{\frac{\lambda}{\eta+\theta}\left[\begin{array}{r} \Upsilon^*(\lambda)(\frac{\eta+\theta}{\lambda} + 1) + \frac{\lambda r}{\theta+\eta}(1 - S_w^*(\theta+\eta)) \\ -\frac{\lambda r}{\delta}S_w^*(\theta+\eta)(1 - S^*(\delta)) + \frac{\eta+\theta}{\delta}\Upsilon^*(\lambda)(1-r) \\ \times(1 - S^*(\delta)) + \frac{\lambda}{\delta}\Upsilon^*(\lambda)(1-r)(1 - S^*(\delta)) \\ +\frac{\lambda}{\theta+\eta}\Upsilon^*(\lambda)(1-r)(1 - S_w^*(\theta+\eta) \\ -\frac{\lambda}{\delta}S_w^*(\theta+\eta)\Upsilon^*(\lambda)(1-r) \end{array}\right]} \tag{31}$$

4 System Performance Measures

When the server is not being utilized,the steady state probability is $\Upsilon(1)$

$$\Upsilon(1) = \frac{(1 - \Upsilon^*(\lambda))\Omega_{0,2}\left[\begin{array}{r} (1 - S_w^*(\theta+\eta)[\frac{\lambda r}{\delta}(1 - S^*(\delta)) + \frac{\lambda r}{\theta+\eta}] \\ +(\frac{(\eta+\theta)r}{\delta})(1 - S^*(\delta) \end{array}\right]}{\Upsilon^*(\lambda) - \frac{\lambda r}{\delta}(1 - S^*(\delta)} \tag{32}$$

When the server is busy, let $\Omega_1(1)$ be the steady state probability.

$$\Omega_1(1) = \frac{(1-S^*(\delta))\Omega_{0,2}\begin{bmatrix} (\eta+\theta)\Upsilon^*(\lambda)-\Upsilon^*(\lambda)(\lambda(S^*_w(\theta+\eta)-1)) \\ +\frac{\lambda^2 r}{\theta+\eta}(1-S^*_w(\theta+\eta)) \end{bmatrix}}{\delta[\Upsilon^*(\lambda)-\frac{\lambda r}{\delta}(1-S^*(\delta)]} \tag{33}$$

When the server is providing slower service, let $\Omega_2(1)$ be the steady state probability.

$$\Omega_2(1) \quad = \quad \frac{\lambda\Omega_{0,2}(1-S^*_w(\theta+\eta))}{\theta+\eta} \tag{34}$$

The busy cycle and busy period's expected durations are $E(T_b)$ and $E(T_c)$. Then

$$\begin{aligned} E(T_b) &= \frac{1}{\lambda}\left[\frac{1}{\Omega_{0,1}}-1\right], \\ E(T_c) &= \frac{1}{\lambda\Omega_{0,1}}, \\ E(T_0) &= \frac{1}{\lambda}. \end{aligned}$$

where the duration of the system's empty state is indicated by the time T_0.

$$E(T_b) = \frac{\begin{bmatrix} \Upsilon^*(\lambda)+\frac{(\eta+\theta)r}{\delta}(1-S^*(\delta))+\frac{\lambda r}{\theta+\eta}(1-S^*_w(\theta+\eta)) \\ +\frac{\eta+\theta}{\delta}\Upsilon^*(\lambda)(1-r)(1-S^*(\delta))-\frac{\lambda r}{\delta}S^*_w(\theta+\eta) \\ \times(1-S^*(\delta))+\frac{\lambda}{\theta+\eta}\Upsilon^*(\lambda)(1-r)(1-S^*_w(\theta+\eta) \\ +\frac{\lambda}{\delta}\Upsilon^*(\lambda)(1-r)(1-S^*(\delta))-\frac{\lambda}{\delta}S^*_w(\theta+\eta)\Upsilon^*(\lambda)(1-r) \end{bmatrix}}{(\theta+\eta)[\Upsilon^*(\lambda)-\frac{\lambda r}{\delta}(1-S^*(\delta))]} \tag{35}$$

$$E(T_c) = \frac{\begin{bmatrix} \Upsilon^*(\lambda)(\frac{\eta+\theta}{\lambda}+1)+\frac{\lambda r}{\theta+\eta}(1-S^*_w(\theta+\eta)) \\ +\frac{\eta+\theta}{\delta}\Upsilon^*(\lambda)(1-r)(1-S^*(\delta))-\frac{\lambda r}{\delta}S^*_w(\theta+\eta) \\ \times(1-S^*(\delta))+\frac{\lambda}{\theta+\eta}\Upsilon^*(\lambda)(1-r)(1-S^*_w(\theta+\eta) \\ +\frac{\lambda}{\delta}\Upsilon^*(\lambda)(1-r)(1-S^*(\delta))-\frac{\lambda}{\delta}S^*_w(\theta+\eta)\Upsilon^*(\lambda)(1-r) \end{bmatrix}}{(\theta+\eta)[\Upsilon^*(\lambda)-\frac{\lambda r}{\delta}(1-S^*(\delta))]} \tag{36}$$

5 Particular Cases

Case(i) Assuming that $r = 1$ then our model reduces to a non Markovian retrial queue with single working vacation, vacation interruption, disaster and working breakdown.
Case(ii) Assuming that if there is no disaster, then our model reduces to a non Markovian retrial queue with Balking, single working vacation and vacation interruption.
Case(iii) Assuming that if there is no disaster, $r = 1$, and no vacation, then our model reduces to a non Markovian retrial queue.

6 Numerical results

In Figure 1 displays the appropriate line graphs and Table 1 contains the values of $E(T_b)$ by fixing the values of $\mu = 4$, $\mu_w = 2$, $\lambda = 3$, $\theta = 6$, and $r = 0.5$ subject to stability conditions and extending the value of η from 1 to 2 increased with 0.2 and θ from the graph suggests that $E(T_b)$ decreases as η increases as would be predicted.

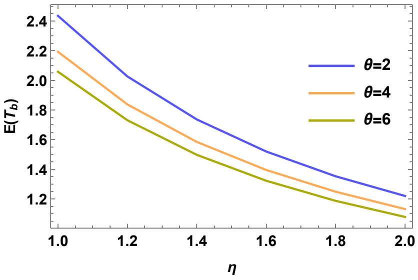

Figure 1: $E(T_b)$ with turn over of η

η	$\theta = 2$	$\theta = 4$	$\theta = 6$
1.0	8.0714	5.1388	4.1767
1.2	6.3738	3.9925	3.2156
1.4	5.3334	3.2963	2.6343
1.6	4.6285	2.8277	2.2444
1.8	4.1185	2.4905	1.9645
2.0	3.7321	2.2361	1.7537

Table 1: $E(T_b)$ with turn over of η

In Figure 2 displays the appropriate line graphs and Table 2 contains the values of $E(T_b)$ subject to stability conditions, by fixing the values of $\mu = 2$, $\mu_w = 1$, $\lambda = 4$, $\theta = 4$, and $r = 0.2$, and extending the values of δ from 1 to 2 increased-with 0.2 and η. The graph suggests that $E(T_b)$ decreases as expected when δ increases.

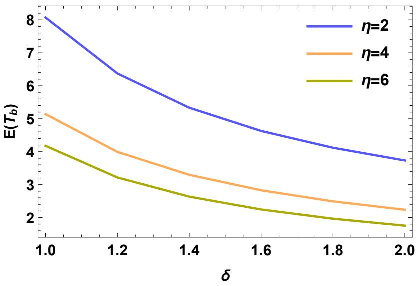

Figure 2: $E(T_b)$ with turn over of δ

δ	$\eta = 2$	$\eta = 4$	$\eta = 6$
1.0	8.0714	5.1388	4.1767
1.2	6.3738	3.9925	3.2156
1.4	5.3334	3.2963	2.6343
1.6	4.6285	2.8277	2.2444
1.8	4.1185	2.4905	1.9645
2.0	3.7321	2.2361	1.7537

Table 2: $E(T_b)$ with turn over of δ

In Figure 3 displays the appropriate line graphs and Table 3 contains the values of $E(T_b)$ by fixing the values of $\mu = 3$, $\mu_w = 2$, $\lambda = 3$, $\theta = 1$, and $r = 0.4$, subject to stability conditions, and extending the values of δ from 1 to 2 incremented with 0.2 and η. From the graph, it can be deduced that $E(T_c)$ decreases as expected when δ increases.

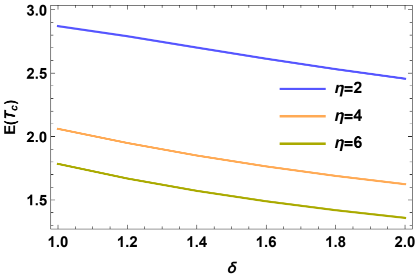

Figure 3: $E(T_c)$ with turn over of δ

δ	$\eta = 2$	$\eta = 4$	$\eta = 6$
1.0	2.8708	2.0610	1.7847
1.2	2.7911	1.9492	1.6691
1.4	2.7016	1.8505	1.5719
1.6	2.6137	1.7646	1.4896
1.8	2.5316	1.6898	1.4194
2.0	2.4564	1.6245	1.3589

Table 3: $E(T_c)$ with turn over of δ

In Figure 4 displays the appropriate line graphs and Table 4 contains the values of $E(T_b)$ subject to stability conditions, by fixing the values of $\mu = 3$, $\mu_w = 2$, $\lambda = 3$, $\theta = 1$, and $r = 0.4$, and extending the values of η from 1 to 2 increased with 0.2 and δ. The graph suggests that $E(T_c)$ decreases as η increases as would be predicted.

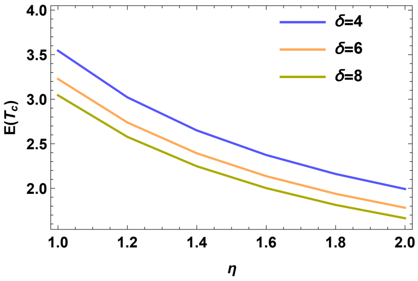

Figure 4: $E(T_c)$ with turn over of η

η	$\delta = 4$	$\delta = 6$	$\delta = 8$
1.0	3.5452	3.2272	3.0440
1.2	3.0212	2.7388	2.5773
1.4	2.6499	2.3931	2.2472
1.6	2.3738	2.1363	2.0022
1.8	2.1609	1.9385	1.8135
2.0	1.9920	1.7818	1.6641

Table 4: $E(T_c)$ with turn over of η

7 Conclusion

In this paper, non Markovian retrial queue, balking, disaster under working breakdown and working vacation is analysed. We discovered the PGF for the total and average number of people in invisible waiting area. We derived some performance measures and deduced some particular cases and illustrated some numerical results.

References

[1] Afthab begum, M.I., Fijy Jose, P., and Bama, S. (2016): An $M^X/G/1$ queue with disasters and working breakdown, Int. Jou. Sci. Res and Pub, Vol. 6, pp. 2250-3153 (2016).

[2] Chandrasekaran, V.M. , Indhira, K. , Saravanarajan, M.C., and Rajadurai, P.: A survey on working vacation queueing models, International Journal of Pure and Applied Mathematics, Vol.106 No.6 ,pp. 33-41 (2016).

[3] Jain, and Sigman.: A Pollaczeck- Khinchine formula for $M/G/1$ queue with disasters, J. Appl. Prob. Vol. 33, pp. 1191-1200 (1996).

[4] Kalidass, K., and Ramanath, K.: A queue with working breakdowns, Computers and Industrial Engineering, Vol 63(4), pp. 779783 (2012).

[5] Kim, B.K., and Lee, D.H.: The $M/G/1$ queue with disasters and working breakdowns, Applied Mathematical Modelling, Vol. 38, pp. 1788-1798 (2014).

[6] Manoharan, P., and Sankarasasi, K.: Analysis of a multitype service of a non-markovian queue with breakdown, delay time and optional vacation, Advances and Applications in Mathematical Sciences, Vol. 20, pp. 975-1001 (2021).

[7] Pazhani Bala Murugan, S., Santhi, K.: An M/G/1 retrial queue with multiple working vacation, International Journal of Mathematics and its Applications, Vol.4, No. 2-D, pp. 35-48 (2016).

[8] Rajadurai P., A study on an M/G/1 retrial G-queue with unreliable server under variant working vacations policy and vacation interruption, *Songklanakarin Journal of Science Technology*, 40(1), pp. 231-242 (2018a).

[9] Rajadurai, P.: Sensitivity analysis of an M/G/1 retrial queueing system with disaster under working vacations and working breakdowns, RAIRO-Operations Res, Vol. 52(1), pp. 35-54 (2018).

[10] Rajadurai P, Chandrasekaran V. M and Saravanarajan M. C., Analysis of an M[X]/G/1 unreliable retrial G-queue with orbital search and feedback under Bernoulli vacation schedule, *OPSEARCH*, 53,pp. 197-223 (2016).

[11] Sennot L. I., Humblet P. A and Tweedi R. L., Mean drifts and the non-Ergodicity of Markov chains. *Oper. Res,* Vol. 31, pp. 783-789 (1983).

[12] Servi, L., Finn, S.: M/M/1 queue with working vacations (M/M/1/WV), Perform. Eval, Vol. 50, pp. 41-52 (2002).

[13] Wu, D., Takagi, H.: M/G/1 queue with multiple working vacations, Perform. Eval, Vol. 63, pp. 654-681 (2006).

J. COMPUTATIONAL ANALYSIS AND APPLICATIONS, VOL. 31, NO. 2, 2023, COPYRIGHT 2023 EUDOXUS PRESS, LLC

A mathematical study of fractional order unsteady natural convective Casson fluid flow past an infinitely vertical plate with heat and mass transfer

Sapna Tyagi [1], **Monika Jain** [1*], **Jagdev Singh**[1]

[1] Department of Mathematics, JECRC University, Jaipur-303905,
Rajasthan, India

tyagisapna1990@gmail.com, monikaj@gmail.com,
jagdevsinghrathore@gmail.com

Abstract. Research on Casson fluid is very important due to its applicability in the progress of industrial and engineering industries. Here, a fractional order model of the Casson fluid over an oscillating plate in the presence of thermal radiation with constant wall temperature and concentration has been considered. The solution of this fractional model is obtained with the help of Laplace transform technique in terms of Wright function. The graphical analysis is also done by making several variations in parametric values including fractional parameter, mass Grashoff number, Prandtl number, velocity, temperature, concentration profiles etc.

1. Introduction

The physical characteristic of non-Newtonian fluid is always a barrier for researchers while solving the problems of non-Newtonian fluid. There is yet no comprehensive model that covers every aspect of a non-Newtonian fluid. Non-Newtonian fluid is widely used in the manufacturing and processing industries, thus researchers are constantly attempting to develop new models. One of the models is the Casson fluid model. In 1959, Casson [22] was the first to present the rheological data of pigment oil suspensions in printing ink.

Khalid et al. [1] studied the Casson fluid across an oscillating vertical plate for Unsteady boundary layer flow with constant wall temperature.

2010 *Mathematics Subject Classification.* 34A34, 26A33.

Key words and phrases. Casson fluid, fractional order, Wright function, Laplace transform.

*Corresponding Author.

Mahantesh et al. [4] studied the convective flow of Casson fluid across an oscillating plate using non-coaxial rotation and quadratic density fluctuation as its boundary conditions. Using variables without dimensions, the governing equations were first transformed into a non - dimensional form. Analytical solutions of the dimensionless momentum, heat, and mass equations were achieved using the Laplace transform method.

Using an exponentially permeable decreasing sheet, Nadeem et al. [25] investigated the boundary layer MHD flow of Casson fluid. The Adomian decomposition method was employed to arrive at the analytical answer to the problem. The velocity distributions resulting from a number of fascinating parameters were displayed and investigated.

The role of the magnetic flux on the three-dimensional Casson fluid flow over the boundary layer of a stretching porous sheet was taken into account in the study by Nadeem et al., [26] . It was discovered that the magnetic field, Casson fluid parameter, and porosity parameter all reduced the velocity profiles in the x and y directions.

The effects of chemical processes and heat generation of MHD convection Casson fluid flow model in a porous media using a revolving vertical plate is provided in the study done by Khan et al. [5].

The unstable MHD free convection flow of Casson fluid through a porous medium past a vertical plate that was moving exponentially was explored by Mohan et al.[24] in the presence of thermal radiation, chemical interaction, and a heat source or sink. They discovered that the velocity profiles decrease when the heat flow, magnetic field parameter, prandtl number, heat source, and Casson parameter increase in value.

Deka [3] has conducted studies of an unstable MHD casson fluid in nanopores with heat transfer through an accelerating vertical plate. It has been discovered that the Casson parameter increases skin friction and fluid velocity. Along with the casson parameter, the surface shear stress also rises.

It is assumed that the Casson fluid, a shear-thinning fluid, has infinite viscosity at zero rate of shear, zero viscosity at infinite rate of shear, and a yield stress below which no flow occurs. A fluid behaves like a solid when it is under conditions where the yield stress is greater than the shear stress. When the applied yield stress is greater than the applied shear stress, the fluid starts to flow. Casson fluid can take the form of things like honey, soup, chocolate, tomato sauce, jelly, blood, sludge, fused polymers, etc. These fluid models have been shown to have important uses in the biomechanics, textile, cosmetic, polymer processing, and pharmaceutical industries.

The Casson fluid flow across an oscillating plate with chemical reaction and sliding phenomenon was expressed by Saqib et al. [16]. The investigation concentrated on the mass and heat transport processes. The Laplace transform method was used to analyse the mathematical model once it had been transformed into dimensionless form. The profiles of velocity, temperature, and concentration were plotted.

Fractional derivatives have recently piqued the interest of many scholars due to the extensive coverage of derivatives and integrals of non-integer order. A variety of physical phenomena or natural circumstances have been studied with the help of fractional calculus, together with the rheological properties of winding polymers, traffic modelling, electric circuits, signal and image processing, electrical networks, stochastic processes and bioengineering.

Imran et al. [18] used two distinct fractional derivatives known as Caputo and Caputo-Fabrizio to study the convection flow of Newtonian fluid.The solutions to the concentration , temperature and velocity profiles were discovered by using the Laplace transform approach. The results were graphically depicted to compare and contrast the two fractional derivatives.

Also, the Caputo time-fractional derivatives are used by Imran et al. [19] to formulate fluid flows with Newtonian heating and arbitrary velocities.It was possible to obtain the dimensionless form of the governing equations by using the specified dimensionless variables. Using the Laplace transform approach, the dimensionless equations were solved.

Numerous scholars have noted the impact of fractional parameters on temperature and velocity characteristics. The computational analysis of fractional diffusion equations occurring in oil pollution has been done by Singh et al., [12].Research by Khan et al.,[11]gives the effect of fractional Caputo time derivatives of general Cassonian fluids with oscillating boundary conditions.

Ali et al. [9] employed the Caputo fractional derivative to examine the blood flow in a horizontal cylinder that was simulated by a Casson fluid. Magnetic particles were present in the fluid flow that was being driven by an oscillating pressure gradient. With the use of finite Hankel and Laplace transformations, the effects of magnetodynamics on Casson's fluids have been investigated and described.

The researchers observed that the fractional order fluid model performs noticeably differently from the conventional model. Several recent important analytical investigations on fluid problems can be found in preceding study [7], [8], [24], and [24].

Atangana-Baleanu and Caputo-Fabrizio are two fractional derivatives that are compared in Sheikh et al. comparative analysis for the convection of Casson's liquid across an infinite vertical flat plate, together with heat and mass transfer[20].

The researchers discovered that for a given unit of time, the velocities calculated using the Caputo-Fabrizio and Atangana-Baleanu operators are the same. Exact solutions for both situations were discovered using the Laplace transform methodology, and the outcomes were compared graphically and in tabular form.On the other hand, when time is less than unity, variance occurs and further differences increase as time increases.
For more definitions and results about the fractional operators, the reader can referes to [5], [13], [14].

2. Mathematical formulation of the problem

The present study takes into account the in compressible Casson fluid flow past an infinitely vertical plate in a free convection flow that is unsteady. Here, the flow range is $y > 0$, and y is the plate's coordinate normal.Primarily, at a time $\tau = 0$, the fluid and the plate are both at rest with a uniform surface concentration of C^*_∞ and temperature T^*_∞. The plate begins to accelerate in its plane at time $\tau > 0$ according to a velocity $A\tau$, where unvarying A represents the plate's acceleration. Both the concentration and plate temperature are increased simultaneously to $T^*_\infty$and C^*_∞ respectively, and then kept constant. The spatial variable y and the time variable t affect the velocity and temperature.

Following the use of the Boussinesq approximation and unidirectional flow, the momentum, energy, and concentration equations acquire the following forms.

$$\rho \tfrac{\partial \mathrm{u}^*}{\partial \tau^*} = \mu \left(1 + \tfrac{1}{\beta}\right) \tfrac{\partial^2 \mathrm{u}^*}{\partial \mathrm{y}^{*2}} + \rho \mathrm{g} \gamma \left(\mathrm{T}^* - \mathrm{T}^*_\infty\right) + \rho \mathrm{g} \beta' \left(\mathrm{C}^* - \mathrm{C}^*_\infty\right), \tag{2.1}$$

$$\rho \mathrm{c_p} \frac{\partial \mathrm{T}^*}{\partial \tau^*} = \mathrm{k} \frac{\partial^2 \mathrm{T}^*}{\partial \mathrm{y}^{*2}} - \frac{\partial \mathrm{q}^*_\mathrm{r}}{\partial \mathrm{y}^*}, \tag{2.2}$$

$$\frac{\partial \mathrm{C}^*}{\partial \tau^*} = \frac{1}{\mathrm{S_c}} \frac{\partial^2 \mathrm{C}^*}{\partial \mathrm{y}^{*2}}. \tag{2.3}$$

Here, β refers Casson parameter, u^* represent fluid in the y-direction, and time variable is denoted by τ^*. The fluid temperature near the plate is T^*, while T^*_∞ refers plate's temperature. ρ denotes fluid density,μ is dynamic viscosity, Y refers to coefficients of the thermal expansion, q^*_r present radiative heat flux, c_p is the heat constant pressure, S_c is Schmidt number, k denotes thermal conductivity.

C^* is the concentration of the fluid near the plate, while C^*_∞ refers concentration of the plate associated with initial and boundary conditions:

$$\left.\begin{array}{c} u^*\left(y^*,0\right)=0, u^*\left(0,\tau^*\right)=\mathrm{F}\tau^{**}; u^*\left(\infty,\tau^*\right)=0 \\ \mathrm{T}^*\left(\mathrm{y}^*,0\right)=\mathrm{T}^*_\infty, \mathrm{T}^*\left(0,\tau^*\right)=\mathrm{T}^*_\mathrm{w}, \mathrm{T}^*\left(\infty,\tau^*\right)=\mathrm{T}^*_\infty \\ \mathrm{C}^*\left(\mathrm{y}^*,0\right)=\mathrm{C}^*_\infty, \mathrm{C}^*\left(0,\tau^*\right)=\mathrm{C}^*_\mathrm{w}, \mathrm{C}^*\left(\infty,\tau^*\right)=\mathrm{C}^*_\infty \end{array}\right\} \tag{2.4}$$

q^*_r is the radiative heat flux in equation (2.2). When q^*_r is differentiated in terms of y using Rosseland's approximation [2],[10],[27],[28], equation (2.2) becomes:

$$\rho c_p \frac{\partial T^*}{\partial \tau^*} = k\frac{\partial^2 T^*}{\partial y^{*2}} - \left(-\frac{16\sigma {T^*_\infty}^3}{3k^*}\right)\frac{\partial^2 T^*}{\partial y^{*2}}. \tag{2.5}$$

3. Problem Solution

The fundamental dimensional equations (2.1), (2.3), and (2.5) are changed into dimensionless equations. The solutions are then derived by employing the Laplace transform approach.
By employing appropriate dimensionless variables,

$$\mathrm{u}=\frac{\mathrm{u}^*}{(\vartheta \mathrm{A})^{\frac{1}{3}}}, \mathrm{t}=\frac{\tau^*(\mathrm{A})^{\frac{2}{3}}}{(\vartheta)^{\frac{1}{3}}}, \mathrm{y}=\frac{\mathrm{y}^*(\mathrm{A})^{\frac{1}{3}}}{(\vartheta)^{\frac{2}{3}}}, \mathrm{T}=\frac{\mathrm{T}^*-\mathrm{T}^*_\infty}{\mathrm{T}^*_\mathrm{w}-\mathrm{T}^*_\infty}\, and\, \mathrm{C}=\frac{\mathrm{C}^*-\mathrm{C}^*_\infty}{\mathrm{C}^*_\mathrm{w}-\mathrm{C}^*_\infty}. \tag{3.1}$$

The governing momentum (2.1), concentration (2.3) and energy (2.5) equations in the dimensionless form in view of (3.1) are

$$\frac{\partial \mathrm{u}}{\partial \mathrm{t}} = \left(1+\frac{1}{\beta}\right)\frac{\partial^2 \mathrm{u}}{\partial \mathrm{y}^2} + \mathrm{GrT} + \mathrm{GmC}, \tag{3.2}$$

$$\mathrm{S_c}\frac{\partial \mathrm{C}}{\partial \mathrm{t}} = \frac{\partial^2 \mathrm{C}}{\partial \mathrm{y}^2}, \tag{3.3}$$

$$\frac{\partial \mathrm{T}}{\partial \mathrm{t}} = \left(\frac{1+\mathrm{N}}{\mathrm{Pr}}\right)\frac{\partial^2 \mathrm{T}}{\partial \mathrm{y}^2}. \tag{3.4}$$

Also the boundary conditions (2.4) takes the form

$$\left.\begin{array}{c} \mathrm{u}\left(\mathrm{y},0\right)=0, \mathrm{u}\left(0,\tau\right)=\mathrm{t}; \mathrm{u}\left(\infty,\tau\right)=0 \\ \mathrm{T}\left(\mathrm{y},0\right)=0, \mathrm{T}\left(0,\tau\right)=1, \mathrm{T}\left(\infty,\tau\right)=0 \\ \mathrm{C}\left(\mathrm{y},0\right)=0, \mathrm{C}\left(0,\tau\right)=1, \mathrm{C}\left(\infty,\tau\right)=0. \end{array}\right\} \tag{3.5}$$

Next, equations (3.2), (3.3), and (3.4) are defined in terms of Caputo fractional derivatives as:

$$\mathrm{D}^\alpha_\mathrm{t}\mathrm{u} = \left(1+\frac{1}{\beta}\right)\frac{\partial^2 \mathrm{u}}{\partial \mathrm{y}^2} + \mathrm{GrT} + \mathrm{GmC}, \tag{3.6}$$

$$\mathrm{S_c D_t^{\alpha} C} = \frac{\partial^2 \mathrm{C}}{\partial \mathrm{y}^2}, \tag{3.7}$$

$$\left(\frac{\mathrm{Pr}}{1+\mathrm{N}}\right) \mathrm{D_t^{\alpha} T} = \frac{\partial^2 \mathrm{T}}{\partial \mathrm{y}^2}, \tag{3.8}$$

where D denotes the differential operator, the fractional operator is α, whereas Gr, N, Pr and Gm are the thermal Grashof number, radiation and Prandtl number and mass Grashof number respectively.

4. Laplace Transform Technique

Unsteady differential equations are frequently solved using the Laplace transform, an integral transform technique. The second order differential equations for the partial differential equations (3.2), (3.3), and (3.4)are generated on using the Laplace transform technique.

$$\left(1+\frac{1}{\beta}\right) \frac{\mathrm{d}^2 \bar{u}}{\mathrm{dy}^2} - \mathrm{s}^{\alpha} \bar{u}\,(\mathrm{y,s}) + \mathrm{Gr}\bar{T} + \mathrm{Gm}\bar{C} = 0, \tag{4.1}$$

$$\frac{\mathrm{d}^2 \bar{C}}{\mathrm{dy}^2} - \mathrm{s}^{\alpha} \mathrm{S_c} \bar{C}\,(\mathrm{y,s}) = 0, \tag{4.2}$$

$$\frac{\mathrm{d}^2 \bar{T}}{\mathrm{dy}^2} - \left(\frac{\mathrm{Pr}}{1+\mathrm{N}}\right) \mathrm{s}^{\alpha} \bar{T}\,(\mathrm{y,s}) = 0. \tag{4.3}$$

Eq. (4.1), (4.2) and (4.3) are then solved by using the undetermined coefficient method and the solutions are presented as

$$\bar{u}\,(\mathrm{y,s}) = \frac{1}{\mathrm{s}^2} \mathrm{e}^{-\mathrm{y}\sqrt{\frac{\mathrm{s}^{\alpha}}{\mathrm{z}}}} + \frac{\mathrm{Gr_0}}{\mathrm{s}^{\alpha+1}} \mathrm{e}^{-\mathrm{y}\sqrt{\frac{\mathrm{s}^{\alpha}}{\mathrm{z}}}} + \frac{\mathrm{Gm_0}}{\mathrm{s}^{\alpha+1}} \mathrm{e}^{-\mathrm{y}\sqrt{\frac{\mathrm{s}^{\alpha}}{\mathrm{z}}}} - \frac{\mathrm{Gr_0}}{\mathrm{s}^{\alpha+1}} \mathrm{e}^{-\mathrm{y}\sqrt{\mathrm{as}^{\alpha}}} - \frac{\mathrm{Gm_0}}{\mathrm{s}^{\alpha+1}} \mathrm{e}^{-\mathrm{y}\sqrt{\mathrm{S_c s}^{\alpha}}}, \tag{4.4}$$

$$\bar{T}\,(\mathrm{y,s}) = \frac{1}{\mathrm{s}} \mathrm{e}^{-\mathrm{y}\sqrt{\mathrm{as}^{\alpha}}}, \tag{4.5}$$

$$\bar{C}\,(\mathrm{y,s}) = \frac{1}{\mathrm{s}} \mathrm{e}^{-\mathrm{y}\sqrt{\mathrm{S_c s}^{\alpha}}}, \tag{4.6}$$

where $\mathrm{z} = \left(1+\frac{1}{\beta}\right), \mathrm{a} = \left(\frac{\mathrm{Pr}}{1+\mathrm{N}}\right), \mathrm{Gr_0} = \frac{\mathrm{Gr}}{(\mathrm{az}-1)}$ and $\mathrm{Gm_0} = \frac{\mathrm{Gm}}{(\mathrm{S_c z}-1)}$. The final solution to the problem is provided by taking inverse Laplace of equations (4.4), (4.5), and (4.6).

$$\begin{aligned} \mathrm{u}\,(\mathrm{y,t}) = {} & \mathrm{t}\varphi\left(2, -\tfrac{\alpha}{2}; -\mathrm{y}\sqrt{\tfrac{\mathrm{s}^{\alpha}}{\mathrm{z}}}\mathrm{t}^{-\frac{\alpha}{2}}\right) + \tfrac{\mathrm{Gr_0}}{\Gamma(\alpha)} \mathrm{t}^{\alpha-1} \varphi\left(1, -\tfrac{\alpha}{2}; -\mathrm{y}\sqrt{\tfrac{\mathrm{s}^{\alpha}}{\mathrm{z}}}\mathrm{t}^{-\frac{\alpha}{2}}\right) \\ & + \tfrac{\mathrm{Gm_0}}{\Gamma(\alpha)} \mathrm{t}^{\alpha-1} \varphi\left(1, -\tfrac{\alpha}{2}; -\mathrm{y}\sqrt{\tfrac{\mathrm{s}^{\alpha}}{\mathrm{z}}}\mathrm{t}^{-\frac{\alpha}{2}}\right) - \tfrac{\mathrm{Gr_0}}{\Gamma(\alpha)} \mathrm{t}^{\alpha-1} \varphi\left(1, -\tfrac{\alpha}{2}; -\mathrm{y}\sqrt{\mathrm{a}}\mathrm{t}^{-\frac{\alpha}{2}}\right) \\ & - \tfrac{\mathrm{Gm_0}}{\Gamma(\alpha)} \mathrm{t}^{\alpha-1} \varphi\left(1, -\tfrac{\alpha}{2}; -\mathrm{y}\sqrt{\mathrm{S_c}}\mathrm{t}^{-\frac{\alpha}{2}}\right), \end{aligned} \tag{4.7}$$

$$\mathrm{C}\left(\mathrm{y},\mathrm{t}\right)=\varphi\left(1,-\frac{\alpha}{2};-\mathrm{y}\sqrt{\mathrm{S_c}}\mathrm{t}^{-\frac{\alpha}{2}}\right), \tag{4.8}$$

$$\mathrm{T}\left(\mathrm{y},\mathrm{t}\right)=\varphi\left(1,-\frac{\alpha}{2};-\mathrm{y}\sqrt{\mathrm{a}}\mathrm{t}^{-\frac{\alpha}{2}}\right), \tag{4.9}$$

where $\varphi\left(a,-\varrho;\zeta\right)=\sum\limits_{n=0}^{\infty}\frac{(\zeta)^n}{n!\Gamma(a-n\varrho)}$ is the Wright function.
Equations (4.7)–(4.9) are bounded by boundary conditions as in (3.5).

5. Result and Discussion

For the free convection flow of a generalised fractional Casson fluid over an accelerating plate, equations (4.4), (4.5), and (4.6) show the closed form. The graphs are generated with varied values of embedded parameters to study how different parameters affect the profiles of velocity, concentration, and temperature. The purpose of the graphs 1-3 is to investigate the impact of the fractional parameter, Prandtl number Pr, and N radiation on temperature profiles with different values.Figures 4–7 display the velocity profile graphs, which were plotted with various fractional parameters, Casson fluid parameters, mass Grashoff number Gm, and time t. In the meantime, Figure 8 shows validation of current solutions.

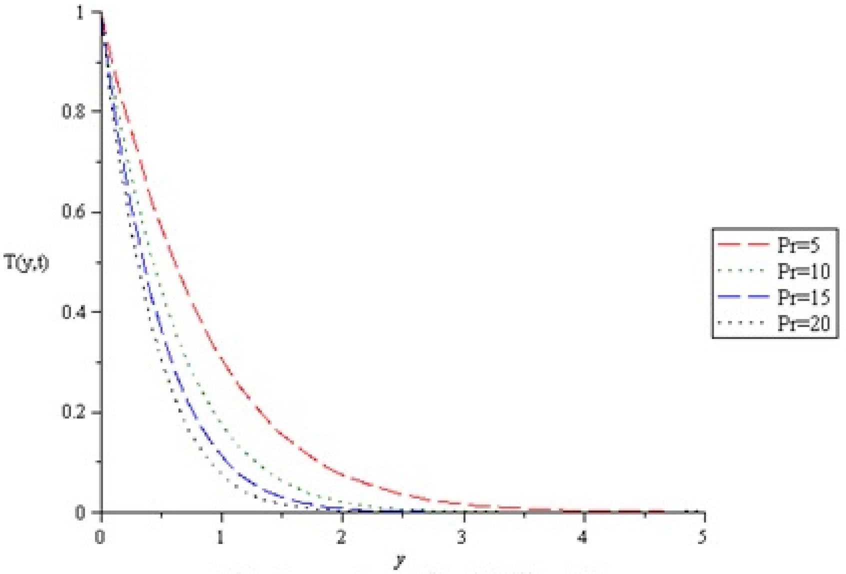

Fig1. Temperature profile with different Pr

The Prandtl number's impact on the temperature distribution is shown in Figure 1. The graph shows that as the value of Pr rises, the temperature profile rapidly falls. The thermal and momentum diffusivity relationship is defined by Prandtl number. Further, the thermal boundary layer thickness is more than the thickness of the momentum boundary layer when Pr , the Prandtl number is small because the fluid travels more slowly than heat transfer. Therefore, for higher Pr fluids, heat can flow from the sheet more quickly. However, a bigger Prandtl number might result in a thinner thermal boundary layer, which would then result in a weaker thermal force for transport and a lower temperature profile.

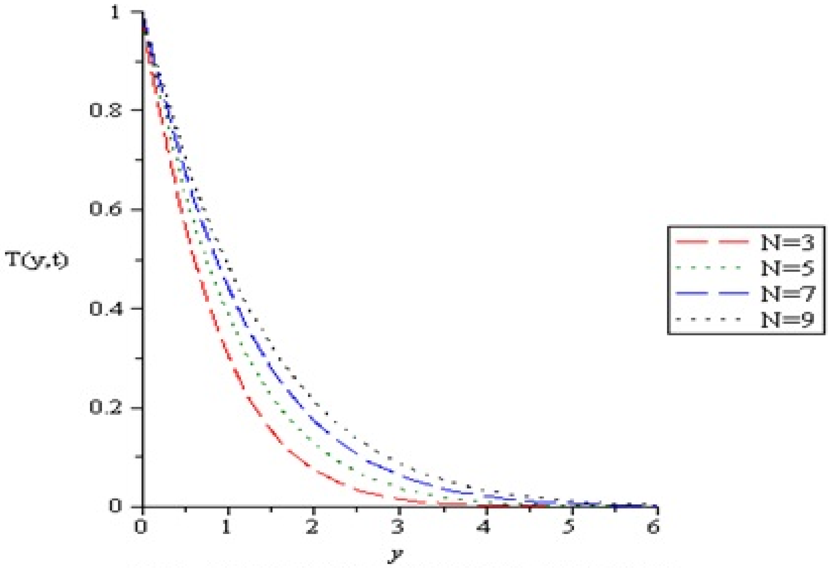

Fig2. Temperature profile with different N

Figure 2 displays the temperature profile of thermal radiation for constant values of Pr and t and various values of N. It is evident that a rise in temperature causes a rise in thermal radiation. The fluid temperature rises as a result of the growing radiation parameter's rising temperatures absorption.

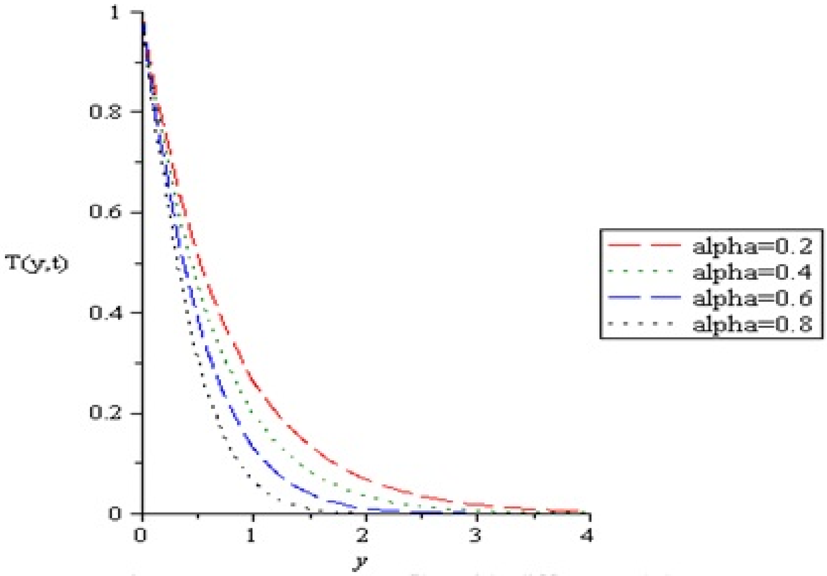

Fig3. Temperature profile with different alpha

Figure 3 illustrates the effect of fractional parameters on temperature. As shown in the figure, the temperature increases monotonically as falls. The outcome here can be helpful for a few real-world issues. By using the computed theoretical results and a suitable fractional mathematical model, the expected outcome and the range for an experimental design are assessed.

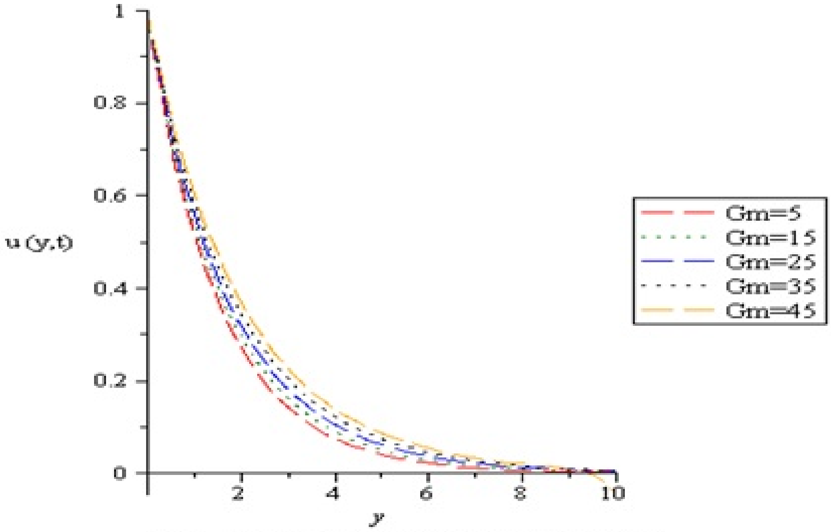

Fig4. Velocity profile with different Gm

The impact of the Grashoff number Gm on the velocity profile is depicted in Figure 4. It is possible to claim that when the value of Gm has been increased, the velocity value also goes up gradually.

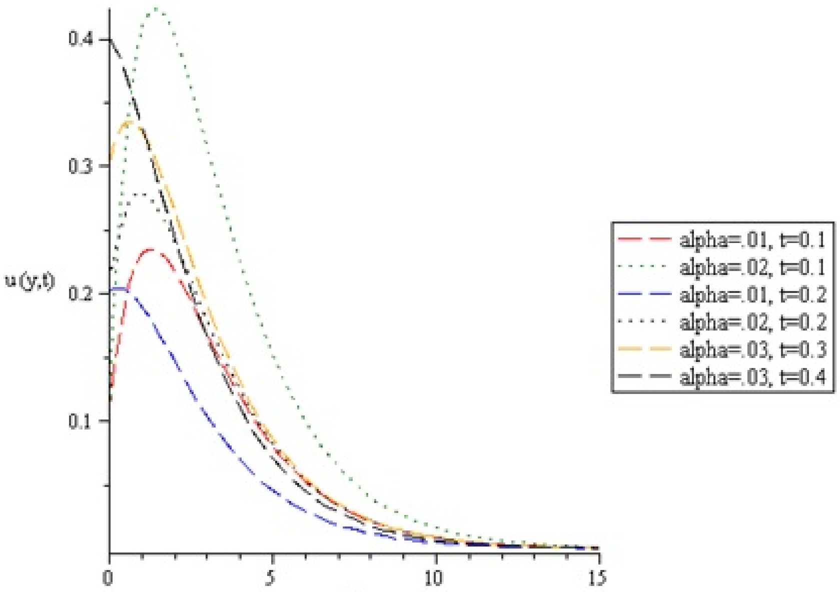

Fig5. Velocity profile with different t & alpha

Figure 5 effects of time and alpha toward the velocity. The velocity increases dramatically in figure 5.

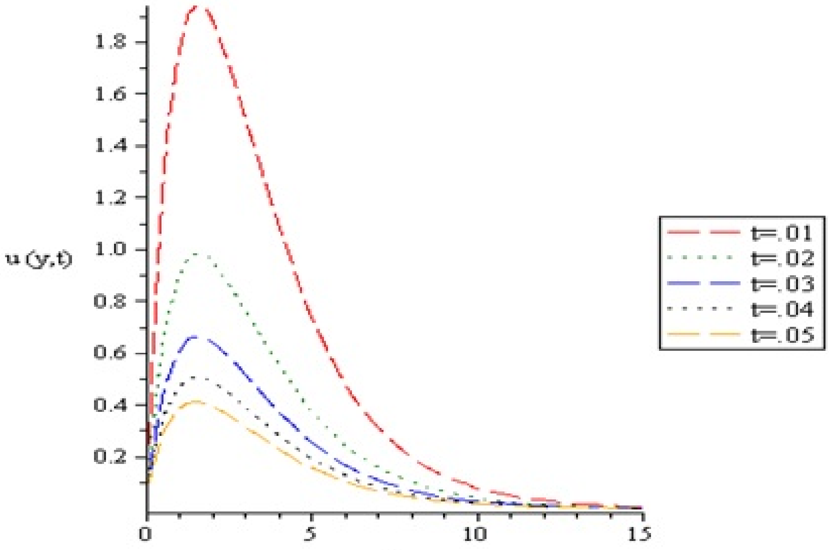

Fig 6. Velocity profile with different t

The impact of time t on velocity profiles is shown in Figure 6. The velocity declines but at a different rate as the value of t rises. The velocity decreases sharply in Figure 6. This tendency can be explained by the graphs' trend which indicates that as t increases, the energy produced by the fluid flow will eventually fall as well.

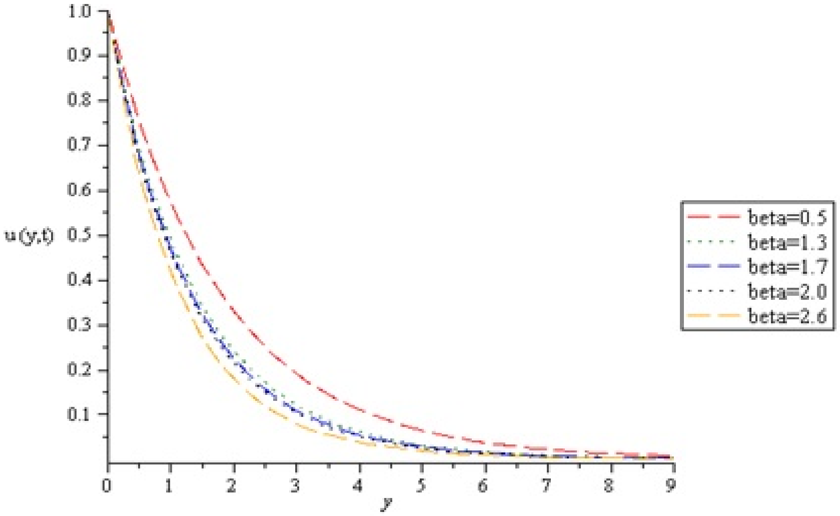

Fig 7. Velocity profile with different beta

The impact of the velocity profile by the Casson parameter is depicted in Figure 7. The velocity initially suffers a falling tendency before progressively increasing.

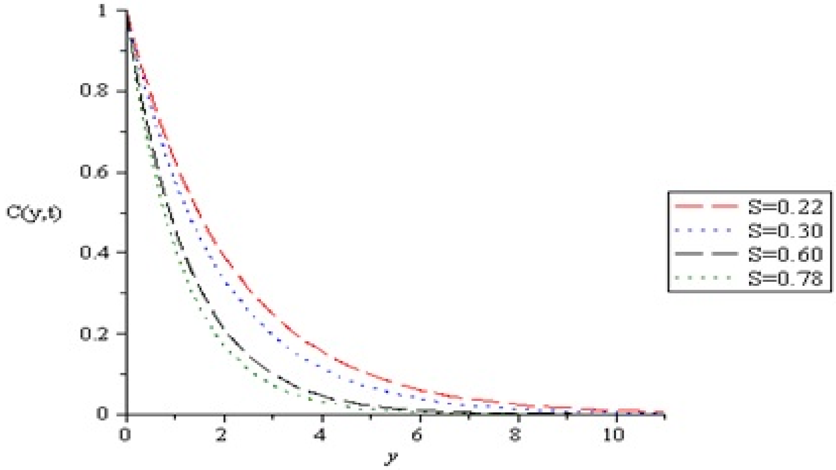

Fig 8. Concentration profile with different Schmidt number (S)

Schmidt number S's impact on the concentration profile may be seen in Figure 8.The value of concentration decrease progressively as the value rise up.

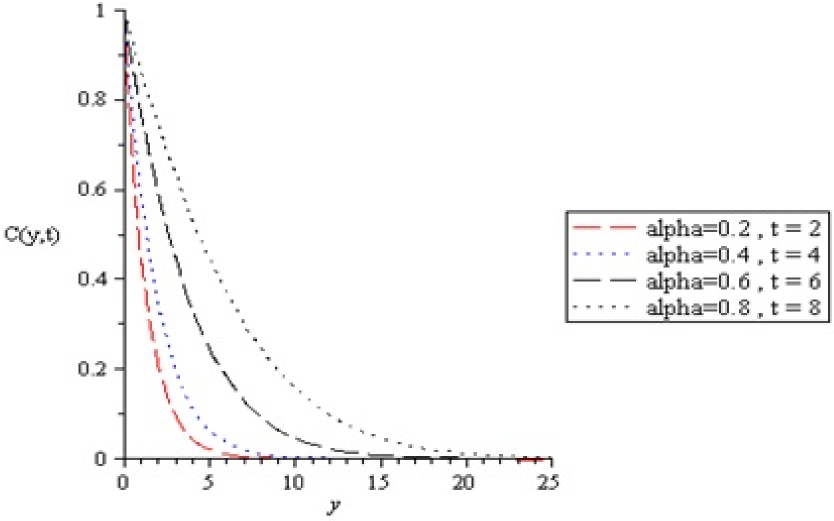

Fig 9. Concentration profile with different alpha and t

Figure 9 shows the effect of t and alpha on the concentration profile. As the value of t and alpha increases, the value of concentration raised steadily.

6. Conclusion

An accelerating plate's free convection flow of fractional order Casson fluid flow has been investigated in the present study. The solutions for velocity and temperature were obtained using the Laplace transform approach.The impact of several parameters on fluid flow, including the Casson fluid parameter, fractional parameter, time, Schmidt number (S), thermal radiation (N), and Prandtl number, is explored. Additionally, it is considered that the obtained results are reliable and provide a new points of view on Casson fluid flow.

References

[1] A. Khalid, I .Khan and S. Shafie, "Unsteady boundary layer flow of a casson fluid past an oscillating vertical plate with constant wall temperature." Malaysian Journal of Fundamental and Applied Science 11, no.1, 28-32(2015).

[2] A.B.M. Raju., P.R. Chandra, B. Malikarjuna and C.S.K. Raju, "Radiation absorption and Soret effects on MHD conducting fluid flow past an exponentially accelerated vertical plate." South East Asian J. Math . Math. Sci., vol. 2'1, no. 1, 1-9 (2020).

[3] A.K. Deka, "In the presence of thermal radiation through porous medium unsteady MHD casson fluid flow past an accelerated vertical plate." International Journal of Statistics and Applied Mathematics 5, no. 4, 213-228 (2020).

[4] B. Mahanthesh, T. Brizlyn, S. Shehzad and B. J. Gireesha, "Nonlinear Thermo-Solution Convective Flow of Casson Fluid over an Oscillating Plate Due to Non-Coaxial Rotation with Quadratic Density Fluctuation Exact Solutions." Multidiscipline Modeling in Materials and Structures 15, 818–8424 (2018).

[5] C. Li, D. Qian and Y. Chen, "On Riemann- Liouville and Caputo Derivative.", Discrete Dynamics in Nature and Society, vol.2011, Article Id 562494, (2011).

[6] D. Khan, A. Khan, I. Khan, F. Ali, F. ul. Karim and I. Tlili, "Effects of relative magnetic field, chemical reaction, heat generation and newtonian heating on convection flow of casson fluid over a moving vertical plate embedded in a porous medium." Scientific Reports 9, no. 1, 1–18(2019).

[7] E.K. Ghiasi and R. Saleh, "Analytical and numerical solutions to the 2d sakiadis flow of casson fluid with cross diffusion, inclined magnetic force, viscous dissipation and thermal radiation based on buongiorno's mathematical model." CFD Letters 11, no. 1, 40–54(2019).

[8] E.K. Mahmoud, "Analytical solution of modified bingham fluid flow through parallel plates channel subjected to forchheimer medium and hall current using linearized differential transformation method." Journal of Advanced Research in Numerical Heat Transfer 4, no. 1, 14–31(2021).

[9] F. Ali, N.A. Sheikh, I. Khan and M. Saqib, "Magnetic field effect on blood flow of Casson fluid in axisymmetric cylindrical tube: A fractional model." Journal of Magnetism and Magnetic Materials 423, 327-336 (2017).

[10] F.S. Ibrahim, A.M. Elaiw and A.A. Bakar, "Effects of the chemical reaction and radition absorption on the unsteady MHD free convection flow past a semi infinite vertical permeable moving plate with heat source and suction." Commun. Nonlinear Sci. Numer. Simul., vol. 13, no. 6, 1056-1066 (2008).

[11] I. Khan, N.A.Shah and D.Vieru, "Unsteady flow of generalized Casson fluid with fractional derivative due to an infinite plate." The European Physical Journal Plus 131, no. 6, 1-12(2016).

[12] J. Singh, A.M. Alshehri, S. M. Momaniand S.B. Hadid, " Computational Analysis of Fractional Diffusion Equations Occurring in Oil Pollution." Mathematics, 10, 20 (2022).

[13] J. Singh, B. Ganbari, D. Kumar and D. Baleanu, "Analysis of fractional model of guava for biological pest control with memory effect." Journal of Advanced Research, 32, 99-108 (2021).

[14] J. Singh, D. Kumar and D. Baleanu, "A new analysis of fractional fish farm model associated with Mittag-Leffler type kernel." International Journal of Biomathematics, vol 13, no. 2(2020).

[15] M. A. Qushairi, N.A. Jaafar, S. Shafie, Z. Ismail and M. Qasim, "Theoretical study on rotating casson fluid in moving channel disk." In Journal of Physics: Conference Series, vol. 1366, no. 1, p. 012039. IOP Publishing, (2019).

[16] M. Saqib, F. Ali, I. Khan and N. A. Sheikh, "Heat and mass transfer phenomena in the flow of Casson fluid over an infinite oscillating plate in the presence of first-order chemical reaction and slip effect.' Neural Computing and Applications 30, no.7, 2159-2172(2018).

[17] M.A. Imran, M. Aleem, M.B. Riaz, R.Ali and I. Khan, "A comprehensive report on convective flow of fractional (ABC) and (CF) MHD viscous fluid subject to generalized boundary conditions." Chaos, Solutions & Fractals, 118, 274-289(2019).

[18] M.A. Imran, N. A.Shah, I. Khan, and M. Aleem, "Applications of non-integer Caputo time fractional derivatives to natural convection flow subject to arbitrary velocity and Newtonian heating." Neural Computing and Applications 30, no. 5, 1589-1599(2018).

[19] M.A. Imran, S. Sarwar, M. Abdullah and I. Khan, "An analysis of the semi-analytic solutions of a viscous fluid with old and new definitions of fractional derivatives." Chinese journal of physics 56, no. 5, 1853-1871(2018).

[20] M.G. Reddy, P.V. Kumari and P. Padma, "Effects of thermal radiation on MHD Casson fluid over a cylinder." J. Nanofluids, vol. 7, 428-438(2018).

[21] N. A. Sheikh, F. Ali, M. Saqib, I. Khan A.S. Alshomrani and M. S Alghamdi, "Comparison and analysis of the atangana–baleanu and caputo–fabrizio fractional derivatives for generalized casson fluid model with heat generation and chemical reaction." Results in Physics 7, 789–800(2017).

[22] N. Casson, "A flow equation for pigment –oil-suspensions of the printing ink type." Rhealogy of Disperse systems (1959).

[23] N. S. Wahid, M. E.H. Hafidzuddin, N. Md. Arifin, M. Turkyilmazoglu and N. A. Abd Rahmin, "Magnetohydrodynamic (MHD) slip darcy flow of viscoelastic fluid over a stretching sheet and heat transfer with thermal radiation and viscous dissipation." CFD Letters 12, no. 1 (2020).

[24] S.Mohan, G.V. Reddy and S. Balakrishna,"An unsteady MHD free convection flow of casson fluid past an exponentially accelerated infinite vertical plate through porous medium in the presence of the thermal radiation, chemical reaction and heat source or sink." International journal of engineering and techniques 4, no. 4, 16-27(2018).

[25] S. Nadeem, R. Ul Haq and C. Lee, "MHD flow of a Casson fluid over an exponentially shrinking sheet." Scientia Iranica 19, no. 6, 1550-1553(2012).

[26] S. Nadeem, R. Ul Haq, N.S. and Z. H. Khan, "MHD three-dimensional Casson fluid flow past a porous linearly stretching sheet." Alexandria Engineering Journal 52, no. 4, 577–882(2013).

[27] S. Pramanik, "Casson fluid flow and heat transfer past exponentially porous stretching surface in presence of thermal radiation." Ain Shams Eng. J., Vol. 5, no. 1, 205-212 (2014).

[28] S.R.Mohan,"Dufour and radiation absorption effects on unsteady MHD free convection casson fluid flow past an exponentially infinite vertical plate through porous medium." Vol. 6, no. 2, 485-512(2019).

[29] V.P. Dubey, J. Singh, A.M. Alshehri and S. Dubey, "Analysis of local fractional coupled Helmholtz and coupled Burgers' equations in fractal media." AIMS Mathematics, 7,5, 8080-8111 (2022).

J. COMPUTATIONAL ANALYSIS AND APPLICATIONS, VOL. 31, NO. 2, 2023, COPYRIGHT 2023 EUDOXUS PRESS, LLC

Effect of the Couple-Stress on Micro Polar Rotating Fluid Flow Saturating a Porous Medium

Devilal Kumawat[1*], Ram Dayal Pankaj[1], and Vijay Mehta[1]

[1]Department of Mathematics and Statistics, Jai Narain Vyas
University, Jodhpur, Rajasthan (INDIA).
*E-mail: devilalkumawat225@gmail.com

December 27, 2022

Abstract - Effect of the couple-stress on micro polar rotating fluid layer heated from below in the presence of varying gravitational field in a porous medium is studied, using normal mode, the problem has been analyzed and it is found that the permeability has destabilizing effect. The rotation, couple-stress parameter and micro-polar parameters have stabilizing effect. The condition of over stability has been found.

Keywords - Micro-Polar Fluid; Couple-Stress; Porous Medium; Rotation

1 Introduction

There are some important classes of fluid in technology areas, one of them being micro-polar fluid. The general theory of micro polar fluid was introduced Eringen[3] . Sharma and Gupta [8] investigated the thermal convection on micro polar fluid in porous medium. Sunil [12] et al. analyzed rotation and different parameters on a micro-polar ferromagnetic fluid flow. Mittal and Rana [5] investigated the medium permeability, suspended particles and other parameters on the micro-polar ferromagnetic fluid.

Stokes [11] study the classical concept of couple-stress fluid. Kumar Pardeep [4] et al. study the rotation on thermal instability in couple-stress viscous elastic fluid. Banyal and Singh [2] investigated the rotation on the couple-stress fluid in a porous medium. Shivakumara et al. [10] used the Galerkin method to investigate the convection in a couple-stress fluid flow. Pundir [6] et al. analyzed the effect of permeability, couple-stress parameter and magnetization. Shah Zahir et al. [7] discussed the effect of couple stress on micro polar fluid flow with hall current. Sharma K. Bhupendra et al. [9] study the effect of porosity, magnetic field and electrically conducting. Aparna P. et al. [1] investigated the couple stress fluid on rotating permeable sphere. Xiong Pei-Ying et al. [13] analyzed the couple stress fluid flow between parallel plates with thermal convection.

Application of this work in geophysics, engineering science, chemical science and industry like as liquid crystal, blood flows, colloids suspensions and clean engine lubricants. In this paper, I attempt to study the couple-stress on micro-polar rotating fluid flow saturating a porous medium. To my knowledge this problem has not yet been investigated using the generalized Darcys model.

2 Mathematical Formulation

An infinite, horizontal, incompressible micro-polar fluid layer of thickness d is assumed and has porosity $\in$ and medium permeability k_1. The upper limit $z = d$ and lower limit $z = 0$ are maintained at constant but varying temperatures T_0 and T_1 such that a study adverse temperature gradient $\beta = \left|\frac{dT}{dz}\right|$ has been continued. The rotation and gravity are applied along z-axis to the system.

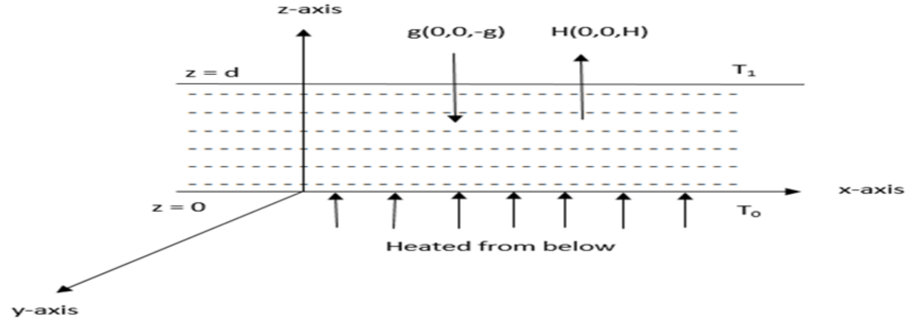

The equation of continuity, momentum, internal angular momentum, temperature and state is

$$\nabla.\vec{q} = o \tag{1}$$

$$\frac{\rho_0}{\in}\left[\frac{\partial\vec{q}}{\partial t} + \frac{1}{\in}\left(\vec{q}.\nabla\right)\vec{q}\right] = -\nabla P - \rho g\hat{e}_z + \left(\mu - \frac{\mu'}{\rho_0}\nabla^2\right)\nabla^2\vec{q} - \frac{1}{k_1}\left(\mu + \varsigma\right)\vec{q} + \varsigma\left(\nabla \times \vec{v}\right) + \frac{2\rho_0}{\in}\left(\vec{q} \times \Omega\right) \tag{2}$$

$$\rho_0 J\left[\frac{\partial\vec{v}}{\partial t} + \frac{1}{\in}\left(\vec{v}.\nabla\right)\vec{v}\right] = \left(\alpha' + \beta'\right)\nabla\left(\nabla.\vec{v}\right) + \gamma'\nabla^2\vec{v} + \frac{\varsigma}{\in}\left(\nabla \times \vec{q}\right) - 2\varsigma\vec{v} \tag{3}$$

$$\left[\in \rho_0 C_v + (1- \in)\rho_s C_s\right]\frac{\partial T}{\partial t} + \rho_0 C_v\left(\vec{q}.\nabla\right)T = \chi\,\nabla^2 T + \delta\left(\nabla \times \vec{v}\right).\nabla T \tag{4}$$

$$\rho = \rho_0\left[1 - \alpha\left(T - T_a\right)\right] \tag{5}$$

Where ρ - Fluid density, ρ_0 Reference density, $\vec{q}$ Filter velocity, $\vec{v}$ Spin (micro rotation), μ - Shear kinematic viscosity coefficient, ς - Coupling viscosity coefficient, P - Pressure, μ' - Couple stress viscosity, $\hat{e}_z$ - Unit vector in z-direction, α' - Bulk spin viscosity coefficient, β' - Shear spin viscosity coefficient, γ' - Micro-polar viscosity coefficient, J - Micro inertia constant, t - time, C_v - Specific heat at constant volume, C_s - Specific heat of solid (Porous Material Matrix), ρ_s - Density of solid matrix, χ - Thermal conductivity, T - Temperature, δ - Micro-polar heat conduction coefficient, α - Coefficient of thermal expansion.

3 Basic State of Problem

The basic state is

$$\vec{q} = \vec{q}_b\left(0,0,0\right),\ \vec{v} = \vec{v}_b\left(0,0,0\right),\ \rho = \rho = \rho_b\left(z\right)\ and\, P = P_b\left(z\right)$$

From equation (1) to (5)

$$\frac{dP_b}{dz} + \rho_b g = 0 \tag{6}$$

$$T = T_b\left(z\right) = -\beta z + T_a \tag{7}$$

$$\rho_b = \rho_0\left(1 + \alpha\beta z\right) \tag{8}$$

4 Linearize Perturbation Equations

$$\nabla.\vec{q}' = o \tag{9}$$

$$\frac{\rho_0}{\in}\frac{\partial \vec{q}'}{\partial t} = -\nabla P' + \alpha\theta g\hat{e}_z + \left(\mu - \frac{\mu'}{\rho_0}\nabla^2\right)\nabla^2\vec{q}' - \frac{1}{k_1}\left(\mu + \varsigma\right)\vec{q}' + \varsigma\left(\nabla\times\vec{v}'\right) + \frac{2\rho_0}{\in}\left(\vec{q}'\times\Omega\right) \tag{10}$$

$$\rho_0 J\frac{\partial \vec{v}'}{\partial t} = \left(\alpha' + \beta'\right)\nabla\left(\nabla.\vec{v}'\right) + \gamma'\nabla^2\vec{v}' + \frac{\varsigma}{\in}\left(\nabla\times\vec{q}'\right) - 2\varsigma\vec{v}' \tag{11}$$

$$E\frac{\partial\theta}{\partial t} + \left(\vec{q}.\nabla\right)T_b = k_T\nabla^2\theta - \frac{\delta}{\rho_0 C_v}\left(\nabla\times\vec{v}'\right)_z\beta + \beta(\vec{q}')_z \tag{12}$$

$$\rho' = -\rho_0\alpha\theta \tag{13}$$

Converting equation (9) to (13) by the following transform $x = dx*$, $y = dy*$, $z = dz*, \vec{q}' = \frac{k_T}{d}\vec{q}*$, $P' = \frac{\mu k_T}{d^2}P*$, $\vec{v}' = \frac{k_T}{d^2}\vec{v}*$, $t = \frac{\rho_0 d^2}{\mu}t*$, $\nabla = \frac{\nabla *}{d}$, $\theta = \beta d\,\theta*$, then we have

$$\nabla.\vec{q} = o \tag{14}$$

$$\frac{1}{\in}\frac{\partial\vec{q}}{\partial t} = -\nabla P + R\theta\hat{e}_z + \left(1 - F\nabla^2\right)\nabla^2\vec{q} - \frac{1}{K_1}\left(1 + K\right)\vec{q} + K\left(\nabla\times\vec{v}\right) + \frac{2}{\in}\left(\vec{q}\times\Omega\right) \tag{15}$$

$$\bar{J}\frac{\partial\vec{v}}{\partial t} = C_1\nabla\left(\nabla.\vec{v}\right) - C_0\nabla\left(\nabla\times\vec{v}\right) + K\left\{\frac{1}{\in}\left(\nabla\times\vec{q}\right) - 2\vec{v}\right\} \tag{16}$$

$$EP_r \frac{\partial \theta}{\partial t} = \nabla^2 \theta - \bar{\delta} (\nabla \times \vec{v})_z + (\vec{q})_z \tag{17}$$

Where $R = \frac{\rho_0 g \alpha \beta d^4}{\mu k_T}$ - Thermal Rayleigh number, $P_r = \frac{\mu}{\rho_0 k_T}$ - Prandtl number, $F = \frac{\mu'}{\rho_0 d^2}$, $E = \in + \frac{(1-\in)\rho_s C_s}{\rho_0 C_v}$, $\bar{J} = \frac{J}{d^2}$, $K_1 = \frac{k_1}{d^2}$, $\bar{\delta} = \frac{\delta}{\rho_0 C_v d^2}$, $C_0 = \frac{\gamma'}{\mu d^2}$, $C_1 = \frac{\alpha' + \beta' + \gamma'}{\mu d^2}$, and $W = \vec{q}.\hat{e}_z$.

5 Boundary conditions

$$W = \frac{d^2 W}{dz^2} = 0,\, \theta = 0 \, at \, z = 0 \, and \, z = d \tag{18}$$

6 Dispersion Relation

Taking curl on both side equation (15) then we have

$$\left[\frac{1}{\in} \frac{\partial}{\partial t} + \left(\frac{1+K}{K_1} \right) - \left(1 - F \nabla^2 \right) \nabla^2 \right] (\nabla \times \vec{q}) = R \left(\frac{\partial \theta}{\partial x} \hat{e}_x + \frac{\partial \theta}{\partial x} \hat{e}_y \right) + K \nabla \times (\nabla \times \vec{v}) + \frac{2}{\in} \nabla \times (\vec{q} \times \Omega) \tag{19}$$

Let $\nabla^2 = \frac{\partial^2}{\partial x^2} + \frac{\partial^2}{\partial y^2} + \frac{\partial^2}{\partial z^2}$, $\nabla_1^2 = \frac{\partial^2}{\partial x^2} + \frac{\partial^2}{\partial y^2}$, $D = \frac{\partial}{\partial z}$, $\zeta_z = (\nabla \times \vec{q})_z$, ${\Omega_z}' = (\nabla \times \vec{v})_z$
Taking curl and z-component of equation (19), (16), then we have

$$\left[\frac{1}{\in} \frac{\partial}{\partial t} + \left(\frac{1+K}{K_1} \right) - \left(1 - F \nabla^2 \right) \nabla^2 \right] \nabla^2 W = R \nabla_1^2 \theta + K \nabla^2 \, {\Omega_z}' \, \hat{e}_z - \frac{2}{\in} \Omega \left(D \zeta_z \right) \tag{20}$$

$$\bar{J} \frac{\partial {\Omega_z}'}{\partial t} = C_0 \nabla^2 {\Omega_z}' - K \left[\frac{1}{\in} \nabla^2 W + 2 {\Omega_z}' \right] \tag{21}$$

Taking z-component of equation (19) and (17) then we have

$$\left[\frac{1}{\in} \frac{\partial}{\partial t} + \left(\frac{1+K}{K_1} \right) - \left(1 - F \nabla^2 \right) \nabla^2 \right] \zeta_z = \frac{2}{\in} \Omega D W \tag{22}$$

$$EP_r \frac{\partial \theta}{\partial t} = \nabla^2 \theta - \bar{\delta} \, {\Omega_z}' + W \tag{23}$$

1. Normal Mode Analysis

Let $\left[W,\, \zeta_z,\, \theta,\, {\Omega_z}' \right] = \left[W(z),\, X(z),\, \Theta(z),\, G(z) \right] \exp . \left[i \, k_x x + i \, k_y y + \sigma t \right]$
Applying normal mode of equation (20) to (23), becomes

$$\left[\frac{\sigma}{\in} + \left(\frac{1+K}{K_1} \right) + F \left(D^2 - a^2 \right)^2 - \left(D^2 - a^2 \right) \right] \left(D^2 - a^2 \right) W = -R a^2 \Theta + K \left(D^2 - a^2 \right) G - \frac{2}{\in} \Omega D X \tag{24}$$

$$\left[\frac{\sigma}{\in}+\left(\frac{1+K}{K_1}\right)+F\left(D^2-a^2\right)^2-\left(D^2-a^2\right)\right]X=\frac{2}{\in}\Omega DW \tag{25}$$

$$\left[m\sigma+2A-\left(D^2-a^2\right)\right]G=-\frac{A}{\in}\left(D^2-a^2\right)W \tag{26}$$

$$\left[EP_r\sigma-\left(D^2-a^2\right)\right]\Theta=-\bar{\delta}G+W \tag{27}$$

Where $a^2=k_x^2+k_y^2$ - wave number, $\sigma=\sigma_r+i\,\sigma_r$ - stability parameter and $m=\frac{\bar{J}A}{K}$, $A=\frac{K}{C_0}$, A - ratio between the micro-polar viscous effect and micro-polar diffusion effects.

$$W=D^2W=0=X=DX=G,\Theta=0\,at\,z=0\,to\,z=1 \tag{28}$$

$$D^{2n}W=0\,at\,z=0\,to\,z=1,\ \text{Where}\ n>0.$$

The solution of equation (28) is

$$W=W_0\,\sin\pi z$$

Eliminating Θ, G, Φ , X from (24) to (27) and put the value of $W\ and\ b=\pi^2+a^2$, then we have

$$\begin{aligned}
&b\left[\frac{\sigma}{\in}+\left(\frac{1+K}{K_1}\right)+Fb^2+b\right]^2[m\sigma+2A+b]\,[EP_r\sigma+b]\\
&\quad=Ra^2\left[\frac{\sigma}{\in}+\left(\frac{1+K}{K_1}\right)+Fb^2+b\right]\left[(m\sigma+2A+b)-\frac{\bar{\delta}Ab}{\in}\right]\\
&\qquad+\frac{KAb^2}{\in}\left[\frac{\sigma}{\in}+\left(\frac{1+K}{K_1}\right)+Fb^2+b\right][EP_r\sigma+b]\\
&\qquad\qquad-\frac{4\Omega^2\pi^2}{\in^2}(m\sigma+2A+b)\,[EP_r\sigma+b]
\end{aligned} \tag{29}$$

7 Stationary Convection

Put the $\rho=0$ in equation (29), then we have

$$\begin{aligned}
R=&\frac{1}{a^2\left[2A+b-\frac{\bar{\delta}Ab}{\in}\right]}\left[b^2\,(2A+b)\left(\frac{1+K}{K_1}+Fb^2+b\right)-\frac{KAb^3}{\in}\right.\\
&\left.+\frac{\frac{4\Omega^2\pi^2}{\in^2}b\,(2A+b)}{\left(\frac{1+K}{K_1}+Fb^2+b\right)}\right]
\end{aligned} \tag{30}$$

To study the behavior of permeability, rotation, couple-stress parameter coupling parameter, micro-polar coefficient, micro-polar heat transfer parameter and find the nature of $\frac{dR}{dK_1}$, $\frac{dR}{d\Omega}$, $\frac{dR}{dF}$, $\frac{dR}{dK}$, $\frac{dR}{dA}\,and\,\frac{dR}{d\bar{\delta}}$ respectively, then

$$\frac{dR}{dK_1}=\frac{-b\,(2A+b)\,(1+K)}{a^2{K_1}^2\left[2A+b-\frac{\bar{\delta}Ab}{\in}\right]}\left[b-\frac{\frac{4\Omega^2\pi^2}{\in^2}}{\left(\frac{1+K}{K_1}+Fb^2+b\right)}\right] \tag{31}$$

$$\frac{dR}{dK_1} < 0\, if\, \frac{4\Omega^2\pi^2}{b} < \in^2\left(\frac{1+K}{K_1} + Fb^2 + b\right)\, and\, \bar{\delta} < \frac{\in}{A}$$

From equation (31), we can say that the permeability has destabilizing effect when $\frac{4\Omega^2\pi^2}{b} < \in^2\left(\frac{1+K}{K_1} + Fb^2 + b\right)\, and\, \bar{\delta} < \frac{\in}{A}$.

$$\frac{dR}{d\Omega} = \frac{8\Omega\pi^2\in^{-2}b\,(2A+b)}{a^2\left(\frac{1+K}{K_1} + Fb^2 + b\right)\left[2A + b - \frac{\bar{\delta}Ab}{\in}\right]} \tag{32}$$

$$\frac{dR}{d\Omega} < 0\, if\;\bar{\delta} < \frac{\in}{A}$$

From equation (32) shows that the rotation has stabilizing effect when $\bar{\delta} < \frac{\in}{A}$.

$$\frac{dR}{dF} = \frac{b^3\,(2A+b)\left[b\left(\frac{1+K}{K_1} + Fb^2 + b\right)^2 - \frac{4\Omega^2\pi^2}{\in^2}\right]}{a^2\left(\frac{1+K}{K} + Fb^2 + b\right)^2\left[2A + b - \frac{\bar{\delta}Ab}{\in}\right]} \tag{33}$$

$$\frac{dR}{dF} > 0\, if\;\left(\frac{1+K}{K_1} + Fb^2 + b\right) > \frac{2\Omega\pi}{\in\sqrt{b}}$$

It is clear that the couple-stress parameter has stabilizing effect when $\left(\frac{1+K}{K_1} + Fb^2 + b\right) > \frac{2\Omega\pi}{\in\sqrt{b}}$.

$$\frac{dR}{dK} = \frac{b\left[Ab\left(\frac{2}{K_1} - \frac{b}{\in}\right)\left(\frac{1+K}{K_1} + Fb^2 + b\right)^2 + \left\{b^2\left(\frac{1+K}{K_1} + Fb^2 + b\right)^2 - \frac{4\Omega^2\pi^2(2A+b)}{\in^2}\right\}\frac{1}{K_1}\right]}{a^2\left(\frac{1+K}{K} + Fb^2 + b\right)^2\left[2A + b - \frac{\bar{\delta}Ab}{\in}\right]} \tag{34}$$

$$\frac{dR}{dK} > 0\, if\, \frac{2}{K_1} > \frac{b}{\in}\, and\, \left(\frac{1+K}{K_1} + Fb^2 + b\right) > \frac{2\Omega\pi\sqrt{(2A+b)}}{\in}$$

Hence the coupling parameter has stabilizing effect when $\frac{2}{K_1} > \frac{b}{\in}\, and\, \left(\frac{1+K}{K_1} + Fb^2 + b\right) > \frac{2\Omega\pi\sqrt{(2A+b)}}{\in}$.

$$\frac{dR}{dA} = \frac{\frac{b^4}{\in}\left(\frac{1+K}{K_1} + Fb^2 + b\right)^2\left[\bar{\delta} - K\left(\frac{1+K}{K_1} + Fb^2 + b\right)\right] + \frac{4\Omega^2\pi^2\bar{\delta}b^3}{\in^3}}{a^2\left(\frac{1+K}{K_1} + Fb^2 + b\right)\left[(2A+b) - \frac{\bar{\delta}Ab}{\in}\right]^2} \tag{35}$$

$$\frac{dR}{dA} > 0\;if\,\bar{\delta} > K\left(\frac{1+K}{K_1} + Fb^2 + b\right)$$

From equation (35), we can say that the micro-polar coefficient has stabilizing effect when $\bar{\delta} > K\left(\frac{1+K}{K_1} + Fb^2 + b\right)$.

$$\frac{dR}{d\bar{\delta}} = \frac{\frac{Ab}{\in}}{a^2\left[(2A+b) - \frac{\bar{\delta}Ab}{\in}\right]^2}\left[b^3\left\{\left(\frac{1+K}{K_1} + Fb^2 + b\right) - \frac{KA}{\in}\right\}\right.$$
$$\left. + 2Ab^2\left(\frac{1+K}{K_1} + Fb^2 + b\right) + \frac{4\Omega^2\pi^2\in^{-2}b\,(2A+b)}{\left(\frac{1+K}{K_1} + Fb^2 + b\right)}\right] \quad (36)$$

$$\frac{dR}{d\bar{\delta}} > 0\, if\ \left(\frac{1+K}{K_1} + Fb^2 + b\right) > \frac{KA}{\in}$$

From equation (36), shows that the micro-polar heat transfer parameter has stabilizing effect when $\left(\frac{1+K}{K_1} + Fb^2 + b\right) > \frac{KA}{\in}$

8 Oscillatory Convection

Putting $\sigma = i\,\sigma_i$ in equation (29) then we get real and imaginary part, eliminating R between them, then we have

$$f_0\sigma_i^4 + f_1\sigma_i^2 + f_2 = 0$$

Put $s = \sigma_i^2$then we have

$$f_0 s^2 + f_1 s + f_2 = 0 \quad (37)$$

Where

$$f_0 = a_1 q_1 - p_1 b_1$$
$$f_1 = a_2 q_1 - p_2 b_1 - p_1 b_2$$
$$f_2 = a_3 q_1 - p_2 b_2$$
$$b_1 = -\frac{ma^2}{\in},\ a_1 = \frac{EP_r mb}{\in^2} \text{ and } b_2 = a^2\,(2A+b)\left\{\frac{1+K}{K_1} + Fb^2 + b\right\}$$

$$a_2 = -\left[\frac{\left\{(2A+b)\,b^2\right\}}{\in^2} + \frac{2b}{\in}\left(\frac{1+K}{K_1} + Fb^2 + b\right)\left\{(2A+b)\,EP_r + mb\right\}\right.$$
$$\left. + \left(\frac{1+K}{K_1} + Fb^2 + b\right)^2 EP_r mb\right] + \frac{KAb^2EP_r}{\in^2} - \frac{4\Omega^2\pi^2EP_r m}{\in^2}$$

$$a_3 = (2A+b)\,b^2\left(\frac{1+K}{K_1} + Fb^2 + b\right)^2 - \frac{KAb^3}{\in}\left(\frac{1+K}{K_1} + Fb^2 + b\right) + \frac{4\Omega^2\pi^2(2A+b)b}{\in^2}$$
$$P_1 = -\frac{1}{\in}\left[\frac{b}{\in}\left\{(2A+b)\,EP_r + mb\right\} + 2EP_r mb\left(\frac{1+K}{K_1} + Fb^2 + b\right)\right]$$

$$\begin{aligned}P_2=\Big[&2\left(2A+b\right)b^2{\in}^{-1}\left(\frac{1+K}{K_1}+Fb^2+b\right)\\&+\left\{\left(2A+b\right)EP_r+mb\right\}b\left(\frac{1+K}{K_1}+Fb^2+b\right)^2\Big]\\&-\frac{KAb^2}{\in}\left(\frac{b}{\in}+EP_r\right)+\frac{4\Omega^2\pi^2}{\in^2}\left[\left(2A+b\right)EP_r+mb\right]\end{aligned}$$

$$q_1=a^2\left[\frac{(2A+b)}{\in}+m\left(\frac{1+K}{K_1}+Fb^2+b\right)-\frac{\bar{\delta}Ab}{\in^2}\right]$$

From (37), we saying that $s=\sigma_i^2$ is positive, equation (37) for the sum of roots is positive, it is not possible if $f_0>0$ and $f_1>0$.
If $f_0>0$ and $f_1>0$ when $\bar{\delta}<\frac{\in}{A}$, $K<4Fb\in$, $KEP_r<4b\,and\,AKb^2<2\pi^2\Omega^2m$.
Above conditions of the overstability.

9 Numerical Calculation

Now we show numerically effect of different parameter from equation (29)

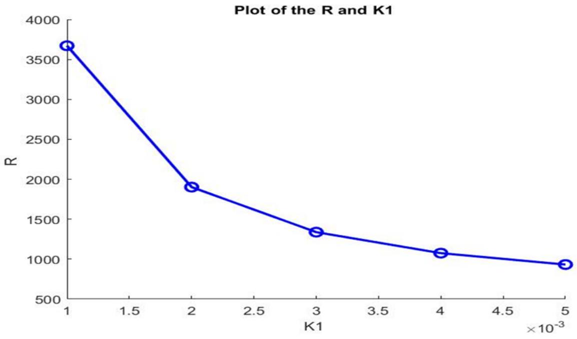

Figure 1:
$E=1,\ \mathrm{P}_r=2,\ \in=0.5,\ A=0.1,\ F=2,\ K=0.2,\ \Omega=10\,and\,\bar{\delta}=0.05.$

Fig 1 shows the variation of Rayleigh number R with respect to medium permeability K_1 i.e. medium permeability K_1 increases then the Rayleigh number R decreases.

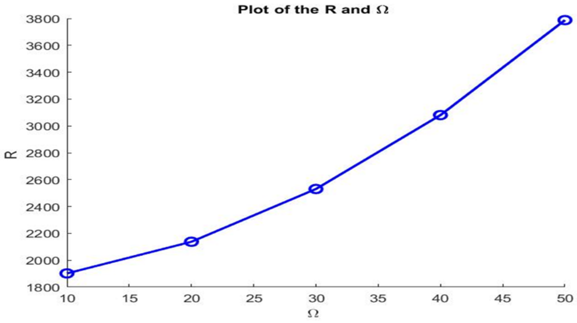

Figure 2:
$E = 1,\ \mathrm{P}_r = 2,\ \in= 0.5,\ A = 0.1,\ F = 2,\ K = 0.2,\ K_1 = 0.002\, and\, \bar{\delta} = 0.05.$

Fig 2 represent the plot of Rayleigh number R versus rotation ω i.e. rotation increases ω then the Rayleigh number R increases.

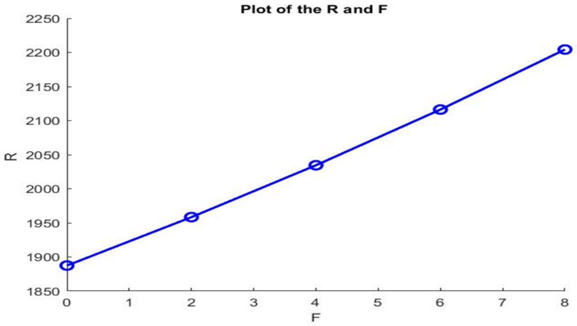

Figure 3:
$E = 1,\ \mathrm{P}_r = 2,\ \in= 0.5,\ A = 0.1,\ \Omega = 10,\ K = 0.2,\ K_1 = 0.002\, and\, \bar{\delta} = 0.05.$

Fig 3 plot between Rayleigh number R and couple-stress parameter F i.e. couple-stress parameter F increases then the Rayleigh number R increases.

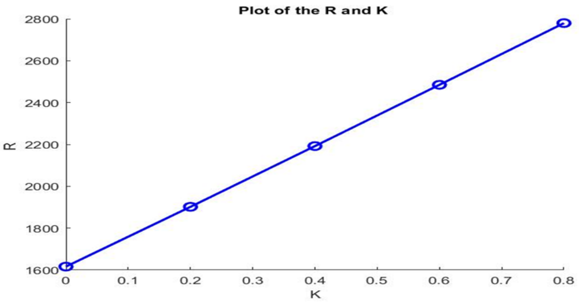

Figure 4:
$E = 1,\ \mathrm{P}_r = 2,\ \in= 0.5,\ A = 0.1,\ \Omega = 10,\ F = 2,\ K_1 = 0.002\, and\, \bar{\delta} = 0.05.$

Fig 4 shows the variation of Rayleigh number R with respect to coupling parameter K i.e. coupling parameter K increases then the Rayleigh number R increases.

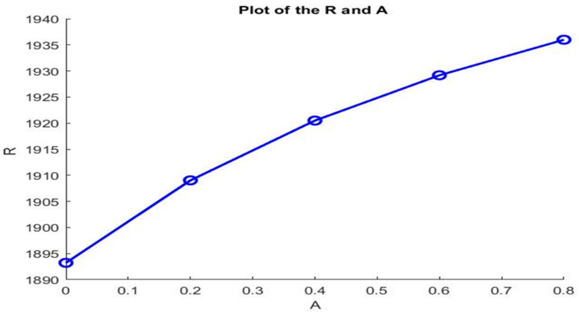

Figure 5:
$E = 1,\ \mathrm{P}_r = 2,\ \in= 0.5,\ K = 0.2,\ \Omega = 10,\ F = 2,\ K_1 = 0.002\, and\, \bar{\delta} = 0.05.$

Fig 5 represent the plot of Rayleigh number R versus micro-polar coefficient i.e. micro-polar coefficient A increases then the Rayleigh number R increases.

10 Conclusions

According to the stationary convection and numerically discussion we found that the effect of permeability is destabilizing. The effect of couple-stress parameter, rotation, coupling parameter, micro-polar coefficient and micro-polar heat conduction are stabilizing. Among them the most important result that the effect of rotation stabilize on the system. The condition of over stability is $\bar{\delta} < \frac{\in}{A}$, $K < 4Fb \in$, $KEP_r < 4b\, and\, AKb^2 < 2\pi^2\Omega^2 m$.

References

[1] Aparna P., Murthy Ramana J.V., Couple on a rotating permeable sphere in a couple stress fluid, Ain shams engineering journal, 2018; 9:665-673.
[2] Banyal S.A. and Singh Kamal A characterization of couple-stress fluid heated from below in a porous medium in the presence of a rotation, International journal of advanced computer and mathematical science, 2012; 3(3): 310-320.
[3] Eringen A.C., Simple microfluids, International journal of engineering science, 1964; 2(2): 205-217.
[4] Kumar pardeep, Lal Roshan and Sharma Poonam, Effect of rotation on thermal instability in couple-stress elastio-viscous fluid, Zeitschrift fur Naturforschung, 2004; 59(a): 407-411.
[5] Mittal Reena and Rana U.S., Effect of dust particles on a layer of micropolar ferromagnetic fluid heated from below saturating a porous medium, Applied Mathematics and computation, 2009; 215:2591-2607.
[6] Pundir K.S., Nadiam K.P. and Pundir R, Effect of hall current on hydromagnetic instability of a couple-stress ferromagnetic fluid in the presence of varying gravitational field through a porous medium, International journal of Statistics and applied mathematics, 2021; 6(4): 01-15.
[7] Shah Zahir, Kumam Poom, Dawar Abdullah, Alzahrani O. Ebraheem and Thounthong Phatiphat, study of the couple stress convective micropolar fluid flow in a hall MHD generator system, Frontiers in physics; 2019, 7:171.
[8] Sharma C.R. and Gupta Urvashi, Thermal convection in micropolar fluids in porous medium, International journal of engineering science, 1995; 33(13): 1887-1892.
[9] Sharma K. Bhupendra, Sharma Kumar Pawan and Chauhan Kumar Sudhir, Effect of MHD on unsteady oscillatory couette flow through porous media, Int. J. of applied mechanics and engineering, 2022; 24(1):188-202
[10] Shivakumara S. Sureshkumar S. and Devaraju N., Effect of Non-uniform temperature gradients on the onset of convection in a couple-stress fluid-saturated porous medium, Journal of applied fluid mechanics, 2012; 5(1): 49-55.
[11] Stokes Kumar Vijay, Couple-stress in fluid, Physics of fluid, 1966; 9(9):1709-1715.
[12] Sunil, Sharma Anu, Bharti K.P., Shandil G.R., Effect of rotation on a layer of micropolar ferromagnetic fluid heated from below saturating a porous medium, International Journal of engineering science, 2006; 44:683-698.
[13] Xiong Pie-Ying, Nazeer Mubbashar, Hussain Farooq, Khan Ijaz M., Saleem Adila, Qayyum Sumaira and Chu Yu-Ming, Two-phase flow of couple stress fluid thermally effected slip boundary conditions: Numerical analysis with variable liquids properties, Alexandria Engineering journal, 2022; 61:3821-3830.

Mathematical Analysis of SEITR Model for Influenza Dynamics

K. Arun Kumar [1] and A.Venkatesh[2*]

[1,2]Department of Mathematics,
AVVM Sri Pushpam College (Affiliated to Bharathidasan University),
Poondi, Thanjavur(Dt), Tamilnadu, India-613 503.

December 28, 2022

Abstract

In order to give timely hospitalisation for infections that are dangerously ill, our primary goal is to reduce the interaction between susceptibles and infections. For this we add treatment T as a fifth compartment to the SEIR model, converting it from SEIR to SEITR. The stabilities of endemic equilibrium and disease-free equilibrium were tested. The next generation matrix method was used to calculate the SEITR model's basic reproduction number. Numerical simulations were also presented to validate our analytic findings. A graphic depicted the impact of parameters on infected populations. It was perceived that, anytime the treatment rate increased, the infected population, exposed population, and treated population all declined but the susceptible population increased.

Keywords: SEITR model, basic reproduction number, stability and numerical simulation.
AMS Subject Classification: 34D20

1 Introduction

Kermack and McKendrick [21] introduced the first mathematical model, SIR (Susceptible-Infectious-Recovered), early in the 20th century. Later Anderson and May[1] were proposed the SEIR model by adding Exposed (E) as fourth compartment to SIR model to define the spread of epidemic. Many authors introduced a numerous extended SEIR models to define the infectious diseases spread and their preventions [7]. ZhilanFeng (2007) [31] developed a SEIR model which has been used to evaluate the electiveness of different control strategies for the size of endemic with separation and isolation. Rafiqul Islam et al [16] was proposed an SEIR model to analysis the influenza in Bangladesh. Vinod kumar bais and Deepak kumar [29] was introduced a model SITR emphasized the condition of the dynamical classic to the transmission populace of H1N1 virus. By combining these two SEIR and SITR models we developed an new SEITR model by including treatment T as a fifth compartment to investigate the dynamics of the influenza epidemic's transmission. Hethcote and Yorke [14] were charity models to analyze the gonorrhea controller techniques, such as showing, outling infectors, post treatment and vaccination.

---

[*] Corresponding author: avenkateshmaths@gmail.com

Chinviriyasit (2007) was introduced a dynamic SIRC model [6] to study the Numerical exhibiting modeling of the spread dynamics of influenza. Samuel Abubakar (2013) was proposed a model [25] to investigation the spread of infectious disease and stability of disease in population. Various researchers such as Andreasen et al. (1997)[2], Hethcote (2000), Earn et al. (2002)[15], Casagrandi et al. (2006)[10], Murray et al. (2008) [23] have been studied the dynamics of influenza and they recommended mathematical models to revision the spread of H1N1 and control the influenza epidemic. Over the past several decades, the field of FDEs has made considerable advancements. To examine the dynamical behaviour of a fish farm in relation to an arbitrary order Atangana-Baleanu derivative, Jagdev et al. [19] suggested a fraction fish farm model. By Jagdev Singh [18], a fractional guava fruit model with memory outcome was introduced. To analyse the COVID-19 trend, Supriya, Yadav et al [28] created the FDE model. A fractional model was created by Jagdev Singh and Arpita Gupta[17] to analyse the results of nonlinear partial modified. To study malaria transmission, Rehman, Attiq ul, et al [**?**] proposed a 9 compartment FDE model. A simple influenza(H1N1) model by means of optimal control studied by Srivastav. A. K et al. (2016) [27], Also Mishra et al. (2013) [22], consume suggested a mathematical model to analyze the spread and control of influenza between two economic groups. Christian Quirouette et al[24] developed to unfolding the localization and spread of influenza virus inside the human breathing area. The Mathematical model [3], plays a crucial role to learning the spread dynamics of the Contagious Disease Influenza, and control the virus through isolation, treatment and vaccination of infected population. Environmental contaminations, global warming, ecosystems, roving etc. are main reasons to spread the contagious diseases. So that certain assumptions and parameters are considered to formulate the model. Influenza is a breathing contagious disease instigated by influenza virus[18], which is also known as flu and it has three kinds A, B and C. This virus spreads easily in the population very fast through the air from coughing, sneezing and through contact by the hands touching our eyes, nose or mouth etc. Communal symptoms of H1N1 are high fever, pain, sore gorge, muscle pain, coughing and weariness [11]. The symptoms were appeared after two days and it has been at most one week [12] but cough may last more than two weeks. Each year individuals are infected by this virus an outbreak particularly in the winter session. The formulation and analysis of the SEITR model were briefly detailed in this article. The analyses of the model, together with the findings on local and global stability, as well as the presence of endemic equilibrium, were investigated. Numerical evidence was used to establish an analytical conclusion. It was seen that if the rate of treatment increased, the susceptible population rose while the infected, exposed, and treated populations all decreased. The limitations of the SEITR model is that it oversimplifies complicated disease processes while still being easily calculable. The SEITR model does take this parameter into account, however additional model extensions would be required.

2 Model Formation

In this study we proposed a new model SEITR by adding treatment T as fifth compartment to SEIR model to analyze the spread dynamics of epidemic Influenza in India. The total populace $N(t)$ at time t is separated into five different populaces , namely, Susceptible populace $S(t)$ at time t, Exposed populace $E(t)$ at time t, Infected inhabitants $I(t)$ at time t, Treatment populace $T(t)$ at time t, and Recovered populace $R(t)$ at time t. The susceptible $(S(t))$ populace are those who are at possibility to become infected by virus. The exposed $(E(t))$ populace are those who are infested by virus but not yet infectious that is not able to infect others. The infected populaces are those who

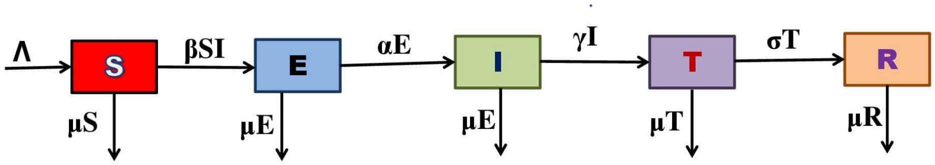

Figure 1: Schematic diagram of SEITR model

are diseased and able to infect others. The treatment populations are those who are infected and taking treatment in hospitals. The recovered populations are those who are recovered after treatment.
The flow diagram of influenza model was presented in fig1.

The susceptible human populace is created by the inflow rate of humans into the populace (at the rate $\wedge$) and the natural death rate μ. Therefore the incidence rate βSI incorporate the transmission frequency at which susceptible individuals becomes exposed and entered exposed populace without being infectious. Thus the rate of change of susceptible human populace is given by

$$\frac{dS}{dt} = \wedge - \beta SI - \mu S$$

The exposed human populace at the rate α be the exposed rate which exposed individuals becomes infected but not infectious and entered into infected populace and the natural death rate μ. Thus the rate of variation of exposed human populace is specified by

$$\frac{dE}{dt} = \beta SI - (\alpha + \mu)\, E$$

The infected human populace at the rate γ be the people are joined in hospital for treatment populace and the natural death rate μ. Thus the rate of variation of infected human populace is specified by

$$\frac{dI}{dt} = \alpha E - (\gamma + \mu)\, I$$

The treatment human populace at the rate σ be a rate at which the treatment individuals recovered and entered into recovered populace. Hence the rate of variation of treatment human populace is specified by

$$\frac{dT}{dt} = \gamma I - (\sigma + \mu)\, T$$

Finally, the rate of variation of recovered human populace is specified by

$$\frac{dR}{dt} = \sigma T - \mu R$$

By using all above assumptions, a nonlinear structure of five differential equations for

Table 1: Complete Description of relative parameters of the SEITR model

Parameter	Depiction
$\wedge$	inflow rate of susceptible individuals
μ	Normal death rate
β	Rate at which susceptible populace becomes exposed
α	Rate at which exposed populace becomes infected
γ	Rate at which infected populace getting treatment
σ	Rate at which treatment populace getting recovered

SEITR model is formed as follows

$$\begin{cases} \frac{dS}{dt} &= \wedge - \beta SI - \mu S \\ \frac{dE}{dt} &= \beta SI - (\alpha+\mu)E \\ \frac{dI}{dt} &= \alpha E - (\gamma+\mu)I \\ \frac{dT}{dt} &= \gamma I - (\sigma+\mu)T \\ \frac{dR}{dt} &= \sigma T - \mu R \end{cases} \tag{1}$$

Where the primary conditions $S(0) \geq 0$, $E(0) \geq 0$, $I(0) \geq 0$, $T(0) \geq 0$ and $R(0) \geq 0$. The total population $N(t) = S(t) + E(t) + I(t) + T(t) + R(t)$ will be assumed as constant.

3 Analysis of the SEITR model

In the segment, the elementary belongings of SEITR model 1 such as positivity and boundedness of the solution, basic reproduction number and stability analysis were discorsed.

3.1 Positivity and boundedness

Theorem 1. *All the solutions $(S(t), E(t), I(t), T(t), R(t)) \in R^5_+$ of the sturcture 1 with primary condition $S(t) \geq 0$, $E(t) \geq 0$, $I(t) \geq 0$, $T(t) \geq 0$, and $R(t) \geq 0$ are nonnegative and uniformly bounded for all $t \geq 0$.*

Proof 1. *Assume that $(S(t), E(t), I(t), T(t), R(t)) \in R^5_+$ is a solution of 1 for $t \in [0, t_0)$, where $t_0 > 0$.*
Through 1^{st} equation of system 1, we get

$$\frac{dS}{dt} = \wedge - \beta^* S^* I - \mu^* S \geq \wedge - \phi(t)^* S.$$

where $\phi(t) = \beta^* I + \mu$
After integration, we get

$$S(t) = S_0 \exp\left(-\int_0^t \phi(s)ds\right) + \wedge \exp\left(-\int_0^t \phi(s)ds\right) \int_0^t e^{\int_0^s \phi(u)du} ds \geq 0 \geq 0.$$

$\Rightarrow S(t) \geq 0$.
From the 2^{nd} equation of system 1, we develop

$$\frac{dE}{dt} = \beta SI - (\alpha+\mu) E \geq -(\alpha+\mu) E$$

Which leads

$$E(t) = E_0 \exp\left(-\int_0^t (\alpha+\mu)\, ds\right) \geq 0$$

$\Rightarrow E(t) \geq 0$

From the 3^{rd} *equation of system 1, we acquire*

$$\frac{dI}{dt} = \alpha E - (\gamma+\mu) \geq -(\gamma+\mu)\, I$$

Which leads

$$I(t) = I_0 \exp\left(-\int_0^t (\gamma+\mu)\, ds\right) \geq 0.$$

$\Rightarrow I(t) \geq 0$

Similarly 4^{th} *and* 5^{th} *equation of system 1*

$$\frac{dT}{dt} = \gamma I - (\sigma+\mu)\, T \geq -(\sigma+\mu)\, T$$

Which leads to

$$T(t) = T_0 \exp\left(-\int_0^t (\sigma+\mu)\right) ds \geq 0$$

$\Rightarrow T(t) \geq 0$

$$\frac{dR}{dt} = \sigma T - \mu R \geq -\mu R$$

which leads to

$$R(t) = R_0 \exp\left(-\int_0^t \mu ds\right) \geq 0$$

$\Rightarrow R(t) \geq 0$

Hence, the results (S, E, I, T, R) of 1 sustaining the primary conditions $S(t) \geq 0$, $E(t) \geq 0$, $I(t) \geq 0$, $T(t) \geq 0$, *and* $R(t) \geq 0$ *for all* $t \in [0, t_0)$ *are nonnegative in the section* $[0, t_0)$.

Now, we demonstrate that the boundedness of clarifications of system 1.

The positivity of the solutions indicates that

$\frac{dS}{dt} \leq \wedge - \mu S$

From the beyond equation, we can write that $\lim_{t\to\infty} \sup S \leq \frac{\wedge}{\mu}$ *and* $S \leq \frac{\wedge}{\mu}$.

Consider the total populations $N = S + E + I + T + R$.

On differentiation gives $\frac{dN}{dt} \leq \wedge - \mu N$ *which leads to* $\lim_{t\to\infty} \sup N \leq \frac{(\wedge)}{(\mu)}$.

Then, we get $N \leq \frac{\wedge}{\mu}$

$\Rightarrow S + E + I + T + R \leq \frac{\wedge}{\mu}$

Therefore all the solution curves (S, E, I, T, R) *sustaining by the primary conditions are consistently bounded in* R_+^5 *and in the section*

$\Omega = \left\{(S, E, I, T, R) \in R_+^5 : 0 \leq (S, E, I, T, R) \leq \frac{\wedge}{\mu}\right\}$.

3.2 Basic Reproduction Number

A crucial factor for communicable disease is the Basic Reproduction Number (R_0) which is distinct as the middling number of subordinate cases obtained by distinct primary case during the infectious dated in a susceptible populace. With R_0, the epidemic growth rate can be estimated and Stability of model will be analyzed [8]. R_0 Value can be determined through approach of Next Generation Matrix method [4], [13].

$R_0 = FV^{-1}$
Where

$$F = \begin{pmatrix} \beta + \mu \\ 0 \\ 0 \end{pmatrix}$$

and

$$V = \begin{pmatrix} (\alpha + \mu) E \\ \alpha E - (\gamma + \mu) I \\ \gamma I - (\sigma + \mu) T \end{pmatrix}$$

The Jacobian of F and V are dual matrices F and V which determined at an disinfection state $E = 0$, $I = 0$ and $T = 0$, we have

$$F = \begin{pmatrix} 0 & \beta & \mu \\ 0 & 0 & 0 \\ 0 & 0 & 0 \end{pmatrix}$$

and

$$V = \begin{pmatrix} (\alpha + \mu) & 0 & \\ \alpha & (\gamma + \mu) & 0 \\ 0 & -\gamma & (\sigma + \mu) \end{pmatrix}$$

FV^{-1} is $\frac{\beta\alpha}{(\alpha+\mu)(\gamma+\mu)} + \frac{\alpha\sigma\mu}{(\alpha+\mu)(\gamma+\mu)(\sigma+\mu)}$
Hence $R_0 = \frac{\beta\alpha}{(\alpha+\mu)(\gamma+\mu)} + \frac{\alpha\sigma\mu}{(\alpha+\mu)(\gamma+\mu)(\sigma+\mu)}$

3.3 Local Stability of Disease Free Equilibrium

Theorem 2. *For $R_0 < 1$, the Disease-Free Equilibrium point $E_0 = (\frac{\triangle}{\mu}, 0, 0, 0, 0)$ was locally asymptotically stable and for $R_0 > 1$, it was unstable [17].*

Proof 2. *The Jacobian matrix corresponding to the structure 1 at disease free equilibrium E_0 is*

$$J(E_0) = \begin{pmatrix} -\mu & 0 & -\beta & 0 & 0 \\ 0 & -(\mu + \alpha) & \beta & 0 & 0 \\ 0 & \alpha & -(\gamma + \mu) & 0 & 0 \\ 0 & 0 & \gamma & -(\sigma + \mu) & 0 \\ 0 & 0 & 0 & \sigma & -\mu \end{pmatrix}$$

The characteristic equation is

$$(\lambda + \mu)^2 (\lambda + (\sigma + \mu)) (\lambda^2 + a_1\lambda + a_2) = 0$$

Where $a_1 = 2\mu + \alpha + \gamma$ and $a_2 = (\mu + \alpha)(\gamma + \mu) - \alpha\beta$.
There are 5 Eigen values for the Jacobian matrix $J(E_0)$ of which first three are -μ, -μ, -$(\sigma + \mu)$, and the remaining two Eigen values are roots of quadratic equation $(\lambda_2 + a_1\lambda + a_2)$ = 0, which are negative.
Through Routh-Hurwitz criterion [20], all the roots of charateristics equation have destructive real part which revenues steady equilibrium if $a_1 > 0$ and $a_2 > 0$.
Since $\mu > 0$, $\alpha > 0$ and $\gamma > 0$, we have $2\mu + \alpha + \gamma > 0$ that is $a_1 > 0$.
Since $(\mu + \alpha)(\gamma + \mu) - \alpha\beta > 0 > 0$ that is $a_2 > 0$.
If $R_0 < 1$, then

$$\frac{\beta\alpha}{(\alpha + \mu)(\gamma + \mu)} + \frac{\alpha\sigma\mu}{(\alpha + \mu)(\gamma + \mu)(\sigma + \mu)(\alpha + \mu)} < 1$$

$$\Rightarrow \frac{\beta\alpha}{(\alpha+\mu)} < \frac{\beta\alpha}{(\alpha+\mu)(\gamma+\mu)} + \frac{\alpha\sigma\mu}{(\alpha+\mu)(\gamma+\mu)(\sigma+\mu)(\alpha+\mu)} < 1$$

$$\Rightarrow \frac{\beta\alpha}{(\alpha+\mu)(\gamma+\mu)} < 1 \Rightarrow \beta\alpha < (\alpha+\mu)(\gamma+\mu)$$

$$\Rightarrow (\mu+\alpha)(\gamma+\mu) - \alpha\beta > 0 thatis a_2 > 0.$$

Therefore, $a_2 > 0$ *if* $R_0 < 1$
Hence by Routh–Hurwitz Criteria, the disease free equilibrium point E_0 *is locally asymptotically stable if* $R_0 < 1$.

3.4 Global Stability of Disease Free Equilibrium

Theorem 3. *The disease-free equilibrium point* $E_0 = (\frac{\triangle}{\mu}, 0, 0, 0, 0)$ *of structure 1 was globally asymptotic stable if* $R_0 < 1$ *[19].*

Proof 3. *It can be detected that from the structure (1), the disease-free sections are S, R and the infected sections are E, I, T. The system of equations (1) will be arranged as*

$$\frac{dU}{dt} = P(U,V), \frac{dV}{dt} = G(U,V), \text{ and } G(U,0) = 0 \tag{2}$$

where $U = (S,R) \in R_+^2$, $V = (A,I,Q,J) \in R_+^3$.
By using the technique introduced by Castillo-Chavez [5], we derived global stability of the disease-free equilibrium point $E_0 = (\frac{\triangle}{\mu}, 0, 0, 0, 0)$. *For the worldwide asymptotic stability of* E_0 *the succeeding two conditions should be satisfied.*
1. $\frac{dU}{dt} = P(U,0)$ *Where* X^* *is world wide asymptotically steady.*
2. $G(U,V) = KV - \hat{G}(U,V)$, $\hat{G}(U,V) \geq 0$, *where* $K = D_V G(U^*,0)$ *is the Metzler Matrix and* $(X,Y) \in \omega$.
If the given system of equations 1 satisfies 2 then the equilibrium point E_0 *is a global asymptotically stable for* $R_0 < 1$.
Hence, the system 1 can be rewritten as

$$P(U,0) = \begin{pmatrix} \wedge - \mu S \\ 0 \end{pmatrix}, K = \begin{pmatrix} (\alpha+\mu) & 0 & 0 \\ \alpha & (\gamma+\mu) & 0 \\ 0 & \gamma & (\sigma+\mu) \end{pmatrix} \text{ and}$$

$$\hat{G}(U,V) = \begin{pmatrix} \beta I (S_0 - S) \\ 0 \\ 0 \end{pmatrix}$$

Since $S_0 > S$, *by observation,* $\hat{G}((U,V)) \geq 0$ $(U,V) \in \Omega$.
We can say that the matrix K is M matrix by the definition of M and also we able to find that $X^* = (\frac{\triangle}{\mu}, 0)$ *is globally asymptotic stable steady state of the limiting structure* $\frac{dU}{dt} = P(U,0)$.
Since the two conditions are fulfilled, disease-free steady state $E_0 = (\frac{\triangle}{\mu}, 0, 0, 0, 0)$ *of structure of equations 1 is globally asymptotic stable if* $R_0 < 1$.

3.5 Local Stability of Endemic Equilibrium point

We conclude the endemic steady state $X^* = (S^* E^*, I^*, T^*, R^*)$ with their possibility conditions are

$$\begin{aligned}
S^* = &\quad \frac{\wedge}{\beta I^* + \mu}, \\
E^* = &\quad \frac{\beta S^* I^*}{(\alpha+\mu)}, \\
T^* = &\quad \frac{\gamma I^*}{(\alpha+\mu)}, \\
R^* = &\quad \frac{\sigma T^*}{\mu}, \\
I^* = &\quad \frac{(\wedge\alpha\beta-\mu(\gamma+\mu))}{(\beta(\gamma+\mu(\sigma+\mu)))} = \frac{(\wedge(R_0-1)-\alpha\sigma\mu)}{(\beta(\gamma+\mu)(\sigma+\mu))}
\end{aligned}$$

Theorem 4. *When $R_0 > 1$,then Endemic Equilibrium point X^* is locally asymptotically steady and unstable if $R_0 < 1$.*

Proof 4. *The Jacobian matrix corresponding to the system 1 at endemic equilibrium point X^* is*

$$J(X^*) = \begin{pmatrix} (-\beta I^* + \mu) & 0 & -\beta S^* & 0 & 0 \\ \beta I^* & -(\mu+\alpha) & \beta S^* & 0 & 0 \\ 0 & \alpha & -(\gamma+\mu) & 0 & 0 \\ 0 & 0 & \gamma & -(\sigma+\mu) & 0 \\ 0 & 0 & 0 & \sigma & -\mu \end{pmatrix}$$

The characteristic equation is

$$(\gamma+\mu)(\gamma+(\sigma+\mu))\left(\lambda^3 + b_1\lambda^2 + b_2\lambda + b_3\right) = 0$$

Where $b_1 = \beta I^* + 3\mu + \alpha + \gamma$,
$b_2 = (\alpha+\mu)(\gamma+\mu) - \alpha\beta S^* + (\gamma+\mu)(\beta I^* + \mu)$ *and*
$b_3 = (\beta I^* + \mu)((\alpha+\mu)(\gamma+\mu) - \alpha\beta S^*) - \beta^2 S^* I^*$
Hence the first two Eigen values are – μ,-$(\sigma+\mu)$ and remaining three Eigen values are the roots of the $\left(\lambda^3 + b_1\lambda^2 + b_2\lambda + b_3\right) = 0$.
Yet over again if the constants of specific equation $a_1 > 0$, $a_2 > 0$, $a_3 > 0$ and $a_1 a_2 > a_3$ are true, formerly by Routh-Hurwitz criterion, altogether the roots of the specific equation have negative real portions and hence a stable equilibrium. Therefore Endemic equilibrium at X^* is locally asymptotically stable if $R_0 > 1$

4 Numerical Simulation

Numerical simulation was performed in order to establish analytical result. We assumed some parameter values and initial conditions of proposed $SEITR$ model and it can be shown table 2.

4.1 Analysis of results

The basic reproduction number for this set of limitation is $R_0 = 2.806$. The dynamical performance of the system will be observed in 2 with the help of MATLAB programming. From Fig. 2, we observed that the dynamics behavior of susceptible, exposed, Infected, treatment and recovered classes. This graph demonstrated that when the treatment rate rose, the infected population decreased and joined either the treatment population or the recovered population.

4.2 Discussion of results

From Fig.3 it was observed that the infected population(Fig.3b), exposed population(Fig.3c) and treatment population(Fig.3d) were decreased while the susceptible population(Fig.3a) was increased whenever the treatment rate increases.

Table 2: Influenza parameters values of the SEITR model

Parameter	Values	Source
β	1.2	[16],[30]
α	0.2	[9],[30]
γ	0.4	[16],[30]
σ	0.1	[16],[30]
μ	0.01	[26],[29]
$S(0)$	1	Assumed
$E(0)$	0.2	Assumed
$I(0)$	0.01	Assumed
$T(0)$	0.4	Assumed
$R(0)$	0.3	Assumed

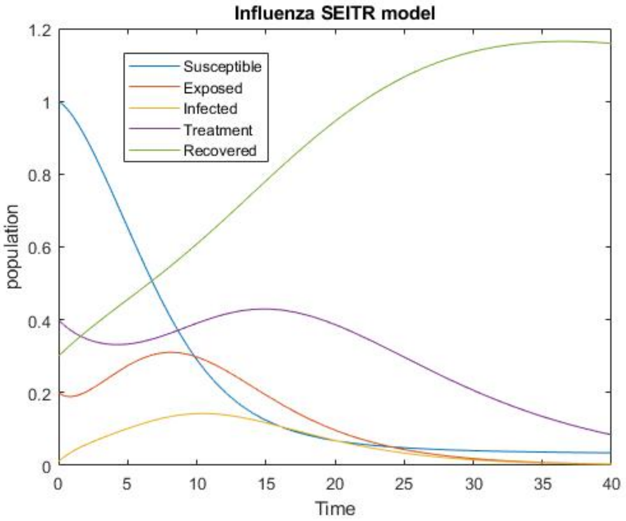

Figure 2: Dynamic behavior various compartments of SEITR model

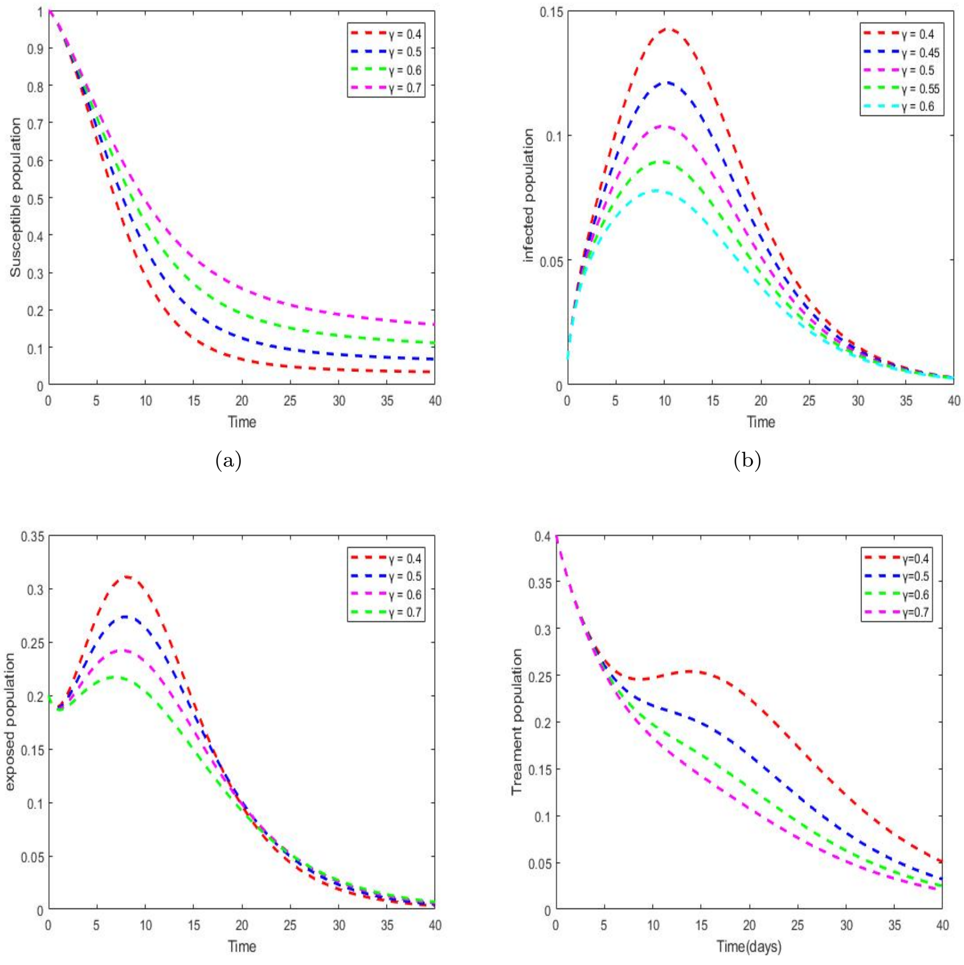

(a)

(b)

(c)

(d)

Figure 3: Effect of treatment rate γ on susceptible, exposed, Infected and treatment population

5 CONCLUSION

The epidemiological models are enabled us a noble knowledge to understanding the spread dynamics of infectious disease in better way. In this article, a five compartment epidemiological model SEITR was proposed and the basic properties were discussed. The basic reproduction number R_0 value was determined. The positivity and uniform boundedness were performed. The existence of disease free equilibrium point E_0 was discussed and showed that it is locally also globally asymptotically stable for $R_0 < 1$. Similarly the endemic equilibrium point X^* be real and local asymptotically stable for $R_0 > 1$. The transmission dynamics of influenza has been observed. The result of treatment rate on the susceptible, exposed, infected and treatment populaces has been examined and it has a positive effect on the infected population. The reproduction number $R_0 = 2.806 > 1$ indicates that the outbreak has gotten out of hand and that there are currently more sick people than ever before. Therefore, the only method to reduce the rate of illness spread is to enhance the rate of treatment, which includes the quick hospitalisation of infections that are dangerously ill. The outcome of the SEITR model on the disease program mechanism can be investigated in next studies. Additionally, future research can be done to ascertain the most effective management strategies for the sickness spread model and the belongings of medications and immunizations on the SEITR model.

References

[1] Anderson. R. M. and May R. M., Infectious Diseases of Humans: Dynamics and Control, Oxford University Press, Oxford, 1991.

[2] Andreasen. V, Lin. J and Levin. S.A, The dynamics of co circulating influenza strains conferring partial cross-immunity. J. Math. Biol., 35, 825-842, 1997.

[3] Attiq ul Rehman, Ram singh, Jagdev Singh, Mathematical analysis of multi-compartmental malaria transmission model with reinfection Chaos, Solitons and Fractals, 163, 2022.

[4] Baojun S. Compute using next generation operator. mtbi, Department of Mathematical Sciences Montclair State University, 12-14, 2013.

[5] Casagrandi. R, Bolzoni. L, Levin. S. A and Andreasen. V, The sirc model and influenza . Math. Biosci. (200) 152-169, 2006.

[6] Chinviriyasit. W, Numerical modelling of the transmission dynamics of influenza, ORSC & APORC, 52-59, 2007.

[7] Coburn. B. J, Wagner B. G. and Blower S., Modeling influenza epidemics and pandemics: insights into the future of swine flu (H1N1), BMC Med, 7(30), 2009.

[8] Dickmann O. and Heeserbeek J. A. P., Mathematical Epidemiology of Infectious Disease: Model Building Analysis and Interpretation, John Wiley, New York, 2000.

[9] Douglas. R, Influenza in man, in: E. Kilbourne (Ed.), The Influenza Viruses and Influenza, Academic Press, New York, USA, 395, 1975.

[10] Earn. D.J.D., Dushoff J. and Levin S.A, Ecology and evolution of the flu, Trends Ecol. Evol., (17) 334-340, 2002.

[11] Eccles. R., Understanding the symptoms of the common cold and influenza, The lancet infectious diseases Vol.5, No.11, 718-25, November 2005.

[12] Gu. Y., Komiya N., Kamiya H., Yasui Y., Taniguchi K., Okabe N., Pandemic A(H1N1) transmission during pre-symptomatic phase, Japan, Emerging infectious diseases, 17(9), September 2011.

[13] Heffernan J.M., Smith R.J. and Wahl L.M, Perspectives on the basic reproductive ratio, Journal of the Royal Society Interface, 2: 281-298, 2005.

[14] Herbert. W. Hethcote, Three basic epidemiological models, Springer - Verlag, NY, 1989.

[15] Hethcote. H.W, The mathematics of infectious diseases, siam rev., 42 599-653, 2000.

[16] Islam, R., Biswas, M. H. A., & Jamali, A. J. U. Mathematical Analysis of Epidemiological Model of Influenza a (H1N1) Virus Transmission Dynamics in Perspective of Bangladesh, GANIT: Journal of Bangladesh Mathematical Society, 37, 39-50, 2018. https://doi.org/10.3329/ganit.v37i0.35724.

[17] Jagdev Singh and Arpita Gupta, Computational analysis of fractional modified Degasperis - Procesi equation with Caputo-Katugampola derivative, AIMS Mathematics, 8(1):194-212, 2022.

[18] Jagdev Singh, Behzad Ganbari, Devendra Kumar, Dumitru Baleanu, Analysis of fractional model of guava for biological pest control with memory effect, Journal of Advanced Research, 32:99-108, 2021.

[19] Jagdev Singh, Devendra Kumar, Dumitru Baleanu, A new analysis of fractional fish farm model associated with Mittag-Leffler type kernel, International Journal of Biomathematics 13(2), 2020.

[20] Jongeun Choi, Lecture on Routh-Hurwitz Stability Criterion, Michigan State University.

[21] Kermack. W. O .and McKendrick A. G, A contribution to the mathematical theory of epidemics, Proc. Roy SocLond, 1927.

[22] Mishra O P, Mishra D K, Spread and control of influenza in two groups: a model, Applied Mathematics and Computation, April,219 (15):7982-7996, 2013.

[23] Murray. E., Alexander M.E., Seyed M., Moghadas S.M., Gergely R. and Jianhong W, A delay differential model for pandemic influenza with antiviral treatment, bull."Math. Biol. 70, 382-396, 2008.

[24] Quirouette C, Younis NP, Reddy MB, Beauchemin CAA (2020) Correction: A mathematical model describing the localization and spread of influenza A virus infection within the human respiratory tract. PLOS Computational Biology 16(11): e1008424. https://doi.org/10.1371/journal.pcbi.1008424

[25] Samuel Abubakar, Bifurcation analysis on the mathematical model of measles disease dynamics, UJAM, 212-216, 2013.

[26] Sanchez Y.G., Sabir Z., Guirao J.L.G. Design of a nonlinear SITR fractal model based on the dynamics of a novel coronavirus (covid -19) Fractals,28(8), 2020.

[27] Srivastav A K, Ghosh M, Analysis of a simple influenza (H1N1) model with optimal control, World Journal of Modelling and Simulation 12(4):307-319, 2016.

[28] Supriya yadav, Devendra Kumar, Jagdev Singh, Dumitru Baleanu, Analysis and Dynamics of Fractional Order Covid-19 Model with Memory Effect, Results in Physics, 24, 2021.

[29] Umar. M, Z. Sabir, M.A.Z. Raja, M. Shoaib, M. Gupta, Y.G. Sánchez, A stochastic intelligent computing with neuro-evolution heuristics for nonlinear SITR system of novel Covid-19, dynamics, Symmetry, 12(10),2020.

[30] Vinod Kumar Bais, and Deepak Kumar, SITR Dynamical Model for Influenza, International Journal of Engineering Technology Science and Research IJETSR,2,2015.

[31] ZhilanFeng, Final and peak epidemic sizes for SEIR models with quarantine and isolation, Mathematical Biosciences and Engineering, 4(4), 2007.

J. COMPUTATIONAL ANALYSIS AND APPLICATIONS, VOL. 31, NO. 2, 2023, COPYRIGHT 2023 EUDOXUS PRESS, LLC

MHD Stagnation Point Flow and Heat Transfer of a Nanofluid Over a Stretching Sheet Fixed in Porous Medium with Effect of Thermal Radiation, Joule Heating and Heat Source/Sink

Ravindra Kumar[1] *Ruchika Mehta*[1*], *Tripti Mehta*[2] *and Sushila*[3]
[1]*Department of Mathematics and Statistics*,
Manipal University Jaipur, Jaipur(Raj.), India
[1]*Department of Mathematics*,
Vivekananda Global University, Jaipur(Raj.), India
[2]*Department of Mathematics*,
S. S. Jain Subodh P. G. College, Jaipur(Raj.), India
[3]*Department of Physics*,
Vivekananda Global University, Jaipur(Raj.), India
ruchika.mehta1981@gmail.com

Abstract

The goal of this research is to see how thermal radiation, joule heating, and heat Source/Sink affect two-dimensional nanofluid stagnation point flow above a stretching sheet fixed in a spongy medium. This research accounts for the magnetic field, and the nonlinear Rosseland approximation is used to calculate heat radiation. The governing equations are converted into a system via similarity transformations in joined nonlinear ordinary differential equations, which are solved numerically using the Runge-Kutta fourth order approach with shooting technique. The numerical results reveal that this method has excellent correctness, good convergence with minimal computational cost, and a lot of promise. The velocity and temperature are also found to increase as a function of the radiation parameter, Eckert number, Brownian motion parameter, Thermophoresis parameter, Biot Number, and thermal buoyancy parameter, as well as the reverse effect in Prandtl numeral. The skin friction, local Nusselt number, and local Sherwood number are increasing functions of the ratio of free stream velocity to stretching sheet velocity parameter, Biot number, Brownian motion parameter, and thermophoresis parameter, with the reverse effect in magnetic parameter, Prandtl number, and permeability parameter.

Keywords: Nanofluid, Stretching Sheet, thermal radiation, joule heating, heat Source/Sink.

1 Introduction:

Nanofluid is a base fluid containing nanometer-sized particles/fibers (water, oil, ethylene glycol, etc.).Al_2O_3, Cu, T_iO_2, Ag, and other materials are commonly utilized for nanoparticles. These liquid combinations were discovered to have excellent assets that could make them useful in a variety of technical and manufacturing applications involving temperature transmission, nuclear reactors, petroleum cells, microelectronics, power production and carrying, space expertise, security and ships, and bony film solar power collectors are only few of the technologies that are being developed. [5] deals with (MHD) nanofluid stream towards a nonlinear extended plane with changeable depth in the company of an electric ground. In the existence of thermal radiation and Joule heating impacts, buoyant MHD nanofluid flow and heat transmission over a stretching sheet are examined [7]. [12] examined the impacts of thermally evolved thermophoresis diffusion and Brownian motion in non-Newtonian nanofluids across an angled extending sheet, as well as the belongings of hotness radiation and chemical response. [14]The influence of thermal radiation on a heat absorbing magneto-viscous nanofluid's dissipative boundary layer flow transversely a holey exponentially overextended pane with thermal slips and Navier's velocity was investigated. When there is a consistent magnetic field present. [15] Entropy generation study of a two-way nanofluid flick stream of Eyringâ€“Powell liquid with warmth and mass transport through an unstable porous stretched sheet was investigated (MHD). [21] The belongings of a magnetic ground and heat rays on the compelled convection stream of CuO-water nano-fluid transversely a stretched pane with a point of stagnation were statistically investigated. The effects of heat radiation on the heat transfer of water-based nanofluids containing exponentially stretched sheets of motile gyrotactic microorganisms were studied by [24]. [26] The authors presented a Form in mathematics for MHD radiative stream of III-grade nanomaterials limited by a nonlinear extending sheet of flexible thickness. [29] investigated the formation of entropy in a II-grade nanofluid MHD stream finished a sheet that is being heated convectively and using nonlinear current radioactivity and viscid .Numerous slip properties on MHD unsteady Maxwell nanofluid stream finished a holey overextended pane with thermal radioactivity and thermo-diffusion in the attendance of chemical response were examined by [1]. In the presence of thermal radiation and a heat source, a 2-way MHD stream of a Jeffery nanofluid transversely a stretched sheet has been quantitatively examined by [2]. In a 2-dimensional accepted convection stream of unstable electrical nanofluid with MHD across a linearly leaky stretched pane, the belongings of suction, as well as current radioactivity, and Joule heating, are investigated by [4]. [18] looked explored the influence of numerous slipups on axisymmetric (MHD) buoyant nano-fluid stream across an extending sheet.[20] The stream of a nanofluid with changeable liquid characteristics done an angled overextended pane in the existence of current energy and chemical response is investigated using unsteady magnetohydrodynamics (MHD). The impact of slip circumstances on the two-way unsteady varied convection stream of electric MHD nanofluid over a stretched sheet in the company of thermal energy, gluey debauchery, and chemical response are the subject of this research. [4]. The effect of nonlinear thermal radiation and spatial and temperature dependent heat generation/absorption on a 3- way MHD Jeffrey liquid stream across a nonlinearly With porous material present, a permeable stretched sheet was investigated. [10]. The current and Joule boiler effect of Casson nanofluid stream with chemical response across an inclined porous stretched surface is investigated in [11]. The effects of buoyancy force on viscoelastic (second grade fluid) magnetized nanofluid were studied by [13]. [19] using a stretched sheet immersed in a porous media generated by suction/blowing, researchers explored the belongings of viscous-Joule boiler, current energy, and warmth production (or absorption) on MHD nanofluid flow. [28] used the power of numerical computing-based Lobatto IIIA method to investigate warmth and mass transmission in 3-D MHD radioactive current of water-based mixture nanofluid across an extended sheet. [30] investigated the three-dimensional border coating stream of Maxwell nanofluid across a extending sheet using magnetohydrodynamic (MHD) warmth and mass transmission. [31] An unsteady magneto-hydrodynamic heat and mass transfer model is used to investigate the heat and mass transfer of a hybrid nanofluid flow across a stretched

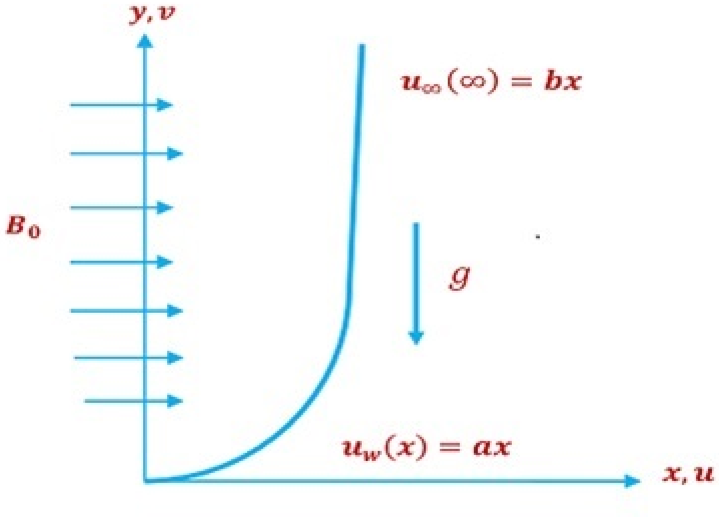

Figure 1: Schematic diagram of the Problem

surface. [32] investigated the heat and mass transfer characteristics of nanofluid flow over a stretched surface embedded in a porous medium in both steady and unsteady cases. [9] examined the effects of solar waves on 2-dimensional a stretched sheet is traversed by nanofluid stagnation-point flow. [16] looked at the heat transport and entropy of an unsteady flow of a non-Newtonian Casson nanofluid. [17] studied for magnetic dipole with stagnation point flow of micropolar nanofluids. [23] warmth and mass transport across a linear extending pane, as well as the essence of nonlinear thermal rays and entropy production for continuous laminar 2-way convective MHD Jeffrey nanofluid stream, were examined. [25]. The effects of convective boundary conditions on MHD Prandtl nanofluid flow over a stretched sheet were investigated.[3]considered the rheological and thermophysical characteristics of a non-Newtonian viscoelastic liquid under stratification over a linearly stretched surface.[27]This pagination's main goal is to outline characteristics of a water-based hybrid nanoliquid flow with single-wall carbon nanotube dispersion.

2 Construction of the Problem:

A steady nanofluid boundary layer flow in two dimensions through an extending sheet is using the speed of $u_w(x) = ax$ wherever a is a constant, as illustrated in Fig.1. A homogenous attractive arena of B_0 upright to the flow direction is supposed to be influenced. Warmth transmission scrutiny is done in the company of viscous dissipation and Joule heating and thermal energy qualities.T_w denotes the convective surface temperature which are based on Fig.1 and T_∞ symbolizes the ambient fluid temperature in the following governing equations. For this nano-fluid flow, the stable border line coat equations for stagnation point flow that is in-compressible:

$$\frac{\partial u}{\partial x} + \frac{\partial v}{\partial y} = 0, \tag{1}$$

$$u\frac{\partial u}{\partial x} + v\frac{\partial u}{\partial y} = u_\infty\frac{\partial u_\infty}{\partial x} + \nu\frac{\partial^2 u}{\partial y^2} - \frac{\sigma {B_0}^2(u - u_\infty)}{\rho} - \frac{\nu}{k}(u - u_\infty) \\ +g\beta_T(T - T_\infty) + g\beta_C(C - C_{\infty)}, \tag{2}$$

Where u_∞ is the free stream velocity, ν means the kinematic viscocity, σ expressions forelectric conduction of liquid, B_0 establishes the unvarying magnetic arena along y-direction, k is used for porosity factor, u and v, respectively, stand for the x- and y-directional velocity components. We have the following border circumstances for the problem under consideration:

$$u = u_w(x) = ax, v = 0, at\ y = 0, and\ u \to u(\infty) = bx, \quad as\ y \to \infty \tag{3}$$

The dimensionless variables are introduced in the form of

$$\eta = \sqrt{\frac{a}{\nu}}y\ , u = \frac{\partial \psi}{\partial y} = axf'(\eta)\ , v = -\frac{\partial \psi}{\partial x} = axf(\eta) \tag{4}$$

Eq. (1) is satisfied in the same way, and Eqs. (2) and (3) can be rewritten as

$$f^{'''} + ff^{''} - f^{'^2} - \ (M + K)(f^{'} - \lambda) + \lambda^2 + \lambda_1\theta + \lambda_2\phi = 0, \tag{5}$$

$$f(0) = 0,\ f^{'}(0) = 1,\ when\ \eta = 0\ and\ f^{'}(\infty) = \lambda,\ as\ \eta \to \infty, \tag{6}$$

where $M = \frac{(\sigma {B_0}^2)}{\rho a}$,is the magnetic restriction, $\lambda = \frac{b}{a}$, represents the share of the rates of unrestricted stream speed to the extending sheet speed, $K = \frac{\nu}{ka}$ is the permeability parameter $\lambda_1 = \frac{G_r}{R_e^2}$ is the thermal buoyancy parameter, where $G_r = g\beta_T(T_w - T_\infty)\frac{x^3}{\nu^2}$ is Grashof numeral, and $Re = \frac{(xU_w)}{\nu}$ is Reynolds number, $\lambda_2 = g\beta_C(C_w - C_\infty)\frac{x^3}{\nu^2}$ is the concentration buoyancy parameter.
Equation of Energy

$$\begin{aligned} u\frac{\partial T}{\partial x} + v\frac{\partial T}{\partial y} = \alpha\frac{\partial^2 T}{\partial y^2} + \frac{\nu}{C_p}(\frac{\partial u}{\partial y})^2 - \frac{1}{\rho c_p}\frac{\partial q_r}{\partial y} + \frac{\sigma {B_0}^2(u - u_\infty)^2}{\rho c_p} \\ + \tau(D_b\frac{\partial T}{\partial y}\frac{\partial C}{\partial y} + \frac{D_T}{T_\infty}(\frac{\partial T}{\partial y})^2) + \frac{Q^*(T - T_\infty)}{\rho c_p} \end{aligned} \tag{7}$$

Equation of Concentration

$$u\frac{\partial C}{\partial x} + v\frac{\partial C}{\partial y} = D_b\frac{\partial^2 C}{\partial y^2} + \frac{D_T}{T_\infty}(\frac{\partial T}{\partial y})^2 \tag{8}$$

where T symbolizes the temperature, C symbolizes the nanoparticles concentration, α is the current diffusivity, D_b and D_T are the Brownian motion coefficient and the thermophoretic dispersal coefficient, correspondingly. $\tau = \frac{(\rho p)_p}{(\rho p)_f}$ is the share of the nanoparticle active warmth size to the base fluid warmth size and q_r states to the radiative warmth flux amount. The radiative heat flux can be calculated using the Rosseland guess for current radiation and applied to optically thick medium as. $q_r = -\frac{4}{3}\frac{\sigma^*}{K^*}\frac{\partial T^4}{\partial y}$ where σ^*, k^* are the Stefan-Boltzman constant and average assimilation coefficient, correspondingly. $T^4 = 4T{T_\infty}^3 - 3T_\infty^4$ is achieved by utilising the Taylor series to expand $T^4$with respect to T_∞while disregarding terms of higher orders. As a result, Eq. (7) is found to be

$$\begin{aligned} u\frac{\partial T}{\partial x} + v\frac{\partial T}{\partial y} = \alpha\frac{\partial^2 T}{\partial y^2} + \frac{\nu}{C_p}(\frac{\partial u}{\partial y})^2 + \frac{16\sigma^* T_\infty^3}{3\rho C_p k^*}\frac{\partial^2 T}{\partial y^2} + \frac{\sigma {B_0}^2(u - u_\infty)^2}{\rho c_p} \\ + \tau(D_b\frac{\partial T}{\partial y}\frac{\partial C}{\partial y} + \frac{D_T}{T_\infty}(\frac{\partial T}{\partial y})^2) + \frac{Q^*(T - T_\infty)}{\rho c_p} \end{aligned} \tag{9}$$

For radiative heat flux modelling, the nonlinear Rosseland guess is used. As an outcome, the relevant convective warmth transport boundary conditions can be presented as.

$$-k\frac{\partial T}{\partial y} = (T - T_W), C = C_w, at\ y = 0, T \to T_\infty,\ C \to C_\infty, as\ \ y \to \infty \tag{10}$$

As a result of specifying the non-dimensional temperature $T = T_\infty + (T_w - T_\infty)\theta(\eta)$ and $C = C_\infty + (C_w - C_\infty)\phi(\eta)$. Eqs. (7) and (8) take the following format:

$$(1 + R_a)\theta^{''} + P_r[f\theta^{'} + ME_c(f^{'} - \lambda)^2 + E_c(f^{''})^2 + (N_b\theta^{'}\phi^{'} + N_t\theta^{'^2}) + \delta\theta\ ] = 0 \tag{11}$$

$$\phi^{''} + L_e f\phi^{'} + \frac{N_t}{N_b}\theta^{''} = 0, \tag{12}$$

and the borderline circumstances

$$\theta^{'}(0) = -(1 - \theta(0))Bi, \phi(0) = 1, \theta(+\infty) \to 0, \phi(+\infty) \to (0), \tag{13}$$

Where $P_r = \frac{\nu}{\alpha}$, is Prandtl number, $R_a = \frac{16\sigma^* T_\infty^3}{3kk^*}$, is radiation parameter, $E_c = \frac{U_w^2}{C_p(T_w - T_\infty)}$, is the Eckert number, $N_b = \frac{\tau D_b(C_W - C_\infty)}{\nu}$,shows the Brownian motion restriction, $N_t = \frac{\tau D_T(T_W - T_\infty)}{\nu T_\infty}$, is thermophoresis restriction,$\delta = \frac{Q^* L}{\rho C_p U_w}$, heat source/sink restriction, $L_e = \dfrac{\nu}{D_b}$, Lewis factor, $Bi = \dfrac{h}{k}\sqrt{\frac{\nu}{a}}$, denotes the Biot number. The three physical measures of our attention are the coefficient of skin friction C_{f_x}, the local Nusselt numberN_{u_x}, and local Sherwood number S_{u_x}, are given as.

$$C_{f_x} = \frac{\tau_w}{\rho U_w^2}, N_{u_x} = \frac{xq_w}{k(T_w - T_\infty)}, S_{u_x} = \frac{xq_m}{D_b(C_w - C_\infty)}, \tag{14}$$

where

$$\tau_w = \mu(\frac{\partial u}{\partial y})_{y=0}, q_w = -k(\frac{\partial T}{\partial y})_{y=0} + (q_r)_{y=0}, q_m = -D_b(\frac{\partial C}{\partial y})_{y=0}, \tag{15}$$

the relations will be.

$$C_{f_x}(R_e)^{\frac{1}{2}} = f^{''}(0),\ N_{u_x}(R_e)^{\frac{-1}{2}} = -(1 + R_a)\theta'(0), S_{u_x}(R_e)^{\frac{1}{2}} = -\phi^{'}(0), \tag{16}$$

The result of equations (4), (11) and (12) jointly through borderline circumstances (5) and (13) is determine through by a systematic numerical method called shooting technique. We translate the nonlinear equivalences into first order regular differential equivalences by labelling the variable quantity i.e.

$f = f_1$, $f^{'} = f_2$, $f^{''} = f_3$, $f^{'''} = f_3^{'}$, $\theta = f_4$, $\theta^{'} = f_5$, $\theta^{''} = f_5'$, $\phi = f_6$,

$\phi^{'} = f_7$, $\phi^{''} = f_7^{'}$, Hence, the system of equations becomes

$$f_1^{'} = f_2, f_2^{'} = f_3, f_3^{'} = [f_2^2 - f_1 f_3 + (M + K)(f_2 - \lambda) - \lambda^2 - \lambda_1 f_4 - \lambda_1 f_6] \tag{17}$$

$$f_4^{'} = f_5, \tag{18}$$

$$f_5^{'} = -(1 + R_a)^{-1} P_r[f_1 f_5 + ME_c(f_2 - \lambda)^2 + E_c f_3^2 + N_b f_5 f_7 + N_t f_5^2 + \delta f_4] \tag{19}$$

$$f_6^{'} = f_7, \tag{20}$$

$$f_7^{'} = -(l_e f_1 f_5 + \frac{N_t}{N_b} f_5^{'}), \tag{21}$$

Subject to the following conditions

$$\begin{gathered} f_1(0) = 0, f_2(0) = 1, f_3(0) = S_1, f_4(0) = (1 + \frac{S_2}{B_i}), f_5(0) = S_2, f_6(0) = 1, \\ f_7(0) = S_3,\ as\ \eta \to 0\ and\ f_2(\infty) = \lambda, f_4(\infty) = 0, f_6(\infty) = 0,\ as\ \eta \to \infty \end{gathered} \tag{22}$$

Now fourth order Runge-Kutta way with shooting technique is follow for stepwise integration and calculations are passed out on MATLAB computer software.

3 Influence of Diverse Restrictions

Ordinary differential equations that are nonlinear. (4), (11) and (12) are numerically solved with the borderline circumstances (5) and (13) using the MATLAB software and the shooting and fourth-order Runga-Kutta method. The obtained results demonstrate the impact of non-dimensional controlling parameters, specifically the magnetic field parameter M, Prandtl numeral P_r, radiation restriction R_a, the proportion of the free stream speed to the extending sheet speed restriction λ, Eckert numeral E_c, Thermophoresis restriction N_t, Brownian motion restriction N_b, Biot Numeral B_i, Lewis factor L_e, Permeability restriction K, thermal buoyancy parameter λ_1, Solutal buoyancy parameter λ_2 and Heat Source/Sink δ. Figures 2 and 3 depict the effect of the magnetic field restriction M on the velocity and temperature field distributions.It's worth noting that when M gets higher, the velocity field gets smaller. A resistive sort of force termed Lorentz force is created in the stream when the magnetic field parameter increases, causing a decrease in velocity field curves. It has been pragmatic that an enhance in magnetic parameters raises the temperature. The Lorentz force causes some additional warmth to be created in the flow. When the magnetic field is increased, the momentum layer thickness decreases while the thermal layer thickness increases. The impact of Prandtl number P_r on the supply of speed and temperature ground is exposed in Fig.4 and 5. It is perceived that growing values of P_r results a decline in velocity and temperature field. Figure 6 and 7 exhibits the significance of the radiation parameter R_a on the velocity and temperature, correspondingly. Figures 6 and 7 show that increasing the radiation parameter increases fluid velocity and temperature. The impact of proportion of the free stream speed to the speed of the extending sheet restriction λ on temperature arena is exposed in Fig.9. escalating values of Λ results a decrement in temperature field. The impact of Eckert number E_c, Brownian motion parameter N_b, Thermophoresis parameter N_t, Biot Numeral B_i on the sharing of speed and warmth field is exposed in Fig. 10, 11, 12, 13, 14, 15 16 and 17It has been observed that rising values of E_c, N_b, N_t and B_i results increment in velocity and temperature field.

4 Conclusions

The influence of thermal radiation, Heat Source/Sink, and joule heating on two-dimensional nanofluid stagnation point stream across a extending pane fixed in porous medium is discussed in this study. The controlling PDEs are changed into nonlinear ODEs using similarity transformations, and then These equations are numerically solved . The effects of a variety of non-dimensional characteristics on velocity and temperature fields are discussed and represented using graphs. The

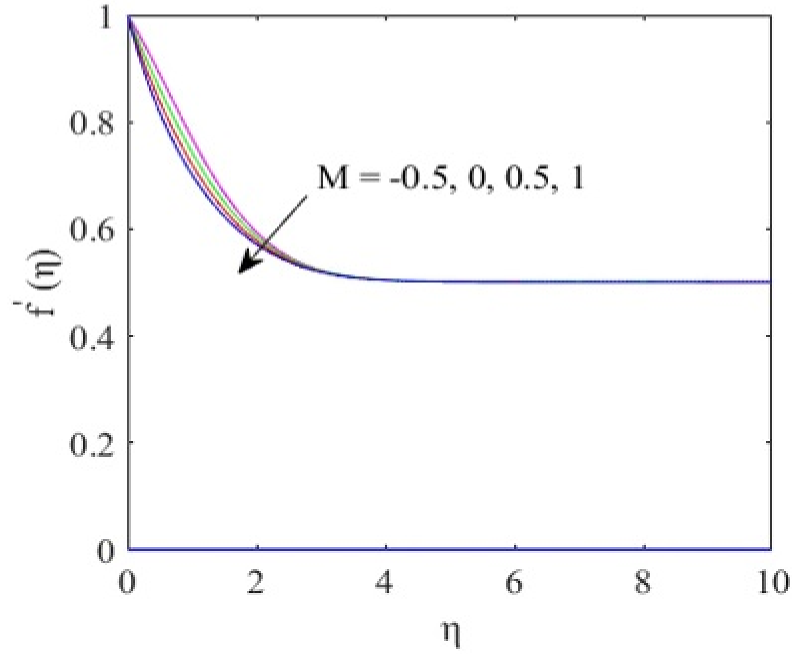

Figure 2: Velocity with η for disparate facts of magnetic restriction M.

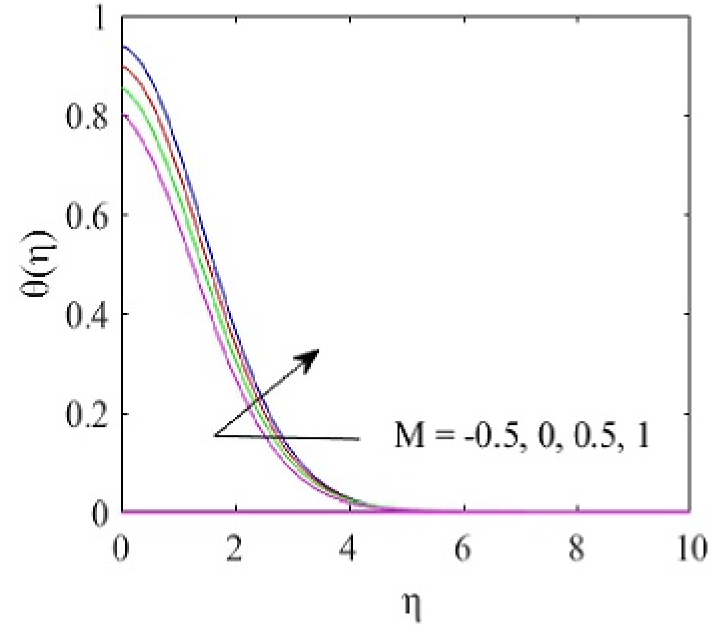

Figure 3: Temperature with η for disparate facts of magnetic restriction M.

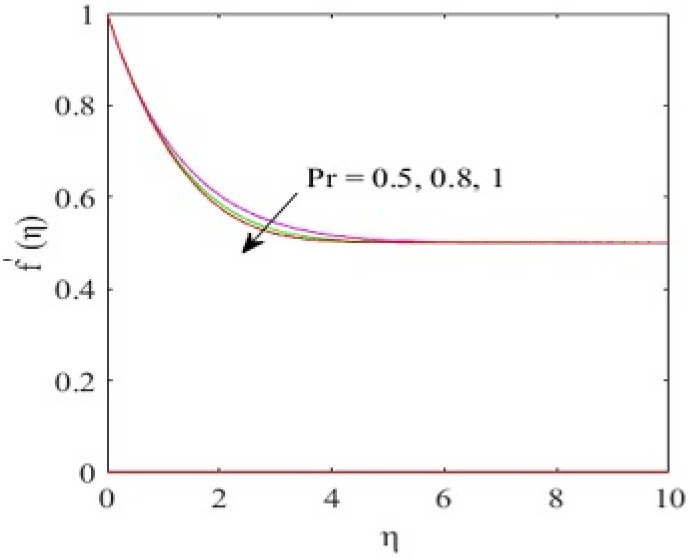

Figure 4: Velocity with η for disparate facts of Prandtl numeral P_r.

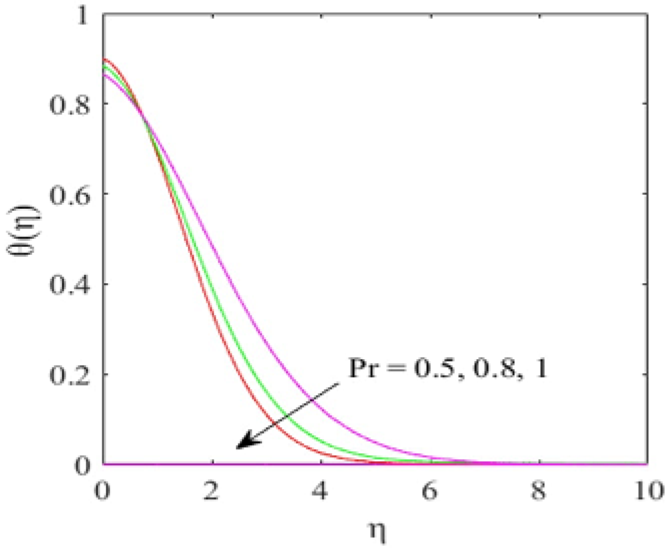

Figure 5: Temperature with η for disparate facts of Prandtl numeral P_r.

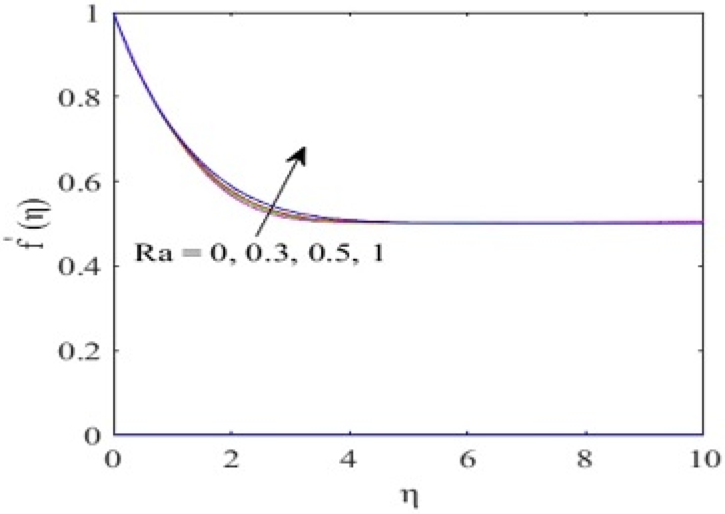

Figure 6: Velocity with η for disparate facts of radiation restriction R_a.

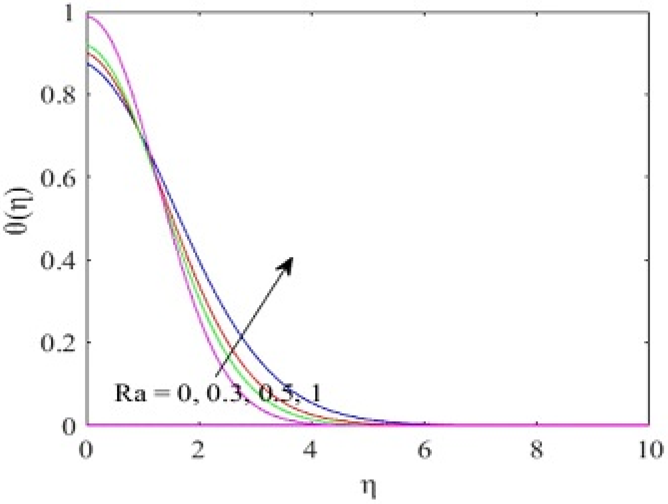

Figure 7: Temperature with η for disparate facts of radiation restriction R_a.

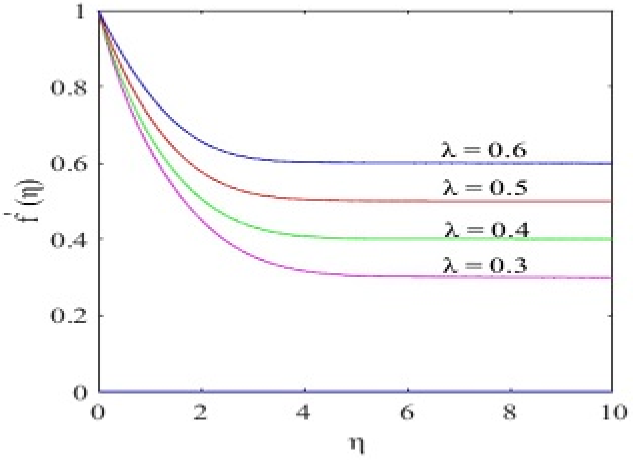

Figure 8: Velocity with η for disparate facts of free stream velocity to stretch sheet restriction velocity ratio of the stretching sheet parameter λ.

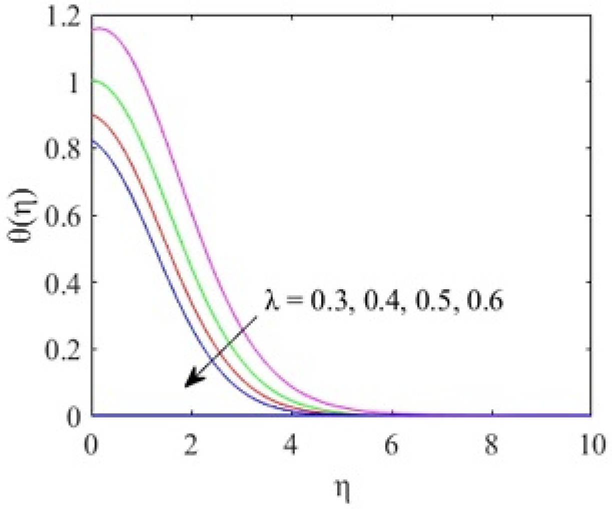

Figure 9: Temperature $\theta(\eta)$ related to η for unlike facts of ratio of the free stream velocity to stretch sheet restriction velocity ratio parameter λ.

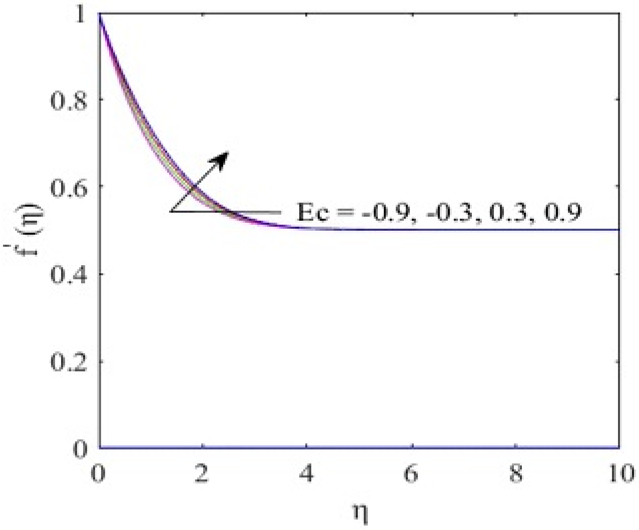

Figure 10: Velocity with η for disparate facts of Eckert numeral E_c.

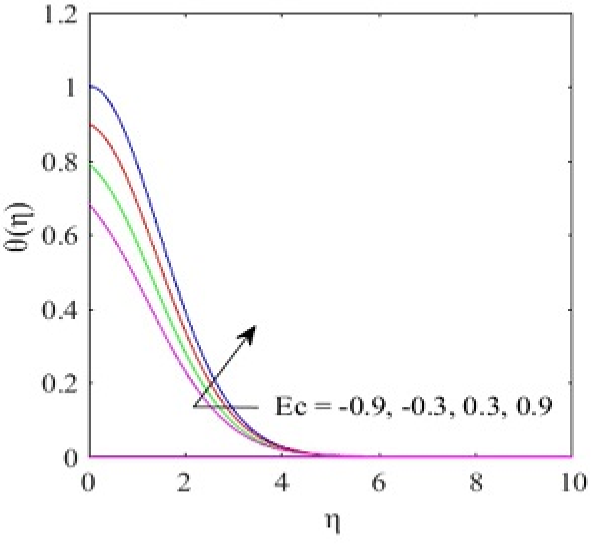

Figure 11: Temperature with η for disparate facts of Eckert numeral E_c.

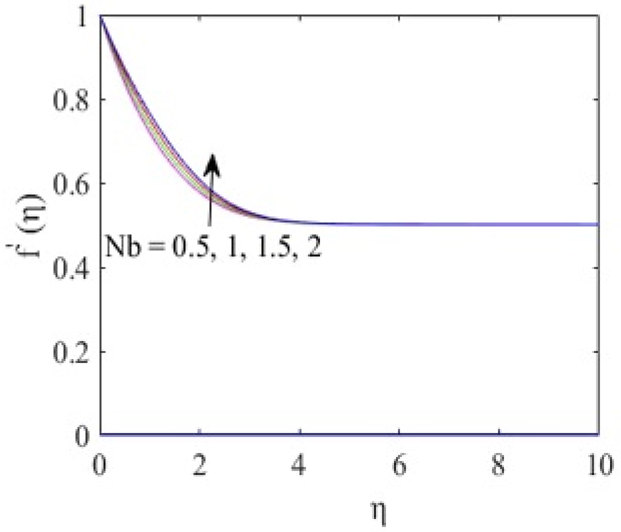

Figure 12: Velocity with η for disparate facts of Brownian motion parameter N_b.

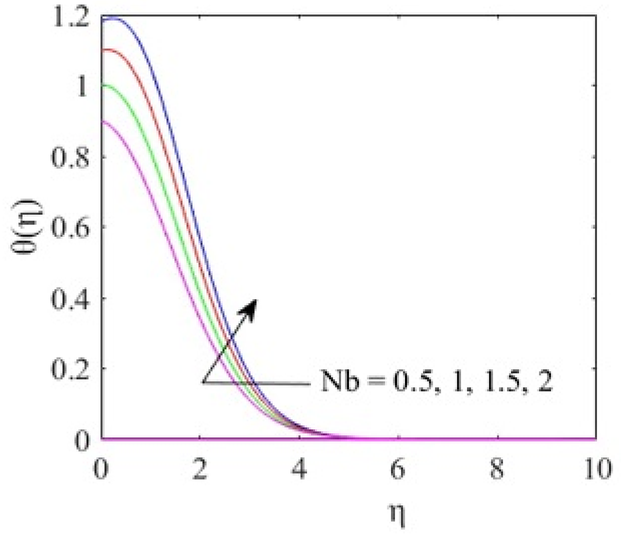

Figure 13: Temperature with η for disparate facts of Brownian motion parameter N_b.

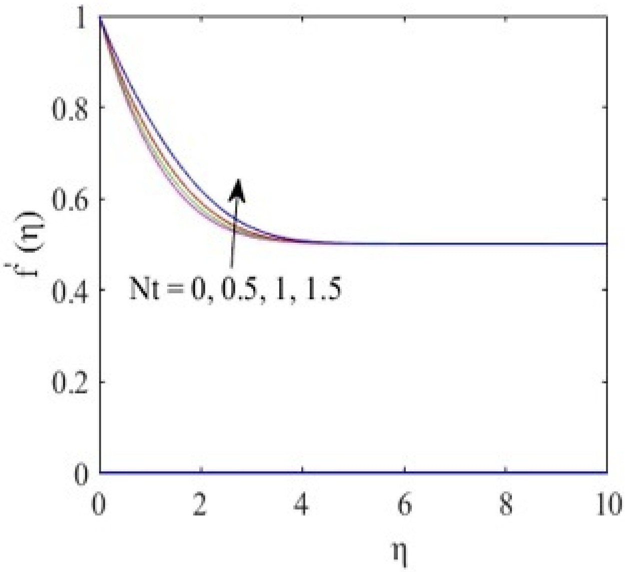

Figure 14: Velocity with η for disparate facts of Thermophoresis parameter N_t.

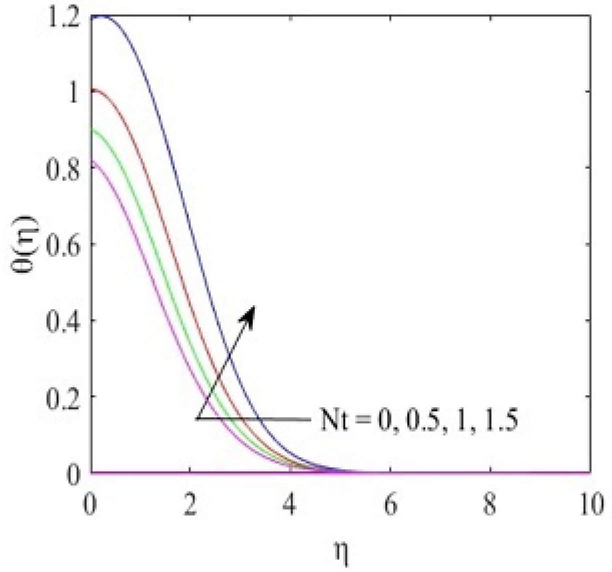

Figure 15: Temperature with η for disparate facts of Thermophoresis parameter N_t.

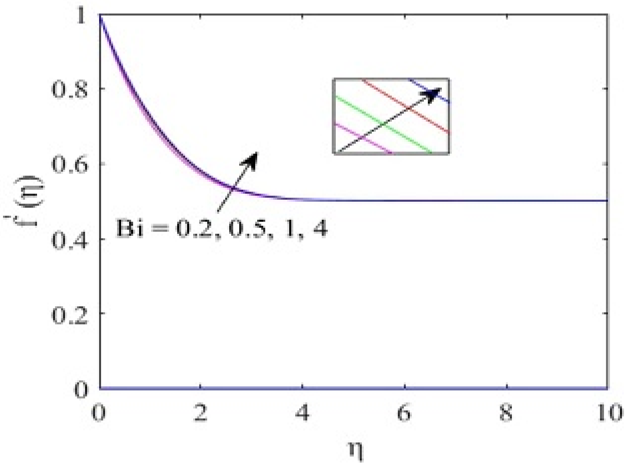

Figure 16: Velocity with η for disparate facts of Biot Numeral Bi.

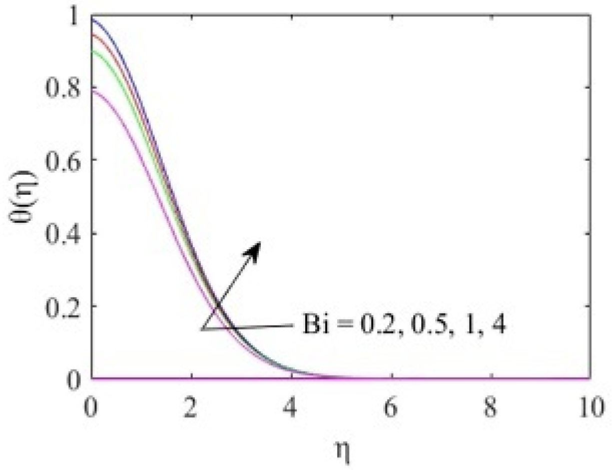

Figure 17: Temperature with η for disparate facts of Biot Numeral Bi.

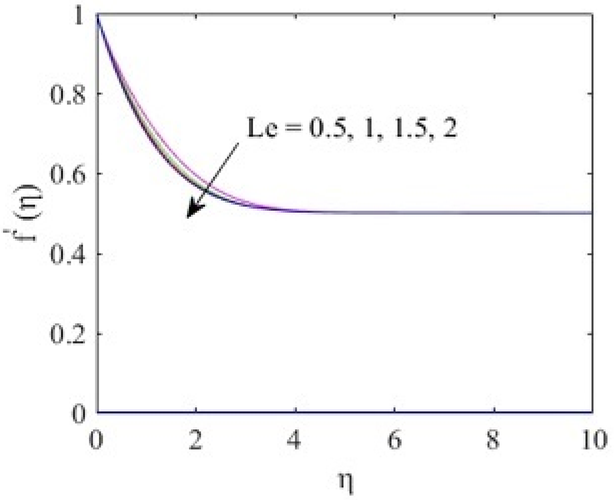

Figure 18: Velocity with η for disparate facts of Lewis factor L_e.

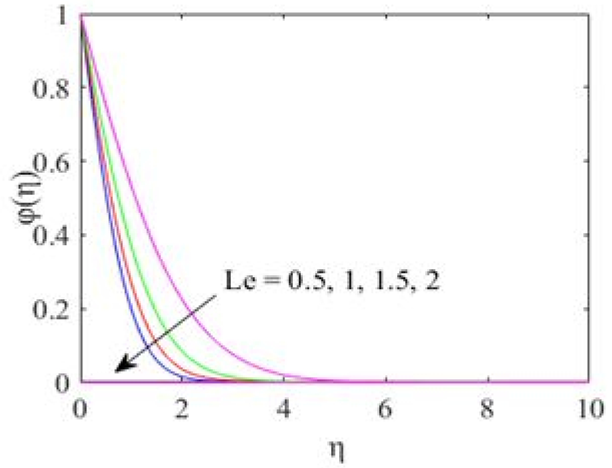

Figure 19: Concentration with η for disparate facts of Lewis factor L_e.

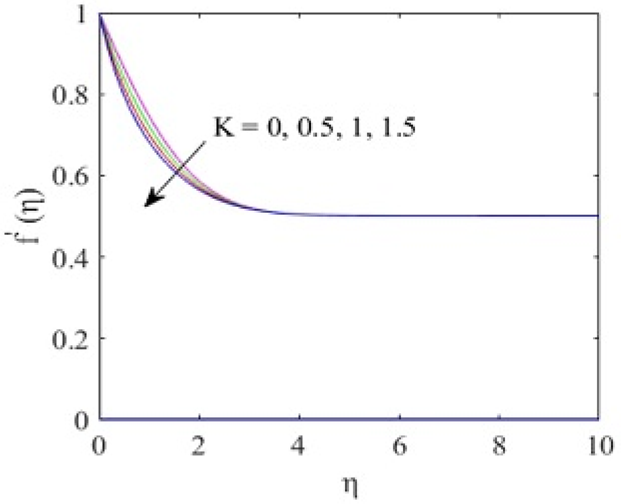

Figure 20: Velocity with η for disparate facts about permeability limitations K.

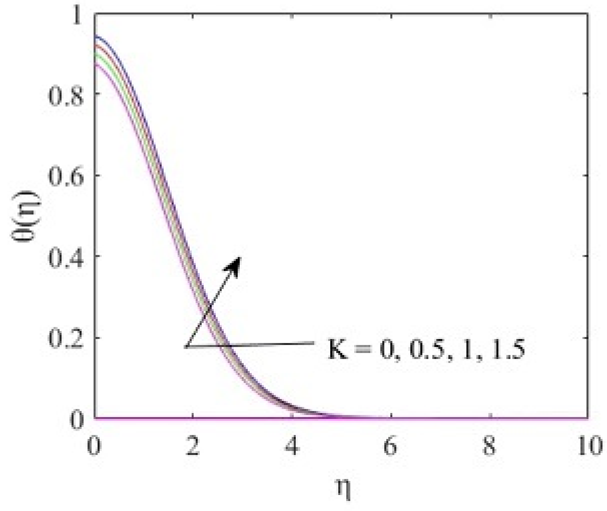

Figure 21: Temperature with η for disparate facts about permeability limitations K.

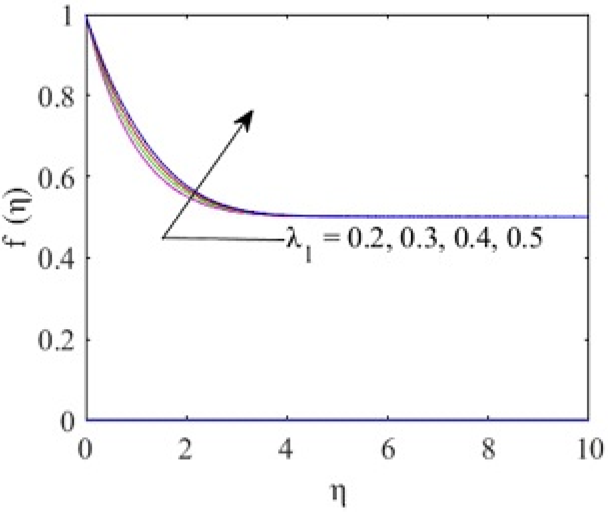

Figure 22: Velocity with η for disparate facts of thermal buoyancy parameter λ_1.

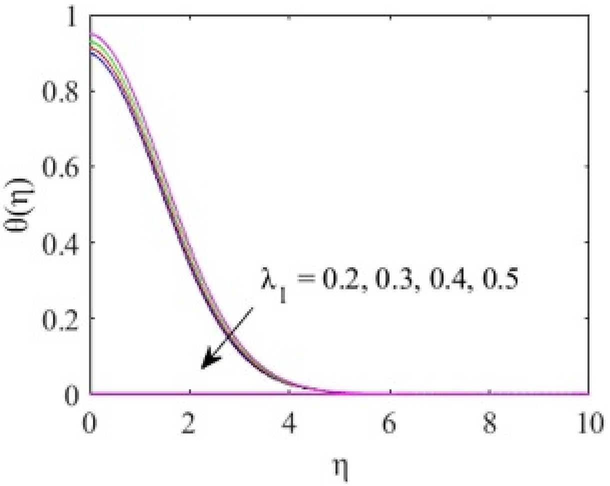

Figure 23: Temperature with η for disparate facts of thermal buoyancy parameter λ_1.

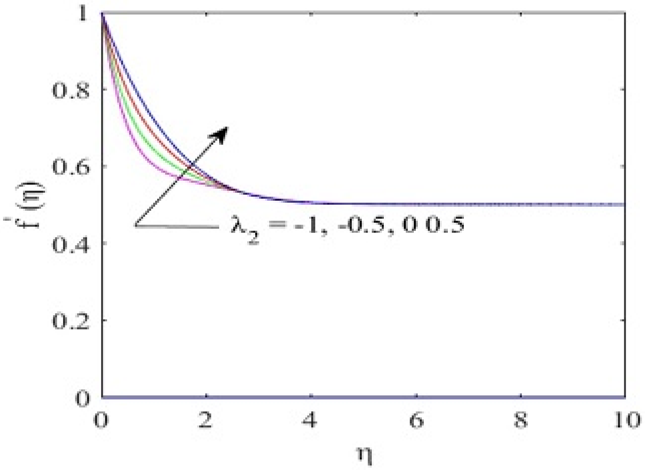

Figure 24: Velocity with η for disparate facts of Solutal buoyancy parameter λ_2.

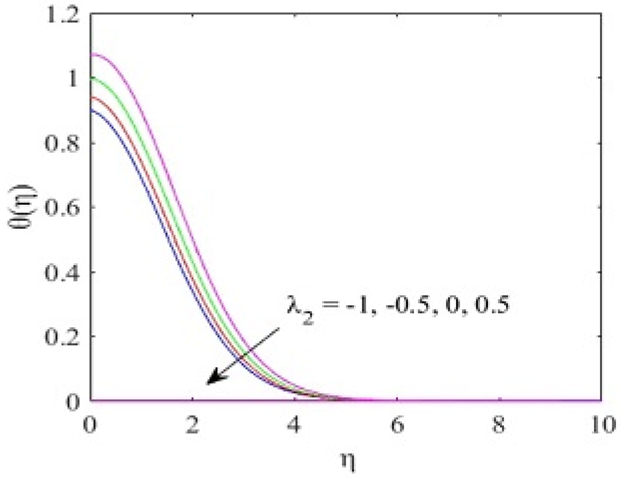

Figure 25: Temperature with η for disparate facts of Solutal buoyancy restriction λ_2.

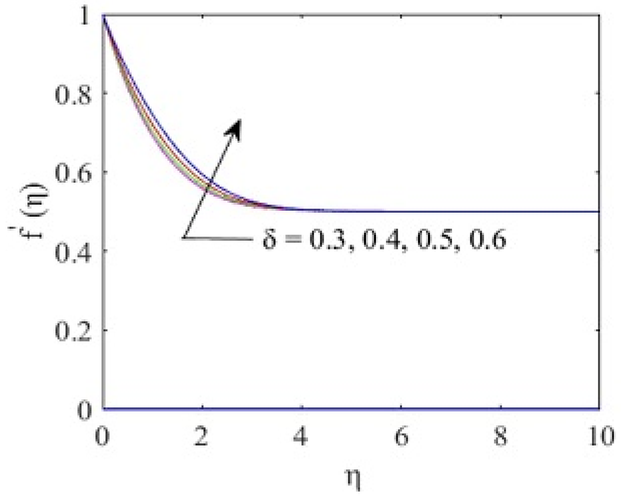

Figure 26: Velocity with η for disparate facts of Heat Source/Sink δ.

Table 1: Encouragement of the three physical dealings are the coefficient of skin friction C_{f_x}, the local Nusselt number N_{u_x} and local Sherwood number S_{u_x}.

Parameter	C_{f_x}	N_{u_x}	S_{u_x}
$M=-0.5$	-0.1951	0.1470	0.7460
$M=0$	-0.2948	0.1080	0.7365
$M=0.5$	-0.3866	0.0749	0.7291
$M=1$	-0.4707	0.0450	0.7222
$P_r=0.5$	-0.3827	0.1008	0.7316
$P_r=0.8$	-0.3861	0.0870	0.7296
$P_r=1$	-0.3866	0.0749	0.7291
$K=0$	-0.2887	0.0930	0.7381
$K=0.5$	-0.3866	0.0749	0.7291
$K=1$	-0.4758	0.0585	0.7217
$K=1.5$	-0.5573	0.0422	0.7160
$\lambda=0.3$	-0.5386	-0.1136	0.7041
$\lambda=0.4$	-0.4778	-0.0015	0.7141
$\lambda=0.5$	-0.3866	0.0749	0.7291
$\lambda=0.6$	-0.2743	0.1320	0.7460
$B_i=0.2$	-0.4161	0.0630	0.7261
$B_i=0.5$	-0.3866	0.0749	0.7291
$B_i=1$	-0.3749	0.0813	0.7315
$B_i=4$	-0.3641	0.0850	0.7326
$\lambda_1=0.2$	-0.5240	0.0369	0.7145
$\lambda_1=0.3$	-0.4762	0.0518	0.7196
$\lambda_1=0.4$	-0.4307	0.0642	0.7251
$\lambda_1=0.5$	-0.3866	0.0749	0.7291
$\lambda_2=-1$	-0.9295	-0.0525	0.6858
$\lambda_2=-0.5$	-0.7493	0.0030	0.7006
$\lambda_2=0.5$	-0.3866	0.0749	0.7291
$E_c=-0.9$	-0.4532	0.2360	0.7191
$E_c=-0.3$	-0.4204	0.1557	0.7241
$E_c=0.3$	-0.3866	0.0749	0.7291
$E_c=0.9$	-0.3546	-0.0021	0.7352
$\delta=0.3$	-0.4505	0.2182	0.7189
$\delta=0.4$	-0.4241	0.1590	0.7231
$\delta=0.5$	-0.3866	0.0749	0.7291
$\delta=0.6$	-0.3283	-0.0563	0.7391
$N_b=0.5$	-0.3866	0.0749	0.7291
$N_b=1$	-0.3519	-0.0014	0.7335
$N_b=1.5$	-0.3180	-0.0732	0.7375
$N_b=2$	-0.2880	-0.1344	0.7406
$N_t=0$	-0.4150	0.1347	0.7225
$N_t=0.5$	-0.3866	0.0749	0.7291
$N_t=1$	-0.3490	-0.0034	0.7398
$N_t=1.5$	-0.2823	-0.1400	0.7571
$R_a=0$	-0.3700	0.0060	0.7301
$R_a=0.3$	-0.3846	0.0527	0.7296
$R_a=0.5$	-0.3866	0.0749	0.7291
$R_a=1$	-0.3879	0.1251	0.7290
$L_e=0.5$	-0.3643	0.0930	0.5055
$L_e=1$	-0.3866	0.0749	0.7291
$L_e=1.5$	-0.4030	0.0696	0.9021
$L_e=2$	-0.4162	0.0681	1.0503

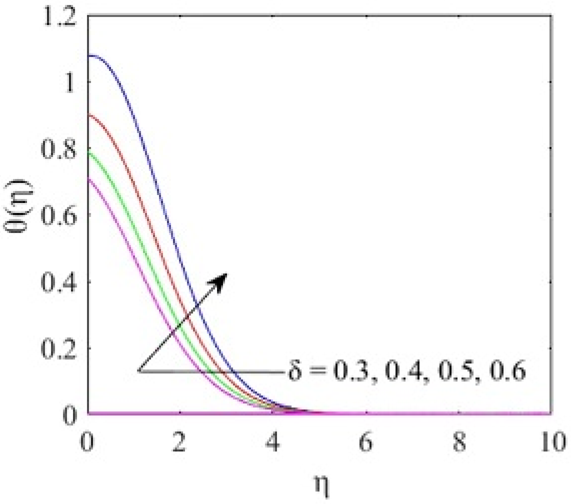

Figure 27: Temperature with η for disparate the Source/Sink facts δ.

table analyses and presents the effect of physical parameters on skin friction, local Nusselt number, and local Sherwood number. The following is a summary of the findings:

- Increasing the magnetic field parameter causes the velocity field to decrease and the temperature distribution to improve.
- The velocity and temperature field both are decrease for Prandtl number but reverse effect is seen in of radiation restriction R_a, Eckert numeral E_c, Thermophoresis limitations N_t,Brownian motion limitations N_b, Biot Numeral B_i and warmth Source/Sink δ.
- The parameter of proportion of the free stream speed to the speed of the stretching sheet λ, decrease the distribution of temperature.
- The Lewis factor decrease the distribution of concentration.
- The Permeability restriction K help to lessening the velocity arena and increase the supply of temperature arena.
- The thermal buoyancy parameter λ_1 an Solutal buoyancy parameter λ_2 help to increase the speed and decrease the temperature field.
- Sherwood number, Skin friction, and Nusselt number are increasing function of proportion of the free stream speed to the speed of the extending sheet restriction λ, Biot Number B_i, thermal buoyancy restriction λ_1 and Solutal buoyancy restriction λ_2 and decreasing function of magnetic field restriction M, Prandtl numeral P_r and Permeability restriction K.
- Skin friction and Sherwood number are increasing function of Eckert number E_c, heat Source/Sink δ, Brownian motion parameter N_b and Thermophoresis parameter N_t. But reverse effect is seen in Nusselt number.

[1] [2] [5] [6] [4] [7] [8] [9] [10] [11] [12] [13] [15] [16] [14] [18] [17] [19] [20] [21] [22] [24] [23] [25] [26] [28] [29] [30] [31] [32] [3] [27]

References

[1] Ali, B., Nie, Y., Khan, S. A., Sadiq, M. T., and Tariq, M. Finite element simulation of multiple slip effects on mhd unsteady maxwell nanofluid flow over a permeable stretching sheet with radiation and thermo-diffusion in the presence of chemical reaction. *Processes 7*, 9 (2019), 628.

[2] Babu, D. H., Ajmath, K., Venkateswarlu, B., and Narayana, P. Thermal radiation and heat source effects on mhd non-newtonian nanofluid flow over a stretching sheet. *Journal of Nanofluids 8*, 5 (2019), 1085–1092.

[3] Bilal, S., Shah, I. A., Akgül, A., Tekin, M. T., Botmart, T., Yahia, I., et al. A comprehensive mathematical structuring of magnetically effected sutterby fluid flow immersed in dually stratified medium under boundary layer approximations over a linearly stretched surface. *Alexandria Engineering Journal 61*, 12 (2022), 11889–11898.

[4] Daniel, Y. S., Aziz, Z. A., Ismail, Z., Bahar, A., and Salah, F. Slip role for unsteady mhd mixed convection of nanofluid over stretching sheet with thermal radiation and electric field. *Indian Journal of Physics 94*, 2 (2020), 195–207.

[5] Daniel, Y. S., Aziz, Z. A., Ismail, Z., and Salah, F. Impact of thermal radiation on electrical mhd flow of nanofluid over nonlinear stretching sheet with variable thickness. *Alexandria Engineering Journal 57*, 3 (2018), 2187–2197.

[6] Daniel, Y. S., Aziz, Z. A., Ismail, Z., and Salah, F. Thermal radiation on unsteady electrical mhd flow of nanofluid over stretching sheet with chemical reaction. *Journal of King Saud University-Science 31*, 4 (2019), 804–812.

[7] Dogonchi, A., and Ganji, D. Effect of cattaneo–christov heat flux on buoyancy mhd nanofluid flow and heat transfer over a stretching sheet in the presence of joule heating and thermal radiation impacts. *Indian Journal of Physics 92*, 6 (2018), 757–766.

[8] Ganesh, N. V., Kameswaran, P., Al-Mdallal, Q. M., Hakeem, A., and Ganga, B. Non-linear thermal radiative marangoni boundary layer flow of gamma al2o3 nanofluids past a stretching sheet. *Journal of Nanofluids 7*, 5 (2018), 944–950.

[9] Ghasemi, S., and Hatami, M. Solar radiation effects on mhd stagnation point flow and heat transfer of a nanofluid over a stretching sheet. *Case Studies in Thermal Engineering 25* (2021), 100898.

[10] Gireesha, B., Umeshaiah, M., Prasannakumara, B., Shashikumar, N., and Archana, M. Impact of nonlinear thermal radiation on magnetohydrodynamic three dimensional boundary layer flow of jeffrey nanofluid over a nonlinearly permeable stretching sheet. *Physica A: Statistical Mechanics and its Applications 549* (2020), 124051.

[11] Goud, B. S., Reddy, Y. D., and Rao, V. S. Thermal radiation and joule heating effects on a magnetohydrodynamic casson nanofluid flow in the presence of chemical reaction through a non-linear inclined porous stretching sheet. *Journal of Naval Architecture and Marine Engineering 17*, 2 (2020), 143–164.

[12] Gupta, S., Kumar, D., and Singh, J. Mhd mixed convective stagnation point flow and heat transfer of an incompressible nanofluid over an inclined stretching sheet with chemical reaction and radiation. *International Journal of Heat and Mass Transfer 118* (2018), 378–387.

[13] Hayat, T., Khan, W., Abbas, S., Nadeem, S., and Ahmad, S. Impact of induced magnetic field on second-grade nanofluid flow past a convectively heated stretching sheet. *Applied Nanoscience 10*, 8 (2020), 3001–3009.

[14] Hussain, S. M., Sharma, R., Seth, G. S., and Mishra, M. R. Thermal radiation impact on boundary layer dissipative flow of magneto-nanofluid over an exponentially stretching sheet. *Int. J. Heat Technol. 36*, 4 (2018), 1163–1173.

[15] Ishaq, M., Ali, G., Shah, Z., Islam, S., and Muhammad, S. Entropy generation on nanofluid thin film flow of eyring–powell fluid with thermal radiation and mhd effect on an unsteady porous stretching sheet. *Entropy 20*, 6 (2018), 412.

[16] Jamshed, W., Goodarzi, M., Prakash, M., Nisar, K. S., Zakarya, M., Abdel-Aty, A.-H., et al. Evaluating the unsteady casson nanofluid over a stretching sheet with solar thermal radiation: An optimal case study. *Case Studies in Thermal Engineering 26* (2021), 101160.

[17] Khan, S. A., Ali, B., Eze, C., Lau, K. T., Ali, L., Chen, J., and Zhao, J. Magnetic dipole and thermal radiation impacts on stagnation point flow of micropolar based nanofluids over a vertically stretching sheet: finite element approach. *Processes 9*, 7 (2021), 1089.

[18] Khan, S. A., Nie, Y., and Ali, B. Multiple slip effects on magnetohydrodynamic axisymmetric buoyant nanofluid flow above a stretching sheet with radiation and chemical reaction. *Symmetry 11*, 9 (2019), 1171.

[19] Mishra, A., and Kumar, M. Thermal performance of mhd nanofluid flow over a stretching sheet due to viscous dissipation, joule heating and thermal radiation. *International Journal of Applied and Computational Mathematics 6*, 4 (2020), 1–17.

[20] Mjankwi, M. A., Masanja, V. G., Mureithi, E. W., and James, M. N. Unsteady mhd flow of nanofluid with variable properties over a stretching sheet in the presence of thermal radiation and chemical reaction. *International Journal of Mathematics and Mathematical Sciences 2019* (2019).

[21] Mohammadein, S., Raslan, K., Abdel-Wahed, M., and Abedel-Aal, E. M. Kkl-model of mhd cuo-nanofluid flow over a stagnation point stretching sheet with nonlinear thermal radiation and suction/injection. *Results in Physics 10* (2018), 194–199.

[22] Muhammad, T., Waqas, H., Farooq, U., and Alqarni, M. Numerical simulation for melting heat transport in nanofluids due to quadratic stretching plate with nonlinear thermal radiation. *Case Studies in Thermal Engineering 27* (2021), 101300.

[23] Pal, D., Mondal, S., and Mondal, H. Entropy generation on mhd jeffrey nanofluid over a stretching sheet with nonlinear thermal radiation using spectral quasilinearisation method. *International Journal of Ambient Energy 42*, 15 (2021), 1712–1726.

[24] Pal, D., and Mondal, S. K. Mhd nanofluid bioconvection over an exponentially stretching sheet in the presence of gyrotactic microorganisms and thermal radiation. *BioNanoScience 8*, 1 (2018), 272–287.

[25] Patil, A. B., Humane, P. P., Patil, V. S., and Rajput, G. R. Mhd prandtl nanofluid flow due to convectively heated stretching sheet below the control of chemical reaction with thermal radiation. *International Journal of Ambient Energy* (2021), 1–13.

[26] Qayyum, S., Hayat, T., and Alsaedi, A. Thermal radiation and heat generation/absorption aspects in third grade magneto-nanofluid over a slendering stretching sheet with newtonian conditions. *Physica B: Condensed Matter 537* (2018), 139–149.

[27] Shah, I. A., Bilal, S., Akgül, A., Tekin, M. T., Botmart, T., Zahran, H. Y., and Yahia, I. S. On analysis of magnetized viscous fluid flow in permeable channel with single wall carbon nano tubes dispersion by executing nano-layer approach. *Alexandria Engineering Journal 61*, 12 (2022), 11737–11751.

[28] Shoaib, M., Raja, M. A. Z., Sabir, M. T., Islam, S., Shah, Z., Kumam, P., and Alrabaiah, H. Numerical investigation for rotating flow of mhd hybrid nanofluid with thermal radiation over a stretching sheet. *Scientific Reports 10*, 1 (2020), 1–15.

[29] Sithole, H., Mondal, H., and Sibanda, P. Entropy generation in a second grade magnetohydrodynamic nanofluid flow over a convectively heated stretching sheet with nonlinear thermal radiation and viscous dissipation. *Results in Physics 9* (2018), 1077–1085.

[30] Sreedevi, P., and Reddy, P. S. Combined influence of brownian motion and thermophoresis on maxwell three-dimensional nanofluid flow over stretching sheet with chemical reaction and thermal radiation. *Journal of Porous Media 23*, 4 (2020).

[31] Sreedevi, P., Sudarsana Reddy, P., and Chamkha, A. Heat and mass transfer analysis of unsteady hybrid nanofluid flow over a stretching sheet with thermal radiation. *SN Applied Sciences 2*, 7 (2020), 1–15.

[32] Sudarsana Reddy, P., and Sreedevi, P. Impact of chemical reaction and double stratification on heat and mass transfer characteristics of nanofluid flow over porous stretching sheet with thermal radiation. *International Journal of Ambient Energy* (2020), 1–11.

J. COMPUTATIONAL ANALYSIS AND APPLICATIONS, VOL. 31, NO. 2, 2023, COPYRIGHT 2023 EUDOXUS PRESS, LLC

Dynamic Mathematical Modelling of Capacitive Pressure Sensors using Different Materials for Healthcare Applications

Suman[1], Deepak Bhatia[1,*] and Devendra Kumar[2]

[1]Department of Electronics Engineering, Rajasthan
Technical University, Kota-324010, Rajasthan, India

[2]Department of Mathematics, University of Rajasthan,
Jaipur-302004, Rajasthan, India
*Corresponding author: dbhatia@rtu.ac.in

December 30, 2022

Abstract

This paper discusses the principle, design and theoretical dynamical modelling of MEMS capacitive pressure sensors with different material properties results that have been simulated as well as compared. The properties of the material ensure that sensor performance analysis for operating pressure range 0-25kPa. This work discusses Timoshenkos plate deflection theory and follows the pull-in phenomenon. One important factor that could influence the performance of a MEMS capacitive pressure sensor is the structure of the diaphragm. The active area of this sensor is made up of 0.5 mm0.5 mm and the cavity size are 2m. According to the simulations, the optimized parameters have higher linearity and greater sensitivity than the initial parameters. The comparison of results shows that Aluminium material gives the highest deflection and better capacitance sensitivities which is about 88 pF/pa and is more linear with the applied pressure than other materials. The behaviour of the touch mode capacitive pressure sensor in terms of the temperature dependence of capacitance is analysed and repeatability error has been reduced. This configuration of touch mode pressure sensor is promising for the use in health monitoring devices like patient blood pressure due to small pressure fluctuation.

Keywords— Capacitive pressure sensor, Linearity, Sensitivity, Range of Blood pressure, Deflections

1 Introduction

Nowadays CPS (Capacitive pressure sensor) is one of the popular MEMS pressure sensors due to their fast dynamic range and less sensitivity to temperature in comparison with piezoresistive pressure sensors and is widely applied in high-performance applications [4, 27, 5, 13] . The capacitive pressure sensor comprises the thin elastic diaphragm and a sealed cavity between the elastic diaphragm and substrate. The thin diaphragm is allowed to contact the substrate and a pair of plates behave as parallel plate capacitors.

Micromachined MEMS CPS can be classified in different ranges such as low, medium, ultra-low and high. Different ranging of pressure can work for different applications like gentle touches use low- a pressure range (1kPa- 10kPa) [3, 24] ,medium pressure range (10kPa -100kPa) can be used for some pressure or movement of the object that is operated by hands [21] . Ultra-low pressure ranging ($< 1Pa$) is used in the progress of the microphone, and touch screen and finger-print recognition. Above these sensors, the range is also used in commercial products like wearable touch keyboards [29, 30] and household appliances. High-pressure ranges ($> 100kPa$) are used in special applications such as industrial robots, colonoscopes [26], etc. MEMS capacitive pressure sensor has a fast-developed product range with brand-new features in contemporary years and covers the foremost part of the sensor market. With the increasing requirements of some sensing applications, great efforts are devoted to the exploration in the direction of the application range of pressure sensors. The main motive of this studies is to find out suitable material for better sensitivity and good linearity. Sensitivity is the most important parameter to judge the quality of pressure sensors [34]. To achieve good sensitivity, conductivity, stability, reproducibility and resolutions. the main aim is to enhance these performance parameters of capacitive pressure sensors. Particularly these parameters are dominantly determined by different two critical factors which are 1) the materials used for conductive electrodes [15, 31] and 2) the shape and structure of the dielectric layer [22, 20, 7, 8, 6, 19] . But there have some limitations of micromachined capacitive pressure sensors have non-linear output and low sensitivity in terms of capacitance [28] . To address this problem, one way is increasing the diaphragm thickness and another way is to expand the middle of the diaphragm membrane in such a way that the output will be more linear concerning the input but capacitive sensitivity reduces due to increasing the stiffness [25, 17].

Many materials have been used as active and non-active components in pressure design applications because the properties of materials play a very significant role in the behaviour of capacitive pressure sensors. Still, one of the main concerns is Material selection for the diaphragm, with rapid development in the world of research, it is not impossible to discover a new material that can compete with the existing materials. In this paper, firstly different capacitive pressure sensors using different diaphragm membrane materials with their different application are investigated and simulated in the same model. Detailed mathematical modelling and simulation results on various characteristics are presented.

2 Design of Pressure Sensors

The diaphragm and substrate are used as mechanical components in many sensors and are the most important part of the system. The size of the thin diaphragm, material

S.NO	Types of pressure sensors	Measurement	Range
1	Absolute	Atmospheric pressure	101.3 kPa
2	Absolute	In-vivo Blood Pressure	80/120 mm
3	Gauge	Intraocular Pressure	15mm Hg
4	Gauge	Tire pressure	30 Psi
5	Differential	Ventilators	25cm H_2O

Table 1: Types of Pressure Sensors with Specific Range and their Applications [2]

selection of the diaphragm, and substrate depend upon the required applications. Some types of pressure sensors along with their application and their pressure range are given in table 1. The deflection of the diaphragm and sensitivity of the sensor is depending upon according to properties of the materials and pressure mounted on the thin membrane.

The design of the diaphragm membrane and structure of MEMS pressure sensor by using finite element simulation software (FEA). MEMS pressure sensors are generally used to measure one parameter at a time, but the value of parameters changes when they operate in complex environments which create a major task for designing a MEMS pressure sensor to achieve good sensitivity with operational precision and speed in harsh environments.

3 Principle and Mathematics background Modelling of the Capacitive Pressure Sensor

MEMS capacitive pressure is work on the principle of the electromechanics interface. By changing applying the pressure to the top of the diaphragm, the membrane moves towards the direction of the substrate. Then performance occurs in terms of diaphragm deflection with thermal considerations. Due to the symmetric nature of the geometry, only a single geometry is used for the analysis [18, 10]. this model contains a thin membrane that is held at a fixed potential of 5V.

$$\frac{\partial^4 w(x,y)}{\partial x^4} + 2\alpha \frac{\partial^4 w(x,y)}{\partial x^2 \partial y^2} + \frac{\partial^4 w(x,y)}{\partial y^4} = \frac{p}{Dh^3} \tag{1}$$

To avoid any connection between substrate and diaphragm membrane insulation connection is provided. Basically, for designing diaphragm capacitive pressure sensors uses the theory of thin plate and small deflection, where the condition of theory plates uses a $h \approx \frac{a}{10}$ and deflection is $w_{max} \approx \frac{h}{4}$ [32] but in case of circular diaphragm r is taken as radius and where h is the thickness and the rectangular diaphragm is taken a is length and b is width. The mathematical expression for calculating diaphragm deflection with a clamped edge due to applied pressure P are governing the fourth-order differential equation in x-y planes (1).

Where w (x, y) is deflection of diaphragm supported with boundary edge condition, a is side of diaphragm, h is the thickness. The following mathematical expression can be used to determine the capacitance of this structure [12].

$$c_0 = \frac{\varepsilon k A}{d_0} \tag{2}$$

Where ε is absolute dielectric permittivity of, k is the relative permittivity of the plates, A is the area of the plates on a squared meters and d0 is the separation between the parallel conducting plates. However, the capacitance cannot be calculated using equation (2) above when the diaphragm's pressure has changed. As a result of uniform pressure being applied, the diaphragm deflects. As can be seen, the deflection with a uniformly loaded square shape plate is utmost at the diaphragm's centre.

$$w_{max} = 0.00126 \frac{L^4 P}{D} \tag{3}$$

Where w_{max} is the maximum deflection, α is the length of the diaphragm membrane, P is the differential pressure, D is the flexural rigidity can be computed by the expression [16, 9, 11] .

$$D = \frac{Eh^3}{12(1-v^2)} \tag{4}$$

Where h is thickness of membrane, E is modulus of elasticity, ν is Poissons ratio [23]. When above equation number 3 is insert in equation number 2 then, maximum deflection occurs.

$$w_{max} = 0.01512(1-v^2)\frac{PL^4}{Eh^3} \tag{5}$$

3.1 Measurements of Capacitance

The mentioned relation (6) can use to find out the change in capacitance and sensitivity of the moving diaphragm towards the cavity after changing the load on the top of the diaphragm.

$$c_f = \varepsilon \int\int \frac{dx.dy}{d - w(x,y)'} \tag{6}$$

$$c_f = \frac{\varepsilon}{d} \int\int \frac{dx.dy}{d - w(x,y)'} \tag{7}$$

Taylor series expansion is given in the following equation,

$$\frac{1}{1+x} = 1 + x + x^2 + x^3, for - 1 < x < 1 \tag{8}$$

Since in this case(w/d=1), therefore formula (8) can be written in the equation (9),

$$c_f = \frac{\varepsilon}{d} \int \int_{-a}^{a} (1 + \frac{w(x,y)}{d} + \frac{w^2(x,y)}{d} + ..) \tag{9}$$

As long as the sensor works with less deflection then, the capacitance, neglecting the higher-order factors, can be calculated by,

$$c_f = \frac{\varepsilon}{d} \int \int_{-a}^{a} (1 + \frac{w(x,y)}{d}) dx.dy \tag{10}$$

By using the binomial expression, the change in capacitance of square shape membrane can be written as [1].

$$c = c_0 (1 + \frac{12.5Pa^4}{2015dh}) \tag{11}$$

Where c is the final calculating capacitance, c_0 is initial capacitance, P is uniform (constant) pressure applied, d is the spacing between the plates and a is the length (size) of the diaphragm. As the zero-pressure capacitance, is given in equations (12),

$$c_0 = \frac{4\varepsilon a^2}{d} \tag{12}$$

Capacitive pressure sensitivity of the square membrane is given by (9).

$$S_A = \frac{49\varepsilon a^6}{2025 d^2 D} \tag{13}$$

3.2 Measurement of Sensitivity

Therefore, Sensitivity of above diaphragm depend upon thickness of membrane and distance between electrodes, influence by applied load and sensitivity of membrane can be expressed as (15).

$$S_c = \frac{dc}{dp} \tag{14}$$

The mechanical sensitivity of a diaphragm is defined as

$$S_M = \frac{dW}{dp} \tag{15}$$

For small deflection, square diaphragm sensitivity is,

$$S_m = \frac{a^2}{3.14h[\frac{4.2Eh^3}{3.14a^2(1-v^2)}]} \tag{16}$$

Thus, the low capacitance will make the device more sensitive. As a result, high displacement will lead to nonlinearity. The segmented or mesh model was created using the FEM (Finite element method) as depicted in figure 2.

4 Simulation Result and Discussion

In this analysis, Diaphragm deflection, capacitance and mechanical sensitivity vary according to the properties and characteristics of materials explained and simulated results of each material are also presented, as well as the equation used for the modelling of pressure to calculate and verify results. The shape of a diaphragm can be square, elliptical and circular but in this paper, the shape of the diaphragm is taken as square and dimensions are $0.5mm \times 0.5mm \times 10\mu m$ made up of different diaphragm material has been examined under the uniform pressure range is 0 to 15kPa, the dimensions of the cavity is 2 m filled with vacuum, silicon is taken substrate is shown in the figure 1 and FEM is used to create the segmented model is depicted in figure 2 and mesh parameter is shown in table 2 and as seen in the diagram boundary condition for the diaphragm deflection of this structure is limited in the z-direction only.

The result shown here in figure 3 is the simulation profile of deformation of the Aluminium membrane at external pressure 15 kPa. The given results proves that maximum deflection is occur at the centre and displacement reduces as moves away from the centre as shown by the vertical line and in order to sustain the linearity moving diaphragm/ plate should not move more than of the distance between the plates. Figure 4. Shows the simulation profile of applied boundary load at 10kPa. The maximum and mean deformations of the square diaphragm membrane at 10 kPa, 3.21 μm and 1.21 μm respectively.

S.NO	Parameter	Size
1	Maximum element size	0.3
2	Minimum element size	0.054
3	Element Growth rate	1.5
4	Curvature factor	0.6
5	Resolution of the regions	0.5
6	Number of iterations	4

Table 2: Mesh Parameter of the Model

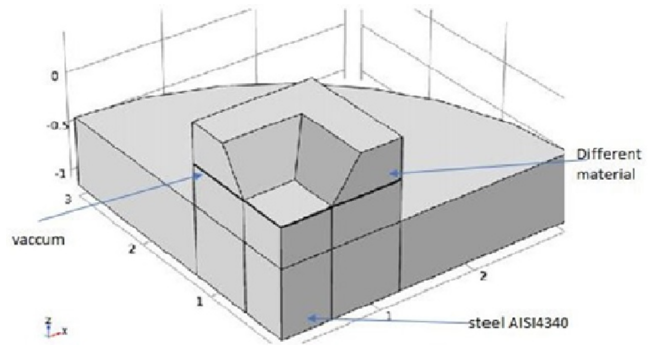

Figure 1: Three -dimensional view of Capacitive Pressure Sensor with different Material

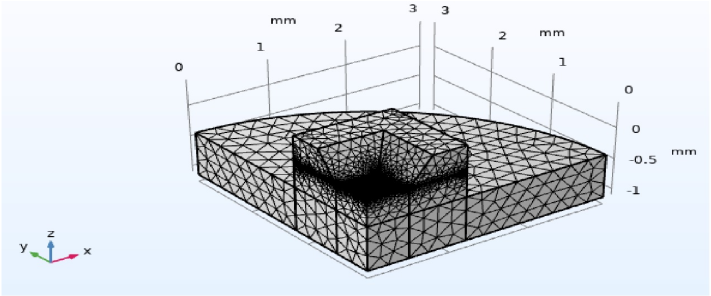

Figure 2: Mesh Model of Capacitive Pressure Sensor

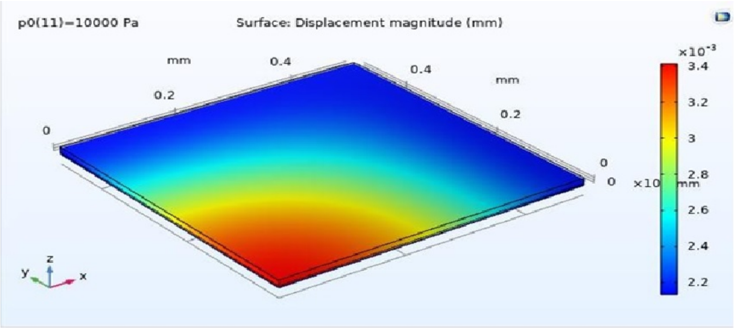

Figure 3: Quadrant Simulation Profile of Deformation of Diaphragm for 0.5mm at 10 kPa pressure

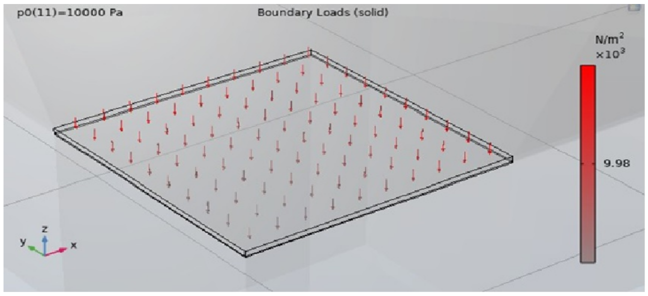

Figure 4: Simulation profile of applied boundary load when applied pressure at 10 kPa

Parameter Name	Value	Units
Youngs modulus	170	GPa
Poissons ratio	0.06	1
Density	2330	Kg/m^3
Relative permittivity	11.7	1
Coefficient of thermal expansion	2.6×10^{-6}	PPM/ $^{\circ}C$

Table 3: Material properties of Si

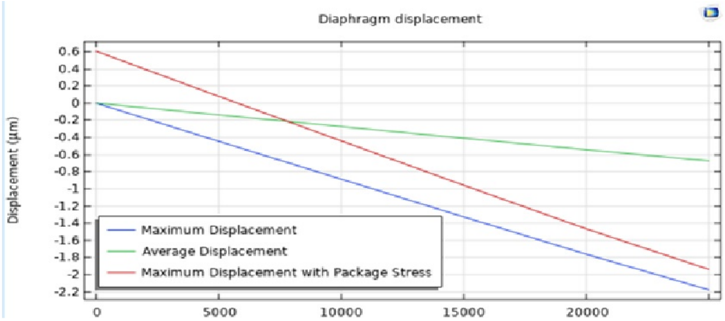

Figure 5: Diaphragm Displacement with Applied Pressure

5 Analysis of Pressure Sensor Performance using Different Materials

Only a few materials are being investigated for capacitive pressure sensors in order to achieve the required application. As three basic requirements of material defined by Mc Donald [33] (a) good electrical and mechanical properties (b) compatible with the fabrication device (c) good intrinsic properties that prevent high stress from developing during processing. Here simulated result of all material is presented.

5.1 Silicon

Silicon material is used as diaphragm material in capacitive pressure sensors due to high melting points and low hysteresis and low thermal expansion. Due to thermal expansion added to the devices, the response of this device is more dependent on the temperature and the capacitive response of the device is nonlinear with gradually increasing the pressure range. the simulated result of capacitance sensitivity is 52.8×10^{-6} pF/Pa and computation time calculated for the whole sensor is 23s. The properties used for the device are shown the table 3 and the graph between diaphragm deflection under applied uniform pressure with and without packaging stress is shown in figure 5.

Parameter Name	Value	Units
Youngs modulus	169	GPa
Poissons ratio	0.22	1
Density	2320	Kg/m^3
Relative permittivity	4.5	1
Coefficient of thermal expansion	2.8×10^{-6}	PPM/$^{\circ}C$

Table 4: Material Properties of Silicon Nanowires

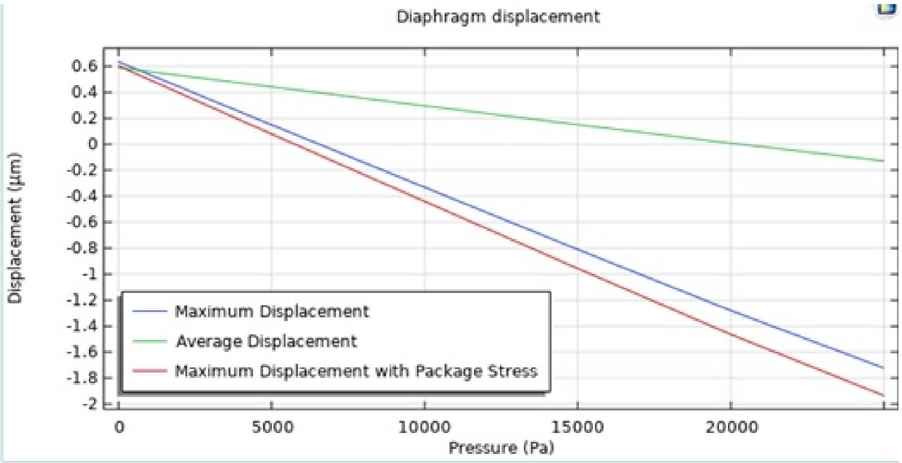

Figure 6: Diaphragm Displacement with Applied Pressure

5.2 Silicon nanowires

Silicon nanowires are used as diaphragm material in capacitive pressure and used low range pressure sensing application that is suitable for blood flow monitoring applications [14]and the simulated result of capacitance sensitivity is 2.3×10^{-6} pF/kPa. The properties used for the device are shown the table 4 and the graph between diaphragm deflection under applied pressure with and without packaging stress is shown in figure 6.

5.3 Titanium

Titanium metal is used as diaphragm material in capacitive pressure and titanium thin films deposited in conjunction with other materials onto a single crystal substrate is being used to create the micro devices. Due to strongest and high fracture toughness, this element is more promising metal substrate. The properties used for the device is shown the table 5 and graph between diaphragm deflection under applied pressure with and without packaging stress is depicted in figure 7.

Parameter Name	Value	Units
Youngs modulus	115.7	GPa
Poissons ratio	00.321	1
Density	4506	Kg/m^3
Relative permittivity	89.1	1
Coefficient of thermal expansion	8.5×10^{-6}	PPM/$^\circ C$

Table 5: Material Properties of Titanium

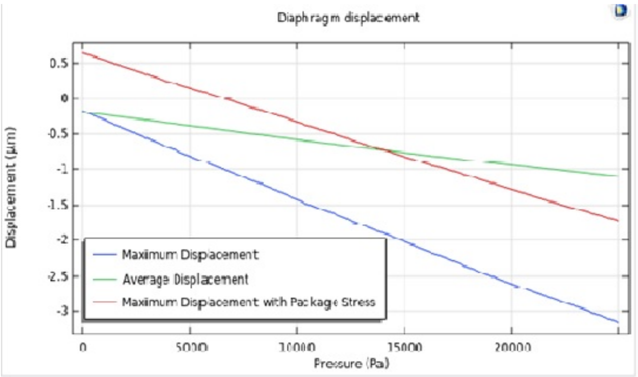

Figure 7: Diaphragm Displacement with Applied Pressure

5.4 Aluminium

Aluminium metal is used as diaphragm material in capacitive pressure and used in IC microelectronics through the integration of CMOS (complementary metal oxide semiconductor) Technology. Capacitive pressure on-chip signal circuitry with aluminium metal gives the highest sensitivity in square shape diaphragms under different pressure ranges. The properties used for the device are shown the table 6 and the graph between diaphragm deflection under applied pressure with and without packaging stress is shown in figure 8.

Parameter Name	Value	Units
Youngs modulus	70	GPa
Poissons ratio	0.35	1
Density	2700	Kg/m^3
Relative permittivity	11.5	1
Coefficient of thermal expansion	25×10^{-6}	PPM/$^\circ C$

Table 6: Material Properties of Aluminium

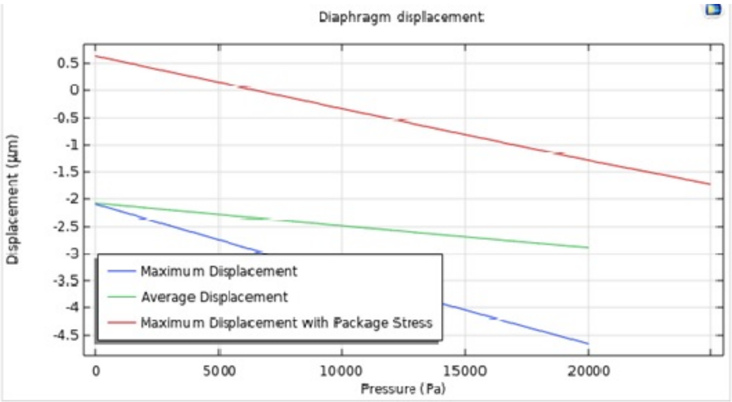

Figure 8: Diaphragm Displacement with Applied Pressure

Parameter Name	Value	Units
Youngs modulus	120	GPa
Poissons ratio	0.34	1
Density	8960	Kg/m^3
Relative permittivity	11.5	1
Coefficient of thermal expansion	25×10^{-6}	PPM/$°C$

Table 7: Material properties of copper

5.5 Copper

Copper metal is used as diaphragm material in capacitive pressure. Although it has good electrical conductivity and high malleable as compared to other materials. it cannot be used in high-pressure applications due to the weak nature of the metal. The properties used for the device are shown in the table 7 and the graph between diaphragm deflection under applied pressure with and without packaging stress is shown in figure 9.

5.6 Comparative Analysis of all Materials

In this paper, different membrane materials were used on the same model and a comparative analysis of touch mode capacitive pressure sensor for different pressure range 0 to 25kPa has been investigated at $10\mu m$ thickness. The average diaphragm deflection and capacitance varied according to the used material properties. The average diaphragm deflection of different membrane materials to different pressure ranges is shown in the figure 10. In, the plots represent that the average deflection of all material is increases with increasing the pressure range in a linear or non-linear manner. On the other hand, among all materials Aluminium material has the highest deflection and more linearity as compared to other materials.

Figure 11. depicts the relationship between the relative capacitance and applied pressure in case of a square diaphragm. This plot represents that the aluminium material has the highest capacitances when compared to other materials. At zero

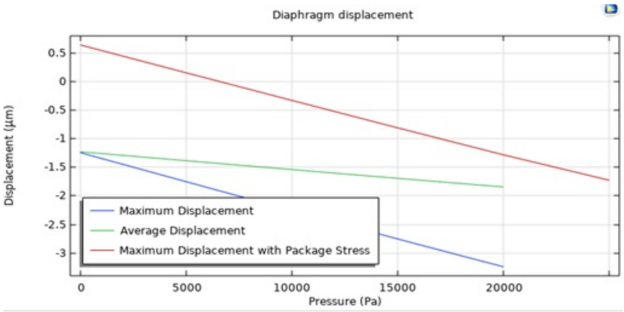

Figure 9: Diaphragm Displacement with Applied Pressure

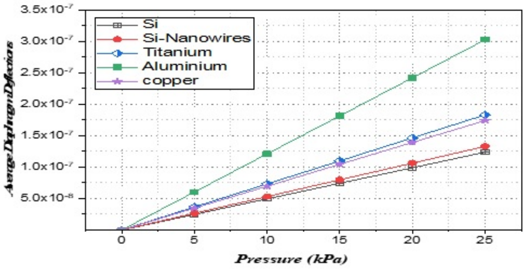

Figure 10: Diaphragm Displacement with Applied Pressure

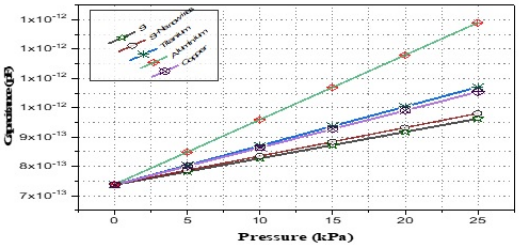

Figure 11: Capacitance changes with Applied Pressure

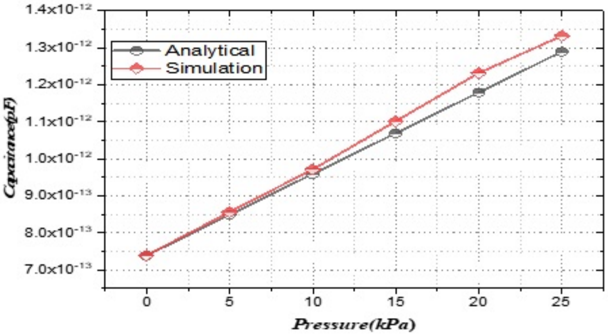

Figure 12: Analytical and Simulation Capacitance with Pressure

applied pressure, the value of capacitances for all the materials is same and gradually increases with applied pressure, but as is shown in the graph, Aluminium material provides better linearity than others materials over the range 0 kPa to 25 kPa

Figure 12 shows the comparison of analytical and simulation results of capacitance with applied pressure of a square diaphragm. This plot indicates that aluminium material provides more accurate and promising result of analytical with simulation result. At 10kPa, the value of capacitance is 9.69×10^{-13} F.

5.7 Sensitivity Analysis

Sensitivity is an important factor for the analysis of the capacitive pressure when membrane deflection and capacitance changes. Here table 8 shows a comparative analysis of the capacitance sensitivity of all Materials of the square diaphragm in which aluminium material provides the highest sensitivity at 10 kPa externally applied pressure is 22×10^{-6} pF/pa (one fourth part of the model) and the overall sensitivity of the model is 88×10^{-6} pF/pa with and without packaging stress.

Material Name	Sensitivity-Quadrant part (pF/pa)	Overall Sensitivity(pF/pa)
Si	9×10^{-6}	36×10^{-6}
Si- Nanowires	9.6×10^{-6}	38.4×10^{-6}
Titanium	13.2×10^{-6}	52.8×10^{-6}
Aluminium	$22.0 \times 1^{0-6}$	88.0×10^{-6}
Copper	12.6×10^{-6}	50.4×10^{-6}

Table 8: Comparative Sensitivity of all Material

6 Conclusion

This paper has described the dynamical modelling of highly sensitive normal and touch mode capacitive pressure sensor was analytically designed and simulated using the finite element method. This sensor comprises of moving top membrane, fixed bottom plate and cavity. In this investigation, the results show that the analytical result is in good agreement with the simulated result. Based on the observed performance its characteristics, accuracy and resolution are improved while repeatability error and computation time are reduced. Aluminium has been found to be more compatible and sensitive than other materials, making it more suitable for the measurement of blood pressure measurement. It also discussed how the reduced cavity size enhanced the sensitivity but this approach is restricted due to pull-in the phenomenon that faces inaccuracies in response time. In addition, these findings open a new route for other medical applications like ICP, IOP.

References

[1] Nisheka Anadkat and M Rangachar. Simulation based analysis of capacitive pressure sensor with comsol multiphysics. *Int. J. Eng. Res. Technol.*, pages 848–852, 2015.

[2] Kirankumar B Balavalad and BG Sheeparamatti. A critical review of mems capacitive pressure sensors. *Sensors & Transducers*, 187(4):120, 2015.

[3] S Bhatter, Kamlesh Jangid, SD Purohit, et al. Fractionalized mathematical models for drug diffusion. *Chaos, Solitons & Fractals*, 165:112810, 2022.

[4] Sung-Pil Chang and Mark G Allen. Demonstration for integrating capacitive pressure sensors with read-out circuitry on stainless steel substrate. *Sensors and Actuators A: Physical*, 116(2):195–204, 2004.

[5] Sarvesh Dubey, Ved Prakash Dubey, Jagdev Singh, Ahmed M. Alshehri, and Devendra Kumar. Computational Study of a Local Fractional Tricomi Equation Occurring in Fractal Transonic Flow. *Journal of Computational and Nonlinear Dynamics*, 17(8), 06 2022. 081006.

[6] Ved Prakash Dubey, Devendra Kumar, Hashim M Alshehri, Sarvesh Dubey, and Jagdev Singh. Computational analysis of local fractional lwr model occurring in a fractal vehicular traffic flow. *Fractal and Fractional*, 6(8):426, 2022.

[7] Ved Prakash Dubey, Devendra Kumar, Hashim M Alshehri, Jagdev Singh, and Dumitru Baleanu. Generalized invexity and duality in multiobjective variational problems involving non-singular fractional derivative. *Open Physics*, 20(1):939–962, 2022.

[8] Ved Prakash Dubey, Devendra Kumar, Jagdev Singh, Ahmed M Alshehri, and Sarvesh Dubey. Analysis of local fractional klein-gordon equations arising in relativistic fractal quantum mechanics. *Waves in Random and Complex Media*, pages 1–21, 2022.

[9] Ved Prakash Dubey, Jagdev Singh, Ahmed M Alshehri, Sarvesh Dubey, and Devendra Kumar. Analysis of local fractional coupled helmholtz and coupled burgers' equations in fractal media. *AIMS Mathematics*, 7(5):8080–8111, 2022.

[10] Ved Prakash Dubey, Jagdev Singh, Ahmed M Alshehri, Sarvesh Dubey, and Devendra Kumar. Forecasting the behavior of fractional order bloch equations appearing in nmr flow via a hybrid computational technique. *Chaos, Solitons & Fractals*, 164:112691, 2022.

[11] Ved Prakash Dubey, Jagdev Singh, Ahmed M Alshehri, Sarvesh Dubey, and Devendra Kumar. A hybrid computational method for local fractional dissipative and damped wave equations in fractal media. *Waves in Random and Complex Media*, pages 1–23, 2022.

[12] BA Ganji and NATERI M SHAMS. Modeling of capacitance and sensitivity of a mems pressure sensor with clamped square diaphragm. 2013.

[13] Xiuchun Hao, Sinya Tanaka, Atsuhiko Masuda, Jun Nakamura, Koichi Sudoh, Kazusuke Maenaka, Hidekuni Takao, and Kohei Higuchi. Application of silicon on nothing structure for developing a novel capacitive absolute pressure sensor. *IEEE Sensors Journal*, 14(3):808–815, 2013.

[14] Wataru Iwasaki, Hirofumi Nogami, Satoshi Takeuchi, Masutaka Furue, Eiji Higurashi, and Renshi Sawada. Detection of site-specific blood flow variation in humans during running by a wearable laser doppler flowmeter. *Sensors*, 15(10):25507–25519, 2015.

[15] Yunsik Joo, Junghwan Byun, Narkhyeon Seong, Jewook Ha, Hyunjong Kim, Sangwoo Kim, Taehoon Kim, Hwarim Im, Donghyun Kim, and Yongtaek Hong. Silver nanowire-embedded pdms with a multiscale structure for a highly sensitive and robust flexible pressure sensor. *Nanoscale*, 7(14):6208–6215, 2015.

[16] Reza Khakpour, Solmaz RM Mansouri, and AR Bahadorimehr. Analytical comparison for square, rectangular and circular diaphragms in mems applications. In *2010 International Conference on Electronic Devices, Systems and Applications*, pages 297–299. IEEE, 2010.

[17] Wen H. Ko. Solid-state capacitive pressure transducers. *Sensors and Actuators*, 10(3):303–320, 1986.

[18] Ali E Kubba, Ahmed Hasson, Ammar I Kubba, and Gregory Hall. A micro-capacitive pressure sensor design and modelling. *Journal of Sensors and Sensor Systems*, 5(1):95–112, 2016.

[19] Shyamsunder Kumawat, S Bhatter, DL Suthar, SD Purohit, and Kamlesh Jangid. Numerical modeling on age-based study of coronavirus transmission. *Applied Mathematics in Science and Engineering*, 30(1):609–634, 2022.

[20] Donguk Kwon, Tae-Ik Lee, Jongmin Shim, Seunghwa Ryu, Min Seong Kim, Seunghwan Kim, Taek-Soo Kim, and Inkyu Park. Highly sensitive, flexible, and wearable pressure sensor based on a giant piezocapacitive effect of three-dimensional microporous elastomeric dielectric layer. *ACS applied materials & interfaces*, 8(26):16922–16931, 2016.

[21] Kin Fong Lei, Kun-Fei Lee, and Ming-Yih Lee. A flexible pdms capacitive tactile sensor with adjustable measurement range for plantar pressure measurement. *Microsystem technologies*, 20(7):1351–1358, 2014.

[22] Tie Li, Hui Luo, Lin Qin, Xuewen Wang, Zuoping Xiong, Haiyan Ding, Yang Gu, Zheng Liu, and Ting Zhang. Flexible capacitive tactile sensor based on micropatterned dielectric layer. *Small*, 12(36):5042–5048, 2016.

[23] Shi-Yu Liu, Jian-Gang Lu, and Han-Ping D Shieh. Influence of permittivity on the sensitivity of porous elastomer-based capacitive pressure sensors. *IEEE Sensors Journal*, 18(5):1870–1876, 2018.

[24] Stefan CB Mannsfeld, Benjamin CK Tee, Randall M Stoltenberg, Christopher V Chen, Soumendra Barman, Beinn VO Muir, Anatoliy N Sokolov, Colin Reese, and Zhenan Bao. Highly sensitive flexible pressure sensors with microstructured rubber dielectric layers. *Nature materials*, 9(10):859–864, 2010.

[25] Manju Mittal, Anurekha Sharma, et al. Virtual prototyping of a mems capacitive pressure sensor for tpms using intellisuite®. In *2012 1st International Symposium on Physics and Technology of Sensors (ISPTS-1)*, pages 25–28. IEEE, 2012.

[26] Lijia Pan, Alex Chortos, Guihua Yu, Yaqun Wang, Scott Isaacson, Ranulfo Allen, Yi Shi, Reinhold Dauskardt, and Zhenan Bao. An ultra-sensitive resistive pressure sensor based on hollow-sphere microstructure induced elasticity in conducting polymer film. *Nature communications*, 5(1):1–8, 2014.

[27] Robert Puers. Capacitive sensors: when and how to use them. *Sensors and Actuators A: Physical*, 37:93–105, 1993.

[28] MJ Sharifi, N Nemati, and A Abedi. A new mems based capacitive differential pressure sensor with acceptable sensitivity and improved linear region. In *2014 22nd Iranian Conference on Electrical Engineering (ICEE)*, pages 29–32. IEEE, 2014.

[29] Ruilong Shi, Zheng Lou, Shuai Chen, and Guozhen Shen. Flexible and transparent capacitive pressure sensor with patterned microstructured composite rubber dielectric for wearable touch keyboard application. *Science China Materials*, 61(12):1587–1595, 2018.

[30] Aarushi Shrivastava, Janki B Sharma, and Sunil D Purohit. Image encryption based on fractional wavelet transform, arnold transform with double random phases in the hsv color domain. *Recent Advances in Computer Science and Communications (Formerly: Recent Patents on Computer Science)*, 15(1):5–13, 2022.

[31] Xingtian Shuai, Pengli Zhu, Wenjin Zeng, Yougen Hu, Xianwen Liang, Yu Zhang, Rong Sun, and Ching-ping Wong. Highly sensitive flexible pressure sensor based on silver nanowires-embedded polydimethylsiloxane electrode with microarray structure. *ACS applied materials & interfaces*, 9(31):26314–26324, 2017.

[32] Stephen Timoshenko, Sergius Woinowsky-Krieger, et al. *Theory of plates and shells*, volume 2. McGraw-hill New York, 1959.

[33] William SN Trimmer. Microrobots and micromechanical systems. *Sensors and actuators*, 19(3):267–287, 1989.

[34] Michael Wehner, Ryan L Truby, Daniel J Fitzgerald, Bobak Mosadegh, George M Whitesides, Jennifer A Lewis, and Robert J Wood. An integrated design and fabrication strategy for entirely soft, autonomous robots. *nature*, 536(7617):451–455, 2016.

TABLE OF CONTENTS, JOURNAL OF COMPUTATIONAL ANALYSIS AND APPLICATIONS, VOL. 31, NO. 2, 2023

Two step Newton's method with multiplicative calculus to solve the non-linear equations, Gurjeet Singh and Sonia Bhalla,……..171

Analysis of Tripled System of Fractional Differential Equation using Certain Fixed Points Theorems with Fractional Boundary Condition, Ashok Kumar Badsara, Jagdev Singh, Richa Sharma, and Virendra Singh Chouhan,……………………………………………………..180

L^1-Convergence of Newly Defined Trigonometric Sums Under Some New Class of Fourier Coefficients, Priyanka, Karannvir Singh,……………………………………………………192

Numerical Study of Heat and Mass Transfer of MHD Casson Fluid Flow with Cross-Diffusion and Heat Source Impacts in presence of Radiation, Shilpa, Ruchika Mehta, Sushila and Renu Sharma,……………………………………………………………………………….204

M/M/1 Retrial Queueing Model with Server Breakdown and Feedback, M.Seenivasan and J.Shiny Epciya,………………………………………………………………………………224

Norm retrieval by vectors and projections, Suman Dowerah and Saikat Mukherjee,…………236

Non Markovian retrial queue, balking, disaster under working breakdown and working vacation, P. Manoharan and S. Subathra,……………………………………………………………244

A mathematical study of fractional order unsteady natural convective Casson fluid flow past an infinitely vertical plate with heat and mass transfer, Sapna Tyagi, Monika Jain, Jagdev Singh,256

Effect of the Couple-Stress on Micro Polar Rotating Fluid Flow Saturating a Porous Medium, Devilal Kumawat, Ram Dayal Pankaj, and Vijay Mehta,………………………………...…270

Mathematical Analysis of SEITR Model for Influenza Dynamics, K. Arun Kumar and A.Venkatesh,……………………………………………………………………………………281

MHD Stagnation Point Flow and Heat Transfer of a Nanofluid Over a Stretching Sheet Fixed in Porous Medium with Effect of Thermal Radiation, Joule Heating and Heat Source/Sink, Ravindra Kumar, Ruchika Mehta, Tripti Mehta, and Sushila,…………………………………294

Dynamic Mathematical Modelling of Capacitive Pressure Sensors using Different Materials for Healthcare Applications, Suman, Deepak Bhatia, and Devendra Kumar,……………………..317

Volume 31, Number 3 September 2023
ISSN:1521-1398 PRINT,1572-9206 ONLINE

Journal of Computational Analysis and Applications

EUDOXUS PRESS,LLC

Journal of Computational Analysis and Applications
ISSNno.'s:1521-1398 PRINT,1572-9206 ONLINE

SCOPE OF THE JOURNAL

An international publication of Eudoxus Press, LLC
(published quarterly) www.eudoxuspress.com.
Editor in Chief: George Anastassiou
Department of Mathematical Sciences,
University of Memphis, Memphis, TN 38152-3240, U.S.A
ganastss@memphis.edu, ganastss2@gmail.com
http://web0.msci.memphis.edu/~ganastss/jocaaa/

The main purpose of "J.Computational Analysis and Applications" is to publish high quality research articles from all subareas of Computational Mathematical Analysis and its many potential applications and connections to other areas of Mathematical Sciences. Any paper whose approach and proofs are computational,using methods from Mathematical Analysis in the broadest sense is suitable and welcome for consideration in our journal, except from Applied Numerical Analysis articles. Also plain word articles without formulas and proofs are excluded. The list of possibly connected mathematical areas with this publication includes, but is not restricted to: Applied Analysis, Applied Functional Analysis, Approximation Theory, Asymptotic Analysis, Difference Equations, Differential Equations, Partial Differential Equations, Fourier Analysis, Fractals, Fuzzy Sets, Harmonic Analysis, Inequalities, Integral Equations, Measure Theory, Moment Theory, Neural Networks, Numerical Functional Analysis, Potential Theory, Probability Theory, Real and Complex Analysis, Signal Analysis, Special Functions, Splines, Stochastic Analysis, Stochastic Processes, Summability, Tomography, Wavelets, any combination of the above, e.t.c.

"J.Computational Analysis and Applications" is a peer-reviewed Journal. See the instructions for preparation and submission **of articles to JOCAAA.**

Journal of Computational Analysis and Applications(JoCAAA) is published by **EUDOXUS PRESS,LLC**,1424 Beaver Trail Drive,Cordova,TN38016,USA,anastassioug@yahoo.com http://www.eudoxuspress.com. **Annual Subscription Prices**:For USA and Canada,Institutional:Print $500, Electronic OPEN ACCESS. Individual:Print $250. For any other part of the world add $150 more(handling and postages) to the above prices for Print. No credit card payments.

Copyright©2023 by Eudoxus Press,LLC,all rights reserved.JoCAAA is printed in USA.

JoCAAA is reviewed and abstracted by Elsevier-Scopus, available also via EBSCO publishing and EBSCO.

It is strictly prohibited the reproduction and transmission of any part of JoCAAA and in any form and by any means without the written permission of the publisher.It is only allowed to educators to Xerox articles for educational purposes.The publisher assumes no responsibility for the content of published papers.

Editorial Board

Associate Editors of Journal of Computational Analysis and Applications

Francesco Altomare
Dipartimento di Matematica
Universita' di Bari
Via E.Orabona, 4
70125 Bari, ITALY
Tel+39-080-5442690 office
+39-080-3944046 home
+39-080-5963612 Fax
altomare@dm.uniba.it
Approximation Theory, Functional Analysis, Semigroups and Partial Differential Equations, Positive Operators.

Ravi P. Agarwal
Department of Mathematics
Texas A&M University - Kingsville
700 University Blvd.
Kingsville, TX 78363-8202
tel: 361-593-2600
Agarwal@tamuk.edu
Differential Equations, Difference Equations, Inequalities

George A. Anastassiou
Department of Mathematical Sciences
The University of Memphis
Memphis, TN 38152,U.S.A
Tel.901-678-3144
e-mail: ganastss@memphis.edu
Approximation Theory, Real Analysis,
Wavelets, Neural Networks, Probability, Inequalities.

J. Marshall Ash
Department of Mathematics
De Paul University
2219 North Kenmore Ave.
Chicago, IL 60614-3504
773-325-4216
e-mail: mash@math.depaul.edu
Real and Harmonic Analysis

Dumitru Baleanu
Department of Mathematics and Computer Sciences,
Cankaya University, Faculty of Art and Sciences,
06530 Balgat, Ankara,
Turkey, dumitru@cankaya.edu.tr
Fractional Differential Equations
Nonlinear Analysis, Fractional Dynamics

Carlo Bardaro
Dipartimento di Matematica e Informatica
Universita di Perugia
Via Vanvitelli 1
06123 Perugia, ITALY
TEL+390755853822
+390755855034
FAX+390755855024
E-mail carlo.bardaro@unipg.it
Web site:
http://www.unipg.it/~bardaro/
Functional Analysis and Approximation Theory, Signal Analysis, Measure Theory, Real Analysis.

Martin Bohner
Department of Mathematics and Statistics, Missouri S&T
Rolla, MO 65409-0020, USA
bohner@mst.edu
web.mst.edu/~bohner
Difference equations, differential equations, dynamic equations on time scale, applications in economics, finance, biology.

Jerry L. Bona
Department of Mathematics
The University of Illinois at Chicago
851 S. Morgan St. CS 249
Chicago, IL 60601
e-mail:bona@math.uic.edu
Partial Differential Equations, Fluid Dynamics

Luis A. Caffarelli
Department of Mathematics
The University of Texas at Austin
Austin, Texas 78712-1082
512-471-3160
e-mail: caffarel@math.utexas.edu
Partial Differential Equations

George Cybenko
Thayer School of Engineering
Dartmouth College
8000 Cummings Hall,
Hanover, NH 03755-8000
603-646-3843 (X 3546 Secr.)
e-mail:george.cybenko@dartmouth.edu
Approximation Theory and Neural
Networks

Sever S. Dragomir
School of Computer Science and
Mathematics, Victoria University,
PO Box 14428,
Melbourne City,
MC 8001, AUSTRALIA
Tel. +61 3 9688 4437
Fax +61 3 9688 4050
e-mail: sever.dragomir@vu.edu.au
Inequalities, Functional Analysis,
Numerical Analysis, Approximations,
Information Theory, Stochastics.

Oktay Duman
TOBB University of Economics and
Technology,
Department of Mathematics, TR-06530, Ankara, Turkey,
e-mail: oduman@etu.edu.tr
Classical Approximation Theory,
Summability Theory, Statistical
Convergence and its Applications

J .A. Goldstein
Department of Mathematical Sciences
The University of Memphis
Memphis, TN 38152
901-678-3130
e-mail: jgoldste@memphis.edu
Partial Differential Equations,
Semigroups of Operators

H. H. Gonska
Department of Mathematics
University of Duisburg
Duisburg, D-47048
Germany
011-49-203-379-3542
e-mail: heiner.gonska@uni-due.de
Approximation Theory, Computer
Aided Geometric Design

John R. Graef
Department of Mathematics
University of Tennessee at
Chattanooga
Chattanooga, TN 37304 USA
e-mail: John-Graef@utc.edu
Ordinary and functional
differential equations, difference
equations, impulsive systems,
differential inclusions, dynamic
equations on time scales, control
theory and their applications

Weimin Han
Department of Mathematics
University of Iowa
Iowa City, IA 52242-1419
319-335-0770
e-mail: whan@math.uiowa.edu
Numerical analysis, Finite element
method, Numerical PDE, Variational
inequalities, Computational
mechanics

Tian-Xiao He
Department of Mathematics and
Computer Science
P.O. Box 2900, Illinois Wesleyan
University
Bloomington, IL 61702-2900, USA
Tel (309)556-3089
Fax (309)556-3864
e-mail: the@iwu.edu
Approximations, Wavelet,
Integration Theory, Numerical
Analysis, Analytic Combinatorics

Margareta Heilmann
Faculty of Mathematics and Natural
Sciences, University of Wuppertal
Gaußstraße 20
D-42119 Wuppertal, Germany,
heilmann@math.uni-wuppertal.de
Approximation Theory (Positive
Linear Operators)

Xing-Biao Hu
Institute of Computational
Mathematics
AMSS, Chinese Academy of Sciences
Beijing, 100190, CHINA
e-mail: hxb@lsec.cc.ac.cn
Computational Mathematics

Seda Karateke
Department of Computer Engineering,
Faculty of Engineering,
Istanbul Topkapi University,
Istanbul, Zeytinburnu 34087, Turkey
e-mail: sedakarateke@topkapi.edu.tr
Approximation Theory, Neural
Networks

Jong Kyu Kim
Department of Mathematics
Kyungnam University
Masan Kyungnam,631-701,Korea
Tel 82-(55)-249-2211
Fax 82-(55)-243-8609
e-mail: jongkyuk@kyungnam.ac.kr
Nonlinear Functional Analysis,
Variational Inequalities, Nonlinear
Ergodic Theory, ODE, PDE,
Functional Equations.

Robert Kozma
Department of Mathematical Sciences
The University of Memphis
Memphis, TN 38152, USA
e-mail: rkozma@memphis.edu
Neural Networks, Reproducing Kernel
Hilbert Spaces,
Neural Percolation Theory

Mustafa Kulenovic
Department of Mathematics
University of Rhode Island
Kingston, RI 02881, USA
e-mail: kulenm@math.uri.edu
Differential and Difference
Equations

Burkhard Lenze
Fachbereich Informatik
Fachhochschule Dortmund
University of Applied Sciences
Postfach 105018
D-44047 Dortmund, Germany
e-mail: lenze@fh-dortmund.de
Real Networks, Fourier Analysis,
Approximation Theory

Alina Alb Lupas
Department of Mathematics and
Computer Science
Faculty of Informatics
University of Oradea
2 Universitatii Street,
410087 Oradea, Romania
e-mail: alblupas@gmail.com
e-mail: dalb@uoradea.ro
Complex Analysis, Topological
Algebra, Mathematical Analysis

Razvan A. Mezei
Computer Science Department
Hal and Inge Marcus School of
Engineering
Saint Martin’s University
Lacey, WA 98503, USA
e-mail: RMezei@stmartin.edu
Numerical Approximation, Fractional
Inequalities.

Hrushikesh N. Mhaskar
Department Of Mathematics
California State University
Los Angeles, CA 90032
626-914-7002
e-mail: hmhaska@gmail.com
Orthogonal Polynomials,
Approximation Theory, Splines,
Wavelets, Neural Networks

Ram N. Mohapatra
Department of Mathematics
University of Central Florida
Orlando, FL 32816-1364
tel.407-823-5080
e-mail: ram.mohapatra@ucf.edu
Real and Complex Analysis,
Approximation Th., Fourier
Analysis, Fuzzy Sets and Systems

Gaston M. N'Guerekata
Department of Mathematics
Morgan State University
Baltimore, MD 21251, USA
tel: 1-443-885-4373
Fax 1-443-885-8216
Gaston.N'Guerekata@morgan.edu
nguerekata@aol.com
Nonlinear Evolution Equations,
Abstract Harmonic Analysis,
Fractional Differential Equations,
Almost Periodicity & Almost
Automorphy

M.Zuhair Nashed
Department Of Mathematics
University of Central Florida
PO Box 161364
Orlando, FL 32816-1364
e-mail: znashed@mail.ucf.edu
Inverse and Ill-Posed problems,
Numerical Functional Analysis,
Integral Equations, Optimization,
Signal Analysis

Mubenga N. Nkashama
Department OF Mathematics
University of Alabama at Birmingham
Birmingham, AL 35294-1170
205-934-2154
e-mail: nkashama@math.uab.edu
Ordinary Differential Equations,
Partial Differential Equations

Vassilis Papanicolaou
Department of Mathematics
National Technical University of Athens
Zografou campus, 157 80
Athens, Greece
tel: +30(210) 772 1722
Fax +30(210) 772 1775
e-mail: papanico@math.ntua.gr
Partial Differential Equations,
Probability

Choonkil Park
Department of Mathematics
Hanyang University
Seoul 133-791
S. Korea,
e-mail: baak@hanyang.ac.kr
Functional Equations

Svetlozar (Zari) Rachev,
Professor of Finance, College of
Business, and Director of
Quantitative Finance Program,
Department of Applied Mathematics &
Statistics
Stonybrook University
312 Harriman Hall, Stony Brook, NY
11794-3775
tel: +1-631-632-1998,
svetlozar.rachev@stonybrook.edu

Alexander G. Ramm
Mathematics Department
Kansas State University
Manhattan, KS 66506-2602
e-mail: ramm@math.ksu.edu
Inverse and Ill-posed Problems,
Scattering Theory, Operator Theory,
Theoretical Numerical Analysis,
Wave Propagation, Signal Processing
and Tomography

Tomasz Rychlik
Polish Academy of Sciences
Instytut Matematyczny PAN
00-956 Warszawa, skr. poczt. 21
ul. Śniadeckich 8
Poland
e-mail: trychlik@impan.pl
Mathematical Statistics,
Probabilistic Inequalities

Boris Shekhtman
Department of Mathematics
University of South Florida
Tampa, FL 33620, USA
Tel 813-974-9710
e-mail: shekhtma@usf.edu
Approximation Theory, Banach
spaces, Classical Analysis

T. E. Simos
Department of Computer
Science and Technology
Faculty of Sciences and Technology
University of Peloponnese
GR-221 00 Tripolis, Greece
Postal Address:
26 Menelaou St.
Anfithea - Paleon Faliron
GR-175 64 Athens, Greece
e-mail: tsimos@mail.ariadne-t.gr
Numerical Analysis

Jagdev Singh
JECRC University, Jaipur, India
jagdevsinghrathore@gmail.com
Fractional Calculus, Mathematical
Modelling, Special Functions,
Numerical Methods

H. M. Srivastava
Department of Mathematics and
Statistics
University of Victoria
Victoria, British Columbia V8W 3R4
Canada
tel.250-472-5313; office,250-477-
6960 home, fax 250-721-8962
e-mail: harimsri@math.uvic.ca
Real and Complex Analysis,
Fractional Calculus and Appl.,
Integral Equations and Transforms,
Higher Transcendental Functions and
Appl.,q-Series and q-Polynomials,
Analytic Number Th.

I. P. Stavroulakis
Department of Mathematics
University of Ioannina
451-10 Ioannina, Greece
e-mail: ipstav@cc.uoi.gr
Differential Equations
Phone +3-065-109-8283

Jessada Tariboon
Department of Mathematics
King Mongut's University of
Technology N. Bangkok
1518 Pracharat 1 Rd., Wongsawang,
Bangsue, Bangkok, Thailand 10800
e-mail: jessada.t@sci.kmutnb.ac.th
Time scales

Differential/Difference Equations,
Fractional Differential Equations

Manfred Tasche
Department of Mathematics
University of Rostock
D-18051 Rostock, Germany
manfred.tasche@mathematik.uni-rostock.de
Numerical Fourier Analysis, Fourier
Analysis, Harmonic Analysis, Signal
Analysis, Spectral Methods,
Wavelets, Splines, Approximation
Theory

Juan J. Trujillo
University of La Laguna
Departamento de Analisis Matematico
C/Astr.Fco.Sanchez s/n
38271. LaLaguna. Tenerife.
SPAIN
Tel/Fax 34-922-318209
e-mail: Juan.Trujillo@ull.es
Fractional: Differential Equations-Operators-Fourier Transforms,
Special functions, Approximations,
and Applications

Xiao-Jun Yang
State Key Laboratory for
Geomechanics and Deep Underground
Engineering, China
University of Mining and
Technology, Xuzhou 221116, China
Local Fractional Calculus and
Applications, Fractional Calculus
and Applications, General
Fractional Calculus and
Applications, Variable-order
Calculus and Applications,
Viscoelasticity and Computational
methods for Mathematical
Physics.dyangxiaojun@163.com

Xiang Ming Yu
Department of Mathematical Sciences
Southwest Missouri State University
Springfield, MO 65804-0094
417-836-5931
e-mail: xmy944f@missouristate.edu
Classical Approximation Theory,
Wavelets

Richard A. Zalik
Department of Mathematics
Auburn University
Auburn University, AL 36849-5310
USA.
Tel 334-844-6557 office
Fax 334-844-6555
e-mail: zalik@auburn.edu
Approximation Theory, Chebychev
Systems, Wavelet Theory

Ahmed I. Zayed
Department of Mathematical Sciences
DePaul University
2320 N. Kenmore Ave.
Chicago, IL 60614-3250
773-325-7808
e-mail: azayed@condor.depaul.edu
Shannon sampling theory, Harmonic
analysis and wavelets, Special
functions and orthogonal
polynomials, Integral transforms

Ding-Xuan Zhou
Department Of Mathematics
City University of Hong Kong
83 Tat Chee Avenue
Kowloon, Hong Kong
852-2788 9708,Fax:852-2788 8561
e-mail: mazhou@cityu.edu.hk
Approximation Theory, Spline
functions, Wavelets

Xin-long Zhou
Fachbereich Mathematik, Fachgebiet
Informatik
Gerhard-Mercator-Universitat
Duisburg
Lotharstr.65, D-47048 Duisburg,
Germany
e-mail:Xzhou@informatik.uni-duisburg.de
Fourier Analysis, Computer-Aided
Geometric Design, Computational
Complexity, Multivariate
Approximation Theory, Approximation
and Interpolation Theory

Instructions to Contributors
Journal of Computational Analysis and Applications

An international publication of Eudoxus Press, LLC, of TN.

Editor in Chief: George Anastassiou

Department of Mathematical Sciences
University of Memphis
Memphis, TN 38152-3240, U.S.A.

1. Manuscripts files in Latex and PDF and in English, should be submitted via email to the Editor-in-Chief:

**Prof.George A. Anastassiou
Department of Mathematical Sciences
The University of Memphis
Memphis,TN 38152, USA.
Tel. 901.678.3144
e-mail: ganastss@memphis.edu**

Authors may want to recommend an associate editor the most related to the submission to possibly handle it.

Also authors may want to submit a list of six possible referees, to be used in case we cannot find related referees by ourselves.

2. Manuscripts should be typed using any of TEX,LaTEX,AMS-TEX,or AMS-LaTEX and according to EUDOXUS PRESS, LLC. LATEX STYLE FILE. (Click HERE to save a copy of the style file.)They should be carefully prepared in all respects. Submitted articles should be brightly typed (not dot-matrix), double spaced, in ten point type size and in 8(1/2)x11 inch area per page. Manuscripts should have generous margins on all sides and should not exceed 24 pages.

3. Submission is a representation that the manuscript has not been published previously in this or any other similar form and is not currently under consideration for publication elsewhere. A statement transferring from the authors(or their employers,if they hold the copyright) to Eudoxus Press, LLC, will be required before the manuscript can be accepted for publication.The Editor-in-Chief will supply the necessary forms for this transfer.Such a written transfer of copyright,which previously was assumed to be implicit in the act of submitting a manuscript,is necessary under the U.S.Copyright Law in order for the publisher to carry through the dissemination of research results and reviews as widely and effective as possible.

4. The paper starts with the title of the article, author's name(s) (no titles or degrees), author's affiliation(s) and e-mail addresses. The affiliation should comprise the department, institution (usually university or company), city, state (and/or nation) and mail code.

The following items, 5 and 6, should be on page no. 1 of the paper.

5. An abstract is to be provided, preferably no longer than 150 words.

6. A list of 5 key words is to be provided directly below the abstract. Key words should express the precise content of the manuscript, as they are used for indexing purposes.

The main body of the paper should begin on page no. 1, if possible.

7. All sections should be numbered with Arabic numerals (such as: 1. INTRODUCTION) .
Subsections should be identified with section and subsection numbers (such as 6.1. Second-Value Subheading).
If applicable, an independent single-number system (one for each category) should be used to label all theorems, lemmas, propositions, corollaries, definitions, remarks, examples, etc. The label (such as Lemma 7) should be typed with paragraph indentation, followed by a period and the lemma itself.

8. Mathematical notation must be typeset. Equations should be numbered consecutively with Arabic numerals in parentheses placed flush right, and should be thusly referred to in the text [such as Eqs.(2) and (5)]. The running title must be placed at the top of even numbered pages and the first author's name, et al., must be placed at the top of the odd numbed pages.

9. Illustrations (photographs, drawings, diagrams, and charts) are to be numbered in one consecutive series of Arabic numerals. The captions for illustrations should be typed double space. All illustrations, charts, tables, etc., must be embedded in the body of the manuscript in proper, final, print position. In particular, manuscript, source, and PDF file version must be at camera ready stage for publication or they cannot be considered.

Tables are to be numbered (with Roman numerals) and referred to by number in the text. Center the title above the table, and type explanatory footnotes (indicated by superscript lowercase letters) below the table.

10. List references alphabetically at the end of the paper and number them consecutively. Each must be cited in the text by the appropriate Arabic numeral in square brackets on the baseline.
References should include (in the following order):
initials of first and middle name, last name of author(s)
title of article,

name of publication, volume number, inclusive pages, and year of publication.

Authors should follow these examples:

Journal Article

1. H.H.Gonska,Degree of simultaneous approximation of bivariate functions by Gordon operators, (journal name in italics) *J. Approx. Theory*, 62,170-191(1990).

Book

2. G.G.Lorentz, (title of book in italics) *Bernstein Polynomials* (2nd ed.), Chelsea,New York,1986.

Contribution to a Book

3. M.K.Khan, Approximation properties of beta operators,in(title of book in italics) *Progress in Approximation Theory* (P.Nevai and A.Pinkus,eds.), Academic Press, New York,1991,pp.483-495.

11. All acknowledgements (including those for a grant and financial support) should occur in one paragraph that directly precedes the References section.

12. Footnotes should be avoided. When their use is absolutely necessary, footnotes should be numbered consecutively using Arabic numerals and should be typed at the bottom of the page to which they refer. Place a line above the footnote, so that it is set off from the text. Use the appropriate superscript numeral for citation in the text.

13. After each revision is made please again submit via email Latex and PDF files of the revised manuscript, including the final one.

14. Effective 1 Nov. 2009 for current journal page charges, contact the Editor in Chief. Upon acceptance of the paper an invoice will be sent to the contact author. The fee payment will be due one month from the invoice date. The article will proceed to publication only after the fee is paid. The charges are to be sent, by money order or certified check, in US dollars, payable to Eudoxus Press, LLC, to the address shown on the Eudoxus homepage.

No galleys will be sent and the contact author will receive one (1) electronic copy of the journal issue in which the article appears.

15. This journal will consider for publication only papers that contain proofs for their listed results.

J. COMPUTATIONAL ANALYSIS AND APPLICATIONS, VOL. 31, NO. 3, 2023, COPYRIGHT 2023 EUDOXUS PRESS, LLC

Generalization of Interval Jacobi and Gauss-Seidel Methods for Interval Linear System

Jahnabi Chakravarty[1]* and Manideepa Saha[2]
Department of Mathematics
National Institute of Technology Meghalaya
Shillong, India-793003
Email: [1]jahnabichakravarty@nitm.ac.in,[2]manideepa.saha@nitm.ac.in

Abstract

The paper presents iterative methods for solving interval linear system of equations. We present a generalization of interval Jacobi method and interval Gauss-Seidel method by generalizing interval diagonal matrices to band interval matrices, and discuss the convergence analysis of the proposed methods. More specifically, we prove that both the proposed methods converge for any initial approximation if the coefficient interval matrix of the system is either an *interval strictly diagonally dominant matrix*, or *interval M-matrix* or *interval H-matrix*. Numerical experiment are carried out to assess the effectiveness of the proposed methods.

Keywords: Convergence, Generalized interval Jacobi method, Generalized interval Gauss-Seidel method, Linear interval systems
2020 Mathematics Subject Classification: 15A30, 65G40, 65H10, 65G30

1 Introduction

Many practical problems involving uncertainties, such as uncertainty in engineering or design problems, global optimization, mathematical programming problems etc., get reduced to solving system of interval equations. We refer to [12, 15, 16, 17, 20, 26] to find the literature on interval analysis dealing with uncertainty. It is worthwhile to mention that the solution set enclosure of interval linear systems, plays a significant role as data are impacted by uncertainty in many real-world problems that involves interval linear systems. However, it is well-known that the interval computations are NP-hard problems. In other words, one cannot expect an algorithm for computing all computations for the interval in less than exponential running time. So the research has been driven for finding a solution set enclosure for the interval linear equations with less computations.

---

*Corresponding author

Interval Jacobi, interval Gauss-Seidel, Bauer-Skeel, Hansen-Bliek-Rohn, Krawczyk iteration methods are among the oldest well-known iterative methods for solving interval linear systems. In [2, 7, 19, 21], authors proved that the above mentioned methods may not produce an optimal enclosure. However Hladík [19] in 2014, proposed a new interval operator that generalizes the interval Gauss-Seidel method, by introducing a new parameter. He further proved both theoretically and numerically that incorporation of such parameter is more effective than the Gauss-Seidel method, and provides tightening solution set enclosure of interval linear systems. Parametric interval linear system of equations were investigated in [18, 6]. In [21], author studied the Hansen-Bliek-Rohn method and the Bauer-Skeel method and their modification based on the preconditioning of the system and on the residual form. The paper aims to develop the iterative methods and their convergency to solve interval linear systems with uncertain coefficients. More specifically, we generalize the interval Jacobi method and interval Gauss-Seidel method for solving interval linear systems and analyze the convergence of these methods.

Throughout the paper, the sets of all real intervals, the set of n-dimensional real interval vectors, and the set of $m\times n$ real interval matrices are denoted by $\mathbb{IR}$, $\mathbb{IR}^n$ and $\mathbb{IR}^{m,n}$, respectively. We write bold letters to represent interval matrices/vectors, whereas normal letters are used to represent real matrices/vectors. A real interval matrix of order $m \times n$ for two real matrices $\underline{A}$ and $\overline{A}$, is defined as $\mathbf{A} = \{A \in \mathbb{R}^{m,n} : \underline{A} \leq A \leq \overline{A}\}$, with componentwise inequality $\underline{A} \leq \overline{A}$.

Consider the following system of interval linear systems of equations

$$\mathbf{A}\mathbf{x} = \mathbf{b} \tag{1}$$

with $\mathbf{A} \in \mathbb{IR}^{n,n}$ and $\mathbf{b} \in \mathbb{IR}^n$ are given interval matrix and interval vector respectively, $\mathbf{x} \in \mathbb{IR}^n$ is unknown. The solution set of (1) is enclosed by

$$\Sigma(\mathbf{A}, \mathbf{b}) := \{\tilde{x} \in \mathbb{R}^n : \tilde{A}\tilde{x} = \tilde{b} \text{ for some } \tilde{A} \in \mathbf{A},\ \tilde{b} \in \mathbf{b}\}$$

The smallest interval enclosure of $\Sigma(\mathbf{A}, \mathbf{b})$ with regard to inclusion is represented by the interval $\mathbf{\Sigma} := \square\Sigma(\mathbf{A}, \mathbf{b}) = [\inf(\Sigma(\mathbf{A}, \mathbf{b})), \sup(\Sigma(\mathbf{A}, \mathbf{b}))]$, is known as the interval hull of the solution set $\Sigma(\mathbf{A}, \mathbf{b})$.

Let $\mathbf{D}$, $-\mathbf{E}$ and $-\mathbf{F}$ be respectively, represent the diagonal part, strictly lower triangular and strictly upper triangular parts of the interval matrix $\mathbf{A}$, so that $\mathbf{A} = \mathbf{D} - \mathbf{E} - \mathbf{F}$. If $0 \notin \mathbf{A}_{ii}$, then the interval Jacobi method and interval Gauss-Seidel method (see [3, 30]) for solving (1) are respectively, given by

$$\begin{aligned} \mathbf{x}^{(k+1)} &= \mathbf{D}^{-1}(\mathbf{E} + \mathbf{F})\mathbf{x}^{(k)} + \mathbf{D}^{-1}\mathbf{b} \\ \mathbf{x}^{(k+1)} &= (\mathbf{D} - \mathbf{E})^{-1}\mathbf{F}\mathbf{x}^{(k)} + (\mathbf{D} - \mathbf{E})^{-1}\mathbf{b}, \end{aligned} \tag{2}$$

We write $\mathbf{H}_J = \mathbf{D}^{-1}(\mathbf{E}+\mathbf{F})$ and $\mathbf{H}_{GS} = (\mathbf{D} - \mathbf{E})^{-1}\mathbf{F}$ to represent the iteration matrices for the interval Jacobi and interval Gauss-Seidel method, respectively. Details of interval Jacobi and Gauss-Seidel method for solving interval linear equations can be found in [3].

It is known from the literature that M-matrices, L-matrices, strictly diagonally dominant (SDD) and symmetric positive definite (SPD) matrices are among the classes of matrices for which both Jacobi and Gauss-Seidel methods converge for any initial guess for a given linear system of equations $Ax = b$. In [4], Salkuyeh generalized the Jacobi and Gauss-Seidel method by generalizing the diagonal matrix to a band matrix, which are given by the following iteration relations

$$x^{(k+1)} = T_m^{-1}(E_m + F_m)x^{(k)} + T_m^{-1}b \tag{3}$$

$$x^{(k+1)} = (T_m - E_m)^{-1}F_m x^{(k)} + (T_m - E_m)^{-1}b \tag{4}$$

where $m \geq 0$ and $F_m = A - T_m - E_m$ and

$$T_m = \begin{bmatrix} a_{1,1} & \cdots & a_{1,m+1} & 0 \\ \vdots & \ddots & \ddots & \\ a_{m+1,1} & & & a_{n-m,n} \\ & \ddots & \ddots & \\ 0 & & a_{n,n-m} & a_{n,n} \end{bmatrix}, \quad E_m = \begin{bmatrix} 0 & \cdots & 0 \\ -a_{m+2,1} & & \\ \vdots & \ddots & \vdots \\ -a_{n,1} & \cdots & -a_{n-m-1,n} \end{bmatrix}$$

Salkuyeh proved that if the coefficient matrix of a system of linear equations is either SDD or an M-matrix, then the generalized Jacobi (GJ) and generalized Gauss-Seidel (GGS) methods converge. In [22], authors proved the convergence of GJ and GGS methods for H-matrices, however both methods may fail to converge for SPD and for L-matrices.

In this paper we generalize the interval Gauss-Seidel and interval Jacobi methods similar to equation (3) and (4), respectively, to obtain a tighter enclosure of the solution set. As mentioned earlier, the iteration schemes defined in (3) and (4) converge for SDD, M-matrices and for H-matrices, so motivated by these results we verify the convergence criteria of both generalized interval Jacobi and interval Gauss-Seidel methods for these classes of interval coefficient matrices.

This paper is organized as follows: In Section 2, we provide the notations and basic definitions related to interval analysis and define various classes of interval matrices under consideration. We also listed a few well-known results that are used in our study. Section 3 introduces the generalization of interval Jacobi method and discuss the convergence analysis of the method for solving (1) for various classes of interval coefficient matrices. In section 4, we describe the generalized interval Gauss-Seidel method and its convergence analysis for various classes of interval coefficient matrices. Numerical experiments are carried out for the proposed methods in Section 5. Finally, Section 6 ends with some concluding remarks.

2 Notation and preliminaries

In accordance with the standard notations, intervals are marked by boldface throughout this article. To represent the lower and upper bounds of intervals respectively, the underscores and overscores notations are used. So, any interval $\mathbf{x}$ is written as $\mathbf{x} = [\underline{x}, \overline{x}]$. For the interval $\mathbf{x}$, *magnitude* and *mignitude* are defined respectively as, $|\mathbf{x}| := \max\{|x| : x \in \mathbf{x}\} = \max\{|\underline{x}|, |\overline{x}|\}$ and $\langle \mathbf{x} \rangle := \min\{|x| : x \in \mathbf{x}\} = \min\{|\underline{x}|, |\overline{x}|\}$. *Magnitude* and *mignitude* of interval matrix $\mathbf{A}$ are defined componentwise, and denoted by corresponding notations as defined for intervals. For a given interval matrix $\mathbf{A} = (\mathbf{A}_{ij}) \in \mathbb{IR}^{n,n}$, we denote $|\mathbf{A}| := (|\mathbf{A}|_{ij}) \in \mathbb{R}^{n,n}$, and the comparison matrix of $\mathbf{A}$ is represented by $\langle \mathbf{A} \rangle$, which has entries $\langle \mathbf{A} \rangle_{ii} = \langle \mathbf{A}_{ii} \rangle$ and $\langle \mathbf{A} \rangle_{ij} = -|\mathbf{A}_{ij}|$, for $i \neq j$. Note that both $|\mathbf{A}|$ and $\langle \mathbf{A} \rangle$ are real matrices. Next we provide some properties of the interval matrices, and define various classes of interval matrices under consideration.

Definition 2.1. [3, 10, 11] An interval matrix $\mathbf{A} \in \mathbb{IR}^{n,n}$ is said to be *regular* if every $A \in \mathbf{A}$ is nonsingular. For a *regular* $\mathbf{A}$, the inverse $\mathbf{A}^{-1}$ is defined as

$$\mathbf{A}^{-1} := \square\{A^{-1} : A \in \mathbf{A}\}$$

where $\square\Sigma := [\inf \Sigma,\ \sup \Sigma]$ denotes the hull of Σ, which is the tightest enclosure for Σ. It is to be noted that the smallest interval matrix $\mathbf{A}^{-1}$ includes the set $\{A^{-1} : A \in \mathbf{A}\}$.

Definition 2.2. [3] For any real intervals $\mathbf{x} = [\underline{x}, \overline{x}], \mathbf{y} = [\underline{y}, \overline{y}]$, interval addition, subtraction and multiplication are defined as

(i) $\mathbf{x} + \mathbf{y} = [\underline{x} + \underline{y},\ \overline{x} + \overline{y}]$

(ii) $\mathbf{x} - \mathbf{y} = [\underline{x} - \overline{y},\ \overline{x} - \underline{y}]$

(iii) The interval multiplication $\mathbf{xy}$ is displayed in the following table:

$*$	$\mathbf{y} \geq 0$	$\mathbf{y} \ni 0$	$\mathbf{y} \leq 0$
$\mathbf{x} \geq 0$	$[\underline{x}\underline{y}, \overline{x}\overline{y}]$	$[\overline{x}\underline{y}, \overline{x}\overline{y}]$	$[\overline{x}\underline{y}, \underline{x}\overline{y}]$
$\mathbf{x} \ni 0$	$[\underline{x}\overline{y}, \overline{x}\overline{y}]$	$[\min\{\underline{x}\overline{y}, \overline{x}\underline{y}\}, \max\{\underline{x}\underline{y}, \overline{x}\overline{y}\}]$	$[\overline{x}\underline{y}, \underline{x}\underline{y}]$
$\mathbf{x} \leq 0$	$[\underline{x}\overline{y}, \overline{x}\underline{y}]$	$[\underline{x}\overline{y}, \underline{x}\underline{y}]$	$[\overline{x}\overline{y}, \underline{x}\underline{y}]$

Definition 2.3. [3] If $\mathbf{A}, \mathbf{B} \in \mathbb{IR}^{m,n}$, addition and subtraction for interval matrices are defined as

(i) $\mathbf{A} + \mathbf{B} = \square\{A + B :\ A \in \mathbf{A},\ B \in \mathbf{B}\}$

(ii) $\mathbf{A} - \mathbf{B} = \square\{A - B :\ A \in \mathbf{A},\ B \in \mathbf{B}\}$

If $\mathbf{A} = [\underline{A}, \overline{A}]$ and $\mathbf{B} = [\underline{B}, \overline{B}]$, then

$$\mathbf{A} + \mathbf{B} = [\underline{A} + \underline{B},\ \overline{A} + \overline{B}] \quad \text{and} \quad \mathbf{A} - \mathbf{B} = [\underline{A} - \overline{B},\ \overline{A} - \underline{B}\ ]$$

Definition 2.4. [3] If $\mathbf{A} \in \mathbb{IR}^{m,n}$ and $\mathbf{B} \in \mathbb{IR}^{n,p}$, then $\mathbf{AB} \in \mathbb{IR}^{m,p}$ is defined as

$$\mathbf{AB} = \square\{\tilde{A}\tilde{B} : \tilde{A} \in \mathbf{A},\ \tilde{B} \in \mathbf{B}\}$$

If $\mathbf{A} = (\mathbf{A}_{ij})$ and $\mathbf{B} = (\mathbf{B}_{ij})$, then $(\mathbf{AB})_{ik} = \sum\limits_{j=1}^{n} \mathbf{A}_{ij}\mathbf{B}_{jk}$

Definition 2.5. [3, 14] Let $\mathbf{A} \in \mathbb{IR}^{n,n}$ and $0 \notin \mathbf{A}_{ii}$ for all i. If the comparison matrix $\langle \mathbf{A} \rangle$ of $\mathbf{A}$ is strictly diagonally dominant,that is, if for all i, $\langle \mathbf{A}_{ii} \rangle > \sum\limits_{j \neq i} |\mathbf{A}_{ij}|$ then $\mathbf{A}$ is known to be an interval *strictly diagonally dominant* (SDD) matrix.

Definition 2.6. [1, 3] A real matrix $A \in \mathbb{R}^{n,n}$ is called an *L-matrix* if it has positive diagonal entries and nonpositive off-diagonal entries. An interval matrix $\mathbf{A} = [\underline{A}, \overline{A}]$ is an *interval L-matrix* if each $A \in \mathbf{A}$ is an L-matrix, equivalently, if $\underline{A}_{ii} > 0$ for all i and $\overline{A}_{ij} \leq 0$, for $i \neq j$.

Definition 2.7. [1] A matrix $A \in \mathbb{R}^{n,n}$ is said to be a *Z-matrix* if A has nonpositive off-diagonal entries. If a Z-matrix A can be written as $A = \alpha I - B$, where $\alpha > \rho(B)$, the spectral radius of B, then A is called an *M-matrix.* Instead of nonsingular M-matrix we write M-matrix for convenience. A *Z-matrix A* becomes an *M-matrix* if and only if there exists a $u > 0$ such that $Au > 0$.

We now state the characterization of M-matrices.

Theorem 2.8. [1] Let $A \in \mathbb{R}^{n,n}$ be a Z-matrix. Then following equivalent conditions hold:

(i) A is an M-matrix.

(ii) $A^{-1} \geq 0$.

(iii) There exists $u > 0$ such that $Au > 0$.

Definition 2.9. [3] An *interval M-matrix* is a square interval matrix $\mathbf{A} \in \mathbb{IR}^{n,n}$ such that $\mathbf{A}_{ik} \leq 0$, that is, every element in $\mathbf{A}_{ik}$ is nonpositive, for all $i \neq k$ and $\mathbf{A}u > 0$ for some real $u > 0$.

Definition 2.10. [3] An *interval H-matrix* $\mathbf{A} \in \mathbb{IR}^{n,n}$ is an interval matrix whose comparison matrix $\langle \mathbf{A} \rangle$ is an M-matrix. Equivalently, we say that $\mathbf{A}$ is an interval H-matrix if and only if $\langle \mathbf{A} \rangle u > 0$ for some $u > 0$.

Definition 2.11. [1] A splitting of a real $n \times n$ matrix A is defined as $A = M - N$, with nonsingular M. A splitting $A = M - N$ of the matrix A is said to be

(i) *regular* if $M^{-1} \geq 0$ and $N \geq 0$.

(ii) *weak regular* if $M^{-1} \geq 0$ and $M^{-1}N \geq 0$.

(iii) *M-splitting* if M is a M-matrix and $N \geq 0$.

Definition 2.12. A *splitting* of a square interval matrix $\mathbf{A} \in \mathbb{IR}^{n,n}$ is defined as $\mathbf{A} = \mathbf{M} - \mathbf{N}$, with regular $\mathbf{M}$.

Next we state few basic results on matrices, that are required to establish our results in the subsequent sections.

Proposition 1. [3, 23] If $A, B \in \mathbb{R}^{n,n}$, and $|A| \leq B$, then $\rho(A) \leq \rho(B)$.

Theorem 2.13. [1] Let A be an M-matrix and let $A = M - N$ be a regular or weak regular splitting of A, then $\rho(M^{-1}N) < 1$.

Theorem 2.14. [27] Let M-splitting of A be $A = M - N$. Then $\rho(M^{-1}N) < 1$ if and only if A is a nonsingular M-matrix.

Theorem 2.15. [1, 13, 23] Let A be a nonnegative matrix. Then

(i) If $\alpha \in \mathbb{R}$ and $Ax \geq \alpha x$, for some positive $x \in \mathbb{R}^n$, then $\rho(A) \geq \alpha$.

(ii) If $Ax \leq \alpha x$ for some $x \geq (\neq) 0$, then $\rho(A) \leq \alpha$.

Theorem 2.16. [23] If A is nonnegative matrix, then $\rho(A)$ is an eigenvalue of A and there is a nonnegative nonzero vector x such that $Ax = \rho(A)x$.

For convenience we have provided some well-known results on interval matrices that will be used to check the convergence of the mentioned methods in next sections of this paper.

Theorem 2.17. [3] Let $\mathbf{A}, \mathbf{B} \in \mathbb{IR}^{n,n}$. Then following conditions hold:

(i) If $\mathbf{A}$ is an M-matrix and $\mathbf{B} \subseteq \mathbf{A}$, then $\mathbf{B}$ is an M-matrix. Each $\tilde{A} \in \mathbf{A}$ in particular, is an M-matrix.

(ii) $\mathbf{A} = [\underline{A},\ \overline{A}]$ is an M-matrix if and only if $\underline{A}$ and $\overline{A}$ are M-matrices.

(iii) Every M-matrix $\mathbf{A} = [\underline{A},\ \overline{A}]$ is regular with $\mathbf{A}^{-1} = [\overline{A}^{-1}, \underline{A}^{-1}] \geq 0$ and $|\mathbf{A}^{-1}| = \langle \mathbf{A} \rangle^{-1}$.

Theorem 2.18. [14] For an interval matrix $\mathbf{A}$ we have

(i) if $\mathbf{A}$ is interval triangular (lower/upper) matrix, then $\mathbf{A}$ is an interval H-matrix.

(ii) if $\mathbf{A}$ is an interval H-matrix, then $|\mathbf{A}^{-1}| \leq \langle \mathbf{A} \rangle^{-1}$. Equality holds if $\mathbf{A}$ is an interval M-matrix.

Proposition 2. [3] For $\mathbf{A}, \mathbf{B} \in \mathbb{IR}^{n,n}$ and $\mathbf{C} \in \mathbb{IR}^{n,q}$, the properties listed below hold:

(i) $\langle \mathbf{A} \rangle = \langle \tilde{A} \rangle$, for some $\tilde{A} \in \mathbf{A}$.

(ii) $|\mathbf{AB}| \leq |\mathbf{A}||\mathbf{B}|$

(iii) $\langle \mathbf{A} \pm \mathbf{B} \rangle \geq \langle \mathbf{A} \rangle - |\mathbf{B}|$.

(iv) $|\mathbf{A}| - |\mathbf{B}| \leq |\mathbf{A} \pm \mathbf{B}| \leq |\mathbf{A}| + |\mathbf{B}|$.

(v) $|\mathbf{AC}| \geq \langle \mathbf{A} \rangle |\mathbf{C}|$.

Theorem 2.19. [14] Let $\mathbf{C}, \mathbf{D} \in \mathbb{IR}^{n,n}$ satisfy $\rho(|\mathbf{C}||\mathbf{D}|) < 1$. Then for any $\mathbf{g} \in \mathbb{IR}^n$, the following statements hold:

(i) The equation $\mathbf{x} = \mathbf{C}(\mathbf{Dx} + \mathbf{g})$ has a unique solution $\mathbf{x} \in \mathbb{IR}^n$

(ii) For any initial vector $\mathbf{x}^0 \in \mathbb{IR}^n$, the iteration

$$\mathbf{x}^{(k+1)} = \mathbf{C}(\mathbf{Dx}^{(k)} + \mathbf{g}),\ k = 0, 1, ...$$

converges to the solution $\mathbf{x}$ of the equation $\mathbf{x} = \mathbf{C}(\mathbf{Dx} + \mathbf{g})$.

3 Generalized Interval Jacobi method

In this section, we propose a generalization of the interval Jacobi method for solving interval linear system similar to that of generalized Jacobi method introduced by Salkuyeh [5] and Saha *et al.* [22] for solving linear systems of matrix equations. Furthermore, we study the convergence properties of the proposed method for solving interval linear system with the coefficient matrix as either an interval SDD matrix, an interval M-matrix or an interval H-matrix.

In Section 2 the splitting of $\mathbf{A}$ for interval Jacobi method for solving (1) is given in equation (2) as $\mathbf{A} = \mathbf{M} - \mathbf{N}$ with $\mathbf{M} = \mathbf{D},\ \mathbf{N} = \mathbf{E} + \mathbf{F}$.

We now propose generalized interval Jacobi (GIJ) method for solving interval linear system similar to (3) and (4), which was introduced by Salkuyeh [4] for general matrices.

Let $\mathbf{A} = [\underline{a_{ij}}, \overline{a_{ij}}]$ be a square interval matrix of order n. Consider an interval band matrix $\mathbf{T}_m = [\underline{t_{ij}}, \overline{t_{ij}}]$ of $2m + 1$ bandwidth, which is characterized as

$$\mathbf{t}_{ij} = \begin{cases} [\underline{a_{ij}}, \overline{a_{ij}}], & \text{if } |i - j| \leq m \\ 0, & \text{elsewhere} \end{cases}$$

For $1 \leq m < n$, interval matrix $\mathbf{A}$ is decomposed as $\mathbf{A} = \mathbf{T}_m - \mathbf{E}_m - \mathbf{F}_m$, with strict lower part -$\mathbf{E}_m$ and strict upper part -$\mathbf{F}_m$ of $\mathbf{A}$. The interval matrices $\mathbf{T}_m,\ \mathbf{E}_m$ and $\mathbf{F}_m$ are expressed as follows

$$\mathbf{T}_m = \begin{bmatrix} & [\underline{a_{11}}, \overline{a_{11}}] & \cdots & [\underline{a_{1,m+1}}, \overline{a_{1,m+1}}] & & 0 \\ & \vdots & \ddots & & \ddots & \\ [\underline{a_{m+1,1}}, \overline{a_{m+1,1}}] & & & & & [\underline{a_{n-m,n}}, \overline{a_{n-m,n}}] \\ & & \ddots & & \ddots & \\ & 0 & & [\underline{a_{n,n-m}}, \overline{a_{n,n-m}}] & & [\underline{a_{n,n}}, \overline{a_{n,n}}] \end{bmatrix},$$

$$\mathbf{E}_m = \begin{bmatrix} & 0 & \cdots & & 0 \\ -[\underline{a_{m+2,1}}, \overline{a_{m+2,1}}] & & & & \\ & \vdots & \ddots & & \vdots \\ & -[\underline{a_{n,1}}, \overline{a_{n,1}}] & \cdots & & -[\underline{a_{n-m-1,n}}, \overline{a_{n-m-1,n}}] \end{bmatrix},$$

$$\mathbf{F}_m = \begin{bmatrix} 0 & -[\underline{a_{1,m+2}}, \overline{a_{1,m+2}}] & & \cdots - [\underline{a_{1,n}}, \overline{a_{1,n}}] \\ \vdots & & \ddots & \vdots \\ 0 & & \cdots & -[\underline{a_{n-m-1,n}}, \overline{a_{n-m-1,n}}] \\ & & & \end{bmatrix} \tag{5}$$

Definition 3.1. Let $\mathbf{T}_m$, $\mathbf{E}_m$ and $\mathbf{F}_m$ be the interval matrices specified in (5). For any $1 \leq m < n$ decompose $\mathbf{A}$ as

$$\mathbf{A} = \mathbf{T}_m - \mathbf{E}_m - \mathbf{F}_m \tag{6}$$

which is corresponding to splitting

$$\mathbf{A} = \mathbf{M}_m - \mathbf{N}_m \tag{7}$$

with $\mathbf{M}_m = \mathbf{T}_m$ and $\mathbf{N}_m = \mathbf{E}_m + \mathbf{F}_m$. Then *generalized interval Jacobi* (GIJ) method to solve (1) is defined as,

$$\mathbf{x}^{(k+1)} = \mathbf{M}_m^{-1} \left(\mathbf{N}_m \mathbf{x}^{(k)} + \mathbf{b}\right) \tag{8}$$

For GIJ method $\mathbf{L} = \mathbf{T}_m^{-1}(\mathbf{E}_m + \mathbf{F}_m)$ is the iteration interval matrix. By decomposing $\mathbf{T}_m = \mathbf{D} + \mathbf{R}_m$, $\mathbf{A}$ can also be written as

$$\mathbf{A} = \mathbf{D} + \mathbf{R}_m - \mathbf{E}_m - \mathbf{F}_m \tag{9}$$

Remark 3.2. From (6), we can decompose $\langle \mathbf{A} \rangle$ as

$$\langle \mathbf{A} \rangle = \langle \mathbf{T}_m \rangle - |\mathbf{E}_m| - |\mathbf{F}_m| = \langle \mathbf{D} \rangle - |\mathbf{R}_m| - |\mathbf{E}_m| - |\mathbf{F}_m| \tag{10}$$

and is associated with the splitting

$$\langle \mathbf{A} \rangle = \langle \mathbf{M}_m \rangle - |\mathbf{N}_m| \tag{11}$$

with $\widetilde{M_1} = \langle \mathbf{M}_m \rangle = \langle \mathbf{T}_m \rangle = \langle \mathbf{D} \rangle - |\mathbf{R}_m|$ and $\widetilde{N}_1 = |\mathbf{N}_m| = |\mathbf{E}_m| + |\mathbf{F}_m|$.

Notation. Throughout the paper following notations are used:

$$\mathbf{R}_m = (\mathbf{R}_{ij}), \quad \mathbf{E}_m = (\mathbf{E}_{ij}), \quad \mathbf{F}_m = (\mathbf{F}_{ij})$$
$$\widetilde{R}_i = \sum_{\substack{j=1\\ j\neq i}}^{n} |\mathbf{R}_{ij}|, \quad \widetilde{E}_i = \sum_{\substack{j=1\\ j\neq i}}^{n} |\mathbf{E}_{ij}|, \quad \widetilde{F}_i = \sum_{\substack{j=1\\ j\neq i}}^{n} |\mathbf{F}_{ij}|$$

3.1 Convergence analysis of GIJ method

In this section we discuss the convergence criterion of GIJ method for solving interval linear system (1) with various classes of coefficient interval matrices. In particular we show that the GIJ method is convergent for interval SDD matrices, interval M-matrices and interval H-matrices using the idea of interval splitting as well as the various characterizations of interval M- and interval H-matrices.

Throughout the section we consider the splitting of $\mathbf{A}$ defined in (7) and (10). More specifically, we write $\mathbf{M}_m := \mathbf{T}_m$ and $\mathbf{N}_m := \mathbf{E}_m + \mathbf{F}_m$. It is known that GIJ method converges if $\rho(|\mathbf{M}_m^{-1}||\mathbf{N}_m|) < 1$ due to Theorem 2.19. Since computing the inverse of interval matrix is NP-hard, so we use the matrix $\widetilde{L}_m = \langle \mathbf{M}_m \rangle^{-1} |\mathbf{N}_m| = \tilde{M}_1^{-1}\tilde{N}_1$ to check the convergence of GIJ method. The following theorem provides a relation between the spectral radius of the iteration matrix $\widehat{L}_m = |\mathbf{M}_m^{-1}||\mathbf{N}_m|$ with $\widetilde{L}_m = \langle \mathbf{M}_m \rangle^{-1} |\mathbf{N}_m| = \tilde{M}_1^{-1}\tilde{N}_1$.

Theorem 3.3. Let $\widehat{L}_m = |\mathbf{M}_m^{-1}||\mathbf{N}_m|$ and $\widetilde{L}_m = \langle \mathbf{M}_m \rangle^{-1} |\mathbf{N}_m| = \widetilde{M_1}^{-1}\widetilde{N}_1$. If $\mathbf{M}_m$ is an interval H-matrix (or interval M-matrix) then the following results hold

(i) $\widehat{L}_m \leq \widetilde{L}_m$ (equality holds if $\mathbf{M}_m$ is an interval M-matrix)

(ii) $\rho(\widehat{L}_m) \leq \rho(\widetilde{L}_m)$.

Proof. (i) As $\mathbf{M}_m$ is given an interval H-matrix, from Theorem 2.18 we have that
$$\widehat{L}_m = |\mathbf{M}_m^{-1}||\mathbf{N}_m| \leq \langle \mathbf{M}_m \rangle^{-1} |\mathbf{N}_m| = \widetilde{L}_m$$

(ii) It follows from (i) and from Proposition 1. □

Remark 3.4. The above theorem shows that if $\rho(\widetilde{L}_m) < 1$, then GIJ converges. This idea has been used to check the convergence of GIJ method in case $\mathbf{M}_m$ is an interval H-(or M-) matrix.

Remark 3.5. [3, 29] Interval SDD matrices are a special case of interval H-matrices, that is, interval SDD matrices $\mathbf{A} = (\mathbf{a}_{ij})$ that satisfy for all i, $\langle \mathbf{A}_{ii} \rangle > \sum_{j\neq i} |\mathbf{A}_{ij}|$, are H-matrices.

Following theorem gives an upper bound for the spectral radius of the matrix $\widetilde{L}_m$ of GIJ method to solve linear interval equations with interval SDD matrix as coefficient interval matrix.

Theorem 3.6. For any $1 \le i \le n$, let $\langle \mathbf{T} \rangle_i = \langle \mathbf{D}_{ii} \rangle - \widetilde{R}_i > 0$. Then

$$\rho(\widetilde{L}_m) \le \max_{i \in \mathbb{N}} \frac{\widetilde{E}_i + \tilde{F}_i}{\langle \mathbf{T} \rangle_i}$$

Proof. Suppose that λ is an eigenvalue of the matrix $\widetilde{L}_m$ satisfying

$$|\lambda| > \max_{i \in \mathbb{N}} \frac{\widetilde{E}_i + \widetilde{F}_i}{\langle \mathbf{T} \rangle_i} = \frac{\widetilde{E}_i + \widetilde{F}_i}{\langle \mathbf{D}_{ii} \rangle - \sum\limits_{\substack{j=1 \\ j \ne i}}^{n} |\mathbf{R}_{ij}|}, \text{ for all } 1 \le i \le n \tag{12}$$

which implies that

$$|\lambda \langle \mathbf{D}_{ii} \rangle| = |\lambda| \langle \mathbf{D}_{ii} \rangle > \widetilde{E}_i + \widetilde{F}_i + |\lambda| \sum_{\substack{j=1 \\ j \ne i}}^{n} |\mathbf{R}_{ij}| \tag{13}$$

Now $\det(\lambda I - \widetilde{L}_m) = 0$ implies $\det(\langle \mathbf{T}_m \rangle^{-1}) \det(C_1) = 0$ where $C_1 = \lambda \langle \mathbf{T}_m \rangle - |\mathbf{E}_m| - |\mathbf{F}_m|$, which again implies that $\det(C_1) = 0$. This is a contradiction to the fact that C_1 is SDD and hence nonsingular. Thus,

$$\rho(\widetilde{L}_m) \le \max_{1 \le i \le n} \frac{\tilde{E}_i + \tilde{F}_i}{\langle \mathbf{T} \rangle_i}$$

□

Following results show the convergence of GIJ for interval SDD matrices.

Theorem 3.7. For interval SDD matrix $\mathbf{A}$, GIJ method (8) converges for any initial guess.

Proof. Let $\mathbf{A}$ be an interval SDD matrix. Decompose $\mathbf{A}$ as in (6). As $\mathbf{A}$ is a SDD matrix, so is the matrix $\mathbf{M}_m$, that is

$$\langle \mathbf{D}_{ii} \rangle > \sum_{j \ne i} |\mathbf{R}_{ij}|$$

Then $\mathbf{M}_m$ is an interval SDD matrix and hence an H-matrix due to the Remark 3.5.

Suppose λ is an eigenvalue of $\widetilde{L}_m$ and $|\lambda| \ge 1$. Then we have that

$$\begin{aligned} \det(\lambda I - \widetilde{L}_m) = 0 &\Rightarrow \det(\lambda \langle \mathbf{M}_m \rangle - |\mathbf{N}_m|) = 0 \\ &\Rightarrow \det(\lambda \langle \mathbf{D} \rangle - \lambda |\mathbf{R}_m| - |\mathbf{N}_m|) = 0 \\ &\Rightarrow \det\left(\langle \mathbf{D} \rangle - |\mathbf{R}_m| - \frac{1}{\lambda} |\mathbf{N}_m|\right) = 0 \\ &\Rightarrow \det\left(\langle \mathbf{D} \rangle - |\mathbf{R}_m| - \frac{1}{\lambda} |\mathbf{E}_m| - \frac{1}{\lambda} |\mathbf{F}_m|\right) = 0 \end{aligned}$$

This shows that the matrix $Q = (\langle \mathbf{D} \rangle - |\mathbf{R}_m| - \frac{1}{\lambda}|\mathbf{E}_m| - \frac{1}{\lambda}|\mathbf{F}_m|)$ is singular. As $|\lambda| \geq 1$, that is, $\frac{1}{|\lambda|} \leq 1$ and hence $\mathbf{A}$ is SDD implies that Q is SDD, a contradiction to the fact that Q is singular. Thus $\rho(\widetilde{L}_m) < 1$ and the result holds for interval SDD matrix. ☐

Next two theorems provide the convergence criteria of GIJ method for two important classes under consideration, namely, the classes of interval M-matrices and interval H-matrices.

Theorem 3.8. GIJ method converges for interval M-matrix $\mathbf{A}$, for any $m \leq n$.

Proof. Let $\mathbf{A}$ be an interval M-matrix of order n. Then by Theorem 2.17 (iii), $\langle \mathbf{A} \rangle^{-1} \geq 0$. Since $\langle \mathbf{A} \rangle$ is a Z-matrix, Theorem 2.8 implies that $\langle \mathbf{A} \rangle$ is an M-matrix. Let $\langle \mathbf{A} \rangle = \widetilde{M}_1 - \widetilde{N}_1$ be the splitting of $\langle \mathbf{A} \rangle$ defined in (11). As $\langle \mathbf{A} \rangle$ is M-matrix, there exists $u > 0$ such that $\langle \mathbf{A} \rangle u > 0$ which implies that $\langle \mathbf{M}_m \rangle u > 0$, that is, $\widetilde{M}_1 u > 0$. Thus $\widetilde{M}_1$ is an M-matrix, by Theorem 2.8. Also, $\widetilde{N}_1 \geq 0$. Therefore, $\langle \mathbf{A} \rangle = \widetilde{M}_1 - \widetilde{N}_1$ is regular splitting, and hence by Theorem 2.13, $\rho(\widetilde{L}_m) < 1$. It is obvious that $\mathbf{M}_m$ is an interval M-matrix and hence Remark 3.4 implies that GIJ converges, for any initial guess. ☐

Theorem 3.9. GIJ method for solving interval linear system converges for interval H-matrix $\mathbf{A}$.

Proof. Let $\mathbf{A}$ be an interval H-matrix, so that the matrix $\langle \mathbf{A} \rangle$ is an M-matrix. Then as shown in Theorem 3.8, it can be proved that $\rho(\widetilde{L}_m) < 1$, which implies that GIJ method converges for interval H-matrix. ☐

4 Generalized interval Gauss-Seidel method

The interval Gauss-Seidel method for solving system of interval linear equations was introduced by Neumaier [3] and Moore [25]. In [4, 22], authors considered generalized Gauss-Seidel method (a particular case of AOR method) and discussed convergence properties thoroughly for various classes of matrices, like, SDD, SPD, M-matrices, L-matrices and for H-matrices as the coefficient matrices of the linear system. Using the similar approach we now propose generalized version of interval Gauss-Seidel (GIGS) method for solving interval linear systems. It is shown in [22] that generalized Gauss-Seidel may not converge for SPD and for L-matrices. Since general matrices are particular case of interval matrices, so this section is emphasised on checking the convergence of generalized interval Gauss-Seidel (GIGS) method, only for interval SDD matrices, interval M-matrices and for interval H-matrices. We now begin with defining iteration steps for generalized interval Gauss-Seidel method.

Definition 4.1. Consider the decomposition of $\mathbf{A}$, defined in equation (7) and the splitting

$$\mathbf{A} = \mathbf{M}_m - \mathbf{N}_m \tag{14}$$

where $\mathbf{M}_m = \mathbf{T}_m - \mathbf{E}_m$ and $\mathbf{N}_m = \mathbf{F}_m$. Then the iteration step for GIGS method to solve the interval linear system (1), is defined as,

$$\mathbf{x}^{(k+1)} = \mathbf{M}_m^{-1}\left(\mathbf{N}_m\mathbf{x}^{(k)} + \mathbf{b}\right) \tag{15}$$

Further decompose $\langle\mathbf{A}\rangle$ same as in (10) and consider the associated splitting (11) where

$$M_1 = \langle\mathbf{M}_m\rangle = \langle\mathbf{T}_m\rangle - |\mathbf{E}_m|, \quad N_1 = |\mathbf{N}_m| = |\mathbf{F}_m| \tag{16}$$

Now we emphasize on the convergence of GIGS method for interval SDD-matrices, interval matrices H-matrices and for interval M-matrices.

4.1 Convergence analysis of GIGS method

Convergence analysis of GIGS method is similar to that of GIJ method discussed in Section 3. For interval Gauss-Seidel method the splitting of $\mathbf{A}$ is considered as $\mathbf{A} = \mathbf{M} - \mathbf{N}$ with $\mathbf{M} = \mathbf{D} - \mathbf{E}$ and $\mathbf{N} = \mathbf{F}$ and the iteration matrix is given by $\mathbf{M}^{-1}\mathbf{N}$. If $\acute{G} := |\mathbf{M}^{-1}||\mathbf{N}|$ and $C := \langle\mathbf{M}\rangle^{-1}|\mathbf{N}|$, then from Theorem 2.19, it is known that interval Gauss-Seidel method converges if $\rho(\acute{G}) < 1$.

Following two results are immediate consequences of Theorem 2.18 and hence the proofs are skipped.

Theorem 4.2. If $\mathbf{M}$ is interval H-matrix then the following results hold

(i) $\acute{G} \leq C$.

(ii) $\rho(\acute{G}) \leq \rho(C)$ (equality holds if $\mathbf{M}$ is an interval M-matrix).

Theorem 4.3. Consider the splitting as given in equation (14) and (16). Let $\widetilde{G} = |\mathbf{M}_m{}^{-1}| \cdot |\mathbf{N}_m|$ and $C_m = \langle\mathbf{M}_m\rangle^{-1}|\mathbf{N}_m| = M_1^{-1}N_1$. If $\mathbf{M}_m$ is an interval H-matrix (or interval M-matrix) then the following results hold:

(i) $\widetilde{G} \leq C_m$ (equality holds if $\mathbf{M}_m$ is an interval M-matrix).

(ii) $\rho(\widetilde{G}) \leq \rho(C_m)$.

Remark 4.4. From the above results, it is obvious that if $\rho(C_m) < 1$ (with $C_0 = C$), then GIGS method converges, which will be used to prove the convergence of GIGS method in the succeeding results.

All through this section, we stick to the following notations:

(i) $\acute{G} := |\mathbf{M}^{-1}||\mathbf{N}|$, with $\mathbf{M} = \mathbf{D} - \mathbf{E}$ and $\mathbf{N} = \mathbf{F}$

(ii) $C := \langle\mathbf{M}\rangle^{-1}|\mathbf{N}|$.

(iii) $\widetilde{G} := |\mathbf{M}_m{}^{-1}| \cdot |\mathbf{N}_m|$, with $\mathbf{M}_m = \mathbf{T}_m - \mathbf{E}_m$ and $\mathbf{N}_m = \mathbf{F}_m$

(iv) $C_m := \langle\mathbf{M}_m\rangle^{-1}|\mathbf{N}_m| = M_1^{-1}N_1$

We begin our results with the following theorem that presents a spectral bound of C_m and hence for $\widetilde{G}$.

Theorem 4.5. Let $\mathbf{A}$ be an interval SDD matrix. Suppose $C_m = \langle \mathbf{T}_m - \mathbf{E}_m \rangle^{-1} |\mathbf{F}_m|$. Let $\widetilde{R}_i, \widetilde{E}_i, \widetilde{F}_i$ be defined same as in Notation 3, and, let $\langle \mathbf{T} \rangle_i = \langle \mathbf{D}_{ii} \rangle - \widetilde{R}_i$. If $\langle \mathbf{T} \rangle_i > \widetilde{E}_i$, $\forall i \in N$ then $\rho(C_m) \leq \max\limits_{i \in \langle n \rangle} \left(\dfrac{\widetilde{F}_i}{\langle \mathbf{T} \rangle_i - \widetilde{E}_i} \right)$, where $\langle n \rangle = \{1, 2, \ldots, n\}$.

Proof. Let λ be an eigenvalue C_m. Choose $x \neq 0 \in \mathbb{R}^n$ such that

$$\begin{aligned} C_m x = \lambda x \quad &\Rightarrow \quad \langle \mathbf{T}_m - \mathbf{E}_m \rangle^{-1} |\mathbf{F}_m| x = \lambda x \\ &\Rightarrow \quad (\lambda \langle \mathbf{T}_m \rangle - \lambda |\mathbf{E}_m| - |\mathbf{F}_m|) x = 0 \\ &\Rightarrow \quad [(\lambda \langle \mathbf{D} \rangle - \lambda |\mathbf{R}_m| - \lambda |\mathbf{E}_m| - |\mathbf{F}_m|] \, x = 0 \\ &\Rightarrow \quad \left[\langle \mathbf{D} \rangle - |\mathbf{R}_m| - |\mathbf{E}_m| - \frac{1}{\lambda} |\mathbf{F}_m| \right] x = 0 \end{aligned}$$

Therefore the matrix $Q = \langle \mathbf{D} \rangle - |\mathbf{R}_m| - |\mathbf{E}_m| - \frac{1}{\lambda} |\mathbf{F}_m|$ is singular, which implies Q is not SDD. Hence there exists an $i \in N$ such that

$$\langle \mathbf{D}_{ii} \rangle \leq \widetilde{R}_i + \widetilde{E}_i + \left| \frac{1}{\lambda} \right| \widetilde{F}_i$$

After simplification we get

$$|\lambda| \leq \max_{i \in \langle n \rangle} \frac{\widetilde{F}_i}{(|\mathbf{D}_{ii}| - \widetilde{R}_i) - \widetilde{E}_i}$$

which implies that

$$\rho(C_m) \leq \max_{i \in \langle n \rangle} \frac{\widetilde{F}_i}{\langle \mathbf{T} \rangle_i - \widetilde{E}_i}$$

□

Note that above theorem provides a spectral upper bound of C_m and hence of the iteration matrix $\widetilde{G}$ of the GIGS method.

Lemma 4.6. If $\mathbf{A} = \mathbf{T}_m - \mathbf{E}_m - \mathbf{F}_m$ be an interval SDD-matrix, then $\mathbf{M}_m = \mathbf{T}_m - \mathbf{E}_m$ is an interval H-matrix.

Proof. As $\mathbf{A}$ is an interval SDD matrix, the comparison matrix $\langle \mathbf{A} \rangle$ of $\mathbf{A}$ satisfies $\langle \mathbf{A}_{ii} \rangle > \sum\limits_{j \neq i} |\mathbf{A}_{ij}|$, for all i. Then

$$\langle \mathbf{A}_{ii} \rangle > \sum_{j \neq i} |\mathbf{A}_{ij}| \geq \sum_{\substack{j \neq i \\ |i-j| \leq m}} |\mathbf{A}_{ij}| + \sum_{i > j+m} |\mathbf{A}_{ij}|$$

which shows that $\mathbf{M}_m$ is an interval SDD matrix, hence an interval H-matrix by Remark 3.5. □

Theorem 4.7. GIGS method given in (2) converges for interval SDD matrix $\mathbf{A}$, for any initial guess.

Proof. Let $\mathbf{A}$ be an interval SDD matrix. Consider the splitting of $\mathbf{A}$ as mentioned in equation (14). Then $\mathbf{M}_m = \mathbf{T}_m - \mathbf{E}_m$ is an interval H-matrix by Lemma 4.6. Thus it suffices to show $\rho(C_m) < 1$.

Suppose that λ is an eigenvalue of C_m and $|\lambda| \geq 1$. Take $Q = \langle \mathbf{D} \rangle - |\mathbf{R}_m| - |\mathbf{E}_m| - \frac{1}{\lambda}|\mathbf{F}_m|$. Now $\frac{1}{|\lambda|} \leq 1$ and $\mathbf{A}$ is SDD imply that Q is SDD. Again as shown in Theorem 4.5, we can prove that $\det(Q) = 0$, which contradicts the fact that Q is SDD. Hence $\rho(C_m) < 1$ and thus the result holds for interval SDD matrix. ☐

The successive two theorems analyze the convergence of GIGS method for interval M-matrices.

Theorem 4.8. GIGS method for solving (1) converges for interval M-matrix $\mathbf{A}$.

Proof. Let $\mathbf{A}$ be an interval M-matrix, then $\langle \mathbf{A} \rangle$ is an M-matrix by Theorem 2.17(iii). Consider the decomposition of $\mathbf{A}$ and $\langle \mathbf{A} \rangle$ respectively, defined in (6) and (10). As $\mathbf{A} = \mathbf{M}_m - \mathbf{N}_m$ is interval M-matrix, there exists $v > 0$ such that $\mathbf{A}v > 0$ which signifies that $\mathbf{M}_m v > 0$, because $\mathbf{N}_m \geq 0$. Hence $\mathbf{M}_m$ is an interval M-matrix. We need to show $\rho(\widetilde{G}) < 1$.

Since $\langle \mathbf{A} \rangle = M_1 - N_1$, where M_1 and N_1 mentioned in equation (16), is an M-matrix, we can choose $u > 0$ such that $\langle \mathbf{A} \rangle u > 0$ which leads to $M_1 u > 0$ that shows M_1 is an M-matrix. By Definition 2.11, $\langle \mathbf{A} \rangle = M_1 - N_1$ is an M-splitting with nonsingular M_1, so Theorem 2.14 gives $\rho(C_m) < 1$. Also using Theorem 4.3 for interval M-matrix $\mathbf{M}_m$ we have $\rho(\widetilde{G}) = \rho(C_m)$. Thus we get $\rho(\widetilde{G}) = \rho(C_m) < 1$. ☐

Theorem 4.9. Let $\mathbf{A}$ be an interval M-matrix. Then $\rho(C_m) \leq \rho(C)$, for any $m \geq 1$.

Proof. By Lemma 4.6, $C = \langle \mathbf{M} \rangle^{-1}|\mathbf{N}|$ is a nonnegative matrix and hence by Perron-Frobenius Theorem $\rho(C)$ is an eigenvalue of C and there is an $x \geq (\neq)0$ such that $Cx = \lambda x$, that is, $\lambda \langle \mathbf{M} \rangle x = |\mathbf{N}|x$.

Let us write $|\mathbf{E}| = |\mathbf{E}_m| + |\mathbf{R}_m^E|$ and $|\mathbf{F}| = |\mathbf{F}_m| + |\mathbf{R}_m^F|$. We now have that

$$\begin{aligned}
\lambda \langle \mathbf{M}_m \rangle x &= \lambda \left(\langle \mathbf{D} \rangle - |\mathbf{E}_m| \right) x \\
&= \lambda \Big(\langle \mathbf{D} \rangle - |\mathbf{E}| + |\mathbf{R}_m^E| \Big) x \\
&= \lambda \langle \mathbf{M} \rangle x + \lambda |\mathbf{R}_m^E| x \\
&\geq |\mathbf{N}|x = |\mathbf{F}|x \\
&= \Big(|\mathbf{F}_m| + |\mathbf{R}_m^F| \Big) x \geq |\mathbf{F}_m|x = |\mathbf{N}_m|x
\end{aligned}$$

As $\langle \mathbf{M}_m \rangle^{-1} \geq 0$, so we have that $\lambda x \geq \langle \mathbf{M}_m \rangle^{-1} |\mathbf{N}_m| x$ and hence by Theorem 2.15 we get

$$\rho(\mathbf{C}_m) = \rho\left(\langle \mathbf{M}_m \rangle^{-1} |\mathbf{N}_m|\right) \leq \lambda = \rho(C).$$

□

Note that Theorem 4.9 leads to the fact that if interval GS method converges, then GIGS method converges for any choice of bandwidth m.

Next theorem is for special case of interval M-matrices, which provides a comparison of spectral radii of iterative matrices of GIGS for different bandwidth. A similar result for AOR method for linear system was presented by Salkuyeh [5].

Theorem 4.10. Let $\mathbf{A}$ be an interval M-matrix. If $C_k = \langle \mathbf{M}_k \rangle^{-1} |\mathbf{N}_k|$, then for any $m \geq p$, $\rho(C_m) \leq \rho(C_p)$.

Proof. As $\mathbf{A}$ is interval M-matrix and so is $\langle \mathbf{M}_p \rangle$, so C_p is nonnegative matrix. Thus by Perron-Frobenius theorem we can choose an eigenvector $x \geq (\neq) 0$ associated with the eigenvalue $\lambda = \rho(C_p)$, so that $C_p x = \lambda x$, that is, $(|\mathbf{N}_p| - \lambda \langle \mathbf{M}_p \rangle) x = 0$.

If we write $\mathbf{T}_p = \mathbf{D} + \mathbf{R}_p$ and $\mathbf{T}_m = \mathbf{D} + \mathbf{R}_m$, then

$$|\mathbf{A}| = |\mathbf{D}| + |\mathbf{R}_m| - |\mathbf{E}_m| - |\mathbf{F}_m| = |\mathbf{D}| + |\mathbf{R}_p| - |\mathbf{E}_p| - |\mathbf{F}_p|$$

which implies that $R + L + U = 0$, where $R = |\mathbf{R}_m| - |\mathbf{R}_p|$, $L = |\mathbf{E}_p| - |\mathbf{E}_m|$ and $U = |\mathbf{F}_p| - |\mathbf{F}_m|$. Since $m \geq p$, so we must have $R \leq 0$, $L \geq 0$ and $U \geq 0$. We now have that

$$\begin{aligned}
C_m x - \lambda x &= \langle \mathbf{M}_m \rangle^{-1} \left(|\mathbf{N}_m| - \lambda \langle \mathbf{M}_m \rangle \right) x \\
&= \langle \mathbf{M}_m \rangle^{-1} \left(|\mathbf{F}_m| - \lambda \langle \mathbf{D} \rangle + \lambda |\mathbf{R}_m| + \lambda |\mathbf{E}_m| \right) x \\
&= \langle \mathbf{M}_m \rangle^{-1} \left(|\mathbf{F}_p| - U - \lambda \langle \mathbf{D} \rangle + \lambda R + \lambda |\mathbf{R}_p| + \lambda |\mathbf{E}_p| - \lambda L \right) x \\
&= \langle \mathbf{M}_m \rangle^{-1} \left(|\mathbf{N}_p| - \lambda \langle \mathbf{M}_p \rangle \right) x - \langle \mathbf{M}_m \rangle^{-1} \left(U + \lambda L - \lambda R \right) x \\
&= -\langle \mathbf{M}_m \rangle^{-1} \left(U + \lambda L - \lambda R \right) x \\
&\leq 0
\end{aligned}$$

Hence $C_m x \leq \lambda x$ and hence $\rho(C_m) \leq \lambda = \rho(C_p)$ by Theorem 2.15. □

Following example validates the above two theorems.

Example 4.11. Consider the interval M-matrix

$$\mathbf{A} = \begin{pmatrix} 4 & [-1,0] & [-1,0] & [-1,0] \\ [-1,0] & 5 & [-1,0] & [-1,0] \\ [-1,0] & [-1,0] & 4 & [-1,0] \\ [-1,0] & [-1,0] & [-1,0] & 5 \end{pmatrix}$$

Then we have that $\rho(C) = 0.4640$, $\rho(C_1) = 0.2749 < 1$ and $\rho(C_2) = 0.1111 < 1$ that is $\rho(C_2) < \rho(C_1) < \rho(C) < 1$ which shows that the above results hold.

We conclude the section by checking the convergence property of GIGS method for interval linear system with coefficient matrix as interval H-matrices.

Theorem 4.12. GIGS method converges for interval H-matrices.

Proof. Let $\mathbf{A}$ be an interval H-matrix, then $\langle \mathbf{A} \rangle$ is an M-matrix. It suffices to prove $\rho(\widetilde{G}) < 1$, where $\widetilde{G} = |{\mathbf{M}_m}^{-1}| \cdot |\mathbf{N}_m|$.

As $\langle \mathbf{A} \rangle = M_1 - N_1$, with M_1 and N_1 are defined in (16), is an M-matrix, so as shown in Theorem 4.8, we can find $u > 0$ such that $M_1 u > 0$. Thus $\langle \mathbf{A} \rangle = M_1 - N_1$ is regular splitting with $M_1^{-1} \geq 0$ and $N_1 > 0$. Hence by Theorem 2.13, $\rho(M_1^{-1} N_1) < 1$. Since $\mathbf{M}_m$ is an interval H-matrix, we have $\rho(\widetilde{G}) \leq \rho(C_m)$ due to Theorem 4.3. Thus we get $\rho(\widetilde{G}) \leq \rho(C_m) < 1$ by Remark 3.4. Hence GIGS method converges for any initial guess. ☐

However, for interval L-matrices GIGS and GIJ methods may not converge. For simplicity we consider examples of interval L-matrix with constant entries to see the convergence behavior of both the methods for interval L-matrices.

Example 4.13. Consider the interval L-matrix (with constant entries)

$$\mathbf{A} = \begin{pmatrix} 2 & -3 & -6 \\ -3 & 1 & -4 \\ -4 & -5 & 3 \end{pmatrix}$$

If $m = 1$ then for GIGS method we get $\rho(\widetilde{G}) = 1.0459 > 1$ and for GIJ method we get $\rho(\widehat{L}_m) = 2.0725 > 1$. Thus it shows GIGS method and GIJ method do not converge for $\mathbf{A}$.

Example 4.14. Consider the interval L-matrix (with constant entries)

$$\mathbf{A} = \begin{pmatrix} 1 & -1 & -1 \\ -3 & 2 & -3 \\ -2 & -1 & 2 \end{pmatrix}$$

If $m = 1$ then GIGS method gives $\rho(\widetilde{G}) = 0.6364 < 1$ but GIJ method gives $\rho(\widehat{L}_m) = 1$. In this case GIGS converges but GIJ method doesn't converge for $\mathbf{A}$.

5 Numerical Illustration

In this section numerical examples are considered to compare the convergence of generalized interval Jacobi method and generalized interval Gauss-Seidel method. In particular, examples are considered with coefficient matrix $\mathbf{A}$ as an interval SDD matrix, interval M-matrix, and an interval H-matrix. The computations are carried out in MATLAB(2021b) with the interval toolbox INTLAB v12 [28] and on a PC-Intel(R) Core(TM) i7-5700U CPU @1.80 GHz, 8 GB RAM. The computations are rounding to four digits and the stopping criteria is chosen as $\|\mathsf{qdist}(\mathbf{x}^{(k+1)},\mathbf{x}^{(k)})\| \leq 10^{-6}$, where $\mathsf{qdist}(\mathbf{x},\mathbf{y}) := \max\{|\underline{x}-\underline{y}|, |\overline{x}-\overline{y}|\}$ represents a measure of distance between the intervals $\mathbf{x} = [\underline{x},\overline{x}]$ and $\mathbf{y} = [\underline{y},\overline{y}]$, and in case $\mathbf{x},\ \mathbf{y} \in \mathbb{IR}^n$, then $\mathsf{qdist}(\mathbf{x},\mathbf{y}) = [\mathsf{qdist}(\mathbf{x}_1,\mathbf{y}_1),\ldots,\mathsf{qdist}(\mathbf{x}_n,\mathbf{y}_n)] \in \mathbb{R}^n$, where $\mathbf{x}_i$ represents the i-th entry of the interval vector $\mathbf{x}$.

We now furnish examples for various classes of interval coefficient matrices, and provide comparisons of our proposed methods with IJ and IGS methods , in terms of no. of iterations, time (in seconds) and $r_k = \|(\mathsf{qdist}(\mathbf{x}^{(\mathsf{k})},\mathbf{x})\|$, where $\mathbf{x}$ is the enclosure obtained by using verifylss.

Example 5.1. Consider the interval linear system (1) with the coefficient interval matrix as interval strictly diagonally dominant matrix mentioned in Neumaier book [3] .

$$\mathbf{A} := \begin{pmatrix} 3 & [-2,2] & 0 \\ 0 & 3 & [-2,2] \\ [-2,2] & 0 & 3 \end{pmatrix}$$

and

$$\mathbf{b} := \begin{pmatrix} [-1,1] \\ [-1,1] \\ 2 \end{pmatrix}$$

Then the function verifylss from the package INTLAB produces the enclosure

$$\mathbf{x} = ([-1.2282, 1.2282], [-1.3423, 1.3423], [-0.1599, 1.4932])^T$$

Taking the initial guess as $\mathbf{x}_0 = ([0,3],[0,3],[0,3])^T$, generalized interval Jacobi converges after 13 iterations and yields the enclosure

$$\mathbf{x}_{\text{GIJ}} = ([-1.2106, 1.2106], [-1.3158, 1.3158], [-0.1404, 1.4737])^T$$

whereas the generalized interval Gauss-Seidel converges after 1 iteration and produces the enclosure

$$\mathbf{x}_{\text{GIGS}} = ([-1.2398, 1.2398], [-1.3481, 1.3481], [-0.1714, 1.5048])^T$$

Table 1 compares GIJ and GIGS methods (taking $m = 1$) with IJ and IGS methods (with $m = 0$) with the initial guess taken as $\mathbf{x}_0 = ([0,3],[0,3],[0,3])^T$.

Iterative method	No. of iterations	r	time in second
GIJ	13	0.0372	0.0225
GIGS	1	0.0173	0.0147
IJ	35	0.0372	0.0437
IGS	24	0.0372	0.0237

Table 1: Numerical result for the interval SDD-matrix with $m = 1$

From the above table we can see that the generalized interval Jacobi method gives the tightest solution set enclosure.

Example 5.2. Consider the interval linear system (1) with the coefficient interval M-matrix

$$\mathbf{A} := \begin{pmatrix} 4 & [-2,0] & [-1,0] \\ [-1,0] & [3,4] & -1 \\ [-2,-1] & [-1,0] & 5 \end{pmatrix}$$

and

$$b := \begin{pmatrix} 1.2 \\ 1.5 \\ 5 \end{pmatrix}$$

then the verifylss function yields the enclosure

$$\mathbf{x} = ([-0.2935, 1.6658], [0.0677, 1.7258], [0.5795, 2.0115])^T$$

Taking initial guess as $\mathbf{x}_0 = ([-1,2], 1, [2,3])^T$, generalized interval Jacobi converges after 16 iterations and provides the enclosure

$$\mathbf{x}_{\mathrm{GIJ}} = ([-0.2935, 1.6658], [0.0677, 1.7258], [0.5795, 2.0115])^T$$

whereas generalized interval Gauss-Seidel converges after 9 iterations and gives the enclosure

$$\mathbf{x}_{\mathrm{GIGS}} = ([-0.2936, 1.6658], [0.0676, 1.7259], [0.5795, 2.0116])^T$$

Table 2 provides a comparison of GIJ and GIGS methods (taking $m = 1$) with IJ and IGS methods (with $m = 0$) with the initial guess taken as $\mathbf{x}_0 = ([-1,2], 1, [2,3])^T$.

Iterative method	No. of iterations	r	time in seconds
GIJ	16	3.23×10^{-5}	0.0272
GIGS	9	1.25×10^{-4}	0.0211
IJ	30	2.38×10^{-5}	0.0443
IGS	18	2.46×10^{-5}	0.0236

Table 2: Numerical result for the interval M-matrix with $m = 1$

This shows that in case of interval M-matrices, generalized interval Jacobi method gives the tightest enclosure of the solution set.

Example 5.3. Consider the interval linear system (1) with the following coefficient interval H-matrix

$$\mathbf{A} := \begin{pmatrix} [4,5] & [-2,2] & [-1,0] \\ [0,1] & [3,5] & [-1,1] \\ [-1,1] & [1,3] & 5 \end{pmatrix}$$

and

$$\mathbf{b} := \begin{pmatrix} [0.1, 0.5] \\ [-0.3, -0.1] \\ [0.3, 0.4] \end{pmatrix}$$

Then the function verifylss from the package INTLAB generates the enclosure

$$\mathbf{x} = ([-0.2425, 0.3967], [-0.3567, 0.2375], [-0.1857, 0.3734])^T$$

Taking the initial guess as $\mathbf{x}_0 = (1, 5, 4)^T$, generalized interval Jacobi converges after 15 iteartions and yields the enclosure

$$\mathbf{x}_{\text{GIJ}} = ([-0.2426, 0.3968], [-0.3567, 0.2375], [-0.1857, 0.3734])^T$$

whereas the generalized interval Gauss-Seidel converges after 9 iterations and produces the enclosure

$$\mathbf{x}_{\text{GIGS}} = ([-0.2425, 0.3967], [-0.3567, 0.2374], [-0.1857, 0.3734])^T$$

We now produce a comparison in Table 3 of GIJ and GIGS methods (taking $m = 1$) with IJ and IGS methods (with $m = 0$) with the initial guess taken as $\mathbf{x}_0 = (1, 5, 4)^T$.

Iterative method	No. of iterations	r	time in seconds
GIJ	15	3.96×10^{-5}	0.0247
GIGS	9	9.73×10^{-6}	0.0209
IJ	45	1.11×10^{-5}	0.0475
IGS	24	1.27×10^{-5}	0.0294

Table 3: Numerical result for the interval H-matrix with $m = 1$

For this example the most tightest enclosure of solution set provided by the generalized interval Gauss-Seidel method.

6 Conclusion

In this paper, we proposed a generalized interval Jacobi (GIJ) method and generalized interval Gauss-Seidel method (GIGS). These methods are generalization of interval Jacobi and interval Gauss-Seidel methods, discussed by Neumaier [3, 25] to solve interval linear system. The GIJ and GIGS methods are proposed similar to that introduced by Salkuyeh in [4], by generalizing the diagonal interval matrix to a band interval matrix. We proved that both the proposed methods converge for interval SDD matrix, interval M-matrix, and for interval H-matrix. Further we found that for interval M-matrices, GIGS method converges for any choice of bandwidth m if interval GS method converges. At last we consider numerical examples to observe that GIJ gives a tighter enclosure for interval M- coefficient matrices, whereas GIGS provides a tighter enclosure of the solution set for interval H-matrices. This leads to the open problem that the same can be concluded in general.

References

[1] A. Berman and R. J. Plemmons, *Nonnegative matrices in the mathematical science*, SIAM, Philadelphia 1979.

[2] A. Neumaier,“New techniques for the analysis of linear interval equations”, *Linear Algebra and its Applications*, **58** (1984) 273–325.

[3] A. Neumaier, *Interval methods for systems of equations*, Cambridge university press, 37, 1990.

[4] D. K. Salkuyeh, “Generalized Jacobi and Gauss-Seidel methods for solving linear system of equations”, *Numer. Math. J. Chinese Univ. (English Ser.)*, **16(2)** (2007) 164–170.

[5] D. K. Salkuyeh,, “Generalized AOR method for solving system of linear equations”, *Australian J. of Basic and Appl. Sci*, **5(3)** (2011) 351–358.

[6] E. D. Popova and M. Hladík, “Outer enclosures to the parametric AE solution set”,*Soft Comput.*, **17** (2013), 1403–1414.

[7] G. Mayer, “Interval analysis: and automatic result verification”, *Walter de Gruyter GmbH & Co KG* (65) (2017).

[8] J. Chakravarty, A. Athikho, and M. Saha, “Convergence of interval AOR method for linear interval equations”, *Numerical Algebra, Control & Optimization* **12(2)** (2022) 293-308.

[9] J. Rohn, “Perron vectors of an irreducible nonnegative interval matrix”, *Linear and Multilinear Algebra* **54(6)** (2006) 399-404.

[10] J. Rohn, “Forty necessary and sufficient conditions for regularity of interval matrices: A survey”, *Electron. J. Linear Algebra*, **18** (2009) 500–512.

[11] J. Rohn and S. Shary, “Interval Matrices: Regularity Generates Singularity”, *Linear Algebra and its Applications* **540** (2018) 149–159.

[12] L. Jaulin, M. Kieffer, O. Didrit and É. Walter, *Applied Interval Analysis*, Springer, London, 2001.

[13] L. Wang and Y. Song, “Preconditioned AOR iterative methods for M-matrices”, *Journal of Computational and Applied Mathematics*, **226(1)** (2009) 114-124.

[14] L. Cvetković and H. Dragoslav, “The AOR method for solving linear interval equations”, *Computing* **41(4)** (1989) 359–364.

[15] M. Allahdadi and H.M. Nehi, “The optimal solution set of the interval linear programming problems”, *Optimization Letters* **7(8)** (2013) 1893–1911.

[16] M. Fiedler, J. Nedoma, J. Ramík, J. Rohn and K. Zimmermann, “Linear optimization problems with inexact data”, *Springer, New York* (2006).

[17] M. Hladík, "Interval linear programming: A survey", *Linear Programming: New Frontiers in Theory and Applications, Nova Science Publishers, New York* Ch2, (2012) 85–120.

[18] M. Hladík, "Enclosures for the solution set of parametric interval linear systems,",*Int. J. Appl. Math. Comput. Sci.*, **22** (2012), 561–574.

[19] M. Hladík, "New Operator and method for solving real interval preconditioned interval linear equations", *SIAM J. Numer. Anal.* ,**52(1)** (2014) 194–206.

[20] M. Hladík, and J. Horáček, "Interval Linear Programming Techniques in Constraint Programming and Global Optimization", *Constraint Programming and Decision Making*, **539** (2014) 44–59.

[21] M. Hladík and I. Skalna, "Relation between various methods for solving linear interval and parametric equations", *Linear Alg. Appl.* **574** (2019) 1–21.

[22] M. Saha and J. Chakravarty, "Convergence of Generalized SOR, Jacobi and Gauss–Seidel Methods for Linear Systems", *International Journal of Applied and Computational Mathematics, Springer* **6** (2020) 1–12.

[23] R. A. Horn and C. R. Johnson, *Matrix Analysis*, Cambridge University Press, 1990.

[24] R. A. Horn and C. R. Johnson, *Topics in Matrix Analysis*, Cambridge University Press, 1994.

[25] R. E. Moore, *Methods and Applications of Interval Analysis*, SIAM, Philadelphia, PA, 1979.

[26] R. Kearfott and V. Kreinovich, *Applications of Interval computations*, Kluwer, Dordrecht, 1996.

[27] R. S. Varga, *Matrix Iterative Analysis*, Prentice-Hall, Englewood Cliffs, NJ, 1962.

[28] S. M. Rump, *INTLAB-INTerval LABoratory*, In Tibor Csendes ed, Developments in Reliable Computing, 77–104. Kluwer Academic Publishers, Dordrecht, 1999. http://www.ti3.tuhh.de/intlab.

[29] S. P. Shary, "Interval Gauss-Seidel method for generalized solution sets to interval linear systems", *Reliable computing*, **7(2)** (2001) 141-155.

[30] T. Nirmala and K. Ganesan, "Solution of interval linear system of equations-an iterative approach", *In AIP conference proceedings,AIP Publishing LLC.* **2112** (2019) 020105.

[31] Y. Saad, *Iterative methods for sparse linear systems*, SIAM, 2003.

J. COMPUTATIONAL ANALYSIS AND APPLICATIONS, VOL. 31, NO. 3, 2023, COPYRIGHT 2023 EUDOXUS PRESS, LLC

Extended Jacobi Elliptic Function Technique: A Tool for Solving Nonlinear Wave Equations with emblematic Software

Ram Dayal Pankaj
Department of Mathematics and Statistics
Jai Narain Vyas University Jodhpur, Rajasthan (India)
Email: drrdpankaj@yahoo.com

Abstract

The Extended Jacobi Elliptic Function Technique (EJET) is a powerful technique for finding the solutions for traveling waves form coming from Non-Linear Waveguides (NLWs). As a result, solitary and shock-wave profiles are obtained simultaneously with corresponding amplitudes and speeds by this method for three types of nonlinear wave equations. A class of nonlinear wave equations of particular interest in mathematical physics have been used to investigate the legality and credibility of this technique. A short script is considered a symbolic software package that calculates traveling wave solutions in exact form.

Key words: Extended Jacobi Elliptic Function Technique; Traveling Waves; solitary and shock-wave profiles; Symbolic Software
Mathematics Subject Classification(2010): 35M10, 65Z05.

[1]

1 Introduction

Nonlinearity is a mesmerizing component of nature, with nonlinear wave phenomena appearing in one way or another in nearly all scientific and engineering fields such as physics (Plasma and Fluid), Ocean Engineering, Chemical Dynamics, Geochemistry and mathematical biology (Population Dynamics) [[1]-[5]] .The nonlinear equations appear in different scenarios in daily real-life situations and very difficult to solve it [[6]-[8]]. Manny method are used to find the solutions (solitary and shock-wave solution) of nonlinear wave phenomena like Tanh-Coth Method [[5],[9]], Expansion method [[10]-[13]] the decomposition method with Integral transformation [[14]-[16]] and so on.
The development of the present paper is as follows. In Section 2, we have outline

---

[1] Email: drrdpankaj@yahoo.com

of EJET for solving NLW. In Section-3 (Application 3.1), we apply this Technique to the second order nonlinear partial differential equations (SONLPDE). And also applied in Section 4 (Application 3.2) K.G. equation and In Section 5 (Application 3.3) Population Dynamics equation. In section 6 discussion and numerical Sketch and in section 6 result and conclusions.

2 Outline of Extended Jacobi Elliptic Function Technique

We now present a brief strategy of the technique. Given non-linear wave equation

$$\Re\left(v, v_t, v_x, v_{tt}, v_{xx}....\right) = 0 \tag{2.1}$$

can be converted to an ordinary differential equation (ODE)

$$P\left(v, v', v'', v'''....\right) = 0 \tag{2.2}$$

upon using a wave variable $z = \alpha\left(x - ct\right)$where α and c are wave number and wave speed respectively. Introducing a new independent variable

$$v(x,t) = v\left(\alpha(x-ct)\right) = v(z)$$

By the Jacobi elliptic function expansion method, $v\left(z\right)$ can be expressed as a finite series in the form of Jacobi elliptic functions[[10],[17]-[18]] ,

$$u\left(z\right) = \sum_{i=0}^{n} \lambda_i (\psi\left(z\right))^i \tag{2.3}$$

is prepared and its highest degree is $O\left\{\psi\left(z\right)\right\} = n.$ where

$$\psi = \psi\left(z\right)$$

satisfies the eq.(2.1) the following auxiliary equation:

$$\frac{\partial}{\partial z}\left(\psi\left(z\right)\right) = \psi'\left(z\right) = \kappa\sqrt{p\,\psi^4(z) + q\,\psi^2\left(z\right) + r} \tag{2.4}$$

Where $\kappa = \pm 1$ and p, q and r are constants. It holds for $\psi\left(z\right)$ as

$$\left.\begin{aligned}
&\frac{\partial^2}{\partial z^2}\left(\psi\left(z\right)\right) = \psi'' = 2p\,\psi^3(z) + q\,\psi(z)\\
&\frac{\partial^3}{\partial z^3}\left(\psi\left(z\right)\right) = \psi''' = \left(6p\,\psi^2(z) + q\,\right)\psi'(z)\\
&\frac{\partial^4}{\partial z^4}\left(\psi\left(z\right)\right) = \psi''''(z) = 24p^2\psi^5(z) + 20p\,q\,\psi^3(z) + \left(12pr + q^2\right)\psi(z)\\
&\frac{\partial^5}{\partial z^5}\left(\psi\left(z\right)\right) = \psi'''''(z) = \left(120p^2\psi^4(z) + 60p\,q\,\psi^2(z) + 12pr + q^2\right)\psi'(z)\\
&...
\end{aligned}\right\} \tag{2.5}$$

we present many closed solutions for eq.(2.4) . In fact, these solutions as $\psi(z)$ = Jacobi elliptic functions, can be casted to hypothesis for more solutions eq.(2.1).$sn(\xi) = sn(\xi, m)$, $dn(\xi) = dn(\xi, m)$and $cn(\xi) = cn(\xi, m)$are the Jacobi elliptic function with modulus m, where $0 < m < 1$. These functions are considerable the resulting formulas:

$$\begin{gathered}
sn^2(\xi) + cn^2(\xi) = 1,\ dn^2(\xi) + m^2 sn^2(\xi) = 1 \\
sn(\xi) = \frac{1}{ns(\xi)},\ cn(\xi) = \frac{1}{nc(\xi)},\ dn(\xi) = \frac{1}{nd(\xi)} \\
cs(\xi) = \frac{sn(\xi)}{cn(\xi)},\ ds(\xi) = \frac{dn(\xi)}{sn(\xi)},\ sd(\xi) = \frac{ns(\xi)}{dn(\xi)} \\
sn'(\xi) = \frac{d(sn(\xi))}{d\xi} = cn(\xi)\, dn(\xi), dn'(\xi) = \frac{d(dn(\xi))}{d\xi} - m^2 cn(\xi)\, sn(\xi), \\
cn'(\xi) = \frac{d(cn(\xi))}{d\xi} - dn(\xi)\, sn(\xi)
\end{gathered}$$

when $m \to 1$; These functions convert to hyperbolic functions as follows:

$$\begin{gathered}
sn(\xi) \to \tanh(\xi),\ \{cn(\xi), dn(\xi)\} \to \operatorname{sech}(\xi), \\
\{sc(\xi), sd(\xi)\} \to \sinh(\xi), \{cd(\xi),\ dc(\xi)\} \to 1 \\
\{ds(\xi), cs(\xi)\} \to \cos ech(\xi), \{nc(\xi), nd(\xi)\} \to \cosh(\xi), \{ns(\xi)\} \to \coth(\xi)
\end{gathered}$$

when $m \to 0$ These functions convert to trigonometric functions as follows:

$$\begin{gathered}
\{sn(\xi), sd(\xi)\} \to \sin(\xi),\ \{cn(\xi), cd(\xi)\} \to \cos(\xi), \\
\{sc(\xi)\} \to \tan(\xi), \{dn(\xi),\ nd(\xi)\} \to 1 \\
\{ns(\xi), ds(\xi)\} \to Cosec(\xi), \{cs(\xi)\} \to \cot(\xi) \{nc(\xi), dc(\xi)\} \to \operatorname{Sec}(\xi)
\end{gathered}$$

Its balancing the highest order derivative term and the nonlinear term and find the value of n in eq. (2.3).

3 Application -3.1

We consider the second order nonlinear partial differential equations with combination Kortewegde Vries (KdV) Equation and BenjaminBonaMahony equation (BBM) Equation of two famous and fundamental nonlinear wave equations. This is as

$$\theta_t + a\,\theta_x + \theta\theta_x + b^2\theta_{x\,x\,x} - c^2\theta_{x\,x\,t} = 0 \tag{3.1}$$

Where $\theta = \theta(x, t)$ unknow wave function with space variable x and time variable t. a, b and c are arbitrary real constant. If $a = 0, c = 0$ then eq. (3.1) is Kortewegde Vries (KdV) Equation, this is one of the most famous non-linear wave equations, it was derived in fluid mechanics to describe shallow water waves in a rectangular channel [[1],[28]]. If $b = 0$ then eq. (3.1) is Benjamin-BonaMahony equation (BBM) Equation, also called regularized long-wave equation (RLWE), this serves as an approximate model in studying the dynamics of small-amplitude surface water waves propagating unidirectionally [[1]]. Suppose that the travelling wave solutions for eq. (3.1) are of the forms as follows

$$\theta(x, t) = \theta(z) = \theta(k(x - \omega t)$$

where k and ω area constant, put in eq. (3.1) then

$$k\,(a-\omega)\;\theta' + k\,\theta\,\theta' + k^3\left(b^2+c^2\omega\right)\theta''' = 0$$

Integral one time, take constant zero

$$k\,(a-\omega)\;\theta + \frac{k^2}{2}\theta^2 + k^3\left(b^2+c^2\omega\right)\theta'' = 0 \tag{3.2}$$

Balancing θ'' with θ^2 in eq. (3.2) gives $2n = n+2$ i.e.,$n = 2$, then

$$\theta\,(z) = \sum_{i=0}^{2}\lambda_i(\psi\,(z))^i = \lambda_0 + \lambda_1\,\psi\,(z) + \lambda_2\,(\psi\,(z))^2 = \lambda_0 + \lambda_1\,\psi + \lambda_2\,\psi^{\,2}$$

$$\theta''\,(z) = \lambda_1\,\psi'' + 2\lambda_2\,\left\{\psi'^{\,2} + \psi\,\psi''\right\}$$

Put these values in eq. (3.2) with eq. (2.5)

$$\begin{gathered}(a-\omega)\left(\lambda_0+\lambda_1\,\psi+\lambda_2\,\psi^2\right)\\ +\frac{k^2}{2}\left(\lambda_0^2+\lambda_1^2\,\psi^2+\lambda_2^2\,\psi^2+2\lambda_0\lambda_1\,\psi+2\lambda_1\lambda_2\,\psi^3+2\lambda_0\lambda_2\,\psi^2\right)\\ +k^3\left(b^2+c^2\omega\right)\left\{2\lambda_2R+\lambda_1\,q\,\psi+2\lambda_2q\,\psi^2+\psi^3\left(2\lambda_1p+2\lambda_2q\right)+\psi^4 6\lambda_2p\right\}=0\end{gathered} \tag{3.3}$$

equating all terms with the powers in ψ , and setting each of the obtained coefficients for ψ to zero, yields the following set of algebraic equations for $\lambda_0, \lambda_1, \lambda_2, k, \omega, a, b\;and\,c$

$$\begin{array}{ll}\psi^0: & \lambda_0 k\,(a-\omega)\,+\frac{k^2\lambda_0^2}{2}+2\lambda_2\,r\,k^3\left(b^2+c^2\omega\right)=0\\ \psi^1: & \lambda_1 k\,(a-\omega)\,+\frac{k^2\lambda_0\lambda_1}{2}+\lambda_1\,q\,k^3\left(b^2+c^2\omega\right)=0\\ \psi^2: & \lambda_2 k\,(a-\omega)\,+\frac{k^2\left(\lambda_1^2+2\lambda_0\lambda_2\right)}{2}+2\lambda_2\,q\,k^3\left(b^2+c^2\omega\right)=0\\ \psi^3: & 2\lambda_2\lambda_1\,+\,k^3\left(b^2+c^2\omega\right)\left(2\lambda_1p+2\lambda_2q\right)=0\\ \psi^4: & \lambda_2^2\,+6\lambda_2pk^3\left(b^2+c^2\omega\right)=0\end{array}$$

One obtains solution

$$\lambda_0 = -\tfrac{k^2\left(b^2+c^2\omega\right)q+(a-\omega)}{k},\quad \lambda_1 = k^2\left(b^2+c^2\omega\right)\sqrt{-12p\,q}$$

$$\lambda_2 = -6k^3\left(b^2+c^2\omega\right)p$$

then

$$\begin{aligned}\theta\,(z) = &-\frac{k^2\left(b^2+c^2\omega\right)q+(a-\omega)}{k}\\ &+\left\{k^2\left(b^2+c^2\omega\right)\sqrt{-12p\,q}\right\}\,\psi(z)\\ &-\left\{6k^3\left(b^2+c^2\omega\right)p\right\}\,(\psi(z)\,)^2\end{aligned}$$

We choose p q and r from [[17],[18]], such that
Solution -1 $p\;:\;\; m^2;\;\; q:\;\; -\left(1+m^2\right)\;\;\; then\;\psi(z) =\;\; sn(z)$ thus

$$\theta\left(z\right) = -\frac{k^2\left(b^2+c^2\omega\right)\left(1+m^2\right)-\left(a-\omega\right)}{k} + \left\{k^2\left(b^2+c^2\omega\right)\sqrt{12m^2\left(1+m^2\right)}\right\} sn(z) - \left\{6k^3\left(b^2+c^2\omega\right)m^2\right\}\left(sn(z)\right)^2$$

Solution -2 $p\ :\ -m^2\ ,\ \ q:\ \left(2m^2-1\right)\ ,\ \ then\ \psi(z)=\ cn(z)$ thus

$$\theta\left(z\right) = -\frac{k^2\left(b^2+c^2\omega\right)\left(2m^2-1\right)+\left(a-\omega\right)}{k} + \left\{k^2\left(b^2+c^2\omega\right)\sqrt{12m^2\ \left(2m^2-1\right)}\right\} cn(z) + \left\{6k^3\left(b^2+c^2\omega\right)m^2\right\}\left(cn(z)\right)^2$$

Solution -3 $p\ :\ -\frac{1}{4}\ ,\ \ q:\ \left(\frac{1+m^2}{2}\right)\ ,\ \ r:\ \left(\frac{1-m^2}{2}\right)^2,\ then\ \psi(z)=mcn(z)\pm dn(z)$ thus

$$\theta\left(z\right) = -\frac{k^2\left(b^2+c^2\omega\right)\left(1+m^2\right)+2\left(a-\omega\right)}{2k} + \left\{k^2\left(b^2+c^2\omega\right)\sqrt{3\ \left(\frac{1+m^2}{2}\right)}\right\}\left(mcn(z)\ \pm\ dn(z)\right) + \left\{\frac{3k^3\left(b^2+c^2\omega\right)}{2}\right\}\left(mcn(z)\ \pm\ dn(z)\right)^2$$

Solution -4 $p\ :\ \frac{m^2}{4}\ ,\ \ q:\ \left(\frac{m^2-2}{2}\right),\ then\ \psi(z)=\ sn(z)+i\,cn(z)$ thus

$$\theta\left(z\right) = -\frac{k^2\left(b^2+c^2\omega\right)\left(m^2-2\right)+2\left(a-\omega\right)}{2k} + \left\{k^2\left(b^2+c^2\omega\right)\sqrt{3m^2\left(\frac{2-m^2}{2}\right)}\right\}\left\{sn(z)\pm i\,cn(z)\right\} - \left\{\frac{3m^2k^3\left(b^2+c^2\omega\right)}{2}\right\}\left(sn(z)\pm i\,cn(z)\right)^2$$

4 Application -3.2

We consider nonlinear KleinGordon (NKG) [[19]-[20]]. The Klein-Gordon equations play a significant role in solid state physics, plasma physics, nonlinear optics and quantum field theory

$$\theta_{tt}-\theta_{xx}+\theta+\beta|\theta|^2\theta=0 \tag{4.1}$$

the travelling wave solutions for Eq. (4.1) are of the forms as follows:

$$\theta\left(x,t\right)=\theta\left(z\right)e^{i\left(\gamma\ \left(\omega x-t\right)\right)}=\theta\left(k(x-\omega t\right)e^{i\left(\gamma\ \left(\omega x-t\right)\right)}$$

where k and ω area constant, put in eq. (2.1) then

$$\left(k^2\omega^2-k^2\right)\theta''+\left\{\gamma^2\left(\omega^2-1\right)+1\right\}\theta+\beta\theta^3=0 \tag{4.2}$$

Balancing θ'' with θ^3 in eq. (4.2) gives $3n=n+2$ i.e.,$n=1$, then

$$\theta\left(z\right)=\sum_{i=0}^{1}\lambda_i\left(\psi\left(z\right)\right)^i=\lambda_0+\lambda_1\,\psi\left(z\right)=\lambda_0+\lambda_1\,\psi$$

Put these values in eq. (4.2)

$$\theta''\left(z\right)=\lambda_1\,\psi''$$

Using eq. (2.5) and equating all terms with the powers in ψ , and setting each of the obtained coefficients for ψ to zero, yields set of algebraic equations for $\lambda_0, \lambda_1 k, \omega\, and\, \gamma$,

One obtains solution

$$\lambda_0^2=-\tfrac{k^2\left(\omega^2-1\right)q+\left\{\gamma^2\left(\omega^2-1\right)+1\right\}}{3\beta},\quad \lambda_1^2=-\tfrac{2k^2\left(\omega^2-1\right)p}{\beta}$$

Then

$$\theta\left(z\right)=\sqrt{-\tfrac{k^2(\omega^2-1)q+\{\gamma^2(\omega^2-1)+1\}}{3\beta}}+\left\{\sqrt{-\tfrac{2k^2(\omega^2-1)p}{\beta}}\right\}\,\psi(z)$$

We choose p, q and r from [[17],[18]], such that

Solution -2.1 $p\ :\ m^2\ ,\quad q:\ -\left(1+m^2\right)\ ,\ then\ \psi(z)=\ sn(z)$ thus

$$\theta\left(z\right)=\left\{\begin{array}{l}\sqrt{-\dfrac{\left\{\gamma^2\left(\omega^2-1\right)+1\right\}-k^2\left(\omega^2-1\right)\left(1+m^2\right)}{3\beta}}\\ +\left\{\sqrt{-\dfrac{2k^2\left(\omega^2-1\right)m^2}{\beta}}\right\}\ sn\left(k(x-\omega t)\right)\end{array}\right\}e^{i(\gamma\ (\omega x-t))}$$

Solution -2.2 $p\ :\ -m^2\ ,\quad q:\ \left(2m^2-1\right)\ ,\ then\ \psi(z)=\ cn(z)$ thus

$$\theta\left(z\right)=\left\{\begin{array}{l}\sqrt{-\dfrac{k^2\left(\omega^2-1\right)\left(2m^2-1\right)+\left\{\gamma^2\left(\omega^2-1\right)+1\right\}}{3\beta}}\\ +\left\{\sqrt{-\dfrac{2k^2\left(1-\omega^2\right)m^2}{\beta}}\right\}\ cn\left(k(x-\omega t)\right)\end{array}\right\}e^{i(\gamma\ (\omega x-t))}$$

Solution -2.3 $p\ :\ \left(\frac{1-m^2}{4}\right)\ ,\ q:\ \left(\frac{1+m^2}{2}\right)\ ,\ ,\ then\ \psi(z)=\frac{cn(z)}{1\pm\,sn(z)}$ thus

$$\theta\left(z\right)=\left\{\begin{array}{l}\sqrt{-\dfrac{k^2\left(\omega^2-1\right)\left(1+m^2\right)\,+2\left\{\gamma^2\left(\omega^2-1\right)+1\right\}}{6\beta}}\\ +\left\{\sqrt{-\dfrac{2k^2\left(\omega^2-1\right)\left(1-m^2\right)}{4\beta}}\right\}\left(\dfrac{cn\left(k(x-\omega t)\right)}{1\pm\ sn(k(x-\omega t))}\right)\end{array}\right\}e^{i(\gamma\ (\omega x-t))}$$

Solution -2.4 $p\ :\ \frac{m^2}{4}\ ,\quad q:\ \left(\frac{m^2-2}{2}\right),\ then\ \psi(z)=\ sn(z)+i\,cn(z)$ thus

$$\theta\left(z\right)=\left\{\begin{array}{l}\sqrt{-\dfrac{\left\{2\gamma^2\left(\omega^2-1\right)+1\right\}+k^2\left(\omega^2-1\right)\left(m^2-2\right)}{6\beta}}\\ +\left\{\sqrt{-\dfrac{2k^2\left(\omega^2-1\right)m^2}{4\beta}}\right\}\left(\,sn(z)+i\,cn(z)\right)\end{array}\right\}e^{i(\gamma\ (\omega x-t))}$$

5 Application -3.3

We consider Fisher equation

$$\theta_t = \delta_1 \, \theta_{xx} + \delta_2 \, \theta \, (1-\theta) \tag{5.1}$$

introduced by Fisher [[21]] to describe the propagation of a virile mutant in an infinitely long habitat. It also represents a model equation for the evolution of a neutron population in a nuclear reactor [[22]-[23]] and a prototype model for a spreading flame [[24]-[25]]. The travelling wave solutions for Eq. (5.1) are of the forms as follows:

$$\theta\,(x,t) = \theta\,(z) = \theta\,(k(x-\omega t)$$

where k and area constant, put in eq. (5.1) then

$$k\omega\theta' + k^2\delta_1\,\theta'' + \delta_2\,\theta - \delta_2\,\theta^2 = 0 \tag{5.2}$$

Balancing θ'' with θ^2 in eq. (5.2) gives $2n = n+2$ i.e.,$n = 2$, then

$$\theta\,(z) = \sum_{i=0}^{2} \lambda_i (\psi\,(z))^i = \lambda_0 + \lambda_1\,\psi\,(z) + \lambda_2\,(\psi\,(z))^2 = \lambda_0 + \lambda_1\,\psi + \lambda_2\,\psi^{\,2}$$

$$\theta''\,(z) = \lambda_1\,\psi'' + 2\lambda_2\,\left\{\psi'^{\,2} + \psi\,\psi''\right\}$$

Put these values in eq. (5.2)

$$(k\omega + \delta_2)\,\left(\lambda_0 + \lambda_1\,\psi + \lambda_2\,\psi^{\,2}\right) + k^2\delta_1\,\left(\lambda_1\,\psi'' + 2\lambda_2\,\left\{\psi'^{\,2} + \psi\,\psi''\right\}\right) - \delta_2\,\left(\lambda_0 + \lambda_1\,\psi + \lambda_2\,\psi^{\,2}\right)^2 = 0 \tag{5.3}$$

Using eq. (2.5) and collecting the coefficients of the same power $\psi^i\,(z)(\psi'(z))^j$ $(j = 0, 1\ i = 0, 1, 2, 3, 4...)$ and setting each of the attained coefficients to be zero we have a set of over determined algebraic equations for $\lambda_0, \lambda_1, \lambda_2, k, \omega, \delta_1\ and\, \delta_2$. One obtains solution

$$\lambda_0 = \tfrac{4k^2\delta_1 q + \delta_2}{2\delta_2},\ \ \lambda_2 = \tfrac{4k^2\delta_1 p}{\delta_2},\ \ \lambda_1 = 2\lambda_2$$

Then

$$\theta\,(z) = \tfrac{4k^2\delta_1 q + \delta_2}{2\delta_2} + \tfrac{4k^2\delta_1 p}{\delta_2}\,\psi(z) + \tfrac{4k^2\delta_1 p}{2\delta_2}\,\psi^2(z)$$

We choose p q and r from [[17]-[18]], such that
Solution -3.1 $p\ :\ m^2\ ,\quad q:\ -\left(1+m^2\right)\ ,\ then\ \psi(z) =\ sn(z)$ thus

$$\theta\,(z) = \tfrac{\delta_2 - 4k^2\delta_1\left(1+m^2\right)}{2\delta_2} + \tfrac{4k^2\delta_1 m^2}{\delta_2}\,sn(z) + \tfrac{4k^2\delta_1 m^2}{2\delta_2}\,sn^2(z)$$

Solution -3.2 $p\ :\ -m^2\ ,\quad q:\ \left(2m^2-1\right)\ ,\ then\ \psi(z) =\ cn(z)$ thus

$$\theta\,(z) = \tfrac{4k^2\delta_1\left(2m^2-1\right) + \delta_2}{2\delta_2} - \tfrac{4k^2\delta_1 m^2}{\delta_2}\,cn(z) - \tfrac{4k^2\delta_1 m^2}{2\delta_2}\,cn^2(z)$$

Solution -3.3 $p\ :\ \left(\frac{1}{4}\right)\ ,\ \ q:\ \ \left(\frac{1-2m^2}{2}\right)\ ,\ \ ,\ then\ \psi(z)=msn(z)\pm i\,dn(z)$thus

$$\theta\left(z\right)=\frac{2k^2\delta_1\left(1-2m^2\right)+\delta_2}{2\delta_2}+\frac{k^2\delta_1}{\delta_2}\left\{m\,sn(z)\pm i\,dn(z)\right\}+\frac{k^2\delta_1}{2\delta_2}\left\{m\,sn(z)\pm i\,dn(z)\right\}^2$$

Solution -3.4 $p\ :\ 1\ ,\ \ q:\ \ \left(2-4m^2\right)\ ,\ \ ,\ then\ \psi(z)=\frac{sn(z)dn(z)}{cn(z)}$thus

$$\theta\left(z\right)=\frac{8k^2\delta_1\left(1-2m^2\right)+\delta_2}{2\delta_2}+\frac{4k^2\delta_1}{\delta_2}\,\frac{sn(z)dn(z)}{cn(z)}+\frac{4k^2\delta_1}{2\delta_2}\left\{\frac{sn(z)dn(z)}{cn(z)}\right\}^2$$

6 Discussion and Numerical Sketch

It should be noted that, although many exact solutions are obtained in this work, it has been proved that some solutions in applications 3.1, 3.2 and 3.3 are equivalent to the solution of in the literature. like solution for 2.1 of application 3.2 [[26]] and solution for 3.2 of application 3.3 [[27]].

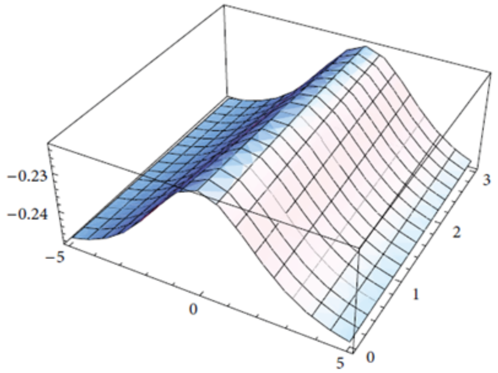

Figure 1: Travelling waves solution for 2 of 3.1 are plotted: bright solitary waves $m\to 1$

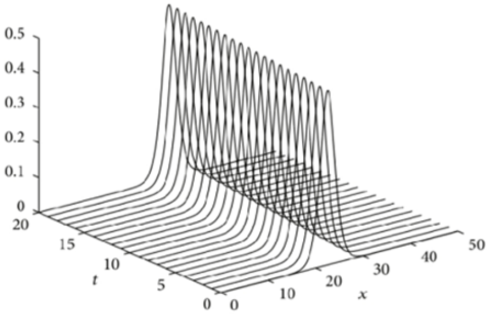

Figure 2: Soliton solution for 2.1 of 3.2 are plotted: solitary waves,$m\to 1$

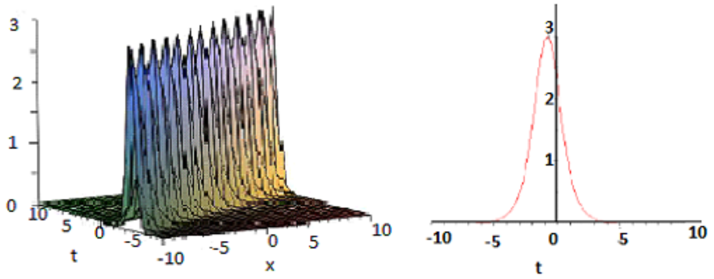

(a) Shape of in 3D (b) Shape of in 2D

Figure 3: Soliton solution for 3.1 of 3.3 are plotted: solitary waves,$m \to 1$

7 Result and Conclusions

The Extended Jacobi Elliptic Function Technique has been successfully applied to obtain exact solution for three nonlinear wave equations. Moreover, the soliton-like solutions and trigonometric-function solutions have been also obtained as limiting cases on Jacobi Elliptic Function as $m \to 1$ and $m \to 0$.All solutions were verified by Maple package program and fig. (1), fig. (2) and fig. (3) are also new solitary wave solution for eq. (6), eq. (9) and eq. (11) respectively.

The main advantage of this method over other methods is that it provides exact solutions for all types, including Jacobian-elliptic functions. Finally, it is pertinent to mention that the proposed method is also a straightforward, short, promising and powerful method for other nonlinear evolution equations in mathematical physics. The algorithm of the method is very applicative and influential to investigate many solutions.

References

[1] Whitham G., (1974) Linear and nonlinear Waves, Wiley, New York,

[2] Gray P. Scott S. (1990) Chemical Oscillations and Instabilities Clarendon Press, Oxford,

[3] Murray J. (1989) Mathematical Biology Springer- Verlag, Berlin.

[4] Malfliet W., (1992) Solitary wave solutions of nonlinear wave equations, Am. J. Phys. 60, 650-654

[5] Malfliet, W. (2004) The tanh method: a tool for solving certain classes of nonlinear evolution and wave equations. Journal of Computational and Applied Mathematics. vol.164-165 pg. 529-541, ISSN 0377-0427 $https://doi.org/10.1016/S0377-0427(03)00645-9$

[6] Pankaj R. D. and S. Chandrawati (2016). Traveling Wave Solutions for Wave-Wave Interaction Model in Ionic Media. International Educational Scientific Research Journal E-ISSN No: 2455-295X 2(6) 70-72

[7] Kumar, A. Pankaj R. D. (2012) Some Solitary and Periodic Solutions of the nonlinear wave Equation by Variational Approach, Journals of Rajasthan Academy of Physical Sciences, Vol. 11(2) pp 133-139, ISSN:0972-6306

[8] Pankaj R. D., Meena M L and Kumar A (2021) New Soliton and Periodic Wave Solutions of Nonlinear Evolution Equations Arising in Wave Interactions. GANITA, Vol.71(1), 257-267 ISSN 0046-5402

[9] Kumar A, Pankaj R. D. (2014) Tanhcoth scheme for traveling wave solutions for Nonlinear Wave Interaction model, Journal of the Egyptian Mathematical Society. 23(2), 282285, ISSN 1110-256X.

[10] Pankaj R. D, Kumar A and Lal C (2022) A novel narration for two long waves interaction through the elaboration scheme, Journal of Interdisciplinary Mathematics, 25(1), 79-88 Print ISSN: 0972-0502 Online ISSN: 2169-012X, DOI : 10.1080/09720502.2021.2010768

[11] Xiang, C. and Wang, H. (2020) Jacobi Elliptic Function Expansion Method for the Nonlinear Vakhnenko Equation. Journal of Applied Mathematics and Physics, 8, 793-798. doi: 10.4236/jamp.2020.85061.

[12] Pankaj R. D (2022) Modelling Shallow Water Waves Propagation Through Natural-Modified Decomposition Method. Advances and Applications in Mathematical Sciences 21(3), Pages 1509-1516. ISSN 0974-6803

[13] Pankaj R. D, Lal C and Kumar A (2021) New Expansion Scheme to Solitary Wave Solutions for a Model of Wave-Wave Interactions in Plasma. Science &Technology Asia Vol.26 (4) 48-58 ISSN 2586-9000

[14] Kumar A, Pankaj R. D.(2012) Laplace-Decomposition Method to Study Solitary Wave Solutions of Coupled Non Linear Partial Differential Equation, International Scholarly Research Network (ISRN) Computational Mathematic Volume 2012, Article ID 423469, 5 pages, ISSN: 2090-7842

[15] Pankaj R. D (2013), Laplace - Modified Decomposition Method to Study Solitary Wave Solutions of Coupled Nonlinear Klein-Gordon Schrdinger Equation, International Journal of Statistika and Mathematika, Volume 5(1) pp 01-05, ISSN: 2277- 2790 E-ISSN: 2249-8605

[16] Kumar, A. Pankaj R. D. (2015) Laplace-Modified Decomposition Method for The Generalized Hiroota-Satauma Coupled KdV Equation CJBAS Vol. 03(04),126-133, ISSN 2292-3381.

[17] Ebaid A mad Aly H. (2012) Exact solutions for the transformed reduced Ostrovsky equation via the F-expansion method in terms of Weierstrass-elliptic and Jacobian-elliptic functions. Wave Motion 49(2):296-308.

[18] Yan Z. (2003) An improved algebra method and its applications in nonlinear wave equations, MM Research Preprints, no. 22, pp. 264274.

[19] Tang S. and Weber R. O. (1990) numerical study of fisher's equation by a petrov-galerkin finite element method australian mathematical society 1991, serial-fee code 0334-2700/91

[20] Hereman, W and Malflietthe W. (2005) tanh method: a tool to solve nonlinear partial differential equations with symbolic software

[21] Fisher R. A. (1936) The wave of advance of advantageous genes", Ann. Of Eugen, 7, 355-69

[22] Canosa J. (1969), Diffusion in nonlinear multiplicative media", J. Math. Phys., 10, 1862-8.

[23] Canosa, J. (1973) On a nonlinear diffusion equation describing population growth", IBM J. Res. Develop, 17 ,307-13

[24] Kolmogoroff, A, Petrovsky I. and Piscounoff N. (1937) Study of the diffusion equation with growth of the quantity of matter and its application to biology problem, Bulletin de 'University d'ilat a Moscou, Serie international, Section A, 1

[25] Zeldovich J. B. and Frank-Kamenetzki D. A., (1938), A theory of thermal propagation of flame, Acta Physicochimica U.R.S.S., 9 (2)

[26] Mirzazadeh, M., Eslami M., Bhrawy A. H., Ahmed B. and Biswas A.7 (2015). Solitons and Other Solutions to Complex-Valued Klein-Gordon Equation in $\Phi - 4$Field Theory. Appl. Math. Inf. Sci. 9, No. 6, 2793-2801

[27] Kudryashov N.A. and Zakharchenko A.S. (2014). A note on solutions of the generalized Fisher equation. Applied Mathematics Letters 32, 53-56, ISSN 0893-9659.

[28] Dubey V. P., Singh J., Ahmed M., Dubey A S and Kumar D (2022) Analysis of local fractional coupled Helmholtz and coupled Burgers' equations in fractal media, AIMS Mathematics, 7(5), 8080-8111.

[29] Singh J., Ahmed M., Dubey A S Hadid M S and Kumar D (2022). Computational Analysis of Fractional Diffusion Equations Occurring in Oil Pollution, Mathematics, 10(20). 3827

[30] Singh J, Ganbari B, Kumar D and Baleanu D. (2021) Analysis of fractional model of guava for biological pest control with memory effect, Journal of Advanced Research, 32, 99-108

[31] Singh J, Kumar D and Baleanu D (2020), A new analysis of fractional fish farm model associated with Mittag-Leffler type kernel, International Journal of Biomathematics 13(2) 2050010.

Laplace Variational Iteration Method for Solving fractional Wave like Equations

Deepika Jain, Alok Bhargava

Department of Mathematics, Swami Keshvanand Institute of Technology, Management and Gramothan, Jaipur

Manipal University Jaipur, Jaipur

30. december 2022

This paper introduces the latest procedure for explaining certain types of fractional wave equations using the variation iteration method (VIM) and Laplace transform. The Laplace variation iteration method is a type of semi-analytical technique applied to both linear and non-linear equations without requiring linearization, discretization, or perturbation. It is not a time-consuming method and converses the solution rapidly with the exact and less error solution. This approach is delineated and then explained through several example cases. The outcomes demonstrate that this alternate strategy yields reliable outcomes and the results are displayed graphically.

1 Introduction

Mathematics, engineering, and sciences are full of amazing phenomena that can be precisely described by using mathematical techniques from fractional calculus, such as the perception of fractional order derivatives and integrals [6,14,15,19]. Differential equations of fractional order [25,26,27,28] have been gaining a lot of attention newly owing to the precise understanding of nonlinear phenomena.

The Wave equations are the linear partial differential equations of the second order. This equation describes the waves, which are a common part of classic physics. These include water waves, sound waves, and light waves. Over the last few years, there has been a new application of wave-like models to physical problems. These models can be used in different fields [2,12,16,17]. Due to the importance of wave-like equations, many researchers [2,20,21] have considered solutions to these equations. For the current issue, we take into consideration the following fractional wave equations with variable

$$D_t^{\alpha} v(x,t) = F(x',y',z')\frac{\partial^2 v}{\partial x'^2} + G(x',y',z')\frac{\partial^2 v}{\partial y'^2} + H(x',y',z')\frac{\partial^2 v}{\partial z'^2}; \quad 1 < \alpha \leq 2 \tag{1}$$

with the initial conditions

$$u(x',y',z',0) = h(x',y',z'), u_t(x',y',z',0) = m(x',y',z') \tag{2}$$

An analytical approach that is more powerful than the traditional variational technique is called the “Variational iteration method” (VIM). It was initially recommended by He [8]. The “Laplace variational iteration method” is a combination of the “Laplace transform” and “variational iteration method.” Applications of VIM to fractional differential equations are slow to converge, mainly because they directly use the Lagrange multipliers of ordinary differential equations (ODEs) [23]. Wu and Baleanu [24] pointed out that it can be difficult to apply integrals by parts of the Riemann-Liouville (RL) integral resulting from the constructed correction function. To overcome this shortcoming, they proposed to identify generalized Lagrange multipliers via the Laplace transform. This method has been utilized by many authors to solve several difficulties [1,3,7]. The novelty of this work lies in applying the “Laplace variational iteration method” (LVIM) for solving heat equations of fractional order.

2 Preliminaries

Definition 1 The Caputo derivative of arbitrary order [4] of function v(x,t) is presented as

$$D_t^{\alpha} v\,(\,x,t\,) = \frac{1}{\Gamma(m-\mu} \int_0^t (t-\delta)^{m-\mu-1}\, v^{(m)}\,(\,x,\delta\,)\, d\delta = J_t^{m-\mu} D^m u(\,v,t\,); \quad m-1<\mu \le\ m, m\in\ N, \tag{3}$$

where $\frac{d^{\alpha}}{dt^{\alpha}}$ and J_t^{α} shows the Riemann- Liouville integral operator of fractional order [19], $\alpha > 0$

$$J_t^{\alpha} v(x,t) = \frac{1}{\Gamma(\alpha)} \int_0^t (t-\delta)^{\alpha-1} v(x,\delta)\, d\delta\ ; m-1<\mu\le m, m\in N \tag{4}$$

Definition 2 The Laplace Transform [18,19] of f(t), $t>0$ is defined as

$$L[f(t)] = F(s) = \int_0^t e^{-st} f(t)\, dt \tag{5}$$

Definition 3 The Laplace transform of $D_t^{\alpha} v(x,t)$ is explained as [18,19]

$$L[D_t^{\alpha} v(x,t)] = L[v(x,t)] - \sum_{n=0}^{m-1} v^n(x,0) s^{\alpha-n-1}; m-1<\alpha\le m, m\in N \tag{6}$$

Definition 4 The Mittag-Leffler function is explained as [18]

$$E_{\alpha}\,(t) = \sum_{n=0}^{\infty} \frac{t^n}{\Gamma\,(\alpha n+1)} \tag{7}$$

$$E_{\alpha,\beta}(t) = \sum_{n=0}^{\infty} \frac{t^n}{\Gamma(\alpha n+\beta)} \tag{8}$$

3 Variational Iteration Method

He [10] established a method VIM for solving problems. This is a common technique used to evaluate solutions for linear and non-linear problems. Illustrate the VIM model, we take into consideration the subsequent non-linear equation with given constraints::

$$Pv(x,t) + Qv(x,t) = f(x,t) \tag{9}$$

where $'v'$ is the unknown function, 'P', 'Q' are linear and nonlinear operators, and f is the source term. The correction functional for (7) is given as follows:

$$v_{n+1}(x,t) = v_n(x,t) + \int_0^t \lambda[Pv_n(\xi,t) + Qv_n(\xi,t) - f(\xi,t)]d\xi \tag{10}$$

where λ is a general Lagrange multiplier that can be identified optimally via the variation theory. The subscript n indicates the nth approximation and u_n is considered as a restricted variation $\delta u_n = 0$.

3.1 Laplace Variational Iteration Method (LVIM)

To demonstrate the elementary purpose of (LVIM), deliberate a general fractional non-linear nonhomogeneous partial differential equation through the primary situations of the type

$$D_t^\alpha v(x,t) + Pv(x,t) + Qv(x,t) = f(x,t); m-1 < \alpha \leq m, m \in N \tag{11}$$

$$v_n(x,0) = h_k(x); n = 0,1,2,3,...m-1 \tag{12}$$

where D_t^α is the Caputo derivative. P and Q are linear and nonlinear operators, respectively, and f is the source term. By applying Laplace transform pertaining to t, on both sides of (9), we get

$$L[v(x,t)] = \frac{1}{s^\alpha}\sum_{n=0}^{m-1} v^n(x,0)s^{\alpha-n-1} + \frac{1}{s^\alpha}L[f(x,t)] - \frac{1}{s^\alpha}L[Pv(x,t) + Qv(x,t)] \tag{13}$$

taking inverse Laplace transform on equation (13)

$$\begin{aligned} v(x,t) = L^{-1}\left[\frac{1}{s^{\alpha}}\sum_{n=0}^{m-1} s^{\alpha-1-n}v^n(x,0) + \frac{1}{s^{\alpha}}L[f(x,t)]\right] - \\ L^{-1}\left[\frac{1}{s^{\alpha}}L[Pv(x,t) + Qv(x,t)]\right] \end{aligned} \tag{14}$$

by differentiating (14), concerning t, we get

$$\begin{aligned} \frac{\partial v(x,t)}{\partial t} = \frac{\partial}{\partial t}\left\{L^{-1}\left[\frac{1}{s^{\alpha}}\sum_{n=0}^{m-1} s^{\alpha-1-n}v^n(x,0) + \frac{1}{s^{\alpha}}L[f(x,t)]\right] - \right. \\ L^{-1}\left[\frac{1}{s^{\alpha}}L[Pv(x,t) + Qv(x,t)]\right] \end{aligned} \tag{15}$$

The correction functional for (15)

$$v_{n+1}(\,x,t\,)=v_n(\,x,t\,)+\int_0^t\lambda\left[\frac{\partial v_n(\,x,\varepsilon\,)}{\partial\varepsilon}-\right.$$
$$\frac{\partial}{\partial\varepsilon}\left\{L^{-1}\left[\frac{1}{s^{\alpha}}\sum_{n=0}^{m-1}s^{\,\alpha-1-n}v^n(\,x,0\,)+\frac{1}{s^{\alpha}}L\left[f(\,x,t\,)\right]\right]\right\}- \tag{16}$$
$$\left.L^{-1}\left[\frac{1}{s^{\alpha}}L\left[Pv(\,x,\varepsilon\,)+Qv(\,x,\varepsilon\,)\right]\right]d\varepsilon\right.$$

The general Lagrange multiplier for (16) can be identified optimally via variation theory to get

$$1+(\lambda)_{\epsilon=t}=0 \tag{17}$$

From (17), we get

$$\lambda=-1 \tag{18}$$

Substituting $\lambda=-1$ into (16), then the iterative formula for $n=0,1,2,$ . . ., as follows:

$$v_{n+1}(\,x,t\,)=v_n(\,x,t\,)-\int_0^t\left[\frac{\partial v_n(\,x,\varepsilon\,)}{\partial\varepsilon}-\frac{\partial}{\partial\varepsilon}\left\{L^{-1}\left[\frac{1}{s^{\alpha}}\sum_{n=0}^{m-1}\right.\right.\right.$$
$$\left.s^{\,\alpha-1-n}v^n(\,x,0\,)+\frac{1}{s^{\alpha}}L\left[f(\,x,t\,)\right]-L^{-1}\left[\frac{1}{s^{\alpha}}L\left[Pv(\,x,\varepsilon\,)+Qv(\,x,\varepsilon\,)\right]\right]d\varepsilon \right. \tag{19}$$

Begin with the early iteration

$$v_0(x,t)=v(x,0)+tv_t(x,0) \tag{20}$$

As a limit of the subsequent approximations, the exact answer is provided $v_n(x,t)$, $n=0,1,2,\ldots$; alternatively in other words

$$v(x,t)=\lim_{n\to\infty}v_n(x,t) \tag{21}$$

3.2 Applications of LVIM for Solving fractional wave-like equations

Problem 1 Deliberate the succeeding 1-D fractional wave-like equation:

$$D_t^{\alpha} v(x,t) = \frac{1}{2} x^2 \frac{\partial^2 v}{\partial x^2}; 1 < \alpha \leq 2 \tag{22}$$

initial condition:

$$v_0(x,y,0) = 0, v_t(x,0) = x^2 \tag{23}$$

taking the Laplace transformation on (22) and result specified by equation (23) we obtain

$$L\left[v(\ x,t\ )\right] = \frac{x}{s} + \frac{x^2}{s^2} + \frac{1}{2s^{\alpha}} x^2 L\left[\frac{\partial^2 u}{\partial x^2}\right] \tag{24}$$

applying inverse Laplace transformation to the Equation (24), we have

$$v(\ x,t\ ) = x + x^2 t + L^{-1}\left[\frac{1}{2s^{\alpha}} x^2 L\left[\frac{\partial^2 v}{\partial x^2}\right]\right] \tag{25}$$

differentiating Equation (25) concerning t, we have

$$\frac{\partial v}{\partial t} = x^2 + \frac{\partial}{\partial t} L^{-1}\left[\frac{1}{2s^{\alpha}} x^2 L\left[\frac{\partial^2 v}{\partial x^2}\right]\right] \tag{26}$$

the correction functional for $\lambda = -1$ is offered by

$$v_{n+1}(\ x,t\ ) = v_n(\ x,t\ ) - \int_0^t \left[\frac{\partial v_n(\ x,\varepsilon\ )}{\partial \varepsilon} - x^2 - \frac{\partial}{\partial \varepsilon} L^{-1}\left\{\frac{1}{2s^{\alpha}} x^2 L\left(\frac{\partial^2 v_n}{\partial x^2}\right)\right\}\right] d\varepsilon \tag{27}$$

the initial iteration

$$v_0(x,0) = x + x^2 t \tag{28}$$

using the equation in equation (26), we have

$$v_0(x,t) = v_0(x,0) = x + x^2 t \tag{29}$$

$$v_1(x,t) = x + x^2 t + x^2 \frac{t^{\alpha+1}}{\Gamma(\alpha+2)} \tag{30}$$

$$v_2(x,t) = x + x^2 t + x^2 \frac{t^{\alpha+1}}{\Gamma(\alpha+2)} + x^2 \frac{t^{2\alpha+1}}{\Gamma(2\alpha+2)} \tag{31}$$

therefore it is expected that the general term in the successive approximation

$$v_n(x,t) = x + x^2[t + \frac{t^{\alpha+1}}{\Gamma(\alpha+2)} + \frac{t^{2\alpha+1}}{\Gamma(2\alpha+2)} + ...] \tag{32}$$

assumed that the solution was in closed form by

$$v(x,t) = \lim_{n\to\infty} v_n(x,t) = x + x^2 t E_{\alpha,2}(t^\alpha) \tag{33}$$

where $E_{\alpha,2}(t^\alpha)$ is the Mittag- Laffler Function defined in equation (6) letting $\alpha = 2$ then

$$v(x,t) == x + x^2 t + \frac{sinht}{t} \tag{34}$$

Numerical and Graphical discussion

In this part we found a record for numerical explanation of equation (31) and plot some graphs for $\alpha = 0.25, 0.5, 0.75, 1$.

Table 1: The values of $v(x,t)$ for $\alpha = 0.25$

$\alpha = 0.25$					
t	X=1	X=3	X=5	X=7	X=9
0	2	12	30	56	90
2	22.907618	50.042141	135.672615	263.118327	432.379275
4	13.010819	111.097371	305.270476	595.530113	981.876342
6	21.343969	186.09572	513.599243	1003.854451	1656.861548
8	30.896476	272.068286	752.411907	1471.927338	2430.614579
10	41.483595	367.352360	1017.089089	1990.696185	3288.171245

Table 2: The values of $v(x,t)$ for $\alpha = 0.50$

$\alpha = 0.50$					
t	X=1	X=3	X=5	X=7	X=9
0	2	12	30	56	90
2	49.149229	58.14922947	133.192304	258.256916	424.343065
4	16.018022	138.162200	380.450555	742.883089	1225.459800
6	31.055812	273.502315	756.395319	1479.734827	2443.520836
8	51.021537	453.193835	1255.538432	2458.055328	4060.744521
10	75.788321	676.094894	1874.708039	3671.627756	6066.854046

Table 3:The values of $v(x,t)$ for $\alpha = 0.75$

$\alpha = 0.75$					
t	X=1	X=3	X=5	X=7	X=9
0	2	12	30	56	90
2	5.239601	41.156416	110.990046	214.740490	352.407748
4	19.958726	173.628535	478.968154	935.977582	1544.656820
6	57.104733	507.942604	1407.618347	2756.131960	4553.483443
8	129.591614	1160.324531	3219.790365	6307.989114	10424.92078
10	251.599886	2258.398981	6269.997168	12286.39445	20307.59083

Table 4:The values of $v(x,t)$ for $\alpha = 1$

$\alpha = 1.0$					
t	X=1	X=3	X=5	X=7	X=9
0	2	12	30	56	90
2	5.33	42	113.33	219.33	360
4	20.66	180	496.66	970.66	1602
6	56	498	1380	2702	4464
8	119.33	1068	2963.33	5805.33	9594
10	218.66	1962	5446.66	10672.66	17640

The solution is graphically presented in Figures 1,2,3, and 4 for various fractional orders of α

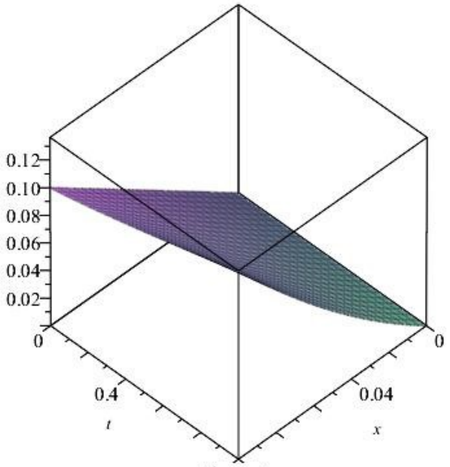

Figure 1
α=0.25

Figur 1: The behaviour of $v(x,t)$ w.r.t. x and t for $\alpha = 0.25$

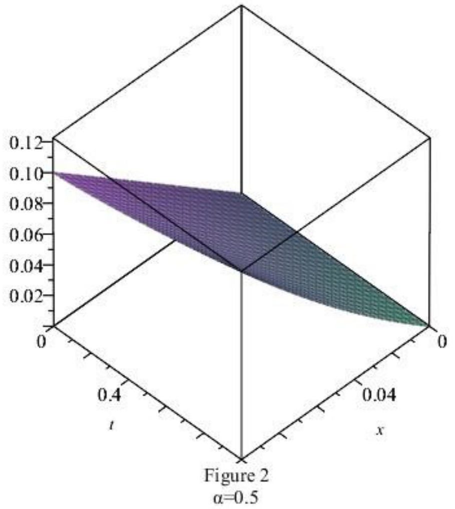

Figur 2: The behaviour of $v(x,t)$ w.r.t. x and t for $\alpha = 0.50$

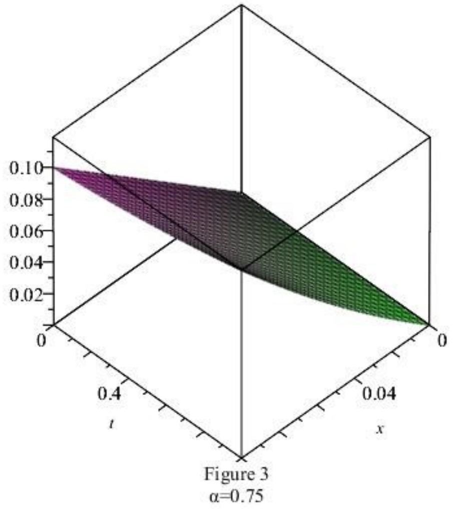

Figur 3: The behaviour of $v(x,t)$ w.r.t. x and t for $\alpha = 0.75$

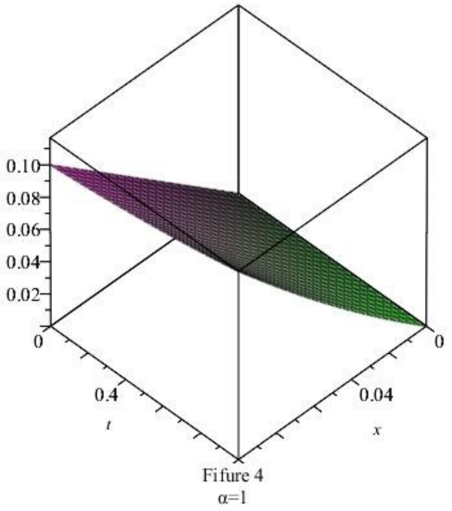

Figur 4: The behaviour of $v(x,t)$ w.r.t x and t for $\alpha = 1$

Problem 2 Deliberate the succeeding 2-D fractional wave-like equation:

$$D_t^{\alpha} v(x,y,t) = \frac{1}{2}[x^2 \frac{\partial^2 v}{\partial x^2} + y^2 \frac{\partial^2 v}{\partial y^2}], 1 < \alpha \leq 2 \tag{35}$$

initial condition:

$$v_0(x,y,0) = x^4, v_t(x,y,0) = y^4 \tag{36}$$

taking the Laplace transformation on (34) and using the result specified by (35), we achieve,

$$v(\ x,y,t\ ) = x^4 + y^4 t + L^{-1}\left[\frac{1}{12 s^{\alpha}} L\left[x^2 \frac{\partial^2 v}{\partial x^2} + y^2 \frac{\partial^2 v}{\partial y^2}\right]\right] \tag{37}$$

apply inverse Laplace transform we have

$$\frac{\partial v}{\partial t} = y^4 + \frac{\partial}{\partial t} L^{-1}\left[\frac{1}{12 s^{\alpha}} L\left[x^2 \frac{\partial^2 v}{\partial x^2} + y^2 \frac{\partial^2 v}{\partial y^2}\right]\right] \tag{38}$$

the correction functional for $\lambda = -1$ is given as follows

$$v_{n+1}(\,x,y,t\,) = v_n(\,x,y,t\,) - \int_0^t \Bigg[\frac{\partial v_n(\,x,y,\varepsilon\,)}{\partial \varepsilon} - y^4 - \\ \frac{\partial}{\partial \varepsilon} L^{-1}\left\{\frac{1}{12s^{\alpha}} L\left(x^2\frac{\partial^2 v_n}{\partial x^2} + y^2\frac{\partial^2 v_n}{\partial y^2}\right)\right\} d\varepsilon \tag{39}$$

the initial iteration

$$v_0(x,y,0) = x^4 + y^4 t \tag{40}$$

using the equation in equation (38), we have

$$v_0(x,y,t) = x^4 + y^4 t \tag{41}$$

$$v_1(x,y,t) = x^4 + y^4 t + x^4\frac{t^{\alpha+1}}{\Gamma(\alpha+1)} + y^4\frac{t^{\alpha+1}}{\Gamma(\alpha+2)} \tag{42}$$

$$v_2(x,y,t) = x^4 + y^4 t + x^4\frac{t^{\alpha+1}}{\Gamma(\alpha+1)} + y^4\frac{t^{\alpha+1}}{\Gamma(\alpha+2)} + x^4\frac{t^{2\alpha}}{\Gamma(2\alpha+1)} + y^4\frac{t^{2\alpha+1}}{\Gamma(\alpha+2)} \tag{43}$$

assumed that the solution was in closed form by

$$v(x,y,t) = \lim_{n\to\infty} v_n(x,y,t) = x^4 E_{\alpha}(t^{\alpha}) + y^4 E_{\alpha,2}(t^{\alpha}) \tag{44}$$

where $E_{\alpha,2}(t^{\alpha})$ is the Mittag- Laffler Function defined in equation (6) letting $\alpha = 2$ then

$$v(x,y,t) == x^4 cosht + y^4 sinht \tag{45}$$

Numerical and Graphical discussion

In this part we found a record for numerical explanation of equation (42) and plot some graphs for $\alpha = 0.25, 0.5, 0.75, 1$.

Table 5: The values of $v(x,y,t)$ for $\alpha = 0.25$

$\alpha = 0.25$					
t	X=1	X=3	X=5	X=7	X=9
0	16	81	625	2401	6561
2	10.723461	322.384991	2448.587477	9388.799277	25645.15124
4	13.010819	111.097371	305.270476	595.530113	981.876342
6	30.834622	470.086827	3457.001819	13208.40076	36049.51540
8	42.943473	524.703270	3814.269888	14553.73738	39709.24682
10	56.013753	578.426352	4130.832026	15728.39172	42893.84687

Table 6:The values of $v(x, y, t)$ for $\alpha = 0.50$

$\alpha = 0.50$					
t	X=1	X=3	X=5	X=7	X=9
0	16	81	625	2401	6561
2	10.723461	378.384991	2878.483393	11040.56935	30158.96889
4	25.274780	605.815447	4553.491981	17441.49478	47629.60945
6	44.819765	825.936021	6137.526560	23478.30743	64096.35272
8	69.213075	1044.536135	7676.732939	29328.90486	80045.70396
10	98.356569	1263.816429	9188.943467	35062.15232	95666.06497

Table 7:The values of $v(x, y, t)$ for $\alpha = 0.75$

$\alpha = 0.75$					
t	X=1	X=3	X=5	X=7	X=9
0	16	81	625	2401	6561
2	9.535236	406.142637	3103.072959	11907.75724	32531.34205
4	23.880947	831.523787	6323.495098	24253.16615	66250.59382
6	44.109711	1342.276394	10169.80983	38989.11017	106493.7576
8	70.420350	1926.202514	14545.52123	55743.88528	152244.5578
10	103.057275	2575.614244	19389.00163	74279.76634	202852.7288

Table 8:The values of $v(x, y, t)$ for $\alpha = 1$

$\alpha = 1.0$					
t	X=1	X=3	X=5	X=7	X=9
0	16	81	625	2401	6561
2	10.33	410.33	3130.33	12010.33	32810.33
4	35.66	1075.66	8147.66	31235.66	85315.66
6	85	2085	15685	60085	164085
8	166.33	3446.33	25750.33	98566.33	269126.33
10	287.66	5167.66	38351.66	146687.66	400447.66

The solution is graphically presented in Figures 5,6,7, and 8 for various fractional orders of α

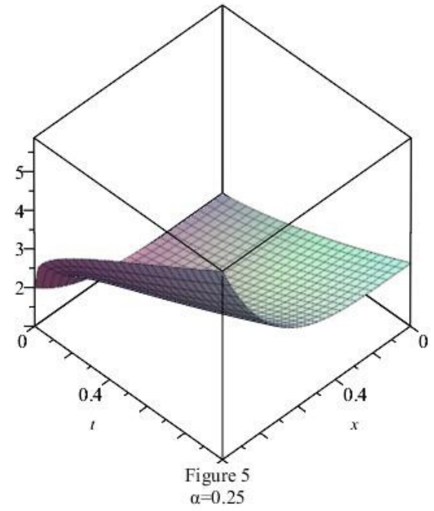

Figur 5: The behaviour of $v(x, y, t)$ w.r.t. x and t for $\alpha = 0.25$

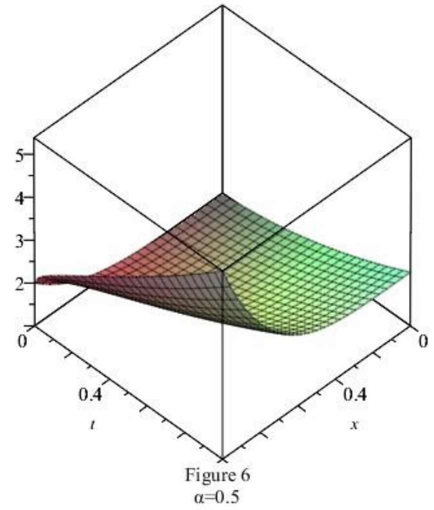

Figur 6: The behaviour of $v(x, y, t)$ w.r.t. x and t for $\alpha = 0.50$

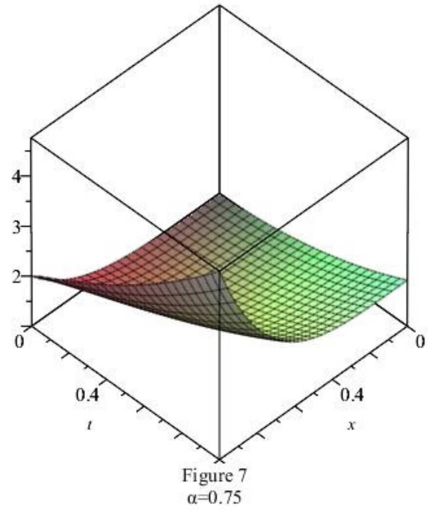

Figur 7: The behaviour of $v(x, y, t)$ w.r.t. x and t for $\alpha = 0.75$

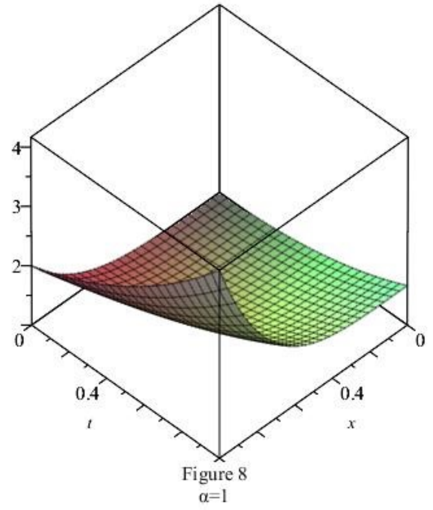

Figur 8: The behaviour of $v(x, y, t)$ w.r.t.x and t for $\alpha = 1$

Problem 3 Deliberate the succeeding 3-D fractional wave-like equation:

$$D_t^{\alpha} v(\, x, y, z, t\,) = x^2 + y^2 + z^2 + \frac{1}{2}\left[x^2 \frac{\partial^2 v}{\partial x^2} + y^2 \frac{\partial^2 v}{\partial y^2} + z^2 \frac{\partial^2 v}{\partial z^2}\right]; 1 < \alpha \leq 2 \quad (46)$$

initial condition:

$$v_0(x,y,z,0)=0, v_t(x,y,z,0)=x^2+y^2-z^2 \tag{47}$$

taking the laplace transform of equation (45) and result obtained by equation (46) we obtain

$$\begin{aligned} L\left[v(\ x,y,z,t\ )\right]=\frac{x^2+y^2-z^2}{s^2}+\frac{1}{s^\alpha}L\left(x^2+y^2+z^2\right)+\\ \frac{1}{2s^\alpha}L\left[x^2\frac{\partial^2 v}{\partial x^2}+y^2\frac{\partial^2 v}{\partial y^2}+z^2\frac{\partial^2 v}{\partial z^2}\right]\end{aligned} \tag{48}$$

apply inverse Laplace transform we have

$$\begin{aligned} v(\ x,y,z,t\ )=t\left(x^2+y^2-z^2\right)+\left(x^2+y^2+z^2\right)\frac{t^\alpha}{\Gamma(\alpha+1)}+\\ L^{-1}\left[\frac{1}{2s^\alpha}L\left[x^2\frac{\partial^2 v}{\partial x^2}+y^2\frac{\partial^2 v}{\partial y^2}+z^2\frac{\partial^2 v}{\partial z^2}\right]\right]\end{aligned} \tag{49}$$

differentiating Equation (48) regarding t, we have

$$\begin{aligned} \frac{\partial v}{\partial t}=\left(x^2+y^2-z^2\right)+\left(x^2+y^2+z^2\right)\alpha\frac{t^{\alpha-1}}{\Gamma(\alpha+1)}+\\ \frac{\partial}{\partial t}\left\{L^{-1}\left[\frac{1}{2s^\alpha}L\left[x^2\frac{\partial^2 v}{\partial x^2}+y^2\frac{\partial^2 v}{\partial y^2}+z^2\frac{\partial^2 v}{\partial z^2}\right]\right]\right\}\end{aligned} \tag{50}$$

the correction functional for $\lambda=-1$ is given as follows

$$\begin{aligned} v_{n+1}\left(x,y,z,t\right)=v_n\left(x,y,z,t\right)-\int_0^t\left[\frac{\partial v_n\left(x,y,z,\varepsilon\right)}{\partial\varepsilon}-\left(x^2+y^2-z^2\right)-\right.\\ \left.\left(x^2+y^2+z^2\right)\frac{\alpha\varepsilon^{\alpha-1}}{\Gamma\left(\alpha+1\right)}-\frac{\partial}{\partial\varepsilon}\left\{L^{-1}\left[\frac{1}{2s^\alpha}L\left[x^2\frac{\partial^2 v_n}{\partial x^2}+y^2\frac{\partial^2 v_n}{\partial y^2}+z^2\frac{\partial^2 v_n}{\partial z^2}\right]\right]\right\}\right] d\varepsilon\end{aligned} \tag{51}$$

the initial iteration

$$v_0(x,y,z,0)=(x^2+y^2-z^2)t+(x^2+y^2+z^2\ )\frac{t^\alpha}{\Gamma(\alpha+1)} \tag{52}$$

then, we have

$$v_1(\ x,y,z,t\ ) = v_0(\ x,y,z,t\ ) - \int_0^t \left[\frac{\partial v_0(\ x,y,z,\ \varepsilon\ )}{\partial \varepsilon} - \left(x^2+y^2-z^2\right) - \left(x^2+y^2+z^2\right)\frac{\alpha\varepsilon^{\alpha-1}}{\Gamma\left(\alpha+1\right)} - \frac{\partial}{\partial\varepsilon}\left\{L^{-1}\left[\frac{1}{2s^\alpha}L\left[x^2\frac{\partial^2 v_0}{\partial x^2}+y^2\frac{\partial^2 v_0}{\partial y^2}+z^2\frac{\partial^2 v_0}{\partial z^2}\right]\right]\right\} d\varepsilon \tag{53}$$

$$v_1(\ x,y,z,t\ ) = t\left(x^2+y^2-z^2\right) + \left(x^2+y^2+z^2\right)\frac{t^\alpha}{\Gamma(\alpha+1)} + \left(x^2+y^2-z^2\right)\frac{t^{\alpha+1}}{\Gamma(\alpha+2)} + \left(x^2+y^2+z^2\right)\frac{t^{2\alpha}}{\Gamma(2\alpha+1)} \tag{54}$$

$$v_2(\ x,y,z,t\ ) = v_1(\ x,y,z,t\ ) - \int_0^t \left[\frac{\partial v_1(x,y,z,\varepsilon)}{\partial \varepsilon} - \left(x^2+y^2-z^2\right) - \left(x^2+y^2+z^2\right)\frac{\alpha\varepsilon^{\alpha-1}}{\Gamma\left(\alpha+1\right)} - \frac{\partial}{\partial\varepsilon}\left\{L^{-1}\left[\frac{1}{2s^\alpha}L\left[x^2\frac{\partial^2 v_1}{\partial x^2}+y^2\frac{\partial^2 v_1}{\partial y^2}+z^2\frac{\partial^2 v_1}{\partial z^2}\right]\right]\right\} d\varepsilon \tag{55}$$

$$v_2(\ x,y,z,t\ ) = t\left(x^2+y^2-z^2\right) + \left(x^2+y^2+z^2\right)\frac{t^\alpha}{\Gamma(\alpha+1)} + \left(x^2+y^2-z^2\right)\frac{t^{\alpha+1}}{\Gamma(\alpha+2)} + \left(x^2+y^2+z^2\right)\frac{t^{2\alpha}}{\Gamma(2\alpha+1)} + \left(x^2+y^2-z^2\right)\frac{t^{2\alpha+1}}{\Gamma(2\alpha+2)} + \left(x^2+y^2+z^2\right)\frac{t^{3\alpha}}{\Gamma(3\alpha+1)} \tag{56}$$

assumed that the solution was in closed form by

$$v(\ x,y,z,t\ ) = limn \rightarrow \infty v_n(\ x,y,z,t\ ) = \ t\left(x^2+y^2-z^2\right)E_{\alpha,2}\left(t^\alpha\right) + \left(x^2+y^2+z^2\right)\left[E_\alpha\left(t^\alpha\right)-1\right] \tag{57}$$

where $E_\alpha\left(t^\alpha\right)$ and $E_{\alpha,2}(t^\alpha)$ are the Mittag-Laffer Function defined in equations (7) and (8) letting $\alpha = 2$ then

$$v(x,y,z,t) = (x^2+y^2)e^t + z^2e^{-t} - (x^2+y^2+z^2) \tag{58}$$

Numerical and Graphical discussion

In this part we found a record for numerical explanation of equation (51) and plot some graphs for different values of $\alpha = 0.25, 0.5, 0.75, 1$.

Table 9:The values of $v(x, y, z, t)$ for $\alpha = 0.25$

$\alpha = 0.25$					
t	X=1	X=3	X=5	X=7	X=9
0	0	0	0	0	0
2	8.513426	60.620834	164.835650	321.157875	529.587508
4	13.992796	109.935171	301.819920	589.647043	973.416542
6	20.636626	169.729635	467.915654	915.194682	36049.51540
8	28.188647	237.697827	656.716187	1285.243727	2123.280446
10	36.506662	312.559961	864.666558	1692.826455	27107.039651

Table 10:The values of $v(x, y, z, t)$ for $\alpha = 0.50$

$\alpha = 0.50$					
t	X=1	X=3	X=5	X=7	X=9
0	0	0	0	0	0
2	9.127692	66.149229	180.192304	351.256916	579.343065
4	21.018022	173.162200	477.450555	933.883089	1542.459800
6	38.05581275	326.502315	903.395319	23478.30743	64096.35272
8	60.021537	524.193835	1452.538432	2845.055328	4701.744521
10	86.788321	765.094894	2121.708039	4156.62775	6869.854046

Table 11 The values of $v(x, y, z, t)$ for $\alpha = 0.75$

$\alpha = 0.75$					
t	X=1	X=3	X=5	X=7	X=9
0	0	0	0	0	0
2	8.793468	63.1412156	171.836710	334.879951	552.270940
4	23.663151	196.968364	543.578790	1063.494429	1756.71528
6	49.835450	432.519053	1197.886259	2345.937068	3876.671480
8	89.129443	786.164995	2180.236099	4271.342754	7059.484963
10	143.116946	1272.052519	3529.923663	6916.730379	903.395319

Table 12:The values of $v(x,y,z,t)$ for $\alpha = 1$

$\alpha = 1.0$					
t	X=1	X=3	X=5	X=7	X=9
0	0	0	0	0	0
2	8.3333	59	160.33	312.33	515
4	25.33	215	593.66	1161.66	1919
6	63	551	1527	2991	4943
8	128.33	1139	3160.33	6192.33	10235
10	229.66	2051	5693.66	11157.66	18443

The solution is graphically presented in Figures 9,10,11, and 12 for various fractional orders of α

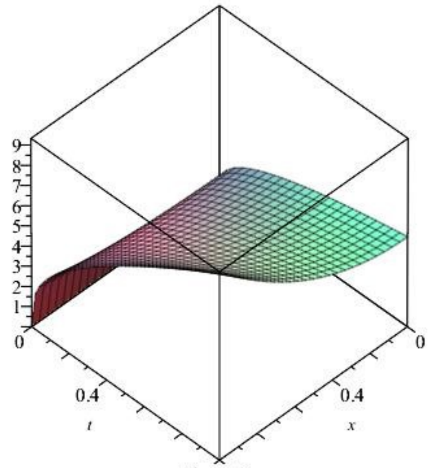

Figure 9
α=0.25

Figur 9: The behaviour of $v(x,y,z,t)$ w.r.t. x and t for $\alpha = 0.25$

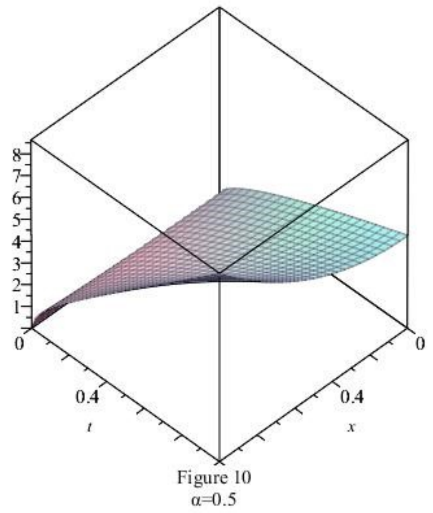

Figur 10: The behaviour of $v(x, y, z, t)$ w.r.t. x and t for $\alpha = 0.50$

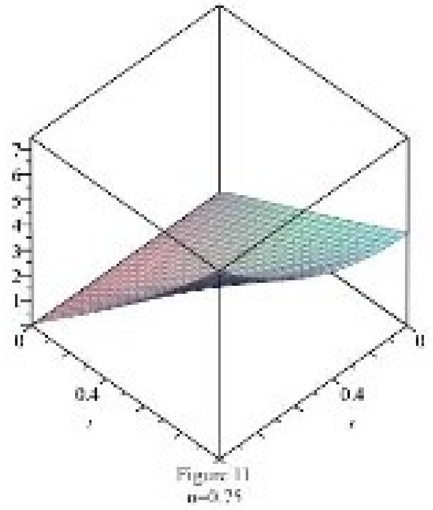

Figur 11: The behaviour of $v(x, y, z, t)$ w.r.t. x and t for $\alpha = 0.75$

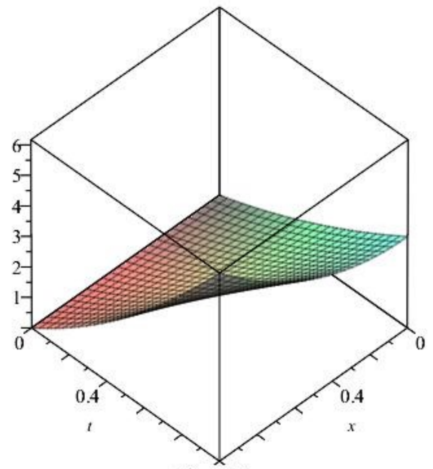

Figure 12
α=1

Figur 12: The behaviour of $v(x, y, z, t)$ w.r.t. x and t for $\alpha = 1$

4 Conclusion:

We review the Laplace variational iteration method to show why it works well for obtaining approximate analytical solutions of nonlinear equations governing nonlinear phenomena. In the conferred document, the “Laplace Variational Iteration Method” is productively executed for the fractional wave equation, wherever we put in the fractional derivative in form of Caputo sense. The analytical, consequent, and comprehensive outcomes have been specified in expressions of a power series that come together to the exact solutions. The graphical consequences of the analysis are also manifested. In the future authors and scholars may use this paper for reference purposes and different values for parameters may be used for the graphical presentation so that the related phenomena may well be understood.

5 References

[1]Abassy, T. A., El-Tawil, M. A., El-Zoheiry, H. (2007). Exact solutions of some nonlinear partial differential equations using the variational iteration method linked with Laplace transforms and the Padé technique. Computers and Mathematics with Applications ,54(7-8), 940-954.

[2]Akhmetov, A. A. (2003). Long current loops as regular solutions of the equation for coupling currents in a flat two-layer superconducting cable. Cryogenics, 43(3-5), 317-322.

[3] Arife, A. S. (2011). New modified variational iteration transforms method (MVITM) for solving eighth-order boundary value problems in one step. In World Appl. Sci. J., 34 (6), 21-30.

[4] Caputo, M. (1969). Elasticita e dissipazione. Zanichelli

[5] Drăgănescu, G. E. (2006). Application of a variational iteration method to linear and nonlinear viscoelastic models with fractional derivatives. Journal of Mathematical Physics, 47(8), 082902.

[6] Gorenflo, R., Mainardi, F. (1997). Fractional calculus. In Fractals and fractional calculus in continuum mechanics (pp. 223-276). Springer, Vienna

[7] Hammouch, Z., Mekkaoui, T. (2010). A Laplace-variational iteration method for solving the homogeneous Smoluchowski coagulation equation.

[8] He, J. H. (1999). Some applications of nonlinear fractional differential equations and their approximations. Bull. Sci. Technol, 15(2), 86-90.

[9] He, J. H. (2012). An approximation to solution of space and time fractional telegraph equations by the variational iteration method. Mathematical Problems in Engineering, 10(5), 212-214.

[10] He, J. H. (1999). Variational iteration method–a kind of non-linear analytical technique: some examples. International journal of non-linear mechanics, 34(4), 699-708.

[11] He, J. H., Wu, X. H. (2007). Variational iteration method: new development and applications. Computers Mathematics with Applications, 54(7-8), 881-894.

[12] Holliday, J. R., Rundle, J. B., Tiampo, K. F., Klein, W., Donnellan, A. (2006). Modification of the pattern informatics method for forecasting large earthquake events using complex eigenfactors. Tectonophysics, 413(1-2), 87-91.

[13] Khuri, S. A., Sayfy, A. (2012). A Laplace variational iteration strategy for the solution of differential equations. Applied Mathematics Letters, 25(12), 2298-2305.

[14] Luchko, Y., Gorenflo, R. (1998). The initial value problem for some fractional differential equations with the Caputo derivatives.

[15] Mainardi, F. (2012). Fractional calculus: some basic problems in continuum and statistical mechanics. arXiv preprint arXiv:1201.0863.

[16] Manolis, G. D., Rangelov, T. V. (2006). Non-homogeneous elastic waves in soils: Notes on the vector decomposition technique. Soil Dynamics

and Earthquake Engineering, 26(10), 952-959.

[17] Merlani, A. L., Natale, G., Salusti, E. (1997). On the theory of pressure and temperature nonlinear waves in compressible fluid-saturated porous rocks. Geophysical Astrophysical Fluid Dynamics, 85(1-2), 97-128.

[18]Miller, K. S., Ross, B. (1993). An introduction to the fractional calculus and fractional differential equations,Wiley.

[19] Podlubny, I. (1998). Fractional differential equations: an introduction to fractional derivatives, fractional differential equations, to methods of their solution and some of their applications. Elsevier.

[20] Sadighi, A., Ganji, D. D., Gorji, M., Tolou, N. (2008, February). Numerical simulation of heat-like models with variable coefficients by the variational iteration method. In Journal of Physics: Conference Series (Vol. 96, No. 1, p. 012083). IOP Publishing

[21]Shou, D. H., He, J. H. (2008). Beyond Adomian method: The variational iteration method for solving heat-like and wave-like equations with variable coefficients. Physics Letters A, 372(3), 233-237.

[22]D.O. Hebb, Wazwaz, A. M. (2010). Partial differential equations and solitary waves theory. Springer Science & Business Media.

[22] Wazwaz, A. M. (2010). Partial differential equations and solitary waves theory. Springer Science Business Media.

[23] JH, H. (1998). Approximate analytical solution for seepage flow with fractional derivatives in porous media. Computer Methods in Applied Mechanics and Engineering, 167(12), 57-68.

[24] Wu, G. C., Baleanu, D. (2013). Variational iteration method for fractional calculus-a universal approach by Laplace transform. Advances in Difference Equations, 2013(1), 1-9.

[25] Dubey, V. P., Singh, J., Alshehri, A. M., Dubey, S., Kumar, D. (2022). Forecasting the behavior of fractional order Bloch equations appearing in NMR flow via a hybrid computational technique. Chaos, Solitons Fractals, 164, 112691.

[26] Dubey, V. P., Kumar, D., Alshehri, H. M., Singh, J., Baleanu, D. (2022). Generalized invexity and duality in multiobjective variational problems involving non-singular fractional derivative. Open Physics, 20(1), 939-962.

[27] Dubey, V. P., Singh, J., Alshehri, A. M., Dubey, S., Kumar, D. (2022). Analysis of local fractional coupled Helmholtz and coupled Burgers' equations in fractal media. AIMS Mathematics, 7(5), 8080-8111.

[28] Dubey, V. P., Singh, J., Alshehri, A. M., Dubey, S., Kumar, D.

(2022). A hybrid computational method for local fractional dissipative and damped wave equations in fractal media. Waves in Random and Complex Media, 1-23.

J. COMPUTATIONAL ANALYSIS AND APPLICATIONS, VOL. 31, NO. 3, 2023, COPYRIGHT 2023 EUDOXUS PRESS, LLC

Boros Integral Involving the Product of Family of Polynomials and the Incomplete I-Function

Sanjay Bhatter[1], Nishant[1,*], Daya Lal Suthar[2] and Sunil Dutt Purohit[3]
[1]Department of Mathematics, Malaviya National Institute of Technology, Jaipur, India.
sbhatter.maths@mnit.ac.in, nishantjangra1996@gmail.com
[2] Department of Mathematics, Wollo University, P.O. Box: 1145, Dessie, Ethiopia.
dlsuthar@gmail.com
[3]Department of HEAS (Mathematics), Rajasthan Technical University, Kota, India.
sunil_a_purohit@yahoo.com

Abstract

The current manuscript's goal is to determine the Boros integral with three parameters, which comprises of the multiplication of the incomplete I-function and a family of polynomials. Some interesting corollaries are provided as a specific case of our primary findings.

Keywords: Incomplete Gamma function, Incomplete I-function, Mellin-Barnes integrals contour, Boros integral, Generalized family of polynomials.
MSC 2010: 33B20, 33C05, 33C60, 33E12.

1 Introduction and Preliminaries

Due to new hurdles in applied science and technology in the present period, the popularity of special functions is growing by the day. Special functions have been used widely in the varity of fields of fluid problems, biological problems, communication and other probelms of physics (see [1, 6–9, 13, 16, 21–24]). However, it has been noted that there are many issues in the fields of astrophysics and heat conduction for which the answers provided by the most prominent groups of special functions are insufficient. In this instance, the illustration makes use of the definition of incomplete gamma functions and its generalisations. So, The investigation of incomplete hypergeometric functions, incomplete H-functions, and incomplete $\overline{H}$-functions has been made possible by the use of incomplete type of gamma functions. For more details, one can see [2, 3] about incomplete functions and their recent applications.

---

[*] Corresponding author

Jangid et al. [10] recently introduced a new category of incomplete I- functions ${}^{\gamma}I_{p,\,q}^{m,\,n}(y)$ and ${}^{\Gamma}I_{p,\,q}^{m,\,n}(y)$, which is the generalization of Rathie's I-function [18] and it is described as:

$$\begin{aligned} {}^{\gamma}I_{p,\,q}^{m,\,n}(y) &= {}^{\gamma}I_{p,\,q}^{m,\,n}\left[y \,\middle|\, \begin{matrix} (f_1, \varsigma_1; \mathcal{F}_1 : t), (f_2, \varsigma_2; \mathcal{F}_2), \cdots, (f_p, \varsigma_p; \mathcal{F}_p) \\ (g_1, \varrho_1; \mathcal{G}_1), \cdots, (g_q, \varrho_q; \mathcal{G}_q) \end{matrix} \right] \\ &= {}^{\gamma}I_{p,\,q}^{m,\,n}\left[y \,\middle|\, \begin{matrix} (f_1, \varsigma_1; \mathcal{F}_1 : t), (f_j, \varsigma_j; \mathcal{F}_j)_{2,\,p} \\ (g_j, \varrho_j; \mathcal{G}_j)_{1,\,q} \end{matrix} \right] = \frac{1}{2\pi i} \int_{\pounds} \phi(r,t)\, y^r \, dr, \end{aligned} \tag{1}$$

and

$$\begin{aligned} {}^{\Gamma}I_{p,\,q}^{m,\,n}(y) &= {}^{\Gamma}I_{p,\,q}^{m,\,n}\left[y \,\middle|\, \begin{matrix} (f_1, \varsigma_1; \mathcal{F}_1 : t), (f_2, \varsigma_2; \mathcal{F}_2), \cdots, (f_p, \varsigma_p; \mathcal{F}_p) \\ (g_1, \varrho_1; \mathcal{G}_1), \cdots, (g_q, \varrho_q; \mathcal{G}_q) \end{matrix} \right] \\ &= {}^{\Gamma}I_{p,\,q}^{m,\,n}\left[y \,\middle|\, \begin{matrix} (f_1, \varsigma_1; \mathcal{F}_1 : t), (f_j, \varsigma_j; \mathcal{F}_j)_{2,\,p} \\ (g_j, \varrho_j; \mathcal{G}_j)_{1,\,q} \end{matrix} \right] = \frac{1}{2\pi i} \int_{\pounds} \Phi(r,t)\, y^r \, dr, \end{aligned} \tag{2}$$

$\forall\ y \neq 0$, where

$$\phi(r,t) = \frac{\{\gamma(1 - f_1 + \varsigma_1 r,\, t)\}^{\mathcal{F}_1} \prod_{j=1}^{m} \{\Gamma(g_j - \varrho_j r)\}^{\mathcal{G}_j} \prod_{j=2}^{n} \{\Gamma(1 - f_j + \varsigma_j r)\}^{\mathcal{F}_j}}{\prod_{j=n+1}^{p} \{\Gamma(f_j - \varsigma_j r)\}^{\mathcal{F}_j} \prod_{j=m+1}^{q} \{\Gamma(1 - g_j + \varrho_j r)\}^{\mathcal{G}_j}}, \tag{3}$$

and

$$\Phi(r,t) = \frac{\{\Gamma(1 - f_1 + \varsigma_1 r,\, t)\}^{\mathcal{F}_1} \prod_{j=1}^{m} \{\Gamma(g_j - \varrho_j r)\}^{\mathcal{G}_j} \prod_{j=2}^{n} \{\Gamma(1 - f_j + \varsigma_j r)\}^{\mathcal{F}_j}}{\prod_{j=n+1}^{p} \{\Gamma(f_j - \varsigma_j r)\}^{\mathcal{F}_j} \prod_{j=m+1}^{q} \{\Gamma(1 - g_j + \varrho_j r)\}^{\mathcal{G}_j}}, \tag{4}$$

where, $\gamma(.,t)$ and $\Gamma(.,t)$ are the lower and upper incomplete gamma functions described in (6) and (7).
The incomplete I-functions ${}^{\gamma}I_{p,\,q}^{m,\,n}(y)$ and ${}^{\Gamma}I_{p,\,q}^{m,\,n}(y)$ exist $\forall\ t \geq 0$ in accordance with Rathie's parameters and contour mentioned in [18] with,

$$\Delta > 0,\ |arg(y)| < \Delta\frac{\pi}{2},$$

where

$$\Delta = \sum_{j'=1}^{m} \mathcal{G}_{j'}\, \varrho_{j'} - \sum_{j'=m+1}^{q} \mathcal{G}_{j'}\, \varrho_{j'} + \sum_{j'=1}^{n} \mathcal{F}_{j'}\, \varsigma_{j'} - \sum_{j'=n+1}^{p} \mathcal{F}_{j'}\, \varsigma_{j'}\,.$$

For $\mathcal{F}_1 = 1$, the following relation is satisfied by the incomplete I-functions:

$${}^{\gamma}I_{p,\,q}^{m,\,n}(y) + {}^{\Gamma}I_{p,\,q}^{m,\,n}(y) = I_{p,\,q}^{m,\,n}(y), \tag{5}$$

for the well known Rathie's I-function [18]. Some additional properties regarding the incomplete I- function can be found in [4].

The incomplete gamma functions $\gamma(r,t)$ and $\Gamma(r,t)$ are described in the following way:

$$\gamma(r,t)=\int_0^t u^{r-1}\,e^{-u}\,du, \qquad \big(t\geqq 0;\Re(r)>0\big), \tag{6}$$

and

$$\Gamma(r,t)=\int_t^\infty u^{r-1}\,e^{-u}\,du, \qquad \big(t\geqq 0;\ \Re(r)>0 \quad \text{when} \quad t=0\big), \tag{7}$$

recognized as the lower and upper incomplete gamma functions respectively. The following relation is satisfied by the incomplete gamma functions.

$$\gamma(r,t)+\Gamma(r,t)=\Gamma(r), \qquad \big(\Re(r)>0\big). \tag{8}$$

A general class of polynomials was studied by the Srivastava [19,20], defined in the following way:

$$S_V^U[t]=\sum_{R=0}^{[V/U]}\frac{(-V)_{UR}}{R!}A_{V,R}\,t^R\,, \tag{9}$$

where $U\in\mathbf{Z}^+$ and $A_{V,\,R}$ are real or complex numbers arbitrary constant. The notations $[k]$ indicates the Floor function and $(\kappa)_\mu$ denote the Pochhammer symbol described by:

$$(\kappa)_0=1 \qquad \text{and} \qquad (\kappa)_\mu=\frac{\Gamma(\kappa+\mu)}{\Gamma(\kappa)} \qquad (\mu\in\mathcal{C}),$$

in the form of the Gamma function.

Lemma 1. *Let $b>0$, $c\geq 0$, $a>-\sqrt{bc}$ and $P>\frac{1}{2}$, we have the integral depending upon the three parameters, see Boros and Molls [5, 14].*

$$\int_0^\infty\left[\frac{h^2}{bh^4+2ah^2+c}\right]^P dh=\frac{B\left(P-\frac{1}{2},\,\frac{1}{2}\right)}{2^{P+1/2}\sqrt{b}\left[a+\sqrt{bc}\right]^{P-1/2}}, \tag{10}$$

where $B(m,\,n)$ denotes the Beta function. Equation (10) can also be expressed in the following way, by using the relation $B(m,n)=\frac{\Gamma(m)\,\Gamma(n)}{\Gamma(m+n)}$.

$$\int_0^\infty\left[\frac{h^2}{bh^4+2ah^2+c}\right]^P dh=\frac{\sqrt{\pi}\,\Gamma\left(P-\frac{1}{2}\right)}{\Gamma(P)\sqrt{b}\,2^{P+\frac{1}{2}}(a+\sqrt{bc})^{P-\frac{1}{2}}}. \tag{11}$$

Concerning the proof, see Boros and Moll [5] and Quershi et al. [17].

Hundreds of special functions have been employed in applied mathematics and computing sciences for many centuries due to their outstanding features and wide range of applications. The application of image formulas involving one or more variable special functions under various definite integrals is crucial from the perspective of the usefulness of these consequences in the evaluation of generalised integrals, applied physics, and many engineering areas. A variety of improper integrals involving incomplete I-functions and the family of polynomials have been examined in this study, primarily motivated by various applications of these findings. A significant amount of additional findings can be constructed as special instances from our main results because of the unified character of our results.

2 Main Results

For $X = \frac{h^2}{bh^4+2ah^2+c}$, the following is the outcomes:

Theorem 1. *For* $c \geq 0, b > 0\,, a > -\sqrt{bc}$, $P > \frac{1}{2}$ *then we have the following result:*

$$\int_0^\infty \left(\frac{h^2}{bh^4+2ah^2+c}\right)^P \, {}^\Gamma I_{p,\,q}^{m,\,n}(X^e\, y)dh = \frac{\sqrt{\pi}}{2\sqrt{b}\left[2\left(a+\sqrt{bc}\right)\right]^{P-\frac{1}{2}}}$$

$$\times\ {}^\Gamma I_{p+1,\,q+1}^{m,\,n+1}\left[y[2(a+\sqrt{bc})]^{-e}\ \middle|\ \begin{matrix}(f_1, \varsigma_1; \mathcal{F}_1 : t), \left(\frac{3}{2}-P,\, e;\, 1\right), (f_j, \varsigma_j; \mathcal{F}_j)_{2,\,p}\\ (1-P,\, e;\, 1), (g_j, \varrho_j; \mathcal{G}_j)_{1,\,q}\end{matrix}\right]. \tag{12}$$

Proof. The LHS of equation (12) is:

$$G^{'} = \int_0^\infty \left(\frac{h^2}{bh^4+2ah^2+c}\right)^P \, {}^\Gamma I_{p,\,q}^{m,\,n}(X^e\, y)dh. \tag{13}$$

Replace the incomplete I- function ${}^\Gamma I_{p,\,q}^{m,\,n}(y)$ by (2), we get:

$$G^{'} = \int_0^\infty X^P \frac{1}{2\pi i}\int_{\pounds} \Phi(r,t)\ (X^e\, y)^r\ dh\, dr, \tag{14}$$

where $\Phi(r,t)$ is given by (4).
Interchange the integration order in the above equation gives:

$$G^{'} = \frac{1}{2\pi i}\int_{\pounds} \frac{\{\Gamma(1-f_1+\varsigma_1 r, t)\}^{\mathcal{F}_1} \prod\limits_{j=1}^{m}\{\Gamma(g_j-\varrho_j r)\}^{\mathcal{G}_j} \prod\limits_{j=2}^{n}\{\Gamma(1-f_j+\varsigma_j r)\}^{\mathcal{F}_j}}{\prod\limits_{j=n+1}^{p}\{\Gamma(f_j-\varsigma_j r)\}^{\mathcal{F}_j} \prod\limits_{j=m+1}^{q}\{\Gamma(1-g_j+\varrho_j r)\}^{\mathcal{G}_j}} y^r$$

$$\times \int_0^\infty X^{P+er}\, dh\, dr. \tag{15}$$

Now with the help of Lemma 1, evaluate the integral, we get:

$$\int_0^\infty X^{P+er} dh = \frac{\sqrt{\pi}\Gamma(P+er-\frac{1}{2})}{\Gamma(P+er)\sqrt{b}\, 2^{P+er+\frac{1}{2}}(a+\sqrt{bc})^{P+er-\frac{1}{2}}}. \tag{16}$$

Put (16) in (15), we get:

$$G^{'} = \frac{\sqrt{\pi}}{2\sqrt{b}\left[2\left(a+\sqrt{bc}\right)\right]^{P-\frac{1}{2}}} \times \frac{1}{2\pi i}$$

$$\int_{\pounds} \frac{\{\Gamma(1-f_1+\varsigma_1 r,t)\}^{\mathcal{F}_1}\{\Gamma\left(P+er-\frac{1}{2}\right)\}\prod\limits_{j=1}^{m}\{\Gamma(g_j-\varrho_j r)\}^{\mathcal{G}_j}\prod\limits_{j=2}^{n}\{\Gamma(1-f_j+\varsigma_j r)\}^{\mathcal{F}_j}}{\prod\limits_{j=n+1}^{p}\{\Gamma(f_j-\varsigma_j r)\}^{\mathcal{F}_j}\prod\limits_{j=m+1}^{q}\{\Gamma(1-g_j+\varrho_j r)\}^{\mathcal{G}_j}\{\Gamma\left(P+er\right)\}}$$

$$\times\, y^r[2(a+\sqrt{bc})]^{-er}\, dr. \tag{17}$$

Now convert equation (17) in incomplete I- function to obtain the desired result.

□

Theorem 2. *For $b>0,\ c\geq 0,\ a>-\sqrt{bc},\ P>\frac{1}{2}$ then we have the following result:*

$$\int_0^\infty \left(\frac{h^2}{h^4+2ah^2+c}\right)^P {}^{\gamma}I_{p,\,q}^{m,\,n}(X^e\, y)dh = \frac{\sqrt{\pi}}{2\sqrt{b}\left[2\left(a+\sqrt{bc}\right)\right]^{P-\frac{1}{2}}}$$

$$\times\ {}^{\gamma}I_{p+1,\,q+1}^{m,\,n+1}\left[y[2(a+\sqrt{bc})]^{-e}\ \middle|\ \begin{matrix}(f_1,\varsigma_1;\mathcal{F}_1:t),\left(\frac{3}{2}-P;\,e,\,1\right),(f_j,\varsigma_j;\mathcal{F}_j)_{2,\,p}\\ (1-P,\,e;\,1),(g_j,\varrho_j;\mathcal{G}_j)_{1,\,q}\end{matrix}\right]. \tag{18}$$

Theorem 2 is proved in the same way as theorem 1 with the same conditions.

Theorem 3. *For $b>0,\ c\geq 0,\ a>-\sqrt{bc},\ P>\frac{1}{2}$ and the coefficient $A_{V,R}$ are real or complex arbitrary constants and $U\in Z^+$ then we have the following result:*

$$\int_0^\infty \left(\frac{h^2}{bh^4+2ah^2+c}\right)^P S_V^U[wX]\ {}^{\Gamma}I_{p,\,q}^{m,\,n}(X^e\, y)dh =$$

$$\frac{\sqrt{\pi}}{2\sqrt{b}\left[2\left(a+\sqrt{bc}\right)\right]^{P-\frac{1}{2}}} \times \sum_{R=0}^{[V/U]}\frac{(-V)_{UR}}{R!}A_{V,R}\, w^R.\ \frac{1}{[2(a+\sqrt{bc})]^R}$$

$$\times\ {}^{\Gamma}I_{p+1,\,q+1}^{m,\,n+1}\left[y[2(a+\sqrt{bc})]^{-e}\ \middle|\ \begin{matrix}(f_1,\varsigma_1;\mathcal{F}_1:t),\left(\frac{3}{2}-P-R,\,e,\,1\right),(f_j,\varsigma_j;\mathcal{F}_j)_{2,\,p}\\ (1-P-R,\,e,\,1),(g_j,\varrho_j;\mathcal{G}_j)_{1,\,q}\end{matrix}\right]. \tag{19}$$

Proof. The LHS of (19) is:

$$G = \int_0^\infty \left(\frac{h^2}{bh^4 + 2ah^2 + c} \right)^P S_V^U[wX] \; {}^{\Gamma}I_{p,\,q}^{m,\,n}(X^e\, y) dh. \tag{20}$$

Replace the Srivastava Polynomial $S_V^U[t]$ and incomplete I- function ${}^{\Gamma}I_{p,\,q}^{m,\,n}(y)$ by (9) and (2) respectively, we get:

$$G = \int_0^\infty X^P \sum_{R=0}^{[V/U]} \frac{(-V)_{UR}}{R!} A_{V,R}\, (w\,X)^R \frac{1}{2\pi i} \int_{\pounds} \Phi(r,t)\; (X^e\, y)^r\; dh\, dr, \tag{21}$$

where $\Phi(r,t)$ is given by (4).
Interchange the integration order in the above equation gives:

$$\sum_{R=0}^{[V/U]} \frac{(-V)_{UR}}{R!} A_{V,R}\, w^R \frac{1}{2\pi i} \int_{\pounds} \frac{\{\Gamma(1 - f_1 + \varsigma_1 r, t)\}^{\mathcal{F}_1} \prod_{j=1}^{m} \{\Gamma(g_j - \varrho_j r)\}^{\mathcal{G}_j} \prod_{j=2}^{n} \{\Gamma(1 - f_j + \varsigma_j r)\}^{\mathcal{F}_j}}{\prod_{j=n+1}^{p} \{\Gamma(f_j - \varsigma_j r)\}^{\mathcal{F}_j} \prod_{j=m+1}^{q} \{\Gamma(1 - g_j + \varrho_j r)\}^{\mathcal{G}_j}}$$

$$\times\, y^r \times \int_0^\infty X^{P+R+er}\, dh\, dr. \tag{22}$$

Now with the help of Lemma 1, evaluate the integral, we get:

$$\int_0^\infty X^{P+R+er} dh = \frac{\sqrt{\pi}\,\Gamma(P + R + er - \frac{1}{2})}{\Gamma(P + R + er)\sqrt{b}\, 2^{P+R+er+\frac{1}{2}} (a + \sqrt{bc})^{P+R+er-\frac{1}{2}}}. \tag{23}$$

Put (23) in (22), we get:

$$\frac{\sqrt{\pi}}{2\sqrt{b} \left[2 \left(a + \sqrt{bc}\right)\right]^{P-\frac{1}{2}}} \times \sum_{R=0}^{[V/U]} \frac{(-V)_{UR}}{R!} A_{V,R}\, w^R \cdot \frac{1}{[2(a + \sqrt{bc})]^R} \times \frac{1}{2\pi i}$$

$$\int_{\pounds} \frac{\{\Gamma(1 - f_1 + \varsigma_1 r, t)\}^{\mathcal{F}_1} \{\Gamma\left(P + R + er - \frac{1}{2}\right)\} \prod_{j=1}^{m} \{\Gamma(g_j - \varrho_j r)\}^{\mathcal{G}_j} \prod_{j=2}^{n} \{\Gamma(1 - f_j + \varsigma_j r)\}^{\mathcal{F}_j}}{\prod_{j=n+1}^{p} \{\Gamma(f_j - \varsigma_j r)\}^{\mathcal{F}_j} \prod_{j=m+1}^{q} \{\Gamma(1 - g_j + \varrho_j r)\}^{\mathcal{G}_j} \{\Gamma\left(P + R + er\right)\}}$$

$$\times\, y^r [2(a + \sqrt{bc})]^{-er}\, dr. \tag{24}$$

Now convert equation (24) in incomplete I- function to obtain the desired result.

□

Theorem 4. *For $b > 0$, $c \geq 0$, $a > -\sqrt{bc}$, $P > \frac{1}{2}$ and the coefficient $A_{V,R}$ are real or complex arbitrary constants and $U \in Z^+$ then we have the following*

result:

$$\int_0^\infty \left(\frac{h^2}{bh^4+2ah^2+c}\right)^P S_V^U[wX]\ {}^{\gamma}I^{m,\,n}_{p,\,q}(X^e\,y)dh =$$
$$\frac{\sqrt{\pi}}{2\sqrt{b}\left[2\left(a+\sqrt{bc}\right)\right]^{P-\frac{1}{2}}} \times \sum_{R=0}^{[V/U]} \frac{(-V)_{UR}}{R!} A_{V,R}\, w^R\, \frac{1}{[2(a+\sqrt{bc})]^R}$$
$$\times\ {}^{\gamma}I^{m,\,n+1}_{p+1,\,q+1}\left[y[2(a+\sqrt{bc})]^{-e}\ \middle|\ \begin{matrix}(f_1,\varsigma_1;\mathcal{F}_1:t),\left(\frac{3}{2}-P-R,\,e,\,1\right),(f_j,\varsigma_j;\mathcal{F}_j)_{2,\,p}\\ (1-P-R,\,e,\,1),(g_j,\varrho_j;\mathcal{G}_j)_{1,\,q}\end{matrix}\right]. \tag{25}$$

Theorem (4) is proved in the same way as theorem (3) with the same conditions.

Remark: If we set $U=1, A_{V,0}=1$ and $A_{V,R}=0\ \forall\ R\neq 0$ in theorem 3 and 4 then the result is same as that of theorem 1 and 2.

3 Special Case

In this section, as a particular instance of Theorem 3 and Theorem 4, we establish the Boros integral for the multiplication of Srivastava polynomial with the incomplete $\bar{I}$- function and the incomplete $\bar{H}$- function. Further, some special value will be given to Srivastava polynomial in order to get the outcomes in the form of Hermite and Laguerre polynomials. If we provide the parameter of particular features, we get the following special cases to delineate the use of fundamental outcomes.

(i) Incomplete $\bar{I}$- function: If we set $\mathcal{G}_j=1$ for $1\le j\le m$ in (2) and making use of the connection, that is (see [11])

$$\begin{aligned}{}^{\Gamma}\overline{I}^{m,\,n}_{p,\,q}(y) &= {}^{\Gamma}\overline{I}^{m,\,n}_{p,\,q}\left[y\ \middle|\ \begin{matrix}(f_1,\varsigma_1;\mathcal{F}_1:t),(f_j,\varsigma_j;\mathcal{F}_j)_{2,\,p}\\ (g_j,\varrho_j;1)_{1,\,m},(g_j,\varrho_j;\mathcal{G}_j)_{m+1,\,q}\end{matrix}\right]\\ &= \frac{1}{2\pi i}\int_{\pounds}\overline{\phi}(r,t)y^r\,dr,\end{aligned} \tag{26}$$

where,

$$\overline{\phi}(r,t) = \frac{\{\Gamma(1-f_1+\varsigma_1 r,t)\}^{\mathcal{F}_1}\prod_{j=1}^{m}\Gamma(g_j-\varrho_j r)\prod_{j=2}^{n}\{\Gamma(1-f_j+\varsigma_j r)\}^{\mathcal{F}_j}}{\prod_{j=n+1}^{p}\{\Gamma(f_j-\varsigma_j r)\}^{\mathcal{F}_j}\prod_{j=m+1}^{q}\{\Gamma(1-g_j+\varrho_j r)\}^{\mathcal{G}_j}}, \tag{27}$$

in (19) and (25), then we obtain the corollaries as follows:

Corollary 1. *For $b>0$, $c\ge 0$, $a>-\sqrt{bc}$, $P>\frac{1}{2}$ and the coefficient $A_{V,R}$ are real or complex arbitrary constants and $U\in Z^+$ then we have the following*

result:

$$\int_0^\infty \left(\frac{h^2}{bh^4+2ah^2+c}\right)^P S_V^U[wX]\ {}^{\Gamma}\bar{I}^{m,\,n}_{p,\,q}(X^e\,y)dh =$$

$$\frac{\sqrt{\pi}}{2\sqrt{b}\left[2\left(a+\sqrt{bc}\right)\right]^{P-\frac{1}{2}}} \times \sum_{R=0}^{[V/U]} \frac{(-V)_{UR}}{R!} A_{V,R}\, w^R\, \frac{1}{[2(a+\sqrt{bc})]^R}$$

$$\times\ {}^{\Gamma}\bar{I}^{m,\,n+1}_{p+1,\,q+1}\left[y[2(a+\sqrt{bc})]^{-e}\ \middle|\ \begin{matrix}(f_1,\varsigma_1;\mathcal{F}_1:t),\left(\frac{3}{2}-P-R,\,e;\,1\right),(f_j,\varsigma_j;\mathcal{F}_j)_{2,\,p}\\ (1-P-R,\,e;\,1),(g_j,\varrho_j;\,1)_{1,\,m},\,(g_j,\varrho_j;\mathcal{G}_j)_{m+1,\,q}\end{matrix}\right]. \tag{28}$$

Corollary 2. *For $b>0$, $c\geq 0$, $a>-\sqrt{bc}$, $P>\frac{1}{2}$ and the coefficient $A_{V,R}$ are real or complex arbitrary constants and $U\in Z^+$ then we have the following result:*

$$\int_0^\infty \left(\frac{h^2}{bh^4+2ah^2+c}\right)^P S_V^U[wX]\ {}^{\gamma}\bar{I}^{m,\,n}_{p,\,q}(X^e\,y)dh =$$

$$\frac{\sqrt{\pi}}{2\sqrt{b}\left[2\left(a+\sqrt{bc}\right)\right]^{P-\frac{1}{2}}} \times \sum_{R=0}^{[V/U]} \frac{(-V)_{UR}}{R!} A_{V,R}\, w^R.\, \frac{1}{[2(a+\sqrt{bc})]^R}$$

$$\times\ {}^{\gamma}\bar{I}^{m,\,n+1}_{p+1,\,q+1}\left[y[2(a+\sqrt{bc})]^{-e}\ \middle|\ \begin{matrix}(f_1,\varsigma_1;\mathcal{F}_1:t),\left(\frac{3}{2}-P-R,\,e;\,1\right),(f_j,\varsigma_j;\mathcal{F}_j)_{2,\,p}\\ (1-P-R,\,e;\,1),(g_j,\varrho_j;\,1)_{1,\,m},\,(g_j,\varrho_j;G_j)_{m+1,\,q}\end{matrix}\right]. \tag{29}$$

(ii) Incomplete $\bar{H}$- function: If we set $\mathcal{F}_j=1$ for $n+1\leq j\leq p$ and $\mathcal{G}_j=1$ for $1\leq j\leq m$ in (2) and making use of the connection, that is (see [12], [15])

$$\begin{aligned}\overline{\Gamma}^{m,\,n}_{p,\,q}(y) &= \overline{\Gamma}^{m,\,n}_{p,\,q}\left[y\ \middle|\ \begin{matrix}(f_1,\varsigma_1;\mathcal{F}_1:t),(f_j,\varsigma_j;\mathcal{F}_j)_{2,\,n}\,,(f_j,\varsigma_j;1)_{n+1,\,p}\\ (g_j,\varrho_j;1)_{1,\,m},(g_j,\varrho_j;\mathcal{G}_j)_{m+1,\,q}\end{matrix}\right]\\ &= \overline{\Gamma}^{m,\,n}_{p,\,q}\left[y\ \middle|\ \begin{matrix}(f_1,\varsigma_1;\mathcal{F}_1:t),(f_j,\varsigma_j;\mathcal{F}_j)_{2,\,n}\,,(f_j,\varsigma_j)_{n+1,\,p}\\ (g_j,\varrho_j)_{1,\,m},(g_j,\varrho_j;\mathcal{G}_j)_{m+1,\,q}\end{matrix}\right]\\ &= \frac{1}{2\pi i}\int_{\pounds}\overline{\psi}(r,t)y^r\,dr,\end{aligned} \tag{30}$$

where,

$$\overline{\psi}(r,t) = \frac{\{\Gamma(1-f_1+\varsigma_1 r,t)\}^{\mathcal{F}_1}\prod\limits_{j=1}^{m}\Gamma(g_j-\varrho_j r)\prod\limits_{j=2}^{n}\{\Gamma(1-f_j+\varsigma_j r)\}^{\mathcal{F}_j}}{\prod\limits_{j=n+1}^{p}\Gamma(f_j-\varsigma_j r)\prod\limits_{j=m+1}^{q}\{\Gamma(1-g_j+\varrho_j r)\}^{\mathcal{G}_j}}, \tag{31}$$

in (19) and (25), then we obtain the corollaries as follows.

Corollary 3. *For $b > 0$, $c \geq 0$, $a > -\sqrt{bc}$, $P > \frac{1}{2}$ and the coefficient $A_{V,R}$ are real or complex arbitrary constants and $U \in Z^+$ then we have the following result:*

$$\begin{aligned}&\int_0^\infty \left(\frac{h^2}{bh^4+2ah^2+c}\right)^P S_V^U[wX]\ \bar{\Gamma}_{p,\,q}^{m,\,n}(X^e\,y)dh\\&= \frac{\sqrt{\pi}}{2\sqrt{b}\left[2\left(a+\sqrt{bc}\right)\right]^{P-\frac{1}{2}}} \times \sum_{R=0}^{[V/U]} \frac{(-V)_{UR}}{R!} A_{V,R}\, w^R\, \frac{1}{[2(a+\sqrt{bc})]^R}\\&\times \bar{\Gamma}^{m,\,n+1}_{p+1,\,q+1}\left[y[2(a+\sqrt{bc})]^{-e}\ \middle|\ \begin{matrix}(f_1,\varsigma_1;\mathcal{F}_1:t),\left(\frac{3}{2}-P-R,\,e,\,1\right),\\ (1-P-R,\,e,\,1),(g_j,\varrho_j;1)_{1,\,m},\end{matrix}\right.\\&\qquad\qquad\left.\begin{matrix}(f_j,\varsigma_j;\mathcal{F}_j)_{2,\,n},\ (f_j,\varsigma_j;1)_{n+1,\,p}\\ (g_j,\varrho_j;\mathcal{G}_j)_{m+1,\,q}\end{matrix}\right].\end{aligned}\tag{32}$$

Corollary 4. *For $b > 0$, $c \geq 0$, $a > -\sqrt{bc}$, $P > \frac{1}{2}$ and the coefficient $A_{V,R}$ are real or complex arbitrary constants and $U \in Z^+$ then we have the following result:*

$$\begin{aligned}&\int_0^\infty \left(\frac{h^2}{bh^4+2ah^2+c}\right)^P S_V^U[wX]\ \bar{\gamma}_{p,\,q}^{m,\,n}(X^e\,y)dh\\&= \frac{\sqrt{\pi}}{2\sqrt{b}\left[2\left(a+\sqrt{bc}\right)\right]^{P-\frac{1}{2}}} \times \sum_{R=0}^{[V/U]} \frac{(-V)_{UR}}{R!} A_{V,R}\, w^R.\, \frac{1}{[2(a+\sqrt{bc})]^R}\\&\times \bar{\gamma}^{m,\,n+1}_{p+1,\,q+1}\left[y[2(a+\sqrt{bc})]^{-e}\ \middle|\ \begin{matrix}(f_1,\varsigma_1;\mathcal{F}_1:t),\left(\frac{3}{2}-P-R,\,e,\,1\right),\\ (1-P-R,\,e,\,1),(g_j,\varrho_j;1)_{1,\,m},\end{matrix}\right.\\&\qquad\qquad\left.\begin{matrix}(f_j,\varsigma_j;\mathcal{F}_j)_{2,\,n},\ (f_j,\varsigma_j;1)_{n+1,\,p}\\ (g_j,\varrho_j;\mathcal{G}_j)_{m+1,\,q}\end{matrix}\right].\end{aligned}\tag{33}$$

(iii) Hermite Polynomial: If we set $A_{V,\,R} = (-1)^R$ and $U = 2$ in (9) then $S_V^2[t] \to t^{V/2} H_V\left(\frac{1}{2\sqrt{t}}\right)$ and making use of the connection, that is (see [20]):

$$H_V(t) = \sum_{R=0}^{[V/2]} (-1)^R \frac{V!}{R!(V-2R)!}(2t)^{V-2R},\tag{34}$$

in (19) and (25), then we obtain the corollaries as follows.

Corollary 5. *For $b > 0$, $c \geq 0$, $a > -\sqrt{bc}$ and $P > \frac{1}{2}$ then we have the following*

result:

$$\int_0^{\infty} \left(\frac{h^2}{bh^4+2ah^2+c}\right)^{P} (Xw)^{\frac{V}{2}}\, H_V\left(\frac{1}{2\sqrt{Xw}}\right)\, {}^{\Gamma}I^{m,\,n}_{p,\,q}(X^e\, y)dh =$$

$$\frac{\sqrt{\pi}}{2\sqrt{b}\left[2\left(a+\sqrt{bc}\right)\right]^{P-\frac{1}{2}}} \times \sum_{R=0}^{[V/2]} \frac{(-1)^R\, V!}{R!\,(V-2R)!}\, w^R \cdot \frac{1}{[2(a+\sqrt{bc})]^R}$$

$$\times\, {}^{\Gamma}I^{m,\,n+1}_{p+1,\,q+1}\left[y[2(a+\sqrt{bc})]^{-e} \,\middle|\, \begin{array}{c} (f_1,\varsigma_1;\mathcal{F}_1:t), \left(\frac{3}{2}-P-R,\, e,\, 1\right), (f_j,\varsigma_j;\mathcal{F}_j)_{2,\,p} \\ (1-P-R,\, e,\, 1), (g_j,\varrho_j;\mathcal{G}_j)_{1,\,q} \end{array} \right]. \tag{35}$$

Corollary 6. *For* $b>0,\ c\geq 0,\ a>-\sqrt{bc}$ *and* $P>\frac{1}{2}$ *then we have the following result:*

$$\int_0^{\infty} \left(\frac{h^2}{bh^4+2ah^2+c}\right)^{P} (Xw)^{\frac{V}{2}}\, H_V\left(\frac{1}{2\sqrt{Xw}}\right)\, {}^{\gamma}I^{m,\,n}_{p,\,q}(X^e\, y)dh =$$

$$\frac{\sqrt{\pi}}{2\sqrt{b}\left[2\left(a+\sqrt{bc}\right)\right]^{P-\frac{1}{2}}} \times \sum_{R=0}^{[V/2]} \frac{(-1)^R\, V!}{R!\,(V-2R)!}\, w^R \cdot \frac{1}{[2(a+\sqrt{bc})]^R}$$

$$\times\, {}^{\gamma}I^{m,\,n+1}_{p+1,\,q+1}\left[y[2(a+\sqrt{bc})]^{-e} \,\middle|\, \begin{array}{c} (f_1,\varsigma_1;\mathcal{F}_1:t), \left(\frac{3}{2}-P-R,\, e,\, 1\right), (f_j,\varsigma_j;\mathcal{F}_j)_{2,\,p} \\ (1-P-R,\, e,\, 1), (g_j,\varrho_j;\mathcal{G}_j)_{1,\,q} \end{array} \right]. \tag{36}$$

(iv) Laguerre Polynomial: If we set $A_{V,\,R}=\binom{V+\alpha}{V}\frac{1}{(\alpha+1)_R}$ and $U=1$ in (9) then $S^1_V[t]\to L^{(\alpha)}_V(t)$ and making use of the connection, that is (see [20]).

$$L^{\alpha}_V(t)=\sum_{R=0}^{V}\binom{V+\alpha}{V-R}\frac{(-t)^R}{R!}, \tag{37}$$

in (19) and (25), then we obtain the corollaries as follows.

Corollary 7. *For* $b>0,\ c\geq 0,\ a>-\sqrt{bc}$ *and* $P>\frac{1}{2}$ *then we have the following result:*

$$\int_0^{\infty} \left(\frac{h^2}{bh^4+2ah^2+c}\right)^{P} L^{(\alpha)}_V[wX]\, {}^{\Gamma}I^{m,\,n}_{p,\,q}(X^e\, y)dh =$$

$$\frac{\sqrt{\pi}}{2\sqrt{b}\left[2\left(a+\sqrt{bc}\right)\right]^{P-\frac{1}{2}}} \times \sum_{R=0}^{V} \binom{V+\alpha}{V-R}\frac{(-w)^R}{R!}\, \frac{1}{[2(a+\sqrt{bc})]^R}$$

$$\times\, {}^{\Gamma}I^{m,\,n+1}_{p+1,\,q+1}\left[y[2(a+\sqrt{bc})]^{-e} \,\middle|\, \begin{array}{c} (f_1,\varsigma_1;\mathcal{F}_1:t), \left(\frac{3}{2}-P-R,\, e,\, 1\right), (f_j,\varsigma_j;\mathcal{F}_j)_{2,\,p} \\ (1-P-R,\, e,\, 1), (g_j,\varrho_j;\mathcal{G}_j)_{1,\,q} \end{array} \right]. \tag{38}$$

Corollary 8. *For $b > 0$, $c \geq 0$, $a > -\sqrt{bc}$ and $P > \frac{1}{2}$ then we have the following result:*

$$\int_0^\infty \left(\frac{h^2}{bh^4 + 2ah^2 + c}\right)^P L_V^{(\alpha)}[wX] \, {}^{\gamma}I_{p,\, q}^{m,\, n}(X^e\, y)dh =$$
$$\frac{\sqrt{\pi}}{2\sqrt{b}\left[2\left(a+\sqrt{bc}\right)\right]^{P-\frac{1}{2}}} \times \sum_{R=0}^{V} \binom{V+\alpha}{V-R} \frac{(-w)^R}{R!} \frac{1}{[2(a+\sqrt{bc})]^R}$$
$$\times\, {}^{\gamma}I_{p+1,\, q+1}^{m,\, n+1}\left[y[2(a+\sqrt{bc})]^{-e} \,\middle|\, \begin{matrix} (f_1, \varsigma_1; \mathcal{F}_1 : t), \left(\frac{3}{2} - P - R,\, e,\, 1\right) (f_j, \varsigma_j; \mathcal{F}_j)_{2,\, p} \\ (1 - P - R,\, e,\, 1), (g_j, \varrho_j; \mathcal{G}_j)_{1,\, q} \end{matrix}\right]. \tag{39}$$

Remark: If we set $U = 1, A_{V,0} = 1$ and $A_{V,R} = 0 \;\forall\; R \neq 0$ for the the first four corollaries (Corollary 1- Corollary 4) then it becomes the special case for Theorem 1 and 2.

4 Concluding Remarks

In this article, we obtain the Boros integral with three parameter for the incomplete I- function which is the extension of the I- function investigated by Jangid et al. [10] and we also study Boros integral for the product of incomplete I- function and Srivastava Polynomial. As the incomplete I- function generalize varity of incomplete functions like: I- function, Meijer G- function, hypergeometric function, H-function, $\bar{I}$- function and many other functions.

Also, Srivastava Polynomial generalize various other polynomial like: Hermite polynomial, Jacobi polynomial, Laguerre polynomial, Gegenbauer polynomial, Legendre polynomial, Tchebycheff polynomial, Gould-Hopper Polynomial and several other polynomials. Our main findings are therefore important and can be used to count the many Boros integral forms associated with various special functions and polynomials.

Acknowledgements

The authors would like to thank anonymous referees for their useful critical comments and suggestions for improving the research paper.

References

[1] Atangana, A., & Baleanu, D. (2016). New fractional derivatives with nonlocal and non-singular kernel: Theory and application to heat transfer model, Therm. Sci. 20(2) 763-769.

[2] Bansal, M. K., Lal, S., Kumar, D., Kumar, S., & Singh, J. (2020). Fractional differential equation pertaining to an integral operator involving incomplete H-function in the kernel. Math. Methods Appl. Sci..

[3] Bansal, M. K., Kumar, D., Singh, J., Tassaddiq, A., & Nisar, K. S. (2020). Some new results for the Srivastava–Luo–Raina M-transform pertaining to the incomplete H-functions. AIMS Math, 5(1), 717-722.

[4] Bhatter, S., Jangid, K., Meena, S., & Purohit, S. D. (2021). Certain Integral Formulae Involving Incomplete I-Functions. Science & Technology Asia, 84-95.

[5] Boros, G., & Moll, V. H. (1998). An integral with three parameters. Siam Review, 40(4), 972-980.

[6] Cattani, C. (2018). A review on harmonic wavelets and their fractional extension. J. Adv. Engg. Comput., 2(4), 224-238.

[7] Dizicheh, A. K., Salahshour, S., Ahmadian, A., & Baleanu, D. (2020). A novel algorithm based on the Legendre wavelets spectral technique for solving the Lane–Emden equations. Appl. Numer. Math. 153, 443-456.

[8] Gao, W., Veeresha, P., Prakasha, D. G., Baskonus, H. M., & Yel, G. (2019). A powerful approach for fractional Drinfeld–Sokolov–Wilson equation with Mittag-Leffler law. Alexandria Engg. J., 58(4), 1301-1311.

[9] Gumah, G., Al-Omari, S., & Baleanu, D. (2020). Soft computing technique for a system of fuzzy Volterra integro-differential equations in a Hilbert space. Appl. Numer. Math., 152, 310-322.

[10] Jangid, K., Bhatter, S., Meena, S. & Purohit, S.D. (2021). Certain classes of the incomplete I- functions and their properties, Discontin. Nonlinearity Complex., accepted.

[11] Jangid, K., Bhatter, S., Meena, S., Baleanu, D., Al Qurashi, M., & Purohit, S. D. (2020). Some fractional calculus findings associated with the incomplete I-functions. Adv. Difference Equ., 2020(1), 1-24.

[12] Kilbas, A. A., Marichev, O. I., & Samko, S. G. (1993). Fractional integrals and derivatives (theory and applications).

[13] Kiryakova, V. S. (1993). Generalized fractional calculus and applications. CRC press.

[14] Kumar, D., Ayant, F., Nirwan, P., & Suthar, D. L. (2022). Boros integral involving the generalized multi-index Mittag-Leffler function and incomplete I-functions. Research in Mathematics, 9(1), 1-7.

[15] Kumar, D., Bansal, M. K., Nisar, K. S., & Singh, J. (2019). Mathematical modelling of internal blood pressure involving incomplete $\overline{H}$-functions. J. Interdiscip. Math., 22(7), 1213-1221.

[16] Mathai, A. M., Saxena, R. K., & Haubold, H. J. (2010). On the H-Function With Applications. In The H-Function (pp. 1-43). Springer, New York, NY.

[17] Qureshi, M. I., Quraishi, K. A., & Pal, R. (2011). Some definite integrals of Gradshteyn-Ryzhil and other integrals. Global Journal of Science Frontier Research, 11(4), 75-80.

[18] Rathie, A.K. (1997). A new generalization of generalized hypergeometric functions, Le Matematiche, 52(2), 297-310.

[19] Sharma, R., Singh, J., Kumar, D., & Singh, Y. (2022). Certain unified integrals associated with product of the general class of polynomials and incomplete I-functions. Int. J. Appl. Comput. Math., 8(1), 1-11.

[20] Srivastava, H.M. & Singh, N.P. (1983). The integration of certain products of the multivariable H-function with a general class of polynomials, Rend. Circ. Mat. Palermo, 32(2), 157-187.

[21] Tuan, N.H., Baleanu, D., Thach, T.N. Regan, D.O. and Can, N.H.(2020). Final value problem for nonlinear time fractional reaction–diffusion equation with discrete data, J. Comput. Appl. Math., 376(1), 112883.

[22] Tyagi, S., Jain, M., & Singh, J. (2021). Application of S-Function and the Aleph Function in the Electric Circuit Theory. Int. J. Appl. Comput. Math., 7(5), 1-10.

[23] Xia, M., Wu, Y. C., & Aissa, S. (2012). Exact outage probability of dual-hop CSI-assisted AF relaying over Nakagami-m fading channels. IEEE Trans. Signal Process, 60(10), 5578-5583.

[24] Yang, X. J., Baleanu, D., Lazaveric, M. P., & Cajic, M. S. (2015). Fractal boundary value problems for integral and differential equations with local fractional operators. Therm. Sci., 19(3):959-66.

J. COMPUTATIONAL ANALYSIS AND APPLICATIONS, VOL. 31, NO. 3, 2023, COPYRIGHT 2023 EUDOXUS PRESS, LLC

Two-State Retrial Queueing Model with Catastrophe

Neelam Singla[1] and Ankita Garg[2*]

[1]Department of Statistics, Punjabi University, Patiala - 147002,
E-mail: neelgagan2k3@pbi.ac.in
[2*]Department of Statistics, Punjabi University, Patiala - 147002,
E-mail: gargankita095@gmail.com

December 29, 2022

Abstract

The present paper discusses a two-state retrial queueing system with catastrophe. If a customer on arrival finds the server free then it is served immediately. Such customer is known as primary customer. Moreover, if the server is busy then the customer joins virtual queue and retries for service after a random amount of time. This customer is called a secondary customer. Primary and secondary customers both follow Poisson processes. Inter arrival times and service times both follow exponential distribution. Catastrophe occurs on a busy server and its occurrence follows a Poisson process. Catastrophe causes the failure of server and so the server is sent for repair after occurrence of catastrophe. The repair times are also exponentially distributed. Time dependent probabilities for exact number of arrivals in the system and departures from the system when the server is idle or busy are obtained by using recursive approach. The probability of server being under repair is also obtained. Verification of results is done. Numerical results are generated and represented graphically to study the effect of various parameters.

Keywords: Retrial, Arrivals, Departures, Catastrophe, Repair.

1 Introduction

In many real life situations it has been observed that a customer does not get the service instantly on arrival. So he tries again for the service after a random period of time which is popularly known as retrial. The queueing systems with these repeated attempts have been used in many fields such as telecommunication, computer networks, data transmission, etc. Analysis of such systems developed a new class of queueing systems which is known as retrial queueing systems. Retrial queue is a model of the system with finite capacity where if the arrival finds a free server, it is served immediately. However, if the server is not free, the customer leaves the service area and joins the virtual queue known as orbit. Thereafter it retries from the orbit after a random amount of time to get service.

Call centers serve as a basic example to retrial systems where call agent is the server and a person who is calling is the customer. If a customer is able to connect the call agent immediately after making a call, he is answered else he has to repeat the call.

[6] is the early work done on retrial queues. [16] discussed some important single server retrial queuing models and represented analytic results. [10] analyzed the single server retrial queue with finite number of sources and established customer's arrival distribution, busy period and waiting time process. An explanation of the retrial queueing system is shown in the following diagram:

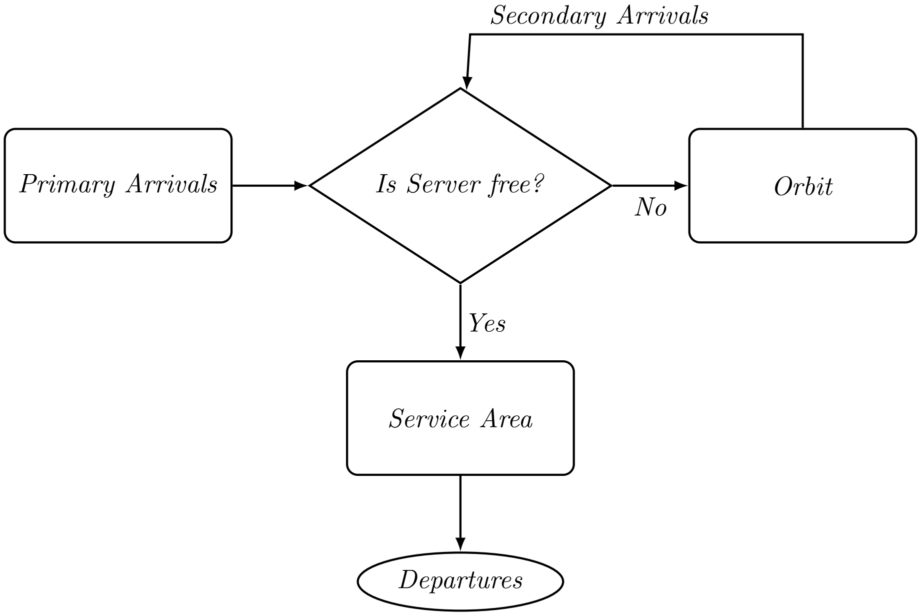

Figure 1. Basic Structure of a Retrial Queueing System

[13] was the first who introduced the concept of two-state in 'Some New Results for the M/M/1 Queue'. In this paper they obtained a closed form solution for the probability that exactly i arrivals and j services occur over a time interval of length t. [14] studied the two-state single server retrial queuing model in which the time dependent probabilities of exact number of arrivals and departures in the system are obtained when the server is free or busy. [15] developed 'A two-state retrial queueing model with feedback having two identical parallel servers' in which transient solution is obtained for the retrial queueing model.

In recent years many researchers have shown interest towards the concept of catastrophe. Catastrophe is a sudden, unexpected failure in a machine, computer network, electronic system, communication system, etc. Catastrophe occurs at random, deletes all the customers present in the system and inactivates the service facilities for a short period of time. Catastrophe resets the system from current state to zero state at random time intervals. Catastrophe may come from outside the system or from another service station. Retrial queueing system with catastrophe can be seen in call centers, computer networks and in telecommunication networks. In population dynamics, catastrophe can be considered as the natural disasters such as floods, storms, etc. On the other hand in the queueing models, catastrophe makes the system empty and causes server's breakdown.

For example: In call centers with the occurrence of catastrophic events like power failure, virus attacks will result in loss of all the calls present at that time and breakdown of the network.

[8], [5] are the works done on Catastrophe occurring in a simple Markovian queue. [11] discussed the asymptotic behavior of the probability of server being free. [12] worked on M/M/1 queuing system with catastrophes. Transient solution is obtained for system with server failure and non-zero repair time.

Furthermore, the server is sent for repair immediately when the failure occurs. After getting repaired, the server comes back to its working position and the system becomes ready to serve new customers. [4] proposed $M/M/\infty$ queueing system with catastrophe and repairable servers.

Following diagram shows the basic structure of retrial queueing system with catastrophe.

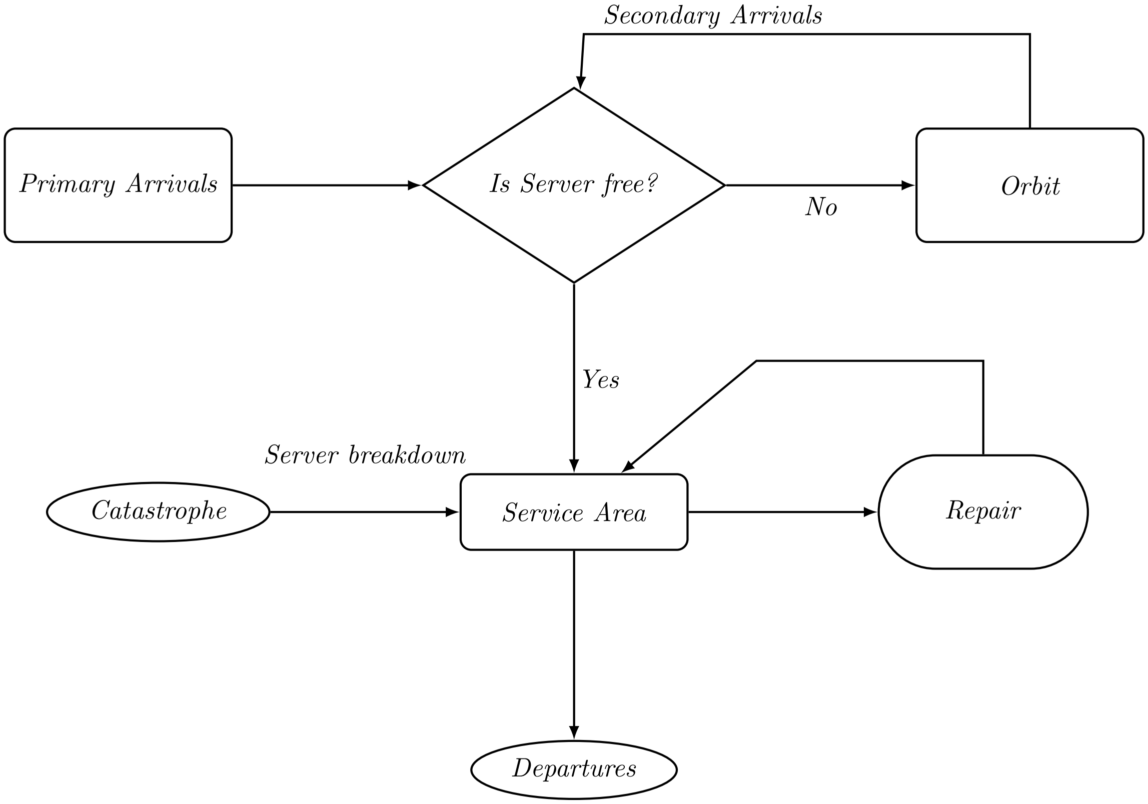

Figure 2. Basic Structure of a Retrial Queue With Catastrophe.

[1] studied the transient behaviour of two-processor heterogeneous system with catastrophes, server failures and repairs. [7] studied a fractional $M/M/1$ queue with catastrophe. [3] obtained transient solution of markovin queues with catastrophe having infinite servers.

The transient solutions are used to study the dynamic behaviour of a system. They are useful to study the characteristics of a system on different time points. Therefore, transient analysis of queueing systems is extremely important from theoretical and practical perspective.

In this paper, we derive two-state time-dependent probabilities for exact number of arrivals to the system and departures from the system by time t when the server is idle or busy for a single server retrial queueing system. The factor two-state makes the results well-quantified as in the case of [13]. Also we obtain the probability of server being under repair when the server fails due to catastrophic events at random time intervals. Besides these theoretical solutions, we present some numerical results graphically to study the effect of various parameters and the behaviour of probabilities with respect to average service times.

The paper has been organized in the following sections:

In section 2 the complete mathematical description of the model is defined. Also, the difference-differential equations are derived in this section. Solution of the model is given in section 3 in which we obtained the transient state probabilities and the probability of server being under repair. In section 4 verification of results is done. The numerical results are obtained and represented graphically in section 5. In section 6 the busy period probabilities of system and the server are obtained numerically and presented graphically. Section 7 discusses the conclusion and in section 8 acknowledgment is given. Finally the references are listed.

2 Model Description

In this paper, we are considering a two-state single server retrial queueing system with catastrophe. In this system, customers arrive according to Poisson process. If on arrival customer finds the server busy, he joins the orbit and retries from the orbit. These retrials are considered to be secondary arrivals. Catastrophe occurs according to Poisson process. We are assuming in our model that catastrophe occurs only when the system is non-empty and when the server is busy. It has no effect on the system when the system is empty. Catastrophe makes system empty and also causes server's breakdown by deleting all the customers present in the system. Once the system becomes empty or when the server breaks down, it is sent for repair immediately. Further, it is assumed that during the repair time no arrival can take place. The detailed description of the model is given as follows:

- Arrival Process: The primary customers arrive at the system according to Poisson process with mean arrival rate λ.
- Retrial Process: The secondary customers arrive at the system according to Poisson process with mean retrial rate θ.
- Service Process: The service times are exponentially distributed with parameter μ.
- Catastrophe: Catastrophe follow Poisson process with mean rate ξ.
- Repair: The repair time is exponentially distributed with parameter τ.

Also, the primary and secondary arrivals, inter-arrival times, service times, departures and catastrophes are mutually independent.

Laplace transformation $\bar{f}(s)$ of $f(t)$ is given by:

$$\bar{f}(s) = \int_0^\infty e^{-st} f(t) dt; \quad Re(s) > 0$$

The Laplace inverse of

$$\frac{Q(p)}{P(p)} = \sum_{k=1}^{n}\sum_{l=1}^{m_k} \frac{t^{m_k-l}e^{a_k t}}{(m_k-l)!(l-1)!} \times \frac{d^{l-1}}{dp^{l-1}}\left(\frac{Q(p)}{P(p)}\right)(p-a_k)^{m_k} \quad \forall p = a_k, \quad a_i \neq a_k \; for \; i \neq k$$

where

$$P(p) = (p-a_1)^{m_1}(p-a_2)^{m_2}.......(p-a_n)^{m_n}$$

Q(p) is a polynomial of degree $< m_1 + m_2 + m_3 + ... + m_n - 1$

$$If \;\; L^{-1}\{f(s)\} = F(t) \;\; and \;\; L^{-1}\{g(s)\} = G(t) \;\; then$$
$$L^{-1}\{f(s)g(s)\} = \int_0^t F(u)G(t-u)du = F * G$$

$F * G$ is called the convolution of F and G.

2.1 The Two-Dimensional State Model

2.1.1 Notations

$P_{i,j,0}(t)$ = Probability that there are exactly i number of arrivals in the system and j number of departures from the system by time t and the server is free.

$P_{i,j,1}(t)$ = Probability that there are exactly i arrivals, j departures from the system by time t and the server is busy.

$Q(t)$=Probability that the server is under repair by time t.

$P_{i,j}(t)$ = Probability that there are exactly i arrivals in the system and j departures from the system by time t.

$$P_{i,j}(t) = P_{i,j,0}(t) + P_{i,j,1}(t) \qquad \forall\, i,j \;\; i \geq j;$$
$$and \qquad P_{i,j,1}(t) = 0,\; i \leq j; \qquad P_{i,j,0}(t) = 0, \quad i < j;$$

Initially

$$P_{0,0,0}(0) = 1; \qquad P_{i,j,0}(0) = 0, \quad P_{i,j,1}(0) = 0,\; i,j \neq 0; \qquad Q(0) = 0;$$

2.1.2 The Difference-Differential equations governing the system are:

$$\frac{d}{dt}P_{i,j,0}(t) = -(\lambda + (i-j)\theta)P_{i,j,0}(t) + \mu P_{i,j-1,1}(t) \qquad i \geq j > 0 \tag{1}$$

$$\frac{d}{dt}P_{0,0,0}(t) = -\lambda P_{0,0,0}(t) + \tau Q(t) \tag{2}$$

$$\frac{d}{dt}P_{i,j,1}(t) = -(\lambda + \mu + \xi)P_{i,j,1}(t) + \lambda P_{i-1,j,0}(t) + \lambda P_{i-1,j,1}(t)(1-\delta_{i-1,j}) + (i-j)\theta P_{i,j,0}(t) \qquad i > j \geq 0 \tag{3}$$

$$\frac{d}{dt}Q(t) = -\tau Q(t) + \xi \sum_{i=1}^{\infty}\sum_{j=0}^{\infty} P_{i,j,1}(t) \tag{4}$$

where

$$\delta_{i-1,j} = \begin{cases} 1 & \text{when } i-1=j \\ 0 & \text{otherwise} \end{cases}$$

Using the Laplace transformation $\bar{f}(s)$ of $f(t)$ given by

$$\bar{f}(s) = \int_0^{\infty} e^{-st} f(t)dt, \quad Re(s) > 0$$

in the equations (1)-(4) along with the initial conditions, we have

$$(s+\lambda+(i-j)\theta)\bar{P}_{i,j,0}(s) = \mu\bar{P}_{i,j-1,1}(s) \qquad i \geq j > 0 \tag{5}$$

$$\begin{aligned}(s+\lambda+\mu+\xi)\bar{P}_{i,j,1}(s) = \lambda\bar{P}_{i-1,j,0}(s) + \lambda\bar{P}_{i-1,j,1}(s)(1-\delta_{i-1,j})+ \\ (i-j)\theta\bar{P}_{i,j,0}(s) \qquad i > j \geq 0\end{aligned} \tag{6}$$

$$(s+\lambda)\bar{P}_{0,0,0}(s) = 1 + \tau\bar{Q}(s) \tag{7}$$

$$(s+\tau)\bar{Q}(s) = \xi \sum_{i=1}^{\infty}\sum_{j=0}^{\infty} \bar{P}_{i,j,1}(s) \tag{8}$$

where

$$\delta_{i-1,j} = \begin{cases} 1 & \text{when } i-1=j \\ 0 & \text{otherwise} \end{cases}$$

3 Solution of the Problem

Solving equations (5)-(8) recursively, we have

$$\bar{P}_{0,0,0}(s) = \frac{1}{s+\lambda} + \frac{\tau}{s+\lambda}\bar{Q}(s) \tag{9}$$

$$\bar{P}_{i,0,1}(s) = \left(\frac{\lambda}{s+\lambda+\mu+\xi}\right)^i \left(\frac{1}{s+\lambda} + \frac{\tau}{s+\lambda}\bar{Q}(s)\right) \qquad i \geq 1 \tag{10}$$

$$\bar{P}_{i,1,0}(s) = \left[\frac{\mu}{s+\lambda+(i-1)\theta}\left(\frac{\lambda}{s+\lambda+\mu+\xi}\right)^i \left(\frac{1}{s+\lambda} + \frac{\tau}{s+\lambda}\bar{Q}(s)\right)\right] \quad i \geq 1 \tag{11}$$

$$\bar{P}_{i,i,0}(s) = \frac{\mu}{s+\lambda}\left[\frac{\lambda}{s+\lambda+\mu+\xi}\bar{P}_{i-1,i-1,0}(s) + \frac{\theta}{s+\lambda+\mu+\xi}\bar{P}_{i,i-1,0}(s)\right] \quad i \geq 2 \tag{12}$$

$$\bar{P}_{i,i-1,1}(s) = \frac{\lambda}{s+\lambda+\mu+\xi}\bar{P}_{i-1,i-1,0}(s) + \frac{\theta}{s+\lambda+\mu+\xi}\bar{P}_{i,i-1,0}(s) \qquad i \geq 2 \tag{13}$$

$$\bar{P}_{i,j,0}(s) = \frac{\mu}{s+\lambda+(i-j)\theta}\Bigg[\sum_{k=1}^{i-j+1}\left(\frac{\lambda}{s+\lambda+\mu+\xi}\right)^{i-j-k+1}\eta_k^{'}(s)\bar{P}_{j+k-1,j-1,0}(s) + \left(\frac{\lambda}{s+\lambda+\mu+\xi}\right)^{i-j}\bar{P}_{j,j-1,1}(s)\Bigg] \qquad i > j > 1 \tag{14}$$

where

$$\eta_k^{'} = \begin{cases} 1 & \text{if } k = 1 \\ 1 + \dfrac{k\theta}{s+\lambda+\mu+\xi} & \text{if } k = 2 \; to \; i-j \\ \dfrac{k\theta}{s+\lambda+\mu+\xi} & \text{if } k = i-j+1 \end{cases}$$

$$\bar{P}_{i,j,1}(s) = \sum_{k=1}^{i-j}\Bigg[\left(\frac{\lambda}{s+\lambda+\mu+\xi}\right)^{i-j-k}\eta_k^{'}(s)\bar{p}_{j+k,j,0}(s)\Bigg] + \left(\frac{\lambda}{s+\lambda+\mu+\xi}\right)^{i-j-1}\bar{P}_{j+1,1,1}(s) \qquad i \geq j+2, j \geq 1 \tag{15}$$

where

$$\eta_k^{'} = \begin{cases} 1 & \text{if } k = 1 \\ 1 + \dfrac{k\theta}{s+\lambda+\mu+\xi} & \text{if } k = 2 \; to \; i-j-1 \\ \dfrac{k\theta}{s+\lambda+\mu+\xi} & \text{if } k = i-j \end{cases}$$

$$\bar{Q}(s) = \frac{\xi}{s+\tau}\sum_{i=1}^{\infty}\sum_{j=0}^{\infty}\bar{P}_{i,j,1}(s) \tag{16}$$

Taking the Inverse Laplace transform of equations (9) − (16), we have

$$P_{0,0,0}(t) = e^{-\lambda t} + \tau e^{-\lambda t} * Q(t) \tag{17}$$

$$P_{i,0,1}(t) = \lambda^i e^{-\lambda t}\Bigg[\frac{1}{(\mu+\xi)^i} - e^{-(\mu+\xi)t}\sum_{r=0}^{i-1}\frac{t^r}{r!}\frac{1}{(\mu+\xi)^{i-r}}\Bigg] + \tau\lambda^i \Bigg[\frac{1}{(\mu+\xi)^i} - e^{-(\mu+\xi)t}\sum_{r=0}^{i-1}\frac{t^r}{r!}\frac{1}{(\mu+\xi)^{i-r}}\Bigg] * Q(t) \qquad i \geq 1 \tag{18}$$

$$P_{i,1,0}(t) = \mu e^{-(\lambda+(i-1)\theta)t} * P_{i,0,1}(t) \qquad i \geq 1 \tag{19}$$

$$\begin{aligned} P_{i,i,0}(t) &= \mu\lambda e^{-\lambda t}\left[\frac{1}{\mu+\xi} - \frac{e^{-(\mu+\xi)t}}{\mu+\xi}\right] * P_{i-1,i-1,0}(t) + \mu\theta e^{-\lambda t} \\ &\quad \left[\frac{1}{\mu+\xi} - \frac{e^{-(\mu+\xi)t}}{\mu+\xi}\right] * P_{i,i-1,0}(t) \qquad i > 1 \end{aligned} \tag{20}$$

$$P_{i,i-1,1}(t) = \lambda e^{-(\lambda+\mu+\xi)t} * P_{i-1,i-1,0}(t) + \theta e^{-(\lambda+\mu+\xi))t} * P_{i,i-1,0}(t) \qquad i > 1 \tag{21}$$

$$\begin{aligned} P_{i,j,0}(t) &= \mu\lambda^{i-j} e^{-(\lambda+(i-j)\theta)t}\left[\frac{1}{(\mu+\xi)^{i-j}} - e^{-(\mu+\xi)t}\sum_{r=0}^{i-j-1}\frac{t^r}{r!}\frac{1}{(\mu+\xi)^{i-j-r}}\right] * P_{j,j-1,0}(t) \\ &\quad + e^{-(\lambda+(i-j)\theta)t}\sum_{k=2}^{i-j}\mu\lambda^{i-j-k+1}\left[\frac{1}{(\mu+\xi)^{i-j-k+1}} - e^{-(\mu+\xi)t}\sum_{r=0}^{i-j-k}\frac{t^r}{r!}\frac{1}{(\mu+\xi)^{i-j-k-r+1}}\right] \\ &\quad * P_{j+k-1,j-1,0}(t) + e^{-(\lambda+(i-j)\theta)t}\sum_{k=2}^{i-j}(\mu k\theta)\lambda^{i-j-k+1}\Bigg[\frac{1}{(\mu+\xi)^{i-j-k+2}} \\ &\quad - e^{-(\mu+\xi)t}\sum_{r=0}^{i-j-k+1}\frac{t^r}{r!}\frac{1}{\mu^{i-j-k-r+2}}\Bigg] * P_{j+k-1,j-1,0}(t) + e^{-(\lambda+(i-j)\theta)t} \\ &\quad ((i-j+1)\mu\theta)\left[\frac{1}{\mu+\xi} - \frac{e^{-(\mu+\xi)t}}{\mu+\xi}\right] * P_{i,j-1,0}(t) + \mu\lambda^{i-j}e^{-(\lambda+(i-j)\theta)t} \\ &\quad \left[\frac{1}{(\mu+\xi)^{i-j}} - e^{-(\mu+\xi)t}\sum_{r=0}^{i-j-1}\frac{t^r}{r!}\frac{1}{(\mu+\xi)^{i-j-r}}\right] * P_{j,j-1,1}(t) \qquad i > j > 1 \end{aligned} \tag{22}$$

$$\begin{aligned} P_{i,j,1}(t) &= \lambda^{i-j-1}e^{-(\lambda+\mu+\xi)t}\frac{t^{i-j-2}}{(i-j-2)!} * P_{j+1,j,0}(t) + e^{-(\lambda+\mu+\xi)t}\sum_{k=2}^{i-j-1}\lambda^{i-j-k} \\ &\quad \frac{t^{i-j-k-1}}{(i-j-k-1)!} * P_{j+k,j,0}(t) + e^{-(\lambda+\mu+\xi)t}\sum_{k=2}^{i-j-1}k\theta\lambda^{i-j-k}\frac{t^{i-j-k}}{(i-j-k)!} * P_{j+k,j,0}(t) + \\ &\quad (i-j)\theta e^{-(\lambda+\mu+\xi)t} * P_{i,j,0}(t) + \lambda^{i-j-1}e^{-(\lambda+\mu+\xi)t}\frac{t^{i-j-2}}{(i-j-2)!} * P_{j+1,j,1}(t) \\ &\quad i \geq j+2, j \geq 1 \end{aligned} \tag{23}$$

$$Q(t) = \xi e^{-\tau t}\sum_{i=1}^{\infty}\sum_{j=0}^{\infty}P_{i,j,1}(t) \tag{24}$$

4 Verification of Results

- Summing equations (9)-(16) over i and j we get,

$$\sum_{i=0}^{\infty}\sum_{j=0}^{i}\left[\bar{P}_{i,j,0}(s)+\bar{P}_{i,j,1}(s)\right]+\bar{Q}(s)=\frac{1}{s}$$

  and hence

$$\sum_{i=0}^{\infty}\sum_{j=0}^{i}\left[P_{i,j,0}(t)+P_{i,j,1}(t)\right]+Q(t)=1$$

  which is the verification of our results.

- Define $U_{n,l}(t)$= Probability that there are n customers in the orbit at time t. The server is idle when $l=0$ and server is busy when $l=1$.
  When the server is idle, it is represented as $U_{n,0}(t)$:

$$U_{n,0}(t)=\sum_{j=0}^{\infty}P_{j+n,j,0}(t)$$

  where n is the number of customers in the orbit, which can be calculated by using the following formula:
  n=(number of arrivals - number of departures).
  When the server is busy, it is represented as $U_{n,1}(t)$:

$$U_{n,1}(t)=\sum_{j=0}^{\infty}P_{j+n+1,j,1}(t)$$

  In this case:
  n= (number of arrivals - number of departures - 1).
  Using the above definitions in (1)-(4) and let $\xi=0$, $\tau=0$ the equations in statistical equilibrium are:

$$(\lambda+n\theta)\,U_{n,0}=\mu\,U_{n,1} \qquad n\geq 0$$

$$(\lambda+\mu)\,U_{n,1}=\lambda(U_{n,0}+U_{n-1,1})+(n+1)\theta\,U_{(n+1),0} \quad n\geq 2$$

  which coincides with the results (1.5) and (1.6) of [9]

5 Numerical Solution and Graphical Representation

The Numerical results are generated using MATLAB programming for the case $\rho=\left(\frac{\lambda}{\mu}\right)$=0.5, $\eta=\left(\frac{\theta}{\mu}\right)$=0.6, $\tau^{'}=\left(\frac{\tau}{\mu}\right)$=0.4, $\xi^{'}=\left(\frac{\xi}{\mu}\right)$=0.3. In following tables, we observe some significant probabilities at various time instants whose sum approaches to 1.

Table I. At time t =1

t	$P_{0,0,0}$	$P_{1,1,0}$	$P_{2,1,0}$	$P_{2,2,0}$	$P_{3,1,0}$	$P_{3,2,0}$	$P_{3,3,0}$	$P_{4,1,0}$	$P_{4,2,0}$	$P_{1,0,1}$	$P_{2,0,1}$	$P_{2,1,1}$	$P_{3,0,1}$	$P_{3,1,1}$	Sum
1	0.6118	0.1029	0.0117	0.0043	0.0012	0.0007	0.0001	0.0001	0.0001	0.1702	0.0335	0.0153	0.0049	0.0032	0.96

Table II. At time t =5

t	$P_{0,0,0}$	$P_{1,1,0}$	$P_{2,1,0}$	$P_{2,2,0}$	$P_{4,1,0}$	$P_{4,2,0}$	$P_{4,3,0}$	$P_{4,4,0}$	$P_{5,1,0}$	$P_{5,2,0}$	$P_{5,3,0}$	$P_{5,4,0}$	$P_{5,5,0}$	$P_{1,0,1}$	$P_{2,0,1}$	$P_{2,1,1}$	$P_{3,0,1}$	$P_{3,1,1}$	$P_{3,2,1}$	$P_{4,0,1}$	$P_{4,1,1}$	$P_{4,2,1}$	$P_{4,3,1}$	$P_{5,0,1}$	$P_{5,1,1}$	$P_{5,2,1}$	$P_{5,3,1}$	$P_{5,4,1}$	$Q(t)$	Sum
5	0.1769	0.1584	0.0205	0.099	0.0009	0.0058	0.0128	0.0096	0.0004	0.0024	0.0063	0.0073	0.0032	0.0546	0.0174	0.0553	0.0057	0.0258	0.0332	0.0019	0.0098	0.0182	0.0118	0.0008	0.0047	0.0104	0.0105	0.0041	0.1663	0.934

Table III. At time t =15

t	$P_{0,0,0}$	$P_{1,1,0}$	$P_{2,1,0}$	$P_{2,2,0}$	$P_{3,1,0}$	$P_{3,2,0}$	$P_{3,3,0}$	$P_{5,1,0}$	$P_{5,2,0}$	$P_{5,3,0}$	$P_{5,4,0}$	$P_{5,5,0}$	$P_{6,5,0}$	$P_{6,6,0}$	$P_{7,3,0}$	$P_{7,4,0}$	$P_{7,5,0}$	$P_{7,6,0}$	$P_{7,7,0}$	$P_{1,0,1}$	$P_{2,0,1}$	$P_{2,1,1}$	$P_{3,0,1}$	$P_{3,1,1}$	$P_{3,2,1}$	$P_{4,0,1}$	$P_{4,1,1}$	$P_{4,2,1}$	$P_{4,3,1}$	$P_{6,0,1}$	$P_{6,1,1}$	$P_{6,2,1}$	$P_{6,3,1}$	$P_{6,4,1}$	$P_{6,5,1}$	$P_{8,2,1}$	$P_{8,4,1}$	$P_{8,5,1}$	$P_{8,6,1}$	$P_{8,7,1}$	$Q(t)$
15	0.1544	0.0866	0.0109	0.0575	0.002	0.011	0.0433	0.0001	0.0006	0.0025	0.0086	0.0271	0.0079	0.0186	0.0002	0.0008	0.0024	0.0061	0.0108	0.043	0.0119	0.0277	0.0033	0.012	0.0199	0.0009	0.0043	0.0104	0.0157	0.0001	0.0005	0.0016	0.004	0.0078	0.0102	0.0003	0.0026	0.0056	0.0095	0.0102	0.1914

$P_{5,0,1}$	$P_{5,1,1}$	$P_{5,2,1}$	$P_{5,3,1}$	$P_{5,4,1}$	$P_{7,3,1}$	$P_{7,4,1}$	$P_{7,5,1}$	$P_{7,6,1}$	Sum
0.0003	0.0014	0.0042	0.0089	0.0129	0.0016	0.0037	0.0065	0.0073	0.8911

Table IV. At time t =25

t	$P_{0,0,0}$	$P_{1,1,0}$	$P_{2,2,0}$	$P_{3,3,0}$	$P_{4,4,0}$	$P_{5,5,0}$	$P_{6,6,0}$	$P_{7,7,0}$	$P_{8,8,0}$	$P_{1,0,1}$	$P_{5,0,1}$
25	0.1391	0.0798	0.0525	0.0369	0.027	0.0204	0.0158	0.0125	0.1515	0.0389	0.0002

$P_{7,5,1}$	$P_{7,6,1}$	$P_{6,4,1}$	$P_{5,3,1}$	$P_{5,4,0}$	$P_{7,6,0}$	$P_{7,5,0}$	$P_{5,4,1}$	$P_{4,1,1}$	$P_{6,5,1}$
0.0048	0.0059	0.0061	0.0077	0.007	0.0044	0.0017	0.0099	0.004	0.0076

$P_{7,4,1}$	$P_{2,1,1}$	$P_{4,2,1}$	$P_{5,2,1}$	$P_{6,5,0}$	$P_{2,0,1}$	$P_{3,2,1}$	$P_{6,3,1}$	$Q(t)$	Sum
0.0029	0.0257	0.0095	0.0039	0.0056	0.0109	0.0181	0.0034	0.1694	0.8831

Table V. At time t =40

t	$P_{6,6,0}$	$P_{7,7,0}$	$P_{5,5,0}$	$P_{5,4,0}$	$P_{3,2,0}$	$P_{7,6,0}$	$P_{4,4,0}$	$P_{6,5,1}$	$P_{7,3,1}$	$P_{7,4,1}$	$P_{7,6,1}$
40	0.0131	0.0101	0.0171	0.0059	0.0085	0.0037	0.0227	0.0064	0.0011	0.0024	0.0049

$P_{0,0,0}$	$P_{1,1,0}$	$P_{1,0,1}$	$P_{2,1,1}$	$P_{3,1,1}$	$P_{4,3,1}$	$P_{4,2,1}$	$P_{5,3,1}$	$P_{5,4,1}$	$P_{7,5,1}$	$P_{2,1,0}$
0.1153	0.0661	0.0323	0.0213	0.0093	0.0111	0.0079	0.0064	0.0083	0.0024	0.0083

$P_{2,2,0}$	$P_{6,4,0}$	$P_{3,3,0}$	$Q(t)$	$P_{3,1,0}$	$P_{4,3,0}$	$P_{5,2,0}$	$P_{5,3,0}$	$P_{8,8,0}$	$P_{2,0,1}$	$P_{3,0,1}$
0.0436	0.0017	0.0309	0.1406	0.0015	0.0073	0.0005	0.0019	0.295	0.0.009	0.0025

$P_{3,2,1}$	$P_{4,0,1}$	$P_{4,1,1}$	Sum
0.0151	0.0.0007	0.0033	0.9382

The probabilities against time are represented graphically in the following figures.

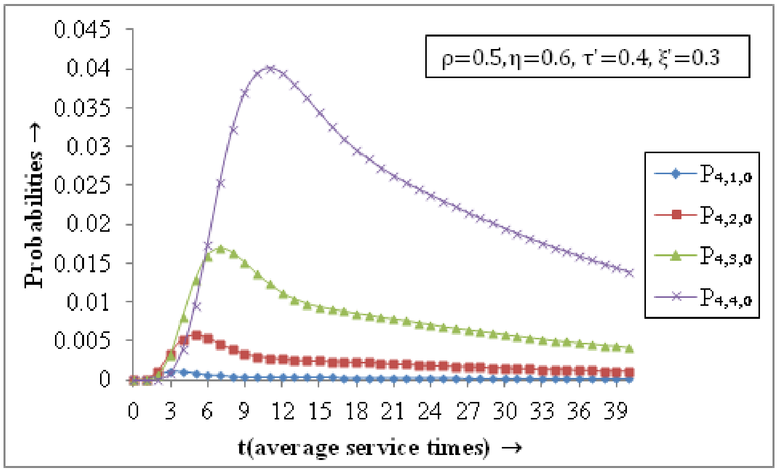

Figure 3. Probabilities $P_{4,1,0}$, $P_{4,2,0}$, $P_{4,3,0}$ and $P_{4,4,0}$ against average service times

In figure 3, the probabilities $P_{4,1,0}$, $P_{4,2,0}$, $P_{4,3,0}$ and $P_{4,4,0}$ are plotted against time t for the given case. It is observed that all the probabilities increase initially and then decrease. Also it can be seen that the probabilities attain higher values for greater number of departures.

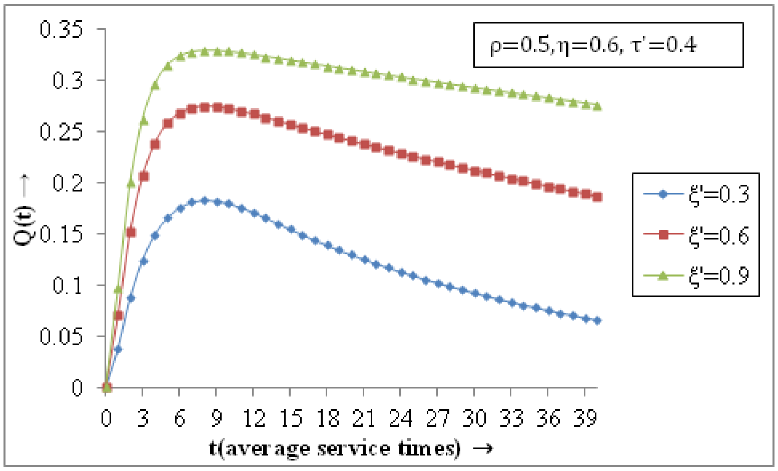

Figure 4. Effect of change in $\xi^{'}$ on the probability $Q(t)$

In figure 4, we study the effect of change in $\xi^{'}$(catastrophe rate per unit service time) on the probability $Q(t)$(probability of server being under repair). From the graph it can be seen that whenever the catastrophe rate per unit service time increases, the probability $Q(t)$ also increases which is as desired.

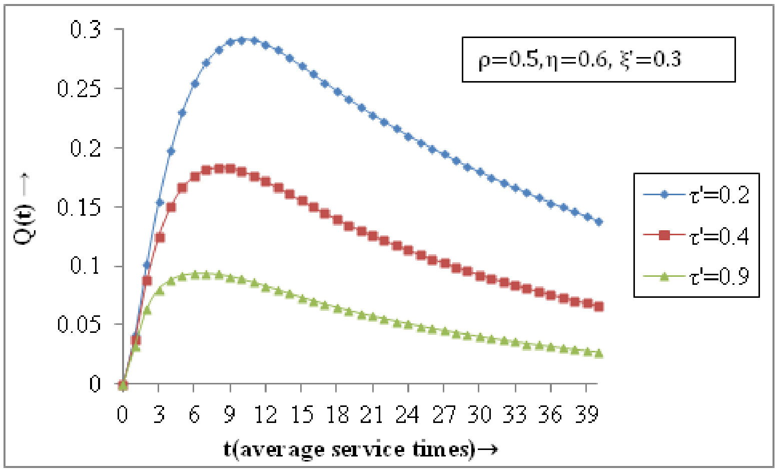

Figure 5. Effect of change in $\tau^{'}$ on the probability $Q(t)$

In figure 5, the effect of change in $\tau^{'}$(repair rate per unit service time) on the probability $Q(t)$ is studied. From the graph it is clearly visible that whenever the repair rate per unit service time increases, the probability $Q(t)$ decreases.

6 Busy Period Probabilities

In this section we discuss the busy period probabilities of the server and the system.
The Probability of busy server is given by:

$$P(Server\ is\ busy) = \sum_{i>j\geq 0} P_{i,j,1}(t) \tag{25}$$

The Probability of busy system is given by:

$$P(System\ is\ busy\ ) = \sum_{i>j\geq 0} \left(P_{i,j,0}(t) + P_{i,j,1}(t) \right) + Q(t) \tag{26}$$

6.1 Numerical and Graphical Representation of Busy Period Probabilities

The numerical results are obtained using MATLAB programming and following [2]. The Probabilities of system busy and server busy are obtained for different values of ρ keeping other parameters constant and are presented in the table given below.

Table VI. Probabilities of System Busy and Server Busy

	Probability(System Busy)			Probability(Server Busy)		
t	$\rho = 0.5$	$\rho = 0.7$	$\rho = 0.9$	$\rho = 0.5$	$\rho = 0.7$	$\rho = 0.9$
0	0	0	0	0	0	0
1	0.2788	0.369	0.4485	0.2286	0.2967	0.3546
2	0.3858	0.5009	0.5956	0.2626	0.3298	0.3827
3	0.4432	0.5683	0.6651	0.2678	0.3315	0.3785
4	0.4779	0.6067	0.7017	0.2689	0.3286	0.3685
5	0.5005	0.6311	0.724	0.2684	0.3226	0.3544
6	0.5171	0.6494	0.7405	0.2662	0.3137	0.338
7	0.5314	0.6654	0.7545	0.2622	0.3026	0.3208
8	0.5453	0.6804	0.7671	0.2565	0.2902	0.3042
9	0.5594	0.6949	0.7786	0.2495	0.2773	0.2885
10	0.5741	0.7086	0.7891	0.2416	0.2645	0.2741

The probabilities of system busy and server busy are also represented graphically.

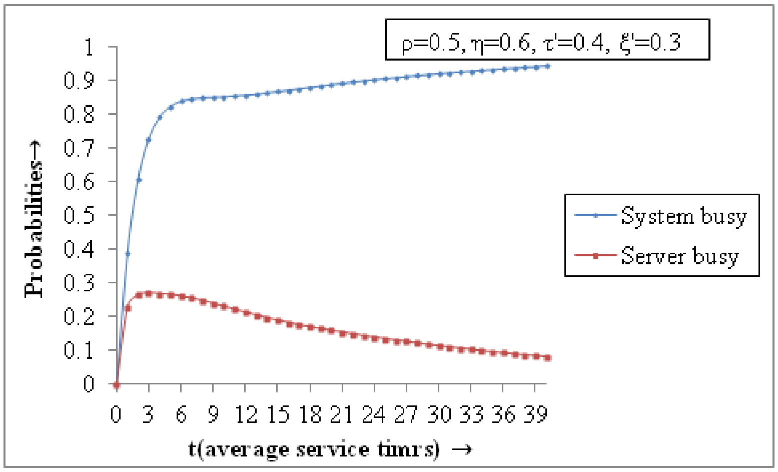

Figure 6. Probabilities of system busy and server busy against average service times

In Figure 6, the probabilities of system busy and server busy are plotted against time t for the case $\rho = 0.7$, $\eta = 0.6$, τ'=0.4, ξ'=0.3. It is clear from the graph that probability of system busy is higher than probability of server busy. The probability of system busy increases rapidly with the increase in time. However, the probability of server busy increases first and then decreases gradually with time.

7 Conclusion

In this paper, we studied a two-state single server retrial queueing system with catastrophe. The catastrophes have significant impact on businesses, computer networks, etc. It is very important to manage the risk of catastrophe for the smooth functioning of the system. Moreover, the two-dimensional state queueing model has been proven to be a viable tool for understanding and quantifying factors. The proposed method is highly applicable in modeling many practical situations like in submitting any application online, ticket booking services using telephone facility, withdrawing cash at an ATM, manufacturing sectors, call centers, etc. In this paper, the transient state probabilities and the probability of server being under repair are obtained. Numerical results and graphical representations are also given.

8 Acknowledgment

The authors are highly thankful to the DST for developing computing facilities in the department of Statistics. The authors have made use of these facilities while doing this research work.

References

[1] S. I. Ammar. Transient behavior of a two-processor heterogeneous system with catastrophes, server failures and repairs. *Applied Mathematical Modelling*, 38(7-8):2224–2234, 2014.

[2] B. D. Bunday. *Basic queueing theory*. Arnold, 1986.

[3] G. S. Bura. Transient solution of an m/m/∞ queue with catastrophes. *Communications in Statistics-Theory and Methods*, 48(14):3439–3450, 2019.

[4] G. S. Bura. M/m/∞ queue with catastrophes and repairable servers. *Reliability: Theory & Applications*, 17(4 (71)):143–153, 2022.

[5] X. Chao. A queueing network model with catastrophes and product form solution. *Operations Research Letters*, 18(2):75–79, 1995.

[6] J. Cohen. Basic problems of telephone traffic theory and the influence of repeated calls. *Philips Telecommunication Review*, 18(2):49–100, 1957.

[7] M. De Oliveira Souza and P. M. Rodriguez. On a fractional queueing model with catastrophes. *Applied Mathematics and Computation*, 410:126468, 2021.

[8] A. Di Crescenzo, V. Giorno, A. G. Nobile, and L. M. Ricciardi. On the m/m/1 queue with catastrophes and its continuous approximation. *Queueing Systems*, 43(4):329–347, 2003.

[9] G. Falin and J. G. Templeton. *Retrial queues*, volume 75. CRC Press, 1997.

[10] G. I. Falin and J. R. Artalejo. A finite source retrial queue. *European Journal of Operational Research*, 108(2):409–424, 1998.

[11] B. K. Kumar and D. Arivudainambi. Transient solution of an m/m/1 queue with catastrophes. *Computers & Mathematics with applications*, 40(10-11):1233–1240, 2000.

[12] B. K. Kumar, A. Krishnamoorthy, S. P. Madheswari, and S. S. Basha. Transient analysis of a single server queue with catastrophes, failures and repairs. *Queueing systems*, 56(3):133–141, 2007.

[13] C. D. Pegden and M. Rosenshine. Some new results for the m/m/1 queue. *Management Science*, 28(7):821–828, 1982.

[14] N. Singla and S. Kalra. Performance analysis of a two-state queueing model with retrials. *Journal of Rajasthan Academy of Physical Sciences*, 17:81–100, 2018.

[15] N. Singla and H. Kaur. A two-state retrial queueing model with feedback having two identical parallel servers. *Indian Journal of Science and Technology*, 14(11):915–931, 2021.

[16] T. Yang and J. G. C. Templeton. A survey on retrial queues. *Queueing systems*, 2(3):201–233, 1987.

J. COMPUTATIONAL ANALYSIS AND APPLICATIONS, VOL. 31, NO. 3, 2023, COPYRIGHT 2023 EUDOXUS PRESS, LLC

Managing Tourism in North East India using Fuzzy Linear Programming

Prabjot Kaur[1,*], Mahuya Deb[2], Arya Shankar[3]
[1,3]Department of Mathematics
Birla Institute of Technology, Mesra, Ranchi, Jharkhand
[2]Department of Advanced Computing
St. Josephss University, Bengaluru
*Corresponding author: prabjotkaur@bitmesra.ac.in

Abstract

The best allocation of limited resources to activities with the aim of accomplishing the desired goal, such as maximization of profit or minimization of cost, is the focus of linear programming. The relationships between activities in linear programming models satisfy the proportionality and additivity requirements since they are linear interactions. This feature of linear programming is extended to the tourism industry which is one of the major industries in the global economy with respect to invested capital and earnings of foreign currencies. In todays era of design thinking, automation, and met averse, there is a very close margin between solutions to similar real-world problems. This is where the need and demand for fuzzy and imprecise linear programming arises. The membership functions provide the model developer the freedom to grade the imprecision as per his/her preference, thereby enabling a unique solution for each problem. While considering the tourism problem a number of factors like natural resources, people, history, culture, security, accommodation, entertainment, political stability, cost of services, tour operator, tour information, and advertisement play an important role in enhancing the sector to a large extent. Combined and classified they come under the following categories like leisure tourism, therapeutic/spa tourism, conference tourism, political tourism, sports/recreational tourism, cultural tourism, social tourism, conference tourism, recreational tourism, sports tourism, religious tourism, health tourism, etc. Each of these sectors requires careful investment on the part of the Government and other stake holders for development purpose. i.e. only a proper marketing mix will ensure a better return for the state. Taking this aspect into consideration the authors decided to introduce a hypothetical LP maximization model for the tourism industry in North East. Cost and space allocation are the constraints in the model. Among the various categories, three tourism forms (heritage, eco-tourism, and pilgrimage tourism) are considered which are used to optimize the allocation of the States marketing budget in tourism in such a way that the appropriate sector provides the greatest likelihood of producing the strongest return on investment. The maximization of profit has been done using various methods, like Werner's, Verdegay's, and Zimmermans. The authors have concluded the results based on the sensitivity analysis that has been done in the process of maximizing profit along with a maximal satisfaction level.

Keywords: Tourism, fuzzy linear programming, optimization, decision making

1 Introduction

The travel, tourism, and hospitality sector in India have the potential to promote grassroots sustainable development and promote economic expansion. Over 39.3 million jobs were created in the sector in 2013, which also brought USD 18.13 billion to foreign currency profits and INR 2.178 lakh crore to India's GDP. However, India only accounts for 0.64% of global tourist visits, despite having enormous potential. According to Public and Social Policies Management (PSPM), YES BANK, December 2014, India is likely the only nation that offers a variety of tourism options. These include beach tourism (India has the longest coastline in the East), spiritual tourism, Ayurveda and other types of Indian medicine, heritage tourism, Eco-tourism, mountain tourism, forest tourism, and adventure tourism. On the basis of their occurrence and the results of engaging in tourism, Professors Bernecker and Kaspar(183) list some more categories of tourism as follows: leisure tourism, therapeutic/spa tourism, conference tourism, political tourism, and sports/recreational tourism. The following additional categories of tourism can also be created depending on the preferences and expectations of the travellers: nature tourism, cultural tourism, social tourism, conference tourism, leisure tourism, sports tourism, religious tourism, health tourism, etc. [Paylos, 2013]. The tourism industry plays a crucial role in the expansion of other vital industries with high growth and employment potential, including those in the healthcare, infrastructure, and education sectors, as well as the alignment of macroeconomic policies with issues of regional development. Important initiatives like the e-Visa, the opening of new airports and rail stations, infrastructure, insurance, and real estate sectors have created viable impetus, essential for continuing critical mass momentum and investment in the under-leveraged inbound segment given the rapid evolution of global travel dynamics. When seen from the perspective of tourism, the North East is certainly a wonderland. For international visitors seeking peace and quiet, the waterfalls, forests, rhinoceroses, colorful birds, nature paths, the sun sinking over the mountains, lush tea gardens, and golf courses with helipads are travelers. The aesthetics and vibrant festivals that take place all year long will be a bonus harvest for them. This massive influx of visitors has profound commercial ramifications in addition to spiritual ones. Following significant government initiatives, a variety of product offers, a growing economy, rising levels of disposable income, and a rise in international tourist inflow, East and North East India have seen an unprecedented 27% gain in foreign tourist inflow. The enormous potential of this resource-rich region is still largely unrealized due to issues with its law and order, poor infrastructure and connection, unemployment, and slow economic growth, among other things.

2 Literature Review

As part of a larger development planning process for changing the area's tourist development, the authors of [5] offer a formulation for linear programming and a vector analysis that assess the available tourism forms in the Dirfis area in Greece. The purpose of the article is to examine how three different types of tourismconference, ecotourism, and pilgrimagecontribute to the local tourism industry in light of the available resources. The authors [6] provide a strategic plan that can aid in the growth of sustainable tourism in popular tourist spots. The A'SWOT (AHP-SWOT) hybrid method was developed by combining the AHP and the SWOT (Strengths, Weaknesses, Opportunities, and Threats) analysis (Analytic Hierarchy Process). The AHP approach was used to prioritise these aspects after a SWOT analysis was conducted to identify the key strategic factors. The researchers [9] investigated the potential applications of LP in the hotel sector. A straightforward optimization problem was attempted to be graphically solved in a hotel's F&B production division, and an ideal solution was obtained. In [11], concepts of revenue optimization are explained with regard to the tourism and hotel industries. Also, deterministic linear programming models of airlines and hotels are presented, and the solution is proposed through a genetic algorithm. Again in [7], a linear programming model is presented as a means to support the formulation of tourist policy in the case of the West Frisian Islands. A model is constructed that calculates the maximum employment effect that can be reached by different levels of government and shows the optimal combination of policy tools in order to achieve this maximum. The researchers discuss the quality of the tourism industry and the programming for its development in Iran in [12]. Based on a case study of all elements of Iran's tourism industry system, this study employs a unified assessment of the industry's quality. SWOT analysis aided in determining the weaknesses and threats, aiming to raise the quality of the indicators. In addition, linear programming from the standpoint of internal and external relations with the national economy has been applied. In [17], the levels of sustainable tourism and environmental sustainability were practically measured in different cities of Kerman Province using a composite indicator, a linear programming model, the Delphi method, and the questionnaire technique. The results of this study showed that the tourism opportunities were not used appropriately in these cities and tourist destinations, and those environmental aspects had very bad situations compared to social and economic aspects. In other words, environmental health had the lowest level of sustainability. The researchers in [19] discussed the concept of over-tourism. It aims to provide more clarity with regard to what tourism entails by placing the concept in a historical context and presenting results from a qualitative investigation among 80 stakeholders in 13 European cities. Seven over-tourism myths are identified that may inhibit a well-rounded understanding of the concept. The researchers in [8] created a model to investigate tourist preferences that used ten attributes of tourist destinations. Fuzzy set theory [2] was adopted as the main analysis method to find the tourists preferences. In [10], a numerical method for solving fuzzy linear programming problems with fuzzy decision variables is proposed. The purpose of this work is to derive the analytic formula of error estimation regarding the approximate optimal solution. In [3], fuzzy set theory is used as a case study in the e-commerce industry for the city of Shiraz. An electronic system in the form of a website is developed, which tourists can use to find appropriate accommodation by inputting data related to their interests and needs. In light of the above literature, the present study is an attempt in this direction to analyze the contribution of different forms of tourism to the overall revenue of the government. Once proper sectors are identified by the authority, proper investment could be made for their further development. Using fuzzy linear programming, the problem is formulated and solved using fuzzy programming techniques. In recent literature very few formulations of single objective linear programming problem under fuzzy environment and application in tourism. The novelty is to improve the quality of policy decisions via optimization approach and allow decision-makers to tap the great tourism resource potentials like geographical, climate, natural attractions, cultural, and ancient heritages. Basically how we will profit from tourism in a remote area via theoretical and then practical ways.The study concludes that the tourist will have approximately 99% satisfaction if parameters are changed from 5% to 20%.This will have very less impact on net profit earned through tourism.

3 Preliminaries

Let X denotes a universal set. Then a fuzzy (Zadeh(1965)) subset A of X is defined by its membership function $\mu_A : X \rightarrow [0,1]$ which assign to each element x in X a real number μ_A in the interval $[0,1]$,where the value of μ_A at x represents the grade of membership of x in A. The nearer the values of μ_A is unity, the higher the grade of membership of x in A.

3.1 Fuzzy Number

Fuzzy Number [22] is a fuzzy set A on R must possess at least the following three properties that A must be a normal fuzzy set; must be a closed interval for every α_A must be a closed interval for every $\alpha \; \epsilon \; (0,1]$; The support of $A, 0+_A$ must be bounded.

4 Linear Programming framework for the Tourism Development Problem

4.1 Model Developments

It is assumed that the State wants to develop a particular area and therefore a proper investment plan has to be decided upon. Based on the available tourist resources, the government or the various stakeholders must design its development policy [5]. For demonstrating the management of the tourism scenario in the state the following assumptions are made:

Decision Variable:

- Number of Heritage and culture sites infrastructures x_1
- Number of eco-tourism sites infrastructures x_2
- Number of infrastructures at pilgrimage locations x_3

Profits per sector are:

- Heritage and culture Tourism: 6 monetary units Eco Tourism: $4mu$
- Pilgrimage Tourism: $3mu$
- The goal of the state is to maximize revenue i.e. $maximize : 6x_1 + 4x_2 + 3x_3$
- The region that can be used to build the ”logistics” infrastructure is $50000m2$.

Constraints:

- The prerequisites for each category are as follows:

- Heritage and Culture Tourism: 800 $\tau\mu$.
- Eco-Tourism: 600 $\tau\mu$.
- Pilgrimage Tourism: 500 $\tau\mu$.

The overall cost of property 39;s maintenance should not be more than the mu. The real cost for each category is: Heritage and culture sites: Tourism: $10mu$ Eco Eco-tourism Tourism: $8mu$ Pilgrimage Tourism: $3mu$ The model can thus be developed now as it has been simplified to a simple linear programming problem. The model can help maximize profit from ecotourism, pilgrimage tourism, and, conference tourism while optimally using important limited resources like land area. The companys objective maximize its gain, i.e.,

$$\begin{aligned} \text{Maximize Z} \quad & 6x_1 + 4x_2 + 3x_3 \\ \text{subject to} \quad & 8x_1 + 6x_2 + 5x_3 \leq 500 \\ & 10x_1 + 8x_2 + 3x_3 \leq 360 \\ & x_1, x_2, x_3 \geq 0 \end{aligned} \tag{1}$$

Two slack variables x_4 and x_5 are introductions for the maximization of the following linear programming problem:

$$\begin{aligned} f(x_1, x_2, x_3, x_4, x_5) = \quad & 6x_1 + 4x_2 + 3x_3 + 0x_4 + 0x_5 \\ \text{where} \quad & 8x_1 + 6x_2 + 5x_3 + x_4 + 0x_5 = 500 \\ & 10x_1 + 8x_2 + 3x_3 + 0x_4 + x_5 = 360 \\ & x_i \geq 0 \qquad i = 1, 2, 3, 4, 5. \end{aligned}$$

Using the simplex algorithm, profit maximization occurs when $x_1 = 11.5$ (i.e. when there are 11 heritage and culture sites), $X_2 = 0$ (i.e. there are no place for eco-tourism) and $X_3 = 81.5$ (i.e 81 pilgrimage areas). Max $Z = 313.5$. Heritage venues won't help maximize profits, thus they are consequently not thought to be relevant. While certainty, reliability and precision are frequently illusory concepts in real-world applications, linear programming models represent real-world situations with some sets of parameters that are determined by experts and decision makers. As a result, experts and decision-makers are often unable to determine the precise value of parameters or may not be able to precisely specify the objective functions or constraints. The use of fuzzy linear programming has the advantage that the decision-maker can model the issue in accordance with the current state of knowledge because it is typically impractical to describe the restrictions and the goal function in precise terms. Many real-world problems find their solution in traditional theory. In original LPP, coefficients and right-hand sides must be well defined. The use of deterministic and stochastic models to model real-world situations necessitates a lot of data processing. In todays era of design thinking, automation and met averse, these is very close margin between solutions of similar real-world problems. Thus the need and demand of fuzzy and imprecise linear programming arises here. Some model parameters can only be approximated roughly in the event of genuine problems. While imprecise input is substituted by average data in classical models, fuzzy models allow decision makers to model their subjective imaginations as exactly as they can explain them. Therefore, the classical LP are not applicable, instead, the Fuzzy Linear Programming [1, 13] is used to model such situations. By introducing fuzziness to LP, such problems can be overcome. When a decision must be made in a fuzzy environment, LP may be modified in one of the three ways listed below. The objective function should not be maximised, to start. In other words, a level of aspiration that cannot be clearly defined as optimal must be reached. Second, the limitations might be ambiguous. The $\leq$ sign might not have a traditional definition or be used in a strictly mathematical sense, but there might be some room for error. When the limitations represent aspirational levels that are not well defined, this can occur. Last but not least, data may be inaccurate due to a lack of precision or some ambiguity in the data collection technique.

4.2 DECISION MAKING IN A FUZZY SCENARIO [18]

Decision making under fuzzy context is the confluence of fuzzy constraints and fuzzy objective functions . The distinction between constraint and goal function vanishes as a fuzzy environment attains ultimate symmetry. Zimmermann (1978) was the first to categorize fuzzy mathematical programming into symmetric and non-symmetric models. Subsequently, it has also been classified by Leung (1998) into four categories: - crisp objective and fuzzy constraints, fuzzy objective and crisp constraints, fuzzy objective and fuzzy constraints and robust programming. Linear programming can also be classified as follows: i. Linear programming problem with uncertain resources ii. A nonsymmetric model by Verdegay iii. Werner's methodology iv. Zimmermann's Model v. Chana's Methodology: A Nonsymmetric Model [4]. In this paper we have considered the objective function, constraints and both constraints and objective fuzzy.The approaches of Werner,Verdegay and Zimmermann depict fuzziness in the model in objectives and constraints.

4.2.1 Werners Method [16]

Werner proposed that the objective function is taken to be fuzzy as the total fuzzy resources or fuzzy inequality constraints. Tolerances given by p_i are fuzzy and given. The construction of membership function μ_0 for objective function is as:

$$\mu_0(x) = \begin{cases} 1 & if cx > Z^1 \\ \dfrac{1-(Z^1-cx)}{Z^1-Z^0} & if Z_0 < cx < Z_1 \\ 0 & if Z_0 < cx \end{cases}$$

where Z_1 and Z_0 are the values obtained after maximization and minimization of the single objective function.
A symmetric model is as

$$\begin{aligned} \text{Max} \quad & \alpha \\ \text{subject to} \quad & \mu_0(x) \geq \alpha \\ & \mu_i(x) \geq \alpha, \quad \forall\, i, \alpha \in [0,1] \; and \; x \geq 0 \end{aligned} \tag{2}$$

4.2.2 Chanas [2] & Verdegays Approach [15, 14]

In the Verdegays approach for non-symmetric model, the constraint is fuzzy while the objective function is not fuzzy. This means that the value of constraint is between 0 and 1 while the objective function has crisp value. The model can be understood as equivalent parametric programming:

$$\begin{aligned} &Maximize && cx \\ &\text{subject to} && (Ax)_j \leq b_i + (1-\alpha)p_i \quad \forall\ i, \alpha \in [0,1]\ and\ x \geq 0 \end{aligned} \tag{3}$$

where p is tolerance parameter and b is basic value.

4.2.3 Solution of Zimmermann [21, 20]

By the Zimmermanns approach,the linear programming problem is solved by adding the objective function cx as a fuzzy goal to the constraints. It is not certain that Zimmermann method (ZM) will give the "best" option when this new LP has alternate optimal solutions (AOS). There are two possibilities: cx might have distinct bounded values for the AOS or it could be unbounded. But since most of the AOS may have same solution, it's possible that we don't offer the best possible solution to the decision maker (DM) unless we check the value of cx for all AOS; it's possible that cx is unbounded yet ZM presents a bounded solution as the best. Zimmermans Approach for solving the fuzzy LPP takes into account a direct relation between α and θ. Further, it takes the variance of tolerance parameter and the graph for same can be obtained.

Let $\alpha = 1 - \theta$ then equaion becomes

$$\begin{aligned} &Min && \theta \\ &\text{subject to} && cx \geq b_0 - \theta\ p_0 \\ & && (Ax)_i \leq b_i + \theta\ p_i, \qquad \forall\ i, \theta \in [0,1]\ and\ x \geq 0 \end{aligned} \tag{4}$$

The above formulated LPP is solved using Verdegay's and Werner approach.

5 PROBLEM WITH VARYING TOLERANCES AND GRAPHICAL INTERPRETATIONS USING WERNERS METHOD

$$\begin{aligned} &MaxZ && 6x_1 + 4x_2 + 3x_3 \\ &\text{subject to} && 8x_1 + 6x_2 + 3x_3 \leq 500 \\ & && 10x_1 + 8x_2 + 3x_3 \leq 360 \\ & && x_1, x_2, x_3 \geq 0 \end{aligned} \tag{5}$$

we get,

$$Z = 313.81 \qquad x_1 = 11.54 \qquad x_2 = 0.00 \qquad x_3 = 81.54$$

Tolerance set at $P_i = 5\%$

$$\begin{aligned} &MaxZ && 6x_1 + 4x_2 + 3x_3 \\ &\text{subject to} && 8x_1 + 6x_2 + 3x_3 \leq 500 + 50\theta \\ & && 10x_1 + 8x_2 + 3x_3 \leq 360 + 18\theta \\ & && x_1, x_2, x_3 \geq 0 \end{aligned}$$

$$\mu_1(x) = \begin{cases} 1 & if g_1(x) < 500 \\ 1 - \dfrac{(g_1(x) - 500)}{25} & if 500 < g_1(x) < 525 \\ 0 & if g_1(x) > 525 \end{cases}$$

$$\mu_2(x) = \begin{cases} 1 & if g_2(x) < 360 \\ 1 - \dfrac{(g_2(x) - 360)}{18} & if 360 < g_2(x) < 378 \\ 0 & if g_2(x) > 378 \end{cases}$$

Table showing the tolerance level set at 5%

θ	x_1	x_2	x_3	Z
0	11.54	0.00	81.54	313.85
0.1	11.60	0.00	81.95	315.42
0.2	11.65	0.00	82.35	316.98
0.3	11.71	0.00	82.76	318.55
0.4	11.77	0.00	83.17	320.12
0.5	11.83	0.00	83.58	321.69
0.6	13.42	0.00	81.52	325.11
0.7	11.94	0.00	84.39	324.83
0.8	12.00	0.00	84.80	326.40
0.9	12.06	0.00	85.21	327.97
1.0	12.12	0.00	85.62	329.54

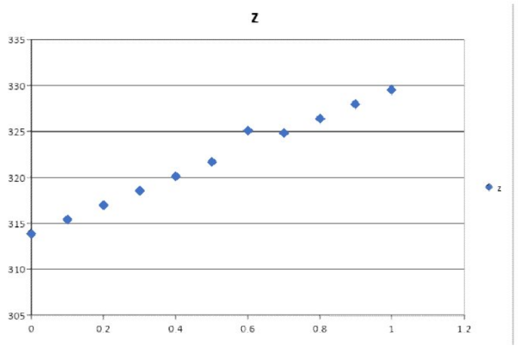

Figure 1: Theta versus z at 5% tolerance parameter.

Tolerance set at $P_i = 10\%, P_1 = 50, P_2 = 36$

$$\begin{aligned} MaxZ \quad & 6x_1 + 4x_2 + 3x_3 \\ \text{subject to} \quad & 8x_1 + 6x_2 + 3x_3 \leq 500 + 50\theta \\ & 10x_1 + 8x_2 + 3x_3 \leq 360 + 36\theta \\ & x_1, x_2, x_3 \geq 0 \end{aligned} \tag{6}$$

θ	x_1	x_2	x_3	Z
0	11.54	0.00	81.54	313.85
0.1	11.65	0.00	82.35	316.98
0.2	11.77	0.00	83.17	320.12
0.3	11.88	0.00	83.98	323.26
0.4	12.00	0.00	84.80	326.40
0.5	14.97	0.00	76.10	318.12
0.6	12.23	0.00	86.43	332.68
0.7	12.35	0.00	87.25	335.82
0.8	12.46	0.00	88.06	338.95
0.9	12.58	0.00	88.88	342.09
1.0	12.69	0.00	89.69	345.23

Table 1: Table showing the tolerance level set at 5%

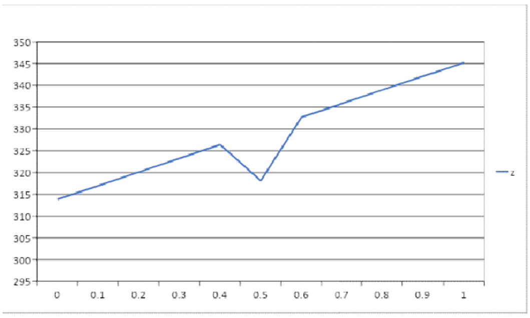

Figure 2: Theta versus z at 10% tolerance parameter.

The next tolerance level is set at $P_i = 15\%, P_1 = 75, P_2 = 54$

$$\begin{aligned} MaxZ \quad & 6x_1 + 4x_2 + 3x_3 \\ \text{subject to} \quad & 8x_1 + 6x_2 + 3x_3 \leq 500 + 75\theta \\ & 10x_1 + 8x_2 + 3x_3 \leq 360 + 54\theta \\ & x_1, x_2, x_3 \geq 0 \end{aligned} \tag{7}$$

θ	x_1	x_2	x_3	Z
0	11.54	0.00	81.54	313.85
0.1	11.71	0.00	82.76	318.55
0.2	71.31	0.00	251.95	323.26
0.3	12.06	0.00	85.21	327.97
0.4	12.23	0.00	86.43	332.62
0.5	12.40	0.00	87.65	337.38
0.6	12.58	0.00	88.88	342.09
0.7	12.75	0.00	90.10	346.80
0.8	12.92	0.00	91.32	351.51
0.9	13.10	0.00	92.55	356.22
1.0	14.13	0.00	90.88	357.46

Table 2: Table showing the tolerance level set at 15%

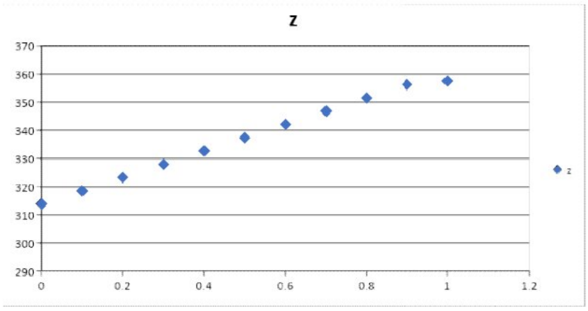

Figure 3: Theta versus z at 15% tolerance parameter.

The next tolerance level is set at $P_i = 20\%, P_1 = 100, P_2 = 72$

$$\begin{aligned} MaxZ \quad & 6x_1 + 4x_2 + 3x_3 \\ \text{subject to} \quad & 8x_1 + 6x_2 + 3x_3 \leq 500 + 100\theta \\ & 10x_1 + 8x_2 + 3x_3 \leq 360 + 72\theta \\ & x_1, x_2, x_3 \geq 0 \end{aligned} \tag{8}$$

θ	x_1	x_2	x_3	Z
0	0.00	0.00	0.00	0.00
0.1	11.77	0.00	83.17	320.12
0.2	12.00	0.00	84.80	326.40
0.3	12.23	0.00	84.43	332.68
0.4	12.46	0.00	88.06	338.95
0.5	12.92	0.00	89.69	345.23
0.6	12.58	0.00	81.52	351.51
0.7	13.15	0.00	92.95	357.78
0.8	13.38	0.00	94.58	364.06
0.9	13.62	0.00	96.22	370.34
1.0	13.85	0.00	97.85	376.62

Table 3: Table showing the tolerance level set at 20%

5.1 Zimmermann Approach [13]

The formulation is that both the objective function and constraints are fuzzy:

$$\begin{aligned} Min \quad & \theta \\ \text{subject to} \quad & cx \geq b_0 - \theta p_0 \\ & (Ax)_i \leq b_i + \theta p_i, \qquad \forall\ i, \theta \in [0,1]\ and x \geq 0 \end{aligned}$$

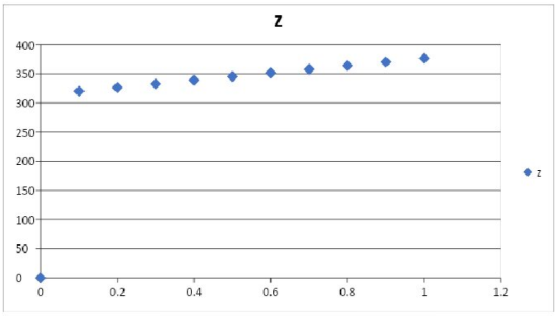

Figure 4: Theta versus z at 20% tolerance parameter.

The value of $\theta \in [0, 1]$ and non -negativity condition $x \geq 0$.
We obtain the formulation for our problem as

$$\begin{aligned}
Min \quad & \theta \\
\text{subject to} \quad & 6x_1 + 13x_2 + 10x_3 + 20x_4 + 25x_5 + 21.25\theta \geq 21.25 \\
& 15x_1 + 3x_2 + 5x_3 + 6x_4 + 10x_5 + 15\theta \geq 15 \\
& x_1 + 3x_2 + 2x_3 + 5x_4 + x_5 + 4\theta \geq 4 \\
& 15x_1 + 3x_2 + 5x_3 + 6x_4 + 10x_5 - 0.75\theta \leq 15 \\
& x_1 + 3x_2 + 2x_3 + 5x_4 + x_5 - 0.2\theta \leq 4 \\
& x_5 - 0.125\theta \leq 0.25 \\
& x_1 + x_2 + x_3 + x_4 + x_5 - 0.50\theta \leq 1
\end{aligned} \tag{9}$$

On solving the above formulation we obtain the table values as:

θ	x_1	x_2	x_3	$\alpha = 1 - \theta$	z
0	11.54	0	81.54	1	313.85
0.1	11.6	0	81.95	0.9	315.42
0.2	11.65	0	82.35	0.8	316.98
0.3	11.71	0	82.76	0.7	318.55
0.4	11.77	0	83.17	0.6	320.12
0.5	11.83	0	83.58	0.5	321.69
0.6	13.42	0	81.52	0.4	325.11
0.7	11.94	0	84.39	0.3	324.83
0.8	12.00	0	84.80	0.2	326.4
0.9	12.06	0	85.21	0.1	327.97
1.0	12.12	0	85.62	0	329.54

Table 4: Values obtained by Zimmermanns method

6 RESULTS AND DISCUSSIONS

As the value of p increases, the consistency of all other parameters increases. At 20% tolerance parameter, the satisfaction level is 100% & the value of $Z = 376.62$. At 15%

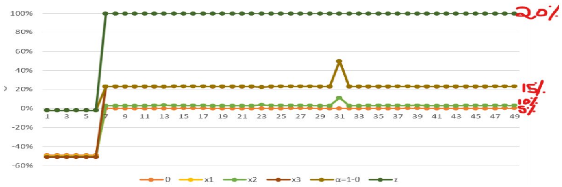

Figure 5: Solution by Zimmermanns approach and values for various tolerance parameters.

tolerance parameter the satisfaction level is 100% & the value of $Z = 357.46$. At 10% tolerance parameter the satisfaction level is 100% & the value of $Z = 345.23$. At 5% tolerance parameter the satisfaction level is 100% & the value of $Z = 329.54$. The decision maker can alter some circumstances whenever he wants to alter the original model and end the solution procedure whenever he is satisfied.

7 Conclusion

A simple linear programming model for revenue optimization of tourism industry is presented in this paper. Henceforth fuzziness is incorporated and their solution obtained through fuzzy linear programming approach. Fuzziness can help to offer a more natural description of uncertain data which depicts the real world phenomenon. Many real-world problems can be solved using general approaches for linear programming, but due to human nature, fuzziness and imprecision make a significant difference to these difficulties. Taking into account the vagueness, Fuzzy Linear Mathematical Programming is able to solve more problems with incremented levels of exactness. They are the mathematical tools which have immense potential for handling uncertainty inherent in real time data. Werners method and Verdegays method do not allow the freedom to solve for desired goal and objective like Zimmermann and Chanas does. In the case study that has been carried out, it can be understood that for various tolerance parameters, the maximum value of objective function changes. Hence, the value of tolerance which yields maximum results is selected. Thus the implementation of this approach can encourage tourism stakeholders such as national and local government, tourism businesses, and local communities to play a guiding role. This technique can improve the quality of policy decisions and allow decision-makers to take advantage of the great tourism resource potential, including geographical, climate, natural attractions, cultural, and ancient heritages. The future scope lies in multiobjective approach to tourism problem with fuzzy linear and non linear membership functions for objectives, constraints or both.

References

[1] R. E. Bellman and L. A. Zadeh. Decision-making in a fuzzy environment. *Management science*, 17(4):B–141, 1970.

[2] S. Chanas. The use of parametric programming in fuzzy linear programming. *Fuzzy sets and systems*, 11(1):243–251, 1983.

[3] J.-R. Chang and B. Chang. The development of a tourism attraction model by using fuzzy theory. *Mathematical Problems in Engineering*, 2015, 2015.

[4] G. B. Dantzig. Linear programming under uncertainty. *Management science*, 1(3-4):197–204, 1955.

[5] S. Karagiannis, D. Apostolou, et al. Regional tourism development using linear programming and vector analysis. *Regional Science Inquiry*, 2(1):25–32, 2010.

[6] N. Kişi. A strategic approach to sustainable tourism development using the awot hybrid method: A case study of zonguldak, turkey. *Sustainability*, 11(4):964, 2019.

[7] E. C. V. D. Knijff and J. Oosterhaven. Optimizing tourist policy: a linear programming approach. *Regional Studies*, 24(1):55–64, 1990.

[8] K. Koens, A. Postma, and B. Papp. Is overtourism overused? understanding the impact of tourism in a city context. *Sustainability*, 10(12):4384, 2018.

[9] S. Rao. Linear programming for revenue management in hotel industry. *Journal of Hospitality Application and Research*, 8(1), 2013.

[10] A. A. Shahraki and I. Ebrahimzadeh. Programming for development of tourism industry using case studies. *Cogent Business & Management*, 2(1):1121638, 2015.

[11] M. Sharma and M. Pooja. Revenue optimization in tourism and hotel industry using genetic algorithm.

[12] H. Shevchenko and M. Petrushenko. Managing change in nature-based tourism: A decision-making model using linear programming1. 2022.

[13] H. Tanaka, T. Okuda, and K. Asai. Fuzzy mathematical programming. *Transactions of the society of instrument and control engineers*, 9(5):607–613, 1973.

[14] J. Verdegay. Applications of fuzzy optimization in operational research. *Control and Cybernetics*, 13(3):229–239, 1984.

[15] J. L. Verdegay. Fuzzy mathematical programming. *Fuzzy information and decision processes*, 231:231–236, 1982.

[16] B. Werners. An interactive fuzzy programming system. *Fuzzy sets and systems*, 23(1):131–147, 1987.

[17] H.-C. Wu. Solving fuzzy linear programming problems with fuzzy decision variables. *Mathematics*, 7(7):569, 2019.

[18] L. A. Zadeh. Fuzzy sets. In *Fuzzy sets, fuzzy logic, and fuzzy systems: selected papers by Lotfi A Zadeh*, pages 394–432. World Scientific, 1996.

[19] M. Ziaabadi, M. Malakootian, M. R. Zare Mehrjerdi, S. A. Jalaee, and H. Mehrabi Boshrabadi. How to use composite indicator and linear programming model for determine sustainable tourism. *Journal of Environmental Health Science and Engineering*, 15(1):1–11, 2017.

[20] H.-J. Zimmermann. Description and optimization of fuzzy systems. *International journal of general System*, 2(1):209–215, 1975.

[21] H.-J. Zimmermann. Applications of fuzzy set theory to mathematical programming. *Information sciences*, 36(1-2):29–58, 1985.

[22] H.-J. Zimmermann. Fuzzy control. In *Fuzzy Set Theoryand Its Applications*, pages 223–264. Springer, 2001.

J. COMPUTATIONAL ANALYSIS AND APPLICATIONS, VOL. 31, NO. 3, 2023, COPYRIGHT 2023 EUDOXUS PRESS, LLC

A homotopy based computational scheme for local fractional Helmholtz and Laplace equations

Jagdev Singh[*], Ritin Babu[†], Ved Prakash Dubey[‡], Devendra Kumar[§¶]

December 31, 2022

In this work, we investigate solutions for the local fractional Helmholtz and Laplace equations on Cantor set having importance in electrostatics, gravitation and fluid dynamics. To find exact solutions, the q-local fractional homotopy analysis transform method (q-LFHATM) has been used. The numerical results computed with the aid of the applied scheme shows that it is an efficient and accurate tool to solve differential equations with local fractional derivatives.

Keywords: Local fractional derivative operator; Partial differential equations; Laplace equation; Helmholtz equation; q-local fractional homotopy analysis transform method.

1 Introduction

The concept of local fractional calculus (LFC) has been used to model and analyze numerous fractal equations some of which are Fokker-Planck equation [1, 2], fractal wave equations [3], fractal-time dynamical systems [4, 5], the local fractional stress strain relations [6], the local fractional heat conduction model [7], local fractional Tricomi equation [8], local fractional Laplace equations [9], the Helmholtz equation associated with local fractional operator [10], fractal signals [11, 12], fractal Fourier analysis [13], Yang Fourier transform [14, 15, 16], Yang-Laplace transform [15, 17], fractal vehicular traffic flow [18], local fractional modelling in growths of population [19], and Boussinesq equation containing local fractional operator [20], etc. Some recent outcomes of different authors on local fractional methods involving local fractional integral transforms can be seen in a series of articles [21, 22, 23].

---

[*] Department of Mathematics, JECRC University, Jaipur-303905, Rajasthan, India

[†] Department of Mathematics, JECRC University, Jaipur-303905, Rajasthan, India

[‡] Faculty of Mathematical and Statistical Sciences, Shri Ramswaroop Memorial University, Barabanki-225003, Uttar Pradesh, India

[§] Department of Mathematics, University of Rajasthan, Jaipur-302004, Rajasthan, India

[¶] Corresponding author: devendra.maths@gmail.com

This work presents a very useful scheme known as the q-local fractional homotopy analysis transform method (q-LFHATM), which is a combination of q-HAM and the local fractional Laplace transform (LFLT). The proposed q-LFHATM is implemented to analyze the local fractional Helmholtz and Laplace equations. The merger of q-HAM and LFLT resulted in lesser C.P.U time (RAM-1 GB or more and Processor 2.65 GHz or more) while solving fractional-order nonlinear problems. The ability of the proposed method to achieve the series solution of local fractional Helmholtz and Laplace equations over a vast domain by picking approximate values for parameters is one of its advantages. El-Tavil & Huseen proposed the q-HAM [24, 25] which is a smooth generalization of the HAM. The HAM was first proposed and used by Liao [26, 27] to solve several problems found in engineering, science and finance.
The rest of the article is organized as follows: Section 2 reports basic definitions and formulae of LFC and LFLT. Section 3, the working of q-LFHATM is explained. The q-LFHATM is utilized to derive the solutions of local fractional Helmholtz and Laplace equations under different fractal conditions in Section 4. Section 5 presents the glimpse of numerical simulation for fractal order $\rho = \ln 2/\ln 3$. At the end, conclusion is reported in Section 6.

2 Preliminaries

Here, we provide certain important concepts of LFC and LFLT.
Definition 2.1. If we have a relation [12, 28]

$$|\theta(t) - \theta(t_0)| < \varepsilon^{\alpha}, 0 < \alpha \le 1, \tag{1}$$

with $|\theta(t) - \theta(t_0)| < \delta$, for $\varepsilon, \alpha \in R$, then the function $\theta(t)$ is said to be local fractional continuous (LFC) at $t = t_0$ and is indicated by $\lim\limits_{t \to t_0} \theta(t) = \theta(t_0)$. Here, $\theta(t)$ is called LFC on (a, b) and is expressed as

$$\theta(t) \in C_{\alpha}(a, b). \tag{2}$$

Definition 2.2. A function $\theta(t)$ is a nondifferentiable function of exponentα $(0 < \alpha \le 1)$ if it satisfies the Hölder function of the exponent α. Then for $t, s \in T$, we have [12, 28]

$$|\theta(t) - \theta(s)| < C|t - s|^{\alpha}. \tag{3}$$

Definition 2.3. $\theta(t)$ is said to be continuous of α, 0<$\alpha \le 1$, or α continuous if there exists the following condition [12] $|\theta(t) - \theta(t_0)| < \varepsilon^{\alpha}$,

$$\theta(t) - \theta(t_0) = o\left((t - t_0)^{\alpha}\right). \tag{4}$$

In view of (4), Eq. (1) presents the standard form of local fractional continuity.
Definition 2.4. If $\theta(t) \in C_{\alpha}(a, b)$, then local fractional derivative (LFD) of $\theta(t)$ of order α at $x = x_0$ is written as [12, 28]:

$$\theta^{(\alpha)}(t_0) = \frac{d^{\alpha}}{dt^{\alpha}} \theta(t)\,|_{t=t_0} = \lim_{t \to t_0} \frac{\Delta^{\alpha}(\theta(t) - \theta(t_0))}{(t - t_0)^{\alpha}}, \tag{5}$$

where $\Delta^{\alpha}\left(\theta\left(t\right)-\theta\left(t_0\right)\right)\cong\Gamma\left(\alpha+1\right)\left(\theta\left(t\right)-\theta\left(t_0\right)\right)$.
For any $t\in(a,b)$, we have $\theta^{(\alpha)}\left(t\right)=D_t^{\alpha}\theta\left(t\right)$. The LFD of $m\alpha$ order is expressed as:

$$\theta^{(m\alpha)}\equiv\overbrace{D_t^{\alpha}....D_t^{\alpha}\theta\left(t\right)}^{\text{m times}},$$

whereas the local fractional partial derivative (LFPD) of $m\alpha$ order is expressed as:

$$\frac{\partial^{m\alpha}\theta\left(t\right)}{\partial t^{m\alpha}}\equiv\overbrace{\frac{\partial^{\alpha}}{\partial t^{\alpha}}....\frac{\partial^{\alpha}}{\partial t^{\alpha}}\theta\left(t\right)}^{\text{m times}}.$$

Definition 2.5. Let $\frac{1}{\Gamma(1+\alpha)}\int_0^{\infty}\left|\theta\left(t\right)\right|\left(dt\right)^{\alpha}<m<\infty$. Then the Yang-Laplace (YL) transform [29, 30] of $\theta\left(t\right)$ is defined as:

$$L_{\alpha}\left\{\theta\left(t\right)\right\}=\theta_s^{L,\alpha}\left(s\right)=\frac{1}{\Gamma\left(1+\alpha\right)}\int_0^{\infty}E_{\alpha}\left(-s^{\alpha}t^{\alpha}\right)\theta\left(t\right)\left(dt\right)^{\alpha},0<\alpha\leq1.\quad(6)$$

Here, the latter integral converges and $s^{\alpha}\in R^{\alpha}$.
Definition 2.6. The inverse of YL transform of $\theta\left(t\right)$ is stated as

$$L_{\alpha}^{-1}\left(\theta_s^{L,\alpha}\left(s\right)\right)=\theta\left(t\right)=\frac{1}{\left(2\pi\right)^{\alpha}}\int_{\upsilon-i\omega}^{\upsilon+i\omega}E_{\alpha}\left(s^{\alpha}t^{\alpha}\right)\theta_s^{L,\alpha}\left(s\right)\left(ds\right)^{\alpha},0<\alpha\leq1,\quad(7)$$

where $s^{\alpha}=\upsilon^{\alpha}+i^{\alpha}\omega^{\alpha}$; fractal imaginary unit i^{α} and $Re\left(s\right)=\alpha>0$.
Some useful formulae of LFLT [11, 12] are mentioned here:

$$L_{\alpha}\left\{a\theta\left(t\right)+b\phi\left(t\right)\right\}=a\theta_s^{L,\alpha}\left(s\right)+b\phi_s^{L,\alpha}\left(s\right),\quad(8)$$

$$L_{\alpha}\left\{E_{\alpha}\left(c^{\alpha}t^{\alpha}\right)\theta\left(t\right)\right\}=\theta_s^{L,\alpha}\left(s-c\right),\quad(9)$$

$$L_{\alpha}\left\{\theta^{(m\alpha)}\left(t\right)\right\}=s^{m\alpha}\theta_s^{L,\alpha}\left(s\right)$$

$$-s^{(m-1)\alpha}\theta\left(0\right)-s^{(m-2)\alpha}\theta^{(\alpha)}\left(0\right)-\cdots-\theta^{((m-1)\alpha)}\left(0\right),\quad(10)$$

$$L_{\alpha}\left\{E_{\alpha}\left(c^{\alpha}t^{\alpha}\right)\right\}=\frac{1}{s^{\alpha}-c^{\alpha}},\quad(11)$$

$$L_{\alpha}\left\{\sin_{\alpha}\left(c^{\alpha}t^{\alpha}\right)\right\}=\frac{c^{\alpha}}{s^{2\alpha}+c^{2\alpha}},\quad(12)$$

$$L_{\alpha}\left\{t^{m\alpha}\right\}=\frac{\Gamma\left(1+m\alpha\right)}{s^{(m+1)\alpha}}.\quad(13)$$

Definition 2.7. The Mittag-Leffler function (MLF) is formulated as [12, 28]

$$E_{\alpha}\left(t^{\alpha}\right)=\sum_{m=0}^{\infty}\frac{t^{m\alpha}}{\Gamma\left(1+m\alpha\right)},0<\alpha\leq1.\quad(14)$$

The following results hold true;

$$\sin_\alpha\left(t^\alpha\right)=\sum_{m=0}^{\infty}(-1)^m\,\frac{t^{(2m+1)\alpha}}{\Gamma\left(1+(2m+1)\,\alpha\right)},$$

$$\cos_\alpha\left(t^\alpha\right)=\sum_{m=0}^{\infty}(-1)^m\,\frac{t^{2m\alpha}}{\Gamma\left(1+2m\alpha\right)},0<\alpha\le 1. \tag{15}$$

Certain fundamental formulas and results used in the work are presented below:

$$\frac{d^\alpha t^{m\alpha}}{dt^\alpha}=\frac{\Gamma\left(1+m\alpha\right)t^{(m-1)\alpha}}{\Gamma\left(1+(m-1)\,\alpha\right)}, \tag{16}$$

$$\frac{d^\alpha E_\alpha\left(t^\alpha\right)}{dt^\alpha}=E_\alpha\left(t^\alpha\right), \tag{17}$$

$$\frac{d^\alpha E_\alpha\left(mt^\alpha\right)}{dt^\alpha}=mE_\alpha\left(mt^\alpha\right). \tag{18}$$

3 Working plan of q-LFHATM

To elucidate the procedure of q-LFHATM, the following nonlinear local fractional partial differential equation (LFPDE) is investigated

$$Ł_\alpha\,\varepsilon(\eta,\kappa)+R_\alpha\,\varepsilon(\eta,\kappa)+N_\alpha\varepsilon(\eta,\kappa)=h(\eta,\kappa),\quad n-1<\alpha\le n, \tag{19}$$

where $Ł_\alpha$ indicates the linear local fractional operator, R_α indicates the remaining local linear differential operator, N_α stands for the nonlinear differential operator and $h(\eta,\kappa)$ signifies the source term.
Operating the LFLT on Eq. (19), we obtain

$$\begin{gathered}L_\alpha\left[\varepsilon(\eta,\kappa)\right]-s^{-\alpha}\varepsilon(\eta,0)-s^{-2\alpha}\varepsilon^{(\alpha)}(\eta,0)-\cdots-s^{-t\alpha}\varepsilon^{((t-1)\alpha)}(\eta,0)\\+s^{-t\alpha}\,L_\alpha\left[R_\alpha\varepsilon(\eta,\kappa)+N_\alpha\,\varepsilon(\eta,\kappa)-h(\eta,\kappa)\right]=0.\end{gathered} \tag{20}$$

We describe the nonlinear operator as:

$$\begin{aligned}N[\psi(\eta,\kappa;l)]&=L_\alpha\left[\psi(\eta,\kappa;l)\right]-s^{-\alpha}\psi(\eta,\kappa;l)(0^+)-s^{-2\alpha}\psi^{(\sigma)}(\eta,\kappa;l)(0^+)-\cdots\\&-s^{-t\alpha}\psi^{((t-1)\alpha)}(\eta,\kappa;l)(0^+)+s^{-t\alpha}L_\alpha\left[R_\alpha\varepsilon(\eta,\kappa)+N_\alpha\,\varepsilon(\eta,\kappa)-h(\eta,\kappa)\right].\end{aligned} \tag{21}$$

In Eq. (21), $l\in[0,\,1/n]$ and $\psi(\eta,\kappa;l)$ is a real valued function of η,κ & l. Now, the homotopy is framed as:

$$(1-nl)\,L_\alpha\left[\left[\psi(\eta,\kappa;l)-\varepsilon_0(\eta,\kappa)\right]=\hbar\,l\,N\left[\varepsilon(\eta,\kappa)\right].\right. \tag{22}$$

In Eq. (22), L_α stands for the LFLT operator, $n\ge 1$,$l\in[0,\,1/n]$ is an embedding variable, $\hbar\ne 0$ stands for an auxiliary parameter, $\varepsilon_0(\eta,\kappa)$ denotes initial guess (IG) of $\varepsilon(\eta,\kappa)$ and $\psi(\eta,\kappa;l)$ is an unidentified function. Clearly, for $l=0$ and $l=\frac{1}{n}$, the results obtained are

$$\psi(\eta,\kappa;0)=\varepsilon_0(\eta,\kappa),\qquad\psi(\eta,\kappa\,;\frac{1}{n})=\varepsilon(\eta,\kappa), \tag{23}$$

respectively. Therefore, when l approaches from 0 to $\frac{1}{n}$, $\psi(\eta,\kappa;l)$ changes from the IG $\varepsilon_0(\eta,\kappa)$ to solution $\varepsilon(\eta,\kappa)$. Taylor series expansion of $\psi(\eta,\kappa;l)$ provides

$$\psi(\eta,\kappa;l)=\sum_{m=0}^{\infty}\varepsilon_m(\eta,\kappa)l^{\,m}. \tag{24}$$

where

$$\varepsilon_m(\eta,\kappa)=\frac{1}{m\,!}\frac{\partial^m\psi(\eta,\kappa;l)}{\partial l^m}\,|_{l=0}. \tag{25}$$

For proper values of $u_0(x,t)$,n and $\hbar$, the series (10) converges for $l=\frac{1}{n}$, then we obtain

$$\varepsilon(\eta,\kappa)=\sum_{m=0}^{\infty}\varepsilon_m(\eta,\kappa)(\frac{1}{n})^m. \tag{26}$$

Now, the set of vectors is characterized as

$$\overrightarrow{\varepsilon}_m=\{\varepsilon_0(\eta,\kappa),\ \varepsilon_1(\eta,\kappa),\cdots,\ \varepsilon_m(\eta,\kappa)\}. \tag{27}$$

Next, the mth-order deformation equation is composed as

$$L_\alpha\left[\varepsilon_m(\eta,\kappa)-\chi_m\varepsilon_{m-1}(\eta,\kappa)\right]=\hbar\,\Re_m(\overrightarrow{\varepsilon}_{m-1}). \tag{28}$$

Operating the inverse LFLT on Eq. (28), we obtain

$$\varepsilon_m(\eta,\kappa)=\chi_m\varepsilon_{m-1}(\eta,\kappa)+\hbar\,{L_\alpha}^{-1}[\Re_m(\overrightarrow{\varepsilon}_{m-1})]. \tag{29}$$

In Eq. (29), the value of $\Re_k(\vec{\phi}_{k-1})$ and χ_k are presented below

$$\Re_m(\overrightarrow{\varepsilon}_{m-1})=\frac{1}{(m-1)!}\frac{\partial^{m-1}N\left[\varepsilon(\eta,\kappa;l)\right]}{\partial l^{m-1}}\,|_{l=0}, \tag{30}$$

and

$$\chi_m=\begin{cases}0, & m\le 1,\\ n, & m>1.\end{cases} \tag{31}$$

4 Illustrative examples

Example 4.1 Let us take the local fractional Helmholtz equation [10] as follows

$$\frac{\partial^{2\rho}\phi(u,v)}{\partial u^{2\rho}}+\frac{\partial^{2\rho}\phi(u,v)}{\partial v^{2\rho}}=\phi(u,v),0<\rho\le 1 \tag{32}$$

with initial-boundary conditions given as:

$$\phi\left(0,v\right)=0,\frac{\partial^{\rho}\phi(0,v)}{\partial u^{\rho}}=E_\rho\left(v^\rho\right). \tag{33}$$

Applying LFLT on Eq. (32), we obtain

$$L_\rho\left\{\phi(u,v)\right\}-s^\rho\phi(0,v)-s^{-2\rho}\frac{\partial^\rho\phi(0,v)}{\partial u^\rho}+s^{-2\rho}L_\rho\left\{\frac{\partial^{2\rho}\phi(u,v)}{\partial^{2\rho}v}-\phi(u,v)\right\}=0,$$

or

$$L_\rho\left\{\phi(u,v)\right\}-s^{-2\rho}E_\rho\left(y^\rho\right)+s^{-2\rho}L_\rho\left\{\frac{\partial^{2\rho}\phi(u,v)}{\partial^{2\rho}v}-\phi(u,v)\right\}=0. \tag{34}$$

The nonlinear operator is defined as

$$N[\psi(\eta,\kappa;l)]=L_\rho\left[\psi(\eta,\kappa;l)\right]-s^{-2\rho}E_\rho\left(y^\rho\right)+s^{-2\rho}L_\beta\left\{\frac{\partial^{2\rho}\psi(\eta,\kappa;l)}{\partial^{2\rho}v}-\psi(\eta,\kappa;l)\right\}, \tag{35}$$

and so

$$\Re_m\left(\vec{\phi}_{m-1}\left(u,v\right)\right)=L_\rho\left\{\phi_{m-1}\left(u,v\right)\right\}$$

$$-\left(1-\frac{\chi_m}{n}\right)s^{-2\rho}E_\rho\left(v^\rho\right)+s^{-2\rho}L_\rho\left[\frac{\partial^{2\rho}\phi_{m-1}\left(u,v\right)}{\partial v^{2\rho}}-\phi_{m-1}\left(u,v\right)\right]. \tag{36}$$

The mth-order deformation equation is built as

$$L_\rho\left\{\phi_m\left(u,v\right)-\chi_m\phi_{m-1}\left(u,v\right)\right\}=\hbar\Re_m\left(\vec{\phi}_{m-1}\left(u,v\right)\right). \tag{37}$$

Applying inverse LFLT on Eq. (37), we obtain

$$\phi_m\left(u,v\right)=\chi_m\phi_{m-1}\left(u,v\right)+\hbar L_\rho^{-1}\left\{\Re_m\left(\vec{\phi}_{m-1}\left(u,v\right)\right)\right\}. \tag{38}$$

For $m=1$, we have

$$\phi_1\left(u,v\right)=\chi_1\phi_0\left(u,v\right)+\hbar L_\rho^{-1}\left\{\Re_1\left(\vec{\phi}_0\left(u,v\right)\right)\right\}$$

or

$$\phi_1\left(u,v\right)=-\hbar E_\rho\left(v^\rho\right)\frac{u^\rho}{\Gamma\left(1+\rho\right)}. \tag{39}$$

For $m=2$, we have

$$\phi_2\left(u,v\right)=\chi_2\phi_1\left(u,v\right)+\hbar L_\rho^{-1}\left\{\Re_2\left(\vec{\phi}_1\left(u,v\right)\right)\right\},$$

or

$$\phi_2\left(u,v\right)=-\left(n+\hbar\right)\hbar E_\rho\left(v^\rho\right)\frac{u^\rho}{\Gamma\left(1+\rho\right)}. \tag{40}$$

For $m=3$, we have

$$\phi_3\left(u,v\right)=\chi_3\phi_2\left(u,v\right)+\hbar L_\rho^{-1}\left\{\Re_3\left(\vec{\phi}_2\left(u,v\right)\right)\right\},$$

or

$$\phi_3\left(u,v\right)=-\left(n+\hbar\right)\hbar^2E_\rho\left(v^\rho\right)\frac{u^\rho}{\Gamma\left(1+\rho\right)}, \tag{41}$$

& so on.

Hence, the nondifferentiable solution is expressed as

$$\phi(u,v)=\sum_{m=0}^{\infty}\phi_m(u,v)(\frac{1}{n})^m.$$

$$\phi(u,v)=\phi_0(u,v)+\frac{\phi_1(u,v)}{n}+\frac{\phi_2(u,v)}{n^2}+\frac{\phi_3(u,v)}{n^3}+\cdots$$

or

$$\phi(u,v)=\frac{1}{n}\left[\hbar E_\rho\left(v^\rho\right)\frac{u^\rho}{\Gamma\left(1+\rho\right)}\right]-\frac{1}{n^2}\left[\left(n+\hbar\right)\hbar E_\rho\left(v^\rho\right)\frac{u^\rho}{\Gamma\left(1+\rho\right)}\right]$$

$$-\frac{1}{n^3}\left[\left(n+\hbar\right)\hbar^2 E_\rho\left(v^\rho\right)\frac{u^\rho}{\Gamma\left(1+\rho\right)}\right]+\cdots. \tag{42}$$

On letting $\hbar=-1$ and $n=1$, one can achieve the result

$$\phi\left(u,v\right)=\frac{u^\rho}{\Gamma\left(1+\rho\right)}E_\rho\left(v^\rho\right). \tag{43}$$

which is the solution of fractal problem (32).

Example 4.2 Take the following local fractional Laplace equation [9]

$$\frac{\partial^{2\rho}\phi(u,v)}{\partial u^{2\rho}}+\frac{\partial^{2\rho}\phi(u,v)}{\partial v^{2\rho}}=0, 0<\rho\leq 1, \tag{44}$$

with initial-boundary conditions given as:

$$\phi\left(0,v\right)=-E_\rho\left(v^\rho\right), \frac{\partial^\rho\phi(0,v)}{\partial u^\rho}=0. \tag{45}$$

Applying LFLT on Eq. (44), we obtain

$$L_\rho\left\{\phi(u,v)\right\}-s^{-\rho}\phi(0,v)-s^{-2\rho}\frac{\partial^\rho\phi(0,v)}{\partial u^\rho}+s^{-2\rho}L_\rho\left\{\frac{\partial^{2\rho}\phi(u,v)}{\partial^{2\rho}v}\right\}=0,$$

or

$$L_\rho\left\{\phi(u,v)\right\}+s^{-\rho}E_\rho\left(y^\rho\right)+s^{-2\rho}L_\rho\left\{\frac{\partial^{2\rho}\phi(u,v)}{\partial^{2\rho}v}\right\}=0. \tag{46}$$

The nonlinear operator is

$$N[\psi(\eta,\kappa;l)]=L_\rho\left[\psi(\eta,\kappa;l)\right]+s^{-\rho}E_\rho\left(y^\rho\right)+s^{-2\rho}L_\beta\left\{\frac{\partial^{2\rho}\psi(\eta,\kappa;l)}{\partial^{2\rho}v}\right\}, \tag{47}$$

and so

$$\Re_m\left(\vec{\phi}_{m-1}(u,v)\right)=L_\rho\left\{\phi_{m-1}(u,v)\right\}$$

$$+\left(1-\frac{\chi_m}{n}\right)s^{-\rho}E_\rho\left(v^\rho\right)+s^{-2\rho}L_\rho\left[\frac{\partial^{2\rho}\phi_{m-1}(u,v)}{\partial v^{2\rho}}\right]. \tag{48}$$

The mth-order deformation equation is constituted as:

$$L_\rho \left\{\phi_m (u,v) - \chi_m \phi_{m-1} (u,v)\right\} = \hbar \Re_m \left(\vec{\phi}_{m-1}(u,v)\right). \tag{49}$$

Operating the inverse LFLT, we obtain

$$\phi_m (u,v) = \chi_m \phi_{m-1} (u,v) + \hbar L_\rho^{-1} \left\{\Re_m \left(\vec{\phi}_{m-1}(u,v)\right)\right\}. \tag{50}$$

Taking $m = 1, 2, 3, \ldots$, we get

For $m = 1$

$$\phi_1 (u,v) = -\hbar E_\rho (v^\rho) \frac{u^{2\rho}}{\Gamma(1+2\rho)}. \tag{51}$$

For $m = 2$

$$\phi_2 (u,v) = -(n+\hbar)\hbar E_\rho (v^\rho) \frac{u^{2\rho}}{\Gamma(1+2\rho)} - \hbar^2 E_\rho (v^\rho) \frac{u^{4\rho}}{\Gamma(1+4\rho)}. \tag{52}$$

For $m = 3$

$$\begin{aligned}\phi_3 (u,v) = &-(n+\hbar)^2 \hbar E_\rho (v^\rho) \frac{u^{2\rho}}{\Gamma(1+2\rho)} - 2(n+\hbar)\hbar^2 E_\rho (v^\rho) \frac{u^{4\rho}}{\Gamma(1+4\rho)} \\ &-\hbar^3 E_\rho (v^\rho) \frac{u^{6\rho}}{\Gamma(1+6\rho)},\end{aligned} \tag{53}$$

& so on.

Hence, the nondifferentiable solution is presented as

$$\begin{aligned}\phi(u,v) = &-\frac{1}{n}\left[\hbar E_\rho (v^\rho) \frac{u^{2\rho}}{\Gamma(1+2\rho)}\right] - \frac{1}{n^2}\left[(n+\hbar)\hbar E_\rho (v^\rho) \frac{u^{2\rho}}{\Gamma(1+2\rho)} - \hbar^2 E_\rho (v^\rho) \frac{u^{4\rho}}{\Gamma(1+4\rho)}\right] \\ &-\frac{1}{n^3}\left[(n+\hbar)^2 \hbar E_\rho (v^\rho) \frac{u^{2\rho}}{\Gamma(1+2\rho)} + 2(n+\hbar)\hbar^2 E_\rho (v^\rho) \frac{u^{4\rho}}{\Gamma(1+4\rho)} + \hbar^3 E_\rho (v^\rho) \frac{u^{6\rho}}{\Gamma(1+6\rho)}\right] + \cdots.\end{aligned} \tag{54}$$

Setting $\hbar = -1$ and $n = 1$, one can have

$$\phi(u,v) = E_\rho (v^\rho) \left(-1 + \frac{u^{2\rho}}{\Gamma(1+2\rho)} - \frac{u^{4\rho}}{\Gamma(1+4\rho)} + \frac{u^{6\rho}}{\Gamma(1+6\rho)} - \cdots\right).$$

It can be written as

$$\phi(u,v) = E_\rho (v^\rho) \left(\sum_{m=0}^{\infty} (-1)^m \frac{u^{2m\rho}}{\Gamma(1+2m\rho)}\right).$$

The solution of Eq. (44) is constituted as

$$\phi(u,v) = E_\rho (v^\rho) \cos_\rho (u^\rho). \tag{55}$$

Example 4.3 Finally, the following Laplace equation with LFD [9] is investigated

$$\frac{\partial^{2\rho}\phi(u,v)}{\partial u^{2\rho}}+\frac{\partial^{2\rho}\phi(u,v)}{\partial v^{2\rho}}=0, 0<\rho\leq 1 \tag{56}$$

with initial-boundary conditions given as:

$$\phi\left(0,v\right)=0, \frac{\partial^{\rho}\phi(0,v)}{\partial u^{\rho}}=-E_{\rho}\left(y^{\rho}\right). \tag{57}$$

Applying LFLT on Eq. (56), we obtain

$$L_{\rho}\left\{\phi(u,v)\right\}-s^{-\rho}\phi(0,v)-s^{-2\rho}\frac{\partial^{\rho}\phi(0,v)}{\partial u^{\rho}}+s^{-2\rho}L_{\rho}\left\{\frac{\partial^{2\rho}\phi(u,v)}{\partial^{2\rho}v}\right\}=0$$

or

$$L_{\rho}\left\{\phi(u,v)\right\}+s^{-2\rho}E_{\rho}\left(y^{\rho}\right)+s^{-2\rho}L_{\rho}\left\{\frac{\partial^{2\rho}\phi(u,v)}{\partial^{2\rho}v}\right\}=0. \tag{58}$$

The nonlinear operator is constituted as

$$N[\psi(\eta,\kappa;l)]=L_{\rho}\left[\psi(\eta,\kappa;l)\right]+s^{-2\rho}E_{\rho}\left(y^{\rho}\right)+s^{-2\rho}L_{\beta}\left\{\frac{\partial^{2\rho}\psi(\eta,\kappa;l)}{\partial^{2\rho}v}\right\}, \tag{59}$$

and so

$$\Re_{m}\left(\vec{\phi}_{m-1}\left(u,v\right)\right)=L_{\rho}\left\{\phi_{m-1}\left(u,v\right)\right\}$$

$$+\left(1-\frac{\chi_{m}}{n}\right)s^{-2\rho}E_{\rho}\left(v^{\rho}\right)+s^{-2\rho}L_{\rho}\left[\frac{\partial^{2\rho}\phi_{m-1}\left(u,v\right)}{\partial v^{2\rho}}\right]. \tag{60}$$

Next, we present the mth-order deformation equation as

$$L_{\rho}\left\{\phi_{m}\left(u,v\right)-\chi_{m}\phi_{m-1}\left(u,v\right)\right\}=\hbar\Re_{m}\left(\vec{\phi}_{m-1}\left(u,v\right)\right). \tag{61}$$

Applying the inverse LFLT, we obtain

$$\phi_{m}\left(u,v\right)=\chi_{m}\phi_{m-1}\left(u,v\right)+\hbar L_{\rho}^{-1}\left\{\Re_{m}\left(\vec{\phi}_{m-1}\left(u,v\right)\right)\right\}. \tag{62}$$

Taking $m=1,2,3,\ldots$, we get
For $m=1$, we have

$$\phi_{1}\left(u,v\right)=\hbar E_{\rho}\left(v^{\rho}\right)\frac{u^{\rho}}{\Gamma\left(1+\rho\right)}. \tag{63}$$

For $m=2$, we obtain

$$\phi_{2}\left(u,v\right)=\left(n+\hbar\right)\hbar E_{\rho}\left(v^{\rho}\right)\frac{u^{\rho}}{\Gamma\left(1+\rho\right)}+\hbar^{2}E_{\rho}\left(v^{\rho}\right)\frac{u^{3\rho}}{\Gamma\left(1+3\rho\right)}. \tag{64}$$

For $m=3$, we find

$$\phi_{3}\left(u,v\right)=\left(n+\hbar\right)^{2}\hbar E_{\rho}\left(v^{\rho}\right)\frac{u^{\rho}}{\Gamma\left(1+\rho\right)}$$

$$+2\left(n+\hbar\right)\hbar^{2}E_{\rho}\left(v^{\rho}\right)\frac{u^{3\rho}}{\Gamma\left(1+3\rho\right)}+\hbar^{3}E_{\rho}\left(v^{\rho}\right)\frac{u^{5\rho}}{\Gamma\left(1+5\rho\right)}, \tag{65}$$

Hence, the nondifferentiable solution is

$$\phi(u,v)=\sum_{m=0}^{\infty}\phi_{m}(u,v)(\frac{1}{n})^{m}.$$

or

$$\phi(u,v)=\frac{1}{n}\left[\hbar E_{\rho}\left(v^{\rho}\right)\frac{u^{\rho}}{\Gamma\left(1+\rho\right)}\right]+\frac{1}{n^{2}}\left[\left(n+\hbar\right)\hbar E_{\rho}\left(v^{\rho}\right)\frac{u^{\rho}}{\Gamma\left(1+\rho\right)}-\hbar^{2}E_{\rho}\left(v^{\rho}\right)\left(\frac{u^{3\rho}}{\Gamma\left(1+3\rho\right)}\right)\right]$$

$$+\frac{1}{n^{3}}\left[\left(n+\hbar\right)^{2}\hbar E_{\rho}\left(v^{\rho}\right)\frac{u^{\rho}}{\Gamma\left(1+\rho\right)}+2\left(n+\hbar\right)\hbar^{2}E_{\rho}\left(v^{\rho}\right)\frac{u^{3\rho}}{\Gamma\left(1+3\rho\right)}+\hbar^{3}E_{\rho}\left(v^{\rho}\right)\frac{u^{5\rho}}{\Gamma\left(1+5\rho\right)}\right]+\cdots. \tag{66}$$

On using the values $\hbar=-1$ and $n=1$, we have

$$\phi\left(u,v\right)=E_{\rho}\left(v^{\rho}\right)\left(-\frac{u^{\rho}}{\Gamma\left(1+\rho\right)}+\frac{u^{3\rho}}{\Gamma\left(1+3\rho\right)}-\frac{u^{5\rho}}{\Gamma\left(1+5\rho\right)}+\cdots\right).$$

The solution of Eq. (56) in closed form is expressed as

$$\phi\left(u,v\right)=E_{\rho}\left(v^{\rho}\right)\left(\sum_{m=0}^{\infty}\left(-1\right)^{m}\frac{u^{(2m+1)\rho}}{\Gamma\left(1+\left(2m+1\right)\rho\right)}\right).$$

or

$$\phi\left(u,v\right)=E_{\rho}\left(v^{\rho}\right)\sin_{\rho}\left(u^{\rho}\right). \tag{67}$$

5 Numerical simulation

This section presents numerical outcomes for fractal problem given in Examples 4.1-4.3 under fractal initial-boundary conditions. The 3D graphs for the local fractional Helmholtz and Laplace equations are demonstrated on the Cantor set for the fractal order $\rho=\ln 2/\ln 3$ via MATLAB. The graphics authenticates that the achieved solutions for Examples 4.1-4.3 depend on the fractal order ρ of the LFD. The 3D graphical visuals show the fractal pattern of the nondifferentiable function $\phi\left(u,\,v\right)$ in Examples 4.1-4.3.

6 Conclusions

In this work, the q-LFHATM is utilized to obtain the nondifferentiable solutions for the Helmholtz and Laplace equation in fractal media. The computed results establish the reliability and efficiency of the proposed technique and the applied method can be used to solve many other LFPDEs arising in fractal media. Finally, the computer simulations are also presented for fractal analysis of local fractional Helmholtz and Laplace models.

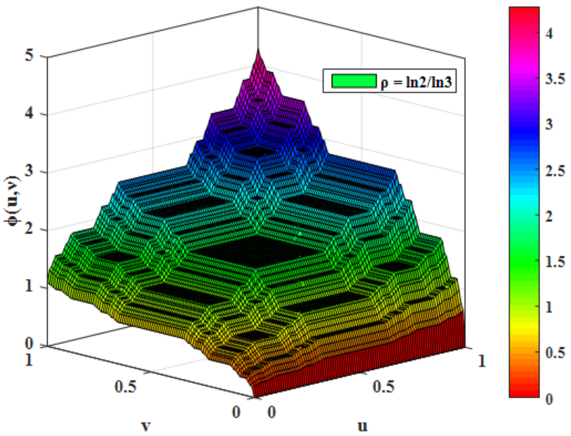

Figure 1: 3D nature of $\phi\left(u,v\right)$ w.r.t. u and v for Example 4.1

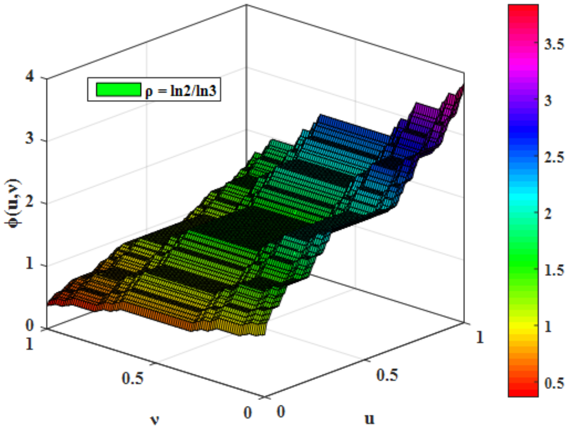

Figure 2: 3D behavior of $\phi\left(u,v\right)$ w.r.t. u and v for Example 4.2

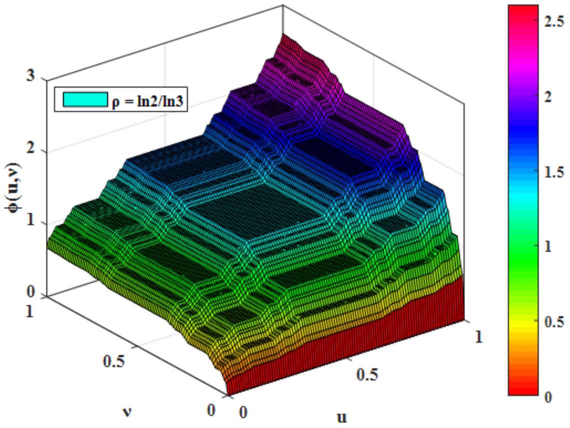

Figure 3: 3D pattern of $\phi\,(u,v)$ w.r.t. u and v for Example 4.3

References

[1] Kolwankar K.M., Gangal A.D., Hölder exponents of irregular signals and local fractional derivatives, *Pramana J. Phys.*, **48** (1997) 49-68.

[2] Kolwankar K.M., Gangal A.D., Local fractional Fokker-Planck equation, *Phys. Rev. Lett.*, **80** (1998) 214-217.

[3] Ahmad J., Mohyud-Din S.T., Solving wave and diffusion equations on Cantor sets, Proc. *Pakistan Acad. Sci.*, **52** (1) (2015) 81-87.

[4] Parvate A., Gangal A.D., Fractal differential equations and fractal time dynamical systems, *Pramana J. Phys*, **64** (3)(2005) 389- 409.

[5] Parvate A., Gangal A.D., Calculus on fractal subsets of real line I: formulation, *Fractals*, **17** (1) (2009) 53- 81.

[6] Carpinteri A., Chiaia B., Cornetti P., Static–kinematic duality and the principle of virtual work in the mechanics of fractal media, *Comput. Method. Appl. Mech. Eng.*, **191** (1-2) (2001) 3-19.

[7] Zhao D., Singh J., Kumar D., Rathore S., Yang X.-J., An efficient computational technique for local fractional heat conduction equations in fractal media, *J. Nonlinear Sci. Appl.*, **10** (4) (2017) 1478-1486.

[8] Singh J., Kumar D., Nieto J.J., A reliable algorithm for local fractional Tricomi equation arising in fractal transonic flow, *Entropy*, **18** (6) 206 (2016) 1-8.

[9] Dubey, V.P., Singh, J., Alshehri, A.M., Dubey, S., Kumar, D., A comparative analysis of two computational schemes for solving local fractional Laplace equations, *Math. Meth. Appl. Sci.*, **44** (17) (2021) 13540–13559.

[10] Yang A.M., Chen, Z., Srivastava, H.M., Yang X.-J., Application of the local fractional series expansion method and the variational iteration method to the Helmholtz equation involving local fractional derivative operators, *Abstr. Appl. Anal.*, **2013** (2013) 259125.

[11] Yang X.-J., Local Fractional Integral Transforms, *Progr. In nonlinear Sci.*, **4** (2011) 12-25.

[12] Yang X.-J., *Local Fractional Functional Analysis and Its Applications*, Asian Academic publisher Limited, Hong Kong (2011).

[13] Yang X.-J., Generalized sampling theorem for fractal signals, *Advances in Digital Multimedia*, **1** (2) (2012) 88-92.

[14] Yang X.-J., The discrete Yang-Fourier transforms in fractal space, *Advances in Electrical Engineering Systems*, **1** (2) (2012) 78-81.

[15] Yang X.-J., Local fractional partial differential equations with boundary problems, *Adv. Comput. Math. Appl.*, **1** (1) (2012) 60-63.

[16] Zhong W.P., Gao F., Shen X.M., Applications of Yang-Fourier transform to local fractional equations with local fractional derivative and local fractional integral, *Advanced Materials Research*, **416** (2012) 306-310.

[17] Guo Y., Local fractional Z transform in fractal space, *Advances in Digital Multimedia*, **1** (2) (2012) 96-102.

[18] Kumar D., Tchier F., Singh J., Baleanu D., An efficient computational technique for fractal vehicular traffic flow, *Entropy* **20**(4) (2018) 259.

[19] Yang X.-J., Machado JAT. A new insight into complexity from the local fractional calculus view point: modelling growths of populations, *Math Methods Appl Sci.*, **40** (17) (2017) 6070-6075.

[20] Yang X.-J., Machado ZAT, Baleanu D. Exact travelling-wave solution for local fractional Boussinesq equation in fractal domain, *Fractals*, **25** (04) (2017) 1740006.

[21] Dubey, V.P., Kumar, D., Singh, J., Alshehri, A.M., Dubey, S., Analysis of local fractional Klein-Gordon equations arising in relativistic fractal quantum mechanics, *Wave Random Complex Media*, (2022) 1-21, doi: 10.1080/17455030.2022.2112993.

[22] Dubey, V.P., Kumar, D., Alshehri, H.M., Dubey, S., Singh, J., Computational analysis of local fractional LWR model occurring in a fractal vehicular traffic flow, *Fractal Fract.*, **6** (2022), 1-19.

[23] Dubey, S., Dubey, V.P., Singh, J., Alshehri, A.M., Kumar, D., Computational study of a local fractional Tricomi equation occurring in fractal transonic flow, *J. Comput. Nonlinear Dynam.*, **17** (2022) 081006, doi: 10.1115/1.4054482.

[24] El-Tawil M.A., Huseen S.N., The q-Homotopy Analysis Method (q-HAM), *Int. J. Appl. Maths. Mech.*, **8** (2012) 51-75.

[25] El-Tawil M.A., Huseen S.N., On convergence of the q-Homotopy Analysis Method(q-HAM), *Int. J. Contemp. Math. Sci.*, **8** (2013) 481-497.

[26] Liao S.J., *The proposed homotopy analysis technique for the solution of nonlinear problems*, Ph.D. Thesis, Shanghai Jiao Tong Univ. (1992).

[27] Liao S.J., *Beyond Perturbation: Introduction to the Homotopy analysis method*, Chapman and Hall/CRC Press, Boca Raton (2003).

[28] Yang, X.-J., *Advanced Local Fractional Calculus and Its Applications*, World Science, New York (2012).

[29] Zhang Y.Z., Yang A.M., Long Y., Initial boundary value problem for fractal heat equation in the semi-infinite region by Yang-Laplace transform, *Thermal Science*, **18** (2) (2014) 677–681.

[30] Zhao C.G., Yang A.M., Jafari H., Haghbin A., The Yang-Laplace transform for solving the IVPs with local fractional derivative, *Abstr. Appl. Anal.*, **2014** (2014) 1-5.

J. COMPUTATIONAL ANALYSIS AND APPLICATIONS, VOL. 31, NO. 3, 2023, COPYRIGHT 2023 EUDOXUS PRESS, LLC

On asymptotic behavior of a quadratic functional equation

Mohamed Sirouni*[1], Muaadh Almahalebi†[2], and Samir Kabbaj‡[3]

[1,2,3]Faculty of Sciences, Department of Mathematics, Ibn Tofail University, BP:14000, Kenitra, Morocco

December 9, 2022

Abstract

The main goal of this paper is to investigate the stability problems for the following quadratic functional equation

$$f(x+y+z)+f(x+y-z)+f(x-y+z)+f(-x+y+z)=4f(x)+4f(y)+4f(z)$$

on an unbounded restricted domain. As a consequence, we can apply the obtained results to obtain some asymptotic behaviors of that equation in normed spaces. Moreover, we introduce a new inequality that characterizes the inner product spaces.

1 Introduction

In 1940, Stanisław Marcin Ulam proposed the following problem [25]:

> Let $(G_1, .)$ be a group and let $(G_2, *)$ be a metric group with the metric $d(.,.)$. Given a real number $\varepsilon > 0$, does there exist a real number $\delta > 0$ such that if a mapping $h: G_1 \to G_2$ satisfies the inequality $d(h(x.y), h(x) * h(y)) \leq \delta$ for all $x, y \in G_1$, then there is a homomorphism $H: G_1 \to G_2$ with $d(h(x), H(x)) \leq \varepsilon$ for all $x \in G_1$?

This problem gave rise to what we now call Ulam's stability of functional equations.

In a later year, an affirmative answer to the Ulam stability problem was given by D. H. Hyers for Banach spaces (see [13]). Several generalizations of this result are discussed. T. Aoki [5] for additive maps and by T.M. Rassias

---

*sirounim@gmail.com
†muaadh1979@hotmail.fr
‡samkabbaj@yahoo.fr

[19] for linear maps considering an unbounded Cauchy difference. P. Găvruţă [12] provided a further generalization of the Rassias' theorem by using a general control function. During the last decades, the stability problems of several functional equations have been extensively investigated by a number of authors (see, [1, 19, 20, 21, 23]).

Throughout the paper, let $(G,+)$ be an Abelian group and Y be a linear space on the field $\mathbb{K} \in \{\mathbb{R},\mathbb{C}\}$.

Let us note that a mapping $q\colon G \to Y$ is called quadratic if q satisfies the well-known quadratic functional equation

$$q(x+y)+q(x-y)=2q(x)+2q(y), \quad x,y \in G. \tag{1.1}$$

Quadratic functional equation (1.1) was used by Jordan and von Neumann [14] to characterize inner product spaces. Several other functional equations are used for this characterization. Maurice Fréchet in [11] obtained a characterization of the inner product spaces among normed linear spaces by using the following functional equation

$$f(x+y+z)+f(x)+f(y)+f(z)=f(x+y)+f(y+z)+f(x+z).$$

Theorem 1.1. *[11] Let $(X,\|.\|)$ be a normed linear space. Then X is an inner product space with respect to $\|.\|$ if and only if*

$$\|x+y+z\|^2+\|x\|^2+\|y\|^2+\|z\|^2=\|x+y\|^2+\|x+z\|^2+\|y+z\|^2, \quad x,y,z \in X.$$

Motivated by this idea, we deal with the following functional equation:

$$\begin{aligned} f(x+y+z)+f(x+y-z)+f(x-y+z)+f(-x+y+z)& \\ =4f(x)+4f(y)+4f(z).& \end{aligned} \tag{1.2}$$

This equation was first introduced and solved by S. Jung [15]. In fact, he proved the following theorem

Theorem 1.2 ([15], Theorem 2.1.)**.** *Let X and Y be vector spaces over fields of characteristic different from 2, respectively. If $f\colon X \to Y$ satisfies the functional equations*

$$f(x+y)+f(x-y)=2f(x)+2f(y), \tag{1.3}$$

$$f(x-y-z)+f(x)+f(y)+f(z)=f(x-y)+f(y+z)+f(z-x) \tag{1.4}$$

and

$$\begin{aligned} f(x+y+z)+f(x+y-z)+f(x-y+z)+f(-x+y+z)& \\ =4f(x)+4f(y)+4f(z),& \end{aligned} \tag{1.5}$$

then each of the equations (1.3), (1.4)*, and* (1.5) *is equivalent to the other.*

Recently, EL-Fassi *et al.* [9] treated the Ulam-type stability of (1.2) in the class of functions from an Abelian group into a Banach space. The method used in [9, Theorem 4] based on a fixed point theorem [7, Theorem 1] and the argument presented is all on the whole set. This aspect of the domain is very important. However if we consider a subset of the domain which does not present all the possibilities when we have on the whole set, is the stability of the equation still valid? Many others studies this question about the stability on restricted domains of some functional equations (see [24, 22]).

Inspired by the works of Hyers [13], Brzdęk [8] and Park [17], and by a direct method, we investigate the stability of (1.2) on a restricted unbounded domain. Then, using these results, we study an asymptotic behavior of this functional equation. We also obtain a new criterion on characterization of inner product spaces by involving our functional equation. Before we state it, let us recall the definitions of quasi-norm and quasi-normed Abelian group.

We recall some basic facts concerning quasi-norm and quasi-normed Abelian group.

Definition 1.3. [4] Let $(G, +)$ be an Abelian group. A function $\rho: G \to \mathbb{R}$ is called a quasi-norm on G if:

1. $0 \leq \rho(x) \leq +\infty$ for all $x \in G$ (positive definite);
2. $\rho(x) = \rho(-x)$ for all $x \in G$ (even);
3. $\rho(x + y) \leq \rho(x) + \rho(y)$ for all $x, y \in G$ (subadditivity);
4. $\rho(0) = 0$.

If $\rho(x) < +\infty$ for all $x \in G$ we say that ρ is a finite quasi-norm. The pair (G, ρ) is called quasi-normed Abelian group if ρ is a quasi-norm on G.

A triplet $(G, +, \delta)$ is called metric Abelian group if $(G, +)$ is an Abelian group and δ is a translation invariant metric on G. This metric can be turned into a quasi-norm $\|.\|_\delta : G \to \mathbb{R}$, via $\|x\|_\delta = \delta(x, 0)$ and the pair $(G, \|.\|_\delta)$ is a quasi-normed Abelian group. For a more detailed definition of such terminology, one can refer to [10, 18].

In this paper, assume that $(G, +)$ be an Abelian group, Y be a linear space on the field $\mathbb{K} \in \{\mathbb{R}, \mathbb{C}\}$. For a given mapping $f: G \longrightarrow Y$, we define the function $\Delta_f: G \times G \times G \longrightarrow Y$ by

$$\begin{aligned}\Delta_f(x, y, z) := {} & f(x + y + z) + f(x + y - z) + f(x - y + z) \\ & + f(-x + y + z) - 4f(x) - 4f(y) - 4f(z), \quad x, y, z \in G.\end{aligned}$$

2 Stability in restricted domains

In this section we study the stability problem of the functional equation (1.2).

Theorem 2.1. *Let $(G,+,\delta)$ be a metric Abelian group, $\|.\|_\delta$ be the induced quasi-norm of δ and $(Y,\|.\|)$ be a Banach space. Let $\varepsilon \geq 0$, $d > 0$ be arbitrary real numbers. Suppose that $f : G \to Y$ is a function satisfies*

$$\|\Delta_f(x,y,z)\| \leq \varepsilon, \quad \|x+y+z\|_\delta \geq d. \tag{2.1}$$

Then, there exists a unique quadratic function $Q : G \to Y$ such that

$$\|Q(x) - f(x)\| \leq \frac{5\varepsilon}{8}, \qquad x \in G. \tag{2.2}$$

Proof. Let $f : G \to Y$ be a function fulfilling (2.1). Taking $x = y = z$ in (2.1), we get

$$\|f(3x) - 9f(x)\| \leq \varepsilon, \quad \|3x\|_\delta \geq d,$$

witch implies

$$\|f(3x) - 9f(x)\| \leq \varepsilon, \quad \|x\|_\delta \geq d.$$

Therefore,

$$\left\| \frac{f(3^{n+1}x)}{9^{n+1}} - \frac{f(3^m x)}{9^m} \right\| \leq \sum_{k=m}^{k=n} \frac{\varepsilon}{9^{k+1}}, \tag{2.3}$$

for all natural numbers ; $n \geq m$, and $\|x\|_\delta \geq d$. Therefore, $\left\{\frac{f(3^n x)}{9^n}\right\}_{n=0}^{\infty}$ is a Cauchy sequence for each $x \in G$ with $\|x\|_\delta \geq d$. It is easily to infer that the sequence $\left\{\frac{f(3^n x)}{9^n}\right\}_n$ is Cauchy in the whole G. As Y is Banach space, this Cauchy sequence is convergent. We define $Q : G \to Y$ by

$$Q(x) := \lim_{n\to+\infty} \frac{f(3^n x)}{9^n}, \quad x \in G. \tag{2.4}$$

For $x \in G \setminus \{0\}$, we choose $N \in \mathbb{N}$ so large that for all $n \geq N$, $\|3^n x\|_\delta \geq d$. By (2.4), we see that

$$\begin{aligned}\|\Delta_Q(x,y,z)\| = \lim_{n\to+\infty} \frac{1}{9^n} \Big\| & f(3^n x + 3^n y + 3^n z) + f(3^n x + 3^n y - 3^n z) \\ & + f(3^n x - 3^n y + 3^n z) + f(-3^n x + 3^n y + 3^n z) \\ & - 4[f(3^n x) + f(3^n y) + f(3^n z)] \Big\| \\ \leq & \lim_{n\to+\infty} \frac{\varepsilon}{9^n} = 0.\end{aligned}$$

Hence, Q fulfills equation (1.2) for all $x \in G \setminus \{0\}$.
Since

$$Q(0) = \lim_{n\to+\infty} \frac{f(0)}{9^n} = 0,$$

the function Q fulfills equation (1.2) for all $x \in G$. Since Q is a solution of (1.2), we infer that Q is a quadratic function in G.

Taking the limit as $n \to +\infty$ and putting $m = 0$, we get from (2.3)

$$\|Q(x) - f(x)\| \leq \frac{\varepsilon}{8}, \quad \|x\|_\delta \geq d. \tag{2.5}$$

Next, we extend (2.5) to the whole G. Let $z \in G$ and choose $\|x\|_\delta \geq \|z\|_\delta + d$ such that $\|y\|_\delta \geq \|z\|_\delta + d$ and $\|x+y\|_\delta \geq \|z\|_\delta + d$. Clearly, $\|x+y\|_\delta \geq d$, $\|x+z\|_\delta \geq d$ and $\|x+y+z\|_\delta \geq d$.Then by (2.5), we get

$$\begin{aligned}
&\|Q(x+y+z) - f(x+y+z)\| \leq \frac{\varepsilon}{8};\\
&\|Q(x+y-z) - f(x+y-z)\| \leq \frac{\varepsilon}{8};\\
&\|Q(x-y+z) - f(x-y+z)\| \leq \frac{\varepsilon}{8};\\
&\|Q(-x+y+z) - f(-x+y+z)\| \leq \frac{\varepsilon}{8};\\
&\|-4Q(x) + 4f(x)\| \leq \frac{4\varepsilon}{8};\\
&\|-4Q(y) + 4f(y)\| \leq \frac{4\varepsilon}{8}.
\end{aligned}$$

Adding these inequalities and applying (2.5) and (2.1), we get

$$\|4Q(z) - 4f(z)\| \leq \varepsilon + \frac{3\varepsilon}{2}.$$

Therefore

$$\|Q(z) - f(z)\| \leq \frac{5\varepsilon}{8},$$

for $z \in G$.

It remains to prove the uniqueness of Q. Assume that $Q' : G \to Y$ is another quadratic function that satisfies inequality (2.2). Then we have

$$\begin{aligned}
\|Q(x) - Q'(x)\| &\leq \|Q(x) - f(x)\| + \|Q'(x) - f(x)\|\\
&\leq \frac{5\varepsilon}{4}, \quad x \in G,
\end{aligned}$$

Since Q and Q' are quadratic, the last inequality implies that

$$\begin{aligned}
\|Q(x) - Q'(x)\| &= \frac{1}{9^n} \|Q(3^n x) - Q'(3^n x)\|\\
&\leq \frac{1}{9^n} \times \frac{5\varepsilon}{4}, \qquad x \in G, n \in \mathbb{N} \setminus \{0\}.
\end{aligned}$$

Taking the limit as $n \longrightarrow \infty$, we obtain $Q(x) = Q'(x)$ for all $x \in G$. This completes the proof. □

3 Asymptotic behavior of the equation

As a consequences, we can prove some corollaries concerning the asymptotic behaviors of the functional equation (1.2).

Corollary 3.1. *Let* $(G,+,\delta)$ *be a metric Abelian group,* $\|.\|_\delta$ *be the induced quasi-norm of* δ *and* $(Y,\|.\|)$ *be a normed space. If a mapping* $f : G \to Y$ *satisfies*

$$\limsup_{\|x+y+z\|_\delta \to +\infty} \Delta_f(x,y,z) = 0, \tag{3.1}$$

then f *is a quadratic function on* X*.*

Proof. Let $f : G \to Y$ be a mapping satisfies (3.1). Then, there exists a sequence $\{d_n\}_{n=1}^{\infty}$ of positive real numbers such that

$$\|\Delta_f(x,y,z)\| \le \frac{1}{n}, \quad \|x+y+z\|_\delta \ge d_n, \quad n > 1.$$

Let $\widetilde{Y}$ be the completion of Y. By Theorem 2.1, there exists a unique quadratic function $Q_n : G \to \widetilde{Y}$ solution of (1.2) and such that

$$\|Q_n(x) - f(x)\| \le \frac{5}{8n}, \quad x \in G, \quad n > 1. \tag{3.2}$$

Let l and m be integers satisfying $m > l > 0$. From (3.2) we obtain

$$\|Q_m(x) - f(x)\| \le \frac{5}{8m} \le \frac{5}{8l}, \quad x \in G.$$

Hence, the uniqueness of Q_n implies that $Q_l = Q_m$ holds for any $l, m \in \mathbb{N}$. Taking the limit as $n \longrightarrow \infty$ in (3.2), we infer that f is quadratic. Then the result follows. $\square$

Using Theorem 2.1, we obtain the results.

Corollary 3.2. *Let* $(G,+,\delta)$ *be a metric Abelian group,* $\|.\|_\delta$ *be the induced quasi-norm of* δ *and* $(Y,\|.\|)$ *be a Banach space. Let* $\psi: G\times G\times G \to [0,+\infty)$*. If a mapping* $f : G \to Y$ *satisfies*

$$\begin{cases} \lim\limits_{\|x+y+z\|_\delta \to +\infty} \psi(x,y,z) = +\infty; \\ \limsup\limits_{\|x+y+z\|_\delta \to +\infty} \psi(x,y,z)\,\|\Delta_f(x,y,z)\| < \infty, \end{cases} \tag{3.3}$$

then f *is a quadratic function on* G*.*

Proof. It follows from (3.3) that there exist constants $s > 0$ and R such that

$$\psi(x,y,z)\,\|\Delta_f(x,y,z)\| < R, \quad \|x+y+z\|_\delta \ge s.$$

Since $\lim_{\|x+y+z\|_\delta \to +\infty} \psi(x,y,z) = +\infty$, then for an arbitrary $\varepsilon > 0$ there is $M > 0$ such that

$$\psi(x,y,z) \geq \frac{R}{\varepsilon}, \quad \|x+y+z\|_\delta \geq M.$$

Then,

$$\|\Delta_f(x,y,z)\| < \varepsilon, \quad \|x+y+z\|_\delta \geq \max\{s, M\}.$$

Let $\widetilde{Y}$ be the completion of Y. Using theorem 2.1, there exists a unique quadratic function $Q : G \to Y$ solution of (1.2) and such that

$$\|Q(x) - f(x)\| \leq \frac{5\varepsilon}{8}, \quad x \in G.$$

Since ε is arbitrary, we infer that $Q(x) = f(x)$ for all $x \in G$. □

Corollary 3.3. *Let $(G, +, \delta)$ be a metric Abelian group, $\|.\|_\delta$ be the induced quasi-norm of δ and $(Y, \|.\|)$ be a Banach space. Let $p < 0$ and $\lambda > 0$ be arbitrary real numbers. If a mapping $f : G \to Y$ satisfies*

$$\|\Delta_f(x,y,z)\| \leq \lambda \|x+y+z\|_\delta^p, \quad x, y, z \in G \setminus \{0\}.$$

Then f is a quadratic function on $G \setminus \{0\}$.

4 Application

Several functional equations were used to characterize inner product spaces from normed spaces, for instance, see [14, 2, 6, 3, 16]. Quadratic functional equation was used to characterize inner product spaces by making use the parallelogram equality [14]:

$$\|x+y\|^2 + \|x-y\|^2 = 2\|x\|^2 + 2\|y\|^2.$$

This characterization gave rise to what we now call Jordan-von Neumann characterization. Other characterization is given by Fréchet in [11], he proved that a normed space $(X, \|.\|)$ is an inner product space if and only if

$$\|x+y+z\|^2 + \|x\|^2 + \|y\|^2 + \|z\|^2 = \|x+y\|^2 + \|x+z\|^2 + \|y+z\|^2, \quad x, y, z \in X.$$

Now, we can apply the functional equation (1.2) in a characterizations of inner product spaces.

Let $\mathbb{K}$ be the field of real or complex numbers. Let $(X, \|.\|)$ be a normed space over $\mathbb{K}$ and $X_0 := X \setminus \{0\}$. Write

$$D(x,y,z) = \|x+y+z\|^2 + \|x+y-z\|^2 + \|x-y+z\|^2 + \|-x+y+z\|^2 - 4\|x\|^2 - 4\|y\|^2 - 4\|z\|^2.$$

Theorem 4.1. *Let* $(X, \|.\|)$ *be a normed space over* $\mathbb{K}$. *Suppose that*

$$D(x, y, z) = 0, \quad x, y, z \in X.$$

Then X *is an inner product space.*

Proof. Let $X \neq \{0\}$ be a normed space over $\mathbb{K}$ such that

$$\|x+y+z\|^2 + \|x+y-z\|^2 + \|x-y+z\|^2 + \|-x+y+z\|^2 \\ - 4\|x\|^2 - 4\|y\|^2 - 4\|z\|^2 = 0, \quad (4.1)$$

for $x, y, z \in X$. Putting $z = 0$ in (4.1), we get

$$\|x+y\|^2 + \|x+y\|^2 + \|x-y\|^2 + \|-x+y\|^2 \; - 4\|x\|^2 - 4\|y\|^2 = 0,$$

for $x, y \in X$, then the Jordan-von Neumann characterization holds

$$\|x+y\|^2 + \|x-y\|^2 = 2\|x\|^2 + 2\|y\|^2 .$$

Consequently, X is an inner product space. □

Theorem 4.2. *Let* $(X, \|.\|)$ *be a normed space over* $\mathbb{K}$. *Suppose that*

$$\sup_{x,y,z\in X} \frac{|D(x,y,z)|}{\lambda \|x+y+z\|^p} < \infty, \quad x+y+z \in X_0, \quad p < 0, \quad \lambda > 0.$$

Then X *is an inner product space.*

Proof. Write $f(x) = \|x\|$ for $x \in X$. From Corollary 3.3 we easily derive that f is a quadratic function, which yields the statement. □

References

[1] M. Akkouchi, Generalized Ulam-Hyers-Rassias stability of a Cauchy type functional equation, *Proyecciones Journal of Mathematics.* 32(1), 15–29(2013).

[2] C. Alsina , P. Cruells, and M. S. Tomás, Characterizations of inner product spaces through an isosceles trapezoid property, *Archivum Mathematicum.* 35(1), 21–27(1999).

[3] D. Amir, *Characterizations of inner product spaces*, Operator theory: Advances and applications, 20, Birkhäuser Verlag, Besel, 1986.

[4] P. Antosik and C. Swartz, The Schur and Phillips lemmas for topological groups, *Journal of mathematical analysis and applications.* 98(1), 179–187(1984).

[5] T. Aoki, On the stability of the linear transformation in Banach spaces, *Journal of the mathematical society of Japan.* 2(1-2), 64–66(1950).

[6] A. Bahyrycz, J. Brzdęk, M. Piszczek, and J. Sikorska, Hyperstability of the Fréchet equation and a characterization of inner product spaces, *Journal of Function Spaces and Applications*. 2013, 01–06(2013).

[7] J. Brzdęk, J. Chudziak, and Z. Páles, A fixed point approach to stability of functional equations, *Nonlinear analysis: theory, methods & applications*. 74(17), 6728–6732(2011).

[8] J. Brzdęk, Z. Leśniak, and R. Malejki, On the stability of a generalized Fréchet functional equation with respect to hyperplanes in the parameter space, *Symmetry*. 13(3), (2013): 384.

[9] I.-i. El-Fassi, C. Park, and G. H. Kim, Stability and hyperstability of a quadratic functional equation and a characterization of inner product spaces, *Demonstratio Mathematica*. 51(1), 295–303(2018).

[10] W. Fechner and Z. Páles, Convexity of sets in metric Abelian groups, in *Forum Mathematicum*, De Gruyter, 2020, pp.1477–1486.

[11] M. Fréchet, Sur la définition axiomatique d'une classe d'espaces vectoriels distanciés applicables vectoriellement sur l'espace de Hilbert, *Annals of Mathematics*. 36(3), 705–718(1935).

[12] P. Găvruţa, A generalization of the Hyers-Ulam-Rassias stability of approximately additive mappings, *Journal of Mathematical Analysis and Applications*. 184(3), 431–436(1994).

[13] D. H. Hyers, On the stability of the linear functional equation, *Proceedings of the National Academy of Sciences of the United States of America*. 27(4), 222–224(1941).

[14] P. Jordan and J. v. Neumann, On inner products in linear, metric spaces, *Annals of Mathematics*. 36(3), 719–723(1935).

[15] S.-M. Jung, Quadratic functional equations of Pexider type, *International Journal of Mathematics and Mathematical Sciences*. 24(5), 351–359(2000).

[16] M. S. Moslehian and J. M. Rassias, A characterization of inner product spaces concerning an Euler-Lagrange identity, *Communications in Mathematical Analysis*. 8(2), 16–21(2010).

[17] C. Park, A. Najati, B. Noori, and M. B. Moghimi, Additive and Fréchet functional equations on restricted domains with some characterizations of inner product spaces, *AIMS Mathematics*. 7(3), 3379–3394(2021).

[18] J. Peetre and G. Sparr, Interpolation of normed Abelian groups, *Annali di Matematica Pura ed Applicata*. 92(1), 217–262(1972).

[19] T. M. Rassias, On the stability of the linear mapping in Banach spaces, *Proceedings of the American mathematical society*. 72(2), 297–300(1978).

[20] T. M. Rassias and K. Shibata, Variational problem of some quadratic functionals in complex analysis, *Journal of Mathematical Analysis and Applications.* 228(1), pp–pp(1998).

[21] T. M. Rassias and P. Šemrl, On the Hyers-Ulam stability of linear mappings, *Journal of Mathematical Analysis and Applications.* 173(2), 325–338(1993).

[22] J. Senasukh and S. Saejung, On the hyperstability of the Drygas functional equation on a restricted domain, *Bulletin of the Australian Mathematical Society.* 102(1), 126–137(2020).

[23] M. Sirouni and S. Kabbaj, A fixed point approach to the hyperstability of Drygas functional equation in metric spaces, *Journal of Mathematical and Computational Science.* 4(4), 705–715(2014).

[24] M. A. Tareeghee, A. Najati, B. Noori, and C. Park, Asymptotic behavior of a generalized functional equation, *AIMS Mathematics.* 7(4), 7001–7011(2022).

[25] S. M. Ulam, *A Collection of Mathematical Problems*, Interscience Publishers, New York, 1960.

TABLE OF CONTENTS, JOURNAL OF COMPUTATIONAL ANALYSIS AND APPLICATIONS, VOL. 31, NO. 3, 2023

Generalization of Interval Jacobi and Gauss-Seidel Methods for Interval Linear System, Jahnabi Chakravarty and Manideepa Saha,……..345

Extended Jacobi Elliptic Function Technique: A Tool for Solving Nonlinear Wave Equations with emblematic Software, Ram Dayal Pankaj,………………………………………………366

Laplace Variational Iteration Method for Solving fractional Wave like Equations, Deepika Jain and Alok Bhargava,………………………………………………………………………377

Boros Integral Involving the Product of Family of Polynomials and the Incomplete I-Function, Sanjay Bhatter, Nishant, Daya Lal Suthar, and Sunil Dutt Purohit,……………………………400

Two-State Retrial Queueing Model with Catastrophe, Neelam Singla and Ankita Garg,……..413

Managing Tourism in North East India using Fuzzy Linear Programming, Prabjot Kaur, Mahuya Deb, and Arya Shankar,…………………………………………………………………..430

A homotopy based computational scheme for local fractional Helmholtz and Laplace equations, Jagdev Singh, Ritin Babu, Ved Prakash Dubey, and Devendra Kumar,……………………….444

On asymptotic behavior of a quadratic functional equation, Mohamed Sirouni, Muaadh Almahalebi, and Samir Kabbaj,…………………………………………………...……458

Volume 31, Number 4 December, 2023
ISSN:1521-1398 PRINT,1572-9206 ONLINE

Journal of Computational Analysis and Applications

EUDOXUS PRESS,LLC

Journal of Computational Analysis and Applications
ISSNno.'s:1521-1398 PRINT,1572-9206 ONLINE

SCOPE OF THE JOURNAL

An international publication of Eudoxus Press, LLC
(published quarterly) www.eudoxuspress.com.

Editor in Chief: George Anastassiou
Department of Mathematical Sciences,
University of Memphis, Memphis, TN 38152-3240, U.S.A
ganastss@memphis.edu, ganastss2@gmail.com
http://web0.msci.memphis.edu/~ganastss/jocaaa/

The main purpose of "J.Computational Analysis and Applications" is to publish high quality research articles from all subareas of Computational Mathematical Analysis and its many potential applications and connections to other areas of Mathematical Sciences. Any paper whose approach and proofs are computational,using methods from Mathematical Analysis in the broadest sense is suitable and welcome for consideration in our journal, except from Applied Numerical Analysis articles. Also plain word articles without formulas and proofs are excluded. The list of possibly connected mathematical areas with this publication includes, but is not restricted to: Applied Analysis, Applied Functional Analysis, Approximation Theory, Asymptotic Analysis, Difference Equations, Differential Equations, Partial Differential Equations, Fourier Analysis, Fractals, Fuzzy Sets, Harmonic Analysis, Inequalities, Integral Equations, Measure Theory, Moment Theory, Neural Networks, Numerical Functional Analysis, Potential Theory, Probability Theory, Real and Complex Analysis, Signal Analysis, Special Functions, Splines, Stochastic Analysis, Stochastic Processes, Summability, Tomography, Wavelets, any combination of the above, e.t.c.

"J.Computational Analysis and Applications" is a peer-reviewed Journal. See the instructions for preparation and submission **of articles to JOCAAA.**

Journal of Computational Analysis and Applications(JoCAAA) is published by **EUDOXUS PRESS,LLC**,1424 Beaver Trail Drive,Cordova,TN38016,USA,anastassioug@yahoo.com http://www.eudoxuspress.com. **Annual Subscription Prices**:For USA and Canada,Institutional:Print $500, Electronic OPEN ACCESS. Individual:Print $250. For any other part of the world add $150 more(handling and postages) to the above prices for Print. No credit card payments.

Copyright©2023 by Eudoxus Press,LLC,all rights reserved.JoCAAA is printed in USA.

JoCAAA is reviewed and abstracted by Elsevier-Scopus, available also via EBSCO publishing and EBSCO.

It is strictly prohibited the reproduction and transmission of any part of JoCAAA and in any form and by any means without the written permission of the publisher.It is only allowed to educators to Xerox articles for educational purposes.The publisher assumes no responsibility for the content of published papers.

Editorial Board

Associate Editors of Journal of Computational Analysis and Applications

Francesco Altomare
Dipartimento di Matematica
Universita' di Bari
Via E.Orabona, 4
70125 Bari, ITALY
Tel+39-080-5442690 office
+39-080-3944046 home
+39-080-5963612 Fax
altomare@dm.uniba.it
Approximation Theory, Functional Analysis, Semigroups and Partial Differential Equations, Positive Operators.

Ravi P. Agarwal
Department of Mathematics
Texas A&M University - Kingsville
700 University Blvd.
Kingsville, TX 78363-8202
tel: 361-593-2600
Agarwal@tamuk.edu
Differential Equations, Difference Equations, Inequalities

George A. Anastassiou
Department of Mathematical Sciences
The University of Memphis
Memphis, TN 38152,U.S.A
Tel.901-678-3144
e-mail: ganastss@memphis.edu
Approximation Theory, Real Analysis,
Wavelets, Neural Networks, Probability, Inequalities.

J. Marshall Ash
Department of Mathematics
De Paul University
2219 North Kenmore Ave.
Chicago, IL 60614-3504
773-325-4216
e-mail: mash@math.depaul.edu
Real and Harmonic Analysis

Dumitru Baleanu
Department of Mathematics and Computer Sciences,
Cankaya University, Faculty of Art and Sciences,
06530 Balgat, Ankara,
Turkey, dumitru@cankaya.edu.tr
Fractional Differential Equations
Nonlinear Analysis, Fractional Dynamics

Carlo Bardaro
Dipartimento di Matematica e Informatica
Universita di Perugia
Via Vanvitelli 1
06123 Perugia, ITALY
TEL+390755853822
+390755855034
FAX+390755855024
E-mail carlo.bardaro@unipg.it
Web site:
http://www.unipg.it/~bardaro/
Functional Analysis and Approximation Theory, Signal Analysis, Measure Theory, Real Analysis.

Martin Bohner
Department of Mathematics and Statistics, Missouri S&T
Rolla, MO 65409-0020, USA
bohner@mst.edu
web.mst.edu/~bohner
Difference equations, differential equations, dynamic equations on time scale, applications in economics, finance, biology.

Jerry L. Bona
Department of Mathematics
The University of Illinois at Chicago
851 S. Morgan St. CS 249
Chicago, IL 60601
e-mail:bona@math.uic.edu
Partial Differential Equations, Fluid Dynamics

Luis A. Caffarelli
Department of Mathematics
The University of Texas at Austin
Austin, Texas 78712-1082
512-471-3160
e-mail: caffarel@math.utexas.edu
Partial Differential Equations

George Cybenko
Thayer School of Engineering
Dartmouth College
8000 Cummings Hall,
Hanover, NH 03755-8000
603-646-3843 (X 3546 Secr.)
e-mail:george.cybenko@dartmouth.edu
Approximation Theory and Neural Networks

Sever S. Dragomir
School of Computer Science and Mathematics, Victoria University,
PO Box 14428,
Melbourne City,
MC 8001, AUSTRALIA
Tel. +61 3 9688 4437
Fax +61 3 9688 4050
e-mail: sever.dragomir@vu.edu.au
Inequalities, Functional Analysis, Numerical Analysis, Approximations, Information Theory, Stochastics.

Oktay Duman
TOBB University of Economics and Technology,
Department of Mathematics, TR-06530, Ankara, Turkey,
e-mail: oduman@etu.edu.tr
Classical Approximation Theory, Summability Theory, Statistical Convergence and its Applications

J .A. Goldstein
Department of Mathematical Sciences
The University of Memphis
Memphis, TN 38152
901-678-3130
e-mail: jgoldste@memphis.edu
Partial Differential Equations, Semigroups of Operators

H. H. Gonska
Department of Mathematics
University of Duisburg
Duisburg, D-47048
Germany
011-49-203-379-3542
e-mail: heiner.gonska@uni-due.de
Approximation Theory, Computer Aided Geometric Design

John R. Graef
Department of Mathematics
University of Tennessee at Chattanooga
Chattanooga, TN 37304 USA
e-mail: John-Graef@utc.edu
Ordinary and functional differential equations, difference equations, impulsive systems, differential inclusions, dynamic equations on time scales, control theory and their applications

Weimin Han
Department of Mathematics
University of Iowa
Iowa City, IA 52242-1419
319-335-0770
e-mail: whan@math.uiowa.edu
Numerical analysis, Finite element method, Numerical PDE, Variational inequalities, Computational mechanics

Tian-Xiao He
Department of Mathematics and Computer Science
P.O. Box 2900, Illinois Wesleyan University
Bloomington, IL 61702-2900, USA
Tel (309)556-3089
Fax (309)556-3864
e-mail: the@iwu.edu
Approximations, Wavelet, Integration Theory, Numerical Analysis, Analytic Combinatorics

Margareta Heilmann
Faculty of Mathematics and Natural Sciences, University of Wuppertal
Gaußstraße 20
D-42119 Wuppertal, Germany,
heilmann@math.uni-wuppertal.de
Approximation Theory (Positive Linear Operators)

Xing-Biao Hu
Institute of Computational Mathematics
AMSS, Chinese Academy of Sciences
Beijing, 100190, CHINA
e-mail: hxb@lsec.cc.ac.cn
Computational Mathematics

Seda Karateke
Department of Computer Engineering,
Faculty of Engineering,
Istanbul Topkapi University,
Istanbul, Zeytinburnu 34087, Turkey
e-mail: sedakarateke@topkapi.edu.tr
Approximation Theory, Neural Networks

Jong Kyu Kim
Department of Mathematics
Kyungnam University
Masan Kyungnam,631-701,Korea
Tel 82-(55)-249-2211
Fax 82-(55)-243-8609
e-mail: jongkyuk@kyungnam.ac.kr
Nonlinear Functional Analysis,
Variational Inequalities, Nonlinear
Ergodic Theory, ODE, PDE,
Functional Equations.

Robert Kozma
Department of Mathematical Sciences
The University of Memphis
Memphis, TN 38152, USA
e-mail: rkozma@memphis.edu
Neural Networks, Reproducing Kernel
Hilbert Spaces,
Neural Percolation Theory

Mustafa Kulenovic
Department of Mathematics
University of Rhode Island
Kingston, RI 02881, USA
e-mail: kulenm@math.uri.edu
Differential and Difference
Equations

Burkhard Lenze
Fachbereich Informatik
Fachhochschule Dortmund
University of Applied Sciences
Postfach 105018
D-44047 Dortmund, Germany
e-mail: lenze@fh-dortmund.de
Real Networks, Fourier Analysis,
Approximation Theory

Alina Alb Lupas
Department of Mathematics and
Computer Science
Faculty of Informatics
University of Oradea
2 Universitatii Street,
410087 Oradea, Romania
e-mail: alblupas@gmail.com
e-mail: dalb@uoradea.ro
Complex Analysis, Topological
Algebra, Mathematical Analysis

Razvan A. Mezei
Computer Science Department
Hal and Inge Marcus School of
Engineering
Saint Martin’s University
Lacey, WA 98503, USA
e-mail: RMezei@stmartin.edu
Numerical Approximation, Fractional
Inequalities.

Hrushikesh N. Mhaskar
Department Of Mathematics
California State University
Los Angeles, CA 90032
626-914-7002
e-mail: hmhaska@gmail.com
Orthogonal Polynomials,
Approximation Theory, Splines,
Wavelets, Neural Networks

Ram N. Mohapatra
Department of Mathematics
University of Central Florida
Orlando, FL 32816-1364
tel.407-823-5080
e-mail: ram.mohapatra@ucf.edu
Real and Complex Analysis,
Approximation Th., Fourier
Analysis, Fuzzy Sets and Systems

Gaston M. N'Guerekata
Department of Mathematics
Morgan State University
Baltimore, MD 21251, USA
tel: 1-443-885-4373
Fax 1-443-885-8216
Gaston.N'Guerekata@morgan.edu
nguerekata@aol.com
Nonlinear Evolution Equations,
Abstract Harmonic Analysis,
Fractional Differential Equations,
Almost Periodicity & Almost
Automorphy

M.Zuhair Nashed
Department Of Mathematics
University of Central Florida
PO Box 161364
Orlando, FL 32816-1364
e-mail: znashed@mail.ucf.edu
Inverse and Ill-Posed problems,
Numerical Functional Analysis,
Integral Equations, Optimization,
Signal Analysis

Mubenga N. Nkashama
Department OF Mathematics
University of Alabama at Birmingham
Birmingham, AL 35294-1170
205-934-2154
e-mail: nkashama@math.uab.edu
Ordinary Differential Equations,
Partial Differential Equations

Vassilis Papanicolaou
Department of Mathematics
National Technical University of Athens
Zografou campus, 157 80
Athens, Greece
tel: +30(210) 772 1722
Fax   +30(210) 772 1775
e-mail: papanico@math.ntua.gr
Partial Differential Equations,
Probability

Choonkil Park
Department of Mathematics
Hanyang University
Seoul 133-791
S. Korea,
e-mail: baak@hanyang.ac.kr
Functional Equations

Svetlozar (Zari) Rachev,
Professor of Finance, College of
Business, and Director of
Quantitative Finance Program,
Department of Applied Mathematics &
Statistics
Stonybrook University
312 Harriman Hall, Stony Brook, NY
11794-3775
tel: +1-631-632-1998,
svetlozar.rachev@stonybrook.edu

Alexander G. Ramm
Mathematics Department
Kansas State University
Manhattan, KS 66506-2602
e-mail: ramm@math.ksu.edu
Inverse and Ill-posed Problems,
Scattering Theory, Operator Theory,
Theoretical Numerical Analysis,
Wave Propagation, Signal Processing
and Tomography

Tomasz Rychlik
Polish Academy of Sciences
Instytut Matematyczny PAN
00-956 Warszawa, skr. poczt. 21
ul. Śniadeckich 8
Poland
e-mail: trychlik@impan.pl
Mathematical Statistics,
Probabilistic Inequalities

Boris Shekhtman
Department of Mathematics
University of South Florida
Tampa, FL 33620, USA
Tel 813-974-9710
e-mail: shekhtma@usf.edu
Approximation Theory, Banach
spaces, Classical Analysis

T. E. Simos
Department of Computer
Science and Technology
Faculty of Sciences and Technology
University of Peloponnese
GR-221 00 Tripolis, Greece
Postal Address:
26 Menelaou St.
Anfithea - Paleon Faliron
GR-175 64 Athens, Greece
e-mail: tsimos@mail.ariadne-t.gr
Numerical Analysis

Jagdev Singh
JECRC University, Jaipur, India
jagdevsinghrathore@gmail.com
Fractional Calculus, Mathematical
Modelling, Special Functions,
Numerical Methods

H. M. Srivastava
Department of Mathematics and
Statistics
University of Victoria
Victoria, British Columbia V8W 3R4
Canada
tel.250-472-5313; office,250-477-
6960 home, fax 250-721-8962
e-mail: harimsri@math.uvic.ca
Real and Complex Analysis,
Fractional Calculus and Appl.,
Integral Equations and Transforms,
Higher Transcendental Functions and
Appl.,q-Series and q-Polynomials,
Analytic Number Th.

I. P. Stavroulakis
Department of Mathematics
University of Ioannina
451-10 Ioannina, Greece
e-mail: ipstav@cc.uoi.gr
Differential Equations
Phone +3-065-109-8283

Jessada Tariboon
Department of Mathematics
King Mongut's University of
Technology N. Bangkok
1518 Pracharat 1 Rd., Wongsawang,
Bangsue, Bangkok, Thailand 10800
e-mail: jessada.t@sci.kmutnb.ac.th
Time scales

Differential/Difference Equations, Fractional Differential Equations

Manfred Tasche
Department of Mathematics
University of Rostock
D-18051 Rostock, Germany
manfred.tasche@mathematik.uni-rostock.de
Numerical Fourier Analysis, Fourier Analysis, Harmonic Analysis, Signal Analysis, Spectral Methods, Wavelets, Splines, Approximation Theory

Juan J. Trujillo
University of La Laguna
Departamento de Analisis Matematico
C/Astr.Fco.Sanchez s/n
38271. LaLaguna. Tenerife.
SPAIN
Tel/Fax 34-922-318209
e-mail: Juan.Trujillo@ull.es
Fractional: Differential Equations-Operators-Fourier Transforms, Special functions, Approximations, and Applications

Xiao-Jun Yang
State Key Laboratory for Geomechanics and Deep Underground Engineering, China
University of Mining and Technology, Xuzhou 221116, China
Local Fractional Calculus and Applications, Fractional Calculus and Applications, General Fractional Calculus and Applications, Variable-order Calculus and Applications, Viscoelasticity and Computational methods for Mathematical Physics.dyangxiaojun@163.com

Xiang Ming Yu
Department of Mathematical Sciences
Southwest Missouri State University
Springfield, MO 65804-0094
417-836-5931
e-mail: xmy944f@missouristate.edu
Classical Approximation Theory, Wavelets

Richard A. Zalik
Department of Mathematics
Auburn University
Auburn University, AL 36849-5310
USA.
Tel 334-844-6557 office
Fax 334-844-6555
e-mail: zalik@auburn.edu
Approximation Theory, Chebychev Systems, Wavelet Theory

Ahmed I. Zayed
Department of Mathematical Sciences
DePaul University
2320 N. Kenmore Ave.
Chicago, IL 60614-3250
773-325-7808
e-mail: azayed@condor.depaul.edu
Shannon sampling theory, Harmonic analysis and wavelets, Special functions and orthogonal polynomials, Integral transforms

Ding-Xuan Zhou
Department Of Mathematics
City University of Hong Kong
83 Tat Chee Avenue
Kowloon, Hong Kong
852-2788 9708,Fax:852-2788 8561
e-mail: mazhou@cityu.edu.hk
Approximation Theory, Spline functions, Wavelets

Xin-long Zhou
Fachbereich Mathematik, Fachgebiet Informatik
Gerhard-Mercator-Universitat Duisburg
Lotharstr.65, D-47048 Duisburg, Germany
e-mail:Xzhou@informatik.uni-duisburg.de
Fourier Analysis, Computer-Aided Geometric Design, Computational Complexity, Multivariate Approximation Theory, Approximation and Interpolation Theory

Instructions to Contributors
Journal of Computational Analysis and Applications

An international publication of Eudoxus Press, LLC, of TN.

Editor in Chief: George Anastassiou

Department of Mathematical Sciences
University of Memphis
Memphis, TN 38152-3240, U.S.A.

1. Manuscripts files in Latex and PDF and in English, should be submitted via email to the Editor-in-Chief:

Prof.George A. Anastassiou
Department of Mathematical Sciences
The University of Memphis
Memphis,TN 38152, USA.
Tel. 901.678.3144
e-mail: ganastss@memphis.edu

Authors may want to recommend an associate editor the most related to the submission to possibly handle it.

Also authors may want to submit a list of six possible referees, to be used in case we cannot find related referees by ourselves.

2. Manuscripts should be typed using any of TEX,LaTEX,AMS-TEX,or AMS-LaTEX and according to EUDOXUS PRESS, LLC. LATEX STYLE FILE. (Click HERE to save a copy of the style file.)They should be carefully prepared in all respects. Submitted articles should be brightly typed (not dot-matrix), double spaced, in ten point type size and in 8(1/2)x11 inch area per page. Manuscripts should have generous margins on all sides and should not exceed 24 pages.

3. Submission is a representation that the manuscript has not been published previously in this or any other similar form and is not currently under consideration for publication elsewhere. A statement transferring from the authors(or their employers,if they hold the copyright) to Eudoxus Press, LLC, will be required before the manuscript can be accepted for publication.The Editor-in-Chief will supply the necessary forms for this transfer.Such a written transfer of copyright,which previously was assumed to be implicit in the act of submitting a manuscript,is necessary under the U.S.Copyright Law in order for the publisher to carry through the dissemination of research results and reviews as widely and effective as possible.

4. The paper starts with the title of the article, author's name(s) (no titles or degrees), author's affiliation(s) and e-mail addresses. The affiliation should comprise the department, institution (usually university or company), city, state (and/or nation) and mail code.

The following items, 5 and 6, should be on page no. 1 of the paper.

5. An abstract is to be provided, preferably no longer than 150 words.

6. A list of 5 key words is to be provided directly below the abstract. Key words should express the precise content of the manuscript, as they are used for indexing purposes.

The main body of the paper should begin on page no. 1, if possible.

7. All sections should be numbered with Arabic numerals (such as: 1. INTRODUCTION) .
Subsections should be identified with section and subsection numbers (such as 6.1. Second-Value Subheading).
If applicable, an independent single-number system (one for each category) should be used to label all theorems, lemmas, propositions, corollaries, definitions, remarks, examples, etc. The label (such as Lemma 7) should be typed with paragraph indentation, followed by a period and the lemma itself.

8. Mathematical notation must be typeset. Equations should be numbered consecutively with Arabic numerals in parentheses placed flush right, and should be thusly referred to in the text [such as Eqs.(2) and (5)]. The running title must be placed at the top of even numbered pages and the first author's name, et al., must be placed at the top of the odd numbed pages.

9. Illustrations (photographs, drawings, diagrams, and charts) are to be numbered in one consecutive series of Arabic numerals. The captions for illustrations should be typed double space. All illustrations, charts, tables, etc., must be embedded in the body of the manuscript in proper, final, print position. In particular, manuscript, source, and PDF file version must be at camera ready stage for publication or they cannot be considered.

Tables are to be numbered (with Roman numerals) and referred to by number in the text. Center the title above the table, and type explanatory footnotes (indicated by superscript lowercase letters) below the table.

10. List references alphabetically at the end of the paper and number them consecutively. Each must be cited in the text by the appropriate Arabic numeral in square brackets on the baseline.
References should include (in the following order):
initials of first and middle name, last name of author(s)
title of article,

name of publication, volume number, inclusive pages, and year of publication.

Authors should follow these examples:

Journal Article

1. H.H.Gonska,Degree of simultaneous approximation of bivariate functions by Gordon operators, (journal name in italics) *J. Approx. Theory*, 62,170-191(1990).

Book

2. G.G.Lorentz, (title of book in italics) *Bernstein Polynomials* (2nd ed.), Chelsea,New York,1986.

Contribution to a Book

3. M.K.Khan, Approximation properties of beta operators,in(title of book in italics) *Progress in Approximation Theory* (P.Nevai and A.Pinkus,eds.), Academic Press, New York,1991,pp.483-495.

11. All acknowledgements (including those for a grant and financial support) should occur in one paragraph that directly precedes the References section.

12. Footnotes should be avoided. When their use is absolutely necessary, footnotes should be numbered consecutively using Arabic numerals and should be typed at the bottom of the page to which they refer. Place a line above the footnote, so that it is set off from the text. Use the appropriate superscript numeral for citation in the text.

13. After each revision is made please again submit via email Latex and PDF files of the revised manuscript, including the final one.

14. Effective 1 Nov. 2009 for current journal page charges, contact the Editor in Chief. Upon acceptance of the paper an invoice will be sent to the contact author. The fee payment will be due one month from the invoice date. The article will proceed to publication only after the fee is paid. The charges are to be sent, by money order or certified check, in US dollars, payable to Eudoxus Press, LLC, to the address shown on the Eudoxus homepage.

No galleys will be sent and the contact author will receive one (1) electronic copy of the journal issue in which the article appears.

15. This journal will consider for publication only papers that contain proofs for their listed results.

J. COMPUTATIONAL ANALYSIS AND APPLICATIONS, VOL. 31, NO. 4, 2023, COPYRIGHT 2023 EUDOXUS PRESS, LLC

Numerical Solutions of Fuzzy Two Coupled Nonlinear Differential Equations

K. Chellapriya[1,*] , M. M. Shanmugapriya[1]
[1,1*] Department of Mathematics,
Karpagam Academy of Higher Education,
Coimbatore,
Tamilnadu, India.
chellapriyavalliappan@gmail.com shanmugapriya.mm@kahedu.edu.in

December 26, 2022

Abstract

In this manuscript, we will use the new modified version of the Runge-Kutta method suitable for solving fuzzy two coupled systems of Nonlinear Ordinary Differential Equations (ODE). With the aid of a numerical example, we will demonstrate the accuracy of the $RK-4$ coupled method for solving these two coupled differential equations. To find the analytical solutions we use Laplace Adomian Decomposition Method since it is a semianalytical method used well in many existing studies on dynamical systems. In order to tell the accuracy, we use the error analysis technique. With the help of numerical simulations, we are able to show at what point of t, both $x(t)$ and $y(t)$ will interact in order to support the theory.

Keywords: New theory of Numerical methods; Analytical Solution; Laplace Adomian Decomposition method; Runge-Kutta method; Two Coupled Differential Equations.

1 Introduction

The equivalence relations to a set of the non-crisp data set called fuzzy sets or fuzzy data set obtained by partisioning the existing relation that will not fail to satisfy the oprations satisfied by the crisp data set. The subsequent of differentiation as well as integration of fuzzy defined equations, and the ever existing theorems on existence and with it the uniqueness of FDE solutions in those space of quotients of fuzzy numbers are presented by various existing studies. The unique solution to the FDE's IVP will be well established if fuzzy normed f satisfies Lipschitz condition.

Many recent studies also developed the fuzzy methods and they have been implemented in so many grounds, such as optimization of multi-objective problems with various decision criteria. The development of mathematics has reached a very high level and is still available today.

The need of RK-4 method was very first arisen at the time of Euler methods to solve ODE numerically. Since it was clearly found very first time by the mathematicians Runge-Kutta, that the convergence of Euler method is only about $O(h^2)$ and error existence affects the coincidense of approximate solutions obtained by Euler with that of Exact solutions. $O(h^2)$ is not a good approximation order. So RK-4 methood was developed and found with $O(h^4)$ which provides the confidence of least error and better approximation that coincdes to atleast four decimal places i.e., $O(h^4)$ for solving linear ode. It also helped the researchers to get the better approximate solutions to that of few non-linear problems like non-linear hybrid differential equations. But for two coupled system of differential equations there are still a research going on many fields like mathematical modelling in poplation dynamics, epidemiology etc.,

There are few noticable works are done on nonlinear epidemic modells and RK-4 methods have also been used but it is also to be mentioned that those modells are not completely three coupled differential equations. After this modell has been developed and if got published we hope strongely that it could be applied to get the solutions of three ccoupled or four coupled DE on the epidemic modells epidemic models. Also, The entire manuscript is brought up by the motivation of well established researches and some of the notable works are Allen, [1] gave his way of introduction mathematical biology. Abbasbandy extended a numerical method called Newtons method to deal with the nonlinear system of equations using modified Adomian Decomposition Method (ADM) in [2]. In [3] Bukley et al., researched on fuzzy differential equations (FDEs). Kermack et al., [4] mathematically analyzed theory of epidemics. Makinde et al., [5] applied ADM to a SIR epidemic model with uniform vaccination therapy. Farman [10] presented solution of SEIR epidemic model of meseales with non- integer time fractional derivatives by using LADM. Ongun [11], applied the LADM for solving a model for HIV infection of $CD4^{+}T$ cells. Palese [12] analysed Variation of Influenza A, B, and C. Saberiad [15] applied of Homotopy Perturbation Method for solving Hybrid Fuzzy Differential Equations. Pederson et al., [19] numerically solved hybrid fuzzy differential equation IVPs by a characterisation theorem. [20] Kandel et al., studied Fuzzy dynamical systems and nature of their solutions. In [21], [22], Lakshmikantham et al., Impulsive hybrid systems and stability theory, Theory of fuzzy differential equations and inclusions. In [23] Seikkala, On the fuzzy initial value problem. [24] Sepahvandzadeh et al., applied Variational Iteration method (VIM) for solving Hybrid Fuzzy Differential Equations. Also there are many researchers who are working on different types fuzzy differential equations in his research on hybrid systems, delay systems, epidemic models etc., in [13, 14], [16],[17, 18], [6, 7], [8, 9]. The manuscript consists of preliminaries in 2, fuzzy-two-coupled non-linear differential equations in 3, Analytical Solution, Semi Analytical Solution in 4, modified Fuzzy RK-4 Algorithm in 5, and finally conclusion in 6

2 Preliminaries

Let E^1 represents the set of functions $q : \mathscr{R} \to [0,1]$ such that

$$q(y) = \begin{cases} 4y-3, & \text{if } \ y \in (0.75, 1], \\ -2y+3, & \text{if } \ y \in (1, 1.5), \\ 0, & \text{if } \ y \notin (0.75, 1.5). \end{cases} \tag{2.1}$$

The r-level set of q in (2.1) can be wriiten as

$$[q; r] = [0.75 + 0.25r, \ 1.5 - 0.5r]. \tag{2.2}$$

We define $\hat{0} \in E^1$ as $\hat{0}(y) = 1$ if $y = 0$ and $\hat{0}(y) = 0$ if $y \neq 0$ for future reference.

From [23] of $y : I \to E^1$ where $I \subset \mathscr{R}$ is an interval. If $\tilde{y}(t) = [\underline{y}(t; r), \overline{y}(t; r)]$ for all $t \in I$ and $r \in [0,1]$, then $\tilde{y}'(t) = [\underline{y}'(t; r), \overline{y}'(t; r)]$, if $y'(t; r) \in E^1$.
Following IVP,

$$y'(t) = g(t, y(t)), \ y(0) = y_0, \tag{2.3}$$

where $g : [0, \infty) \times \mathscr{R} \to \mathscr{R}$ is continuous. We would like to interpret (2.3) using the Seikkala's derivative and $y_0 \in E^1$. Let $\tilde{y}_0 = [\underline{y}(0; r), \overline{y}(0; r)]$ and $\tilde{y}(t) = [\underline{y}(t; r), \overline{y}(t; r)]$.

2.1 Definitions and Basic Results

This secion consits of important results considered from [25, 23, 3, 26] "Let $G_k(\mathscr{R}^n)$ represents the house of complete nonempty, compacted, convex collection of subsets of $\mathscr{R}^n$. Sum and product in $G_k(\mathscr{R}^n)$ are existing as usual. Let y be a point in $\mathscr{R}^n$ and B be a non-empty sub set of $\mathscr{R}^n$. The distance $D(y, B)$ from y to B is defined by

$$D(y, B) = \inf_{b \in B} \{\|y - b\|\}$$

Let M and N be two nonempty bounded subsets of $\mathscr{R}^n$. The Housdorff separation of M from N is defined by

$$D_H^*(M, N) = \sup_{\mu \in M} \{d(\mu, \nu)\},$$

The Housdorff separation of N from M is defined by

$$D_H^*(N, M) = \sup_{\nu \in N} \{d(\nu, \mu)\},$$

The distance of separation between M and N as understood by the Housdorff sense

$$D_H(M, N) = \max\left\{ \sup_{m \in M} \inf_{n \in N} \|m - n\|, \sup_{n \in M} \inf_{m \in M} \|m - n\| \right\},$$

where $\| \cdot \|$ is the traditional Euclidean norm $||.||$ in $\mathscr{R}^n$. Then it is clear that $(F_k(\mathscr{R}^n), D)$ becomes a complete metric space.

A fuzzy subset of $\mathscr{R}^n$ is explained in terms of a membership arguments which coins to each point $x \in \mathscr{R}^n$, a grade of membership in the fuzzy set. Such a membership function $q : \mathscr{R}^n \to I \in [0, 1]$ is used to denote the corresponding fuzzy set.

To every $r \in (0, 1]$, the r- level set $[q]^r$ of a fuzzy set u is the subset of values $y \in \mathscr{R}^n$ with memberships $q(y)$ of r powers, that is $[q]^r = \{y \in \mathscr{R}^n : q(y) \geq r\}$. The support $[q]^0$ of a fuzzy set is then defined as the closure of the union of all its level sets, that is, $[q]^0 = \overline{\bigcup_{r \in (0,1]} [q]^r}$. An inclusion result arrives spontaneously from the above definitions.

Result 1
To every $0 \leq r_1 \leq r_2 \leq 1$, $[q]^{r_2} \subseteq [q]^{r_1} \subseteq [q]^0$.

Universally, some level sets usually be null in a ordinary fuzzy set. Particularly, the triviality arise when $q(y) \equiv 0$ for all $y \in \mathscr{R}^n$, though the support is null: q is null fuzzy set in this sense. Here we shall pay focus only to the normal fuzzy sets which satisfy.

In view of Result 1. we have

Result 2
$[q]^r$ is a compact subset of $\mathscr{R}^n$ for all $r \in I$.

Result 3
"If u is fuzzy convex, then $[q]^r$ is convex for each $r \in I$.

Let $I = [0, 1] \subseteq R$ be as compact interval and let E^n denote the set of all $q : \mathscr{R}^n \to I$ such that q satisfies the following conditions.
(i) q is normal, that is, there exist an $q_0 \in \mathscr{R}^n$ such that $q_0 = 1$,
(ii) q is fuzzy convex,
(iii) q is upper semicontinuous,

(iv) $[q]^0 \equiv$ closure of $\{q \in \mathscr{R}^n : q(x) > 0\}$ is compact.
Then, from $(1) - (4)$, it follows that the r-level set $[q]^r \in P_k(\mathscr{R}^1)$ for all $0 \leq r \leq 1$. If $g : \mathscr{R}^n \times \mathscr{R}^n \to \mathscr{R}^n$ is a function, then using Zadeh's extension principle we can extend g to $E^n \times E^n \to E^n$ by the equation"

$$\tilde{g}(q_1, q_2)(z) = \sup_{z=g(x,y)} \min\{q_1(x), q_2(y)\}. \tag{2.4}$$

It is well known that$[\tilde{g}(q_1, q_2)]^r = g([q_1]^r, [q_2]^r)$, for all $q_1, q_2 \in E^n$, $0 \leq r \leq 1$, and continuous function g. Further we have

$$\begin{aligned} [q_1^r + q_2^r] &= ([q_1]^r + [q_2]^r), & (2.5)\\ [kq]^r &= k[q]^r, & (2.6) \end{aligned}$$

where $k \in \mathscr{R}$. The real numbers can be embedded in E^n by the rule $c \to \hat{c}(t)$", where,

$$\hat{c}(t) = \begin{cases} 1 & for \quad t = c, \\ 0 & elsewhere. \end{cases}$$

3 Fuzzy-Two-Coupled Non-linear Differential Equations

For preliminary definitins of fuzzy differential equations authors are encouraged to go through [25, 26], [18], etc., Two Coupled differential Equations have wide range of applications in any mathematicall modell of physical phenomena in epidemiology, ecology,etc., By the application of fuzzy it is used to eliminate the randomness and vagueness that arises in any dynamics of the system.

$$\begin{cases} x'(t) = c_1 x(t) y(t),\ t_0 \leq t \leq t_n \\ y'(t) = c_2 x(t) y(t),\ t_0 \leq t \leq t_n \\ x(t_0) = x_0, \\ y(t_0) = y_0 \end{cases} \tag{3.1}$$

where c_1, c_2 are numeric constants such that they are not equal to zero and also $c_1 \neq c_2$. By using the concept fuzzy, the equation (3.1) becomes,

$$\begin{cases} \tilde{x}'(t) = c_1 \tilde{x}(t) \tilde{y}(t),\ t_0 \leq t \leq t_n \\ \tilde{y}'(t) = c_2 \tilde{x}(t) \tilde{y}(t),\ t_0 \leq t \leq t_n \\ \tilde{x}(t_0) = x_0, \\ \tilde{y}(t_0) = y_0 \end{cases} \tag{3.2}$$

Such that $\tilde{x}(t) = [\underline{x}(t;r), \overline{x}(t;r)]$. In the same way for $\tilde{y}(t)\,\tilde{x}'(t)\,\tilde{y}'(t)$ and also for $\tilde{x}_0$, $\tilde{y}(0)$

4 Analytical Solution, Semi Analytical Solution

The analytical Solution of the system (3.2) is given by

$$\begin{aligned} \tilde{x}(t) &= \tilde{x}_0 e^{c_1 \int_0^t y(s) ds} \\ \tilde{y}(t) &= \tilde{y}_0 e^{c_2 \int_0^t x(s) ds} \end{aligned} \tag{4.1}$$

In order to obtain the semi analytical solution we are here by making use of well known Laplace Adomian Decomposition method (LADM). We prefer this method to compare the solutions of nonlinear coupled differential equations. The method is already defined and described in somany papers previously whereas the RK-4 algorith or method for nonlinear coupled differential equations is not defined clearly yet but found traces of the authors try over it in the literature. The method is taken since we are unable to process the analytical solutions even though its structure is expalined above.

4.1 Fuzzy Laplace Adomian Decomposition Method

$$\begin{aligned} X(k+1) &= L^{-1}(c_1/s \times L(A_k)) \\ Y(k+1) &= L^{-1}(c_2/s^{\alpha 2} \times L(A_k)) \end{aligned} \tag{4.2}$$

Where (A_k) is an Adomian polynomial defined by $A_k = \frac{1}{k!}\frac{d^k}{\lambda^k}(\sum_{l=0}^{k}(\lambda^l.x_l\lambda^l.y_l)|_{\lambda=0}$ i.e.,
$A_0 = x_0y_0$
$A_1 = x_0y_1 + x_1y_0$
$A_2 = x_0y_2 + x_1y_1 + x_2y_0$ and so on.
$x(t) = \sum_{k=0}^{\infty}(x(k))$
$y(t) = \sum_{k=0}^{\infty}(y(k))$

5 Modified Fuzzy RK-4 Algorithm:

We are at present sharing the new algorithm for novel RK-4 method for solving nonlinear coupled differential equations. In this section we are using the fourth order Runge-Kutta method (RK-4). We are finding the values of $\tilde{x}(t)$,$\tilde{y}(t)$, at $h = 0.1$ for the best approximation. For $0 \leq r \leq 1$.

To evaluate x(t), and y(t):
Consider,

$$\begin{aligned} \tilde{x}(t+1) &= (\tilde{x}(t) + (1/6(A_1 + 2A_2 + 2A_3 + K_4))) \\ \tilde{y}(t+1) &= (\tilde{y}(t) + (1/6(L_1 + 2B_2 + 2B_3 + B_4))) \end{aligned} \tag{5.1}$$

To estimate (5.1), consider the following.

$$\begin{aligned} \tilde{A}_1 &= h \times c_1((\tilde{x}(t))(\tilde{y}(t)) \\ \tilde{B}_1 &= h \times c_2((\tilde{x}(t))(\tilde{y}(t)) \\ \tilde{A}_2 &= h \times c_1(\tilde{x}(t) + (\tilde{A}_1/2))(\tilde{y}(t) + (\tilde{B}_1/2)) \\ \tilde{B}_2 &= h \times c_2(\tilde{x}(t) + (\tilde{A}_1/2))(\tilde{y}(t) + (\tilde{B}_1/2)) \\ \tilde{A}_3 &= h \times c_1(\tilde{x}(t) + (\tilde{A}_2/2))(\tilde{y}(t) + (\tilde{B}_2/2)) \\ \tilde{B}_3 &= h \times c_2(\tilde{x}(t) + (\tilde{A}_2/2))(\tilde{y}(t) + (\tilde{B}_2/2)) \\ \tilde{A}_4 &= h \times c_1(\tilde{x}(t) + (\tilde{A}_3))(\tilde{y}(t) + (\tilde{B}_3)) \\ \tilde{B}_4 &= h \times c_2(\tilde{x}(t) + (\tilde{A}_3))(\tilde{y}(t) + (\tilde{B}_3)) \end{aligned} \tag{5.2}$$

For $1 \leq p \leq 4$ and $0 \leq r \leq 1$,
$\tilde{A}_p = \tilde{A}_p(t;r) = [\underline{A}_p(t;r), \overline{A}_p(t;r)]$,
$\tilde{B}_p = \tilde{B}_p(t;r) = [\underline{B}_p(t;r), \overline{B}_p(t;r)]$,
For $0 \leq t \leq n$, $n = 1, 2, 3, ...,$,
and for $\underline{q} = t$, $\overline{q} = t+1$, $t = 0, 1, 2, 3, ...$
$\tilde{x}(q) = \tilde{x}(q)(t;r) = [\underline{x}_q(t;r), \overline{x}_q(t;r)]$,
$\tilde{y}(q) = \tilde{y}(q)(t;r) = [\underline{y}_q(t;r), \overline{y}_q(t;r)]$,
Where, $[\underline{f}(t;r), \overline{f}(t;r)] = [0.75 + 0.25r, 1.125 - 0.125r]f(t)$.

Table 1: Approximate solution by RK-4 for non-fuzzy case

t	LADM-4		RK-4		Error	
	x(t)	y(t)	x(t)	y(t)	x(t)	y(t)
0	5	3	5	3	0	0
0.1	4.991	3.0045	5.006	2.99325	0.015	0.01125
0.2	4.98201	3.009	4.99701	2.99775	0.015	0.01125
0.3	4.97301	3.01349	4.98802	3.00224	0.01501	0.01125
0.4	4.96402	3.01799	4.97904	3.00673	0.01502	0.01126
0.5	4.95503	3.02248	4.97006	3.01122	0.01503	0.01126
0.6	4.94605	3.02697	4.96108	3.01571	0.01503	0.01126
0.7	4.93707	3.03147	4.9521	3.0202	0.01503	0.01127
0.8	4.92809	3.03595	4.94313	3.02469	0.01504	0.01126
0.9	4.91912	3.04044	4.93416	3.02917	0.01504	0.01127
1.0	4.91014	3.04493	4.92519	3.03366	0.01505	0.01127

Table 2: Approximate solution by RK-4 for fuzzy case

r	x(t;r)		y(t;r)	
	min	max	min	max
0	3.6939	5.625	2.27524	3.41286
0.1	3.81703	5.56917	2.35108	3.37494
0.2	3.94016	5.49671	2.42692	3.33702
0.3	4.06329	5.42447	2.50277	3.2991
0.4	4.18641	5.35246	2.57861	3.26118
0.5	4.30954	5.28068	2.65445	3.22326
0.6	4.43267	5.20913	2.73029	3.18534
0.7	4.5558	5.13781	2.80613	3.14742
0.8	4.67893	5.06671	2.88197	3.1095
0.9	4.80206	4.99584	2.95781	3.07158
1	4.92519	4.92519	3.03366	3.03366

5.1 An Example

Let us consider the following problem and compare the results of the method LADM RKM-4 in both non-fuzzy and as well as fuzzy. In Table 1, we are presenting the values of $x(t)$, $y(t)$, in non fuzzy by means of LADM-4 and RK-4, and also the error analysis between them. In table 1, we have presented only the values for $t \in [0, 1]$ but one can estimate the values for $t \in [0, 100]$. In that way we found that at $t = 15.5$, $x(t) = 3.66502$, $y(t) = 3.66749$, i.e $x(t) \approx y(t)$, $t = 20.$, there is a interaction between $x(t)$, and $y(t)$.

$$\begin{cases} \tilde{x}'(t) = -0.006\tilde{x}(t)\tilde{y}(t),\ 0 \le t \le 1 \\ \tilde{y}'(t) = 0.003\tilde{x}(t)\tilde{y}(t),\ 0 \le t \le 1 \\ \tilde{x}(0) = 5, \\ \tilde{y}(0) = 3. \end{cases} \tag{5.3}$$

We calculate error by means of $Error = |(LADM - 4) - (RK - 4)|$ Let us present below the table value of $x(t)$ and $y(t)$ in terms of fuzzy in Table 2. So that we have $x(t;r)$ and $y(t;r)$ for $t \in [0, 1]$ and $r \in [0, 1]$.

5.2 Numerical Simlations

For non-Fuzzy coupled case of above example:
For Fuzzy coupled case of above example:

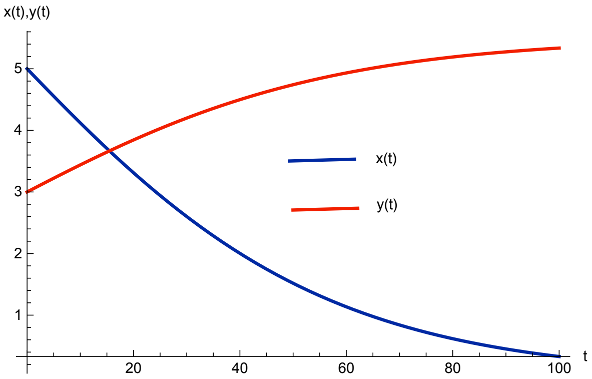

Figure 1: Non-Fuzzy Nonlinear Two Coupled Differential Systems

By the above figures, Figure1 and 2 we are able to understand the travel of solutions in $t \in 0, 100$ for non-fuzzy case and for $t \in [0, 1]$ and $r \in [0, 1]$ for fuzzy case respectively.

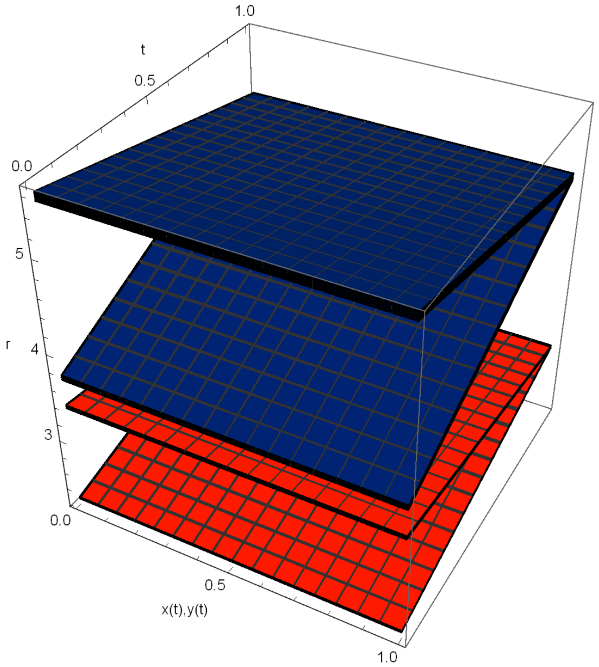

Figure 2: Fuzzy Nonlinear Two Coupled Differential Systems

6 Conclusion

There are numerous numerical methods that one want to use other than Rung-Kutta method when it comes to the need to solve the function with non-linear

ODE especially for coupled differential equaions we are having so many applications but the methods like Laplace Adomian Decomposition method etc., are used as presented in earlier section. But now we had presented the new coupled form of RK-4 algorithm for solving any kind of nonlinear two coupled nonlinear ODE. We recommend this RK-4 algorithm since its accuracy is of about $O(h^1)$ or one decimal place when it is compared with semianalytical method like LADM. The important aspect is that one can easily see the interaction between $x(t)$ and $y(t)$ in figure 1 which tells us at $t = 15.5$, $x(t) \approx y(t)$. As a future work, we will present this approach on completely coupled fuzzy disease modelling problems.

References

[1] L.J.S. Allen, An introduction to mathematical biology, NJ: Prentice Hall: 2007.

[2] S. Abbasbandy Extended Newtons method for a system of nonlinear equations by modified Adomian Decomposition Method,*Applied Mathematics and computation*,170(2005), 648-656

[3] J.J. Bukley and T. Feuring, Fuzzy differential equations, *Fuzzy Sets and Systems*, 110 (2000), 43-54.

[4] W.O. Kermack and A.G. Mckendrick, Contribution to the Mathematical Theory of Epidemics, *Proc.Roy.Soc.Lond.A*, 115, 700-721 (1927).

[5] O.D. Makinde, Adomian Decomposition approach to a SIR epidemic model with constant vaccination Strategy,*Applied Mathematics and Computation*, 184(2) (2007) 842-848.

[6] P.B. Dhandapani, D. Baleanu, J. Thippan, and V. Sivakumar, Fuzzy Type RK4 Solutions to Fuzzy Hybrid Retarded Delay Differential Equations, *Frontiers in Physics*, 7:168, (2019), 1-6.

[7] P.B. Dhandapni, D. Baleanu, J. Thippan, and V. Sivakumar, New Fuzzy Fractional Epidemic Model Involving Death Population, *Computer Systems Science and Engineering*, 37(3), (2021), 331-346.

[8] P.B. Dhandapani, T. Jayakumar, and S. Vinoth, Existence and Uniqueness of Solutions for Fuzzy Mixed Type of Delay Differential Equations, *Journal of Applied Nonlinear Dynamics*, 10(1), (2021), 187-196.

[9] P.B. Dhandapani, J. Thippan, C. Martin-Barreiro, V. Leiva, C. Chesneau, Numerical Solutions of a Differential System Considering a Pure Hybrid Fuzzy Neutral Delay Theory. Electronics 2022, 11, 1478.

[10] Muhammad Farman, Muhammed Umer Saleem, Aqueel Ahmed, M.O. Ahamed, Analysis and Numerical solution of SEIR epidemic model of meseales with non- integer time fractional derivatives by using Laplace Adomian Decomposition Method, *Ain Shams Engineering Journal*, 9(2018) 3391-3397.

[11] M.Y. Ongun, The Laplace Adomian Decomposition Method for solving a model for HIV infection of $CD4^{+}T$ cells. *Mathematical and Computer Modelling*, 53(2011) 597-603.

[12] P.Palese and J.F Young, Variation of Influenza A, B, and C*Science*, 215(4539), (1982) 1468-1474.

[13] Prasantha Bharathi. D, Baleanu. D, Jayakumar. T, and Vinoth. S., On Stiff Fuzzy IRD-14 day average transmission model of COVID-19 pandemic disease, *AIMS Bioengineering*, 7(4), (2020),208-223.

[14] D.P. Bharathi, T. Jayakumar, and S. Vinoth, Numerical Solution of Hybrid Fuzzy Mixed Delay Differential Equation by Fourth Order Runge-Kutta Method, *Discontinuity, Nonlinearity and Complexity*, 10(1), (2021), 77-86.

[15] F. Saberiad, S.M. Karbassi, M. Heydari, S.M.M. Hosseini, Application of Homotopy Perturbation Method for solving Hybrid Fuzzy Differential Equations, Journal of Mathematical Extension, 12(1) (2018), 113-145.

[16] D.P. Bharathi, T. Jayakumar, and S. Vinoth, Numerical Solution of Fuzzy Mixed Delay Differential Equations Via Runge-Kutta Method of Order Four, *International Journal of Applied Engineering Research*, 14(3),(Special Issue) (2019), 70-74.

[17] D.P. Bharathi, T. Jayakumar, and S. Vinoth, Numerical Solution of Fuzzy Multiple Hybrid Single Retarded Delay Differential Equations, *International Journal of Recent Technology and Engineering*, 8(3), (2019), 1946-1949.

[18] D.P. Bharathi, T. Jayakumar, and S. Vinoth, Numerical Solutions of Fuzzy Multiple Hybrid Single Neutral Delay Differential Equations, *International Journal of Scientific & Technology Research*, 8(09), (2019), 520-523.

[19] S.Pederson and M. Sambandham, Numerical Solution of hybrid fuzzy differential equation IVPs by a characterisation theorem, Information Sciences, 179 (2009), 319-328.

[20] A. Kandel, Fuzzy dynamical systems and the nature of their solutions, in: P.P. Wang, S.K. Chang(Eds.), Fuzzy Sets: Theory and Application to Policy Analysis and Information Systems, Plenum Press, New York, (1980), 93-122.

[21] V. Lakshmikantham and X.Z. Liu, Impulsive hybrid systems and stability theory, International Journal of Nonlinear Differential Equations, 5 (1999), 9-17.

[22] V. Lakshmikantham and R.N. Mohapatra, Theory of fuzzy differential equations and inclusions, Taylor and Francis, United Kingdom, 2003.

[23] S.Seikkala, On the fuzzy initial value problem, Fuzzy Sets and Systems, 24 (1987) 319-330.

[24] A. Sepahvandzadeh and B. Ghazanfari, Variational Iternation method for solving Hybri Fuzzy Differential Equations. Journal of Mathematical Extension,10 (4) (2016), 75-85.

[25] L.A. Zadeh, Fuzzy sets, Information and Control,8(1965), 338-353.

[26] R. Goetschel and W. Voxman, Elementary fuzzy calculus,*Fuzzy Sets and Systems,* 18(1986), 31-43.

Formatting of Funding Sources:
This research did not receive any specific grant from funding agencies in the public, commercial, or not-for-profit sectors.

J. COMPUTATIONAL ANALYSIS AND APPLICATIONS, VOL. 31, NO. 4, 2023, COPYRIGHT 2023 EUDOXUS PRESS, LLC

Parametrized hyperbolic tangent based Banach space valued multivariate multi layer neural network approximations

George A. Anastassiou
Department of Mathematical Sciences
University of Memphis
Memphis, TN 38152, U.S.A.
ganastss@memphis.edu

Seda Karateke
Department of Computer Engineering, Faculty of Engineering,
Istanbul Topkapı University, Istanbul, Zeytinburnu 34087, Turkey.
sedakarateke@topkapi.edu.tr

Abstract

Here we examine the multivariate quantitative approximations of Banach space valued continuous multivariate functions on a box or $\mathbb{R}^N$, $N \in \mathbb{N}$, by the multivariate normalized, quasi-interpolation, Kantorovich type and quadrature type neural network operators. We research also the case of approximation by iterated operators of the last four types, that is multi hidden layer approximations. These approximations are achieved by establishing multidimensional Jackson type inequalities involving the multivariate modulus of continuity of the engaged function or its high order Fréchet derivatives. Our multivariate operators are defined by using a multidimensional density function induced by a parametrized hyperbolic tangent sigmoid function. The approximations are pointwise, uniform and L_p. The related feed-forward neural networks are with one or multi hidden layers.

2020 AMS Mathematics Subject Classification: 41A17, 41A25, 41A30, 41A36.

Keywords and Phrases: multi layer approximation, parametrized hyperbolic tangent sigmoid function, multivariate neural network approximation, quasi-interpolation operator, Kantorovich type operator, quadrature type operator, multivariate modulus of continuity, abstract approximation, iterated and

L_p approximations.

1 Introduction

G.A. Anastassiou in [2] and [3], see chapters 2-5, was the first to establish neural network approximations to continuous functions with rates by very specifically defined neural network operators of Cardaliaguet-Euvrard and "Squashing" types, by employing the modulus of continuity of the engaged function or its high order derivative, and producing very tight Jackson type inequalities. He treats there both the univariate and multivariate cases. The defining these operators "bell-shaped" and "squashing" functions are assumed to be of compact support. Also in [3] he gives the Nth order asymptotic expansion for the error of weak approximation of these two operators to a special natural class of smooth functions, see chapters 4-5 there.

Motivations for this work are the article [22] of Z. Chen and F. Cao, and [4]-[19], [23], [24].

Here we perform a parametrized hyperbolic tangent sigmoid function based neural network multivariate approximation to continuous functions over boxes or over the whole $\mathbb{R}^N$, $N \in \mathbb{N}$, and also iterated, multi layer and L_p approximations. All convergences here are with rates expressed via the multivariate modulus of continuity of the involved function or its high order Fréchet derivative and given by very tight multidimensional Jackson type inequalities.

We come up with the "right" precisely defined multivariate normalized, quasi-interpolation neural network operators related to boxes or $\mathbb{R}^N$, as well as Kantorovich type and quadrature type related operators on $\mathbb{R}^N$. Our boxes are not necessarily symmetric to the origin. In preparation to prove our results we establish important properties of the basic multivariate density function induced by a parametrized hyperbolic tangent sigmoid function.

Feed-forward neural networks (FNNs) with one hidden layer, the only type of networks we deal with in this article, are mathematically expressed as

$$N_n(x) = \sum_{j=0}^{n} c_j \sigma\left(\langle a_j \cdot x \rangle + b_j\right), \quad x \in \mathbb{R}^s, \quad s \in \mathbb{N},$$

where for $0 \leq j \leq n$, $b_j \in \mathbb{R}$ are the thresholds, $a_j \in \mathbb{R}^s$ are the connection weights, $c_j \in \mathbb{R}$ are the coefficients, $\langle a_j \cdot x \rangle$ is the inner product of a_j and x, and σ is the activation function of the network. In many fundamental neural network models, the activation function is based on the hyperbolic tangent sigmoid function. About neural networks read [25]-[27].

2 Background

We consider here the generalized hyperbolic tangent function $\tanh \lambda x$, $x \in \mathbb{R}$, $\lambda > 0$:

$$\tanh \lambda x = \frac{e^{\lambda x} - e^{-\lambda x}}{e^{\lambda x} + e^{-\lambda x}}. \tag{1}$$

It is $\tanh \lambda 0 = 0, -1 < \tanh \lambda x < 1, \forall\ x \in \mathbb{R}$, and $\tanh \lambda (-x) = -\tanh \lambda x$. Furthermore we have $\tanh \lambda (\infty) = 1$ and $\tanh \lambda (-\infty) = -1$, and $\tanh \lambda x$ is strictly increasing on $\mathbb{R}$, with

$$\frac{d}{dx} \tanh \lambda x = \frac{\lambda}{\cos^2 \lambda x} > 0. \tag{2}$$

The induced activation function will be

$$\theta (x) := \frac{1}{4} (\tanh \lambda (x+1) - \tanh \lambda (x-1)) > 0, \forall x \in \mathbb{R}, \tag{3}$$

with $\theta (x) = \theta (-x)$.

Clearly $\theta (x)$ is differentiable and thus it is continuous.

Proposition 1 *$\theta (x)$ is strictly decrasing on $(0, \infty)$ and strictly increasing on $(-\infty, 0]$. We have that $\theta (-\infty) = \theta (\infty) = 0$. So that θ has the bell shape with horizontal asymptote the x-axis. The maximum of θ is*

$$\theta (0) = \frac{\tanh \lambda}{2}. \tag{4}$$

We mention

Theorem 2 *([20]) It holds*

$$\sum_{i=-\infty}^{\infty} \theta (x - i) = 1, \ \ \forall\ x \in \mathbb{R}. \tag{5}$$

Theorem 3 *([20]) We have that*

$$\int_{-\infty}^{\infty} \theta (x)\, dx = 1. \tag{6}$$

So that θ is a density function on $\mathbb{R}$.

Theorem 4 *([20]) Let $0 < \alpha < 1$, $\lambda > 0$ and $n \in \mathbb{N}$. It holds*

$$\sum_{\begin{cases} k = -\infty \\ : |nx - k| \geq n^{1-\alpha} \end{cases}}^{\infty} \theta (nx - k) < e^{4\lambda} e^{-2\lambda n^{(1-\alpha)}}. \tag{7}$$

Denote by $\lfloor \cdot \rfloor$ the integral part of the number and by $\lceil \cdot \rceil$ the ceiling of the number.

Theorem 5 *([20]) Let $x \in [a,b] \subset \mathbb{R}$ and $n \in \mathbb{N}$, so that $\lceil na \rceil \leq \lfloor nb \rfloor$. Then*

$$\frac{1}{\sum_{k=\lceil na \rceil}^{\lfloor nb \rfloor} \theta\left(nx-k\right)} < \frac{4}{\tanh 2\lambda} = \frac{1}{\theta\left(1\right)}. \tag{8}$$

We make

Remark 6 *([20])*

(i) We have that

$$\lim_{n\to\infty} \sum_{k=\lceil na \rceil}^{\lfloor nb \rfloor} \theta\left(nx-k\right) \neq 1, \tag{9}$$

for at least some $x \in [a,b]$.

(ii) Let $[a,b] \subset \mathbb{R}$. For large n we always have $\lceil na \rceil \leq \lfloor nb \rfloor$. Also $a \leq \frac{k}{n} \leq b$, iff $\lceil na \rceil \leq k \leq \lfloor nb \rfloor$.

In general it holds

$$\sum_{k=\lceil na \rceil}^{\lfloor nb \rfloor} \theta\left(nx-k\right) \leq 1. \tag{10}$$

We introduce

$$Z\left(x_1,...,x_N\right) := Z\left(x\right) := \prod_{i=1}^{N} \theta\left(x_i\right), \quad x = \left(x_1,...,x_N\right) \in \mathbb{R}^N, \;\; N \in \mathbb{N}. \tag{11}$$

It has the properties:

(i) $Z\left(x\right) > 0, \;\; \forall\, x \in \mathbb{R}^N$,

(ii)

$$\sum_{k=-\infty}^{\infty} Z\left(x-k\right) := \sum_{k_1=-\infty}^{\infty} \sum_{k_2=-\infty}^{\infty} ... \sum_{k_N=-\infty}^{\infty} Z\left(x_1-k_1,...,x_N-k_N\right) = 1, \tag{12}$$

where $k := \left(k_1,...,k_n\right) \in \mathbb{Z}^N$, $\forall\, x \in \mathbb{R}^N$,

hence

(iii)

$$\sum_{k=-\infty}^{\infty} Z\left(nx-k\right) = 1, \tag{13}$$

$\forall\, x \in \mathbb{R}^N$; $n \in \mathbb{N}$,

and

(iv)

$$\int_{\mathbb{R}^N} Z(x)\,dx = 1, \tag{14}$$

that is Z is a multivariate density function.

Here denote $\|x\|_\infty := \max\{|x_1|,...,|x_N|\}$, $x \in \mathbb{R}^N$, also set $\infty := (\infty,...,\infty)$, $-\infty := (-\infty,...,-\infty)$ upon the multivariate context, and

$$\begin{gathered}\lceil na \rceil := (\lceil na_1 \rceil,...,\lceil na_N \rceil),\\ \lfloor nb \rfloor := (\lfloor nb_1 \rfloor,...,\lfloor nb_N \rfloor),\end{gathered} \tag{15}$$

where $a := (a_1,...,a_N)$, $b := (b_1,...,b_N)$.

We obviously see that

$$\sum_{k=\lceil na \rceil}^{\lfloor nb \rfloor} Z(nx-k) = \sum_{k=\lceil na \rceil}^{\lfloor nb \rfloor} \left(\prod_{i=1}^{N} \theta(nx_i - k_i)\right) =$$

$$\sum_{k_1=\lceil na_1 \rceil}^{\lfloor nb_1 \rfloor} ... \sum_{k_N=\lceil na_N \rceil}^{\lfloor nb_N \rfloor} \left(\prod_{i=1}^{N} \theta(nx_i - k_i)\right) = \prod_{i=1}^{N} \left(\sum_{k_i=\lceil na_i \rceil}^{\lfloor nb_i \rfloor} \theta(nx_i - k_i)\right). \tag{16}$$

For $0 < \beta < 1$ and $n \in \mathbb{N}$, a fixed $x \in \mathbb{R}^N$, we have that

$$\sum_{k=\lceil na \rceil}^{\lfloor nb \rfloor} Z(nx-k) =$$

$$\sum_{\begin{cases} k = \lceil na \rceil \\ \left\|\frac{k}{n} - x\right\|_\infty \le \frac{1}{n^\beta} \end{cases}}^{\lfloor nb \rfloor} Z(nx-k) + \sum_{\begin{cases} k = \lceil na \rceil \\ \left\|\frac{k}{n} - x\right\|_\infty > \frac{1}{n^\beta} \end{cases}}^{\lfloor nb \rfloor} Z(nx-k). \tag{17}$$

In the last two sums the counting is over disjoint vector sets of k's, because the condition $\left\|\frac{k}{n} - x\right\|_\infty > \frac{1}{n^\beta}$ implies that there exists at least one $\left|\frac{k_r}{n} - x_r\right| > \frac{1}{n^\beta}$, where $r \in \{1,...,N\}$.

(v) As in, Theorem 4 we derive that

$$\sum_{\begin{cases} k = \lceil na \rceil \\ \left\|\frac{k}{n} - x\right\|_\infty > \frac{1}{n^\beta} \end{cases}}^{\lfloor nb \rfloor} Z(nx-k) \overset{(7)}{<} e^{4\lambda} e^{-2\lambda n^{(1-\beta)}}, \ \ 0 < \beta < 1, \ \lambda > 0. \tag{18}$$

with $n \in \mathbb{N} : n^{1-\beta} > 2$, $x \in \prod_{i=1}^{N} [a_i, b_i]$.

(vi) By Theorem 5 we get that

$$0 < \frac{1}{\sum_{k=\lceil na \rceil}^{\lfloor nb \rfloor} Z(nx-k)} < \left(\frac{4}{\tanh 2\lambda}\right)^N, \tag{19}$$

$\lambda > 0$, $\forall\, x \in \left(\prod_{i=1}^{N} [a_i, b_i]\right)$, $n \in \mathbb{N}$.

It is also clear that

(vii)

$$\sum_{\begin{cases} k=-\infty \\ \left\| \frac{k}{n} - x \right\|_{\infty} > \frac{1}{n^{\beta}} \end{cases}}^{\infty} Z(nx-k) < e^{4\lambda} e^{-2\lambda n^{(1-\beta)}}, \tag{20}$$

$\lambda > 0, 0 < \beta < 1$, $n \in \mathbb{N} : n^{1-\beta} > 2$, $x \in \mathbb{R}^N$.

Furthermore it holds

$$\lim_{n\to\infty} \sum_{k=\lceil na \rceil}^{\lfloor nb \rfloor} Z(nx-k) \neq 1, \tag{21}$$

for at least some $x \in \left(\prod_{i=1}^{N} [a_i, b_i]\right)$.

Here $\left(X, \|\cdot\|_{\gamma}\right)$ is a Banach space.

Let $f \in C\left(\prod_{i=1}^{N} [a_i, b_i], X\right)$, $x = (x_1, ..., x_N) \in \prod_{i=1}^{N} [a_i, b_i]$, $n \in \mathbb{N}$ such that $\lceil na_i \rceil \leq \lfloor nb_i \rfloor$, $i = 1, ..., N$.

We introduce and define the following multivariate linear normalized neural network operator ($x := (x_1, ..., x_N) \in \left(\prod_{i=1}^{N} [a_i, b_i]\right)$):

$$A_n(f, x_1, ..., x_N) := A_n(f, x) := \frac{\sum_{k=\lceil na \rceil}^{\lfloor nb \rfloor} f\left(\frac{k}{n}\right) Z(nx-k)}{\sum_{k=\lceil na \rceil}^{\lfloor nb \rfloor} Z(nx-k)} =$$

$$\frac{\sum_{k_1=\lceil na_1 \rceil}^{\lfloor nb_1 \rfloor} \sum_{k_2=\lceil na_2 \rceil}^{\lfloor nb_2 \rfloor} ... \sum_{k_N=\lceil na_N \rceil}^{\lfloor nb_N \rfloor} f\left(\frac{k_1}{n}, ..., \frac{k_N}{n}\right) \left(\prod_{i=1}^{N} \theta(nx_i - k_i)\right)}{\prod_{i=1}^{N} \left(\sum_{k_i=\lceil na_i \rceil}^{\lfloor nb_i \rfloor} \theta(nx_i - k_i)\right)}. \tag{22}$$

For large enough $n \in \mathbb{N}$ we always obtain $\lceil na_i \rceil \leq \lfloor nb_i \rfloor$, $i = 1, ..., N$. Also $a_i \leq \frac{k_i}{n} \leq b_i$, iff $\lceil na_i \rceil \leq k_i \leq \lfloor nb_i \rfloor$, $i = 1, ..., N$.

When $g \in C\left(\prod_{i=1}^{N} [a_i, b_i]\right)$ we define the companion operator

$$\widetilde{A}_n(g, x) := \frac{\sum_{k=\lceil na \rceil}^{\lfloor nb \rfloor} g\left(\frac{k}{n}\right) Z(nx-k)}{\sum_{k=\lceil na \rceil}^{\lfloor nb \rfloor} Z(nx-k)}. \tag{23}$$

Clearly $\widetilde{A}_n$ is a positive linear operator. We have that

$$\widetilde{A}_n(1, x) = 1, \ \forall\, x \in \left(\prod_{i=1}^{N} [a_i, b_i]\right).$$

Notice that $A_n(f) \in C\left(\prod_{i=1}^{N} [a_i, b_i], X\right)$ and $\widetilde{A}_n(g) \in C\left(\prod_{i=1}^{N} [a_i, b_i]\right)$.

Furthermore it holds

$$\left\|A_n(f,x)\right\|_\gamma \leq \frac{\sum_{k=\lceil na\rceil}^{\lfloor nb\rfloor}\left\|f\left(\frac{k}{n}\right)\right\|_\gamma Z(nx-k)}{\sum_{k=\lceil na\rceil}^{\lfloor nb\rfloor} Z(nx-k)} = \widetilde{A}_n\left(\|f\|_\gamma, x\right), \tag{24}$$

$\forall\ x \in \prod_{i=1}^{N}[a_i,b_i]$.

Clearly $\|f\|_\gamma \in C\left(\prod_{i=1}^{N}[a_i,b_i]\right)$.

So, we have that

$$\left\|A_n(f,x)\right\|_\gamma \leq \widetilde{A}_n\left(\|f\|_\gamma, x\right), \tag{25}$$

$\forall\ x \in \prod_{i=1}^{N}[a_i,b_i]$, $\forall\ n \in \mathbb{N}$, $\forall\ f \in C\left(\prod_{i=1}^{N}[a_i,b_i], X\right)$.

Let $c \in X$ and $g \in C\left(\prod_{i=1}^{N}[a_i,b_i]\right)$, then $cg \in C\left(\prod_{i=1}^{N}[a_i,b_i], X\right)$.

Furthermore it holds

$$A_n(cg,x) = c\widetilde{A}_n(g,x), \ \ \forall\ x \in \prod_{i=1}^{N}[a_i,b_i]. \tag{26}$$

Since $\widetilde{A}_n(1) = 1$, we get that

$$A_n(c) = c, \ \ \forall\ c \in X. \tag{27}$$

We call $\widetilde{A}_n$ the companion operator of A_n.

For convenience we call

$$A_n^*(f,x) := \sum_{k=\lceil na\rceil}^{\lfloor nb\rfloor} f\left(\frac{k}{n}\right) Z(nx-k) =$$

$$\sum_{k_1=\lceil na_1\rceil}^{\lfloor nb_1\rfloor}\sum_{k_2=\lceil na_2\rceil}^{\lfloor nb_2\rfloor}\dots\sum_{k_N=\lceil na_N\rceil}^{\lfloor nb_N\rfloor} f\left(\frac{k_1}{n},\dots,\frac{k_N}{n}\right)\left(\prod_{i=1}^{N}\theta(nx_i-k_i)\right), \tag{28}$$

$\forall\ x \in \left(\prod_{i=1}^{N}[a_i,b_i]\right)$.

That is

$$A_n(f,x) := \frac{A_n^*(f,x)}{\sum_{k=\lceil na\rceil}^{\lfloor nb\rfloor} Z(nx-k)}, \tag{29}$$

$\forall\ x \in \left(\prod_{i=1}^{N}[a_i,b_i]\right)$, $n \in \mathbb{N}$.

Hence

$$A_n(f,x) - f(x) = \frac{A_n^*(f,x) - f(x)\left(\sum_{k=\lceil na\rceil}^{\lfloor nb\rfloor} Z(nx-k)\right)}{\sum_{k=\lceil na\rceil}^{\lfloor nb\rfloor} Z(nx-k)}. \tag{30}$$

Consequently we derive

$$\left\|A_n(f,x)-f(x)\right\|_\gamma \overset{(19)}{\leq} \left(\frac{4}{\tanh 2\lambda}\right)^N \left\|A_n^*(f,x)-f(x)\sum_{k=\lceil na\rceil}^{\lfloor nb\rfloor} Z(nx-k)\right\|_\gamma, \tag{31}$$

$\forall\ x \in \left(\prod_{i=1}^N [a_i,b_i]\right).$

We will estimate the right hand side of (31).

For the last and others we need

Definition 7 *([15], p. 274) Let M be a convex and compact subset of $\left(\mathbb{R}^N, \|\cdot\|_p\right)$, $p\in[1,\infty]$, and $\left(X,\|\cdot\|_\gamma\right)$ be a Banach space. Let $f\in C(M,X)$. We define the first modulus of continuity of f as*

$$\omega_1(f,\delta) := \sup_{\substack{x,y\in M:\\ \|x-y\|_p\leq\delta}} \|f(x)-f(y)\|_\gamma,\ \ 0<\delta\leq diam(M). \tag{32}$$

If $\delta > diam(M)$, then

$$\omega_1(f,\delta) = \omega_1(f, diam(M)). \tag{33}$$

Notice $\omega_1(f,\delta)$ is increasing in $\delta>0$. For $f\in C_B(M,X)$ (continuous and bounded functions) $\omega_1(f,\delta)$ is defined similarly.

Lemma 8 *([15], p. 274) We have $\omega_1(f,\delta)\to 0$ as $\delta\downarrow 0$, iff $f\in C(M,X)$, where M is a convex compact subset of $\left(\mathbb{R}^N,\|\cdot\|_p\right)$, $p\in[1,\infty]$.*

Clearly we have also: $f\in C_U\left(\mathbb{R}^N,X\right)$ (uniformly continuous functions), iff $\omega_1(f,\delta)\to 0$ as $\delta\downarrow 0$, where ω_1 is defined similarly to (32). The space $C_B\left(\mathbb{R}^N,X\right)$ denotes the continuous and bounded functions on $\mathbb{R}^N$.

When $f\in C_B\left(\mathbb{R}^N,X\right)$ we define,

$$B_n(f,x) := B_n(f,x_1,...,x_N) := \sum_{k=-\infty}^{\infty} f\left(\frac{k}{n}\right) Z(nx-k) :=$$

$$\sum_{k_1=-\infty}^{\infty}\sum_{k_2=-\infty}^{\infty}...\sum_{k_N=-\infty}^{\infty} f\left(\frac{k_1}{n},\frac{k_2}{n},...,\frac{k_N}{n}\right)\left(\prod_{i=1}^N \theta(nx_i-k_i)\right), \tag{34}$$

$n\in\mathbb{N}$, $\forall\ x\in\mathbb{R}^N$, $N\in\mathbb{N}$, the multivariate quasi-interpolation neural network operator.

Also for $f\in C_B\left(\mathbb{R}^N,X\right)$ we define the multivariate Kantorovich type neural network operator

$$C_n(f,x) := C_n(f,x_1,...,x_N) := \sum_{k=-\infty}^{\infty}\left(n^N\int_{\frac{k}{n}}^{\frac{k+1}{n}} f(t)\,dt\right) Z(nx-k) =$$

$$\sum_{k_1=-\infty}^{\infty}\sum_{k_2=-\infty}^{\infty}\ldots\sum_{k_N=-\infty}^{\infty}\left(n^N\int_{\frac{k_1}{n}}^{\frac{k_1+1}{n}}\int_{\frac{k_2}{n}}^{\frac{k_2+1}{n}}\ldots\int_{\frac{k_N}{n}}^{\frac{k_N+1}{n}}f\left(t_1,\ldots,t_N\right)dt_1\ldots dt_N\right)$$

$$\cdot\left(\prod_{i=1}^{N}\theta\left(nx_i-k_i\right)\right), \tag{35}$$

$n\in\mathbb{N},\ \forall\ x\in\mathbb{R}^N$.

Again for $f\in C_B\left(\mathbb{R}^N,X\right)$, $N\in\mathbb{N}$, we define the multivariate neural network operator of quadrature type $D_n\left(f,x\right)$, $n\in\mathbb{N}$, as follows.

Let $\theta=\left(\theta_1,\ldots,\theta_N\right)\in\mathbb{N}^N$, $r=\left(r_1,\ldots,r_N\right)\in\mathbb{Z}_+^N$, $w_r=w_{r_1,r_2,\ldots r_N}\geq 0$, such that $\sum\limits_{r=0}^{\theta}w_r=\sum\limits_{r_1=0}^{\theta_1}\sum\limits_{r_2=0}^{\theta_2}\ldots\sum\limits_{r_N=0}^{\theta_N}w_{r_1,r_2,\ldots r_N}=1$; $k\in\mathbb{Z}^N$ and

$$\delta_{nk}\left(f\right):=\delta_{n,k_1,k_2,\ldots,k_N}\left(f\right):=\sum_{r=0}^{\theta}w_rf\left(\frac{k}{n}+\frac{r}{n\theta}\right)=$$

$$\sum_{r_1=0}^{\theta_1}\sum_{r_2=0}^{\theta_2}\ldots\sum_{r_N=0}^{\theta_N}w_{r_1,r_2,\ldots r_N}f\left(\frac{k_1}{n}+\frac{r_1}{n\theta_1},\frac{k_2}{n}+\frac{r_2}{n\theta_2},\ldots,\frac{k_N}{n}+\frac{r_N}{n\theta_N}\right), \tag{36}$$

where $\frac{r}{\theta}:=\left(\frac{r_1}{\theta_1},\frac{r_2}{\theta_2},\ldots,\frac{r_N}{\theta_N}\right)$.

We set

$$D_n\left(f,x\right):=D_n\left(f,x_1,\ldots,x_N\right):=\sum_{k=-\infty}^{\infty}\delta_{nk}\left(f\right)Z\left(nx-k\right)= \tag{37}$$

$$\sum_{k_1=-\infty}^{\infty}\sum_{k_2=-\infty}^{\infty}\ldots\sum_{k_N=-\infty}^{\infty}\delta_{n,k_1,k_2,\ldots,k_N}\left(f\right)\left(\prod_{i=1}^{N}\theta\left(nx_i-k_i\right)\right),$$

$\forall\ x\in\mathbb{R}^N$.

In this article we study the approximation properties of A_n,B_n,C_n, D_n neural network operators and as well of their iterates. That is, the quantitative pointwise and uniform convergence of these operators to the unit operator I.

3 Multivariate Parametrized Hyperbolic Tangent Induced Banach Space Valued Network Approximations

Here we present several vectorial neural network approximations to Banach space valued functions given with rates.

We give

Theorem 9 *Let* $f \in C\left(\prod_{i=1}^{N}[a_i,b_i], X\right)$, $0<\beta<1$, $\lambda>0$, $x \in \left(\prod_{i=1}^{N}[a_i,b_i]\right)$, $N,n \in \mathbb{N}$ *with* $n^{1-\beta}>2$. *Then*

1)

$$\left\|A_n(f,x)-f(x)\right\|_\gamma \leq \left(\frac{4}{\tanh 2\lambda}\right)^N \left[\omega_1\left(f,\frac{1}{n^\beta}\right)+\frac{2e^{4\lambda}\left\|\left\|f\right\|_\gamma\right\|_\infty}{e^{2\lambda\left(n^{1-\beta}\right)}}\right] =: \Omega_1(n), \tag{38}$$

and

2)

$$\left\|\left\|A_n(f)-f\right\|_\gamma\right\|_\infty \leq \Omega_1(n). \tag{39}$$

We notice that $\lim_{n\to\infty} A_n(f) \overset{\|\cdot\|_\gamma}{=} f$, *pointwise and uniformly.*

Above ω_1 *is with respect to* $p=\infty$ *and the speed of convergence is* $\max\left(\frac{1}{n^\beta},\frac{1}{e^{2\lambda n^{(1-\beta)}}}\right)=\frac{1}{n^\beta}$.

Proof. We observe that

$$\Delta(x) := A_n^*(f,x)-f(x)\sum_{k=\lceil na\rceil}^{\lfloor nb\rfloor} Z(nx-k) =$$

$$\sum_{k=\lceil na\rceil}^{\lfloor nb\rfloor} f\left(\frac{k}{n}\right)Z(nx-k)-\sum_{k=\lceil na\rceil}^{\lfloor nb\rfloor} f(x)Z(nx-k) =$$

$$\sum_{k=\lceil na\rceil}^{\lfloor nb\rfloor}\left(f\left(\frac{k}{n}\right)-f(x)\right)Z(nx-k). \tag{40}$$

Thus

$$\left\|\Delta(x)\right\|_\gamma \leq \sum_{k=\lceil na\rceil}^{\lfloor nb\rfloor}\left\|f\left(\frac{k}{n}\right)-f(x)\right\|_\gamma Z(nx-k) =$$

$$\sum_{\substack{\begin{cases} k=\lceil na\rceil \\ \left\|\frac{k}{n}-x\right\|_\infty \leq \frac{1}{n^\beta}\end{cases}}}^{\lfloor nb\rfloor}\left\|f\left(\frac{k}{n}\right)-f(x)\right\|_\gamma Z(nx-k)+$$

$$\sum_{\substack{\begin{cases} k=\lceil na\rceil \\ \left\|\frac{k}{n}-x\right\|_\infty > \frac{1}{n^\beta}\end{cases}}}^{\lfloor nb\rfloor}\left\|f\left(\frac{k}{n}\right)-f(x)\right\|_\gamma Z(nx-k) \overset{(13)}{\leq}$$

$$\omega_1\left(f, \frac{1}{n^{\beta}}\right) + 2\left\| \|f\|_{\gamma} \right\|_{\infty} \sum_{\begin{cases} k = \lceil na \rceil \\ \left\| \frac{k}{n} - x \right\|_{\infty} > \frac{1}{n^{\beta}} \end{cases}}^{\lfloor nb \rfloor} Z\left(nx - k\right) \overset{(18)}{\leq}$$

$$\omega_1\left(f, \frac{1}{n^{\beta}}\right) + 2\left\| \|f\|_{\gamma} \right\|_{\infty} e^{4\lambda} e^{-2\lambda n^{(1-\beta)}}, \ 0 < \beta < 1, \ \lambda > 0. \tag{41}$$

So that

$$\left\|\Delta\left(x\right)\right\|_{\gamma} \leq \omega_1\left(f, \frac{1}{n^{\beta}}\right) + \frac{2e^{4\lambda}\left\| \|f\|_{\gamma} \right\|_{\infty}}{e^{2\lambda n^{(1-\beta)}}}. \tag{42}$$

Now using (31) we finish the proof. ■

We make

Remark 10 *([15], pp. 263-266) Let* $\left(\mathbb{R}^N, \|\cdot\|_p\right)$, $N \in \mathbb{N}$; *where* $\|\cdot\|_p$ *is the* L_p-*norm,* $1 \leq p \leq \infty$. $\mathbb{R}^N$ *is a Banach space, and* $\left(\mathbb{R}^N\right)^j$ *denotes the* j-*fold product space* $\mathbb{R}^N \times ... \times \mathbb{R}^N$ *endowed with the max-norm* $\|x\|_{(\mathbb{R}^N)^j} := \max_{1 \leq \rho \leq j} \|x_{\rho}\|_p$, *where* $x := (x_1, ..., x_j) \in \left(\mathbb{R}^N\right)^j$.

Let $\left(X, \|\cdot\|_{\gamma}\right)$ *be a general Banach space. Then the space* $V_j := V_j\left(\left(\mathbb{R}^N\right)^j; X\right)$ *of all* j-*multilinear continuous maps* $g : \left(\mathbb{R}^N\right)^j \to X$, $j = 1, ..., m$, *is a Banach space with norm*

$$\|g\| := \|g\|_{V_j} := \sup_{\left(\|x\|_{(\mathbb{R}^N)^j} = 1\right)} \|g\left(x\right)\|_{\gamma} = \sup \frac{\|g\left(x\right)\|_{\gamma}}{\|x_1\|_p \cdots \|x_j\|_p}. \tag{43}$$

Let M *be a non-empty convex and compact subset of* $\mathbb{R}^N$ *and* $x_0 \in M$ *is fixed.*

Let O *be an open subset of* $\mathbb{R}^N : M \subset O$. *Let* $f : O \to X$ *be a continuous function, whose Fréchet derivatives (see [28])* $f^{(j)} : O \to V_j = V_j\left(\left(\mathbb{R}^N\right)^j; X\right)$ *exist and are continuous for* $1 \leq j \leq m$, $m \in \mathbb{N}$.

Call $(x - x_0)^j := (x - x_0, ..., x - x_0) \in \left(\mathbb{R}^N\right)^j$, $x \in M$.

We will work with $f|_M$.

Then, by Taylor's formula ([21]), ([28], p. 124), we get

$$f\left(x\right) = \sum_{j=0}^{m} \frac{f^{(j)}\left(x_0\right)\left(x - x_0\right)^j}{j!} + R_m\left(x, x_0\right), \quad all\ x \in M, \tag{44}$$

where the remainder is the Riemann integral

$$R_m\left(x, x_0\right) := \int_0^1 \frac{\left(1 - u\right)^{m-1}}{(m-1)!}\left(f^{(m)}\left(x_0 + u\left(x - x_0\right)\right) - f^{(m)}\left(x_0\right)\right)\left(x - x_0\right)^m du, \tag{45}$$

here we set $f^{(0)}(x_0)(x-x_0)^0 = f(x_0)$.

We consider

$$\omega := \omega_1\left(f^{(m)}, h\right) := \sup_{\substack{x,y\in M: \\ \|x-y\|_p \leq h}} \left\| f^{(m)}(x) - f^{(m)}(y) \right\|, \tag{46}$$

$h > 0$.

We obtain

$$\left\| \left(f^{(m)}(x_0 + u(x-x_0)) - f^{(m)}(x_0) \right)(x-x_0)^m \right\|_\gamma \leq$$

$$\left\| f^{(m)}(x_0 + u(x-x_0)) - f^{(m)}(x_0) \right\| \cdot \|x-x_0\|_p^m \leq$$

$$\omega \|x-x_0\|_p^m \left\lceil \frac{u\|x-x_0\|_p}{h} \right\rceil, \tag{47}$$

by Lemma 7.1.1, [1], p. 208, where $\lceil\cdot\rceil$ *is the ceiling.*

Therefore for all $x \in M$ *(see [1], pp. 121-122):*

$$\|R_m(x,x_0)\|_\gamma \leq \omega \|x-x_0\|_p^m \int_0^1 \left\lceil \frac{u\|x-x_0\|_p}{h} \right\rceil \frac{(1-u)^{m-1}}{(m-1)!} du$$

$$= \omega \Phi_m\left(\|x-x_0\|_p\right) \tag{48}$$

by a change of variable, where

$$\Phi_m(t) := \int_0^{|t|} \left\lceil \frac{s}{h} \right\rceil \frac{(|t|-s)^{m-1}}{(m-1)!} ds = \frac{1}{m!}\left(\sum_{j=0}^{\infty} (|t| - jh)_+^m \right), \quad \forall\, t \in \mathbb{R}, \tag{49}$$

is a (polynomial) spline function, see [1], p. 210-211.

Also from there we get

$$\Phi_m(t) \leq \left(\frac{|t|^{m+1}}{(m+1)!h} + \frac{|t|^m}{2m!} + \frac{h|t|^{m-1}}{8(m-1)!} \right), \quad \forall\, t \in \mathbb{R}, \tag{50}$$

with equality true only at $t = 0$.

Therefore it holds

$$\|R_m(x,x_0)\|_\gamma \leq \omega \left(\frac{\|x-x_0\|_p^{m+1}}{(m+1)!h} + \frac{\|x-x_0\|_p^m}{2m!} + \frac{h\|x-x_0\|_p^{m-1}}{8(m-1)!} \right), \quad \forall\, x \in M. \tag{51}$$

We have found that

$$\left\| f(x) - \sum_{j=0}^{m} \frac{f^{(j)}(x_0)(x-x_0)^j}{j!} \right\|_\gamma \leq$$

$$\omega_1\left(f^{(m)},h\right)\left(\frac{\|x-x_0\|_p^{m+1}}{(m+1)!h}+\frac{\|x-x_0\|_p^{m}}{2m!}+\frac{h\,\|x-x_0\|_p^{m-1}}{8\,(m-1)!}\right)<\infty, \tag{52}$$

$\forall\ x,x_0\in M$.

Here $0<\omega_1\left(f^{(m)},h\right)<\infty$, *by* M *being compact and* $f^{(m)}$ *being continuous on* M.

One can rewrite (52) as follows:

$$\left\|f(\cdot)-\sum_{j=0}^{m}\frac{f^{(j)}(x_0)(\cdot-x_0)^j}{j!}\right\|_\gamma\leq$$

$$\omega_1\left(f^{(m)},h\right)\left(\frac{\|\cdot-x_0\|_p^{m+1}}{(m+1)!h}+\frac{\|\cdot-x_0\|_p^{m}}{2m!}+\frac{h\,\|\cdot-x_0\|_p^{m-1}}{8\,(m-1)!}\right),\ \forall\ x_0\in M, \tag{53}$$

a pointwise functional inequality on M.

Here $(\cdot-x_0)^j$ *maps* M *into* $\left(\mathbb{R}^N\right)^j$ *and it is continuous, also* $f^{(j)}(x_0)$ *maps* $\left(\mathbb{R}^N\right)^j$ *into* X *and it is continuous. Hence their composition* $f^{(j)}(x_0)(\cdot-x_0)^j$ *is continuous from* M *into* X.

Clearly $f(\cdot)-\sum_{j=0}^{m}\frac{f^{(j)}(x_0)(\cdot-x_0)^j}{j!}\in C(M,X)$, *hence* $\left\|f(\cdot)-\sum_{j=0}^{m}\frac{f^{(j)}(x_0)(\cdot-x_0)^j}{j!}\right\|_\gamma\in C(M)$.

Let $\left\{\widetilde{S}_N\right\}_{N\in\mathbb{N}}$ *be a sequence of positive linear operators mapping* $C(M)$ *into* $C(M)$.

Therefore we obtain

$$\left(\widetilde{S}_N\left(\left\|f(\cdot)-\sum_{j=0}^{m}\frac{f^{(j)}(x_0)(\cdot-x_0)^j}{j!}\right\|_\gamma\right)\right)(x_0)\leq$$

$$\omega_1\left(f^{(m)},h\right)\left[\frac{\left(\widetilde{S}_N\left(\|\cdot-x_0\|_p^{m+1}\right)\right)(x_0)}{(m+1)!h}+\frac{\left(\widetilde{S}_N\left(\|\cdot-x_0\|_p^{m}\right)\right)(x_0)}{2m!}+\right.$$

$$\left.\frac{h\left(\widetilde{S}_N\left(\|\cdot-x_0\|_p^{m-1}\right)\right)(x_0)}{8\,(m-1)!}\right], \tag{54}$$

$\forall\ N\in\mathbb{N},\ \forall\ x_0\in M$.

Clearly (54) is valid when $M=\prod_{i=1}^{N}[a_i,b_i]$ and $\widetilde{S}_n=\widetilde{A}_n$, see (23).

All the above is preparation for the following theorem, where we assume Fréchet differentiability of functions.

This will be a direct application of Theorem 10.2, [15], pp. 268-270. The operators A_n, $\widetilde{A}_n$ fulfill its assumptions, see (22), (23), (25), and (26).

We present the following high order approximation results.

Theorem 11 *Let O open subset of $\left(\mathbb{R}^N, \|\cdot\|_p\right)$, $p \in [1,\infty]$, such that $\prod_{i=1}^{N}[a_i,b_i] \subset O \subseteq \mathbb{R}^N$, and let $\left(X, \|\cdot\|_\gamma\right)$ be a general Banach space. Let $m \in \mathbb{N}$ and $f \in C^m(O,X)$, the space of m-times continuously Fréchet differentiable functions from O into X. We study the approximation of $f|_{\prod_{i=1}^{N}[a_i,b_i]}$. Let $x_0 \in \left(\prod_{i=1}^{N}[a_i,b_i]\right)$ and $r > 0$. Then*

1)

$$\left\|(A_n(f))(x_0) - \sum_{j=0}^{m}\frac{1}{j!}\left(A_n\left(f^{(j)}(x_0)(\cdot - x_0)^j\right)\right)(x_0)\right\|_\gamma \leq$$

$$\frac{\omega_1\left(f^{(m)}, r\left(\left(\widetilde{A}_n\left(\|\cdot - x_0\|_p^{m+1}\right)\right)(x_0)\right)^{\frac{1}{m+1}}\right)}{rm!}\left(\left(\widetilde{A}_n\left(\|\cdot - x_0\|_p^{m+1}\right)\right)(x_0)\right)^{\left(\frac{m}{m+1}\right)}$$
$$\left[\frac{1}{(m+1)} + \frac{r}{2} + \frac{mr^2}{8}\right], \tag{55}$$

2) additionally if $f^{(j)}(x_0) = 0$, $j = 1,\ldots,m$, we have

$$\|(A_n(f))(x_0) - f(x_0)\|_\gamma \leq$$

$$\frac{\omega_1\left(f^{(m)}, r\left(\left(\widetilde{A}_n\left(\|\cdot - x_0\|_p^{m+1}\right)\right)(x_0)\right)^{\frac{1}{m+1}}\right)}{rm!}\left(\left(\widetilde{A}_n\left(\|\cdot - x_0\|_p^{m+1}\right)\right)(x_0)\right)^{\left(\frac{m}{m+1}\right)} \tag{56}$$
$$\left[\frac{1}{(m+1)} + \frac{r}{2} + \frac{mr^2}{8}\right],$$

3)

$$\|(A_n(f))(x_0) - f(x_0)\|_\gamma \leq \sum_{j=1}^{m}\frac{1}{j!}\left\|\left(A_n\left(f^{(j)}(x_0)(\cdot - x_0)^j\right)\right)(x_0)\right\|_\gamma +$$

$$\frac{\omega_1\left(f^{(m)}, r\left(\left(\widetilde{A}_n\left(\|\cdot - x_0\|_p^{m+1}\right)\right)(x_0)\right)^{\frac{1}{m+1}}\right)}{rm!}\left(\left(\widetilde{A}_n\left(\|\cdot - x_0\|_p^{m+1}\right)\right)(x_0)\right)^{\left(\frac{m}{m+1}\right)} \tag{57}$$
$$\left[\frac{1}{(m+1)} + \frac{r}{2} + \frac{mr^2}{8}\right],$$

and

4)

$$\left\|\|A_n(f) - f\|_\gamma\right\|_{\infty, \prod_{i=1}^{N}[a_i,b_i]} \leq$$

$$\sum_{j=1}^{m}\frac{1}{j!}\left\|\left\|\left(A_n\left(f^{(j)}(x_0)(\cdot-x_0)^j\right)\right)(x_0)\right\|_\gamma\right\|_{\infty,x_0\in\prod_{i=1}^{N}[a_i,b_i]}+$$

$$\frac{\omega_1\left(f^{(m)},r\left\|\left(\widetilde{A}_n\left(\|\cdot-x_0\|_p^{m+1}\right)\right)(x_0)\right\|_{\infty,x_0\in\prod_{i=1}^{N}[a_i,b_i]}^{\frac{1}{m+1}}\right)}{rm!}$$

$$\left\|\left(\widetilde{A}_n\left(\|\cdot-x_0\|_p^{m+1}\right)\right)(x_0)\right\|_{\infty,x_0\in\prod_{i=1}^{N}[a_i,b_i]}^{\left(\frac{m}{m+1}\right)} \tag{58}$$

$$\left[\frac{1}{(m+1)}+\frac{r}{2}+\frac{mr^2}{8}\right].$$

We need

Lemma 12 *The function* $\left(\widetilde{A}_n\left(\|\cdot-x_0\|_p^m\right)\right)(x_0)$ *is continuous in* $x_0\in\left(\prod_{i=1}^{N}[a_i,b_i]\right)$, $m\in\mathbb{N}$.

Proof. By Lemma 10.3, [15], p. 272.

Remark 13 *By Remark 10.4 [15], p.273, we get that*

$$\left\|\left(\widetilde{A}_n\left(\|\cdot-x_0\|_p^k\right)\right)(x_0)\right\|_{\infty,x_0\in\prod_{i=1}^{N}[a_i,b_i]}\leq\left\|\left(\widetilde{A}_n\left(\|\cdot-x_0\|_p^{m+1}\right)\right)(x_0)\right\|_{\infty,x_0\in\prod_{i=1}^{N}[a_i,b_i]}^{\left(\frac{k}{m+1}\right)}, \tag{59}$$

for all $k=1,...,m$.

■

We give

Corollary 14 *(to Theorem 11, case of* $m=1$*) Then*

1)

$$\|(A_n(f))(x_0)-f(x_0)\|_\gamma\leq\left\|\left(A_n\left(f^{(1)}(x_0)(\cdot-x_0)\right)\right)(x_0)\right\|_\gamma+$$

$$\frac{1}{2r}\omega_1\left(f^{(1)},r\left(\left(\widetilde{A}_n\left(\|\cdot-x_0\|_p^2\right)\right)(x_0)\right)^{\frac{1}{2}}\right)\left(\left(\widetilde{A}_n\left(\|\cdot-x_0\|_p^2\right)\right)(x_0)\right)^{\frac{1}{2}} \tag{60}$$

$$\left[1+r+\frac{r^2}{4}\right],$$

and

2)

$$\left\|\|(A_n(f))-f\|_\gamma\right\|_{\infty,\prod_{i=1}^{N}[a_i,b_i]}\leq$$

$$\left\|\left\|\left(A_n\left(f^{(1)}(x_0)(\cdot - x_0)\right)\right)(x_0)\right\|_{\gamma}\right\|_{\infty, x_0 \in \prod_{i=1}^{N}[a_i,b_i]} +$$

$$\frac{1}{2r}\omega_1\left(f^{(1)}, r\left\|\left(\widetilde{A}_n\left(\|\cdot - x_0\|_p^2\right)\right)(x_0)\right\|^{\frac{1}{2}}_{\infty, x_0 \in \prod_{i=1}^{N}[a_i,b_i]}\right)$$

$$\left\|\left(\widetilde{A}_n\left(\|\cdot - x_0\|_p^2\right)\right)(x_0)\right\|^{\frac{1}{2}}_{\infty, x_0 \in \prod_{i=1}^{N}[a_i,b_i]}\left[1 + r + \frac{r^2}{4}\right], \tag{61}$$

$r > 0$.

We make

Remark 15 *We estimate* $0 < \alpha < 1$, $\lambda > 0$, $m, n \in \mathbb{N} : n^{1-\alpha} > 2$,

$$\widetilde{A}_n\left(\|\cdot - x_0\|_\infty^{m+1}\right)(x_0) = \frac{\sum_{k=\lceil na \rceil}^{\lfloor nb \rfloor}\left\|\frac{k}{n} - x_0\right\|_\infty^{m+1} Z(nx_0 - k)}{\sum_{k=\lceil na \rceil}^{\lfloor nb \rfloor} Z(nx_0 - k)} \overset{(19)}{<}$$

$$\left(\frac{4}{\tanh 2\lambda}\right)^N \sum_{k=\lceil na \rceil}^{\lfloor nb \rfloor}\left\|\frac{k}{n} - x_0\right\|_\infty^{m+1} Z(nx_0 - k) = \tag{62}$$

$$\left(\frac{4}{\tanh 2\lambda}\right)^N \left\{ \sum_{\substack{k = \lceil na \rceil \\ : \left\|\frac{k}{n} - x_0\right\|_\infty \le \frac{1}{n^\alpha}}}^{\lfloor nb \rfloor} \left\|\frac{k}{n} - x_0\right\|_\infty^{m+1} Z(nx_0 - k) + \right.$$

$$\left. \sum_{\substack{k = \lceil na \rceil \\ : \left\|\frac{k}{n} - x_0\right\|_\infty > \frac{1}{n^\alpha}}}^{\lfloor nb \rfloor} \left\|\frac{k}{n} - x_0\right\|_\infty^{m+1} Z(nx_0 - k) \right\} \overset{(20)}{\le}$$

$$\left(\frac{4}{\tanh 2\lambda}\right)^N \left\{\frac{1}{n^{\alpha(m+1)}} + \frac{e^{4\lambda}\|b - a\|_\infty^{m+1}}{e^{2\lambda(n^{1-\beta})}}\right\}, \tag{63}$$

(where $b - a = (b_1 - a_1, ..., b_N - a_N)$*).*

We have proved that ($\forall\ x_0 \in \prod_{i=1}^{N}[a_i, b_i]$)

$$\widetilde{A}_n\left(\|\cdot - x_0\|_\infty^{m+1}\right)(x_0) < \left(\frac{4}{\tanh 2\lambda}\right)^N \left\{\frac{1}{n^{\alpha(m+1)}} + \frac{e^{4\lambda}\|b - a\|_\infty^{m+1}}{e^{2\lambda(n^{1-\beta})}}\right\} =: \Lambda_1(n) \tag{64}$$

($0<\alpha<1$, $m,n\in\mathbb{N}:n^{1-\alpha}>2$, $\lambda>0$).

And, consequently it holds

$$\left\|\widetilde{A}_n\left(\|\cdot-x_0\|_\infty^{m+1}\right)(x_0)\right\|_{\infty,x_0\in\prod_{i=1}^{N}[a_i,b_i]}<$$

$$\left(\frac{4}{\tanh 2\lambda}\right)^N\left\{\frac{1}{n^{\alpha(m+1)}}+\frac{e^{4\lambda}\|b-a\|_\infty^{m+1}}{e^{2\lambda(n^{1-\beta})}}\right\}=\Lambda_1(n)\to 0,\quad as\ n\to+\infty. \tag{65}$$

So, we have that $\Lambda_1(n)\to 0$, as $n\to+\infty$. Thus, when $p\in[1,\infty]$, from Theorem 11 we have the convergence to zero in the right hand sides of parts (1), (2).

Next we estimate $\left\|\left(\widetilde{A}_n\left(f^{(j)}(x_0)(\cdot-x_0)^j\right)\right)(x_0)\right\|_\gamma$.

We have that

$$\left(\widetilde{A}_n\left(f^{(j)}(x_0)(\cdot-x_0)^j\right)\right)(x_0)=\frac{\sum_{k=\lceil na\rceil}^{\lfloor nb\rfloor}f^{(j)}(x_0)\left(\frac{k}{n}-x_0\right)^jZ(nx_0-k)}{\sum_{k=\lceil na\rceil}^{\lfloor nb\rfloor}Z(nx_0-k)}. \tag{66}$$

When $p=\infty$, $j=1,...,m$, we obtain

$$\left\|f^{(j)}(x_0)\left(\frac{k}{n}-x_0\right)^j\right\|_\gamma\le\left\|f^{(j)}(x_0)\right\|\left\|\frac{k}{n}-x_0\right\|_\infty^j. \tag{67}$$

We further have that

$$\left\|\left(\widetilde{A}_n\left(f^{(j)}(x_0)(\cdot-x_0)^j\right)\right)(x_0)\right\|_\gamma\overset{(19)}{<}$$

$$\left(\frac{4}{\tanh 2\lambda}\right)^N\left(\sum_{k=\lceil na\rceil}^{\lfloor nb\rfloor}\left\|f^{(j)}(x_0)\left(\frac{k}{n}-x_0\right)^j\right\|_\gamma Z(nx_0-k)\right)\le$$

$$\left(\frac{4}{\tanh 2\lambda}\right)^N\left(\sum_{k=\lceil na\rceil}^{\lfloor nb\rfloor}\left\|f^{(j)}(x_0)\right\|\left\|\frac{k}{n}-x_0\right\|_\infty^jZ(nx_0-k)\right)= \tag{68}$$

$$\left(\frac{4}{\tanh 2\lambda}\right)^N\left\|f^{(j)}(x_0)\right\|\left(\sum_{k=\lceil na\rceil}^{\lfloor nb\rfloor}\left\|\frac{k}{n}-x_0\right\|_\infty^jZ(nx_0-k)\right)=$$

$$\left(\frac{4}{\tanh 2\lambda}\right)^N\left\|f^{(j)}(x_0)\right\|\left\{\sum_{\substack{k=\lceil na\rceil\\ :\left\|\frac{k}{n}-x_0\right\|_\infty\le\frac{1}{n^\alpha}}}^{\lfloor nb\rfloor}\left\|\frac{k}{n}-x_0\right\|_\infty^jZ(nx_0-k)\right.$$

17

$$\left. + \sum_{\substack{k = \lceil na \rceil \\ : \left\| \frac{k}{n} - x_0 \right\|_\infty > \frac{1}{n^\alpha}}}^{\lfloor nb \rfloor} \left\| \frac{k}{n} - x_0 \right\|_\infty^j Z(nx_0 - k) \right\} \overset{(20)}{\leq} \tag{69}$$

$$\left(\frac{4}{\tanh 2\lambda} \right)^N \left\| f^{(j)}(x_0) \right\| \left\{ \frac{1}{n^{\alpha j}} + \frac{e^{4\lambda} \|b - a\|_\infty^j}{e^{2\lambda(n^{1-\beta})}} \right\} \to 0, \text{ as } n \to \infty.$$

That is

$$\left\| \left(\widetilde{A}_n \left(f^{(j)}(x_0) (\cdot - x_0)^j \right) \right) (x_0) \right\|_\gamma \to 0, \text{ as } n \to \infty.$$

Therefore when $p = \infty$*, for* $j = 1, ..., m$*, we have proved:*

$$\left\| \left(\widetilde{A}_n \left(f^{(j)}(x_0) (\cdot - x_0)^j \right) \right) (x_0) \right\|_\gamma <$$

$$\left(\frac{4}{\tanh 2\lambda} \right)^N \left\| f^{(j)}(x_0) \right\| \left\{ \frac{1}{n^{\alpha j}} + \frac{e^{4\lambda} \|b - a\|_\infty^j}{e^{2\lambda(n^{1-\beta})}} \right\} \leq$$

$$\left(\frac{4}{\tanh 2\lambda} \right)^N \left\| f^{(j)}(x_0) \right\|_\infty \left\{ \frac{1}{n^{\alpha j}} + \frac{e^{4\lambda} \|b - a\|_\infty^j}{e^{2\lambda(n^{1-\beta})}} \right\} =: \Lambda_{2j}(n) < \infty, \tag{70}$$

and converges to zero, as $n \to \infty$.

We conclude:

In Theorem 11, the right hand sides of (57) and (58) converge to zero as $n \to \infty$, for any $p \in [1, \infty]$.

Also in Corollary 14, the right hand sides of (60) and (61) converge to zero as $n \to \infty$, for any $p \in [1, \infty]$.

Conclusion 16 *We have proved that the left hand sides of (55), (56), (57), (58) and (60), (61) converge to zero as* $n \to \infty$*, for* $p \in [1, \infty]$*. Consequently* $A_n \to I$ *(unit operator) pointwise and uniformly, as* $n \to \infty$*, where* $p \in [1, \infty]$*. In the presence of initial conditions we achieve a higher speed of convergence, see (56). Higher speed of convergence happens also to the left hand side of (55).*

We further give

Corollary 17 *(to Theorem 11) Let* O *open subset of* $\left(\mathbb{R}^N, \|\cdot\|_\infty\right)$*, such that* $\prod_{i=1}^N [a_i, b_i] \subset O \subseteq \mathbb{R}^N$*, and let* $\left(X, \|\cdot\|_\gamma\right)$ *be a general Banach space. Let* $m \in \mathbb{N}$ *and* $f \in C^m(O, X)$*, the space of* m*-times continuously Fréchet differentiable functions from* O *into* X*. We study the approximation of* $f|_{\prod_{i=1}^N [a_i, b_i]}$*. Let* $x_0 \in$

$\left(\prod_{i=1}^{N}[a_i,b_i]\right)$ and $r>0$. Here $\Lambda_1(n)$ as in (65) and $\Lambda_{2j}(n)$ as in (70), where $n\in\mathbb{N}: n^{1-\alpha}>2$, $0<\alpha<1$, $\lambda>0$, $j=1,\dots,m$. Then

1)

$$\left\|(A_n(f))(x_0)-\sum_{j=0}^{m}\frac{1}{j!}\left(A_n\left(f^{(j)}(x_0)(\cdot-x_0)^j\right)\right)(x_0)\right\|_\gamma\le$$

$$\frac{\omega_1\left(f^{(m)},r(\Lambda_1(n))^{\frac{1}{m+1}}\right)}{rm!}(\Lambda_1(n))^{\left(\frac{m}{m+1}\right)}\left[\frac{1}{(m+1)}+\frac{r}{2}+\frac{mr^2}{8}\right],\tag{71}$$

2) additionally, if $f^{(j)}(x_0)=0$, $j=1,\dots,m$, we have

$$\|(A_n(f))(x_0)-f(x_0)\|_\gamma\le$$

$$\frac{\omega_1\left(f^{(m)},r(\Lambda_1(n))^{\frac{1}{m+1}}\right)}{rm!}(\Lambda_1(n))^{\left(\frac{m}{m+1}\right)}\left[\frac{1}{(m+1)}+\frac{r}{2}+\frac{mr^2}{8}\right],\tag{72}$$

3)

$$\left\|\|A_n(f)-f\|_\gamma\right\|_{\infty,\prod_{i=1}^{N}[a_i,b_i]}\le\sum_{j=1}^{m}\frac{\Lambda_{2j}(n)}{j!}+$$

$$\frac{\omega_1\left(f^{(m)},r(\Lambda_1(n))^{\frac{1}{m+1}}\right)}{rm!}(\Lambda_1(n))^{\left(\frac{m}{m+1}\right)}$$

$$\left[\frac{1}{(m+1)}+\frac{r}{2}+\frac{mr^2}{8}\right]=:\Lambda_3(n)\to 0,\text{ as } n\to\infty.\tag{73}$$

We continue with

Theorem 18 *Let $f\in C_B(\mathbb{R}^N,X)$, $0<\beta<1$, $\lambda>0$, $x\in\mathbb{R}^N, N,n\in\mathbb{N}$ with $n^{1-\beta}>2$, ω_1 is for $p=\infty$. Then*

1)

$$\|B_n(f,x)-f(x)\|_\gamma\le\omega_1\left(f,\frac{1}{n^\beta}\right)+\frac{e^{4\lambda}\left\|\|f\|_\gamma\right\|_\infty}{e^{2\lambda(n^{1-\beta})}}=:\Omega_2(n),\tag{74}$$

2)

$$\left\|\|B_n(f)-f\|_\gamma\right\|_\infty\le\Omega_2(n).\tag{75}$$

Given that $f\in\left(C_U(\mathbb{R}^N,X)\cap C_B(\mathbb{R}^N,X)\right)$, we obtain $\lim_{n\to\infty}B_n(f)=f$, uniformly. The speed of convergence above is $\max\left(\frac{1}{n^\beta},\frac{1}{e^{2\lambda n^{(1-\beta)}}}\right)=\frac{1}{n^\beta}$.

Proof. We have that

$$B_n(f,x) - f(x) \overset{(13)}{=} \sum_{k=-\infty}^{\infty} f\left(\frac{k}{n}\right) Z(nx-k) - f(x) \sum_{k=-\infty}^{\infty} Z(nx-k) = \tag{76}$$

$$\sum_{k=-\infty}^{\infty} \left(f\left(\frac{k}{n}\right) - f(x) \right) Z(nx-k).$$

Hence

$$\left\| B_n(f,x) - f(x) \right\|_\gamma \leq \sum_{k=-\infty}^{\infty} \left\| f\left(\frac{k}{n}\right) - f(x) \right\|_\gamma Z(nx-k) =$$

$$\sum_{\substack{k=-\infty \\ \left\| \frac{k}{n} - x \right\|_\infty \leq \frac{1}{n^\beta}}}^{\infty} \left\| f\left(\frac{k}{n}\right) - f(x) \right\|_\gamma Z(nx-k) +$$

$$\sum_{\substack{k=-\infty \\ \left\| \frac{k}{n} - x \right\|_\infty > \frac{1}{n^\beta}}}^{\infty} \left\| f\left(\frac{k}{n}\right) - f(x) \right\|_\gamma Z(nx-k) \overset{(13)}{\leq}$$

$$\omega_1\left(f, \frac{1}{n^\beta}\right) + 2 \left\| \|f\|_\gamma \right\|_\infty \sum_{\substack{k=-\infty \\ \left\| \frac{k}{n} - x \right\|_\infty > \frac{1}{n^\beta}}}^{\infty} Z(nx-k) \overset{(20)}{\leq}$$

$$\omega_1\left(f, \frac{1}{n^\beta}\right) + \frac{2e^{4\lambda} \left\| \|f\|_\gamma \right\|_\infty}{e^{2\lambda\left(n^{1-\beta}\right)}}, \tag{77}$$

proving the claim. ■

We give

Theorem 19 *Let $f \in C_B\left(\mathbb{R}^N, X\right)$, $0 < \beta < 1$, $x \in \mathbb{R}^N$, $\lambda > 0, N, n \in \mathbb{N}$ with $n^{1-\beta} > 2$, ω_1 is for $p = \infty$. Then*

1)

$$\left\| C_n(f,x) - f(x) \right\|_\gamma \leq \omega_1\left(f, \frac{1}{n} + \frac{1}{n^\beta}\right) + \frac{2e^{4\lambda} \left\| \|f\|_\gamma \right\|_\infty}{e^{2\lambda\left(n^{1-\beta}\right)}} =: \Omega_3(n), \tag{78}$$

2)

$$\left\| \left\| C_n(f) - f \right\|_\gamma \right\|_\infty \leq \Omega_3(n). \tag{79}$$

Given that $f \in \left(C_U\left(\mathbb{R}^N, X\right) \cap C_B\left(\mathbb{R}^N, X\right)\right)$, we obtain $\lim_{n\to\infty} C_n(f) = f$, uniformly.

Proof. We notice that

$$\int_{\frac{k}{n}}^{\frac{k+1}{n}} f(t)\,dt = \int_{\frac{k_1}{n}}^{\frac{k_1+1}{n}} \int_{\frac{k_2}{n}}^{\frac{k_2+1}{n}} ... \int_{\frac{k_N}{n}}^{\frac{k_N+1}{n}} f(t_1, t_2, ..., t_N)\,dt_1 dt_2 ... dt_N =$$

$$\int_0^{\frac{1}{n}} \int_0^{\frac{1}{n}} ... \int_0^{\frac{1}{n}} f\left(t_1 + \frac{k_1}{n}, t_2 + \frac{k_2}{n}, ..., t_N + \frac{k_N}{n}\right) dt_1 ... dt_N = \int_0^{\frac{1}{n}} f\left(t + \frac{k}{n}\right) dt. \tag{80}$$

Thus it holds (by (35))

$$C_n(f, x) = \sum_{k=-\infty}^{\infty} \left(n^N \int_0^{\frac{1}{n}} f\left(t + \frac{k}{n}\right) dt\right) Z(nx - k). \tag{81}$$

We observe that

$$\|C_n(f, x) - f(x)\|_\gamma =$$

$$\left\| \sum_{k=-\infty}^{\infty} \left(n^N \int_0^{\frac{1}{n}} f\left(t + \frac{k}{n}\right) dt\right) Z(nx - k) - \sum_{k=-\infty}^{\infty} f(x) Z(nx - k) \right\|_\gamma =$$

$$\left\| \sum_{k=-\infty}^{\infty} \left(\left(n^N \int_0^{\frac{1}{n}} f\left(t + \frac{k}{n}\right) dt\right) - f(x)\right) Z(nx - k) \right\|_\gamma =$$

$$\left\| \sum_{k=-\infty}^{\infty} \left(n^N \int_0^{\frac{1}{n}} \left(f\left(t + \frac{k}{n}\right) - f(x)\right) dt\right) Z(nx - k) \right\|_\gamma \leq \tag{82}$$

$$\sum_{k=-\infty}^{\infty} \left(n^N \int_0^{\frac{1}{n}} \left\| f\left(t + \frac{k}{n}\right) - f(x) \right\|_\gamma dt\right) Z(nx - k) =$$

$$\sum_{\begin{cases} k = -\infty \\ \left\|\frac{k}{n} - x\right\|_\infty \leq \frac{1}{n^\beta} \end{cases}}^{\infty} \left(n^N \int_0^{\frac{1}{n}} \left\| f\left(t + \frac{k}{n}\right) - f(x) \right\|_\gamma dt\right) Z(nx - k) +$$

$$\sum_{\begin{cases} k = -\infty \\ \left\|\frac{k}{n} - x\right\|_\infty > \frac{1}{n^\beta} \end{cases}}^{\infty} \left(n^N \int_0^{\frac{1}{n}} \left\| f\left(t + \frac{k}{n}\right) - f(x) \right\|_\gamma dt\right) Z(nx - k) \leq$$

$$\sum_{\begin{cases} k = -\infty \\ \left\|\frac{k}{n} - x\right\|_\infty \leq \frac{1}{n^\beta} \end{cases}}^{\infty} \left(n^N \int_0^{\frac{1}{n}} \omega_1\left(f, \|t\|_\infty + \left\|\frac{k}{n} - x\right\|_\infty\right) dt\right) Z(nx - k) +$$

21

$$2\left\|\|f\|_{\gamma}\right\|_{\infty}\left(\sum_{\substack{k=-\infty \\ \left\|\frac{k}{n}-x\right\|_{\infty}>\frac{1}{n^{\beta}}}}^{\infty} Z(|nx-k|)\right)\leq$$

$$\omega_{1}\left(f,\frac{1}{n}+\frac{1}{n^{\beta}}\right)+\frac{2e^{4\lambda}\left\|\|f\|_{\gamma}\right\|_{\infty}}{e^{2\lambda\left(n^{1-\beta}\right)}}, \tag{83}$$

proving the claim. ■

We also present

Theorem 20 *Let* $f\in C_{B}\left(\mathbb{R}^{N},X\right)$, $0<\beta<1$, $x\in\mathbb{R}^{N}$, $\lambda>0, N,n\in\mathbb{N}$ *with* $n^{1-\beta}>2$, ω_{1} *is for* $p=\infty$. *Then*

1)

$$\left\|D_{n}(f,x)-f(x)\right\|_{\gamma}\leq\omega_{1}\left(f,\frac{1}{n}+\frac{1}{n^{\beta}}\right)+\frac{2e^{4\lambda}\left\|\|f\|_{\gamma}\right\|_{\infty}}{e^{2\lambda\left(n^{1-\beta}\right)}}=:\Omega_{4}(n), \tag{84}$$

2)

$$\left\|\left\|D_{n}(f)-f\right\|_{\gamma}\right\|_{\infty}\leq\Omega_{4}(n). \tag{85}$$

Given that $f\in\left(C_{U}\left(\mathbb{R}^{N},X\right)\cap C_{B}\left(\mathbb{R}^{N},X\right)\right)$, *we obtain* $\lim_{n\to\infty}D_{n}(f)=f$, *uniformly.*

Proof. We have that (by (37))

$$\left\|D_{n}(f,x)-f(x)\right\|_{\gamma}=\left\|\sum_{k=-\infty}^{\infty}\delta_{nk}(f)Z(nx-k)-\sum_{k=-\infty}^{\infty}f(x)Z(nx-k)\right\|_{\gamma}=$$

$$\left\|\sum_{k=-\infty}^{\infty}\left(\delta_{nk}(f)-f(x)\right)Z(nx-k)\right\|_{\gamma}=\left\|\sum_{k=-\infty}^{\infty}\omega_{r}\left(f\left(\frac{k}{n}+\frac{r}{n\theta}\right)-f(x)\right)Z(nx-k)\right\|_{\gamma}\leq$$

$$\sum_{k=-\infty}^{\infty}\left(\sum_{r=0}^{\theta}\omega_{r}\left\|f\left(\frac{k}{n}+\frac{r}{n\theta}\right)-f(x)\right\|_{\gamma}\right)Z(nx-k)=$$

$$\sum_{\substack{k=-\infty \\ \left\|\frac{k}{n}-x\right\|_{\infty}\leq\frac{1}{n^{\beta}}}}^{\infty}\left(\sum_{r=0}^{\theta}\omega_{r}\left\|f\left(\frac{k}{n}+\frac{r}{n\theta}\right)-f(x)\right\|_{\gamma}\right)Z(nx-k)+$$

22

$$\sum_{\begin{cases} k=-\infty \\ \left\|\frac{k}{n}-x\right\|_{\infty} > \frac{1}{n^{\beta}} \end{cases}}^{\infty} \left(\sum_{r=0}^{\theta} \omega_r \left\| f\left(\frac{k}{n}+\frac{r}{n\theta}\right) - f(x) \right\|_{\gamma} \right) Z(nx-k) \leq$$

$$\sum_{\begin{cases} k=-\infty \\ \left\|\frac{k}{n}-x\right\|_{\infty} \leq \frac{1}{n^{\beta}} \end{cases}}^{\infty} \left(\sum_{r=0}^{\theta} \omega_r \left\| f\left(\frac{k}{n}+\frac{r}{n\theta}\right) - f(x) \right\|_{\gamma} \right) Z(nx-k) +$$

$$2\left\| \|f\|_{\gamma} \right\|_{\infty} \left(\sum_{\begin{cases} k=-\infty \\ \left\|\frac{k}{n}-x\right\|_{\infty} > \frac{1}{n^{\beta}} \end{cases}}^{\infty} (Z(nx-k)) \right) \leq$$

$$\omega_1\left(f, \frac{1}{n}+\frac{1}{n^{\beta}}\right) + \frac{2e^{4\lambda}\left\| \|f\|_{\gamma} \right\|_{\infty}}{e^{2\lambda\left(n^{1-\beta}\right)}} = \Omega_4(n),$$

proving the claim. ■

Next we perform multi layer neural network approximations.

We make

Definition 21 *Let* $f \in C_B\left(\mathbb{R}^N, X\right)$, $N \in \mathbb{N}$, *where* $\left(X, \|\cdot\|_{\gamma}\right)$ *is a Banach space. We define the general neural network operator*

$$F_n(f,x) := \sum_{k=-\infty}^{\infty} l_{nk}(f)\, Z(nx-k) =$$

$$\begin{cases} B_n(f,x), & \text{if } l_{nk}(f) = f\left(\frac{k}{n}\right), \\ C_n(f,x), & \text{if } l_{nk}(f) = n^N \int_{\frac{k}{n}}^{\frac{k+1}{n}} f(t)\,dt, \\ D_n(f,x), & \text{if } l_{nk}(f) = \delta_{nk}(f). \end{cases} \tag{86}$$

Clearly $l_{nk}(f)$ is an X-valued bounded linear functional such that $\|l_{nk}(f)\|_{\gamma} \leq \left\| \|f\|_{\gamma} \right\|_{\infty}$.

Hence $F_n(f)$ is a bounded linear operator with $\left\| \|F_n(f)\|_{\gamma} \right\|_{\infty} \leq \left\| \|f\|_{\gamma} \right\|_{\infty}$.

We need

Theorem 22 *Let* $f \in C_B\left(\mathbb{R}^N, X\right)$, $N \geq 1$. *Then* $F_n(f) \in C_B\left(\mathbb{R}^N, X\right)$.

Proof. Lengthy and similar to the proof of Theorem 11 of [18], as such is omitted. ■

Remark 23 *By (22) it is obvious that* $\left\| \left\| A_n(f) \right\|_\gamma \right\|_\infty \leq \left\| \left\| f \right\|_\gamma \right\|_\infty < \infty$, *and* $A_n(f) \in C\left(\prod_{i=1}^{N} [a_i, b_i], X\right)$, *given that* $f \in C\left(\prod_{i=1}^{N} [a_i, b_i], X\right)$.

Call K_n *any of the operators* A_n, B_n, C_n, D_n.

Clearly then

$$\left\| \left\| K_n^2(f) \right\|_\gamma \right\|_\infty = \left\| \left\| K_n(K_n(f)) \right\|_\gamma \right\|_\infty \leq \left\| \left\| K_n(f) \right\|_\gamma \right\|_\infty \leq \left\| \left\| f \right\|_\gamma \right\|_\infty, \tag{87}$$

etc.

Therefore we get

$$\left\| \left\| K_n^k(f) \right\|_\gamma \right\|_\infty \leq \left\| \left\| f \right\|_\gamma \right\|_\infty, \ \forall\, k \in \mathbb{N}, \tag{88}$$

the contraction property.

Also we see that

$$\left\| \left\| K_n^k(f) \right\|_\gamma \right\|_\infty \leq \left\| \left\| K_n^{k-1}(f) \right\|_\gamma \right\|_\infty \leq \ldots \leq \left\| \left\| K_n(f) \right\|_\gamma \right\|_\infty \leq \left\| \left\| f \right\|_\gamma \right\|_\infty. \tag{89}$$

Here K_n^k *are bounded linear operators.*

Notation 24 *Here* $N \in \mathbb{N}$, $0 < \beta < 1$. *Denote by*

$$c_N := \begin{cases} \left(\frac{4}{\tanh 2\lambda}\right)^N, & \text{if } K_n = A_n, \\ 1, & \text{if } K_n = B_n, C_n, D_n, \end{cases} \tag{90}$$

$$\Lambda(n) := \begin{cases} \frac{1}{n^\beta}, & \text{if } K_n = A_n,\ B_n, \\ \frac{1}{n} + \frac{1}{n^\beta}, & \text{if } K_n = C_n, D_n, \end{cases} \tag{91}$$

$$\Gamma := \begin{cases} C\left(\prod_{i=1}^{N} [a_i, b_i], X\right), & \text{if } K_n = A_n, \\ C_B\left(\mathbb{R}^N, X\right), & \text{if } K_n = B_n, C_n, D_n, \end{cases} \tag{92}$$

and

$$Y := \begin{cases} \prod_{i=1}^{N} [a_i, b_i], & \text{if } K_n = A_n, \\ \mathbb{R}^N, & \text{if } K_n = B_n, C_n, D_n. \end{cases} \tag{93}$$

We give the condensed

Theorem 25 *Let* $f \in \Gamma$, $0 < \beta < 1$, $x \in Y$; $n, \lambda > 0$; $N \in \mathbb{N}$ *with* $n^{1-\beta} > 2$. *Then*

(i)

$$\left\| K_n(f, x) - f(x) \right\|_\gamma \leq c_N \left[\omega_1(f, \Lambda(n)) + \frac{2e^{4\lambda} \left\| \left\| f \right\|_\gamma \right\|_\infty}{e^{2\lambda(n^{1-\beta})}} \right] =: \tau(n), \tag{94}$$

24

where ω_1 *is for* $p = \infty$,

and

(ii)

$$\left\| \left\| K_n(f) - f \right\|_\gamma \right\|_\infty \leq \tau(n) \to 0, \text{ as } n \to \infty. \tag{95}$$

For f *uniformly continuous and in* Γ *we obtain*

$$\lim_{n\to\infty} K_n(f) = f,$$

pointwise and uniformly.

Proof. By Theorems 9, 18, 19, 20. ■

Next we do iterated, multi layer neural network approximation. (see also [10]).

We make

Remark 26 *Let* $r \in \mathbb{N}$ *and* K_n *as above. We observe that*

$$K_n^r f - f = \left(K_n^r f - K_n^{r-1} f\right) + \left(K_n^{r-1} f - K_n^{r-2} f\right) +$$

$$\left(K_n^{r-2} f - K_n^{r-3} f\right) + ... + \left(K_n^2 f - K_n f\right) + \left(K_n f - f\right).$$

Then

$$\left\| \left\| K_n^r f - f \right\|_\gamma \right\|_\infty \leq \left\| \left\| K_n^r f - K_n^{r-1} f \right\|_\gamma \right\|_\infty + \left\| \left\| K_n^{r-1} f - K_n^{r-2} f \right\|_\gamma \right\|_\infty +$$

$$\left\| \left\| K_n^{r-2} f - K_n^{r-3} f \right\|_\gamma \right\|_\infty + ... + \left\| \left\| K_n^2 f - K_n f \right\|_\gamma \right\|_\infty + \left\| \left\| K_n f - f \right\|_\gamma \right\|_\infty =$$

$$\left\| \left\| K_n^{r-1}(K_n f - f) \right\|_\gamma \right\|_\infty + \left\| \left\| K_n^{r-2}(K_n f - f) \right\|_\gamma \right\|_\infty + \left\| \left\| K_n^{r-3}(K_n f - f) \right\|_\gamma \right\|_\infty + ... +$$

$$\left\| \left\| K_n(K_n f - f) \right\|_\gamma \right\|_\infty + \left\| \left\| K_n f - f \right\|_\gamma \right\|_\infty \leq r \left\| \left\| K_n f - f \right\|_\gamma \right\|_\infty.$$

That is

$$\left\| \left\| K_n^r f - f \right\|_\gamma \right\|_\infty \leq r \left\| \left\| K_n f - f \right\|_\gamma \right\|_\infty. \tag{96}$$

We give

Theorem 27 *All here as in Theorem 25 and* $r \in \mathbb{N}$, $\tau(n)$ *as in (94). Then*

$$\left\| \left\| K_n^r f - f \right\|_\gamma \right\|_\infty \leq r\tau(n). \tag{97}$$

So that the speed of convergence to the unit operator of K_n^r *is not worse than of* K_n.

Proof. As similar to [18] is omitted. ■

Remark 28 *Let* $m_1, m_2, ..., m_r \in \mathbb{N} : m_1 \leq m_2 \leq ... \leq m_r$, $0 < \beta < 1, \lambda > 0$, $f \in \Gamma$. *Then*

$$\Lambda(m_1) \geq \Lambda(m_2) \geq ... \geq \Lambda(m_r), \ \Lambda \text{ as in (91).}$$

Therefore

$$\omega_1(f, \Lambda(m_1)) \geq \omega_1(f, \Lambda(m_2)) \geq ... \geq \omega_1(f, \Lambda(m_r)).$$

Assıme further that $m_i^{(1-\beta)} > 2$, $i = 1, ..., r$. *Then*

$$\frac{e^{4\lambda}}{e^{2\lambda m_1^{(1-\beta)}}} \geq \frac{e^{4\lambda}}{e^{\lambda m_2^{(1-\beta)}}} \geq ... \geq \frac{e^{4\lambda}}{e^{\lambda m_r^{(1-\beta)}}}.$$

Let K_{m_i} *as above,* $i = 1, ..., r$, *all of the same kind. We write*

$$K_{m_r}\left(K_{m_{r-1}}\left(...K_{m_2}\left(K_{m_1 f}\right)\right)\right) - f =$$

$$K_{m_r}\left(K_{m_{r-1}}\left(...K_{m_2}\left(K_{m_1 f}\right)\right)\right) - K_{m_r}\left(K_{m_{r-1}}\left(...K_{m_2} f\right)\right) +$$
$$K_{m_r}\left(K_{m_{r-1}}\left(...K_{m_2} f\right)\right) - K_{m_r}\left(K_{m_{r-1}}\left(...K_{m_3} f\right)\right) +$$
$$K_{m_r}\left(K_{m_{r-1}}\left(...K_{m}3f\right)\right) - K_{m_r}\left(K_{m_{r-1}}\left(...K_{m_4} f\right)\right) + ...+$$
$$K_{m_r}\left(K_{m_{r-1}} f\right) - K_{m_r} f + K_{m_r} f - f =$$
$$K_{m_r}\left(K_{m_{r-1}}\left(...K_{m_2}\right)\right)\left(K_{m_1} f - f\right) + K_{m_r}\left(K_{m_{r-1}}\left(...K_{m_3}\right)\right)\left(K_{m_2} f - f\right) +$$
$$K_{m_r}\left(K_{m_{r-1}}\left(...K_{m_4}\right)\right)\left(K_{m}3f - f\right) + ... + K_{m_r}\left(K_{m_{r-1}} f - f\right) + K_{m_r} f - f.$$

Hence by the triangle inequality of $\left\|\left\|\cdot\right\|_\gamma\right\|_\infty$ *we get*

$$\left\|\left\|K_{m_r}\left(K_{m_{r-1}}\left(...K_{m_2}\left(K_{m_1} f\right)\right)\right) - f\right\|_\gamma\right\|_\infty \leq$$

$$\left\|\left\|K_{m_r} K_{m_{r-1}} ...K_{m_2}\left(K_{m_1} f - f\right)\right\|_\gamma\right\|_\infty +$$

$$\left\|\left\|K_{m_r} K_{m_{r-1}} ...K_{m_2}\left(K_{m_1} f - f\right)\right\|_\gamma\right\|_\infty +$$

$$\left\|\left\|K_{m_r}\left(K_{m_{r-1}}\left(...K_{m_4}\right)\right)\left(K_{m}3f - f\right)\right\|_\gamma\right\|_\infty + ...+$$

$$\left\|\left\|K_{m_r}\left(K_{m_{r-1}} f - f\right)\right\|_\gamma\right\|_\infty + \left\|\left\|K_{m_r} f - f\right\|_\gamma\right\|_\infty \leq$$

(repeatedly applying (87))

$$\left\|\left\|K_{m_1} f - f\right\|_\gamma\right\|_\infty + \left\|\left\|K_{m_2} f - f\right\|_\gamma\right\|_\infty + \left\|\left\|K_{m_3} f - f\right\|_\gamma\right\|_\infty + ...+$$

$$\left\|\left\|K_{m_{r-1}} f - f\right\|_\gamma\right\|_\infty + \left\|\left\|K_{m_2} f - f\right\|_\gamma\right\|_\infty + \left\|\left\|K_{m_3} f - f\right\|_\gamma\right\|_\infty + ...+$$

$$\left\|\left\|K_{m_{r-1}}f-f\right\|_{\gamma}\right\|_{\infty}+\left\|\left\|K_{m_r}f-f\right\|_{\gamma}\right\|_{\infty}=_{i=1}^{r}\left\|\left\|K_{m_i}f-f\right\|_{\gamma}\right\|_{\infty}.$$

That is, we proved

$$\left\|\left\|K_{m_r}\left(K_{m_{r-1}}\left(...K_{m_2}\left(K_{m_1}f\right)\right)\right)-f\right\|_{\gamma}\right\|_{\infty}\leq_{i=1}^{r}\left\|\left\|K_{m_i}f-f\right\|_{\gamma}\right\|_{\infty}. \quad (98)$$

We also present

Theorem 29 *Let* $f\in\Gamma$; m, N, $m_1,m_2,...,m_r\in\mathbb{N}:m_1\leq m_2\leq...\leq m_r$, $0<\beta<1,\lambda>0$; $m_i^{(1-\beta)}>2$, $i=1,...,r$, $x\in Y$, *and let* $\left(K_{m_1},...,K_{m_r}\right)$ *as* $\left(A_{m_1},...,A_{m_r}\right)$ *or* $\left(B_{m_1},...,B_{m_r}\right)$ *or* $\left(C_{m_1},...,C_{m_r}\right)$ *or* $\left(D_{m_1},...,D_{m_r}\right)$, $p=\infty$. *Then*

$$\left\|K_{m_r}\left(K_{m_{r-1}}\left(...K_{m_2}\left(K_{m_1}f\right)\right)\right)(x)-f(x)\right\|_{\gamma}\leq$$

$$\left\|\left\|K_{m_r}\left(K_{m_{r-1}}\left(...K_{m_2}\left(K_{m_1}f\right)\right)\right)-f\right\|_{\gamma}\right\|_{\infty}\leq$$

$$\sum_{i=1}^{r}\left\|\left\|K_{m_i}f-f\right\|_{\gamma}\right\|_{\infty}\leq$$

$$c_N\sum_{i=1}^{r}\left[\omega_1\left(f,\Lambda\left(m_i\right)\right)+\frac{2e^{4\lambda}\left\|\left\|f\right\|_{\gamma}\right\|_{\infty}}{e^{2\lambda m_i^{(1-\beta)}}}\right]\leq$$

$$rc_N\left[\omega_1\left(f,\Lambda\left(m_1\right)\right)+\frac{2e^{4\lambda}\left\|\left\|f\right\|_{\gamma}\right\|_{\infty}}{e^{2\lambda m_1^{(1-\beta)}}}\right]. \quad (99)$$

Clearly, we notice that the speed of convergence to the unit operator of the multiply iterated multi layer operator is not worse than the speed of K_{m_1}.

Proof. As similar to [18] is omitted. ■

We continue with

Theorem 30 *Let all as in Corollary 17, and* $r\in\mathbb{N}$. *Here* $\Lambda_3(n)$ *is as in (73). Then*

$$\left\|\left\|A_n^r f-f\right\|_{\gamma}\right\|_{\infty}\leq r\left\|\left\|A_n f-f\right\|_{\gamma}\right\|_{\infty}\leq r\Lambda_3(n). \quad (100)$$

Proof. As similar to [18] is omitted. ■

Next we present some L_{p_1}, $p_1\geq1$, approximation related results.

Theorem 31 *Let* $p_1\geq1$, $f\in C\left(\prod_{i=1}^{n}\left[a_i,b_i\right],X\right)$, $0<\beta<1,\lambda>0$; $N,n\in\mathbb{N}$ *with* $n^{1-\beta}>2$, *and* $\Omega_1(n)$ *as in (38),* ω_1 *is for* $p=\infty$. *Then*

$$\left\|\left\|A_n f-f\right\|_{\gamma}\right\|_{p_1,\prod_{i=1}^{n}\left[a_i,b_i\right]}\leq\Omega_1(n)\left(\prod_{i=1}^{n}\left(b_i-a_i\right)\right)^{\frac{1}{p_1}}. \quad (101)$$

We notice that $\lim_{n\to\infty}\left\|\left\|A_n f-f\right\|_{\gamma}\right\|_{p_1,\prod_{i=1}^{n}\left[a_i,b_i\right]}=0$.

Proof. Obvious, by integrating (38), etc. ■

It follows

Theorem 32 *Let* $p_1 \geq 1$, $f \in C_B\left(\mathbb{R}^N, X\right)$, $0 < \beta < 1, \lambda > 0$; $N, n \in \mathbb{N}$ *with* $n^{1-\beta} > 2$, *and* ω_1 *is for* $p = \infty$; $\Omega_2(n)$ *as in (74) and* P *a compact set of* $\mathbb{R}^N$. *Then*

$$\left\| \left\| B_n f - f \right\|_\gamma \right\|_{p_1,\ P} \leq \Omega_2(n) \left| P \right|^{\frac{1}{p_1}}, \tag{102}$$

where $|P| < \infty$, *is the Lebesgue measure of* P. *We notice that* $\lim\limits_{n \to \infty} \left\| \left\| B_n f - f \right\|_\gamma \right\|_{p_1, P} = 0$ *for* $f \in \left(C_U\left(\mathbb{R}^N, X\right) \cap C_B\left(\mathbb{R}^N, X\right)\right)$.

Proof. By integrating (74), etc. ■

Next come

Theorem 33 *All as in Theorem 32, but we use* $\Omega_3(n)$ *of (78). Then*

$$\left\| \left\| C_n f - f \right\|_\gamma \right\|_{p_1,\ P} \leq \Omega_3(n) \left| P \right|^{\frac{1}{p_1}}. \tag{103}$$

We have that $\lim\limits_{n \to \infty} \left\| \left\| C_n f - f \right\|_\gamma \right\|_{p_1,\ P} = 0$ *for* $f \in \left(C_U\left(\mathbb{R}^N, X\right) \cap C_B\left(\mathbb{R}^N, X\right)\right)$.

Proof. By (78). ■

Theorem 34 *All as in Theorem 32, but we use* $\Omega_4(n)$ *of (84). Then*

$$\left\| \left\| D_n f - f \right\|_\gamma \right\|_{p_1,\ P} \leq \Omega_4(n) \left| P \right|^{\frac{1}{p_1}}. \tag{104}$$

We have that $\lim\limits_{n \to \infty} \left\| \left\| D_n f - f \right\|_\gamma \right\|_{p_1,\ P} = 0$ *for* $f \in \left(C_U\left(\mathbb{R}^N, X\right) \cap C_B\left(\mathbb{R}^N, X\right)\right)$.

Proof. By (84). ■

Application 35 *A typical application of all of our results is when* $\left(X, \left\|\cdot\right\|_\gamma\right) = (\mathbb{C}, |\cdot|)$, *where* $\mathbb{C}$ *is the set of the complex numbers.*

References

[1] G.A. Anastassiou, *Moments in Probability and Approximation Theory*, Pitman Research Notes in Math., Vol. 287, Longman Sci. & Tech., Harlow, U.K., 1993.

[2] G.A. Anastassiou, *Rate of convergence of some neural network operators to the unit-univariate case*, J. Math. Anal. Appli. 212 (1997), 237-262.

[3] G.A. Anastassiou, *Quantitative Approximations*, Chapman&Hall/CRC, Boca Raton, New York, 2001.

[4] G.A. Anastassiou, *Intelligent Systems: Approximation by Artificial Neural Networks*, Intelligent Systems Reference Library, Vol. 19, Springer, Heidelberg, 2011.

[5] G.A. Anastassiou, *Univariate hyperbolic tangent neural network approximation*, Mathematics and Computer Modelling, 53(2011), 1111-1132.

[6] G.A. Anastassiou, *Multivariate hyperbolic tangent neural network approximation*, Computers and Mathematics 61(2011), 809-821.

[7] G.A. Anastassiou, *Multivariate sigmoidal neural network approximation*, Neural Networks 24(2011), 378-386.

[8] G.A. Anastassiou, *Univariate sigmoidal neural network approximation*, J. of Computational Analysis and Applications, Vol. 14, No. 4, 2012, 659-690.

[9] G.A. Anastassiou, *Fractional neural network approximation*, Computers and Mathematics with Applications, 64 (2012), 1655-1676.

[10] G.A. Anastassiou, *Approximation by neural networks iterates,* Advances in Applied Mathematics and Approximation Theory, pp. 1-20, Springer Proceedings in Math. & Stat., Springer, New York, 2013, Eds. G. Anastassiou, O. Duman.

[11] G.A. Anastassiou, *Intelligent Systems II: Complete Approximation by Neural Network Operators*, Springer, Heidelberg, New York, 2016.

[12] G.A. Anastassiou, *Strong Right Fractional Calculus for Banach space valued functions*, ‘Revista Proyecciones, Vol. 36, No. 1 (2017), 149-186.

[13] G.A. Anastassiou, *Vector fractional Korovkin type Approximations*, Dynamic Systems and Applications, 26(2017), 81-104.

[14] G.A. Anastassiou, *A strong Fractional Calculus Theory for Banach space valued functions*, Nonlinear Functional Analysis and Applications (Korea), 22(3) (2017), 495-524.

[15] G.A. Anastassiou, *Intelligent Computations: Abstract Fractional Calculus, Inequalities, Approximations*, Springer, Heidelberg, New York, 2018.

[16] G.A. Anastassiou, *Nonlinearity: Ordinary and Fractional Approximations by Sublinear and Max-Product Operators*, Springer, Heidelberg, New York, 2018.

[17] G.A. Anastassiou, *Algebraic function based Banach space valued ordinary and fractional neural network approximations*, New Trends in Mathematical Sciences, 10 special issue (1) (2022), 100-125.

[18] G.A. Anastassiou, *General multimariate arctangent function activated neural network approximations*, Journal of Numerical Analysis and Approximation Theory 51(1) (2022), 37-66.

[19] G.A. Anastassiou, *Abstract multivariate algebraic function activated neural network approximations*, accepted to Journal of Computational Analysis and Applications, 2022.

[20] G.A. Anastassiou and S. Karateke, *Parametrized hyperbolic tangent induced Banach space valued ordinary and fractional neural network approximation, submitted*, 2022.

[21] H. Cartan, *Differential Calculus*, Hermann, Paris, 1971.

[22] Z. Chen and F. Cao, *The approximation operators with sigmoidal functions*, Computers and Mathematics with Applications, 58 (2009), 758-765.

[23] D. Costarelli and R. Spigler, *Approximation results for neural network operators activated by sigmoidal functions*, Neural Networks 44 (2013), 101-106.

[24] D. Costarelli and R. Spigler, *Multivariate neural network operators with sigmoidal activation functions*, Neural Networks 48 (2013), 72-77.

[25] S. Haykin, *Neural Networks: A Comprehensive Foundation* (2 ed.), Prentice Hall, New York, 1998.

[26] W. McCulloch and W. Pitts, *A logical calculus of the ideas immanent in nervous activity*, Bulletin of Mathematical Biophysics, 7 (1943), 115-133.

[27] T.M. Mitchell, *Machine Learning*, WCB-McGraw-Hill, New York, 1997.

[28] L.B. Rall, *Computational Solution of Nonlinear Operator Equations*, John Wiley & Sons, New York, 1969.

General sigmoid based Banach space valued neural network approximation

George A. Anastassiou
Department of Mathematical Sciences
University of Memphis
Memphis, TN 38152, U.S.A.
ganastss@memphis.edu

Abstract

Here we study the univariate quantitative approximation of Banach space valued continuous functions on a compact interval or all the real line by quasi-interpolation Banach space valued neural network operators. We perform also the related Banach space valued fractional approximation. These approximations are derived by establishing Jackson type inequalities involving the modulus of continuity of the engaged function or its Banach space valued high order derivative or fractional derivaties. Our operators are defined by using a density function induced by a general sigmoid function. The approximations are pointwise and with respect to the uniform norm. The related Banach space valued feed-forward neural networks are with one hidden layer. We finish with a convergence analysis.

2020 AMS Mathematics Subject Classification: 26A33, 41A17, 41A25, 41A30, 46B25.

Keywords and Phrases: general sigmoid function, Banach space valued neural network approximation, Banach space valued quasi-interpolation operator, modulus of continuity, Banach space valued Caputo fractional derivative, Banach space valued fractional approximation.

1 Introduction

The author in [1] and [2], see Chapters 2-5, was the first to establish neural network approximation to continuous functions with rates by very specifically defined neural network operators of Cardaliagnet-Euvrard and "Squashing" types, by employing the modulus of continuity of the engaged function or its high order derivative, and producing very tight Jackson type inequalities. He treats there both the univariate and multivariate cases. The defining these operators "bell-shaped" and "squashing" functions are assumed to be of compact suport. Also in [2] he gives the Nth order asymptotic expansion for the error of weak approximation of these two operators to a special natural class of smooth functions, see Chapters 4-5 there.

The author inspired by [14], continued his studies on neural networks approximation by introducing and using the proper quasi-interpolation operators of sigmoidal and hyperbolic tangent type which resulted into [3], [4], [5],[6], [7], by treating both the univariate and multivariate cases. He did also the corresponding fractional case [8].

In this article we are greatly inspired by the related works [15], [16].

The author here performs general sigmoid function based neural network approximations to continuous functions over compact intervals of the real line or over the whole $\mathbb{R}$ with values to an arbitrary Banach space $(X, \|\cdot\|)$. Finally he treats completely the related X-valued fractional approximation. All convergences here are with rates expressed via the modulus of continuity of the involved function or its X-valued high order derivative, or X-valued fractional derivatives and given by very tight Jackson type inequalities.

Our compact intervals are not necessarily symmetric to the origin. Some of our upper bounds to error quantity are very flexible and general. In preparation to prove our results we establish important properties of the basic density function defining our operators which is induced by a general sigmoid function.

Feed-forward X-valued neural networks (FNNs) with one hidden layer, the only type of networks we deal with in this article, are mathematically expressed as

$$N_n(x) = \sum_{j=0}^{n} c_j \sigma\left(\langle a_j \cdot x\rangle + b_j\right), \quad x \in \mathbb{R}^s, \, s \in \mathbb{N},$$

where for $0 \leq j \leq n$, $b_j \in \mathbb{R}$ are the thresholds, $a_j \in \mathbb{R}^s$ are the connection weights, $c_j \in X$ are the coefficients, $\langle a_j \cdot x\rangle$ is the inner product of a_j and x, and σ is the activation function of the network. In many fundamental neural network models, the activation function is derived from various specific sigmoid functions. Here we work for a general sigmoid function. About neural networks in general read [17], [18], [20]. See also [9] for a complete study of real valued approximation by neural network operators.

2 Basics

Let $h : \mathbb{R} \to [-1, 1]$ be a general sigmoid function, such that it is strictly increasing, $h(0) = 0$, $h(-x) = -h(x)$, $h(+\infty) = 1$, $h(-\infty) = -1$. Also h is strictly convex over $(-\infty, 0]$ and striclty concave over $[0, +\infty)$, with $h^{(2)} \in C(\mathbb{R})$.

We consider the activation function

$$\psi(x) := \frac{1}{4}\left(h(x+1) - h(x-1)\right), \quad x \in \mathbb{R}, \tag{1}$$

As in [13], p. 285, we get that $\psi(-x) = \psi(x)$, thus ψ is an even function. Since $x+1 > x-1$, then $h(x+1) > h(x-1)$, and $\psi(x) > 0$, all $x \in \mathbb{R}$.

We see that

$$\psi(0) = \frac{h(1)}{2}. \tag{2}$$

Let $x > 1$, we have that

$$\psi'(x) = \frac{1}{4}\left(h'(x+1) - h'(x-1)\right) < 0,$$

by h' being strictly decreasing over $[0, +\infty)$.

Let now $0 < x < 1$, then $1 - x > 0$ and $0 < 1 - x < 1 + x$. It holds $h'(x-1) = h'(1-x) > h'(x+1)$, so that again $\psi'(x) < 0$. Consequently ψ is stritly decreasing on $(0, +\infty)$.

Clearly, ψ is strictly increasing on $(-\infty, 0)$, and $\psi'(0) = 0$.

See that

$$\lim_{x \to +\infty} \psi(x) = \frac{1}{4}\left(h(+\infty) - h(+\infty)\right) = 0, \tag{3}$$

and

$$\lim_{x \to -\infty} \psi(x) = \frac{1}{4}\left(h(-\infty) - h(-\infty)\right) = 0. \tag{4}$$

That is the x-axis is the horizontal asymptote on ψ.

Conclusion, ψ is a bell symmetric function with maximum

$$\psi(0) = \frac{h(1)}{2}.$$

We need

Theorem 1 *We have that*

$$\sum_{i=-\infty}^{\infty} \psi(x - i) = 1, \quad \forall\, x \in \mathbb{R}. \tag{5}$$

Proof. As exactly the same as in [13], p. 286 is omitted. ■

Theorem 2 *It holds*

$$\int_{-\infty}^{\infty} \psi(x)\, dx = 1. \tag{6}$$

Proof. Similar to [13], p. 287. It is omitted. ■

Thus $\psi(x)$ is a density function on $\mathbb{R}$.

We give

Theorem 3 *Let $0 < \alpha < 1$, and $n \in \mathbb{N}$ with $n^{1-\alpha} > 2$. It holds*

$$\sum_{\begin{cases} k=-\infty \\ : |nx-k| \geq n^{1-\alpha} \end{cases}}^{\infty} \psi(nx-k) < \frac{\left(1-h\left(n^{1-\alpha}-2\right)\right)}{2}. \tag{7}$$

Notice that

$$\lim_{n\to+\infty} \frac{\left(1-h\left(n^{1-\alpha}-2\right)\right)}{2} = 0.$$

Proof. Let $x \geq 1$. That is $0 \leq x-1 < x+1$. Applying the mean value theorem we get

$$\psi(x) \overset{(1)}{=} \frac{1}{4} \cdot 2 \cdot h'(\xi) = \frac{h'(\xi)}{2}, \tag{8}$$

for some $x-1 < \xi < x+1$.

Since h' is strictly decreasing we obtain $h'(\xi) < h'(x-1)$ and

$$\psi(x) < \frac{h'(x-1)}{2}, \ \forall\, x \geq 1. \tag{9}$$

Therefore we have

$$\sum_{\begin{cases} k=-\infty \\ : |nx-k| \geq n^{1-\alpha} \end{cases}}^{\infty} \psi(nx-k) = \sum_{\begin{cases} k=-\infty \\ : |nx-k| \geq n^{1-\alpha} \end{cases}}^{\infty} \psi(|nx-k|) <$$

$$\frac{1}{2} \sum_{\begin{cases} k=-\infty \\ : |nx-k| \geq n^{1-\alpha} \end{cases}}^{\infty} h'(|nx-k|-1) \leq \frac{1}{2} \int_{(n^{1-\alpha}-1)}^{+\infty} h'(x-1)\, d(x-1) =$$

$$\frac{1}{2} \left(h(x-1) \Big|_{(n^{1-\alpha}-1)}^{+\infty} \right) = \frac{1}{2} \left[h(+\infty) - h\left(n^{1-\alpha}-2\right) \right] = \frac{1}{2} \left(1 - h\left(n^{1-\alpha}-2\right)\right). \tag{10}$$

The claim is proved. ■

Denote by $\lfloor \cdot \rfloor$ the integral part of the number and by $\lceil \cdot \rceil$ the ceiling of the number.

We further give

Theorem 4 *Let $x \in [a,b] \subset \mathbb{R}$ and $n \in \mathbb{N}$ so that $\lceil na \rceil \leq \lfloor nb \rfloor$. It holds*

$$\frac{1}{\sum_{k=\lceil na \rceil}^{\lfloor nb \rfloor} \psi(nx-k)} < \frac{1}{\psi(1)}, \quad \forall\, x \in [a,b]. \tag{11}$$

Proof. As similar to [13], p. 289 is omitted. ■

Remark 5 *We have that*

$$\lim_{n\to\infty} \sum_{k=\lceil na\rceil}^{\lfloor nb\rfloor} \psi(nx-k) \neq 1, \tag{12}$$

for at least some $x \in [a,b]$*.*

See [13], p. 290, same reasoning.

Note 6 *For large enough* n *we always obtain* $\lceil na\rceil \leq \lfloor nb\rfloor$*. Also* $a \leq \frac{k}{n} \leq b$*, iff* $\lceil na\rceil \leq k \leq \lfloor nb\rfloor$*. In general it holds (by (5))*

$$\sum_{k=\lceil na\rceil}^{\lfloor nb\rfloor} \psi(nx-k) \leq 1. \tag{13}$$

Let $(X, \|\cdot\|)$ be a Banach space.

Definition 7 *Let* $f \in C([a,b], X)$ *and* $n \in \mathbb{N} : \lceil na\rceil \leq \lfloor nb\rfloor$*. We introduce and define the* X*-valued linear neural network operators*

$$A_n(f,x) := \frac{\sum_{k=\lceil na\rceil}^{\lfloor nb\rfloor} f\left(\frac{k}{n}\right)\psi(nx-k)}{\sum_{k=\lceil na\rceil}^{\lfloor nb\rfloor} \psi(nx-k)}, \quad x \in [a,b]. \tag{14}$$

Clearly here $A_n(f,x) \in C([a,b], X)$. For convenience we use the same A_n for real valued function when needed. We study here the pointwise and uniform convergence of $A_n(f,x)$ to $f(x)$ with rates.

For convenience also we call

$$A_n^*(f,x) := \sum_{k=\lceil na\rceil}^{\lfloor nb\rfloor} f\left(\frac{k}{n}\right)\psi(nx-k), \tag{15}$$

(similarly A_n^* can be defined for real valued function) that is

$$A_n(f,x) = \frac{A_n^*(f,x)}{\sum_{k=\lceil na\rceil}^{\lfloor nb\rfloor} \psi(nx-k)}. \tag{16}$$

So that

$$A_n(f,x) - f(x) = \frac{A_n^*(f,x)}{\sum_{k=\lceil na\rceil}^{\lfloor nb\rfloor} \psi(nx-k)} - f(x)$$

$$= \frac{A_n^*(f,x) - f(x)\left(\sum_{k=\lceil na\rceil}^{\lfloor nb\rfloor} \psi(nx-k)\right)}{\sum_{k=\lceil na\rceil}^{\lfloor nb\rfloor} \psi(nx-k)}. \tag{17}$$

Consequently we derive

$$\|A_n(f,x) - f(x)\| \leq \frac{1}{\psi(1)} \left\| A_n^*(f,x) - f(x)\left(\sum_{k=\lceil na\rceil}^{\lfloor nb\rfloor} \psi(nx-k)\right)\right\|. \tag{18}$$

That is

$$\left\| A_n(f,x) - f(x) \right\| \leq \frac{1}{\psi(1)} \left\| \sum_{k=\lceil na \rceil}^{\lfloor nb \rfloor} \left(f\left(\frac{k}{n}\right) - f(x) \right) \psi(nx-k) \right\|. \qquad (19)$$

We will estimate the right hand side of (19).

For that we need, for $f \in C([a,b],X)$ the first modulus of continuity

$$\omega_1(f,\delta)_{[a,b]} := \omega_1(f,\delta) := \sup_{\substack{x,y \in [a,b] \\ |x-y| \leq \delta}} \|f(x) - f(y)\|, \quad \delta > 0. \qquad (20)$$

Similarly, it is defined ω_1 for $f \in C_{uB}(\mathbb{R},X)$ (uniformly continuous and bounded functions from $\mathbb{R}$ into X), for $f \in C_B(\mathbb{R},X)$ (continuous and bounded X-valued) and for $f \in C_u(\mathbb{R},X)$ (uniformly continuous).

The fact $f \in C([a,b],X)$ or $f \in C_u(\mathbb{R},X)$, is equivalent to $\lim_{\delta \to 0} \omega_1(f,\delta) = 0$, see [11].

Definition 8 *When $f \in C_{uB}(\mathbb{R},X)$, or $f \in C_B(\mathbb{R},X)$, we define*

$$\overline{A}_n(f,x) := \sum_{k=-\infty}^{\infty} f\left(\frac{k}{n}\right) \psi(nx-k), \quad n \in \mathbb{N}, \ x \in \mathbb{R}, \qquad (21)$$

the X-valued quasi-interpolation neural network operator.

Remark 9 *We have that*

$$\left\| f\left(\frac{k}{n}\right) \right\| \leq \|f\|_{\infty,\mathbb{R}} < +\infty,$$

and

$$\left\| f\left(\frac{k}{n}\right) \right\| \psi(nx-k) \leq \|f\|_{\infty,\mathbb{R}} \psi(nx-k), \qquad (22)$$

and

$$\sum_{k=-\lambda}^{\lambda} \left\| f\left(\frac{k}{n}\right) \right\| \psi(nx-k) \leq \|f\|_{\infty,\mathbb{R}} \left(\sum_{k=-\lambda}^{\lambda} \psi(nx-k) \right),$$

and finally

$$\sum_{k=-\infty}^{\infty} \left\| f\left(\frac{k}{n}\right) \right\| \psi(nx-k) \leq \|f\|_{\infty,\mathbb{R}}, \qquad (23)$$

a convergent in $\mathbb{R}$ series.

So the series $\sum_{k=-\infty}^{\infty} f\left(\frac{k}{n}\right) \psi(nx-k)$ is absolutely convergent in X, hence it is convergent in X and $\overline{A}_n(f,x) \in X$.

We denote by $\|f\|_{\infty} := \sup_{x \in [a,b]} \|f(x)\|$, for $f \in C([a,b],X)$, similarly is defined for $f \in C_B(\mathbb{R},X)$.

3 Main Results

We present a series of X-valued neural network approximations to a function given with rates.

We first give

Theorem 10 *Let $f \in C([a,b], X)$, $0<\alpha<1$, $n \in \mathbb{N} : n^{1-\alpha} > 2$, $x \in [a,b]$. Then*

i)

$$\|A_n(f,x) - f(x)\| \leq \frac{1}{\psi(1)} \left[\omega_1\left(f, \frac{1}{n^{\alpha}}\right) + \left(1 - h\left(n^{1-\alpha} - 2\right)\right) \|f\|_{\infty} \right] =: \rho, \tag{24}$$

and

ii)

$$\|A_n(f) - f\|_{\infty} \leq \rho. \tag{25}$$

We notice $\lim_{n\to\infty} A_n(f) = f$, pointwise and uniformly.

The speed of convergence is $\max\left(\frac{1}{n^{\alpha}}, \left(1 - h\left(n^{1-\alpha} - 2\right)\right)\right)$.

Proof. As similar to [13], p. 293 is omitted. ■

Next we give

Theorem 11 *Let $f \in C_B(\mathbb{R}, X)$, $0<\alpha<1$, $n \in \mathbb{N} : n^{1-\alpha} > 2$, $x \in \mathbb{R}$. Then*

i)

$$\left\|\overline{A}_n(f,x) - f(x)\right\| \leq \omega_1\left(f, \frac{1}{n^{\alpha}}\right) + \left(1 - h\left(n^{1-\alpha} - 2\right)\right) \|f\|_{\infty} =: \mu, \tag{26}$$

and

ii)

$$\left\|\overline{A}_n(f) - f\right\|_{\infty} \leq \mu. \tag{27}$$

For $f \in C_{uB}(\mathbb{R}, X)$ we get $\lim_{n\to\infty} \overline{A}_n(f) = f$, pointwise and uniformly.

The speed of convergence is $\max\left(\frac{1}{n^{\alpha}}, \left(1 - h\left(n^{1-\alpha} - 2\right)\right)\right)$.

Proof. As similar to [13], p. 294 is omitted. ■

In the next we discuss high order neural network X-valued approximation by using the smoothness of f.

Theorem 12 *Let $f \in C^N([a,b], X)$, $n, N \in \mathbb{N}$, $0<\alpha<1$, $x \in [a,b]$ and $n^{1-\alpha} > 2$. Then*

i)

$$\|A_n(f,x) - f(x)\| \leq \frac{1}{\psi(1)} \left\{ \sum_{j=1}^{N} \frac{\left\|f^{(j)}(x)\right\|}{j!} \left[\frac{1}{n^{\alpha j}} + \frac{\left(1 - h\left(n^{1-\alpha} - 2\right)\right)}{2} (b-a)^j \right] + \right. \tag{28}$$

$$\left[\omega_1\left(f^{(N)}, \frac{1}{n^{\alpha}}\right)\frac{1}{n^{\alpha N}N!} + \frac{\left(1-h\left(n^{1-\alpha}-2\right)\right)\left\|f^{(N)}\right\|_{\infty}(b-a)^N}{N!}\right]\Bigg\}$$

ii) assume further $f^{(j)}(x_0) = 0$*,* $j = 1, ..., N$*, for some* $x_0 \in [a,b]$*, it holds*

$$\|A_n(f, x_0) - f(x_0)\| \leq \frac{1}{\psi(1)}$$

$$\left\{\omega_1\left(f^{(N)}, \frac{1}{n^{\alpha}}\right)\frac{1}{n^{\alpha N}N!} + \frac{\left(1-h\left(n^{1-\alpha}-2\right)\right)\left\|f^{(N)}\right\|_{\infty}(b-a)^N}{N!}\right\}, \tag{29}$$

and

iii)

$$\|A_n(f) - f\|_{\infty} \leq \frac{1}{\psi(1)}\left\{\sum_{j=1}^{N}\frac{\left\|f^{(j)}\right\|_{\infty}}{j!}\left[\frac{1}{n^{\alpha j}} + \frac{\left(1-h\left(n^{1-\alpha}-2\right)\right)}{2}(b-a)^j\right] +\right.$$

$$\left.\left[\omega_1\left(f^{(N)}, \frac{1}{n^{\alpha}}\right)\frac{1}{n^{\alpha N}N!} + \frac{\left(1-h\left(n^{1-\alpha}-2\right)\right)\left\|f^{(N)}\right\|_{\infty}(b-a)^N}{N!}\right]\right\}. \tag{30}$$

Again we obtain $\lim_{n\to\infty} A_n(f) = f$*, pointwise and uniformly.*

Proof. As similar to [13], pp. 296-301 is omitted. ■

All integrals from now on are of Bochner type [19].

We need

Definition 13 *([12]) Let* $[a,b] \subset \mathbb{R}$*,* X *be a Banach space,* $\alpha > 0$*;* $m = \lceil \alpha \rceil \in \mathbb{N}$*, (*$\lceil \cdot \rceil$ *is the ceiling of the number),* $f : [a,b] \to X$*. We assume that* $f^{(m)} \in L_1([a,b], X)$*. We call the Caputo-Bochner left fractional derivative of order* α*:*

$$\left(D_{*a}^{\alpha}f\right)(x) := \frac{1}{\Gamma(m-\alpha)}\int_a^x (x-t)^{m-\alpha-1} f^{(m)}(t)\,dt, \quad \forall\ x \in [a,b]. \tag{31}$$

If $\alpha \in \mathbb{N}$*, we set* $D_{*a}^{\alpha}f := f^{(m)}$ *the ordinary* X*-valued derivative (defined similar to numerical one, see [21], p. 83), and also set* $D_{*a}^{0}f := f$*.*

By [12], $\left(D_{*a}^{\alpha}f\right)(x)$ exists almost everywhere in $x \in [a,b]$ and $D_{*a}^{\alpha}f \in L_1([a,b], X)$.

If $\left\|f^{(m)}\right\|_{L_{\infty}([a,b],X)} < \infty$, then by [12], $D_{*a}^{\alpha}f \in C([a,b], X)$, hence $\left\|D_{*a}^{\alpha}f\right\| \in C([a,b])$.

We mention

Lemma 14 *([11]) Let* $\alpha > 0$*,* $\alpha \notin \mathbb{N}$*,* $m = \lceil \alpha \rceil$*,* $f \in C^{m-1}([a,b], X)$ *and* $f^{(m)} \in L_{\infty}([a,b], X)$*. Then* $D_{*a}^{\alpha}f(a) = 0$*.*

We mention

Definition 15 *([10]) Let $[a,b] \subset \mathbb{R}$, X be a Banach space, $\alpha > 0$, $m := \lceil \alpha \rceil$. We assume that $f^{(m)} \in L_1([a,b], X)$, where $f : [a,b] \to X$. We call the Caputo-Bochner right fractional derivative of order α:*

$$\left(D_{b-}^{\alpha} f \right)(x) := \frac{(-1)^m}{\Gamma(m-\alpha)} \int_x^b (z-x)^{m-\alpha-1} f^{(m)}(z)\, dz, \quad \forall\ x \in [a,b]. \tag{32}$$

We observe that $\left(D_{b-}^{m} f \right)(x) = (-1)^m f^{(m)}(x)$, for $m \in \mathbb{N}$, and $\left(D_{b-}^{0} f \right)(x) = f(x)$.

By [10], $\left(D_{b-}^{\alpha} f \right)(x)$ exists almost everywhere on $[a,b]$ and $\left(D_{b-}^{\alpha} f \right) \in L_1([a,b], X)$.

If $\left\| f^{(m)} \right\|_{L_\infty([a,b],X)} < \infty$, and $\alpha \notin \mathbb{N}$, by [10], $D_{b-}^{\alpha} f \in C([a,b], X)$, hence $\left\| D_{b-}^{\alpha} f \right\| \in C([a,b])$.

We need

Lemma 16 *([11]) Let $f \in C^{m-1}([a,b], X)$, $f^{(m)} \in L_\infty([a,b], X)$, $m = \lceil \alpha \rceil$, $\alpha > 0$, $\alpha \notin \mathbb{N}$. Then $D_{b-}^{\alpha} f(b) = 0$.*

Convention 17 *We assume that*

$$D_{*x_0}^{\alpha} f(x) = 0, \text{ for } x < x_0, \tag{33}$$

and

$$D_{x_0-}^{\alpha} f(x) = 0, \text{ for } x > x_0, \tag{34}$$

for all $x, x_0 \in [a,b]$.

We mention

Proposition 18 *([11]) Let $f \in C^n([a,b], X)$, $n = \lceil \nu \rceil$, $\nu > 0$. Then $D_{*a}^{\nu} f(x)$ is continuous in $x \in [a,b]$.*

Proposition 19 *([11]) Let $f \in C^m([a,b], X)$, $m = \lceil \alpha \rceil$, $\alpha > 0$. Then $D_{b-}^{\nu} f(x)$ is continuous in $x \in [a,b]$.*

We also mention

Proposition 20 *([11]) Let $f \in C^{m-1}([a,b], X)$, $f^{(m)} \in L_\infty([a,b], X)$, $m = \lceil \alpha \rceil$, $\alpha > 0$ and*

$$D_{*x_0}^{\alpha} f(x) = \frac{1}{\Gamma(m-\alpha)} \int_{x_0}^{x} (x-t)^{m-\alpha-1} f^{(m)}(t)\, dt, \tag{35}$$

for all $x, x_0 \in [a,b] : x \geq x_0$.

Then $D_{*x_0}^{\alpha} f(x)$ is continuous in x_0.

Proposition 21 *([11]) Let* $f \in C^{m-1}([a,b], X)$*,* $f^{(m)} \in L_\infty([a,b], X)$*,* $m = \lceil \alpha \rceil$*,* $\alpha > 0$ *and*

$$D^\alpha_{x_0-} f(x) = \frac{(-1)^m}{\Gamma(m-\alpha)} \int_x^{x_0} (\zeta - x)^{m-\alpha-1} f^{(m)}(\zeta)\, d\zeta, \tag{36}$$

for all $x, x_0 \in [a,b] : x_0 \geq x$.

Then $D^\alpha_{x_0-} f(x)$ *is continuous in* x_0.

Corollary 22 *([11]) Let* $f \in C^m([a,b], X)$*,* $m = \lceil \alpha \rceil$*,* $\alpha > 0$*,* $x, x_0 \in [a,b]$*. Then* $D^\alpha_{*x_0} f(x)$*,* $D^\alpha_{x_0-} f(x)$ *are jointly continuous functions in* (x, x_0) *from* $[a,b]^2$ *into* X*,* X *is a Banach space.*

We need

Theorem 23 *([11]) Let* $f : [a,b]^2 \to X$ *be jointly continuous,* X *is a Banach space. Consider*

$$G(x) = \omega_1(f(\cdot, x), \delta, [x,b]), \tag{37}$$

$\delta > 0$, $x \in [a,b]$.

Then G *is continuous on* $[a,b]$.

Theorem 24 *([11]) Let* $f : [a,b]^2 \to X$ *be jointly continuous,* X *is a Banach space. Then*

$$H(x) = \omega_1(f(\cdot, x), \delta, [a,x]), \tag{38}$$

$x \in [a,b]$*, is continuous in* $x \in [a,b]$*,* $\delta > 0$.

We present the following X-valued fractional approximation result by neural networks.

Theorem 25 *Let* $\alpha > 0$*,* $N = \lceil \alpha \rceil$*,* $\alpha \notin \mathbb{N}$*,* $f \in C^N([a,b], X)$*,* $0 < \beta < 1$*,* $x \in [a,b]$*,* $n \in \mathbb{N} : n^{1-\beta} > 2$*. Then*

i)

$$\left\| A_n(f,x) - \sum_{j=1}^{N-1} \frac{f^{(j)}(x)}{j!} A_n\left((\cdot - x)^j\right)(x) - f(x) \right\| \leq$$

$$\frac{(\psi(1))^{-1}}{\Gamma(\alpha+1)} \left\{ \frac{\left(\omega_1\left(D^\alpha_{x-} f, \frac{1}{n^\beta}\right)_{[a,x]} + \omega_1\left(D^\alpha_{*x} f, \frac{1}{n^\beta}\right)_{[x,b]}\right)}{n^{\alpha\beta}} + \right.$$

$$\left. \left(\frac{1 - h\left(n^{1-\beta} - 2\right)}{2}\right) \left(\left\| D^\alpha_{x-} f \right\|_{\infty,[a,x]} (x-a)^\alpha + \left\| D^\alpha_{*x} f \right\|_{\infty,[x,b]} (b-x)^\alpha \right) \right\}, \tag{39}$$

ii) if $f^{(j)}(x)=0$*, for* $j=1,...,N-1$*, we have*

$$\|A_n(f,x)-f(x)\| \leq \frac{(\psi(1))^{-1}}{\Gamma(\alpha+1)}$$

$$\left\{ \frac{\left(\omega_1\left(D^{\alpha}_{x-}f,\frac{1}{n^{\beta}}\right)_{[a,x]}+\omega_1\left(D^{\alpha}_{*x}f,\frac{1}{n^{\beta}}\right)_{[x,b]}\right)}{n^{\alpha\beta}}+\right.$$

$$\left.\left(\frac{1-h\left(n^{1-\beta}-2\right)}{2}\right)\left(\left\|D^{\alpha}_{x-}f\right\|_{\infty,[a,x]}(x-a)^{\alpha}+\left\|D^{\alpha}_{*x}f\right\|_{\infty,[x,b]}(b-x)^{\alpha}\right)\right\}, \tag{40}$$

iii)

$$\|A_n(f,x)-f(x)\| \leq (\psi(1))^{-1}$$

$$\left\{\sum_{j=1}^{N-1}\frac{\left\|f^{(j)}(x)\right\|}{j!}\left\{\frac{1}{n^{\beta j}}+(b-a)^{j}\left(\frac{1-h\left(n^{1-\beta}-2\right)}{2}\right)\right\}+\right.$$

$$\frac{1}{\Gamma(\alpha+1)}\left\{\frac{\left(\omega_1\left(D^{\alpha}_{x-}f,\frac{1}{n^{\beta}}\right)_{[a,x]}+\omega_1\left(D^{\alpha}_{*x}f,\frac{1}{n^{\beta}}\right)_{[x,b]}\right)}{n^{\alpha\beta}}+\right.$$

$$\left.\left.\left(\frac{1-h\left(n^{1-\beta}-2\right)}{2}\right)\left(\left\|D^{\alpha}_{x-}f\right\|_{\infty,[a,x]}(x-a)^{\alpha}+\left\|D^{\alpha}_{*x}f\right\|_{\infty,[x,b]}(b-x)^{\alpha}\right)\right\}\right\}, \tag{41}$$

$\forall\ x\in[a,b]$,

and

iv)

$$\|A_nf-f\|_{\infty} \leq (\psi(1))^{-1}$$

$$\left\{\sum_{j=1}^{N-1}\frac{\left\|f^{(j)}\right\|_{\infty}}{j!}\left\{\frac{1}{n^{\beta j}}+(b-a)^{j}\left(\frac{1-h\left(n^{1-\beta}-2\right)}{2}\right)\right\}+\right.$$

$$\frac{1}{\Gamma(\alpha+1)}\left\{\frac{\left(\sup_{x\in[a,b]}\omega_1\left(D^{\alpha}_{x-}f,\frac{1}{n^{\beta}}\right)_{[a,x]}+\sup_{x\in[a,b]}\omega_1\left(D^{\alpha}_{*x}f,\frac{1}{n^{\beta}}\right)_{[x,b]}\right)}{n^{\alpha\beta}}+\right.$$

$$\left.\left.\left(\frac{1-h\left(n^{1-\beta}-2\right)}{2}\right)(b-a)^{\alpha}\left(\sup_{x\in[a,b]}\left\|D^{\alpha}_{x-}f\right\|_{\infty,[a,x]}+\sup_{x\in[a,b]}\left\|D^{\alpha}_{*x}f\right\|_{\infty,[x,b]}\right)\right\}\right\}. \tag{42}$$

Above, when $N=1$ *the sum* $\sum_{j=1}^{N-1}\cdot=0$.

As we see here we obtain X*-valued fractionally type pointwise and uniform convergence with rates of* $A_n\to I$ *the unit operator, as* $n\to\infty$.

Proof. It is very lengthy, as similar to [13], pp. 305-316, is omitted. ■

Next we apply Theorem 25 for $N = 1$.

Theorem 26 *Let* $0 < \alpha, \beta < 1$, $f \in C^1([a,b], X)$, $x \in [a,b]$, $n \in \mathbb{N} : n^{1-\beta} > 2$. *Then*

i)

$$\|A_n(f,x) - f(x)\| \leq$$

$$\frac{(\psi(1))^{-1}}{\Gamma(\alpha+1)} \left\{ \frac{\left(\omega_1\left(D_{x-}^{\alpha} f, \frac{1}{n^\beta}\right)_{[a,x]} + \omega_1\left(D_{*x}^{\alpha} f, \frac{1}{n^\beta}\right)_{[x,b]}\right)}{n^{\alpha\beta}} + \right.$$

$$\left. \left(\frac{1 - h\left(n^{1-\beta} - 2\right)}{2}\right) \left(\left\|D_{x-}^{\alpha} f\right\|_{\infty,[a,x]} (x-a)^\alpha + \left\|D_{*x}^{\alpha} f\right\|_{\infty,[x,b]} (b-x)^\alpha\right) \right\}, \tag{43}$$

and

ii)

$$\|A_n f - f\|_\infty \leq \frac{(\psi(1))^{-1}}{\Gamma(\alpha+1)}$$

$$\left\{ \frac{\left(\sup_{x\in[a,b]} \omega_1\left(D_{x-}^{\alpha} f, \frac{1}{n^\beta}\right)_{[a,x]} + \sup_{x\in[a,b]} \omega_1\left(D_{*x}^{\alpha} f, \frac{1}{n^\beta}\right)_{[x,b]}\right)}{n^{\alpha\beta}} + \right.$$

$$\left. \left(\frac{1 - h\left(n^{1-\beta} - 2\right)}{2}\right) (b-a)^\alpha \left(\sup_{x\in[a,b]} \left\|D_{x-}^{\alpha} f\right\|_{\infty,[a,x]} + \sup_{x\in[a,b]} \left\|D_{*x}^{\alpha} f\right\|_{\infty,[x,b]}\right) \right\}. \tag{44}$$

When $\alpha = \frac{1}{2}$ we derive

Corollary 27 *Let* $0 < \beta < 1$, $f \in C^1([a,b], X)$, $x \in [a,b]$, $n \in \mathbb{N} : n^{1-\beta} > 2$. *Then*

i)

$$\|A_n(f,x) - f(x)\| \leq$$

$$\frac{2(\psi(1))^{-1}}{\sqrt{\pi}} \left\{ \frac{\left(\omega_1\left(D_{x-}^{\frac{1}{2}} f, \frac{1}{n^\beta}\right)_{[a,x]} + \omega_1\left(D_{*x}^{\frac{1}{2}} f, \frac{1}{n^\beta}\right)_{[x,b]}\right)}{n^{\frac{\beta}{2}}} + \right.$$

$$\left. \left(\frac{1 - h\left(n^{1-\beta} - 2\right)}{2}\right) \left(\left\|D_{x-}^{\frac{1}{2}} f\right\|_{\infty,[a,x]} \sqrt{(x-a)} + \left\|D_{*x}^{\frac{1}{2}} f\right\|_{\infty,[x,b]} \sqrt{(b-x)}\right) \right\}, \tag{45}$$

and

ii)

$$\|A_n f - f\|_\infty \leq \frac{2(\psi(1))^{-1}}{\sqrt{\pi}}$$

$$\left\{ \frac{\left(\sup_{x\in[a,b]} \omega_1 \left(D_{x-}^{\frac{1}{2}} f, \frac{1}{n^\beta} \right)_{[a,x]} + \sup_{x\in[a,b]} \omega_1 \left(D_{*x}^{\frac{1}{2}} f, \frac{1}{n^\beta} \right)_{[x,b]} \right)}{n^{\frac{\beta}{2}}} + \right.$$

$$\left. \left(\frac{1-h(n^{1-\beta}-2)}{2} \right) \sqrt{(b-a)} \left(\sup_{x\in[a,b]} \left\| D_{x-}^{\frac{1}{2}} f \right\|_{\infty,[a,x]} + \sup_{x\in[a,b]} \left\| D_{*x}^{\frac{1}{2}} f \right\|_{\infty,[x,b]} \right) \right\} < \infty. \tag{46}$$

We finish with

Remark 28 *Some convergence analysis follows:*

Let $0<\beta<1$, $f \in C^1([a,b],X)$, $x\in[a,b]$, $n\in\mathbb{N} : n^{1-\beta} > 2$. *We elaborate on (46). Assume that*

$$\omega_1 \left(D_{x-}^{\frac{1}{2}} f, \frac{1}{n^\beta} \right)_{[a,x]} \leq \frac{K_1}{n^\beta}, \tag{47}$$

and

$$\omega_1 \left(D_{*x}^{\frac{1}{2}} f, \frac{1}{n^\beta} \right)_{[x,b]} \leq \frac{K_2}{n^\beta}, \tag{48}$$

$\forall\, x\in[a,b]$, $\forall\, n\in\mathbb{N}$, *where* $K_1, K_2 > 0$.

Then it holds

$$\frac{\left[\sup_{x\in[a,b]} \omega_1 \left(D_{x-}^{\frac{1}{2}} f, \frac{1}{n^\beta} \right)_{[a,x]} + \sup_{x\in[a,b]} \omega_1 \left(D_{*x}^{\frac{1}{2}} f, \frac{1}{n^\beta} \right)_{[x,b]} \right]}{n^{\frac{\beta}{2}}} \leq$$

$$\frac{\frac{(K_1+K_2)}{n^\beta}}{n^{\frac{\beta}{2}}} = \frac{(K_1+K_2)}{n^{\frac{3\beta}{2}}} = \frac{K}{n^{\frac{3\beta}{2}}}, \tag{49}$$

where $K := K_1 + K_2 > 0$.

The other summand of the right hand side of (46), for large enough n, *converges to zero at the speed* $\left(\frac{1-h(n^{1-\beta}-2)}{2} \right)$.

Then, for large enough $n\in\mathbb{N}$, *by (46) and (49) and the last comment, we obtain that*

$$\|A_n f - f\|_\infty \leq M \max\left(\frac{1}{n^{\frac{3\beta}{2}}}, \left(\frac{1-h(n^{1-\beta}-2)}{2} \right) \right), \tag{50}$$

where $M > 0$.

If $\frac{1}{n^{\frac{3\beta}{2}}} \geq \left(\frac{1-h\left(n^{1-\beta}-2\right)}{2}\right)$, *then* $\frac{1}{n^{\beta}} \geq \left(\frac{1-h\left(n^{1-\beta}-2\right)}{2}\right)$, *and consequently* $\left\|A_n f - f\right\|_{\infty}$ *in (50) converges to zero faster than in Theorem 10. This because the differentiability of* f.

References

[1] G.A. Anastassiou, *Rate of convergence of some neural network operators to the unit-univariate case*, J. Math. Anal. Appl, 212 (1997), 237-262.

[2] G.A. Anastassiou, *Quantitative Approximations*, Chapman & Hall / CRC, Boca Raton, New York, 2001.

[3] G.A. Anastassiou, *Univariate hyperbolic tangent neural network approximation*, Mathematics and Computer Modelling, 53 (2011), 1111-1132.

[4] G.A. Anastassiou, *Multivariate hyperbolic tangent neural network approximation*, Computers and Mathematics, 61 (2011), 809-821.

[5] G.A. Anastassiou, *Multivariate sigmoidal neural network approximation*, Neural Networks, 24 (2011), 378-386.

[6] G.A. Anastassiou, *Inteligent Systems: Approximation by Artificial Neural Networks*, Intelligent Systems Reference Library, Vol. 19, Springer, Heidelberg, 2011.

[7] G.A. Anastassiou, *Univariate sigmoidal neural network approximation*, J. of Computational Analysis and Applications, Vol. 14, No. 4, 2012, 659-690.

[8] G.A. Anastassiou, *Fractional neural network approximation*, Computers and Mathematics with Applications, 64 (2012), 1655-1676.

[9] G.A. Anastassiou, *Intelligent Systems II: Complete Approximation by Neural Network Operators*, Springer, Heidelberg, New York, 2016.

[10] G.A. Anastassiou, *Strong Right Fractional Calculus for Banach space valued functions*, ‘Revista Proyecciones, Vol. 36, No. 1 (2017), 149-186.

[11] G.A. Anastassiou, *Vector fractional Korovkin type Approximations*, Dynamic Systems and Applications, 26 (2017), 81-104.

[12] G.A. Anastassiou, *A strong Fractional Calculus Theory for Banach space valued functions*, Nonlinear Functional Analysis and Applications (Korea), 22(3)(2017), 495-524.

[13] G.A. Anastassiou, *Intelligent Computations: Abstract Fractional Calculus, Inequalities, Approximations*, Springer, Heidelberg, Neq York, 2018.

[14] Z. Chen and F. Cao, *The approximation operators with sigmoidal functions*, Computers and Mathematics with Applications, 58 (2009), 758-765.

[15] D. Costarelli, R. Spigler, *Approximation results for neural network operators activated by sigmoidal functions*, Neural Networks 44 (2013), 101-106.

[16] D. Costarelli, R. Spigler, *Multivariate neural network operators with sigmoidal activation functions*, Neural Networks 48 (2013), 72-77.

[17] S. Haykin, *Neural Networks: A Comprehensive Foundation* (2 ed.), Prentice Hall, New York, 1998.

[18] W. McCulloch and W. Pitts, *A logical calculus of the ideas immanent in nervous activity*, Bulletin of Mathematical Biophysis, 7 (1943), 115-133.

[19] J. Mikusinski, *The Bochner integral*, Academic Press, New York, 1978.

[20] T.M. Mitchell, *Machine Learning*, WCB-McGraw-Hill, New York, 1997.

[21] G.E. Shilov, *Elementary Functional Analysis*, Dover Publications, Inc., New York, 1996.

J. COMPUTATIONAL ANALYSIS AND APPLICATIONS, VOL. 31, NO. 4, 2023, COPYRIGHT 2023 EUDOXUS PRESS, LLC

Approximation of Time Separating Stochastic Processes by Neural Networks

George A. Anastassiou

Department of Mathematical Sciences
University of Memphis, Memphis, TN 38152, U.S.A.
ganastss@memphis.edu

Dimitra Kouloumpou

Section of Mathematics
Hellenic Naval Academy, Piraeus, 18539, Greece
dimkouloumpou@hna.gr

Abstract

Here we study the univariate quantitative approximation of time separating stochastic process over a compact interval or all the real line by quasi-interpolation neural network operators. We perform also the related fractional approximation. These approximations are derived by establishing Jackson type inequalities involving the modulus of continuity of the engaged stochastic function or its high order derivative or fractional derivatives. Our operators are defined by using a density function induced by a general sigmoid function. The approximations are pointwise and with respect to the uniform norm. The feed-forward neural networks are with one hidden layer. We finish with a lot of interesting applications.

2020 AMS Subject Classification: 26A33, 41A17, 41A25

Keywords and Phrases: general sigmoid function, time separating stochastic process, neural network approximation, quasi-interpolation operator, modulus of continuity, Caputo fractional derivative, fractional approximation.

1 Introduction

The first author in [1] and [2], see Chapters 2-5, was the first to establish neural network approximation to continuous functions with rates by very specifically defined neural network operators of Cardaliaguet-Euvrard and "Squashing" types, by employing the modulus of continuity of the engaged function or its high order derivative, and producing very tight Jackson type inequalities. He treats there both the univariate and multivariate cases. The defining these operators "bell-shaped" and "squashing" functions are assumed to be of compact suport. Also in [2] he gives the Nth order asymptotic expansion for the error of weak approximation of these two operators to a special natural class of smooth functions, see Chapters 4-5 there. The first author inspired by [15], continued his studies on neural networks approximation by introducing and using the proper quasi interpolation operators of sigmoidal and hyperbolic tangent type which resulted into

[3]-[7], by treating both the univariate and multivariate cases. He did also the corresponding fractional case [8]. In this article we are also inspired by the related works [16], [17]. The authors here use general sigmoid function based neural network quantitative approximations to continuous functions over compact intervals of the real line or over the whole $\mathbb{R}$ with values to $\mathbb{R}$. All convergences here are with rates expressed via the modulus of continuity of the involved function or its high order derivative, or fractional derivatives and given by very tight Jackson type inequalities. More precisely, here we perform quantitative approximations of time separating stochastic processes by neural networks. We give plenty of varied and interesting applications. Specific motivations came by:

1. Stationary Gaussian processes with an explicit representation such as

$$X_t = \cos(\alpha t)\,\xi_1 + \sin(\alpha t)\,\xi_2, \alpha \in \mathbb{R},$$

   where ξ_1, ξ_2 are independent random variables with the standard normal distribution, see [19],

2. by the "Fourier model" of a stationary process, see [20].

Feed-forward neural networks (FNNs) with one hidden layer, the only type of networks we deal with in this article, are mathematically expressed as

$$N_n(x) = \sum_{j=0}^{n} c_j \sigma\left(\langle a_j \cdot x\rangle + b_j\right), \;\; x \in \mathbb{R}^s, s \in \mathbb{N},$$

where for $0 \leq j \leq n$, $b_j \in \mathbb{R}$ are the thresholds, $a_j \in \mathbb{R}^s$ are the connection weights, $c_j \in X$ are the coefficients, $\langle a_j \cdot x\rangle$ is the inner product of a_j and x, and σ is the activation function of the network. In many fundamental neural network models, the activation function is derived from various specific sigmoid functions. Here we work for a general sigmoid function. About neural networks in general read [18], [21],[23]. See also [9] for a complete study of real valued approximation by neural network operators.

2 Background

Here we follow [14].

2.1 Basics on Neural Network

Let $h : \mathbb{R} \to [-1, 1]$ be a general sigmoid function, such that it is strictly increasing, $h(0) = 0, h(-x) = -h(x)$ for every $x \in \mathbb{R}$, $h(+\infty) = 1, h(-\infty) = -1$. Also h is strictly convex over $(-\infty, 0]$ and strictly concave over $[0, +\infty)$, with $h^{(2)} \in C(\mathbb{R})$.
Some examples of related sigmoid functions follow: $\frac{1}{1+e^{-x}}$; $\tanh x$; $\frac{2}{\pi}\arctan\left(\frac{\pi}{2}x\right)$; $\frac{x}{\sqrt[2m]{1+x^{2m}}}, m \in \mathbb{N}$; $\frac{2}{\pi} gd(x)$; $\frac{x}{\left(1+|x|^{\lambda}\right)^{\frac{1}{\lambda}}}$, λ is odd ; $erf\left(\frac{\sqrt{\pi}}{2}x\right)$; $\frac{1}{1+e^{-\mu x}}$; $\tanh(\mu x), \mu > 0$ for all $x \in \mathbb{R}$

We consider the activation function

$$\psi(x) := \frac{1}{4}\left(h(x+1) - h(x-1)\right), x \in \mathbb{R}, , \tag{1}$$

As in [13], p.285, we get that

$$\psi(-x) = \psi(x), \text{ for every } x \in \mathbb{R}.$$

Thus ψ is an even function.
Since $x+1>x-1$, then $h(x+1)>h(x-1)$, and $\psi(x)>0$, for all $x\in\mathbb{R}$.
We see that

$$\psi(0)=\frac{h(1)}{2}. \tag{2}$$

Let $x>1$, we have that

$$\psi'(x)=\frac{1}{4}\left(h'(x+1)-h'(x-1)\right)<0, \tag{3}$$

by h' be strictly decreasing on $[0,+\infty)$.
Let now $0<x<1$, then $1-x>0$ and $0<1-x<1+x$. It holds $h'(x-1)=h'(1-x)>h'(x+1)$, so that again $\psi'(x)<0$. Consequently ψ is strictly decreasing on $(0,+\infty)$. Clearly ψ is strictly increasing on $(-\infty,0)$ and $\psi'(0)=0$. See that

$$\begin{gathered}\lim_{x\to+\infty}\psi(x)=\frac{1}{4}\left(h(+\infty)-h(+\infty)\right)=0,\\ \text{and}\\ \lim_{x\to-\infty}\psi(x)=\frac{1}{4}\left(h(-\infty)-h(-\infty)\right)=0.\end{gathered} \tag{4}$$

That is the x-axis is the horizontal asymptote on ψ .
Conclusion, ψ is a bell symmetric function with maximum $\psi(0)=\frac{h(1)}{2}$.
We need

Theorem 1. *([14]) We have that*

$$\sum_{i=-\infty}^{+\infty}\psi(x-i)=1,\ \textit{for every}\ x\in\mathbb{R}. \tag{5}$$

Theorem 2. *([14]) It holds*

$$\int_{-\infty}^{+\infty}\psi(x)dx=1. \tag{6}$$

Thus, $\psi(x)$ is a density function on $\mathbb{R}$.
We give

Theorem 3. *([14]) Let $0<\alpha<1$, and $n\in\mathbb{N}$ with $n^{1-\alpha}>2$. It holds*

$$\sum_{\left\{\begin{array}{l}k=-\infty\\ :|nx-k|\geq n^{1-\alpha}\end{array}\right.}^{\infty}\psi\left(nx-k\right)<\frac{\left(1-h\left(n^{1-\alpha}-2\right)\right)}{2}. \tag{7}$$

Notice that

$$\lim_{n\to+\infty}\frac{\left(1-h\left(n^{1-\alpha}-2\right)\right)}{2}=0.$$

Denote by $\lfloor\cdot\rfloor$ the integral part of the number and by $\lceil\cdot\rceil$ the ceiling of the number.
We further give

Theorem 4. *([14])Let $x\in[a,b]\subset\mathbb{R}$ and $n\in\mathbb{N}$ so that $\lceil na\rceil\leq\lfloor nb\rfloor$. It holds*

$$\frac{1}{\sum_{k=\lceil na\rceil}^{\lfloor nb\rfloor}\psi\left(nx-k\right)}<\frac{1}{\psi\left(1\right)},\quad\forall\ x\in\left[a,b\right]. \tag{8}$$

Remark 5. *We have that*

$$\lim_{n\to\infty}\sum_{k=\lceil na\rceil}^{\lfloor nb\rfloor}\psi(nx-k)\neq 1, \tag{9}$$

for at least some $x\in[a,b]$. See [13], p. 290, same reasoning.

Note 6. *For large enough n we always obtain $\lceil na\rceil\leq\lfloor nb\rfloor$. Also $a\leq\frac{k}{n}\leq b$, if and only if $\lceil na\rceil\leq k\leq\lfloor nb\rfloor$. In general it holds (by (5))*

$$\sum_{k=\lceil na\rceil}^{\lfloor nb\rfloor}\psi(nx-k)\leq 1. \tag{10}$$

Let $(X,\|\cdot\|)$ be a Banach space.

Definition 7. *([14]) Let $f\in C([a,b],X)$ and $n\in\mathbb{N}:\lceil na\rceil\leq\lfloor nb\rfloor$. We introduce and define the X-valued linear neural network operators*

$$A_n(f,x):=\frac{\sum_{k=\lceil na\rceil}^{\lfloor nb\rfloor}f\left(\frac{k}{n}\right)\psi(nx-k)}{\sum_{k=\lceil na\rceil}^{\lfloor nb\rfloor}\psi(nx-k)},\quad x\in[a,b]. \tag{11}$$

Clearly here $A_n(f,x)\in C([a,b],X)$. For convenience we use the same A_n for real valued function when needed. We mention here the pointwise and uniform convergence of $A_n(f,x)$ to $f(x)$ with rates. For convenience also we call

$$A_n^*(f,x):=\sum_{k=\lceil na\rceil}^{\lfloor nb\rfloor}f\left(\frac{k}{n}\right)\psi(nx-k), \tag{12}$$

(similarly A_n^* can be defined for real valued function) that is

$$A_n(f,x)=\frac{A_n^*(f,x)}{\sum_{k=\lceil na\rceil}^{\lfloor nb\rfloor}\psi(nx-k)}. \tag{13}$$

So that

$$A_n(f,x)-f(x)=\frac{A_n^*(f,x)}{\sum_{k=\lceil na\rceil}^{\lfloor nb\rfloor}\psi(nx-k)}-f(x)$$

$$=\frac{A_n^*(f,x)-f(x)\left(\sum_{k=\lceil na\rceil}^{\lfloor nb\rfloor}\psi(nx-k)\right)}{\sum_{k=\lceil na\rceil}^{\lfloor nb\rfloor}\psi(nx-k)}. \tag{14}$$

Consequently we derive

$$\|A_n(f,x)-f(x)\|\leq\frac{1}{\psi(1)}\left\|A_n^*(f,x)-f(x)\left(\sum_{k=\lceil na\rceil}^{\lfloor nb\rfloor}\psi(nx-k)\right)\right\|. \tag{15}$$

That is

$$\|A_n(f,x)-f(x)\|\leq\frac{1}{\psi(1)}\left\|\sum_{k=\lceil na\rceil}^{\lfloor nb\rfloor}\left(f\left(\frac{k}{n}\right)-f(x)\right)\psi(nx-k)\right\|. \tag{16}$$

We will estimate the right hand side of (16).

For that we need, for $f\in C([a,b],X)$ the first modulus of continuity

$$\omega_1(f,\delta)_{[a,b]}:=\omega_1(f,\delta):=\sup_{\substack{x,y\in[a,b]\\|x-y|\leq\delta}}\|f(x)-f(y)\|,\quad\delta>0. \tag{17}$$

Similarly, it is defined ω_1 for $f \in C_{uB}(\mathbb{R}, X)$ (uniformly continuous and bounded functions from $\mathbb{R}$ into X), for $f \in C_B(\mathbb{R}, X)$ (continuous and bounded X-valued) and for $f \in C_u(\mathbb{R}, X)$ (uniformly continuous). The fact $f \in C([a,b], X)$ or $f \in C_u(\mathbb{R}, X)$, is equivalent to $\lim_{\delta \to 0} \omega_1(f, \delta) = 0$, see [11].

Definition 8. *([14]) When $f \in C_{uB}(\mathbb{R}, X)$, or $f \in C_B(\mathbb{R}, X)$, we define*

$$\overline{A}_n(f,x) := \sum_{k=-\infty}^{\infty} f\left(\frac{k}{n}\right) \psi(nx-k), \quad n \in \mathbb{N}, \ x \in \mathbb{R}, \tag{18}$$

the X-valued quasi-interpolation neural network operator.

Remark 9. *([14]) We have that the series*

$$\sum_{k=-\infty}^{+\infty} f\left(\frac{k}{n}\right) \psi(nx-k)$$

is absolutely convergent in X, hence it is convergent in X and $\overline{A}_n(f,x) \in X$.

We denote by $\|f\|_\infty := \sup_{x\in[a,b]} \|f(x)\|$, for $f \in C([a,b], X)$, similarly is defined for $f \in C_B(\mathbb{R}, X)$. We mention a series of X-valued neural network approximations to a function given with rates. We first give

Theorem 10. *([14]). Let $f \in C([a,b], X)$, $0 < \alpha < 1$, $n \in \mathbb{N} : n^{1-\alpha} > 2$, $x \in [a,b]$. Then*

i)

$$\|A_n(f,x) - f(x)\| \leq \frac{1}{\psi(1)} \left[\omega_1\left(f, \frac{1}{n^\alpha}\right) + \left(1 - h\left(n^{1-\alpha} - 2\right)\right) \|f\|_\infty\right] =: \rho, \tag{19}$$

and

ii)

$$\|A_n(f) - f\|_\infty \leq \rho. \tag{20}$$

We notice $\lim_{n\to\infty} A_n(f) = f$, pointwise and uniformly.
The speed of convergence is $\max\left(\frac{1}{n^\alpha}, \left(1 - h\left(n^{1-\alpha} - 2\right)\right)\right)$.

Next we give

Theorem 11. *([14]). Let $f \in C_B(\mathbb{R}, X)$, $0 < \alpha < 1$, $n \in \mathbb{N} : n^{1-\alpha} > 2$, $x \in \mathbb{R}$. Then*

i)

$$\left\|\overline{A}_n(f,x) - f(x)\right\| \leq \omega_1\left(f, \frac{1}{n^\alpha}\right) + \left(1 - h\left(n^{1-\alpha} - 2\right)\right) \|f\|_\infty =: \mu, \tag{21}$$

and

ii)

$$\left\|\overline{A}_n(f) - f\right\|_\infty \leq \mu. \tag{22}$$

For $f \in C_{uB}(\mathbb{R}, X)$ we get $\lim_{n\to\infty} \overline{A}_n(f) = f$, pointwise and uniformly. The speed of convergence is

$$\max\left(\frac{1}{n^\alpha}, \left(1 - h\left(n^{1-\alpha} - 2\right)\right)\right).$$

In the next we discuss high order neural network X-valued approximation by using the smoothness of f. The X-valued derivatives are as the numerical ones, see ([24]).

Theorem 12. *([14])Let $f \in C^N([a,b],X)$, $n, N \in \mathbb{N}$, $0<\alpha<1$, $x \in [a,b]$ and $n^{1-\alpha} > 2$. Then*

i)

$$\|A_n(f,x) - f(x)\| \leq \frac{1}{\psi(1)} \left\{ \sum_{j=1}^{N} \frac{\|f^{(j)}(x)\|}{j!} \left[\frac{1}{n^{\alpha j}} + \frac{\left(1 - h\left(n^{1-\alpha} - 2\right)\right)}{2} (b-a)^j \right] + \left[\omega_1\left(f^{(N)}, \frac{1}{n^\alpha}\right) \frac{1}{n^{\alpha N} N!} + \frac{\left(1 - h\left(n^{1-\alpha} - 2\right)\right) \|f^{(N)}\|_\infty (b-a)^N}{N!} \right] \right\}. \tag{23}$$

ii) Assume further $f^{(j)}(x_0) = 0$, $j = 1, ..., N$, for some $x_0 \in [a,b]$, it holds

$$\|A_n(f,x_0) - f(x_0)\| \leq \frac{1}{\psi(1)} \left\{ \omega_1\left(f^{(N)}, \frac{1}{n^\alpha}\right) \frac{1}{n^{\alpha N} N!} + \frac{\left(1 - h\left(n^{1-\alpha} - 2\right)\right) \|f^{(N)}\|_\infty (b-a)^N}{N!} \right\}, \tag{24}$$

and

iii)

$$\|A_n(f) - f\|_\infty \leq \frac{1}{\psi(1)} \left\{ \sum_{j=1}^{N} \frac{\|f^{(j)}\|_\infty}{j!} \left[\frac{1}{n^{\alpha j}} + \frac{\left(1 - h\left(n^{1-\alpha} - 2\right)\right)}{2} (b-a)^j \right] + \left[\omega_1\left(f^{(N)}, \frac{1}{n^\alpha}\right) \frac{1}{n^{\alpha N} N!} + \frac{\left(1 - h\left(n^{1-\alpha} - 2\right)\right) \|f^{(N)}\|_\infty (b-a)^N}{N!} \right] \right\}. \tag{25}$$

Again we obtain $\lim_{n\to\infty} A_n(f) = f$, pointwise and uniformly.

All integrals from now on are of Bochner type [22].
We need

Definition 13. *([12]) Let $[a,b] \subset \mathbb{R}$, X be a Banach space, $\alpha > 0$; $m = \lceil \alpha \rceil \in \mathbb{N}$, ($\lceil \cdot \rceil$ is the ceiling of the number), $f : [a,b] \to X$. We assume that $f^{(m)} \in L_1([a,b],X)$. We call the Caputo-Bochner left fractional derivative of order α:*

$$\left(D_{*a}^{\alpha} f\right)(x) := \frac{1}{\Gamma(m-\alpha)} \int_a^x (x-t)^{m-\alpha-1} f^{(m)}(t)\, dt, \quad \forall\, x \in [a,b]. \tag{26}$$

If $\alpha \in \mathbb{N}$, we set $D_{*a}^{\alpha} f := f^{(m)}$ the ordinary X-valued derivative (defined similar to numerical one, see [24], p. 83), and also set $D_{*a}^0 f := f$.

By [12], $\left(D_{*a}^{\alpha} f\right)(x)$ exists almost everywhere in $x \in [a,b]$ and $D_{*a}^{\alpha} f \in L_1([a,b],X)$.

If $\left\|f^{(m)}\right\|_{L_\infty([a,b],X)} < \infty$, then by [12], $D_{*a}^{\alpha} f \in C([a,b],X)$, hence $\|D_{*a}^{\alpha} f\| \in C([a,b])$.

Definition 14. *([10]) Let $[a,b] \subset \mathbb{R}$, X be a Banach space, $\alpha > 0$, $m := \lceil \alpha \rceil$. We assume that $f^{(m)} \in L_1([a,b],X)$, where $f : [a,b] \to X$. We call the Caputo-Bochner right fractional derivative of order α:*

$$\left(D_{b-}^{\alpha} f\right)(x) := \frac{(-1)^m}{\Gamma(m-\alpha)} \int_x^b (z-x)^{m-\alpha-1} f^{(m)}(z)\, dz, \quad \forall\, x \in [a,b]. \tag{27}$$

We observe that $\left(D_{b-}^{m} f\right)(x) = (-1)^m f^{(m)}(x)$, for $m \in \mathbb{N}$, and $\left(D_{b-}^{0} f\right)(x) = f(x)$.

By [10], $\left(D_{b-}^{\alpha}f\right)(x)$ exists almost everywhere on $[a,b]$ and $\left(D_{b-}^{\alpha}f\right) \in L_1([a,b],X)$. If $\left\|f^{(m)}\right\|_{L_\infty([a,b],X)} < \infty$, and $\alpha \notin \mathbb{N}$, by [10], $D_{b-}^{\alpha}f \in C([a,b],X)$, hence $\left\|D_{b-}^{\alpha}f\right\| \in C([a,b])$.
In the next $\omega_1(f,\delta)_{[a,b]}$ refers to a modulus of continuity. ω_1 defined over $[a,b]$.
We mention the following $X-$valued fractional approximation result by neural networks.

Theorem 15. *([14]). Let $\alpha > 0$, $N = \lceil \alpha \rceil$, $\alpha \notin \mathbb{N}$, $f \in C^N([a,b],X)$, $0 < \beta < 1$, $x \in [a,b]$, $n \in \mathbb{N} : n^{1-\beta} > 2$. Then*

i)

$$\left\|A_n(f,x) - \sum_{j=1}^{N-1} \frac{f^{(j)}(x)}{j!} A_n\left((\cdot - x)^j\right)(x) - f(x)\right\| \leq$$

$$\frac{(\psi(1))^{-1}}{\Gamma(\alpha+1)} \left\{ \frac{\left(\omega_1\left(D_{x-}^{\alpha}f, \frac{1}{n^\beta}\right)_{[a,x]} + \omega_1\left(D_{*x}^{\alpha}f, \frac{1}{n^\beta}\right)_{[x,b]}\right)}{n^{\alpha\beta}} + \right.$$

$$\left. \left(\frac{1-h\left(n^{1-\beta}-2\right)}{2}\right)\left(\left\|D_{x-}^{\alpha}f\right\|_{\infty,[a,x]}(x-a)^\alpha + \left\|D_{*x}^{\alpha}f\right\|_{\infty,[x,b]}(b-x)^\alpha\right)\right\}, \tag{28}$$

ii) if $f^{(j)}(x) = 0$, for $j = 1,...,N-1$, we have

$$\|A_n(f,x) - f(x)\| \leq \frac{(\psi(1))^{-1}}{\Gamma(\alpha+1)}$$

$$\left\{ \frac{\left(\omega_1\left(D_{x-}^{\alpha}f, \frac{1}{n^\beta}\right)_{[a,x]} + \omega_1\left(D_{*x}^{\alpha}f, \frac{1}{n^\beta}\right)_{[x,b]}\right)}{n^{\alpha\beta}} + \right.$$

$$\left. \left(\frac{1-h\left(n^{1-\beta}-2\right)}{2}\right)\left(\left\|D_{x-}^{\alpha}f\right\|_{\infty,[a,x]}(x-a)^\alpha + \left\|D_{*x}^{\alpha}f\right\|_{\infty,[x,b]}(b-x)^\alpha\right)\right\}, \tag{29}$$

iii)

$$\|A_n(f,x) - f(x)\| \leq (\psi(1))^{-1}$$

$$\left\{ \sum_{j=1}^{N-1} \frac{\left\|f^{(j)}(x)\right\|}{j!} \left\{ \frac{1}{n^{\beta j}} + (b-a)^j \left(\frac{1-h\left(n^{1-\beta}-2\right)}{2}\right)\right\} + \right.$$

$$\frac{1}{\Gamma(\alpha+1)} \left\{ \frac{\left(\omega_1\left(D_{x-}^{\alpha}f, \frac{1}{n^\beta}\right)_{[a,x]} + \omega_1\left(D_{*x}^{\alpha}f, \frac{1}{n^\beta}\right)_{[x,b]}\right)}{n^{\alpha\beta}} + \right.$$

$$\left.\left. \left(\frac{1-h\left(n^{1-\beta}-2\right)}{2}\right)\left(\left\|D_{x-}^{\alpha}f\right\|_{\infty,[a,x]}(x-a)^\alpha + \left\|D_{*x}^{\alpha}f\right\|_{\infty,[x,b]}(b-x)^\alpha\right)\right\}\right\}, \tag{30}$$

$\forall\ x \in [a,b]$,

and

iv)

$$\|A_n f - f\|_\infty \leq (\psi(1))^{-1}$$

$$\left\{ \sum_{j=1}^{N-1} \frac{\left\|f^{(j)}\right\|_\infty}{j!} \left\{ \frac{1}{n^{\beta j}} + (b-a)^j \left(\frac{1-h\left(n^{1-\beta}-2\right)}{2}\right)\right\} + \right.$$

$$\frac{1}{\Gamma(\alpha+1)}\left\{\frac{\left(\sup_{x\in[a,b]}\omega_1\left(D^{\alpha}_{x-}f,\frac{1}{n^{\beta}}\right)_{[a,x]}+\sup_{x\in[a,b]}\omega_1\left(D^{\alpha}_{*x}f,\frac{1}{n^{\beta}}\right)_{[x,b]}\right)}{n^{\alpha\beta}}+\right.$$

$$\left.\left(\frac{1-h\left(n^{1-\beta}-2\right)}{2}\right)(b-a)^{\alpha}\left(\sup_{x\in[a,b]}\left\|D^{\alpha}_{x-}f\right\|_{\infty,[a,x]}+\sup_{x\in[a,b]}\left\|D^{\alpha}_{*x}f\right\|_{\infty,[x,b]}\right)\right\}\Bigg\}. \tag{31}$$

Above, when $N=1$ *the sum* $\sum_{j=1}^{N-1}\cdot=0$.

As we see here we obtain X*-valued fractionally type pointwise and uniform convergence with rates of* $A_n\to I$ *the unit operator, as* $n\to\infty$.

Next we apply Theorem 15 for $N=1$.

Corollary 16. *([14]) Let* $0<\alpha,\beta<1$, $f\in C^1([a,b],X)$, $x\in[a,b]$, $n\in\mathbb{N}:n^{1-\beta}>2$. *Then*

i)

$$\|A_n(f,x)-f(x)\|\leq$$

$$\frac{(\psi(1))^{-1}}{\Gamma(\alpha+1)}\left\{\frac{\left(\omega_1\left(D^{\alpha}_{x-}f,\frac{1}{n^{\beta}}\right)_{[a,x]}+\omega_1\left(D^{\alpha}_{*x}f,\frac{1}{n^{\beta}}\right)_{[x,b]}\right)}{n^{\alpha\beta}}+\right.$$

$$\left.\left(\frac{1-h\left(n^{1-\beta}-2\right)}{2}\right)\left(\left\|D^{\alpha}_{x-}f\right\|_{\infty,[a,x]}(x-a)^{\alpha}+\left\|D^{\alpha}_{*x}f\right\|_{\infty,[x,b]}(b-x)^{\alpha}\right)\right\}, \tag{32}$$

and

ii)

$$\|A_nf-f\|_{\infty}\leq\frac{(\psi(1))^{-1}}{\Gamma(\alpha+1)}$$

$$\left\{\frac{\left(\sup_{x\in[a,b]}\omega_1\left(D^{\alpha}_{x-}f,\frac{1}{n^{\beta}}\right)_{[a,x]}+\sup_{x\in[a,b]}\omega_1\left(D^{\alpha}_{*x}f,\frac{1}{n^{\beta}}\right)_{[x,b]}\right)}{n^{\alpha\beta}}+\right.$$

$$\left.\left(\frac{1-h\left(n^{1-\beta}-2\right)}{2}\right)(b-a)^{\alpha}\left(\sup_{x\in[a,b]}\left\|D^{\alpha}_{x-}f\right\|_{\infty,[a,x]}+\sup_{x\in[a,b]}\left\|D^{\alpha}_{*x}f\right\|_{\infty,[x,b]}\right)\right\}. \tag{33}$$

When $\alpha=\frac{1}{2}$ we derive

Corollary 17. *([14]) Let* $0<\beta<1$, $f\in C^1([a,b],X)$, $x\in[a,b]$, $n\in\mathbb{N}:n^{1-\beta}>2$. *Then*

i)

$$\|A_n(f,x)-f(x)\|\leq$$

$$\frac{2(\psi(1))^{-1}}{\sqrt{\pi}}\left\{\frac{\left(\omega_1\left(D^{\frac{1}{2}}_{x-}f,\frac{1}{n^{\beta}}\right)_{[a,x]}+\omega_1\left(D^{\frac{1}{2}}_{*x}f,\frac{1}{n^{\beta}}\right)_{[x,b]}\right)}{n^{\frac{\beta}{2}}}+\right.$$

$$\left.\left(\frac{1-h\left(n^{1-\beta}-2\right)}{2}\right)\left(\left\|D^{\frac{1}{2}}_{x-}f\right\|_{\infty,[a,x]}\sqrt{(x-a)}+\left\|D^{\frac{1}{2}}_{*x}f\right\|_{\infty,[x,b]}\sqrt{(b-x)}\right)\right\}, \tag{34}$$

and

ii)

$$\|A_n f - f\|_{\infty} \leq \frac{2\left(\psi\left(1\right)\right)^{-1}}{\sqrt{\pi}}$$

$$\left\{ \frac{\left(\sup_{x\in[a,b]} \omega_1 \left(D_{x-}^{\frac{1}{2}} f, \frac{1}{n^{\beta}} \right)_{[a,x]} + \sup_{x\in[a,b]} \omega_1 \left(D_{*x}^{\frac{1}{2}} f, \frac{1}{n^{\beta}} \right)_{[x,b]} \right)}{n^{\frac{\beta}{2}}} + \right.$$

$$\left. \left(\frac{1 - h\left(n^{1-\beta} - 2\right)}{2} \right) \sqrt{(b-a)} \left(\sup_{x\in[a,b]} \left\| D_{x-}^{\frac{1}{2}} f \right\|_{\infty,[a,x]} + \sup_{x\in[a,b]} \left\| D_{*x}^{\frac{1}{2}} f \right\|_{\infty,[x,b]} \right) \right\} < \infty. \tag{35}$$

From now on we set $X = \mathbb{R}$.

2.2 Time Seperating Stochastic Processes

Let $(\Omega, \mathcal{F}, P)$ be a probability space, $\omega \in \Omega; Y_1, Y_2, \ldots, Y_m, m \in \mathbb{N}$, be real-valued random variables on Ω with finite expectations, and $h_1(t), h_2(t), \ldots h_m(t) : I \to \mathbb{R}$, where I is an infinite subset of $\mathbb{R}$. Typically here I is an infinite length interval of $\mathbb{R}$, usualy $I = \mathbb{R}$ or $I = \mathbb{R}_+$.

Clearly, then

$$Y\left(t, \omega\right) := \sum_{i=1}^{m} h_i(t) Y_i(\omega), t \in I, \tag{36}$$

is a quite common stochastic process separating time.

We can assume that $h_i \in C^r(I), i = 1, 2, ..., m; r \in \mathbb{N}$. Consequently, we have that the expectation

$$\left(EY\right)\left(t\right) = \sum_{i=1}^{m} h_i(t) EY_i \in C(I) \text{ or } C^r(I). \tag{37}$$

A classical example of a stochastic process separating time is

$$\left(\sin t\right) Y_1(\omega) + \left(\cos t\right) Y_2(\omega), t \in I.$$

Notice that $|\sin t| \leq 1$ and $|\cos t| \leq 1$.

Another typical example is

$$\sinh(t) Y_1(\omega) + \cosh(t) Y_2(\omega), t \in I. \tag{38}$$

In this article we will apply the main results of section 2.1, to $f(t) = \left(EY\right)\left(t\right)$. We will finish with several applications. See the related [19], [20].

3 Main Results

We present the following general approximation of the seperating stochastic processes by neural network operators.

Theorem 18. *Let* $(EY)(t)$ *as in (37),* $t \in [t_1, t_2]$, *where* $t_1, t_2 \in \mathbb{R}$, *with* $t_1 < t_2, h_i \in C\left([t_1, t_2]\right)$ *for every* $i = 1, 2, ..., m, 0 < \alpha < 1, n \in \mathbb{N} : n^{1-\alpha} > 2$. *Then* *i)*

$$\left|A_n\left(\left(EY\right),t\right)-\left(EY\right)(t)\right| \leq \frac{1}{\psi(1)}\left[\omega_1\left(EY,\frac{1}{n^{\alpha}}\right)+\left(1-h\left(n^{1-\alpha}-2\right)\right)\|EY\|_{\infty}\right] =: \rho, \tag{39}$$

and

ii)

$$\left\|A_n\left(EY\right)-EY\right\|_{\infty} \leq \rho. \tag{40}$$

We have that $\lim_{n\to\infty} A_n\left(EY\right)=EY$, *pointwise and uniformly.*
The speed of convergence is $\max\left(\frac{1}{n^{\alpha}},\left(1-h\left(n^{1-\alpha}-2\right)\right)\right)$.

Proof. Notice that when $h_i \in C\left(\left[t_1,t_2\right]\right)$ for every $i=1,2,...,m$, then $\left(EY\right)(t) \in C\left(\left[t_1,t_2\right]\right)$. Thus, the conclusion comes from Theorem 10. □
We continue with,

Theorem 19. *Let* $(EY)(t)$ *as in (37),* $h_i \in C_B\left(\mathbb{R}\right)$ *for every* $i=1,2,...,m, 0<\alpha<1$, $n\in\mathbb{N}: n^{1-\alpha}>2$, $t\in\mathbb{R}$. *Then*

i)

$$\left|\overline{A}_n\left(EY,t\right)-\left(EY\right)(t)\right| \leq \omega_1\left(EY,\frac{1}{n^{\alpha}}\right)+\left(1-h\left(n^{1-\alpha}-2\right)\right)\|EY\|_{\infty} =: \mu, \tag{41}$$

and

ii)

$$\left\|\overline{A}_n\left(EY\right)-EY\right\|_{\infty} \leq \mu. \tag{42}$$

For $EY \in C_{uB}\left(\mathbb{R}\right)$ *we get* $\lim_{n\to\infty}\overline{A}_n\left(EY\right)=EY$, *pointwise and uniformly. The speed of convergence is* $\max\left(\frac{1}{n^{\alpha}},\left(1-h\left(n^{1-\alpha}-2\right)\right)\right)$.

Proof. Since that $h_i \in C_B\left(\mathbb{R}\right)$ for every $i=1,2,...,m$ and $t\in\mathbb{R}$, then $EX \in C_B\left(\mathbb{R}\right)$. Therefore the results come from Theorem 11. □
Furthermore, we have

Theorem 20. *Let* $(EY)(t)$ *as in (37),* $t\in\left[t_1,t_2\right]$, *where* $t_1,t_2\in\mathbb{R}$, *with* $t_1<t_2, h_i\in C^N\left(\left[t_1,t_2\right]\right)$ *for every* $i=1,2,...,m,n,N\in\mathbb{N}$, $0<\alpha<1$, *and* $n^{1-\alpha}>2$. *Then*

i)

$$\left|A_n\left(EY,t\right)-\left(EY\right)(t)\right| \leq \frac{1}{\psi(1)}\left\{\sum_{j=1}^{N}\frac{\left|\left(EY\right)^{(j)}(t)\right|}{j!}\left[\frac{1}{n^{\alpha j}}+\frac{\left(1-h\left(n^{1-\alpha}-2\right)\right)}{2}\left(t_2-t_1\right)^j\right]+\right. \tag{43}$$

$$\left.\left[\omega_1\left(\left(EY\right)^{(N)},\frac{1}{n^{\alpha}}\right)\frac{1}{n^{\alpha N}N!}+\frac{\left(1-h\left(n^{1-\alpha}-2\right)\right)\left\|\left(EY\right)^{(N)}\right\|_{\infty}\left(t_2-t_1\right)^N}{N!}\right]\right\}.$$

ii) Assume further $\left(EY\right)^{(j)}\left(t_0\right)=0$, $j=1,...,N$, *for some* $t_0\in\left[t_1,t_2\right]$, *it holds*

$$\left|A_n\left(EY,t_0\right)-\left(EY\right)\left(t_0\right)\right| \leq \frac{1}{\psi(1)}$$

$$\left\{\omega_1\left(\left(EY\right)^{(N)}, \frac{1}{n^{\alpha}}\right)\frac{1}{n^{\alpha N}N!} + \frac{\left(1-h\left(n^{1-\alpha}-2\right)\right)\left\|\left(EY\right)^{(N)}\right\|_{\infty}\left(t_2-t_1\right)^N}{N!}\right\}, \tag{44}$$

and

iii)

$$\left\|A_n\left(EY\right)-EY\right\|_{\infty} \leq \frac{1}{\psi\left(1\right)}\left\{\sum_{j=1}^{N}\frac{\left\|\left(EY\right)^{(j)}\right\|_{\infty}}{j!}\left[\frac{1}{n^{\alpha j}}+\frac{\left(1-h\left(n^{1-\alpha}-2\right)\right)}{2}\left(t_2-t_1\right)^j\right]+\right.$$

$$\left.\left[\omega_1\left(\left(EY\right)^{(N)}, \frac{1}{n^{\alpha}}\right)\frac{1}{n^{\alpha N}N!}+\frac{\left(1-h\left(n^{1-\alpha}-2\right)\right)\left\|\left(EY\right)^{(N)}\right\|_{\infty}\left(t_2-t_1\right)^N}{N!}\right]\right\}. \tag{45}$$

Again we obtain $\lim_{n\to\infty} A_n\left(EY\right) = EY$*, pointwise and uniformly.*

Proof. By Theorem 12. □

We also present

Theorem 21. *Let* $\alpha > 0, N = \lceil\alpha\rceil, \alpha \notin \mathbb{N}, 0 < \beta < 1, t \in [t_1, t_2]$ *where* $t_1, t_2 \in \mathbb{R}$*, with* $t_1 < t_2$*,* $n \in \mathbb{N} : n^{1-\beta} > 2$*. Then*

i)

$$\left|A_n\left(EY,t\right)-\sum_{j=1}^{N-1}\frac{\left(EY\right)^{(j)}\left(t\right)}{j!}A_n\left(\left(\cdot-t\right)^j\right)\left(t\right)-\left(EY\right)\left(t\right)\right| \leq$$

$$\frac{\left(\psi\left(1\right)\right)^{-1}}{\Gamma\left(\alpha+1\right)}\left\{\frac{\left(\omega_1\left(D_{t-}^{\alpha}\left(EY\right), \frac{1}{n^{\beta}}\right)_{[t_1,t]}+\omega_1\left(D_{*t}^{\alpha}\left(EY\right), \frac{1}{n^{\beta}}\right)_{[t,t_2]}\right)}{n^{\alpha\beta}}+\right.$$

$$\left.\left(\frac{1-h\left(n^{1-\beta}-2\right)}{2}\right)\left(\left\|D_{t-}^{\alpha}\left(EY\right)\right\|_{\infty,[t_1,t]}\left(t-t_1\right)^{\alpha}+\left\|D_{*t}^{\alpha}\left(EY\right)\right\|_{\infty,[t,t_2]}\left(t_2-t\right)^{\alpha}\right)\right\}, \tag{46}$$

ii) if $\left(EY\right)^{(j)}\left(t\right)=0$*, for* $j=1,...,N-1$*, we have*

$$\left|A_n\left(EY,t\right)-\left(EY\right)\left(t\right)\right| \leq \frac{\left(\psi\left(1\right)\right)^{-1}}{\Gamma\left(\alpha+1\right)}$$

$$\left\{\frac{\left(\omega_1\left(D_{t-}^{\alpha}\left(EY\right), \frac{1}{n^{\beta}}\right)_{[t_1,t]}+\omega_1\left(D_{*t}^{\alpha}\left(EY\right), \frac{1}{n^{\beta}}\right)_{[t,t_2]}\right)}{n^{\alpha\beta}}+\right.$$

$$\left.\left(\frac{1-h\left(n^{1-\beta}-2\right)}{2}\right)\left(\left\|D_{t-}^{\alpha}\left(EY\right)\right\|_{\infty,[t_1,t]}\left(t-t_1\right)^{\alpha}+\left\|D_{*t}^{\alpha}\left(EY\right)\right\|_{\infty,[t,t_2]}\left(t_2-t\right)^{\alpha}\right)\right\}, \tag{47}$$

iii)

$$\left\|A_n\left(EY,t\right)-\left(EY\right)\left(t\right)\right\| \leq \left(\psi\left(1\right)\right)^{-1}$$

$$\left\{\sum_{j=1}^{N-1}\frac{\left|\left(EY\right)^{(j)}\left(t\right)\right|}{j!}\left\{\frac{1}{n^{\beta j}}+\left(t_2-t_1\right)^j\left(\frac{1-h\left(n^{1-\beta}-2\right)}{2}\right)\right\}+\right.$$

$$\frac{1}{\Gamma\left(\alpha+1\right)}\left\{\frac{\left(\omega_1\left(D_{t-}^{\alpha}\left(EY\right), \frac{1}{n^{\beta}}\right)_{[t_1,t]}+\omega_1\left(D_{*t}^{\alpha}\left(EY\right), \frac{1}{n^{\beta}}\right)_{[t,t_2]}\right)}{n^{\alpha\beta}}+\right.$$

$$\left(\frac{1-h\left(n^{1-\beta}-2\right)}{2}\right)\left(\left\|D_{t-}^{\alpha}\left(EY\right)\right\|_{\infty,[t_1,t]}\left(t-t_1\right)^{\alpha}+\left\|D_{*t}^{\alpha}\left(EY\right)\right\|_{\infty,[t,t_2]}\left(t_2-t\right)^{\alpha}\right)\Bigg\}\Bigg\}, \tag{48}$$

$\forall\ t\in[t_1,t_2]$,

and

iv)

$$\left\|A_n\left(EY\right)-EY\right\|_{\infty}\leq\left(\psi\left(1\right)\right)^{-1}$$

$$\left\{\sum_{j=1}^{N-1}\frac{\left\|\left(EY\right)^{(j)}\right\|_{\infty}}{j!}\left\{\frac{1}{n^{\beta j}}+\left(t_2-t_1\right)^{j}\left(\frac{1-h\left(n^{1-\beta}-2\right)}{2}\right)\right\}+\right.$$

$$\frac{1}{\Gamma\left(\alpha+1\right)}\left\{\frac{\left(\sup_{x\in[t_1,t_2]}\omega_1\left(D_{t-}^{\alpha}\left(EY\right),\frac{1}{n^{\beta}}\right)_{[t_1,t]}+\sup_{t\in[t_1,t_2]}\omega_1\left(D_{*t}^{\alpha}\left(EY\right),\frac{1}{n^{\beta}}\right)_{[t,t_2]}\right)}{n^{\alpha\beta}}+\right.$$

$$\left.\left.\left(\frac{1-h\left(n^{1-\beta}-2\right)}{2}\right)\left(t_2-t_1\right)^{\alpha}\left(\sup_{t\in[t_1,t_2]}\left\|D_{t-}^{\alpha}\left(EY\right)\right\|_{\infty,[t_1,t]}+\sup_{t\in[t_1,t_2]}\left\|D_{*t}^{\alpha}\left(EY\right)\right\|_{\infty,[t,t_2]}\right)\right\}\right\}. \tag{49}$$

Above, when $N=1$ the sum $\sum_{j=1}^{N-1}\cdot=0$.

As we see here we obtain t-valued fractionally type pointwise and uniform convergence with rates of $A_n\rightarrow I$ the unit operator, as $n\rightarrow\infty$.

Proof. By Theorem 15. □

Next we apply Theorem 21 for $N=1$.

Corollary 22. *Let $(EY)(t)$ as in (37), $0<\alpha,\beta<1$, $t\in[t_1,t_2]$, where $t_1,t_2\in\mathbb{R}$, with $t_1<t_2$,$n\in\mathbb{N}:n^{1-\beta}>2$. and $h_i\in C\left([t_1,t_2]\right)$ for every $i=1,2,...,m$. Then*

i)

$$\left|A_n\left(EY,t\right)-\left(EY\right)(t)\right|\leq$$

$$\frac{\left(\psi\left(1\right)\right)^{-1}}{\Gamma\left(\alpha+1\right)}\left\{\frac{\left(\omega_1\left(D_{t-}^{\alpha}\left(EY\right),\frac{1}{n^{\beta}}\right)_{[t_1,t]}+\omega_1\left(D_{*t}^{\alpha}\left(EY\right),\frac{1}{n^{\beta}}\right)_{[t,t_2]}\right)}{n^{\alpha\beta}}+\right.$$

$$\left.\left(\frac{1-h\left(n^{1-\beta}-2\right)}{2}\right)\left(\left\|D_{t-}^{\alpha}\left(EY\right)\right\|_{\infty,[t_1,t]}\left(t-t_1\right)^{\alpha}+\left\|D_{*t}^{\alpha}\left(EY\right)\right\|_{\infty,[t,t_2]}\left(t_2-t\right)^{\alpha}\right)\right\}, \tag{50}$$

and

ii)

$$\left\|A_n\left(EY\right)-\left(EY\right)\right\|_{\infty}\leq\frac{\left(\psi\left(1\right)\right)^{-1}}{\Gamma\left(\alpha+1\right)}$$

$$\left\{\frac{\left(\sup_{t\in[t_1,t_2]}\omega_1\left(D_{t-}^{\alpha}\left(EY\right),\frac{1}{n^{\beta}}\right)_{[t_1,t]}+\sup_{t\in[t_1,t_2]}\omega_1\left(D_{*t}^{\alpha}\left(EY\right),\frac{1}{n^{\beta}}\right)_{[t,t_2]}\right)}{n^{\alpha\beta}}+\right.$$

$$\left.\left(\frac{1-h\left(n^{1-\beta}-2\right)}{2}\right)\left(t_2-t_1\right)^{\alpha}\left(\sup_{t\in[t_1,t_2]}\left\|D_{t-}^{\alpha}\left(EY\right)\right\|_{\infty,[t_1,t]}+\sup_{x\in[t_1,t_2]}\left\|D_{*t}^{\alpha}\left(EY\right)\right\|_{\infty,[t,t_2]}\right)\right\}. \tag{51}$$

When $\alpha = \frac{1}{2}$ we derive

Corollary 23. *Assume again $(EY)(t)$ as in (37). Let $0 < \beta < 1$, $t \in [t_1, t_2]$, where $t_1, t_2 \in \mathbb{R}$, with $t_1 < t_2$, $n \in \mathbb{N} : n^{1-\beta} > 2$ and $h_i \in C([t_1, t_2])$ for every $i = 1, 2, ..., m$. Then*

i)

$$\left|A_n(EY,t) - (EY)(t)\right| \leq$$

$$\frac{2(\psi(1))^{-1}}{\sqrt{\pi}} \left\{ \frac{\left(\omega_1\left(D_{t-}^{\frac{1}{2}}(EY), \frac{1}{n^{\beta}}\right)_{[t_1,t]} + \omega_1\left(D_{*t}^{\frac{1}{2}}(EY), \frac{1}{n^{\beta}}\right)_{[t,t_2]} \right)}{n^{\frac{\beta}{2}}} + \right.$$

$$\left. \left(\frac{1 - h\left(n^{1-\beta} - 2\right)}{2}\right) \left(\left\| D_{t-}^{\frac{1}{2}}(EY) \right\|_{\infty,[t_1,t]} \sqrt{(t - t_1)} + \left\| D_{*t}^{\frac{1}{2}}(EY) \right\|_{\infty,[t,t_2]} \sqrt{(t_2 - t)} \right) \right\}, \tag{52}$$

and

ii)

$$\left\|A_n(EY) - (EY)\right\|_{\infty} \leq \frac{2(\psi(1))^{-1}}{\sqrt{\pi}}$$

$$\left\{ \frac{\left(\sup_{t \in [t_1,t_2]} \omega_1\left(D_{t-}^{\frac{1}{2}}(EY), \frac{1}{n^{\beta}}\right)_{[t_1,t]} + \sup_{t \in [t_1,t_2]} \omega_1\left(D_{*t}^{\frac{1}{2}}(EY), \frac{1}{n^{\beta}}\right)_{[t,t_2]} \right)}{n^{\frac{\beta}{2}}} + \right.$$

$$\left. \left(\frac{1 - h\left(n^{1-\beta} - 2\right)}{2}\right) \sqrt{(t_2 - t_1)} \left(\sup_{t \in [t_1,t_2]} \left\| D_{t-}^{\frac{1}{2}}(EY) \right\|_{\infty,[t_1,t]} + \sup_{t \in [t_1,t_2]} \left\| D_{*t}^{\frac{1}{2}}(EY) \right\|_{\infty,[t,t_2]} \right) \right\} < \infty. \tag{53}$$

4 Applications

For the next applications we consider (Ω, F, P) be a probability space and Y_0, Y_1, Y_2 be real valued random variables on Ω with finite expectations. We consider the stochastic processes $Z_i(t, \omega)$ for $i = 1, 2, \ldots, 9$, where $t \in \mathbb{R}$ and $\omega \in \Omega$ as follows:

$$Z_1(t, \omega) = \left[(t - t_0)^{\mu+1} + 1\right] Y_0(\omega), \tag{54}$$

where $t_0 \in \mathbb{R}$ and $\mu \in \mathbb{N}$ are fixed;

$$Z_2(t, \omega) = \sin(\xi t) Y_1(\omega) + \cos(\xi t) Y_2(\omega), \tag{55}$$

where $\xi > 0$ is fixed;

$$Z_3(t, \omega) = \sinh(\mu t) Y_1(\omega) + \cosh(\mu t) Y_2(\omega), \tag{56}$$

where $\mu > 0$ is fixed;

$$Z_4(t, \omega) = sech(\mu t) Y_1(\omega) + \tanh(\mu t) Y_2(\omega), \tag{57}$$

where $\mu > 0$ is fixed.
Here $sechx := \frac{1}{\cosh x} = \frac{2}{e^x + e^{-x}}, x \in \mathbb{R}$.

$$Z_5(t, \omega) = e^{-\ell_1 t} Y_1(\omega) + e^{-\ell_2 t} Y_2(\omega), \tag{58}$$

where $\ell_1, \ell_2 > 0$ are fixed;

$$Z_6(t,\omega) = \frac{1}{1+e^{-\ell_1 t}} Y_1(\omega) + \frac{1}{1+e^{-\ell_2 t}} Y_2(\omega), \tag{59}$$

where $\ell_1, \ell_2 > 0$ are fixed;

$$Z_7(t,\omega) = e^{-e^{-\mu_1 t}} Y_1(\omega) + e^{-e^{-\mu_2 t}} Y_2(\omega), \tag{60}$$

where $\mu_1, \mu_2 > 0$ are fixed;

$$Z_8(t,\omega) = P_m(\ell_1 t) Y_1(\omega) + P_m(\ell_2 t) Y_2(\omega), \tag{61}$$

where $\ell_1, \ell_2 > 0$ and $m \in \mathbb{N}$ are fixed.
Here $P_m(x)$ is the Legendre Polynomial of degree $m \in \mathbb{N}$, i.e

$$P_m : [-1,1] \longrightarrow [-1,1]$$

such that,

$$P_m(x) = \frac{1}{2^m m!} \frac{d^m}{dx^m} \left(x^2 - 1\right)^m = \frac{1}{2^m} \sum_{k=0}^{m} \binom{m}{k}^2 (x-1)^{m-k} (x+1)^k, x \in [-1,1].$$

To define the stochastic process $Z_9(t,\omega)$, we consider the Cauchy function

$$\hat{f}(x) = \begin{cases} e^{-\frac{1}{x^2}}, & x \neq 0 \\ 0, & x = 0 \end{cases}.$$

Notice that, $\hat{f} \in C^{\infty}(\mathbb{R})$ and it has $\hat{f}^{(i)}(0) = 0$, for all $i = 1, 2, \ldots, \infty$.
We set,

$$Z_9(t,\omega) = \hat{f}(t) Y_0(\omega), \tag{62}$$

The expectations of $Z_i, i = 1, 2, ..., 9$ are

$$(EZ_1)(t) = \left[(t-t_0)^{\mu+1} + 1\right] E(Y_0), \tag{63}$$

$$(EZ_2)(t) = \sin(\xi t) E(Y_1) + \cos(\xi t) E(Y_2), \tag{64}$$

$$(EZ_3)(t) = \sinh(\mu t) E(Y_1) + \cosh(\mu t) E(Y_2), \tag{65}$$

$$(EZ_4)(t) = sech(\mu t) E(Y_1) + \tanh(\mu t) E(Y_2), \tag{66}$$

$$(EZ_5)(t) = e^{-\ell_1 t} E(Y_1) + e^{-\ell_2 t} E(Y_2), \tag{67}$$

$$(EZ_6)(t) = \frac{1}{1+e^{-\ell_1 t}} E(Y_1) + \frac{1}{1+e^{-\ell_2 t}} E(Y_2), \tag{68}$$

$$(EZ_7)(t) = e^{-e^{-\mu_1 t}} E(Y_1) + e^{-e^{-\mu_2 t}} E(Y_2), \tag{69}$$

$$(EZ_8)(t) = P_m(\ell_1 t) E(Y_1) + P_m(\ell_2 t) E(Y_2), \tag{70}$$

$$(EZ_9)(t) = \hat{f}(t) E(Y_0), \tag{71}$$

For the next $(EZ_i)(t), i = 1, 2, \ldots, 9$ are as defined in relations between (63) and (71) respectively.
We present the following result.

Proposition 24. *Let $t \in [t_1, t_2]$, where $t_1, t_2 \in \mathbb{R}$, with $t_1 < t_2, 0 < \alpha < 1, n \in \mathbb{N} : n^{1-\alpha} > 2$. Then for $i = 1, 2, \ldots, 9$*

i)

$$\left|A_n\left(\left(EZ_i\right), t\right) - \left(EZ_i\right)(t)\right| \leq \frac{1}{\psi(1)}\left[\omega_1\left(EZ_i, \frac{1}{n^\alpha}\right) + \left(1 - h\left(n^{1-\alpha} - 2\right)\right)\left\|EZ_i\right\|_\infty\right] =: \rho, \tag{72}$$

and

ii)

$$\left\|A_n\left(EZ_i\right) - EZ_i\right\|_\infty \leq \rho. \tag{73}$$

We have that $\lim_{n\to\infty} A_n\left(EZ_i\right) = EZ_i$, *pointwise and uniformly.*
The speed of convergence is $\max\left(\frac{1}{n^\alpha}, \left(1 - h\left(n^{1-\alpha} - 2\right)\right)\right)$.

Proof. From Theorem 18. □
In the cases of stochastic processes $Z_i(t, \omega)$, for $i = 2, 4, 6, 7$ we have the next

Proposition 25. *Let $i \in \{2, 4, 6, 7\}, 0 < \alpha < 1, n \in \mathbb{N} : n^{1-\alpha} > 2, t \in \mathbb{R}$. Then*

i)

$$\left|\overline{A}_n\left(EZ_i, t\right) - \left(EZ_i\right)(t)\right| \leq \omega_1\left(EZ_i, \frac{1}{n^\alpha}\right) + \left(1 - h\left(n^{1-\alpha} - 2\right)\right)\left\|EZ_i\right\|_\infty =: \mu, \tag{74}$$

and

ii)

$$\left\|\overline{A}_n\left(EZ_i\right) - EZ_i\right\|_\infty \leq \mu. \tag{75}$$

For $EZ_i \in C_{uB}(\mathbb{R})$ we get $\lim_{n\to\infty} \overline{A}_n\left(EZ_i\right) = EZ_i$, *pointwise and uniformly.*
The speed of convergence is $\max\left(\frac{1}{n^\alpha}, \left(1 - h\left(n^{1-\alpha} - 2\right)\right)\right)$.

Proof. Notice that for every $t \in \mathbb{R}$ we have that:

for $Z_2(t, \omega)$, $|\sin(\xi t)| \leq 1$ and $|\cos(\xi t)| \leq 1$,

for $Z_4(t, \omega)$, $|sech(\mu t)| \leq 1$ and $|tanh(\mu t)| \leq 1$,

for $Z_6(t, \omega)$, $0 < \frac{1}{1+e^{-\ell_1 t}} < 1$ and $0 < \frac{1}{1+e^{-\ell_2 t}} < 1$,

for $Z_7(t, \omega)$, $0 < e^{-e^{-\mu_1 t}} < 1$ and $0 < e^{-e^{-\mu_2 t}} < 1$.

Thus, the results come from Theorem 19. □
Moreover, we present the next

Proposition 26. *Let $i = 1, 2, \ldots, 9, t \in [t_1, t_2]$, where $t_1, t_2 \in \mathbb{R}$, with $t_1 < t_2, 0 < \alpha < 1$, and $n^{1-\alpha} > 2$. Then*

i)

$$\left|A_n\left(EZ_i, t\right) - \left(EZ_i\right)(t)\right| \leq \frac{1}{\psi(1)}\left\{\sum_{j=1}^{N} \frac{\left|\left(EZ_i\right)^{(j)}(t)\right|}{j!}\left[\frac{1}{n^{\alpha j}} + \frac{\left(1 - h\left(n^{1-\alpha} - 2\right)\right)}{2}\left(t_2 - t_1\right)^j\right] + \right. \tag{76}$$

$$\left.\left[\omega_1\left(\left(EZ_i\right)^{(N)}, \frac{1}{n^\alpha}\right)\frac{1}{n^{\alpha N} N!} + \frac{\left(1 - h\left(n^{1-\alpha} - 2\right)\right)\left\|\left(EZ_i\right)^{(N)}\right\|_\infty\left(t_2 - t_1\right)^N}{N!}\right]\right\}.$$

ii) Assume further $(EZ_i)^{(j)}(t_a) = 0$, $j = 1, ..., N$, *for some* $t_a \in [t_1, t_2]$, *it holds*

$$|A_n(EZ_i, t_a) - (EZ_i)(t_a)| \leq \frac{1}{\psi(1)}$$

$$\left\{ \omega_1\left((EZ_i)^{(N)}, \frac{1}{n^\alpha} \right) \frac{1}{n^{\alpha N} N!} + \frac{\left(1 - h\left(n^{1-\alpha} - 2\right)\right) \left\| (EZ_i)^{(N)} \right\|_\infty (t_2 - t_1)^N}{N!} \right\}, \tag{77}$$

and

iii)

$$\|A_n(EZ_i) - EZ_i\|_\infty \leq \frac{1}{\psi(1)} \left\{ \sum_{j=1}^{N} \frac{\left\| (EZ_i)^{(j)} \right\|_\infty}{j!} \left[\frac{1}{n^{\alpha j}} + \frac{\left(1 - h\left(n^{1-\alpha} - 2\right)\right)}{2} (t_2 - t_1)^j \right] + \right.$$

$$\left. \left[\omega_1\left((EZ_i)^{(N)}, \frac{1}{n^\alpha} \right) \frac{1}{n^{\alpha N} N!} + \frac{\left(1 - h\left(n^{1-\alpha} - 2\right)\right) \left\| (EZ_i)^{(N)} \right\|_\infty (t_2 - t_1)^N}{N!} \right] \right\}. \tag{78}$$

Again we obtain $\lim_{n \to \infty} A_n(EZ_i) = EZ_i$, *pointwise and uniformly.*

Proof. By Theorem 20. □

We also present

Proposition 27. *Let* $i = 1, 2, \ldots, 9, \alpha > 0, N = \lceil \alpha \rceil, \alpha \notin \mathbb{N}, 0 < \beta < 1, t \in [t_1, t_2]$ *where* $t_1, t_2 \in \mathbb{R}$, *with* $t_1 < t_2$, $n \in \mathbb{N} : n^{1-\beta} > 2$. *Then*

i)

$$\left| A_n(EZ_i, t) - \sum_{j=1}^{N-1} \frac{(EZ_i)^{(j)}(t)}{j!} A_n\left((\cdot - t)^j\right)(t) - (EZ_i)(t) \right| \leq$$

$$\frac{(\psi(1))^{-1}}{\Gamma(\alpha+1)} \left\{ \frac{\left(\omega_1\left(D_{t-}^\alpha(EZ_i), \frac{1}{n^\beta}\right)_{[t_1,t]} + \omega_1\left(D_{*t}^\alpha(EZ_i), \frac{1}{n^\beta}\right)_{[t,t_2]} \right)}{n^{\alpha\beta}} + \right.$$

$$\left. \left(\frac{1 - h\left(n^{1-\beta} - 2\right)}{2} \right) \left(\left\| D_{t-}^\alpha(EZ_i) \right\|_{\infty,[t_1,t]} (t - t_1)^\alpha + \left\| D_{*t}^\alpha(EZ_i) \right\|_{\infty,[t,t_2]} (t_2 - t)^\alpha \right) \right\}, \tag{79}$$

ii) if $(EZ_i)^{(j)}(t) = 0$, *for* $j = 1, ..., N-1$, *we have*

$$|A_n(EZ_i, t) - (EZ_i)(t)| \leq \frac{(\psi(1))^{-1}}{\Gamma(\alpha+1)}$$

$$\left\{ \frac{\left(\omega_1\left(D_{t-}^\alpha(EZ_i), \frac{1}{n^\beta}\right)_{[t_1,t]} + \omega_1\left(D_{*t}^\alpha(EZ_i), \frac{1}{n^\beta}\right)_{[t,t_2]} \right)}{n^{\alpha\beta}} + \right.$$

$$\left. \left(\frac{1 - h\left(n^{1-\beta} - 2\right)}{2} \right) \left(\left\| D_{t-}^\alpha(EZ_i) \right\|_{\infty,[t_1,t]} (t - t_1)^\alpha + \left\| D_{*t}^\alpha(EZ_i) \right\|_{\infty,[t,t_2]} (t_2 - t)^\alpha \right) \right\}, \tag{80}$$

iii)

$$\|A_n(EZ_i, t) - (EZ_i)(t)\| \leq (\psi(1))^{-1}$$

$$\left\{\sum_{j=1}^{N-1}\frac{\left|(EZ_i)^{(j)}(t)\right|}{j!}\left\{\frac{1}{n^{\beta j}}+(t_2-t_1)^j\left(\frac{1-h\left(n^{1-\beta}-2\right)}{2}\right)\right\}+\frac{1}{\Gamma(\alpha+1)}\left\{\frac{\left(\omega_1\left(D_{t-}^{\alpha}(EZ_i),\frac{1}{n^{\beta}}\right)_{[t_1,t]}+\omega_1\left(D_{*t}^{\alpha}(EZ_i),\frac{1}{n^{\beta}}\right)_{[t,t_2]}\right)}{n^{\alpha\beta}}+\left(\frac{1-h\left(n^{1-\beta}-2\right)}{2}\right)\left(\left\|D_{t-}^{\alpha}(EZ_i)\right\|_{\infty,[t_1,t]}(t-t_1)^{\alpha}+\left\|D_{*t}^{\alpha}(EZ_i)\right\|_{\infty,[t,t_2]}(t_2-t)^{\alpha}\right)\right\}\right\}, \tag{81}$$

$\forall\ t\in[t_1,t_2]$,

and

iv)

$$\|A_n(EZ_i)-EZ_i\|_{\infty}\leq(\psi(1))^{-1}\left\{\sum_{j=1}^{N-1}\frac{\left\|(EZ_i)^{(j)}\right\|_{\infty}}{j!}\left\{\frac{1}{n^{\beta j}}+(t_2-t_1)^j\left(\frac{1-h\left(n^{1-\beta}-2\right)}{2}\right)\right\}+\frac{1}{\Gamma(\alpha+1)}\left\{\frac{\left(\sup_{x\in[t_1,t_2]}\omega_1\left(D_{t-}^{\alpha}(EZ_i),\frac{1}{n^{\beta}}\right)_{[t_1,t]}+\sup_{t\in[t_1,t_2]}\omega_1\left(D_{*t}^{\alpha}(EZ_i),\frac{1}{n^{\beta}}\right)_{[t,t_2]}\right)}{n^{\alpha\beta}}+\left(\frac{1-h\left(n^{1-\beta}-2\right)}{2}\right)(t_2-t_1)^{\alpha}\left(\sup_{t\in[t_1,t_2]}\left\|D_{t-}^{\alpha}(EZ_i)\right\|_{\infty,[t_1,t]}+\sup_{t\in[t_1,t_2]}\left\|D_{*t}^{\alpha}(EZ_i)\right\|_{\infty,[t,t_2]}\right)\right\}\right\}. \tag{82}$$

Above, when $N=1$ *the sum* $\sum_{j=1}^{N-1}\cdot=0$.

As we see here we obtain t*-valued fractionally type pointwise and uniform convergence with rates of* $A_n\rightarrow I$ *the unit operator, as* $n\rightarrow\infty$.

Proof. By Theorem 21. □

Next we apply Proposition 27 for $N=1$.

Corollary 28. *Let* $i=1,2,\ldots,9$, $0<\alpha,\beta<1$, $t\in[t_1,t_2]$, *where* $t_1,t_2\in\mathbb{R}$, *with* $t_1<t_2$,$n\in\mathbb{N}:n^{1-\beta}>2$. *Then*

i)

$$|A_n(EZ_i,t)-(EZ_i)(t)|\leq\frac{(\psi(1))^{-1}}{\Gamma(\alpha+1)}\left\{\frac{\left(\omega_1\left(D_{t-}^{\alpha}(EZ_i),\frac{1}{n^{\beta}}\right)_{[t_1,t]}+\omega_1\left(D_{*t}^{\alpha}(EZ_i),\frac{1}{n^{\beta}}\right)_{[t,t_2]}\right)}{n^{\alpha\beta}}+\left(\frac{1-h\left(n^{1-\beta}-2\right)}{2}\right)\left(\left\|D_{t-}^{\alpha}(EZ_i)\right\|_{\infty,[t_1,t]}(t-t_1)^{\alpha}+\left\|D_{*t}^{\alpha}(EZ_i)\right\|_{\infty,[t,t_2]}(t_2-t)^{\alpha}\right)\right\}, \tag{83}$$

and

ii)

$$\|A_n(EZ_i)-(EZ_i)\|_{\infty}\leq\frac{(\psi(1))^{-1}}{\Gamma(\alpha+1)}$$

$$\left\{ \frac{\left(\sup_{t\in[t_1,t_2]} \omega_1 \left(D^{\alpha}_{t-}\left(EZ_i\right), \frac{1}{n^{\beta}}\right)_{[t_1,t]} + \sup_{t\in[t_1,t_2]} \omega_1 \left(D^{\alpha}_{*t}\left(EZ_i\right), \frac{1}{n^{\beta}}\right)_{[t,t_2]} \right)}{n^{\alpha\beta}} + \right.$$

$$\left. \left(\frac{1-h\left(n^{1-\beta}-2\right)}{2}\right)\left(t_2-t_1\right)^{\alpha}\left(\sup_{t\in[t_1,t_2]}\left\|D^{\alpha}_{t-}\left(EZ_i\right)\right\|_{\infty,[t_1,t]}+\sup_{x\in[t_1,t_2]}\left\|D^{\alpha}_{*t}\left(EZ_i\right)\right\|_{\infty,[t,t_2]}\right)\right\}. \tag{84}$$

When $\alpha = \frac{1}{2}$ we derive

Corollary 29. *Assume $i = 1, 2, \ldots, 9$. Let $0 < \beta < 1$, $t \in [t_1, t_2]$, where $t_1, t_2 \in \mathbb{R}$, with $t_1 < t_2$, and $n \in \mathbb{N} : n^{1-\beta} > 2$. Then*

i)

$$\left|A_n\left(EZ_i,t\right)-\left(EZ_i\right)(t)\right| \leq$$

$$\frac{2\left(\psi(1)\right)^{-1}}{\sqrt{\pi}} \left\{ \frac{\left(\omega_1 \left(D^{\frac{1}{2}}_{t-}\left(EZ_i\right), \frac{1}{n^{\beta}}\right)_{[t_1,t]} + \omega_1 \left(D^{\frac{1}{2}}_{*t}\left(EZ_i\right), \frac{1}{n^{\beta}}\right)_{[t,t_2]} \right)}{n^{\frac{\beta}{2}}} + \right.$$

$$\left. \left(\frac{1-h\left(n^{1-\beta}-2\right)}{2}\right)\left(\left\|D^{\frac{1}{2}}_{t-}\left(EZ_i\right)\right\|_{\infty,[t_1,t]}\sqrt{(t-t_1)}+\left\|D^{\frac{1}{2}}_{*t}\left(EZ_i\right)\right\|_{\infty,[t,t_2]}\sqrt{(t_2-t)}\right)\right\}, \tag{85}$$

and

ii)

$$\left\|A_n\left(EZ_i\right)-\left(EZ_i\right)\right\|_{\infty} \leq \frac{2\left(\psi(1)\right)^{-1}}{\sqrt{\pi}}$$

$$\left\{ \frac{\left(\sup_{t\in[t_1,t_2]} \omega_1 \left(D^{\frac{1}{2}}_{t-}\left(EZ_i\right), \frac{1}{n^{\beta}}\right)_{[t_1,t]} + \sup_{t\in[t_1,t_2]} \omega_1 \left(D^{\frac{1}{2}}_{*t}\left(EZ_i\right), \frac{1}{n^{\beta}}\right)_{[t,t_2]} \right)}{n^{\frac{\beta}{2}}} + \right.$$

$$\left. \left(\frac{1-h\left(n^{1-\beta}-2\right)}{2}\right)\sqrt{(t_2-t_1)}\left(\sup_{t\in[t_1,t_2]}\left\|D^{\frac{1}{2}}_{t-}\left(EZ_i\right)\right\|_{\infty,[t_1,t]}+\sup_{t\in[t_1,t_2]}\left\|D^{\frac{1}{2}}_{*t}\left(EZ_i\right)\right\|_{\infty,[t,t_2]}\right)\right\} < \infty. \tag{86}$$

5 Specific Applications

Let $(\Omega, \mathcal{F}, P)$, where Ω is the set of non-negative integers, be a probability space, $Y_{1,1}, Y_{2,1}$ be real-valued random variables on Ω following Poisson distributions with parameters $\lambda_1, \lambda_2 \in (0, \infty)$ respectively.
We consider the stochastic processes $Z_{i,1}(t, \omega)$ for $i = 1, 2, 3, 5$, where $t \in \mathbb{R}$ and $\omega \in \Omega$ as follows:

$$Z_{1,1}(t,\omega) = \left[(t-t_0)^{\mu+1}+1\right]Y_{1,1}(\omega), \tag{87}$$

where $t_0 \in \mathbb{R}$ and $\mu \in \mathbb{N}$ are fixed;

$$Z_{2,1}(t,\omega) = \sin(\xi t)\,Y_{1,1}(\omega) + \cos(\xi t)\,Y_{2,1}(\omega), \tag{88}$$

where $\xi > 0$ is fixed;

$$Z_{3,1}(t,\omega) = \sinh(\mu t)\,Y_{1,1}(\omega) + \cosh(\mu t)\,Y_{2,1}(\omega), \tag{89}$$

where $\mu > 0$ is fixed;

$$Z_{5,1}(t,\omega) = e^{-\ell_1 t} Y_{1,1}(\omega) + e^{-\ell_2 t} Y_{2,1}(\omega), \tag{90}$$

where $\ell_1, \ell_2 > 0$ are fixed.
Since $E(Y_{1,1}) = \lambda_1$ and $E(Y_{2,1}) = \lambda_2$, the expectations of $Z_{i,1}, i = 1,2,3,5$, are

$$(EZ_{1,1})(t) = \lambda_1 \left[(t - t_0)^{\mu+1} + 1 \right], \tag{91}$$

$$(EZ_{2,1})(t) = \lambda_1 \sin(\xi t) + \lambda_2 \cos(\xi t), \tag{92}$$

$$(EZ_{3,1})(t) = \lambda_1 \sinh(\mu t) + \lambda_2 \cosh(\mu t), \tag{93}$$

$$(EZ_{5,1})(t) = \lambda_1 e^{-\ell_1 t} + \lambda_2 e^{-\ell_2 t}, \tag{94}$$

For the next we consider $(\Omega, \mathcal{F}, P)$, where $\Omega = \mathbb{R}$, be a probability space, $Y_{1,2}, Y_{2,2}$ be real-valued random variables on Ω following Gaussian distributions with expectations $\hat{\mu}_1, \hat{\mu}_2 \in \mathbb{R}$ respectively.
We consider the stochastic processes $Z_{i,2}(t,\omega)$ for $i = 1,2,3,5$, where $t \in \mathbb{R}$ and $\omega \in \Omega$ as follows:

$$Z_{1,2}(t,\omega) = \left[(t - t_0)^{\mu+1} + 1 \right] Y_{1,2}(\omega), \tag{95}$$

where $t_0 \in \mathbb{R}$ and $\mu \in \mathbb{N}$ are fixed;

$$Z_{2,2}(t,\omega) = \sin(\xi t) Y_{1,2}(\omega) + \cos(\xi t) Y_{2,2}(\omega), \tag{96}$$

where $\xi > 0$ is fixed;

$$Z_{3,2}(t,\omega) = \sinh(\mu t) Y_{1,2}(\omega) + \cosh(\mu t) Y_{2,2}(\omega), \tag{97}$$

where $\mu > 0$ is fixed;

$$Z_{5,2}(t,\omega) = e^{-\ell_1 t} Y_{1,2}(\omega) + e^{-\ell_2 t} Y_{2,2}(\omega), \tag{98}$$

where $\ell_1, \ell_2 > 0$ are fixed.
Since $E(Y_{1,2}) = \hat{\mu}_1$ and $E(Y_{2,2}) = \hat{\mu}_2$, The expectations of $Z_{i,2}, i = 1,2,3,5$ are

$$(EZ_{1,2})(t) = \hat{\mu}_1 \left[(t - t_0)^{\mu+1} + 1 \right], \tag{99}$$

$$(EZ_{2,2})(t) = \hat{\mu}_1 \sin(\xi t) + \hat{\mu}_2 \cos(\xi t), \tag{100}$$

$$(EZ_{3,2})(t) = \hat{\mu}_1 \sinh(\mu t) + \hat{\mu}_2 \cosh(\mu t), \tag{101}$$

$$(EZ_{5,2})(t) = \hat{\mu}_1 e^{-\ell_1 t} + \hat{\mu}_2 e^{-\ell_2 t}. \tag{102}$$

Furthermore, we consider $(\Omega, \mathcal{F}, P)$, where $\Omega = [0, \infty)$, be a probability space, $Y_{1,3}, Y_{2,3}$ be real-valued random variables on Ω following Weibull distributions with scale parameters 1 and shape parameters $\gamma_1, \gamma_2 \in (0, \infty)$ respectively.
We consider the stochastic processes $Z_{i,3}(t,\omega)$ for $i = 1,2,3,5$, where $t \in \mathbb{R}$ and $\omega \in \Omega$ as follows:

$$Z_{1,3}(t,\omega) = \left[(t - t_0)^{\mu+1} + 1 \right] Y_{1,3}(\omega), \tag{103}$$

where $t_0 \in \mathbb{R}$ and $\mu \in \mathbb{N}$ are fixed;

$$Z_{2,3}(t,\omega) = \sin(\xi t) Y_{1,3}(\omega) + \cos(\xi t) Y_{2,3}(\omega), \tag{104}$$

where $\xi > 0$ is fixed;

$$Z_{3,3}(t,\omega) = \sinh(\mu t) Y_{1,3}(\omega) + \cosh(\mu t) Y_{2,3}(\omega), \tag{105}$$

where $\mu > 0$ is fixed;

$$Z_{5,3}(t,\omega) = e^{-\ell_1 t} Y_{1,3}(\omega) + e^{-\ell_2 t} Y_{2,3}(\omega), \tag{106}$$

where $\ell_1, \ell_2 > 0$ are fixed.
Since $E\left(Y_{1,3}\right) = \Gamma\left(1 + \frac{1}{\gamma_1}\right)$ and $E\left(Y_{2,3}\right) = \Gamma\left(1 + \frac{1}{\gamma_2}\right)$, where $\Gamma\left(\cdot\right)$ is the Gamma function, The expectations of $Z_{i,3}, i = 1,2,3,5,$ are

$$\left(EZ_{1,3}\right)(t) = \Gamma\left(1 + \frac{1}{\gamma_1}\right)\left[(t - t_0)^{\mu+1} + 1\right], \tag{107}$$

$$\left(EZ_{2,3}\right)(t) = \Gamma\left(1 + \frac{1}{\gamma_1}\right)\sin\left(\xi t\right) + \Gamma\left(1 + \frac{1}{\gamma_2}\right)\cos\left(\xi t\right), \tag{108}$$

$$\left(EZ_{3,3}\right)(t) = \Gamma\left(1 + \frac{1}{\gamma_1}\right)\sinh\left(\mu t\right) + \Gamma\left(1 + \frac{1}{\gamma_2}\right)\cosh\left(\mu t\right), \tag{109}$$

$$\left(EZ_{5,3}\right)(t) = \Gamma\left(1 + \frac{1}{\gamma_1}\right)e^{-\ell_1 t} + \Gamma\left(1 + \frac{1}{\gamma_2}\right)e^{-\ell_2 t}, \tag{110}$$

We present the following result.

Proposition 30. *Let $t \in [t_1, t_2]$, where $t_1, t_2 \in \mathbb{R}$, with $t_1 < t_2, 0 < \alpha < 1, n \in \mathbb{N} : n^{1-\alpha} > 2$. Then for $i = 1,2,3,5$ and $k = 1,2,3$*
i)

$$\left|A_n\left(\left(EZ_{i,k}\right), t\right) - \left(EZ_{i,k}\right)(t)\right| \leq \frac{1}{\psi(1)}\left[\omega_1\left(EZ_{i,k}, \frac{1}{n^\alpha}\right) + \left(1 - h\left(n^{1-\alpha} - 2\right)\right)\left\|EZ_{i,k}\right\|_\infty\right] =: \rho, \tag{111}$$

and

ii)

$$\left\|A_n\left(EZ_{i,k}\right) - EZ_{i,k}\right\|_\infty \leq \rho. \tag{112}$$

We have that $\lim_{n\to\infty} A_n\left(EZ_{i,k}\right) = EZ_{i,k}$, pointwise and uniformly.
The speed of convergence is $\max\left(\frac{1}{n^\alpha}, \left(1 - h\left(n^{1-\alpha} - 2\right)\right)\right)$.

Proof. From Proposition 24. □
In the cases of stochastic processes $Z_{2,k}(t,\omega)$, for $k = 1,2,3$ we have the next

Proposition 31. *Let $k \in \{1,2,3\}, 0 < \alpha < 1, n \in \mathbb{N} : n^{1-\alpha} > 2, t \in \mathbb{R}$. Then*

i)

$$\left|\overline{A}_n\left(EZ_{2,k}, t\right) - \left(EZ_{2,k}\right)(t)\right| \leq \omega_1\left(EZ_{2,k}, \frac{1}{n^\alpha}\right) + \left(1 - h\left(n^{1-\alpha} - 2\right)\right)\left\|EZ_{2,k}\right\|_\infty =: \mu, \tag{113}$$

and

ii)

$$\left\|\overline{A}_n\left(EZ_{2,k}\right) - EZ_{2,k}\right\|_\infty \leq \mu. \tag{114}$$

For $EZ_{2,k} \in C_{uB}(\mathbb{R})$ we get $\lim_{n\to\infty} \overline{A}_n\left(EZ_{2,k}\right) = EZ_{2,k}$, pointwise and uniformly.
The speed of convergence is $\max\left(\frac{1}{n^\alpha}, \left(1 - h\left(n^{1-\alpha} - 2\right)\right)\right)$.

Proof. The results come from Proposition 25. □
Moreover, we present the next

Corollary 32. *Assume* $i = 1, 2, 3, 5$ *and* $k = 1, 2, 3$. *Let* $0 < \beta < 1$, $t \in [t_1, t_2]$, *where* $t_1, t_2 \in \mathbb{R}$, *with* $t_1 < t_2$, *and* $n \in \mathbb{N} : n^{1-\beta} > 2$. *Then*

i)

$$\left|A_n\left(EZ_{i,k}, t\right) - \left(EZ_{i,k}\right)(t)\right| \leq$$

$$\frac{2(\psi(1))^{-1}}{\sqrt{\pi}} \left\{ \frac{\left(\omega_1\left(D_{t-}^{\frac{1}{2}}\left(EZ_{i,k}\right), \frac{1}{n^{\beta}}\right)_{[t_1,t]} + \omega_1\left(D_{*t}^{\frac{1}{2}}\left(EZ_{i,k}\right), \frac{1}{n^{\beta}}\right)_{[t,t_2]}\right)}{n^{\frac{\beta}{2}}} + \right.$$

$$\left.\left(\frac{1 - h\left(n^{1-\beta} - 2\right)}{2}\right)\left(\left\|D_{t-}^{\frac{1}{2}}\left(EZ_{i,k}\right)\right\|_{\infty,[t_1,t]} \sqrt{(t - t_1)} + \left\|D_{*t}^{\frac{1}{2}}\left(EZ_{i,k}\right)\right\|_{\infty,[t,t_2]} \sqrt{(t_2 - t)}\right)\right\}, \quad (115)$$

and

ii)

$$\left\|A_n\left(EZ_{i,k}\right) - \left(EZ_{i,k}\right)\right\|_{\infty} \leq \frac{2(\psi(1))^{-1}}{\sqrt{\pi}}$$

$$\left\{ \frac{\left(\sup_{t\in[t_1,t_2]} \omega_1\left(D_{t-}^{\frac{1}{2}}\left(EZ_{i,k}\right), \frac{1}{n^{\beta}}\right)_{[t_1,t]} + \sup_{t\in[t_1,t_2]} \omega_1\left(D_{*t}^{\frac{1}{2}}\left(EZ_{i,k}\right), \frac{1}{n^{\beta}}\right)_{[t,t_2]}\right)}{n^{\frac{\beta}{2}}} + \right.$$

$$\left.\left(\frac{1 - h\left(n^{1-\beta} - 2\right)}{2}\right)\sqrt{(t_2 - t_1)}\left(\sup_{t\in[t_1,t_2]}\left\|D_{t-}^{\frac{1}{2}}\left(EZ_{i,k}\right)\right\|_{\infty,[t_1,t]} + \sup_{t\in[t_1,t_2]}\left\|D_{*t}^{\frac{1}{2}}\left(EZ_{i,k}\right)\right\|_{\infty,[t,t_2]}\right)\right\} < \infty. \quad (116)$$

Proof. From Corollary 29. □

References

[1] G.A. Anastassiou, *Rate of convergence of some neural network operators to the unit-univariate case*, J. Math. Anal. Appl, 212 (1997), 237-262.

[2] G.A. Anastassiou, *Quantitative Approximations*, Chapman & Hall / CRC, Boca Raton, New York, 2001.

[3] G.A. Anastassiou, *Univariate hyperbolic tangent neural network approximation*, Mathematics and Computer Modelling, 53 (2011), 1111-1132.

[4] G.A. Anastassiou, *Multivariate hyperbolic tangent neural network approximation*, Computers and Mathematics, 61 (2011), 809-821.

[5] G.A. Anastassiou, *Multivariate sigmoidal neural networkapproximation*, Neural Networks, 24 (2011), 378-386.

[6] G.A. Anastassiou, *Inteligent Systems: Approximation by Artificial Neural Networks*, Intelligent Systems Reference Library, Vol. 19, Springer, Heidelberg, 2011.

[7] G.A. Anastassiou, *Univariate sigmoidal neural network approximation*, J. of Computational Analysis and Applications, Vol. 14, No.4, 2012, 659-690.

[8] G.A. Anastassiou, *Fractional neural network approximation*, Computers and Mathematics with Applications, 64 (2012), 1655-1676.

[9] G.A. Anastassiou, *Intelligent Systems II: Complete Approximation by Neural Network Operators*, Springer, Heidelberg, New York, 2016.

[10] G.A. Anastassiou, *Strong Right Fractional Calculus for Banach space valued functions*, Revista Proyecciones, Vol. 36, No. 1 (2017), 149-186.

[11] G.A. Anastassiou, *Vector fractional Korovkin type Approximations*, Dynamic Systems and Applications, 26 (2017), 81-104.

[12] G.A. Anastassiou, *A strong Fractional Calculus Theory for Banach space valued functions*, Nonlinear Functional Analysis and Applications (Korea), 22(3)(2017), 495-524.

[13] G.A. Anastassiou, *Intelligent Computations: Abstract Fractional Calculus, Inequalities, Approximations*, Springer, Heidelberg, New York, 2018.

[14] G.A. Anastassiou,*General sigmoid based Banach space valued neural network approximation*, Journal of Computational Analysis and Applications, Accepted, 2022.

[15] Z. Chen and F. Cao, *The approximation operators with sigmoidal functions*, Computers and Mathematics with Applications, 58 (2009), 758-765.

[16] D. Costarelli, R. Spigler, *Approximation results for neural network operators activated by sigmoidal functions*, Neural Networks 44 (2013), 101-106.

[17] D. Costarelli, R. Spigler, *Multivariate neural network operators with sigmoidal activation functions*, Neural Networks 48 (2013), 72-77.

[18] S. Haykin, *Neural Networks: A Comprehensive Foundation* (2 ed.), Prentice Hall, New York, 1998.

[19] M. Kac , A.J.F. Siegert, *An explicit representation of a stationary Gaussian process*, The Annals of Mathematical Statistics, 18 (3) (1947), 438-442.

[20] Yuriy Kozachenko et al, *Simulation of stochastic processes with given accuracy and reliability*, Elsevier (2016), pp.71-104.

[21] W. McCulloch and W. Pitts, *A logical calculus of the ideas immanent in nervous activity*, Bulletin of Mathematical Biophysis, 7 (1943), 115-133.

[22] J. Mikusinski, *The Bochner integral*, Academic Press, New York, 1978.

[23] T.M. Mitchell, *Machine Learning*, WCB-McGraw-Hill, New York, 1997.

[24] G.E. Shilov, *Elementary Functional Analysis*, Dover Publications, Inc., New York, 1996.

J. COMPUTATIONAL ANALYSIS AND APPLICATIONS, VOL. 31, NO. 4, 2023, COPYRIGHT 2023 EUDOXUS PRESS, LLC

Multivariate Gudermannian function based neural network approximation

George A. Anastassiou
Department of Mathematical Sciences
University of Memphis
Memphis, TN 38152, U.S.A.
ganastss@memphis.edu

Abstract

Here we present multivariate quantitative approximations of Banach space valued continuous multivariate functions on a box or $\mathbb{R}^N$, $N \in \mathbb{N}$, by the multivariate normalized, quasi-interpolation, Kantorovich type and quadrature type neural network operators. We examine also the case of approximation by iterated operators of the last four types. These approximations are achieved by establishing multidimensional Jackson type inequalities involving the multivariate modulus of continuity of the engaged function or its high order Fréchet derivatives. Our multivariate operators are defined by using a multidimensional density function induced by the Gudermannian sigmoid function. The approximations are pointwise and uniform. The related feed-forward neural network is with one hidden layer.

2020 AMS Mathematics Subject Classification: 41A17, 41A25, 41A30, 41A36.

Keywords and Phrases: Gudermannian sigmoid function, multivariate neural network approximation, quasi-interpolation operator, Kantorovich type operator, quadrature type operator, multivariate modulus of continuity, abstract approximation, iterated approximation.

1 Introduction

G.A. Anastassiou in [2] and [3], see chapters 2-5, was the first to establish neural network approximations to continuous functions with rates by very specifically defined neural network operators of Cardaliaguet-Euvrard and "Squashing" types, by employing the modulus of continuity of the engaged function or its high order derivative, and producing very tight Jackson type inequalities.

He treats there both the univariate and multivariate cases. The defining these operators "bell-shaped" and "squashing" functions are assumed to be of compact support. Also in [3] he gives the Nth order asymptotic expansion for the error of weak approximation of these two operators to a special natural class of smooth functions, see chapters 4-5 there.

Motivations for this work are the article [17] of Z. Chen and F. Cao, and [4], [5], [6], [7], [8], [9], [10], [11], [12], [14], [15], [18], [19].

Here we perform multivariate Gudermannian sigmoid function based neural network approximations to continuous functions over boxes or over the whole $\mathbb{R}^N$, $N \in \mathbb{N}$, and also iterated approximations. All convergences here are with rates expressed via the multivariate modulus of continuity of the involved function or its high order Fréchet derivative and given by very tight multidimensional Jackson type inequalities.

We come up with the "right" precisely defined multivariate normalized, quasi-interpolation neural network operators related to boxes or $\mathbb{R}^N$, as well as Kantorovich type and quadrature type related operators on $\mathbb{R}^N$. Our boxes are not necessarily symmetric to the origin. In preparation to prove our results we establish important properties of the basic multivariate density function induced by Gudermannian sigmoid function and defining our operators.

Feed-forward neural networks (FNNs) with one hidden layer, the only type of networks we deal with in this article, are mathematically expressed as

$$N_n(x) = \sum_{j=0}^{n} c_j \sigma\left(\langle a_j \cdot x \rangle + b_j\right), \quad x \in \mathbb{R}^s, \quad s \in \mathbb{N},$$

where for $0 \leq j \leq n$, $b_j \in \mathbb{R}$ are the thresholds, $a_j \in \mathbb{R}^s$ are the connection weights, $c_j \in \mathbb{R}$ are the coefficients, $\langle a_j \cdot x \rangle$ is the inner product of a_j and x, and σ is the activation function of the network. In many fundamental network models, the activation function is the Gudermannian sigmoid function. About neural networks see [20], [21], [22].

2 Background

See also [13], [24].

Here we consider $gd(x)$ the Gudermannian function [24], which is a sigmoid function, as a generator function:

$$\sigma(x) = 2\arctan\left(\tanh\left(\frac{x}{2}\right)\right) = \int_0^x \frac{dt}{\cosh t} =: gd(x), \; x \in \mathbb{R}. \tag{1}$$

Let the normalized generator sigmoid function

$$f(x) := \frac{2}{\pi}\sigma(x) = \frac{2}{\pi}\int_0^x \frac{dt}{\cosh t} = \frac{4}{\pi}\int_0^x \frac{1}{e^t + e^{-t}}dt, \quad x \in \mathbb{R}. \tag{2}$$

Here

$$f'(x) = \frac{2}{\pi \cosh x} > 0, \quad \forall\, x \in \mathbb{R},$$

hence $f$is strictly increasing on $\mathbb{R}$.

Notice that $\tanh(-x) = -\tanh x$ and $\arctan(-x) = -\arctan x$, $x \in \mathbb{R}$.

So, here the neural network activation function will be:

$$W(x) = \frac{1}{4}\left[f(x+1) - f(x-1)\right], \; x \in \mathbb{R}. \tag{3}$$

By [3], we get that

$$W(x) = W(-x), \quad \forall\, x \in \mathbb{R}, \tag{4}$$

i.e. it is even and symmetric with respect to the y-axis. Here we have $f(+\infty) = 1$, $f(-\infty) = -1$ and $f(0) = 0$. Clearly it is

$$f(-x) = -f(x), \; \forall\, x \in \mathbb{R}, \tag{5}$$

an odd function, symmetric with respect to the origin. Since $x+1 > x-1$, and $f(x+1) > f(x-1)$, we obtain $W(x) > 0$, $\forall\, x \in \mathbb{R}$.

By [13], we have that

$$W(0) = \frac{1}{\pi} gd(1) \cong 0.2757. \tag{6}$$

By [13] W is strictly decreasing on $(0, +\infty)$, and strictly increasing on $(-\infty, 0)$, and $W'(0) = 0$.

Also we have that

$$\lim_{x \to +\infty} W(x) = \lim_{x \to -\infty} W(x) = 0, \tag{7}$$

that is the x-axis is the horizontal asymptote for W.

Conclusion, W is a bell shaped symmetric function with maximum $W(0) \cong 0.2757$.

We need

Theorem 1 *([13]) It holds that*

$$\sum_{i=-\infty}^{\infty} W(x-i) = 1, \; \forall\, x \in \mathbb{R}. \tag{8}$$

Theorem 2 *([13]) We have that*

$$\int_{-\infty}^{\infty} W(x)\, dx = 1. \tag{9}$$

So $W(x)$ is a density function.

Theorem 3 *([13]) Let $0 < \alpha < 1$, and $n \in \mathbb{N}$ with $n^{1-\alpha} > 2$. It holds*

$$\sum_{\begin{cases} k = -\infty \\ : |nx - k| \geq n^{1-\alpha} \end{cases}}^{\infty} W(nx - k) < \frac{2}{\pi e^{(n^{1-\alpha}-2)}} = \frac{2e^2}{\pi e^{n^{1-\alpha}}}. \tag{10}$$

Denote by $\lfloor \cdot \rfloor$ the integral part of the number and by $\lceil \cdot \rceil$ the ceiling of the number.

Theorem 4 *([13]) Let $[a, b] \subset \mathbb{R}$ and $n \in \mathbb{N}$, so that $\lceil na \rceil \leq \lfloor nb \rfloor$. It holds*

$$\frac{1}{\sum_{k=\lceil na \rceil}^{\lfloor nb \rfloor} W(nx - k)} < \frac{2\pi}{gd(2)} \cong 4.824, \tag{11}$$

$\forall\, x \in [a, b]$.

We make

Remark 5 *([13])*

(i) We have that

$$\lim_{n \to \infty} \sum_{k=\lceil na \rceil}^{\lfloor nb \rfloor} W(nx - k) \neq 1, \tag{12}$$

for at least some $x \in [a, b]$.

(ii) Let $[a, b] \subset \mathbb{R}$. For large n we always have $\lceil na \rceil \leq \lfloor nb \rfloor$. Also $a \leq \frac{k}{n} \leq b$, iff $\lceil na \rceil \leq k \leq \lfloor nb \rfloor$.

In general it holds

$$\sum_{k=\lceil na \rceil}^{\lfloor nb \rfloor} W(nx - k) \leq 1. \tag{13}$$

We introduce

$$Z(x_1, ..., x_N) := Z(x) := \prod_{i=1}^{N} W(x_i), \quad x = (x_1, ..., x_N) \in \mathbb{R}^N, \ N \in \mathbb{N}. \tag{14}$$

It has the properties:

(i) $Z(x) > 0, \ \forall\, x \in \mathbb{R}^N$,

(ii)

$$\sum_{k=-\infty}^{\infty} Z(x - k) := \sum_{k_1=-\infty}^{\infty} \sum_{k_2=-\infty}^{\infty} ... \sum_{k_N=-\infty}^{\infty} Z(x_1 - k_1, ..., x_N - k_N) = 1, \tag{15}$$

where $k := (k_1, ..., k_n) \in \mathbb{Z}^N$, $\forall\ x \in \mathbb{R}^N$,

hence

(iii)

$$\sum_{k=-\infty}^{\infty} Z(nx-k) = 1, \tag{16}$$

$\forall\ x \in \mathbb{R}^N$; $n \in \mathbb{N}$,

and

(iv)

$$\int_{\mathbb{R}^N} Z(x)\, dx = 1, \tag{17}$$

that is Z is a multivariate density function.

Here denote $\|x\|_\infty := \max\{|x_1|, ..., |x_N|\}$, $x \in \mathbb{R}^N$, also set $\infty := (\infty, ..., \infty)$, $-\infty := (-\infty, ..., -\infty)$ upon the multivariate context, and

$$\begin{gathered} \lceil na \rceil := (\lceil na_1 \rceil, ..., \lceil na_N \rceil), \\ \lfloor nb \rfloor := (\lfloor nb_1 \rfloor, ..., \lfloor nb_N \rfloor), \end{gathered} \tag{18}$$

where $a := (a_1, ..., a_N)$, $b := (b_1, ..., b_N)$.

We obviously see that

$$\sum_{k=\lceil na \rceil}^{\lfloor nb \rfloor} Z(nx-k) = \sum_{k=\lceil na \rceil}^{\lfloor nb \rfloor} \left(\prod_{i=1}^{N} W(nx_i - k_i) \right) =$$

$$\sum_{k_1=\lceil na_1 \rceil}^{\lfloor nb_1 \rfloor} \cdots \sum_{k_N=\lceil na_N \rceil}^{\lfloor nb_N \rfloor} \left(\prod_{i=1}^{N} W(nx_i - k_i) \right) = \prod_{i=1}^{N} \left(\sum_{k_i=\lceil na_i \rceil}^{\lfloor nb_i \rfloor} W(nx_i - k_i) \right). \tag{19}$$

For $0 < \beta < 1$ and $n \in \mathbb{N}$, a fixed $x \in \mathbb{R}^N$, we have that

$$\sum_{k=\lceil na \rceil}^{\lfloor nb \rfloor} Z(nx-k) =$$

$$\sum_{\begin{cases} k = \lceil na \rceil \\ \left\| \frac{k}{n} - x \right\|_\infty \le \frac{1}{n^\beta} \end{cases}}^{\lfloor nb \rfloor} Z(nx-k) + \sum_{\begin{cases} k = \lceil na \rceil \\ \left\| \frac{k}{n} - x \right\|_\infty > \frac{1}{n^\beta} \end{cases}}^{\lfloor nb \rfloor} Z(nx-k). \tag{20}$$

In the last two sums the counting is over disjoint vector sets of k's, because the condition $\left\| \frac{k}{n} - x \right\|_\infty > \frac{1}{n^\beta}$ implies that there exists at least one $\left| \frac{k_r}{n} - x_r \right| > \frac{1}{n^\beta}$, where $r \in \{1, ..., N\}$.

(v) As in [10], pp. 379-380, we derive that

$$\sum_{\substack{\left\{\begin{array}{l} k=\lceil na\rceil \\ \left\|\frac{k}{n}-x\right\|_{\infty}>\frac{1}{n^{\beta}} \end{array}\right.}}^{\lfloor nb\rfloor} Z(nx-k) \overset{(10)}{<} \frac{2e^{2}}{\pi e^{n^{1-\beta}}},\ \ 0<\beta<1,\ \ m\in\mathbb{N}, \tag{21}$$

with $n\in\mathbb{N}: n^{1-\beta}>2$, $x\in\prod_{i=1}^{N}[a_i,b_i]$.

(vi) By Theorem 4 we get that

$$0<\frac{1}{\sum_{k=\lceil na\rceil}^{\lfloor nb\rfloor} Z(nx-k)}<\left(\frac{2\pi}{gd(2)}\right)^{N}\cong(4.824)^{N}, \tag{22}$$

$\forall\ x\in\left(\prod_{i=1}^{N}[a_i,b_i]\right),\ \ n\in\mathbb{N}$.

It is also clear that

(vii)

$$\sum_{\substack{\left\{\begin{array}{l} k=-\infty \\ \left\|\frac{k}{n}-x\right\|_{\infty}>\frac{1}{n^{\beta}} \end{array}\right.}}^{\infty} Z(nx-k)<\frac{2e^{2}}{\pi e^{n^{1-\beta}}}, \tag{23}$$

$0<\beta<1$, $n\in\mathbb{N}: n^{1-\beta}>2$, $x\in\mathbb{R}^{N}$, $m\in\mathbb{N}$.

Furthermore it holds

$$\lim_{n\to\infty}\sum_{k=\lceil na\rceil}^{\lfloor nb\rfloor} Z(nx-k)\neq 1, \tag{24}$$

for at least some $x\in\left(\prod_{i=1}^{N}[a_i,b_i]\right)$.

Here $\left(X,\|\cdot\|_{\gamma}\right)$ is a Banach space.

Let $f\in C\left(\prod_{i=1}^{N}[a_i,b_i],X\right)$, $x=(x_1,...,x_N)\in\prod_{i=1}^{N}[a_i,b_i]$, $n\in\mathbb{N}$ such that $\lceil na_i\rceil\leq\lfloor nb_i\rfloor$, $i=1,...,N$.

We introduce and define the following multivariate linear normalized neural network operator ($x:=(x_1,...,x_N)\in\left(\prod_{i=1}^{N}[a_i,b_i]\right)$):

$$A_n(f,x_1,...,x_N):=A_n(f,x):=\frac{\sum_{k=\lceil na\rceil}^{\lfloor nb\rfloor} f\left(\frac{k}{n}\right)Z(nx-k)}{\sum_{k=\lceil na\rceil}^{\lfloor nb\rfloor} Z(nx-k)}=$$

$$\frac{\sum_{k_1=\lceil na_1\rceil}^{\lfloor nb_1\rfloor}\sum_{k_2=\lceil na_2\rceil}^{\lfloor nb_2\rfloor}...\sum_{k_N=\lceil na_N\rceil}^{\lfloor nb_N\rfloor} f\left(\frac{k_1}{n},...,\frac{k_N}{n}\right)\left(\prod_{i=1}^{N}W(nx_i-k_i)\right)}{\prod_{i=1}^{N}\left(\sum_{k_i=\lceil na_i\rceil}^{\lfloor nb_i\rfloor}W(nx_i-k_i)\right)}. \tag{25}$$

For large enough $n\in\mathbb{N}$ we always obtain $\lceil na_i\rceil\leq\lfloor nb_i\rfloor$, $i=1,...,N$. Also $a_i\leq\frac{k_i}{n}\leq b_i$, iff $\lceil na_i\rceil\leq k_i\leq\lfloor nb_i\rfloor$, $i=1,...,N$.

When $g \in C\left(\prod_{i=1}^{N}[a_i,b_i]\right)$ we define the companion operator

$$\widetilde{A}_n(g,x) := \frac{\sum_{k=\lceil na\rceil}^{\lfloor nb\rfloor} g\left(\frac{k}{n}\right) Z(nx-k)}{\sum_{k=\lceil na\rceil}^{\lfloor nb\rfloor} Z(nx-k)}. \tag{26}$$

Clearly $\widetilde{A}_n$ is a positive linear operator. We have that

$$\widetilde{A}_n(1,x) = 1, \ \forall\ x \in \left(\prod_{i=1}^{N}[a_i,b_i]\right).$$

Notice that $A_n(f) \in C\left(\prod_{i=1}^{N}[a_i,b_i], X\right)$ and $\widetilde{A}_n(g) \in C\left(\prod_{i=1}^{N}[a_i,b_i]\right)$.

Furthermore it holds

$$\|A_n(f,x)\|_\gamma \leq \frac{\sum_{k=\lceil na\rceil}^{\lfloor nb\rfloor} \left\|f\left(\frac{k}{n}\right)\right\|_\gamma Z(nx-k)}{\sum_{k=\lceil na\rceil}^{\lfloor nb\rfloor} Z(nx-k)} = \widetilde{A}_n\left(\|f\|_\gamma, x\right), \tag{27}$$

$\forall\ x \in \prod_{i=1}^{N}[a_i,b_i]$.

Clearly $\|f\|_\gamma \in C\left(\prod_{i=1}^{N}[a_i,b_i]\right)$.

So, we have that

$$\|A_n(f,x)\|_\gamma \leq \widetilde{A}_n\left(\|f\|_\gamma, x\right), \tag{28}$$

$\forall\ x \in \prod_{i=1}^{N}[a_i,b_i]$, $\forall\ n \in \mathbb{N}$, $\forall\ f \in C\left(\prod_{i=1}^{N}[a_i,b_i], X\right)$.

Let $c \in X$ and $g \in C\left(\prod_{i=1}^{N}[a_i,b_i]\right)$, then $cg \in C\left(\prod_{i=1}^{N}[a_i,b_i], X\right)$.

Furthermore it holds

$$A_n(cg,x) = c\widetilde{A}_n(g,x), \ \forall\ x \in \prod_{i=1}^{N}[a_i,b_i]. \tag{29}$$

Since $\widetilde{A}_n(1) = 1$, we get that

$$A_n(c) = c, \ \forall\ c \in X. \tag{30}$$

We call $\widetilde{A}_n$ the companion operator of A_n.

For convinience we call

$$A_n^*(f,x) := \sum_{k=\lceil na\rceil}^{\lfloor nb\rfloor} f\left(\frac{k}{n}\right) Z(nx-k) =$$

$$\sum_{k_1=\lceil na_1\rceil}^{\lfloor nb_1\rfloor} \sum_{k_2=\lceil na_2\rceil}^{\lfloor nb_2\rfloor} \ldots \sum_{k_N=\lceil na_N\rceil}^{\lfloor nb_N\rfloor} f\left(\frac{k_1}{n}, \ldots, \frac{k_N}{n}\right)\left(\prod_{i=1}^{N} W(nx_i-k_i)\right), \tag{31}$$

$\forall\ x \in \left(\prod_{i=1}^{N} [a_i, b_i] \right)$.

That is

$$A_n(f, x) := \frac{A_n^*(f, x)}{\sum_{k=\lceil na \rceil}^{\lfloor nb \rfloor} Z(nx - k)}, \tag{32}$$

$\forall\ x \in \left(\prod_{i=1}^{N} [a_i, b_i] \right)$, $n \in \mathbb{N}$.

Hence

$$A_n(f, x) - f(x) = \frac{A_n^*(f, x) - f(x) \left(\sum_{k=\lceil na \rceil}^{\lfloor nb \rfloor} Z(nx - k) \right)}{\sum_{k=\lceil na \rceil}^{\lfloor nb \rfloor} Z(nx - k)}. \tag{33}$$

Consequently we derive

$$\|A_n(f, x) - f(x)\|_\gamma \overset{(22)}{\leq} (4.824)^N \left\| A_n^*(f, x) - f(x) \sum_{k=\lceil na \rceil}^{\lfloor nb \rfloor} Z(nx - k) \right\|_\gamma, \tag{34}$$

$\forall\ x \in \left(\prod_{i=1}^{N} [a_i, b_i] \right)$.

We will estimate the right hand side of (34).

For the last and others we need

Definition 6 *([11], p. 274) Let M be a convex and compact subset of $\left(\mathbb{R}^N, \|\cdot\|_p\right)$, $p \in [1, \infty]$, and $\left(X, \|\cdot\|_\gamma\right)$ be a Banach space. Let $f \in C(M, X)$. We define the first modulus of continuity of f as*

$$\omega_1(f, \delta) := \sup_{\substack{x, y \in M: \\ \|x - y\|_p \leq \delta}} \|f(x) - f(y)\|_\gamma, \quad 0 < \delta \leq diam(M). \tag{35}$$

If $\delta > diam(M)$, then

$$\omega_1(f, \delta) = \omega_1(f, diam(M)). \tag{36}$$

Notice $\omega_1(f, \delta)$ is increasing in $\delta > 0$. For $f \in C_B(M, X)$ (continuous and bounded functions) $\omega_1(f, \delta)$ is defined similarly.

Lemma 7 *([11], p. 274) We have $\omega_1(f, \delta) \to 0$ as $\delta \downarrow 0$, iff $f \in C(M, X)$, where M is a convex compact subset of $\left(\mathbb{R}^N, \|\cdot\|_p\right)$, $p \in [1, \infty]$.*

Clearly we have also: $f \in C_U\left(\mathbb{R}^N, X\right)$ (uniformly continuous functions), iff $\omega_1(f, \delta) \to 0$ as $\delta \downarrow 0$, where ω_1 is defined similarly to (35). The space $C_B\left(\mathbb{R}^N, X\right)$ denotes the continuous and bounded functions on $\mathbb{R}^N$.

When $f \in C_B\left(\mathbb{R}^N, X\right)$ we define,

$$B_n(f,x) := B_n(f,x_1,...,x_N) := \sum_{k=-\infty}^{\infty} f\left(\frac{k}{n}\right) Z(nx-k) :=$$

$$\sum_{k_1=-\infty}^{\infty} \sum_{k_2=-\infty}^{\infty} ... \sum_{k_N=-\infty}^{\infty} f\left(\frac{k_1}{n}, \frac{k_2}{n}, ..., \frac{k_N}{n}\right) \left(\prod_{i=1}^{N} W(nx_i - k_i)\right), \tag{37}$$

$n \in \mathbb{N}$, $\forall\ x \in \mathbb{R}^N$, $N \in \mathbb{N}$, the multivariate quasi-interpolation neural network operator.

Also for $f \in C_B\left(\mathbb{R}^N, X\right)$ we define the multivariate Kantorovich type neural network operator

$$C_n(f,x) := C_n(f,x_1,...,x_N) := \sum_{k=-\infty}^{\infty} \left(n^N \int_{\frac{k}{n}}^{\frac{k+1}{n}} f(t)\,dt\right) Z(nx-k) =$$

$$\sum_{k_1=-\infty}^{\infty} \sum_{k_2=-\infty}^{\infty} ... \sum_{k_N=-\infty}^{\infty} \left(n^N \int_{\frac{k_1}{n}}^{\frac{k_1+1}{n}} \int_{\frac{k_2}{n}}^{\frac{k_2+1}{n}} ... \int_{\frac{k_N}{n}}^{\frac{k_N+1}{n}} f(t_1,...,t_N)\,dt_1...dt_N\right)$$

$$\cdot \left(\prod_{i=1}^{N} W(nx_i - k_i)\right), \tag{38}$$

$n \in \mathbb{N}$, $\forall\ x \in \mathbb{R}^N$.

Again for $f \in C_B\left(\mathbb{R}^N, X\right)$, $N \in \mathbb{N}$, we define the multivariate neural network operator of quadrature type $D_n(f,x)$, $n \in \mathbb{N}$, as follows.

Let $\theta = (\theta_1, ..., \theta_N) \in \mathbb{N}^N$, $r = (r_1, ..., r_N) \in \mathbb{Z}_+^N$, $w_r = w_{r_1,r_2,...r_N} \geq 0$, such that $\sum\limits_{r=0}^{\theta} w_r = \sum\limits_{r_1=0}^{\theta_1} \sum\limits_{r_2=0}^{\theta_2} ... \sum\limits_{r_N=0}^{\theta_N} w_{r_1,r_2,...r_N} = 1$; $k \in \mathbb{Z}^N$ and

$$\delta_{nk}(f) := \delta_{n,k_1,k_2,...,k_N}(f) := \sum_{r=0}^{\theta} w_r f\left(\frac{k}{n} + \frac{r}{n\theta}\right) =$$

$$\sum_{r_1=0}^{\theta_1} \sum_{r_2=0}^{\theta_2} ... \sum_{r_N=0}^{\theta_N} w_{r_1,r_2,...r_N} f\left(\frac{k_1}{n} + \frac{r_1}{n\theta_1}, \frac{k_2}{n} + \frac{r_2}{n\theta_2}, ..., \frac{k_N}{n} + \frac{r_N}{n\theta_N}\right), \tag{39}$$

where $\frac{r}{\theta} := \left(\frac{r_1}{\theta_1}, \frac{r_2}{\theta_2}, ..., \frac{r_N}{\theta_N}\right)$.

We set

$$D_n(f,x) := D_n(f,x_1,...,x_N) := \sum_{k=-\infty}^{\infty} \delta_{nk}(f) Z(nx-k) = \tag{40}$$

$$\sum_{k_1=-\infty}^{\infty} \sum_{k_2=-\infty}^{\infty} ... \sum_{k_N=-\infty}^{\infty} \delta_{n,k_1,k_2,...,k_N}(f) \left(\prod_{i=1}^{N} W(nx_i - k_i)\right),$$

$\forall\ x \in \mathbb{R}^N$.

In this article we study the approximation properties of $A_n, B_n, C_n,\ D_n$ neural network operators and as well of their iterates. That is, the quantitative pointwise and uniform convergence of these operators to the unit operator I.

3 Multivariate general Neural Network Approximations

Here we present several vectorial neural network approximations to Banach space valued functions given with rates.

We give

Theorem 8 *Let* $f \in C\left(\prod_{i=1}^{N}\left[a_i, b_i\right], X\right)$, $0 < \beta < 1$, $x \in \left(\prod_{i=1}^{N}\left[a_i, b_i\right]\right)$, $m, N, n \in \mathbb{N}$ *with* $n^{1-\beta} > 2$. *Then*

1)

$$\left\|A_n(f, x) - f(x)\right\|_\gamma \leq (4.824)^N \left[\omega_1\left(f, \frac{1}{n^\beta}\right) + \frac{4e^2 \left\|\left\|f\right\|_\gamma\right\|_\infty}{\pi e^{n^{1-\beta}}}\right] =: \lambda_1(n), \tag{41}$$

and

2)

$$\left\|\left\|A_n(f) - f\right\|_\gamma\right\|_\infty \leq \lambda_1(n). \tag{42}$$

We notice that $\lim_{n\to\infty} A_n(f) \overset{\|\cdot\|_\gamma}{=} f$, *pointwise and uniformly.*

Above ω_1 *is with respect to* $p = \infty$.

Proof. We observe that

$$\Delta(x) := A_n^*(f, x) - f(x) \sum_{k=\lceil na \rceil}^{\lfloor nb \rfloor} Z(nx - k) =$$

$$\sum_{k=\lceil na \rceil}^{\lfloor nb \rfloor} f\left(\frac{k}{n}\right) Z(nx - k) - \sum_{k=\lceil na \rceil}^{\lfloor nb \rfloor} f(x) Z(nx - k) =$$

$$\sum_{k=\lceil na \rceil}^{\lfloor nb \rfloor} \left(f\left(\frac{k}{n}\right) - f(x)\right) Z(nx - k). \tag{43}$$

Thus

$$\left\|\Delta(x)\right\|_\gamma \leq \sum_{k=\lceil na \rceil}^{\lfloor nb \rfloor} \left\|f\left(\frac{k}{n}\right) - f(x)\right\|_\gamma Z(nx - k) =$$

$$\sum_{\left\{\begin{array}{c} k=\lceil na\rceil \\ \left\|\frac{k}{n}-x\right\|_\infty \leq \frac{1}{n^\beta}\end{array}\right.}^{\lfloor nb\rfloor} \left\|f\left(\frac{k}{n}\right)-f(x)\right\|_\gamma Z(nx-k)+$$

$$\sum_{\left\{\begin{array}{c} k=\lceil na\rceil \\ \left\|\frac{k}{n}-x\right\|_\infty > \frac{1}{n^\beta}\end{array}\right.}^{\lfloor nb\rfloor} \left\|f\left(\frac{k}{n}\right)-f(x)\right\|_\gamma Z(nx-k) \overset{(16)}{\leq}$$

$$\omega_1\left(f,\frac{1}{n^\beta}\right)+2\left\|\|f\|_\gamma\right\|_\infty \sum_{\left\{\begin{array}{c} k=\lceil na\rceil \\ \left\|\frac{k}{n}-x\right\|_\infty > \frac{1}{n^\beta}\end{array}\right.}^{\lfloor nb\rfloor} Z(nx-k) \overset{(21)}{\leq}$$

$$\omega_1\left(f,\frac{1}{n^\beta}\right)+\frac{4e^2\left\|\|f\|_\gamma\right\|_\infty}{\pi e^{n^{1-\beta}}}. \tag{44}$$

So that

$$\|\Delta(x)\|_\gamma \leq \omega_1\left(f,\frac{1}{n^\beta}\right)+\frac{4e^2\left\|\|f\|_\gamma\right\|_\infty}{\pi e^{n^{1-\beta}}}. \tag{45}$$

Now using (34) we finish the proof. ■

We make

Remark 9 *([11], pp. 263-266) Let* $\left(\mathbb{R}^N, \|\cdot\|_p\right)$, $N\in\mathbb{N}$*; where* $\|\cdot\|_p$ *is the* L_p*-norm,* $1\leq p\leq\infty$. $\mathbb{R}^N$ *is a Banach space, and* $\left(\mathbb{R}^N\right)^j$ *denotes the* j*-fold product space* $\mathbb{R}^N\times...\times\mathbb{R}^N$ *endowed with the max-norm* $\|x\|_{(\mathbb{R}^N)^j} := \max_{1\leq\lambda\leq j}\|x_\lambda\|_p$*, where* $x:=(x_1,...,x_j)\in\left(\mathbb{R}^N\right)^j$.

Let $\left(X,\|\cdot\|_\gamma\right)$ *be a general Banach space. Then the space* $L_j := L_j\left(\left(\mathbb{R}^N\right)^j; X\right)$ *of all* j*-multilinear continuous maps* $g:\left(\mathbb{R}^N\right)^j\to X$, $j=1,...,m$*, is a Banach space with norm*

$$\|g\| := \|g\|_{L_j} := \sup_{\left(\|x\|_{(\mathbb{R}^N)^j}=1\right)}\|g(x)\|_\gamma = \sup\frac{\|g(x)\|_\gamma}{\|x_1\|_p\cdots\|x_j\|_p}. \tag{46}$$

Let M *be a non-empty convex and compact subset of* $\mathbb{R}^N$ *and* $x_0\in M$ *is fixed.*

Let O *be an open subset of* $\mathbb{R}^N : M\subset O$*. Let* $f:O\to X$ *be a continuous function, whose Fréchet derivatives (see [23])* $f^{(j)}:O\to L_j=L_j\left(\left(\mathbb{R}^N\right)^j;X\right)$ *exist and are continuous for* $1\leq j\leq m$, $m\in\mathbb{N}$.

Call $(x-x_0)^j := (x-x_0,...,x-x_0)\in\left(\mathbb{R}^N\right)^j$, $x\in M$.

We will work with $f|_M$.

Then, by Taylor's formula ([16]), ([23], p. 124), we get

$$f(x)=\sum_{j=0}^{m}\frac{f^{(j)}(x_0)(x-x_0)^j}{j!}+R_m(x,x_0),\quad \text{all } x\in M, \tag{47}$$

where the remainder is the Riemann integral

$$R_m(x,x_0):=\int_0^1\frac{(1-u)^{m-1}}{(m-1)!}\left(f^{(m)}(x_0+u(x-x_0))-f^{(m)}(x_0)\right)(x-x_0)^m du, \tag{48}$$

here we set $f^{(0)}(x_0)(x-x_0)^0=f(x_0)$.

We consider

$$w:=\omega_1\left(f^{(m)},h\right):=\sup_{\substack{x,y\in M:\\ \|x-y\|_p\le h}}\left\|f^{(m)}(x)-f^{(m)}(y)\right\|, \tag{49}$$

$h>0$.

We obtain

$$\left\|\left(f^{(m)}(x_0+u(x-x_0))-f^{(m)}(x_0)\right)(x-x_0)^m\right\|_\gamma\le$$
$$\left\|f^{(m)}(x_0+u(x-x_0))-f^{(m)}(x_0)\right\|\cdot\|x-x_0\|_p^m\le$$
$$w\|x-x_0\|_p^m\left\lceil\frac{u\|x-x_0\|_p}{h}\right\rceil, \tag{50}$$

by Lemma 7.1.1, [1], p. 208, where $\lceil\cdot\rceil$ *is the ceiling.*

Therefore for all $x\in M$ *(see [1], pp. 121-122):*

$$\|R_m(x,x_0)\|_\gamma\le w\|x-x_0\|_p^m\int_0^1\left\lceil\frac{u\|x-x_0\|_p}{h}\right\rceil\frac{(1-u)^{m-1}}{(m-1)!}du$$
$$=w\Phi_m\left(\|x-x_0\|_p\right) \tag{51}$$

by a change of variable, where

$$\Phi_m(t):=\int_0^{|t|}\left\lceil\frac{s}{h}\right\rceil\frac{(|t|-s)^{m-1}}{(m-1)!}ds=\frac{1}{m!}\left(\sum_{j=0}^{\infty}(|t|-jh)_+^m\right),\quad\forall\, t\in\mathbb{R}, \tag{52}$$

is a (polynomial) spline function, see [1], p. 210-211.

Also from there we get

$$\Phi_m(t)\le\left(\frac{|t|^{m+1}}{(m+1)!h}+\frac{|t|^m}{2m!}+\frac{h|t|^{m-1}}{8(m-1)!}\right),\quad\forall\, t\in\mathbb{R}, \tag{53}$$

with equality true only at $t=0$.

Therefore it holds

$$\left\|R_m(x,x_0)\right\|_\gamma \leq w\left(\frac{\|x-x_0\|_p^{m+1}}{(m+1)!h}+\frac{\|x-x_0\|_p^{m}}{2m!}+\frac{h\|x-x_0\|_p^{m-1}}{8(m-1)!}\right), \quad \forall\, x\in M. \tag{54}$$

We have found that

$$\left\|f(x)-\sum_{j=0}^{m}\frac{f^{(j)}(x_0)(x-x_0)^j}{j!}\right\|_\gamma \leq$$

$$\omega_1\left(f^{(m)},h\right)\left(\frac{\|x-x_0\|_p^{m+1}}{(m+1)!h}+\frac{\|x-x_0\|_p^{m}}{2m!}+\frac{h\|x-x_0\|_p^{m-1}}{8(m-1)!}\right)<\infty, \tag{55}$$

$\forall\, x,x_0\in M$.

Here $0<\omega_1\left(f^{(m)},h\right)<\infty$, *by* M *being compact and* $f^{(m)}$ *being continuous on* M.

One can rewrite (55) as follows:

$$\left\|f(\cdot)-\sum_{j=0}^{m}\frac{f^{(j)}(x_0)(\cdot-x_0)^j}{j!}\right\|_\gamma \leq$$

$$\omega_1\left(f^{(m)},h\right)\left(\frac{\|\cdot-x_0\|_p^{m+1}}{(m+1)!h}+\frac{\|\cdot-x_0\|_p^{m}}{2m!}+\frac{h\|\cdot-x_0\|_p^{m-1}}{8(m-1)!}\right), \ \forall\, x_0\in M, \tag{56}$$

a pointwise functional inequality on M.

Here $(\cdot-x_0)^j$ *maps* M *into* $\left(\mathbb{R}^N\right)^j$ *and it is continuous, also* $f^{(j)}(x_0)$ *maps* $\left(\mathbb{R}^N\right)^j$ *into* X *and it is continuous. Hence their composition* $f^{(j)}(x_0)(\cdot-x_0)^j$ *is continuous from* M *into* X.

Clearly $f(\cdot)-\sum_{j=0}^{m}\frac{f^{(j)}(x_0)(\cdot-x_0)^j}{j!}\in C(M,X)$, *hence* $\left\|f(\cdot)-\sum_{j=0}^{m}\frac{f^{(j)}(x_0)(\cdot-x_0)^j}{j!}\right\|_\gamma\in C(M)$.

Let $\left\{\widetilde{L}_N\right\}_{N\in\mathbb{N}}$ *be a sequence of positive linear operators mapping* $C(M)$ *into* $C(M)$.

Therefore we obtain

$$\left(\widetilde{L}_N\left(\left\|f(\cdot)-\sum_{j=0}^{m}\frac{f^{(j)}(x_0)(\cdot-x_0)^j}{j!}\right\|_\gamma\right)\right)(x_0)\leq$$

$$\omega_1\left(f^{(m)},h\right)\left[\frac{\left(\widetilde{L}_N\left(\|\cdot-x_0\|_p^{m+1}\right)\right)(x_0)}{(m+1)!h}+\frac{\left(\widetilde{L}_N\left(\|\cdot-x_0\|_p^{m}\right)\right)(x_0)}{2m!}\right.$$

$$\left. + \frac{h\left(\widetilde{L}_N\left(\|\cdot - x_0\|_p^{m-1}\right)\right)(x_0)}{8(m-1)!}\right], \tag{57}$$

$\forall\ N \in \mathbb{N}$, $\forall\ x_0 \in M$.

Clearly (57) is valid when $M = \prod_{i=1}^{N} [a_i, b_i]$ and $\widetilde{L}_n = \widetilde{A}_n$, see (26).

All the above is preparation for the following theorem, where we assume Fréchet differentiability of functions.

This will be a direct application of Theorem 10.2, [11], pp. 268-270. The operators A_n, $\widetilde{A}_n$ fulfill its assumptions, see (25), (26), (28), (29) and (30).

We present the following high order approximation results.

Theorem 10 *Let O open subset of $\left(\mathbb{R}^N, \|\cdot\|_p\right)$, $p \in [1, \infty]$, such that $\prod_{i=1}^{N} [a_i, b_i] \subset O \subseteq \mathbb{R}^N$, and let $\left(X, \|\cdot\|_\gamma\right)$ be a general Banach space. Let $m \in \mathbb{N}$ and $f \in C^m(O, X)$, the space of $\overline{m}$-times continuously Fréchet differentiable functions from O into X. We study the approximation of $f|_{\prod_{i=1}^{N}[a_i,b_i]}$. Let $x_0 \in \left(\prod_{i=1}^{N} [a_i, b_i]\right)$ and $r > 0$. Then*

1)

$$\left\| (A_n(f))(x_0) - \sum_{j=0}^{m} \frac{1}{j!}\left(A_n\left(f^{(j)}(x_0)(\cdot - x_0)^j\right)\right)(x_0) \right\|_\gamma \leq$$

$$\frac{\omega_1\left(f^{(m)}, r\left(\left(\widetilde{A}_n\left(\|\cdot - x_0\|_p^{m+1}\right)\right)(x_0)\right)^{\frac{1}{m+1}}\right)}{rm!}\left(\left(\widetilde{A}_n\left(\|\cdot - x_0\|_p^{m+1}\right)\right)(x_0)\right)^{\left(\frac{m}{m+1}\right)}$$

$$\left[\frac{1}{(m+1)} + \frac{r}{2} + \frac{mr^2}{8}\right], \tag{58}$$

2) additionally if $f^{(j)}(x_0) = 0$, $j = 1, ..., \overline{m}$, we have

$$\|(A_n(f))(x_0) - f(x_0)\|_\gamma \leq$$

$$\frac{\omega_1\left(f^{(m)}, r\left(\left(\widetilde{A}_n\left(\|\cdot - x_0\|_p^{m+1}\right)\right)(x_0)\right)^{\frac{1}{m+1}}\right)}{rm!}\left(\left(\widetilde{A}_n\left(\|\cdot - x_0\|_p^{m+1}\right)\right)(x_0)\right)^{\left(\frac{m}{m+1}\right)} \tag{59}$$

$$\left[\frac{1}{(m+1)} + \frac{r}{2} + \frac{mr^2}{8}\right],$$

3)

$$\|(A_n(f))(x_0) - f(x_0)\|_\gamma \leq \sum_{j=1}^{m} \frac{1}{j!}\left\|\left(A_n\left(f^{(j)}(x_0)(\cdot - x_0)^j\right)\right)(x_0)\right\|_\gamma +$$

$$\frac{\omega_1\left(f^{(m)}, r\left(\left(\widetilde{A}_n\left(\|\cdot - x_0\|_p^{m+1}\right)\right)(x_0)\right)^{\frac{1}{m+1}}\right)}{rm!}\left(\left(\widetilde{A}_n\left(\|\cdot - x_0\|_p^{m+1}\right)\right)(x_0)\right)^{\left(\frac{m}{m+1}\right)} \tag{60}$$
$$\left[\frac{1}{(m+1)} + \frac{r}{2} + \frac{mr^2}{8}\right],$$

and

4)

$$\left\|\|A_n(f) - f\|_\gamma\right\|_{\infty, \prod_{i=1}^{N}[a_i,b_i]} \leq$$
$$\sum_{j=1}^{m}\frac{1}{j!}\left\|\left\|\left(A_n\left(f^{(j)}(x_0)(\cdot - x_0)^j\right)\right)(x_0)\right\|_\gamma\right\|_{\infty, x_0\in\prod_{i=1}^{N}[a_i,b_i]} +$$
$$\frac{\omega_1\left(f^{(m)}, r\left\|\left(\widetilde{A}_n\left(\|\cdot - x_0\|_p^{m+1}\right)\right)(x_0)\right\|_{\infty, x_0\in\prod_{i=1}^{N}[a_i,b_i]}^{\frac{1}{m+1}}\right)}{rm!}$$
$$\left\|\left(\widetilde{A}_n\left(\|\cdot - x_0\|_p^{m+1}\right)\right)(x_0)\right\|_{\infty, x_0\in\prod_{i=1}^{N}[a_i,b_i]}^{\left(\frac{m}{m+1}\right)} \tag{61}$$
$$\left[\frac{1}{(m+1)} + \frac{r}{2} + \frac{mr^2}{8}\right].$$

We need

Lemma 11 *The function* $\left(\widetilde{A}_n\left(\|\cdot - x_0\|_p^m\right)\right)(x_0)$ *is continuous in* $x_0 \in \left(\prod_{i=1}^{N}[a_i,b_i]\right)$, $m \in \mathbb{N}$.

Proof. By Lemma 10.3, [11], p. 272. ■

We give

Corollary 12 *(to Theorem 10, case of* $m = 1$*) Then*

1)

$$\|(A_n(f))(x_0) - f(x_0)\|_\gamma \leq \left\|\left(A_n\left(f^{(1)}(x_0)(\cdot - x_0)\right)\right)(x_0)\right\|_\gamma +$$
$$\frac{1}{2r}\omega_1\left(f^{(1)}, r\left(\left(\widetilde{A}_n\left(\|\cdot - x_0\|_p^2\right)\right)(x_0)\right)^{\frac{1}{2}}\right)\left(\left(\widetilde{A}_n\left(\|\cdot - x_0\|_p^2\right)\right)(x_0)\right)^{\frac{1}{2}} \tag{62}$$
$$\left[1 + r + \frac{r^2}{4}\right],$$

and

2)

$$\left\| \left\| \left(A_n (f) \right) - f \right\|_\gamma \right\|_{\infty, \prod_{i=1}^{N} [a_i, b_i]} \leq$$

$$\left\| \left\| \left(A_n \left(f^{(1)} (x_0) (\cdot - x_0) \right) \right) (x_0) \right\|_\gamma \right\|_{\infty, x_0 \in \prod_{i=1}^{N} [a_i, b_i]} +$$

$$\frac{1}{2r} \omega_1 \left(f^{(1)}, r \left\| \left(\widetilde{A}_n \left(\| \cdot - x_0 \|_p^2 \right) \right) (x_0) \right\|_{\infty, x_0 \in \prod_{i=1}^{N} [a_i, b_i]}^{\frac{1}{2}} \right)$$

$$\left\| \left(\widetilde{A}_n \left(\| \cdot - x_0 \|_p^2 \right) \right) (x_0) \right\|_{\infty, x_0 \in \prod_{i=1}^{N} [a_i, b_i]}^{\frac{1}{2}} \left[1 + r + \frac{r^2}{4} \right], \tag{63}$$

$r > 0$.

We make

Remark 13 *We estimate* $0 < \alpha < 1$, $m, n \in \mathbb{N} : n^{1-\alpha} > 2$,

$$\widetilde{A}_n \left(\| \cdot - x_0 \|_\infty^{m+1} \right) (x_0) = \frac{\sum_{k=\lceil na \rceil}^{\lfloor nb \rfloor} \left\| \frac{k}{n} - x_0 \right\|_\infty^{m+1} Z(nx_0 - k)}{\sum_{k=\lceil na \rceil}^{\lfloor nb \rfloor} Z(nx_0 - k)} \overset{(22)}{<}$$

$$(4.824)^N \sum_{k=\lceil na \rceil}^{\lfloor nb \rfloor} \left\| \frac{k}{n} - x_0 \right\|_\infty^{m+1} Z(nx_0 - k) = \tag{64}$$

$$(4.824)^N \left\{ \sum_{\substack{k = \lceil na \rceil \\ : \left\| \frac{k}{n} - x_0 \right\|_\infty \leq \frac{1}{n^\alpha}}}^{\lfloor nb \rfloor} \left\| \frac{k}{n} - x_0 \right\|_\infty^{m+1} Z(nx_0 - k) + \right.$$

$$\left. \sum_{\substack{k = \lceil na \rceil \\ : \left\| \frac{k}{n} - x_0 \right\|_\infty > \frac{1}{n^\alpha}}}^{\lfloor nb \rfloor} \left\| \frac{k}{n} - x_0 \right\|_\infty^{m+1} Z(nx_0 - k) \right\} \overset{(23)}{\leq}$$

$$(4.824)^N \left\{ \frac{1}{n^{\alpha(m+1)}} + \frac{2e^2 \| b - a \|_\infty^{m+1}}{\pi e^{n^{1-\alpha}}} \right\}, \tag{65}$$

(where $b - a = (b_1 - a_1, ..., b_N - a_N)$*).*

We have proved that ($\forall\ x_0 \in \prod_{i=1}^{N} [a_i, b_i]$)

$$\widetilde{A}_n \left(\|\cdot - x_0\|_\infty^{m+1} \right)(x_0) < (4.824)^N \left\{ \frac{1}{n^{\alpha(m+1)}} + \frac{2e^2 \|b-a\|_\infty^{m+1}}{\pi e^{n^{1-\alpha}}} \right\} =: \varphi_1(n) \tag{66}$$

($0 < \alpha < 1$, $m, n \in \mathbb{N} : n^{1-\alpha} > 2$).

And, consequently it holds

$$\left\| \widetilde{A}_n \left(\|\cdot - x_0\|_\infty^{m+1} \right)(x_0) \right\|_{\infty, x_0 \in \prod_{i=1}^{N} [a_i, b_i]} <$$

$$(4.824)^N \left\{ \frac{1}{n^{\alpha(m+1)}} + \frac{2e^2 \|b-a\|_\infty^{m+1}}{\pi e^{n^{1-\alpha}}} \right\} = \varphi_1(n) \to 0, \quad \text{as } n \to +\infty. \tag{67}$$

So, we have that $\varphi_1(n) \to 0$, *as* $n \to +\infty$. *Thus, when* $p \in [1, \infty]$, *from Theorem 10 we have the convergence to zero in the right hand sides of parts (1), (2).*

Next we estimate $\left\| \left(\widetilde{A}_n \left(f^{(j)}(x_0)(\cdot - x_0)^j \right) \right)(x_0) \right\|_\gamma$.

We have that

$$\left(\widetilde{A}_n \left(f^{(j)}(x_0)(\cdot - x_0)^j \right) \right)(x_0) = \frac{\sum_{k=\lceil na \rceil}^{\lfloor nb \rfloor} f^{(j)}(x_0) \left(\frac{k}{n} - x_0 \right)^j Z(nx_0 - k)}{\sum_{k=\lceil na \rceil}^{\lfloor nb \rfloor} Z(nx_0 - k)}. \tag{68}$$

When $p = \infty$, $j = 1, ..., m$, *we obtain*

$$\left\| f^{(j)}(x_0) \left(\frac{k}{n} - x_0 \right)^j \right\|_\gamma \le \left\| f^{(j)}(x_0) \right\| \left\| \frac{k}{n} - x_0 \right\|_\infty^j. \tag{69}$$

We further have that

$$\left\| \left(\widetilde{A}_n \left(f^{(j)}(x_0)(\cdot - x_0)^j \right) \right)(x_0) \right\|_\gamma \overset{(22)}{<}$$

$$(4.824)^N \left(\sum_{k=\lceil na \rceil}^{\lfloor nb \rfloor} \left\| f^{(j)}(x_0) \left(\frac{k}{n} - x_0 \right)^j \right\|_\gamma Z(nx_0 - k) \right) \le$$

$$(4.824)^N \left(\sum_{k=\lceil na \rceil}^{\lfloor nb \rfloor} \left\| f^{(j)}(x_0) \right\| \left\| \frac{k}{n} - x_0 \right\|_\infty^j Z(nx_0 - k) \right) = \tag{70}$$

$$(4.824)^N \left\| f^{(j)}(x_0) \right\| \left(\sum_{k=\lceil na \rceil}^{\lfloor nb \rfloor} \left\| \frac{k}{n} - x_0 \right\|_\infty^j Z(nx_0 - k) \right) =$$

$$(4.824)^N \left\| f^{(j)}(x_0) \right\| \left\{ \sum_{\substack{k=\lceil na \rceil \\ : \left\| \frac{k}{n} - x_0 \right\|_\infty \leq \frac{1}{n^\alpha}}}^{\lfloor nb \rfloor} \left\| \frac{k}{n} - x_0 \right\|_\infty^j Z(nx_0 - k) \right.$$

$$\left. + \sum_{\substack{k=\lceil na \rceil \\ : \left\| \frac{k}{n} - x_0 \right\|_\infty > \frac{1}{n^\alpha}}}^{\lfloor nb \rfloor} \left\| \frac{k}{n} - x_0 \right\|_\infty^j Z(nx_0 - k) \right\} \overset{(23)}{\leq} \tag{71}$$

$$(4.824)^N \left\| f^{(j)}(x_0) \right\| \left\{ \frac{1}{n^{\alpha j}} + \frac{2e^2 \|b-a\|_\infty^j}{\pi e^{n^{1-\alpha}}} \right\} \to 0, \text{ as } n \to \infty.$$

That is

$$\left\| \left(\widetilde{A}_n \left(f^{(j)}(x_0)(\cdot - x_0)^j \right) \right)(x_0) \right\|_\gamma \to 0, \text{ as } n \to \infty.$$

Therefore when $p = \infty$, for $j = 1, ..., m$, we have proved:

$$\left\| \left(\widetilde{A}_n \left(f^{(j)}(x_0)(\cdot - x_0)^j \right) \right)(x_0) \right\|_\gamma <$$

$$(4.824)^N \left\| f^{(j)}(x_0) \right\| \left\{ \frac{1}{n^{\alpha j}} + \frac{2e^2 \|b-a\|_\infty^j}{\pi e^{n^{1-\alpha}}} \right\} \leq \tag{72}$$

$$(4.824)^N \left\| f^{(j)} \right\|_\infty \left\{ \frac{1}{n^{\alpha j}} + \frac{2e^2 \|b-a\|_\infty^j}{\pi e^{n^{1-\alpha}}} \right\} =: \varphi_{2j}(n) < \infty,$$

and converges to zero, as $n \to \infty$.

We conclude:

In Theorem 10, the right hand sides of (60) and (61) converge to zero as $n \to \infty$, for any $p \in [1, \infty]$.

Also in Corollary 12, the right hand sides of (62) and (63) converge to zero as $n \to \infty$, for any $p \in [1, \infty]$.

Conclusion 14 *We have proved that the left hand sides of (58), (59), (60), (61) and (62), (63) converge to zero as $n \to \infty$, for $p \in [1, \infty]$. Consequently $A_n \to I$ (unit operator) pointwise and uniformly, as $n \to \infty$, where $p \in [1, \infty]$. In the presence of initial conditions we achieve a higher speed of convergence, see (59). Higher speed of convergence happens also to the left hand side of (58).*

We further give

Corollary 15 *(to Theorem 10) Let* O *open subset of* $\left(\mathbb{R}^N, \|\cdot\|_\infty\right)$, *such that* $\prod_{i=1}^{N} [a_i, b_i] \subset O \subseteq \mathbb{R}^N$, *and let* $\left(X, \|\cdot\|_\gamma\right)$ *be a general Banach space. Let* $m \in \mathbb{N}$ *and* $f \in C^m(O, X)$, *the space of* $\overline{m}$*-times continuously Fréchet differentiable functions from* O *into* X. *We study the approximation of* $f|_{\prod_{i=1}^{N}[a_i,b_i]}$. *Let* $x_0 \in \left(\prod_{i=1}^{N} [a_i, b_i]\right)$ *and* $r > 0$. *Here* $\varphi_1(n)$ *as in (67) and* $\varphi_{2j}(n)$ *as in (72), where* $n \in \mathbb{N} : n^{1-\alpha} > 2$, $0 < \alpha < 1$, $j = 1, ..., m$. *Then*

1)

$$\left\| (A_n(f))(x_0) - \sum_{j=0}^{m} \frac{1}{j!} \left(A_n \left(f^{(j)}(x_0)(\cdot - x_0)^j \right) \right)(x_0) \right\|_\gamma \leq$$

$$\frac{\omega_1\left(f^{(m)}, r(\varphi_1(n))^{\frac{1}{m+1}}\right)}{rm!} (\varphi_1(n))^{\left(\frac{m}{m+1}\right)} \left[\frac{1}{(m+1)} + \frac{r}{2} + \frac{mr^2}{8} \right], \tag{73}$$

2) additionally, if $f^{(j)}(x_0) = 0$, $j = 1, ..., \overline{m}$, *we have*

$$\|(A_n(f))(x_0) - f(x_0)\|_\gamma \leq$$

$$\frac{\omega_1\left(f^{(m)}, r(\varphi_1(n))^{\frac{1}{m+1}}\right)}{rm!} (\varphi_1(n))^{\left(\frac{m}{m+1}\right)} \left[\frac{1}{(m+1)} + \frac{r}{2} + \frac{mr^2}{8} \right], \tag{74}$$

3)

$$\left\| \|A_n(f) - f\|_\gamma \right\|_{\infty, \prod_{i=1}^{N}[a_i,b_i]} \leq \sum_{j=1}^{m} \frac{\varphi_{2j}(n)}{j!} +$$

$$\frac{\omega_1\left(f^{(m)}, r(\varphi_1(n))^{\frac{1}{m+1}}\right)}{rm!} (\varphi_1(n))^{\left(\frac{m}{m+1}\right)} \tag{75}$$

$$\left[\frac{1}{(m+1)} + \frac{r}{2} + \frac{mr^2}{8} \right] =: \varphi_3(n) \to 0, \text{ as } n \to \infty.$$

We continue with

Theorem 16 *Let* $f \in C_B\left(\mathbb{R}^N, X\right)$, $0 < \beta < 1$, $x \in \mathbb{R}^N$, $m, N, n \in \mathbb{N}$ *with* $n^{1-\beta} > 2$, ω_1 *is for* $p = \infty$. *Then*

1)

$$\|B_n(f, x) - f(x)\|_\gamma \leq \omega_1\left(f, \frac{1}{n^\beta}\right) + \frac{4e^2 \left\| \|f\|_\gamma \right\|_\infty}{\pi e^{n^{1-\beta}}} =: \lambda_2(n), \tag{76}$$

2)

$$\left\| \|B_n(f) - f\|_\gamma \right\|_\infty \leq \lambda_2(n). \tag{77}$$

Given that $f \in \left(C_U\left(\mathbb{R}^N, X\right) \cap C_B\left(\mathbb{R}^N, X\right)\right)$, *we obtain* $\lim_{n\to\infty} B_n(f) = f$, *uniformly.*

Proof. We have that

$$B_n(f,x) - f(x) \overset{(16)}{=} \sum_{k=-\infty}^{\infty} f\left(\frac{k}{n}\right) Z(nx-k) - f(x) \sum_{k=-\infty}^{\infty} Z(nx-k) = \tag{78}$$

$$\sum_{k=-\infty}^{\infty} \left(f\left(\frac{k}{n}\right) - f(x)\right) Z(nx-k).$$

Hence

$$\|B_n(f,x) - f(x)\|_\gamma \leq \sum_{k=-\infty}^{\infty} \left\| f\left(\frac{k}{n}\right) - f(x)\right\|_\gamma Z(nx-k) =$$

$$\sum_{\substack{k=-\infty \\ \left\|\frac{k}{n}-x\right\|_\infty \leq \frac{1}{n^\beta}}}^{\infty} \left\| f\left(\frac{k}{n}\right) - f(x)\right\|_\gamma Z(nx-k) +$$

$$\sum_{\substack{k=-\infty \\ \left\|\frac{k}{n}-x\right\|_\infty > \frac{1}{n^\beta}}}^{\infty} \left\| f\left(\frac{k}{n}\right) - f(x)\right\|_\gamma Z(nx-k) \overset{(16)}{\leq}$$

$$\omega_1\left(f, \frac{1}{n^\beta}\right) + 2\left\|\|f\|_\gamma\right\|_\infty \sum_{\substack{k=-\infty \\ \left\|\frac{k}{n}-x\right\|_\infty > \frac{1}{n^\beta}}}^{\infty} Z(nx-k) \overset{(23)}{\leq}$$

$$\omega_1\left(f, \frac{1}{n^\beta}\right) + \frac{4e^2\left\|\|f\|_\gamma\right\|_\infty}{\pi e^{n^{1-\beta}}}, \tag{79}$$

proving the claim. ■

We give

Theorem 17 *Let* $f \in C_B\left(\mathbb{R}^N, X\right)$, $0 < \beta < 1$, $x \in \mathbb{R}^N$, $m, N, n \in \mathbb{N}$ *with* $n^{1-\beta} > 2$, ω_1 *is for* $p = \infty$. *Then*

1)

$$\|C_n(f,x) - f(x)\|_\gamma \leq \omega_1\left(f, \frac{1}{n} + \frac{1}{n^\beta}\right) + \frac{4e^2\left\|\|f\|_\gamma\right\|_\infty}{\pi e^{n^{1-\beta}}} =: \lambda_3(n), \tag{80}$$

2)

$$\left\|\|C_n(f) - f\|_\gamma\right\|_\infty \leq \lambda_3(n). \tag{81}$$

Given that $f \in \left(C_U\left(\mathbb{R}^N, X\right) \cap C_B\left(\mathbb{R}^N, X\right)\right)$, *we obtain* $\lim_{n\to\infty} C_n(f) = f$, *uniformly.*

Proof. We notice that

$$\int_{\frac{k}{n}}^{\frac{k+1}{n}} f(t)\,dt = \int_{\frac{k_1}{n}}^{\frac{k_1+1}{n}} \int_{\frac{k_2}{n}}^{\frac{k_2+1}{n}} \dots \int_{\frac{k_N}{n}}^{\frac{k_N+1}{n}} f(t_1, t_2, \dots, t_N)\, dt_1 dt_2 \dots dt_N =$$

$$\int_0^{\frac{1}{n}} \int_0^{\frac{1}{n}} \dots \int_0^{\frac{1}{n}} f\left(t_1 + \frac{k_1}{n}, t_2 + \frac{k_2}{n}, \dots, t_N + \frac{k_N}{n}\right) dt_1 \dots dt_N = \int_0^{\frac{1}{n}} f\left(t + \frac{k}{n}\right) dt. \tag{82}$$

Thus it holds (by (38))

$$C_n(f, x) = \sum_{k=-\infty}^{\infty} \left(n^N \int_0^{\frac{1}{n}} f\left(t + \frac{k}{n}\right) dt\right) Z(nx - k). \tag{83}$$

We observe that

$$\|C_n(f, x) - f(x)\|_\gamma =$$

$$\left\| \sum_{k=-\infty}^{\infty} \left(n^N \int_0^{\frac{1}{n}} f\left(t + \frac{k}{n}\right) dt\right) Z(nx - k) - \sum_{k=-\infty}^{\infty} f(x) Z(nx - k) \right\|_\gamma =$$

$$\left\| \sum_{k=-\infty}^{\infty} \left(\left(n^N \int_0^{\frac{1}{n}} f\left(t + \frac{k}{n}\right) dt\right) - f(x) \right) Z(nx - k) \right\|_\gamma =$$

$$\left\| \sum_{k=-\infty}^{\infty} \left(n^N \int_0^{\frac{1}{n}} \left(f\left(t + \frac{k}{n}\right) - f(x)\right) dt\right) Z(nx - k) \right\|_\gamma \leq \tag{84}$$

$$\sum_{k=-\infty}^{\infty} \left(n^N \int_0^{\frac{1}{n}} \left\| f\left(t + \frac{k}{n}\right) - f(x)\right\|_\gamma dt\right) Z(nx - k) =$$

$$\sum_{\begin{cases} k = -\infty \\ \left\|\frac{k}{n} - x\right\|_\infty \leq \frac{1}{n^\beta} \end{cases}}^{\infty} \left(n^N \int_0^{\frac{1}{n}} \left\| f\left(t + \frac{k}{n}\right) - f(x)\right\|_\gamma dt\right) Z(nx - k) +$$

$$\sum_{\begin{cases} k = -\infty \\ \left\|\frac{k}{n} - x\right\|_\infty > \frac{1}{n^\beta} \end{cases}}^{\infty} \left(n^N \int_0^{\frac{1}{n}} \left\| f\left(t + \frac{k}{n}\right) - f(x)\right\|_\gamma dt\right) Z(nx - k) \leq$$

$$\sum_{\begin{cases} k = -\infty \\ \left\|\frac{k}{n} - x\right\|_\infty \leq \frac{1}{n^\beta} \end{cases}}^{\infty} \left(n^N \int_0^{\frac{1}{n}} \omega_1\left(f, \|t\|_\infty + \left\|\frac{k}{n} - x\right\|_\infty\right) dt\right) Z(nx - k) +$$

$$2\left\|\|f\|_{\gamma}\right\|_{\infty}\left(\sum_{\substack{k=-\infty \\ \left\|\frac{k}{n}-x\right\|_{\infty}>\frac{1}{n^{\beta}}}}^{\infty} Z\left(|nx-k|\right)\right)\leq$$

$$\omega_1\left(f,\frac{1}{n}+\frac{1}{n^{\beta}}\right)+\frac{4e^2\left\|\|f\|_{\gamma}\right\|_{\infty}}{\pi e^{n^{1-\beta}}}, \tag{85}$$

proving the claim. ■

We also present

Theorem 18 *Let* $f\in C_B\left(\mathbb{R}^N,X\right)$, $0<\beta<1$, $x\in\mathbb{R}^N$, $m,N,n\in\mathbb{N}$ *with* $n^{1-\beta}>2$, ω_1 *is for* $p=\infty$. *Then*

1)

$$\left\|D_n(f,x)-f(x)\right\|_{\gamma}\leq\omega_1\left(f,\frac{1}{n}+\frac{1}{n^{\beta}}\right)+\frac{4e^2\left\|\|f\|_{\gamma}\right\|_{\infty}}{\pi e^{n^{1-\beta}}}=\lambda_4(n), \tag{86}$$

2)

$$\left\|\left\|D_n(f)-f\right\|_{\gamma}\right\|_{\infty}\leq\lambda_4(n). \tag{87}$$

Given that $f\in\left(C_U\left(\mathbb{R}^N,X\right)\cap C_B\left(\mathbb{R}^N,X\right)\right)$, *we obtain* $\lim_{n\to\infty}D_n(f)=f$, *uniformly.*

Proof. Similar to the proof of Theorem 17, as such is omitted. ■

We make

Definition 19 *Let* $f\in C_B\left(\mathbb{R}^N,X\right)$, $N\in\mathbb{N}$, *where* $\left(X,\|\cdot\|_{\gamma}\right)$ *is a Banach space. We define the general neural network operator*

$$F_n(f,x):=\sum_{k=-\infty}^{\infty} l_{nk}(f)\,Z(nx-k)=$$

$$\begin{cases} B_n(f,x), & \text{if } l_{nk}(f)=f\left(\frac{k}{n}\right),\\ C_n(f,x), & \text{if } l_{nk}(f)=n^N\int_{\frac{k}{n}}^{\frac{k+1}{n}} f(t)\,dt,\\ D_n(f,x), & \text{if } l_{nk}(f)=\delta_{nk}(f). \end{cases} \tag{88}$$

Clearly $l_{nk}(f)$ is an X-valued bounded linear functional such that $\left\|l_{nk}(f)\right\|_{\gamma}\leq\left\|\|f\|_{\gamma}\right\|_{\infty}$.

Hence $F_n(f)$ is a bounded linear operator with $\left\|\left\|F_n(f)\right\|_{\gamma}\right\|_{\infty}\leq\left\|\|f\|_{\gamma}\right\|_{\infty}$.

We need

Theorem 20 *Let* $f \in C_B\left(\mathbb{R}^N, X\right)$, $N \geq 1$. *Then* $F_n(f) \in C_B\left(\mathbb{R}^N, X\right)$.

Proof. Lengthy and similar to the proof of Theorem 21 of [14], as such is omitted. ■

Remark 21 *By (25) it is obvious that* $\left\| \|A_n(f)\|_\gamma \right\|_\infty \leq \left\| \|f\|_\gamma \right\|_\infty < \infty$, *and* $A_n(f) \in C\left(\prod_{i=1}^{N}[a_i, b_i], X\right)$, *given that* $f \in C\left(\prod_{i=1}^{N}[a_i, b_i], X\right)$.

Call L_n *any of the operators* A_n, B_n, C_n, D_n.

Clearly then

$$\left\| \|L_n^2(f)\|_\gamma \right\|_\infty = \left\| \|L_n(L_n(f))\|_\gamma \right\|_\infty \leq \left\| \|L_n(f)\|_\gamma \right\|_\infty \leq \left\| \|f\|_\gamma \right\|_\infty, \tag{89}$$

etc.

Therefore we get

$$\left\| \|L_n^k(f)\|_\gamma \right\|_\infty \leq \left\| \|f\|_\gamma \right\|_\infty, \ \forall\, k \in \mathbb{N}, \tag{90}$$

the contraction property.

Also we see that

$$\left\| \|L_n^k(f)\|_\gamma \right\|_\infty \leq \left\| \|L_n^{k-1}(f)\|_\gamma \right\|_\infty \leq \ldots \leq \left\| \|L_n(f)\|_\gamma \right\|_\infty \leq \left\| \|f\|_\gamma \right\|_\infty. \tag{91}$$

Here L_n^k *are bounded linear operators.*

Notation 22 *Here* $N \in \mathbb{N}$, $0 < \beta < 1$. *Denote by*

$$c_N := \begin{cases} (4.824)^N, & \text{if } L_n = A_n, \\ 1, & \text{if } L_n = B_n, C_n, D_n, \end{cases} \tag{92}$$

$$\varphi(n) := \begin{cases} \frac{1}{n^\beta}, & \text{if } L_n = A_n,\ B_n, \\ \frac{1}{n} + \frac{1}{n^\beta}, & \text{if } L_n = C_n, D_n, \end{cases} \tag{93}$$

$$\Omega := \begin{cases} C\left(\prod_{i=1}^{N}[a_i, b_i], X\right), & \text{if } L_n = A_n, \\ C_B\left(\mathbb{R}^N, X\right), & \text{if } L_n = B_n, C_n, D_n, \end{cases} \tag{94}$$

and

$$Y := \begin{cases} \prod_{i=1}^{N}[a_i, b_i], & \text{if } L_n = A_n, \\ \mathbb{R}^N, & \text{if } L_n = B_n, C_n, D_n. \end{cases} \tag{95}$$

We give the condensed

Theorem 23 *Let $f \in \Omega$, $0 < \beta < 1$, $x \in Y$; n, m, $N \in \mathbb{N}$ with $n^{1-\beta} > 2$. Then*
(i)

$$\left\| L_n(f,x) - f(x) \right\|_\gamma \leq c_N \left[\omega_1(f, \varphi(n)) + \frac{4e^2 \left\| \|f\|_\gamma \right\|_\infty}{\pi e^{n^{1-\beta}}} \right] =: \tau(n), \tag{96}$$

where ω_1 is for $p = \infty$,
and
(ii)

$$\left\| \left\| L_n(f) - f \right\|_\gamma \right\|_\infty \leq \tau(n) \to 0, \text{ as } n \to \infty. \tag{97}$$

For f uniformly continuous and in Ω we obtain

$$\lim_{n\to\infty} L_n(f) = f,$$

pointwise and uniformly.

Proof. By Theorems 8, 16, 17, 18. ∎

Next we talk about iterated neural network approximation (see also [9]).

We give

Theorem 24 *All here as in Theorem 23 and $r \in \mathbb{N}$, $\tau(n)$ as in (96). Then*

$$\left\| \left\| L_n^r f - f \right\|_\gamma \right\|_\infty \leq r\tau(n). \tag{98}$$

So that the speed of convergence to the unit operator of L_n^r is not worse than of L_n.

Proof. As similar to [14] is omitted. ∎

We also present

Theorem 25 *Let $f \in \Omega$; m, N, $m_1, m_2, ..., m_r \in \mathbb{N} : m_1 \leq m_2 \leq ... \leq m_r$, $0 < \beta < 1$; $m_i^{1-\beta} > 2$, $i = 1, ..., r$, $x \in Y$, and let $(L_{m_1}, ..., L_{m_r})$ as $(A_{m_1}, ..., A_{m_r})$ or $(B_{m_1}, ..., B_{m_r})$ or $(C_{m_1}, ..., C_{m_r})$ or $(D_{m_1}, ..., D_{m_r})$, $p = \infty$. Then*

$$\left\| L_{m_r}\left(L_{m_{r-1}}\left(...L_{m_2}\left(L_{m_1} f\right)\right)\right)(x) - f(x) \right\|_\gamma \leq$$

$$\left\| \left\| L_{m_r}\left(L_{m_{r-1}}\left(...L_{m_2}\left(L_{m_1} f\right)\right)\right) - f \right\|_\gamma \right\|_\infty \leq$$

$$\sum_{i=1}^{r} \left\| \left\| L_{m_i} f - f \right\|_\gamma \right\|_\infty \leq$$

$$c_N \sum_{i=1}^{r} \left[\omega_1(f, \varphi(m_i)) + \frac{4e^2 \left\| \|f\|_\gamma \right\|_\infty}{\pi e^{m_i^{1-\beta}}} \right] \leq$$

$$rc_N \left[\omega_1 \left(f, \varphi \left(m_1 \right) \right) + \frac{4e^2 \left\| \left\| f \right\|_\gamma \right\|_\infty}{\pi e^{m_1^{1-\beta}}} \right]. \tag{99}$$

Clearly, we notice that the speed of convergence to the unit operator of the multiply iterated operator is not worse than the speed of L_{m_1}.

Proof. As similar to [14] is omitted. ■

We also give

Theorem 26 *Let all as in Corollary 15, and* $r \in \mathbb{N}$. *Here* $\varphi_3(n)$ *is as in (75). Then*

$$\left\| \left\| A_n^r f - f \right\|_\gamma \right\|_\infty \leq r \left\| \left\| A_n f - f \right\|_\gamma \right\|_\infty \leq r \varphi_3(n). \tag{100}$$

Proof. As similar to [14] is omitted. ■

Application 27 *A typical application of all of our results is when* $\left(X, \|\cdot\|_\gamma \right) = (\mathbb{C}, |\cdot|)$, *where* $\mathbb{C}$ *are the complex numbers.*

References

[1] G.A. Anastassiou, *Moments in Probability and Approximation Theory*, Pitman Research Notes in Math., Vol. 287, Longman Sci. & Tech., Harlow, U.K., 1993.

[2] G.A. Anastassiou, *Rate of convergence of some neural network operators to the unit-univariate case*, J. Math. Anal. Appli. 212 (1997), 237-262.

[3] G.A. Anastassiou, *Quantitative Approximations*, Chapman&Hall/CRC, Boca Raton, New York, 2001.

[4] G.A. Anastassiou, *Inteligent Systems: Approximation by Artificial Neural Networks*, Intelligent Systems Reference Library, Vol. 19, Springer, Heidelberg, 2011.

[5] G.A. Anastassiou, *Univariate hyperbolic tangent neural network approximation*, Mathematics and Computer Modelling, 53(2011), 1111-1132.

[6] G.A. Anastassiou, *Multivariate hyperbolic tangent neural network approximation*, Computers and Mathematics 61(2011), 809-821.

[7] G.A. Anastassiou, *Multivariate sigmoidal neural network approximation*, Neural Networks 24(2011), 378-386.

[8] G.A. Anastassiou, *Univariate sigmoidal neural network approximation*, J. of Computational Analysis and Applications, Vol. 14, No. 4, 2012, 659-690.

[9] G.A. Anastassiou, *Approximation by neural networks iterates,* Advances in Applied Mathematics and Approximation Theory, pp. 1-20, Springer Proceedings in Math. & Stat., Springer, New York, 2013, Eds. G. Anastassiou, O. Duman.

[10] G.A. Anastassiou, *Intelligent Systems II: Complete Approximation by Neural Network Operators*, Springer, Heidelberg, New York, 2016.

[11] G.A. Anastassiou, *Intelligent Computations: Abstract Fractional Calculus, Inequalities, Approximations*, Springer, Heidelberg, New York, 2018.

[12] G.A. Anastassiou, *Algebraic function based Banach space valued ordinary and fractional neural network approximations*, New Trends in Mathematical Sciences, 10 special issue (1) (2022), 100-125.

[13] G.A. Anastassiou, *Gudermannian function activated Banach space valued ordinary and fractional neural network approximation*, Advances in Nonlinear Variational Inequalities, 25 (2) (2022), 27-64.

[14] G.A. Anastassiou, *General multimariate arctangent function activated neural network approximations*, submitted, 2022.

[15] G.A. Anastassiou, *Abstract multivariate algebraic function activated neural network approximations*, submitted, 2022.

[16] H. Cartan, *Differential Calculus*, Hermann, Paris, 1971.

[17] Z. Chen and F. Cao, *The approximation operators with sigmoidal functions*, Computers and Mathematics with Applications, 58 (2009), 758-765.

[18] D. Costarelli, R. Spigler, *Approximation results for neural network operators activated by sigmoidal functions*, Neural Networks 44 (2013), 101-106.

[19] D. Costarelli, R. Spigler, *Multivariate neural network operators with sigmoidal activation functions*, Neural Networks 48 (2013), 72-77.

[20] S. Haykin, *Neural Networks: A Comprehensive Foundation* (2 ed.), Prentice Hall, New York, 1998.

[21] W. McCulloch and W. Pitts, *A logical calculus of the ideas immanent in nervous activity*, Bulletin of Mathematical Biophysics, 7 (1943), 115-133.

[22] T.M. Mitchell, *Machine Learning*, WCB-McGraw-Hill, New York, 1997.

[23] L.B. Rall, *Computational Solution of Nonlinear Operator Equations*, John Wiley & Sons, New York, 1969.

[24] E.W. Weisstein, *Gudermannian*, MathWorld.

J. COMPUTATIONAL ANALYSIS AND APPLICATIONS, VOL. 31, NO. 4, 2023, COPYRIGHT 2023 EUDOXUS PRESS, LLC

p-Schatten norm generalized Canavati fractional Ostrowski, Opial and Grüss type inequalities involving several functions

George A. Anastassiou
Department of Mathematical Sciences
University of Memphis
Memphis, TN 38152, U.S.A.
ganastss@memphis.edu

Abstract

Using generalized Canavati fractional left and right vectorial Taylor formulae we establish generalized fractional Ostrowski, Opial and Grüss type inequalities for several functions that take values in the von Neumann-Schatten class $\mathcal{B}_p(H)$, $1 \leq p < \infty$. The estimates are with respect to all p-Schatten norms, $1 \leq p < \infty$. We finish with applications.

2020 Mathematics Subject Classification : 26A33, 26D10, 26D15, 47A60, 47A63.
Keywords and Phrases: p-Schatten norms, von Neumann-Schatten class, Ostrowski, Opial and Grüss inequalities, generalized Canavati fractional derivative, generalized Canavati fractional inequalities.

1 Introduction

The following results inspire our work.

Theorem 1 *(1938, Ostrowski [16]) Let $f : [a,b] \to \mathbb{R}$ be continuous on $[a,b]$ and differentiable on (a,b) whose derivative $f' : (a,b) \to \mathbb{R}$ is bounded on (a,b), i.e., $\|f'\|_{\infty}^{\sup} := \sup_{t \in (a,b)} |f'(t)| < +\infty$. Then*

$$\left| \frac{1}{b-a} \int_a^b f(t)\,dt - f(x) \right| \leq \left[\frac{1}{4} + \frac{\left(x - \frac{a+b}{2}\right)^2}{(b-a)^2} \right] (b-a) \|f'\|_{\infty}^{\sup}, \qquad (1)$$

for any $x \in [a,b]$. The constant $\frac{1}{4}$ is the best possible.

Ostrowski type inequalities have great applications to integral approximations in Numerical Analysis.

We mention

Theorem 2 *(1882, Čebyšev [8]) Let $f, g : [a, b] \to \mathbb{R}$ be absolutely continuous functions with $f', g' \in L_\infty([a, b])$. Then*

$$\left| \frac{1}{b-a} \int_a^b f(x) g(x) dx - \left(\frac{1}{b-a} \int_a^b f(x) dx \right) \left(\frac{1}{b-a} \int_a^b g(x) dx \right) \right|$$

$$\leq \frac{1}{12} (b-a)^2 \|f'\|_\infty \|g'\|_\infty . \tag{2}$$

The above integrals are assumed to exist.

The related Grüss type inequalities have many applications to Probability Theory. We presented also ([3], Ch. 8,9) mixed fractional Ostrowski and Grüss-Cebysev type inequalities for several functions, acting to all possible directions. The estimates involve the left and right Caputo fractional derivatives. See also the monographs written by the author [1], Chapters 24-26 and [2], Chapters 2-6.

We are motivated also by S. Dragomir [11] recent work:

An operator $A \in \mathcal{B}(H)$ is said to belong to the von Neumann-Schatten class $\mathcal{B}_p(H)$, $1 \leq p < \infty$ if the p-Schatten norm is finite

$$\|A\|_p := [tr(|A|^p)]^{\frac{1}{p}} < \infty.$$

Assume that $A : [a, b] \to \mathcal{B}_p(H)$, $B : [a, b] \to \mathcal{B}_q(H)$, $p, q > 1$ with $\frac{1}{p} + \frac{1}{q} = 1$, are continuous and B is strongly differentiable on (a, b), then

$$\left\| \int_a^b A(t) B(t) dt - \left(\int_a^b A(s) ds \right) B(u) \right\|_1 \leq$$

$$\sup_{t \in [a,b]} \|B'(t)\|_q \times \begin{cases} \left[\frac{1}{2}(b-a) + \left| u - \frac{a+b}{2} \right| \right] \int_a^b \|A(t)\|_p dt, \\ \left[\frac{(u-a)^{\beta+1} + (b-u)^{\beta+1}}{\beta+1} \right]^{\frac{1}{\beta}} \left(\int_a^b \|A(t)\|_p^\alpha \right)^{\frac{1}{\alpha}}, \\ \text{for } \alpha, \beta > 1 \text{ with } \frac{1}{\alpha} + \frac{1}{\beta} = 1 \\ \left[\frac{1}{4}(b-a)^2 + \left(u - \frac{a+b}{2} \right)^2 \right] \sup\limits_{t \in [a,b]} \|A(t)\|_p , \end{cases} \tag{3}$$

for all $u \in [a, b]$, an Ostrowski type inequality.

Further inspiration comes from S. Dragomir [12] recent work on Grüss inequalities:

For two continuous functions $A, B : [a,b] \to \mathcal{B}(H)$ we define the noncommutative Cebysev fractional

$$D(A,B) := (b-a)\int_a^b A(t)\,B(t)\,dt - \int_a^b A(t)\,dt \int_a^b B(t)\,dt.$$

If $p, q > 1$ with $\frac{1}{p}+\frac{1}{q}=1$, let $A : [a,b] \to \mathcal{B}_p(H)$, $B : [a,b] \to \mathcal{B}_q(H)$ be strongly differentiable functions on the interval (a,b), then

$$\|D(A,B)\|_1 \leq D\left(\int_a^b \|A'(u)\|_p\,du, \int_a^b \|B'(u)\|_q\,du\right) \leq \tag{4}$$

$$\frac{1}{4}(b-a)^2 \int_a^b \|A'(u)\|_p\,du \int_a^b \|B'(u)\|_q\,du.$$

We are also inspired by Z. Opial [15], 1960, famous inequality.

Theorem 3 *Let $x(t) \in C^1([0,h])$ be such that $x(0) = x(h) = 0$, and $x(t) > 0$ in $(0,h)$. Then*

$$\int_0^h |x(t)\,x'(t)|\,dt \leq \frac{h}{4}\int_0^h (x'(t))^2\,dt. \tag{5}$$

In (5), the constant $\frac{h}{4}$ is the best possible. Inequality (5) holds as equality for the optimal function

$$x(t) = \begin{cases} ct, & 0 \leq t \leq \frac{h}{2}, \\ c(h-t), & \frac{h}{2} \leq t \leq h, \end{cases} \tag{6}$$

where $c > 0$ is an arbitrary constant.

Opial-type inequalities are used a lot in proving uniqueness of solutions to differential equations and also to give upper bounds to their solutions.

For an extensive study about fractional Opial inequalities see the author's monograph [1].

In this article we generalize [3], Ch. 8,9 for several Banach algebra $\mathcal{B}_p(H)$ valued functions, in the sense of developing fractional Ostrowski, Opial and Grüss type inequalities. Now our left and right generalized Canavati fractional derivatives are for Banach space valued functions and our integrals are of Bochner type [13]. Applications finish the article.

2 Background on Vectorial generalized Canavati fractional calculus

All in this section come from [5], pp. 109-115 and [4].

Let $g : [a, b] \to \mathbb{R}$ be a strictly increasing function. such that $g \in C^1([a, b])$, and $g^{-1} \in C^n([g(a), g(b)])$, $n \in \mathbb{N}$, $(X, \|\cdot\|)$ is a Banach space. Let $f \in C^n([a, b], X)$, and call $l := f \circ g^{-1} : [g(a), g(b)] \to X$. It is clear that $l, l', ..., l^{(n)}$ are continuous functions from $[g(a), g(b)]$ into $f([a, b]) \subseteq X$.

Let $\nu \geq 1$ such that $[\nu] = n$, $n \in \mathbb{N}$ as above, where $[\cdot]$ is the integral part of the number.

Clearly when $0 < \nu < 1$, $[\nu] = 0$.

I) Let $h \in C([g(a), g(b)], X)$, we define the left Riemann-Liouville Bochner fractional integral as

$$\left(J_{\nu}^{z_0} h\right)(z) := \frac{1}{\Gamma(\nu)} \int_{z_0}^{z} (z - t)^{\nu - 1} h(t)\, dt, \tag{7}$$

for $g(a) \leq z_0 \leq z \leq g(b)$, where Γ is the gamma function; $\Gamma(\nu) = \int_0^{\infty} e^{-t} t^{\nu - 1} dt$. We set $J_0^{z_0} h = h$.

Let $\alpha := \nu - [\nu]$ $(0 < \alpha < 1)$. We define the subspace $C_{g(x_0)}^{\nu}([g(a), g(b)], X)$ of $C^{[\nu]}([g(a), g(b)], X)$, where $x_0 \in [a, b]$ as:

$$C_{g(x_0)}^{\nu}([g(a), g(b)], X) =$$

$$\left\{ h \in C^{[\nu]}([g(a), g(b)], X) : J_{1-\alpha}^{g(x_0)} h^{([\nu])} \in C^1([g(x_0), g(b)], X) \right\}. \tag{8}$$

So let $h \in C_{g(x_0)}^{\nu}([g(a), g(b)], X)$, we define the left g-generalized X-valued fractional derivative of h of order ν, of Canavati type, over $[g(x_0), g(b)]$ as

$$D_{g(x_0)}^{\nu} h := \left(J_{1-\alpha}^{g(x_0)} h^{([\nu])} \right)'. \tag{9}$$

Clearly, for $h \in C_{g(x_0)}^{\nu}([g(a), g(b)], X)$, there exists

$$\left(D_{g(x_0)}^{\nu} h \right)(z) = \frac{1}{\Gamma(1 - \alpha)} \frac{d}{dz} \int_{g(x_0)}^{z} (z - t)^{-\alpha} h^{([\nu])}(t)\, dt, \tag{10}$$

for all $g(x_0) \leq z \leq g(b)$.

In particular, when $f \circ g^{-1} \in C_{g(x_0)}^{\nu}([g(a), g(b)], X)$, we have that

$$\left(D_{g(x_0)}^{\nu} \left(f \circ g^{-1} \right) \right)(z) = \frac{1}{\Gamma(1 - \alpha)} \frac{d}{dz} \int_{g(x_0)}^{z} (z - t)^{-\alpha} \left(f \circ g^{-1} \right)^{([\nu])}(t)\, dt, \tag{11}$$

for all $g(x_0) \leq z \leq g(b)$. We have that $D_{g(x_0)}^{n} \left(f \circ g^{-1} \right) = \left(f \circ g^{-1} \right)^{(n)}$ and $D_{g(x_0)}^{0} \left(f \circ g^{-1} \right) = f \circ g^{-1}$, see [4].

By [4], we have for $f \circ g^{-1} \in C_{g(x_0)}^{\nu}([g(a), g(b)], X)$, where $x_0 \in [a, b]$ the following left generalized g-fractional, of Canavati type,X-valued Taylor's formula:

Theorem 4 *Let* $f \circ g^{-1} \in C^{\nu}_{g(x_0)}([g(a), g(b)], X)$, *where* $x_0 \in [a,b]$ *is fixed.*

(i) If $\nu \geq 1$, *then*

$$f(x) - f(x_0) = \sum_{k=1}^{[\nu]-1} \frac{\left(f \circ g^{-1}\right)^{(k)}(g(x_0))}{k!} (g(x) - g(x_0))^k +$$

$$\frac{1}{\Gamma(\nu)} \int_{g(x_0)}^{g(x)} (g(x) - t)^{\nu-1} \left(D^{\nu}_{g(x_0)}\left(f \circ g^{-1}\right)\right)(t)\, dt, \tag{12}$$

for all $x_0 \leq x \leq b$.

(ii) If $0 < \nu < 1$, *we get*

$$f(x) = \frac{1}{\Gamma(\nu)} \int_{g(x_0)}^{g(x)} (g(x) - t)^{\nu-1} \left(D^{\nu}_{g(x_0)}\left(f \circ g^{-1}\right)\right)(t)\, dt, \tag{13}$$

for all $x_0 \leq x \leq b$.

II) Let $h \in C([g(a), g(b)], X)$, we define the right Riemann-Liouville Bochner fractional integral as

$$\left(J^{\nu}_{z_0-}h\right)(z) := \frac{1}{\Gamma(\nu)} \int_{z}^{z_0} (t - z)^{\nu-1} h(t)\, dt, \tag{14}$$

for $g(a) \leq z \leq z_0 \leq g(b)$. We set $J^{0}_{z_0-}h = h$.

Let $\alpha := \nu - [\nu]$ $(0 < \alpha < 1)$. We define the subspace $C^{\nu}_{g(x_0)-}([g(a), g(b)], X)$ of $C^{[\nu]}([g(a), g(b)], X)$, where $x_0 \in [a,b]$ as:

$$C^{\nu}_{g(x_0)-}([g(a), g(b)], X) :=$$

$$\left\{h \in C^{[\nu]}([g(a), g(b)], X) : J^{1-\alpha}_{g(x_0)-}h^{([\nu])} \in C^{1}([g(a), g(x_0)], X)\right\}. \tag{15}$$

So let $h \in C^{\nu}_{g(x_0)-}([g(a), g(b)], X)$, we define the right g-generalized X-valued fractional derivative of h of order ν, of Canavati type, over $[g(a), g(x_0)]$ as

$$D^{\nu}_{g(x_0)-}h := (-1)^{n-1}\left(J^{1-\alpha}_{g(x_0)-}h^{([\nu])}\right)'. \tag{16}$$

Clearly, for $h \in C^{\nu}_{g(x_0)-}([g(a), g(b)], X)$, there exists

$$\left(D^{\nu}_{g(x_0)-}h\right)(z) = \frac{(-1)^{n-1}}{\Gamma(1-\alpha)} \frac{d}{dz} \int_{z}^{g(x_0)} (t - z)^{-\alpha} h^{([\nu])}(t)\, dt, \tag{17}$$

for all $g(a) \leq z \leq g(x_0) \leq g(b)$.

In particular, when $f \circ g^{-1} \in C^{\nu}_{g(x_0)-}([g(a), g(b)], X)$, we have that

$$\left(D^{\nu}_{g(x_0)-}\left(f \circ g^{-1}\right)\right)(z) = \frac{(-1)^{n-1}}{\Gamma(1-\alpha)} \frac{d}{dz} \int_{z}^{g(x_0)} (t - z)^{-\alpha} \left(f \circ g^{-1}\right)^{([\nu])}(t)\, dt, \tag{18}$$

for all $g(a) \leq z \leq g(x_0) \leq g(b)$.

We get that

$$\left(D^n_{g(x_0)-}\left(f \circ g^{-1}\right)\right)(z) = (-1)^n \left(f \circ g^{-1}\right)^{(n)}(z) \tag{19}$$

and $\left(D^0_{g(x_0)-}\left(f \circ g^{-1}\right)\right)(z) = \left(f \circ g^{-1}\right)(z)$, all $z \in [g(a), g(b)]$, see [4].

By [4], we have for $f \circ g^{-1} \in C^{\nu}_{g(x_0)-}([g(a), g(b)], X)$, where $x_0 \in [a, b]$ is fixed, the following right generalized g-fractional, of Canavati type, X-valued Taylor's formula:

Theorem 5 *Let $f \circ g^{-1} \in C^{\nu}_{g(x_0)-}([g(a), g(b)], X)$, where $x_0 \in [a, b]$ is fixed.*

(i) If $\nu \geq 1$, then

$$f(x) - f(x_0) = \sum_{k=1}^{[\nu]-1} \frac{\left(f \circ g^{-1}\right)^{(k)}(g(x_0))}{k!}(g(x) - g(x_0))^k +$$

$$\frac{1}{\Gamma(\nu)} \int_{g(x)}^{g(x_0)} (t - g(x))^{\nu-1} \left(D^{\nu}_{g(x_0)-}\left(f \circ g^{-1}\right)\right)(t)\, dt, \tag{20}$$

for all $a \leq x \leq x_0$,

(ii) If $0 < \nu < 1$, we get

$$f(x) = \frac{1}{\Gamma(\nu)} \int_{g(x)}^{g(x_0)} (t - g(x))^{\nu-1} \left(D^{\nu}_{g(x_0)-}\left(f \circ g^{-1}\right)\right)(t)\, dt, \tag{21}$$

all $a \leq x \leq x_0$.

III) Denote by

$$D^{m\nu}_{g(x_0)} = D^{\nu}_{g(x_0)} D^{\nu}_{g(x_0)} \ldots D^{\nu}_{g(x_0)} \quad (m\text{-times}),\ m \in \mathbb{N}. \tag{22}$$

We mention the following modified and generalized left X-valued fractional Taylor's formula of Canavati type:

Theorem 6 *Let $f \in C^1([a, b], X)$, $g \in C^1([a, b])$, strictly increasing: $g^{-1} \in C^1([g(a), g(b)])$. Assume that $\left(D^{i\nu}_{g(x_0)}\left(f \circ g^{-1}\right)\right) \in C^{\nu}_{g(x_0)}([g(a), g(b)], X)$, $0 < \nu < 1$, $x_0 \in [a, b]$, for $i = 0, 1, \ldots, m$. Then*

$$f(x) = \frac{1}{\Gamma((m+1)\nu)} \int_{g(x_0)}^{g(x)} (g(x) - z)^{(m+1)\nu-1} \left(D^{(m+1)\nu}_{g(x_0)}\left(f \circ g^{-1}\right)\right)(z)\, dz, \tag{23}$$

all $x_0 \leq x \leq b$.

IV) Denote by

$$D_{g(x_0)-}^{m\nu} = D_{g(x_0)-}^{\nu} D_{g(x_0)-}^{\nu} ... D_{g(x_0)-}^{\nu} \quad (m \text{ times}),\ m \in \mathbb{N}. \tag{24}$$

We mention the following modified and generalized right X-valued fractional Taylor's formula of Canavati type:

Theorem 7 *Let $f \in C^1([a,b], X)$, $g \in C^1([a,b])$, strictly increasing: $g^{-1} \in C^1([g(a), g(b)])$. Assume that $\left(D_{g(x_0)-}^{i\nu}(f \circ g^{-1})\right) \in C_{g(x_0)-}^{\nu}([g(a), g(b)], X)$, $0 < \nu < 1$, $x_0 \in [a,b]$, for all $i = 0, 1, ..., m$. Then*

$$f(x) = \frac{1}{\Gamma((m+1)\nu)} \int_{g(x)}^{g(x_0)} (z - g(x))^{(m+1)\nu - 1} \left(D_{g(x_0)-}^{(m+1)\nu}(f \circ g^{-1})\right)(z)\, dz, \tag{25}$$

all $a \leq x \leq x_0 \leq b$.

3 Basic Banach Algebras background

All here come from [17].

We need

Definition 8 *([17], p. 245) A complex algebra is a vector space A over the complex filed $\mathbb{C}$ in which a multiplication is defined that satisfies*

$$x(yz) = (xy)z, \tag{26}$$

$$(x+y)z = xz + yz, \quad x(y+z) = xy + xz, \tag{27}$$

and

$$\alpha(xy) = (\alpha x)y = x(\alpha y), \tag{28}$$

for all x, y and z in A and for all scalars α.

Additionally if A is a Banach space with respect to a norm that satisfies the multiplicative inequality

$$\|xy\| \leq \|x\| \|y\| \quad (x \in A,\ y \in A) \tag{29}$$

and if A contains a unit element e such that

$$xe = ex = x \quad (x \in A) \tag{30}$$

and

$$\|e\| = 1, \tag{31}$$

then A is called a Banach algebra.

A is commutative iff $xy = yx$ for all $x, y \in A$.

We make

Remark 9 *Commutativity of A is explicited stated when needed.*

There exists at most one $e \in A$ that satisfies (30).

Inequality (29) makes multiplication to be continuous, more precisely left and right continuous, see [17], p. 246.

Multiplication in A is not necessarily the numerical multiplication, it is something more general and it is defined abstractly, that is for $x, y \in A$ we have $xy \in A$, e.g. composition or convolution, etc.

For nice examples about Banach algebras see [17], p. 247-248, § 10.3.

We also make

Remark 10 *Next we mention about integration of A-valued functions, see [17], p. 259, § 10.22:*

If A is a Banach algebra and f is a continuous A-valued function on some compact Hausdorff space Q on which a complex Borel measure μ is defined, then $\int f d\mu$ exists and has all the properties that were discussed in Chapter 3 of [17], simply because A is a Banach space. However, an additional property can be added to these, namely: If $x \in A$, then

$$x \int_Q f \; d\mu = \int_Q x f(p) \; d\mu(p) \tag{32}$$

and

$$\left(\int_Q f \; d\mu \right) x = \int_Q f(p) \, x \; d\mu(p) . \tag{33}$$

The Bochner integrals we will involve in our article follow (32) and (33). Also, let $f \in C([a,b], X)$, where $[a,b] \subset \mathbb{R}$, $(X, \|\cdot\|)$ is a Banach space. By [5], p. 3, f is Bochner integrable.

4 p-Schatten norms background

In this advanced section all come from [11].

Let $(H, \langle \cdot, \cdot \rangle)$ be a complex Hilbert space and $\mathcal{B}(H)$ the Banach algebra of all bounded linear operators on H. If $\{e_i\}_{i \in I}$ an orthonormal basis of H, we say that $A \in \mathcal{B}(H)$ is of trace class if

$$\|A\|_1 := \sum_{i \in I} \langle |A| e_i, e_i \rangle < \infty. \tag{34}$$

The definition of $\|A\|_1$ does not depend on the choice of the orthornormal basis $\{e_i\}_{i \in I}$. We denote by $\mathcal{B}_1(H)$ the set of trace class operators in $\mathcal{B}(H)$.

We define the trace of a trace class operator $A \in \mathcal{B}_1(H)$ to be

$$tr(A) := \sum_{i \in I} \langle Ae_i, e_i \rangle, \tag{35}$$

where $\{e_i\}_{i \in I}$ an orthonormal basis of H. Note that this coincides with the usual definition of the trace if H is finite-dimensional. We observe that the series (35) converges absolutely and it is independent from the choice of basis.

The following result collects some properties of the trace:

Theorem 11 *We have:*

(i) If $A \in \mathcal{B}_1(H)$ then $A^* \in \mathcal{B}_1(H)$ and

$$tr(A^*) = \overline{tr(A)}; \tag{36}$$

(ii) If $A \in \mathcal{B}_1(H)$ and $T \in \mathcal{B}(H)$, then AT, $TA \in \mathcal{B}_1(H)$ and

$$tr(AT) = tr(TA) \quad and \quad |tr(AT)| \le \|A\|_1 \|T\|; \tag{37}$$

(iii) $tr(\cdot)$ is a bounded linear functional on $\mathcal{B}_1(H)$ with $\|tr\| = 1$;

(iv) If $A, B \in \mathcal{B}_2(H)$ then AB, $BA \in \mathcal{B}_1(H)$ and $tr(AB) = tr(BA)$;

(v) $\mathcal{B}_{fin}(H)$ (finite rank operators) is a dense subspace of $\mathcal{B}_1(H)$.

An operator $A \in \mathcal{B}(H)$ is said to belong to the von Neumann-Schatten class $\mathcal{B}_p(H)$, $1 \le p < \infty$ if the p-Schatten norm is finite [19, p. 60-64]

$$\|A\|_p := [tr(|A|^p)]^{\frac{1}{p}} < \infty,$$

$|A|^p$ is an operator notation and not a power.

For $1 < p < q < \infty$ we have that

$$\mathcal{B}_1(H) \subset \mathcal{B}_p(H) \subset \mathcal{B}_q(H) \subset \mathcal{B}(H) \tag{38}$$

and

$$\|A\|_1 \ge \|A\|_p \ge \|A\|_q \ge \|A\|. \tag{39}$$

For $p \ge 1$ the functional $\|\cdot\|_p$ is a norm on the $*$-ideal $\mathcal{B}_p(H)$, which is a Banach algebra, and $\left(\mathcal{B}_p(H), \|\cdot\|_p\right)$ is a Banach space.

Also, see for instance [19, p. 60-64], for $p \ge 1$,

$$\|A\|_p = \|A^*\|_p, \quad A \in \mathcal{B}_p(H) \tag{40}$$

$$\|AB\|_p \le \|A\|_p \|B\|_p, \quad A, B \in \mathcal{B}_p(H) \tag{41}$$

and

$$\|AB\|_p \le \|A\|_p \|B\|, \quad \|BA\|_p \le \|B\| \|A\|_p, \quad A \in \mathcal{B}_p(H), B \in \mathcal{B}(H). \tag{42}$$

This implies that

$$\|CAB\|_p \leq \|C\| \, \|A\|_p \, \|B\| \, , \ \ A \in \mathcal{B}_p(H) \, , \ B, C \in \mathcal{B}(H) \, . \tag{43}$$

In terms of p-Schatten norm we have the Hölder inequality for $p, q > 1$ with $\frac{1}{p} + \frac{1}{q} = 1$:

$$(|tr(AB)| \leq) \, \|AB\|_1 \leq \|A\|_p \, \|B\|_q \, , \quad A \in \mathcal{B}_p(H) \, , \ B \in \mathcal{B}_q(H) \, . \tag{44}$$

For the theory of trace functionals and their applications the interested reader is referred to [18] and [19].

For some classical trace inequalities see [9], [10] and [14], which are continuations of the work of Bellman [7].

5 Main Results

We start with 1-Schatten norm weighted mixed generalized Canavati fractional Ostrowski type inequalities involving several functions taking values in the Banach algebra $\mathcal{B}_2(H) \subset \mathcal{B}(H)$:

Theorem 12 *Let the $*$-ideal $\mathcal{B}_2(H)$, which $(\mathcal{B}_2(H), \|\cdot\|_2)$ is a Banach algebra; $x_0 \in [a,b] \subset \mathbb{R}$, $\nu \geq 1$, $n = [\nu]$; $f_i \in C^n([a,b], \mathcal{B}_2(H))$, $i = 1, ..., r \in \mathbb{N} - \{1\}$; $g \in C^1([a,b])$, strictly increasing such that $g^{-1} \in C^n([g(a), g(b)])$, with $\left(f_i \circ g^{-1}\right)^{(k)}(g(x_0)) = 0$, $k = 1, ..., n-1$; $i = 1, ..., r$. Assume further that $f_i \circ g^{-1} \in C^{\nu}_{g(x_0)-}([g(a), g(b)], \mathcal{B}_2(H)) \cap C^{\nu}_{g(x_0)}([g(a), g(b)], \mathcal{B}_2(H))$, $i = 1, ..., r$.*

Denote by

$$K(f_1, ..., f_r)(x_0) :=$$
$$\sum_{i=1}^{r} \left[\int_a^b \left(\prod_{\substack{j=1 \\ j \neq i}}^{r} f_j(x) \right) f_i(x) \, dx - \left(\int_a^b \left(\prod_{\substack{j=1 \\ j \neq i}}^{r} f_j(x) \right) dx \right) f_i(x_0) \right]. \tag{45}$$

Then

$$\|K(f_1, ..., f_r)(x_0)\|_1 \leq \frac{1}{\Gamma(\nu+1)} \sum_{i=1}^{r} \left[\left[\left\| \left\| D^{\nu}_{g(x_0)-} \left(f_i \circ g^{-1}\right) \right\|_2 \right\|_{\infty, [g(a), g(x_0)]} \right.\right.$$
$$\left. (g(x_0) - g(a))^{\nu} \left(\int_a^{x_0} \left(\prod_{\substack{j=1 \\ j \neq i}}^{r} \|f_j(x)\|_2 \right) dx \right) \right] + \tag{46}$$
$$\left.\left[\left\| \left\| D^{\nu}_{g(x_0)} \left(f_i \circ g^{-1}\right) \right\|_2 \right\|_{\infty, [g(x_0), g(b)]} (g(b) - g(x_0))^{\nu} \left(\int_{x_0}^{b} \left(\prod_{\substack{j=1 \\ j \neq i}}^{r} \|f_j(x)\|_2 \right) dx \right) \right] \right].$$

Proof. Since $\left(f_i \circ g^{-1}\right)^{(k)}(g(x_0)) = 0$, $k = 1, ..., [\nu]-1$; $i = 1, ..., r$; we have by Theorem 4 that

$$f_i(x) - f_i(x_0) = \frac{1}{\Gamma(\nu)} \int_{g(x_0)}^{g(x)} (g(x) - t)^{\nu-1} \left(D^{\nu}_{g(x_0)}\left(f_i \circ g^{-1}\right)\right)(t)\, dt, \quad (47)$$

$\forall\ x \in [x_0, b]$,

and by Theorem 5 that

$$f_i(x) - f_i(x_0) = \frac{1}{\Gamma(\nu)} \int_{g(x)}^{g(x_0)} (t - g(x))^{\nu-1} \left(D^{\nu}_{g(x_0)-}\left(f_i \circ g^{-1}\right)\right)(t)\, dt, \quad (48)$$

$\forall\ x \in [a, x_0]$, for all $i = 1, ..., r$.

Left multiplying (47) and (48) with $\left(\prod_{\substack{j=1 \\ j \neq i}}^{r} f_j(x)\right)$ we get, respectively,

$$\left(\prod_{\substack{j=1 \\ j \neq i}}^{r} f_j(x)\right) f_i(x) - \left(\prod_{\substack{j=1 \\ j \neq i}}^{r} f_j(x)\right) f_i(x_0) =$$

$$\frac{\left(\prod_{\substack{j=1 \\ j \neq i}}^{r} f_j(x)\right)}{\Gamma(\nu)} \int_{g(x_0)}^{g(x)} (g(x) - t)^{\nu-1} \left(D^{\nu}_{g(x_0)}\left(f_i \circ g^{-1}\right)\right)(t)\, dt, \quad (49)$$

$\forall\ x \in [x_0, b]$,

and

$$\left(\prod_{\substack{j=1 \\ j \neq i}}^{r} f_j(x)\right) f_i(x) - \left(\prod_{\substack{j=1 \\ j \neq i}}^{r} f_j(x)\right) f_i(x_0) = \quad (50)$$

$$\frac{\left(\prod_{\substack{j=1 \\ j \neq i}}^{r} f_j(x)\right)}{\Gamma(\nu)} \int_{g(x)}^{g(x_0)} (t - g(x))^{\nu-1} \left(D^{\nu}_{g(x_0)-}\left(f_i \circ g^{-1}\right)\right)(t)\, dt,$$

$\forall\ x \in [a, x_0]$, for all $i = 1, ..., r$.

Adding (49) and (50) as separate groups, we obtain

$$\sum_{i=1}^{r} \left(\prod_{\substack{j=1 \\ j \neq i}}^{r} f_j(x)\right) f_i(x) - \sum_{i=1}^{r} \left(\prod_{\substack{j=1 \\ j \neq i}}^{r} f_j(x)\right) f_i(x_0) =$$

$$\frac{1}{\Gamma(\nu)} \sum_{i=1}^{r} \left(\prod_{\substack{j=1 \\ j \neq i}}^{r} f_j(x)\right) \int_{g(x_0)}^{g(x)} (g(x) - t)^{\nu-1} \left(D^{\nu}_{g(x_0)}\left(f_i \circ g^{-1}\right)\right)(t)\, dt, \quad (51)$$

$\forall\ x \in [x_0, b]$,

and

$$\sum_{i=1}^{r}\left(\prod_{\substack{j=1\\ j\neq i}}^{r} f_j(x)\right) f_i(x) - \sum_{i=1}^{r}\left(\prod_{\substack{j=1\\ j\neq i}}^{r} f_j(x)\right) f_i(x_0) =$$

$$\frac{1}{\Gamma(\nu)}\sum_{i=1}^{r}\left(\prod_{\substack{j=1\\ j\neq i}}^{r} f_j(x)\right)\int_{g(x)}^{g(x_0)} (t-g(x))^{\nu-1}\left(D_{g(x_0)-}^{\nu}\left(f_i\circ g^{-1}\right)\right)(t)\,dt, \quad (52)$$

$\forall\ x \in [a, x_0]$.

Next, we integrate (51) and (52) with respect to $x \in [a,b]$. We have

$$\sum_{i=1}^{r}\int_{x_0}^{b}\left(\prod_{\substack{j=1\\ j\neq i}}^{r} f_j(x)\right) f_i(x)\,dx - \sum_{i=1}^{r}\left(\int_{x_0}^{b}\left(\prod_{\substack{j=1\\ j\neq i}}^{r} f_j(x)\right) dx\right) f_i(x_0) =$$

$$\frac{1}{\Gamma(\nu)}\sum_{i=1}^{r}\left[\int_{x_0}^{b}\left(\prod_{\substack{j=1\\ j\neq i}}^{r} f_j(x)\right)\left(\int_{g(x_0)}^{g(x)} (g(x)-t)^{\nu-1}\left(D_{g(x_0)}^{\nu}\left(f_i\circ g^{-1}\right)\right)(t)\,dt\right) dx\right], \quad (53)$$

and

$$\sum_{i=1}^{r}\int_{a}^{x_0}\left(\prod_{\substack{j=1\\ j\neq i}}^{r} f_j(x)\right) f_i(x)\,dx - \sum_{i=1}^{r}\left(\int_{a}^{x_0}\left(\prod_{\substack{j=1\\ j\neq i}}^{r} f_j(x)\right) dx\right) f_i(x_0) =$$

$$\frac{1}{\Gamma(\nu)}\sum_{i=1}^{r}\left[\int_{a}^{x_0}\left(\prod_{\substack{j=1\\ j\neq i}}^{r} f_j(x)\right)\left(\int_{g(x)}^{g(x_0)} (t-g(x))^{\nu-1}\left(D_{g(x_0)-}^{\nu}\left(f_i\circ g^{-1}\right)\right)(t)\,dt\right) dx\right], \quad (54)$$

Finally, adding (53) and (54) we obtain the useful identity

$$K(f_1,\ldots,f_r)(x_0) :=$$

$$\sum_{i=1}^{r}\left[\int_{a}^{b}\left(\prod_{\substack{j=1\\ j\neq i}}^{r} f_j(x)\right) f_i(x)\,dx - \left(\int_{a}^{b}\left(\prod_{\substack{j=1\\ j\neq i}}^{r} f_j(x)\right) dx\right) f_i(x_0)\right] =$$

$$\frac{1}{\Gamma(\nu)}\sum_{i=1}^{r}\left[\left[\int_{a}^{x_0}\left(\prod_{\substack{j=1\\ j\neq i}}^{r} f_j(x)\right)\left(\int_{g(x)}^{g(x_0)} (t-g(x))^{\nu-1}\left(D_{g(x_0)-}^{\nu}\left(f_i\circ g^{-1}\right)\right)(t)\,dt\right) dx\right]\right.$$

$$+\left[\int_{x_0}^{b}\left(\prod_{\substack{j=1\\ j\neq i}}^{r} f_j\left(x\right)\right)\left(\int_{g(x_0)}^{g(x)}\left(g\left(x\right)-t\right)^{\nu-1}\left(D_{g(x_0)}^{\nu}\left(f_i\circ g^{-1}\right)\right)\left(t\right)dt\right)dx\right]\Bigg]. \tag{55}$$

Therefore, we get that

$$\left\|K\left(f_1,...,f_r\right)\left(x_0\right)\right\|_1 =$$

$$\left\|\sum_{i=1}^{r}\left[\int_a^b\left(\prod_{\substack{j=1\\ j\neq i}}^{r} f_j\left(x\right)\right)f_i\left(x\right)dx-\left(\int_a^b\left(\prod_{\substack{j=1\\ j\neq i}}^{r} f_j\left(x\right)\right)dx\right)f_i\left(x_0\right)\right]\right\|_1 \leq \frac{1}{\Gamma\left(\nu\right)}$$

$$\sum_{i=1}^{r}\left[\left\|\left[\int_a^{x_0}\left(\prod_{\substack{j=1\\ j\neq i}}^{r} f_j\left(x\right)\right)\left(\int_{g(x)}^{g(x_0)}\left(t-g\left(x\right)\right)^{\nu-1}\left(D_{g(x_0)-}^{\nu}\left(f_i\circ g^{-1}\right)\right)\left(t\right)dt\right)dx\right]\right\|_1\right. \tag{56}$$

$$\left.+\left\|\left[\int_{x_0}^{b}\left(\prod_{\substack{j=1\\ j\neq i}}^{r} f_j\left(x\right)\right)\left(\int_{g(x_0)}^{g(x)}\left(g\left(x\right)-t\right)^{\nu-1}\left(D_{g(x_0)}^{\nu}\left(f_i\circ g^{-1}\right)\right)\left(t\right)dt\right)dx\right]\right\|_1\right] \leq$$

$$\frac{1}{\Gamma\left(\nu\right)}\sum_{i=1}^{r}\left[\left[\int_a^{x_0}\left\|\left(\prod_{\substack{j=1\\ j\neq i}}^{r} f_j\left(x\right)\right)\left(\int_{g(x)}^{g(x_0)}\left(t-g\left(x\right)\right)^{\nu-1}\left(D_{g(x_0)-}^{\nu}\left(f_i\circ g^{-1}\right)\right)\left(t\right)dt\right)\right\|_1 dx\right]\right. \tag{57}$$

$$\left.+\left[\int_{x_0}^{b}\left\|\left(\prod_{\substack{j=1\\ j\neq i}}^{r} f_j\left(x\right)\right)\left(\int_{g(x_0)}^{g(x)}\left(g\left(x\right)-t\right)^{\nu-1}\left(D_{g(x_0)}^{\nu}\left(f_i\circ g^{-1}\right)\right)\left(t\right)dt\right)\right\|_1 dx\right]\right] \leq$$

$$\frac{1}{\Gamma\left(\nu\right)}\sum_{i=1}^{r}\left[\left[\int_a^{x_0}\left(\prod_{\substack{j=1\\ j\neq i}}^{r}\left\|f_j\left(x\right)\right\|_2\right)\left(\int_{g(x)}^{g(x_0)}\left(t-g\left(x\right)\right)^{\nu-1}\left\|\left(D_{g(x_0)-}^{\nu}\left(f_i\circ g^{-1}\right)\right)\left(t\right)\right\|_2 dt\right)dx\right]\right. \tag{58}$$

$$\left.+\left[\int_{x_0}^{b}\left(\prod_{\substack{j=1\\ j\neq i}}^{r}\left\|f_j\left(x\right)\right\|_2\right)\left(\int_{g(x_0)}^{g(x)}\left(g\left(x\right)-t\right)^{\nu-1}\left\|\left(D_{g(x_0)}^{\nu}\left(f_i\circ g^{-1}\right)\right)\left(t\right)\right\|_2 dt\right)dx\right]\right] =: \left(*\right).$$

Hence it holds

$$\left\|K\left(f_1,...,f_r\right)\left(x_0\right)\right\|_1 \leq \left(*\right). \tag{59}$$

We have that

$$\left(*\right) \leq \frac{1}{\Gamma\left(\nu+1\right)}$$

$$\sum_{i=1}^{r}\left[\left[\left\Vert\left\Vert\left(D_{g(x_0)-}^{\nu}\left(f_i\circ g^{-1}\right)\right)\right\Vert_2\right\Vert_{\infty,[g(a),g(x_0)]}\int_a^{x_0}\left(\prod_{\substack{j=1\\j\neq i}}^{r}\left\Vert f_j\left(x\right)\right\Vert_2\right)\left(g\left(x_0\right)-g\left(x\right)\right)^{\nu}dx\right]\right.$$

$$\left.+\left[\left\Vert\left\Vert\left(D_{g(x_0)}^{\nu}\left(f_i\circ g^{-1}\right)\right)\right\Vert_2\right\Vert_{\infty,[g(x_0),g(b)]}\int_{x_0}^{b}\left(\prod_{\substack{j=1\\j\neq i}}^{r}\left\Vert f_j\left(x\right)\right\Vert_2\right)\left(g\left(x\right)-g\left(x_0\right)\right)^{\nu}dx\right]\right]\leq \tag{60}$$

$$\frac{1}{\Gamma\left(\nu+1\right)}\sum_{i=1}^{r}\left[\left[\left\Vert\left\Vert\left(D_{g(x_0)-}^{\nu}\left(f_i\circ g^{-1}\right)\right)\right\Vert_2\right\Vert_{\infty,[g(a),g(x_0)]}\right.\right.$$

$$\left.\left(g\left(x_0\right)-g\left(a\right)\right)^{\nu}\left(\int_a^{x_0}\left(\prod_{\substack{j=1\\j\neq i}}^{r}\left\Vert f_j\left(x\right)\right\Vert_2\right)dx\right)\right]+ \tag{61}$$

$$\left.\left[\left\Vert\left\Vert\left(D_{g(x_0)}^{\nu}\left(f_i\circ g^{-1}\right)\right)\right\Vert_2\right\Vert_{\infty,[g(x_0),g(b)]}\left(g\left(b\right)-g\left(x_0\right)\right)^{\nu}\left(\int_{x_0}^{b}\left(\prod_{\substack{j=1\\j\neq i}}^{r}\left\Vert f_j\left(x\right)\right\Vert_2\right)dx\right)\right]\right],$$

proving (46). ■

Next comes an L_1 estimate.

Theorem 13 *All as in Theorem 12. Then*

$$\Vert|K\left(f_1,...,f_r\right)\left(x_0\right)\Vert_1\leq\frac{1}{\Gamma\left(\nu\right)}$$

$$\sum_{i=1}^{r}\left[\left[\left\Vert\left\Vert\left(D_{g(x_0)-}^{\nu}\left(f_i\circ g^{-1}\right)\right)\right\Vert_2\right\Vert_{L_1([g(a),g(x_0)])}\int_a^{x_0}\left(\prod_{\substack{j=1\\j\neq i}}^{r}\left\Vert f_j\left(x\right)\right\Vert_2\right)\left(g\left(x_0\right)-g\left(x\right)\right)^{\nu-1}dx\right]\right. \tag{62}$$

$$\left.+\left[\left\Vert\left\Vert\left(D_{g(x_0)}^{\nu}\left(f_i\circ g^{-1}\right)\right)\right\Vert_2\right\Vert_{L_1([g(x_0),g(b)])}\int_{x_0}^{b}\left(\prod_{\substack{j=1\\j\neq i}}^{r}\left\Vert f_j\left(x\right)\right\Vert_2\right)\left(g\left(x\right)-g\left(x_0\right)\right)^{\nu-1}dx\right]\right].$$

Proof. We observe that (by (58), (59))

$$(*)\leq\frac{1}{\Gamma\left(\nu\right)}$$

$$\sum_{i=1}^{r}\left[\left[\left\Vert\left\Vert\left(D_{g(x_0)-}^{\nu}\left(f_i\circ g^{-1}\right)\right)\right\Vert_2\right\Vert_{L_1([g(a),g(x_0)])}\int_a^{x_0}\left(\prod_{\substack{j=1\\j\neq i}}^{r}\left\Vert f_j\left(x\right)\right\Vert_2\right)\left(g\left(x_0\right)-g\left(x\right)\right)^{\nu-1}dx\right]\right. \tag{63}$$

$$+\left[\left\|\left\|\left(D^{\nu}_{g(x_0)}\left(f_i\circ g^{-1}\right)\right)\right\|_2\right\|_{L_1([g(x_0),g(b)])}\int_{x_0}^{b}\left(\prod_{\substack{j=1\\j\neq i}}^{r}\|f_j(x)\|_2\right)(g(x)-g(x_0))^{\nu-1}dx\right]\Bigg],$$

proving (62). ■

An L_p estimate follows.

Theorem 14 *All as in Theorem 12. Let now* $p,q>1:\frac{1}{p}+\frac{1}{q}=1$. *Then*

$$\|K(f_1,...,f_r)(x_0)\|_1\leq\frac{1}{(p(\nu-1)+1)^{\frac{1}{p}}\Gamma(\nu)}$$

$$\sum_{i=1}^{r}\left[\left[\left\|\left\|\left(D^{\nu}_{g(x_0)-}\left(f_i\circ g^{-1}\right)\right)\right\|_2\right\|_{q,[g(a),g(x_0)]}\left(\int_a^{x_0}(g(x_0)-g(x))^{\nu-\frac{1}{q}}\left(\prod_{\substack{j=1\\j\neq i}}^{r}\|f_j(x)\|_2\right)dx\right)\right]\right.$$

$$(64)$$

$$\left.+\left[\left\|\left\|\left(D^{\nu}_{g(x_0)}\left(f_i\circ g^{-1}\right)\right)\right\|_2\right\|_{q,[g(x_0),g(b)]}\left(\int_{x_0}^{b}(g(x)-g(x_0))^{\nu-\frac{1}{q}}\left(\prod_{\substack{j=1\\j\neq i}}^{r}\|f_j(x)\|_2\right)dx\right)\right]\right].$$

Proof. We have that (by (58), (59))

$$(*)\leq\frac{1}{\Gamma(\nu)}\sum_{i=1}^{r}\left[\left[\int_a^{x_0}\left(\prod_{\substack{j=1\\j\neq i}}^{r}\|f_j(x)\|_2\right)\left(\int_{g(x)}^{g(x_0)}(t-g(x))^{p(\nu-1)}dt\right)^{\frac{1}{p}}\right.\right.$$

$$\left.\left(\int_{g(x)}^{g(x_0)}\left\|\left(D^{\nu}_{g(x_0)-}\left(f_i\circ g^{-1}\right)\right)(t)\right\|_2^q dt\right)^{\frac{1}{q}}dx\right]+$$

$$\left[\int_{x_0}^{b}\left(\prod_{\substack{j=1\\j\neq i}}^{r}\|f_j(x)\|_2\right)\left(\int_{g(x_0)}^{g(x)}(g(x)-t)^{p(\nu-1)}dt\right)^{\frac{1}{p}}\right.$$

$$\left.\left.\left(\int_{g(x)}^{g(x_0)}\left\|\left(D^{\nu}_{g(x_0)}\left(f_i\circ g^{-1}\right)\right)(t)\right\|_2^q dt\right)^{\frac{1}{q}}dx\right]\right]\leq\qquad(65)$$

$$\frac{1}{\Gamma(\nu)}\sum_{i=1}^{r}\left[\left[\int_a^{x_0}\left(\prod_{\substack{j=1\\j\neq i}}^{r}\|f_j(x)\|_2\right)\frac{(g(x_0)-g(x))^{\nu-1+\frac{1}{p}}}{(p(\nu-1)+1)^{\frac{1}{p}}}\left\|\left\|\left(D^{\nu}_{g(x_0)-}\left(f_i\circ g^{-1}\right)\right)\right\|_2\right\|_{q,[g(a),g(x_0)]}dx\right]\right.$$

$$+\left[\int_{x_0}^{b}\left(\prod_{\substack{j=1\\j\neq i}}^{r}\|f_j(x)\|_2\right)\frac{(g(x)-g(x_0))^{\nu-1+\frac{1}{p}}}{(p(\nu-1)+1)^{\frac{1}{p}}}\left\|\left\|\left(D_{g(x_0)}^{\nu}\left(f_i\circ g^{-1}\right)\right)(z)\right\|_2\right\|_{q,[g(x_0),g(b)]}dx\right]\Bigg]$$

$$=\frac{1}{(p(\nu-1)+1)^{\frac{1}{p}}\Gamma(\nu)}$$

$$\sum_{i=1}^{r}\left[\left\|\left\|\left(D_{g(x_0)-}^{\nu}\left(f_i\circ g^{-1}\right)\right)\right\|_2\right\|_{q,[g(a),g(x_0)]}\left(\int_a^{x_0}(g(x_0)-g(x))^{\nu-\frac{1}{q}}\left(\prod_{\substack{j=1\\j\neq i}}^{r}\|f_j(x)\|_2\right)dx\right)\right.$$

$$\left.+\left\|\left\|\left(D_{g(x_0)}^{\nu}\left(f_i\circ g^{-1}\right)\right)\right\|_2\right\|_{q,[g(x_0),g(b)]}\left(\int_{x_0}^{b}(g(x)-g(x_0))^{\nu-\frac{1}{q}}\left(\prod_{\substack{j=1\\j\neq i}}^{r}\|f_j(x)\|_2\right)dx\right)\right], \tag{66}$$

proving (64). ■

We continue with γ-Schatten norm related Ostrowski fractional inequalities:

Theorem 15 *Let $\gamma\geq 1$, the $*$-ideal $\mathcal{B}_\gamma(H)$, which $\left(\mathcal{B}_\gamma(H),\|\cdot\|_\gamma\right)$ is a Banach algebra; $x_0\in[a,b]\subset\mathbb{R}$, $\nu\geq 1$, $n=[\nu]$; $f_i\in C^n([a,b],\mathcal{B}_\gamma(H))$, $i=1,...,r\in\mathbb{N}-\{1\}$; $g\in C^1([a,b])$, strictly increasing such that $g^{-1}\in C^n([g(a),g(b)])$, with $\left(f_i\circ g^{-1}\right)^{(k)}(g(x_0))=0$, $k=1,...,n-1$; $i=1,...,r$. Assume further that $f_i\circ g^{-1}\in C_{g(x_0)-}^{\nu}([g(a),g(b)],\mathcal{B}_\gamma(H))\cap C_{g(x_0)}^{\nu}([g(a),g(b)],\mathcal{B}_\gamma(H))$, $i=1,...,r$.*

Here $K(f_1,...,f_r)(x_0)$ is as in (45). Then

$$\|K(f_1,...,f_r)(x_0)\|_\gamma\leq\frac{1}{\Gamma(\nu+1)}\sum_{i=1}^{r}\left[\left[\left\|\left\|D_{g(x_0)-}^{\nu}\left(f_i\circ g^{-1}\right)\right\|_\gamma\right\|_{\infty,[g(a),g(x_0)]}\right.\right.$$

$$\left.(g(x_0)-g(a))^{\nu}\left(\int_a^{x_0}\left(\prod_{\substack{j=1\\j\neq i}}^{r}\|f_j(x)\|_\gamma\right)dx\right)\right]+ \tag{67}$$

$$\left.\left[\left\|\left\|D_{g(x_0)}^{\nu}\left(f_i\circ g^{-1}\right)\right\|_\gamma\right\|_{\infty,[g(x_0),g(b)]}(g(b)-g(x_0))^{\nu}\left(\int_{x_0}^{b}\left(\prod_{\substack{j=1\\j\neq i}}^{r}\|f_j(x)\|_\gamma\right)dx\right)\right]\right].$$

Proof. As similar to Theorem 12 is omitted. Use of (41). ■

An L_1 estimate follows:

Theorem 16 *All as in Theorem 15. Then*

$$|\|K\left(f_{1},...,f_{r}\right)\left(x_{0}\right)\|_{\gamma}\leq\frac{1}{\Gamma\left(\nu\right)}$$

$$\sum_{i=1}^{r}\left[\left[\left\|\left\|\left(D_{g(x_{0})-}^{\nu}\left(f_{i}\circ g^{-1}\right)\right)\right\|_{\gamma}\right\|_{L_{1}([g(a),g(x_{0})])}\int_{a}^{x_{0}}\left(\prod_{\substack{j=1\\j\neq i}}^{r}\left\|f_{j}\left(x\right)\right\|_{\gamma}\right)\left(g\left(x_{0}\right)-g\left(x\right)\right)^{\nu-1}dx\right]\right.$$

$$\left.+\left[\left\|\left\|\left(D_{g(x_{0})}^{\nu}\left(f_{i}\circ g^{-1}\right)\right)\right\|_{\gamma}\right\|_{L_{1}([g(x_{0}),g(b)])}\int_{x_{0}}^{b}\left(\prod_{\substack{j=1\\j\neq i}}^{r}\left\|f_{j}\left(x\right)\right\|_{\gamma}\right)\left(g\left(x\right)-g\left(x_{0}\right)\right)^{\nu-1}dx\right]\right]. \tag{68}$$

Proof. As similar to Theorem 13 is omitted. ■

An L_p estimate follows.

Theorem 17 *All as in Theorem 15. Let now* $p,q>1:\frac{1}{p}+\frac{1}{q}=1$. *Then*

$$\left\|K\left(f_{1},...,f_{r}\right)\left(x_{0}\right)\right\|_{\gamma}\leq\frac{1}{\left(p\left(\nu-1\right)+1\right)^{\frac{1}{p}}\Gamma\left(\nu\right)}$$

$$\sum_{i=1}^{r}\left[\left[\left\|\left\|\left(D_{g(x_{0})-}^{\nu}\left(f_{i}\circ g^{-1}\right)\right)\right\|_{\gamma}\right\|_{q,[g(a),g(x_{0})]}\left(\int_{a}^{x_{0}}\left(g\left(x_{0}\right)-g\left(x\right)\right)^{\nu-\frac{1}{q}}\left(\prod_{\substack{j=1\\j\neq i}}^{r}\left\|f_{j}\left(x\right)\right\|_{\gamma}\right)dx\right)\right]\right.$$

$$\left.+\left[\left\|\left\|\left(D_{g(x_{0})}^{\nu}\left(f_{i}\circ g^{-1}\right)\right)\right\|_{\gamma}\right\|_{q,[g(x_{0}),g(b)]}\left(\int_{x_{0}}^{b}\left(g\left(x\right)-g\left(x_{0}\right)\right)^{\nu-\frac{1}{q}}\left(\prod_{\substack{j=1\\j\neq i}}^{r}\left\|f_{j}\left(x\right)\right\|_{\gamma}\right)dx\right)\right]\right]. \tag{69}$$

Proof. As similar to Theorem 14 is omitted. ■

When $r=2$ we derive the following p-Schatten norm operator related Ostrowski type Canavati fractional inequalities.

Theorem 18 *Let* $p,q>1:\frac{1}{p}+\frac{1}{q}=1$, *and let the* $*$*-ideals* $\mathcal{B}_{p}\left(H\right)$, $\mathcal{B}_{q}\left(H\right)$, *for which* $\left(\mathcal{B}_{p}\left(H\right),\left\|\cdot\right\|_{p}\right)$, $\left(\mathcal{B}_{q}\left(H\right),\left\|\cdot\right\|_{q}\right)$ *are Banach algebras;* $x_{0}\in\left[a,b\right]\subset\mathbb{R}$, $\alpha\geq1$, $n=\left[\alpha\right]$; $A_{1}\in C^{n}\left(\left[a,b\right],\mathcal{B}_{p}\left(H\right)\right)$, $A_{2}\in C^{n}\left(\left[a,b\right],\mathcal{B}_{q}\left(H\right)\right)$; $g\in C^{1}\left(\left[a,b\right]\right)$, *strictly increasing, such that* $g^{-1}\in C^{n}\left(\left[g\left(a\right),g\left(b\right)\right]\right)$, *with* $\left(A_{i}\circ g^{-1}\right)^{(k)}\left(g\left(x_{0}\right)\right)=0$, $k=1,...,n-1$; $i=1,2$. *Assume further that* $A_{1}\circ g^{-1}\in C_{g(x_{0})-}^{\alpha}\left(\left[g\left(a\right),g\left(b\right)\right],\mathcal{B}_{p}\left(H\right)\right)\cap C_{g(x_{0})}^{\alpha}\left(\left[g\left(a\right),g\left(b\right)\right],\mathcal{B}_{p}\left(H\right)\right)$, *and* $A_{2}\circ g^{-1}\in C_{g(x_{0})-}^{\alpha}\left(\left[g\left(a\right),g\left(b\right)\right],\mathcal{B}_{q}\left(H\right)\right)\cap C_{g(x_{0})}^{\alpha}\left(\left[g\left(a\right),g\left(b\right)\right],\mathcal{B}_{q}\left(H\right)\right)$. *Then*

1) it holds

$$\Phi\left(A_1, A_2\right)\left(x_0\right) := \int_a^b A_2\left(x\right) A_1\left(x\right) + \int_a^b A_1\left(x\right) A_2\left(x\right) dx -$$

$$\left(\int_a^b A_2\left(x\right) dx\right) A_1\left(x_0\right) - \left(\int_a^b A_1\left(x\right) dx\right) A_2\left(x_0\right) =$$

$$\frac{1}{\Gamma\left(\alpha\right)} \left\{ \left[\int_a^{x_0} A_2\left(x\right) \left(\int_{g(x)}^{g(x_0)} \left(z - g\left(x\right)\right)^{\alpha-1} \left(D^{\alpha}_{g(x_0)-} \left(A_1 \circ g^{-1}\right)\right)\left(z\right) dz \right) dx \right] + \right.$$

$$\left[\int_{x_0}^{b} A_2\left(x\right) \left(\int_{g(x_0)}^{g(x)} \left(g\left(x\right) - z\right)^{\alpha-1} \left(D^{\alpha}_{g(x_0)} \left(A_1 \circ g^{-1}\right)\right)\left(z\right) dz \right) dx \right] + \tag{70}$$

$$\left[\int_a^{x_0} A_1\left(x\right) \left(\int_{g(x)}^{g(x_0)} \left(z - g\left(x\right)\right)^{\alpha-1} \left(D^{\alpha}_{g(x_0)-} \left(A_2 \circ g^{-1}\right)\right)\left(z\right) dz \right) dx \right] +$$

$$\left. \left[\int_{x_0}^{b} A_1\left(x\right) \left(\int_{g(x_0)}^{g(x)} \left(g\left(x\right) - z\right)^{\alpha-1} \left(D^{\alpha}_{g(x_0)} \left(A_2 \circ g^{-1}\right)\right)\left(z\right) dz \right) dx \right] \right\},$$

2) for $\gamma, \delta > 1 : \frac{1}{\gamma} + \frac{1}{\delta} = 1$, we have that

$$\left\|\Phi\left(A_1, A_2\right)\left(x_0\right)\right\|_1 \leq \frac{1}{\Gamma\left(\alpha\right)\left(\gamma\left(\alpha-1\right)+1\right)^{\frac{1}{\gamma}}}$$

$$\left\{ \left[\left\| \left\| D^{\alpha}_{g(x_0)-} \left(A_1 \circ g^{-1}\right) \right\|_p \right\|_{\delta,[g(a),g(x_0)]} \int_a^{x_0} \left\|A_2\left(x\right)\right\|_q \left(g\left(x_0\right) - g\left(x\right)\right)^{\alpha-\frac{1}{\delta}} dx \right] + \right.$$

$$\left[\left\| \left\| D^{\alpha}_{g(x_0)} \left(A_1 \circ g^{-1}\right) \right\|_p \right\|_{\delta,[g(x_0),g(b)]} \int_{x_0}^{b} \left\|A_2\left(x\right)\right\|_q \left(g\left(x\right) - g\left(x_0\right)\right)^{\alpha-\frac{1}{\delta}} dx \right] + \tag{71}$$

$$\left[\left\| \left\| D^{\alpha}_{g(x_0)-} \left(A_2 \circ g^{-1}\right) \right\|_q \right\|_{\delta,[g(a),g(x_0)]} \int_a^{x_0} \left\|A_1\left(x\right)\right\|_p \left(g\left(x_0\right) - g\left(x\right)\right)^{\alpha-\frac{1}{\delta}} dx \right] +$$

$$\left. \left[\left\| \left\| D^{\alpha}_{g(x_0)} \left(A_2 \circ g^{-1}\right) \right\|_q \right\|_{\delta,[g(x_0),g(b)]} \int_{x_0}^{b} \left\|A_1\left(x\right)\right\|_p \left(g\left(x\right) - g\left(x_0\right)\right)^{\alpha-\frac{1}{\delta}} dx \right] \right\},$$

3) we also obtain

$$\left\|\Phi\left(A_1, A_2\right)\left(x_0\right)\right\|_1 \leq \frac{1}{\Gamma\left(\alpha\right)}$$

$$\left\{ \left[\left\| \left\| D^{\alpha}_{g(x_0)-} \left(A_1 \circ g^{-1}\right) \right\|_p \right\|_{L_1([g(a),g(x_0)])} \int_a^{x_0} \left\|A_2\left(x\right)\right\|_q \left(g\left(x_0\right) - g\left(x\right)\right)^{\alpha-1} dx \right] + \right.$$

$$\left[\left\|\left\|D^{\alpha}_{g(x_0)}\left(A_1\circ g^{-1}\right)\right\|_p\right\|_{L_1([g(x_0),g(b)])}\int_{x_0}^{b}\left\|A_2(x)\right\|_q\left(g(x)-g(x_0)\right)^{\alpha-1}dx\right]+$$

$$\left[\left\|\left\|D^{\alpha}_{g(x_0)-}\left(A_2\circ g^{-1}\right)\right\|_q\right\|_{L_1([g(a),g(x_0)])}\int_{a}^{x_0}\left\|A_1(x)\right\|_p\left(g(x_0)-g(x)\right)^{\alpha-1}dx\right]+$$

$$\left.\left[\left\|\left\|D^{\alpha}_{g(x_0)}\left(A_2\circ g^{-1}\right)\right\|_q\right\|_{L_1([g(x_0),g(b)])}\int_{x_0}^{b}\left\|A_1(x)\right\|_p\left(g(x)-g(x_0)\right)^{\alpha-1}dx\right]\right\}, \tag{72}$$

and

4)

$$\left\|\Phi\left(A_1,A_2\right)(x_0)\right\|_1\leq\frac{1}{\Gamma(\alpha+1)}$$

$$\left\{\left[\left\|\left\|D^{\alpha}_{g(x_0)-}\left(A_1\circ g^{-1}\right)\right\|_p\right\|_{\infty,[g(a),g(x_0)]}\int_{a}^{x_0}\left\|A_2(x)\right\|_q\left(g(x_0)-g(x)\right)^{\alpha}dx\right]+\right.$$

$$\left[\left\|\left\|D^{\alpha}_{g(x_0)}\left(A_1\circ g^{-1}\right)\right\|_p\right\|_{\infty,[g(x_0),g(b)]}\int_{x_0}^{b}\left\|A_2(x)\right\|_q\left(g(x)-g(x_0)\right)^{\alpha}dx\right]+$$

$$\left[\left\|\left\|D^{\alpha}_{g(x_0)-}\left(A_2\circ g^{-1}\right)\right\|_q\right\|_{\infty,[g(a),g(x_0)]}\int_{a}^{x_0}\left\|A_1(x)\right\|_p\left(g(x_0)-g(x)\right)^{\alpha}dx\right]+$$

$$\left.\left[\left\|\left\|D^{\alpha}_{g(x_0)}\left(A_2\circ g^{-1}\right)\right\|_q\right\|_{\infty,[g(x_0),g(b)]}\int_{x_0}^{b}\left\|A_1(x)\right\|_p\left(g(x)-g(x_0)\right)^{\alpha}dx\right]\right\}. \tag{73}$$

Proof. Here we have that (acting as in the proof of Theorem 12 for $r=2$)

$$\Phi\left(A_1,A_2\right)(x_0):=\int_a^b A_2(x)\,A_1(x)+\int_a^b A_1(x)\,A_2(x)\,dx-$$

$$\left(\int_a^b A_2(x)\,dx\right)A_1(x_0)-\left(\int_a^b A_1(x)\,dx\right)A_2(x_0)\overset{(55)}{=}$$

$$\frac{1}{\Gamma(\alpha)}\left\{\left[\int_a^{x_0}A_2(x)\left(\int_{g(x)}^{g(x_0)}(z-g(x))^{\alpha-1}\left(D^{\alpha}_{g(x_0)-}\left(A_1\circ g^{-1}\right)\right)(z)\,dz\right)dx\right]+\right.$$

$$\left[\int_{x_0}^{b}A_2(x)\left(\int_{g(x_0)}^{g(x)}(g(x)-z)^{\alpha-1}\left(D^{\alpha}_{g(x_0)}\left(A_1\circ g^{-1}\right)\right)(z)\,dz\right)dx\right]+$$

$$\left[\int_a^{x_0}A_1(x)\left(\int_{g(x)}^{g(x_0)}(z-g(x))^{\alpha-1}\left(D^{\alpha}_{g(x_0)-}\left(A_2\circ g^{-1}\right)\right)(z)\,dz\right)dx\right]+$$

$$\left.\left[\int_{x_0}^{b}A_1(x)\left(\int_{g(x_0)}^{g(x)}(g(x)-z)^{\alpha-1}\left(D^{\alpha}_{g(x_0)}\left(A_2\circ g^{-1}\right)\right)(z)\,dz\right)dx\right]\right\}. \tag{74}$$

Therefore it holds by taking the 1-Schatten norm that

$$\|\Phi(A_1, A_2)(x_0)\|_1 = \left\| \int_a^b A_2(x) A_1(x) + \int_a^b A_1(x) A_2(x) dx - \right.$$

$$\left. \left(\int_a^b A_2(x) dx \right) A_1(x_0) - \left(\int_a^b A_1(x) dx \right) A_2(x_0) \right\|_1 \leq$$

$$\frac{1}{\Gamma(\alpha)} \left\{ \left[\left\| \int_a^{x_0} A_2(x) \left(\int_{g(x)}^{g(x_0)} (z - g(x))^{\alpha-1} \left(D_{g(x_0)-}^{\alpha} (A_1 \circ g^{-1}) \right)(z) dz \right) dx \right\|_1 \right] + \right.$$

$$\left[\left\| \int_{x_0}^b A_2(x) \left(\int_{g(x_0)}^{g(x)} (g(x) - z)^{\alpha-1} \left(D_{g(x_0)}^{\alpha} (A_1 \circ g^{-1}) \right)(z) dz \right) dx \right\|_1 \right] +$$

$$\left[\left\| \int_a^{x_0} A_1(x) \left(\int_{g(x)}^{g(x_0)} (z - g(x))^{\alpha-1} \left(D_{g(x_0)-}^{\alpha} (A_2 \circ g^{-1}) \right)(z) dz \right) dx \right\|_1 \right] +$$

$$\left. \left[\left\| \int_{x_0}^b A_1(x) \left(\int_{g(x_0)}^{g(x)} (g(x) - z)^{\alpha-1} \left(D_{g(x_0)}^{\alpha} (A_2 \circ g^{-1}) \right)(z) dz \right) dx \right\|_1 \right] \right\} \leq \tag{75}$$

$$\frac{1}{\Gamma(\alpha)} \left\{ \left[\int_a^{x_0} \left\| A_2(x) \left(\int_{g(x)}^{g(x_0)} (z - g(x))^{\alpha-1} \left(D_{g(x_0)-}^{\alpha} (A_1 \circ g^{-1}) \right)(z) dz \right) \right\|_1 dx \right] + \right.$$

$$\left[\int_{x_0}^b \left\| A_2(x) \left(\int_{g(x_0)}^{g(x)} (g(x) - z)^{\alpha-1} \left(D_{g(x_0)}^{\alpha} (A_1 \circ g^{-1}) \right)(z) dz \right) \right\|_1 dx \right] +$$

$$\left[\int_a^{x_0} \left\| A_1(x) \left(\int_{g(x)}^{g(x_0)} (z - g(x))^{\alpha-1} \left(D_{g(x_0)-}^{\alpha} (A_2 \circ g^{-1}) \right)(z) dz \right) \right\|_1 dx \right] +$$

$$\left. \left[\int_{x_0}^b \left\| A_1(x) \left(\int_{g(x_0)}^{g(x)} (g(x) - z)^{\alpha-1} \left(D_{g(x_0)}^{\alpha} (A_2 \circ g^{-1}) \right)(z) dz \right) \right\|_1 dx \right] \right\} \leq \tag{76}$$

(by using the p-Schatten norm and Hölder's type inequality (44) for $p, q > 1$: $\frac{1}{p} + \frac{1}{q} = 1$)

$$\frac{1}{\Gamma(\alpha)} \left\{ \left[\int_a^{x_0} \|A_2(x)\|_q \left\| \left(\int_{g(x)}^{g(x_0)} (z - g(x))^{\alpha-1} \left(D_{g(x_0)-}^{\alpha} (A_1 \circ g^{-1}) \right)(z) dz \right) \right\|_p dx \right] + \right.$$

$$\left[\int_{x_0}^b \|A_2(x)\|_q \left\| \left(\int_{g(x_0)}^{g(x)} (g(x) - z)^{\alpha-1} \left(D_{g(x_0)}^{\alpha} (A_1 \circ g^{-1}) \right)(z) dz \right) \right\|_p dx \right] +$$

$$\left[\int_a^{x_0}\|A_1(x)\|_p\left\|\left(\int_{g(x)}^{g(x_0)}(z-g(x))^{\alpha-1}\left(D^{\alpha}_{g(x_0)-}\left(A_2\circ g^{-1}\right)\right)(z)\,dz\right)\right\|_q dx\right]+$$

$$\left.\left[\int_{x_0}^{b}\|A_1(x)\|_p\left\|\left(\int_{g(x_0)}^{g(x)}(g(x)-z)^{\alpha-1}\left(D^{\alpha}_{g(x_0)}\left(A_2\circ g^{-1}\right)\right)(z)\,dz\right)\right\|_q dx\right]\right\}\leq \tag{77}$$

$$\frac{1}{\Gamma(\alpha)}\left\{\left[\int_a^{x_0}\|A_2(x)\|_q\left(\int_{g(x)}^{g(x_0)}(z-g(x))^{\alpha-1}\left\|\left(D^{\alpha}_{g(x_0)-}\left(A_1\circ g^{-1}\right)\right)(z)\right\|_p dz\right)dx\right]+\right.$$

$$\left[\int_{x_0}^{b}\|A_2(x)\|_q\left(\int_{g(x_0)}^{g(x)}(g(x)-z)^{\alpha-1}\left\|\left(D^{\alpha}_{g(x_0)}\left(A_1\circ g^{-1}\right)\right)(z)\right\|_p dz\right)dx\right]+$$

$$\left[\int_a^{x_0}\|A_1(x)\|_p\left(\int_{g(x)}^{g(x_0)}(z-g(x))^{\alpha-1}\left\|\left(D^{\alpha}_{g(x_0)-}\left(A_2\circ g^{-1}\right)\right)(z)\right\|_q dz\right)dx\right]+$$

$$\left.\left[\int_{x_0}^{b}\|A_1(x)\|_p\left(\int_{g(x_0)}^{g(x)}(g(x)-z)^{\alpha-1}\left\|\left(D^{\alpha}_{g(x_0)}\left(A_2\circ g^{-1}\right)\right)(z)\right\|_q dz\right)dx\right]\right\}. \tag{78}$$

We have proved, so far, that

$$\|\Phi(A_1,A_2)(x_0)\|_1\leq$$

$$\frac{1}{\Gamma(\alpha)}\left\{\left[\int_a^{x_0}\|A_2(x)\|_q\left(\int_{g(x)}^{g(x_0)}(z-g(x))^{\alpha-1}\left\|\left(D^{\alpha}_{g(x_0)-}\left(A_1\circ g^{-1}\right)\right)(z)\right\|_p dz\right)dx\right]+\right.$$

$$\left[\int_{x_0}^{b}\|A_2(x)\|_q\left(\int_{g(x_0)}^{g(x)}(g(x)-z)^{\alpha-1}\left\|\left(D^{\alpha}_{g(x_0)}\left(A_1\circ g^{-1}\right)\right)(z)\right\|_p dz\right)dx\right]+$$

$$\left[\int_a^{x_0}\|A_1(x)\|_p\left(\int_{g(x)}^{g(x_0)}(z-g(x))^{\alpha-1}\left\|\left(D^{\alpha}_{g(x_0)-}\left(A_2\circ g^{-1}\right)\right)(z)\right\|_q dz\right)dx\right]+$$

$$\left.\left[\int_{x_0}^{b}\|A_1(x)\|_p\left(\int_{g(x_0)}^{g(x)}(g(x)-z)^{\alpha-1}\left\|\left(D^{\alpha}_{g(x_0)}\left(A_2\circ g^{-1}\right)\right)(z)\right\|_q dz\right)dx\right]\right\}=:(\lambda). \tag{79}$$

Let now $\gamma,\delta>1$ such that $\frac{1}{\gamma}+\frac{1}{\delta}=1$, and we apply the usual Hölder's inequality in (79). Then we have that

$$\|\Phi(A_1,A_2)(x_0)\|_1\leq(\lambda)\leq\frac{1}{\Gamma(\alpha)(\gamma(\alpha-1)+1)^{\frac{1}{\gamma}}}$$

$$\left\{\left[\int_a^{x_0}\|A_2(x)\|_q(g(x_0)-g(x))^{\frac{\gamma(\alpha-1)+1}{\gamma}}\left(\int_{g(x)}^{g(x_0)}\left\|\left(D^{\alpha}_{g(x_0)-}\left(A_1\circ g^{-1}\right)\right)(z)\right\|_p^{\delta}dz\right)^{\frac{1}{\delta}}dx\right]+\right.$$

$$\left[\int_{x_0}^{b}\left\|A_2(x)\right\|_q\left(g(x)-g(x_0)\right)^{\frac{\gamma(\alpha-1)+1}{\gamma}}\left(\int_{g(x_0)}^{g(x)}\left\|\left(D_{g(x_0)}^{\alpha}\left(A_1\circ g^{-1}\right)\right)(z)\right\|_p^{\delta}dz\right)^{\frac{1}{\delta}}dx\right]+$$

$$\left[\int_{a}^{x_0}\left\|A_1(x)\right\|_p\left(g(x_0)-g(x)\right)^{\frac{\gamma(\alpha-1)+1}{\gamma}}\left(\int_{g(x)}^{g(x_0)}\left\|\left(D_{g(x_0)-}^{\alpha}\left(A_2\circ g^{-1}\right)\right)(z)\right\|_q^{\delta}dz\right)^{\frac{1}{\delta}}dx\right]+ \tag{80}$$

$$\left.\left[\int_{x_0}^{b}\left\|A_1(x)\right\|_p\left(g(x)-g(x_0)\right)^{\frac{\gamma(\alpha-1)+1}{\gamma}}\left(\int_{g(x_0)}^{g(x)}\left\|\left(D_{g(x_0)}^{\alpha}\left(A_2\circ g^{-1}\right)\right)(z)\right\|_q^{\delta}dz\right)^{\frac{1}{\delta}}dx\right]\right\}$$

$$\leq\frac{1}{\Gamma(\alpha)\left(\gamma(\alpha-1)+1\right)^{\frac{1}{\gamma}}}$$

$$\left\{\left[\left\|\left\|D_{g(x_0)-}^{\alpha}\left(A_1\circ g^{-1}\right)\right\|_p\right\|_{\delta,[g(a),g(x_0)]}\int_a^{x_0}\left\|A_2(x)\right\|_q\left(g(x_0)-g(x)\right)^{\alpha-\frac{1}{\delta}}dx\right]+\right.$$

$$\left[\left\|\left\|D_{g(x_0)}^{\alpha}\left(A_1\circ g^{-1}\right)\right\|_p\right\|_{\delta,[g(x_0),g(b)]}\int_{x_0}^{b}\left\|A_2(x)\right\|_q\left(g(x)-g(x_0)\right)^{\alpha-\frac{1}{\delta}}dx\right]+ \tag{81}$$

$$\left[\left\|\left\|D_{g(x_0)-}^{\alpha}\left(A_2\circ g^{-1}\right)\right\|_q\right\|_{\delta,[g(a),g(x_0)]}\int_a^{x_0}\left\|A_1(x)\right\|_p\left(g(x_0)-g(x)\right)^{\alpha-\frac{1}{\delta}}dx\right]+$$

$$\left.\left[\left\|\left\|D_{g(x_0)}^{\alpha}\left(A_2\circ g^{-1}\right)\right\|_q\right\|_{\delta,[g(x_0),g(b)]}\int_{x_0}^{b}\left\|A_1(x)\right\|_p\left(g(x)-g(x_0)\right)^{\alpha-\frac{1}{\delta}}dx\right]\right\},$$

proving (71).

We also obtain

$$\left\|\Phi(A_1,A_2)(x_0)\right\|_1\leq(\lambda)\leq\frac{1}{\Gamma(\alpha)}$$

$$\left\{\left[\left\|\left\|D_{g(x_0)-}^{\alpha}\left(A_1\circ g^{-1}\right)\right\|_p\right\|_{L_1([g(a),g(x_0)])}\int_a^{x_0}\left\|A_2(x)\right\|_q\left(g(x_0)-g(x)\right)^{\alpha-1}dx\right]+\right.$$

$$\left[\left\|\left\|D_{g(x_0)}^{\alpha}\left(A_1\circ g^{-1}\right)\right\|_p\right\|_{L_1([g(x_0),g(b)])}\int_{x_0}^{b}\left\|A_2(x)\right\|_q\left(g(x)-g(x_0)\right)^{\alpha-1}dx\right]+$$

$$\left[\left\|\left\|D_{g(x_0)-}^{\alpha}\left(A_2\circ g^{-1}\right)\right\|_q\right\|_{L_1([g(a),g(x_0)])}\int_a^{x_0}\left\|A_1(x)\right\|_p\left(g(x_0)-g(x)\right)^{\alpha-1}dx\right]+ \tag{82}$$

$$\left.\left[\left\|\left\|D_{g(x_0)}^{\alpha}\left(A_2\circ g^{-1}\right)\right\|_q\right\|_{L_1([g(x_0),g(b)])}\int_{x_0}^{b}\left\|A_1(x)\right\|_p\left(g(x)-g(x_0)\right)^{\alpha-1}dx\right]\right\},$$

proving (72).

At last we derive

$$\left\|\Phi\left(A_1,A_2\right)\left(x_0\right)\right\|_1 \leq (\lambda) \leq \frac{1}{\Gamma\left(\alpha+1\right)}$$

$$\left\{\left[\left\|\left\|D^{\alpha}_{g(x_0)-}\left(A_1\circ g^{-1}\right)\right\|_p\right\|_{\infty,[g(a),g(x_0)]}\int_a^{x_0}\left\|A_2\left(x\right)\right\|_q\left(g\left(x_0\right)-g\left(x\right)\right)^{\alpha}dx\right]+\right.$$
$$\left[\left\|\left\|D^{\alpha}_{g(x_0)}\left(A_1\circ g^{-1}\right)\right\|_p\right\|_{\infty,[g(x_0),g(b)]}\int_{x_0}^{b}\left\|A_2\left(x\right)\right\|_q\left(g\left(x\right)-g\left(x_0\right)\right)^{\alpha}dx\right]+$$
$$\left[\left\|\left\|D^{\alpha}_{g(x_0)-}\left(A_2\circ g^{-1}\right)\right\|_q\right\|_{\infty,[g(a),g(x_0)]}\int_a^{x_0}\left\|A_1\left(x\right)\right\|_p\left(g\left(x_0\right)-g\left(x\right)\right)^{\alpha}dx\right]+$$
$$\left.\left[\left\|\left\|D^{\alpha}_{g(x_0)}\left(A_2\circ g^{-1}\right)\right\|_q\right\|_{\infty,[g(x_0),g(b)]}\int_{x_0}^{b}\left\|A_1\left(x\right)\right\|_p\left(g\left(x\right)-g\left(x_0\right)\right)^{\alpha}dx\right]\right\}, \tag{83}$$

proving (73).

The theorem is proved. ■

Next we present p-Schatten left and right generalized Canavati fractional Opial type inequalities:

Theorem 19 *Let the $*$-ideal $\mathcal{B}_2\left(H\right)$, which $\left(\mathcal{B}_2\left(H\right),\left\|\cdot\right\|_2\right)$ is a Banach algebra; $x_0\in\left[a,b\right]\subset\mathbb{R}$, $\nu\geq1$, $n=\left[\nu\right]$; $f\in C^n\left(\left[a,b\right],\mathcal{B}_2\left(H\right)\right)$, $g\in C^1\left(\left[a,b\right]\right)$, strictly increasing such that $g^{-1}\in C^n\left(\left[g\left(a\right),g\left(b\right)\right]\right)$, with $\left(f\circ g^{-1}\right)^{(k)}\left(g\left(x_0\right)\right)=0$, $k=0,1,...,n-1$. Assume further that $f\circ g^{-1}\in C^{\nu}_{g(x_0)}\left(\left[g\left(a\right),g\left(b\right)\right],\mathcal{B}_2\left(H\right)\right)$.*

Let also $p,q>1:\frac{1}{p}+\frac{1}{q}=1$. Then

$$\int_{g(x_0)}^{z}\left\|\left(\left(f\circ g^{-1}\right)\left(w\right)\right)\left(\left(D^{\nu}_{g(x_0)}\left(f\circ g^{-1}\right)\right)\left(w\right)\right)\right\|_1dw\leq \tag{84}$$

$$\frac{2^{-\frac{1}{q}}\left(z-g\left(x_0\right)\right)^{\nu+\frac{1}{p}-\frac{1}{q}}}{\Gamma\left(\nu\right)\left[\left(p\left(\nu-1\right)+1\right)\left(p\left(\nu-1\right)+2\right)\right]^{\frac{1}{p}}}\left(\int_{g(x_0)}^{z}\left\|\left(D^{\nu}_{g(x_0)}\left(f\circ g^{-1}\right)\right)\left(w\right)\right\|_2^q dw\right)^{\frac{2}{q}},$$

for all $g\left(x_0\right)\leq z\leq g\left(b\right)$.

Proof. Very similar to the proof of Theorem 13 of [6]. Use of (44) for $p=q=2$. ■

A similar result comex next:

Theorem 20 *Let $\gamma\geq1$, the $*$-ideal $\mathcal{B}_{\gamma}\left(H\right)$, which $\left(\mathcal{B}_{\gamma}\left(H\right),\left\|\cdot\right\|_{\gamma}\right)$ is a Banach algebra; $x_0\in\left[a,b\right]\subset\mathbb{R}$, $\nu\geq1$, $n=\left[\nu\right]$; $f\in C^n\left(\left[a,b\right],\mathcal{B}_{\gamma}\left(H\right)\right)$, $g\in C^1\left(\left[a,b\right]\right)$, strictly increasing such that $g^{-1}\in C^n\left(\left[g\left(a\right),g\left(b\right)\right]\right)$, with $\left(f\circ g^{-1}\right)^{(k)}\left(g\left(x_0\right)\right)=0$, $k=0,1,...,n-1$. Assume further that $f\circ g^{-1}\in C^{\nu}_{g(x_0)}\left(\left[g\left(a\right),g\left(b\right)\right],\mathcal{B}_{\gamma}\left(H\right)\right)$.*

Let also $p, q > 1 : \frac{1}{p} + \frac{1}{q} = 1$. *Then*

$$\int_{g(x_0)}^{z} \left\| \left(\left(f \circ g^{-1} \right)(w) \right) \left(\left(D_{g(x_0)}^{\nu} \left(f \circ g^{-1} \right) \right)(w) \right) \right\|_{\gamma} dw \leq \tag{85}$$

$$\frac{2^{-\frac{1}{q}} \left(z - g(x_0) \right)^{\nu + \frac{1}{p} - \frac{1}{q}}}{\Gamma(\nu) \left[\left(p(\nu - 1) + 1 \right) \left(p(\nu - 1) + 2 \right) \right]^{\frac{1}{p}}} \left(\int_{g(x_0)}^{z} \left\| \left(D_{g(x_0)}^{\nu} \left(f \circ g^{-1} \right) \right)(w) \right\|_{\gamma}^{q} dw \right)^{\frac{2}{q}},$$

for all $g(x_0) \leq z \leq g(b)$.

Proof. Very similar to the proof of Theorem 13 of [6]. Use of (41) for $p = \gamma$.

■

It follows the corresponding right side fractional Opial type inequalities:

Theorem 21 *All as in Theorem 19, however now it is* $f \circ g^{-1} \in C_{g(x_0)-}^{\nu}\left([g(a), g(b)], \mathcal{B}_2(H) \right)$. *Then*

$$\int_{z}^{g(x_0)} \left\| \left(\left(f \circ g^{-1} \right)(w) \right) \left(\left(D_{g(x_0)-}^{\nu} \left(f \circ g^{-1} \right) \right)(w) \right) \right\|_{1} dw \leq$$

$$\frac{2^{-\frac{1}{q}} \left(g(x_0) - z \right)^{\nu + \frac{1}{p} - \frac{1}{q}}}{\Gamma(\nu) \left[\left(p(\nu - 1) + 1 \right) \left(p(\nu - 1) + 2 \right) \right]^{\frac{1}{p}}} \left(\int_{z}^{g(x_0)} \left\| \left(D_{g(x_0)-}^{\nu} \left(f \circ g^{-1} \right) \right)(t) \right\|_{2}^{q} dt \right)^{\frac{2}{q}}, \tag{86}$$

for all $g(a) \leq z \leq g(x_0)$.

Proof. Based on (20), and as similar to the proof of Theorem 19 is omitted.

■

Next comes another right ride fractional Opial type inequality:

Theorem 22 *All as in Theorem 20, however now it is* $f \circ g^{-1} \in C_{g(x_0)-}^{\nu}\left([g(a), g(b)], \mathcal{B}_{\gamma}(H) \right)$. *Then*

$$\int_{z}^{g(x_0)} \left\| \left(\left(f \circ g^{-1} \right)(w) \right) \left(\left(D_{g(x_0)-}^{\nu} \left(f \circ g^{-1} \right) \right)(w) \right) \right\|_{\gamma} dw \leq$$

$$\frac{2^{-\frac{1}{q}} \left(g(x_0) - z \right)^{\nu + \frac{1}{p} - \frac{1}{q}}}{\Gamma(\nu) \left[\left(p(\nu - 1) + 1 \right) \left(p(\nu - 1) + 2 \right) \right]^{\frac{1}{p}}} \left(\int_{z}^{g(x_0)} \left\| \left(D_{g(x_0)-}^{\nu} \left(f \circ g^{-1} \right) \right)(t) \right\|_{\gamma}^{q} dt \right)^{\frac{2}{q}}, \tag{87}$$

for all $g(a) \leq z \leq g(x_0)$.

Proof. Based on (20), and as similar to the proof of Theorem 19 is omitted.

■

It follows the modified generalized left $\mathcal{B}_2(H)$-valued fractional Opial inequality:

Theorem 23 *All as in Theorem 6, where* $X=\mathcal{B}_2(H)$ *and let* $p,q>1:\frac{1}{p}+\frac{1}{q}=1$. *Here we assume that* $\frac{1}{(m+1)q}<\nu<1$. *Then*

$$\int_{g(x_0)}^{z}\left\|\left(\left(f\circ g^{-1}\right)(w)\right)\left(\left(D_{g(x_0)}^{(m+1)\nu}\left(f\circ g^{-1}\right)\right)(w)\right)\right\|_1 dw\leq \tag{88}$$

$$\frac{2^{-\frac{1}{q}}\left(z-g(x_0)\right)^{(m+1)\nu+\frac{1}{p}-\frac{1}{q}}}{\Gamma((m+1)\nu)\left[\left(p\left((m+1)\nu-1\right)+1\right)\left(p\left((m+1)\nu-1\right)+2\right)\right]^{\frac{1}{p}}}$$

$$\left(\int_{g(x_0)}^{z}\left\|\left(D_{g(x_0)}^{(m+1)\nu}\left(f\circ g^{-1}\right)\right)(t)\right\|_2^q dt\right)^{\frac{2}{q}},$$

for all $g(x_0)\leq z\leq g(b)$.

Proof. As in Theorem 19. ■

Next comes another modified generalized left $\mathcal{B}_\gamma(H)$-valued fractional Opial inequality:

Theorem 24 *All as in Theorem 6, where* $X=\mathcal{B}_\gamma(H)$ *and let* $p,q>1:\frac{1}{p}+\frac{1}{q}=1$. *Here we assume that* $\frac{1}{(m+1)q}<\nu<1$. *Then*

$$\int_{g(x_0)}^{z}\left\|\left(\left(f\circ g^{-1}\right)(w)\right)\left(\left(D_{g(x_0)}^{(m+1)\nu}\left(f\circ g^{-1}\right)\right)(w)\right)\right\|_\gamma dw\leq \tag{89}$$

$$\frac{2^{-\frac{1}{q}}\left(z-g(x_0)\right)^{(m+1)\nu+\frac{1}{p}-\frac{1}{q}}}{\Gamma((m+1)\nu)\left[\left(p\left((m+1)\nu-1\right)+1\right)\left(p\left((m+1)\nu-1\right)+2\right)\right]^{\frac{1}{p}}}$$

$$\left(\int_{g(x_0)}^{z}\left\|\left(D_{g(x_0)}^{(m+1)\nu}\left(f\circ g^{-1}\right)\right)(t)\right\|_\gamma^q dt\right)^{\frac{2}{q}},$$

for all $g(x_0)\leq z\leq g(b)$.

Proof. As in Theorem 19. ■

The corresponding modified generalized right $\mathcal{B}_2(H)$-valued fractional Opial inequality comes next:

Theorem 25 *All as in Theorem 7, where* $X=\mathcal{B}_2(H)$ *and let* $p,q>1:\frac{1}{p}+\frac{1}{q}=1$. *Here we assume that* $\frac{1}{(m+1)q}<\nu<1$. *Then*

$$\int_{z}^{g(x_0)}\left\|\left(\left(f\circ g^{-1}\right)(w)\right)\left(\left(D_{g(x_0)-}^{(m+1)\nu}\left(f\circ g^{-1}\right)\right)(w)\right)\right\|_1 dw\leq \tag{90}$$

$$\frac{2^{-\frac{1}{q}}\left(g(x_0)-z\right)^{(m+1)\nu+\frac{1}{p}-\frac{1}{q}}}{\Gamma((m+1)\nu)\left[\left(p\left((m+1)\nu-1\right)+1\right)\left(p\left((m+1)\nu-1\right)+2\right)\right]^{\frac{1}{p}}}$$

$$\left(\int_{z}^{g(x_0)}\left\|\left(D_{g(x_0)-}^{(m+1)\nu}\left(f\circ g^{-1}\right)\right)(t)\right\|_2^q dt\right)^{\frac{2}{q}},$$

for all $g(a)\leq z\leq g(x_0)$.

Proof. As in Theorem 19. ■

The corresponding modified generalized right $\mathcal{B}_\gamma(H)$-valued fractional Opial inequality comes next:

Theorem 26 *All as in Theorem 7, where* $X=\mathcal{B}_\gamma(H)$ *and let* $p,q>1:\frac{1}{p}+\frac{1}{q}=1$. *Here we assume that* $\frac{1}{(m+1)q}<\nu<1$. *Then*

$$\int_{z}^{g(x_0)}\left\|\left(\left(f\circ g^{-1}\right)(w)\right)\left(\left(D_{g(x_0)-}^{(m+1)\nu}\left(f\circ g^{-1}\right)\right)(w)\right)\right\|_\gamma dw\leq \tag{91}$$

$$\frac{2^{-\frac{1}{q}}\left(g(x_0)-z\right)^{(m+1)\nu+\frac{1}{p}-\frac{1}{q}}}{\Gamma((m+1)\nu)\left[\left(p((m+1)\nu-1)+1\right)\left(p((m+1)\nu-1)+2\right)\right]^{\frac{1}{p}}}$$

$$\left(\int_{z}^{g(x_0)}\left\|\left(D_{g(x_0)-}^{(m+1)\nu}\left(f\circ g^{-1}\right)\right)(t)\right\|_\gamma^q dt\right)^{\frac{2}{q}},$$

for all $g(a)\leq z\leq g(x_0)$.

Proof. As in Theorem 19. ■

We make

Remark 27 *(to Theorem 12)*

Case of inequality (46):

Call and assume

$$M_1(f_1,...,f_r):= \tag{92}$$

$$\max_{i=1,...,r}\left\{\sup_{x_0\in[a,b]}\left\|\left\|D_{g(x_0)-}^{\nu}\left(f_i\circ g^{-1}\right)\right\|_2\right\|_{\infty,[g(a),g(x_0)]},\right.$$

$$\left.\sup_{x_0\in[a,b]}\left\|\left\|D_{g(x_0)}^{\gamma}\left(f_i\circ g^{-1}\right)\right\|_2\right\|_{\infty,[g(x_0),g(b)]}\right\}<+\infty.$$

Then

$$\|K(f_1,...,f_r)(x_0)\|_1\leq \textit{Right hand side (46)}\ \leq$$

$$\frac{M_1(f_1,...,f_r)\left(g(b)-g(a)\right)^\nu}{\Gamma(\nu+1)}\sum_{i=1}^{r}\left(\int_a^b\left(\prod_{\substack{j=1\\ j\neq i}}^{r}\|f_j(x)\|_2\right)dx\right). \tag{93}$$

We make

Remark 28 *(to Theorem 13)*

Case of inequality (62):

Call and assume

$$M_2\left(f_1,...,f_r\right) := \tag{94}$$

$$\max_{i=1,...,r}\left\{\sup_{x_0\in[a,b]}\left\|\left\|D^{\nu}_{g(x_0)-}\left(f_i\circ g^{-1}\right)\right\|_2\right\|_{L_1([g(a),g(x_0)])},\right.$$

$$\left.\sup_{x_0\in[a,b]}\left\|\left\|D^{\nu}_{g(x_0)}\left(f_i\circ g^{-1}\right)\right\|_2\right\|_{L_1([g(x_0),g(b)])}\right\} < +\infty.$$

Then

$$\left\|K\left(f_1,...,f_r\right)\left(x_0\right)\right\|_1 \leq \textit{Right hand side (62)} \leq$$

$$\frac{M_2\left(f_1,...,f_r\right)\left(g\left(b\right)-g\left(a\right)\right)^{\nu-1}}{\Gamma\left(\nu\right)}\sum_{i=1}^{r}\left(\int_a^b\left(\prod_{\substack{j=1\\j\neq i}}^{r}\left\|f_j\left(x\right)\right\|_2\right)dx\right). \tag{95}$$

We make

Remark 29 *(to Theorem 14)*

Case of inequality (64):

Call and assume $(p,q>1:\frac{1}{p}+\frac{1}{q}=1)$*:*

$$M_3\left(f_1,...,f_r\right) := \tag{96}$$

$$\max_{i=1,...,r}\left\{\sup_{x_0\in[a,b]}\left\|\left\|D^{\nu}_{g(x_0)-}\left(f_i\circ g^{-1}\right)\right\|_2\right\|_{q,([g(a),g(x_0)])},\right.$$

$$\left.\sup_{x_0\in[a,b]}\left\|\left\|D^{\nu}_{g(x_0)}\left(f_i\circ g^{-1}\right)\right\|_2\right\|_{q,([g(x_0),g(b)])}\right\} < +\infty.$$

Then

$$\left\|K\left(f_1,...,f_r\right)\left(x_0\right)\right\|_1 \leq \textit{Right hand side (64)} \leq$$

$$\frac{M_3\left(f_1,...,f_r\right)\left(g\left(b\right)-g\left(a\right)\right)^{\nu-\frac{1}{q}}}{\left(p\left(\nu-1\right)+1\right)^{\frac{1}{p}}\Gamma\left(\nu\right)}\sum_{i=1}^{r}\left(\int_a^b\left(\prod_{\substack{j=1\\j\neq i}}^{r}\left\|f_j\left(x\right)\right\|_2\right)dx\right). \tag{97}$$

We make

Remark 30 *(to Theorem 15)* $(\gamma\geq 1)$

Case of inequality (67):

Call and assume

$$M_1^{\gamma}\left(f_1,...,f_r\right) := \tag{98}$$

$$\max_{i=1,\ldots,r}\left\{\sup_{x_0\in[a,b]}\left\|\left\|D^{\nu}_{g(x_0)-}\left(f_i\circ g^{-1}\right)\right\|_{\gamma}\right\|_{\infty,[g(a),g(x_0)]},\right.$$

$$\left.\sup_{x_0\in[a,b]}\left\|\left\|D^{\gamma}_{g(x_0)}\left(f_i\circ g^{-1}\right)\right\|_{\gamma}\right\|_{\infty,[g(x_0),g(b)]}\right\}<+\infty.$$

Then

$$\left\|K\left(f_1,...,f_r\right)(x_0)\right\|_{\gamma}\leq \textit{Right hand side (67)} \leq$$

$$\frac{M_1^{\gamma}\left(f_1,...,f_r\right)\left(g\left(b\right)-g\left(a\right)\right)^{\nu}}{\Gamma\left(\nu+1\right)}\sum_{i=1}^{r}\left(\int_a^b\left(\prod_{\substack{j=1\\j\neq i}}^{r}\left\|f_j\left(x\right)\right\|_{\gamma}\right)dx\right). \tag{99}$$

We make

Remark 31 *(to Theorem 16) ($\gamma \geq 1$)*

Case of inequality (68):

Call and assume:

$$M_2^{\gamma}\left(f_1,...,f_r\right):= \tag{100}$$

$$\max_{i=1,\ldots,r}\left\{\sup_{x_0\in[a,b]}\left\|\left\|D^{\nu}_{g(x_0)-}\left(f_i\circ g^{-1}\right)\right\|_{\gamma}\right\|_{L_1([g(a),g(x_0)])},\right.$$

$$\left.\sup_{x_0\in[a,b]}\left\|\left\|D^{\nu}_{g(x_0)}\left(f_i\circ g^{-1}\right)\right\|_{\gamma}\right\|_{L_1([g(x_0),g(b)])}\right\}<+\infty.$$

Then

$$\left\|K\left(f_1,...,f_r\right)(x_0)\right\|_{\gamma}\leq \textit{Right hand side (68)} \leq$$

$$\frac{M_2^{\gamma}\left(f_1,...,f_r\right)\left(g\left(b\right)-g\left(a\right)\right)^{\nu-1}}{\Gamma\left(\nu\right)}\sum_{i=1}^{r}\left(\int_a^b\left(\prod_{\substack{j=1\\j\neq i}}^{r}\left\|f_j\left(x\right)\right\|_{\gamma}\right)dx\right). \tag{101}$$

We make

Remark 32 *(to Theorem 17) ($\gamma \geq 1$)*

Case of inequality (69):

Call and assume ($p,q>1:\frac{1}{p}+\frac{1}{q}=1$):

$$M_3^{\gamma}\left(f_1,...,f_r\right):= \tag{102}$$

$$\max_{i=1,\ldots,r}\left\{\sup_{x_0\in[a,b]}\left\|\left\|D^{\nu}_{g(x_0)-}\left(f_i\circ g^{-1}\right)\right\|_{\gamma}\right\|_{q,([g(a),g(x_0)])},\right.$$

$$\left.\sup_{x_0\in[a,b]}\left\|\left\|D^{\nu}_{g(x_0)}\left(f_i\circ g^{-1}\right)\right\|_{\gamma}\right\|_{q,([g(x_0),g(b)])}\right\}<+\infty.$$

Then

$$\left\|K\left(f_1,...,f_r\right)\left(x_0\right)\right\|_{\gamma}\leq \textit{Right hand side (69)} \ \leq$$

$$\frac{M_3^{\gamma}\left(f_1,...,f_r\right)\left(g\left(b\right)-g\left(a\right)\right)^{\nu-\frac{1}{q}}}{\left(p\left(\nu-1\right)+1\right)^{\frac{1}{p}}\Gamma\left(\nu\right)}\sum_{i=1}^{r}\left(\int_a^b\left(\prod_{\substack{j=1\\ j\neq i}}^{r}\left\|f_j\left(x\right)\right\|_{\gamma}\right)dx\right). \tag{103}$$

Remark 33 *(to Theorem 18)*

i) for $\gamma,\delta>1:\frac{1}{\gamma}+\frac{1}{\delta}=1$, *case of inequality (71):*

Call and assume

$$N_1\left(A_1,A_2\right):=$$

$$\max\left\{\sup_{x_0\in[a,b]}\left\|\left\|D^{\nu}_{g(x_0)-}\left(A_1\circ g^{-1}\right)\right\|_p\right\|_{\delta,[g(a),g(x_0)]},\ \sup_{x_0\in[a,b]}\left\|\left\|D^{\nu}_{g(x_0)}\left(A_1\circ g^{-1}\right)\right\|_p\right\|_{\delta,[g(x_0),g(b)]},\right.$$

$$\left.\sup_{x_0\in[a,b]}\left\|\left\|D^{\nu}_{g(x_0)-}\left(A_2\circ g^{-1}\right)\right\|_q\right\|_{\delta,[g(a),g(x_0)]},\ \sup_{x_0\in[a,b]}\left\|\left\|D^{\nu}_{g(x_0)}\left(A_2\circ g^{-1}\right)\right\|_q\right\|_{\delta,[g(x_0),g(b)]}\right\}<+\infty. \tag{104}$$

Then

$$\left\|\Phi\left(A_1,A_2\right)\left(x_0\right)\right\|_1\leq \textit{right hand side (71)} \ \leq$$

$$\frac{N_1\left(A_1,A_2\right)\left(g\left(b\right)-g\left(a\right)\right)^{\alpha-\frac{1}{\delta}}}{\Gamma\left(\alpha\right)\left(\gamma\left(\alpha-1\right)+1\right)^{\frac{1}{\gamma}}}\left[\int_a^b\left\|A_1\left(x\right)\right\|_p dx+\int_a^b\left\|A_2\left(x\right)\right\|_q dx\right]. \tag{105}$$

ii) case of inequality (72):

Call and assume

$$N_2\left(A_1,A_2\right):= \tag{106}$$

$$\max\left\{\sup_{x_0\in[a,b]}\left\|\left\|D^{\nu}_{g(x_0)-}\left(A_1\circ g^{-1}\right)\right\|_p\right\|_{L_1([g(a),g(x_0)])},\ \sup_{x_0\in[a,b]}\left\|\left\|D^{\nu}_{g(x_0)}\left(A_1\circ g^{-1}\right)\right\|_p\right\|_{L_1([g(x_0),g(b)])},\right.$$

$$\left.\sup_{x_0\in[a,b]}\left\|\left\|D^{\nu}_{g(x_0)-}\left(A_2\circ g^{-1}\right)\right\|_q\right\|_{L_1([g(a),g(x_0)])},\ \sup_{x_0\in[a,b]}\left\|\left\|D^{\nu}_{g(x_0)}\left(A_2\circ g^{-1}\right)^{-1}\right\|_q\right\|_{L_1([g(x_0),g(b)])}\right\}<+\infty.$$

Then

$$\left\|\Phi\left(A_1,A_2\right)\left(x_0\right)\right\|_1\leq \textit{right hand side (72)} \ \leq$$

$$\frac{N_2\left(A_1,A_2\right)\left(g\left(b\right)-g\left(a\right)\right)^{\alpha-1}}{\Gamma\left(\alpha\right)}\left[\int_a^b\left\|A_1\left(x\right)\right\|_p dx+\int_a^b\left\|A_2\left(x\right)\right\|_q dx\right]. \tag{107}$$

iii) case of inequality (73):

Call and assume

$$N_3\left(A_1,A_2\right):= \tag{108}$$

$$\max\left\{\sup_{x_0\in[a,b]}\left\|\left\|D^{\nu}_{g(x_0)-}\left(A_1\circ g^{-1}\right)\right\|_p\right\|_{\infty,[g(a),g(x_0)]},\ \sup_{x_0\in[a,b]}\left\|\left\|D^{\nu}_{g(x_0)}\left(A_1\circ g^{-1}\right)\right\|_p\right\|_{\infty,[g(x_0),g(b)]},\right.$$

$$\sup_{x_0\in[a,b]}\left\|\left\|D^{\nu}_{g(x_0)-}\left(A_2\circ g^{-1}\right)\right\|_q\right\|_{\infty,[g(a),g(x_0)]},\sup_{x_0\in[a,b]}\left\|\left\|D^{\nu}_{g(x_0)}\left(A_2\circ g^{-1}\right)^{-1}\right\|_q\right\|_{\infty,[g(x_0),g(b)]}\Bigg\}<+\infty.$$

Then

$$\left\|\Phi\left(A_1,A_2\right)(x_0)\right\|_1 \leq \textit{right hand side (73)} \leq$$

$$\frac{N_3\left(A_1,A_2\right)\left(g(b)-g(a)\right)^{\alpha}}{\Gamma(\alpha+1)}\left[\int_a^b\left\|A_1(x)\right\|_p dx+\int_a^b\left\|A_2(x)\right\|_q dx\right]. \tag{109}$$

We need

Remark 34 *(i) This is regarding Theorems 12-17. Here* $K\left(f_1,...,f_r\right)(x_0)$, $x_0\in[a,b]$, *is as in (45). Next we denote and have (case of* $1\leq\nu<2$*):*

$$\Delta\left(f_1,...,f_r\right):=\int_a^b K\left(f_1,...,f_r\right)(x_0)\,dx_0=$$

$$\sum_{i=1}^{r}\left[(b-a)\int_a^b\left(\prod_{\substack{j=1\\ j\neq i}}^{r}f_j(x)\right)f_i(x)\,dx-\left(\int_a^b\left(\prod_{\substack{j=1\\ j\neq i}}^{r}f_j(x)\right)dx\right)\left(\int_a^b f_i(x)\,dx\right)\right], \tag{110}$$

(ii) This is regarding Theorem 18. Here $\Phi\left(A_1,A_2\right)(x_0)$, $x_0\in[a,b]$, *is as in (70). Next we denote and have (case of* $1\leq\alpha<2$*):*

$$\Delta\left(A_1,A_2\right):=\int_a^b\Phi\left(A_1,A_2\right)(x_0)\,dx_0=$$

$$(b-a)\left(\int_a^b A_2(x)A_1(x)\,dx+\int_a^b A_1(x)A_2(x)\,dx\right)- \tag{111}$$

$$\left(\int_a^b A_2(x)\,dx\right)\left(\int_a^b A_1(x)\,dx\right)-\left(\int_a^b A_1(x)\,dx\right)\left(\int_a^b A_2(x)\,dx\right).$$

(iii) for $\gamma\geq1$, *it holds*

$$\left\|\Delta\left(f_1,...,f_r\right)\right\|_{\gamma}\leq\int_a^b\left\|K\left(f_1,...,f_r\right)(x)\right\|_{\gamma}dx, \tag{112}$$

and

$$\left\|\Delta\left(A_1,A_2\right)\right\|_1\leq\int_a^b\left\|\Phi\left(A_1,A_2\right)(x)\right\|_1 dx. \tag{113}$$

We give the following set of γ-Schatten norm generalized Canavati type fractional Grüss type inequalities involving several functions over $\mathcal{B}_{\gamma}(H)$, $\gamma\geq1$.

Theorem 35 *All as in Theorem 12, with $1 \leq \nu < 2$ (i.e. $n = 1$). Then*

i)

$$\|\Delta(f_1, ..., f_r)\|_1 \leq \frac{M_1(f_1, ..., f_r)(g(b) - g(a))^{\nu}(b-a)^2}{\Gamma(\nu+1)}$$

$$\sum_{i=1}^{r}\left(\left\|\prod_{\substack{j=1 \\ j\neq i}}^{r}\|f_j(x)\|_2\right\|_{\infty,[a,b]}\right), \tag{114}$$

where $M_1(f_1, ..., f_r)$ is as in (92),

ii)

$$\|\Delta(f_1, ..., f_r)\|_1 \leq \frac{M_2(f_1, ..., f_r)(g(b) - g(a))^{\nu-1}(b-a)^2}{\Gamma(\nu)}$$

$$\sum_{i=1}^{r}\left(\left\|\prod_{\substack{j=1 \\ j\neq i}}^{r}\|f_j(x)\|_2\right\|_{\infty,[a,b]}\right), \tag{115}$$

where $M_2(f_1, ..., f_r)$ is as in (94),

iii) when $p, q > 1 : \frac{1}{p} + \frac{1}{q} = 1$, we have

$$\|\Delta(f_1, ..., f_r)\|_1 \leq \frac{M_3(f_1, ..., f_r)(g(b) - g(a))^{\nu-\frac{1}{q}}(b-a)^2}{(p(\nu-1)+1)^{\frac{1}{p}}\Gamma(\nu)}$$

$$\sum_{i=1}^{r}\left(\left\|\prod_{\substack{j=1 \\ j\neq i}}^{r}\|f_j(x)\|_2\right\|_{\infty,[a,b]}\right), \tag{116}$$

where $M_3(f_1, ..., f_r)$ is as in (96).

Proof. By Remarks 34, 27-29 and that

$$\int_a^b\left(\prod_{\substack{j=1 \\ j\neq i}}^{r}\|f_j(x)\|_2\right)dx \leq (b-a)\left\|\prod_{\substack{j=1 \\ j\neq i}}^{r}\|f_j(x)\|_2\right\|_{\infty,[a,b]}.$$

■

We continue with

Theorem 36 *All as in Theorem 15, with $1 \leq \nu < 2$ (i.e. $n = 1$), $\gamma \geq 1$. Then*

i)

$$\|\Delta(f_1, ..., f_r)\|_{\gamma} \leq \frac{M_1^{\gamma}(f_1, ..., f_r)(g(b) - g(a))^{\nu}(b-a)^2}{\Gamma(\nu+1)}$$

$$\sum_{i=1}^{r}\left(\left\|\prod_{\substack{j=1\\j\neq i}}^{r}\left\|f_j(x)\right\|_\gamma\right\|_{\infty,[a,b]}\right), \tag{117}$$

where $M_1^\gamma(f_1,...,f_r)$ is as in (98),

ii)

$$\left\|\Delta(f_1,...,f_r)\right\|_\gamma \leq \frac{M_2^\gamma(f_1,...,f_r)(g(b)-g(a))^{\nu-1}(b-a)^2}{\Gamma(\nu)}$$

$$\sum_{i=1}^{r}\left(\left\|\prod_{\substack{j=1\\j\neq i}}^{r}\left\|f_j(x)\right\|_\gamma\right\|_{\infty,[a,b]}\right), \tag{118}$$

where $M_2^\gamma(f_1,...,f_r)$ is as in (100),

iii) when $p,q>1:\frac{1}{p}+\frac{1}{q}=1$, we have

$$\left\|\Delta(f_1,...,f_r)\right\|_\gamma \leq \frac{M_3^\gamma(f_1,...,f_r)(g(b)-g(a))^{\nu-\frac{1}{q}}(b-a)^2}{(p(\nu-1)+1)^{\frac{1}{p}}\Gamma(\nu)}$$

$$\sum_{i=1}^{r}\left(\left\|\prod_{\substack{j=1\\j\neq i}}^{r}\left\|f_j(x)\right\|_\gamma\right\|_{\infty,[a,b]}\right), \tag{119}$$

where $M_3^\gamma(f_1,...,f_r)$ is as in (102).

Proof. By Remarks 34, 30-32 and that

$$\int_a^b\left(\prod_{\substack{j=1\\j\neq i}}^{r}\left\|f_j(x)\right\|_\gamma\right)dx \leq (b-a)\left\|\prod_{\substack{j=1\\j\neq i}}^{r}\left\|f_j(x)\right\|_\gamma\right\|_{\infty,[a,b]}.$$

■

Furthermore we have ($r=2$ case of p-Schatten norm Grüss inequalities)

Theorem 37 *All as in Theorem 18, with $1\leq\alpha<2$ (i.e. $[\alpha]=1$). Then*

i) for $\gamma,\delta>1:\frac{1}{\gamma}+\frac{1}{\delta}=1$, we have

$$\left\|\Delta(A_1,A_2)\right\|_1 \leq \frac{N_1(A_1,A_2)(g(b)-g(a))^{\alpha-\frac{1}{\delta}}(b-a)}{\Gamma(\alpha)(\gamma(\alpha-1)+1)^{\frac{1}{\gamma}}}$$

$$\left[\int_a^b\left\|A_1(x)\right\|_p dx+\int_a^b\left\|A_2(x)\right\|_q dx\right], \tag{120}$$

where $N_1(A_1,A_2)$ *is as in (104),*

ii)

$$\|\Delta(A_1,A_2)\|_1 \leq \frac{N_2(A_1,A_2)(g(b)-g(a))^{\alpha-1}(b-a)}{\Gamma(\alpha)}$$
$$\left[\int_a^b \|A_1(x)\|_p\,dx + \int_a^b \|A_2(x)\|_q\,dx\right], \tag{121}$$

where $N_2(A_1,A_2)$ *is as in (106),*

and

iii)

$$\|\Delta(A_1,A_2)\|_1 \leq \frac{N_3(A_1,A_2)(g(b)-g(a))^{\alpha}(b-a)}{\Gamma(\alpha+1)}$$
$$\left[\int_a^b \|A_1(x)\|_p\,dx + \int_a^b \|A_2(x)\|_q\,dx\right], \tag{122}$$

where $N_3(A_1,A_2)$ *is as in (108).*

Proof. By Remarks 34, 33. ■

6 Applications

We start with applications on Ostrowski type inequalities:

Corollary 38 *(to Theorems 12-14) All as in Theorem 12 for* $g(t)=t$. *Then*

i)

$$\|K(f_1,...,f_r)(x_0)\|_1 \leq \frac{1}{\Gamma(\nu+1)}$$
$$\sum_{i=1}^{r}\left[\left[\left\|\left\|\left(D_{x_0-}^{\nu}f_i\right)\right\|_2\right\|_{\infty,[a,x_0]}(x_0-a)^{\nu}\left(\int_a^{x_0}\left(\prod_{\substack{j=1\\ j\neq i}}^{r}\|f_j(x)\|_2\right)dx\right)\right]+\right. \tag{123}$$
$$\left.\left[\left\|\left\|\left(D_{x_0}^{\nu}f_i\right)\right\|_2\right\|_{\infty,[x_0,b]}(b-x_0)^{\nu}\left(\int_{x_0}^{b}\left(\prod_{\substack{j=1\\ j\neq i}}^{r}\|f_j(x)\|_2\right)dx\right)\right]\right],$$

ii)

$$\|K(f_1,...,f_r)(x_0)\|_1 \leq \frac{1}{\Gamma(\nu)}$$
$$\sum_{i=1}^{r}\left[\left[\left\|\left\|\left(D_{x_0-}^{\nu}f_i\right)\right\|_2\right\|_{L_1([a,x_0])}\int_a^{x_0}\left(\prod_{\substack{j=1\\ j\neq i}}^{r}\|f_j(x)\|_2\right)(x_0-x)^{\nu-1}dx\right]+\right.$$

$$\left[\left\|\left\|\left(D_{x_0}^{\nu} f_i\right)\right\|_2\right\|_{L_1([x_0,b])} \int_{x_0}^{b} \left(\prod_{\substack{j=1\\ j\neq i}}^{r} \left\|f_j(x)\right\|_2\right) (x-x_0)^{\nu-1}\, dx\right]\Bigg], \tag{124}$$

iii) when $p,q>1:\frac{1}{p}+\frac{1}{q}=1$*, we have*

$$\left\|K(f_1,...,f_r)(x_0)\right\|_1 \leq \frac{1}{(p(\nu-1)+1)^{\frac{1}{p}}\,\Gamma(\nu)}$$

$$\sum_{i=1}^{r}\Bigg[\left[\left\|\left\|\left(D_{x_0-}^{\nu} f_i\right)\right\|_2\right\|_{q,[a,x_0]} \left(\int_a^{x_0} (x_0-x)^{\nu-\frac{1}{q}} \left(\prod_{\substack{j=1\\ j\neq i}}^{r} \left\|f_j(x)\right\|_2\right) dx\right)\right] +$$

$$\left[\left\|\left\|\left(D_{x_0}^{\nu} f_i\right)\right\|_2\right\|_{q,[x_0,b]} \left(\int_{x_0}^{b} (x-x_0)^{\nu-\frac{1}{q}} \left(\prod_{\substack{j=1\\ j\neq i}}^{r} \left\|f_j(x)\right\|_2\right) dx\right)\right]\Bigg]. \tag{125}$$

It follows:

Corollary 39 *(to Theorems 15-17) All as in Theorem 15 for* $g(t)=t$*,* $\gamma\geq 1$*. Then*

i)

$$\left\|K(f_1,...,f_r)(x_0)\right\|_\gamma \leq \frac{1}{\Gamma(\nu+1)}$$

$$\sum_{i=1}^{r}\Bigg[\left[\left\|\left\|\left(D_{x_0-}^{\nu} f_i\right)\right\|_\gamma\right\|_{\infty,[a,x_0]} (x_0-a)^{\nu} \left(\int_a^{x_0} \left(\prod_{\substack{j=1\\ j\neq i}}^{r} \left\|f_j(x)\right\|_\gamma\right) dx\right)\right] +$$

$$\left[\left\|\left\|\left(D_{x_0}^{\nu} f_i\right)\right\|_\gamma\right\|_{\infty,[x_0,b]} (b-x_0)^{\nu} \left(\int_{x_0}^{b} \left(\prod_{\substack{j=1\\ j\neq i}}^{r} \left\|f_j(x)\right\|_\gamma\right) dx\right)\right]\Bigg], \tag{126}$$

ii)

$$\left\|K(f_1,...,f_r)(x_0)\right\|_\gamma \leq \frac{1}{\Gamma(\nu)}$$

$$\sum_{i=1}^{r}\Bigg[\left[\left\|\left\|\left(D_{x_0-}^{\nu} f_i\right)\right\|_\gamma\right\|_{L_1([a,x_0])} \int_a^{x_0} \left(\prod_{\substack{j=1\\ j\neq i}}^{r} \left\|f_j(x)\right\|_\gamma\right) (x_0-x)^{\nu-1}\, dx\right] +$$

$$\left[\left\|\left\|\left(D_{x_0}^{\nu} f_i\right)\right\|_\gamma\right\|_{L_1([x_0,b])} \int_{x_0}^{b} \left(\prod_{\substack{j=1\\ j\neq i}}^{r} \left\|f_j(x)\right\|_\gamma\right) (x-x_0)^{\nu-1}\, dx\right]\Bigg], \tag{127}$$

iii) when $p,q>1:\frac{1}{p}+\frac{1}{q}=1$, *we have*

$$\left\|K\left(f_1,...,f_r\right)\left(x_0\right)\right\|_\gamma \le \frac{1}{\left(p\left(\nu-1\right)+1\right)^{\frac{1}{p}}\Gamma\left(\nu\right)}$$

$$\sum_{i=1}^{r}\left[\left[\left\|\left\|\left(D^{\nu}_{x_0-}f_i\right)\right\|_\gamma\right\|_{q,[a,x_0]}\left(\int_a^{x_0}\left(x_0-x\right)^{\nu-\frac{1}{q}}\left(\prod_{\substack{j=1\\ j\neq i}}^{r}\left\|f_j\left(x\right)\right\|_\gamma\right)dx\right)\right]+\right.$$

$$\left.\left[\left\|\left\|\left(D^{\nu}_{x_0}f_i\right)\right\|_\gamma\right\|_{q,[x_0,b]}\left(\int_{x_0}^{b}\left(x-x_0\right)^{\nu-\frac{1}{q}}\left(\prod_{\substack{j=1\\ j\neq i}}^{r}\left\|f_j\left(x\right)\right\|_\gamma\right)dx\right)\right]\right]. \tag{128}$$

We continue with

Corollary 40 *(to Theorem 18) All as in Theorem 18, with* $g\left(t\right)=e^t$. *Then*

i) for $\gamma,\delta>1:\frac{1}{\gamma}+\frac{1}{\delta}=1$, *we have*

$$\left\|\Phi\left(A_1,A_2\right)\left(x_0\right)\right\|_1 \le \frac{1}{\Gamma\left(\alpha\right)\left(\gamma\left(\alpha-1\right)+1\right)^{\frac{1}{\gamma}}}$$

$$\left\{\left[\left\|\left\|D^{\alpha}_{e^{x_0}-}\left(A_1\circ\log\right)\right\|_p\right\|_{\delta,[e^a,e^{x_0}]}\int_a^{x_0}\left\|A_2\left(x\right)\right\|_q\left(e^{x_0}-e^x\right)^{\alpha-\frac{1}{\delta}}dx\right]+\right.$$

$$\left[\left\|\left\|D^{\alpha}_{e^{x_0}}\left(A_1\circ\log\right)\right\|_p\right\|_{\delta,[e^{x_0},e^b]}\int_{x_0}^{b}\left\|A_2\left(x\right)\right\|_q\left(e^{x}-e^{x_0}\right)^{\alpha-\frac{1}{\delta}}dx\right]+$$

$$\left[\left\|\left\|D^{\alpha}_{e^{x_0}-}\left(A_2\circ\log\right)\right\|_q\right\|_{\delta,[e^a,e^{x_0}]}\int_a^{x_0}\left\|A_1\left(x\right)\right\|_p\left(e^{x_0}-e^x\right)^{\alpha-\frac{1}{\delta}}dx\right]+$$

$$\left.\left[\left\|\left\|D^{\alpha}_{e^{x_0}}\left(A_2\circ\log\right)\right\|_q\right\|_{\delta,[e^{x_0},e^b]}\int_{x_0}^{b}\left\|A_1\left(x\right)\right\|_p\left(e^{x}-e^{x_0}\right)^{\alpha-\frac{1}{\delta}}dx\right]\right\}, \tag{129}$$

ii) it holds

$$\left\|\Phi\left(A_1,A_2\right)\left(x_0\right)\right\|_1 \le \frac{1}{\Gamma\left(\alpha\right)}$$

$$\left\{\left[\left\|\left\|D^{\alpha}_{e^{x_0}-}\left(A_1\circ\log\right)\right\|_p\right\|_{L_1([e^a,e^{x_0}])}\int_a^{x_0}\left\|A_2\left(x\right)\right\|_q\left(e^{x_0}-e^x\right)^{\alpha-1}dx\right]+\right.$$

$$\left[\left\|\left\|D^{\alpha}_{e^{x_0}}\left(A_1\circ\log\right)\right\|_p\right\|_{L_1([e^{x_0},e^b])}\int_{x_0}^{b}\left\|A_2\left(x\right)\right\|_q\left(e^{x}-e^{x_0}\right)^{\alpha-1}dx\right]+$$

$$\left[\left\|\left\|D^{\alpha}_{e^{x_0}-}\left(A_2\circ\log\right)\right\|_q\right\|_{L_1([e^a,e^{x_0}])}\int_a^{x_0}\left\|A_1\left(x\right)\right\|_p\left(e^{x_0}-e^x\right)^{\alpha-1}dx\right]+ \tag{130}$$

$$\left[\left\| \left\| D_{e^{x_0}}^{\alpha} \left(A_2 \circ \log \right) \right\|_q \right\|_{L_1([e^{x_0}, e^b])} \int_{x_0}^{b} \left\| A_1 (x) \right\|_p \left(e^x - e^{x_0} \right)^{\alpha - 1} dx \right] \right\},$$

and

iii)

$$\left\| \Phi \left(A_1, A_2 \right) (x_0) \right\|_1 \leq \frac{1}{\Gamma (\alpha + 1)}$$

$$\left\{ \left[\left\| \left\| D_{e^{x_0}-}^{\alpha} \left(A_1 \circ \log \right) \right\|_p \right\|_{\infty, [e^a, e^{x_0}]} \int_a^{x_0} \left\| A_2 (x) \right\|_q \left(e^{x_0} - e^x \right)^{\alpha} dx \right] + \right.$$

$$\left[\left\| \left\| D_{e^{x_0}}^{\alpha} \left(A_1 \circ \log \right) \right\|_p \right\|_{\infty, [e^{x_0}, e^b]} \int_{x_0}^{b} \left\| A_2 (x) \right\|_q \left(e^x - e^{x_0} \right)^{\alpha} dx \right] +$$

$$\left[\left\| \left\| D_{e^{x_0}-}^{\alpha} \left(A_2 \circ \log \right) \right\|_q \right\|_{\infty, [e^a, e^{x_0}]} \int_a^{x_0} \left\| A_1 (x) \right\|_p \left(e^{x_0} - e^x \right)^{\alpha} dx \right] +$$

$$\left. \left[\left\| \left\| D_{e^{x_0}}^{\alpha} \left(A_2 \circ \log \right) \right\|_q \right\|_{\infty, [e^{x_0}, e^b]} \int_{x_0}^{b} \left\| A_1 (x) \right\|_p \left(e^x - e^{x_0} \right)^{\alpha} dx \right] \right\}. \tag{131}$$

We continue with applications on Opial inequalities

Corollary 41 *(to Theorem 19) All as in Theorem 19 with $g(t) = t$. Let $p, q > 1 : \frac{1}{p} + \frac{1}{q} = 1$. Then*

$$\int_{x_0}^{z} \left\| f(w) \left(D_{x_0}^{\nu} f \right)(w) \right\|_1 dw \leq$$

$$\frac{2^{-\frac{1}{q}} (z - x_0)^{\nu + \frac{1}{p} - \frac{1}{q}}}{\Gamma(\nu) \left[\left(p(\nu - 1) + 1 \right) \left(p(\nu - 1) + 2 \right) \right]^{\frac{1}{p}}} \left(\int_{x_0}^{z} \left\| \left(D_{x_0}^{\nu} f \right)(w) \right\|_2^q dw \right)^{\frac{2}{q}}, \tag{132}$$

for all $x_0 \leq z \leq b$.

It follows:

Corollary 42 *(to Theorem 20) All as in Theorem 20, $\gamma \geq 1$, with $g(t) = e^t$. Let also $p, q > 1 : \frac{1}{p} + \frac{1}{q} = 1$. Then*

$$\int_{e^{x_0}}^{z} \left\| \left((f \circ \log)(w) \right) \left(\left(D_{e^{x_0}}^{\nu} (f \circ \log) \right)(w) \right) \right\|_{\gamma} dw \leq$$

$$\frac{2^{-\frac{1}{q}} (z - e^{x_0})^{\nu + \frac{1}{p} - \frac{1}{q}}}{\Gamma(\nu) \left[\left(p(\nu - 1) + 1 \right) \left(p(\nu - 1) + 2 \right) \right]^{\frac{1}{p}}} \left(\int_{e^{x_0}}^{z} \left\| \left(D_{e^{x_0}}^{\nu} (f \circ \log) \right)(w) \right\|_{\gamma}^q dw \right)^{\frac{2}{q}}, \tag{133}$$

for all $e^{x_0} \leq z \leq e^b$.

We finish with applications on Grüss inequalities:

Corollary 43 *(to Theorem 35) All as in Theorem 35 with* $g(t)=t$ $(1\leq\nu<2)$. *Then*

i)

$$\left\|\Delta\left(f_1,...,f_r\right)\right\|_1\leq\frac{M_1\left(f_1,...,f_r\right)(b-a)^{\nu+2}}{\Gamma(\nu+1)}\sum_{i=1}^{r}\left(\left\|\prod_{\substack{j=1\\j\neq i}}^{r}\left\|f_j(x)\right\|_2\right\|_{\infty,[a,b]}\right), \tag{134}$$

where $M_1\left(f_1,...,f_r\right)$ *is as in (92),*

ii)

$$\left\|\Delta\left(f_1,...,f_r\right)\right\|_1\leq\frac{M_2\left(f_1,...,f_r\right)(b-a)^{\nu+1}}{\Gamma(\nu)}\sum_{i=1}^{r}\left(\left\|\prod_{\substack{j=1\\j\neq i}}^{r}\left\|f_j(x)\right\|_2\right\|_{\infty,[a,b]}\right), \tag{135}$$

where $M_2\left(f_1,...,f_r\right)$ *is as in (94),*

iii) when $p,q>1:\frac{1}{p}+\frac{1}{q}=1$, *we have*

$$\left\|\Delta\left(f_1,...,f_r\right)\right\|_1\leq\frac{M_3\left(f_1,...,f_r\right)(b-a)^{\nu+1+\frac{1}{p}}}{(p(\nu-1)+1)^{\frac{1}{p}}\Gamma(\nu)}\sum_{i=1}^{r}\left(\left\|\prod_{\substack{j=1\\j\neq i}}^{r}\left\|f_j(x)\right\|_2\right\|_{\infty,[a,b]}\right), \tag{136}$$

where $M_3\left(f_1,...,f_r\right)$ *is as in (96).*

It follows ($r=2$ case)

Corollary 44 *(to Theorem 37) All as in Theorem 37, with* $[a,b]\subset\mathbb{R}_+-\{0\}$, *and* $g(t)=\log t$. *Then*

i) for $\gamma,\delta>1:\frac{1}{\gamma}+\frac{1}{\delta}=1$, *we have*

$$\left\|\Delta\left(A_1,A_2\right)\right\|_1\leq\frac{N_1\left(A_1,A_2\right)\left(\log\frac{b}{a}\right)^{\alpha-\frac{1}{\delta}}(b-a)}{\Gamma(\alpha)(\gamma(\alpha-1)+1)^{\frac{1}{\gamma}}}$$

$$\left[\int_a^b\left\|A_1(x)\right\|_p dx+\int_a^b\left\|A_2(x)\right\|_q dx\right], \tag{137}$$

where $N_1\left(A_1,A_2\right)$ *is as in (104),*

ii)

$$\left\|\Delta\left(A_1,A_2\right)\right\|_1\leq\frac{N_2\left(A_1,A_2\right)\left(\log\frac{b}{a}\right)^{\alpha-1}(b-a)}{\Gamma(\alpha)}$$

$$\left[\int_a^b \left\|A_1(x)\right\|_p dx + \int_a^b \left\|A_2(x)\right\|_q dx\right], \tag{138}$$

where $N_2(A_1, A_2)$ *is as in (106),*

and

iii)

$$\left\|\Delta(A_1, A_2)\right\|_1 \leq \frac{N_3(A_1, A_2)\left(\log \frac{b}{a}\right)^{\alpha}(b-a)}{\Gamma(\alpha+1)}$$

$$\left[\int_a^b \left\|A_1(x)\right\|_p dx + \int_a^b \left\|A_2(x)\right\|_q dx\right], \tag{139}$$

where $N_3(A_1, A_2)$ *is as in (108).*

References

[1] G.A. Anastassiou, *Fractional Differentiation Inequalities*, Research Monograph, Springer, New York, 2009.

[2] G.A. Anastassiou, *Advances on Fractional Inequalities*, Research Monograph, Springer, New York, 2011.

[3] G.A. Anastassiou, *Intelligent Comparisons: Analytic Inequalities*, Springer, Heidelberg, New York, 2016.

[4] G.A. Anastassiou, *Strong mixed and generalized fractional calculus for Banach space valued functions*, Mat. Vesnik, 69(3) (2017), 176-191.

[5] G.A. Anastassiou, *Intelligent Computations: Abstract Fractional Calculus, Inequalities, Approximations*, Springer, Heidelberg, New York, 2018.

[6] G.A. Anastassiou, *Generalized Canavati Fractional Ostrowski, Opial and Grüss type inequalities for Banach algebra valued functions*, submitted, 2021.

[7] R. Bellman, *Some inequalities for positive definite matrices*, in E.F. Beckenbach (Ed.), General Inequalities 2, Proceedings of the 2nd International Conference on General Inequalities, Birkhauser, Basel, 1980, 89-90.

[8] Čebyšev, *Sur les expressions approximatives des intégrales définies par les aures prises entre les mêmes limites*, Proc. Math. Soc. Charkov, 2(1882), 93-98.

[9] D. Chang, *A matrix trace inequality for products of Hermitian matrices*, J. Math. Anal. Appl., 237 (1999), 721-725.

[10] I.D. Coop, *On matrix trace inequalities and related topics for products of Hermitian matrix*, J. Math. Anal. Appl. 188 (1994), 999-1001.

[11] S.S. Dragomir, *p-Schatten norm inequalities of Ostrowski's type*, RGMIA Res. Rep. Coll. 24 (2021), Art. 108, 19 pp.

[12] S.S. Dragomir, *p-Schatten norm inequalities of Grüss type*, RGMIA Res. Rep. Coll. 24 (2021), Art. 115, 16 pp.

[13] J. Mikusinski, *The Bochner integral*, Academic Press, New York, 1978.

[14] H. Neudecker, *A matrix trace inequality*, J. Math. Anal. Appl., 166 (1992), 302-303.

[15] Z. Opial, *Sur une inegalite*, Ann. Polon. Math. 8(1960), 29-32.

[16] A. Ostrowski, *Über die Absolutabweichung einer differentiabaren Funcktion von ihrem Integralmittelwert*, Comment. Math. Helv., 10 (1938), 226-227.

[17] W. Rudin, *Functional Analysis*, Second Edition, McGraw-Hill, Inc., New York, 1991.

[18] B. Simon, *Trace ideals and Their Applications*, Cambridge University Press, Cambridge, 1979.

[19] V.A. Zagrebvov, *Gibbs Semigroups*, Operator Theory: Advances and Applications, Volume 273, Birkhauser, 2019.

J. COMPUTATIONAL ANALYSIS AND APPLICATIONS, VOL. 31, NO. 4, 2023, COPYRIGHT 2023 EUDOXUS PRESS, LLC

Abstract multivariate algebraic function activated neural network approximations

George A. Anastassiou, Robert Kozma
Department of Mathematical Sciences
University of Memphis
Memphis, TN 38152, U.S.A.
ganastss@memphis.edu

Abstract

Here we exhibit multivariate quantitative approximations of Banach space valued continuous multivariate functions on a box or $\mathbb{R}^N$, $N \in \mathbb{N}$, by the multivariate normalized, quasi-interpolation, Kantorovich type and quadrature type neural network operators. We study also the case of approximation by iterated operators of the last four types. These approximations are achieved by establishing multidimensional Jackson type inequalities involving the multivariate modulus of continuity of the engaged function or its high order Fréchet derivatives. Our multivariate operators are defined by using a multidimensional density function induced by the algebraic sigmoid function. The approximations are pointwise and uniform. The related feed-forward neural network is with one hidden layer.

2020 AMS Mathematics Subject Classification: 41A17, 41A25, 41A30, 41A36.

Keywords and Phrases: algebraic sigmoid function, multivariate neural network approximation, quasi-interpolation operator, Kantorovich type operator, quadrature type operator, multivariate modulus of continuity, abstract approximation, iterated approximation.

1 Introduction

G.A. Anastassiou in [2] and [3], see chapters 2-5, was the first to establish neural network approximations to continuous functions with rates by very specifically defined neural network operators of Cardaliagnet-Euvrard and "Squashing" types, by employing the modulus of continuity of the engaged function or its high order derivative, and producing very tight Jackson type inequalities. He treats there both the univariate and multivariate cases. The defining these operators "bell-shaped" and "squashing" functions are assumed to be of compact support. Also in [3] he gives the Nth order asymptotic expansion for the error of weak approximation of these two operators to a special natural class of smooth functions, see chapters 4-5 there.

Motivations for this work are the article [15] of Z. Chen and F. Cao, and [4], [5], [6], [7], [8], [9], [10], [11], [12], [13], [16], [17].

Here we perform multivariate algebraic sigmoid function based neural network approximations to continuous functions over boxes or over the whole $\mathbb{R}^N$, $N \in \mathbb{N}$, and also iterated approximations. All convergences here are with rates expressed via the multivariate modulus of continuity of the involved function or its high order Fréchet derivative and given by very tight multidimensional Jackson type inequalities.

We come up with the "right" precisely defined multivariate normalized, quasi-interpolation neural network operators related to boxes or $\mathbb{R}^N$, as well as Kantorovich type and quadrature type related operators on $\mathbb{R}^N$. Our boxes are not necessarily symmetric to the origin. In preparation to prove our results we establish important properties of the basic multivariate density function induced by algebraic sigmoid function and defining our operators.

Feed-forward neural networks (FNNs) with one hidden layer, the only type of networks we deal with in this article, are mathematically expressed as

$$N_n(x) = \sum_{j=0}^{n} c_j \sigma\left(\langle a_j \cdot x\rangle + b_j\right), \quad x \in \mathbb{R}^s, \quad s \in \mathbb{N},$$

where for $0 \leq j \leq n$, $b_j \in \mathbb{R}$ are the thresholds, $a_j \in \mathbb{R}^s$ are the connection weights, $c_j \in \mathbb{R}$ are the coefficients, $\langle a_j \cdot x\rangle$ is the inner product of a_j and x, and σ is the activation function of the network. In many fundamental network models, the activation function is the algebrai sigmoid function. About neural networks see [18], [19], [20].

2 Basic

Here see also [12].

We consider the generator algebraic function

$$\varphi(x) = \frac{x}{\sqrt[2m]{1+x^{2m}}}, \quad m \in \mathbb{N}, x \in \mathbb{R}, \tag{1}$$

which is a sigmoid type of function and is a strictly increasing function.

We see that $\varphi(-x) = -\varphi(x)$ with $\varphi(0) = 0$. We get that

$$\varphi'(x) = \frac{1}{\left(1+x^{2m}\right)^{\frac{2m+1}{m}}} > 0, \ \forall \, x \in \mathbb{R}, \tag{2}$$

proving φ as strictly increasing over $\mathbb{R}, \varphi'(x) = \varphi'(-x)$. We easily find that $\lim_{x \to +\infty} \varphi(x) = 1$, $\varphi(+\infty) = 1$, and $\lim_{x \to -\infty} \varphi(x) = -1$, $\varphi(-\infty) = -1$.

We consider the activation function

$$\Phi(x) = \frac{1}{4}\left[\varphi(x+1) - \varphi(x-1)\right]. \tag{3}$$

Clearly it is $\Phi(x) = \Phi(-x)$, $\forall\ x \in \mathbb{R}$, so that Φ is an even function and symmetric with respect to the y-axis. Clearly $\Phi(x) > 0$, $\forall\ x \in \mathbb{R}$.

Also it is

$$\Phi(0) = \frac{1}{2\sqrt[2m]{2}}. \tag{4}$$

By [12], we have that $\Phi'(x) < 0$ for $x > 0$. That is Φ is strictly decreasing over $(0, +\infty)$.

Clearly, Φ is strictly increasing over $(-\infty, 0)$ and $\Phi'(0) = 0$.

Furthermore we obtain that

$$\lim_{x \to +\infty} \Phi(x) = \frac{1}{4}\left[\varphi(+\infty) - \varphi(+\infty)\right] = 0, \tag{5}$$

and

$$\lim_{x \to -\infty} \Phi(x) = \frac{1}{4}\left[\varphi(-\infty) - \varphi(-\infty)\right] = 0. \tag{6}$$

That is the x-axis is the horizontal asymptote of Φ.

Conclusion, Φ is a bell shape symmetric function with maximum

$$\Phi(0) = \frac{1}{2\sqrt[2m]{2}}, \quad m \in \mathbb{N}. \tag{7}$$

We need

Theorem 1 *([12]) We have that*

$$\sum_{i=-\infty}^{\infty} \Phi(x - i) = 1, \quad \forall\ x \in \mathbb{R}. \tag{8}$$

Theorem 2 *([12]) It holds*

$$\int_{-\infty}^{\infty} \Phi(x)\, dx = 1. \tag{9}$$

Theorem 3 *([12]) Let $0 < \alpha < 1$, and $n \in \mathbb{N}$ with $n^{1-\alpha} > 2$. It holds*

$$\sum_{\begin{cases} k = -\infty \\ : |nx - k| \geq n^{1-\alpha} \end{cases}}^{\infty} \Phi(nx - k) < \frac{1}{4m\left(n^{1-\alpha} - 2\right)^{2m}}, \quad m \in \mathbb{N}. \tag{10}$$

Denote by $\lfloor\cdot\rfloor$ the integral part of the number and by $\lceil\cdot\rceil$ the ceiling of the number.

We need

Theorem 4 *([12]) Let $[a,b]\subset\mathbb{R}$ and $n\in\mathbb{N}$ so that $\lceil na\rceil\leq\lfloor nb\rfloor$. It holds*

$$\frac{1}{\sum_{k=\lceil na\rceil}^{\lfloor nb\rfloor}\Phi(nx-k)}<2\left(\sqrt[2m]{1+4^m}\right), \tag{11}$$

$\forall\ x\in[a,b]$, $m\in\mathbb{N}$.

Note 5 *1) By [12] we have that*

$$\lim_{n\to\infty}\sum_{k=\lceil na\rceil}^{\lfloor nb\rfloor}\Phi(nx-k)\neq 1, \tag{12}$$

for at least some $x\in[a,b]$.

2) Let $[a,b]\subset\mathbb{R}$. For large $n\in\mathbb{N}$ we always have $\lceil na\rceil\leq\lfloor nb\rfloor$. Also $a\leq\frac{k}{n}\leq b$, iff $\lceil na\rceil\leq k\leq\lfloor nb\rfloor$.

In general it holds that

$$\sum_{k=\lceil na\rceil}^{\lfloor nb\rfloor}\Phi(nx-k)\leq 1. \tag{13}$$

We introduce

$$Z(x_1,...,x_N):=Z(x):=\prod_{i=1}^{N}\Phi(x_i),\quad x=(x_1,...,x_N)\in\mathbb{R}^N,\ N\in\mathbb{N}. \tag{14}$$

It has the properties:

(i) $Z(x)>0,\ \ \forall\ x\in\mathbb{R}^N$,

(ii)

$$\sum_{k=-\infty}^{\infty}Z(x-k):=\sum_{k_1=-\infty}^{\infty}\sum_{k_2=-\infty}^{\infty}...\sum_{k_N=-\infty}^{\infty}Z(x_1-k_1,...,x_N-k_N)=1, \tag{15}$$

where $k:=(k_1,...,k_n)\in\mathbb{Z}^N$, $\forall\ x\in\mathbb{R}^N$,

hence

(iii)

$$\sum_{k=-\infty}^{\infty}Z(nx-k)=1, \tag{16}$$

$\forall\ x\in\mathbb{R}^N$; $n\in\mathbb{N}$,

and
(iv)

$$\int_{\mathbb{R}^N} Z(x)\, dx = 1, \tag{17}$$

that is Z is a multivariate density function.

Here denote $\|x\|_\infty := \max\{|x_1|, ..., |x_N|\}$, $x \in \mathbb{R}^N$, also set $\infty := (\infty, ..., \infty)$, $-\infty := (-\infty, ..., -\infty)$ upon the multivariate context, and

$$\begin{gathered} \lceil na \rceil := (\lceil na_1 \rceil, ..., \lceil na_N \rceil), \\ \lfloor nb \rfloor := (\lfloor nb_1 \rfloor, ..., \lfloor nb_N \rfloor), \end{gathered} \tag{18}$$

where $a := (a_1, ..., a_N)$, $b := (b_1, ..., b_N)$.

We obviously see that

$$\sum_{k=\lceil na \rceil}^{\lfloor nb \rfloor} Z(nx-k) = \sum_{k=\lceil na \rceil}^{\lfloor nb \rfloor} \left(\prod_{i=1}^{N} \Phi(nx_i - k_i) \right) =$$

$$\sum_{k_1=\lceil na_1 \rceil}^{\lfloor nb_1 \rfloor} ... \sum_{k_N=\lceil na_N \rceil}^{\lfloor nb_N \rfloor} \left(\prod_{i=1}^{N} \Phi(nx_i - k_i) \right) = \prod_{i=1}^{N} \left(\sum_{k_i=\lceil na_i \rceil}^{\lfloor nb_i \rfloor} \Phi(nx_i - k_i) \right). \tag{19}$$

For $0 < \beta < 1$ and $n \in \mathbb{N}$, a fixed $x \in \mathbb{R}^N$, we have that

$$\sum_{k=\lceil na \rceil}^{\lfloor nb \rfloor} Z(nx-k) =$$

$$\sum_{\substack{k = \lceil na \rceil \\ \left\| \frac{k}{n} - x \right\|_\infty \leq \frac{1}{n^\beta}}}^{\lfloor nb \rfloor} Z(nx-k) + \sum_{\substack{k = \lceil na \rceil \\ \left\| \frac{k}{n} - x \right\|_\infty > \frac{1}{n^\beta}}}^{\lfloor nb \rfloor} Z(nx-k). \tag{20}$$

In the last two sums the counting is over disjoint vector sets of k's, because the condition $\left\| \frac{k}{n} - x \right\|_\infty > \frac{1}{n^\beta}$ implies that there exists at least one $\left| \frac{k_r}{n} - x_r \right| > \frac{1}{n^\beta}$, where $r \in \{1, ..., N\}$.

(v) As in [10], pp. 379-380, we derive that

$$\sum_{\substack{k = \lceil na \rceil \\ \left\| \frac{k}{n} - x \right\|_\infty > \frac{1}{n^\beta}}}^{\lfloor nb \rfloor} Z(nx-k) \overset{(10)}{<} \frac{1}{4m\left(n^{1-\beta} - 2\right)^{2m}}, \quad 0 < \beta < 1, \; m \in \mathbb{N}, \tag{21}$$

with $n \in \mathbb{N} : n^{1-\beta} > 2$, $x \in \prod_{i=1}^{N} [a_i, b_i]$.

(vi) By Theorem 4 we get that

$$0 < \frac{1}{\sum_{k=\lceil na \rceil}^{\lfloor nb \rfloor} Z(nx-k)} < \frac{1}{(\Phi(1))^N} \cong \left[2\left(\sqrt[2m]{1+4^m}\right)\right]^N, \tag{22}$$

$\forall\, x \in \left(\prod_{i=1}^N [a_i, b_i]\right)$, $n \in \mathbb{N}$.

It is also clear that

(vii)

$$\sum_{\begin{cases} k=-\infty \\ \left\|\frac{k}{n}-x\right\|_\infty > \frac{1}{n^\beta} \end{cases}}^{\infty} Z(nx-k) < \frac{1}{4m(n^{1-\beta}-2)^{2m}}, \tag{23}$$

$0 < \beta < 1$, $n \in \mathbb{N} : n^{1-\beta} > 2$, $x \in \mathbb{R}^N$, $m \in \mathbb{N}$.

Furthermore it holds

$$\lim_{n\to\infty} \sum_{k=\lceil na \rceil}^{\lfloor nb \rfloor} Z(nx-k) \neq 1, \tag{24}$$

for at least some $x \in \left(\prod_{i=1}^N [a_i, b_i]\right)$.

Here $\left(X, \|\cdot\|_\gamma\right)$ is a Banach space.

Let $f \in C\left(\prod_{i=1}^N [a_i, b_i], X\right)$, $x = (x_1, ..., x_N) \in \prod_{i=1}^N [a_i, b_i]$, $n \in \mathbb{N}$ such that $\lceil na_i \rceil \leq \lfloor nb_i \rfloor$, $i = 1, ..., N$.

We introduce and define the following multivariate linear normalized neural network operator ($x := (x_1, ..., x_N) \in \left(\prod_{i=1}^N [a_i, b_i]\right)$):

$$A_n(f, x_1, ..., x_N) := A_n(f, x) := \frac{\sum_{k=\lceil na \rceil}^{\lfloor nb \rfloor} f\left(\frac{k}{n}\right) Z(nx-k)}{\sum_{k=\lceil na \rceil}^{\lfloor nb \rfloor} Z(nx-k)} =$$

$$\frac{\sum_{k_1=\lceil na_1 \rceil}^{\lfloor nb_1 \rfloor} \sum_{k_2=\lceil na_2 \rceil}^{\lfloor nb_2 \rfloor} ... \sum_{k_N=\lceil na_N \rceil}^{\lfloor nb_N \rfloor} f\left(\frac{k_1}{n}, ..., \frac{k_N}{n}\right) \left(\prod_{i=1}^N \Phi(nx_i - k_i)\right)}{\prod_{i=1}^N \left(\sum_{k_i=\lceil na_i \rceil}^{\lfloor nb_i \rfloor} \Phi(nx_i - k_i)\right)}. \tag{25}$$

For large enough $n \in \mathbb{N}$ we always obtain $\lceil na_i \rceil \leq \lfloor nb_i \rfloor$, $i = 1, ..., N$. Also $a_i \leq \frac{k_i}{n} \leq b_i$, iff $\lceil na_i \rceil \leq k_i \leq \lfloor nb_i \rfloor$, $i = 1, ..., N$.

When $g \in C\left(\prod_{i=1}^N [a_i, b_i]\right)$ we define the companion operator

$$\widetilde{A}_n(g, x) := \frac{\sum_{k=\lceil na \rceil}^{\lfloor nb \rfloor} g\left(\frac{k}{n}\right) Z(nx-k)}{\sum_{k=\lceil na \rceil}^{\lfloor nb \rfloor} Z(nx-k)}. \tag{26}$$

Clearly $\widetilde{A}_n$ is a positive linear operator. We have that

$$\widetilde{A}_n(1,x)=1,\ \ \forall\ x\in\left(\prod_{i=1}^{N}[a_i,b_i]\right).$$

Notice that $A_n(f)\in C\left(\prod_{i=1}^{N}[a_i,b_i],X\right)$ and $\widetilde{A}_n(g)\in C\left(\prod_{i=1}^{N}[a_i,b_i]\right)$.

Furthermore it holds

$$\left\|A_n(f,x)\right\|_{\gamma}\leq\frac{\sum_{k=\lceil na\rceil}^{\lfloor nb\rfloor}\left\|f\left(\frac{k}{n}\right)\right\|_{\gamma}Z(nx-k)}{\sum_{k=\lceil na\rceil}^{\lfloor nb\rfloor}Z(nx-k)}=\widetilde{A}_n\left(\|f\|_{\gamma},x\right), \tag{27}$$

$\forall\ x\in\prod_{i=1}^{N}[a_i,b_i]$.

Clearly $\|f\|_{\gamma}\in C\left(\prod_{i=1}^{N}[a_i,b_i]\right)$.

So, we have that

$$\left\|A_n(f,x)\right\|_{\gamma}\leq\widetilde{A}_n\left(\|f\|_{\gamma},x\right), \tag{28}$$

$\forall\ x\in\prod_{i=1}^{N}[a_i,b_i]$, $\forall\ n\in\mathbb{N}$, $\forall\ f\in C\left(\prod_{i=1}^{N}[a_i,b_i],X\right)$.

Let $c\in X$ and $g\in C\left(\prod_{i=1}^{N}[a_i,b_i]\right)$, then $cg\in C\left(\prod_{i=1}^{N}[a_i,b_i],X\right)$.

Furthermore it holds

$$A_n(cg,x)=c\widetilde{A}_n(g,x),\ \ \forall\ x\in\prod_{i=1}^{N}[a_i,b_i]. \tag{29}$$

Since $\widetilde{A}_n(1)=1$, we get that

$$A_n(c)=c,\ \ \forall\ c\in X. \tag{30}$$

We call $\widetilde{A}_n$ the companion operator of A_n.

For convinience we call

$$A_n^{*}(f,x):=\sum_{k=\lceil na\rceil}^{\lfloor nb\rfloor}f\left(\frac{k}{n}\right)Z(nx-k)=$$

$$\sum_{k_1=\lceil na_1\rceil}^{\lfloor nb_1\rfloor}\sum_{k_2=\lceil na_2\rceil}^{\lfloor nb_2\rfloor}\cdots\sum_{k_N=\lceil na_N\rceil}^{\lfloor nb_N\rfloor}f\left(\frac{k_1}{n},...,\frac{k_N}{n}\right)\left(\prod_{i=1}^{N}\Phi(nx_i-k_i)\right), \tag{31}$$

$\forall\ x\in\left(\prod_{i=1}^{N}[a_i,b_i]\right)$.

That is

$$A_n(f,x):=\frac{A_n^{*}(f,x)}{\sum_{k=\lceil na\rceil}^{\lfloor nb\rfloor}Z(nx-k)}, \tag{32}$$

$\forall\ x \in \left(\prod_{i=1}^{N}\left[a_i, b_i\right]\right)$, $n \in \mathbb{N}$.

Hence

$$A_n\left(f,x\right) - f\left(x\right) = \frac{A_n^*\left(f,x\right) - f\left(x\right)\left(\sum_{k=\lceil na\rceil}^{\lfloor nb\rfloor} Z\left(nx-k\right)\right)}{\sum_{k=\lceil na\rceil}^{\lfloor nb\rfloor} Z\left(nx-k\right)}. \tag{33}$$

Consequently we derive

$$\left\|A_n\left(f,x\right) - f\left(x\right)\right\|_\gamma \overset{(22)}{\leq} \left[2\left(\sqrt[2m]{1+4^m}\right)\right]^N \left\|A_n^*\left(f,x\right) - f\left(x\right)\sum_{k=\lceil na\rceil}^{\lfloor nb\rfloor} Z\left(nx-k\right)\right\|_\gamma, \tag{34}$$

$\forall\ x \in \left(\prod_{i=1}^{N}\left[a_i, b_i\right]\right)$.

We will estimate the right hand side of (34).

For the last and others we need

Definition 6 *([11], p. 274) Let M be a convex and compact subset of $\left(\mathbb{R}^N, \left\|\cdot\right\|_p\right)$, $p \in [1,\infty]$, and $\left(X, \left\|\cdot\right\|_\gamma\right)$ be a Banach space. Let $f \in C\left(M,X\right)$. We define the first modulus of continuity of f as*

$$\omega_1\left(f,\delta\right) := \sup_{\substack{x,y \in M:\\ \left\|x-y\right\|_p \leq \delta}} \left\|f\left(x\right) - f\left(y\right)\right\|_\gamma, \quad 0 < \delta \leq diam\left(M\right). \tag{35}$$

If $\delta > diam\left(M\right)$, then

$$\omega_1\left(f,\delta\right) = \omega_1\left(f, diam\left(M\right)\right). \tag{36}$$

Notice $\omega_1\left(f,\delta\right)$ is increasing in $\delta > 0$. For $f \in C_B\left(M,X\right)$ (continuous and bounded functions) $\omega_1\left(f,\delta\right)$ is defined similarly.

Lemma 7 *([11], p. 274) We have $\omega_1\left(f,\delta\right) \to 0$ as $\delta \downarrow 0$, iff $f \in C\left(M,X\right)$, where M is a convex compact subset of $\left(\mathbb{R}^N, \left\|\cdot\right\|_p\right)$, $p \in [1,\infty]$.*

Clearly we have also: $f \in C_U\left(\mathbb{R}^N, X\right)$ (uniformly continuous functions), iff $\omega_1\left(f,\delta\right) \to 0$ as $\delta \downarrow 0$, where ω_1 is defined similarly to (35). The space $C_B\left(\mathbb{R}^N, X\right)$ denotes the continuous and bounded functions on $\mathbb{R}^N$.

When $f \in C_B\left(\mathbb{R}^N, X\right)$ we define,

$$B_n\left(f,x\right) := B_n\left(f,x_1,...,x_N\right) := \sum_{k=-\infty}^{\infty} f\left(\frac{k}{n}\right) Z\left(nx-k\right) :=$$

$$\sum_{k_1=-\infty}^{\infty}\sum_{k_2=-\infty}^{\infty}...\sum_{k_N=-\infty}^{\infty} f\left(\frac{k_1}{n}, \frac{k_2}{n}, ..., \frac{k_N}{n}\right)\left(\prod_{i=1}^{N}\Phi\left(nx_i - k_i\right)\right), \tag{37}$$

$n \in \mathbb{N}$, $\forall\ x \in \mathbb{R}^N$, $N \in \mathbb{N}$, the multivariate quasi-interpolation neural network operator.

Also for $f \in C_B\left(\mathbb{R}^N, X\right)$ we define the multivariate Kantorovich type neural network operator

$$C_n(f,x) := C_n(f,x_1,...,x_N) := \sum_{k=-\infty}^{\infty}\left(n^N \int_{\frac{k}{n}}^{\frac{k+1}{n}} f(t)\,dt\right) Z(nx-k) =$$

$$\sum_{k_1=-\infty}^{\infty}\sum_{k_2=-\infty}^{\infty}...\sum_{k_N=-\infty}^{\infty}\left(n^N \int_{\frac{k_1}{n}}^{\frac{k_1+1}{n}}\int_{\frac{k_2}{n}}^{\frac{k_2+1}{n}}...\int_{\frac{k_N}{n}}^{\frac{k_N+1}{n}} f(t_1,...,t_N)\,dt_1...dt_N\right)$$

$$\cdot\left(\prod_{i=1}^{N}\Phi(nx_i-k_i)\right), \tag{38}$$

$n \in \mathbb{N}$, $\forall\ x \in \mathbb{R}^N$.

Again for $f \in C_B\left(\mathbb{R}^N, X\right)$, $N \in \mathbb{N}$, we define the multivariate neural network operator of quadrature type $D_n(f,x)$, $n \in \mathbb{N}$, as follows.

Let $\theta = (\theta_1,...,\theta_N) \in \mathbb{N}^N$, $r = (r_1,...,r_N) \in \mathbb{Z}_+^N$, $w_r = w_{r_1,r_2,...r_N} \geq 0$, such that $\sum\limits_{r=0}^{\theta} w_r = \sum\limits_{r_1=0}^{\theta_1}\sum\limits_{r_2=0}^{\theta_2}...\sum\limits_{r_N=0}^{\theta_N} w_{r_1,r_2,...r_N} = 1$; $k \in \mathbb{Z}^N$ and

$$\delta_{nk}(f) := \delta_{n,k_1,k_2,...,k_N}(f) := \sum_{r=0}^{\theta} w_r f\left(\frac{k}{n}+\frac{r}{n\theta}\right) =$$

$$\sum_{r_1=0}^{\theta_1}\sum_{r_2=0}^{\theta_2}...\sum_{r_N=0}^{\theta_N} w_{r_1,r_2,...r_N} f\left(\frac{k_1}{n}+\frac{r_1}{n\theta_1},\frac{k_2}{n}+\frac{r_2}{n\theta_2},...,\frac{k_N}{n}+\frac{r_N}{n\theta_N}\right), \tag{39}$$

where $\frac{r}{\theta} := \left(\frac{r_1}{\theta_1},\frac{r_2}{\theta_2},...,\frac{r_N}{\theta_N}\right)$.

We set

$$D_n(f,x) := D_n(f,x_1,...,x_N) := \sum_{k=-\infty}^{\infty}\delta_{nk}(f)\,Z(nx-k) = \tag{40}$$

$$\sum_{k_1=-\infty}^{\infty}\sum_{k_2=-\infty}^{\infty}...\sum_{k_N=-\infty}^{\infty}\delta_{n,k_1,k_2,...,k_N}(f)\left(\prod_{i=1}^{N}\Phi(nx_i-k_i)\right),$$

$\forall\ x \in \mathbb{R}^N$.

In this article we study the approximation properties of $A_n, B_n, C_n,\ D_n$ neural network operators and as well of their iterates. That is, the quantitative pointwise and uniform convergence of these operators to the unit operator I.

3 Multivariate general Neural Network Approximations

Here we present several vectorial neural network approximations to Banach space valued functions given with rates.

We give

Theorem 8 *Let* $f \in C\left(\prod_{i=1}^{N}[a_i,b_i], X\right)$, $0<\beta<1$, $x \in \left(\prod_{i=1}^{N}[a_i,b_i]\right)$, $m, N, n \in \mathbb{N}$ *with* $n^{1-\beta}>2$. *Then*

1)

$$\|A_n(f,x)-f(x)\|_\gamma \leq \left[2\left(\sqrt[2m]{1+4^m}\right)\right]^N \left[\omega_1\left(f,\frac{1}{n^\beta}\right)+\frac{\left\|\|f\|_\gamma\right\|_\infty}{2m\left(n^{1-\beta}-2\right)^{2m}}\right] =: \lambda_1(n), \tag{41}$$

and

2)

$$\left\|\|A_n(f)-f\|_\gamma\right\|_\infty \leq \lambda_1(n). \tag{42}$$

We notice that $\lim_{n\to\infty} A_n(f) \overset{\|\cdot\|_\gamma}{=} f$, *pointwise and uniformly.*

Above ω_1 *is with respect to* $p=\infty$.

Proof. We observe that

$$\Delta(x) := A_n^*(f,x) - f(x)\sum_{k=\lceil na\rceil}^{\lfloor nb\rfloor} Z(nx-k) =$$

$$\sum_{k=\lceil na\rceil}^{\lfloor nb\rfloor} f\left(\frac{k}{n}\right) Z(nx-k) - \sum_{k=\lceil na\rceil}^{\lfloor nb\rfloor} f(x) Z(nx-k) =$$

$$\sum_{k=\lceil na\rceil}^{\lfloor nb\rfloor}\left(f\left(\frac{k}{n}\right)-f(x)\right) Z(nx-k). \tag{43}$$

Thus

$$\|\Delta(x)\|_\gamma \leq \sum_{k=\lceil na\rceil}^{\lfloor nb\rfloor}\left\|f\left(\frac{k}{n}\right)-f(x)\right\|_\gamma Z(nx-k) =$$

$$\sum_{\substack{k=\lceil na\rceil \\ \left\|\frac{k}{n}-x\right\|_\infty \leq \frac{1}{n^\beta}}}^{\lfloor nb\rfloor} \left\|f\left(\frac{k}{n}\right)-f(x)\right\|_\gamma Z(nx-k) +$$

$$\sum_{\begin{cases} k = \lceil na \rceil \\ \left\| \frac{k}{n} - x \right\|_{\infty} > \frac{1}{n^{\beta}} \end{cases}}^{\lfloor nb \rfloor} \left\| f\left(\frac{k}{n}\right) - f(x) \right\|_{\gamma} Z(nx-k) \overset{(16)}{\leq}$$

$$\omega_1\left(f, \frac{1}{n^{\beta}}\right) + 2\left\| \|f\|_{\gamma} \right\|_{\infty} \sum_{\begin{cases} k = \lceil na \rceil \\ \left\| \frac{k}{n} - x \right\|_{\infty} > \frac{1}{n^{\beta}} \end{cases}}^{\lfloor nb \rfloor} Z(nx-k) \overset{(21)}{\leq}$$

$$\omega_1\left(f, \frac{1}{n^{\beta}}\right) + \frac{2\left\| \|f\|_{\gamma} \right\|_{\infty}}{4m\left(n^{1-\beta}-2\right)^{2m}}. \tag{44}$$

So that

$$\|\Delta(x)\|_{\gamma} \leq \omega_1\left(f, \frac{1}{n^{\beta}}\right) + \frac{\left\| \|f\|_{\gamma} \right\|_{\infty}}{2m\left(n^{1-\beta}-2\right)^{2m}}. \tag{45}$$

Now using (34) we finish the proof. ■

We make

Remark 9 *([11], pp. 263-266) Let* $\left(\mathbb{R}^N, \|\cdot\|_p\right)$, $N \in \mathbb{N}$*; where* $\|\cdot\|_p$ *is the* L_p*-norm,* $1 \leq p \leq \infty$. $\mathbb{R}^N$ *is a Banach space, and* $\left(\mathbb{R}^N\right)^j$ *denotes the* j*-fold product space* $\mathbb{R}^N \times ... \times \mathbb{R}^N$ *endowed with the max-norm* $\|x\|_{(\mathbb{R}^N)^j} := \max_{1 \leq \lambda \leq j} \|x_{\lambda}\|_p$*, where* $x := (x_1, ..., x_j) \in \left(\mathbb{R}^N\right)^j$.

Let $\left(X, \|\cdot\|_{\gamma}\right)$ *be a general Banach space. Then the space* $L_j := L_j\left(\left(\mathbb{R}^N\right)^j; X\right)$ *of all* j*-multilinear continuous maps* $g : \left(\mathbb{R}^N\right)^j \to X$, $j = 1, ..., m$*, is a Banach space with norm*

$$\|g\| := \|g\|_{L_j} := \sup_{\left(\|x\|_{(\mathbb{R}^N)^j} = 1\right)} \|g(x)\|_{\gamma} = \sup \frac{\|g(x)\|_{\gamma}}{\|x_1\|_p ... \|x_j\|_p}. \tag{46}$$

Let M *be a non-empty convex and compact subset of* $\mathbb{R}^N$ *and* $x_0 \in M$ *is fixed.*

Let O *be an open subset of* $\mathbb{R}^N : M \subset O$*. Let* $f : O \to X$ *be a continuous function, whose Fréchet derivatives (see [21])* $f^{(j)} : O \to L_j = L_j\left(\left(\mathbb{R}^N\right)^j; X\right)$ *exist and are continuous for* $1 \leq j \leq \overline{m}$, $\overline{m} \in \mathbb{N}$.

Call $(x - x_0)^j := (x - x_0, ..., x - x_0) \in \left(\mathbb{R}^N\right)^j$, $x \in M$.

We will work with $f|_M$.

Then, by Taylor's formula ([14]), ([21], p. 124), we get

$$f(x) = \sum_{j=0}^{\overline{m}} \frac{f^{(j)}(x_0)(x-x_0)^j}{j!} + R_{\overline{m}}(x, x_0), \quad \text{all } x \in M, \tag{47}$$

where the remainder is the Riemann integral

$$R_{\overline{m}}(x,x_0) := \int_0^1 \frac{(1-u)^{\overline{m}-1}}{(\overline{m}-1)!}\left(f^{(\overline{m})}(x_0+u(x-x_0)) - f^{(\overline{m})}(x_0)\right)(x-x_0)^{\overline{m}}\,du, \tag{48}$$

here we set $f^{(0)}(x_0)(x-x_0)^0 = f(x_0)$.

We consider

$$w := \omega_1\left(f^{(\overline{m})},h\right) := \sup_{\substack{x,y\in M:\\ \|x-y\|_p\le h}} \left\|f^{(\overline{m})}(x) - f^{(\overline{m})}(y)\right\|, \tag{49}$$

$h > 0$.

We obtain

$$\left\|\left(f^{(\overline{m})}(x_0+u(x-x_0)) - f^{(\overline{m})}(x_0)\right)(x-x_0)^{\overline{m}}\right\|_\gamma \le$$
$$\left\|f^{(\overline{m})}(x_0+u(x-x_0)) - f^{(\overline{m})}(x_0)\right\|\cdot\|x-x_0\|_p^{\overline{m}} \le$$
$$w\,\|x-x_0\|_p^{\overline{m}}\left\lceil\frac{u\,\|x-x_0\|_p}{h}\right\rceil, \tag{50}$$

by Lemma 7.1.1, [1], p. 208, where $\lceil\cdot\rceil$ *is the ceiling.*

Therefore for all $x\in M$ *(see [1], pp. 121-122):*

$$\|R_{\overline{m}}(x,x_0)\|_\gamma \le w\,\|x-x_0\|_p^{\overline{m}}\int_0^1\left\lceil\frac{u\,\|x-x_0\|_p}{h}\right\rceil\frac{(1-u)^{\overline{m}-1}}{(\overline{m}-1)!}du$$
$$= \overline{w}\Phi_{\overline{m}}\left(\|x-x_0\|_p\right) \tag{51}$$

by a change of variable, where

$$\Phi_{\overline{m}}(t) := \int_0^{|t|}\left\lceil\frac{s}{h}\right\rceil\frac{(|t|-s)^{\overline{m}-1}}{(\overline{m}-1)!}ds = \frac{1}{\overline{m}!}\left(\sum_{j=0}^{\infty}(|t|-jh)_+^{\overline{m}}\right),\quad \forall\ t\in\mathbb{R}, \tag{52}$$

is a (polynomial) spline function, see [1], p. 210-211.

Also from there we get

$$\Phi_{\overline{m}}(t) \le \left(\frac{|t|^{\overline{m}+1}}{(\overline{m}+1)!h} + \frac{|t|^{\overline{m}}}{2\overline{m}!} + \frac{h\,|t|^{\overline{m}-1}}{8(\overline{m}-1)!}\right),\quad \forall\ t\in\mathbb{R}, \tag{53}$$

with equality true only at $t=0$.

Therefore it holds

$$\|R_{\overline{m}}(x,x_0)\|_\gamma \le w\left(\frac{\|x-x_0\|_p^{\overline{m}+1}}{(\overline{m}+1)!h} + \frac{\|x-x_0\|_p^{\overline{m}}}{2\overline{m}!} + \frac{h\,\|x-x_0\|_p^{\overline{m}-1}}{8(\overline{m}-1)!}\right),\quad \forall\ x\in M. \tag{54}$$

We have found that

$$\left\Vert f(x)-\sum_{j=0}^{\overline{m}}\frac{f^{(j)}(x_0)(x-x_0)^j}{j!}\right\Vert_{\gamma}\leq$$

$$\omega_1\left(f^{(\overline{m})},h\right)\left(\frac{\Vert x-x_0\Vert_p^{\overline{m}+1}}{(\overline{m}+1)!h}+\frac{\Vert x-x_0\Vert_p^{\overline{m}}}{2\overline{m}!}+\frac{h\Vert x-x_0\Vert_p^{\overline{m}-1}}{8(\overline{m}-1)!}\right)<\infty, \tag{55}$$

$\forall\ x,x_0\in M$.

Here $0<\omega_1\left(f^{(\overline{m})},h\right)<\infty$, *by* M *being compact and* $f^{(\overline{m})}$ *being continuous on* M.

One can rewrite (55) as follows:

$$\left\Vert f(\cdot)-\sum_{j=0}^{\overline{m}}\frac{f^{(j)}(x_0)(\cdot-x_0)^j}{j!}\right\Vert_{\gamma}\leq$$

$$\omega_1\left(f^{(\overline{m})},h\right)\left(\frac{\Vert\cdot-x_0\Vert_p^{\overline{m}+1}}{(\overline{m}+1)!h}+\frac{\Vert\cdot-x_0\Vert_p^{\overline{m}}}{2\overline{m}!}+\frac{h\Vert\cdot-x_0\Vert_p^{\overline{m}-1}}{8(\overline{m}-1)!}\right),\ \forall\ x_0\in M, \tag{56}$$

a pointwise functional inequality on M.

Here $(\cdot-x_0)^j$ *maps* M *into* $\left(\mathbb{R}^N\right)^j$ *and it is continuous, also* $f^{(j)}(x_0)$ *maps* $\left(\mathbb{R}^N\right)^j$ *into* X *and it is continuous. Hence their composition* $f^{(j)}(x_0)(\cdot-x_0)^j$ *is continuous from* M *into* X.

Clearly $f(\cdot)-\sum_{j=0}^{\overline{m}}\frac{f^{(j)}(x_0)(\cdot-x_0)^j}{j!}\in C(M,X)$, *hence* $\left\Vert f(\cdot)-\sum_{j=0}^{\overline{m}}\frac{f^{(j)}(x_0)(\cdot-x_0)^j}{j!}\right\Vert_{\gamma}\in C(M)$.

Let $\left\{\widetilde{L}_N\right\}_{N\in\mathbb{N}}$ *be a sequence of positive linear operators mapping* $C(M)$ *into* $C(M)$.

Therefore we obtain

$$\left(\widetilde{L}_N\left(\left\Vert f(\cdot)-\sum_{j=0}^{\overline{m}}\frac{f^{(j)}(x_0)(\cdot-x_0)^j}{j!}\right\Vert_{\gamma}\right)\right)(x_0)\leq$$

$$\omega_1\left(f^{(\overline{m})},h\right)\left[\frac{\left(\widetilde{L}_N\left(\Vert\cdot-x_0\Vert_p^{\overline{m}+1}\right)\right)(x_0)}{(\overline{m}+1)!h}+\frac{\left(\widetilde{L}_N\left(\Vert\cdot-x_0\Vert_p^{\overline{m}}\right)\right)(x_0)}{2\overline{m}!}\right.$$
$$\left.+\frac{h\left(\widetilde{L}_N\left(\Vert\cdot-x_0\Vert_p^{\overline{m}-1}\right)\right)(x_0)}{8(\overline{m}-1)!}\right], \tag{57}$$

$\forall\ N\in\mathbb{N},\ \forall\ x_0\in M$.

Clearly (57) is valid when $M = \prod_{i=1}^{N} [a_i, b_i]$ and $\widetilde{L}_n = \widetilde{A}_n$, see (26).

All the above is preparation for the following theorem, where we assume Fréchet differentiability of functions.

This will be a direct application of Theorem 10.2, [11], pp. 268-270. The operators A_n, $\widetilde{A}_n$ fulfill its assumptions, see (25), (26), (28), (29) and (30).

We present the following high order approximation results.

Theorem 10 *Let O open subset of $\left(\mathbb{R}^N, \|\cdot\|_p\right)$, $p \in [1, \infty]$, such that $\prod_{i=1}^{N} [a_i, b_i] \subset O \subseteq \mathbb{R}^N$, and let $\left(X, \|\cdot\|_\gamma\right)$ be a general Banach space. Let $\overline{m} \in \mathbb{N}$ and $f \in C^{\overline{m}}(O, X)$, the space of $\overline{m}$-times continuously Fréchet differentiable functions from O into X. We study the approximation of $f|_{\prod_{i=1}^{N} [a_i, b_i]}$. Let $x_0 \in \left(\prod_{i=1}^{N} [a_i, b_i]\right)$ and $r > 0$. Then*

1)

$$\left\| (A_n(f))(x_0) - \sum_{j=0}^{\overline{m}} \frac{1}{j!} \left(A_n \left(f^{(j)}(x_0)(\cdot - x_0)^j \right) \right)(x_0) \right\|_\gamma \leq$$

$$\frac{\omega_1 \left(f^{(\overline{m})}, r \left(\left(\widetilde{A}_n \left(\|\cdot - x_0\|_p^{\overline{m}+1} \right) \right)(x_0) \right)^{\frac{1}{\overline{m}+1}} \right)}{r \overline{m}!} \left(\left(\widetilde{A}_n \left(\|\cdot - x_0\|_p^{\overline{m}+1} \right) \right)(x_0) \right)^{\left(\frac{\overline{m}}{\overline{m}+1}\right)}$$

$$\left[\frac{1}{(\overline{m}+1)} + \frac{r}{2} + \frac{\overline{m} r^2}{8} \right], \tag{58}$$

2) additionally if $f^{(j)}(x_0) = 0$, $j = 1, ..., \overline{m}$, we have

$$\|(A_n(f))(x_0) - f(x_0)\|_\gamma \leq$$

$$\frac{\omega_1 \left(f^{(\overline{m})}, r \left(\left(\widetilde{A}_n \left(\|\cdot - x_0\|_p^{\overline{m}+1} \right) \right)(x_0) \right)^{\frac{1}{\overline{m}+1}} \right)}{r \overline{m}!} \left(\left(\widetilde{A}_n \left(\|\cdot - x_0\|_p^{\overline{m}+1} \right) \right)(x_0) \right)^{\left(\frac{\overline{m}}{\overline{m}+1}\right)} \tag{59}$$

$$\left[\frac{1}{(\overline{m}+1)} + \frac{r}{2} + \frac{\overline{m} r^2}{8} \right],$$

3)

$$\|(A_n(f))(x_0) - f(x_0)\|_\gamma \leq \sum_{j=1}^{\overline{m}} \frac{1}{j!} \left\| \left(A_n \left(f^{(j)}(x_0)(\cdot - x_0)^j \right) \right)(x_0) \right\|_\gamma +$$

$$\frac{\omega_1 \left(f^{(\overline{m})}, r \left(\left(\widetilde{A}_n \left(\|\cdot - x_0\|_p^{\overline{m}+1} \right) \right)(x_0) \right)^{\frac{1}{\overline{m}+1}} \right)}{r \overline{m}!} \left(\left(\widetilde{A}_n \left(\|\cdot - x_0\|_p^{\overline{m}+1} \right) \right)(x_0) \right)^{\left(\frac{\overline{m}}{\overline{m}+1}\right)} \tag{60}$$

$$\left[\frac{1}{(\overline{m}+1)}+\frac{r}{2}+\frac{\overline{m}r^2}{8}\right],$$

and

4)

$$\left\|\left\|A_n(f)-f\right\|_\gamma\right\|_{\infty,\prod_{i=1}^N[a_i,b_i]}\leq$$

$$\sum_{j=1}^{\overline{m}}\frac{1}{j!}\left\|\left\|\left(A_n\left(f^{(j)}(x_0)(\cdot-x_0)^j\right)\right)(x_0)\right\|_\gamma\right\|_{\infty,x_0\in\prod_{i=1}^N[a_i,b_i]}+$$

$$\frac{\omega_1\left(f^{(\overline{m})},r\left\|\left(\widetilde{A}_n\left(\|\cdot-x_0\|_p^{\overline{m}+1}\right)\right)(x_0)\right\|_{\infty,x_0\in\prod_{i=1}^N[a_i,b_i]}^{\frac{1}{\overline{m}+1}}\right)}{r\overline{m}!}$$

$$\left\|\left(\widetilde{A}_n\left(\|\cdot-x_0\|_p^{\overline{m}+1}\right)\right)(x_0)\right\|_{\infty,x_0\in\prod_{i=1}^N[a_i,b_i]}^{\left(\frac{\overline{m}}{\overline{m}+1}\right)} \quad (61)$$

$$\left[\frac{1}{(\overline{m}+1)}+\frac{r}{2}+\frac{\overline{m}r^2}{8}\right].$$

We need

Lemma 11 *The function* $\left(\widetilde{A}_n\left(\|\cdot-x_0\|_p^{\overline{m}}\right)\right)(x_0)$ *is continuous in* $x_0\in\left(\prod_{i=1}^N[a_i,b_i]\right)$, $\overline{m}\in\mathbb{N}$.

Proof. By Lemma 10.3, [11], p. 272. ■

We give

Corollary 12 *(to Theorem 10, case of* $\overline{m}=1$*) Then*

1)

$$\|(A_n(f))(x_0)-f(x_0)\|_\gamma\leq\left\|\left(A_n\left(f^{(1)}(x_0)(\cdot-x_0)\right)\right)(x_0)\right\|_\gamma+$$

$$\frac{1}{2r}\omega_1\left(f^{(1)},r\left(\left(\widetilde{A}_n\left(\|\cdot-x_0\|_p^2\right)\right)(x_0)\right)^{\frac{1}{2}}\right)\left(\left(\widetilde{A}_n\left(\|\cdot-x_0\|_p^2\right)\right)(x_0)\right)^{\frac{1}{2}} \quad (62)$$

$$\left[1+r+\frac{r^2}{4}\right],$$

and

2)

$$\left\|\left\|(A_n(f))-f\right\|_\gamma\right\|_{\infty,\prod_{i=1}^N[a_i,b_i]}\leq$$

$$\left\|\left\|\left(A_n\left(f^{(1)}\left(x_0\right)\left(\cdot-x_0\right)\right)\right)\left(x_0\right)\right\|_\gamma\right\|_{\infty, x_0 \in \prod_{i=1}^N\left[a_i, b_i\right]}+$$

$$\frac{1}{2 r} \omega_1\left(f^{(1)}, r\left\|\left(\widetilde{A}_n\left(\|\cdot-x_0\|_p^2\right)\right)\left(x_0\right)\right\|_{\infty, x_0 \in \prod_{i=1}^N\left[a_i, b_i\right]}^{\frac{1}{2}}\right)$$

$$\left\|\left(\widetilde{A}_n\left(\|\cdot-x_0\|_p^2\right)\right)\left(x_0\right)\right\|_{\infty, x_0 \in \prod_{i=1}^N\left[a_i, b_i\right]}^{\frac{1}{2}}\left[1+r+\frac{r^2}{4}\right], \tag{63}$$

$r>0$.

We make

Remark 13 *We estimate* $0<\alpha<1$, $m, \overline{m}, n \in \mathbb{N}: n^{1-\alpha}>2$,

$$\widetilde{A}_n\left(\|\cdot-x_0\|_{\infty}^{\overline{m}+1}\right)\left(x_0\right)=\frac{\sum_{k=\lceil n a\rceil}^{\lfloor n b\rfloor}\left\|\frac{k}{n}-x_0\right\|_{\infty}^{\overline{m}+1} Z\left(n x_0-k\right)}{\sum_{k=\lceil n a\rceil}^{\lfloor n b\rfloor} Z\left(n x_0-k\right)} \overset{(22)}{<}$$

$$\left[2\left(\sqrt[2m]{1+4^m}\right)\right]^N \sum_{k=\lceil n a\rceil}^{\lfloor n b\rfloor}\left\|\frac{k}{n}-x_0\right\|_{\infty}^{\overline{m}+1} Z\left(n x_0-k\right)= \tag{64}$$

$$\left[2\left(\sqrt[2m]{1+4^m}\right)\right]^N\left\{\sum_{\left\{\begin{array}{c}k=\lceil n a\rceil \\ :\left\|\frac{k}{n}-x_0\right\|_{\infty} \leq \frac{1}{n^\alpha}\end{array}\right.}^{\lfloor n b\rfloor}\left\|\frac{k}{n}-x_0\right\|_{\infty}^{\overline{m}+1} Z\left(n x_0-k\right)+\right.$$

$$\left.\sum_{\left\{\begin{array}{c}k=\lceil n a\rceil \\ :\left\|\frac{k}{n}-x_0\right\|_{\infty}>\frac{1}{n^\alpha}\end{array}\right.}^{\lfloor n b\rfloor}\left\|\frac{k}{n}-x_0\right\|_{\infty}^{\overline{m}+1} Z\left(n x_0-k\right)\right\} \overset{(23)}{\leq}$$

$$\left[2\left(\sqrt[2m]{1+4^m}\right)\right]^N\left\{\frac{1}{n^{\alpha(\overline{m}+1)}}+\frac{\|b-a\|_{\infty}^{\overline{m}+1}}{4 m\left(n^{1-\alpha}-2\right)^{2 m}}\right\}, \tag{65}$$

(where $b-a=\left(b_1-a_1, \ldots, b_N-a_N\right)$*).*

We have proved that ($\forall$ $x_0 \in \prod_{i=1}^N\left[a_i, b_i\right]$)

$$\widetilde{A}_n\left(\|\cdot-x_0\|_{\infty}^{\overline{m}+1}\right)\left(x_0\right)<\left[2\left(\sqrt[2m]{1+4^m}\right)\right]^N\left\{\frac{1}{n^{\alpha(\overline{m}+1)}}+\frac{\|b-a\|_{\infty}^{\overline{m}+1}}{4 m\left(n^{1-\alpha}-2\right)^{2 m}}\right\}=: \varphi_1(n) \tag{66}$$

($0<\alpha<1$*,* $m,\overline{m},n\in\mathbb{N}:n^{1-\alpha}>2$*).*

And, consequently it holds

$$\left\|\widetilde{A}_n\left(\|\cdot-x_0\|_\infty^{\overline{m}+1}\right)(x_0)\right\|_{\infty,x_0\in\prod_{i=1}^N[a_i,b_i]}<$$

$$\left[2\left(\sqrt[2m]{1+4^m}\right)\right]^N\left\{\frac{1}{n^{\alpha(\overline{m}+1)}}+\frac{\|b-a\|_\infty^{\overline{m}+1}}{4m\left(n^{1-\alpha}-2\right)^{2m}}\right\}=\varphi_1(n)\to 0,\quad as\ n\to+\infty. \tag{67}$$

So, we have that $\varphi_1(n)\to 0$*, as* $n\to+\infty$*. Thus, when* $p\in[1,\infty]$*, from Theorem 10 we have the convergence to zero in the right hand sides of parts (1), (2).*

Next we estimate $\left\|\left(\widetilde{A}_n\left(f^{(j)}(x_0)(\cdot-x_0)^j\right)\right)(x_0)\right\|_\gamma$.

We have that

$$\left(\widetilde{A}_n\left(f^{(j)}(x_0)(\cdot-x_0)^j\right)\right)(x_0)=\frac{\sum_{k=\lceil na\rceil}^{\lfloor nb\rfloor}f^{(j)}(x_0)\left(\frac{k}{n}-x_0\right)^jZ(nx_0-k)}{\sum_{k=\lceil na\rceil}^{\lfloor nb\rfloor}Z(nx_0-k)}. \tag{68}$$

When $p=\infty$*,* $j=1,...,\overline{m}$*, we obtain*

$$\left\|f^{(j)}(x_0)\left(\frac{k}{n}-x_0\right)^j\right\|_\gamma\leq\left\|f^{(j)}(x_0)\right\|\left\|\frac{k}{n}-x_0\right\|_\infty^j. \tag{69}$$

We further have that

$$\left\|\left(\widetilde{A}_n\left(f^{(j)}(x_0)(\cdot-x_0)^j\right)\right)(x_0)\right\|_\gamma\overset{(22)}{<}$$

$$\left[2\left(\sqrt[2m]{1+4^m}\right)\right]^N\left(\sum_{k=\lceil na\rceil}^{\lfloor nb\rfloor}\left\|f^{(j)}(x_0)\left(\frac{k}{n}-x_0\right)^j\right\|_\gamma Z(nx_0-k)\right)\leq$$

$$\left[2\left(\sqrt[2m]{1+4^m}\right)\right]^N\left(\sum_{k=\lceil na\rceil}^{\lfloor nb\rfloor}\left\|f^{(j)}(x_0)\right\|\left\|\frac{k}{n}-x_0\right\|_\infty^jZ(nx_0-k)\right)= \tag{70}$$

$$\left[2\left(\sqrt[2m]{1+4^m}\right)\right]^N\left\|f^{(j)}(x_0)\right\|\left(\sum_{k=\lceil na\rceil}^{\lfloor nb\rfloor}\left\|\frac{k}{n}-x_0\right\|_\infty^jZ(nx_0-k)\right)=$$

$$\left[2\left(\sqrt[2m]{1+4^m}\right)\right]^N\left\|f^{(j)}(x_0)\right\|\left\{\sum_{\begin{cases}k=\lceil na\rceil\\:\left\|\frac{k}{n}-x_0\right\|_\infty\leq\frac{1}{n^\alpha}\end{cases}}^{\lfloor nb\rfloor}\left\|\frac{k}{n}-x_0\right\|_\infty^jZ(nx_0-k)\right.$$

$$+\left.\sum_{\substack{k=\lceil na\rceil \\ :\left\|\frac{k}{n}-x_0\right\|_{\infty}>\frac{1}{n^{\alpha}}}}^{\lfloor nb\rfloor}\left\|\frac{k}{n}-x_0\right\|_{\infty}^{j}Z\left(nx_0-k\right)\right\}\overset{(21)}{\leq} \tag{71}$$

$$\left[2\left(\sqrt[2m]{1+4^m}\right)\right]^N\left\|f^{(j)}\left(x_0\right)\right\|\left\{\frac{1}{n^{\alpha j}}+\frac{\|b-a\|_{\infty}^{j}}{4m\left(n^{1-\alpha}-2\right)^{2m}}\right\}\rightarrow 0,\ as\ n\rightarrow\infty.$$

That is

$$\left\|\left(\widetilde{A}_n\left(f^{(j)}\left(x_0\right)\left(\cdot-x_0\right)^j\right)\right)\left(x_0\right)\right\|_{\gamma}\rightarrow 0,\ as\ n\rightarrow\infty.$$

Therefore when $p=\infty$, *for* $j=1,...,\overline{m}$, *we have proved:*

$$\left\|\left(\widetilde{A}_n\left(f^{(j)}\left(x_0\right)\left(\cdot-x_0\right)^j\right)\right)\left(x_0\right)\right\|_{\gamma}<$$

$$\left[2\left(\sqrt[2m]{1+4^m}\right)\right]^N\left\|f^{(j)}\left(x_0\right)\right\|\left\{\frac{1}{n^{\alpha j}}+\frac{\|b-a\|_{\infty}^{j}}{4m\left(n^{1-\alpha}-2\right)^{2m}}\right\}\leq \tag{72}$$

$$\left[2\left(\sqrt[2m]{1+4^m}\right)\right]^N\left\|f^{(j)}\right\|_{\infty}\left\{\frac{1}{n^{\alpha j}}+\frac{\|b-a\|_{\infty}^{j}}{4m\left(n^{1-\alpha}-2\right)^{2m}}\right\}=:\varphi_{2j}\left(n\right)<\infty,$$

and converges to zero, as $n\rightarrow\infty$.

We conclude:

In Theorem 10, the right hand sides of (60) and (61) converge to zero as $n\rightarrow\infty$, for any $p\in[1,\infty]$.

Also in Corollary 12, the right hand sides of (62) and (63) converge to zero as $n\rightarrow\infty$, for any $p\in[1,\infty]$.

Conclusion 14 *We have proved that the left hand sides of (58), (59), (60), (61) and (62), (63) converge to zero as* $n\rightarrow\infty$, *for* $p\in[1,\infty]$. *Consequently* $A_n\rightarrow I$ *(unit operator) pointwise and uniformly, as* $n\rightarrow\infty$, *where* $p\in[1,\infty]$. *In the presence of initial conditions we achieve a higher speed of convergence, see (59). Higher speed of convergence happens also to the left hand side of (58).*

We further give

Corollary 15 *(to Theorem 10) Let* O *open subset of* $\left(\mathbb{R}^N,\|\cdot\|_{\infty}\right)$, *such that* $\prod_{i=1}^{N}[a_i,b_i]\subset O\subseteq\mathbb{R}^N$, *and let* $\left(X,\|\cdot\|_{\gamma}\right)$ *be a general Banach space. Let* $\overline{m}\in\mathbb{N}$ *and* $f\in C^{\overline{m}}(O,X)$, *the space of* $\overline{m}$*-times continuously Fréchet differentiable functions from* O *into* X. *We study the approximation of* $f|_{\prod_{i=1}^{N}[a_i,b_i]}$. *Let* $x_0\in$

$\left(\prod_{i=1}^{N}[a_i,b_i]\right)$ *and* $r>0$. *Here* $\varphi_1(n)$ *as in (66) and* $\varphi_{2j}(n)$ *as in (72), where* $n\in\mathbb{N}:n^{1-\alpha}>2$, $0<\alpha<1$, $j=1,...,\overline{m}$. *Then*

1)

$$\left\|\left(A_n(f)\right)(x_0)-\sum_{j=0}^{\overline{m}}\frac{1}{j!}\left(A_n\left(f^{(j)}(x_0)(\cdot-x_0)^j\right)\right)(x_0)\right\|_{\gamma}\leq$$

$$\frac{\omega_1\left(f^{(\overline{m})},r(\varphi_1(n))^{\frac{1}{\overline{m}+1}}\right)}{r\overline{m}!}(\varphi_1(n))^{\left(\frac{\overline{m}}{\overline{m}+1}\right)}\left[\frac{1}{(\overline{m}+1)}+\frac{r}{2}+\frac{\overline{m}r^2}{8}\right], \tag{73}$$

2) additionally, if $f^{(j)}(x_0)=0$, $j=1,...,\overline{m}$, *we have*

$$\left\|\left(A_n(f)\right)(x_0)-f(x_0)\right\|_{\gamma}\leq$$

$$\frac{\omega_1\left(f^{(\overline{m})},r(\varphi_1(n))^{\frac{1}{\overline{m}+1}}\right)}{r\overline{m}!}(\varphi_1(n))^{\left(\frac{\overline{m}}{\overline{m}+1}\right)}\left[\frac{1}{(\overline{m}+1)}+\frac{r}{2}+\frac{\overline{m}r^2}{8}\right], \tag{74}$$

3)

$$\left\|\left\|A_n(f)-f\right\|_{\gamma}\right\|_{\infty,\prod_{i=1}^{N}[a_i,b_i]}\leq\sum_{j=1}^{\overline{m}}\frac{\varphi_{2j}(n)}{j!}+$$

$$\frac{\omega_1\left(f^{(\overline{m})},r(\varphi_1(n))^{\frac{1}{\overline{m}+1}}\right)}{r\overline{m}!}(\varphi_1(n))^{\left(\frac{\overline{m}}{\overline{m}+1}\right)} \tag{75}$$

$$\left[\frac{1}{(\overline{m}+1)}+\frac{r}{2}+\frac{\overline{m}r^2}{8}\right]=:\varphi_3(n)\to0,\text{ as }n\to\infty.$$

We continue with

Theorem 16 *Let* $f\in C_B\left(\mathbb{R}^N,X\right)$, $0<\beta<1$, $x\in\mathbb{R}^N$, $m,N,n\in\mathbb{N}$ *with* $n^{1-\beta}>2$, ω_1 *is for* $p=\infty$. *Then*

1)

$$\left\|B_n(f,x)-f(x)\right\|_{\gamma}\leq\omega_1\left(f,\frac{1}{n^{\beta}}\right)+\frac{\left\|\left\|f\right\|_{\gamma}\right\|_{\infty}}{2m\left(n^{1-\beta}-2\right)^{2m}}=:\lambda_2(n), \tag{76}$$

2)

$$\left\|\left\|B_n(f)-f\right\|_{\gamma}\right\|_{\infty}\leq\lambda_2(n). \tag{77}$$

Given that $f\in\left(C_U\left(\mathbb{R}^N,X\right)\cap C_B\left(\mathbb{R}^N,X\right)\right)$, *we obtain* $\lim_{n\to\infty}B_n(f)=f$, *uniformly.*

Proof. We have that

$$B_n(f,x) - f(x) \overset{(16)}{=} \sum_{k=-\infty}^{\infty} f\left(\frac{k}{n}\right) Z(nx-k) - f(x) \sum_{k=-\infty}^{\infty} Z(nx-k) = \tag{78}$$

$$\sum_{k=-\infty}^{\infty} \left(f\left(\frac{k}{n}\right) - f(x)\right) Z(nx-k).$$

Hence

$$\left\|B_n(f,x) - f(x)\right\|_\gamma \leq \sum_{k=-\infty}^{\infty} \left\|f\left(\frac{k}{n}\right) - f(x)\right\|_\gamma Z(nx-k) =$$

$$\sum_{\begin{cases} k=-\infty \\ \left\|\frac{k}{n}-x\right\|_\infty \leq \frac{1}{n^\beta} \end{cases}}^{\infty} \left\|f\left(\frac{k}{n}\right) - f(x)\right\|_\gamma Z(nx-k) +$$

$$\sum_{\begin{cases} k=-\infty \\ \left\|\frac{k}{n}-x\right\|_\infty > \frac{1}{n^\beta} \end{cases}}^{\infty} \left\|f\left(\frac{k}{n}\right) - f(x)\right\|_\gamma Z(nx-k) \overset{(16)}{\leq}$$

$$\omega_1\left(f, \frac{1}{n^\beta}\right) + 2\left\|\|f\|_\gamma\right\|_\infty \sum_{\begin{cases} k=-\infty \\ \left\|\frac{k}{n}-x\right\|_\infty > \frac{1}{n^\beta} \end{cases}}^{\infty} Z(nx-k) \overset{(23)}{\leq}$$

$$\omega_1\left(f, \frac{1}{n^\beta}\right) + \frac{\left\|\|f\|_\gamma\right\|_\infty}{2m\left(n^{1-\beta}-2\right)^{2m}}, \tag{79}$$

proving the claim. ■

We give

Theorem 17 *Let $f \in C_B\left(\mathbb{R}^N, X\right)$, $0 < \beta < 1$, $x \in \mathbb{R}^N$, $m, N, n \in \mathbb{N}$ with $n^{1-\beta} > 2$, ω_1 is for $p = \infty$. Then*

1)

$$\left\|C_n(f,x) - f(x)\right\|_\gamma \leq \omega_1\left(f, \frac{1}{n} + \frac{1}{n^\beta}\right) + \frac{\left\|\|f\|_\gamma\right\|_\infty}{2m\left(n^{1-\beta}-2\right)^{2m}} =: \lambda_3(n), \tag{80}$$

2)

$$\left\|\left\|C_n(f) - f\right\|_\gamma\right\|_\infty \leq \lambda_3(n). \tag{81}$$

Given that $f \in \left(C_U\left(\mathbb{R}^N, X\right) \cap C_B\left(\mathbb{R}^N, X\right)\right)$, we obtain $\lim_{n\to\infty} C_n(f) = f$, uniformly.

Proof. We notice that

$$\int_{\frac{k}{n}}^{\frac{k+1}{n}} f(t)\,dt = \int_{\frac{k_1}{n}}^{\frac{k_1+1}{n}} \int_{\frac{k_2}{n}}^{\frac{k_2+1}{n}} \ldots \int_{\frac{k_N}{n}}^{\frac{k_N+1}{n}} f(t_1, t_2, \ldots, t_N)\, dt_1 dt_2 \ldots dt_N =$$

$$\int_0^{\frac{1}{n}} \int_0^{\frac{1}{n}} \ldots \int_0^{\frac{1}{n}} f\left(t_1 + \frac{k_1}{n}, t_2 + \frac{k_2}{n}, \ldots, t_N + \frac{k_N}{n}\right) dt_1 \ldots dt_N = \int_0^{\frac{1}{n}} f\left(t + \frac{k}{n}\right) dt. \tag{82}$$

Thus it holds (by (38))

$$C_n(f,x) = \sum_{k=-\infty}^{\infty} \left(n^N \int_0^{\frac{1}{n}} f\left(t + \frac{k}{n}\right) dt\right) Z(nx-k). \tag{83}$$

We observe that

$$\|C_n(f,x) - f(x)\|_\gamma =$$

$$\left\| \sum_{k=-\infty}^{\infty} \left(n^N \int_0^{\frac{1}{n}} f\left(t + \frac{k}{n}\right) dt\right) Z(nx-k) - \sum_{k=-\infty}^{\infty} f(x) Z(nx-k) \right\|_\gamma =$$

$$\left\| \sum_{k=-\infty}^{\infty} \left(\left(n^N \int_0^{\frac{1}{n}} f\left(t + \frac{k}{n}\right) dt\right) - f(x) \right) Z(nx-k) \right\|_\gamma =$$

$$\left\| \sum_{k=-\infty}^{\infty} \left(n^N \int_0^{\frac{1}{n}} \left(f\left(t + \frac{k}{n}\right) - f(x)\right) dt\right) Z(nx-k) \right\|_\gamma \leq \tag{84}$$

$$\sum_{k=-\infty}^{\infty} \left(n^N \int_0^{\frac{1}{n}} \left\|f\left(t + \frac{k}{n}\right) - f(x)\right\|_\gamma dt\right) Z(nx-k) =$$

$$\sum_{\substack{k=-\infty \\ \left\|\frac{k}{n} - x\right\|_\infty \leq \frac{1}{n^\beta}}}^{\infty} \left(n^N \int_0^{\frac{1}{n}} \left\|f\left(t + \frac{k}{n}\right) - f(x)\right\|_\gamma dt\right) Z(nx-k) +$$

$$\sum_{\substack{k=-\infty \\ \left\|\frac{k}{n} - x\right\|_\infty > \frac{1}{n^\beta}}}^{\infty} \left(n^N \int_0^{\frac{1}{n}} \left\|f\left(t + \frac{k}{n}\right) - f(x)\right\|_\gamma dt\right) Z(nx-k) \leq$$

$$\sum_{\substack{k=-\infty \\ \left\|\frac{k}{n} - x\right\|_\infty \leq \frac{1}{n^\beta}}}^{\infty} \left(n^N \int_0^{\frac{1}{n}} \omega_1\left(f, \|t\|_\infty + \left\|\frac{k}{n} - x\right\|_\infty\right) dt\right) Z(nx-k) +$$

$$2\left\|\left\|f\right\|_{\gamma}\right\|_{\infty}\left(\sum_{\left\{\begin{array}{c}k=-\infty\\ \left\|\frac{k}{n}-x\right\|_{\infty}>\frac{1}{n^{\beta}}\end{array}\right.}^{\infty} Z\left(\left|nx-k\right|\right)\right)\leq$$

$$\omega_{1}\left(f,\frac{1}{n}+\frac{1}{n^{\beta}}\right)+\frac{\left\|\left\|f\right\|_{\gamma}\right\|_{\infty}}{2m\left(n^{1-\beta}-2\right)^{2m}}, \tag{85}$$

proving the claim. ■

We also present

Theorem 18 *Let* $f\in C_{B}\left(\mathbb{R}^{N},X\right)$, $0<\beta<1$, $x\in\mathbb{R}^{N}$, $m,N,n\in\mathbb{N}$ *with* $n^{1-\beta}>2$, ω_{1} *is for* $p=\infty$. *Then*

1)

$$\left\|D_{n}\left(f,x\right)-f\left(x\right)\right\|_{\gamma}\leq\omega_{1}\left(f,\frac{1}{n}+\frac{1}{n^{\beta}}\right)+\frac{\left\|\left\|f\right\|_{\gamma}\right\|_{\infty}}{2m\left(n^{1-\beta}-2\right)^{2m}}=\lambda_{4}\left(n\right), \tag{86}$$

2)

$$\left\|\left\|D_{n}\left(f\right)-f\right\|_{\gamma}\right\|_{\infty}\leq\lambda_{4}\left(n\right). \tag{87}$$

Given that $f\in\left(C_{U}\left(\mathbb{R}^{N},X\right)\cap C_{B}\left(\mathbb{R}^{N},X\right)\right)$, *we obtain* $\lim_{n\rightarrow\infty}D_{n}\left(f\right)=f$, *uniformly.*

Proof. We have that (by (40))

$$\left\|D_{n}\left(f,x\right)-f\left(x\right)\right\|_{\gamma}=\left\|\sum_{k=-\infty}^{\infty}\delta_{nk}\left(f\right)Z\left(nx-k\right)-\sum_{k=-\infty}^{\infty}f\left(x\right)Z\left(nx-k\right)\right\|_{\gamma}= \tag{88}$$

$$\left\|\sum_{k=-\infty}^{\infty}\left(\delta_{nk}\left(f\right)-f\left(x\right)\right)Z\left(nx-k\right)\right\|_{\gamma}=$$

$$\left\|\sum_{k=-\infty}^{\infty}\left(\sum_{r=0}^{\theta}w_{r}\left(f\left(\frac{k}{n}+\frac{r}{n\theta}\right)-f\left(x\right)\right)\right)Z\left(nx-k\right)\right\|_{\gamma}\leq$$

$$\sum_{k=-\infty}^{\infty}\left(\sum_{r=0}^{\theta}w_{r}\left\|f\left(\frac{k}{n}+\frac{r}{n\theta}\right)-f\left(x\right)\right\|_{\gamma}\right)Z\left(nx-k\right)=$$

$$\sum_{\left\{\begin{array}{c}k=-\infty\\ \left\|\frac{k}{n}-x\right\|_{\infty}\leq\frac{1}{n^{\beta}}\end{array}\right.}^{\infty}\left(\sum_{r=0}^{\theta}w_{r}\left\|f\left(\frac{k}{n}+\frac{r}{n\theta}\right)-f\left(x\right)\right\|_{\gamma}\right)Z\left(nx-k\right)+$$

$$\sum_{\begin{cases} k=-\infty \\ \left\|\frac{k}{n}-x\right\|_{\infty}>\frac{1}{n^{\beta}} \end{cases}}^{\infty} \left(\sum_{r=0}^{\theta} w_r \left\| f\left(\frac{k}{n}+\frac{r}{n\theta}\right)-f(x)\right\|_{\gamma}\right) Z(nx-k) \leq$$

$$\sum_{\begin{cases} k=-\infty \\ \left\|\frac{k}{n}-x\right\|_{\infty}\leq\frac{1}{n^{\beta}} \end{cases}}^{\infty} \left(\sum_{r=0}^{\theta} w_r \omega_1\left(f, \left\|\frac{k}{n}-x\right\|_{\infty}+\left\|\frac{r}{n\theta}\right\|_{\infty}\right)\right) Z(nx-k)+$$

$$2\left\|\|f\|_{\gamma}\right\|_{\infty}\left(\sum_{\begin{cases} k=-\infty \\ \left\|\frac{k}{n}-x\right\|_{\infty}>\frac{1}{n^{\beta}} \end{cases}}^{\infty} Z(nx-k)\right) \leq$$

$$\omega_1\left(f,\frac{1}{n}+\frac{1}{n^{\beta}}\right)+\frac{\left\|\|f\|_{\gamma}\right\|_{\infty}}{2m\left(n^{1-\beta}-2\right)^{2m}}, \tag{89}$$

proving the claim. ■

We make

Definition 19 *Let $f \in C_B\left(\mathbb{R}^N, X\right)$, $N \in \mathbb{N}$, where $\left(X, \|\cdot\|_{\gamma}\right)$ is a Banach space. We define the general neural network operator*

$$F_n(f,x) := \sum_{k=-\infty}^{\infty} l_{nk}(f)\, Z(nx-k) =$$

$$\begin{cases} B_n(f,x), & \text{if } l_{nk}(f) = f\left(\frac{k}{n}\right), \\ C_n(f,x), & \text{if } l_{nk}(f) = n^N \int_{\frac{k}{n}}^{\frac{k+1}{n}} f(t)\,dt, \\ D_n(f,x), & \text{if } l_{nk}(f) = \delta_{nk}(f). \end{cases} \tag{90}$$

Clearly $l_{nk}(f)$ is an X-valued bounded linear functional such that $\|l_{nk}(f)\|_{\gamma} \leq \left\|\|f\|_{\gamma}\right\|_{\infty}$.

Hence $F_n(f)$ is a bounded linear operator with $\left\|\|F_n(f)\|_{\gamma}\right\|_{\infty} \leq \left\|\|f\|_{\gamma}\right\|_{\infty}$.

We need

Theorem 20 *Let $f \in C_B\left(\mathbb{R}^N, X\right)$, $N \geq 1$. Then $F_n(f) \in C_B\left(\mathbb{R}^N, X\right)$.*

Proof. Clearly $F_n(f)$ is a bounded function.

Next we prove the continuity of $F_n(f)$. Notice for $N=1$, $Z=\Phi$ by (14).

We will use the generalized Weierstrass M test: If a sequence of positive constants $M_1, M_2, M_3, \ldots$, can be found such that in some interval

(a) $\|u_n(x)\|_\gamma \leq M_n, \ n = 1, 2, 3, ...$

(b) $\sum M_n$ converges,

then $\sum u_n(x)$ is uniformly and absolutely convergent in the interval.

Also we will use:

If $\{u_n(x)\}$, $n = 1, 2, 3, ...$ are continuous in $[a, b]$ and if $\sum u_n(x)$ converges uniformly to the sum $S(x)$ in $[a, b]$, then $S(x)$ is continuous in $[a, b]$. I.e. a uniformly convergent series of continuous functions is a continuous function. First we prove claim for $N = 1$.

We will prove that $\sum_{k=-\infty}^{\infty} l_{nk}(f)\, \Phi(nx - k)$ is continuous in $x \in \mathbb{R}$.

There always exists $\lambda \in \mathbb{N}$ such that $nx \in [-\lambda, \lambda]$.

Since $nx \leq \lambda$, then $-nx \geq -\lambda$ and $k - nx \geq k - \lambda \geq 0$, when $k \geq \lambda$. Therefore

$$\sum_{k=\lambda}^{\infty} \Phi(nx - k) = \sum_{k=\lambda}^{\infty} \Phi(k - nx) \leq \sum_{k=\lambda}^{\infty} \Phi(k - \lambda) = \sum_{k'=0}^{\infty} \Phi(k') \leq 1. \tag{91}$$

So for $k \geq \lambda$ we get

$$\|l_{nk}(f)\|_\gamma \, \Phi(nx - k) \leq \left\| \|f\|_\gamma \right\|_\infty \Phi(k - \lambda),$$

and

$$\left\| \|f\|_\gamma \right\|_\infty \sum_{k=\lambda}^{\infty} \Phi(k - \lambda) \leq \left\| \|f\|_\gamma \right\|_\infty.$$

Hence by the generalized Weierstrass M test we obtain that $\sum_{k=\lambda}^{\infty} l_{nk}(f)\, \Phi(nx - k)$ is uniformly and absolutely convergent on $\left[-\frac{\lambda}{n}, \frac{\lambda}{n}\right]$.

Since $l_{nk}(f)\, \Phi(nx - k)$ is continuous in x, then $\sum_{k=\lambda}^{\infty} l_{nk}(f)\, \Phi(nx - k)$ is continuous on $\left[-\frac{\lambda}{n}, \frac{\lambda}{n}\right]$.

Because $nx \geq -\lambda$, then $-nx \leq \lambda$, and $k - nx \leq k + \lambda \leq 0$, when $k \leq -\lambda$. Therefore

$$\sum_{k=-\infty}^{-\lambda} \Phi(nx - k) = \sum_{k=-\infty}^{-\lambda} \Phi(k - nx) \leq \sum_{k=-\infty}^{-\lambda} \Phi(k + \lambda) = \sum_{k'=-\infty}^{0} \Phi(k') \leq 1.$$

So for $k \leq -\lambda$ we get

$$\|l_{nk}(f)\|_\gamma \, \Phi(nx - k) \leq \left\| \|f\|_\gamma \right\|_\infty \Phi(k + \lambda), \tag{92}$$

and

$$\left\| \|f\|_\gamma \right\|_\infty \sum_{k=-\infty}^{-\lambda} \Phi(k + \lambda) \leq \left\| \|f\|_\gamma \right\|_\infty.$$

Hence by Weierstrass M test we obtain that $\sum_{k=-\infty}^{-\lambda} l_{nk}(f)\, \Phi(nx - k)$ is uniformly and absolutely convergent on $\left[-\frac{\lambda}{n}, \frac{\lambda}{n}\right]$.

Since $l_{nk}(f)\Phi(nx-k)$ is continuous in x, then $\sum_{k=-\infty}^{-\lambda} l_{nk}(f)\Phi(nx-k)$ is continuous on $\left[-\frac{\lambda}{n},\frac{\lambda}{n}\right]$.

So we proved that $\sum_{k=\lambda}^{\infty} l_{nk}(f)\Phi(nx-k)$ and $\sum_{k=-\infty}^{-\lambda} l_{nk}(f)\Phi(nx-k)$ are continuous on $\mathbb{R}$. Since $\sum_{k=-\lambda+1}^{\lambda-1} l_{nk}(f)\Phi(nx-k)$ is a finite sum of continuous functions on $\mathbb{R}$, it is also a continuous function on $\mathbb{R}$.

Writing

$$\sum_{k=-\infty}^{\infty} l_{nk}(f)\Phi(nx-k)=\sum_{k=-\infty}^{-\lambda} l_{nk}(f)\Phi(nx-k)+$$

$$\sum_{k=-\lambda+1}^{\lambda-1} l_{nk}(f)\Phi(nx-k)+\sum_{k=\lambda}^{\infty} l_{nk}(f)\Phi(nx-k) \tag{93}$$

we have it as a continuous function on $\mathbb{R}$. Therefore $F_n(f)$, when $N=1$, is a continuous function on $\mathbb{R}$.

When $N=2$ we have

$$F_n(f,x_1,x_2)=\sum_{k_1=-\infty}^{\infty}\sum_{k_2=-\infty}^{\infty} l_{nk}(f)\Phi(nx_1-k_1)\Phi(nx_2-k_2)=$$

$$\sum_{k_1=-\infty}^{\infty}\Phi(nx_1-k_1)\left(\sum_{k_2=-\infty}^{\infty} l_{nk}(f)\Phi(nx_2-k_2)\right)$$

(there always exist $\lambda_1,\lambda_2\in\mathbb{N}$ such that $nx_1\in[-\lambda_1,\lambda_1]$ and $nx_2\in[-\lambda_2,\lambda_2]$)

$$=\sum_{k_1=-\infty}^{\infty}\Phi(nx_1-k_1)\left[\sum_{k_2=-\infty}^{-\lambda_2} l_{nk}(f)\Phi(nx_2-k_2)+\right.$$

$$\left.\sum_{k_2=-\lambda_2+1}^{\lambda_2-1} l_{nk}(f)\Phi(nx_2-k_2)+\sum_{k_2=\lambda_2}^{\infty} l_{nk}(f)\Phi(nx_2-k_2)\right]=$$

$$=\sum_{k_1=-\infty}^{\infty}\sum_{k_2=-\infty}^{-\lambda_2} l_{nk}(f)\Phi(nx_1-k_1)\Phi(nx_2-k_2)+$$

$$\sum_{k_1=-\infty}^{\infty}\sum_{k_2=-\lambda_2+1}^{\lambda_2-1} l_{nk}(f)\Phi(nx_1-k_1)\Phi(nx_2-k_2)+$$

$$\sum_{k_1=-\infty}^{\infty}\sum_{k_2=\lambda_2}^{\infty} l_{nk}(f)\Phi(nx_1-k_1)\Phi(nx_2-k_2)=:(*).$$

(For convenience call

$$F(k_1,k_2,x_1,x_2):=l_{nk}(f)\Phi(nx_1-k_1)\Phi(nx_2-k_2).\ )$$

Thus

$$(*) = \sum_{k_1=-\infty}^{-\lambda_1}\sum_{k_2=-\infty}^{-\lambda_2} F(k_1,k_2,x_1,x_2) + \sum_{k_1=-\lambda_1+1}^{\lambda_1-1}\sum_{k_2=-\infty}^{-\lambda_2} F(k_1,k_2,x_1,x_2) +$$

$$\sum_{k_1=\lambda_1}^{\infty}\sum_{k_2=-\infty}^{-\lambda_2} F(k_1,k_2,x_1,x_2) + \sum_{k_1=-\infty}^{-\lambda_1}\sum_{k_2=-\lambda_2+1}^{\lambda_2-1} F(k_1,k_2,x_1,x_2) +$$

$$\sum_{k_1=-\lambda_1+1}^{\lambda_1-1}\sum_{k_2=-\lambda_2+1}^{\lambda_2-1} F(k_1,k_2,x_1,x_2) + \sum_{k_1=\lambda_1}^{\infty}\sum_{k_2=-\lambda_2+1}^{\lambda_2-1} F(k_1,k_2,x_1,x_2) +$$

$$\sum_{k_1=-\infty}^{-\lambda_1}\sum_{k_2=\lambda_2}^{\infty} F(k_1,k_2,x_1,x_2) + \sum_{k_1=-\lambda_1+1}^{\lambda_1-1}\sum_{k_2=\lambda_2}^{\infty} F(k_1,k_2,x_1,x_2) + \tag{94}$$

$$\sum_{k_1=\lambda_1}^{\infty}\sum_{k_2=\lambda_2}^{\infty} F(k_1,k_2,x_1,x_2).$$

Notice that the finite sum of continuous functions $F(k_1,k_2,x_1,x_2)$, $\sum_{k_1=-\lambda_1+1}^{\lambda_1-1}\sum_{k_2=-\lambda_2+1}^{\lambda_2-1} F(k_1,k_2,x_1,x_2)$ is a continuous function.

The rest of the summands of $F_n(f,x_1,x_2)$ are treated all the same way and similarly to the case of $N=1$. The method is demonstrated as follows.

We will prove that $\sum_{k_1=\lambda_1}^{\infty}\sum_{k_2=-\infty}^{-\lambda_2} l_{nk}(f)\,\Phi(nx_1-k_1)\,\Phi(nx_2-k_2)$ is continuous in $(x_1,x_2)\in\mathbb{R}^2$.

The continuous function

$$\|l_{nk}(f)\|_{\gamma}\,\Phi(nx_1-k_1)\,\Phi(nx_2-k_2) \leq \left\|\|f\|_{\gamma}\right\|_{\infty}\Phi(k_1-\lambda_1)\,\Phi(k_2+\lambda_2),$$

and

$$\left\|\|f\|_{\gamma}\right\|_{\infty}\sum_{k_1=\lambda_1}^{\infty}\sum_{k_2=-\infty}^{-\lambda_2}\Phi(k_1-\lambda_1)\,\Phi(k_2+\lambda_2) =$$

$$\left\|\|f\|_{\gamma}\right\|_{\infty}\left(\sum_{k_1=\lambda_1}^{\infty}\Phi(k_1-\lambda_1)\right)\left(\sum_{k_2=-\infty}^{-\lambda_2}\Phi(k_2+\lambda_2)\right) \leq$$

$$\left\|\|f\|_{\gamma}\right\|_{\infty}\left(\sum_{k_1'=0}^{\infty}\Phi(k_1')\right)\left(\sum_{k_2'=-\infty}^{0}\Phi(k_2')\right) \leq \left\|\|f\|_{\gamma}\right\|_{\infty}.$$

So by the Weierstrass M test we get that $\sum_{k_1=\lambda_1}^{\infty}\sum_{k_2=-\infty}^{-\lambda_2} l_{nk}(f)\,\Phi(nx_1-k_1)\,\Phi(nx_2-k_2)$ is uniformly and absolutely convergent. Therefore it is continuous on $\mathbb{R}^2$.

Next we prove continuity on $\mathbb{R}^2$ of $\sum_{k_1=-\lambda_1+1}^{\lambda_1-1}\sum_{k_2=-\infty}^{-\lambda_2} l_{nk}(f)\,\Phi(nx_1-k_1)\,\Phi(nx_2-k_2)$.

Notice here that

$$\left\|l_{nk}(f)\right\|_{\gamma}\Phi(nx_1-k_1)\Phi(nx_2-k_2)\leq\left\|\|f\|_{\gamma}\right\|_{\infty}\Phi(nx_1-k_1)\Phi(k_2+\lambda_2)$$

$$\leq\left\|\|f\|_{\gamma}\right\|_{\infty}\Phi(0)\Phi(k_2+\lambda_2)=\frac{1}{2\sqrt[2m]{2}}\cdot\left\|\|f\|_{\gamma}\right\|_{\infty}\Phi(k_2+\lambda_2),$$

and

$$\frac{1}{2\sqrt[2m]{2}}\cdot\left\|\|f\|_{\gamma}\right\|_{\infty}\left(\sum_{k_1=-\lambda_1+1}^{\lambda_1-1}1\right)\left(\sum_{k_2=-\infty}^{-\lambda_2}\Phi(k_2+\lambda_2)\right)=$$

$$\frac{1}{2\sqrt[2m]{2}}\cdot\left\|\|f\|_{\gamma}\right\|_{\infty}(2\lambda_1-1)\left(\sum_{k_2'=-\infty}^{0}\Phi(k_2')\right)\leq\frac{1}{2\sqrt[2m]{2}}\cdot(2\lambda_1-1)\left\|\|f\|_{\gamma}\right\|_{\infty}. \tag{95}$$

So the double series under consideration is uniformly convergent and continuous. Clearly $F_n(f,x_1,x_2)$ is proved to be continuous on $\mathbb{R}^2$.

Similarly reasoning one can prove easily now, but with more tedious work, that $F_n(f,x_1,...,x_N)$ is continuous on $\mathbb{R}^N$, for any $N\geq 1$. We choose to omit this similar extra work. ■

Remark 21 *By (25) it is obvious that* $\left\|\|A_n(f)\|_{\gamma}\right\|_{\infty}\leq\left\|\|f\|_{\gamma}\right\|_{\infty}<\infty$, *and* $A_n(f)\in C\left(\prod_{i=1}^{N}[a_i,b_i],X\right)$, *given that* $f\in C\left(\prod_{i=1}^{N}[a_i,b_i],X\right)$.

Call L_n *any of the operators* A_n,B_n,C_n,D_n.

Clearly then

$$\left\|\|L_n^2(f)\|_{\gamma}\right\|_{\infty}=\left\|\|L_n(L_n(f))\|_{\gamma}\right\|_{\infty}\leq\left\|\|L_n(f)\|_{\gamma}\right\|_{\infty}\leq\left\|\|f\|_{\gamma}\right\|_{\infty}, \tag{96}$$

etc.

Therefore we get

$$\left\|\|L_n^k(f)\|_{\gamma}\right\|_{\infty}\leq\left\|\|f\|_{\gamma}\right\|_{\infty},\ \ \forall\ k\in\mathbb{N}, \tag{97}$$

the contraction property.

Also we see that

$$\left\|\|L_n^k(f)\|_{\gamma}\right\|_{\infty}\leq\left\|\|L_n^{k-1}(f)\|_{\gamma}\right\|_{\infty}\leq...\leq\left\|\|L_n(f)\|_{\gamma}\right\|_{\infty}\leq\left\|\|f\|_{\gamma}\right\|_{\infty}. \tag{98}$$

Here L_n^k *are bounded linear operators.*

Notation 22 *Here* $N\in\mathbb{N}$, $0<\beta<1$. *Denote by*

$$c_N:=\begin{cases}\left[2\left(\sqrt[2m]{1+4^m}\right)\right]^N, & \text{if } L_n=A_n,\\ 1, & \text{if } L_n=B_n,C_n,D_n,\end{cases} \tag{99}$$

$$\varphi(n) := \begin{cases} \frac{1}{n^\beta}, & \text{if } L_n = A_n,\ B_n, \\ \frac{1}{n} + \frac{1}{n^\beta}, & \text{if } L_n = C_n, D_n, \end{cases} \tag{100}$$

$$\Omega := \begin{cases} C\left(\prod_{i=1}^{N}[a_i,b_i], X\right), & \text{if } L_n = A_n, \\ C_B\left(\mathbb{R}^N, X\right), & \text{if } L_n = B_n, C_n, D_n, \end{cases} \tag{101}$$

and

$$Y := \begin{cases} \prod_{i=1}^{N}[a_i,b_i], & \text{if } L_n = A_n, \\ \mathbb{R}^N, & \text{if } L_n = B_n, C_n, D_n. \end{cases} \tag{102}$$

We give the condensed

Theorem 23 *Let $f \in \Omega$, $0 < \beta < 1$, $x \in Y$; n, m, $N \in \mathbb{N}$ with $n^{1-\beta} > 2$. Then*
(i)

$$\|L_n(f,x) - f(x)\|_\gamma \leq c_N \left[\omega_1(f, \varphi(n)) + \frac{\left\| \|f\|_\gamma \right\|_\infty}{2m\left(n^{1-\beta}-2\right)^{2m}}\right] =: \tau(n), \tag{103}$$

where ω_1 is for $p = \infty$,
and
(ii)

$$\left\| \|L_n(f) - f\|_\gamma \right\|_\infty \leq \tau(n) \to 0, \text{ as } n \to \infty. \tag{104}$$

For f uniformly continuous and in Ω we obtain

$$\lim_{n\to\infty} L_n(f) = f,$$

pointwise and uniformly.

Proof. By Theorems 8, 16, 17, 18. ■

Next we do iterated neural network approximation (see also [9]).

We make

Remark 24 *Let $r \in \mathbb{N}$ and L_n as above. We observe that*

$$L_n^r f - f = \left(L_n^r f - L_n^{r-1} f\right) + \left(L_n^{r-1} f - L_n^{r-2} f\right) +$$

$$\left(L_n^{r-2} f - L_n^{r-3} f\right) + \ldots + \left(L_n^2 f - L_n f\right) + \left(L_n f - f\right).$$

Then

$$\left\| \|L_n^r f - f\|_\gamma \right\|_\infty \leq \left\| \|L_n^r f - L_n^{r-1} f\|_\gamma \right\|_\infty + \left\| \|L_n^{r-1} f - L_n^{r-2} f\|_\gamma \right\|_\infty +$$

$$\left\| \|L_n^{r-2} f - L_n^{r-3} f\|_\gamma \right\|_\infty + \ldots + \left\| \|L_n^2 f - L_n f\|_\gamma \right\|_\infty + \left\| \|L_n f - f\|_\gamma \right\|_\infty =$$

$$\left\| \left\| L_n^{r-1} \left(L_n f - f \right) \right\|_\gamma \right\|_\infty + \left\| \left\| L_n^{r-2} \left(L_n f - f \right) \right\|_\gamma \right\|_\infty + \left\| \left\| L_n^{r-3} \left(L_n f - f \right) \right\|_\gamma \right\|_\infty$$

$$+ ... + \left\| \left\| L_n \left(L_n f - f \right) \right\|_\gamma \right\|_\infty + \left\| \left\| L_n f - f \right\|_\gamma \right\|_\infty \leq r \left\| \left\| L_n f - f \right\|_\gamma \right\|_\infty . \quad (105)$$

That is

$$\left\| \left\| L_n^r f - f \right\|_\gamma \right\|_\infty \leq r \left\| \left\| L_n f - f \right\|_\gamma \right\|_\infty . \quad (106)$$

We give

Theorem 25 *All here as in Theorem 23 and* $r \in \mathbb{N}$, $\tau(n)$ *as in (104). Then*

$$\left\| \left\| L_n^r f - f \right\|_\gamma \right\|_\infty \leq r \tau(n) . \quad (107)$$

So that the speed of convergence to the unit operator of L_n^r *is not worse than of* L_n*.*

Proof. By (106) and (104). ■

We make

Remark 26 *Let* $m, m_1, ..., m_r \in \mathbb{N} : m_1 \leq m_2 \leq ... \leq m_r$, $0 < \beta < 1$, $f \in \Omega$. *Then* $\varphi(m_1) \geq \varphi(m_2) \geq ... \geq \varphi(m_r)$, φ *as in (100).*

Therefore

$$\omega_1(f, \varphi(m_1)) \geq \omega_1(f, \varphi(m_2)) \geq ... \geq \omega_1(f, \varphi(m_r)) . \quad (108)$$

Assume further that $m_i^{1-\beta} > 2$, $i = 1, ..., r$. *Then*

$$\frac{1}{4m\left(m_1^{1-\beta} - 2\right)^{2m}} \geq \frac{1}{4m\left(m_2^{1-\beta} - 2\right)^{2m}} \geq ... \geq \frac{1}{4m\left(m_r^{1-\beta} - 2\right)^{2m}} . \quad (109)$$

Let L_{m_i} *as above,* $i = 1, ..., r$, *all of the same kind.*

We write

$$\begin{gathered} L_{m_r}\left(L_{m_{r-1}}\left(...L_{m_2}\left(L_{m_1} f\right)\right)\right) - f = \\ L_{m_r}\left(L_{m_{r-1}}\left(...L_{m_2}\left(L_{m_1} f\right)\right)\right) - L_{m_r}\left(L_{m_{r-1}}\left(...L_{m_2} f\right)\right) + \\ L_{m_r}\left(L_{m_{r-1}}\left(...L_{m_2} f\right)\right) - L_{m_r}\left(L_{m_{r-1}}\left(...L_{m_3} f\right)\right) + \\ L_{m_r}\left(L_{m_{r-1}}\left(...L_{m_3} f\right)\right) - L_{m_r}\left(L_{m_{r-1}}\left(...L_{m_4} f\right)\right) + ... + \quad (110) \\ L_{m_r}\left(L_{m_{r-1}} f\right) - L_{m_r} f + L_{m_r} f - f = \\ L_{m_r}\left(L_{m_{r-1}}\left(...L_{m_2}\right)\right)\left(L_{m_1} f - f\right) + L_{m_r}\left(L_{m_{r-1}}\left(...L_{m_3}\right)\right)\left(L_{m_2} f - f\right) + \\ L_{m_r}\left(L_{m_{r-1}}\left(...L_{m_4}\right)\right)\left(L_{m_3} f - f\right) + ... + L_{m_r}\left(L_{m_{r-1}} f - f\right) + L_{m_r} f - f. \end{gathered}$$

Hence by the triangle inequality property of $\left\| \left\| \cdot \right\|_\gamma \right\|_\infty$ *we get*

$$\left\| \left\| L_{m_r}\left(L_{m_{r-1}}\left(...L_{m_2}\left(L_{m_1} f\right)\right)\right) - f \right\|_\gamma \right\|_\infty \leq$$

$$\left\| \left\| L_{m_r}\left(L_{m_{r-1}}\left(...L_{m_2}\right)\right)\left(L_{m_1}f-f\right)\right\|_\gamma \right\|_\infty +$$

$$\left\| \left\| L_{m_r}\left(L_{m_{r-1}}\left(...L_{m_3}\right)\right)\left(L_{m_2}f-f\right)\right\|_\gamma \right\|_\infty +$$

$$\left\| \left\| L_{m_r}\left(L_{m_{r-1}}\left(...L_{m_4}\right)\right)\left(L_{m_3}f-f\right)\right\|_\gamma \right\|_\infty + ...+$$

$$\left\| \left\| L_{m_r}\left(L_{m_{r-1}}f-f\right)\right\|_\gamma \right\|_\infty + \left\| \left\| L_{m_r}f-f\right\|_\gamma \right\|_\infty$$

(repeatedly applying (96))

$$\leq \left\| \left\| L_{m_1}f-f\right\|_\gamma \right\|_\infty + \left\| \left\| L_{m_2}f-f\right\|_\gamma \right\|_\infty + \left\| \left\| L_{m_3}f-f\right\|_\gamma \right\|_\infty + ...+$$

$$\left\| \left\| L_{m_{r-1}}f-f\right\|_\gamma \right\|_\infty + \left\| \left\| L_{m_r}f-f\right\|_\gamma \right\|_\infty = \sum_{i=1}^{r} \left\| \left\| L_{m_i}f-f\right\|_\gamma \right\|_\infty . \tag{111}$$

That is, we proved

$$\left\| \left\| L_{m_r}\left(L_{m_{r-1}}\left(...L_{m_2}\left(L_{m_1}f\right)\right)\right)-f\right\|_\gamma \right\|_\infty \leq \sum_{i=1}^{r} \left\| \left\| L_{m_i}f-f\right\|_\gamma \right\|_\infty . \tag{112}$$

We give

Theorem 27 *Let $f \in \Omega$; m, N, $m_1, m_2, ..., m_r \in \mathbb{N} : m_1 \leq m_2 \leq ... \leq m_r$, $0 < \beta < 1$; $m_i^{1-\beta} > 2$, $i = 1, ..., r$, $x \in Y$, and let $(L_{m_1}, ..., L_{m_r})$ as $(A_{m_1}, ..., A_{m_r})$ or $(B_{m_1}, ..., B_{m_r})$ or $(C_{m_1}, ..., C_{m_r})$ or $(D_{m_1}, ..., D_{m_r})$, $p = \infty$. Then*

$$\left\| L_{m_r}\left(L_{m_{r-1}}\left(...L_{m_2}\left(L_{m_1}f\right)\right)\right)(x)-f(x)\right\|_\gamma \leq$$

$$\left\| \left\| L_{m_r}\left(L_{m_{r-1}}\left(...L_{m_2}\left(L_{m_1}f\right)\right)\right)-f\right\|_\gamma \right\|_\infty \leq$$

$$\sum_{i=1}^{r} \left\| \left\| L_{m_i}f-f\right\|_\gamma \right\|_\infty \leq$$

$$c_N \sum_{i=1}^{r} \left[\omega_1\left(f, \varphi\left(m_i\right)\right) + \frac{\left\| \left\| f \right\|_\gamma \right\|_\infty}{2m\left(m_i^{1-\beta}-2\right)^{2m}} \right] \leq$$

$$r c_N \left[\omega_1\left(f, \varphi\left(m_1\right)\right) + \frac{\left\| \left\| f \right\|_\gamma \right\|_\infty}{2m\left(m_1^{1-\beta}-2\right)^{2m}} \right] . \tag{113}$$

Clearly, we notice that the speed of convergence to the unit operator of the multiply iterated operator is not worse than the speed of L_{m_1}.

Proof. Using (112), (108), (109) and (103), (104). ■

We continue with

Theorem 28 *Let all as in Corollary 15, and* $r \in \mathbb{N}$. *Here* $\varphi_3(n)$ *is as in (75). Then*

$$\left\| \|A_n^r f - f\|_\gamma \right\|_\infty \leq r \left\| \|A_n f - f\|_\gamma \right\|_\infty \leq r\varphi_3(n). \tag{114}$$

Proof. By (106) and (75). ■

Application 29 *A typical application of all of our results is when* $\left(X, \|\cdot\|_\gamma\right) = (\mathbb{C}, |\cdot|)$, *where* $\mathbb{C}$ *are the complex numbers.*

References

[1] G.A. Anastassiou, *Moments in Probability and Approximation Theory*, Pitman Research Notes in Math., Vol. 287, Longman Sci. & Tech., Harlow, U.K., 1993.

[2] G.A. Anastassiou, *Rate of convergence of some neural network operators to the unit-univariate case*, J. Math. Anal. Appli. 212 (1997), 237-262.

[3] G.A. Anastassiou, *Quantitative Approximations*, Chapman&Hall/CRC, Boca Raton, New York, 2001.

[4] G.A. Anastassiou, *Inteligent Systems: Approximation by Artificial Neural Networks*, Intelligent Systems Reference Library, Vol. 19, Springer, Heidelberg, 2011.

[5] G.A. Anastassiou, *Univariate hyperbolic tangent neural network approximation*, Mathematics and Computer Modelling, 53(2011), 1111-1132.

[6] G.A. Anastassiou, *Multivariate hyperbolic tangent neural network approximation*, Computers and Mathematics 61(2011), 809-821.

[7] G.A. Anastassiou, *Multivariate sigmoidal neural network approximation*, Neural Networks 24(2011), 378-386.

[8] G.A. Anastassiou, *Univariate sigmoidal neural network approximation*, J. of Computational Analysis and Applications, Vol. 14, No. 4, 2012, 659-690.

[9] G.A. Anastassiou, *Approximation by neural networks iterates,* Advances in Applied Mathematics and Approximation Theory, pp. 1-20, Springer Proceedings in Math. & Stat., Springer, New York, 2013, Eds. G. Anastassiou, O. Duman.

[10] G.A. Anastassiou, *Intelligent Systems II: Complete Approximation by Neural Network Operators*, Springer, Heidelberg, New York, 2016.

[11] G.A. Anastassiou, *Intelligent Computations: Abstract Fractional Calculus, Inequalities, Approximations*, Springer, Heidelberg, New York, 2018.

[12] G.A. Anastassiou, *Algebraic function based Banach space valued ordinary and fractional neural network approximations*, New Trends in Mathematical Sciences, 10 special issue (1) (2022), 100-125.

[13] G.A. Anastassiou, *General multimariate arctangent function activated neural network approximations*, submitted, 2022.

[14] H. Cartan, *Differential Calculus*, Hermann, Paris, 1971.

[15] Z. Chen and F. Cao, *The approximation operators with sigmoidal functions*, Computers and Mathematics with Applications, 58 (2009), 758-765.

[16] D. Costarelli, R. Spigler, *Approximation results for neural network operators activated by sigmoidal functions*, Neural Networks 44 (2013), 101-106.

[17] D. Costarelli, R. Spigler, *Multivariate neural network operators with sigmoidal activation functions*, Neural Networks 48 (2013), 72-77.

[18] S. Haykin, *Neural Networks: A Comprehensive Foundation* (2 ed.), Prentice Hall, New York, 1998.

[19] W. McCulloch and W. Pitts, *A logical calculus of the ideas immanent in nervous activity*, Bulletin of Mathematical Biophysics, 7 (1943), 115-133.

[20] T.M. Mitchell, *Machine Learning*, WCB-McGraw-Hill, New York, 1997.

[21] L.B. Rall, *Computational Solution of Nonlinear Operator Equations*, John Wiley & Sons, New York, 1969.

TABLE OF CONTENTS, JOURNAL OF COMPUTATIONAL ANALYSIS AND APPLICATIONS, VOL. 31, NO. 4, 2023

Numerical Solutions of Fuzzy Two Coupled Nonlinear Differential Equations, K. Chellapriya and M. M. Shanmugapriya,……..481

Parametrized hyperbolic tangent based Banach space valued multivariate multi layer neural network approximations, George A. Anastassiou and Seda Karateke,…………………………490

General sigmoid based Banach space valued neural network approximation, George A. Anastassiou,………………………………………………………………………………..…520

Approximation of Time Separating Stochastic Processes by Neural Networks, George A. Anastassiou and Dimitra Kouloumpou,……………………………………………………...…535

Multivariate Gudermannian function based neural network approximation, George A. Anastassiou,……………………………………………………………………………………….557

p-Schatten norm generalized Canavati fractional Ostrowski, Opial and Grüss type inequalities involving several functions, George A. Anastassiou,………………………………………….583

Abstract multivariate algebraic function activated neural network approximations, George A. Anastassiou and Robert Kozma,………………………………………………………………..622